



MASARYKOVA UNIVERZITA  
PŘÍRODOVĚDECKÁ FAKULTA  
ÚSTAV CHEMIE

---



# **New organic compounds with targeted biological activity**

Kamil Paruch

Brno 2016

## Contents

<b>Aims and scope of the work</b>	<b>1</b>
<b>Part 1</b>	
1a. Versatile templates for the development of novel kinase inhibitors: discovery of novel CDK inhibitors	<b>20</b>
1b. Pyrazolo[1,5- <i>a</i> ]pyrimidines as orally available inhibitors of cyclin-dependent kinase 2	<b>31</b>
1c. Discovery of dinaciclib (SCH 727965): a potent and selective inhibitor of cyclin-dependent kinases	<b>38</b>
1d. Dinaciclib (SCH 727965), a novel and potent cyclin-dependent kinase inhibitor	<b>50</b>
<b>Part 2</b>	
2a. Discovery of pyrazolo[1,5- <i>a</i> ]pyrimidine-based CHK1 inhibitors: a template-based approach-part 1	<b>69</b>
2b. Discovery of pyrazolo[1,5- <i>a</i> ]pyrimidine-based CHK1 inhibitors: a template-based approach-part 2	<b>80</b>
2c. Targeting the replication checkpoint using SCH 900776, a potent and functionally selective CHK1 inhibitor identified via high content screening	<b>90</b>
2d. Discovery of pyrazolo[1,5- <i>a</i> ]pyrimidine-based Pim inhibitors: a template-based approach	<b>113</b>
<b>Part 3</b>	
3a. Cyclin-dependent kinase inhibitors inspired by roscovitine: purine bioisosteres	<b>125</b>
3b. Fuopyridines as inhibitors of protein kinases	<b>141</b>
<b>Part 4</b>	
4a. Syntheses of 5'-amino-2',5'-dideoxy-2', 2'-difluorocytidine derivatives as novel anticancer nucleoside analogs	<b>243</b>
4b. New carbocyclic nucleosides: synthesis of carbocyclic pseudoisocytidine and its analogs	<b>253</b>
4c. Highly diastereoselective flexible synthesis of new carbocyclic C-nucleosides	<b>284</b>
<b>Part 5</b>	
Synthesis of carbocyclic analogs of dehydroaltenusin: identification of a stable inhibitor of calf DNA polymerase $\alpha$	<b>353</b>

## Aims and scope of the work

Small organic molecules, i.e. compounds with molecular weight less than 1000 g/mol, are ubiquitous in nature. Their biological activity can be multifaceted: e. g., they can bind to receptors, modulate activity of enzymes, get incorporated into membranes etc.<sup>1</sup> Despite the rapid development of therapeutics based on biomolecules, small-molecule organic compounds still represent the majority of clinically used substances.<sup>2</sup>

In addition to their medicinal use, selective organic compounds can be utilized as chemical biology probes that enable elucidation of fundamental biological processes.<sup>3</sup> Information obtained by the chemical biology approach can be of crucial importance, given the recent concerns of possibly misleading phenotypes upon elimination of a protein (e. g., by RNAi-mediated knock-down), rather than just inhibiting its function while preserving the protein's abundance, interactions and compartmentalization, thereby avoiding the otherwise potentially non-physiological or compensatory substitutions by other proteins.<sup>4</sup>

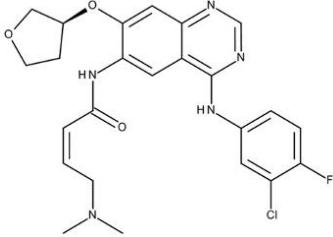
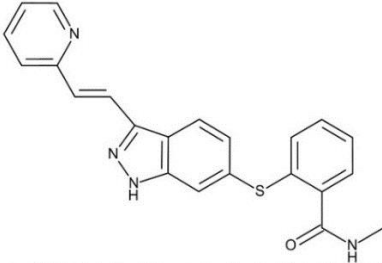
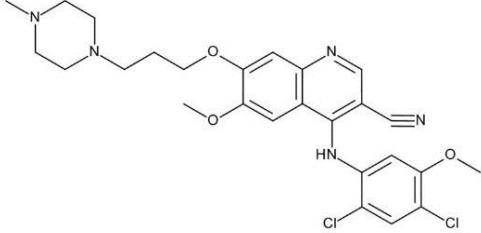
Protein kinases form a large family of ATP-dependent phosphotransferases, encoded by over 500 genes.<sup>5</sup> Protein kinases catalyze reversible phosphorylation on the hydroxyl group of tyrosine, serine, or threonine residues of protein substrates. Reversible phosphorylation is a major post-translational signaling mechanism which is involved in many regulatory pathways that control a diverse set of cellular processes. Modulation of activity of some protein kinases can be in principle utilized in modern anti-cancer therapy as well as for treatment of other diseases such as rheumatoid arthritis, cardiovascular diseases, diabetes, diabetic complications and Alzheimer's disease.<sup>6</sup>

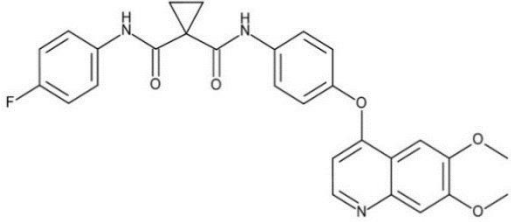
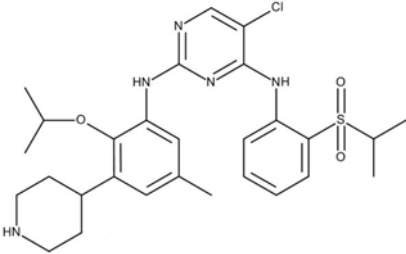
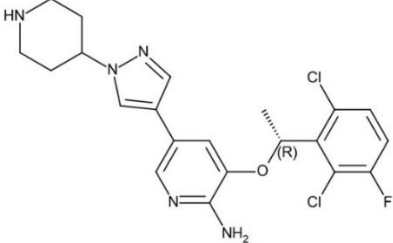
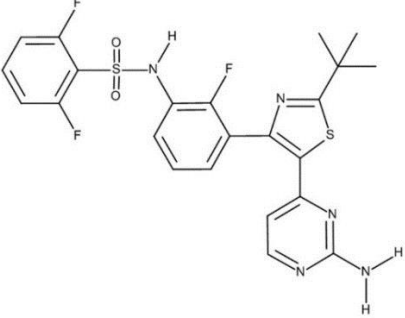
It has been estimated that protein kinases represent ca. 20 % of the druggable genome.<sup>7</sup> Accordingly, development of new protein kinase inhibitors has been one of the most active fields in the academic as well as in the industrial sector. Massive effort in the last two decades has enabled clinical development of new substances for therapeutical use.<sup>8</sup>

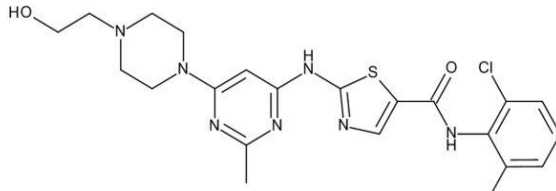
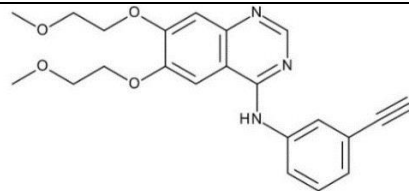
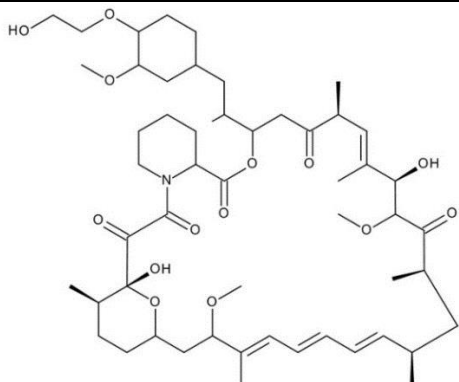
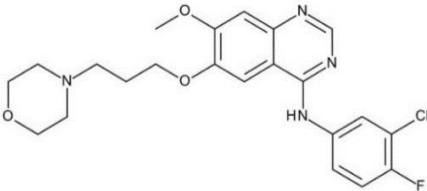
Table 1 summarizes all current clinically used protein kinase inhibitors; including recently approved palbociclib (February 2015) and lenvatinib (February 2015).<sup>9</sup> Except for the Janus kinase inhibitor tofacitinib, all inhibitors have been approved for treatment of different malignancies. It should be noted that in some cases inhibition of several targets is necessary in order to achieve optimal therapeutic outcome; therefore, some inhibitors are relatively non-selective.<sup>10</sup> In other cases, however, inhibition of a particular pathway is sufficient and high selectivity is required to minimize side effects.<sup>11</sup> Typically, protein kinase inhibitors are often well tolerated and possess overall better safety

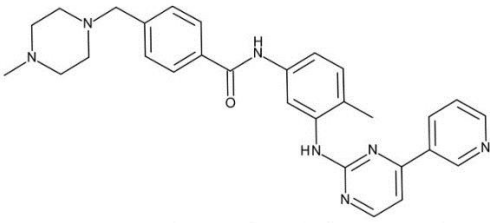
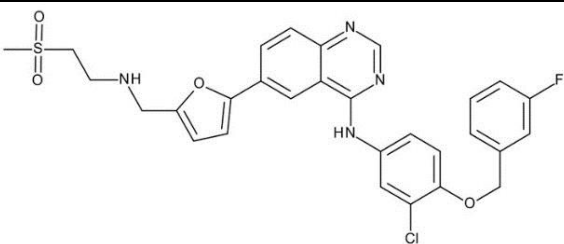
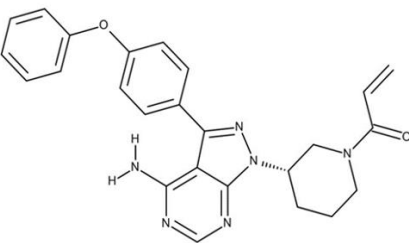
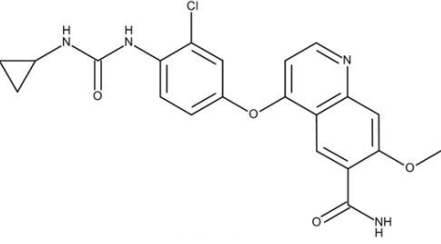
profiles than classical cytotoxic chemotherapies, with toxicities and side effects that are generally more manageable and reversible.

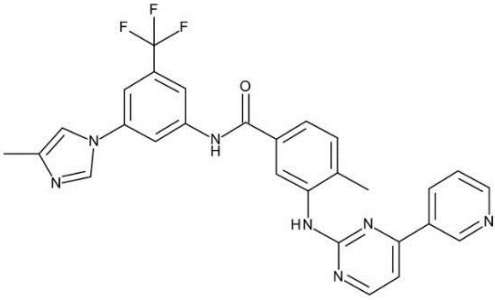
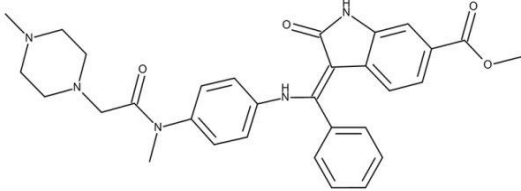
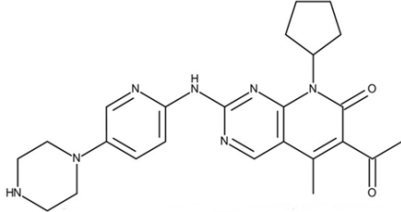
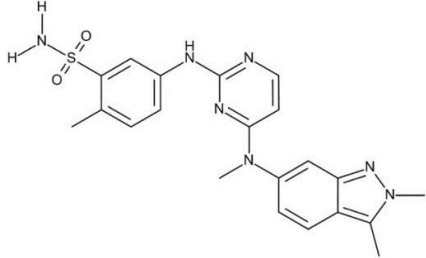
**Table 1.** Clinically used protein kinase inhibitors, year of their approval and their known biological targets.<sup>9</sup>

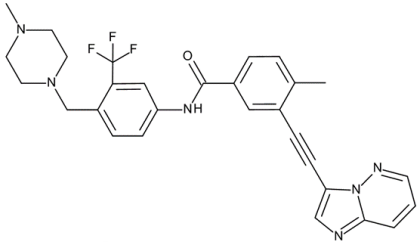
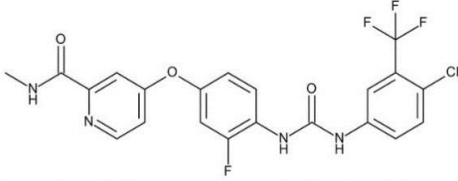
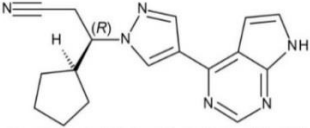
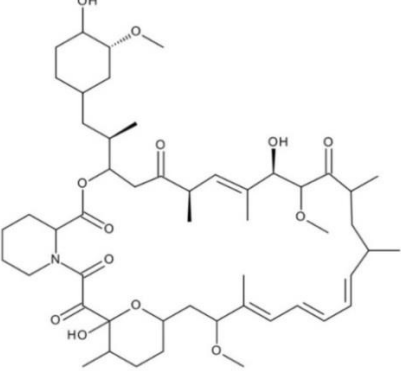
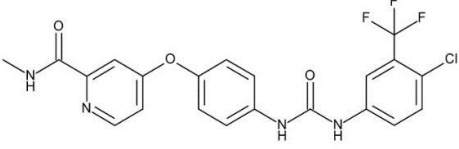
Structure	Year	Known targets
 <p style="text-align: center;"><b>afatinib</b></p>	2013	EGFR
 <p style="text-align: center;"><b>axitinib</b></p>	2012	VEGFR1/2/3
 <p style="text-align: center;"><b>bosutinib</b></p>	2012	BCR-Abl, Src, Lyn, and Hck

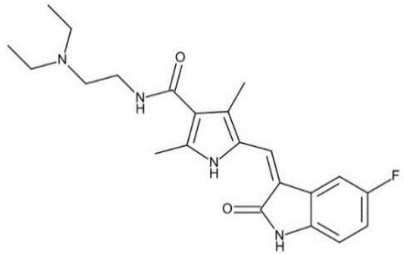
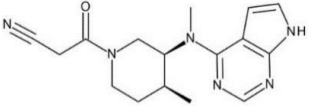
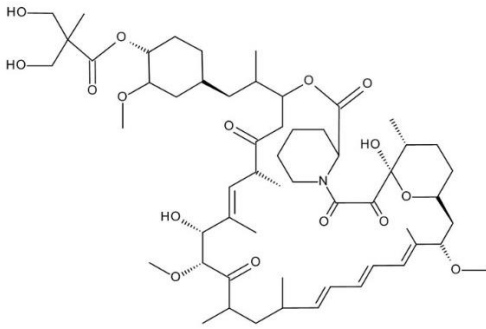
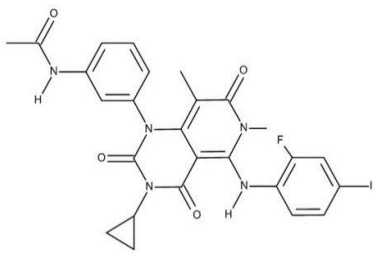
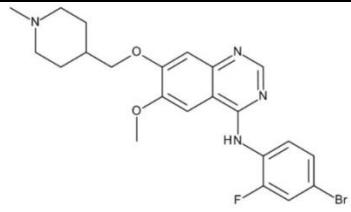
 <p><b>cabozantinib</b></p>	2012	RET, Met, VEGFR1/2/3, Kit, TrkB, Flt3, Axl, Tie2
 <p><b>ceritinib</b></p>	2014	ALK, IGF-1R, InsR, ROS1
 <p><b>crizotinib</b></p>	2011	ALK, c-Met (HGFR), and Ros
 <p><b>dabrafenib</b></p>	2013	B-raf

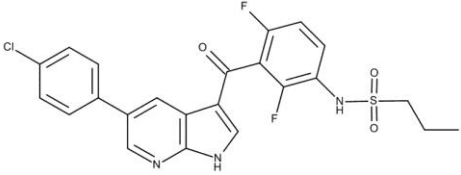
 <p><b>dasatinib</b></p>	2006	BCR-Abl, Src, Lck, Yes, Fyn, Kit, EphA2, and PDGFR $\beta$
 <p><b>erlotinib</b></p>	2004	EGFR
 <p><b>everolimus</b></p>	2009	FKBP12/mTOR
 <p><b>gefitinib</b></p>	2003	EGFR

 <p><b>imatinib</b></p>	2001	BCR-Abl, Kit, and PDGFR
 <p><b>lapatinib</b></p>	2007	EGFR and ErbB2
 <p><b>ibrutinib</b></p>	2013	Bruton's kinase
 <p><b>lenvatinib</b></p>	2015	VEGFRs/FGFRs/ PDGFR/Kit/RET

 <p><b>nilotinib</b></p>	2007	BCR-Abl, PDGFR
 <p><b>nintedanib</b></p>	2014	VEGFR, FGFR, PDGFR
 <p><b>palbociclib</b></p>	2015	CDK4/6
 <p><b>pazopanib</b></p>	2009	VEGFR1/2/3, PDGFR $\alpha/\beta$ , FGFR1/3, Kit, Lck, Fms, and Itk

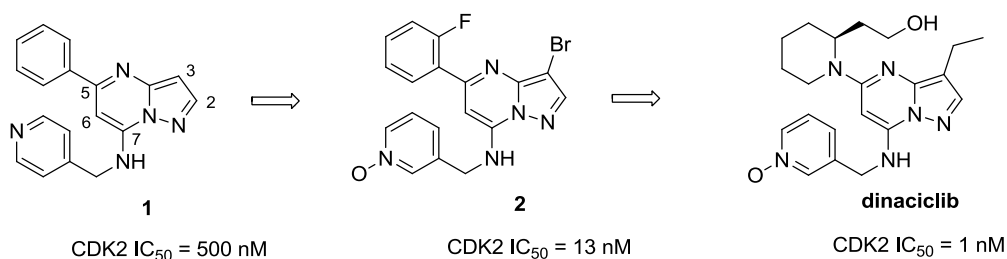
 <p><b>ponatinib</b></p>	2012	BCR-Abl, BCR-Abl T315I, VEGFR, PDGFR, FGFR, Eph, Src family kinases, Kit, RET, Tie2, and Flt3
 <p><b>regorafenib</b></p>	2012	VEGFR1/2/3, BCR-Abl, B-Raf, B-Raf(V600E), Kit, PDGFR $\alpha/\beta$ , RET, FGFR1/2, Tie2
 <p><b>ruxolitinib</b></p>	2011	JAK1/2
 <p><b>sirolimus</b></p>	1999	FKBP12/mTOR
 <p><b>sorafenib</b></p>	2005	C-Raf, B-Raf, B-Raf (V600E), Kit, Flt3, RET, VEGFR1/2/3, and PDGFR $\alpha/\beta$

 <p><b>sunitinib</b></p>	2006	<p>PDGFR<math>\alpha/\beta</math>, VEGFR1/2/3, Kit, Flt3, CSF-1R, and RET</p>
 <p><b>tofacitinib</b></p>	2012	JAK3
 <p><b>temsirolimus</b></p>	2007	FKBP12/mTOR
 <p><b>trametinib</b></p>	2013	MEK1/2
 <p><b>vandetanib</b></p>	2011	<p>EGFRs, VEGFRs, RET, Brk, Tie2, EphRs, and Src family kinases</p>

 <p style="text-align: center;"><b>vemurafenib</b></p>	2011	A/B/C-Raf and B-Raf (V600E)
---	------	--------------------------------

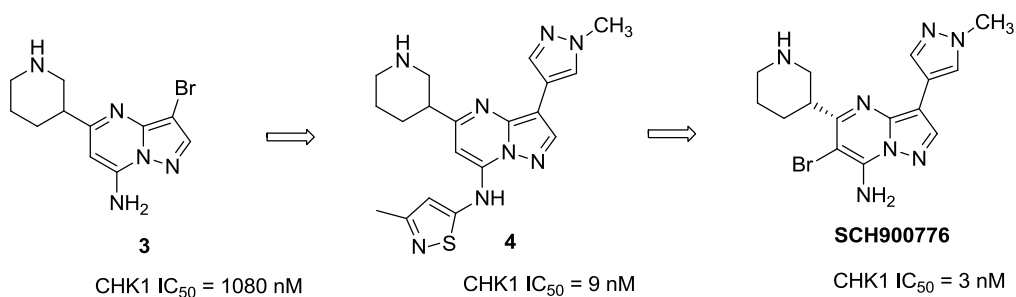
The overarching theme of this work is the search for new organic compounds with defined biological activity that can be used in modern oncology either as single agents or in combination with other therapeutics.

**Part 1** of the work describes discovery of potent cyclin-dependent kinase (CDK) inhibitors with the pyrazolo[1,5-*a*]pyrimidine core. First, the pyrazolo[1,5-*a*]pyrimidine motif, exemplified by compound **1**, was identified among several purine bioisosteres as optimal scaffold (**Part 1a**). Early SAR development around the core led to identification of potent bioavailable inhibitors of CDKs (e. g., compound **2**) that were used in proof-of-concept studies *in vivo* (**Part 1b**). Further optimization of the substituents enabled discovery of extremely potent sub-series with aminoalcohols at position 5 of the pyrazolo[1,5-*a*]pyrimidines core (**Part 1c**), which included SCH727965 (dinaciclib).

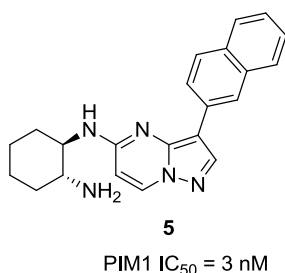


Based on optimal therapeutic index, dinaciclib was chosen for further preclinical progression (**Part 1d**) and later entered clinical trials. Currently, dinaciclib is profiled in Phase III clinical trials as an agent against chronic lymphocytic leukemia (CLL).<sup>12</sup>

**Part 2** describes discovery of potent and selective inhibitors of kinases CHK1 and PIM. Due to the enzyme's central role in the cell cycle, inhibition of CHK1 was identified as an attractive component for therapeutic regimes that utilize the concept of *synthetic lethality*, where the required phenotype (apoptosis and cell death of tumor cells) is caused by a synergic modulation of two or more biological processes.<sup>13</sup> High throughput screening of differently substituted pyrazolo[1,5-*a*]pyrimidines revealed hits; e. g., compound **3**. Modification of the substitution pattern at positions 3, 5, 6, and 7 of the central pyrazolo[1,5-*a*]pyrimidine core yielded the sub-series (exemplified by compound **4**) with significantly reduced activity towards CDKs and single-digit nanomolar activity against CHK1 (**Part 2a** and **Part 2b**). High content cell-based screening then allowed identification of SCH900776, which was further preclinically profiled (**Part 2c**). Since it showed encouraging efficacy in *in vivo* models, SCH900776 later entered clinical trials.



Similarly, exploration of the SAR around the positions 3 and 5 of the pyrazolo[1,5-*a*]pyrimidine core yielded a series of potent and selective inhibitors of PIM kinases; e. g., compound **5** (**Part 2d**).



The strategy utilized the atypical cavity present in the ATP-binding site of PIM kinases; the inhibitors possessing large hydrophobic motifs at position 3 bind to the enzymes via an alternative mode, which is different from the “canonical” one observed for the inhibitors of CDKs and CHK1 described above (Figure 1).

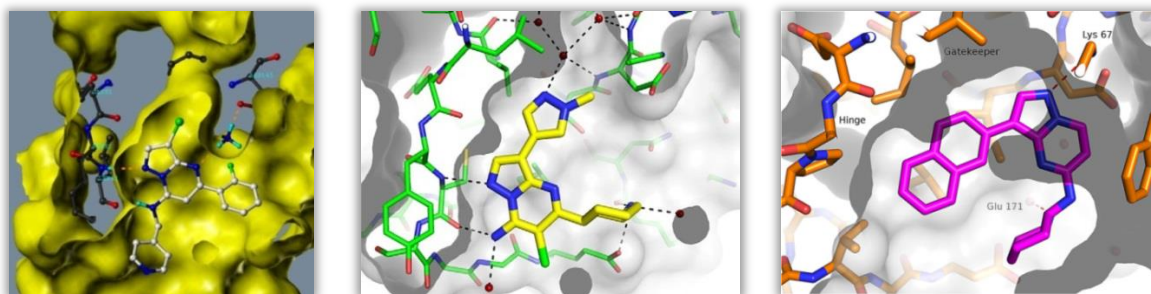
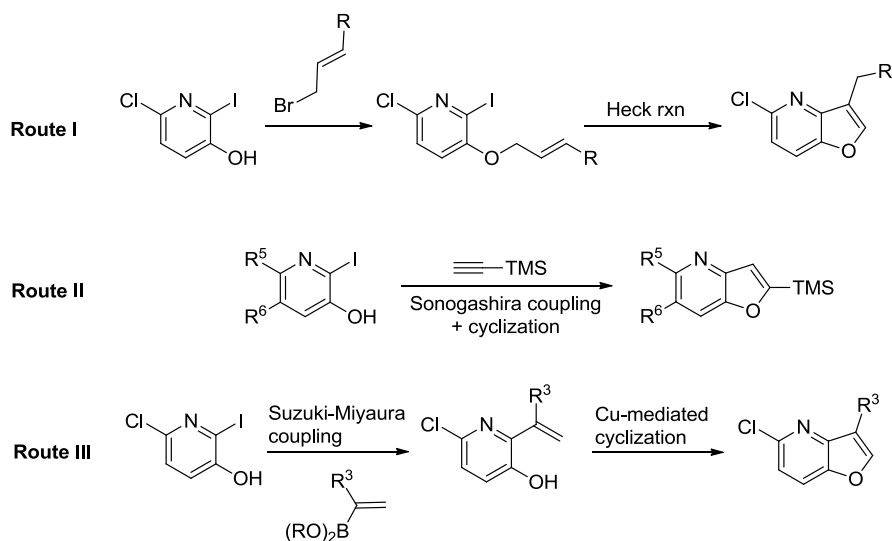


**Figure 1.** Binding modes of pyrazolo[1,5-*a*]pyrimidine-based inhibitors of CDK (left), CHK1 (middle), and PIM (right); the “hinge” regions of the kinases are in compatible orientation.

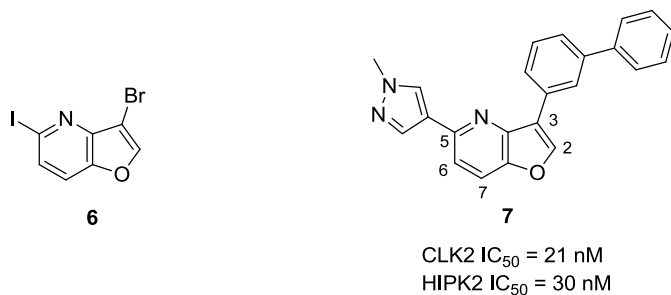
**Part 3** covers our efforts to identify new central pharmacophores as alternatives to the pyrazolo[1,5-*a*]pyrimidine scaffold. Analysis of various bioisosteres of the purine-based CDK inhibitor roscovitine revealed the fact that only certain bicyclic condensed heterocycles are suitable to replace the central purine scaffold (**Part 3a**).

The main aim of the project described in **Part 3b** was to find out whether the furo[3,2-*b*]pyridine scaffold can be used as a central pharmacophore for inhibitors of protein kinases. In order to prepare a sufficiently diverse set of compounds for initial “unbiased” screen, we optimized two known methods (Route I and Route II in Scheme 1) to assemble the furo[3,2-*b*]pyridine core and developed one new annulation methodology (Route III).



**Scheme 1:** Three different strategies for the construction of the furo[3,2-*b*]pyridine scaffold.

Thorough profiling of the starting set our heretofore unknown furo[3,2-*b*]pyridines against 206 human kinases (in the Merck Millipore KinaseProfiler) revealed early leads. We further elaborated the sub-series with proper substituents at positions 3 and 5 of the furo[3,2-*b*]pyridine scaffold, utilizing especially our newly developed annulation methodology to flexibly install a variety of substituents at the two positions. We prepared heretofore unknown compound **6**, which proved to be a valuable intermediate as it could be used for orthogonal manipulation of position 5 and (then) position 3 via sequential Suzuki couplings. This enabled us to identify some *very potent* ( $IC_{50} < 50$  nM) and *selective inhibitors of CLK and HIPK kinases*, exemplified by compound **7**.



CLK and HIPK kinases have emerged only recently as possible therapeutic targets and in terms of activity, some of our compounds are at least comparable to the known inhibitors of these enzymes.

**Part 4** is focused on synthesis and biological profiling of new nucleoside analogs. Due to their multifaceted function nucleosides and their analogs remain attractive molecules to scientist across life sciences.<sup>14</sup> Currently, 29 nucleoside analogs are used as medicaments and numerous others are in clinical trials; especially as antivirals (Figure 2) and chemotherapeutic agents in oncology, including in synthetic lethal combinations with inhibitors of CHK1 kinase (Figure 3).

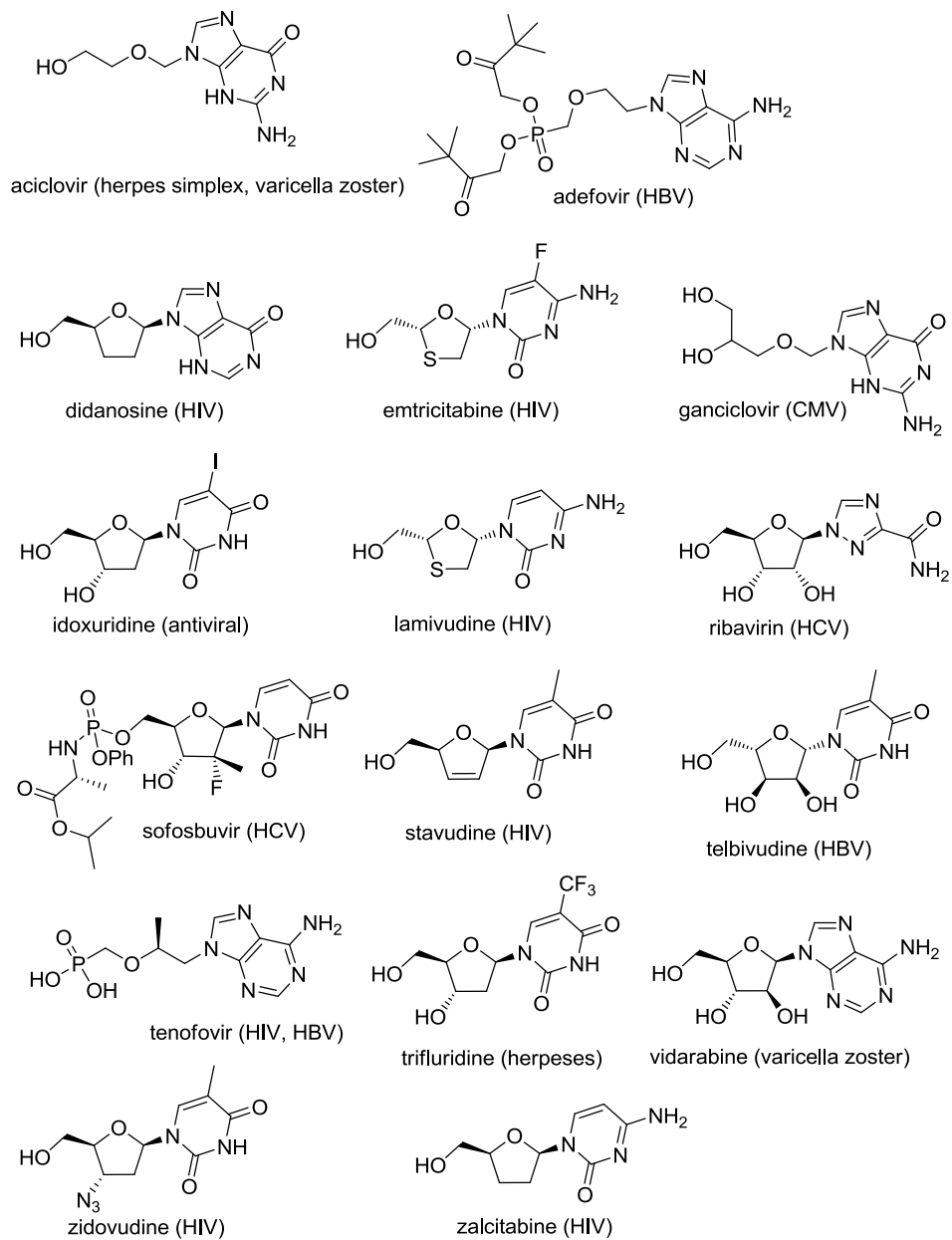


**Figure 2.** Antiviral nucleoside analogs.

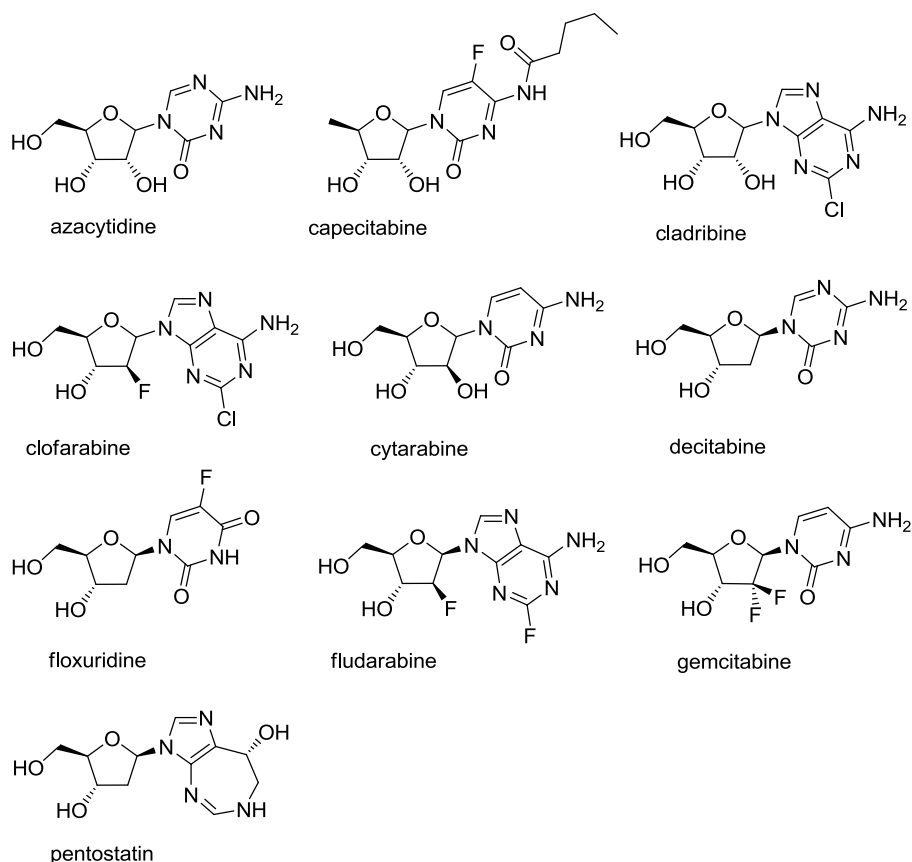
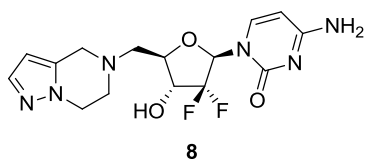


**Figure 3.** Anticancer nucleoside analogs.

However, the biology and the corresponding potential use of nucleosides in therapy are usually not straightforward due to several factors: (i) many nucleoside analogs are not effectively phosphorylated by the cellular kinases; (ii) metabolic stability toward deaminases, hydrolysis of nucleoside-base linkage and sugar ring opening are also limiting for many of analogs; and (iii) the resulting metabolites of mostly unidentified structures can be potentially toxic. These factors often complicate the testing and interpretation of nucleosides' biological activity.<sup>15</sup> On the other hand, the biological activity of nucleoside analogs with non-phosphorylatable substituents at position 5' should be significantly easier to decipher as the biological effects of the compounds would not rely on the full complex scenario described above.

Along this line, **Part 4a** describes identification of analogs of gemcitabine with non-hydroxylic substituents at position 5' of the ribose scaffold; exemplified by compound **8**. Interestingly, despite the fact that the compounds cannot undergo metabolic phosphorylation, they are capable of inhibition of ribonucleotide reductase (RNR) in the cell<sup>16</sup> and could be therefore used as potential partners for synthetic lethal treatment in combination with CHK1 inhibitors.<sup>17</sup>



Classical nucleosides (structure **A** in Figure 1) possess the hemiaminal motif; their chemical and metabolic stability is therefore often limited and the resulting metabolites can be a source of undesired side effects.<sup>18</sup> Significant effort has thus been invested into identification of more stable analogs while preserving the biological activity. Two main strategies involve replacement of the C-N bond between sugar and base by the more stable C-C bond (C-nucleosides, structure **B** in Figure 1)<sup>19</sup> and replacement of the tetrahydrofuran motif by a carbocyclic ring (e. g., cyclopentane), which leads to carbocyclic N-nucleosides (structure **C** in Figure 1).<sup>20</sup>

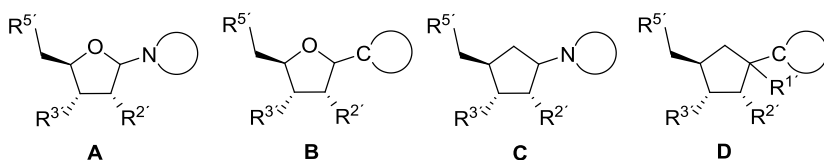
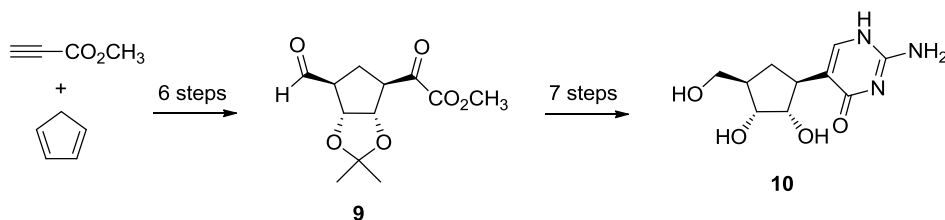


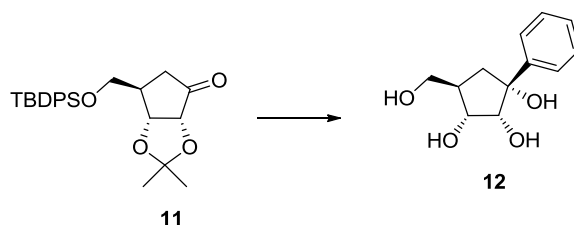
**Figure 4.** Generic structures of natural nucleosides (**A**), C-nucleosides (**B**), carbocyclic N-nucleosides (**C**), and carbocyclic C-nucleosides (**D**).

Structure **D** in Figure 4 combines the stabilizing elements of structures **B** and **C** (i. e. C-C connection between the (heterocyclic) base and the carbocyclic scaffold) and represents carbocyclic C-nucleosides, which are *only sporadically documented in the literature*. It is conceivable that, at least in some cases, those compounds might be more robust versions of nucleoside analogs **B** and **C**. In addition, installation of certain substituents (e. g.  $R^{1'} = \text{OH}$ ) is meaningful only in this series, as this would lead to chemically unstable ketals and aminals in the other analog series.

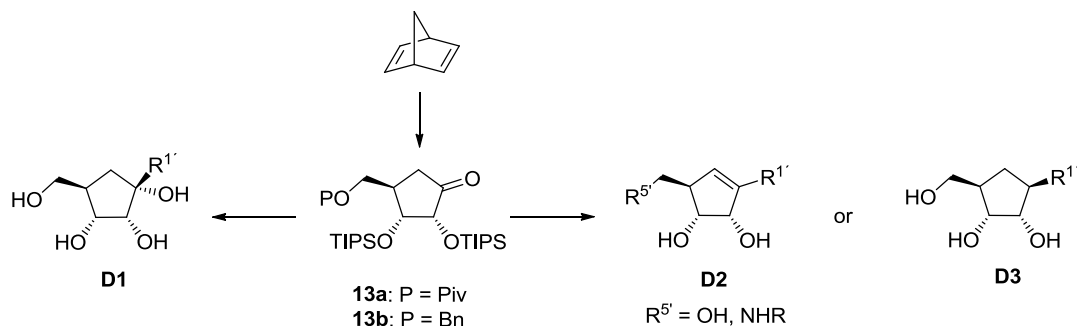
**Part 4b** includes our target-oriented synthesis of racemic carbocyclic pseudoisocytidine (**10**) and its analogs, which were prepared in 13 steps from cyclopentadiene and methyl propiolate via ketoester **9**.



We also prepared versatile cyclopentanone intermediate **11**, which we converted into novel carbocyclic nucleosides *via* highly stereoselective addition of organometallic nucleophiles. Reaction with phenyllithium led to target compound **12** (the stereochemistry was confirmed by X-ray crystallography), which inhibits human glycosylase NEIL1 in a dose-dependent manner.

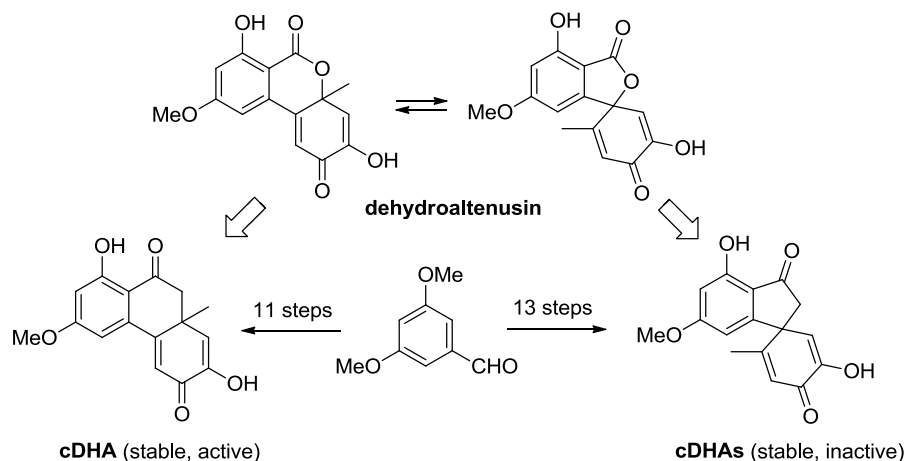


**Part 4c** describes our modular and highly diastereoselective synthesis of three classes of new carbocyclic C-nucleosides, represented by generic structures **D1**, **D2** and **D3**.



Our route enables flexible preparation of three classes of these nucleoside analogs from common precursors – properly substituted cyclopentanones **13a** and **13b**, which can be prepared racemic (in six steps) or optically pure (in ten steps) from inexpensive norbornadiene. The methodology allows flexible manipulation of individual positions around the cyclopentane ring, namely highly diastereoselective installation of carbo- and heterocyclic substituents at position 1', orthogonal functionalization of position 5', and efficient inversion of stereochemistry at position 2'. *The methodology represents, to our knowledge, first sufficiently flexible synthetic approach to carbocyclic C-nucleosides.*

**Part 5** includes synthesis and biological profiling of heretofore unknown carbocyclic analogs of dehydroaltenusin. The project was part of our efforts to identify suitable new substances for synthetic lethal treatments in combination with CHK1 inhibitors. Dehydroaltenusin is one of the very few known inhibitors of DNA polymerase  $\alpha$ , whose depletion has been shown to afford the synthetic lethal phenotype in combination with co-depletion or pharmacological inhibition of CHK1 kinase.<sup>21</sup> However, chemical stability of dehydroaltenusin is limited, as it undergoes a rearrangement in aqueous solutions to give a mixture of the spirocyclic and non-spirocyclic forms (structures **DHAs** and **DHA** in Scheme 1; absolute configurations are not known).<sup>22</sup> It is not clear which of these forms is active and it has been suggested that the rearrangement o-quinone intermediate might be also responsible for the inhibitory activity.<sup>23</sup> In order to help elucidate this issue, we decided to carry out bioisosteric replacement of the lactone ring oxygen by methylene group and prepare the carbocyclic analogs of the spirocyclic and non-spirocyclic forms of dehydroaltenusin - **cDHAs** and **cDHA**, respectively (Scheme 1). These compounds were envisioned to be significantly more stable and resistant to the rearrangement.



**Scheme 1.** Design and synthesis of carbocyclic analogs of both forms of dehydroaltenusin.

The target compounds **cDHA** and **cDHAs** were prepared from 3,5-dimethoxybenzaldehyde in 11 and 13 steps, respectively. Unlike dehydroaltenusin, both **cDHA** and **cDHAs** are stable and their structures were confirmed by X-ray crystallography. Compound **cDHA** was found to be active against calf DNA polymerase  $\alpha$  but not related isozymes, while the spirocyclic analog **cDHAs** was inactive.

Bioisosteric replacement of oxygen atom by the methylene group is commonly used in medicinal chemistry;<sup>24</sup> however, in the context of this project, it enabled not only identification of more stable analogs, but also provided significant (albeit indirect) information on which of the dehydroaltenusin isomers is responsible for its biological activity. Our observation of the dramatic difference in activities of **cdHA** and **cdHAs** strongly suggests that dehydroaltenusin's inhibitory activity toward polymerases is due to its non-spirocyclic form and while the presence reactive o-quinone intermediate may contribute to dehydroaltenusin's inhibitory activity, it may not be absolutely required.

Our results could be used to guide further development of potent and selective inhibitors of mammalian polymerases, namely DNA polymerase  $\alpha$ , exploiting the recently published crystal structure.<sup>25</sup>

## References and notes

1. Ganellin, C. R.; Jefferis, R.; Roberts, S. M. *Introduction to Biological and Small Molecule Drug Research and Development: Theory and Case Studies*; Elsevier Science, **2013**.
2. (a) *Chem. Eng. News* **2016**, *94*, 12. (b) <http://www.economist.com/news/business/21637387-wave-new-medicines-known-biologics-will-be-good-drugmakers-may-not-be-so-good>
3. (a) Schreiber, S. L.; Kapoor, T. M.; Wess, G. *Chemical Biology: From Small Molecules to Systems Biology and Drug Design*; Ed.: Wiley-VCH, **2007**. (b) Waldmann, H.; Janning, P. *Chemical Biology*; Ed.: Wiley-VCH, **2009**.
4. Weiss, W. A.; Taylor, S. S.; Shokat, K. M. *Nat. Chem. Biol.* **2007**, *3*, 739.
5. Grant, S. K. *Cell. Mol. Life Sci.* **2009**, *66*, 1163.
6. Saitoh, M.; Kunitomo, J.; Kimura, E.; Iwashita, H.; Uno, Y.; Onishi, T.; Uchiyama, N.; Kawamoto, T.; Tanaka, T.; Mol, C. D.; Dougan, D. R.; Textor, G. P.; Snell, G. P.; Takizawa, M.; Itoh, F.; Kori, M. *J. Med. Chem.* **2009**, *52*, 6270.
7. Lim, F. P.; Dolzhenko, A. V. *Eur. J. Med. Chem.* **2014**, *85*, 371.
8. Matthews, D. J.; Gerritsen, M. E. *Targeting Protein Kinases for Cancer Therapy*; Wiley, **2010**.
9. <http://www.brimr.org/PKI/PKIs.htm>
10. Legraverend, M.; Grierson, D. S. *Bioorg. Med. Chem.* **2006**, *14*, 3987.
11. Koch, P.; Gehringer, M.; Laufer, S. A. *J. Med. Chem.* **2015**, *58*, 72.
12. <https://ash.confex.com/ash/2015/webprogram/Paper79907.html>

13. (a) Kaelin, W. G. *Nat. Rev. Cancer* **2005**, *5*, 689. (b) Benson, J. D.; Chen, Y.-N. P.; Cornell-Kennon, S. A.; Dorsch, M.; Kim, S.; Leszcznicka, M.; Sellers, W. R.; Lengauer, C. *Nature*, **2006**, *441*, 451. (c) Arlander, S. J. H.; Greene, B. T.; Innes, C. L.; Paules, R. S. *Cancer Res.* **2008**, *68*, 89. (d) Banerjee, S.; Kaye, S. B.; Ashworth, A. *Nat. Rev. Clin. Oncol.* **2010**, *7*, 508.
14. Herdewijn, P. *Modified Nucleosides in Biochemistry, Biotechnology and Medicine*; Ed.: Wiley-VCH, **2008**.
15. Park, W. B. *Chem. Rev.* **2009**, *109*, 2880.
16. Labroli, M. A.; Dwyer, M. P.; Shen, R.; Popovici-Muller, J.; Pu, Q.; Wyss, D.; McCoy, M.; Barrett, D.; Davis, N.; Seghezzi, W.; Shanahan, F.; Taricani, L.; Beaumont, M.; Malinao, M.-C.; Parry, D.; Guzi, T. J. *Bioorg. Med. Chem.* **2014**, *22*, 2303.
17. Taricani, L.; Shanahan, F.; Malinao, M.-C.; Beaumont, M.; Parry, D. *PLoS ONE* **2014**, *9*: e111714.
18. (a) Kawaguchi, T.; Fukushima, S.; Ohmura, M.; Mishima, M.; Nakano, M. *Chem. Pharm. Bull.* **1989**, *37*, 1944. b) Azuma, A.; Hanaoka, K.; Kurihara, A.; Kobayashi, T.; Miyauchi, S.; Kamo, N.; Tanaka, M.; Sasaki, T.; Matsuda, A. *J. Med. Chem.* **1995**, *38*, 3391.
19. Štambaský, J.; Hocek, M.; Kočovský, P. *Chem. Rev.* **2009**, *109*, 6729.
20. (a) Crimmins, M. T. *Tetrahedron*, **1998**, *54*, 9229. b) Jenkins, G. M.; Turner, N. J. *Chem. Soc. Rev.* **1995**, *24*, 169. c) Agrofoglio, L. A.; Suhas, E.; Farese, A.; Condom, R.; Challand, S. R.; Earl, R. A.; Guedj, R. *Tetrahedron*, **1994**, *50*, 10611. d) Zhu, X. F. *Nucleos. Nucleot. Nucl.* **2000**, *19*, 651. e) Agrofoglio, L. A. *Curr. Org. Chem.* **2006**, *10*, 333. f) Ichikawa, E.; Kato, K. *Curr. Med. Chem.* **2001**, *8*, 385. g) Schneller, S. W. *Curr. Top. Med. Chem.* **2002**, *2*, 1087. Boutureira, O.; Matheu, M. I.; Díaz, Y.; Castellón, S. *Chem. Soc. Rev.* **2013**, *42*, 5056.
21. Taricani, L.; Shanahan, F.; Parry, D. *Cell Cycle* **2009**, *8*, 482-489.
22. Kamisuki, S.; Takahashi, S.; Mizushina, Y.; Sakaguchi, K.; Nakata, T.; Sugawara, F. *Bioorg. Med. Chem.* **2004**, *12*, 5355-5359.
23. Kuramochi, K.; Fukudome, K.; Kuryiama, I.; Takeuchi, T.; Sato, Y.; Kamisuki, S.; Tsubaki, K.; Sugawara, F.; Yoshida, H.; Mizushina, Y. *Bioorg. Med. Chem.* **2009**, *17*, 7227-7238.
24. Brown, N. *Bioisosteres in Medicinal Chemistry*; Ed.: Wiley-VCH, **2012**.
25. Baranovskiy, A. G.; Babayeva, N. D.; Suwa, Y.; Gu, J.; Pavlov, Y. I.; Tahirov, T. H. *Nucleic Acids Res.* **2014**, *42*, 14013.

**Part 1a**  
**Versatile templates for the development of novel kinase  
inhibitors: discovery of novel CDK inhibitors\***

\*published as:

Dwyer, M. P.;\* Paruch, K.;\* Alvarez, C.; Doll, R. J.; Keertikar, K.; Duca, J.; Fischmann, T.; Hruza, A.;  
Madison, V.; Lees, E.; Parry, D.; Sgambellone, N.; Seghezzi, W.; Shanahan, F.; Wiswell, D.; Guzi, T. J.  
Versatile Templates for the Development of Novel Kinase Inhibitors: Discovery of Novel CDK Inhibitors.  
*Bioorg. Med. Chem. Lett.* **2007**, *17*, 6216.

The cyclin-dependent kinases (CDKs) are a family of serine/threonine kinases that function as critical regulators of the mammalian cell cycle which integrates extracellular signaling, DNA synthesis, and mitosis.<sup>1</sup> Dysregulation of cell cycle control is a hallmark of all human cancers and is frequently associated with aberrant activation/regulation of cyclin-dependent kinases (CDKs).<sup>2</sup> While coordinated CDK2/CDK1 activity is required for appropriate regulation of S-phase entry (DNA synthesis), suppression of apoptosis in late S-phase, S-phase exit and entry into mitosis, it has been illustrated that inhibition of CDK2/CDK1 in tumors provokes cell cycle arrest and apoptosis.<sup>3</sup> Hence, inhibition of the essential, rate-limiting activities of CDK2 and CDK1 represents an attractive therapeutic strategy for oncology indications.<sup>4</sup>

Several CDK inhibitors are currently under clinical evaluation including flavopiridol ( **1**),<sup>5</sup> roscovitine ( **2**),<sup>6</sup> BMS

387032 ( **3**),<sup>7</sup> R547 ( **4**),<sup>8</sup> and PD0332991 ( **5**) (Fig. 1).<sup>9</sup> However, opportunities exist to identify and develop additional novel CDK inhibitors that may possess superior biological profiles to current candidates. One considerable challenge that exists in this area is the identification of novel core structures for the development of selective kinase inhibitors. Toward this end, the targeting of ATP competitive inhibitors of the CDKs has emerged as the mainstay of this area with several classes of compounds having been developed.<sup>10</sup>

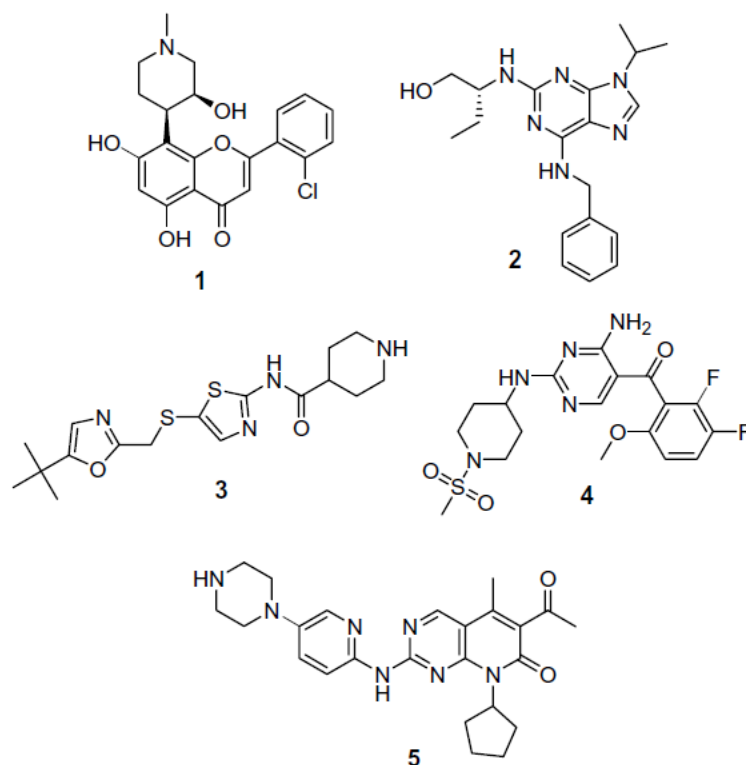


**Figure 1.** CDK inhibitors currently under clinical evaluation.

Herein, we report our initial efforts exploring the utility of several bicyclic cores toward the development of novel ATP-competitive kinase inhibitors of the CDKs. In the early course of our CDK program, two lead classes of compounds emerged from our in-house screening: the pyrazolo[1,5-*a*]pyrimidine **6**<sup>11</sup> and the imidazo[1,2-*a*]pyrazine **7** both of which possessed submicromolar potency in a cyclin A/CDK2 kinase biochemical assay<sup>12</sup> (Fig. 2).

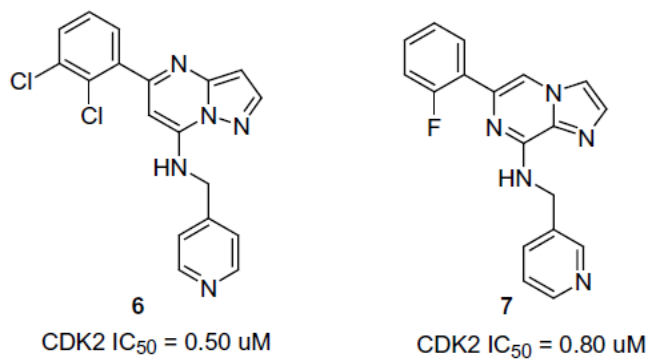


**Figure 2.** Pyrazolo[1,5-*a*]pyrimidine **6** and imidazo[1,2-*a*]pyrazine **7** lead structures from library screening.

Owing to the structural similarities of **6** with the purine CDK2 inhibitor roscovitine (**2**) (Fig. 1), initial C3 bromide substitution of **8** yielded compound **9** which demonstrated over 10-fold improvement of potency in the biochemical assay<sup>12</sup> (Fig. 3).

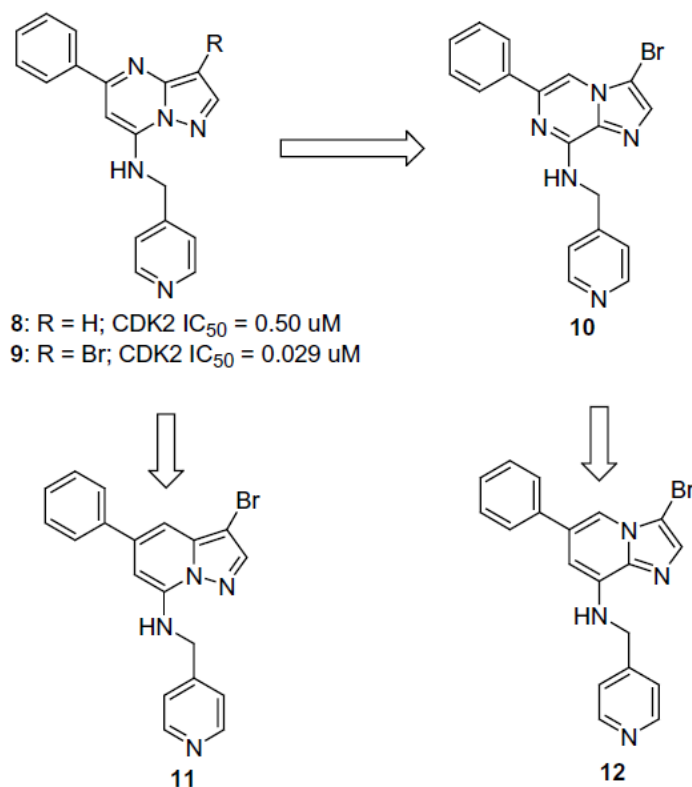
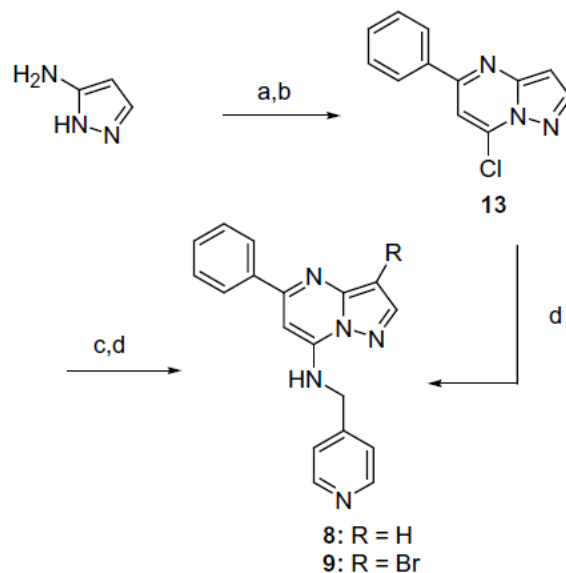


**Figure 3.** Four bicyclic cores of interest as potential CDK inhibitors.

Having achieved reasonable potency in compound **9**, efforts were undertaken to explore the potential utility of other bicyclic cores outside those represented by **6** and **7**. Toward this end, we targeted two additional cores besides the pyrazolo- [1,5-*a*]pyrimidine derivative **9** and the imidazo[1,2-*a*]pyrazine **10** to include: pyrazolo[1,5-*a*]pyridine **11**; and imidazo[1,2-*a*]pyridine **12** (Fig. 3). Each of these compounds was prepared bearing identical substitution and subsequent biological evaluation would allow for the identification of the best CDK bicyclic scaffold.

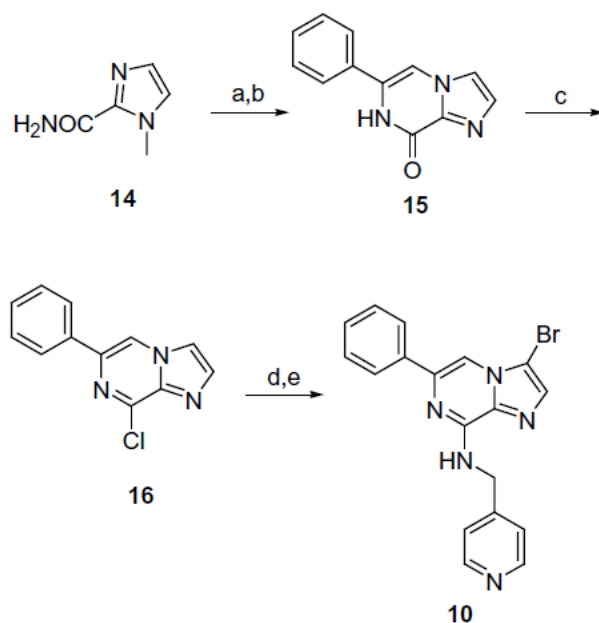
The preparation of the individual core molecules **8-12** is shown in Schemes 1–4.

Preparation of the pyrazolo[1,5-*a*]pyrimidine derivatives **8** and **9** was achieved by treatment of 3-aminopyrazole with ethyl benzoylacetate under acid conditions followed by chlorination under standard conditions to afford compound **13** (Scheme 1).<sup>13</sup> Regioselective bromination followed by displacement with 4-pyridylmethylamine afforded the title compound **9** while treatment with the amine directly on **13** afforded compound **8**.



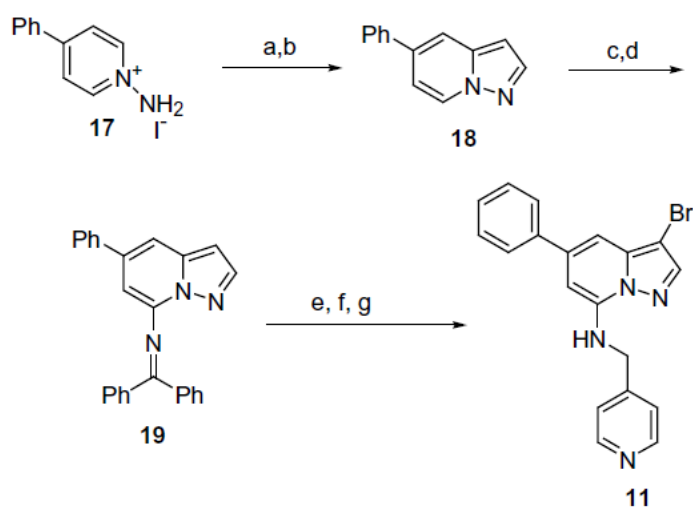
**Scheme 1.** Reagents and condition: (a) ethyl benzoylacetate, AcOH, 100 °C; (b) POCl<sub>3</sub>, pyridine, DMAP; (c) NBS, CH<sub>3</sub>CN; (d) 4-pyridylmethylamine, DIPEA, dioxane.

Preparation of the imidazo[1,2-*a*]pyrazine analog **10** was carried out in an analogous fashion to the protocol depicted in Scheme 1. Treatment of 1-methyl-1H-imidazole-2-carboxamide **14**<sup>14</sup> with  $\alpha$ -bromomethylphenyl ketone followed by dealkylation of the resultant quaternary salt with imidazole afforded compound **15** (Scheme 2).<sup>14</sup> Conversion to chloride **16** followed by regioselective bromination and amine displacement yielded title compound **10**.



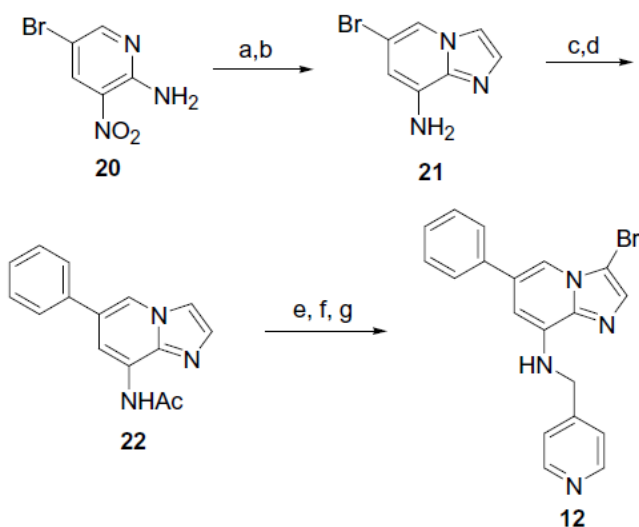
**Scheme 2.** Reagents and condition: (a)  $\alpha$ -bromomethylphenyl ketone,  $\text{CH}_3\text{CN}$ ; (b) imidazole, heat; (c)  $\text{POCl}_3$ , pyridine, DMAP; (d) NBS,  $\text{CH}_3\text{CN}$ ; (e) 4-pyridylmethylamine, DIPEA, dioxane.

Preparation of the pyrazolo[1,5-a]pyridine analog **11** began with cyclization of the known 1-aminopyridinium adduct **17**<sup>15</sup> with ethyl propiolate under basic conditions followed by acid-catalyzed decarboxylation to afford cycloadduct **18** (Scheme 3).<sup>16</sup> Regioselective iodination<sup>17</sup> followed by Pd-catalyzed amination afforded imine **19**. Regioselective bromination, imine deprotection, followed by  $\text{ZnCl}_2$ -promoted reductive amination afforded the title compound **11**.



**Scheme 3.** Reagents and conditions: (a) ethyl propiolate,  $K_2CO_3$ , air; (b)  $H_2SO_4$ , heat; (c) *n*-BuLi, diiodoethane; (d)  $Ph_2CNH$ ,  $Pd(OAc)_2$ , BINAP,  $Cs_2CO_3$ , toluene; (e) NBS,  $CH_3CN$ ; (f)  $NH_2OH$ , NaOAc; (g) 4-pyridinecarboxaldehyde,  $ZnCl_2$  then  $NaBH_3CN$ .

Preparation of the imidazo[1,2-*a*]pyridine adduct **12** began with treatment of nitro adduct **20** under reductive conditions<sup>18</sup> followed by cyclization with in-situ generated bromoacetaldehyde to afford **21**.<sup>19</sup> Suzuki coupling with phenyl boronic acid followed by acetylation afforded **22**. Regioselective bromination, deprotection, and reductive amination afforded the title compound **12**.



**Scheme 4.** Reagents: (a) SnCl<sub>2</sub>, H<sub>2</sub>O, EtOH; (b) BrCH<sub>2</sub>CHO, K<sub>2</sub>CO<sub>3</sub>; (c) PhB(OH)<sub>2</sub>, Pd(PPh<sub>3</sub>)<sub>4</sub>, K<sub>3</sub>PO<sub>4</sub>, DME/H<sub>2</sub>O; (d) AcCl, pyridine; (e) NBS, CH<sub>3</sub>CN; (f) aq. HCl, EtOH; (g) 4-pyridinecarboxaldehyde, ZnCl<sub>2</sub> then NaBH<sub>3</sub>CN.

The targets described above were assayed in a biochemical assay for the inhibition of cyclin A/CDK2.<sup>12</sup> Analogs that demonstrated reasonable potency in the biochemical assay were advanced into a thymidine incorporation assay<sup>20</sup> which was used to measure the ability of the compounds to inhibit asynchronously growing A2780 ovarian carcinoma cells. The data generated for compounds **9-12** and flavopiridol are summarized in Table 1.

Table 1. Cyclin A/CDK2 assay<sup>12</sup> and thymidine incorporation assay<sup>20</sup> for analogs **9-12** and flavopiridol.

Compound	Cyclin A/CDK2 IC <sub>50</sub> (μM) <sup>a</sup>	Thymidine incorporation IC <sub>50</sub> (μM) <sup>a,b</sup>
<b>9</b>	0.029	0.6
<b>10</b>	0.44	2.0
<b>11</b>	4.5	—
<b>12</b>	0.70	—
Flavopiridol	0.012	—

<sup>a</sup> All IC<sub>50</sub> values are means of at least two determinations.

<sup>b</sup> Assay conditions listed in Ref. 20.

In Table 1, incorporation of a C3 bromide into imidazo[1,2-*a*]pyrazine series (**7-10**) showed a clear improvement in in-vitro potency (twofold) but to a lesser extent as was observed in the pyrazolo[1,5-*a*]pyrimidine series (represented by **9**). Modification of the bicyclic core had a much more dramatic effect on the CDK2 in-vitro potency as displayed in Table 1. Deletion of the N6 nitrogen in the imidazo[1,2-*a*]pyrazine adduct **10** yielded imidazo[1,2-*a*]pyridine **12** which led to a twofold loss in *in vitro* potency. More noticeably, the deletion of the N4 nitrogen of pyrazolo[1,5-*a*]pyrimidine **9** afforded pyrazolo[1,5-*a*]pyridine **11** which suffered a 100-fold loss in *in vitro* potency. The great disparity in potency based upon the nature of the bicyclic core is suggestive that the placement of N atoms in cores such as **9** and **10** is imperative. This functionality may play a role in mediating the H-bond donor/acceptor capability of the core or possibly pick up additional interactions with the protein. Our in house X-ray data<sup>21</sup> for compound **9** bound to CDK2 elucidated several key polar interactions

between the 7-NH and Leu83 backbone carbonyl and the pyrazole N and Leu83 backbone NH in a purine-like binding mode (Figure 4).

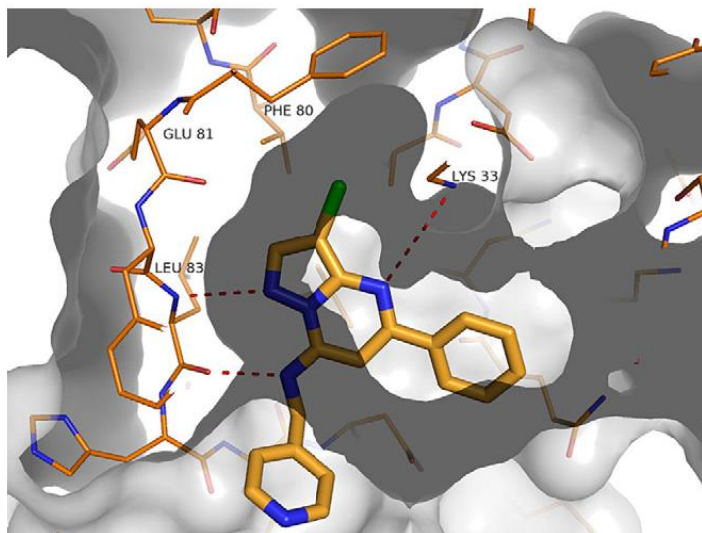


**Figure 4.** X-ray structure of **9** bound to CDK2.<sup>21</sup> Red dotted lines represent key polar interactions.

Recent X-ray data of related pyrazolo[1,5-*a*]pyrimidine analogs<sup>11</sup> are consistent with these results while additional computational and X-ray structural data rationalizing the dramatic potency differences between the core structures

**9–12** will be reported in due course.<sup>22</sup> The two most potent analogs (**9** and **10**) were further evaluated for their ability to alter uptake and incorporation of radioactively labeled thymidine by living cells. In line with the observed *in vitro* potency trends in Table 1, pyrazolo[1,5-*a*]pyrimidine adduct **9** possessed superior activity in the thymidine incorporation assay with an  $IC_{50} = 0.6 \mu M$  versus the comparable imidazo[1,2-*a*]pyrazine adduct **10**. As summarized in Table 1, pyrazolo[1,5-*a*]pyrimidine adduct **9** displayed comparable *in vitro* potency in the cyclin A/CDK2 assay to the known CDK inhibitor flavopiridol (**1**) shown in Figure 1. In summary, four bicyclic cores were designed and prepared bearing identical functionality based upon early screening hits. Based upon both *in vitro* and cell-based data, the pyrazolo[1,5-*a*]pyrimidine core (represented by **9**) emerged from these efforts as the preferred bicyclic motif for our CDK2 program. Further optimization of the pyrazolo[1,5-*a*]pyrimidine series as CDK2 inhibitors appears in the accompanying paper.<sup>23</sup>

## References and notes

1. Murray, A. W. *Cell* **2004**, *116*, 221.
2. (a) Sherr, C. J. *Cancer Res.* **2000**, *60*, 3689; (b) Nevins, J. R. *Hum. Mol. Genet.* **2001**, *10*, 699.
3. Webster, K. R.; Kimball, D. *Emerging Drugs* **2000**, *5*, 45.
4. (a) Thomas, M. P.; McInnes, C. *IDrugs* **2006**, *9*, 273; (b) Shapiro, G. I. *J. Clin. Oncol.* **2006**, *24*, 1770; (c) Fischer, P. *M. Drugs Future* **2005**, *30*, 911; (d) Fischer, P. M. *Cell Cycle* **2004**, *3*, 742.
5. Bible, K. C.; Lensing, J. L.; Nelson, S. A.; Lee, Y. K.; Reid, J. M.; Ames, M. M.; Isham, C. R.; Piens, J.; Rubin, S. L.; Rubin, J.; Kaufmann, S. H.; Atherton, P. J.; Sloan, J. A.; Daiss, M. K.; Adjei, A. A.; Erlichman, C. *Clin. Cancer Res.* **2005**, *11*, 5935.
6. McClue, S. J.; Blake, D.; Clarke, R.; Cowan, A.; Cummings, L.; Fischer, P. M.; MacKenzie, M.; Melville, J.; Stewart, K.; Wang, S.; Zhelev, N.; Zheleva, D.; Lane, D. P. *Int. J. Cancer* **2002**, *102*, 463.
7. Misra, R. N.; Xiao, H.; Kim, K. S.; Lu, S.; Han, W.-C.; Barbosa, S. A.; Hunt, J. T.; Rawlins, D. B.; Shan, W.; Ahmed, S. Z.; Qian, L.; Chen, B.-C.; Zhao, R.; Bednarz, M. S.; Kellar, K. A.; Mulheron, J. G.; Batorsky, R.; Roongta, U.; Kamath, A.; Marathe, P.; Ranadive, S. A.; Sack, J. S.; Tokarski, J. S.; Pavletich, N. P.; Lee, F. Y. F.; Webster, K. R.; Kimball, S. D. *J. Med. Chem.* **2004**, *47*, 1719.
8. Chu, X.-J.; DePinto, W.; Bartkovitz, D.; Sung-Sau, S.; Vu, B. T.; Packman, K.; Luckacs, C.; Ding, Q.; Jiang, N.; Wang, K.; Goelzer, P.; Yin, X.; Smith, M. A.; Higgins, B. X.; Chen, Y.; Xiang, Q.; Moliterni, J.; Kaplan, G.; Graves, B.; Lovey, A.; Fotouhi, N. *J. Med. Chem.* **2006**, *49*, 6549.
9. Toogood, P. L.; Harvey, P. J.; Repine, J. T.; Sheehan, D. J.; VanderWel, S. N.; Zhou, H.; Keller, P. R.; McNamara, D. J.; Fry, D. W. *J. Med. Chem.* **2005**, *48*, 2388.
10. (a) Hirai, H.; Kawanishi, N.; Iwasawa, Y. *Curr. Top. Med. Chem.* **2005**, *5*, 167; (b) McInnes, C.; Fischer, P. M. *Curr. Pharm. Des.* **2005**, *11*, 1845; (c) Fischer, P. M. *Curr. Med. Chem.* **2004**, *11*, 1563.
11. For a recent report on pyrazolo[1,5-a]pyrimidine-based CDK2 inhibitors, see: Williamson, D. S.; Parratt, M. J.; Bower, J. F.; Moore, J. D.; Richardson, C. M.; Dokurno, P.; Cansfield, A. D.; Francis, G. L.; Hebdon, R. J.; Howes, R.; Jackson, P. S.; Lockie, A. M.; Murray, J. B.; Nunns, C. L.; Powles, J.; Robertson, A.; Surgenor, A. E.; Torrance, C. J. *Bioorg. Med. Chem. Lett.* **2005**, *15*, 863.
12. Cyclin A/CDK2 kinase assay. Recombinant baculoviruses were purified from Sf9 cells engineered to express cyclin A and CDK2. Cyclin A/CDK2 enzyme was diluted to a final concentration of 50 µg/mL in kinase buffer containing 50 mM Tris, pH 8.0, 10 mM MgCl<sub>2</sub>, 1 mM DTT, and 0.1 mM sodium orthovanadate. For each kinase reaction, 1 µg of enzyme and 20 µL of 2

$\mu\text{M}$  substrate solution (a biotinylated peptide derived from Histone H1; Amersham, UK) were mixed and combined with 10  $\mu\text{L}$  of diluted compound. The reaction was started by addition of 50  $\mu\text{L}$  of 2  $\mu\text{M}$  ATP and 0.1  $\mu\text{Ci}$  of  $^{33}\text{P}$ -ATP (Amersham, UK). Kinase reactions ran for 1 h at room temperature and were stopped by the addition of 0.1% Triton X-100, 1 mM ATP, 5 mM EDTA, and 5 mg/mL streptavidin-coated SPA beads (Amersham, UK). SPA beads were captured using a 96-well GF/B filter plate (Packard/Perkin Elmer Life Sciences) and a Filtermate universal harvester (Packard/Perkin-Elmer Life Sciences.) Beads were washed twice with 2M NaCl and twice with 2 M NaCl with 1% phosphoric acid. Signal was then assayed using a TopCount 96-well liquid scintillation counter (Packard/Perkin-Elmer Life Sciences). Dose–response curves were generated from duplicate 8 point serial dilutions of inhibitory compounds.  $\text{IC}_{50}$  values were derived by nonlinear regression analysis.

13. Senga, K.; Novinson, T.; Wilson, H. R.; Robins, R. K. *J. Med. Chem.* **1981**, *24*, 610.

14. Davey, D. D. *J. Org. Chem.* **1987**, *57*, 4379.

15. Larson, S. D.; Spilman, C. H. *WO 1993/25553*.

16. Lober, S.; Huber, H.; Utz, W.; Gmeiner, P. *J. Med. Chem.* **2001**, *44*, 2941.

17. Aboul-Fadl, T.; Lober, S.; Gmeiner, P. *Synthesis* **2000**, 1727.

18. Cai, S. X.; Huang, J.-C.; Espitia, S. A.; Tran, M.; Ilyin, V. I.; Hawkinson, J. E.; Woodward, R. M.; Weber, E.; Keana, J. F. W. *J. Med. Chem.* **1997**, *40*, 3679.

19. Hand, E. S.; Paudler, W. W. *J. Org. Chem.* **1978**, *43*, 2906.

20. Thymidine uptake growth inhibition assay. The thymidine incorporation assay was used to measure inhibition of asynchronously growing A2780 ovarian carcinoma cells exposed to test compound. These cells were maintained in DMEM (Cellgro) plus 10% fetal bovine serum (HyClone) and passaged twice a week by detaching the monolayer with Trypsin-EDTA (Gibco). One hundred microliters of A2780 cells (5000 cells/well) was added per well to a 96 well Cytostar T plate (Amersham, UK) and incubated for 16–24 h at 37 °C. Compounds were serially diluted in complete media plus 2%  $^{14}\text{C}$ -labeled thymidine (Amersham, UK). Media were removed from Cytostar T plate, 200  $\mu\text{L}$  of compound dilution was added in quadruplicate and incubated for 24 h at 37 °C. Accumulated incorporation of radiolabel was assayed using scintillation proximity and measured on TopCount (Packard/Perkin-Elmer Life Sciences). Percentage inhibitions, relative to vehicle controls, were calculated and plotted on log-linear plots to allow derivation of  $\text{IC}_{50}$  values.

21. The X-ray coordinates for compound **9** bound to CDK2 have been deposited in the ProteinDataBank (PDB ID code: 2R3R).

22. Duca, J.; Fischmann, T. O.; Hruza, A.; Madison, V. *Unpublished results*.

23. Paruch, K.; Dwyer, M. P.; Alvarez, C.; Brown, C.; Chan, T.-Y.; Doll, R. J.; Keertikar, K.; Knutson, C.; McKittrick, B.; Rivera, J.; Rossman, R.; Tucker, G.; Fischmann, T. O.; Hruza, A.;

Madison, V.; Nomeir, A. A.; Wang, Y.; Lees, E.; Parry, D.; Sgambellone, N.; Seghezzi, W.; Schultz, L.; Shanahan, F.; Wiswell, D.; Xu, X.; Zhou, Q.; James, R. A.; Paradkar, V. M.; Park, H.; Rokosz, L. R.; Stauffer, T. M.; Guzi, T. J. *Bioorg. Med. Chem. Lett.* **2007**. doi:10.1016/j.bmcl.2007.09.017, subsequent paper.

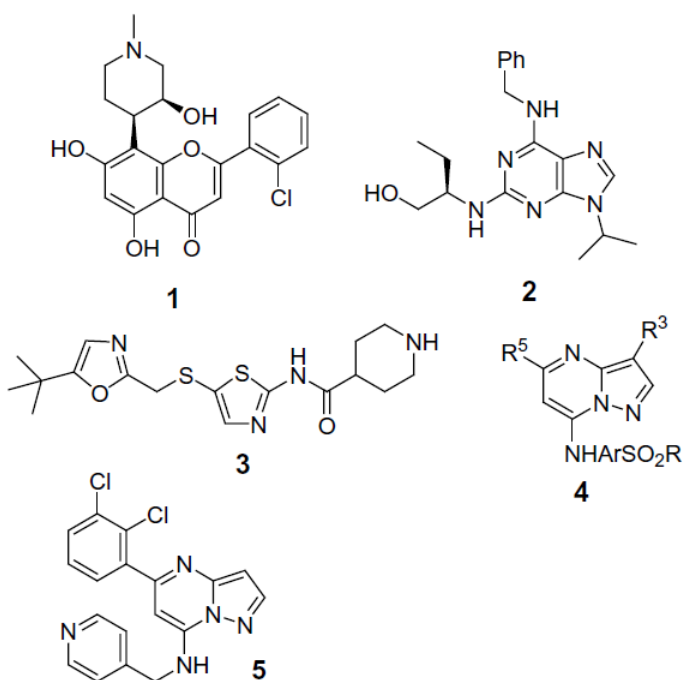
**Note:** Experimental details can be found in our publicly available patents WO 2004/022062 A1, WO 2004/026310 A1, WO 2004/026867 A1, WO 2004/026872 A1, and WO 2004/026877 A1.

**Part 1b**  
**Pyrazolo[1,5-*a*]pyrimidines as orally available inhibitors**  
**of cyclin-dependent kinase 2\***

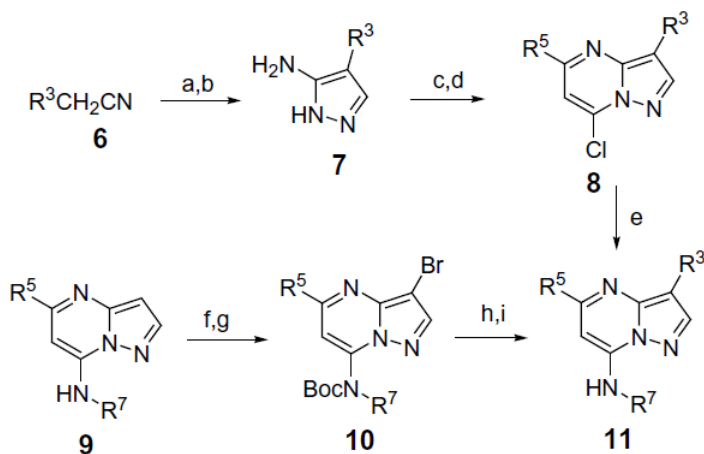
\*published as:

Paruch, K.; \* Dwyer, M. P.; \* Alvarez, C.; Brown, C.; Chan, T.-Y.; Doll, R. J.; Keertikar, K.; Knutson, C.; McKittrick, B.; Rivera, J.; Rossman, R.; Tucker, G.; Fischmann, T.; Hruza, A.; Madison, V.; Nomeir, A. A.; Wang, Y.; Lees, E.; Parry, D.; Sgambellone, N.; Seghezzi, W.; Schultz, L.; Shanahan, F.; Wiswell, D.; Xu, X.; Zhou, Q.; James, R. A.; Paradkar, V. M.; Park, H.; Rokosz, L. R.; Stauffer, T. M.; Guzi, T. J. Pyrazolo[1,5-*a*]pyrimidines as Orally Available Inhibitors of Cyclin-Dependent Kinase 2. *Bioorg. Med. Chem. Lett.* **2007**, *17*, 6220.

One of the characteristics of cancer is uncontrolled cell growth and proliferation. Cyclin-dependent kinases (CDKs) are key regulators of the cell cycle<sup>1</sup> and the proper regulation of CDK activity is crucial for the ordered execution of the phases of the cycle. A large number of human neoplasias show overexpression of positive regulators of CDKs and/or decrease in negative regulators.<sup>2</sup> Abnormal expression of CDK2/cyclin E has been detected in colorectal, ovarian, breast, and prostate cancers.<sup>3</sup> CDK inhibitors have been shown to induce apoptosis in different tumor cell lines.<sup>4</sup> Therefore, CDK inhibitors have the potential to enlarge the group of anticancer agents. A number of more or less selective CDK inhibitors have been described in the literature<sup>5</sup>; those undergoing clinical trials are flavopiridol (**1**),<sup>6</sup> roscovitine (**2**),<sup>7</sup> and BMS 387032 (**3**).<sup>8</sup> Recently, an article on a series of pyrazolo[ 1,5-*a*]pyrimidines (**4**) (with amines linked through NH or O at the 5-position and arylsulfones at the 7-position NH) possessing CDK2 inhibitory activity has been published.<sup>9</sup> Herein, pyrazolo[1,5-*a*]pyrimidines with benzylic substituents at the 7-position are described. The selectivity and pharmacokinetic profiles of these compounds are significantly different from those with N-aryl substitution at the 7-position.<sup>9</sup>



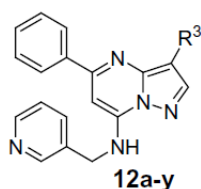
Our effort had started by identification of a relatively weak inhibitor **5** (CDK2/cyclinA  $IC_{50}$  = 500 nM). A number of pyrazolo[1,5-*a*]pyrimidines were synthesized from appropriately substituted acetonitriles and  $\beta$ -ketoesters as shown in Scheme 1. Desired substitution at the 3-position was achieved by choosing properly substituted acetonitriles **6** or via Pd-catalyzed coupling of intermediate **10**.



**Scheme 1.** Reagents: (a)  $HCO_2Et$ , *t*-BuOK, THF; (b)  $N_2H_4$ , AcOH, EtOH; (c)  $R^5COCH_2CO_2Me$ ,  $PhCH_3$ ; (d)  $POCl_3$ , *N,N*-dimethylaniline; (e)  $R^7NH_2$ , DIPEA, dioxane; (f)  $Boc_2O$ , DMAP,  $CH_2Cl_2$ ; (g) NBS,  $CH_3CN$ ; (h)  $R^3B(OH)_2$ ,  $Pd[PPh_3]_4$ ,  $Na_2CO_3$ , DME,  $H_2O$  or  $R^3SnBu_3$ ,  $Pd[PPh_3]_4$ , dioxane; (i) TFA,  $CH_2Cl_2$ .

Incorporation of halogens and other small substituents at the 3-position resulted in significant improvement of potency (Table 1). Most active compounds were selective against GSK3 $\beta$  and MAPK kinases. **12b** exhibited activity in cells (measured by incorporation of radiolabeled thymidine) with IC<sub>50</sub> = 350 nM. The X-ray crystal structure of **13** in CDK2 (without cyclin) given in Figure 1 is consistent with the observed SAR—only a relatively small cavity occupied by 3-substituents is available in the vicinity of Phe 80; (**13** CDK2/cyclinA IC<sub>50</sub> = 49 nM). Thus, only small non-polar substituents (H, Br, Me, Et, *c*-Pr, and SCH<sub>3</sub>) were tolerated; incorporation of large (Ph, Bn) or polar (NO<sub>2</sub>, CH<sub>2</sub>OH) motifs resulted in a sharp drop of activity.

**Table 1.** CDK2 inhibitory activity of pyrazolo[1,5-*a*]pyrimidines **12a–12y**.



Compound	R <sup>3</sup>	CDK2/cyclin A IC <sub>50</sub> (μM)	GSK3 $\beta$ IC <sub>50</sub> (μM)	MAPK IC <sub>50</sub> (μM)
<b>12a</b>	H	0.25	—	—
<b>12b</b>	Br	0.011	0.57	0.37
<b>12c</b>	Me	0.072	—	1.40
<b>12d</b>	Et	0.008	2.80	2.00
<b>12e</b>	Pr	0.890	—	—
<b>12f</b>	Bu	1.20	—	—
<b>12g</b>	Ethynyl	0.048	9.82	7.48
<b>12h</b>	Vinyl	0.090	—	—
<b>12i</b>	Propynyl	0.84	—	—
<b>12j</b>	<i>c</i> -Pr	0.071	—	—
<b>12k</b>	CF <sub>3</sub>	0.095	—	—
<b>12l</b>	CH <sub>2</sub> CF <sub>3</sub>	0.71	—	—
<b>12m</b>	SCH <sub>3</sub>	0.007	1.80	0.90
<b>12n</b>	OCH <sub>3</sub>	1.10	—	—
<b>12o</b>	CH <sub>2</sub> OH	2.17	—	—
<b>12p</b>	CH(OH)CF <sub>3</sub>	3.40	—	—
<b>12q</b>	<i>i</i> -Pr	0.37	—	—
<b>12r</b>	Ph	>50	—	—
<b>12s</b>	CH <sub>2</sub> Ph	16.0	—	—
<b>12t</b>	NO <sub>2</sub>	>50	—	—
<b>12u</b>	CH <sub>2</sub> N(Me) <sub>2</sub>	34.0	—	—
<b>12v</b>	COCH <sub>3</sub>	>50	—	—
<b>12w</b>	S(CH <sub>2</sub> ) <sub>2</sub> NHAc	0.002	0.034	12.00
<b>12x</b>	S(CH <sub>2</sub> ) <sub>2</sub> OH	0.030	—	—
<b>12y</b>	CH <sub>2</sub> CN	0.049	1.10	1.33

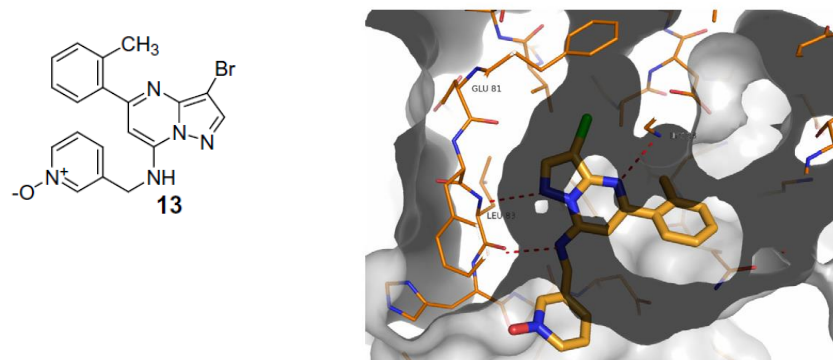
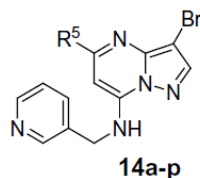


**Figure 1.** X-ray of crystal structure of **13** in CDK2.

Exploration of the 5-position led to a variety of inhibitors whose  $IC_{50}$ s were below 50 nM (Table 2). A somewhat greater differentiation was noted in the cell-based assay, where the compounds with relatively non-polar substituents showed best potency. Notable exceptions are piperidine-containing compounds **14l** and **14m**; the presence of the piperidine moiety, however, resulted in somewhat inconsistent SAR across the series. **14g**, **14h**, **14i**, and **14n** were prepared from 5,7-dichloro[1,5-*a*]pyrimidine by sequential displacements at the 7-position with 3-(aminomethyl)pyridine and at the 5-position with the corresponding nucleophiles followed by bromination with NBS.

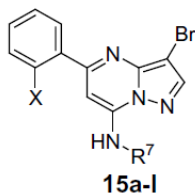
**Table 2.** CDK2 inhibitory activity of pyrazolo[1,5-*a*]pyrimidines **14a–14p**.



Compound	R <sup>5</sup>	CDK2/cyclin A IC <sub>50</sub> (μM)	GSK3β IC <sub>50</sub> (μM)	Thym IC <sub>50</sub> (μM)
<b>14a</b>	Me	0.060	3.53	1.80
<b>14b</b>	Et	0.018	0.92	0.52
<b>14c</b>	<i>i</i> -Pr	0.017	0.42	0.95
<b>14d</b>	CycloPr	0.045	1.13	1.50
<b>14e</b>	CH(CH <sub>3</sub> )OH	0.038	0.50	1.40
<b>14f</b>	CO <sub>2</sub> Et	0.089	0.79	2.90
<b>14g</b>	NHCH <sub>3</sub>	0.043	4.6	1.20
<b>14h</b>	OCH <sub>3</sub>	0.035	1.41	2.00
<b>14i</b>	SCH <sub>3</sub>	0.038	1.18	0.99
<b>14j</b>	Ph-2-Cl	0.003	0.054	0.50
<b>14k</b>	Cyclohexyl	0.004	0.027	0.20
<b>14l</b>	3-Piperidinyl	0.008	0.18	0.06
<b>14m</b>	4-Piperidinyl	0.016	0.41	0.16
<b>14n</b>	Piperazine	0.210	—	—
<b>14o</b>	2-Furyl	0.008	0.31	15.19
<b>14p</b>	2-Thienyl	0.013	0.48	0.75

A variety of substituents were tolerated at the 7-position (Table 3), which is close to the solvent-exposed part of the enzyme. The best cell activity (measured by radiolabeled thymidine uptake) was noted for the subclass containing pyridines and pyridine-N-oxides. In addition, unlike the aniline series, those compounds exhibited good oral PK profile.

**Table 3.** CDK2 inhibitory activity of pyrazolo[1,5-*a*]pyrimidines **15a–15l**.



Compound	X	R <sup>7</sup>	CDK2/cyclin A IC <sub>50</sub> (μM)	GSK3β IC <sub>50</sub> (μM)	Thym IC <sub>50</sub> (μM)
<b>15a</b>	H	H	0.25	—	—
<b>15b</b>	Cl	Me	0.020	0.247	1.80
<b>15c</b>	Cl	Pr	0.163	—	—
<b>15d</b>	Cl	<i>c</i> -Pr	0.825	—	—
<b>15e</b>	F	Ph	0.408	13.31	—
<b>15f</b>	Cl	Ph-4-SO <sub>2</sub> CH <sub>3</sub>	0.35	0.45	0.90
<b>15g</b>	F	Bn	0.300	15.2	—
<b>15h</b>	Cl	CH <sub>2</sub> -3Pyr	0.004	0.054	0.50
<b>15i</b>	Cl	CH <sub>2</sub> -3Pyr-O	0.011	0.035	0.17
<b>15j</b>	F	CH <sub>2</sub> -3Pyr-O	0.013	0.13	0.21
<b>15k</b>	H	CH <sub>2</sub> -3Pyr-O	0.034	0.60	0.14
<b>15l</b>	H	CH(Me)-3Pyr	3.000	—	—

Compound **15j** was profiled further: it was screened against a panel of 50 kinases (e.g. cSRC, JNK1, PDK1, PKB, ROCK-II) without observing any non-CDK cross-reactivity. The compound is moderately protein-bound (mouse: 90%, rat: 85%, monkey: 89%, dog: 93%, human: 95%). **15j** was active against a panel of 17 different tumor cell lines in the clonogenicity assay with IC<sub>50</sub>s in the range of 120–390 nM. The compound is orally available and its PK parameters are summarized in Table 4.

**Table 4.** Pharmacokinetic parameters of **15j**.

Species	Dose, mpk vehicle	AUC ( $\mu\text{M h}$ )	$c_{\text{max}}$ ( $\mu\text{M}$ )	$t_{\text{max}}$ (h)
Rat	10	16.4	2.29	2.0
Mouse	40 0.4% MC	17.9	6.81	2.0
	20% HPBCD			
Dog	5 20% HPBCD	2.44	2.58	
Monkey	10	43.0	3.2	3.3
	0.4% HPMC			

Compound **15j** demonstrated efficacy in a staged A2780 tumor xenograft model in the mouse (Fig. 2). The dose of 40 mpk, qd, PO for 10 days caused 96% tumor growth inhibition with observed tumor regression in 9 of 10 animals. The compound was well tolerated and only a moderate and reversible decrease of white blood cells was observed.

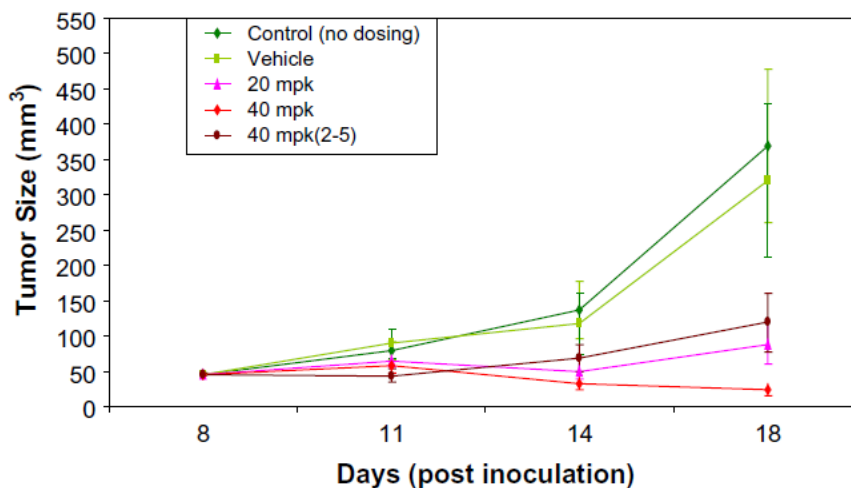


**Figure 2.** Efficacy of **15j** in A2780 xenograft model (mouse).

In conclusion, we demonstrated that properly substituted pyrazolo[1,5-*a*]pyrimidines can serve as potent, selective, and efficacious orally available CDK2 inhibitors.

## References and notes

1. Murray, A. W. *Cell* **2004**, *116*, 221.
2. Carnero, A. *Br. J. Cancer* **2002**, *87*, 129.
3. Webster, K. R.; Kimball, D. *Emerging Drugs* **2000**, *5*, 45.
4. Cai, D.; Byth, K. F.; Shapiro, G. I. *Cancer Res.* **2006**, *66*, 435.
5. Kong, N.; Fotouhi, N.; Wovkulich, P. M.; Roberts, J. *Drugs Fut.* **2003**, *28*, 881.
6. Bible, K. C.; Lensing, J. L.; Nelson, S. A.; Lee, Y. K.; Reid, J. M.; Ames, M. M.; Isham, C. R.; Piens, J.; Rubin, S. L.; Rubin, J.; Kaufmann, S. H.; Atherton, P. J.; Sloan, J. A.; Daiss, M. K.; Adjei, A. A.; Erlichman, C. *Clin. Cancer Res.* **2005**, *11*, 5935.
7. McClue, S. J.; Blake, D.; Clarke, R.; Cowan, A.; Cummings, L.; Fischer, P. M.; MacKenzie, M.; Melville, J.; Stewart, K.; Wang, S.; Zhelev, N.; Zheleva, D.; Lane, D. P. *Int. J. Cancer.* **2002**, *102*, 463.
8. Misra, R. N.; Xiao, H.; Kim, K. S.; Lu, S.; Han, W.-C.; Barbosa, S. A.; Hunt, J. T.; Rawlins, D. B.; Shan, W.; Ahmed, S. Z.; Qian, L.; Chen, B.-C.; Zhao, R.; Bednarz, M. S.; Kellar, K. A.; Mulheron, J. G.; Batorsky, R.; Roongta, U.; Kamath, A.; Marathe, P.; Ranadive, S. A.; Sack, J. S.; Tokarski, J. S.; Pavletich, N. P.; Lee, F. Y. F.; Webster, K. R.; Kimball, S. D. *J. Med. Chem.* **2004**, *47*, 1719.
9. Williamson, D. S.; Parratt, M. J.; Bower, J. F.; Moore, J. D.; Richardson, C. M.; Dokurno, P.; Cansfield, A. D.; Francis, G. L.; Hebdon, R. J.; Howes, R.; Jackson, P. S.; Lockie, A. M.; Murray, J. B.; Nunns, C. L.; Powles, J.; Robertson, A.; Surgenor, A. E.; Torrance, C. J. *Bioorg. Med. Chem. Lett.* **2005**, *15*, 863.

**Note:** Experimental details can be found in our publicly available patents WO 2004/022062 A1, WO 2004/022559 A1, WO 2004/022560 A1, WO 2004/022561 A1, and WO 2004/026229 A1.

**Part 1c**  
**Discovery of dinaciclib (SCH 727965): a potent and  
selective inhibitor of cyclin-dependent kinases\***

\*published as:

Paruch, K.; Dwyer, M. P.; Alvarez, C.; Brown, C.; Chan T.-Y.; Doll, R. J.; Keertikar K.; Knutson, C.; McKittrick, B.; Rivera, J.; Rossman, R.; Tucker, G.; Fishmann, T.; Hruza, A.; Madison, V.; Nomeir, A. A.; Wang, Y.; Kirschmeier, P.; Lees, E.; Parry, D.; Sgambellone, N.; Seghezzi, W.; Schultz, L.; Shanahan, F.; Wiswell, D.; Xu, X.; Zhou, Q.; James, R. A.; Paradkar, V. M.; Park, H.; Rokosz, L. R.; Stauffer, T. M.; Guzi, T. J.\* Discovery of Dinaciclib (SCH 727965): A Potent and Selective Inhibitor of Cyclin-Dependent Kinases. *ACS Med. Chem. Lett.* **2010**, *1*, 204.

The mammalian cell cycle is a nonredundant process that integrates extracellular signaling, DNA synthesis, and mitosis.<sup>1</sup> Loss of cell cycle control is a hallmark of all human cancers and is frequently associated with aberrant activation of cyclin-dependent kinases (CDKs).<sup>2,3</sup> The CDKs are a well-characterized family of serine/threonine kinases that regulate cell cycle progression by phosphorylation and inactivation of the retinoblastoma tumor suppressor gene product (Rb) throughout late-G1, S, and G2/M phases as well as playing a role in the G2/M checkpoint and progression through mitosis.<sup>4-9</sup> Other members of the CDK family have also been shown to have functions beyond cell cycle regulation. For example, CDK5 is involved in neuronal function and  $\tau$  phosphorylation,<sup>10</sup> and CDK7, CDK8, and CDK9 have been implicated in transcriptional regulation.<sup>11,12</sup> Inhibition of multiple members of the CDK family has been shown to induce therapeutically desirable phenotypes such as inhibition of proliferation and apoptosis. For example, expression of dominant negative forms of CDK2 and combinatorial silencing of CDK1 and CDK2 via siRNA generates cell cycle arrest and apoptosis.<sup>13-17</sup> Likewise, inhibition of the noncell cycle-related CDKs, CDK7 and CDK9, depress transcriptional regulation a variety of targets including several antiapoptotic proteins.<sup>8,17</sup> Moreover, inhibition of CDK8 modulates B-catenin function, resulting in decreased proliferation of colon cancer cells.<sup>18,19</sup> Thus, inhibition of the essential, rate-limiting activities of multiple members of the CDK family represents an attractive therapeutic strategy for oncology indications.

A number of diverse CDK inhibitors have progressed into clinical development (Figure 1).<sup>20-23</sup> Flavopiridol has been the most clinically studied CDK inhibitor, and several phase II trials targeting a

variety of indications have been completed. Thus far, the most significant activity has been reported in chronic lymphocytic leukemia.<sup>24</sup>

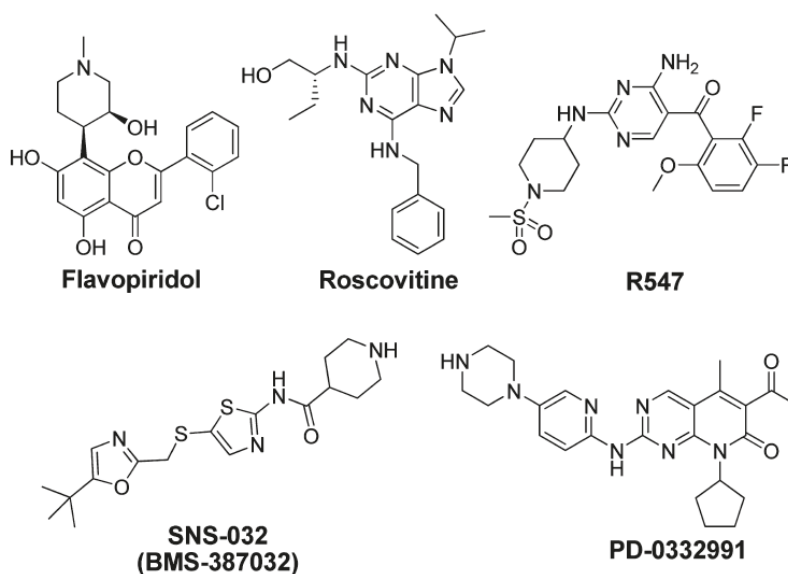
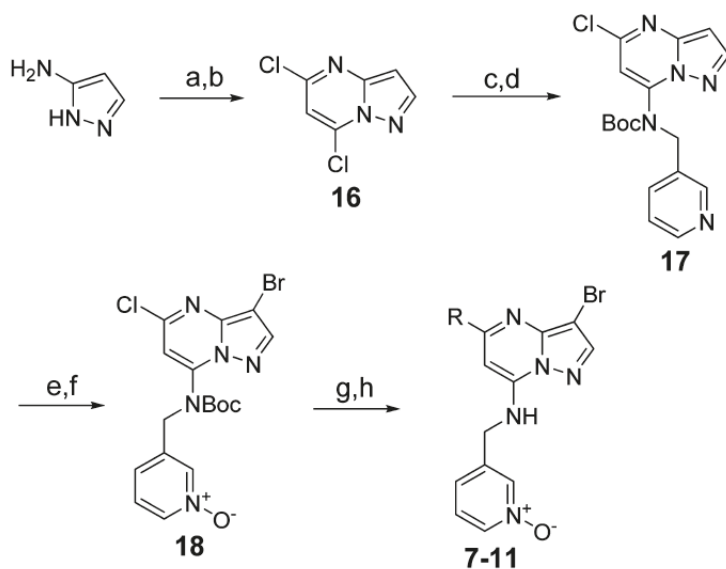


**Figure 1.** Representative CDK inhibitors in clinical trials.

Efforts in applying an *in vivo* screening system to select candidate CDK inhibitors with the optimal combination of potency, pharmacokinetic, efficacy, and safety parameters are herein described. This functional approach allowed rapid differentiation within a discrete series of compounds as well as benchmarking against flavopiridol. Ultimately, this approach led to the identification of SCH 727965, which is currently in phase II clinical trials.

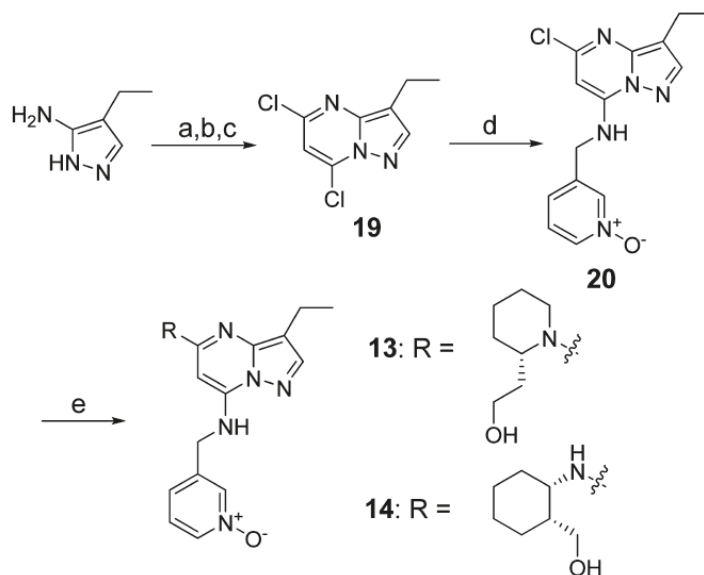
The utility of the pyrazolo[1,5-*a*]pyrimidine scaffold as a basis for the development of novel CDK inhibitors has previously been described.<sup>25,26</sup> From these efforts, compound **6** was identified as a novel CDK inhibitor, which was effective at reducing tumor burden *in vivo* upon oral delivery. In an effort to further expand the understanding of the impact of positional substitution on activity, structure-activity relationship development was expanded around each position in the pyrazolo[1,5-*a*]pyrimidine core. The preparation of these novel pyrazolo[1,5-*a*]pyrimidine CDK inhibitors is outlined in Schemes 1 and 2. The synthesis of these analogues for the 3-bromo series began with treatment of 3-aminopyrazole with diethylmalonate under basic conditions followed by chlorination to afford **16**. Treatment with 3-aminomethylpyridine followed by Boc protection afforded intermediate **17**. Bromination with NBS followed by oxidation yielded **18**, which was treated with commercially available amines and deprotected under basic conditions to afford the title compounds **7-11**.



**Scheme 1.** Preparation of 3-Bromo Derivatives **7-11**.<sup>a</sup>

<sup>a</sup> Reagents and conditions: (a) Na, EtOH, diethylmalonate, reflux. (b) POCl<sub>3</sub>, dimethylaniline, 60 °C. (c) 3-aminomethyl pyridine, DIPEA, dioxane. (d) Boc<sub>2</sub>O, DMAP, CH<sub>2</sub>Cl<sub>2</sub>. (e) NBS, CH<sub>3</sub>CN, 0 °C. (f) MCPBA, CH<sub>2</sub>Cl<sub>2</sub>. (g) HNR<sup>1</sup>R<sup>2</sup>, DIPEA, dioxane, 90 °C. (h) KOH, EtOH/H<sub>2</sub>O, 100 °C.

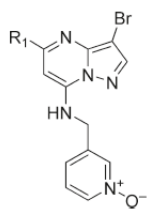
The corresponding 3-ethyl derivatives were prepared by cyclization of 3-amino-4-ethyl pyrazole with dimethylmalonate under basic conditions followed by chlorination, which afforded **19** (Scheme 2). Treatment of **19** with 3-(aminomethyl) pyridine N-oxide monohydrochloride under basic conditions yielded **20** followed by treatment with known amino alcohols, which afforded title compounds **13** and **14**. The preparation of **6** and **12** has been previously described.<sup>26,27</sup>

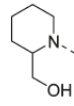
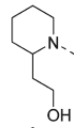
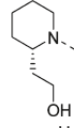
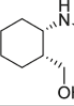


**Scheme 2.** Preparation of 3-Ethyl Aminoalcohol Derivatives **13** and **14**.<sup>a</sup>

<sup>a</sup> Reagents and conditions: (a) Dimethylmalonate, reflux. (b) NaOMe, MeOH, reflux. (c) POCl<sub>3</sub>, dimethylaniline, reflux. (d) 3-Aminomethyl pyridine N-oxide hydrochloride, NaHCO<sub>3</sub>, CH<sub>3</sub>CN, reflux. (e) HNR<sup>1</sup>R<sup>2</sup>, NaHCO<sub>3</sub>, NMP, 150 °C.

As illustrated in Table 1, a key observation made in the 3-bromo series was the marked improvement in potency by replacement of the aryl functionality at the 5-position of **6** with N-linked motifs bearing hydroxy substitution such as **8**. Furthermore, with correct positioning of this functionality, additional improvements in both kinase activity as well as inhibition of cell growth were observed in **9-11**.

**Table 1.** Optimization in the 5-Position.<sup>a</sup>

Compound	R <sub>1</sub>	A/CDK2 <sup>a</sup> IC <sub>50</sub> (uM)	In-cell <sup>b</sup> IC <sub>50</sub> (uM)
6		0.03	0.2
7		0.03	0.2
8		0.018	0.025
9		0.001	0.003
10		0.001	0.004
11		0.001	0.003

<sup>a</sup> Dose-response curves were generated from duplicate 8-point serial dilutions of inhibitory compounds. IC<sub>50</sub> values were derived by nonlinear regression analysis.

<sup>b</sup> Thymidine uptake growth inhibition assay in A2780 cells. Percentage inhibitions, relative to vehicle controls, were calculated and plotted on log-linear plots to allow derivation of IC<sub>50</sub> values.<sup>25,26</sup>

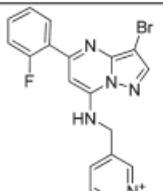
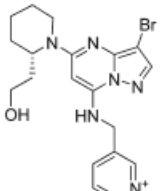
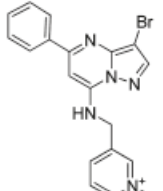
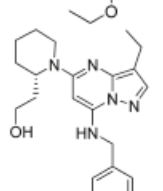
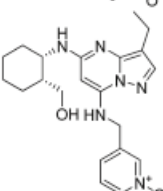
The structural basis for these improvements in activity can be readily explained by interactions revealed in the X-ray crystal structure of this series of compounds bound to CDK2 and the CDK2/cyclin A complex.<sup>28</sup> A detailed description of these findings will be published in due course. The initial goal of these efforts was to identify a novel inhibitor of CDK1 and CDK2. Because of the high degree of homology within the CDK family, inhibition of additional CDKs within this series of compound was also observed (data not shown). Thus, there exists a realistic likelihood that these small molecule inhibitors of the CDKs would exert their effects via compound-specific, combinatorial inhibition of multiple members of the family. This expected multitargeted nature of CDK inhibitors places a premium on maintaining an adequate therapeutic index *in vivo*. In this context, a critical issue in the development of CDK inhibitors is the relationship between desirable on-target effects and the

onset of off-target tolerability issues that might adversely affect clinical dose escalation. Ultimately, a screening system reminiscent of the historical standard paradigm for cytotoxic drug discovery, which evaluated the tolerability versus activity *in vivo*, was implemented.

Simply, this *in vivo* system sought to establish the ratio of maximally tolerated and minimally effective doses in the A2780 ovarian carcinoma xenograft model. It was reasoned that through the application of this screening system, a compound could be identified that might give the best opportunity to achieve pharmacologically relevant doses clinically before the manifestation of toxicity. Hence, the maximally tolerated dose (MTD) was determined by intraperitoneal administration of compound to nude mice on a fixed, QDx7 schedule at varying dose levels. In these experiments, the MTD was defined as the dose on the QDx7 schedule required to reduce body weight by 20%. In parallel, the minimum effective doses (MEDs) were established on the same schedule. The MED was defined as the dose given QDx7 that was associated with >50% tumor growth inhibition. Pharmacokinetic parameters were also established to enable calibration of effects on the basis of systemic exposure. Thus, a series of compounds comprised of diverse structures, potency, and pharmacokinetic parameters were selected in an attempt to identify the optimal profile for a CDK inhibitor within this class of compound.

Through the application of this *in vivo* screen, clear trends emerged among compounds of diverse structures and ranges of potency (Table 2).

**Table 2.** Relative Therapeutic Indices from the *in Vivo* Screening Paradigm.

Compound	A/CDK2 IC <sub>50</sub> <sup>a</sup> (uM)	In-Cell IC <sub>50</sub> <sup>b</sup> (uM)	MTD <sup>c</sup> (mg/kg)	MED <sup>c</sup> (mg/kg)	TI <sup>c</sup> (MTD/MED)	
<b>6</b>		0.03	0.2	40 (po)	20 (po)	2
<b>10</b>		0.001	0.003	20	4	5
<b>12</b>		0.018	0.025	5	5	1
<b>13</b>		0.001	0.004	60	5	>10
<b>14</b>		0.001	0.003	<20	ND	ND
<b>15</b>	Flavopiridol	0.012	0.07	<10	10	<1

<sup>a</sup> Dose-response curves were generated from duplicate 8-point serial dilutions of inhibitory compounds. IC<sub>50</sub> values were derived by nonlinear regression analysis.

<sup>b</sup> Thymidine uptake growth inhibition assay in A2780 cells. Percentage inhibitions, relative to vehicle controls, were calculated and plotted on log-linear plots to allow derivation of IC<sub>50</sub> values.

<sup>c</sup> Relative therapeutic indices following intraperitoneal (IP) dosing using the *in vivo* screening paradigm (MTD=20% weight loss; MED = 50% inhibition of tumor growth; and QDx7 = once a day dosing for 7 consecutive days).<sup>25,26</sup>

Compound **12**, an analog with improved in-cell activity relative to the previously described **6**, was found to have an MED of 5 mpk with an MTD of 5 mpk, giving a putative therapeutic index of 1. In contrast, the more highly potent compound **10** displayed a relative therapeutic index of 5. Interestingly, simple modification of substitution within this highly potent series of inhibitor induced significant differences in relative therapeutic indices. For example, incorporation of a 3-ethyl substituent as in **13** resulted in an improved overall profile relative to **10**. Conversely, the aminocyclohexyl methyl alcohol **14** gave a decreased tolerability profile relative to the piperidine ethanol derivative **13**. Notably, these compounds displayed no significant differences in pharmacokinetic profile (Table 3) or kinase cross reactivity across a set of diverse kinases (data not shown).

Table 3. Exposure parameters.<sup>a</sup>

compd	AUC <sup>b</sup> ( $\mu\text{M h}$ )	C <sub>max</sub> <sup>c</sup> ( $\mu\text{M}$ )
<b>6</b>	8	6
<b>10</b>	1.4	6
<b>12</b>	10	8
<b>13</b>	0.8	0.8
<b>14</b>	0.5	0.9
<b>15</b>	N/A	N/A

<sup>a</sup> Plasma samples from mice were collected at various times after intraperitoneal administration at 5 mg/kg and analyzed by liquid chromatography-tandem mass spectrometry. Pharmacokinetic variables were estimated from the plasma concentration data.

<sup>b</sup> The area under the plasma concentration vs time curve (AUC) was calculated using the linear trapezoidal rule.

<sup>c</sup> Cmax values (maximum plasma concentration) were taken directly from the plasma concentration-time profiles.<sup>26,29</sup>

We also benchmarked flavopiridol **15**. The ratio of MTD to MED for flavopiridol was <1, indicating that in this screening system minimal antitumor efficacy was attained before the onset of toxicity. While ramifications of these findings are unknown, it is compelling to hypothesize that a compound such as **13** may have increased potential to achieve a more robustly active dose range prior to the manifestation of dose-limiting toxicities. Several unexpected trends emerged from the utilization of

this screening system. Namely, compounds with very high levels of potency tended to give improved therapeutic indices relative to those with lower affinity. Interestingly, these compounds displayed lower exposure and higher clearance rates relative to those with lower therapeutic indices. Taken together, short exposures to highly potent CDK inhibitors appear to induce long-lasting effects and have the potential to do so with improved

tolerability. This stands in contrast to efforts in earlier stages of the program, which had been more focused on chronic exposure to induce continual CDK inhibition. Additionally, within this series of compounds, small changes in substitution had a large impact on overall activity and tolerability relationships that were not predictable from simple *in vitro* and pharmacokinetic profiling.

In summary, a series of pyrazolo[1,5-*a*]pyrimidine CDK inhibitors, which display a range of potency and pharmacokinetic parameters, were identified. Utilizing a functional *in vivo* screen, compounds were readily differentiated on the basis of efficacy versus tolerability profiles even in those structures with remarkably similar substitution and *in vitro* and pharmacokinetic profiles. A key observation arising from the application of this approach was that highly potent, rapidly cleared CDK inhibitors appear to give an optimal balance between efficacy and tolerability. Within compounds of this profile, **13** was selected as a candidate CDK inhibitor suitable for progression. In-depth evaluation of the *in vitro* and *in vivo* properties further supported the conclusion that **13** had the appropriate qualities for a development candidate.<sup>29</sup> Compound **13** (SCH 727965) is currently undergoing phase II clinical trials.

## References

- (1) Murray, A. W. Recycling the cell cycle: Cyclins revisited. *Cell* **2004**, *116*, 221–234.
- (2) Sherr, C. J. Cancer cell cycles. *Science* **1996**, *274*, 1672–1677.
- (3) Hall, M.; Peters, G. Genetic alterations of cyclins, cyclin-dependent kinases and CDK inhibitors in human cancer. *Adv. Cancer Res.* **1996**, *68*, 67–108.
- (4) Hunter, T.; Pines, J. Cyclins and cancer II: Cyclin D and CDK inhibitors come of age. *Cell* **1994**, *79*, 573–582.
- (5) Ewen, M. E. The cell cycle and the retinoblastoma protein family. *Cancer Metastasis Rev.* **1994**, *13*, 45–66.
- (6) Ewen, M. E. Regulation of the cell cycle by the Rb tumor suppressor family. *Results Probl. Cell Differ.* **1998**, *22*, 149–179.
- (7) Shapiro, G. I. Cyclin-dependent kinase pathways as targets for cancer treatment. *J. Clin. Oncol.* **2006**, *24*, 1770–1783.
- (8) Malumbres, M.; Pevarello, P.; Barbacid, M.; Bischoff, J. R. CDK inhibitors in cancer therapy. What is next?. *Trends Pharmacol. Sci.* **2007**, *29*, 16–21.
- (9) Satyanarayana, A; Kaldis, P. Mammalian cell-cycle regulation: Several Cdks, numerous cyclins and compensatory mechanisms. *Oncogene* **2009**, *28*, 2925–2939.
- (10) Wei, F. Y.; Tomizawa, K. Cyclin-dependent kinase 5 (Cdk5): A potential therapeutic target for the treatment of neurodegenerative diseases and diabetes mellitus. *Mini Rev. Med. Chem.* **2007**, *7*, 1070–1074.
- (11) Bregman, D. B.; Pestell, R. G.; Kidd, V. J. Cell cycle regulation and RNA polymerase II. *Front. Biosci.* **2000**, *5*, D244–D257.
- (12) Oelgeschlager, T. Regulation of RNA polymerase II activity by CTD phosphorylation and cell cycle control. *J. Cell Physiol.* **2002**, *190*, 160–169.
- (13) van den Heuvel, S.; Harlow, E. Distinct roles for cyclin-dependent kinases in cell cycle control. *Science* **1993**, *262*, 2050–2054.
- (14) Hu, B.; Mitra, J.; van den Heuvel, S.; Enders, G. H. S and G2 phase roles for Cdk2 revealed by inducible expression of a dominant-negative mutant in human cells. *Mol. Cell. Biol.* **2001**, *21*, 2755–2766.
- (15) L'Italien, L.; Tanudji, M.; Russell, L.; Schebye, X. M. Unmasking the redundancy between Cdk1 and Cdk2 at G2 phase in human cancer cell lines. *Cell Cycle* **2006**, *5*, 984–993.
- (16) Webster, K. R.; Kimball, D. Novel drugs targeting the cell cycle. *Emerging Drugs* **2000**, *5*, 45–59.

- (17) Cai, D.; Latham, V. M., Jr.; Zhang, X.; Shapiro, G. I. Combined depletion of cell cycle and transcriptional cyclin dependent kinase activities induces apoptosis in cancer cells. *Cancer Res.* **2006**, *66*, 9270–9280.
- (18) Firestein, R.; Bass, A. J.; Kim, S. Y.; Dunn, I. F.; Silver, S. J.; Guney, I.; Freed, E.; Ligon, A. H.; Vena, N.; Ogino, S.; Chheda, M. G.; Tamayo, P.; Finn, S.; Shrestha, Y.; Boehm, J. S.; Jain, S.; Bojarski, E.; Mermel, C.; Barretina, J.; Chan, J. A.; Baselga, J.; Taberero, J.; Root, D. E.; Fuchs, C. S.; Loda, M.; Shivdasani, R. A.; Meyerson, M.; Hahn, W. C. CDK8 is a colorectal cancer oncogene that regulates beta-catenin activity. *Nature* **2008**, *455*, 547–551.
- (19) Morris, E. J.; Ji, J.-Y.; Yang, F.; Di Stefano, L.; Herr, A.; Moon, N.-S.; Kwon, E.-J.; Haigis, K. M.; Naar, A. M.; Dyson, N. J. E2F1 represses beta-catenin transcription and is antagonized by both pRB and CDK8. *Nature* **2008**, *455*, 552–556.
- (20) McInnes, C. Progress in the evaluation of CDK inhibitors as anti-tumor agents. *Drug Discovery Today* **2008**, *13*, 875–881.
- (21) DePinto, W.; Chu, X.-J.; Yin, X.; Smith, M.; Packman, K.; Goelzer, P.; Lovey, A.; Chen, Y.; Qian, H.; Hamid, R.; Xiang, Q.; Tovar, C.; Blain, R.; Nevisn, T.; Higgins, B.; Luistro, L.; Kolinsky, K.; Felix, B.; Hussain, S.; Heimbrook, D. In vitro and in vivo activity of R547: a potent and selective cyclin-dependent kinase inhibitor currently in phase I clinical trials. *Mol. Cancer Ther.* **2006**, *5*, 2644–2658.
- (22) Wyatt, P. G.; Woodhead, A. J.; Berdini, V.; Boulstridge, J. A.; Carr, M. G.; Cross, D. M.; Davis, D. J.; Devine, L. A.; Early, T. R.; Feltell, R. E.; Lewis, E. J.; McMenamain, R. L.; Navarro, E. F.; O'Brien, M. A.; O'Reilly, M.; Reule, M.; Saxty, G.; Seavers, L. C. A.; Smith, D.-M.; Squires, M. S.; Trewartha, G.; Walker, M. T.; Woolford, A. J.-A. Identification of N-(4-piperidinyl)-4-(2,6-dichlorobenzoylamino)-1H-pyrazole-3-carboxamide (AT7519), a novel cyclin dependent kinase inhibitor using fragment-based X-ray crystallography and structure based drug design. *J. Med. Chem.* **2008**, *51*, 4986–4999.
- (23) Misra, R. N.; Xiao, H.; Kim, K. S.; Lu, S.; Han, W.-C.; Barbosa, S. A.; Hunt, J. T.; Rawlins, D. B.; Shan, W.; Ahmed, S. Z.; Qian, L.; Chen, B.-C.; Zhao, R.; Bednarz, M. S.; Kellar, K. A.; Mulheron, J. G.; Batorsky, R.; Roongta, U.; Kamath, A.; Marathe, P.; Ranadive, S. A.; Sack, J. S.; Tokarski, J. S.; Pavletich, N. P.; Lee, F. Y. F.; Webster, K. R.; Kimball, S. D. N-(Cycloalkylamino)acyl-2-aminothiazole inhibitors of cyclin-dependent kinase 2. N-[5-[[[5-(1,1-Dimethylethyl)-2-oxazolyl]methyl]thio]-2-thiazolyl]-4-piperidinecarboxamide (BMS-387032), a highly efficacious and selective antitumor agent. *J. Med. Chem.* **2004**, *47*, 1719–1728.
- (24) Christian, B. A.; Grever, M. R.; Byrd, J. C.; Lin, T. S. Flavopiridol in the treatment of chronic lymphocytic leukemia. *Curr. Opin. Oncol.* **2007**, *19*, 573–578.

(25) Dwyer, M. P.; Paruch, P.; Alvarez, C.; Doll, R. J.; Keertikar, K.; Duca, J.; Fischmann, T. O.; Hruza, A.; Madison, V.; Lees, E.; Parry, D.; Seghezzi, W.; Sgambellone, N.; Shanahan, F.; Wiswell, D.; Guzi, T. J. Versatile templates for the development of novel kinase inhibitors: discovery of novel CDK inhibitors. *Bioorg. Med. Chem. Lett.* **2007**, *17*, 6216–6219.

(26) Paruch, P.; Dwyer, M. P.; Alvarez, C.; Brown, C.; Chan, T.-Y.; Doll, R. J.; Keertikar, K.; Knutson, C.; McKittrick, B.; Rivera, J.; Rossman, R.; Tucker, G.; Fischmann, T.O.; Hruza, A.; Madison, V.; Nomeir, A.; Wang, Y.; Lees, E.; Parry, D.; Sgambellone, N.; Seghezzi, W.; Schultz, L.; Shanahan, F.; Wiswell, D.; Xu, X.; Zho, Q.; James, R. A.; Paradkar, V.; Park, H.; Roskosz, L.; Stauffer, T.; Guzi, T. J. Pyrazolo[1,5-a]pyrimidines as orally available inhibitors of cyclin-dependent kinase 2. *Bioorg. Med. Chem. Lett.* **2007**, *17*, 6220–6223.

(27) Full experimental details for the preparation of compounds **6** and **12** can be found in the Supporting Information.

(28) Fischmann, T. O.; Hruza, A.; Duca, J. S.; Ramanathan, L.; Mayhood, T.; Windsor, W. T.; Le, H. V.; Guzi, T. J.; Dwyer, M. P.; Paruch, K.; Doll, R. J.; Lees, E.; Parry, D.; Seghezzi, W.; Madison, V. Structure-guided discovery of cyclin-dependent kinase inhibitors. *Biopolymers* **2008**, *89*, 372–379.

(29) Parry, D.; Guzi, T.; Shanahan, F.; Davis, N.; Prabhavalkar, D.; Wiswell, D.; Seghezzi, W.; Paruch, K.; Dwyer, M. P.; Doll, R.; Nomeir, A.; Windsor, W.; Fischmann, T.; Wang, Y.; Oft, M.; Chen, T.; Kirschmeier, P.; Lees, E. SCH 727965, a novel and potent cyclin-dependent kinase inhibitor. *Mol. Cancer Ther.* Submitted for publication.

## Part 1d

### Dinaciclib (SCH 727965), a novel and potent cyclin-dependent kinase inhibitor\*

\*published as:

Parry, D.;\* Guzi, T. J.; Shanahan, F.; Davis, N.; Prabhavalkar, D.; Wiswell, D; Seghezzi, W.; Paruch, K.; Dwyer, M. P.; Doll, R. J.; Nomeir, A. A.; Windsor, W.; Fischmann, T.; Wang, Y.; Oft, M.; Chen, T.; Kirschmeier, P.; Lees, E. M. Dinaciclib (SCH 727965), a Novel and Potent Cyclin-Dependent Kinase Inhibitor. *Mol. Cancer Ther.* **2010**, *9*, 2344.

The mammalian cell cycle is a nonredundant process that integrates extracellular signaling, DNA synthesis, and mitosis.<sup>1,2</sup> Dysregulation of cell cycle control is a hallmark of all human cancers and is frequently associated with selective, aberrant activation of cyclin-dependent kinases (CDK).<sup>3,4</sup> Several members of the CDK family are critical regulators of cell cycle progression. CDK2 and CDK1 are two closely related kinases that play overlapping roles during cell division, contributing to the phosphorylation and inactivation of the retinoblastoma (Rb) tumor suppressor gene product throughout late G<sub>1</sub>, S, and G<sub>2</sub>-M phases.<sup>5-7</sup> Other CDK family members play important roles outside of direct regulation of cell cycle progression. For instance, CDK7, CDK8, and CDK9 contribute to the regulation of RNA polymerase II and the control of cellular transcription.<sup>8,9</sup>

Inhibition of CDK activities represents an attractive therapeutic strategy in oncology. Indeed, expression of dominant-negative forms of CDK2 or combinatorial silencing of CDK1 and CDK2 through small interfering RNA generates therapeutically relevant phenotypes, such as cell cycle arrest.<sup>10-12</sup> Suppression of CDK9 using RNAi has desirable therapeutic effects *in vitro*.<sup>13</sup> Similarly, inhibition of CDK9 and the subsequent suppression of MCL1 transcription are proposed as a potential mechanism-of-action for the pan-CDK inhibitor flavopiridol in chronic lymphocytic leukemia.<sup>14,15</sup> Finally, CDK8 is a key modulator of  $\beta$ -catenin function, and the *CDK8* gene is amplified in some human colorectal cancers.<sup>16,17</sup> Furthermore, the lack of appropriate cell cycle regulation in tumor cells predicts their increased propensity for apoptosis, compared with normal tissue.<sup>18</sup>

Based on the intriguing and multifaceted attributes of the CDK target class, several small-molecule CDK inhibitors have entered clinical development.<sup>19</sup> However, due to the high degree of structural homology within the CDK protein family, putative small-molecule CDK inhibitors may exert their effects through combinatorial inhibition of multiple CDKs and other closely related serine/threonine kinases. Hence, the almost inevitable multitargeted nature of CDK inhibitors places a high premium

on maintaining an adequate therapeutic index *in vivo*. A critical issue for the successful development of CDK inhibitors (and indeed the majority of cytoreductive agents) is, therefore, the relationship between desirable, target-specific effects and the onset of nonspecific adverse events that might negatively influence clinical dose escalation.<sup>20</sup> Selection of dinaciclib (SCH 727965; Fig. 1A) for clinical development was facilitated by a range of diverse assays and included an *in vivo* screening strategy that identified candidate compounds with the optimal combination of pharmacokinetic, efficacy, and safety characteristics.<sup>21</sup> This highly effective, functional approach allowed for rapid benchmarking against known CDK inhibitors with undesirable side effects, such as flavopiridol (Fig. 1B), and showed SCH 727965 to be a compound with a significantly superior therapeutic profile.

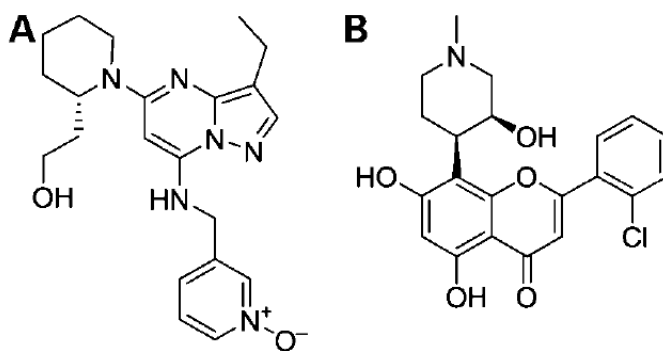


**Figure 1.** Structures of SCH 727965 (A) and flavopiridol (B).

## Materials and Methods

### *Experimental and control agents*

SCH 727965 ((*S*)-(-)-2-(1-{3-ethyl-7-[(1-oxy-pyridin-3-ylmethyl)amino] pyrazolo[1,5-a]pyrimidin-5-yl}piperidin-2-yl)ethanol) and flavopiridol (2-(2-chlorophenyl)-5,7-dihydroxy-8-[(3*S*,4*R*)-3-hydroxy-1-methyl-4-piperidinyl]-4-chromenone) were supplied by Schering-Plough Research Institute. Paclitaxel was purchased from Sigma. The vehicle for these agents, except paclitaxel, was 20% hydroxypropyl- $\beta$ -cyclodextrin. The vehicle for paclitaxel was Cremophor. Dosing volume was 0.2 mL per injection.

### *Cyclin/CDK kinase assay*

Recombinant cyclin/CDK holoenzymes were purified from Sf9 cells engineered to produce baculoviruses that express a specific cyclin or CDK. Cyclin/CDK complexes were typically diluted to a final concentration of 50  $\mu$ g/mL in a kinase reaction buffer containing 50 mmol/L Tris-HCl (pH

8.0), 10 mmol/L MgCl<sub>2</sub>, 1 mmol/L DTT, and 0.1 mmol/L sodium orthovanadate. For each kinase reaction, 1 µg of enzyme and 20 µL of a 2-µmol/L substrate solution (a biotinylated peptide derived from histone H1; Amersham) were mixed and combined with 10 µL of diluted SCH 727965. The reaction was started by the addition of 50 µL of 2 µmol/L ATP and 0.1 µCi of <sup>33</sup>P-ATP (Amersham). Kinase reactions were incubated for 1 hour at room temperature and were stopped by the addition of 0.1% Triton X-100, 1 mmol/L ATP, 5 mmol/L EDTA, and 5 mg/mL streptavidin-coated SPA beads (Amersham). SPA beads were captured using a 96-well GF/B filter plate (Packard/Perkin-Elmer Life Sciences) and a Filtermate universal harvester (Packard/Perkin-Elmer Life Sciences.) Beads were washed twice with 2 mol/L NaCl and twice with 2 mol/L NaCl containing 1% phosphoric acid. The signal was then assayed using a TopCount 96-well liquid scintillation counter (Packard/Perkin-Elmer Life Sciences). Dose-response curves were generated from duplicate, eight-point serial dilutions of inhibitory compounds. IC<sub>50</sub> values were derived by nonlinear regression analysis.

#### ***Kinase counter-screening***

SCH 727965 and flavopiridol were counter-screened using the Millipore Kinase Profiler service. Both compounds were tested at 1.0 and 10.0 µmol/L against a panel of diverse kinases, using a fixed (10 µmol/L) concentration of ATP.

#### ***Cell lines and cell culture***

The majority of the tumor cell lines were obtained from the American Type Culture Collection and propagated under the suggested growth conditions. Mantle cell lymphoma cell lines were generously provided by Dr. Geoffrey Shapiro (Dana-Farber Cancer Institute, Boston, MA).

#### ***dThd uptake growth inhibition assay***

A2780 cells were maintained in DMEM (Cellgro) plus 10% fetal bovine serum (HyClone) and passaged twice weekly by detaching the monolayer with trypsin-EDTA (Life Technologies). One hundred microliters of A2780 cells ( $5 \times 10^3$  cells) were added per well to a 96-well Cytostar-T plate (Amersham) and incubated for 16 to 24 hours at 37 °C. Compounds were serially diluted in complete media plus 2% <sup>14</sup>C-labeled dThd (Amersham). Media were removed from the Cytostar T plate; 200 µL of various compound dilutions were added in quadruplicate; and the cells were incubated for 24 hours at 37 °C. Accumulated incorporation of radiolabel was assayed using scintillation proximity and measured on a TopCount (Packard/Perkin-Elmer Life Sciences). The percentage of dThd uptake inhibition, relative to a vehicle control, was calculated and plotted on log-linear plots to allow derivation of IC<sub>50</sub> values.

### ***Bromodeoxyuridine incorporation assay***

A2780 cells were plated into six-well tissue culture dishes and allowed to adhere. Cells were then exposed to differing concentrations of SCH 727965 or a DMSO control vehicle for 24 hours, followed by a brief (30 min) pulsed exposure to bromodeoxyuridine (BrdUrd). Cells were then harvested, immunostained using FITC-conjugated antibodies specific for BrdUrd (BD Biosciences), counter-stained with propidium iodide/RNase A solution (BD Biosciences), and analyzed using flow cytometry. Fluorescence-activated cell sorting analyses were done on a FACSCalibur instrument (Becton Dickinson). FITC-positive BrdUrd staining and propidium iodide signal allowed assessment of ongoing DNA replication and the cell cycle stage. Percentages of the cell population in each cell cycle stage were plotted for each test article concentration.

### ***Immunoblotting***

Asynchronously growing tumor cell lines were exposed to differing concentrations of SCH 727965. Subsequently, cells were harvested and lysed in a 50 mmol/L Tris-HCl buffer containing 350 mmol/L NaCl, 0.1% NP40, 1 mmol/L DTT, and a cocktail of protease and phosphatase inhibitors (Calbiochem). Following protein concentration determination (Bio-Rad), cell lysates were separated on reducing SDS-PAGE gels and immunoblotted with antisera specific for Rb phosphorylated on serines 807, 811 (Cell Signaling), hypophosphorylated Rb (Cell Signaling), or the p85 poly ADP ribose polymerase (PARP) caspase cleavage product (Promega).

### ***Induction of apoptosis assessed by activated caspase***

Assays of caspase activation were done using the Beckman Coulter CellProbe HT Caspase-3/7 Whole Cell Assay system. Asynchronously growing cells were plated into 96-well plates and allowed to adhere. Cells were exposed to differing concentrations of SCH 727965 or vehicle for 24 hours. Cells were subsequently incubated with a fluorescently labeled caspase substrate (CellProbe); uptake and fluorescence of the substrate within cells correlate with the level of activated caspases. The caspase activity was determined using an Analyst AD 96.384 fluorometer (485 nm excitation and 530 nm emission).

### ***Clonogenicity and alamarBlue viability assays***

Cells were plated onto tissue culture dishes and propagated with the appropriate growth media. Growing cultures were exposed to increasing concentrations of SCH 727965 or a vehicle control, typically for 7 days. After removing the medium, cells were fixed with 50% methanol/50% acetone

for 5 minutes and stained with 0.2% crystal violet (Fisher) in 2% ethanol for 5 minutes. Following staining, cells were washed with 5 to 10 mL of water. Stained cells were solubilized in 1% deoxycholic acid (Sigma), and the absorbance of the resulting solution was measured at 600 nm using a SOFTmax PRO 4.3 plate reader (Molecular Devices). Absorbance of SCH 727965–treated samples was plotted as a percent of that of a vehicle-treated control, and data were reported as an IC<sub>50</sub> value relative to these controls. For suspension cell lines, assessments of cell viability were obtained using the alamarBlue Cell Viability Assay kit (Biotium), using the manufacturers' recommended protocol.

### ***Experimental mice***

All mouse strains were obtained from Charles River Laboratories. Female nude mice age 9 to 14 week or female BALB/c mice age 6 to 14 weeks were used. Animals were housed in an Association for Assessment and Accreditation of Laboratory Animal Care-accredited animal facility at Schering-Plough Biopharma, Palo Alto, CA, and Schering-Plough Research Institute, Kenilworth, NJ. Conventional animal chow and water were provided *ad libitum*. All protocols related to experiments using animals have been approved by the appropriate Institutional Animal Care and Use Committee.

### ***In vivo tumor growth assessments***

For tumor implantation, specific cell lines were grown *in vitro*, washed once with PBS, and resuspended in 50% Matrigel (BD Biosciences) in PBS to a final concentration of  $4 \times 10^7$  to  $5 \times 10^7$  cells per milliliter. Nude mice were injected with 0.1 mL of this suspension s.c. in the flank region. Tumor length (*L*), width (*W*), and height (*H*) were measured by a caliper twice weekly on each mouse and then used to calculate tumor volume using the formula  $(L \times W \times H)/2$ . When the tumor volume reached  $\sim 100 \text{ mm}^3$ , the animals were randomized to treatment groups (10 mice/group) and treated i.p. with either SCH 727965 or individual chemotherapeutic agents according to the dosing schedule indicated in table and figure legends. Tumor volumes and body weights were measured during and after the treatment periods. Data were expressed as means  $\pm$  SEM. Animals were euthanized according to the Institutional Animal Care and Use Committee guidelines.

### ***Immunohistochemical staining of phospho-Rb protein***

Samples were harvested from the nude mice skin at various time points following administration of a single 40-mg/kg dose of SCH 727965. The samples were fixed overnight in 10% formaldehyde, washed in 70% ethanol, and processed in a tissue processor (Thermo Electronic Co.); the tissues were dehydrated in graded ethanol solutions, cleared in three changes of xylene, and penetrated in heated paraffin (at 56–58 °C). The tissues were embedded in paraffin, cut into 4- to 6- $\mu\text{m}$  sections, and

placed onto slides. Before staining, the slides were placed in a chamber containing 1× Reveal Solution (BioCare Medical) for deparaffinization and antigen retrieval. The slides were rinsed in hot water, placed in PBS for 15 minutes at room temperature, and loaded onto a DAKO automated immunostainer. Endogenous hydrogen peroxidase activity was blocked with hydrogen peroxide for 10 minutes followed by rinsing with a Tris-HCl buffered saline solution containing 0.5% Tween 20 (TBST; Sigma). The slides were then sequentially incubated with avidin, rinsed in TBST, treated with biotin, and rinsed again in TBST (avidin/biotin block kit; Vector Laboratories). Nonspecific binding sites were blocked with 1× blocking buffer (Sigma) for 20 minutes. The slides were then incubated with anti-phospho Rb 807/811 (Cell Signaling) diluted 1:75 or rabbit control antisera at 1 µg/mL for 45 minutes, rinsed with TBST, and incubated with biotinylated goat anti-rabbit IgG (Elite ABC kit; Vector Laboratories) for 30 minutes. The slides were rinsed again with TBST and treated with ABC complex (Elite ABC kit; Vector Laboratories) for 30 minutes, followed by another TBST rinse. The slides were developed in 3,3'-diaminobenzidine (Dakocytomation) for 5 minutes, rinsed with TBST, and incubated for 2 minutes with hematoxylin (Dakocytomation). Finally, the slides were rinsed in distilled water, dehydrated in graded ethanol solutions, cleared in xylene using a Leica autostainer, and cover slipped in a Leica Cover slipper.

#### ***Assessments of SCH 727965 effects on hematologic parameters***

A daily dose of SCH 727965 (40 mg/kg) was administered i.p. to BALB/c mice for 5 days. Blood was collected on day 6 and day 13 (1st and 7th day after the final dose, respectively), diluted 1:5 in PBS, and immediately analyzed on an Advia 120 hematology analyzer (with differential).

#### ***Pharmacokinetic determinations***

Plasma samples from mice were collected at various times after i.p. administration of SCH 727965. At each time point, blood samples from three animals were combined and analyzed for SCH 727965 by liquid chromatography-tandem mass spectrometry. Pharmacokinetic variables were estimated from the plasma concentration data. Maximum plasma concentration values were taken directly from the plasma concentration time profiles, and the area under the plasma concentration versus time curve (0–24 h) was calculated using the linear trapezoidal rule.

## Results

### *SCH 727965 selection using a mouse tumor xenograft model*

SCH 727965 was selected as the optimal drug candidate for clinical development by screening individual, diversely substituted compounds against the A2780 ovarian carcinoma mouse xenograft model, using flavopiridol as a benchmark control agent. This system established the ratio of maximum tolerated dose (MTD) and minimum effective dose (MED) for each tested compound. MTD was determined following i.p. administration of each compound to nude mice at varying dose levels once daily for 7 days and defined as the dose associated with a body weight reduction of 20%. In parallel, MED was defined as the dose, given by the same schedule, associated with >50% tumor growth inhibition. Promising compounds were further profiled in rats and dogs (21). The screening data pertinent to SCH 727965 are outlined in Table 1. Thus, MTD and MED of SCH 727965 were >60 and 5 mg/kg, respectively; in contrast, MTD and MED of flavopiridol were <10 and 10 mg/kg, respectively. Therefore, a screening therapeutic index (MTD/MED ratio) of SCH 727965 was >10, whereas the index of flavopiridol was <1, indicating that minimal antitumor efficacy was not attained with flavopiridol before the onset of dose-limiting toxicity. These data indicated that SCH 727965 has an attractive *in vivo* profile that is superior to flavopiridol.

**Table 1.** Comparison between SCH 727965 and flavopiridol: inhibition of CDKs, dThd incorporation, and activity in a mouse tumor xenograft.

Compound	CDK2	CDK5	CDK1	CDK9	dThd incorporation	MTD*	MED†	(MTD/MED)‡
	IC <sub>50</sub> (nmol/L)					(mg/kg)		
SCH 727965	1	1	3	4	4	60	5	>10
Flavopiridol	12	14	3	4	70	<10	10	<1

\*MTD: 20% weight loss.  
†MED: >50% inhibition of tumor growth (both administered i.p. once daily for 7 d).  
‡Screening therapeutic index.

### *SCH 727965 is a potent and selective inhibitor of CDKs*

Inhibition of the kinase activity of various cyclin/CDKs was examined using isolated, baculovirus-expressed holoenzymes *in vitro*. SCH 727965 inhibits CDK2, CDK5, CDK1, and CDK9 with IC<sub>50</sub>

values of 1, 1, 3, and 4 nmol/L, respectively. Compared with flavopiridol and assayed under identical conditions, SCH 727965 is an equally potent inhibitor of CDK1 and CDK9 but a 12- and 14-fold stronger inhibitor of CDK2 and CDK5, respectively (Table 1). SCH 727965 was found to be a potent DNA replication inhibitor that blocked thymidine (dThd) DNA incorporation in A2780 cells with an IC<sub>50</sub> of 4 nmol/L. In contrast, flavopiridol had an ~16-fold lesser potency in that assay. These data show that SCH 727965's stronger and more selective inhibition of CDKs translates into its more potent inhibition of DNA synthesis compared with flavopiridol in cell-based assays (Table 1).

SCH 727965 is not a general kinase inhibitor (Supplementary Table S1) and, in a series of additional kinase counter-screens (Table 2), was shown to be more selective or the CDK family, compared with flavopiridol. These data showed that flavopiridol affects a broader range of serine/threonine and tyrosine kinases (e.g., c-Src), which may contribute to its poor screening therapeutic index compared with that of SCH 727965.

**Table 2.** Millipore kinase profiler counter-screening for SCH 727965 and flavopiridol.

Kinase	SCH 727965		Flavopiridol	
	1	10	1	10
	μmol/L	μmol/L	μmol/L	μmol/L
<b>Kinase activity remaining (%)</b>				
AMPK	94	62	67	20
Blk	69	100	73	26
CaMKII	102	91	44	30
CDK6/cyclin D3	12	3	25	6
CDK7/cyclin H1/MAT1	7	4	16	6
c-Src	117	111	3	4
Fes	87	91	44	13
Lyn	108	110	73	18
MSK1	94	97	74	37
PKC α	96	94	65	20
PKC β II	110	113	75	26
PKC ε	93	88	45	9
PKC θ	95	95	23	5
RSK2	104	76	65	16
Yes	92	98	68	40

***SCH 727965 inhibits phosphorylation of the Rb tumor suppressor protein and induces accumulation of the p85 PARP caspase cleavage product***

Inhibition of CDK-specific serine 807 and 811 (Ser 807/811) phosphorylation on the Rb tumor suppressor protein and accumulation of p85 PARP caspase cleavage product (p85 PARP) were selected as mechanism-based markers. These were used to explore the mechanism of dThd uptake inhibition observed upon cell exposure to SCH 727965 or flavopiridol, and correlate onset of apoptosis with inhibition of CDKs (Fig. 2). Lysates from asynchronously growing A2780 cells treated with increasing concentrations of SCH 727965 or flavopiridol for 16 hours were analyzed on SDS-PAGE and immunoblotted with Ser 807/811 Rb-specific antisera or with p85 PARP-specific antisera.

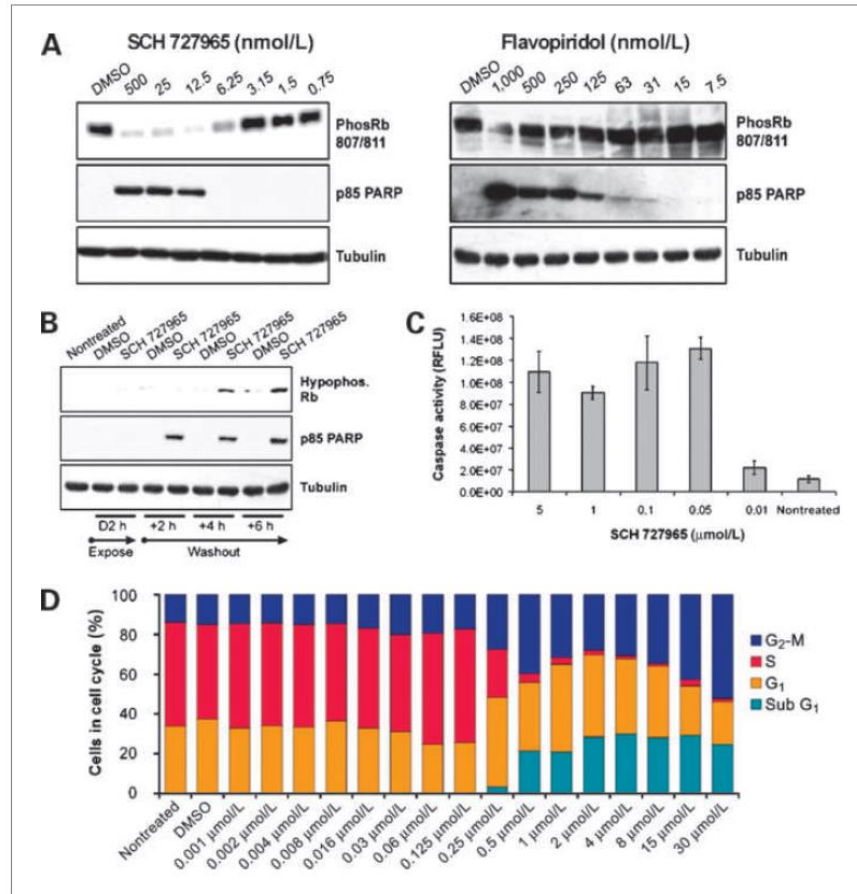


**Figure 2.** Mechanism-based marker analyses in human cancer cells.

A, asynchronously growing A2780 cells were treated for 16 h with increasing concentrations of SCH 727965 (left) or flavopiridol (right), as indicated. Cell lysates were immunoblotted with anti-phospho Rb 807/811, a marker of cellular CDK activity, anti-p85 PARP caspase cleavage product, a marker indicating activation of caspases, and anti-tubulin, a loading control.

B, short treatment with SCH 727965 induces mechanism-based effects in human cancer cells. Lysates from asynchronously growing A2780 cells exposed to 100 nmol/L SCH 727965 for 2 h were separated on PAGE-SDS and immunoblotted with antisera specific for hypophosphorylated Rb, p85 PARP caspase cleavage product, and tubulin as a control.

C, caspase activation analysis using a quantitative fluorometric analysis. A2780 cells were exposed to increasing concentrations of SCH 727965, as indicated, for 2 h, and analyzed 6 h after the drug washout. Caspase activation was observed following exposure to 50 nmol/L of SCH 727965 and did not increase with elevated levels of SCH 727965 (up to 5  $\mu\text{mol/L}$ ).

D, cell cycle distribution following short treatment with SCH 727965. Asynchronously growing A2780 cells were exposed to increasing concentrations of SCH 727965 for 2 h, cultured for an additional 24 h in drug-free medium, and then pulsed for 30 min with BrdUrd. A 2-h exposure to  $\leq 500$   $\mu\text{mol/L}$  SCH 727965 was sufficient to suppress  $>90\%$  of BrdUrd incorporation 24 h later.

SCH 727965 strongly suppressed phosphorylation of Rb on Ser 807/811 at concentrations  $>6.25$  nmol/L, which is in accord with the observation that 4 nmol/L concentrations are required for 50% inhibition of dThd DNA incorporation in the same cell model as previously described. Significantly, complete suppression of Rb phosphorylation was correlated with the onset of apoptosis, as indicated by the appearance of the p85 PARP cleavage product in cells exposed to  $>6.25$  nmol/L SCH 727965 (Fig. 2A, left). No evidence of apoptosis induction was detectable before the complete suppression of Rb phosphorylation. In contrast, flavopiridol was less effective at inducing significant suppression of Rb phosphorylation, and concentrations approaching 1  $\mu\text{mol/L}$  were required to induce detectable effects on phospho-Rb Ser 807/811 levels (Fig. 2A, right). Of note, flavopiridol stimulated the accumulation of the p85 PARP cleavage product concentrations otherwise insufficient to inhibit Rb phosphorylation, suggesting a poor correlation between flavopiridol-induced apoptosis and Rb phosphorylation status. In contrast, the cytotoxic activity of SCH 727965 and its effect on Rb phosphorylation correlate with its proposed mechanism of action based on selective inhibition of CDKs.

#### ***Mechanism of action-based effects following a short cellular SCH 727965 exposure***

To determine whether short exposures to SCH 727965 were able to induce responses similar to those following 16- to 24-hour exposures described above, A2780 cells were treated with 100 nmol/L SCH 727965 for 2 hours, washed out and supplied with a drug-free medium. Cell lysates from a time course of 2-hour intervals were then separated on SDS-PAGE and immunoblotted with antisera specific for hypophosphorylated Rb and p85 PARP; this allowed the assessment of CDK inhibition and apoptosis activation. A 2-hour exposure to 100 nmol/L SCH 727965 was sufficient to induce suppression of Rb phosphorylation and caspase activation, detectable up to 6 hours later (Fig. 2B). Induction of apoptosis was confirmed using a quantitative, fluorometric cell-based assay of caspase activation following short exposures to as little as 50 nmol/L of SCH 727965 (Fig. 2C).

To examine the effects of a short SCH 727965 exposure on cell cycle, asynchronously growing A2780 cells treated with increasing concentrations of SCH 727965 for 2 hours were maintained for

24 hours in a drug-free medium, then pulse labeled with BrdUrd to establish the percentage of cells undergoing active DNA replication, before analysis by fluorescence-activated cell sorting. Under these conditions, cells exposed to 125 to 250 nmol/L SCH 727965 for 2 hours partially suppressed DNA synthesis and BrdUrd incorporation for 24 hours (Fig. 2D). Higher exposures ( $\leq 500$  nmol/L) were sufficient to completely suppress DNA synthesis for 24 hours and were correlated with the accumulation of apoptotic (sub-G<sub>1</sub>) cells. Overall, these data show that short exposures to SCH 727965 can induce long-lasting effects in target cells and imply that continuous exposure to SCH 727965 may not be required for sustained activity *in vivo*.

### ***SCH 727965 activity in a panel of tumor cell lines***

CDK inhibitors are expected to have broad antiproliferative activity against a wide range of tumor cells. SCH 727965 antiproliferative activity (clonogenicity, alamarBlue viability assay, dThd and BrdUrd incorporation, and p85 PARP marker analysis) was examined in an extended panel of human tumor cell lines that included the full NCI-60 screening set and an additional 47 cell lines procured to expand representation of small-cell lung cancer, lymphoma, leukemia, prostate, and pancreatic cancers. The broad range of transformed cellular backgrounds (p53, pRB, p16, c-Myc, K-Ras, etc.) allowed SCH 727965 testing in diverse settings. Tumor cell line origin and response characteristics are summarized in Table 3.

**Table 3.** SCH 727965 is active against a broad spectrum of human tumor cell lines.

<b>Table 3.</b> SCH 727965 is active against a broad spectrum of human tumor cell lines		
<b>Tumor cell line</b>	<b>Mean in-cell IC<sub>50</sub> (clonogenicity; nmol/L)</b>	<b>Detectable caspase activation* (single exposure)</b>
Prostate	12	4 of 5
Breast	8	6 of 7
Colon	17	5 of 9
SCLC	14	8 of 9
SCLC	6	2 of 6
Ovarian	14	5 of 7
Pancreatic	15	11 of 15
Melanoma	9	9 of 9
Leukemia	6	5 of 6
Bladder	10	1 of 2
Liver	8	2 of 2
Mantle cell lymphoma	7	3 of 4
Lymphoma (NHL)	7	8 of 8

Abbreviations: SCLC, small-cell lung cancer; NHL, non-Hodgkin lymphoma.  
\*Data indicate the number of caspase-positive cell lines out of total number of cell lines from each tumor cell line type tested.

The mean and median IC<sub>50</sub> values across this cell line panel were 10 and 11 nmol/L, respectively. Complete suppression of BrdUrd incorporation in the tested cell lines was typically apparent at concentrations that induce inhibition of clonogenicity by 90% (20–25 nmol/L; data not shown). Following exposure to SCH 727965, all tested human tumor cell lines underwent cell cycle arrest, and no selectivity toward a specific tumor type was observed. Furthermore, apoptosis, which was determined by the appearance of the p85 PARP cleavage product on Western blots following a single exposure to SCH 727965 at concentrations <100 nmol/L, was detected in >85% of the cell lines tested. Approximately 50% of cell lines from the NCI-60 screening panel express multiple drug resistance gene 1, and it is noteworthy that multiple drug resistance gene 1 status did not significantly influence sensitivity to SCH 727965. Overall, these data suggest that SCH 727965 has antiproliferative activity across a broad range of tumor types and genetic backgrounds.

#### ***SCH 727965 efficacy and tolerability in vivo***

The previously described A2780 ovarian cancer mouse xenograft model developed for initial selection of active agents was used for further assessment of SCH 727965 efficacy and tolerability; paclitaxel was a positive control. Nude mice with ~100 mm<sup>3</sup> A2780 tumors were randomized into groups of 10 animals ~7 days after initial s.c. cell inoculation and assigned to each SCH 727965 dosage group, paclitaxel, or vehicle control. SCH 727965 i.p. administration at 8, 16, 32, and 48 mg/kg daily for 10 days resulted in tumor inhibition by 70%, 70%, 89%, and 96%, respectively; paclitaxel i.p. administration at 20 mg/kg twice weekly inhibited tumor growth by 63% (Fig. 3A). Consistent with earlier *in vivo* screening data, SCH 727965 MED appears to be <8 mg/kg. SCH 727965 was well tolerated, and the maximum body weight loss in the highest dosage group was 5% (data not shown). This is well below the MTD defined as 20% loss of body weight over the course of this experiment. Taken together, the data show that SCH 727965 has dose-dependent antitumor activity *in vivo*, and that nearly complete inhibition of tumor growth occurs at a dose level below the MTD (Table 4; Fig. 3A).

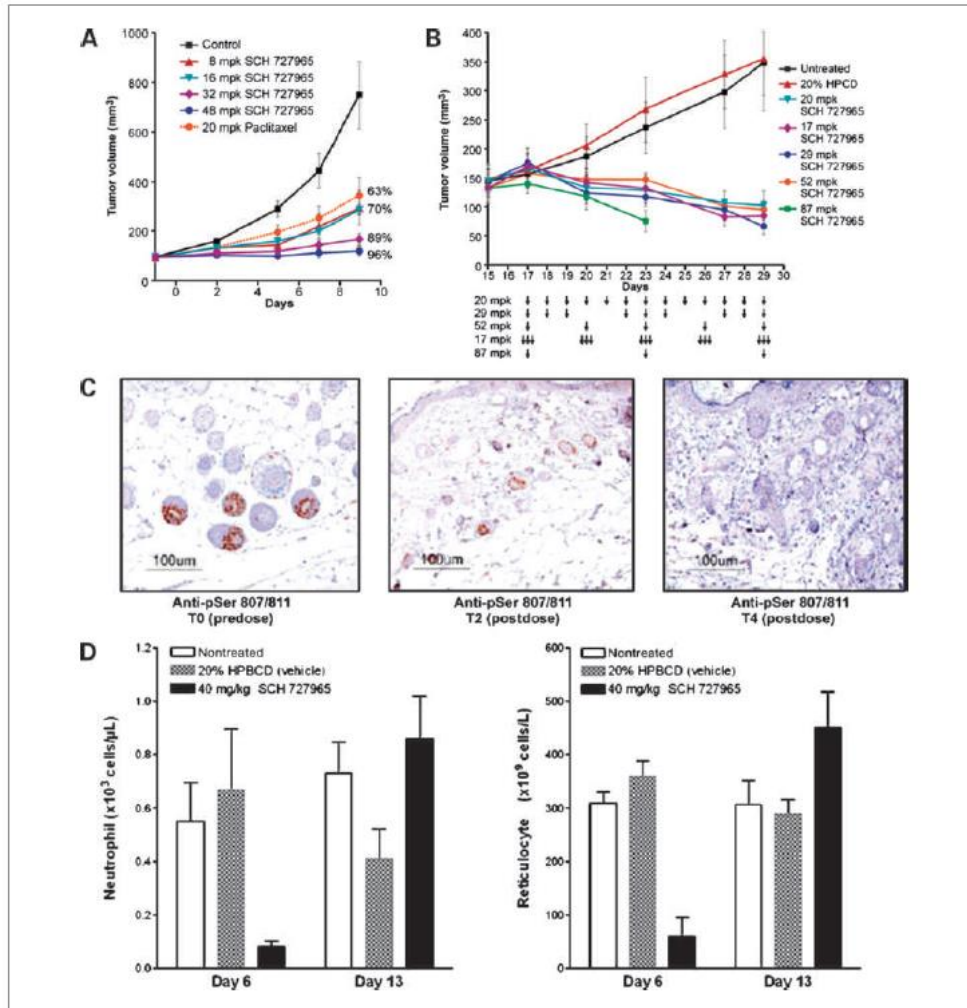


**Figure 3.**

A, SCH 727965 efficacy in a mouse xenograft model. Nude mice inoculated s.c. with A2780 cells were treated with SCH 727965, paclitaxel, or vehicle control when tumor volume reached  $\sim 100 \text{ mm}^3$ ,  $\sim 7$  d after inoculation. SCH 727965 was administered at 8, 16, 32, and 48 mg/kg i.p. daily for 10 d; paclitaxel was administered at 20 mg/kg i.p. twice weekly. Left, growth curves; right, percent tumor growth inhibition (%TGI) and percent of maximally tolerated dose (%MTD).

B, SCH 727965 is active using intermittent dosing schedules in mice. A total dose equivalent to 20 mg/kg daily for 13 days (260 mg/kg) was fractionated over several diverse schedules and administered to nude mice bearing established A549 xenografts. SCH 727965 (87 mg/kg) exceeded the MTD ( $>20\%$  body weight loss) when given on a once-weekly schedule. Similar regressions were observed on all schedules.

C, SCH 727965 induces mechanism-based systemic effects *in vivo*. SCH 727965 induced rapid and sustained suppression of phospho-Rb within the proliferating epithelial cells of the basal epithelium and hair follicles. Skin samples were obtained from mice before treatment (T0, predose) or 2 and 4 h following administration of

40 mg/kg SCH 727965 i.p. (T2 and T4 postdose). Samples were stained with phospho-Rb Ser 807/811 specific antisera.

D, SCH 727965 induces reversible hematologic effects. BALB/c mice were treated with SCH 727965 at 40 mg/kg on a dose-intense, daily for 5 days schedule. To determine blood cell count nadirs and reversibility, blood samples were obtained from mice on the day after the last SCH 727965 dose (day 6) and then 7 d later (day 13). Absolute neutrophil (left) and reticulocyte responses (right) are shown compared with BALB/c mice that were administered vehicle (20% hydroxypropyl- $\beta$ -cyclodextrin) or left nontreated. Neutrophil and reticulocyte nadirs were observed on day 6. By day 13, counts neutrophil and reticulocyte counts in SCH 727965-treated animals had returned to levels similar to those observed in vehicle-treated or nontreated mice. There were no detectable effects on platelets or RBC during the duration of this time course (data not shown).

**Table 4.** Dose dependent antitumor activity of SCH 727965.

<b>Compound (dose)</b>	<b>% MTD</b>	<b>% TGI</b>
Paclitaxel (20 mg/kg, i.p., 2x weekly)	~50%	63%
SCH 727965 (8 mg/kg, i.p., QD)	13%	70%
SCH 727965 (16 mg/kg, i.p., QD)	27%	70%
SCH 727965 (32 mg/kg, i.p., QD)	53%	90%
SCH 727965 (48 mg/kg, i.p., QD)	80%	96%

Abbreviation: QD, once daily.

***SCH 727965 has antitumor activity on various intermittent schedules***

Pharmacokinetic studies showed that SCH 727965 has a short plasma half-life in mouse. Thus, a dose of 5 mg/kg SCH 727965 given i.p. in mice was associated with a plasma half-life of ~0.25 hour (Supplementary Table S2), perhaps suggesting a need for frequent dosing. However, previous results imply that continuous SCH 727965 exposure may not be a prerequisite for antiproliferative activity because short treatments with the drug induce long-term effects *in vitro* and *in vivo*. To test that hypothesis, a total SCH 727965 dose of 260 mg/kg, equivalent to 20 mg/kg once daily for 13 days, was fractionated over several diverse schedules and administered to nude mice bearing established

(>100 mm<sup>3</sup>) A549 tumor xenografts (Fig. 3B; dosing days are indicated by arrows). Primary end points for this study were tumor volume/mass and body weight. SCH 727965 dosing of 87 mg/kg given once weekly exceeded the MTD and was terminated early. Similar tumor regressions were observed for all schedules. These data agree with earlier observations and indicate that similar *in vivo* responses can be generated on a wide range of intermittent SCH 727965 dosing schedules.

### ***Mechanism-based systemic effects in vivo following exposure to SCH 727965***

In this study, phospho-Rb 807/811 has been used as a surrogate marker of CDK engagement and mechanism-based SCH 727965 activity. To show that 20-mg/kg to 60-mg/kg doses of SCH 727965 previously exhibiting significant antitumor activity in a mouse xenograft model are associated with modulation of the CDK mechanism, the expression of phospho-Rb 807/811 was analyzed in skin samples taken from SCH 727965–treated, tumor-naïve nude mice. Skin and hair follicles are an excellent peripheral source of surrogate proliferating (nontumor) tissue. Skin punch biopsies were harvested at various time points following the administration of SCH 727965. Immunohistochemical staining of murine skin indicates that a single 40-mg/kg SCH 727965 dose induces rapid and sustained suppression of phospho-Rb 807/811 within the proliferating epithelial cells of the basal epithelium and hair follicles (Fig. 3C). These observations suggest that doses of SCH 727965 associated with regressions in the A549 xenograft model (Fig. 3B) are correlated with the modulation of a mechanism-based marker in proliferating surrogate tissues. These data are consistent with the hypothesis that inhibition of CDKs can induce inhibition of cell cycle within proliferating normal tissues and suggest that proliferating compartments will likely be sensitive to SCH 727965.

To assess effects of SCH 727965 on hematologic parameters, BALB/c mice were i.p. dosed daily with 40 mg/kg for 5 days, with controls nontreated or dosed with a vehicle, 20% hydroxypropyl- $\beta$ -cyclodextran. Blood samples were obtained 1 day after administration of the last dose (day 6) as well as 7 days later (day 13). Blood cells were counted (with differential) to examine nadir and rebound kinetics of several hematologic parameters. Neutrophils and reticulocytes were most sensitive to SCH 727965, and nadirs in their absolute counts were detected on day 6 (Fig. 3D). Significantly, absolute neutrophil counts (Fig. 3D, left) and reticulocyte counts (Fig. 3D, right) returned to normal levels by day 13. No detectable effects on platelets or RBC over this time course were observed (data not shown). These results are consistent with the mechanism-based activity of SCH 727965 within the examined dose range and suggest that cell cycle inhibition effects are transient and reversible in proliferating normal cell compartments.

## Discussion

SCH 727965 was selected for clinical development following a functional *in vivo* screen that integrated both efficacy and tolerability of tested compounds. This rapid and discriminatory approach identified a candidate for clinical development that was significantly more effective and better tolerated than flavopiridol. SCH 727965 has several distinct *in vitro* properties consistent with an improved *in vivo* therapeutic index. Notably, the compound exhibits strong selectivity for the CDK family. These data suggest the activated CDK conformation has unique structural aspects, not present in closely related serine/threonine kinases (such as the extracellular signal-regulated kinase and GSK3 families), thus providing a potential explanation for the observed excellent selectivity and tolerability profiles of SCH 727965.

*In vitro* and *in vivo* analyses presented in this study support the conclusion that SCH 727965 has the potential to inhibit the growth of a broad spectrum of human cancers. SCH 727965 induced mechanism-based apoptosis in the vast majority of tested human tumor cell lines of diverse origin, following a single exposure. In agreement, SCH 727965 was effective at doses below the MTD level in multiple *in vivo* models and induced regression in several xenografts using continuous or intermittent schedules. Under similar conditions, the observed xenograft efficacy profiles of SCH 727965 were consistently superior to those achieved using approved benchmark agents, such as taxanes. Moreover, in mechanism-based biomarker studies, effective doses of the drug were sufficient to suppress phosphorylated Rb levels in surrogate tissues, such as skin and hair follicles. Likewise, active dose levels in the mouse were also associated with reversible effects on hematologic parameters. Quantitative tracking of leukocyte cell counts may offer an additional approach for tracking mechanism-based pharmacodynamic effects of SCH 727965.

Interestingly, the *in vivo* activity of SCH 727965 observed in murine systems was readily detectable despite rapid clearance of the parent compound from mouse plasma, indicating that continual exposure to SCH 727965 was not necessary for activity *in vivo*. Consistent with this, short exposure to SCH 727965 can induce long-lasting pharmacodynamic effects *in vitro*. Thus, a 2-hour exposure to  $\leq 500$  nmol/L SCH 727965 was sufficient to suppress BrdUrd incorporation 24 hours later. Similarly, transient *in vitro* exposure to SCH 727965 induced suppression of Rb phosphorylation that was correlated with induction of apoptosis. Significantly, escalation of SCH 727965 exposure ( $\leq 30$   $\mu\text{mol/L}$ ) did not augment apoptotic phenotypes, suggesting a relative lack of nonspecific or off-target cytotoxicity. Taken together, the available *in vitro* and *in vivo* data show that long-lasting therapeutic effects can be induced within sensitive cells following short exposures to SCH 727965. It is possible

that selecting compounds for further development solely on the basis of pharmacokinetic parameters would not have facilitated selection of SCH 727965 for clinical development. In summary, the approach of *in vivo* screening in mice ultimately led to the selection of a compound with attractive biochemical and pharmacologic properties.

Inhibitors of the CDK family have been proposed as attractive drug targets and pursued for oncology indications for several years, and several candidate molecules have entered clinical studies. In the case of flavopiridol, a combination of suboptimal selectivity, poor drug-like qualities, and adverse side effects may ultimately obscure any potentially desirable mechanism-based activities of this agent. In this study, we have described the novel pharmacologic properties of SCH 727965, a highly potent and selective CDK inhibitor that is differentiated from first generation CDK inhibitor compounds, such as flavopiridol. SCH 727965 is currently undergoing clinical testing against a range of solid and hematologic malignancies. The overall excellent profile of SCH 727965 suggests this molecule has the necessary properties to allow further pharmacologic exploration of the cell cycle mechanism in oncology.

## References

1. Sherr, C. J. Growth factor-regulated G1 cyclins. *Stem Cells* **1994**, *12 Suppl 1*, 47–55.
2. Pines, J. Protein kinases and cell cycle control. *Semin. Cell Biol.* **1994**, *5*, 399–408.
3. Hall, M.; Peters, G. Genetic alterations of cyclins, cyclin-dependent kinases, and Cdk inhibitors in human cancer. *Adv. Cancer Res.* **1996**, *68*, 67–108.
4. Sherr, C. J. Cancer cell cycles. *Science* **1996**, *274*, 1672–7.
5. Hunter, T.; Pines, J. Cyclins and cancer II: cyclin D and CDK inhibitors come of age. *Cell* **1994**, *79*, 573–82.
6. Ewen, M. E. The cell cycle and the retinoblastoma protein family. *Cancer Metastasis Rev.* **1994**, *13*, 45–66.
7. Ewen, M. E. Regulation of the cell cycle by the Rb tumor suppressor family. *Results Probl. Cell Differ.* **1998**, *22*, 149–79.
8. Bregman, D. B.; Pestell, R. G.; Kidd, V. J. Cell cycle regulation and RNA polymerase II. *Front. Biosci.* **2000**, *5*, D244–57.
9. Oelgeschlager, T. Regulation of RNA polymerase II activity by CTD phosphorylation and cell cycle control. *J. Cell. Physiol.* **2002**, *190*, 160–9.

10. van den Heuvel, S.; Harlow, E. Distinct roles for cyclin-dependent kinases in cell cycle control. *Science* **1993**, *262*, 2050–4.
11. Hu, B.; Mitra, J.; van den Heuvel, S.; Enders, G. H. S and G2 phase roles for Cdk2 revealed by inducible expression of a dominant-negative mutant in human cells. *Mol. Cell. Biol.* **2001**, *21*, 2755–66.
12. L'Italien, L.; Tanudji, M.; Russell, L.; Schebye, X. M. Unmasking the redundancy between Cdk1 and Cdk2 at G2 phase in human cancer cell lines. *Cell Cycle* **2006**, *5*, 984–93.
13. Cai, D.; Latham, V. M Jr.; Zhang, X. Shapiro, G. I. Combined depletion of cell cycle and transcriptional cyclin-dependent kinase activities induces apoptosis in cancer cells 10.1158/0008-5472.CAN-06-1758. *Cancer Res.* **2006**, *66*, 9270–80.
14. Gojo, I.; Zhang, B.; Fenton, R. G. The cyclin-dependent kinase inhibitor flavopiridol induces apoptosis in multiple myeloma cells through transcriptional repression and down-regulation of Mcl-1. *Clin. Cancer Res.* **2002**, *8*, 3527–38.
15. Chen, R.; Keating, M. J.; Gandhi, V.; Plunkett, W. Transcription inhibition by flavopiridol: mechanism of chronic lymphocytic leukemia cell death 10.1182/blood-2005-04-1678. *Blood* **2005**, *106*, 2513–9.
16. Firestein, R.; Bass, A. J.; Kim, S. Y. et al. CDK8 is a colorectal cancer oncogene that regulates [bgr]-catenin activity. 2008 2008/09/14/online.
17. Morris, E. J.; Ji, J.-Y.; Yang, F. et al. E2F1 represses [bgr]-catenin transcription and is antagonized by both pRB and CDK8. 2008 2008/09/14/online.
18. Chen, Y. N.; Sharma, S. K.; Ramsey, T. M. et al. Selective killing of transformed cells by cyclin/cyclin-dependent kinase 2 antagonists. *Proc. Natl. Acad. Sci. U S A* **1999**, *96*, 4325–9.
19. Shapiro, G. I. Cyclin-dependent kinase pathways as targets for cancer treatment 10.1200/JCO.2005.03.7689. *J. Clin. Oncol.* **2006**, *24*, 1770–83.
20. Kummar, S.; Gutierrez, M.; Doroshow, J. H.; Murgo, A. J. Drug development in oncology: classical cytotoxics and molecularly targeted agents. *Br. J. Clin. Pharmacol.* **2006**, *62*, 15–26.
21. Paruch, K.; Dwyer, M. P.; Alvarez, C. et al. Discovery of dinaciclib (SCH 727965): a potent and selective inhibitor of cyclin-dependent kinases. *ACS Med. Chem. Lett.* **2010**. Epub ahead of print.

## Part 2a

### Discovery of pyrazolo[1,5-*a*]pyrimidine-based CHK1 inhibitors: a template-based approach-part 1\*

\*published as:

Dwyer, M. P.;\* Paruch, K.; Labroli, M.; Alvarez, C.; Keertikar, K. M.; Poker, C.; Rossman, R.; Fischmann, T. O.; Duca, J. S.; Madison, V.; Parry, D.; Davis, N.; Seghezzi, W.; Wiswell, D.; Guzi, T. J. Discovery of pyrazolo[1,5-*a*]pyrimidine-based CHK1 inhibitors: A template-based approach-Part 1. *Bioorg. Med. Chem. Lett.* **2011**, *21*, 467.

Checkpoint kinase 1 (CHK1) is a serine/threonine kinase that controls the cellular response to DNA damage. In response to a DNA-damaging agent, CHK1 is activated by phosphorylation via ATR and ATM to arrest cells at various cell-cycle checkpoints (G1, S and G2) in order to initiate the DNA repair process.<sup>1</sup> Inhibition of CHK1 abrogates cell-cycle arrest resulting in genomic instability and ultimately progression into mitosis and cell death.<sup>2</sup> The inhibition of CHK1 creates a ‘synthetic lethal’ response by which aberrant cells cannot replicate which should impede the progression of cancer. In contrast, normal cells still arrest at the G1 checkpoint, via p53, to repair the DNA damage caused by these agents. Due to the fact that inhibition of CHK1 represents a targeted approach to enhance the cytotoxicity of DNA-damaging agents toward tumor cells while having a lesser effect on normal cells, it has been an attractive target in the oncology field.<sup>3</sup> A number of small-molecule CHK1 inhibitors have been described recently and several comprehensive reviews have provided overviews of the emerging CHK1 small-molecule chemotypes.<sup>4</sup> In addition, several checkpoint kinase inhibitors, such as PF-00477736 (**1**)<sup>5</sup> and AZD7762 (**2**)<sup>6</sup> (Fig. 1), have recently entered the clinic in combination with various DNA-damaging agents. Due to the therapeutic value of a CHK1 inhibitor as a chemopotentiator,<sup>7</sup> efforts were directed towards the identification of additional, novel CHK1 inhibitors.

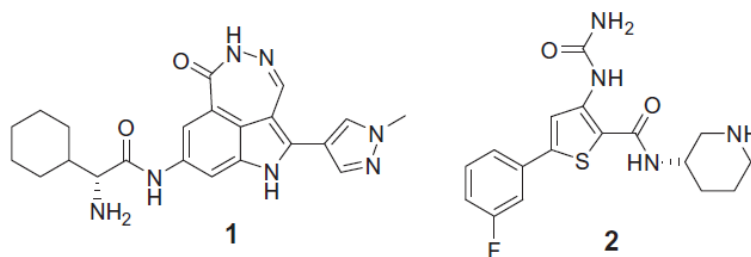


**Figure 1.** CHK1 inhibitors currently under clinical evaluation.

Screening of an internal compound library identified compounds **3** and **4**, as early CHK1 program hits (Fig. 2). While these initial hits possessed better *in vitro* potency versus CDK2 than CHK1, it was rationalized that proper substitution around the pyrazolo[1,5-*a*]pyrimidine core might improve the potency and selectivity of this series for CHK1. Previously, the pyrazolo[1,5-*a*]pyrimidine core was shown to be a viable template for the preparation of CDK2 inhibitors such as compound **5** which was orally bioavailable and found to be efficacious in a mouse tumor xenograft model (Fig. 2).<sup>8</sup>

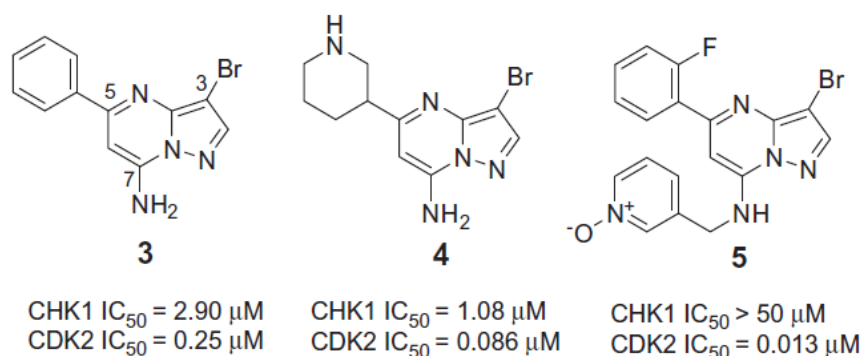
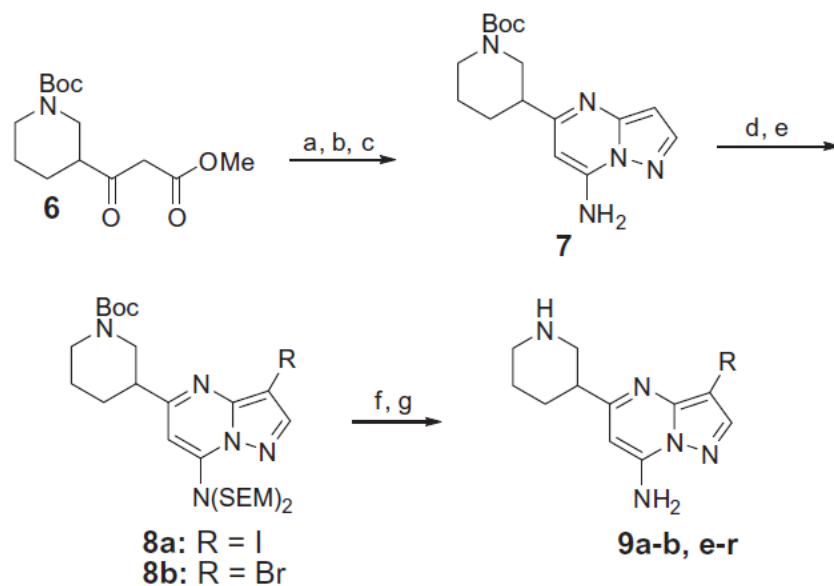


**Figure 2.** Initial pyrazolo[1,5-*a*]pyrimidine CHK1 Hits.

With compound **4** as a starting point, we focused upon making systematic modifications around the pyrazolo[1,5-*a*]pyrimidine core in order to enhance the *in vitro* potency for CHK1 while monitoring the selectivity versus CDK2. It was rationalized that selectivity for CHK1 over CDK2 was required since the inhibition of the CDK function may antagonize CHK1 ablation/inhibition phenotypes.<sup>9</sup>

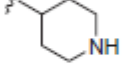
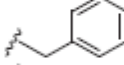
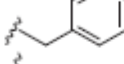
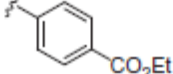
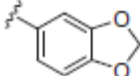
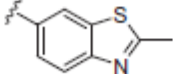
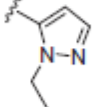
Since a limited set of substituents had been tolerated at the C3 position in the pyrazolo[1,5-*a*]pyrimidine core in our previous CDK2 program,<sup>8</sup> initial synthetic efforts focused upon modifications of the 3-position of compound **4** to further explore potential differences in this region for CHK1. The preparation of C3 analogs of compound **4** is illustrated in Schemes 1 and 2.<sup>10</sup>



**Scheme 1.** Reagents and conditions: (a) 3-aminopyrazole, PhCH<sub>3</sub>, 73%; (b) POCl<sub>3</sub>, N,N-dimethylaniline, 71%; (c) NH<sub>3</sub>, 2-propanol, H<sub>2</sub>O, 98%; (d) SEMCl, DIPEA, (CH<sub>2</sub>Cl)<sub>2</sub>, 76%; (e) NBS, CH<sub>3</sub>CN or NIS, CH<sub>3</sub>CN, 92%; (f) RB(OH)<sub>2</sub>, PdCl<sub>2</sub>dppf, K<sub>3</sub>PO<sub>4</sub>, DME/H<sub>2</sub>O or Bu<sub>3</sub>SnR, Pd[PPh<sub>3</sub>]<sub>4</sub>, dioxane, 29–89%; (g) 3 N HCl/EtOH, 23–78%.

Cyclization of β-keto ester **6** with 3-aminopyrazole followed by chlorination and amination afforded **7**. Diprotection of the resultant C7 amino group<sup>11</sup> followed by introduction of either the C3 iodide via NIS treatment or C3 bromide via NBS treatment afforded intermediates **8a** or **8b**. Treatment of **8a**, **b** under either Suzuki or Stille coupling conditions followed by global deprotection with 3 N HCl in EtOH afforded the C3 analogs **9a–b**, **e–r** which are summarized in Table 1.

**Table 1.** CHK1 and CDK2 inhibitory activity of C3 substituted pyrazolo[1,5-*a*]pyrimidines **9a-r**.

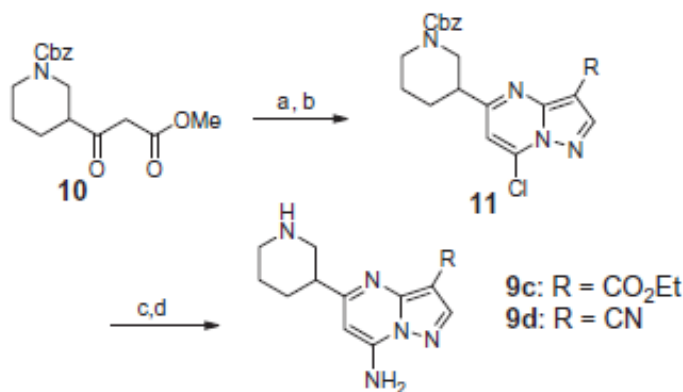
Compd	R	CHK1 IC <sub>50</sub> <sup>a</sup> (μM)	CDK2/cyclin A IC <sub>50</sub> <sup>b</sup> (μM)
<b>9</b>	H	0.06	6.06
<b>7a</b>	Me	0.14	na
<b>7b</b>	Et	0.48	na
<b>7c</b>		1.5	na
<b>17d</b>		5.0	na
<b>17e</b>		6.8	na
<b>17f</b>		1.0	31
<b>17g</b>		0.86	na
<b>17h</b>		0.41	na
<b>17i</b>		0.087	na
<b>17j</b>		0.051	na
<b>17k</b>		0.39	na
<b>17l</b>		0.61	na
<b>17m</b>		34	nt
<b>17n</b>		2.2	na
<b>17o</b>		0.028	na
<b>17p</b>		0.028	na
<b>17q</b>		0.021	na
<b>17r</b>		0.009	40

nt = not tested; values are means of two experiments.

<sup>a</sup> Assay conditions can be found in Ref. 12.

<sup>b</sup> Assay conditions can be found in Ref. 8a.

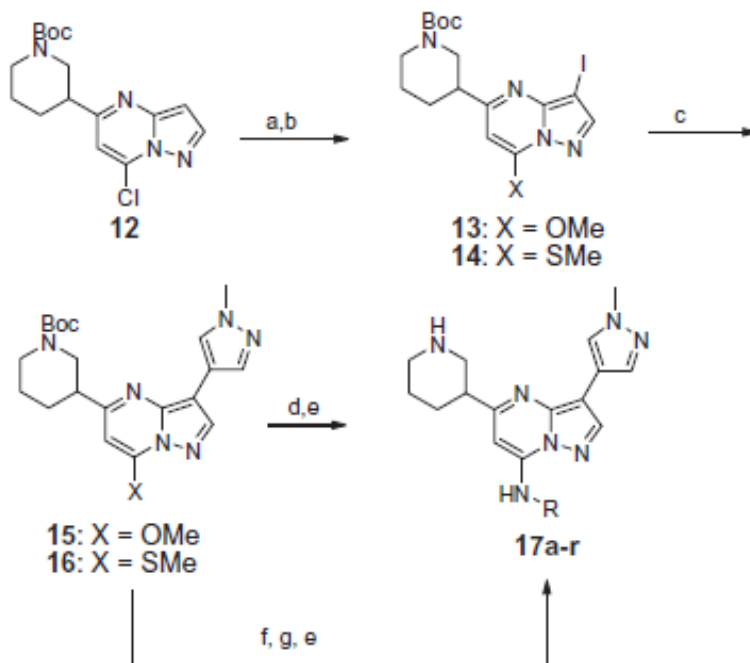
Alternatively in Scheme 2, cyclization of the Cbz-protected  $\beta$ -keto ester with either the cyano or ethyl ester substituted pyrazole followed by subsequent chlorination under standard conditions afforded **11**. Treatment with  $\text{NH}_3$  in isopropanol followed by Cbz deprotection with TMSI afforded the final adducts **9c** and **9d**.



**Scheme 2.** Reagents and conditions: (a) 3-aminopyrazole-4-carbonitrile or 3-amino-4-carboethoxypyrazole,  $\text{PhCH}_3$ , 41–61%; (b)  $\text{POCl}_3$ , *N,N*-dimethylaniline, 91–98%; (c)  $\text{NH}_3$ , 2-propanol,  $\text{H}_2\text{O}$ , 82–90%; (d) TMSI, MeOH, 31–45%.

As shown in Table 1, small linear substituents (**9b–f**) at the C3 position improved the CHK1 potency versus the 3-H adduct (**9a**) with the exception of ester **9c**. Despite the potency improvements for CHK1, these analogs also retained good potency for CDK2. Incorporation of aryl (**9g, h**) and heteroaryl substituents into the C3 position substituents (**9i–n**) resulted in marked improvement in CHK1 potency and selectivity versus CDK2 in the biochemical assay. Additionally, several heteroaryl derivatives in Table 1 (**9o, p**) showed weaker CHK1 activity which suggested that the proper placement of heteroatoms in the heteroaryl ring at C3 is critical to retain CHK1 potency. From this SAR survey of the C3 position, compound **9q** emerged as a key compound which demonstrated good CHK1 potency ( $\text{IC}_{50} = 60 \text{ nM}$ ) and nearly 100-fold selectivity for CHK1 over CDK2. Compound **9q** was selected as a lead structure for further SAR optimization efforts.

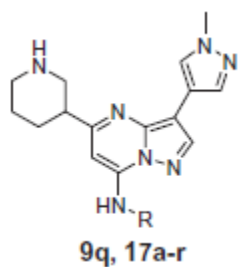
With compound **9q** in hand, attention turned toward the exploration of additional substitution of the primary amine located at the C7 position of this compound. The preparation of these analogs is outlined in Scheme 3.<sup>10</sup>



**Scheme 3.** Reagents and conditions: (a) NIS, CH<sub>3</sub>CN, 97%; (b) NaOMe or NaSMe, THF, 85–97%; (c) 1-methylpyrazole-4-boronic acid pinacol ester, PdCl<sub>2</sub>dppf, K<sub>3</sub>PO<sub>4</sub>, DME/H<sub>2</sub>O, 52–75%; (d) H<sub>2</sub>NR, NaH, DMF, 38–98%; (e) TFA, CH<sub>2</sub>Cl<sub>2</sub>, 13–98%; (f) MCPBA, CH<sub>2</sub>Cl<sub>2</sub>, 85%; (g) H<sub>2</sub>NR, n-BuOH, 100 °C, 21–85%.

Iodination of **12** followed by treatment with either sodium methoxide or sodium thiomethoxide in THF afforded compounds **13** or **14**, respectively. Treatment of **13** or **14** with 1-methylpyrazole-4-boronic acid pinacol ester under Suzuki coupling conditions afforded the corresponding coupled products **15** and **16**, respectively. For the preparation of C7 amino derivatives bearing either aryl or heteroaryl functionality, compound **15** was treated with the anion of the anilinic/heteroaryl coupling partners using NaH followed by TFA treatment to afford the title compounds **17i-r** (Table 2).

**Table 2.** CHK1 and CDK2 inhibitory activity of C7 substituted amino pyrazolo[1,5-*a*]pyrimidines.



Compd	R	CHK1 IC <sub>50</sub> <sup>a</sup> (μM)	CDK2/cyclin A IC <sub>50</sub> <sup>b</sup> (μM)
<b>9q</b>	H	0.06	6.06
<b>17a</b>	Me	0.14	na
<b>17b</b>	Et	0.48	na
<b>17c</b>		1.5	na
<b>17d</b>		5.0	na
<b>17e</b>		6.8	na
<b>17f</b>		1.0	31
<b>17g</b>		0.86	na
<b>17h</b>		0.41	na
<b>17i</b>		0.087	na
<b>17j</b>		0.051	na
<b>17k</b>		0.39	na
<b>17l</b>		0.61	na
<b>17m</b>		34	nt
<b>17n</b>		2.2	na
<b>17o</b>		0.028	na
<b>17p</b>		0.028	na
<b>17q</b>		0.021	na
<b>17r</b>		0.009	40

na = not active up to >50 μM; nt = not tested.

<sup>a</sup> Assay conditions can be found in Ref. 12.

<sup>b</sup> Assay conditions can be found in Ref. 8a.

Surprisingly, treatment of **15** with simple alkyl and benzyl amines with heating yielded none of the desired addition product but only the demethylated (7-OH) adduct. This issue was circumvented by utilization of the corresponding thiomethyl adduct **16**. Oxidation of the thiomethyl group with mCPBA afforded a mixture of sulfoxide/sulfone which was treated with either alkyl or branched alkyl amine derivatives in hot n-BuOH in the presence of Et<sub>3</sub>N to afford the desired addition products.

Deprotection of the intermediate Boc adducts with TFA afforded the C7 substituted amino derivatives **17a–h** listed in Table 2. As summarized in Table 2, incorporation of simple alkyl, branched alkyl, and cycloalkyl groups at the C7 amino group (**17a–e**) resulted in poorer in vitro potency for CHK1 versus the parent NH<sub>2</sub> derivative (**9q**). Simple alkyl modifications with pendant functionality (**17f–h**) resulted in derivatives with modest CHK1 activity. All of the C7 substituted amino derivatives in Table 2 demonstrated improved selectivity versus CDK2 (IC<sub>50</sub> >30 μM). While simple aryl derivatives or heteroaryl derivatives demonstrated good CHK1 activity (**17i–j**, **o–p**), the proper placement of heteroatom functionality in these motifs was important for retaining CHK1 potency as illustrated by **17k–n**. Aminoisothiazole **17r** emerged from the SAR work at the C7 position with excellent potency for CHK1 (<10 nM) and very good selectivity over CDK2. In order to better understand the SAR trends observed in Tables 1 and 2, a single crystal X-ray structure of **17r** bound to CHK1 (shown in Fig. 3) was obtained.<sup>13</sup>

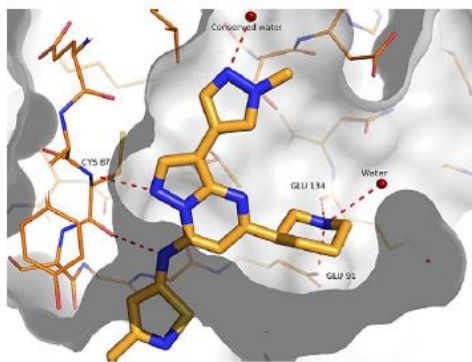


**Figure 3.** X-ray of crystal structure of **17r** in CHK1.<sup>13</sup>

In the X-ray structure, three key interactions were observed between **17r** and the CHK1 protein. First, the N1 moiety and C7 NH of the pyrazolo[1,5-*a*]pyrimidine core bind to the peptide backbone in the hinge area. Secondly, the 1-methylpyrazole moiety at the C3 position interacts with an array of ordered water molecules in the kinase specificity domain of CHK1. The SAR observed for the C3 heterocyclic derivatives shown in Table 1 may be explained in part by the propensity of these motifs to interact favorably with these water molecules which may mediate interactions with other amino acids. Lastly, the C5 piperidine nitrogen interacts with the carboxylate of Glu 91 as well as the amide carbonyl of Glu 134. Interestingly, the SAR observed at the C7 amino group (Table 2) is difficult to rationalize since this substitution projects into the solvent-exposed region based upon the X-ray structure depicted in Figure 3. Additional SAR efforts directed toward trying to elucidate the structural/electronic requirements in this region of this class of CHK1 inhibitors will be discussed in the accompanying manuscript.<sup>14</sup>

In summary, systematic optimization of both the C3 and C7 positions of pyrazolo[1,5-*a*]pyrimidine CHK1 hit **4** led to the discovery of potent, selective CHK1 inhibitors represented by **17r**. Single X-ray crystallography of **17r** in CHK1 elucidated several key interactions with the protein that appear to be critical to the improvement of CHK1 potency and selectivity versus CDK2 for this class of compounds. Additional SAR development and further analysis of this novel class of CHK1 inhibitors is found in the accompanying paper.<sup>14</sup>

## References and notes

1. (a) Sancar, A.; Lindsey-Boltz, L. A.; Unsal-Kacmaz, K.; Linn, S. *Annu. Rev. Biochem.* **2004**, *73*, 39; (b) Kastan, M. B.; Bartek, J. *Nature* **2004**, *432*, 316.
2. (a) Bucher, N.; Britten, C. D. *Br. J. Cancer* **2008**, *98*, 523; (b) Luo, Y.; Levenson, J. D. *Expert Rev. Anticancer Ther.* **2005**, *5*, 333.
3. (a) Powell, S. N.; DeFrank, J. S.; Connell, P.; Eogan, M.; Preffer, F.; Dombkowski, D.; Tang, W.; Friend, S. *Cancer Res.* **1995**, *55*, 1643; (b) Zhou, B.-B. S.; Elledge, S. J. *Nature* **2000**, *408*, 433; (c) Li, Q.; Zhu, G.-D. *Curr. Top. Med. Chem.* **2002**, *2*, 939.
4. (a) Matthews, T. P.; Klair, S.; Burns, S.; Boxall, K.; Cherry, M.; Fisher, M.; Westwood, I. M.; Walton, M. I.; McHardy, T.; Cheung, K.-M. J.; Van Montfort, R.; Williams, D.; Aherne, G. W.; Garrett, M. D.; Reader, J.; Collins, I. *J. Med. Chem.* **2009**, *52*, 4810. and references cited therein; (b) Janetka, J. W.; Ashwell, S. *Expert Opin. Ther. Patents* **2009**, *19*, 165; (c) Janetka, J. W.; Ashwell, S.; Zabludoff, S.; Lyne, P. *Curr. Opin. Drug Discov. Dev.* **2007**, *10*, 473; (d) Arrington, K. L.; Dudkin, V. Y. *ChemMedChem* **2007**, *2*, 1571.
5. Blasina, A.; Hallin, J.; Chen, E.; Arango, M. E.; Kraynov, E.; Register, J.; Gant, S.; Ninkovic, S.; Chen, P.; Nichols, T.; O'Connor, P.; Anderas, K. *Mol. Cancer Ther.* **2008**, *7*, 2394.
6. Zabludoff, S. D.; Deng, C.; Grondine, M. R.; Sheehy, A. M.; Ashwell, S.; Caleb, B. L.; Green, S.; Haye, H. R.; Horn, C. L.; Janetka, J. W.; Liu, D.; Mouchet, E.; Ready, S.; Rosenthal, J. L.; Queva, C.; Schwartz, G. K.; Taylor, K. J.; Tse, A. N.; Walker, G. E.; White, A. M. *Mol. Cancer Ther.* **2008**, *7*, 2955.
7. (a) Tao, Z.-F.; Lin, N.-H. *Anti-Cancer Agents Med. Chem.* **2006**, *6*, 377; (b) Prudhomme, M. *Recent Patents Anti-Cancer Drug Discov.* **2006**, *11*, 55.
8. (a) Dwyer, M. P.; Paruch, K.; Alvarez, C.; Doll, R. J.; Keertikar, K.; Duca, J.; Fischmann, T. O.; Hruza, A.; Madison, V.; Lees, E.; Parry, D.; Seghezzi, W.; Sgambellone, N.; Shanahan, F.; Wiswell, D.; Guzi, T. J. *Bioorg. Med. Chem. Lett.* **2007**, *17*, 6216; (b) Paruch, K.; Dwyer, M. P.; Alvarez, C.; Brown, C.; Chan, T.-Y.; Doll, R. J.; Keertikar, K.; Knutson, C.; McKittrick, B.; Rivera, J.; Rossman, R.; Tucker, G.; Fischmann, T.; Hruza, A.; Madison, V.; Nomeir, A. A.; Wang, Y.; Lees, E.; Parry, D.; Sgambellone, N.; Seghezzi, W.; Schultz, L.; Shanahan, F.; Wiswell, D.; Xu, X.; Zhou, Q.; James, R. A.; Paradkar, V. M.; Park, H.; Rokosz, L. R.; Stauffer, T. M.; Guzi, T. J. *Bioorg. Med. Chem. Lett.* **2007**, *17*, 6220; (c) Paruch, K.; Dwyer, M. P.; Alvarez, C.; Brown, C.; Chan, T.-Y.; Doll, R. J.; Keertikar, K.; Knutson, C.; McKittrick, B.; Rivera, J.; Rossman, R.; Tucker, G.; Fischmann, T.; Hruza, A.; Madison, V.; Nomeir, A. A.; Wang, Y.; Kirschmeier, P.; Lees, E.; Parry, D.; Sgambellone, N.; Seghezzi, W.; Schultz, L.; Shanahan, F.; Wiswell, D.; Xu, X.; Zhou, Q.; James, R. A.; Paradkar, V. M.; Park, H.; Rokosz, L. R.; Stauffer, T. M.; Guzi, T. J. *ACS Med. Chem. Lett.* **2010**, *1*, 204.

9. Walton, M. I.; Eve, P. D.; Hayes, A.; Valenti, M.; De Haven Brandon, A.; Box, G.; Boxall, K. J.; Aherne, G. W.; Eccles, S. A.; Raynaud, F. I.; Williams, D. H.; Reader, J. C.; Collins, I.; Garrett, M. M. D. *Mol. Cancer Ther.* **2010**, *9*, 89.
10. Full experimental details have appeared elsewhere: Guzi, T. J.; Paruch, K.; Dwyer, M. P.; Parry, D. A. *US 2007/0082900*.
11. Protection of the C7 amino group as the di-SEM analog proved to be optimal for efficient coupling reactions using either the Suzuki or Stille coupling protocols.
12. CHK1 SPA assay. An in vitro assay utilizing recombinant His-CHK1 expressed in the baculovirus expression system as an enzyme source and biotinylated peptide based upon CDC25C as substrate. His-CHK1 was diluted to 32 nM in kinase buffer containing 50 mM Tris pH 8.0, 10 mM MgCl<sub>2</sub>, and 1 mM DTT. CDC25C (CDC25 Ser216 C-term biotinylated peptide, Research Genetics) peptide was diluted to 1.93 μM in kinase buffer. For each kinase reaction, 20 μL of 32 nM CHK1 enzyme solution and 20 μL of 1.926 μM substrate solution were mixed and combined with 10 μL of compound diluted in 10% DMSO, making final reaction concentrations of 6.2 nM CHK1, 385 nM CDC25C and 1% DMSO after addition of start solution. The reaction was started by addition of 50 μL of start solution consisting of 2 μM ATP and 0.2 μCi of <sup>33</sup>PATP (Amersham, UK), making a final reaction concentration of 1 μM ATP, with 0.2 μCi of <sup>33</sup>P-ATP per reaction. Kinase reactions ran for 2 h at room temperature and were stopped by the addition of 100 μL of stop solution consisting of 2 M NaCl, 1% H<sub>3</sub>PO<sub>4</sub>, and 5 mg/mL Streptavidin-coated SPA beads (Amersham, UK). SPA beads were captured using a 96-well GF/B filter plate (Packard/Perkin Elmer Life Sciences) and a Filtermate universal harvester (Packard/Perkin Elmer Life Sciences). Beads were washed twice with 2 M NaCl and twice with 2 M NaCl with 1% phosphoric acid. Signal was then assayed using a TopCount 96-well liquid scintillation counter (Packard/Perkin Elmer Life Sciences). Dose–response curves were generated from duplicate 8 point serial dilutions of inhibitory compounds. IC<sub>50</sub> values were derived by nonlinear regression analysis.
13. The coordinates of compound **17r** bound to CHK1 have been deposited in the Protein Databank: pdb ID 3OT8.
14. Labroli, M.; Paruch, K.; Dwyer, M. P.; Alvarez, C.; Keertikar, K.; Poker, C.; Rossman, R.; Fischmann, T. O.; Duca, J. A.; Madison, V.; Parry, D.; Davis, N.; Seghezzi, W.; Wiswell, D.; Guzi, T. J. *Bioorg. Med. Chem. Lett.* **2010**, *21*, 471.

**Note:** Experimental details can be found in our publicly available patents WO 2007/041712 A1 and WO 2008/153870 A1.

## Part 2b

### Discovery of pyrazolo[1,5-*a*]pyrimidine-based CHK1 inhibitors: a template-based approach-part 2\*

\*published as:

Labroli, M.;\* Paruch, K.; Dwyer, M. P.; Alvarez, C.; Keertikar, K. M.; Poker, C.; Rossman, R.; Fischmann, T. O.; Duca, J. S.; Madison, V.; Parry, D.; Davis, N.; Seghezzi, W.; Wiswell, D.; Guzi, T. J. Discovery of pyrazolo[1,5-*a*]pyrimidine-based CHK1 inhibitors: A template-based approach-Part 2. *Bioorg. Med. Chem. Lett.* **2011**, *21*, 471.

As one of the key regulators of the cell cycle progression, CHK1 is a serine/threonine kinase which has been an attractive target in oncology.<sup>1</sup> A number of small-molecule ATP-competitive CHK1 inhibitors have been described<sup>2</sup> and several compounds have recently entered the clinic including PF-00477736 (**1**)<sup>3</sup> and AZD7762 (**2**)<sup>4</sup> (Fig. 1).

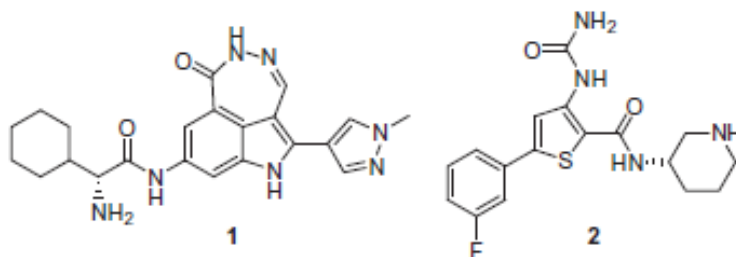


**Figure 1.** CHK1 inhibitors currently under clinical evaluation.

Herein, we describe our continued SAR development of the pyrazolo[1,5-*a*]pyrimidine core to develop potent and selective CHK1 inhibitors. Initial screening of our internal compound library identified compound **3** as a CHK1 program hit which was derived from an earlier CDK program (Fig. 2).

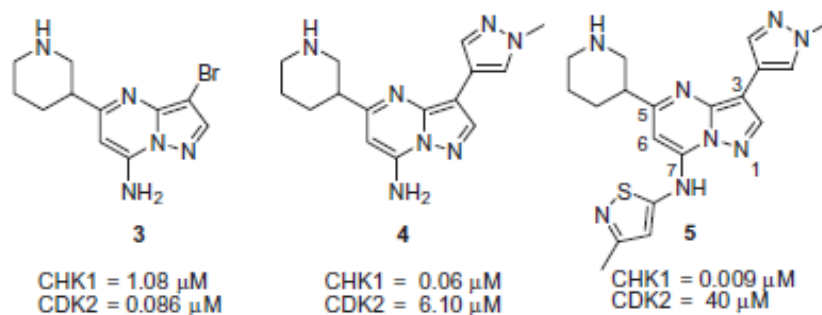
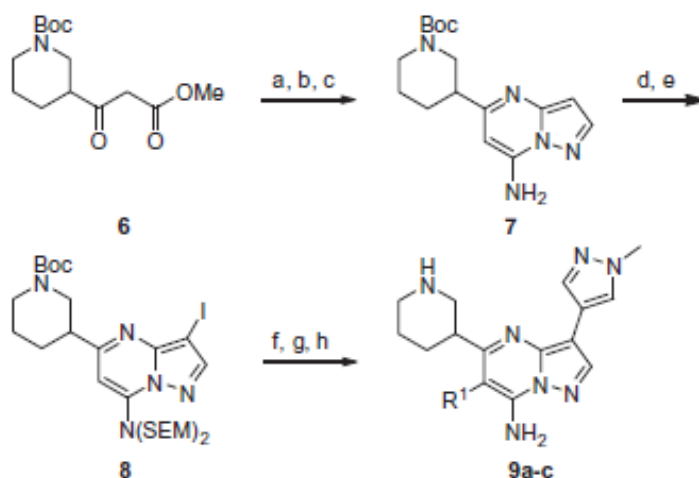


**Figure 2.** Pyrazolo[1,5-*a*]pyrimidine hits for CHK1 program.

Initial SAR optimization work on the pyrazolo[1,5-*a*]pyrimidine scaffold at both the C3 and C7–NH2 positions led to several promising targets, including **4** and **5**, which displayed improved in vitro potency for CHK1 and increased selectivity against CDK2 versus the early hit **3** (Fig. 2).<sup>5</sup> As discussed in the preceding Letter,<sup>5</sup> the SAR study of the C3 position demonstrated that the 4-*N*-methylpyrazole moiety conferred optimal CHK1 potency while maintaining selectivity against CDK2. Additionally, structural modifications of the C7–NH2 position were extremely challenging as a majority of substituents incorporated in this region displayed a loss in CHK1 potency versus the C7–NH2 analog with the exception of compound **5**. These observations could, in part, be attributed to the deleterious effect of the C7–NH2 substituents on the crucial H-bonding motif in the hinge region.<sup>5</sup> In light of these observations, we felt there might be additional opportunities to explore the solvent exposed region using C6 substitution. Initial synthetic efforts focused upon the preparation of the 6-halo compounds **9a–c** which maintained key functionality at C3 (*N*-methyl pyrazole) and C5 (3-piperidine) that was previously noted for CHK1 potency.<sup>5</sup> It was envisioned that the C6 halo functionality could serve as handles for further elaboration at the C6 position. The preparation of these analogs was discussed previously and shown in Scheme 1.<sup>5,6</sup>



**Scheme 1.** Reagents: (a) 3-aminopyrazole, PhCH<sub>3</sub>, 75%; (b) POCl<sub>3</sub>, N,N-dimethylaniline, 71%; (c) NH<sub>3</sub>, 2-propanol, H<sub>2</sub>O, 98%; (d) SEMCl, DIPEA (CH<sub>2</sub>Cl)<sub>2</sub>, 76%; (e) NIS, CH<sub>3</sub>CN, 92%; (f) 1-methyl-4-(4,4,4,5-tetramethyl-1,3,2-dioxaborolan-2-yl)-1H-pyrazole, PdCl<sub>2</sub>dppf, K<sub>3</sub>PO<sub>4</sub>, DME, 81%; (g) HCl, EtOH, 90%; (h) NCS, CH<sub>3</sub>CN, 72% or NBS or Br<sub>2</sub>, t-BuNH<sub>2</sub>, CH<sub>2</sub>Cl<sub>2</sub>, 73% or NIS, CH<sub>3</sub>CN, 83%.

Interestingly, the 6-halo compounds **9a–c** demonstrated a 20-fold improvement in CHK1 activity relative to the parent compound **4** (Table 1).

**Table 1.** CHK1 and CDK2 inhibitory activity of pyrazolo[1,5-*a*]pyrimidines **4** and **9a–p**.

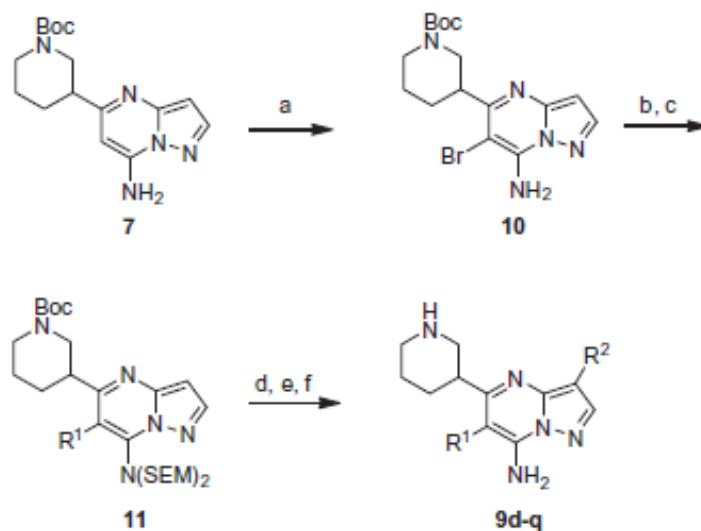
Compds	R <sup>1</sup>	CHK1 IC <sub>50</sub> <sup>a</sup> (μM)	CDK2/cyclin A IC <sub>50</sub> <sup>b</sup> (μM)
<b>4</b>	H	0.060	6.1
<b>9a</b>	Cl	0.003	0.31
<b>9b</b>	Br	0.003	0.16
<b>9c</b>	I	0.003	0.33
<b>9d</b>	Et	0.031	0.33
<b>9e</b>	Propynyl	0.045	0.52
<b>9f</b>	Cypr	0.017	0.17
<b>9g</b>	(CH <sub>2</sub> ) <sub>2</sub> OH	0.026	0.048
<b>9h</b>	CH=CH-CH <sub>2</sub> OMe	0.052	2.2
<b>9i</b>	CN	0.10	1.7
<b>9j</b>	Ph	0.56	8.3
<b>9k</b>	2-Thienyl	0.086	0.99
<b>9l</b>	3-Thienyl	0.16	2.2
<b>9m</b>	3-Furyl	0.34	2.3
<b>9n</b>	3-Pyridyl	0.51	1.5
<b>9o</b>	4-Pyridyl	0.23	11
<b>9p</b>	4- <i>N</i> -Methylpyrazolyl	0.10	22

Values reported are means of two experiments.

<sup>a</sup> Assay conditions can be found in Ref. 5.

<sup>b</sup> Assay conditions can be found in Ref. 10.

Unfortunately, all attempts to install additional functionality at the C6 position via the 6-halo precursors using either Suzuki or Stille coupling protocols were unsuccessful (not shown). While the limitations of using these coupling protocols in sterically congested systems has been documented,<sup>7</sup> the initial synthetic route had to be modified to allow for more facile incorporation of substituents at the C6 position which is shown in Scheme 2. Treatment of **7** with bromine in *t*-butylamine<sup>8</sup> yielded the corresponding 6-bromo derivative **10** for further elaboration (Scheme 2). Bisprotection of **10** with SEMCl<sup>9</sup> followed by Pd-mediated couplings introduced desired substitution at the C6 position to yield compound **11**. Functionalization of the C3 position was achieved by bromination, Suzuki or Stille coupling with the appropriate heteroaromatic group, and global deprotection to afford targets **9d–q**.



**Scheme 2.** Reagents: (a) Br<sub>2</sub>, *t*-BuNH<sub>2</sub>, CH<sub>2</sub>Cl<sub>2</sub>, 79%; (b) SEMCl, DIPEA (CH<sub>2</sub>Cl)<sub>2</sub>, 39%; (c) R<sup>1</sup>B(OH)<sub>2</sub>, PdCl<sub>2</sub>dppf, K<sub>3</sub>PO<sub>4</sub>, DME, H<sub>2</sub>O or Bu<sub>3</sub>SnR<sup>1</sup>, Pd(PPh<sub>3</sub>)<sub>4</sub>, dioxane, 27–83%; (d) NBS, CH<sub>3</sub>CN, 66–92%; (e) R<sup>2</sup>B(OH)<sub>2</sub>, PdCl<sub>2</sub>dppf, K<sub>3</sub>PO<sub>4</sub>, DME, H<sub>2</sub>O or Bu<sub>3</sub>SnR<sup>2</sup>, Pd[PPh<sub>3</sub>]<sub>4</sub>, dioxane, 41–90%; (f) HCl, EtOH, 17–80%.

The biochemical assay results for both CHK1 and CDK2 are summarized in Table 1 for compounds **4** and **9a–q**. As evident from Table 1, small alkyl or cycloalkyl substituents at the C6 position retained reasonable CHK1 potency with varying levels of CDK2 selectivity (**9d–i**) similar to the 6-halo compounds **9a–c**. Incorporation of either aryl or heteroaryl derivatives at the C6 position generally led to a loss of CHK1 potency versus the smaller substituents while maintaining some selectivity over

CDK2 (**9j–p**). Although it appears that the solvent exposed region would be more accommodating to a variety of substituents, the SAR observed at the C6 position may be a combination of both size and polarity requirements of the substituents. Additionally, the electron withdrawing substituents such as the 6-halo derivatives **9a–c** seem to be preferred at this position and may in fact play a role in modulating the acidity of the adjacent C7–NH<sub>2</sub> group.

Based upon the SAR observed in Table 1, we decided to briefly investigate a series of C3 heteroaromatic groups bearing the C6–Br to determine if we were maintaining optimal potency and selectivity among the C3, C6, and C7 substituents. Representative examples are depicted in Table 2.

**Table 2.** CHK1 and CDK2 inhibitory activity of C3-substituted pyrazolo[1,5-*a*]pyrimidines **9b** and **12a–c**.

Compds	R <sup>2</sup>	CHK1 IC <sub>50</sub> <sup>a</sup> (μM)	CDK2/cyclin A IC <sub>50</sub> <sup>b</sup> (μM)
<b>9b</b>		0.003	0.16
<b>12a</b>		0.017	0.17
<b>12b</b>		0.025	0.10
<b>12c</b>		0.008	0.20

Values reported are means of two experiments.

a Assay conditions can be found in Ref. 5.

b Assay conditions can be found in Ref. 10.

Although compound **9b** remained the most potent analog, other C3 heteroaromatic groups, for example, **12c**, demonstrated comparable CHK1 potency with a comparable selectivity profile against CDK2. With the initial SAR investigations at the C3, C6, and C7–NH<sub>2</sub> positions of the pyrazolo[1,5-*a*]pyrimidine core complete, attention was turned toward exploration of the C5 position. From the X-ray structure of compound **5** bound to CHK1,<sup>5</sup> the NH of the C5 3-piperidinyl group was observed to form several key hydrogen bond interactions with several acidic residues as well as a conserved water molecule in this region. Initial SAR efforts at the C5 position focused upon further optimization of this key H-bonding interaction. In order to more rapidly examine the SAR in this region, an alternative synthesis was developed taking into account the optimal substituents at the C3, C6, and C7 positions of the pyrazolo[1,5-*a*]pyrimidine core. Retrosynthetically, we envisioned a more convergent

assembly of the pyrazolo[1,5-*a*]pyrimidine core (e. g., **4**) via the cyclocondensation of  $\beta$ -keto nitrile **13** and 3-amino-1-methyl-1H-1',4,4'-bispyrazole **14** (Fig. 3).

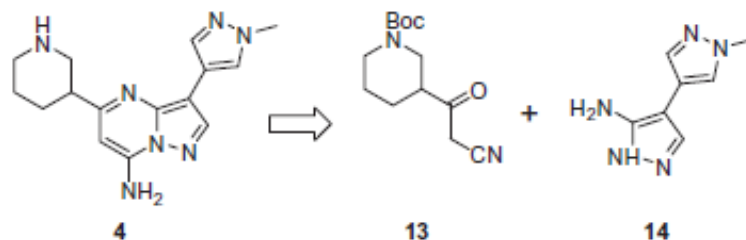
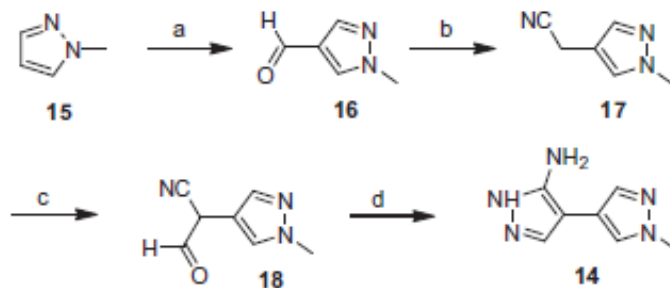


**Figure 3.** Retrosynthetic analysis of **4**.

The preparation of aminopyrazole **14**<sup>11</sup> began with Vilsmeier-Haack formylation of *N*-methyl-1H-pyrazole **15** to afford aldehyde **16** (Scheme 3). Treatment of **16** with tosyl methyl isocyanide<sup>12</sup> (TosMIC) in the presence of potassium *t*-butoxide in DME resulted in the one-step homologation and cyanation process to yield the acetonitrile **17**.  $\alpha$ -Formylation, followed by cyclization with hydrazine monohydrochloride in ethanol yielded the final bispyrazole **14**.

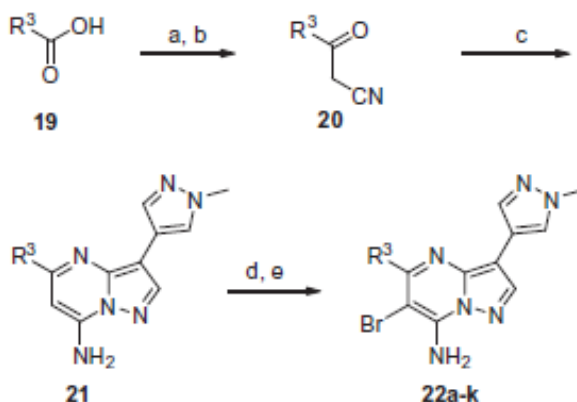


**Scheme 3.** Reagents: (a) POCl<sub>3</sub>, DMF, 50%; (b) KO-*t*-Bu, TosMIC, DME, 65%; (c) ethyl formate, KO-*t*-Bu, DME, 82%; (d) N<sub>2</sub>H<sub>4</sub>-HCl, EtOH, 90%.

It should be noted that this preparation of bispyrazole **14** was amenable to large-scale synthesis and the use of TosMIC avoids the need for toxic cyanide reagents commonly employed in other cyanation protocols.

With the bispyrazole **14** in hand, the syntheses of the C5 targets **22a–k** were accomplished utilizing the route displayed in Scheme 4. Treatment of acids **19** with 1,1-carbonyldiimidazole followed by

addition of the anion of acetonitrile provided the substituted  $\beta$ -keto nitriles **20** in good yield. Cyclocondensation of **20** with bispyrazole **14** from Scheme 4 in EtOH or toluene provided the core **21**. Regioselective bromination with NBS followed by acid deprotection of Boc intermediates, when necessary, provided the desired targets **22a–k** listed in Table 2.



**Scheme 4.** Reagents and conditions: (a) CDI, THF; (b) LiHMDS, CH<sub>3</sub>CN, THF, -78 °C, 22–78% overall for two steps; (c) **14**, EtOH, 45 °C, or toluene, 115 °C, 37–87%; (d) NBS, DCM, 71–89%; (e) TFA, DCM, 39–93%.

As summarized in Table 3, the SAR at C5 clearly demonstrates the necessity of both the proper positioning and basicity of the piperidine NH for optimal CHK1 potency and selectivity against other kinases, specifically CDK2. Loss of the piperidine NH (e.g., **22a**) as well as different positional isomers (**22b, c**) led to a loss of CHK1 potency. Additional heteroatoms are tolerated with varying degrees of CHK1 potency (e.g., **22d, e**) while ring-contracted (**22f**) or the acyclic amine derivative (**22g**) generally showed reduced CHK1 potency. Several homologated analogs (**22i, j**) as well as exocyclic amine analog **22k** demonstrated comparable CHK1 potency to **9b** with a comparable or improved selectivity profile against CDK2 (Table 3).

**Table 3.** CHK1 and CDK2 inhibitory activity of C5-substituted pyrazolo[1,5-*a*]pyrimidines **9b** and **22a–k**.

Comps	R <sup>3</sup>	CHK1 IC <sub>50</sub> <sup>a</sup> (μM)	CDK2/cyclin A IC <sub>50</sub> <sup>b</sup> (μM)
<b>9b</b>		0.003	0.16
<b>22a</b>		4.0	1.3
<b>22b</b>		2.9	28.7
<b>22c</b>		0.035	0.49
<b>22d</b>		0.13	1.2
<b>22e</b>		0.006	0.15
<b>22f</b>		0.031	0.51
<b>22g</b>		0.034	0.92
<b>22h</b>		0.087	2.8
<b>22i</b>		0.007	0.84
<b>22j</b>		0.007	2.4
<b>22k<sup>c</sup></b>		0.005	0.44

Values reported are means of two experiments.

<sup>a</sup> Assay conditions can be found in Ref. 5.

<sup>b</sup> Assay conditions can be found in Ref. 10.

A single X-ray crystal structure of **22k** bound to CHK1 (Fig. 4) was obtained which confirmed a similar binding mode to that observed for compound **5**.<sup>5</sup> From Figure 4, the key H-bond network from the C3 pyrazole in **22k** with ordered waters is maintained while the C7-NH<sub>2</sub> maintains a key hinge contact with the C6-Br group projecting into the solvent exposed region as expected. Interestingly, the exocyclic NH<sub>2</sub> of **22k** occupies a similar position as the piperidine NH of **5** to maintain the key interactions with an acidic group and a conserved water molecule which is imperative for CHK1 potency as demonstrated in Table 3.

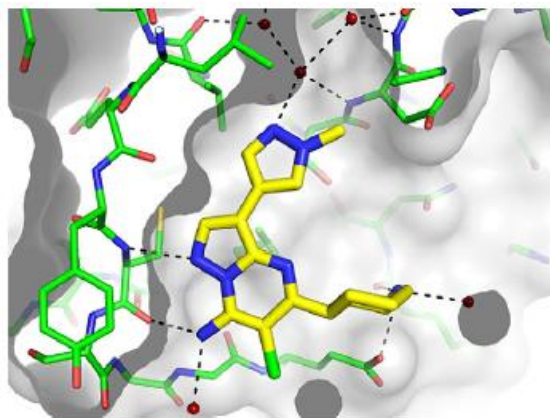


**Figure 4.** X-ray of crystal structure of **22k** in CHK1.<sup>13</sup>

Starting with a CDK2 selective pyrazolo[1,5-*a*]pyrimidine CHK1 lead **3**, systematic SAR studies of the C3, C5, C6, and C7-NH<sub>2</sub> positions of the core led to the identification of potent and selective CHK1 inhibitors, for example, **5**, **9a-c**, **12c**, and **22i-k**.<sup>5</sup> Interestingly, potent CHK1 inhibition can be retained through the appropriate combination of C6 substitution with a primary amine at C7. Approaches to differentiate between this novel class of pyrazolo[1,5-*a*]pyrimidines and those identified in the preceding Letter<sup>5</sup> as well as to calibrate the extent of CDK2 selectivity required in a CHK1 inhibitor utilizing a mechanistically based in-cell evaluation assay will be the subject of a future Letter.

## References and notes

1. Zhou, B.-B. S.; Elledge, S. J. *Nature* **2000**, *408*, 433.
2. (a) Janetka, J. W.; Ashwell, S.; Zabludoff, S.; Lyne, P. *Curr. Opin. Drug Discov. Devel.* **2007**, *10*, 473; (b) Matthews, T. P.; Klair, S.; Burns, S.; Boxall, K.; Cherry, M.; Fisher, M.; Westwood, I. M.; Walton, M. I.; McHardy, T.; Cheung, K.-M. J.; Van Montfort, R.; Williams, D.; Aherne, G. W.; Garrett, M. D.; Reader, J.; Collins, I. *J. Med. Chem.* **2009**, *52*, 4810. and references cited therein.
3. Blasina, A.; Hallin, J.; Chen, E.; Arango, M. E.; Kraynov, E.; Register, J.; Gant, S.; Ninkovic, S.; Chen, P.; Nichols, T.; O'Connor, P.; Anderas, K. *Mol. Cancer Ther.* **2008**, *7*, 2394.
4. Zabludoff, S. D.; Deng, C.; Grondine, M. R.; Sheehy, A. M.; Ashwell, S.; Caleb, B. L.; Green, S.; Haye, H. R.; Horn, C. L.; Janetka, J. W.; Liu, D.; Mouchet, E.; Ready, S.; Rosenthal, J. L.; Queva, C.; Schwartz, G. K.; Taylor, K. J.; Tse, A. N.; Walker, G. E.; White, A. M. *Mol. Cancer Ther.* **2008**, *7*, 2955.
5. Dwyer, M. P.; Paruch, K.; Labroli, M. A.; Alvarez, C.; Keertikar, K.; Poker, C.; Rossman, R.; Duca, J. A.; Madison, V.; Parry, D.; Davis, N.; Seghezzi, W.; Wiswell, D.; Guzi, T. J. *Bioorg. Med. Chem. Lett.* **2010**, *21*, 467.
6. Full experimental details have appeared elsewhere: Guzi, T. J.; Paruch, K.; Dwyer, M. P.; Parry, D. A. *US 2007/0082900*.
7. (a) Mei, X.; Martin, R. M.; Wolf, C. *J. Org. Chem.* **2006**, *71*, 2854; (b) Johnson, M. G.; Foglesong, R. J. *Tetrahedron Lett.* **1997**, *38*, 7001.
8. (a) Pearson, D. E.; Wysong, R. D.; Breder, C. V. *J. Org. Chem.* **1967**, *32*, 2358; (b) Ishizaki, M.; Ozaki, K.; Kanematsu, A.; Isoda, T.; Hoshino, O. *J. Org. Chem.* **1993**, *58*, 3877.
9. Protection of the 7-amino group as the di-SEM analog proved to be optimal as it was shown that this protection was imperative for efficient coupling reactions via either the Suzuki or Stille couplings.
10. Dwyer, M. P.; Paruch, K.; Alvarez, C.; Doll, R. J.; Keertikar, K.; Duca, J.; Fischmann, T. O.; Hruza, A.; Madison, V.; Lees, E.; Parry, D.; Seghezzi, W.; Sgambellone, N.; Shanahan, F.; Wiswell, D.; Guzi, T. J. *Bioorg. Med. Chem. Lett.* **2007**, *17*, 6216.
11. Labroli, M. A.; Poker, C.; Guzi, T. J.; Paruch, K.; Dwyer, M. P.; Keertikar, K. M.; Alvarez, C. S. Process for preparation of substituted 3-aminopyrazoles via formylation, cyanation, and cyclocondensation reactions. *PCT Int. Appl. WO 2008153873*.
12. van Leusen, A. M.; Oomkes, P. G. *Synth. Commun.* **1980**, *10*, 399.
13. The co-ordinates of **22k** bound to CHK1 have been deposited in the Protein Databank pdb 3OT3.  
**Note:** Experimental details can be found in our publicly available patents WO 2007/041712 A1 and WO 2008/153870 A1.

**Part 2c**  
**Targeting the replication checkpoint using SCH 900776, a  
potent and functionally selective CHK1 inhibitor identified  
via high content screening\***

\*published as:

Guzi, T.; Paruch, K.; Dwyer, M.; Labroli, M.; Shanahan, F.; Davis, N.; Taricani, L.; Wiswell, D.; Seghezzi, W.; Penafior, E.; Bhagwat, B.; Wang, W.; Gu, D.; Hsieh, Y.; Lee, S.; Liu, M.; Parry, D. \* Targeting the Replication Checkpoint Using SCH 900776, a Potent and Functionally Selective CHK1 Inhibitor Identified Via High Content Screening. *Mol. Cancer Ther.* **2011**, *10*, 591.

## **Introduction**

DNA antimetabolite drugs are used extensively in modern clinical oncology.<sup>1</sup> A primary mechanism of action of DNA antimetabolite drugs is to suppress DNA synthesis, which leads to stalled replication forks and activation of the replication checkpoint.<sup>2, 3</sup> This checkpoint is critical for maintaining viability, acting to stabilize and preserve replication fork complexes.<sup>4-6</sup> Replication fork collapse is an irretrievable and catastrophic event and the serine/threonine kinase checkpoint kinase 1 (CHK1) is an essential mediator of the mammalian replication checkpoint.<sup>5</sup> Thus, CHK1 is associated with key mediators of DNA replication and, following exposure to hydroxyurea, is activated in this context in a manner that requires TopBP1 and ataxia telangiectasia-related protein.<sup>7</sup> Activation of CHK1 ultimately causes inactivation of cyclin-dependent kinases (CDK) leading to appropriately controlled delays in downstream cell cycle progression.<sup>8-10</sup>

Ablation of CHK1 using short interfering RNA (siRNA) during hydroxyurea exposure led to rapid generation of double-strand DNA breaks and subsequent cell death. In addition, tumor cells lacking CHK1 were unable to resume DNA synthesis following withdrawal of hydroxyurea and underwent apoptosis in a manner independent of CHK2 or p53 status. Hence, CHK1 appears essential for suppression of DNA damage and maintains viability during replication stress.<sup>5</sup> By extension, the nonredundant function of CHK1 at the replication checkpoint appears mechanistically distinct from the previously characterized role at the G<sub>2</sub>-M or DNA damage checkpoint.<sup>9, 11</sup> Significantly, similar phenotypes were not observed following depletion of CHK1 in nontransformed, diploid fibroblasts.<sup>5</sup>

In this study, we once more focus on the role of CHK1 at the replication checkpoint and describe the use of mechanism-based phenotypic screening to identify and discriminate between potent CHK1

inhibitor compounds. The cellular  $\gamma$ -H2AX biomarker of double-strand DNA break accumulation was a key component of this highly functional approach.<sup>12</sup> Using this marker, the relative contributions of CHK1, CHK2, and the CDKs to the replication checkpoint were assessed.<sup>13</sup> These experiments prompted a deeper understanding of the inhibitory profile required in a fully functional CHK1 inhibitor and led to the identification of SCH 900776.

## **Materials and Methods**

### ***Experimental compounds and siRNAs***

Experimental compounds A, B, C, D, E, SCH 900776, and SCH 727965 were synthesized and purified as described previously.<sup>14-17</sup> Clinical formulations of gemcitabine and pemetrexed were obtained from Eli Lilly (Gemzar, Alimta, Eli Lilly). SN38, the active metabolite of CPT-11, was purchased from Tocris Biosciences. Other reagents were obtained from Sigma-Aldrich Chemical Company. Characterization of CHK1, CHK2, CDK siRNAs, and transfection conditions have been described previously.<sup>5, 7, 18</sup>

### ***Cell lines and cell culture***

Tumor cell lines were obtained from the American Type Culture Collection and the Schering Plough cell line repository (no authentication was done by the authors).

### ***Immunoblotting***

Cells were harvested and lysed in a 50 mmol/L Tris-HCl buffer containing 350 mmol/L NaCl, 0.1% NP40, 1 mmol/L dithiothreitol, and a cocktail of protease and phosphatase inhibitors (Calbiochem). Following protein concentration determination (Biorad), cell lysates were separated on reducing SDS-PAGE gels and immunoblotted with antisera specific for CDK1 (cell signaling), CDK2 (cell signaling), CHK1 pS345 (cell signaling), CHK1 pS296 (cell signaling), total CHK1 (7), and phospho-replication protein A (RPA) (Bethel Labs).

### ***Kinase assays***

CHK1, CHK2, and CDK kinase assays have been described previously.<sup>14-17, 19, 20</sup> The Millipore Kinase Profiler service was used to generate general selectivity data for SCH 900776 against a broad range of serine/threonine and tyrosine kinases. Assays were typically run at two concentrations of

SCH 900776 (0.5 and 5  $\mu\text{mol/L}$ ), at a fixed (10  $\mu\text{mol/L}$ ) concentration of ATP. Data were provided as percent activity remaining, relative to uninhibited controls.

#### ***Affinity assessment using temperature-dependent fluorescence***

An amount of 1  $\mu\text{mol/L}$  CHK1 recombinant kinase domain protein (amino acid residues 2–274) was mixed with micromolar concentrations (usually 1–50  $\mu\text{mol/L}$ ) of compounds in 20  $\mu\text{L}$  of assay buffer (25 mmol/L HEPES, pH 7.4, 300 mmol/L NaCl, 5 mmol/L dithiothreitol, 2% dimethyl sulfoxide, Sypro Orange 5x) in a white 96-well PCR plate. The plate was sealed by clear strips and placed in a thermocycler (Chromo4, BioRad). The fluorescence intensities were monitored at every 0.5  $^{\circ}\text{C}$  increment during melting from 25  $^{\circ}\text{C}$  to 95  $^{\circ}\text{C}$ . The data were exported into Excel and were subject to proprietary custom curve fitting algorithm (unpublished) to derive temperature-dependent fluorescence (TdF)  $K_{\text{d}}$  values. For CHK1 TdF data, a two-state binding model (compound binding to both the native and thermally unfolded molten globule state) is routinely used. Compound binding to the molten globule state of the target kinase is usually over 1,000-fold weaker than to the native state. All TdF  $K_{\text{d}}$  values have an error margin of  $\sim 50\%$  due to uncertainty with the enthalpy change of binding.

#### ***$\gamma$ -H2AX assay***

Briefly, cells were exposed to an antimetabolite to induce the activation of CHK1. Control populations were left untreated. SCH 900776 was then titrated onto cells over a 2-hour exposure window (in the presence of the antimetabolite). Following the 2-hour coexposure to SCH 900776, cells were fixed and permeabilized (70% ethanol) before staining with a fluorescein isothiocyanate (FITC)-conjugated anti- $\gamma$ -H2AX monoclonal antibody (cell signaling). Cells were counterstained with propidium iodide and subsequently analyzed using flow cytometry (Becton Dickinson LSR II) or the Discovery 1 immunofluorescence platform (Molecular Devices). Experiments were typically done in triplicate and data are presented as the percentage of  $\gamma$ -H2AX positive cells, and thus reflect the overall penetrance of the  $\gamma$ -H2AX phenotype.

#### ***Induction of apoptosis assessed by active caspase***

Assays of caspase activation were done using the Beckman Coulter CellProbe HT Caspase 3/7 Whole Cell Assay system. Briefly, cells were exposed to an antimetabolite (hydroxyurea) overnight and then differing concentrations of SCH 900776 over a 2-hour exposure window. Cells were then washed to remove all antimetabolite and SCH 900776. Caspase activity was assessed at this point ( $T_0$ , or release) and further assays were done at  $T + 24$  and  $T + 48$  hours. Cells were subsequently incubated

with a fluorescently labeled caspase substrate (CellProbe); uptake and fluorescence of the substrate within cells correlate with the level of activated caspases. The percentage of cells expressing activated caspases was then determined by flow cytometry.

#### ***Bromodeoxyuridine incorporation assay***

Cells were plated into 10 cm tissue culture dishes and allowed to adhere. Cells were exposed over 2 hours to differing concentrations of SCH 900776 either with, or without, prior antimetabolite exposure. Cells were then washed and allowed to attempt resumption of S-phase for 24 hours. This was followed by a brief (30 minute) exposure to bromodeoxyuridine (BrdU) to assess the percentage of cells that were capable of re-entering the cell cycle in a viable manner. Cells were then harvested, fixed, and permeabilized. This was followed by an acid denaturation step to expose incorporated BrdU epitopes within the genomic DNA, after which samples were immunostained with a FITC-conjugated monoclonal antibody specific for BrdU (BD Biosciences). Cells were then counterstained with propidium iodide to allow assessment of DNA content and analyzed using flow cytometry. Bivariate analysis of positive BrdU staining and propidium iodide signal allowed assessment of the number of cells undergoing DNA synthesis and the overall cell cycle distribution of the cell line ( $G_1$ , S,  $G_2$ -M, and sub- $G_1$ ). Percentages of each population at each concentration of the test article were plotted.

#### ***Experimental animals***

Strains used were typically 6- to 8-week old, female nude mice, Sprague-Dawley rats and beagle dogs. Animals were housed in an Association Assessment and Accreditation of Laboratory Animal Care accredited animal facilities (Merck Research Laboratories; Xenometrics). All protocols using animals were approved by the relevant Institutional Animal Care and Use Committee.

#### ***In vivo tumor growth assessments, sampling, and skin biopsies***

For tumor implantation, specific cell lines were grown *in vitro*, washed once with PBS and resuspended in 50% Matrigel (BD Biosciences) in PBS to a final concentration of  $4 \times 10^7$  to  $5 \times 10^7$  cells per mL. Nude mice were injected with 0.1 mL of this suspension subcutaneously in the flank region. Tumor length ( $L$ ), width ( $W$ ), and height ( $H$ ) were measured by a caliper twice a week on each mouse and then used to calculate tumor volume using the formula:  $(L \times W \times H)/2$ . Animals ( $N = 10$ ) were randomized to treatment groups and treated intraperitoneally with either SCH 900776 (formulated in 20% hydroxypropyl  $\beta$ -cyclodextrin) or individual chemotherapeutic agents, formulated as recommended. Tumor volumes and body weights were measured during and after the treatment

periods. Data were recorded as means  $\pm$  SEM before being normalized to starting volume. Time to progression to 10x starting volume (TTP 10x) was monitored in some experiments. Animals were euthanized according to Institutional Animal Care and Use Committee guidelines. For pharmacodynamic marker analyses in mice, tumors and adjacent skin were collected at necropsy, fixed overnight in 10% formalin, and washed/stored in 70% ethanol. For skin punch biopsies, an area of approximately 4 square inches was shaved. Rats were anesthetized using inhaled isoflurane and dogs were locally anesthetized using subcutaneous administration of lidocaine. Samples were collected using a 4 mm biopsy punch. Skin punches were fixed in 10% formalin overnight before washing/storage in 70% ethanol.

### ***Immunohistochemistry***

Fixed samples were processed in a tissue processor (Thermo Electronic Co.). Tissues were dehydrated in graded ethanol solutions, cleared in 3 changes of xylene, and penetrated in heated paraffin (at 56 °C–58 °C). The tissues were embedded in paraffin, cut into 4- to 6- $\mu$ m sections, and placed onto slides. Before staining, deparaffinization and rehydration was done in a Leica autostainer (65 °C, 20'; xylene 5', x3; 100% ethanol 1', x3; 95% ethanol 1', x2; 70% ethanol 1'; distilled water, 5'). Antigen retrieval was done via pressure cooker. Slides were incubated in 1x target retrieval solution (Dako) at 120°C for 4 minutes at 18 to 20 psi. The pressure cooker was returned to 0 PSI and 89°C before opening. Slides were then rinsed in water and PBS (5' each). Slides were stained using polymer detection (Envision, Dako) on a Dako automated immunostainer. Endogenous hydrogen peroxidase activity was blocked with hydrogen peroxide for 10 minutes followed by rinsing with wash buffer (Dako). Slides were incubated with antibodies (e.g.,  $\gamma$ -H2AX clone 20E3 and CHK1 pS345 clone 133D3; cell signaling) diluted 1:250 in wash buffer for 60'. Alternatively, slides were incubated with appropriate isotype controls, diluted similarly. Slides were washed and incubated with anti-rabbit horseradish peroxidase polymer for 30', followed by a further wash. Slides were developed using 3,3'-diaminobenzidine (DAB)<sup>+</sup> chromogen (Dako) for 10' and washed with water. After staining, slides were counterstained, dehydrated, and cleared using a Leica autostainer (Dako hematoxylin, 5'; distilled water, 1'; Richard Allen Blueing Reagent, 1'; distilled water, 1'; 95% ethanol, 1' x1' 100% ethanol, 1' x2; xylene, 1' x3). Finally, slides were cover-slipped with mounting reagent (Permount, Fisher).

### ***Peripheral hematological parameters***

Blood samples were obtained from mice, diluted 1 to 5 in PBS, and immediately analyzed on an Advia 120 hematology analyzer. A full differential blood count was done, in particular red blood cell

analysis (including reticulocyte, variant count, and hemoglobin analyses), white blood cell analysis (including differential lineage counts and peroxidase staining), and a thrombopoiesis analysis.

### ***Pharmacokinetic determinations***

Plasma samples from test species were collected at various times after administration of SCH 900776. At each time-point, blood samples from 3 animals were combined and analyzed for SCH 900776 by LC/MS. Pharmacokinetic variables were estimated from the plasma concentration data.  $C_{max}$  values (maximum plasma concentration) were taken directly from the plasma concentration-time profiles, and the area under the plasma concentration versus time curve area under curve (AUC) was calculated using the linear trapezoidal rule.<sup>21</sup>

## **Results**

### ***Contributions of CHK1, CHK2, and CDKs to replication checkpoint override phenotypes***

Exposure to hydroxyurea induced activation of CHK1 in U2OS cells and depletion of CHK1 in this context led to accumulation of  $\gamma$ -H2AX signal in ~62% of the cell culture population (refs. 5; Table 1 and Supplementary Fig. S1A and B). In contrast, depletion of CHK2 did not significantly enhance the hydroxyurea phenotype and combinatorial depletion of CHK1 and CHK2 was not beneficial, appearing inferior to single CHK1 ablation (Table 1). This led to an examination of other possible antagonistic mechanisms, in particular the CDKs. A consequence of checkpoint activation is suppression of downstream CDK activity.<sup>8,9,22</sup> Therefore, inhibition of CDK function might antagonize CHK1 ablation/inhibition phenotypes. Indeed, codepletion of CDK2 or CDK1 with CHK1 suppressed  $\gamma$ -H2AX signals and combined ablation of CDK2 and CDK1 further exacerbated suppression (Table 1). Knockdowns in each case were confirmed by Western blotting (data not shown). Additionally, simultaneous addition of SCH 727965 (a potent CDK inhibitor; refs. 15, 20) during hydroxyurea exposure also suppressed accumulation of  $\gamma$ -H2AX, in a dose-dependent manner (Table 1). Representative fluorescence-activated cell sorter plots stemming from these experiments are shown in Supplementary Fig. S1C to E. Taken together, these data suggested a requirement for sufficient CHK1 versus CDK selectivity, whilst the CHK2 observations implied the existence of additional antagonistic pathways. Global counter screening for kinase cross-reactivity is impractical and the degree of selectivity required in each case is inherently unpredictable. To circumvent this, we devised a high content/high throughput, single-cell assay to track anticipated mechanism-based effects following override of the hydroxyurea-mediated replication checkpoint.

**Table 1.** Contributions of CHK1, CHK2, and the CDKs to replication checkpoint control assessed using siRNAs directed against CHK1, CHK2, CDK1, and CDK2 or pharmacological inhibition of the CDKs using SCH 727965.

**Table 1.** Comparison between SCH 727965 and flavopiridol: inhibition of CDKs, dThd incorporation, and activity in a mouse tumor xenograft

Compound	IC <sub>50</sub> (nmol/L)					MTD* MED <sup>†</sup>		(MTD/MED) <sup>‡</sup>
	CDK2	CDK5	CDK1	CDK9	dThd incorporation	(mg/kg)		
SCH 727965	1	1	3	4	4	60	5	>10
Flavopiridol	12	14	3	4	70	<10	10	<1

\*MTD: 20% weight loss.  
<sup>†</sup>MED: >50% inhibition of tumor growth (both administered i.p. once daily for 7 d).  
<sup>‡</sup>Screening therapeutic index.

### **SAR trends and selection of SCH 900776 using the Discovery 1 $\gamma$ -H2AX assay**

Pyrazolo[1,5-*a*]pyrimidines have been established as a viable core for the development of potent and selective CDK inhibitors.<sup>14, 19, 20, 23</sup> Through a focused medicinal chemistry effort, substitution patterns were identified that showed improved CHK1 inhibition *in vitro*.<sup>16, 17</sup> To calibrate this *in vitro* activity and determine if this series was able to reveal the desired mechanism-based effects, the  $\gamma$ -H2AX fluorescence-activated cell sorter based assay was adapted for quantitative, high throughput immunofluorescence (Fig. 1A). A functionally selective CHK1 inhibitor would not be expected to suppress  $\gamma$ -H2AX accumulation at higher concentrations. In agreement with the hypothesis that individual compounds have varying degrees of on-target and off-target (antagonistic) properties, bell-shaped responses were observed within this series of compounds (Fig. 1). Ultimately, SCH 900776 (Fig. 1G) was identified as a candidate for additional evaluation.

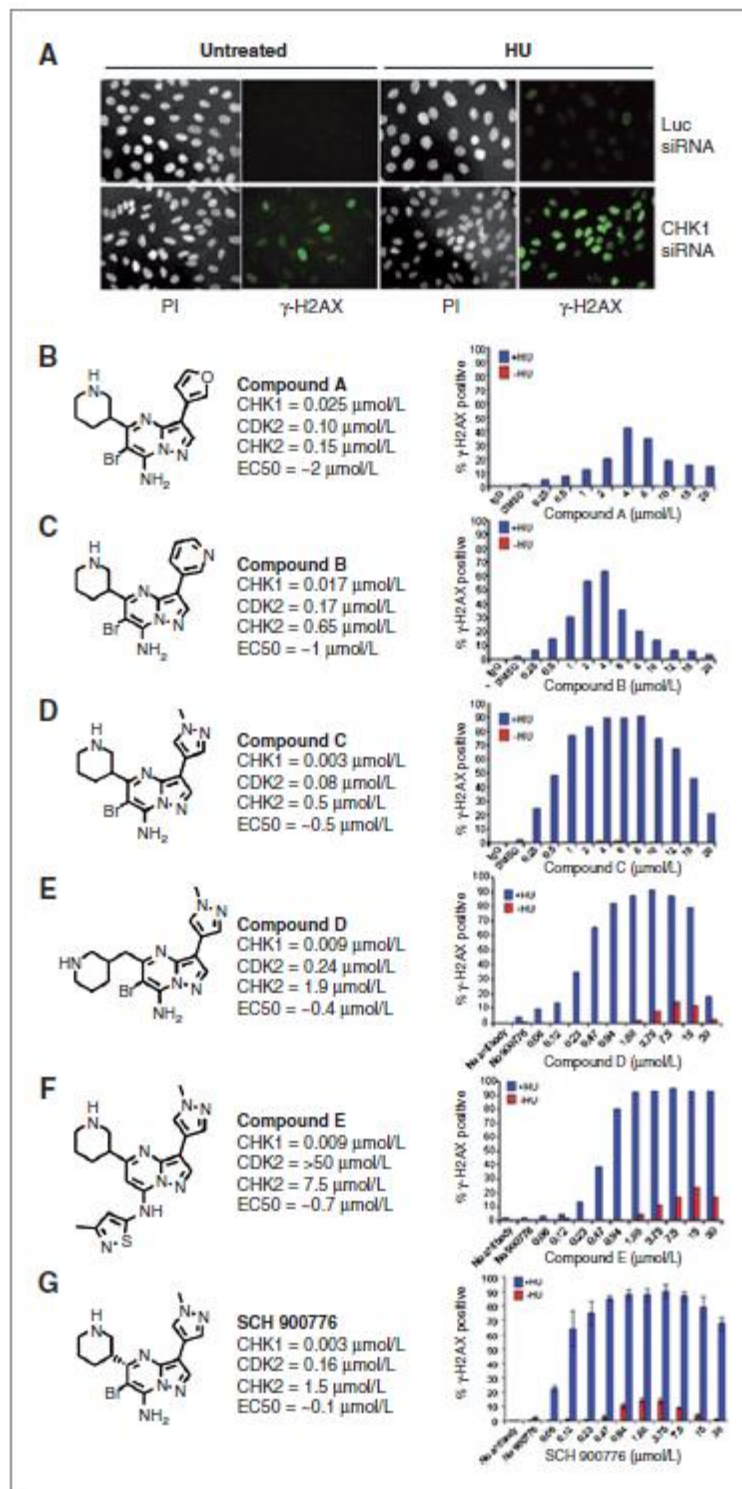


**Figure 1.**

Discovery 1  $\gamma$ -H2AX assay and structure-activity-relationships within the pyrazolopyrimidine lead series. A, Discovery 1 immunofluorescence images of U2OS cells stained with PI and  $\gamma$ -H2AX following transfection

with luciferase or CHK1 siRNAs and hydroxyurea exposure, as indicated. HU, hydroxyurea. B–G, structures of compounds A, B, C, D, E, and SCH 900776 with respective CHK1, CHK2, CDK2 kinase IC<sub>50</sub>s, and Discovery 1  $\gamma$ -H2AX EC<sub>50</sub>s. Graphical representations of the Discovery 1 titration profiles, assessed in the presence or absence of hydroxyurea (blue and red bars, respectively), are shown on the right of each compound. HU, hydroxyurea.

SCH 900776 (Fig. 1G) is a potent and functionally selective inhibitor of CHK1. In direct binding studies, the K<sub>d</sub> (TdF methodology) of SCH 900776 for the CHK1 kinase domain was determined to be 2 nmol/L, in agreement with the enzymatically determined IC<sub>50</sub>. SCH 900776 is not a potent inhibitor of CHK2 and is a weak inhibitor of CDK2 (Fig. 1F). The overall kinase selectivity profile of SCH 900776 was further characterized via the Millipore Kinase Profiling service (Supplementary Table S1). SCH 900776 is not highly protein bound (Supplementary Table S2) and showed no significant inhibition of cytochrome P450 human liver microsomal isoforms 1A2, 2C9, 2C19, 2D6, and 3A4 (Supplementary Table S3). The solubility of SCH 900776 in buffers representing the physiologically acceptable pH range indicates suitability for aqueous based formulation (Supplementary Table S4).

### ***In-cell profile of SCH 900776***

Checkpoint override phenotypes following hydroxyurea exposure were confirmed using  $\gamma$ -H2AX staining and flow cytometry. SCH 900776 exhibits an approximate EC<sub>50</sub> of 60 nmol/L under these conditions, in good agreement with those obtained via Discovery 1 (Fig. 2A). Next, to assess potential off-target activities in a functional manner, BrdU incorporation following SCH 900776 exposure was measured. CHK1 siRNA treatment does not suppress entry into DNA synthesis (Supplementary Fig. 2A). In agreement, treatment of U2OS cells with increasing concentrations of SCH 900776 did not decrease BrdU incorporation (Supplementary Fig. 2B).

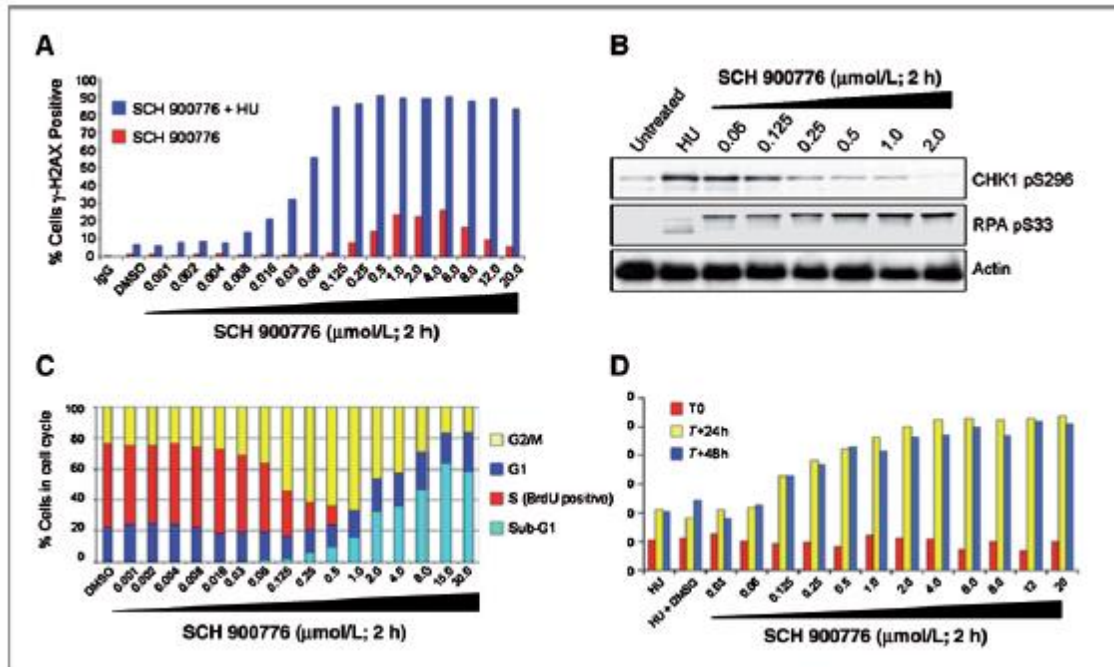


**Figure 2.**

In-cell activities of SCH 900776. A, confirmation of SCH 900776  $\gamma$ -H2AX profile using flow cytometry in the presence and absence of hydroxyurea (blue and red bars, as indicated). B, SCH 900776 rapidly suppresses accumulation of the CHK1 p296 auto-phosphorylation epitope (top) with concomitant accumulation of DNA damage (RPA pS33; center). C, short-term exposure to SCH 900776 following hydroxyurea treatment induces long-term loss of BrdU incorporation capacity (red bars) and leads to accumulation of cells with a sub-G<sub>1</sub> DNA content (light blue bars). D, short-term exposure to SCH 900776 following hydroxyurea treatment induces caspase activation. U2OS cells were exposed to hydroxyurea overnight and then to increasing concentrations of SCH 900776 for 2 hours. Cells were harvested immediately (T0; red bars) or cultured for an additional 24 or 48 hours in drug-free medium before being assayed for activated caspases (T24 and T48; yellow and blue bars, respectively). HU, hydroxyurea.

Serine 296 of CHK1 has been proposed as a site of CHK1 autophosphorylation.<sup>13, 24, 25</sup> Following exposure to hydroxyurea, U2OS cells accumulate CHK1 pS296, and 2 hour exposures to SCH 900776 induced dose-dependent suppression of CHK1 pS296 and concomitant accumulation of phospho-RPA signal (Fig. 2B), suggestive of DNA damage.

Cells lacking CHK1 following siRNA treatment cannot efficiently resume DNA synthesis. Rather, these cells accumulate double-strand DNA breaks and undergo cell death.<sup>5</sup> SCH 900776 induced a

dose-dependent loss of DNA replication capability 24 hours after hydroxyurea exposure (Fig. 2C, red bars). An increase in the sub-G<sub>1</sub> population was also observed, suggestive of cell death within the culture (Fig. 2C, light blue bars). In agreement, SCH 900776 exposure enhanced apoptosis for at least 48 hours following release from hydroxyurea blockade (Fig. 2D). These data are consistent with the observed increase in the sub-G<sub>1</sub> populations and are suggestive of cell death within the culture.

### ***In vivo modeling of SCH 900776: gemcitabine combinations***

CHK1 ablation can phenotypically enhance hydroxyurea, 5-fluoruracil, and cytarabine  $\gamma$ -H2AX profiles.<sup>5, 26</sup> To extend these observations pharmacologically, SCH 900776 was used in combination with a range of diverse agents. SCH 900776 enhanced the  $\gamma$ -H2AX response of all the agents tested (Supplementary Fig. S3A-I). Strong combination responses were observed following exposure to nucleoside DNA antimetabolites and antifolates. Gemcitabine (like hydroxyurea) is an inhibitor of ribonucleotide reductase (27) that activates CHK1 (Supplementary Fig. S4A), and was selected as the partner chemotherapy during *in vivo* modeling of SCH 900776 activities.

To confirm activation of CHK1 *in vivo*, gemcitabine (25, 75, and 150 mg/kg) was used in the A2780 xenograft model. Immunohistochemical staining revealed dose-dependent activation of the CHK1 pS345 marker within 2 hours (Supplementary Fig. S4B to E). The threshold dose of SCH 900776 associated with intratumoral induction of  $\gamma$ -H2AX was then determined in established A2780 xenografts (~250 mm<sup>3</sup>), in combination with 150 mg/kg gemcitabine. SCH 900776 was administered 30 minutes after gemcitabine. Animals were scheduled to receive 3 cycles of treatment on an every fifth day regimen before cessation of dosing and monitoring of regression response. Satellite animals were sacrificed 2 hours after the first dosing cycle for  $\gamma$ -H2AX marker analyses. Thus, 4 mg/kg SCH 900776 was sufficient to induce the  $\gamma$ -H2AX biomarker (Fig. 3D) while 8 mg/kg led to enhanced tumor pharmacodynamic and regression responses relative to gemcitabine or SCH 900776 alone (Fig. 3E and H). Dose escalation of SCH 900776 (16 and 32 mg/kg) induced incremental improvements in tumor response (Fig. 3F to H). The approximate  $C_{max}$  plasma concentration in mice following IP administration of 10 mg/kg SCH 900776 was ~0.6  $\mu$ mol/L and the plasma AUC was ~0.9  $\mu$ mol/L.h (Supplementary Table S5). Therefore, rapid and pronounced modulation of the CHK1 mechanism *in vivo* is associated with low doses and exposures of SCH 900776.

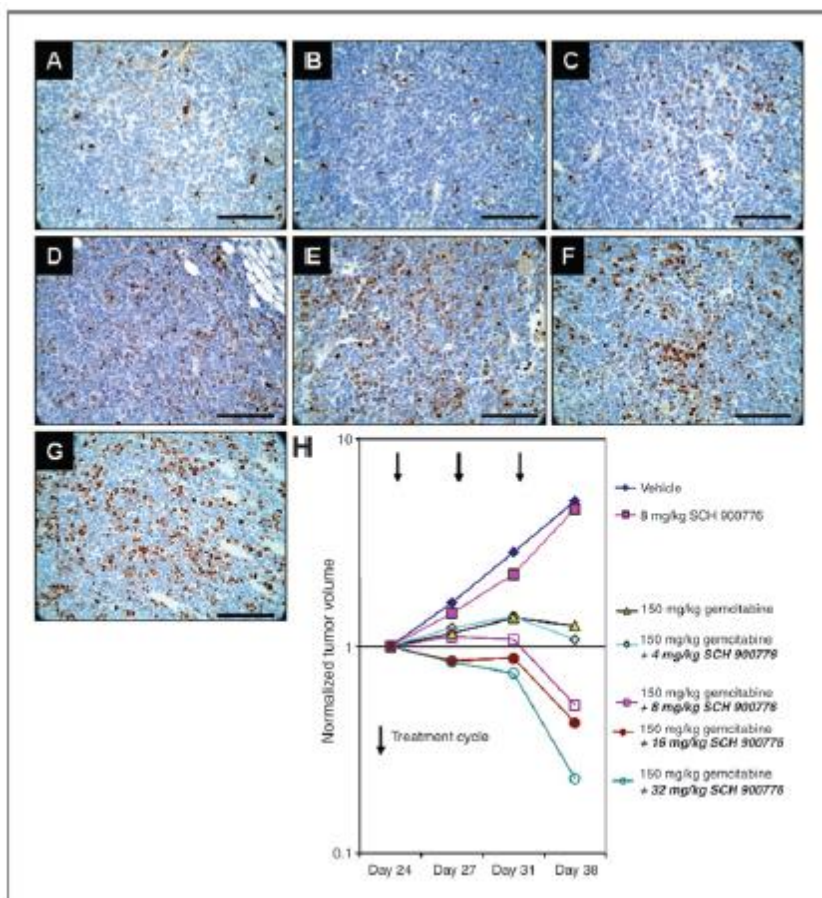


**Figure 3.**

Active dose threshold of SCH 900776 in combination with gemcitabine (A2780). Representative images from tumor sections stained for  $\gamma$ -H2AX 2 hours after dosing. A, vehicle. B, 8 mg/kg SCH 900776. C, 150 mg/kg gemcitabine. D, 150 mg/kg gemcitabine with 4 mg/kg SCH 900776. E, 150 mg/kg gemcitabine with 8 mg/kg SCH 900776. F, 150 mg/kg gemcitabine with 16 mg/kg SCH 900776. G, 150 mg/kg gemcitabine with 32 mg/kg SCH 900776. Scale bars represent 100  $\mu$ m. H, tumor regression responses after 3 cycles of treatment (dose groups as indicated).

To test the hypothesis that SCH 900776 effects *in vivo* are also dependent on the dose of CHK1-activating partner chemotherapy, 25, 75, and 150 mg/kg doses of gemcitabine were combined with a fixed dose of SCH 900776 (50 mg/kg). A2780 xenografts were staged at  $\sim 50$  mm<sup>3</sup>. Mice were given two cycles of treatment, with pharmacodynamic sampling done 2 hours after the first cycle. Exposure to single agent SCH 900776 or gemcitabine induced minor  $\gamma$ -H2AX responses (Supplementary Fig. S5B and C). In contrast, combination of 50 mg/kg SCH 900776 with 25, 75, or 150 mg/kg gemcitabine was sufficient to enhance the  $\gamma$ -H2AX staining pattern at 2 hours post dose

(Supplementary Fig. S5D to F). Mice were given a second and final cycle of treatment 3 days later and TTP 10x was monitored (Supplementary Fig. S5G). Improvements in progression kinetics driven by SCH 900776 were clearly dependent on the dose of gemcitabine and likely reflect the overall penetrance of the initial CHK1 activation within these xenografts.

MiaPaca2 is a slow growing pancreatic xenograft that progresses during gemcitabine treatment, implying a degree of resistance to the cytotoxic effects of this agent.<sup>28</sup> However, gemcitabine can suppress BrdU incorporation in MiaPaCa2 cells (Supplementary Fig. S6A). Furthermore, combination with SCH 900776 induces  $\gamma$ -H2AX in MiaPaCa2 cells at concentrations of gemcitabine associated with suppression of BrdU incorporation (Supplementary Fig. S6B), consistent with an active replication checkpoint. Gemcitabine (150 mg/kg) was administered to staged ( $\sim 50$  mm<sup>3</sup>) MiaPaCa2 tumors followed by escalating doses of SCH 900776 (8, 20, and 50 mg/kg). Satellite animals were again used for pharmacodynamic marker analyses following the first cycle of dosing and TTP 10x was followed after 4 cycles of dosing. Gemcitabine retains activity in MiaPaCa2, as CHK1 pS345 was readily detectable within 2 hours of dosing (Supplementary Fig. S7B). SCH 900776 or gemcitabine dosed as monotherapy induced minimal  $\gamma$ -H2AX signal as a monotherapy in MiaPaCa2 tumors. However, administration of 8, 20, or 50 mg/kg SCH 900776 to animals previously dosed with gemcitabine augmented the  $\gamma$ -H2AX response (Supplementary Fig. S7D to H). TTP 10x was then tracked in each dose cohort. Single agent SCH 900776 (50 mg/kg) was nonefficacious on this schedule. Administration of gemcitabine or the combination of 150 mg/kg of gemcitabine with 8 mg/kg SCH 900776 both induced a similar TTP 10x benefit of  $\sim 9$  days. Escalation of SCH 900776 dose to 20 and 50 mg/kg in combination with gemcitabine led to improvements in TTP 10x (Supplementary Fig. S7I). Summaries of the preclinical xenograft modeling are provided in Table 2 and Supplementary Tables S6 to 8.

**Table 2.** Summary of *in vivo* studies utilizing SCH 900776 and gemcitabine in the A2780 and MiaPaCa2 xenograft systems.

Study	Dose and schedule	$\gamma$ -H2AX, IHC, +/- (after first dose)	Best response (after last dose)	% Starting volume (after last dose)	TTP 10x (after first dose; days)
A2780 Ovarian xenograft (>250 mm <sup>3</sup> ) Fixed dose: gemcitabine; Titrated dose: SCH 900776					
	20% HP $\beta$ CD q5dx3	(-)	P	503	N/D
	50 mg/kg SCH 900776 q5dx3	(-/+)	P	466	N/D
	150 mg/kg gemcitabine q5dx3	(-)	SD	102	N/D
	150 mg/kg gemcitabine q5dx3 + 4 mg/kg SCH 900776	(+)	SD	107	N/D
	150 mg/kg gemcitabine q5dx3 + 8 mg/kg SCH 900776	(+)	R	52	N/D
	150 mg/kg gemcitabine q5dx3 + 16 mg/kg SCH 900776	(+)	R	41	N/D
	150 mg/kg gemcitabine q5dx3 + 32 mg/kg SCH 900776	(+)	R	23	N/D
A2780 ovarian xenograft (~50 mm <sup>3</sup> ) Fixed dose: SCH 900776; Titrated dose: gemcitabine					
	20% HP $\beta$ CD q3dx2	(-)	P	580	10
	50 mg/kg SCH 900776 q3dx2	(-/+)	P	425	10
	150 mg/kg gemcitabine q3dx2	(-/+)	P	188	17
	25 mg/kg gemcitabine + 50 mg/kg SCH 900776 q3dx2	(+)	P/SD	138	17
	75 mg/kg gemcitabine + 50 mg/kg SCH 900776 q3dx2	(+)	SD/R	97	27
	150 mg/kg gemcitabine + 50 mg/kg SCH 900776 q3dx2	(+)	R	71	>34
MiaPaCa2 pancreatic xenograft (~50 mm <sup>3</sup> ) Fixed dose: gemcitabine; Titrated dose: SCH 900776					
	20% HP $\beta$ CD q3dx4	(-)	P	457	40
	50 mg/kg SCH 900776 q3dx4	(-/+)	P	352	40
	150 mg/kg gemcitabine q3dx4	(-)	P	217	50
	150 mg/kg gemcitabine q3dx4 + 8 mg/kg SCH 900776	(-/+)	P	151	50
	150 mg/kg gemcitabine q3dx4 + 20 mg/kg SCH 900776	(+)	P/SD	138	57
	150 mg/kg gemcitabine q3dx4 + 50 mg/kg SCH 900776	(+)	P/SD	133	71

Abbreviations: q5dx3, every fifth day for 3 cycles; q3dx2, every third day for 2 cycles; q3dx4, every third day for 4 cycles; P, progressive disease; SD, stable disease; R, regression; N/D, not determined.

### ***Replication checkpoint override phenotypes in nontransformed cells***

SCH 900776 in combination with hydroxyurea did not lead to a dramatic increase in  $\gamma$ -H2AX signal in WS1 diploid fibroblasts (ref. 5; Supplementary Fig. S8), consistent with earlier data using CHK1 siRNA. Furthermore, in a survey of several diverse hematological parameters in BALB/c mice (neutrophils, lymphocytes, red blood cells, and platelets), SCH 900776 did not exacerbate the myelosuppressive effects of gemcitabine (Table 3). Three days post dosing, gemcitabine (400 mg/kg;

1200 mg/m<sup>2</sup>) rapidly induced nadirs in total white cell, absolute neutrophil, and absolute lymphocyte counts. Counts typically rebounded to within the normal range over 7 days and consistently attained control levels by day 14. Administration of SCH 900776 to animals previously exposed to gemcitabine did not adversely alter the severity of the nadirs or subsequent rebound kinetics. Platelet and red blood cell counts were not significantly affected by any dose level of gemcitabine, SCH 900776, or the combination. In summary, combination of gemcitabine at clinically relevant levels with active doses of SCH 900776 was not associated with synergistic myelosuppression in BALB/c mice.

**Table 3.** Effects of SCH 900776, gemcitabine, and the combination on hematological parameters in BALB/c mice.

Treatment and parameter	Day 0	Day 3	Day 7	Day 14
<b>No treatment</b>				
Absolute neutrophils, cells/mm <sup>3</sup>	1238 <sup>a</sup> (765)	1080 (706)	580 (390)	640 (301)
Absolute lymphocytes, cells/mm <sup>3</sup>	8950 <sup>a</sup> (2641)	7110 (1540)	5920 (1608)	6540 (2395)
RBC, x10 <sup>6</sup> /mm <sup>3</sup>	10.33 <sup>a</sup> (1.79)	8.46 (2.62)	9.35 (1.58)	9.94 (1.21)
Platelets, per μL	871 <sup>a</sup> (382)	1361 (439)	1140 (442)	1449 (211)
<b>50 mg/kg SCH 900776, i.p. (~150 mg/m<sup>2</sup>)</b>				
Absolute neutrophils, cells/mm <sup>3</sup>	370 (44)	450 (200)	528 (380)	700 (462)
Absolute lymphocytes, cells/mm <sup>3</sup>	8710 (2323)	6550 (1980)	5520 (1148)	6760 (700)
RBC, x10 <sup>6</sup> /mm <sup>3</sup>	9.95 (2.01)	7.93 (0.79)	10.07 (1.14)	10.70 (0.29)
Platelets, per μL	1234 (226)	1045 (388)	1481 (387)	1670 (143)
<b>400 mg/kg gemcitabine, i.p. (~1200 mg/m<sup>2</sup>)</b>				
Absolute neutrophils, cells/mm <sup>3</sup>	670 (470)	80 (44)	980 (513)	660 (399)
Absolute lymphocytes, cells/mm <sup>3</sup>	8410 (1731)	2780 (514)	4380 (660)	6600 (1082)
RBC, x10 <sup>6</sup> /mm <sup>3</sup>	10.74 (0.40)	8.75 (1.13)	9.14 (0.36)	10.57 (0.34)
Platelets, per μL	1202 (226)	1180 (130)	1849 (119)	1425 (185)
<b>400 mg/kg gemcitabine, i.p. + 50 mg/kg SCH 900776, i.p. (~1200 mg/m<sup>2</sup> + ~150 mg/m<sup>2</sup>)</b>				
Absolute neutrophils, cells/mm <sup>3</sup>	1020 (859)	170 (57)	884 (337)	610 (479)
Absolute lymphocytes, cells/mm <sup>3</sup>	7450 (2292)	3460 (502)	5162 (1368)	6450 (2066)
RBC, x10 <sup>6</sup> /mm <sup>3</sup>	10.18 (1.21)	9.11 (0.45)	9.85 (0.92)	9.35 (2.63)
Platelets, per μL	1190 (334)	997 (195)	1254 (662)	1237 (522)

NOTE: Animals (N = 5, unless otherwise indicated) were administered treatments as indicated on day 0. Day 0 values represent the predose (baseline) status for each parameter. To track nadirs/rebounds of sensitive parameters, complete blood cell counts were done on day 3, day 7, and day 14 following each treatment. Values in parentheses denote SD.

<sup>a</sup>N = 4.

### *In vivo assessment of SCH 900776 active dose range skin biopsies in toxicology species*

During clinical trials, it will be important to demonstrate active doses of SCH 900776 can be safely attained in combination with partner chemotherapy. A biomarker strategy that indicates engagement

of CHK1 is therefore critical. CHK1 is an essential kinase and exposure to CHK1 siRNA or SCH 900776 as monotherapy induces intra-S phase DNA damage (ref. 5; Supplementary Fig. S9A and B). Hence, DNA damage biomarkers (e.g.,  $\gamma$ -H2AX and CHK1 pS345) may be useful readouts for SCH 900776-driven target engagement.<sup>29</sup> Indeed, SCH 900776 induces dose-dependent accumulation of CHK1 pS345 in proliferating WS1 cells (Supplementary Fig. S9C). Furthermore, CHK1 pS345 positive cells were detected in skin punch biopsies taken from mice at SCH 900776 doses  $\leq 25$  mg/kg (75 mg/m<sup>2</sup>), in rats dosed IV at 5 and 10 mg/kg (30 and 60 mg/m<sup>2</sup>) and from dogs dosed IV at 2.5 and 5 mg/kg (45 and 89 mg/m<sup>2</sup>; Supplementary Fig. S10A to C). These data and the associated plasma exposures are summarized in Table 4 and comprise a pharmacological audit trail (30) of SCH 900776 activity in three relevant preclinical species.

**Table 4.** Dose, pharmacodynamic, pharmacokinetic, and tolerability relationships of SCH 900776 in mouse, rat, and dog.

Species tested	Dose in mg/m <sup>2</sup> (route, schedule)	Xenograft profile in combination with gemcitabine (A2780) ( $\gamma$ -H2AX IHC, +/-; tumor response)	$\sim C_{max}$ , $\mu$ mol/L	$\sim AUC$ , $\mu$ mol/L.h	Skin Bx pharmacodynamic profile as monotherapy (CHK1 pS345 IHC, +/-)	DLT
Mouse	12 IP, bolus	+ <i>stable disease</i>	ND	ND	-	None
	24 IP, bolus	+ <i>regression</i>	ND	ND	-	None
	30 IP, bolus	+ <i>regression</i>	0.6	0.9	-	None
	75 IP, bolus	+ <i>regression</i>	3.6	ND	+	None
Rat	15 IV, 2 min	NA	0.1	0.3	-	None
	30 IV, 2 min	NA	0.5	1.5	+	None
	60 IV, 2 min	NA	2.9	5.4	+	None
Dog	18 IV, 15 min	NA	0.9	2.4	-	None
	45 IV, 15 min	NA	2.8	6.4	+	None
	89 IV, 15 min	NA	4.7	15.8	+	None

Abbreviations: DLT, dose limiting toxicity; NA, not applicable; ND, no data.

## Discussion

CHK1 preserves tumor cell viability by suppressing the catastrophic accumulation of DNA damage that would ensue following replication fork collapse.<sup>4-6,31,32</sup> This is in contrast to the role of CHK1 in the DNA damage checkpoint, wherein CHK1 is activated in response to pre-existing DNA lesions.<sup>33</sup> Hence, dramatic accumulation of DNA damage is predicted to be a signature phenotype of CHK1 inhibition during replication checkpoint override. SCH 900776 is a potent and functionally selective CHK1 inhibitor currently in clinical development. This molecule was identified using a mechanism-of-action related biomarker ( $\gamma$ -H2AX) in a functional screen that was highly discriminatory. Moreover, this assay allowed a functional assessment of the CHK1 pathway and other, potentially antagonistic, mechanisms. Thus, via a combination of siRNA and medicinal chemistry approaches, the relative contributions of CHK1, CHK2, and CDKs to the replication checkpoint were assessed. These experiments revealed absolute antagonism following CDK inhibition and suggested CHK2 inhibition to be neither necessary nor desirable. Intriguingly, the functional approach highlighted a dilemma often faced during the discovery of targeted kinase inhibitors. Prospective reliance on comprehensive *in vitro* kinase counter screening may not have identified a CHK1 inhibitor with the mechanism-based characteristics exhibited by SCH 900776. In contrast, the high content functional approach identified molecules with the necessary selectivity characteristics against all kinases (more accurately, those expressed within the screening cell line), as well as other potential nonkinase antagonistic mechanisms; *in vitro* kinase selectivity was then determined *post hoc*. Taken together, it is clear CHK1 selectivity is an important component in clinical compounds targeting this mechanism. SCH 900776 is also of low molecular weight (<300 Da), is not highly protein bound (~50% protein bound in human plasma), is highly soluble in aqueous buffers at neutral pH, and does not significantly inhibit a diverse range of P450 enzymes. In summary, SCH 900776 is a drug-like compound with the key characteristics required for replication checkpoint override.

SCH 900776 recapitulates the key replication checkpoint override phenotypes described following CHK1 ablation with siRNA. Thus, in combination with an antimetabolite, SCH 900776 induces accumulation of  $\gamma$ -H2AX within 2 hours, indicative of replication fork collapse and double stranded DNA breaks. Additionally, SCH 900776 suppressed accumulation of the CHK1 pS296 autophosphorylation epitope in a dose-dependent manner, once more within a 2 hour exposure window. The rapid onset of these phenotypes was intimately linked to a long-term loss of DNA synthetic capacity and cytotoxicity, suggesting little need for continual exposure when used in combination. This was confirmed in a series of *in vivo* studies wherein SCH 900776 activity appeared correlated with the penetrance of CHK1 activation driven by gemcitabine. Moreover, intermittent

schedules, low doses, and low exposures of SCH 900776 were associated with modulation of mechanism-based biomarkers and enhancement of gemcitabine response. Importantly, similar biomarker activation and enhancement of gemcitabine response were observed in gemcitabine sensitive (A2780) and gemcitabine refractory (MiaPaCa2) models. The scheduling strategy used was designed to target the replication checkpoint. Thus, SCH 900776 was administered within 30 minutes of gemcitabine during the window of CHK1 activation induced by replication fork stalling. This is in contrast to checkpoint inhibition strategies that target the role of CHK1 at the G<sub>2</sub>-M DNA damage checkpoint in p53 mutant tumor cells. In this setting, delayed administration of the CHK1 inhibitor is necessary to allow accumulation of cells at the G<sub>2</sub>-M boundary.<sup>34-36</sup> Targeting the replication checkpoint represents a mechanistically distinct approach to CHK1 inhibition. Moreover, this strategy offers several advantages; notably lack of dependence on p53 status<sup>5</sup> and, importantly, patient convenience.

Target organs of DNA antimetabolites include the blood and immune systems. These effects are generally reversible, clinically manageable mechanism-based toxicities. Importantly, doses of SCH 900776 associated with robust biomarker activation and improved tumor response were not associated with enhanced toxicity of gemcitabine on hematological parameters in BALB/c mice. These data (and those derived *in vitro* using WS1 cells) imply an interesting difference between SCH 900776 responses in normal and transformed backgrounds, in the context of partner chemotherapy combinations.

Interestingly, exposure of proliferating WS1 cells to SCH 900776 as a single agent was associated with rapid, dose-dependent accumulation of CHK1 pS345. These data raised the possibility that cycling populations of normal cells induce CHK1 pS345 following exposure to SCH 900776 as part of a futile cycle, perhaps driven by AT-family kinases and DNA-PK (refs. 6, 29, 32, 37-40; Supplementary Fig. S9D). During these experiments, we noted that monotherapy doses of SCH 900776 associated with detection of CHK1 pS345 in skin were moderately in excess of those associated with  $\gamma$ -H2AX modulation and enhanced response within xenografts (Table 4), suggesting doses of SCH 900776 sufficient to induce CHK1 pS345 in skin punch biopsies are likely to be equal to or greater than those required in combination with agents such as gemcitabine. Significantly, monotherapy doses of SCH 900776 sufficient to induce biomarker responses in skin punch biopsies taken from rats and dogs were achieved with no dose limiting toxicities. Hence, active doses of SCH 900776 are readily attainable in relevant toxicology species. These observations led to a clinically tractable biomarker strategy and prompted the design of a 2-stage phase 1 protocol to establish the

safety and activity of SCH 900776, initially as a lead-in monotherapy, before determining safety of the same SCH 900776 dose in combination with gemcitabine.<sup>41</sup>

Multiple chemotherapeutic agents that impact DNA replication provoke synergistic accumulation of  $\gamma$ -H2AX when combined with SCH 900776. These agents include nucleoside antimetabolites, antifolates, and alkylators. Interestingly, combination with topoisomerase I inhibitors such as SN38, did not induce  $\gamma$ -H2AX to a similar extent. These studies are far from comprehensive but they illuminate a number of other potential SCH 900776 combination strategies. Importantly, under some circumstances tumors described as nonresponsive to antimetabolites may retain the ability to cease DNA synthesis following rechallenge.<sup>42-44</sup> This suggests such tumors still exhibit the primary response to these agents (suppression of S-phase) but are perhaps better able to tolerate long-term intra-S phase arrest, thus avoiding cell death. Hence, the lack of overall response to agents like cytarabine or gemcitabine in a resistant setting may not necessarily be a result of the chemotherapeutic being inactive. Rather, this may reflect selection of cells more tolerant of the primary mechanistic effect (e.g., stalled replication forks; ref. 45). CHK1 inhibition may represent a novel opportunity to regenerate meaningful responses on repeat antimetabolite therapy within this target patient population, by redirecting the mechanism of action of this successful class of drugs toward tumor-targeted cytotoxicity.

## References

1. Haskell, C. *Cancer Treatment*. 5th ed. Philadelphia: Saunders; 2001.
2. Shi, Z.; Azuma, A.; Sampath, D.; Li, Y. X.; Huang, P.; Plunkett, W. S-Phase arrest by nucleoside analogues and abrogation of survival without cell cycle progression by 7-hydroxystaurosporine. *Cancer Res.* **2001**, *61*, 1065–72.
3. Zhang, Y. W.; Hunter, T.; Abraham, R. T. Turning the replication checkpoint on and off. *Cell Cycle* **2006**, *5*, 125–8.
4. Zachos, G.; Rainey, M. D.; Gillespie, D. A. Chk1-deficient tumour cells are viable but exhibit multiple checkpoint and survival defects. *EMBO J.* **2003**, *22*, 713–23.
5. Cho, S. H.; Toouli, C. D.; Fujii, G. H.; Crain, C.; Parry, D. Chk1 is essential for tumor cell viability following activation of the replication checkpoint. *Cell Cycle* **2005**, *4*, 131–9.
6. Syljuasen, R. G.; Sorensen, C. S.; Hansen, L. T.; Fugger, K.; Lundin, C.; Johansson, F. et al. Inhibition of human Chk1 causes increased initiation of DNA replication, phosphorylation of ATR targets, and DNA breakage. *Mol. Cell. Biol.* **2005**, *25*, 3553–62.
7. Taricani, L.; Shanahan, F.; Parry, D. Replication stress activates DNA polymerase alpha-associated Chk1. *Cell Cycle* **2009**, *8*, 482–9.
8. Furnari, B.; Rhind, N.; Russell, P. Cdc25 mitotic inducer targeted by chk1 DNA damage checkpoint kinase. *Science* **1997**, *277*, 1495–7.
9. O'Connell, M. J.; Raleigh, J. M.; Verkade, H. M.; Nurse, P. Chk1 is a wee1 kinase in the G2 DNA damage checkpoint inhibiting cdc2 by Y15 phosphorylation. *EMBO J.* **1997**, *16*, 545–54.
10. Sanchez, Y.; Wong, C.; Thoma, R. S.; Richman, R. Wu, Z.; Piwnicka-Worms, H. Conservation of the Chk1 checkpoint pathway in mammals: linkage of DNA damage to Cdk regulation through Cdc25. *Science* **1997**, *277*, 1497–501.
11. Liu, Q.; Guntuku, S.; Cui, X. S.; Matsuoka, S.; Cortez, D.; Tamai, K. et al. Chk1 is an essential kinase that is regulated by Atr and required for the G(2)/M DNA damage checkpoint. *Genes Dev.* **2000**, *14*, 1448–59.
12. Ewald, B.; Sampath, D.; Plunkett, W. H2AX phosphorylation marks gemcitabine-induced stalled replication forks and their collapse upon S-phase checkpoint abrogation. *Mol. Cancer Ther.* **2007**, *6*, 1239–48.
13. Walton, M. I.; Eve, P. D.; Hayes, A.; Valenti, M.; De Haven, B.; Brandon, A.; Box, G. et al. The preclinical pharmacology and therapeutic activity of the novel CHK1 inhibitor SAR-020106. *Mol. Cancer Ther.* **2010**, *9*, 89–100.

14. Dwyer, M. P.; Paruch, K.; Alvarez, C.; Doll, R. J.; Keertikar, K.; Duca, J. et al. Versatile templates for the development of novel kinase inhibitors: discovery of novel CDK inhibitors. *Bioorg. Med. Chem. Lett.* **2007**, *17*, 6216–9.
15. Paruch, K.; Dwyer, M. P.; Alvarez, C.; Brown, C.; Chan, T. Y.; Doll, R. J. et al. Discovery of dinaciclib (SCH 727965): a potent and selective inhibitor of cyclin-dependent kinases. *ACS Med. Chem. Lett.* **2010**, *1*, 204–8.
16. Dwyer, M.; Paruch, K.; Labroli, M.; Alvarez, C.; Keertikar, K.; Poker, C. et al. Discovery of pyrazolo[1,5-a]pyrimidine-based CHK1 inhibitors: A template-based approach – part 1. *Bioorg. Med. Chem. Lett.* **2010**. Available from: <http://dx.doi.org/10.1016/j.bmcl.2010.10.113>.
17. Labroli, M.; Dwyer, M. P.; Paruch, K.; Dwyer, M. P.; Alvarez, C.; Keertikar, K. et al. Discovery of pyrazolo[1,5-a]pyrimidine-based CHK1 inhibitors: A template-based approach – part 2. *Bioorg. Med. Chem. Lett.* **2010**. Available from: <http://dx.doi.org/10.1016/j.bmcl.2010.10.114>.
18. L'Italien, L.; Tanudji, M.; Russell, L.; Schebye, X. M. Unmasking the redundancy between Cdk1 and Cdk2 at G2 phase in human cancer cell lines. *Cell Cycle* **2006**, *5*, 984–93.
19. Paruch, K.; Dwyer, M. P.; Alvarez, C.; Brown, C.; Chan, T. Y.; Doll, R. J. et al. Pyrazolo[1,5-a]pyrimidines as orally available inhibitors of cyclin-dependent kinase 2. *Bioorg. Med. Chem. Lett.* **2007**, *17*, 6220–3.
20. Parry, D.; Guzi, T.; Shanahan, F. et al. Dinaciclib (SCH 727965), a novel and potent cyclin-dependent kinase inhibitor. *Mol. Cancer Ther.* **2010**, *9*, 2344–53.
21. Hsieh, Y.; Korfmacher, W. The role of hyphenated chromatography-mass spectrometry techniques in exploratory drug metabolism and pharmacokinetics. *Curr. Pharm. Des.* **2009**, *15*, 2251–61.
22. Sampath, D.; Shi, Z.; Plunkett, W. Inhibition of cyclin-dependent kinase 2 by the Chk1-Cdc25A pathway during the S-phase checkpoint activated by fludarabine: dysregulation by 7-hydroxystaurosporine. *Mol. Pharmacol.* **2002**, *62*, 680–8.
23. Fischmann, T. O.; Hruza, A.; Duca, J. S.; Ramanathan, L.; Mayhood, T.; Windsor, W. T. et al. Structure-guided discovery of cyclin-dependent kinase inhibitors. *Biopolymers* **2008**, *89*, 372–9.
24. Smits, V. A. Spreading the signal: dissociation of Chk1 from chromatin. *Cell Cycle* **2006**, *5*, 1039–43.
25. Clarke, C. A.; Clarke, P. R. DNA-dependent phosphorylation of Chk1 and Claspin in a human cell-free system. *Biochem. J.* **2005**, *388*, 705–12.

26. Jardim, M. J.; Wang, Q.; Furumai, R.; Wakeman, T.; Goodman, B. K.; Wang, X. F. Reduced ATR or Chk1 expression leads to chromosome instability and chemosensitization of mismatch repair-deficient colorectal cancer cells. *Mol. Biol. Cell* **2009**, *20*, 3801–9.
27. Plunkett, W.; Huang, P.; Searcy, C. E.; Gandhi, V. Gemcitabine: preclinical pharmacology and mechanisms of action. *Semin. Oncol.* **1996**, *23Suppl 10*, 3–15.
28. Arumugam, T.; Ramachandran, V.; Fournier, K. F.; Wang, H.; Marquis, L.; Abbruzzese, J. L. et al. Epithelial to mesenchymal transition contributes to drug resistance in pancreatic cancer. *Cancer Res.* **2009**, *69*, 5820–8.
29. Zabludoff, S. D.; Deng, C.; Grondine, M. R.; Sheehy, A. M.; Ashwell, S.; Caleb, B. L. et al. AZD7762, a novel checkpoint kinase inhibitor, drives checkpoint abrogation and potentiates DNA-targeted therapies. *Mol. Cancer Ther.* **2008**, *7*, 2955–66.
30. Workman, P. How much gets there and what does it do?: The need for better pharmacokinetic and pharmacodynamic endpoints in contemporary drug discovery and development. *Curr. Pharm. Des.* **2003**, *9*, 891–902.
31. Feijoo, C.; Hall-Jackson, C.; Wu, R.; Jenkins, D.; Leitch, J.; Gilbert, D. M. et al. Activation of mammalian Chk1 during DNA replication arrest: a role for Chk1 in the intra-S phase checkpoint monitoring replication origin firing. *J. Cell Biol.* **2001**, *154*, 913–23.
32. McNeely, S.; Conti, C.; Sheikh, T.; Patel, H.; Zabludoff, S.; Pommier, Y. et al. Chk1 inhibition after replicative stress activates a double strand break response mediated by ATM and DNA-dependent protein kinase. *Cell Cycle* **2010**, *9*, 995–1004.
33. Bartek, J.; Lukas, J. Chk1 and Chk2 kinases in checkpoint control and cancer. *Cancer Cell* **2003**, *3*, 421–9.
34. Wang, Q.; Fan, S.; Eastman, A.; Worland, P. J.; Sausville, E. A.; O'Connor, P. M. UCN-01: a potent abrogator of G2 checkpoint function in cancer cells with disrupted p53. *J. Natl. Cancer Inst.* **1996**, *88*, 956–65.
35. Sugiyama K, Shimizu M, Akiyama T, Tamaoki T, Yamaguchi K, Takahashi R, et al. UCN-01 selectively enhances mitomycin C cytotoxicity in p53 defective cells which is mediated through S and/or G(2) checkpoint abrogation. *Int. J. Cancer* **2000**, *85*, 703–9.
36. Blasina, A.; Hallin, J.; Chen, E.; Arango, M. E.; Kraynov, E.; Register, J. et al. Breaching the DNA damage checkpoint via PF-00477736, a novel small-molecule inhibitor of checkpoint kinase 1. *Mol. Cancer Ther.* **2008**, *7*, 2394–404.
37. Zhao, H.; Piwnicka-Worms, H. ATR-mediated checkpoint pathways regulate phosphorylation and activation of human Chk1. *Mol. Cell Biol.* **2001**, *21*, 4129–39.

38. Lupardus, P. J.; Byun, T.; Yee, M. C.; Hekmat-Nejad, M.; Cimprich, K. A. A requirement for replication in activation of the ATR-dependent DNA damage checkpoint. *Genes Dev.* **2002**, *16*, 2327–32.
39. Liu, S.; Bekker-Jensen, S.; Mailand, N.; Lukas, C.; Bartek, J.; Lukas, J. Claspin operates downstream of TopBP1 to direct ATR signaling towards Chk1 activation. *Mol. Cell Biol.* **2006**, *26*, 6056–64.
40. Paulsen, R. D.; Cimprich, K. A. The ATR pathway: fine-tuning the fork. *DNA Repair (Amst)* **2007**, *6*, 953–66.
41. Available from: <http://www.clinicaltrials.gov>.
42. Gandhi, V.; Plunkett, W.; Du, M.; Ayres, M.; Estey, E. H. Prolonged infusion of gemcitabine: clinical and pharmacodynamic studies during a phase I trial in relapsed acute myelogenous leukemia. *J. Clin. Oncol.* **2002**, *20*, 665–73.
43. Gandhi, V.; Kantarjian, H.; Faderl, S.; Bonate, P.; Du, M.; Ayres, M. et al. Pharmacokinetics and pharmacodynamics of plasma clofarabine and cellular clofarabine triphosphate in patients with acute leukemias. *Clin. Cancer Res.* **2003**, *9*, 6335–42.
44. Sampath, D.; Cortes, J.; Estrov, Z.; Du, M.; Shi, Z.; Andreeff, M. et al. Pharmacodynamics of cytarabine alone and in combination with 7-hydroxystaurosporine (UCN-01) in AML blasts *in vitro* and during a clinical trial. *Blood* **2006**, *107*, 2517–24.
45. Cavalier, C.; Didier, C.; Prade, N.; Mansat-De Mas, V.; Manenti, S.; Recher, C. et al. Constitutive activation of the DNA damage signaling pathway in acute myeloid leukemia with complex karyotype: potential importance for checkpoint targeting therapy. *Cancer Res.* **2009**, *69*, 8652–61.

**Part 2d**  
**Discovery of pyrazolo[1,5-*a*]pyrimidine-based Pim inhibitors:**  
**a template-based approach\***

\*published as:

Dwyer, M. P.;\* Keertikar, K.;\* Paruch, K.; Alvarez, C.; Labroli, M.; Poker, C.; Fischmann, T. O.; Mayer-Ezell, R.; Bond, R.; Wang, Y.; Azevedo, R.; Guzi, T. J. Discovery of Pyrazolo[1,5- *a*]pyrimidine-based Pim Inhibitors: A Template-Based Approach. *Bioorg. Med. Chem. Lett.* **2013**, *23*, 6178.

The Pim kinases are a family of serine/threonine kinases in the CAMK (calmodulin-dependent protein kinase) family consisting of three members Pim-1, Pim-2, and Pim-3.<sup>1</sup> There is a high level of sequence homology between these family members which is suggestive of functional redundancy.<sup>2</sup> Both Pim-1 and Pim-2 have been shown to be overexpressed in a number of human hematopoietic malignancies such as myeloid leukemia and lymphomas.<sup>3</sup> In addition, DNA microarray analyses demonstrated that Pim-1 is overexpressed in human prostate cancer and correlates with disease outcome.<sup>4</sup> In animal models, overexpression of Pim-1 and Pim-2 in human prostate cancer cells enhances their growth in nude mice.<sup>5</sup> These observations suggest that Pim-1 and/or Pim-2 inhibitor may be effective in the treatment for hematologic malignancies.

In 2005, Knapp and co-workers described the first small molecule Pim inhibitors<sup>6</sup> represented by 1 (Fig. 1). Since these initial reports, several additional small molecule Pim inhibitor classes<sup>7-13</sup> have been reported and several excellent reviews of recent Pim inhibitor chemotypes have appeared.<sup>14</sup>

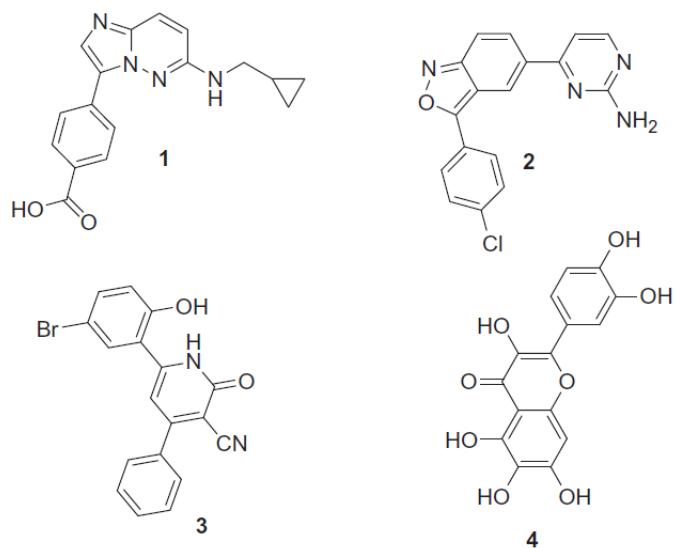


**Figure 1.** Representative Pim inhibitors 1–4.

In addition, several X-ray structures of Pim-1 co-crystallized with inhibitors point to some very unique structural features for this family of kinases: the hinge region. The unique hinge region for Pim-1 contains an extra residue, proline-123, which allows for the formation of only a single hydrogen bond with either ATP or ATP mimetics. With this information in hand, we set about identifying novel Pim inhibitors that may serve as effective agents for the treatment of hematologic malignancies.

Initial HTS screening of our internal compound collection identified pyrazolo[1,5-*a*]pyrimidines **5** and **6**<sup>15</sup> as early Pim program hits (Figure 2). These initial hits possessed sub-micromolar potency for Pim-1, and **5** showed good selectivity versus both CDK2 and CHK1. We found this chemotype was of particular interest due to our long standing efforts utilizing the pyrazolo[1,5-*a*]pyrimidine core for the identification of selective cell-cycle kinase inhibitors of CDK (dinaciclib)<sup>16</sup> and CHK1 (SCH 900776)<sup>17</sup> which are currently under clinical evaluation.

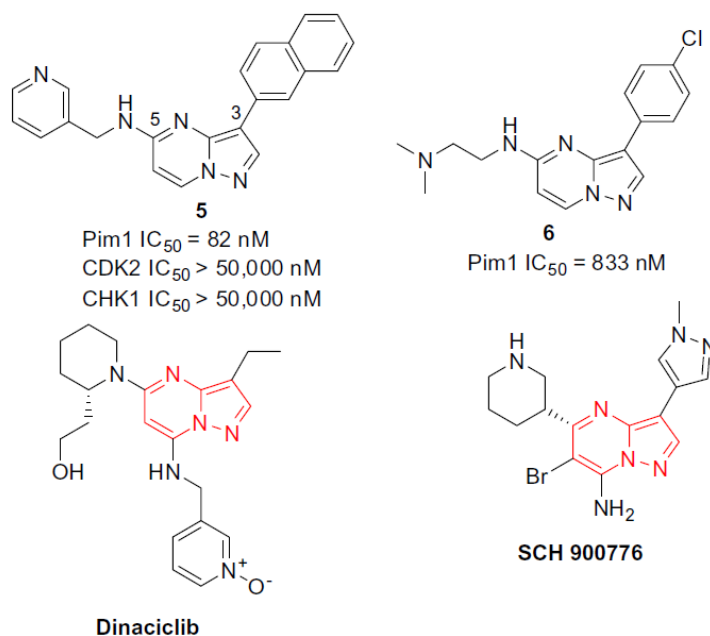
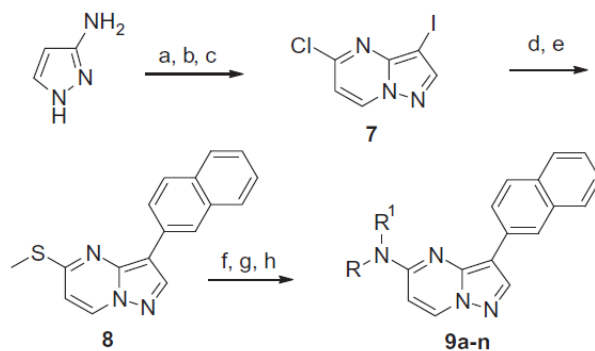


**Figure 2.** Pyrazolo[1,5-*a*]pyrimidine-based Pim hits and pyrazolo[1,5-*a*]pyrimidine-based cell-cycle kinase inhibitors.

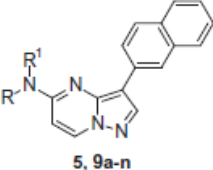
With these initial screening hits in hand (Fig. 2), efforts were initiated to conduct systematic modifications around the pyrazolo[1,5-*a*]pyrimidine core to enhance in-vitro potency against Pim-1 as well as other family members such as Pim-2.

It was not clear at the outset of the program whether a Pim isoform selective inhibitor or a pan-Pim inhibitor would be more desirable. The ability to access compounds that possessed either profile was of interest for biology validation studies. Initial chemistry efforts focused upon structural modifications of the C5 position of naphthyl derivative **5** to explore the SAR around this region. The synthetic preparation of the C5 derivatives is depicted in Scheme 1. Condensation of 3-aminopyrazole with 1,3-dimethyl uracil<sup>18,19</sup> followed by treatment with POCl<sub>3</sub> and iodination afforded compound **7**. Treatment with sodium thiomethoxide followed by Suzuki coupling with 2-naphthyl boronic acid under standard conditions afforded **8**. Oxidation of the thiomethyl moiety with mCPBA afforded roughly a 1:1 mixture of the intermediate sulfoxide/sulfone which was treated directly with amines in NMP to afford the title compounds **9a–e**, **k**, **m–n** found in Table 1. The Boc protected diamine intermediates were treated with TFA to afford final compounds **9f–j**, **l** (Scheme 1).

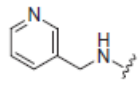
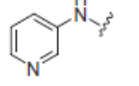
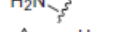
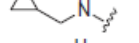
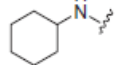
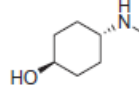
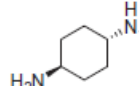
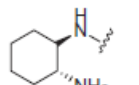
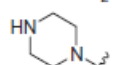
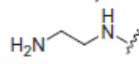
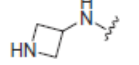
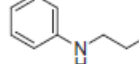
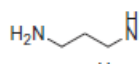
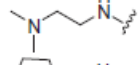
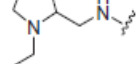


**Scheme 1.** (a) 1,3-dimethyluracil, NaOMe; (b) POCl<sub>3</sub>; (c) NIS; 55% (3 steps) (d) NaSMe, THF; (e) 2-naphthyl boronic acid, PdCl<sub>2</sub>(dppf), K<sub>3</sub>PO<sub>4</sub>, DME/H<sub>2</sub>O 65% (2 steps) (f) mCPBA, CH<sub>2</sub>Cl<sub>2</sub>; (g) HNRR<sup>1</sup>, NMP, 20–62% (two steps): (h) TFA, CH<sub>2</sub>Cl<sub>2</sub>; 85–96%.

As depicted in Table 1, simple shortening of the chain or elimination of the pyridyl functionality from compound **5** resulted in a dramatic loss in both Pim-1 and Pim-2 potency. While simple alkyl or cycloalkyl functionality (**9c** and **d**) did not retain potency versus either Pim isoform, incorporation of polar functionality particularly a primary amine moiety resulted in a dramatic improvement in potency for both Pim-1 and Pim-2 as demonstrated by compound **9f**. While the pendant amino functionality could be moved around and retain reasonable Pim-1 activity, the Pim-2 activity seemed to be very sensitive towards the steric environment. This modification resulted in the identification of extremely selective Pim-1 compounds such as compounds **9m** and **9n**. Owing to our interest in obtaining a pan-Pim inhibitor for a tool compound for biological studies, we chose to further explore SAR around compound **9i** which represented the best pan-Pim profile in Table 1 as measured by the Pim-1 and Pim-2 in-vitro assays.

**Table 1.** Pim-1 and Pim-2 in vitro activity of N5 pyrazolo[1,5-*a*]pyrimidines **5**, **9a–n**.

Chemical structure of the N5 pyrazolo[1,5-*a*]pyrimidine core, labeled **5, 9a–n**. It features a pyrazolo[1,5-*a*]pyrimidine ring system with an R<sup>1</sup> group on the N5 nitrogen and a biphenyl-2-yl group at the C3 position.

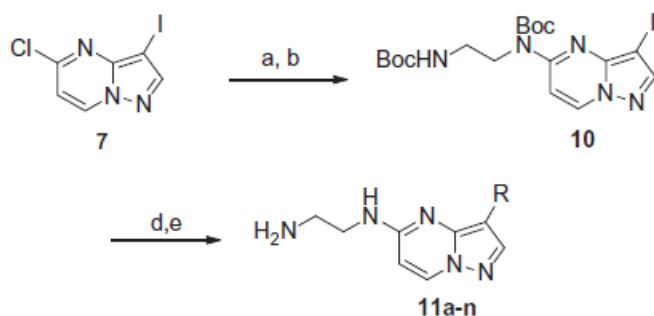
Compd	NRR <sup>1</sup>	Pim-1 IC <sub>50</sub> <sup>a</sup> (nM)	Pim-2 IC <sub>50</sub> <sup>a</sup> (nM)
<b>5</b>		87	na <sup>b</sup>
<b>9a</b>		1527	na <sup>b</sup>
<b>9b</b>		804	na <sup>b</sup>
<b>9c</b>		718	na <sup>b</sup>
<b>9d</b>		na <sup>b</sup>	na <sup>b</sup>
<b>9e</b>		18	na <sup>b</sup>
<b>9f</b>		3.1	190
<b>9g</b>		2.9	157
<b>9h</b>		6.8	1462
<b>9i</b>		1.5	87
<b>9j</b>		25	781
<b>9k</b>		1618	na <sup>b</sup>
<b>9l</b>		5.1	2302
<b>9m</b>		5.0	na <sup>b</sup>
<b>9n</b>		1.6	4308

<sup>a</sup> Values are the mean of two ( $n = 2$ ) runs. See Ref. 20 for assay details.

<sup>b</sup> na = Not active at >5000 nM.

With compound **9i** in hand, efforts were directed towards the exploration of additional C3 modifications, particularly around bicyclic and biaryl motifs.<sup>21</sup> The preparation of these C3 analogs is shown in Scheme 2. Treatment of iodide **7** with tert-butyl(2-aminoethyl) carbamate followed by subsequent Boc protection afforded **10**. Using **10** as a common starting material, Suzuki coupling

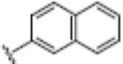
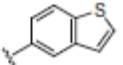
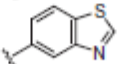
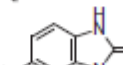
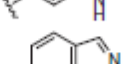
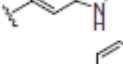
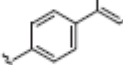
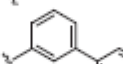
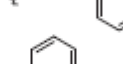
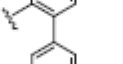
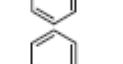
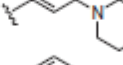
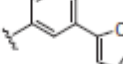
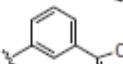
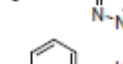
with various boronic acids/boronates under standard conditions followed by TFA-mediated Boc deprotection afforded the title compounds **11a–n** (Table 2).



**Scheme 2.** (a) tert-Butyl(2-aminoethyl)carbamate, NMP; (b) Boc<sub>2</sub>O, DMAP; 60% (two steps) (c) RB(OH)<sub>2</sub>, PdCl<sub>2</sub>(dppf), K<sub>3</sub>PO<sub>4</sub>, DME/H<sub>2</sub>O; (d) TFA, CH<sub>2</sub>Cl<sub>2</sub>, 40–65% (two steps).

As summarized in Table 2, simple replacement of the naphthyl motif with either a benzothiophene (**11a**) or benzothiazole (**11b**) resulted in very comparable Pim in vitro profiles to the compound **9i**. However, incorporation of polar functionality such as a benzimidazolone (**11c**) or indazole (**11d**) resulted in 3–4 fold improvement in Pim-2 activity while retaining good Pim-1 potency. Systematic exploration of placement of biaryl functionality demonstrated that meta-substituted derivatives (**11f**) were far superior to both ortho and para-substituted derivatives. The pendant ring of the biaryl motif of **11f** was found to be tolerant of certain heterocyclic rings such as a 1,2,4-oxadiazole (**11j**) and furan (**11i**) while the 2-imidazole derivative (**11k**) was completely devoid of Pim activity, illustrating the stringent structural requirements for this ring. In this vein, attempted replacement of the pendant ring with heteroatom linked rings or O-tethered functionality led to a loss in Pim potency while replacement of the proximal ring of **11f** was generally not well tolerated as illustrated by compounds **11m** and **11n**.

**Table 2.** Pim-1 and Pim-2 *in vitro* activity of C3 pyrazolo[1,5-*a*]pyrimidines **9i**, **11a–n**.

Compd	R	Pim-1 IC <sub>50</sub> (nM) <sup>a</sup>	Pim-2 IC <sub>50</sub> (nM) <sup>a</sup>
<b>9i</b>		1.5	87
<b>11a</b>		2	114
<b>11b</b>		7	212
<b>11c</b>		7.2	19
<b>11d</b>		9.4	24
<b>11e</b>		247	na <sup>b</sup>
<b>11f</b>		10	137
<b>11g</b>		834	na <sup>b</sup>
<b>11h</b>		3511	na <sup>b</sup>
<b>11i</b>		4.5	89
<b>11j</b>		1.3	7.3
<b>11k</b>		na <sup>b</sup>	na <sup>b</sup>
<b>11l</b>		136	886
<b>11m</b>		162	na <sup>b</sup>
<b>11n</b>		834	na <sup>b</sup>

<sup>a</sup> Values are the mean of two (n = 2) runs. See Ref.20 for assay details.

<sup>b</sup> na = Not active at >5000 nM.

As depicted in Table 2, compound **11j** emerged as a lead pan-Pim inhibitor based upon the single digit nanomolar potency it demonstrated versus both Pim-1 and Pim-2. Further evaluation of this compound across a battery of kinases summarized in Table 3 reinforces the pan Pim activity (including Pim-3) of **11j** while demonstrating excellent selectivity versus several other kinases.

**Table 3.** Kinase selectivity of compound **11j**.

Kinase	IC <sub>50</sub> (nM)
Pim-3	1.8
CHK1	7100
CDK2	580
PEK	>3000
mTor	>3000
CK2	950

This compound was found to be clean in both CYP P450 evaluation (3A4, 2D6 and 2C9 > 20 10 μM and hERG ion channel evaluation (11% inhibition @ 10 μM)

In order to better understand the SAR trends observed in Tables 1 and 2 for this class of compounds, X-ray co-crystal structures of two compounds (**11o**<sup>22</sup> and **9g**) bearing different functionality at C3 and C5 bound to Pim-1 (shown in Figs. 3 and 4) were obtained.

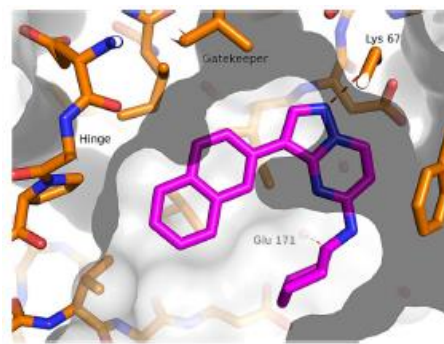
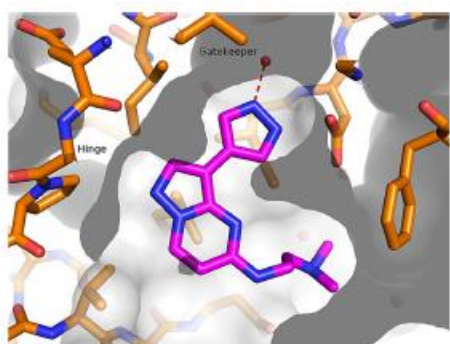


**Figure 3.** X-ray of crystal structure of **11o** bound to Pim-1.<sup>23</sup> **Figure 4.** X-ray of crystal structure of **9g** in Pim-1.<sup>24</sup>

In Figure 3, compound **11o** does not make contact with the hinge area of the Pim-1 protein but makes only a single hydrogen bond to a water molecule found in the kinase specificity pocket. The canonical binding mode observed for **11o** in Pim-1 is consistent with the orientation observed for most other pyrazolo[1,5-*a*]pyrimidine derivatives from both our CDK and CHK1 programs.<sup>16,17</sup>

In Figure 4, the larger C3 naphthyl group in **9g** induces a flip from the canonical binding mode observed for **11o** shown in Figure 3. The N1 moiety of the pyrazolo[1,5-*a*]pyrimidine acts as a H-bond acceptor for Lys57 with the C3 naphthyl group oriented parallel to the hinge region of the protein. In addition, the primary amine on the cyclohexyl ring of **9g** makes a H-bond contact with the oxygen of Glu171. The binding mode observed for **9g** is consistent with an X-ray structure for a structurally related imidazo[1,2-*b*]pyridazine bound to Pim-1.<sup>6</sup> While a X-ray co-crystal structure of compound **11j** bound to Pim-1 could not be obtained, it can be rationalized this compound might bind in a similar fashion to **9g** with the large C3 group oriented along the hinge region.

In summary, systematic optimization of both the C3 and C5 position of pyrazolo[1,5-*a*]pyrimidine Pim hit **5** led to the discovery of potent, pan Pim inhibitors represented by **11j**. Modifications of either the C3 or C5 functionality of this series were shown to play a critical role in determining the ultimate selectivity versus the various Pim isoforms. In addition, single X-ray crystallography of several members of the pyrazolo[1,5-*a*]pyrimidine series bound to Pim-1 illustrated several unique binding modes which seem to be driven by the size of the C3 substituent. This work further validates the utility of the pyrazolo[1,5-*a*]pyrimidine core toward the development of additional classes of kinase inhibitors. Additional evaluation of this class of Pim inhibitors<sup>25</sup> including compound **11j** will be reported in due course.

## References and notes

1. Bachmann, M.; Moroy, T. *Int. J. Biochem. Cell Biol.* **2005**, *37*, 726.
2. van der Lugt, N. M.; Domen, J.; Verhoeven, E.; Linders, K.; van der Gulden, H.; Allen, J.; Berns, A. *EMBO J.* **1995**, *14*, 2536.
3. (a) Amson, R.; Sigaux, F.; Przedborski, S.; Flandrin, G.; Givol, D.; Telerman, A. *Proc. Natl. Acad. Sci. U.S.A.* **1989**, *86*, 8857; (b) Cohen, A. M.; Grinblat, B.; Bessler, H.; Kristt, D. A.; Kremer, A.; Shalom, S.; Schwartz, A.; Halperin, M.; Merkel, D.; Don, J. *Leuk. Lymphoma* **2004**, *45*, 951.
4. Fox, C. J.; Hammerman, P. S.; Thompson, C. B. *J. Exp. Med.* **2005**, *201*, 259.
5. Chen, W. W.; Chan, D. C.; Donald, C.; Lilly, M. B.; Kraft, A. S. *Mol. Cancer Res.* **2005**, *3*, 443.
6. (a) Bullock, A. N.; Debreczeni, J. E.; Federov, O. Y.; Nelson, A.; Marsden, B. D.; Knapp, S. *J. Med. Chem.* **2005**, *48*, 7604; (b) Pogacic, V.; Bullock, A. N.; Fedorov, O.; Filippakopoulos, P.; Gasser, C.; Biondi, A.; Meyer-Mondard, S.; Knapp, S.; Schwaller, J. *Cancer Res.* **2007**, *67*, 6916.
7. Cheney, I. W.; Yan, S.; Appleby, T.; Walker, H.; Vo, T.; Yao, N.; Hamatake, R.; Hong, Z.; Wu, J. *Z. Bioorg. Med. Chem. Lett.* **2007**, *17*, 1679.
8. Tong, Y.; Stewart, K. D.; Thomas, S.; Przytulinska, M.; Johnson, E. F.; Klinghofer, V.; Levenson, J.; McCall, O.; Soni, N. B.; Luo, Y.; Lin, N.-H.; Sowin, T. J.; Giranda, V. L.; Penning, T. D. *Bioorg. Med. Chem. Lett.* **2008**, *18*, 5206.
9. Pierce, A. C.; Jacobs, M.; Stuver-Moody, C. *J. Med. Chem.* **1972**, *2008*, 51.
10. Grey, R.; Pierce, A. C.; Bemis, G. W.; Jacobs, M. D.; Stuver-Moody, C.; Jajoo, R.; Mohal, N.; Green, J. *Bioorg. Med. Chem. Lett.* **2009**, *19*, 3019.
11. Xia, Z.; Knaak, C.; Ma, J.; Beharry, Z. M.; McInnes, C.; Wang, W.; Kraft, A. S.; Smith, C. D. *J. Med. Chem.* **2009**, *52*, 74.
12. Qian, K.; Wang, L.; Cywin, C. L.; Farmer, B. T., II; Hickey, E.; Homon, C.; Jakes, S.; Kashem, M. A.; Lee, G.; Leonard, S.; Li, J.; Magboo, R.; Mao, W.; Pack, E.; Peng, C.; Prokopowicz, A., III; Welzel, M.; Wolak, J.; Morwick, T. *J. Med. Chem.* **2009**, *52*, 1814.
13. Beharry, Z.; Zemskova, M.; Mahajan, S.; Zhang, F.; Ma, J.; Xia, Z.; Lilly, M.; Smith, C. D.; Kraft, A. S. *Mol. Cancer Ther.* **2009**, *8*, 1473.
14. (a) Morwick, T. *Expert Opin. Ther. Pat.* **2010**, *20*, 193; (b) Anizon, F. S.; Shtil, A. A.; Danilenko, V. N.; Moreau, P. *Curr. Med. Chem.* **2010**, *17*, 4114; (c) Drygin, D.; Haddach, M.; Pierre, F.; Rychman, D. M. *J. Med. Chem.* **2012**, *55*, 8199.
15. The first pyrazolo[1,5-a]pyrimidine-based Pim inhibitor was reported by Knapp and co-workers: See Ref.6
16. (a) Dwyer, M. P.; Paruch, K.; Alvarez, C.; Doll, R. J.; Keertikar, K.; Duca, J.; Fischmann, T. O.; Hruza, A.; Madison, V.; Lees, E.; Parry, D.; Seghezzi, W.; Sgambellone, N.; Shanahan, F.; Wiswell,

D.; Guzi, T. J. *Bioorg. Med. Chem. Lett.* **2007**, *17*, 6216; (b) Paruch, K.; Dwyer, M. P.; Alvarez, C.; Brown, C.; Chan, T.-Y.; Doll, R. J.; Keertikar, K.; Knutson, C.; McKittrick, B.; Rivera, J.; Rossman, R.; Tucker, G.; Fischmann, T.; Hruza, A.; Madison, V.; Nomeir, A. A.; Wang, Y.; Lees, E.; Parry, D.; Sgambellone, N.; Seghezzi, W.; Schultz, L.; Shanahan, F.; Wiswell, D.; Xu, X.; Zhou, Q.; James, R. A.; Paradkar, V. M.; Park, H.; Rokosz, L. R.; Stauffer, T. M.; Guzi, T. J. *Bioorg. Med. Chem. Lett.* **2007**, *17*, 6220; (c) Paruch, K.; Dwyer, M. P.; Alvarez, C.; Brown, C.; Chan, T.-Y.; Doll, R. J.; Keertikar, K.; Knutson, C.; McKittrick, B.; Rivera, J.; Rossman, R.; Tucker, G.; Fischmann, T. O.; Hruza, A.; Madison, V.; Nomeir, A. A.; Wang, Y.; Lees, E.; Parry, D.; Sgambellone, N.; Seghezzi, W.; Schultz, L.; Shanahan, F.; Wiswell, D.; Xu, X.; Zhou, Q.; James, R. A.; Paradkar, V. M.; Park, H.; Rokosz, L. R.; Stauffer, T. M.; Guzi, T. J. *ACS Med. Chem. Lett.* **2010**, *1*, 204–208.

17. (a) Dwyer, M. P.; Paruch, K.; Labroli, M.; Alvarez, C.; Keertikar, K.; Poker, C.; Rossman, R.; Fischmann, T. O.; Duca, J. S.; Madison, V.; Parry, D.; Davis, N.; Seghezzi, W.; Wiswell, D.; Guzi, T. J. *Bioorg. Med. Chem. Lett.* **2011**, *21*, 467; (b) Labroli, M.; Paruch, K.; Dwyer, M. P.; Alvarez, C.; Keertikar, K.; Poker, C.; Rossman, R.; Duca, J. S.; Fischmann, T. O.; Madison, V.; Parry, D.; Davis, N.; Seghezzi, W.; Wiswell, D.; Guzi, T. J. *Bioorg. Med. Chem. Lett.* **2011**, *21*, 471–474; (c) Guzi, T. J.; Paruch, K.; Dwyer, M. P.; Labroli, M.; Shanahan, F.; Davis, N.; Taricani, L.; Wiswell, D.; Seghezzi, W.; Penafior, E.; Bhagwat, B.; Wang, W.; Gu, D.; Hsieh, Y.; Lee, S.; Liu, M.; Parry, D. *Mol. Cancer Ther.* **2011**, *10*, 591.

18. It should be noted that this original paper describing the regiochemical outcome of the cyclization of 3-aminopyrazole with 1,3-dimethyl uracil assigned the product as the 7-OH pyrazolo[1,5-*a*]pyrimidine. More recent examination of this reaction by Gavrin and coworkers (Ref.19) found this cyclization in fact affords the 5-OH pyrazolo[1,5-*a*]pyrimidine instead of the 7-OH analog first reported by Cutler and coworkers. Independent X-ray analysis conducted in our research laboratories of a derivative prepared via this method (unpublished results) supports the revised assignment as the 5-OH pyrazolo[1,5-*a*]pyrimidine core as proposed by Gavrin and coworkers.

Chu, C. K.; Suh, J. J.; Mesbah, M.; Cutler, S. J. *J. Heterocycl. Chem.* **1986**, *23*, 349.

19. Gavrin, L. K.; Lee, A.; Provencher, B. A.; Masefski, W. W.; Huhn, S. D.; Ciszewski, G. M.; Cole, D. C.; McKew, J. C. *J. Org. Chem.* **2007**, *72*, 1043.

20. Pim-1, -2, -3 kinase assays: Pim1, 2, and 3 activity were measured using CisBio KinEASE HTRF assays (catalog # 62ST3PEC) with substrates STK3 (Pim1) or STK1 (Pim2 & 3), anti-phospho Ser/Thr Cryptate and streptavidin-XL-665 in Corning black LVP 384 well plates (Fisher Catalog # 3676). (Pim 1 and 3 are from Millipore catalog #s 14–573 and 14–738, Pim 2 is from Invitrogen catalog # PV4036). Briefly, 0.75 ng/well enzyme was added in 7  $\mu$ l kinase buffer (10 mM HEPES pH 7, 0.02% sodium azide, 0.01% BSA, 0.1 mM orthovanadate, 1 mM DTT, 10 mM MgCl<sub>2</sub>) followed by

3  $\mu\text{l}$  of compound diluted from DMSO 1:6 with kinase buffer. After a 30 min preincubation, the reaction was started by adding 2  $\mu\text{l}$  of 6ATP/STK mix (final concentrations for Pim 1: 25  $\mu\text{M}$  ATP and 200 nM STK3; Pim 2: 5  $\mu\text{M}$  ATP and 700 nM STK1; Pim 3: 10  $\mu\text{M}$  ATP and 300 nM STK1). Reactions were run at room temperature for 45 min (Pim 1) or 60 min (Pim 2 and 3) and stopped by addition of 10  $\mu\text{l}$  detection buffer containing 50 nM, 175 nM, or 75 nM SAXL665 for Pims 1, 2, and 3 respectively and anti-phospho Ser/Thr Cryptate at 1:100. Fluorescence at 620 nM (Cryptate) and 665 nM (XL665) were measured on a Pherastar (BMG Labtech) and the 665/620 ratio x 10,000 was used for data analysis (ABASE). Dose–response curves were generated from duplicate 8 point serial dilutions of inhibitory compounds.  $\text{IC}_{50}$  values were derived by nonlinear regression analysis.

21. Early SAR efforts around the C3 monocyclic aryl motifs as found in compound **6** did not yield significant improvements in the *in vitro* potency (unpublished results).

22. Compound **11o** was prepared according to the synthetic route outlined in Scheme 2 by substituting dimethylethylamine and Bocpyrazole boronic acid to afford the final compound. The binding assay data for **11o** is Pim-1  $\text{IC}_{50} = 7$  nM and Pim-2  $\text{IC}_{50} = 185$  nM.

23. The X-ray coordinates for compound **11o** bound to Pim-1 have been deposited in the ProteinDataBank (PDB ID code: 4MBI).

24. The X-ray coordinates for compound **9g** bound to Pim-1 have been deposited in the ProteinDataBank (PDB ID code: 4MBL).

25. A series of potent 3-carboxamido pyrazolo[1,5-*a*]pyrimidine Pim inhibitors has been recently disclosed: Wang, X.; Magnuson, S.; Pastor, R.; Fan, E.; Hu, H.; Tsui, V.; Deng, W.; Murray, J.; Steffek, M.; Wallweber, H.; Moffat, J.; Drummond, J.; Chan, G.; Harstad, E.; Ebens, A. J. *Bioorg. Med. Chem. Lett.* **2013**, *23*, 3149.

**Part 3a**  
**Cyclin-dependent kinase inhibitors inspired by roscovitine:**  
**purine bioisosteres\***

\*published as:

Jorda, R.; Paruch, K.; Krystof, V. \* Cyclin-dependent Kinase Inhibitors Inspired by Roscovitine: Purine Bioisosteres. *Curr. Pharm. Design* **2012**, *18*, 2974.

### **Introduction**

Since their discovery as key elements of the cell cycle regulatory machinery, cyclin-dependent kinases (CDKs) have been considered to be potential targets for drugs against proliferative diseases.<sup>1</sup> Indeed, the first small molecule inhibitors of CDKs were found to block proliferation in a variety of cellular models and induce cell death in transformed cell lines.<sup>2,3</sup> Moreover, several cyclins and CDKs were shown to be oncogenes, while their natural peptide inhibitors (and some of their substrates) proved to be tumour suppressors.<sup>4,5</sup> Taken together, these findings prompted a number of extensive research programs focused on identifying novel CDK inhibitors as drug candidates for oncology. Historically, many inhibitors were discovered during random screening programs. Notable examples include flavopiridol and roscovitine, two of the most well-known first-generation CDK inhibitors to have undergone clinical trials.<sup>6-8</sup> Other compounds were developed via structure-based design using a number of three dimensional structures of individual CDKs, with or without ligands.<sup>9,10</sup> To the best of our knowledge, only one successful compound has been developed by fragment-based inhibitor discovery the aminopyrazole derivative AT7519.<sup>11</sup> The most extensively used approach is ligand-based rational design and synthesis of different analogs based on targeted modifications of early leads and bioisosteric replacements of their functional groups. This approach has yielded structurally diverse CDK inhibitors that have successfully passed through preclinical testing, such as P276-00 (a derivative of flavopiridol<sup>12</sup>) and ZK 304709 (which is based on the scaffold of the indigoid dye indirubin<sup>13</sup>). In addition, PHA-848125 could be regarded as a bioisostere of PD-0332991, although both drugs were apparently developed independently.<sup>14,15</sup> This review focuses specifically on CDK inhibitors developed as bioisosteres of roscovitine.

### **Roscovitine and its analogues**

Systematic structural modifications of the 2,6,9-trisubstituted purine derivative olomoucine, which was identified during random screening, lead to the development of roscovitine<sup>16-18</sup>, one of the first

CDK inhibitors to enter clinical trials.<sup>19,20</sup> Roscovitine is a pan-selective inhibitor of CDK 1/2/5/7/9<sup>21,22</sup> whose antiproliferative activities correlate with dephosphorylation of the retinoblastoma protein and the down-regulation of CDKs and cyclins.<sup>23-27</sup> It also influences global transcription by inhibiting CDK7 and CDK9 and thereby inhibiting the activity of RNA polymerase II (RNAP II).<sup>24,28</sup> This causes down-regulation of proteins with short half-lives, including several anti-apoptotic proteins. The reduced abundance of anti-apoptotic proteins alters the balance between cell survival and apoptosis.

Roscovitine is currently undergoing Phase 2 clinical trials as a single agent against non-small cell lung carcinoma and nasopharyngeal cancer. It is also being used in combination with other drugs in two Phase I trials. In the first, it is being evaluated with sapacitabine to treat patients with advanced solid tumours, while in the second it is being tested in combination with liposomal doxorubicin to treat patients with metastatic triple negative breast cancer.<sup>29,30</sup>

The success of roscovitine has prompted attempts to develop related CDK inhibitors by

- i) optimizing the substituents of the purine,
- ii) changing the positions and ratios of nitrogen and carbon atoms in the heterocyclic core,
- iii) using a combination of the two approaches discussed above.

The first approach resulted in the development of many highly potent purine CDK inhibitors (Fig. 1), including H717<sup>31</sup>, purvalanol A<sup>32,33</sup>, MDLI08522<sup>34</sup>, 3-chloranilino derivatives<sup>35</sup>, the cyclohexylmethoxy compounds NU2058 and NU6102<sup>9,36</sup>, CR8<sup>37</sup>, and other biaryl derivatives<sup>38-40</sup> (Fig. 1). With the exception of the NU-series, all of these compounds retain similar C2-, C6-, and N9substituents, i.e. a small hydrophobic chain (isopropyl or cyclopentyl) at N9, an aromatic side chain coupled through the secondary amino group at C6, and a polar alkyl- or cycloalkylamine at C2. Many of these compounds are at least a hundred-fold more potent CDK inhibitors than roscovitine.

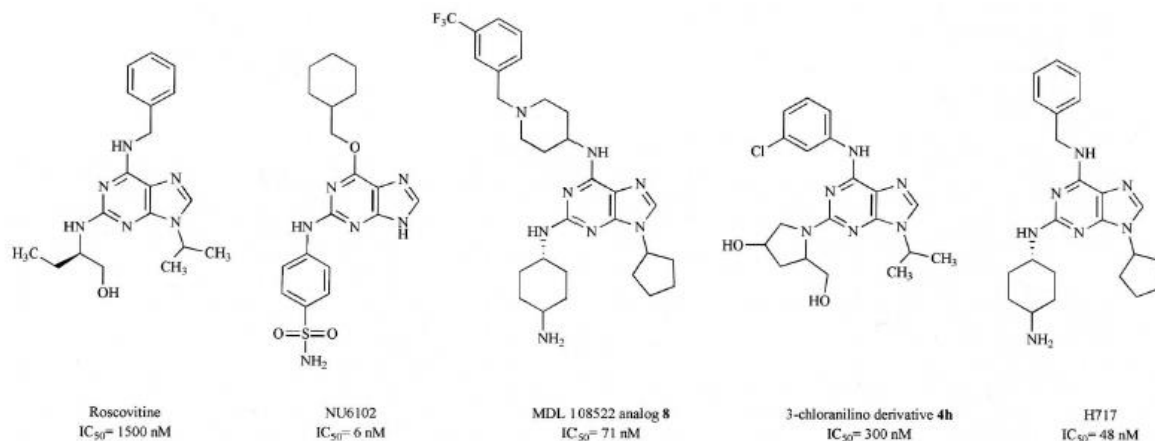


**Figure 1.** Roscovitine and related purine inhibitors of CDK2. This selection of compounds summarizes structure-activity relationships within the class and demonstrates the diversity of acceptable substitutions.

More synthetically challenging modifications of the purine core have led to the discovery of several groups of purine bioisosteres (Fig. 2). Purine isomers retaining all four nitrogens (4N) comprise the largest group, but several types of bioisosteres with two (2N) and three nitrogens (3N) have also been developed, along with one group having 5 nitrogens (5N). Many of these bioisosteres can replace purine without sacrificing activity, including imidazo[2, 1-*f*]-1,2,4-triazines<sup>41,42</sup>, pyrrolo[3,2-*d*]pyrimidines<sup>43</sup>, triazolo[1,5-*a*]pyrimidines<sup>44,45</sup>, imidazo[4,5-*d*]pyridines<sup>46</sup>, imidazo[1,2-*a*]pyrazines<sup>47</sup> and imidazo[1,2-*a*]pyridines<sup>48,49</sup>. However, the use of pyrazolo[3,4-*d*]pyrimidines<sup>50</sup>, triazolo[4,5-*d*]pyrimidines (8-azapurines)<sup>51</sup> and benzo[*d*]imidazoles<sup>52</sup> resulted in the loss of CDK inhibitory potential. Notably, four classes of bioisosteres that yield improved potency relative to purine have been described: pyrazolo[1,5-*a*]-1,3,5-triazines<sup>41,42,53</sup>, pyrazolo[1,5-*a*]pyrimidines<sup>54-60</sup>, pyrazolo[1,5-*a*]pyridines<sup>48</sup> and pyrazolo[4,3-*d*]pyrimidines.<sup>61-63</sup> Unfortunately, because the structure-activity relationships within each group of purine bioisosteres have been studied in different levels of detail, it is difficult to directly compare their activity. Specifically, only six types of direct roscovitine analogues have been prepared and evaluated biochemically side by side with roscovitine (Table 1).

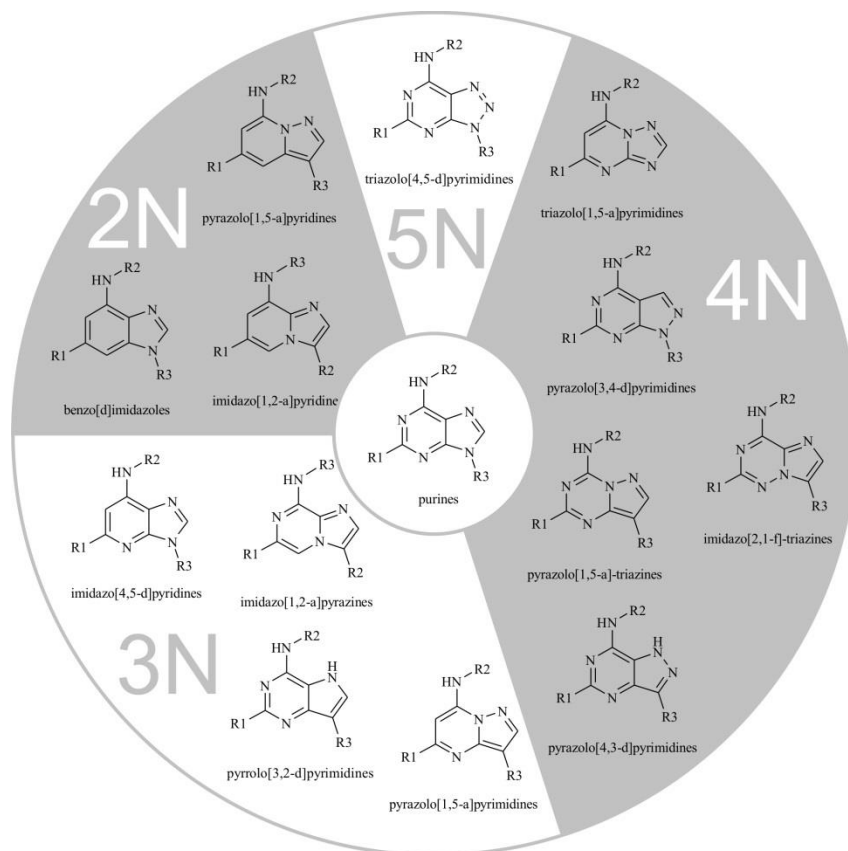


**Figure 2.** Structural motifs of known purine bioisosteres primarily designed as CDK inhibitors.

**Table 1.** CDK Inhibitory and Antiproliferative Activity of Selected Roscovitine Bioisosteres.

Type of Bioisostere	Compound	CDK2/CYCA1C50 (pM)	CDK21CYCE IC <sub>50</sub> (pM)	Average of the growth inhibition [IC <sub>50</sub> ] Number of tested cancer cell lines	Refs.
purine	R-roscovitine	0.22	0.15	19.3 / 60	41,42
pyrazolo[1,5- <i>a</i> ]-1,3,5-triazine	<b>7a</b> <sup>§</sup>	0.04	0.026	1.41 / 60	41,42
imidazo[2,1- <i>f</i> ]-1,2,4-triazine	<b>13</b> <sup>§</sup>	0.22	0.16	25.0 / 6	41
pyrazolo[3,4- <i>d</i> ]pyrimidine	<b>33a</b>	0.5	n.a.	76.3 / 3	50
pyrazolo[1,5- <i>a</i> ]pyrimidine	BS193 <sup>§</sup>	> 1	n.a.	>100 / 1	59
pyrazolo[1,5- <i>a</i> ]pyrimidine	BS181	n.a.	0.88	19.3 / 18	54
pyrazolo[1,5- <i>a</i> ]pyrimidine	<b>13</b> (SCH727965)	0.001	n.a.	0.01 / 13	64,65
imidazo[4,5- <i>d</i> ]pyridine	<b>1a</b> <sup>§</sup>	0.3	0.18	16.1 / 5	46
triazolo[4,5- <i>a</i> ]pyrimidine	<b>79</b> <sup>§</sup>	5.05	n.a.	n.a. / n.a.	44
triazolo[1,5- <i>a</i> ]pyrimidine	<b>6</b>	0.35	0.35	25 / 1	45
triazolo[4,5- <i>d</i> ]pyrimidine	<b>4</b> <sup>§</sup>	n.a.	4.1	82.75 / 4	51
triazolo[4,5- <i>d</i> ]pyrimidine	<b>19</b>	n.a.	1.1	7.6 / 17	51
imidazo[1,2- <i>a</i> ]pyridine	<b>105</b>	n.a.	0.12	n.a. / n.a.	48,49
imidazo[1,2- <i>a</i> ]pyrazine	<b>2</b>	n.a.	0.8	n.a. / n.a.	48
pyrazolo[4,3- <i>d</i> ]pyrimidine	<b>7</b> <sup>§</sup>	n.a.	0.04	10.2 / 60	61
Pyrazolo[4,3- <i>d</i> ]pyrimidine	LGRI406	1.0	0.6	n.a. / n.a.	63

\*compound identifiers refer to those used in original publications; <sup>§</sup> direct analogue of roscovitine (all side chains identical); \* compound closely related to roscovitine (at least two side chains identical).

### Two-nitrogen purine bioisosteres (2N)

While there are many possible two-nitrogen purine bioisosteres, only three groups have been prepared and described to date: imidazo[1,2-*a*]pyridines, pyrazolo[1,5-*a*]pyridines and benzo[*d*]imidazoles.<sup>49,52,66</sup> The CDK inhibitory activity of imidazo[1,2-*a*]pyridines and pyrazolo[1,5-*a*]pyridines is worse than that of pyrazolo[1,5-*a*]pyrimidines and imidazo[1,2-*a*]pyrazines despite the fact that their modes of binding to CDK2 are identical.<sup>48</sup> The 6-O- linked series of benzo[*d*]imidazoles were

designed as potential CDK5 inhibitors, but the direct analogue of roscovitine from this series (**4**) is less potent than the parent compound.<sup>52</sup>

### Three-nitrogen purine bioisosteres (3N)

#### Pyrazolo[1,5-*a*]pyrimidines

Numerous pyrazolo[1,5-*a*]pyrimidines with nanomolar activity against CDK2 have been synthesized to date.<sup>56,58,60,67</sup> The most potent pyrazolo[1,5-*a*]pyrimidines **15j**<sup>58</sup> and **4k** (Fig. 3)<sup>56</sup> were tested on different tumour cell lines (average IC<sub>50</sub>-250 nM). Their mode of binding to CDK2 was studied with several compounds, including **4k** (PDB: 3NS9)<sup>56</sup> and the related **9a** (PDB: 1Y91)<sup>60</sup>, **13** (PDB: 2R3Q)<sup>58</sup> and **9** (PDB: 2R3R).<sup>67</sup> In order to differentiate between series with different pharmacokinetic profiles and *in vitro* activities, an *in vivo* screening approach with integrated efficacy and tolerability parameters was adopted. SCH727965 (Dinaciclib) (Fig. 3) had the best therapeutic index of the tested compounds and was therefore selected for clinical progression.<sup>58,64</sup>

A computer-aided approach yielded a series of pyrazolo[1,5-*a*]pyrimidine-based CDK7 inhibitors.<sup>54,59</sup> The most potent compound was BS-181 (Fig. 3), which strongly inhibits CDK7 (IC<sub>50</sub> = 21 nM), weakly inhibits CDK2 (IC<sub>50</sub> = 0.88 μM), and has no effect on 69 other kinases.<sup>54</sup> It is considered to be the first potent and selective CDK7 inhibitor.<sup>54</sup> The roscovitine analog for this series, BS193, was synthesized but unfortunately did not exhibit any significant selective CDK inhibition.<sup>54</sup>



**Figure 3.** Examples of interesting pyrazolo[1,5-*a*]pyrimidine CDK inhibitors.

### **Imidazo[4,5-*d*]pyridines**

Elimination of the nitrogen atom from position 1 of the purine skeleton (purine numbering) generates the imidazo[4,5-*d*]pyridines. CDK inhibitors of this type have been described in a patent.<sup>46</sup> In general, the activity and selectivity of these compounds is similar to that of the analogous purines, including both enantiomers of roscovitine.

### **Pyrrolo[3,2-*d*]pyrimidines**

Removal of the nitrogen in position 9 (purine numbering) yielded the pyrrolo[3,2-*d*]pyrimidines (9-deazapurines) prepared by Capek *et al.*<sup>43</sup> The olomoucine isostere **1** was synthesized, but did not significantly affect cell growth in a primary biological activity screen.

### **Imidazo[1,2-*a*]pyrazines**

Only a little information is available about the imidazo[1,2-*a*]pyrazines.<sup>47</sup> CDK inhibition data for several derivatives suggest that imidazo[1,2-*a*]pyrazines do not have greater activity than purines even though *ab initio* results indicated that the scaffold would bind more tightly to the hinge region than pyrazolo[1,5-*a*]pyrimidines.<sup>48</sup> The binding mode of some of these compounds to CDK2 (PDB: 2R3G, 2R3H) was recently studied alongside that of other purine bioisosteres such as pyrazolo[1,5-*a*]pyrimidines, pyrazolo[1,5-*a*]pyridines and imidazo[1,2-*a*]pyridines<sup>48</sup>; compound **2** was suggested to have an unusual mode of binding due to the interaction of the fluorophenyl group with the hinge region (Fig. 4).

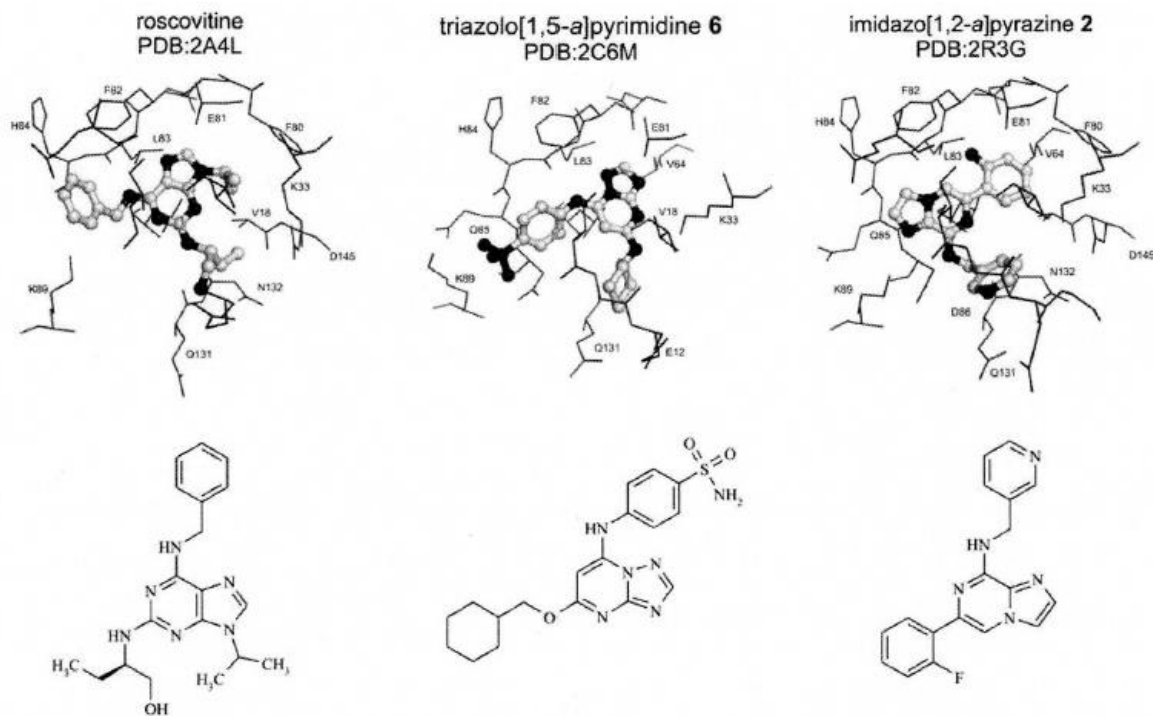


**Figure 4.** Binding modes of roscovitine and some purine bioisosteres in the active site of CDK2. Lines represent amino acid residues of CDK2 with a distance of 4 Å from the ligand. Ligands are shown in a ball and stick representation, with all heteroatoms shown in black.

#### Four-nitrogen purine bioisosteres (4N)

##### Pyrazolo[1,5-*a*]-1,3,5-triazines

Shifting the nitrogen atom at position 9 of the purine skeleton to position 5 yields the pyrazolo[1,5-*a*]-1,3,5-triazines. A large number of those derivatives have been prepared, including analogs of roscovitine and purvalanol.<sup>42</sup> The roscovitine bioisostere **7a** (N-&-NI, GP0210, NSC 743927) was reported to be a pan-selective CDK inhibitor with 2-3 times more activity than roscovitine. However, both **7a** and roscovitine appear to have very similar modes of binding to CDK2 as judged by a superimposition of their conformations in the active site.<sup>41</sup> On average, compound **7a** is 14 times more potent than roscovitine against the NCI panel of 60 tumour cell lines and does not appear to have any bias towards specific types of tumour.<sup>42</sup> Its pharmacokinetic profile is similar to that of roscovitine.<sup>41</sup>

### **Imidazo[2,1-f]-1,2,4-triazines**

A series of imidazo[2,1-*f*]-1,2,4-triazines was prepared, including roscovitine analog **13**. Unfortunately, **13** is a less effective CDK inhibitor than roscovitine<sup>41,42</sup>: it was only observed to have activity against CDKs or to induce antiproliferative effects (as judged by the dephosphorylation of the retinoblastoma protein and changes in the expression of the anti-apoptotic protein Mel-1) at mid-micromolar concentrations.

### **Pyrazolo[3,4-*d*]pyrimidines**

Replacing the pyrazole-like part of the roscovitine purine skeleton with an imidazole yields trisubstituted pyrazolo[3,4-*d*]pyrimidines; a series of olomoucine analogues with this skeleton have been prepared.<sup>50</sup> Most of these compounds did not show any kinase inhibitory activity. This is probably due to the absence of a nitrogen atom at the 7 position (purine numbering), which is crucial for binding to the CDK active site.

### **Triazolo[1,5-*a*]pyrimidines**

The successful identification of potent pyrazolo[1,5-*a*]pyrimidine-based CDK2 inhibitors<sup>60</sup> probably inspired the investigation of the closely related triazolo[1,5-*a*]pyrimidine series.<sup>44,45</sup> A docking study on the pyrazolo[1,5-*a*]pyrimidines suggested that replacing the ligand C3 atom with nitrogen might increase the compounds' potency.<sup>45</sup> Compounds **5** and **6** are analogues of purines NU6102 and H717.<sup>45</sup> Importantly, compound **6** (Fig. 4) showed improved potency for CDK2 inhibition (32-fold) and also showed good activity against CDKI (IC<sub>50</sub> = 140 nM). These findings were supported by X-ray structures of the compound bound to CDK2 (PDB: 2C6M).

### **Pyrazolo[4,3-*d*]pyrimidines**

The first series of pyrazolo[4,3-*d*]pyrimidines prepared contained only two substituents, at the 3- and 7-positions.<sup>68</sup> As those compounds were more potent than the corresponding purines, 3,5,7-trisubstituted derivatives were subsequently synthesized.<sup>69</sup> While comprehensive data on the

structure-activity relationships of these purine bioisosteres have not been published, the anti-cancer/anti-kinase activities of some compounds from this family have been described.<sup>61,63</sup> Compound LGR1406 was examined as a potential inhibitor of abnormal vascular smooth muscle cell proliferation, which contributes to the pathogenesis of restenosis. Compared to roscovitine, LGR1406 is not a more potent CDK inhibitor but it arrested smooth muscle cell proliferation at one fifth of the dosage.<sup>63</sup> The protein kinase selectivity profile and anti-cancer activity of the pyrazolo[4,3-*d*]pyrimidine-based analogue of roscovitine are better than those of roscovitine itself.<sup>61</sup> An X-ray crystal structure of compound **7** bound to CDK2 (PDB: 3PJ8) revealed that its binding mode resembles that of roscovitine.

### **Five-nitrogen purine bioisosteres (5N)**

To date, only one group of purine bioisosteres containing five nitrogen atoms has been reported in the literature: the 1,2,3- triazolo[4,5-*d*]pyrimidines.<sup>51</sup> All of the compounds in this class that have been prepared (including the roscovitine analogue) showed significantly reduced CDK inhibitory activity.<sup>51</sup> Apparently, the nitrogen atom at the 2-position interacts unfavourably with the Glu81 residue of the CDK2 active site.

### **Conclusions**

Of the purine bioisosteres described above, only four classes exhibited better CDK inhibition and/or cytotoxicity than the corresponding purines: the pyrazolo[1,5-*a*] -1,3,5-triazines, pyrazolo[4,3-*d*]pyrimidines, pyrazolo[1,5-*a*]pyrimidines, and pyrazolo[1,5-*a*]pyridines. The greater potency of those analogues is apparently due to the arrangement and number of nitrogen atoms in the five-membered ring that makes direct contact with the hinge region of CDK2:

- The importance of the nitrogen atom at position 7 (purine numbering) is evident from the binding modes of roscovitine and other purine inhibitors in the active site of CDK2.<sup>9</sup> This atom participates in a hydrogen bond with the amino group of Leu83 and, together with the hydrogen at N6 that interacts with carbonyl group of Leu83, creates an optimal donor-acceptor motif in the hinge region of CDK2. Replacing this nitrogen with carbon (to give pyrazolo[3,4-*d*]pyrimidines) yields significantly less effective CDK inhibitors.<sup>50</sup>
- The position of the second nitrogen in the five-membered ring is apparently also important in determining the CDK affinity of purine bioisosteres. The presence of a second nitrogen adjacent to

the 7 position in the heterocyclic core (i.e. at position 5 or 8 of the purine skeleton) has a modest effect on the compounds' electrostatic potential<sup>41</sup> and markedly increases the CDK2 affinity of all four listed groups of bioisosteres.

- The number of nitrogen atoms in the five-membered ring seems to be an important variable in determining inhibitory activity: all active inhibitors have only 2 nitrogens here. As demonstrated by the triazolo[1,5-*a*]pyrimidines and triazolo[4,5-*d*]pyrimidines, adding a third nitrogen to ring generates less effective inhibitors.<sup>45,51</sup>

In sum, ligand-based design has yielded new structurally diverse CDK inhibitors with improved biochemical and biological properties in some cases. As demonstrated for the heterocyclic skeleton of the purine-related CDK inhibitors, bioisosteric replacement represents a valid strategy for innovating from the structures of known drugs. The structure-activity relationships summarized in this review suggest that the pyrazolo[1,5-*a*]pyrimidine derivative dinaciclib, which is currently going through phase II clinical trials, can be considered a bioisostere of roscovitine, one of the best known CDK inhibitors.

## References

1. Lapenna, S.; Giordano, A. Cell cycle kinases as therapeutic targets for cancer. *Nat. Rev. Drug Discov.* **2009**, *8*, 547-66.
2. Knockaert, M.; Greengard, P.; Meijer, L. Pharmacological inhibitors of cyclin-dependent kinases. *Trends Pharmacol. Sci.* **2002**, *23*, 417-25.
3. Senderowicz, A. M. Small molecule modulators of cyclin-dependent kinases for cancer therapy. *Oncogene* **2000**, *19*, 6600-6.
4. Malumbres, M.; Camero, A. Cell cycle deregulation: a common motif in cancer. *Prog. Cell Cycle Res.* **2003**, *5*, 5-18.
5. Malumbres, M.; Barbacid, M. Cell cycle, CDKs and cancer: a changing paradigm. *Nat. Rev. Cancer* **2009**, *9*, 153-66.
6. Blagosklonny, M. V. Flavopiridol, an inhibitor of transcription: implications, problems and solutions. *Cell Cycle* **2004**, *3*, 1537-42.
7. Meijer, L.; Bettayeb, K.; Galons, H. (R)-Roscovitine (CYC202, Seliciclib). In: Smith, P. J; Yue, E. W., Eds. *Inhibitors of cyclin-dependent kinases as anti-tumor agents*. Boca Raton, FL: CRC Press, **2006**, pp 187-226.
8. Sedlacek, H. H. Mechanisms of action of flavopiridol. *Crit. Rev. Oncol. Hematol.* **2001**, *38*, 139-70.
9. Davies, T. G.; Pratt, O. J.; Endicott, J. A.; Johnson, L. N.; Noble, M. E. Structure-based design of cyclin-dependent kinase inhibitors. *Pharmacol. Ther.* **2002**, *93*, 125-33.
10. Honma, T.; Hayashi, K.; Aoyama, T. *et al.*. Structure-based generation of a new class of potent Cdk4 inhibitors: new de novo design strategy and library design. *J. Med. Chem.* **2001**, *44*, 4615-27.
11. Wyatt, P. G.; Woodhead, A. J.; Berdini, V. *et al.* Identification of N-(4-piperidinyl)-4-(2,6-dichlorobenzoylamino)-1H-pyrazole-3-carboxamide (AT7519), a novel cyclin dependent kinase inhibitor using fragment-based X-ray crystallography and structure based drug design. *J. Med. Chem.* **2008**, *51*, 4986-99.
12. Joshi, K. S.; Rathos, M. J.; Joshi, R. D. *et al.* *In vitro* antitumor properties of a novel cyclin-dependent kinase inhibitor, P276-00. *Mol. Cancer Ther.* **2007**, *6*, 918-25.
13. Siemeister, G.; Luecking, U.; Wagner, C.; Detjen, K.; Me, C. C.; Bosslet, K. Molecular and pharmacodynamic characteristics of the novel multi-target tumor growth inhibitor ZK 304709. *Biomed. Pharmacother.* **2006**, *60*, 269-72.
14. Brasca, M. G.; Amboldi N.; Ballinari, D. *et al.* Identification of N,1,4,4-tetramethyl-8-[[4-(4-methylpiperazin-1-yl)phenyl]amino]-4,5-dihydro-1H-pyrazolo[4,3-h]quinazoline-3-carboxamide (PHA-848125), a potent, orally available cyclin dependent kinase inhibitor. *J. Med. Chem.* **2009**, *52*,

5152-63.

15. Fry, O. W.; Harvey, P. J.; Keller, P. R. *et al.* Specific inhibition of cyclin- dependent kinase 4/6 by PD 0332991 and associated antitumor activity in human tumor xenografts. *Mol. Cancer Ther.* **2004**, *3*, 1427-38.
16. Havlicek, L.; Hanus, J.; Vesely, J. *et al.* Cytokinin-derived cyclin- dependent kinase inhibitors: synthesis and cdc2 inhibitory activity of olomoucine and related compounds. *J. Med. Chem.* **1997**, *40*, 408-12.
17. Meijer, L.; Borgne, A.; Mulner, O. *et al.* Biochemical and cellular effects of roscovitine, a potent and selective inhibitor of the cyclin- dependent kinases cdc2, cdk2 and cdk5. *Eur. J. Biochem.* **1997**, *243*, 527-36.
18. Vesely, J.; Havlicek, L.; Strnad, M. *et al.* Inhibition of cyclin-dependent kinases by purine analogues. *Eur. J. Biochem.* **1994**, *224*, 771-86.
19. Guzi, T. CYC-202 Cyclacel. *Curr. Opin. Investig. Drugs* **2004**, *5*, 1311-8.
20. Meijer, L.; Raymond, E. Roscovitine and other purines as kinase inhibitors. From starfish oocytes to clinical trials. *Acc. Chem. Res.* **2003**, *36*, 417-25.
21. Krystof, V.; McNae, I. W.; Walkinshaw, M. D. *et al.* Antiproliferative activity of olomoucine II, a novel 2,6,9-trisubstituted purine cyclin- dependent kinase inhibitor. *Cell. Mol. Life Sci.* **2005**, *62*, 1763-71.
22. McClue, S. J, Blake, D.; Clarke, R. *et al.* In vitro and in vivo antitumor properties of the cyclin dependent kinase inhibitor CYC202 (R- roscovitine). *Int. J. Cancer* **2002**, *102*, 463-8.
23. Barrie, S. E.; Eno-Amooquaye, E.; Hardcastle, A. *et al.* High-throughput screening for the identification of small-molecule inhibitors of retinoblastoma protein phosphorylation in cells. *Anal. Biochem.* **2003**, *320*, 66-74.
24. MacCallum, D. E.; Melville, J.; Frame, S. *et al.* Seliciclib (CYC202, R-Roscovitine) induces cell death in multiple myeloma cells by inhibition of RNA polymerase II-dependent transcription and down-regulation of Mcl-1 . *Cancer Res.* **2005**, *65*, 5399-407.
25. Paprskarova, M.; Krystof, V.; Jorda, R. *et al.* Functional p53 in cells contributes to the anticancer effect of the cyclin-dependent kinase inhibitor roscovitine. *J. Cell Biochem.* **2009**, *107*, 428-37.
26. Raynaud, F. I.; Whittaker, S. R.; Fischer, P. M. *et al.* In vitro and in vivo pharmacokinetic-pharmacodynamic relationships for the trisubstituted aminopurine cyclin-dependent kinase inhibitors olomoucine, bohemine and CYC202. *Clin. Cancer Res.* **2005**, *11*, 4875-87.
27. Whittaker, S R.; Walton, M. I.; Garrett, M. D.; Workman, P. The Cyclin-dependent kinase inhibitor CYC202 (R-roscovitine) inhibits retinoblastoma protein phosphorylation, causes loss of Cyclin D1, and activates the mitogen-activated protein kinase pathway. *Cancer Res.* **2004**, *64*, 262-

72.

28. Ljungman, M.; Paulsen, M. T. The cyclin-dependent kinase inhibitor roscovitine inhibits RNA synthesis and triggers nuclear accumulation of p53 that is unmodified at Ser15 and Lys382. *Mol. Pharmacol.* **2001**, *60*, 785-9.

29. Cyclacel Pharmaceuticals [homepage on the Internet] Berkeley Heights, NJ 07922, United States of America. Available from <http://cyclacel.com>.

30. Clinical trials [homepage on the internet], U.S. National Library of Medicine, 8600 Rockville Pike, Bethesda, MD 20894. Available from <http://clinicaltrials.gov>.

31. Dreyer, M. K.; Borcharding, D. R.; Dumont, J. A. *et al.* Crystal structure of human cyclin-dependent kinase 2 in complex with the adenine-derived inhibitor H717. *J. Med. Chem.* **2001**, *44*, 524-30.

32. Chang, Y. T.; Gray, N. S.; Rosania, G. R. *et al.* Synthesis and application of functionally diverse 2,6,9-trisubstituted purine libraries as CDK inhibitors. *Chem. Biol.* **1999**, *6*, 361-75.

33. Gray, N. S.; Wodicka, L.; Thunnissen, A. M. *et al.* Exploiting chemical libraries, structure, and genomics in the search for kinase inhibitors. *Science* **1998**, *281*, 533-8.

34. Shum, P. W.; Peet, N. P.; Weintraub, P. M. *et al.* The design and synthesis of purine inhibitors of CDK2. III. *Nucleosides Nucleotides Nucleic Acids* **2001**, *20*, 1067-78.

35. Oh, C. H.; Kim, H. K.; Lee, S. C. *et al.* Synthesis and biological properties of C-2, C-8, N-9 substituted 6-(3-chloroanilino)purine derivatives as cyclin-dependent kinase inhibitors. Part II. *Arch. Pharm. (Weinheim)* **2001**, *334*, 345-50.

36. Hardcastle, I. R.; Arris, C. E.; Bentley, J. *et al.* N2-substituted O6-cyclohexylmethylguanine derivatives: potent inhibitors of cyclin-dependent kinases 1 and 2. *J. Med. Chem.* **2004**, *47*, 3710-22.

37. Bettayeb, K.; Oumata, N.; Echalié, A. *et al.* CR8, a potent and selective, roscovitine-derived inhibitor of cyclin-dependent kinases. *Oncogene* **2008**, *27*, 5797-807.

38. Oumata, N.; Bettayeb, K.; Ferandin, Y. *et al.* Roscovitine-derived, dual-specificity inhibitors of cyclin-dependent kinases and casein kinases 1. *J. Med. Chem.* **2008**, *51*, 5229-42.

39. Trova, M. P.; Barnes, K. D.; Alicea, L. *et al.* Heterobiaryl purine derivatives as potent antiproliferative agents: inhibitors of cyclin dependent kinases. Part 11. *Bioorg. Med. Chem. Lett.* **2009**, *19*, 6613-7.

40. Trova, M. P.; Barnes, K. D.; Barford, C. *et al.* Biaryl purine derivatives as potent antiproliferative agents: inhibitors of cyclin dependent kinases. Part I. *Bioorg. Med. Chem. Lett.* **2009**, *19*, 6608-12.

41. Bettayeb, K.; Sallam, H.; Ferandin, Y. *et al.* N-&-N, a new class of cell death-inducing kinase inhibitors derived from the purine roscovitine. *Mol. Cancer Ther.* **2008**, *7*, 2713-24.

42. Popowycz, F.; Fournet, G.; Schneider, C. *et al.* Pyrazolo[1,5-a]-1,3,5-triazine as a purine

bioisostere: access to potent cyclin-dependent kinase inhibitor (R)-roscovitine analogue. *J. Med. Chem.* **2009**, *52*, 655-63.

43. Capek, P.; Otrnar, M.; Masojdkova, M.; Votruba, I.; Holy, A. A facile synthesis of 9-deaza analogue of olomoucine. *Coll. Czech. Chem. Commun.* **2003**, *68*, 779-91 .

44. Bower, J. F.; Cansfield, A.; Jordan, A.; Parrat, M.; Walmsley, L.; Williamson, D. inventors; Triazolo[1,5-a]pyrimidines and their use in medicine. *WO 2004/108136*. 2004 Dec 16.

45. Richardson, C. M.; Williamson, D. S.; Parratt, M. J. *et al.* Triazolo[1,5-a]pyrimidines as novel CDK2 inhibitors: protein structure-guided design and SAR. *Bioorg. Med. Chem. Lett.* **2006**, *16*, 1353-7.

46. Meijer, L.; Bettayeb, K.; Galons, H.; Demange, L.; Oumata, N. inventors; Perharidines as CDK inhibitors. *WO 2009/034411*. 2009 Mar 19.

47. Paruch, K.; Guzi, T. J.; Dwyer, M. P.; Doll, R. J.; Girijavallabhan, V. M.; Mallams, A. K. inventors; Imidazopyrazines as cyclin dependent kinase inhibitors. *WO 2004/026877*. 2004 Apr 1.

48. Fischmann, T. O.; Hruza, A.; Duca, J. S. *et al.* Structure-guided discovery of cyclin-dependent kinase inhibitors. *Biopolymers* **2008**, *89*, 372-9.

49. Dwyer, M. P.; Guzi, T. J.; Paruch, K.; Doll, R. J.; Keertikar, K. M.; Girijavallabhan, V. M. inventors; Novel imidazopyridines as cyclin- dependent kinase inhibitors. *WO 2004/026867*. 2004 Apr 1.

50. Kim, D. C.; Lee, Y. R.; Yang, B. S.; Shin, K. J.; Kim, O. J.; Chung, B. Y.; Yoo, K. H. Synthesis and biological evaluations of pyrazolo[3,4-d]pyrimidines as cyclin-dependent kinase 2 inhibitors. *Eur. J. Med. Chem.* **2003**, *38*, 525-32.

51. Havlicek, L.; Fuksova, K.; Krystof, V.; Orsag, M.; Vojtesek, B.; Strnad, M. 8-Azapurines as new inhibitors of cyclin-dependent kinases. *Bioorg. Med. Chem.* **2005**, *13*, 5399-407.

52. Jain, P.; Flaherty, P. T.; Yi, S. *et al.* Design, synthesis, and testing of an 6-O-linked series of benzimidazole based inhibitors of CDK5/p25. *Bioorg. Med. Chem.* **2011**, *19*, 359-73.

53. Guzi, T. J.; Paruch, K. inventors; Pyrazolotriazines as kinase inhibitors. *WO 2005/082908*. 2005 Sep 9.

54. Ali, S.; Heathcote, D. A.; Kroll, S. H. *et al.* The development of a selective cyclin-dependent kinase inhibitor that shows antitumor activity. *Cancer Res.* **2009**, *69*, 6208-15.

55. Chen, F. X.; Keertikar, K.; Kuo, S. *et al.* inventors; Process and intermediates for the synthesis of (3-alkyl-5-piperidin-1-yl-3,3a-dihydropyrazolo[1,5-a]-pyrimidin-7-yl)-aminoderivatives and intermediates. *WO 2008/027220*. 2008 Mar 6.

56. Heathcote, D. A.; Patel, H.; Kroll, S. H. *et al.* A novel pyrazolo[1,5-a]pyrimidine is a potent inhibitor of cyclin-dependent protein kinases 1, 2, and 9, which demonstrates antitumor effects in

- human tumor xenografts following oral administration. *J. Med. Chem.* **2010**, *53*, 8508-22.
57. Parratt, M. J.; Bower, J. F.; Williams, J. W.; Cansfield, A. D. inventors; Pyrazolopyrimidine compounds and their use in medicine. *WO 2004/087707*. 2004 Oct 14.
58. Paruch, K.; Dwyer, M. P.; Alvarez, C. *et al.* Pyrazolo[1,5-a]pyrimidines as orally available inhibitors of cyclin-dependent kinase 2. *Bioorg. Med. Chem. Lett.* **2007**, *17*, 6220-3.
59. Snyder, J. P.; Liotta, D. C.; Barrett, A. G. *et al.* inventors; Selective inhibitors for cyclin-dependent kinases. *WO 20081151304*. 2008 Dec 11.
60. Williamson, O. S.; Parratt, M. J.; Bower, J. F. *et al.* Structure-guided design of pyrazolo[1,5-a]pyrimidines as inhibitors of human cyclin-dependent kinase 2. *Bioorg. Med. Chem. Lett.* **2005**, *15*, 863-7.
61. Jorda, R.; Havlicek L.; McNae, I. W. *et al.* Pyrazolo[4,3-d]pyrimidine bioisostere of roscovitine: evaluation of a novel selective inhibitor of cyclin-dependent kinases with antiproliferative activity. *J. Med. Chem.* **2011**, *54*, 2980-93.
62. Krystof, V.; Moravcova, D.; Paprskarova, M. *et al.* Synthesis and biological activity of 8-azapurine and pyrazolo[4,3-d]pyrimidine analogues of myoseverin. *Eur. J. Med. Chem.* **2006**, *41*, 1405-11.
63. Sroka, I. M.; Heiss, E. H.; Havlicek, L. *et al.* A novel roscovitine derivative potently induces G1-phase arrest in platelet-derived growth factor-BB-activated vascular smooth muscle cells. *Mol. Pharmacol.* **2010**, *77*, 255-61.
64. Parry, D.; Guzi, T.; Shanahan, F. *et al.* Dinaciclib (SCH 727965), a novel and potent cyclin-dependent kinase inhibitor. *Mol. Cancer Ther.* **2010**, *9*, 2344-53.
65. Paruch, K.; Dwyer, M. P.; Alvarez, C. *et al.* Discovery of Dinaciclib (SCH 727965): A Potent and Selective Inhibitor of Cyclin- Dependent Kinases. *ACS Med. Chem. Lett.* **2010**, *1*, 204-8.
66. Dwyer, M. P.; Guzi, T. J.; Paruch, K.; Doll, R. J.; Keertikar, K. M.; Girijavallabhan, V. M. inventors; Pyrazolopyridines as cyclin-dependent kinase inhibitors. *WO 2004/026872*. 2004 Apr I.
67. Dwyer, M. P.; Paruch, K.; Alvarez, C. *et al.* Versatile templates for the development of novel kinase inhibitors: Discovery of novel CDK inhibitors. *Bioorg. Med. Chem. Lett.* **2007**, *17*, 6216-9.
68. Moravcova, D.; Krystof, V.; Havlicek, L.; Moravec, J.; Lenobel, R.; Strnad, M. Pyrazolo[4,3-d]pyrimidines as new generation of cyclin-dependent kinase inhibitors. *Bioorg. Med. Chem. Lett.* **2003**, *13*, 2989-92.
69. Moravcova, D.; Havlicek, L.; Krystof, V.; Lenobel, R.; Strnad, M. inventors; Novel pyrazolo[4,3-d]pyrimidines, processes for their preparation and method for therapy. *WO 2003/082872*. 2003 Oct 9.

## Part 3b

### Fuopyridines as inhibitors of protein kinases\*

\*published as:

Paruch, K.;\* Petruřjová, M.; Němec, V. Fuopyridines as inhibitors of protein kinases *PCT Int. Appl.* **2015**, *WO 2015165428 A1*.

#### Field of the Invention

The present invention relates to substituted furo[3,2-*b*]pyridines as inhibitors of various protein kinases, regulators or modulators, pharmaceutical compositions containing the compounds, and pharmaceutical use of the compounds and compositions in the treatment of the diseases such as, for example, cancer, inflammation, pain, neurodegenerative diseases or viral infections.

#### Background

Protein kinases are involved in regulation of practically all processes that are central to the growth, development, and homeostasis of eukaryotic cells. In addition, some protein kinases have an important role in oncogenesis and tumor progression and several kinase inhibitors are now approved for the treatment of cancer (D. J. Matthews and M. E. Gerritsen: *Targeting protein kinases for cancer therapy*, Wiley, 2010).

Examples of kinase inhibitors that are used in modern oncology include: imatinib (treatment of CML); dasatinib (CML with resistance to prior treatment, including imatinib); nilotinib (CML); bosutinib (CML); gefitinib (non-small cell lung cancer); erlotinib (non-small cell lung cancer and pancreatic cancer); lapatinib (breast cancer); sorafenib (metastatic renal cell carcinoma, hepatocellular cancer); vandetanib (metastatic medullary thyroid cancer); vemurafenib (inoperable or metastatic melanoma); crizotinib (non-small cell lung cancer); sunitinib (metastatic renal cell carcinoma, gastrointestinal stromal tumor that is not responding to imatinib, or pancreatic neuroendocrine tumors); pazopanib (renal cell carcinoma and advanced soft tissue sarcoma); regorafenib (metastatic colorectal cancer); cabozantinib (metastatic medullary thyroid cancer); dabrafenib (BRAF V600E mutation-positive advanced melanoma); and trametinib (in combination with dabrafenib for the treatment of BRAF V600E/K-mutant metastatic melanoma).

Various kinases are regarded as good targets for pharmacological inhibition in order to treat proliferative and/or neurodegenerative diseases. Biological and potential therapeutic significance of some selected kinases is briefly summarized below.

The regulation of splice site usage provides a versatile mechanism for controlling gene expression and for the generation of proteome diversity, playing an essential role in many biological processes. The importance of alternative splicing is further illustrated by the increasing number of human diseases that have been attributed to mis-splicing events. Appropriate spatial and temporal generation of splicing variants demands that alternative splicing be subjected to extensive regulation, similar to transcriptional control. The CLK (Cdc2-like kinase) family has been implicated in splicing control (*Experimental Cell Research* **1998**, 241, 300.). Pharmacological inhibition of CLK1/Sty results in blockage of SF2/ASF-dependent splicing of beta-globin pre-mRNA *in vitro* by suppression of CLK-mediated phosphorylation. It also suppresses dissociation of nuclear speckles as well as CLK1/Sty-dependent alternative splicing in mammalian cells and was shown to rescue the embryonic defects induced by excessive CLK activity in *Xenopus* (*Journal of Biological Chemistry* **2004**, 279, 24246.).

Alternative mRNA splicing is a mechanism to regulate protein isoform expression and is regulated by alternative splicing factors. The alternative splicing factor 45 (SPF45) is overexpressed in cancer and its overexpression enhances two processes that are important for metastasis, i.e. cell migration and invasion, dependent on biochemical regulation by CLK1 (*Nucleic Acids Research* **2013**, 41, 4949.). CLK1 phosphorylates SPF45 on eight serine residues. CLK1 expression enhances, whereas CLK1 inhibition reduces, SPF45-induced exon 6 exclusion from Fas mRNA. Inhibition of CLK1 increases SPF45 degradation through a proteasome-dependent pathway. In addition, small-molecule inhibitors of specific CLKs can suppress HIV-1 gene expression and replication (*Retrovirology* **2011**, 8, 47.), which could be used in concert with current drug combinations to achieve more efficient treatment of the infection. Inhibition of CLK1 can be applicable in the treatment of Alzheimer's disease (*Current Drug Targets* **2014**, 15, 539.).

DYRK (dual specificity tyrosine phosphorylation-regulated kinase) family enzymes are essential components of important signaling cascades in the pathophysiology of cancer and Alzheimer's disease and their biological expression levels regulate key signaling processes in these diseases. In particular, DYRK2 is over-expressed in adenocarcinomas of the esophagus and lung (*Cancer Research* **2003**, 63, 4136.) and DYRK1A in glioblastoma where its inhibition compromised tumors' survival and produced a profound decrease in tumor burden (*Journal of Clinical Investigation* **2013**, 123, 2475.). DYRK1B activation that is induced by microtubule damage triggers microtubule

stabilization and promotes the mitochondrial translocation of p21Cip1/waf1 to suppress apoptosis. Its inhibition caused reduced viability of cancer cells (*ACS Chemical Biology* **2014**, *9*, 731.). Correspondingly, it has been understood that inhibition of DYRK kinases alone or in combination with other chemotherapeutic drugs may have tumor suppression effect and the enzymes are therefore appropriate targets for pharmacological inhibition (*Bioorganic & Medicinal Chemistry Letters* **2013**, *23*, 6610.; *Medicinal Chemistry Research* **2014**, *23*, 1925.).

In addition, DYRK kinases are also over-expressed in neurodegenerative diseases such as Alzheimer's disease, Parkinson's disease, Huntington's disease, and Pick disease (*Neurobiology of Disease* **2005**, *20*, 392.; *Cellular and Molecular Life Sciences* **2009**, *66*, 3235.).

HIPK2 (homeodomain-interacting protein kinase) is a tumor suppressor and functions as an evolutionary conserved regulator of signaling and gene expression. This kinase regulates a vast array of biological processes that range from the DNA damage response and apoptosis to hypoxia signaling and cell proliferation. Recent studies showed the tight control of HIPK2 by hierarchically occurring posttranslational modifications such as phosphorylation, small ubiquitin-like modifier modification, acetylation, and ubiquitination. Dysregulation of HIPK2 can result in increased proliferation of cell populations as it occurs in cancer or fibrosis. Inappropriate expression, modification, or localization of HIPK2 can be a driver for these proliferative diseases (*Journal of Molecular Medicine* **2013**, *91*, 1051.).

FMS-like tyrosine kinase 3 (FLT3), a receptor tyrosine kinase (RTK), is a membrane-bound receptor with an intrinsic tyrosine kinase domain. Its activation regulates a number of cellular processes (e.g. phospholipid metabolism, transcription, proliferation, and apoptosis), and through these processes, FLT3 activation plays a critical role in governing normal hematopoiesis and cellular growth. Expression of FLT3 has been evaluated in hematologic malignancies. The majority of B-cell acute lymphocytic leukemia (ALL) and acute myeloid leukemia (AML) blasts (> 90%) express FLT3 at various levels (*Clinical Cancer Research* **2009**, *15*, 4263.). Overexpression or/and activating mutation of FLT3 kinase play a major driving role in the pathogenesis of acute myeloid leukemia (AML). Hence, pharmacologic inhibitors of FLT3 are of therapeutic potential for AML treatment (*Oncologist* **2011**, *16*, 1162.; *PLoS One* **2014**, *9*, e83160/1.; *Leukemia Lymphoma* **2014**, *55*, 243.).

Tropomyosin-related kinase (TRK) is a family of three RTKs (TRK-A, TRK-B, TRK-C) regulating several signaling pathways that are important for survival and differentiation of neurons. TRK-A regulates proliferation and is important for development and maturation of the nervous system, promotes survival of cells from death. Point mutations, deletions and chromosomal rearrangements

cause ligand-independent receptor dimerization and activation of TRK-A. In mutated version of TRK, abnormal function will render cells unable to undergo differentiation in response to ligand in their microenvironment, so they would continue to grow when they should differentiate, and survive when they should die.

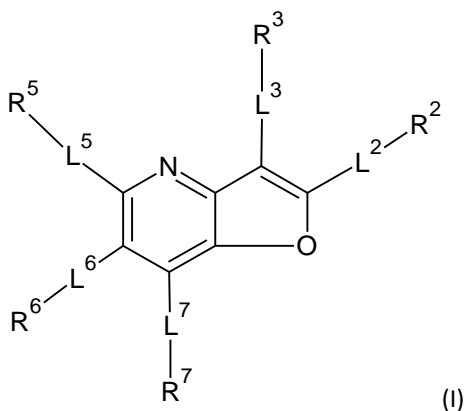
Activated TRK-A oncogenes have been associated with several human malignancies, e.g., breast, colon, prostate, thyroid carcinomas and AML (*Cell Cycle* **2005**, 4, 8.; *Cancer Letters* **2006**, 232, 90.). In addition, inhibition of TRK can be relevant for the treatment of inflammation (*PLoS One* **2013**, 8, e83380.) and pain (*Expert Opinion on Therapeutic Patents* **2009**, 19, 305.).

In summary, there is a need for inhibitors of different protein kinases in order to treat or prevent disease states associated with abnormal regulation of the kinases-mediated biological processes.

## Disclosure of the Invention

The present invention provides substituted furo[3,2-*b*]pyridine compounds, methods of preparing such compounds, pharmaceutical compositions comprising one or more of such compounds, and their use in the treatment, prevention, inhibition or amelioration of one or more diseases associated with protein kinases using such compounds or pharmaceutical compositions.

The present invention provides compounds represented by the structural formula (I):



or a pharmaceutically acceptable salt, solvate or a prodrug thereof, wherein:

L<sup>5</sup> is selected from the group consisting of a bond, -N(R<sup>11</sup>)-;

L<sup>2</sup> is selected from the group consisting of a bond, -O-;

L<sup>3</sup> is selected from the group consisting of a bond, -N(R<sup>11</sup>)-, -O-;

L<sup>6</sup> is selected from the group consisting of a bond, -O-;

L<sup>7</sup> is selected from the group consisting of a bond, -N(R<sup>11</sup>)-;

R<sup>5</sup> is selected from the group consisting of C<sub>1</sub>-C<sub>6</sub> alkyl; aryl; heteroaryl; biaryl; bi(heteroaryl); cycloalkylaryl; heterocyclaryl; heteroarylaryl; arylheteroaryl; cycloalkylheteroaryl; heterocyclheteroaryl; wherein each of the substituent moieties can be unsubstituted or optionally substituted;

R<sup>2</sup> is selected from the group consisting of H; -CF<sub>3</sub>; NH<sub>2</sub>; -Cl; -Br; -F; C<sub>1</sub>-C<sub>6</sub> alkyl;

R<sup>3</sup> is selected from the group consisting of H; C<sub>1</sub>-C<sub>6</sub> alkyl; aryl; cycloalkyl; heteroaryl; biaryl; heteroarylaryl; arylheteroaryl; wherein each of the substituent moieties can be unsubstituted or optionally substituted;

R<sup>6</sup> is selected from the group consisting of H; -CF<sub>3</sub>; NH<sub>2</sub>; -Cl; -Br; -F; C<sub>1</sub>-C<sub>6</sub> alkyl; aryl; heteroaryl; wherein each of the substituent moieties can be unsubstituted or optionally substituted;

R<sup>7</sup> is selected from the group consisting of H; C<sub>1</sub>-C<sub>6</sub> alkyl; aryl; cycloalkyl; heteroaryl; biaryl; heteroarylaryl; arylheteroaryl; wherein each of the substituent moieties can be unsubstituted or optionally substituted;

R<sup>11</sup> is selected from the group consisting of H, C<sub>1</sub>-C<sub>6</sub> alkyl;

provided that the substituent in position 5 (L5-R5) is not oxadiazolyl or methyl-oxadiazolyl.

As used in this disclosure, the following terms, unless otherwise indicated, have the following meanings:

“alkyl” means an aliphatic hydrocarbon group which may be straight or branched and contains 1 to 6 carbon atoms, more preferably 1 to 4 carbon atoms in the chain. Examples of suitable alkyls are methyl, ethyl, propyl, isopropyl, butyl, isobutyl, tert-butyl, pentyl, isopentyl, hexyl. The alkyl can be unsubstituted or optionally substituted by one or more substituents which can be the same or different, each substituent being independently selected from the group consisting of F, Cl, Br, CF<sub>3</sub>, OCF<sub>3</sub>, OR<sup>9</sup>, SR<sup>9</sup>, SOH, SO<sub>2</sub>H, SO<sub>2</sub>N(H, C<sub>1</sub>-C<sub>4</sub> alkyl)<sub>2</sub>, CHO, COO(H, C<sub>1</sub>-C<sub>4</sub> alkyl), COH, C(O)N(H, C<sub>1</sub>-C<sub>4</sub> alkyl), O(CH<sub>2</sub>)<sub>p</sub>N(CH<sub>3</sub>)<sub>2</sub> and NR<sup>9</sup>R<sup>10</sup>;

“aryl” means an aromatic monocyclic or polycyclic ring system containing 6 to 14 carbon atoms, preferably 6 to 10 carbon atoms. Examples of suitable aryls are phenyl, naphthyl. The aryl can be unsubstituted or optionally substituted by one or more substituents which can be the same or different, each substituent being independently selected from the group consisting of F, Cl, Br, CF<sub>3</sub>, OCF<sub>3</sub>, OR<sup>9</sup>, SR<sup>9</sup>, SOH, SO<sub>2</sub>H, SO<sub>2</sub>N(H, C<sub>1</sub>-C<sub>4</sub> alkyl)<sub>2</sub>, CHO, COO(H, C<sub>1</sub>-C<sub>4</sub> alkyl), COH, C(O)N(H, C<sub>1</sub>-C<sub>4</sub> alkyl), NR<sup>9</sup>R<sup>10</sup>, -(CR<sup>9</sup>R<sup>10</sup>)<sub>p</sub>R<sup>9a</sup>, O(CH<sub>2</sub>)<sub>p</sub>N(CH<sub>3</sub>)<sub>2</sub> and -(CR<sup>9</sup>R<sup>10</sup>)<sub>p</sub>OR<sup>9a</sup>;

“cycloalkyl” means an aliphatic monocyclic or bicyclic ring system comprising 3 to 10 carbon atoms, preferably 5 to 7 carbon atoms. Suitable examples include cyclopentyl, cyclohexyl, cycloheptyl, 1-decalinyl, norbornyl, adamantyl. The cycloalkyl can be unsubstituted or optionally substituted by one or more substituents which can be the same or different, each substituent being independently selected from the group consisting of F, Cl, Br, CF<sub>3</sub>, OCF<sub>3</sub>, OR<sup>9</sup>, SR<sup>9</sup>, SOH, SO<sub>2</sub>H, SO<sub>2</sub>N(H, C<sub>1</sub>-C<sub>4</sub> alkyl)<sub>2</sub>, CHO, COO(H, C<sub>1</sub>-C<sub>4</sub> alkyl), COH, C(O)N(H, C<sub>1</sub>-C<sub>4</sub> alkyl), NR<sup>9</sup>R<sup>10</sup>, -(CR<sup>9</sup>R<sup>10</sup>)<sub>p</sub>R<sup>9a</sup>, O(CH<sub>2</sub>)<sub>p</sub>N(CH<sub>3</sub>)<sub>2</sub> and -(CR<sup>9</sup>R<sup>10</sup>)<sub>p</sub>OR<sup>9a</sup>;

“heterocyclyl” means an aliphatic monocyclic or bicyclic ring system containing 3 to 10 carbon atoms, preferably 4 to 8 carbon atoms, and at least one heteroatom selected from the group consisting of nitrogen, oxygen and sulfur. Suitable examples include piperazinyl and morpholinyl. Preferably, heterocyclyl is not a bicyclic ring system containing only N heteroatoms. The heterocyclyl can be unsubstituted or optionally substituted by one or more substituents which can

be the same or different, each substituent being independently selected from the group consisting of F, Cl, Br, CF<sub>3</sub>, OCF<sub>3</sub>, OR<sup>9</sup>, SR<sup>9</sup>, SOH, SO<sub>2</sub>H, SO<sub>2</sub>N(H, C<sub>1</sub>-C<sub>4</sub> alkyl)<sub>2</sub>, CHO, COO(H, C<sub>1</sub>-C<sub>4</sub> alkyl), COH, C(O)N(H, C<sub>1</sub>-C<sub>4</sub> alkyl), NR<sup>9</sup>R<sup>10</sup>, -(CR<sup>9</sup>R<sup>10</sup>)<sub>p</sub>R<sup>9a</sup>, O(CH<sub>2</sub>)<sub>p</sub>N(CH<sub>3</sub>)<sub>2</sub> and -(CR<sup>9</sup>R<sup>10</sup>)<sub>p</sub>OR<sup>9a</sup>;

“heteroaryl” means an aromatic monocyclic or bicyclic ring system containing 1 to 14 carbon atoms, preferably 3 to 7 carbon atoms, most preferably 3 to 5 carbon atoms, and at least one heteroatom selected from the group consisting of nitrogen, oxygen and sulfur. Examples of suitable heteroaryls are pyrazolyl, pyridyl, pyrimidinyl, pyrazinyl, furanyl, thienyl, oxazolyl, thiazolyl, isothiazolyl, isoxazolyl, pyrrolyl, imidazolyl. Preferably, heteroaryl is not indolyl, indolinolyl or imidazopyridazinyl. The heteroaryl can be unsubstituted or optionally substituted by one or more substituents which can be the same or different, each substituent being independently selected from the group consisting of F, Cl, Br, CF<sub>3</sub>, OCF<sub>3</sub>, OR<sup>9</sup>, SR<sup>9</sup>, SOH, SO<sub>2</sub>H, SO<sub>2</sub>N(H, C<sub>1</sub>-C<sub>4</sub> alkyl)<sub>2</sub>, CHO, COO(H, C<sub>1</sub>-C<sub>4</sub> alkyl), COH, C(O)N(H, C<sub>1</sub>-C<sub>4</sub> alkyl), NR<sup>9</sup>R<sup>10</sup>, -(CR<sup>9</sup>R<sup>10</sup>)<sub>p</sub>R<sup>9a</sup>, O(CH<sub>2</sub>)<sub>p</sub>N(CH<sub>3</sub>)<sub>2</sub> and -(CR<sup>9</sup>R<sup>10</sup>)<sub>p</sub>OR<sup>9a</sup>;

“biaryl” means an aryl-aryl- group in which each of the aryls is independently as previously described. An example is biphenyl;

“bi(heteroaryl)” means a heteroaryl-heteroaryl- group in which each of the heteroaryls is independently as previously described;

“cycloalkylaryl” means a cycloalkyl-aryl- group in which the cycloalkyl and aryl are as previously described;

“heterocyclaryl” means a heterocycl-aryl- group in which the heterocycl and aryl are as previously described;

“heteroarylaryl” means a heteroaryl-aryl- group in which the heteroaryl and aryl are as previously described;

“arylheteroaryl” means a aryl-heteroaryl- group in which the aryl and heteroaryl are as previously described;

“cycloalkylheteroaryl” means a cycloalkyl-heteroaryl- group in which the heteroaryl and cycloalkyl are as previously described;

“heterocyclheteroaryl” means a heterocycl-heteroaryl- group in which the heterocycl and heteroaryl are as previously described;

wherein

each of aryl, cycloalkyl, heterocyclyl, heteroaryl, biaryl, bi(heteroaryl), cycloalkylaryl, heterocyclylaryl, heteroarylaryl, arylheteroaryl, cycloalkylheteroaryl, and heterocyclylheteroaryl can be bound directly or via a methylene or ethylene spacer;

p is an integer in the range of from 1 to 7, more preferably from 1 to 5, even more preferably 1 to 3;

R<sup>9</sup> is H or C1-C6 alkyl, unsubstituted or optionally substituted by -OH, -NH<sub>2</sub>, -N(CH<sub>3</sub>)<sub>2</sub>;

R<sup>9a</sup> is H or C1-C6 alkyl, unsubstituted or optionally substituted by -OH, -NH<sub>2</sub>, -N(CH<sub>3</sub>)<sub>2</sub>;

R<sup>10</sup> is H or C1-C6 alkyl, unsubstituted or optionally substituted by -OH, -NH<sub>2</sub>, -N(CH<sub>3</sub>)<sub>2</sub>.

In a preferred embodiment, R<sup>5</sup> is selected from the group consisting of aryl; heteroaryl; heterocyclylaryl; heteroarylaryl; arylheteroaryl; heterocyclylheteroaryl; wherein each of the substituent moieties can be unsubstituted or optionally substituted, preferably by at least one substituent selected from the group consisting of F, Cl, Br, methyl, ethyl, propyl, isopropyl, butyl, isobutyl, tert-butyl, methoxy, ethoxy, propoxy, isopropoxy, OH, NH<sub>2</sub>, N(CH<sub>3</sub>)<sub>2</sub>, O(CH<sub>2</sub>)<sub>p</sub>N(CH<sub>3</sub>)<sub>2</sub>. More preferably, R<sup>5</sup> is selected from the group consisting of aryl; heteroaryl; wherein each of the substituent moieties can be unsubstituted or optionally substituted, preferably by at least one substituent selected from the group consisting of F, Cl, Br, methyl, ethyl, propyl, isopropyl, butyl, isobutyl, tert-butyl, methoxy, ethoxy, propoxy, isopropoxy, OH, NH<sub>2</sub>, N(CH<sub>3</sub>)<sub>2</sub>, O(CH<sub>2</sub>)<sub>p</sub>N(CH<sub>3</sub>)<sub>2</sub>. Even more preferably, the heteroaryl in R<sup>5</sup> is pyrazolyl.

In a preferred embodiment, any of L<sup>5</sup>, L<sup>7</sup> is independently selected from the group consisting of a bond, -NH-.

In another preferred embodiment, any of L<sup>2</sup>, L<sup>6</sup> is a bond.

In yet another preferred embodiment, L<sup>3</sup> is a bond or -O-.

In a preferred embodiment, R<sup>3</sup> is selected from the group consisting of aryl; heteroaryl; biaryl; wherein each of the substituent moieties can be unsubstituted or optionally substituted, preferably by at least one substituent selected from the group consisting of F, Cl, Br, methyl, ethyl, propyl, isopropyl, butyl, isobutyl, tert-butyl, methoxy, ethoxy, propoxy, isopropoxy, OH, NH<sub>2</sub>, N(CH<sub>3</sub>)<sub>2</sub>,

$O(CH_2)_pN(CH_3)_2$ . Even more preferably, the aryl in  $R^3$  is phenyl, naphthyl (e.g., 2-naphthyl) and the biaryl in  $R^3$  is biphenyl (e.g., 3-biphenyl).

In a preferred embodiment,  $R^6$  is selected from the group consisting of H; -Cl; -Br; -F; -OH; -NH<sub>2</sub>; or methyl.

In a preferred embodiment,  $R^2$  is selected from the group consisting of H; -Cl; -Br; -F; -OH; -NH<sub>2</sub>; or methyl.

In a preferred embodiment,  $R^7$  is selected from the group consisting of H; C<sub>1</sub>-C<sub>6</sub> alkyl; aryl; heteroaryl; wherein each of the substituent moieties can be unsubstituted or optionally substituted, preferably by at least one substituent selected from the group consisting of F, Cl, Br, methyl, ethyl, propyl, isopropyl, butyl, isobutyl, tert-butyl, methoxy, ethoxy, propoxy, isopropoxy, OH, NH<sub>2</sub>, N(CH<sub>3</sub>)<sub>2</sub>,  $O(CH_2)_pN(CH_3)_2$ .

Preferably, at least one of  $R^3$  and  $R^7$  is not H when the corresponding L (i.e., L<sup>3</sup> or L<sup>7</sup>, respectively) is a bond.

In a preferred embodiment, -L<sup>2</sup>-R<sup>2</sup>, -L<sup>6</sup>-R<sup>6</sup>, -L<sup>7</sup>-R<sup>7</sup> are hydrogens and -L<sup>3</sup>-R<sup>3</sup> is not hydrogen.

In one preferred embodiment, -L<sup>2</sup>-R<sup>2</sup>, -L<sup>6</sup>-R<sup>6</sup>, -L<sup>7</sup>-R<sup>7</sup> are hydrogens, -L<sup>3</sup>-R<sup>3</sup> is aryl or biaryl (optionally substituted) and -L<sup>5</sup>-R<sup>5</sup> is heteroaryl (optionally substituted).

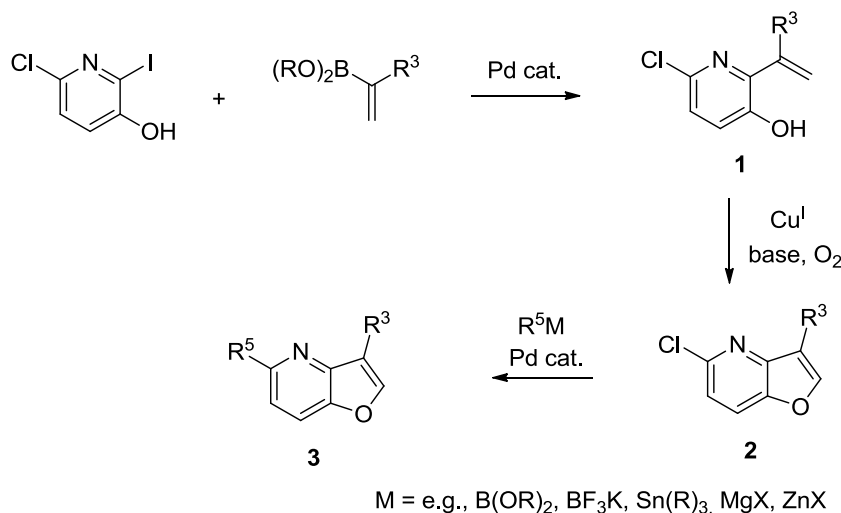
In a preferred embodiment, any of aryl; cycloalkyl; heterocyclyl; heteroaryl; biaryl; bi(heteroaryl); cycloalkylaryl; heterocyclylaryl; heteroarylaryl; arylheteroaryl; cycloalkylheteroaryl; heterocyclylheteroaryl is unsubstituted or substituted with at least one substituent selected from the group consisting of NH<sub>2</sub>, N(CH<sub>3</sub>)<sub>2</sub>, OH, methoxy, ethoxy, propoxy, isopropoxy, methyl, ethyl, propyl, isopropyl, butyl, isobutyl and tert-butyl.

In another preferred embodiment, any of  $-L^2-R^2$ ,  $-L^3-R^3$ ,  $-L^6-R^6$ ,  $-L^7-R^7$ ,  $-L^5-R^5$  can be hydroxy(C<sub>1</sub>-C<sub>6</sub>)alkylamino, amino(C<sub>1</sub>-C<sub>6</sub>)alkylamino or dimethylamino(C<sub>1</sub>-C<sub>6</sub>)alkylamino.

Pharmaceutically acceptable salts are salts with acids or bases, or acid addition salts. The acids and bases can be inorganic or organic acids and bases commonly used in the art of formulation, such as hydrochloride, hydrobromide, sulfate, bisulfate, phosphate, hydrogen phosphate, acetate, benzoate, succinate, fumarate, maleate, lactate, citrate, tartarate, gluconate, methanesulfonate, benzenesulfonate, para-toluenesulfonate, primary, secondary and tertiary amides, ammonia.

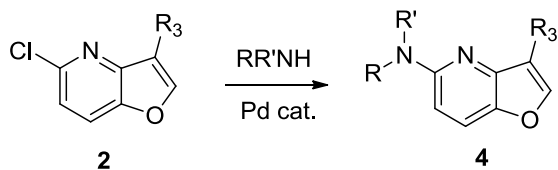
In general, the compounds described in this invention can be prepared through the general routes described below in Schemes 1-6.

Pd-catalyzed coupling of 6-chloro-2-iodopyridin-3-ol with vinyl boronates provides intermediate **1** (as shown in Scheme 1), whose copper-mediated closure provides the furopyridine system in intermediate **2**. Subsequent Pd-catalyzed coupling of intermediate **2** with proper C-nucleophiles leads to compounds **3** with R<sup>5</sup> substituent attached via C-C bond.



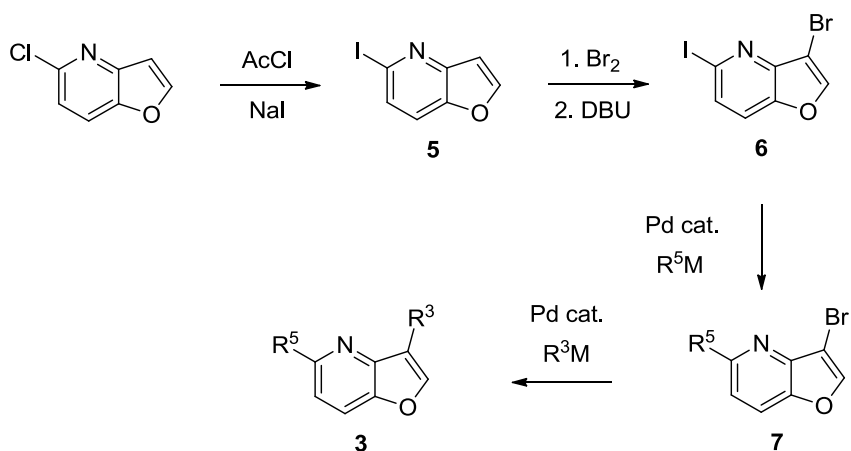
**Scheme 1**

Alternatively, intermediate **2** can be subjected to amination to yield amine-containing compounds **4** depicted in Scheme 2.



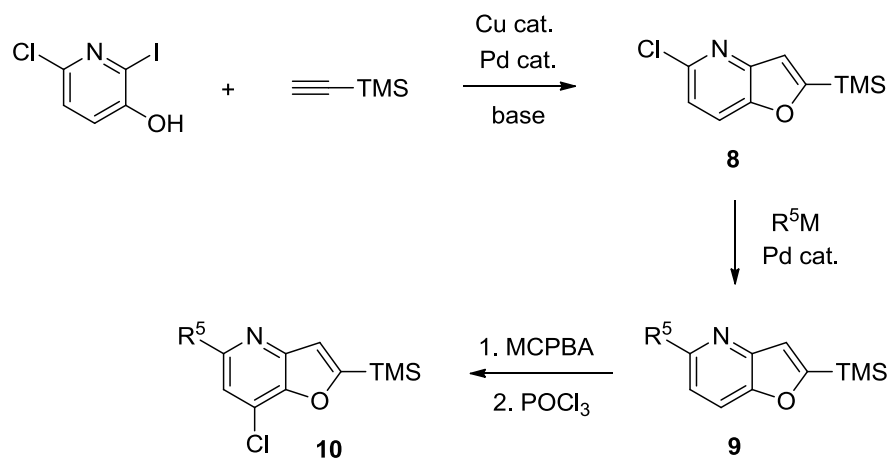
**Scheme 2**

Also, 5-chlorofuro[3,2-*b*]pyridine can be converted into iodide **5**, which can be brominated to yield intermediate **6** (Scheme 3). Sequential chemoselective Pd-catalyzed couplings provide target compounds **3** where  $R^5$  and  $R^3$  are different aryls or heteroaryls (Scheme 3).



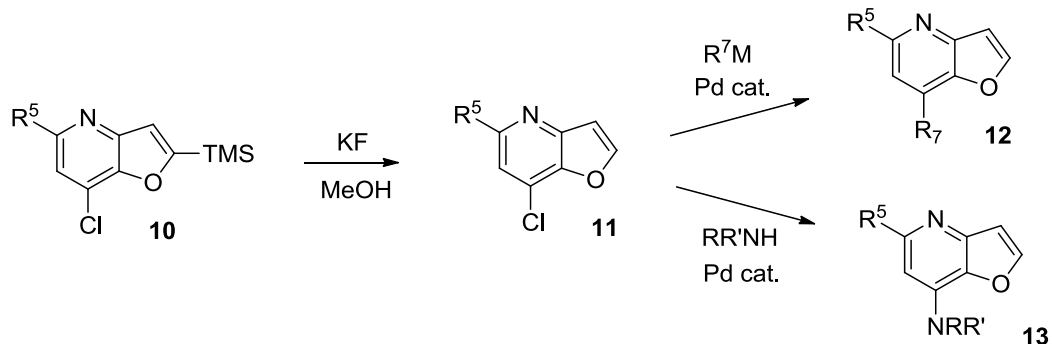
**Scheme 3**

Reaction of 6-chloro-2-iodopyridin-3-ol with trimethylsilylacetylene gives the furopyridine intermediate **8**, which can be subjected to a Pd-catalyzed coupling (e.g. Suzuki reaction) and subsequent N-oxidation followed by the treatment with  $\text{POCl}_3$  to yield chlorinated intermediate **10**, as illustrated in Scheme 4.



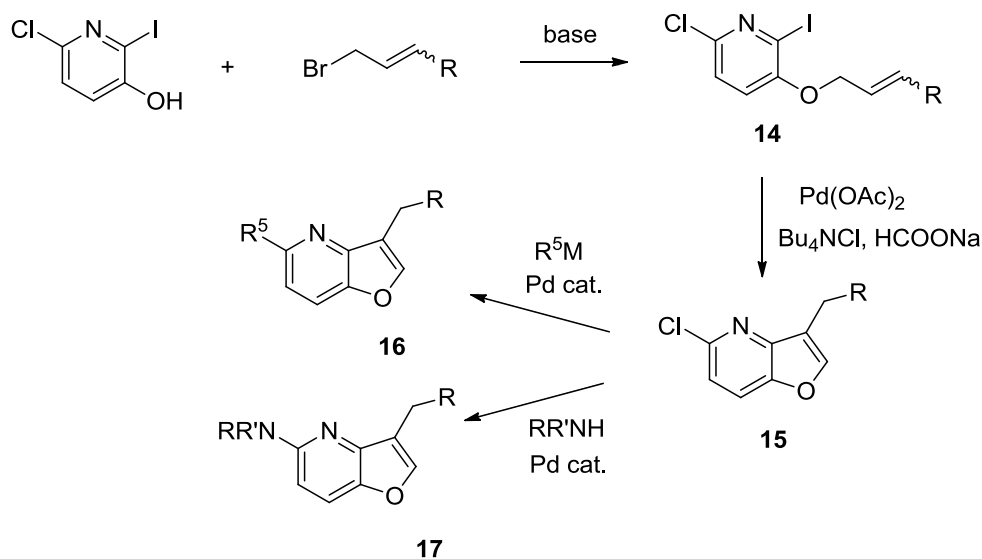
**Scheme 4**

The TMS group in **10** can be removed by KF in methanol to yield intermediate **11**, which can be subjected to Pd-catalyzed C-C bond formation or amination (indicated in Scheme 5) to yield compounds **12** and **13**, respectively.



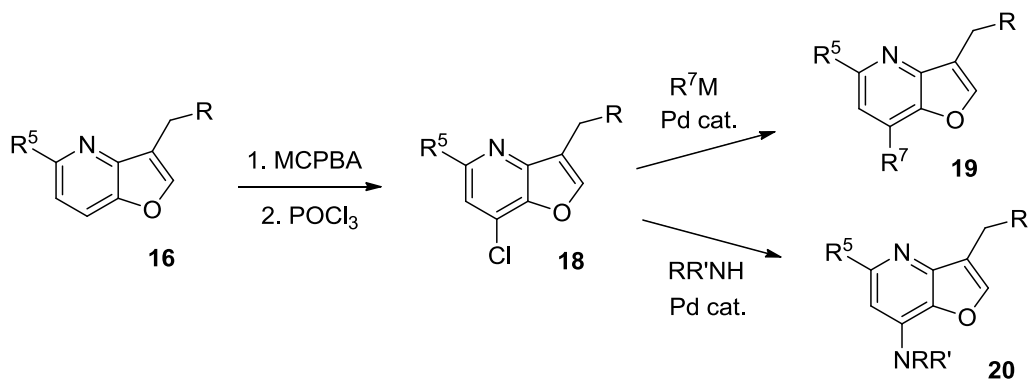
**Scheme 5**

As depicted in Scheme 6, 6-chloro-2-iodopyridin-3-ol can be allylated to give intermediate **14**, which can be cyclized to furopyridine intermediate **15**, which upon Pd-catalyzed C-C bond formation or amination yields compounds **16** and **17**, respectively.



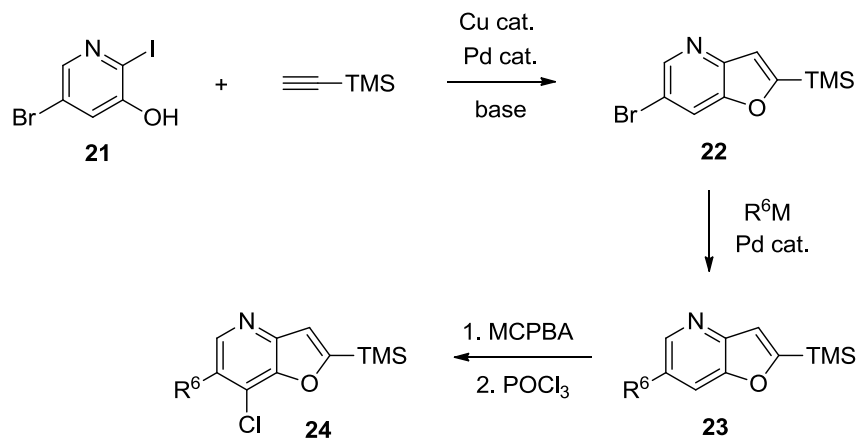
**Scheme 6**

Compounds **16** can be further elaborated (shown in Scheme 7) by N-oxidation-chlorination sequence to yield chlorinated intermediate **18**, which can be subjected to Pd-catalyzed C-C bond formation or amination to yield compounds **19** and **20**, respectively.



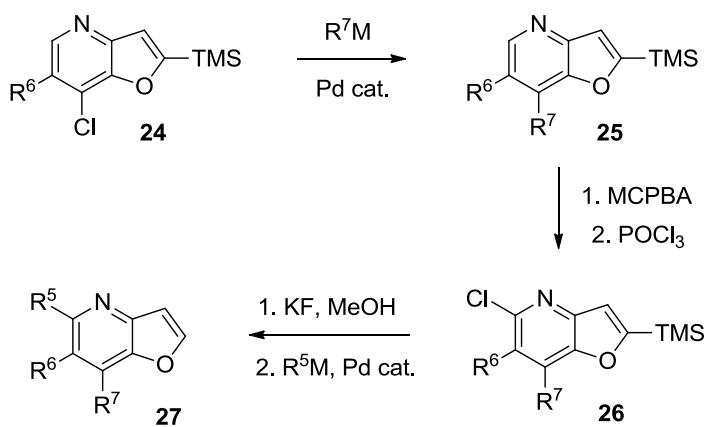
**Scheme 7**

In addition, iodination of 5-bromopyridin-3-ol provides intermediate **21**, which can be converted into compound **22**. Subsequent Pd-catalyzed coupling followed by N-oxidation and regioselective chlorination yield chloride **24** (Scheme 8).



**Scheme 8**

Another Pd-catalyzed coupling on intermediate **24**, followed by the by N-oxidation-chlorination sequence and another Pd-catalyzed coupling provide intermediate **26**. Removal of the TMS group, followed by final Pd-catalyzed coupling provide target compounds **27** with substituents at positions 7- and 5, respectively (Scheme 9).



**Scheme 9**

The compounds of formula (I) can be useful as protein kinase inhibitors and can be useful in the treatment and prevention of proliferative diseases, e.g. cancer, inflammation and arthritis, neurodegenerative diseases such as Alzheimer's disease, cardiovascular diseases, viral diseases, and fungal diseases. In one preferred embodiment, the protein kinase is not GSK3. In another preferred embodiment, the protein kinase is selected from CLK2, CLK4, HIPK1, HIPK2, HIPK3, FLT3, TRKA and DYRK2.

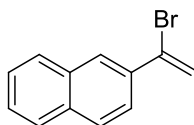
The present invention thus provides the compounds of formula (I) for use as medicaments. More specifically, it provides the compounds of formula (I) for use in the treatment and prevention of conditions selected from proliferative diseases, neurodegenerative diseases, cardiovascular diseases, pain, viral diseases, and fungal diseases.

The present invention also provides a method for treatment, inhibition, amelioration or prevention of a condition selected from proliferative diseases, neurodegenerative diseases, cardiovascular diseases, pain, viral diseases, and fungal diseases, in a patient suffering from such condition, comprising the step of administering at least one compound of formula (I) to said patient.

The present invention further includes pharmaceutical compositions comprising at least one compound of formula (I) and at least one pharmaceutically acceptable auxiliary compound. The auxiliary compounds may include, e.g., carriers, diluents, fillers, preservatives, stabilisers, binders, wetting agents, emulsifiers, buffers, etc. Suitable auxiliary compounds are well known to those skilled in the art of formulation. The pharmaceutical compositions are prepared by known methods, e.g., mixing, dissolving etc.

## Examples of carrying out the Invention

### Preparative Example 1



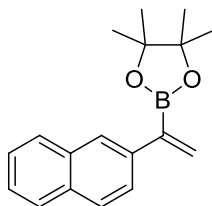
To a solution of  $(\text{PhO})_3\text{P}$  (2.09 g; 6.75 mmol) in anhydrous  $\text{CH}_2\text{Cl}_2$  (10 mL) was added  $\text{Br}_2$  (0.380 mL; 7.38 mmol) dropwise under Ar atmosphere at  $-60\text{ }^\circ\text{C}$ . Then triethylamine (1.10 mL; 7.89 mmol) and a solution of 2-acetonaphthone (1.03 g; 6.05 mmol) in anhydrous  $\text{CH}_2\text{Cl}_2$  (5 mL) were added. The resulting reaction mixture was stirred under Ar for 18 h, while warming to  $25\text{ }^\circ\text{C}$ , and then heated to reflux for additional 2 h. Then, the  $\text{CH}_2\text{Cl}_2$  and excess of triethylamine and  $\text{Br}_2$  were evaporated and the residue was purified by column chromatography on silica gel (eluent: hexane/ $\text{CH}_2\text{Cl}_2$  – 2:1). The product was obtained as a pale orange solid (0.947 g; 67 %).

$^1\text{H}$  NMR (500 MHz,  $\text{CDCl}_3$ )  $\delta$  8.07 (d,  $J = 1.55$  Hz, 1H); 7.87-7.77 (m, 3H); 7.69-7.66 (m, 1H); 7.52-7.46 (m, 2H); 6.25 (d,  $J = 2.10$  Hz, 1H); 5.87 (d,  $J = 2.10$  Hz, 1H).

$^{13}\text{C}$  NMR (126 MHz,  $\text{CDCl}_3$ )  $\delta$  135.9, 133.7, 133.2, 131.3, 128.8, 128.1, 127.8, 127.1, 126.9, 124.4, 118.2.

HRMS (APCI): calcd. for  $\text{C}_{12}\text{H}_{10}\text{Br}$   $[\text{M}+\text{H}]^+ = 232.9960$ ; found  $[\text{M}+\text{H}]^+ = 232.9958$ .

### Preparative Example 2A



A mixture of vinyl bromide from Preparative Example 1 (0.947 g; 4.06 mmol), bis(pinacolato)diboron (1.140 g; 4.49 mmol),  $\text{PPh}_3$  (0.066 g; 0.25 mmol), potassium phenolate (0.809 g; 6.12 mmol) and  $\text{PdCl}_2(\text{PPh}_3)_2$  (0.089 g; 0.13 mmol) in anhydrous toluene (20 mL) was stirred under  $\text{N}_2$  at  $50\text{ }^\circ\text{C}$  for 24 h. The crude mixture was then cooled to  $25\text{ }^\circ\text{C}$ , poured into water (100 mL)

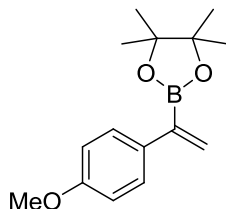
and extracted with EtOAc (3×80 mL). The organic extracts were washed with brine (80 mL), dried over Na<sub>2</sub>SO<sub>4</sub>, filtered, and the solvent was evaporated. The obtained oil was purified by column chromatography on silica gel (eluent: hexane/CH<sub>2</sub>Cl<sub>2</sub> – 2:1) to yield the product as a pale orange solid (0.460 g; 40 %).

<sup>1</sup>H NMR (500 MHz, CDCl<sub>3</sub>) δ 7.94 (s, 1H); 7.84-7.75 (m, 3H); 7.61 (dd, *J* = 1.50 Hz, 8.54 Hz, 1H); 7.46-7.38 (m, 2H); 6.20 (d, *J* = 2.29 Hz, 1H); 6.14 (d, *J* = 2.73 Hz, 1H); 1.35 (s, 12H).

<sup>13</sup>C NMR (126 MHz, CDCl<sub>3</sub>) δ 139.1, 133.8, 132.9, 131.4, 128.5, 127.8, 127.7, 126.4, 126.0, 125.8, 84.1, 25.1.

HRMS (APCI): calcd. for C<sub>18</sub>H<sub>22</sub>BO<sub>2</sub> [M+H]<sup>+</sup> = 281.1711; found [M+H]<sup>+</sup> = 281.1708.

### Preparative Example 2B



A heatgun-dried round bottom flask containing Ni(dppp)Cl<sub>2</sub> (0.251 g; 0.46 mmol) was flushed with N<sub>2</sub>, anhydrous THF (24 mL) was added, followed by dropwise addition of DIBAL-H (1.0 M solution in heptane; 20 mL; 20 mmol) at 25 °C. The mixture was cooled to 0 °C and 4-ethynylanisole (2.0 mL; 15.4 mmol) was added slowly over 5 min. The resulting black solution was allowed to warm to 25 °C and stirred for additional 2 h. Then, 2-methoxy-4,4,5,5-tetramethyl-1,3,2-dioxaborolane (7.6 mL; 46.4 mmol) was added dropwise at 0 °C and the resulting reaction mixture was stirred under N<sub>2</sub> at 80 °C for 15 h. The reaction was then quenched by dropwise addition of water (50 mL) at 0 °C, allowed to warm to 25 °C and stirred for additional 1 h. The mixture was poured into saturated aqueous solution of potassium sodium tartarate (200 mL) and extracted with Et<sub>2</sub>O (3×150 mL). The extracts were washed with brine (200 mL), dried over MgSO<sub>4</sub>, filtered and the solvent was evaporated. The resulting oil was purified by column chromatography on silica gel (eluent: hexane/EtOAc – 10:1) to yield the product as a pale yellow solid (3.22 g; 80 %).

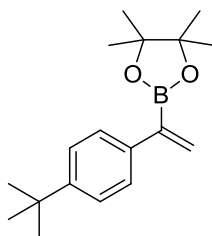
<sup>1</sup>H NMR (500 MHz, CDCl<sub>3</sub>) δ 7.45-7.41 (m, 2H); 6.87-6.82 (m, 2H); 5.99 (d, *J* = 2.65 Hz, 1H); 5.94 (d, *J* = 2.82 Hz, 1H); 3.79 (s, 3H); 1.31 (s, 12H).

<sup>13</sup>C NMR (126 MHz, CDCl<sub>3</sub>) δ 159.1, 134.2, 129.2, 128.5, 113.9, 84.0, 77.5, 77.2, 77.0, 55.5, 25.0.

HRMS (APCI): calcd. for  $C_{15}H_{22}BO_3$   $[M+H]^+ = 260.1693$ ; found  $[M+H]^+ = 260.1696$ .

### Preparative Example 2C

By essentially same procedure set forth in Preparative Example 2B, using 1-(tert-butyl)-4-ethynylbenzene, the compound given below was prepared.



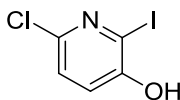
White solid.

$^1H$  NMR (500 MHz,  $CDCl_3$ )  $\delta$  7.44 (d,  $J = 8.5$  Hz, 2H), 7.35 (d,  $J = 8.5$  Hz, 2H), 6.08 (d,  $J = 2.8$  Hz, 1H), 6.02 (d,  $J = 3.0$  Hz, 1H), 1.36 – 1.30 (m, 21H).

$^{13}C$  NMR (126 MHz,  $CDCl_3$ )  $\delta$  150.0, 138.5, 130.2, 126.9, 125.2, 83.8, 34.6, 31.5, 25.0.

HRMS (APCI): calcd. for  $C_{18}H_{27}BO_2$   $[M+H]^+ = 286.2213$ ; found  $[M+H]^+ = 286.2213$ .

### Preparative Example 3



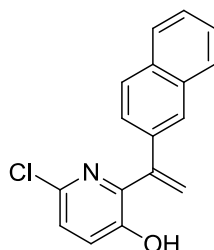
To a stirred solution of 2-chloro-5-hydroxypyridine (6.0 g, 46.3 mmol) in  $H_2O$  (80 mL) were added  $Na_2CO_3$  (10.3 g, 97.3 mmol) and  $I_2$  (11.8 g, 46.3 mmol). The resulting mixture was stirred at 25 °C under  $N_2$  for 2 h. Then it was neutralized by HCl (1M, approx. 50 mL) to pH=7 and extracted with EtOAc ( $3 \times 110$  mL). The organic extracts were washed with brine (150 mL), dried over  $Na_2SO_4$ , filtered, and the solvent was evaporated. The product was obtained as a pale yellow solid (11.1 g, 94 %).

$^1H$  NMR (500 MHz,  $DMSO-d_6$ )  $\delta$  11.10 (s, 1H); 7.30 (d,  $J = 8.40$  Hz, 1H); 7.18 (d,  $J = 8.40$  Hz, 1H).

$^{13}C$  NMR (126 MHz,  $DMSO-d_6$ )  $\delta$  153.9, 138.1, 124.0, 123.9, 107.7.

HRMS (APCI): calcd. for  $C_5H_4ClINO$   $[M+H]^+ = 255.9021$ ; found  $[M+H]^+ = 255.9018$ .

### Preparative Example 4A



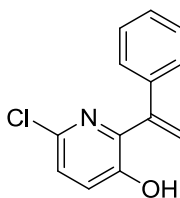
To a mixture of vinyl boronate from Preparative Example 2A (0.460 g; 1.64 mmol), pyridinol from Preparative Example 3 (0.349 g; 1.37 mmol),  $K_3PO_4$  (1.196 g; 5.64 mmol) and  $PdCl_2.dppf$  (0.063 g; 0.068 mmol) were added under  $N_2$  1,2-dimethoxyethane (8 mL) and water (2 mL). The resulting reaction mixture was refluxed for 15 h. Then it was cooled to 25 °C, poured into brine (80 mL) and extracted with  $CH_2Cl_2$  (3×60 mL). The organic extracts were dried over  $Na_2SO_4$ , filtered, and the solvent was evaporated. The residue was purified by column chromatography on silica gel (eluent:  $CH_2Cl_2$ ) to yield the product as a pale yellow solid (0.105 g; 27 %).

$^1H$  NMR (500 MHz,  $CDCl_3$ )  $\delta$  7.85-7.75 (m, 3H); 7.72 (d,  $J = 1.33$  Hz, 1H); 7.52 (dd,  $J = 1.86$  Hz, 8.57 Hz, 1H); 7.50-7.45 (m, 2H); 7.26-7.22 (m, 2H); 6.06 (s, 1H); 5.79 (s, 1H); 5.07 (s, 1H).

$^{13}C$  NMR (126 MHz,  $CDCl_3$ )  $\delta$  149.6, 145.6, 143.8, 142.3, 134.9, 133.7, 133.6, 129.1, 128.7, 127.9, 127.4, 127.0, 126.9, 126.8, 125.0, 124.5, 120.9.

### Preparative Example 4B

By essentially same procedure set forth in Preparative Example 4A, using 1-phenylvinylboronic acid pinacol ester instead of vinyl boronate from Preparative Example 2A, the compound given below was prepared.



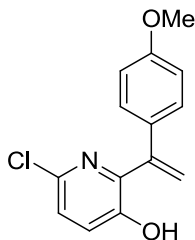
$^1\text{H}$  NMR (500 MHz,  $\text{CDCl}_3$ )  $\delta$  7.39-7.31 (m, 5H); 7.23-7.18 (m, 2H); 5.93 (d,  $J = 0.73$  Hz, 1H); 5.71 (d,  $J = 0.68$  Hz, 1H); 5.00 (brs, 1H).

$^{13}\text{C}$  NMR (126 MHz,  $\text{CDCl}_3$ )  $\delta$  149.5, 145.5, 143.8, 142.2, 137.6, 129.3, 129.3, 127.3, 127.2, 125.0, 120.1.

HRMS (APCI): calcd. for  $\text{C}_{13}\text{H}_{11}\text{ClNO}$   $[\text{M}+\text{H}]^+ = 232.0524$ ; found  $[\text{M}+\text{H}]^+ = 232.0525$ .

### Preparative Example 4C

By essentially same procedure set forth in Preparative Example 4A, using the vinyl boronate from Preparative Example 2B, the compound given below was prepared.

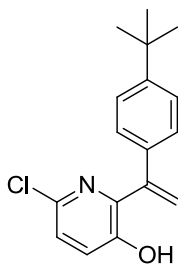


$^1\text{H}$  NMR (500 MHz,  $\text{CDCl}_3$ )  $\delta$  7.30-7.25 (m, 2H); 7.23-7.17 (m, 2H); 6.89-6.85 (m, 2H); 5.83 (d,  $J = 0.65$  Hz, 1H); 5.59 (d,  $J = 0.52$  Hz, 1H); 5.10 (brs, 1H); 3.80 (s, 3H).

$^{13}\text{C}$  NMR (126 MHz,  $\text{CDCl}_3$ )  $\delta$  160.6, 149.5, 145.8, 143.1, 142.1, 129.8, 128.6, 127.2, 124.9, 118.3, 114.7, 55.6.

HRMS (APCI): calcd. for  $\text{C}_{14}\text{H}_{13}\text{ClNO}_2$   $[\text{M}+\text{H}]^+ = 262.0629$ ; found  $[\text{M}+\text{H}]^+ = 262.0631$ .

### Preparative Example 4D



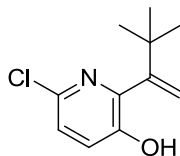
The product from Preparative Example 3 (1.16 g, 4.53 mmol), the product from Preparative Example 2C (1.18 g, 4.12 mmol),  $K_3PO_4$  (3.5 g, 16.5 mmol), DMF (5.5 mL) and  $PdCl_2(dppf)$  (150 mg, 0.206 mmol) were placed into a 50 mL round bottom flask and the mixture was stirred under  $N_2$  at 80 °C for 14 h. The solvent was evaporated and the residue was loaded on silica gel and purified by column chromatography ( $CH_2Cl_2$ /hexane; 4:1). The product was obtained as a white solid (492 mg, 41 %).

$^1H$  NMR (500 MHz,  $CDCl_3$ )  $\delta$  7.42 – 7.37 (m, 2H), 7.32 – 7.28 (m, 2H), 7.24 – 7.20 (m, 2H), 5.92 (d,  $J = 0.8$  Hz, 1H), 5.69 (d,  $J = 0.7$  Hz, 1H), 5.04 (s, 1H), 1.32 (s, 9H).

$^{13}C$  NMR (126 MHz,  $CDCl_3$ )  $\delta$  152.5, 149.4, 145.5, 143.4, 142.0, 134.3, 127.1, 126.8, 126.2, 124.7, 119.3, 34.8, 31.4.

HRMS (APCI): calcd. for  $C_{17}H_{18}ClNO$   $[M+H]^+ = 288.1150$ ; found  $[M+H]^+ = 288.1148$ .

#### Preparative Example 4E



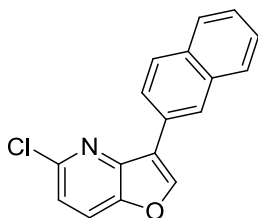
2-(3,3-dimethylbut-1-en-2-yl)-4,4,5,5-tetramethyl-1,3,2-dioxaborolane (400 mg, 1.90 mmol), DMF (7 mL),  $K_3PO_4$  (1.2 g, 5.72 mmol), the product from Preparative Example 3 (584 mg, 2.28 mmol) and  $PdCl_2(dppf)$  (69 mg, 95  $\mu$ mol) were placed into a 25 mL round bottom flask. The mixture was stirred under  $N_2$  at 80 °C for 9 h. Then, additional  $PdCl_2(dppf)$  (47 mg, 64  $\mu$ mol) was added and the mixture was stirred at 90 °C for additional 45 h. The solvent was evaporated and the residue was loaded on silica gel and purified by column chromatography (from EtOAc/hexane; 1:20 to EtOAc). The product was obtained as a white solid (40 mg, 10 %) of limited stability.

$^1H$  NMR (300 MHz,  $CDCl_3$ )  $\delta$  7.22 (d,  $J = 8.5$  Hz, 1H), 7.12 (d,  $J = 8.5$  Hz, 1H), 5.62 (s, 1H), 5.35 (s, 1H), 5.15 (s, 1H), 1.20 (s, 9H).

$^{13}C$  NMR (126 MHz,  $CDCl_3$ )  $\delta$  153.4, 148.6, 147.7, 140.8, 125.8, 123.8, 116.0, 37.2, 29.6.

HRMS (APCI): calcd. for  $C_{11}H_{14}ClNO$   $[M+H]^+ = 212.0837$ ; found  $[M+H]^+ = 212.0835$ .

### Preparative Example 5A



A mixture of the product from Preparative Example 4A (0.105 g; 0.37 mmol), copper(I) acetate (0.029 g; 0.24 mmol), 8-hydroxyquinoline (0.037 g; 0.25 mmol) and  $K_2CO_3$  (0.067 g; 0.48 mmol) in anhydrous *N,N*-dimethylacetamide (1.5 mL) was stirred under  $O_2$  at 140 °C for 18 h. Then the reaction mixture was concentrated under reduce pressure, the residual oil was poured into water (50 mL) and extracted with EtOAc (3×30 mL). The organic extracts were washed with brine (40 mL), dried over  $MgSO_4$ , filtered and the solvent was evaporated. The resulting residue was purified by column chromatography on silica gel (eluent: hexane/ $CH_2Cl_2$  – 1:1) to yield the product as a pale solid product (0.037 g; 36 %).

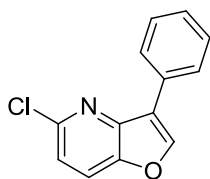
$^1H$  NMR (500 MHz,  $CDCl_3$ )  $\delta$  8.67 (s, 1H); 8.23 (s, 1H); 8.01-7.93 (m, 2H); 7.90 (d,  $J$  = 8.53 Hz, 1H); 7.85-7.82 (m, 1H); 7.75 (d,  $J$  = 8.60 Hz, 1H); 7.53-7.45 (m, 2H); 7.29 (d,  $J$  = 8.59 Hz, 1H).

$^{13}C$  NMR (126 MHz,  $CDCl_3$ )  $\delta$  148.0, 147.3, 146.4, 146.0, 133.9, 133.2, 128.7, 128.7, 127.9, 127.3, 126.5, 126.4, 126.4, 124.9, 121.7, 121.3, 119.9.

HRMS (APCI): calcd. for  $C_{17}H_{10}ClNO$   $[M+H]^+$  = 280.0524; found  $[M+H]^+$  = 280.0526.

### Preparative Example 5B

By essentially same procedure set forth in Preparative Example 5A, using product from Preparative Example 4B, the compound given below was prepared.



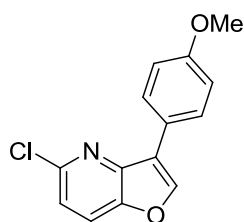
$^1H$  NMR (500 MHz,  $CDCl_3$ )  $\delta$  8.12 (s, 1H); 8.04-7.99 (m, 2H); 7.73 (d,  $J$  = 8.61 Hz, 1H); 7.49-7.43 (m, 2H); 7.37-7.32 (m, 1H); 7.27 (d,  $J$  = 8.60 Hz, 1H).

$^{13}\text{C}$  NMR (126 MHz,  $\text{CDCl}_3$ )  $\delta$  147.9, 147.3, 146.1, 145.9, 129.9, 129.1, 128.2, 127.3, 121.8, 121.3, 119.8.

HRMS (APCI): calcd. for  $\text{C}_{13}\text{H}_9\text{ClNO}$   $[\text{M}+\text{H}]^+ = 230.0367$ ; found  $[\text{M}+\text{H}]^+ = 230.0365$ .

### Preparative Example 5C

By essentially same procedure set forth in Preparative Example 5A, using the product from Preparative Example 4C, the compound given below was prepared.

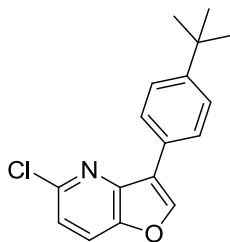


$^1\text{H}$  NMR (500 MHz,  $\text{CDCl}_3$ )  $\delta$  8.05 (s, 1H); 7.97-7.93 (m, 2H); 7.71 (d,  $J = 8.59$  Hz, 1H); 2.25 (d,  $J = 8.59$  Hz, 1H); 7.01-6.97 (m, 2H); 3.84 (s, 3H).

$^{13}\text{C}$  NMR (126 MHz,  $\text{CDCl}_3$ )  $\delta$  159.7, 147.9, 147.1, 146.0, 145.2, 128.5, 122.4, 121.5, 121.2, 119.6, 114.6, 55.6.

HRMS (APCI): calcd. for  $\text{C}_{14}\text{H}_{11}\text{ClNO}_2$   $[\text{M}+\text{H}]^+ = 260.0473$ ; found  $[\text{M}+\text{H}]^+ = 260.0469$ .

### Preparative Example 5D



The product from Preparative Example 4D (470 mg, 1.63 mmol),  $\text{Cu}(\text{OAc})_2$  (148 mg, 0.816 mmol), quinolin-8-ol (118 mg, 0.816 mmol),  $\text{K}_2\text{CO}_3$  (248 mg, 1.79 mmol) were placed into a 50 mL round bottom flask. The flask was filled with  $\text{O}_2$ . Then, *N,N*-dimethylacetamide (4 mL) was added and the mixture was stirred at 140 °C for 75 min. The solvent was evaporated and the residue was loaded on silica gel and purified by column chromatography ( $\text{CH}_2\text{Cl}_2$ /hexane; 1:1). The product was obtained as an orange solid (378 mg, 74 %).

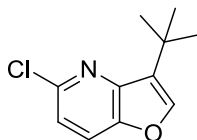
$^1\text{H}$  NMR (500 MHz,  $\text{CDCl}_3$ )  $\delta$  8.11 (s, 1H), 7.94 (d,  $J = 8.5$  Hz, 2H), 7.74 (d,  $J = 8.6$  Hz, 1H), 7.51 (d,  $J = 8.5$  Hz, 2H), 7.28 (d,  $J = 8.6$  Hz, 1H), 1.36 (s, 9H).

$^{13}\text{C}$  NMR (126 MHz,  $\text{CDCl}_3$ )  $\delta$  151.2, 147.8, 147.1, 146.0, 145.7, 127.0, 126.8, 126.0, 121.7, 121.1, 119.6, 34.8, 31.5.

HRMS (APCI): calcd. for  $\text{C}_{17}\text{H}_{16}\text{ClNO}$   $[\text{M}+\text{H}]^+ = 286.0993$ ; found  $[\text{M}+\text{H}]^+ = 286.0991$ .

### Preparative Example 5E

By essentially same procedure set forth in Preparative Example 5D, using the product from Preparative Example 4E, the compound given below was prepared.



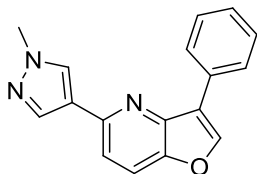
White solid.

$^1\text{H}$  NMR (500 MHz,  $\text{CDCl}_3$ )  $\delta$  7.63 (d,  $J = 8.6$  Hz, 1H), 7.56 (s, 1H), 7.17 (d,  $J = 8.6$  Hz, 1H), 1.48 (s, 9H).

$^{13}\text{C}$  NMR (126 MHz,  $\text{CDCl}_3$ )  $\delta$  147.7, 147.0, 145.8, 144.3, 131.0, 120.6, 118.8, 31.0, 29.6.

HRMS (APCI): calcd. for  $[\text{M}+\text{H}]^+ = 210.0680$ ; found  $[\text{M}+\text{H}]^+ = 210.0682$ .

### Preparative Example 6A



To a mixture of the product from Preparative Example 5B (0.052 g; 0.23 mmol), 1-methylpyrazole-4-boronic acid pinacol ester (0.059 g; 0.28 mmol),  $\text{K}_3\text{PO}_4$  (0.227 g; 1.07 mmol) and  $\text{PdCl}_2(\text{dppf})$  (0.011 g; 0.015 mmol) were added under  $\text{N}_2$  1,2-dimethoxyethane (2 mL) and water (0.5 mL). The resulting reaction mixture was refluxed for 18 h. Then it was cooled to 25  $^\circ\text{C}$ , diluted with EtOAc (10 mL),

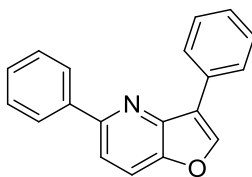
poured into brine (25 mL) and extracted with EtOAc (3×10 mL). The organic extracts were dried over Na<sub>2</sub>SO<sub>4</sub>, filtered, and the solvent was evaporated. The residue was purified by column chromatography on silica gel (eluent: CH<sub>2</sub>Cl<sub>2</sub>/EtOAc – 2:1) to yield the product as a pale orange solid (0.051 g; 81 %).

<sup>1</sup>H NMR (500 MHz, CDCl<sub>3</sub>) δ 8.17-8.13 (m, 2H); 8.09 (s, 1H); 7.99 (d, *J* = 5.58 Hz, 2H); 7.72 (d, *J* = 8.61 Hz, 1H); 7.50-7.744 (m, 2H); 7.42 (d, *J* = 8.60 Hz; 1H); 7.37-7.32 (m, 1H); 3.96 (s, 3H).

<sup>13</sup>C NMR (126 MHz, CDCl<sub>3</sub>) δ 148.9, 147.7, 145.9, 145.2, 137.7, 131.0, 129.1, 128.9, 127.8, 127.3, 124.4, 121.7, 119.2, 115.8, 39.4.

HRMS (APCI): calcd. for C<sub>17</sub>H<sub>14</sub>N<sub>3</sub>O [M+H]<sup>+</sup> = 276.1131; found [M+H]<sup>+</sup> = 276.1128.

### Preparative Example 6B



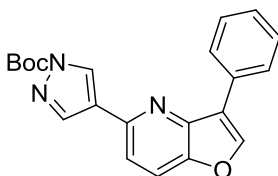
To a mixture of the product from Preparative Example 5B (0.311 g; 1.36 mmol), phenylboronic acid pinacol ester (0.225 g; 1.85 mmol), K<sub>3</sub>PO<sub>4</sub> (1.20 g; 5.64 mmol) and PdCl<sub>2</sub>.dppf (0.062 g; 0.084 mmol) were added under N<sub>2</sub> 1,2-dimethoxyethane (8 mL) and water (2 mL). The reaction mixture was refluxed under N<sub>2</sub> for 19 h. Then it was cooled to 25 °C, diluted with EtOAc (40 mL), poured into brine (50 mL) and extracted with EtOAc (3×40 mL). The organic extracts were dried over Na<sub>2</sub>SO<sub>4</sub>, filtered, and the solvent was evaporated. The residue was purified by column chromatography on silica gel (eluent: hexane/EtOAc – 5:1) to yield the product as a pale yellow wax (0.262 g; 71 %).

<sup>1</sup>H NMR (500 MHz, CDCl<sub>3</sub>) δ 8.26-8.19 (m, 2H); 8.17-8.10 (m, 3H); 7.83 (d, *J* = 8.66 Hz, 1H); 7.73 (d, *J* = 8.67 Hz, 1H); 7.54-7.46 (m, 4H); 7.45-7.33 (m, 2H).

<sup>13</sup>C NMR (126 MHz, CDCl<sub>3</sub>) δ 154.3, 148.3, 146.1, 145.4, 140.0, 130.9, 129.0, 128.9, 128.8, 127.9, 127.4, 127.3, 122.0, 119.2, 116.8.

HRMS (APCI): calcd. for C<sub>19</sub>H<sub>14</sub>NO [M+H]<sup>+</sup> = 272.1070; found [M+H]<sup>+</sup> = 272.1074.

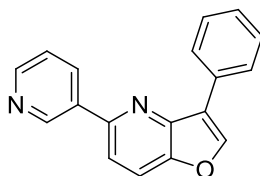
### Preparative Example 6C



To a mixture of the product from Preparative Example 5B (0.078 g; 0.34 mmol), 1-Boc-pyrazole-4-boronic acid pinacol ester (0.122 g; 0.42 mmol),  $K_3PO_4$  (0.282 g; 1.33 mmol) and palladium catalyst  $PdCl_2.dppf$  (0.018 g; 0.024 mmol) were added under  $N_2$  1,2-dimethoxyethane (2 mL) and water (0.5 mL). The reaction mixture was refluxed under  $N_2$  for 15 h. Then it was cooled to 25 °C, diluted with EtOAc (15 mL), poured into brine (25 mL) and extracted with EtOAc (3×15 mL). The organic extracts were dried over  $Na_2SO_4$ , filtered, and the solvent was evaporated. The residue was purified by column chromatography on silica gel (eluent: hexane/EtOAc – 2:1) to yield the product as a pale yellow solid (0.047 g; 38 %).

$^1H$  NMR (300 MHz,  $CDCl_3$ )  $\delta$  8.27 (s, 1H); 8.18-8.11 (m, 3H); 7.78 (d,  $J = 8.59$  Hz, 1H); 7.53-7.44 (m, 3H); 7.40-7.32 (m, 1H); 1.68 (s, 9H).

### Preparative Example 6D



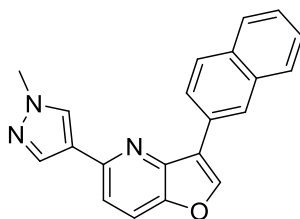
To a mixture of the product from Preparative Example 5B (0.088 g; 0.38 mmol), 3-pyridineboronic acid pinacol ester (0.098 g; 0.48 mmol),  $K_3PO_4$  (0.336 g; 1.58 mmol) and palladium catalyst  $PdCl_2.dppf$  (0.019 g; 0.026 mmol) were added under  $N_2$  1,2-dimethoxyethane (2 mL) and water (0.5 mL). The reaction mixture was refluxed under  $N_2$  for 19 h. Then it was cooled to 25 °C, diluted with EtOAc (15 mL), poured into brine (25 mL) and extracted with EtOAc (3×15 mL). The organic extracts were dried over  $Na_2SO_4$ , filtered, and the solvent was evaporated. The residue was purified by column chromatography on silica gel (eluent:  $CH_2Cl_2/MeOH$  – 15:1) to yield the product as a pale brown solid (0.087 g; 83 %).

$^1\text{H}$  NMR (500 MHz,  $\text{CDCl}_3$ )  $\delta$  9.43 (brs, 1H); 8.73 (brs, 1H); 8.44 (d,  $J = 7.88$  Hz, 1H); 8.23-8.15 (m, 3H); 7.87 (d,  $J = 8.57$  Hz, 1H); 7.74 (d,  $J = 8.61$  Hz, 1H); 7.53-7.34 (m, 4H).

$^{13}\text{C}$  NMR (126 MHz,  $\text{CDCl}_3$ )  $\delta$  151.5, 149.6, 148.7, 148.6, 146.6, 145.8, 135.8, 134.8, 130.6, 129.1, 128.1, 127.3, 124.2, 122.0, 119.5, 116.7.

HRMS (APCI): calcd. for  $\text{C}_{18}\text{H}_{13}\text{N}_2\text{O}$   $[\text{M}+\text{H}]^+ = 273.1022$ ; found  $[\text{M}+\text{H}]^+ = 273.1022$ .

### Preparative Example 7A



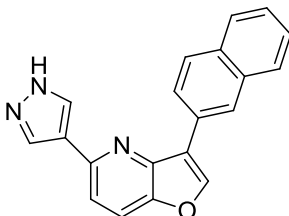
To a mixture of Preparative Example 5A (0.053 g; 0.19 mmol), 1-methylpyrazole-4-boronic acid pinacol ester (0.048 g; 0.23 mmol),  $\text{K}_3\text{PO}_4$  (0.177 g; 0.83 mmol) and  $\text{PdCl}_2\cdot\text{dppf}$  (0.010 g; 0.014 mmol) were added under  $\text{N}_2$  1,2-dimethoxyethane (2 mL) and water (0.5 mL). The reaction mixture was refluxed for 19 h. Then it was cooled to 25 °C, diluted with EtOAc (10 mL), poured into brine (25 mL) and extracted with EtOAc ( $3 \times 10$  mL). The organic extracts were dried over  $\text{Na}_2\text{SO}_4$ , filtered and the solvent was evaporated. The residue was purified by column chromatography on silica gel (eluent: EtOAc/MeOH – 20:1) to yield the product as a pale yellow solid (0.049 g; 79 %).

$^1\text{H}$  NMR (500 MHz,  $\text{CDCl}_3$ )  $\delta$  8.86 (s, 1H); 8.21 (s, 1H); 8.11-7.99 (m, 3H); 7.97-7.89 (m, 2H); 7.85 (d,  $J = 7.82$  Hz, 1H); 7.76 (d,  $J = 8.26$  Hz, 1H); 7.54-7.42 (m, 3H); 3.99 (s, 3H).

$^{13}\text{C}$  NMR (126 MHz,  $\text{CDCl}_3$ )  $\delta$  148.9, 147.8, 145.9, 145.6, 137.8, 133.9, 133.1, 129.2, 128.6, 128.5, 128.3, 128.0, 126.5, 126.2, 125.1, 124.4, 121.6, 119.4, 116.0, 39.5.

HRMS (APCI): calcd. for  $\text{C}_{21}\text{H}_{16}\text{N}_3\text{O}$   $[\text{M}+\text{H}]^+ = 326.1288$ ; found  $[\text{M}+\text{H}]^+ = 326.1284$ .

### Preparative example 7B



Tert-butyl 4-(4,4,5,5-tetramethyl-1,3,2-dioxaborolan-2-yl)-1H-pyrazole-1-carboxylate (77 mg, 0.26 mmol), the product from Preparative Example 5A (61 mg, 0.22 mmol),  $K_3PO_4$  (180 mg, 0.85 mmol), 1,2-dimethoxyethane (2 mL),  $H_2O$  (0.5 mL) and  $PdCl_2(dppf)$  (1.8 mg, 0.008 mmol) were added into a 25 mL round bottom flask. The mixture was refluxed under  $N_2$  for 18 h, then saturated aqueous solution of  $NH_4Cl$  (15 mL) was added, the mixture was extracted with EtOAc (10 mL) and then with  $CH_2Cl_2$  (2×20 mL). The organic extracts were dried over  $Na_2SO_4$ , filtered, and the solvents were evaporated. The residue was loaded on silica gel and purified by column chromatography (EtOAc/hexane; 5:4) to afford the product as a light yellow solid (47 mg, 69 %).

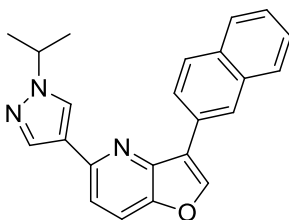
$^1H$  NMR (500 MHz,  $CDCl_3$ )  $\delta$  8.94 (s, 1H), 8.32 – 8.20 (m, 3H), 8.11 (d,  $J = 8.6$  Hz, 1H), 8.00 – 7.91 (m, 2H), 7.87 (d,  $J = 7.8$  Hz, 1H), 7.81 (d,  $J = 8.6$  Hz, 1H), 7.56 – 7.47 (m, 3H).

$^1H$  NMR (300 MHz, DMSO- $d_6$ )  $\delta$  13.04 (b, 1H), 9.12 (s, 1H), 8.95 (s, 1H), 8.52 – 8.20 (m, 3H), 8.14 – 7.99 (m, 3H), 7.99 – 7.90 (m, 1H), 7.78 (d,  $J = 8.7$  Hz, 1H), 7.63 – 7.49 (m, 2H).

$^{13}C$  NMR (126 MHz,  $CDCl_3$ )  $\delta$  148.6, 147.8, 146.0, 145.5, 133.8, 133.0, 128.5, 128.4, 128.2, 127.9, 126.4, 126.1, 124.9, 121.5, 119.2, 116.1.

HRMS (APCI): calcd. for  $C_{20}H_{13}N_3O$   $[M+H]^+ = 312.1131$ ; found  $[M+H]^+ = 312.1129$ .

### Preparative example 7C



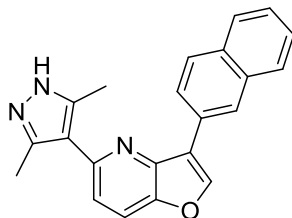
1-isopropyl-4-(4,4,5,5-tetramethyl-1,3,2-dioxaborolan-2-yl)-1H-pyrazole (41 mg, 0.17 mmol), the product from Preparative Example 5A (40 mg, 0.14 mmol),  $K_3PO_4$  (91 mg, 0.43 mmol), 1,2-dimethoxyethane (2 mL),  $H_2O$  (0.5 mL) and  $PdCl_2(dppf)$  (3.1 mg, 4.3  $\mu$ mol) were added into a 25 mL round bottom flask and the mixture was refluxed under  $N_2$  for 2 h. The solvent was evaporated and the residue was loaded on silica gel and purified by column chromatography (EtOAc/hexane; 1:1) to yield the product as a light yellow wax (40 mg, 79 %).

$^1H$  NMR (500 MHz,  $CDCl_3$ )  $\delta$  8.91 (s, 1H), 8.23 (s, 1H), 8.13 – 8.07 (m, 3H), 7.98 – 7.92 (m, 2H), 7.87 (d,  $J = 8.0$  Hz, 1H), 7.78 (d,  $J = 8.6$  Hz, 1H), 7.55 – 7.47 (m, 3H), 4.60 (sep,  $J = 13.4, 6.7$  Hz, 1H), 1.62 (s, 3H), 1.60 (s, 3H).

$^{13}C$  NMR (126 MHz,  $CDCl_3$ )  $\delta$  149.1, 147.6, 145.9, 145.3, 137.3, 133.8, 133.0, 128.4, 128.4, 128.3, 127.8, 126.3, 126.0, 125.4, 125.0, 123.6, 121.5, 119.2, 115.8, 54.2, 23.1.

HRMS (APCI): calcd. for  $C_{23}H_{19}N_3O$   $[M+H]^+ = 354.1601$ ; found  $[M+H]^+ = 354.1596$ .

#### Preparative example 7D



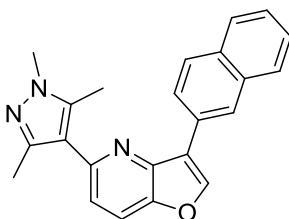
Tert-butyl 3,5-dimethyl-4-(4,4,5,5-tetramethyl-1,3,2-dioxaborolan-2-yl)-1H-pyrazole-1-carboxylate (55 mg, 0.17 mmol), the product from Preparative Example 5A (40 mg, 0.14 mmol),  $K_3PO_4$  (91 mg, 0.43 mmol), 1,2-dimethoxyethane (2 mL),  $H_2O$  (0.5 mL) and  $PdCl_2(dppf)$  (3.1 mg, 4.3  $\mu$ mol) were added into a 25 mL round bottom flask and the mixture was refluxed under  $N_2$  for 24 h. Then, additional tert-butyl 3,5-dimethyl-4-(4,4,5,5-tetramethyl-1,3,2-dioxaborolan-2-yl)-1H-pyrazole-1-carboxylate (30 mg, 0.09 mmol) and  $PdCl_2(dppf)$  (4 mg, 5.4  $\mu$ mol) were added and the mixture was refluxed under  $N_2$  for additional 24 h. The solvent was evaporated and the residue was loaded on silica gel and purified by column chromatography (EtOAc/MeOH; 30:1) and then re-chromatographed (EtOAc/hexane; 1:1). So obtained material was purified by preparative TLC (EtOAc/hexane; 1:1) and then by another preparative TLC ( $CH_2Cl_2/MeOH$ ; 15:1). The product was obtained as a colorless wax (7.2 mg, 29 % yield).

$^1\text{H}$  NMR (300 MHz,  $\text{CDCl}_3$ )  $\delta$  8.99 (s, 1H), 8.28 (s, 1H), 8.06 (dd,  $J = 8.6, 1.6$  Hz, 1H), 7.99 – 7.79 (m, 4H), 7.57 – 7.43 (m, 2H), 7.39 (d,  $J = 8.6$  Hz, 1H), 2.62 (s, 6H).

$^{13}\text{C}$  NMR (126 MHz,  $\text{CDCl}_3$ )  $\delta$  150.4, 147.0, 145.8, 145.3, 144.7, 143.4, 133.8, 132.9, 128.4, 128.3, 128.2, 127.8, 126.4, 126.3, 126.0, 124.7, 121.6, 118.9, 118.8, 118.1, 12.9, 12.3.

HRMS (APCI): calcd. for  $\text{C}_{22}\text{H}_{17}\text{N}_3\text{O}$   $[\text{M}+\text{H}]^+ = 340.1444$ ; found  $[\text{M}+\text{H}]^+ = 340.1441$ .

### Preparative example 7E



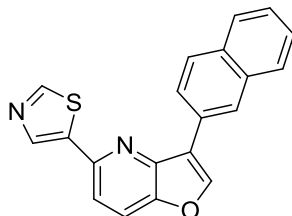
(1,3,5-trimethyl-1H-pyrazol-4-yl)boronic acid (33 mg, 0.21 mmol), the product from Preparative Example 5A (50 mg, 0.18 mmol),  $\text{K}_3\text{PO}_4$  (133 mg, 0.63 mmol), 1,2-dimethoxyethane (2.4 mL),  $\text{H}_2\text{O}$  (0.6 mL) and  $\text{PdCl}_2(\text{dppf})$  (6.5 mg, 8.9  $\mu\text{mol}$ ) were added into a 10 mL round bottom flask and the mixture was refluxed under  $\text{N}_2$  for 18 h. Additional  $\text{PdCl}_2(\text{dppf})$  (4 mg, 5.4  $\mu\text{mol}$ ) and  $\text{K}_3\text{PO}_4$  (118 mg, 0.56 mmol) were added and the mixture was refluxed for additional 12 h. Then, another portion of  $\text{PdCl}_2(\text{dppf})$  (4 mg, 5.4  $\mu\text{mol}$ ) was added and the mixture was refluxed for additional 10 h. The solvent was evaporated and the residue was loaded on silica gel and purified by column chromatography (EtOAc/hexane; from 1:1 to 2:1) and then by preparative TLC ( $\text{CH}_2\text{Cl}_2/\text{MeOH}$ ; 15:1) to yield the product as a colorless wax (5 mg, 8 %).

$^1\text{H}$  NMR (500 MHz,  $\text{CDCl}_3$ )  $\delta$  8.99 (s, 1H), 8.28 (s, 1H), 8.06 (dd,  $J = 8.5, 1.7$  Hz, 1H), 7.94 – 7.88 (m, 2H), 7.88 – 7.82 (m, 2H), 7.54 – 7.44 (m, 2H), 7.35 (d,  $J = 8.6$  Hz, 1H), 3.85 (s, 3H), 2.59 (s, 3H), 2.51 (s, 3H).

$^{13}\text{C}$  NMR (126 MHz,  $\text{CDCl}_3$ )  $\delta$  150.7, 147.0, 145.9, 145.8, 145.3, 138.1, 133.9, 132.9, 128.4, 128.3, 128.2, 127.8, 126.4, 126.3, 126.0, 124.7, 121.6, 119.2, 118.9, 118.8, 36.1, 13.7, 11.2.

HRMS (APCI): calcd. for  $\text{C}_{23}\text{H}_{19}\text{N}_3\text{O}$   $[\text{M}+\text{H}]^+ = 354.1601$ ; found  $[\text{M}+\text{H}]^+ = 354.1599$ .

### Preparative example 7F



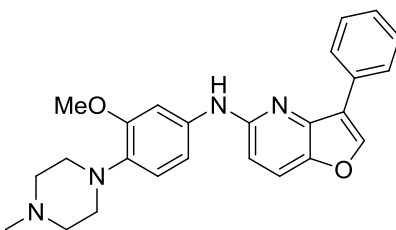
A mixture of 5-thiazole boronic acid MIDA ester (69 mg, 0.29 mmol), the product from Preparative Example 5A (62 mg, 0.22 mmol),  $K_3PO_4$  (165 mg, 0.78 mmol), 1,2-dimethoxyethane (2 mL),  $H_2O$  (0.5 mL) and  $PdCl_2(dppf)$  (8.1 mg, 11  $\mu mol$ ) was stirred at 60 °C under  $N_2$  for 2 h and then at 80 °C for 7 h. Additional  $PdCl_2(dppf)$  (4 mg, 5.4  $\mu mol$ ), the mixture was refluxed for 27 h, then additional  $PdCl_2(PPh_3)_2$  (4 mg, 5.7  $\mu mol$ ) was added and the mixture was refluxed for additional 24 h. Then, additional  $Pd(PPh_3)_4$  (5 mg, 4.3  $\mu mol$ ) and 5-thiazole boronic acid MIDA ester (20 mg, 0.083 mmol) were added and the mixture was refluxed for additional 24 h. The solvent was evaporated and the residue was loaded on silica gel and purified by column chromatography (EtOAc/hexane; from 1:2 to 1:1) and then by preparative TLC (EtOAc/hexane; 1:1). The product was obtained as a light yellow solid (7 mg, 10%).

$^1H$  NMR (300 MHz,  $CDCl_3$ )  $\delta$  8.98 (s, 1H), 8.88 (s, 1H), 8.41 (s, 1H), 8.30 (s, 1H), 8.07 (dd,  $J = 8.6$ , 1.7 Hz, 1H), 8.03 – 7.84 (m, 4H), 7.74 (d,  $J = 8.6$  Hz, 1H), 7.58 – 7.48 (m, 2H).

$^{13}C$  NMR (126 MHz,  $CDCl_3$ )  $\delta$  154.4, 148.4, 147.0, 146.3, 146.1, 141.4, 139.7, 133.8, 133.0, 128.6, 128.5, 127.8, 127.7, 126.5, 126.5, 126.3, 124.6, 121.4, 119.5, 116.0.

HRMS (APCI): calcd. for  $C_{20}H_{12}N_2OS$   $[M+H]^+ = 329.0743$ ; found  $[M+H]^+ = 329.0747$ .

### Preparative Example 8A



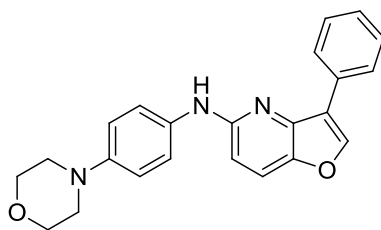
To a freshly prepared solution of (*S*)-1-[(*R<sub>p</sub>*)-2-(dicyclohexylphosphino)ferrocenyl]ethyl-di-*tert*-butylphosphine (0.013 g; 0.023 mmol) and Pd(OAc)<sub>2</sub> (0.007 g; 0.030 mmol) in anhydrous 1,2-dimethoxyethane (2 mL) were added the product from Preparative Example 5B (0.053 g; 0.23 mmol), *t*-BuOK (0.036 g; 0.32 mmol) and 3-methoxy-4-(4-methylpiperazin-1-yl)aniline (0.064 g; 0.29 mmol) and the resulting mixture was stirred under N<sub>2</sub> at 100 °C for 16 h. Then it was cooled to 25 °C, diluted with EtOAc (10 mL), poured into brine (25 mL) and extracted with EtOAc (3×10 mL). The organic extracts were dried over MgSO<sub>4</sub>, filtered and the solvent was evaporated. The residue was purified by column chromatography on silica gel (eluent: CH<sub>2</sub>Cl<sub>2</sub>/7N NH<sub>3</sub> in MeOH – 30:1) to yield the product as a dark orange semi – solid (0.079 g; 83 %).

<sup>1</sup>H NMR (500 MHz, CDCl<sub>3</sub>) δ 8.05-8.02 (m, 2H); 7.99 (s, 1H); 7.59 (d, *J* = 8.93 Hz, 1H); 7.44-7.39 (m, 2H); 7.33-7.27 (m, 2H); 6.91-6.81 (m, 2H); 6.70 (d, *J* = 8.94 Hz, 1H); 6.49 (brs, 1H); 3.80 (s, 3H); 3.10 (s, 4H); 2.68 (s, 4H); 2.38 (s, 3H).

<sup>13</sup>C NMR (126 MHz, CDCl<sub>3</sub>) δ 154.0, 153.1, 144.6, 143.7, 137.3, 136.6, 131.3, 128.9, 127.6, 127.2, 121.5, 121.0, 118.9, 112.3, 106.5, 104.8, 55.8, 55.6, 50.9, 46.2.

HRMS (APCI): calcd. for C<sub>25</sub>H<sub>27</sub>N<sub>4</sub>O<sub>2</sub> [M+H]<sup>+</sup> = 415.2129; found [M+H]<sup>+</sup> = 415.2129.

### Preparative Example 8B



To a freshly prepared solution of (*S*)-1-[(*R<sub>p</sub>*)-2-(dicyclohexylphosphino)ferrocenyl]ethyl-di-*tert*-butylphosphine (0.007 g; 0.012 mmol) and Pd(OAc)<sub>2</sub> (0.004 g; 0.018 mmol) in anhydrous 1,2-dimethoxyethane (2 mL) were added the product from Preparative Example 5B (0.067 g; 0.29 mmol), *t*-BuOK (0.041 g; 0.43 mmol) and 4-morpholinoaniline (0.062 g; 0.35 mmol) and the resulting mixture was stirred under N<sub>2</sub> at 100 °C for 14 h. Then it was cooled to 25 °C, diluted with EtOAc (10 mL), poured into brine (25 mL) and extracted with EtOAc (3×10 mL). The organic extracts were dried over MgSO<sub>4</sub>, filtered, and the solvent was evaporated. The residue was purified

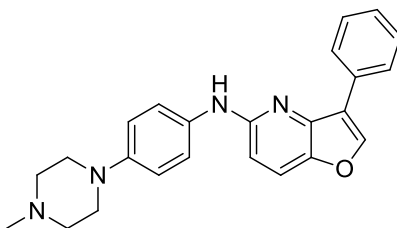
by column chromatography on silica gel (eluent: CH<sub>2</sub>Cl<sub>2</sub>/MeOH – 50:1) to yield the product as an orange solid (0.062 g; 58 %).

<sup>1</sup>H NMR (500 MHz, DMSO-d<sub>6</sub>) δ 8.92 (s, 1H); 8.59 (s, 1H); 8.25-8.20 (m, 2H); 7.84 (d, *J* = 9.01 Hz, 1H); 7.72-7.66 (m, 2H); 7.54-7.47 (m, 2H); 7.38-7.31 (m, 1H); 6.98-6.91 (m, 2H); 6.79 (d, *J* = 9.04 Hz, 1H); 3.78-3.72 (m, 4H); 3.08-3.03 (m, 4H).

<sup>13</sup>C NMR (126 MHz, DMSO-d<sub>6</sub>) δ 153.6, 145.3, 145.0, 143.0, 141.6, 134.6, 131.0, 128.5, 127.0, 126.2, 121.0, 119.7, 118.9, 115.8, 107.7, 66.1, 49.4.

HRMS (APCI): calcd. for C<sub>23</sub>H<sub>22</sub>N<sub>3</sub>O<sub>2</sub> [M+H]<sup>+</sup> = 372.1707; found [M+H]<sup>+</sup> = 372.1704.

### Preparative Example 8C



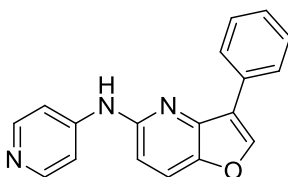
To a freshly prepared solution of (*S*)-1-[(*R<sub>p</sub>*)-2-(dicyclohexylphosphino)ferrocenyl]ethyl-di-*tert*-butylphosphine (0.008 g; 0.014 mmol) and Pd(OAc)<sub>2</sub> (0.010 g; 0.042 mmol) in anhydrous 1,2-dimethoxyethane (2 mL) were added the product from Preparative Example 5B (0.061 g; 0.26 mmol), *t*-BuOK (0.038 g; 0.40 mmol) and 4-(4-methyl-1-piperazinyl)aniline (0.057 g; 0.30 mmol) and the resulting mixture was stirred under N<sub>2</sub> at 100 °C for 19 h. Then it was cooled to 25 °C, diluted with EtOAc (15 mL), poured into brine (25 mL) and extracted with EtOAc (3×15 mL). The organic extracts were dried over MgSO<sub>4</sub>, filtered and the solvent was evaporated. The resulting residue was purified by column chromatography on silica gel (eluent: CH<sub>2</sub>Cl<sub>2</sub>/7N NH<sub>3</sub> in MeOH – 15:1) to yield the product as a pale brown solid (0.069 g; 68 %).

<sup>1</sup>H NMR (500 MHz, CDCl<sub>3</sub>) δ 8.08-8.04 (m, 2H); 7.99 (s, 1H); 7.56 (d, *J* = 8.96 Hz, 1H); 7.46-7.41 (m, 2H); 7.37-7.28 (m, 3H); 6.93 (d, *J* = 5.55 Hz, 2H); 6.66 (d, *J* = 8.61 Hz, 1H); 6.41 (brs, 1H); 3.18 (brs, 4H); 2.63-2.57 (m, 4H); 2.36 (s, 3H).

<sup>13</sup>C NMR (126 MHz, CDCl<sub>3</sub>) δ 147.8, 144.5, 143.8, 134.0, 131.3, 128.9, 127.5, 127.2, 122.8, 122.7, 121.3, 120.9, 117.5, 105.4, 55.4, 50.0, 46.3.

HRMS (APCI): calcd. for C<sub>24</sub>H<sub>25</sub>N<sub>4</sub>O [M+H]<sup>+</sup> = 385.2023; found [M+H]<sup>+</sup> = 385.2030.

### Preparative Example 8D



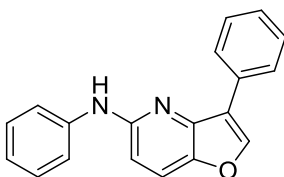
To a freshly prepared solution of (*S*)-1-[(*R<sub>p</sub>*)-2-(dicyclohexylphosphino)ferrocenyl]ethyl-di-*tert*-butylphosphine (0.009 g; 0.016 mmol) and Pd(OAc)<sub>2</sub> (0.015 g; 0.068 mmol) in anhydrous 1,2-dimethoxyethane (2 mL) were added the product from Preparative Example 5B (0.054 g; 0.23 mmol), *t*-BuOK (0.033 g; 0.34 mmol) and 4-aminopyridine (0.024 g; 0.26 mmol) and the resulting mixture was stirred under N<sub>2</sub> at 100 °C for 14 h. Then it was cooled to 25 °C, diluted with EtOAc (10 mL), poured into brine (25 mL) and extracted with EtOAc (3×10 mL). The organic extracts were dried over MgSO<sub>4</sub>, filtered and the solvent was evaporated. The residue was purified by column chromatography on silica gel (eluent: CH<sub>2</sub>Cl<sub>2</sub>/7N NH<sub>3</sub> in MeOH – 10:1) to yield the product as a pale yellow solid (0.034 g; 50 %).

<sup>1</sup>H NMR (500 MHz, DMSO-d<sub>6</sub>) δ 9.71 (s, 1H); 8.71 (s, 1H); 8.35 (d, *J* = 5.44 Hz, 2H); 8.19 (d, *J* = 7.31, 2H); 8.02 (d, *J* = 8.93 Hz, 1H); 7.77 (d, *J* = 5.66 Hz, 2H); 7.58-7.50 (m, 3H); 7.41-7.35 (m, 1H); 6.98 (d, *J* = 8.94 Hz, 1H).

<sup>13</sup>C NMR (126 MHz, DMSO-d<sub>6</sub>) δ 152.0, 149.7, 147.8, 145.9, 143.8, 141.8, 130.5, 128.6, 127.3, 126.3, 121.5, 120.0, 111.3, 109.2.

HRMS (APCI): calcd. for C<sub>18</sub>H<sub>14</sub>N<sub>3</sub>O [M+H]<sup>+</sup> = 288.1131; found [M+H]<sup>+</sup> = 288.1131.

### Preparative Example 8E



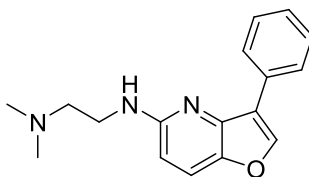
To a freshly prepared solution of (*S*)-1-[(*R<sub>p</sub>*)-2-(dicyclohexylphosphino)ferrocenyl]ethyl-di-*tert*-butylphosphine (0.011 g; 0.020 mmol) and palladium catalyst Pd(OAc)<sub>2</sub> (0.008 g; 0.033 mmol) in anhydrous 1,2-dimethoxyethane (2 mL) were added the product from Preparative Example 5B (0.053 g; 0.23 mmol), *t*-BuOK (0.032 g; 0.34 mmol) and aniline (0.025 mL; 0.27 mmol) and the resulting mixture was stirred under N<sub>2</sub> at 100 °C for 15 h. Then it was cooled to 25 °C, diluted with EtOAc (10 mL), poured into brine (25 mL) and extracted with EtOAc (3×10 mL). The organic extracts were dried over MgSO<sub>4</sub>, filtered and the solvent was evaporated. The residue was purified by column chromatography on silica gel (eluent: hexane/EtOAc – 5:1) to yield the product as a brownish semi – solid (0.050 g; 76 %).

<sup>1</sup>H NMR (500 MHz, CDCl<sub>3</sub>) δ 8.08-8.04 (m, 2H); 8.02 (s, 1H); 7.64 (d, *J* = 8.96 Hz, 1H); 7.49-7.43 (m, 4H); 7.37-7.29 (m, 3H); 7.07-7.00 (m, 1H); 6.81 (d, *J* = 8.96 Hz, 1H).

<sup>13</sup>C NMR (126 MHz, CDCl<sub>3</sub>) δ 153.4, 144.8, 144.7, 141.2, 130.9, 129.4, 129.0, 127.8, 127.2, 122.7, 121.3, 119.9, 106.5.

HRMS (APCI): calcd. for C<sub>19</sub>H<sub>15</sub>N<sub>2</sub>O [M+H]<sup>+</sup> = 287.1179; found [M+H]<sup>+</sup> = 287.1180.

### Preparative Example 8F



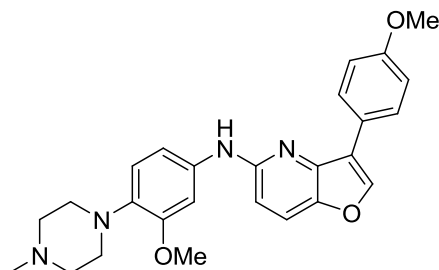
To a solution of the product from Preparative Example 5B (0.045 g; 0.20 mmol), (*R*)-BINAP (0.017 g; 0.027 mmol), Pd<sub>2</sub>(dba)<sub>3</sub> (0.014 g; 0.015 mmol) and *t*-BuOK (0.033 g; 0.29 mmol) in anhydrous toluene (2 mL) was added *N,N*-dimethylethylenediamine (0.022 mL; 0.20 mmol) and the resulting mixture was stirred under N<sub>2</sub> at 80 °C for 20 h. Then it was cooled to 25 °C, diluted with EtOAc (10 mL), poured into water (25 mL) and extracted with EtOAc (3×10 mL). The organic extracts were washed with brine (15 mL), dried over MgSO<sub>4</sub>, filtered and the solvent was evaporated. The residue was purified by preparative TLC (eluent: CH<sub>2</sub>Cl<sub>2</sub>/7N NH<sub>3</sub> in MeOH – 17:1) to yield the product as an orange wax (0.024 g; 43 %).

<sup>1</sup>H NMR (500 MHz, CDCl<sub>3</sub>) δ 8.13-8.08 (m, 2H); 7.96 (s, 1H); 7.51 (d, *J* = 8.93 Hz, 1H); 7.45-7.39 (m, 2H); 7.32-7.26 (m, 1H); 6.39 (d, *J* = 8.93 Hz, 1H); 5.04-4.95 (m, 1H); 3.50 (dd, *J* = 5.71 Hz, 11.41 Hz, 2H); 2.60 (t, *J* = 6.06 Hz, 2H); 2.29 (s, 3H).

$^{13}\text{C}$  NMR (126 MHz,  $\text{CDCl}_3$ )  $\delta$  156.9, 143.9, 143.8, 143.5, 131.7, 128.8, 127.3, 127.0, 121.1, 120.7, 105.4, 58.6, 45.6, 40.1.

HRMS (APCI): calcd. for  $\text{C}_{17}\text{H}_{20}\text{N}_3\text{O}$   $[\text{M}+\text{H}]^+ = 282.1601$ ; found  $[\text{M}+\text{H}]^+ = 282.1600$ .

### Preparative Example 8G



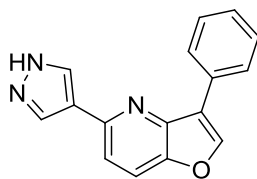
To a freshly prepared solution of (*S*)-1-[(*R<sub>P</sub>*)-2-(dicyclohexylphosphino)ferrocenyl]ethyl-di-*tert*-butylphosphine (0.011 g; 0.023 mmol) and  $\text{Pd}(\text{OAc})_2$  (0.007 g; 0.030 mmol) in anhydrous 1,2-dimethoxyethane (2 mL) were added the product from Preparative Example 5C (0.054 g; 0.22 mmol), *t*-BuONa (0.030 g; 0.31 mmol) and 3-methoxy-4-(4-methylpiperazin-1-yl)aniline (0.056 g; 0.25 mmol) and the resulting mixture was stirred under  $\text{N}_2$  at 100 °C for 18 h. Then it was cooled to 25 °C, diluted with EtOAc (10 mL), poured into brine (25 mL) and extracted with EtOAc (3×10 mL). The organic extracts were dried over  $\text{MgSO}_4$ , filtered, and the solvent was evaporated. The residue was purified by column chromatography on silica gel (eluent:  $\text{CH}_2\text{Cl}_2/7\text{N NH}_3$  in MeOH – 17:1) to yield the product as a pale orange foam (0.041 g; 42 %).

$^1\text{H}$  NMR (500 MHz,  $\text{CDCl}_3$ )  $\delta$  7.99-7.95 (m, 2H); 7.91 (s, 1H); 7.56 (d,  $J = 8.92$  Hz, 1H); 7.27-7.22 (m, 1H); 6.91-6.81 (m, 2H); 6.68 (d,  $J = 8.93$  Hz, 1H); 6.50 (brs, 1H); 3.83 (s, 3H); 3.80 (s, 3H); 3.08 (brs, 4H); 2.64 (brs, 4H); 2.36 (s, 3H).

$^{13}\text{C}$  NMR (126 MHz,  $\text{CDCl}_3$ )  $\delta$  159.2, 153.9, 153.1, 144.4, 143.7, 137.3, 136.6, 128.4, 123.8, 121.1, 120.9, 118.8, 114.3, 112.3, 106.3, 104.8, 55.7, 55.6, 55.5, 51.1, 46.3.

HRMS (APCI): calcd. for  $\text{C}_{26}\text{H}_{29}\text{N}_4\text{O}_3$   $[\text{M}+\text{H}]^+ = 445.2234$ ; found  $[\text{M}+\text{H}]^+ = 445.2235$ .

### Preparative Example 9



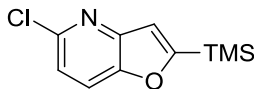
To a stirred solution of the product from Preparative Example 6C (0.049 g; 0.14 mmol) in ethanol (2 mL) was added aqueous solution of HCl (3M; 0.9 mL; 2.7 mmol) and the resulting mixture was stirred under N<sub>2</sub> at 60 °C for 8 h. Then, the ethanol and HCl were evaporated and the oily residue was mixed with CH<sub>2</sub>Cl<sub>2</sub> (2 mL), MeOH (1mL) and Na<sub>2</sub>CO<sub>3</sub> (200 mg) and the mixture was stirred at 25 °C. After 20 min., the solvents were evaporated and the solid residue was purified by column chromatography on silica gel (eluent: CH<sub>2</sub>Cl<sub>2</sub>/7N NH<sub>3</sub> in MeOH – 10:1) to yield the product as a pale yellow solid (0.026 g; 75 %).

<sup>1</sup>H NMR (500 MHz, CD<sub>3</sub>OD) δ 8.36 (s, 1H); 8.31-8.08 (m, 4H); 7.85 (d, *J* = 8.64 Hz, 1H); 7.63 (d, *J* = 8.64 Hz, 1H); 7.49-7.44 (m, 2H); 7.36-7.31 (m, 1H).

<sup>13</sup>C NMR (126 MHz, CD<sub>3</sub>OD) δ 150.2, 149.0, 147.1, 146.8, 138.6, 132.2, 129.7, 128.6, 128.1, 122.5, 120.3, 117.2.

HRMS (APCI): calcd. for C<sub>16</sub>H<sub>12</sub>N<sub>3</sub>O [M+H]<sup>+</sup> = 262.0975; found [M+H]<sup>+</sup> = 262.0976.

### Preparative Example 10



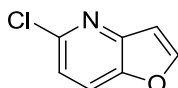
The product from Preparative Example 3 (4.5 g; 17.62 mmol) was placed into a 250 mL round bottom flask. TEA (32 mL) and 1,4-dioxane (32 mL) were added and the mixture was purged with N<sub>2</sub>. Ethynyltrimethylsilane (2.25 g; 22.9 mmol), CuI (0.168 g; 0.881 mmol) and PdCl<sub>2</sub>(PPh<sub>3</sub>)<sub>2</sub> (0.247 mg, 0.352 mmol) were added and the mixture was stirred at 45 °C under N<sub>2</sub> for 2.5 h. The solvent was evaporated and the residue was purified by column chromatography (hexane/EtOAc; from 15:1 to 10:1) to yield the product as an orange solid (2.90 g; 73 % yield).

$^1\text{H}$  NMR (500 MHz,  $\text{CDCl}_3$ )  $\delta$  7.67 (dd,  $J = 0.85$  Hz, 8.56 Hz, 1H); 7.17 (d,  $J = 8.56$  Hz, 1H); 7.03 (d,  $J = 0.84$  Hz, 1H); 0.35 (m, 9H).

$^{13}\text{C}$  NMR (126 MHz,  $\text{CDCl}_3$ )  $\delta$  170.8, 149.9, 148.5, 146.7, 120.7, 119.1, 116.8, -1.9.

HRMS (APCI): calcd. for  $\text{C}_{10}\text{H}_{13}\text{ClNOSi}$   $[\text{M}+\text{H}]^+ = 226.0449$ ; found  $[\text{M}+\text{H}]^+ = 226.0446$ .

### Preparative Example 11



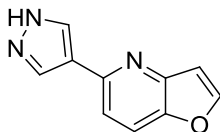
To a solution of the product from Preparative Example 10 (1.013 g; 4.49 mmol) in methanol (20 mL) was added KF (0.803 g; 13.82 mmol) and the resulting mixture was stirred under  $\text{N}_2$  at 60 °C for 15 h. Then it was cooled to 25 °C, poured into aqueous solution of HCl (0.1M; 100 mL) and extracted with EtOAc (3×60 mL). The organic extracts were dried over  $\text{Na}_2\text{SO}_4$ , filtered, and the solvent was evaporated. The residue was purified by column chromatography on silica gel (eluent: hexane/ EtOAc – 10:1) to yield the product as a pale yellow solid (0.579 g; 84 %).

$^1\text{H}$  NMR (500 MHz,  $\text{CDCl}_3$ )  $\delta$  7.84 (d,  $J = 2.28$  Hz, 1H); 7.70 (dd,  $J = 0.84$  Hz, 8.60 Hz, 1H); 7.21 (d,  $J = 8.60$  Hz, 1H); 6.90 (dd,  $J = 0.84$  Hz, 2.26 Hz, 1H).

$^{13}\text{C}$  NMR (126 MHz,  $\text{CDCl}_3$ )  $\delta$  150.3, 147.6, 147.2, 146.9, 121.1, 119.5, 108.1.

HRMS (APCI): calcd. for  $\text{C}_7\text{H}_5\text{ClNO}$   $[\text{M}+\text{H}]^+ = 154.0054$ ; found  $[\text{M}+\text{H}]^+ = 154.0055$ .

### Preparative Example 12A



To a mixture of the product from Preparative Example 11 (0.201 g; 0.89 mmol), 1-Boc-pyrazole-4-boronic acid pinacol ester (0.0317 g; 1.07 mmol),  $\text{K}_3\text{PO}_4$  (0.781 g; 3.68 mmol) and  $\text{PdCl}_2\text{.dppf}$  (0.039 g; 0.053 mmol) were added under  $\text{N}_2$  1,2-dimethoxyethane (4 mL) and water (1 mL). The reaction mixture was refluxed for 19 h. Then it was cooled to 25 °C, diluted with EtOAc (20 mL),

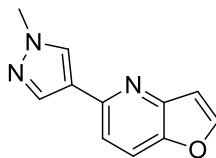
poured into brine (30 mL) and extracted with EtOAc (3×20 mL). The organic extracts were dried over Na<sub>2</sub>SO<sub>4</sub>, filtered and the solvent was evaporated. The residue was purified by column chromatography on silica gel (eluent: CH<sub>2</sub>Cl<sub>2</sub>/MeOH – 15:1). So obtained solid was further purified by preparative TLC (eluent: CH<sub>2</sub>Cl<sub>2</sub>/MeOH – 15:1) to yield the pale yellow crystalline product (0.080 g; 49 %).

<sup>1</sup>H NMR (500 MHz, CD<sub>3</sub>OD) δ 8.17 (s, 2H); 8.04 (d, *J* = 2.28 Hz, 1H); 7.89 (dd, *J* = 0.83 Hz, 8.64 Hz, 1H); 7.62 (d, *J* = 8.65 Hz, 1H); 6.96 (dd, *J* = 0.85 Hz, 2.26 Hz, 1H); 4.86 (brs, 1H).

<sup>13</sup>C NMR (126 MHz, CD<sub>3</sub>OD) δ 151.4, 150.1, 148.2, 148.1, 133.4, 123.8, 120.9, 117.7, 108.2.

HRMS (APCI): calcd. for C<sub>10</sub>H<sub>8</sub>N<sub>3</sub>O [M+H]<sup>+</sup> = 186.0662; found [M+H]<sup>+</sup> = 186.0659.

### Preparative Example 12B



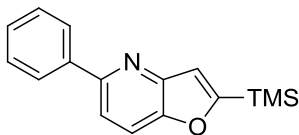
To a mixture of the product from Preparative Example 11 (0.052 g; 0.34 mmol), 1-methylpyrazole-4-boronic acid pinacol ester (0.092 g; 0.44 mmol), K<sub>3</sub>PO<sub>4</sub> (0.308 g; 1.45 mmol) and PdCl<sub>2</sub>.dppf (0.017 g; 0.023 mmol) were added under N<sub>2</sub> 1,2-dimethoxyethane (2 mL) and water (0.5 mL). The reaction mixture was refluxed for 14 h. Then it was cooled to 25 °C, diluted with EtOAc (15 mL), poured into brine (25 mL) and extracted with EtOAc (3×15 mL). The organic extracts were dried over Na<sub>2</sub>SO<sub>4</sub>, filtered and the solvent was evaporated. The residue was purified by column chromatography on silica gel (eluent: CH<sub>2</sub>Cl<sub>2</sub>/MeOH – 10:1) to yield the product as a brown solid (0.045 g; 66 %).

<sup>1</sup>H NMR (500 MHz, CDCl<sub>3</sub>) δ 7.94 (s, 2H); 7.80 (d, *J* = 2.21 Hz, 1H); 7.72 (d, *J* = 8.53 Hz, 1H); 7.39 (d, *J* = 8.59 Hz, 1H); 6.95 (d, *J* = 1.64 Hz, 1H); 3.94 (s, 3H).

<sup>13</sup>C NMR (126 MHz, CDCl<sub>3</sub>) δ 149.3, 149.0, 147.5, 146.7, 137.7, 128.9, 124.1, 119.2, 116.0, 108.3, 39.4.

HRMS (APCI): calcd. for C<sub>11</sub>H<sub>10</sub>N<sub>3</sub>O [M+H]<sup>+</sup> = 200.0818; found [M+H]<sup>+</sup> = 200.0817.

### Preparative Example 13



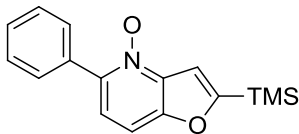
To a mixture of the product from Preparative Example 10 (1.62 g; 7.16 mmol), phenylboronic acid (1.13 g; 9.26 mmol), triethylamine (10 mL; 71.8 mmol) and PdCl<sub>2</sub>.dppf (0.160 g; 0.22 mmol) were added under N<sub>2</sub> 1,2-dimethoxyethane (12 mL) and water (3 mL). The reaction mixture was refluxed under N<sub>2</sub> for 20 h. Then it was cooled to 25 °C, diluted with EtOAc (70 mL), poured into brine (90 mL) and extracted with EtOAc (3×70 mL). The organic extracts were dried over Na<sub>2</sub>SO<sub>4</sub>, filtered and the solvent was evaporated. The residue was purified by column chromatography on silica gel (eluent: hexane/EtOAc – 15:1) to yield the product as a pale yellow solid (1.61 g; 84 %).

<sup>1</sup>H NMR (500 MHz, CDCl<sub>3</sub>) δ 8.01-7.96 (m, 2H); 7.78 (dd, *J* = 0.93 Hz, 8.61 Hz, 1H); 7.61 (d, *J* = 8.62 Hz, 1H); 7.49-7.43 (m, 2H); 7.41-7.35 (m, 1H); 7.20 (d, *J* = 0.81 Hz, 1H); 0.39-0.39 (m, 9H).

<sup>13</sup>C NMR (126 MHz, CDCl<sub>3</sub>) δ 169.5, 154.3, 150.3, 148.6, 140.3, 128.9, 128.6, 127.5, 118.7, 117.6, 116.9, -1.8.

HRMS (APCI): calcd. for C<sub>16</sub>H<sub>18</sub>NOSi [M+H]<sup>+</sup> = 268.1152; found [M+H]<sup>+</sup> = 268.1153.

### Preparative Example 14



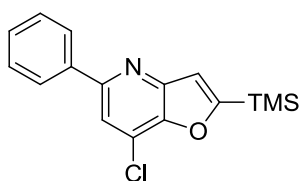
To a stirred solution of the product from Preparative Example 13 (1.61 g, 6.02 mmol) in anhydrous CH<sub>2</sub>Cl<sub>2</sub> (20 ml) was added MCPBA (1.88 g, 10.9 mmol) and the resulting mixture was stirred under N<sub>2</sub> at 25 °C for 72 h. Then it was poured into saturated aqueous solution of NaHCO<sub>3</sub> (110 mL) and extracted with CH<sub>2</sub>Cl<sub>2</sub> (3×60 mL). The organic extracts were washed with brine (50 mL), dried over Na<sub>2</sub>SO<sub>4</sub>, filtered and the solvent was evaporated. The residue was purified by column chromatography on silica gel (eluent: CH<sub>2</sub>Cl<sub>2</sub>/MeOH – 12:1) to yield the product as a pale yellow solid (1.60 g; 94 %).

$^1\text{H}$  NMR (500 MHz,  $\text{CDCl}_3$ )  $\delta$  7.86-7.80 (m, 2H); 7.50-7.39 (m, 5H); 7.30 (d,  $J = 8.58$  Hz, 1H); 0.38-0.36 (m, 9H).

$^{13}\text{C}$  NMR (126 MHz,  $\text{CDCl}_3$ )  $\delta$  169.0, 153.2, 144.7, 139.6, 133.1, 129.8, 129.4, 128.5, 122.2, 112.0, 110.4, -1.9.

HRMS (APCI): calcd. for  $\text{C}_{16}\text{H}_{17}\text{NO}_2\text{Si}$   $[\text{2M}+\text{H}]^+ = 567.213$ ; found  $[\text{2M}+\text{H}]^+ = 567.2134$ .

### Preparative Example 15



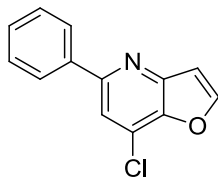
To a stirred solution of the product from Preparative Example 14 (0.575 g, 2.03 mmol) in  $\text{CHCl}_3$  (10 ml) was added  $\text{POCl}_3$  (3.4 mL; 36.5 mmol) and the resulting mixture was refluxed under  $\text{N}_2$  for 1 h. Then, the  $\text{CHCl}_3$  and  $\text{POCl}_3$  were evaporated under reduced pressure. The dark oily residue was diluted with  $\text{CH}_2\text{Cl}_2$  (50 mL), poured into saturated aqueous solution of  $\text{NaHCO}_3$  (200 mL) and extracted with  $\text{CH}_2\text{Cl}_2$  ( $3 \times 70$  mL). The organic extracts were washed with water (50 mL), brine (80 mL), dried over  $\text{Na}_2\text{SO}_4$ , filtered, and the solvent was evaporated. The residue was purified by column chromatography on silica gel (eluent: hexane/ $\text{CH}_2\text{Cl}_2$  – 1:1) to yield the product as a colorless wax (0.339 g; 55 %).

$^1\text{H}$  NMR (500 MHz,  $\text{CDCl}_3$ )  $\delta$  7.99-7.94 (m, 2H); 7.63 (s, 1H); 7.49-7.44 (m, 2H); 7.42-7.37 (m, 1H); 7.20 (s, 1H); 0.41-0.38 (m, 9H).

$^{13}\text{C}$  NMR (126 MHz,  $\text{CDCl}_3$ )  $\delta$  170.6, 155.4, 149.8, 146.8, 139.3, 129.1, 129.0, 127.4, 126.5, 118.1, 117.3, -1.8.

HRMS (APCI): calcd. for  $\text{C}_{16}\text{H}_{16}\text{ClNOSi}$   $[\text{M}+\text{H}]^+ = 302.0762$ ; found  $[\text{M}+\text{H}]^+ = 302.0764$ .

### Preparative Example 16



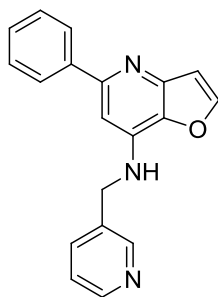
To a solution of the product from Preparative Example 15 (1.11 g; 3.68 mmol) in methanol (10 mL) was added KF (0.646 g; 11.1 mmol) and the resulting mixture was stirred under N<sub>2</sub> at 60 °C for 20 h. Then it was cooled to 25 °C, poured into aqueous solution of HCl (0.1M; 40 mL) and extracted with EtOAc (3×30 mL). The organic extracts were washed with brine (30 mL), dried over Na<sub>2</sub>SO<sub>4</sub>, filtered and the solvent was evaporated. The residue was purified by column chromatography on silica gel (eluent: CH<sub>2</sub>Cl<sub>2</sub>/ MeOH – 20:1) to yield the product as a white solid (0.796 g; 94 %).

<sup>1</sup>H NMR (500 MHz, CDCl<sub>3</sub>) δ 7.99-7.95 (m, 2H); 7.90 (d, *J* = 2.18 Hz, 1H); 7.68 (s, 1H); 7.51-7.44 (m, 2H); 7.43-7.39 (m, 1H); 7.09 (d, *J* = 2.15 Hz, 1H).

<sup>13</sup>C NMR (126 MHz, CDCl<sub>3</sub>) δ 155.8, 150.2, 148.8, 144.0, 138.8, 129.4, 129.1, 127.5, 127.0, 117.6, 109.2.

HRMS (APCI): calcd. for C<sub>13</sub>H<sub>9</sub>ClNO [M+H]<sup>+</sup> = 230.0367; found [M+H]<sup>+</sup> = 230.0365.

### Preparative Example 17A



To a solution of the product from Preparative Example 16 (0.103 g; 0.45 mmol), (*R*)-BINAP (0.016 g; 0.026 mmol), Pd(dba)<sub>2</sub> (0.017 g; 0.030 mmol) and *t*-BuOK (0.078 g; 0.69 mmol) in anhydrous toluene (3 mL) was added 3-picolylamine (0.050 mL; 0.49 mmol) and the resulting mixture was stirred under N<sub>2</sub> at 80 °C for 17 h. Then it was cooled to 25 °C, diluted with EtOAc (10 mL), poured into water (25 mL) and extracted with EtOAc (3×10 mL). The organic extracts were washed with

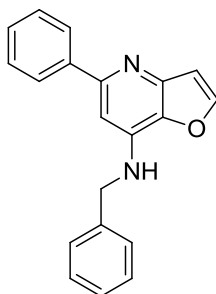
brine (15 mL), dried over MgSO<sub>4</sub>, filtered, and the solvent was evaporated. The residue was purified by column chromatography on silica gel (eluent: CH<sub>2</sub>Cl<sub>2</sub>/ MeOH – 10:1) to yield the product as an orange foam (0.056 g; 42 %).

<sup>1</sup>H NMR (500 MHz, CDCl<sub>3</sub>) δ 8.62 (d, *J* = 59.05 Hz, 2H); 7.84 (d, *J* = 7.29 Hz, 2H); 7.75-7.66 (m, 2H); 7.44-7.25 (m, 4H); 6.96 (d, *J* = 2.02 Hz, 1H); 6.81 (s, 1H); 5.09 (brs, 1H); 4.63 (d, *J* = 5.71 Hz, 2H).

<sup>13</sup>C NMR (126 MHz, CDCl<sub>3</sub>) δ 156.5, 149.5, 149.3, 147.5, 146.7, 140.8, 139.4, 136.8, 135.2, 133.7, 128.8, 128.6, 127.5, 124.0, 109.1, 99.6, 45.0.

HRMS (APCI): calcd. for C<sub>19</sub>H<sub>16</sub>N<sub>3</sub>O [M+H]<sup>+</sup> = 302.1288; found [M+H]<sup>+</sup> = 302.1285.

### Preparative Example 17B



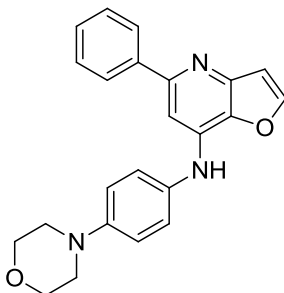
To a solution of the product from Preparative Example 16 (0.207 g; 0.90 mmol), (*R*)-BINAP (0.035 g; 0.056 mmol), Pd(dba)<sub>2</sub> (0.050 g; 0.087 mmol) and *t*-BuOK (0.146 g; 1.30 mmol) in anhydrous toluene (3 mL) was added benzylamine (0.120 mL; 1.10 mmol) and the resulting mixture was stirred under N<sub>2</sub> at 80 °C for 17 h. Then it was cooled to 25 °C, diluted with EtOAc (10 mL), poured into water (25 mL) and extracted with EtOAc (3×10 mL). The organic extracts were washed with brine (15 mL), dried over MgSO<sub>4</sub>, filtered and the solvent was evaporated. The residue was purified by column chromatography on silica gel (eluent: CH<sub>2</sub>Cl<sub>2</sub>/ MeOH – 15:1). So obtained solid was further purified by preparative TLC (eluent: CH<sub>2</sub>Cl<sub>2</sub>/MeOH – 20:1) to yield the product as a brownish foam (0.233 g; 86 %).

<sup>1</sup>H NMR (500 MHz, CDCl<sub>3</sub>) δ 7.90-7.85 (m, 2H); 7.69 (d, *J* = 2.19 Hz, 1H); 7.44-7.28 (m, 8H); 6.95 (d, *J* = 2.19 Hz, 1H); 6.85 (s, 1H); 4.96 (t, *J* = 5.13 Hz, 1H); 4.59 (d, *J* = 5.63 Hz, 2H).

$^{13}\text{C}$  NMR (126 MHz,  $\text{CDCl}_3$ )  $\delta$  156.6, 147.2, 146.7, 141.2, 139.7, 138.1, 136.9, 129.1, 128.7, 128.4, 128.0, 127.7, 127.6, 109.2, 99.5, 47.4.

HRMS (APCI): calcd. for  $\text{C}_{20}\text{H}_{17}\text{N}_2\text{O}$   $[\text{M}+\text{H}]^+ = 301.1335$ ; found  $[\text{M}+\text{H}]^+ = 301.1335$ .

### Preparative Example 17C



To a freshly prepared solution of xantphos (0.012 g; 0.021 mmol) and  $\text{Pd}_3(\text{dba})_2$  (0.022 g; 0.024 mmol) in anhydrous 1,2-dimethoxyethane (2 mL) were added the product from Preparative Example 16 (0.049 g; 0.22 mmol), *t*-BuOK (0.052 g; 0.46 mmol) and 4-morpholinoaniline (0.048 g; 0.27 mmol) and the resulting mixture was stirred under  $\text{N}_2$  at 100 °C for 16 h. Then it was cooled to 25 °C, diluted with EtOAc (15 mL), poured into brine (25 mL) and extracted with EtOAc (3×15 mL). The organic extracts were dried over  $\text{MgSO}_4$ , filtered, and the solvent was evaporated. The residue was purified by column chromatography on silica gel (eluent:  $\text{CH}_2\text{Cl}_2/\text{MeOH} - 15:1$ ). So obtained oil was further purified by preparative TLC (eluent:  $\text{CH}_2\text{Cl}_2/\text{MeOH} - 20:1$ ) to yield the product as a brownish solid (0.018 g; 22 %).

$^1\text{H}$  NMR (500 MHz,  $\text{CDCl}_3$ )  $\delta$  7.86-7.83 (m, 2H); 7.74 (d,  $J = 2.20$  Hz, 1H); 7.42-7.37 (m, 2H); 7.36-7.31 (m, 1H); 7.26-7.21 (m, 2H); 7.15 (s, 1H); 6.99 (d,  $J = 2.20$  Hz, 1H); 6.97-6.93 (m, 2H); 6.34 (brs, 1H); 3.90-3.85 (m, 4H); 3.20-3.14 (m, 4H).

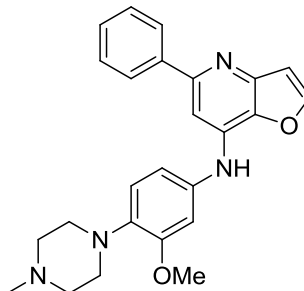
$^{13}\text{C}$  NMR (126 MHz,  $\text{CDCl}_3$ )  $\delta$  156.3, 149.1, 147.5, 147.2, 140.9, 137.9, 137.0, 131.4, 128.7, 128.5, 127.6, 124.7, 116.9, 109.2, 100.3, 67.1, 49.8.

HRMS (APCI): calcd. for  $\text{C}_{23}\text{H}_{22}\text{N}_3\text{O}_2$   $[\text{M}+\text{H}]^+ = 372.1707$ ; found  $[\text{M}+\text{H}]^+ = 372.1707$ .

### Preparative Examples 17D-17I

By essentially same procedure set forth in Preparative Example 17C, using proper amines instead of 4-morpholinoaniline, the compounds given below were prepared.

#### Preparative Example 17D



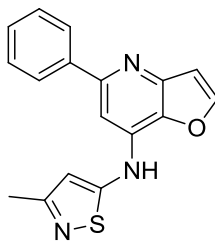
Brown semi – solid.

$^1\text{H}$  NMR (500 MHz,  $\text{CDCl}_3$ )  $\delta$  7.87-7.83 (m, 2H); 7.74 (d,  $J = 2.21$  Hz, 1H); 7.42-7.37 (m, 2H); 7.35-7.31 (m, 1H); 7.25 (s, 1H); 6.98 (d,  $J = 2.20$  Hz, 1H); 6.95 (d,  $J = 8.36$  Hz, 1H); 6.87 (dd,  $J = 2.33$  Hz, 8.36 Hz, 1H); 6.83 (d,  $J = 2.33$  Hz, 1H); 6.38 (brs, 1H); 3.84 (s, 3H); 3.20-3.02 (m, 4H); 2.69-2.58 (m, 4H); 2.36 (s, 3H).

$^{13}\text{C}$  NMR (126 MHz,  $\text{CDCl}_3$ )  $\delta$  156.4, 153.3, 147.6, 147.4, 140.9, 138.8, 137.4, 137.0, 134.4, 128.7, 128.5, 127.5, 119.2, 115.3, 109.3, 107.1, 100.6, 55.9, 55.6, 50.9, 46.3.

HRMS (APCI): calcd. for  $\text{C}_{25}\text{H}_{27}\text{N}_4\text{O}_2$   $[\text{M}+\text{H}]^+ = 415.2129$ ; found  $[\text{M}+\text{H}]^+ = 415.2130$ .

#### Preparative Example 17E



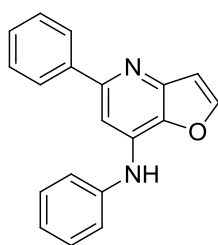
Orange solid.

$^1\text{H}$  NMR (500 MHz, DMSO- $d_6$ )  $\delta$  8.36 (d,  $J = 2.26$  Hz, 1H); 8.01-7.97 (m, 2H); 7.93 (s, 1H); 7.61-7.50 (m, 3H); 7.48-7.43 (m, 1H); 7.38 (s, 1H); 7.21 (d,  $J = 2.25$  Hz, 1H); 2.33 (s, 3H).

$^{13}\text{C}$  NMR (126 MHz, DMSO- $d_6$ )  $\delta$  168.5, 153.3, 150.6, 146.5, 143.5, 138.8, 130.8, 128.7, 128.7, 126.6, 121.5, 110.7, 108.0, 53.7, 20.0.

HRMS (APCI): calcd. for  $\text{C}_{17}\text{H}_{14}\text{N}_3\text{OS}$   $[\text{M}+\text{H}]^+ = 308.0852$ ; found  $[\text{M}+\text{H}]^+ = 308.0850$ .

### Preparative Example 17F



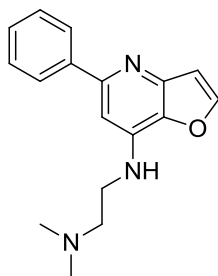
Pale yellow solid.

$^1\text{H}$  NMR (500 MHz,  $\text{CDCl}_3$ )  $\delta$  7.89-7.86 (m, 2H); 7.76 (d,  $J = 2.21$  Hz, 1H); 7.44-7.29 (m, 8H); 7.18-7.14 (m, 1H); 7.00 (d,  $J = 2.22$  Hz, 1H); 6.48 (brs, 1H).

$^{13}\text{C}$  NMR (126 MHz,  $\text{CDCl}_3$ )  $\delta$  156.4, 147.7, 147.6, 140.9, 139.5, 137.2, 136.4, 129.9, 128.8, 128.5, 127.5, 124.5, 121.8, 109.3, 101.0.

HRMS (APCI): calcd. for  $\text{C}_{19}\text{H}_{15}\text{N}_2\text{O}$   $[\text{M}+\text{H}]^+ = 287.1179$ ; found  $[\text{M}+\text{H}]^+ = 287.1178$ .

### Preparative Example 17G



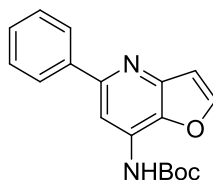
Orange semi – solid.

$^1\text{H}$  NMR (500 MHz,  $\text{CDCl}_3$ )  $\delta$  7.95-7.90 (m, 2H); 7.69 (d,  $J = 2.17$  Hz, 1H); 7.46-7.40 (m, 2H); 7.38-7.33 (m, 1H); 6.94 (d,  $J = 2.17$  Hz, 1H); 6.81 (s, 1H); 5.36-5.23 (m, 1H); 3.43 (dd,  $J = 5.19$  Hz, 11.56 Hz, 2H); 2.69-2.62 (m, 2H); 2.30 (s, 6H).

$^{13}\text{C}$  NMR (126 MHz,  $\text{CDCl}_3$ )  $\delta$  156.4, 147.1, 146.6, 141.3, 140.1, 137.0, 128.7, 128.4, 127.6, 109.0, 99.5, 57.8, 45.3, 40.2.

HRMS (APCI): calcd. for  $\text{C}_{17}\text{H}_{20}\text{N}_3\text{O}$   $[\text{M}+\text{H}]^+ = 282.1601$ ; found  $[\text{M}+\text{H}]^+ = 282.1602$ .

### Preparative Example 17H



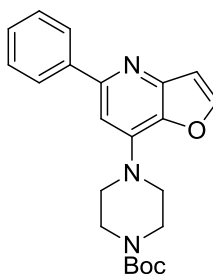
Pale yellow solid foam.

$^1\text{H}$  NMR (500 MHz,  $\text{CDCl}_3$ )  $\delta$  8.41 (s, 1H); 8.03-7.98 (m, 2H); 7.76 (d,  $J = 2.21$  Hz, 1H); 7.46-7.42 (m, 2H); 7.39-7.35 (m, 1H); 7.15 (brs, 1H); 7.02 (d,  $J = 2.21$  Hz, 1H); 1.57 (s, 9H).

$^{13}\text{C}$  NMR (126 MHz,  $\text{CDCl}_3$ )  $\delta$  156.5, 152.0, 148.1, 147.3, 140.3, 136.9, 131.4, 128.8, 128.8, 127.7, 109.4, 105.5, 82.4, 28.5.

HRMS (APCI): calcd. for  $\text{C}_{18}\text{H}_{19}\text{N}_2\text{O}_3$   $[\text{M}+\text{H}]^+ = 311.1390$ ; found  $[\text{M}+\text{H}]^+ = 311.1394$ .

### Preparative Example 17I



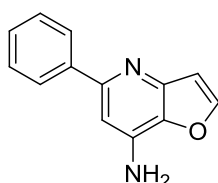
Orange wax.

$^1\text{H}$  NMR (500 MHz,  $\text{CDCl}_3$ )  $\delta$  7.93-7.89 (m, 2H); 7.73 (d,  $J = 2.22$  Hz, 1H); 7.47-7.41 (m, 2H), 7.40-7.35 (m, 1H); 6.99 (d,  $J = 1.60$  Hz, 1H); 6.92 (s, 1H); 3.67-3.60 (m, 8H); 1.48 (s, 9H).

$^{13}\text{C}$  NMR (126 MHz,  $\text{CDCl}_3$ )  $\delta$  156.3, 154.9, 147.2, 142.3, 138.0, 128.8, 128.7, 127.6, 108.9, 102.9, 80.4, 48.1, 28.7.

HRMS (APCI): calcd. for  $\text{C}_{22}\text{H}_{26}\text{N}_3\text{O}_3$   $[\text{M}+\text{H}]^+ = 380.1969$ ; found  $[\text{M}+\text{H}]^+ = 380.1970$ .

### Preparative Example 18A



To a stirred solution of the product from Preparative Example 17H (0.031 g; 0.10 mmol) in ethanol (2 mL) was added aqueous solution of HCl (3M; 0.7 mL; 2.1 mmol) and the resulting mixture was stirred under  $\text{N}_2$  at 60 °C for 18 h. Then the ethanol and HCl were evaporated and the oily residue was treated with  $\text{CH}_2\text{Cl}_2$  (2 mL), MeOH (1mL) and  $\text{Na}_2\text{CO}_3$  (200 mg) and the mixture was stirred at 25 °C. After 20 min., the solvents were evaporated and the solid residue was purified by preparative TLC (eluent:  $\text{CH}_2\text{Cl}_2/7\text{N NH}_3$  in MeOH – 50:1) to yield the product as a white solid (0.019 g; 88 %).

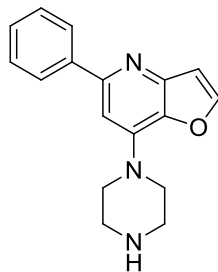
$^1\text{H}$  NMR (500 MHz,  $\text{CDCl}_3$ )  $\delta$  7.92-7.87 (m, 2H); 7.72 (d,  $J = 2.20$  Hz, 1H); 7.45-7.40 (m, 2H); 7.38-7.33 (m, 1H); 6.95 (d,  $J = 2.20$  Hz, 1H); 6.92 (s, 1H); 4.49 (brs, 2H).

$^{13}\text{C}$  NMR (126 MHz,  $\text{CDCl}_3$ )  $\delta$  156.1, 147.8, 147.5, 140.6, 138.5, 137.0, 128.8, 128.5, 127.5, 109.0, 103.2.

HRMS (APCI): calcd. for  $\text{C}_{13}\text{H}_{11}\text{N}_2\text{O}$   $[\text{M}+\text{H}]^+ = 211.0866$ ; found  $[\text{M}+\text{H}]^+ = 211.0866$ .

### Preparative Example 18B

By essentially same procedure set forth in Preparative Example 18A, using the product from Preparative Example 17I, the compound given below was prepared.



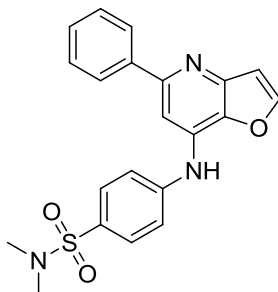
Pale yellow semi – solid.

$^1\text{H}$  NMR (500 MHz,  $\text{CDCl}_3$ )  $\delta$  7.93-7.89 (m, 2H); 7.71 (d,  $J = 2.21$  Hz, 1H); 7.46-7.40 (m, 2H); 7.38-7.34 (m, 1H); 6.96 (d,  $J = 2.22$  Hz, 1H); 6.92 (s, 1H); 3.65-3.60 (m, 4H); 3.13-3.04 (m, 4H).

$^{13}\text{C}$  NMR (126 MHz,  $\text{CDCl}_3$ )  $\delta$  156.4, 148.4, 146.9, 142.7, 141.0, 138.2, 128.8, 128.5, 127.6, 108.9, 102.8, 49.2, 46.0.

HRMS (APCI): calcd. for  $\text{C}_{17}\text{H}_{18}\text{N}_3\text{O}$   $[\text{M}+\text{H}]^+ = 280.1444$ ; found  $[\text{M}+\text{H}]^+ = 280.1443$ .

#### Preparative Example 19A



To a freshly prepared solution of (*S*)-1-[(*R<sub>P</sub>*)-2-(dicyclohexylphosphino)ferrocenyl]ethyl-di-*tert*-butylphosphine (0.012 g; 0.022 mmol) and  $\text{Pd}(\text{OAc})_2$  (0.008 g; 0.037 mmol) in anhydrous 1,2-dimethoxyethane (2 mL) were added the product from Preparative Example 16 (0.049 g; 0.21 mmol), *t*-BuOK (0.038 g; 0.34 mmol) and 4-amino-*N,N*-dimethyl-benzenesulfonamide (0.051 g; 0.25 mmol) and the resulting mixture was stirred under  $\text{N}_2$  at 100 °C for 16 h. Then it was diluted with EtOAc (15 mL), poured into brine (25 mL) and extracted with EtOAc (3×15 mL). The organic extracts were dried over  $\text{MgSO}_4$ , filtered and the solvent was evaporated. The residue was purified by column chromatography on silica gel (eluent:  $\text{CH}_2\text{Cl}_2/\text{MeOH} - 15:1$ ). So obtained oil was further purified by preparative TLC (eluent:  $\text{CH}_2\text{Cl}_2/\text{MeOH} - 20:1$ ) to yield the yellow semi – solid product (0.036 g; 43 %).

$^1\text{H}$  NMR (500 MHz,  $\text{CDCl}_3$ )  $\delta$  7.90-7.86 (m, 2H); 7.78-7.71 (m, 3H); 7.49 (s, 1H); 7.45-7.32 (m, 5H); 7.03 (brs, 1H); 7.00 (d,  $J = 2.15$  Hz, 1H); 2.72 (s, 6H).

$^{13}\text{C}$  NMR (126 MHz,  $\text{CDCl}_3$ )  $\delta$  156.4, 148.3, 148.3, 144.5, 140.3, 137.6, 134.1, 129.8, 129.2, 128.9, 128.9, 127.5, 118.8, 109.2, 103.2, 38.2.

HRMS (APCI): calcd. for  $\text{C}_{21}\text{H}_{20}\text{N}_3\text{O}_3\text{S}$   $[\text{M}+\text{H}]^+ = 394.1220$ ; found  $[\text{M}+\text{H}]^+ = 394.1217$ .

### Preparative Example 19B

By essentially same procedure set forth in Preparative Example 19A, using cyclohexylamine instead of 4-amino-*N,N*-dimethyl-benzenesulfonamide, the compound given below was prepared.



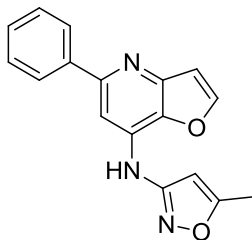
Yellow wax.

$^1\text{H}$  NMR (500 MHz,  $\text{CDCl}_3$ )  $\delta$  7.92-7.87 (m, 2H); 7.66 (d,  $J = 2.17$  Hz, 1H); 7.45-7.39 (m, 2H); 7.38-7.32 (m, 1H); 6.96 (d,  $J = 2.17$  Hz, 1H); 6.81 (s, 1H); 4.70 (brs, 1H); 3.65-3.52 (m, 1H); 2.16-2.05 (m, 2H); 1.84-1.75 (m, 2H); 1.71-1.62 (m, 1H); 1.48-1.36 (m, 2H); 1.35-1.19 (m, 4H).

$^{13}\text{C}$  NMR (126 MHz,  $\text{CDCl}_3$ )  $\delta$  156.0, 147.1, 146.0, 140.8, 139.4, 136.7, 128.7, 128.5, 127.6, 108.8, 99.5, 51.5, 33.4, 25.8, 25.0.

HRMS (APCI): calcd. for  $\text{C}_{19}\text{H}_{21}\text{N}_2\text{O}$   $[\text{M}+\text{H}]^+ = 293.1648$ ; found  $[\text{M}+\text{H}]^+ = 293.1647$ .

### Preparative Example 19C



Degassed 1,2-dimethoxyethane (2.5 mL) was added under N<sub>2</sub> into a 10 mL round bottom flask containing Pd<sub>2</sub>(dba)<sub>3</sub> (15.9 mg, 0.017 mmol) and SPhos (7.1 mg, 0.017 mmol). After 5 min, the product from Preparative Example 16 (40 mg, 0.17 mmol), 5-methylisoxazol-3-amine (20 mg, 0.212 mmol) and Cs<sub>2</sub>CO<sub>3</sub> (125 mg, 0.383 mmol) were added. The mixture was stirred at 80 °C under N<sub>2</sub> for 24 h, then the temperature was elevated to 120 °C and the mixture was stirred for additional 24 h. H<sub>2</sub>O (15 mL) was added and the mixture was extracted with EtOAc (3×25 mL). The organic phase was dried over Na<sub>2</sub>SO<sub>4</sub>, filtered, and then the solvent was evaporated. The residue was purified by column chromatography (CH<sub>2</sub>Cl<sub>2</sub>/EtOAc; 2:1) and then by preparative TLC (CH<sub>2</sub>Cl<sub>2</sub>/EtOAc; 2:1). The product was obtained as a colorless wax (14 mg, 30 % yield).

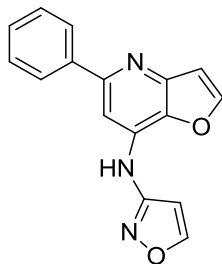
<sup>1</sup>H NMR (300 MHz, CDCl<sub>3</sub>) δ 8.21 (s, 1H), 8.03 (d, *J* = 7.9 Hz, 2H), 7.77 (d, *J* = 1.7 Hz, 1H), 7.54 – 7.34 (m, 3H), 7.09 – 6.96 (m, 2H), 5.92 (s, 1H), 2.42 (s, 3H).

<sup>13</sup>C NMR (126 MHz, CDCl<sub>3</sub>) δ 169.4, 159.5, 156.4, 147.6, 146.7, 140.0, 136.4, 132.8, 128.5, 128.4, 127.3, 109.0, 104.3, 94.8, 12.4.

HRMS (APCI): calcd. for C<sub>17</sub>H<sub>13</sub>N<sub>3</sub>O<sub>2</sub> [M+H]<sup>+</sup> = 292.1081; found [M+H]<sup>+</sup> = 292.1082.

### Preparative Example 19D

By essentially same procedure set forth in Preparative Example 19C, using isoxazol-3-amine instead of 5-methylisoxazol-3-amine, the compound given below was prepared.



Colorless wax.

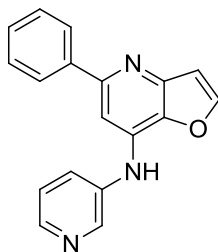
$^1\text{H}$  NMR (500 MHz,  $\text{CDCl}_3$ )  $\delta$  8.30 (d,  $J = 1.7$  Hz, 1H), 8.28 (s, 1H), 8.07 – 8.01 (m, 2H), 7.78 (d,  $J = 2.2$  Hz, 1H), 7.52 – 7.44 (m, 2H), 7.44 – 7.37 (m, 1H), 7.14 (s, 1H), 7.04 (d,  $J = 2.2$  Hz, 1H), 6.28 (d,  $J = 1.7$  Hz, 1H).

$^{13}\text{C}$  NMR (126 MHz,  $\text{CDCl}_3$ )  $\delta$  158.2, 157.6, 155.8, 146.8, 146.1, 139.3, 135.6, 131.8, 127.7, 127.7, 126.6, 108.3, 103.7, 97.0.

HRMS (APCI): calcd. for  $\text{C}_{16}\text{H}_{11}\text{N}_3\text{O}_2$   $[\text{M}+\text{H}]^+ = 278.0924$ ; found  $[\text{M}+\text{H}]^+ = 278.0926$ .

### Preparative Example 19E

By essentially same procedure set forth in Preparative Example 19C, using pyridin-3-amine instead of 5-methylisoxazol-3-amine, the compound given below was prepared.



Colorless wax.

$^1\text{H}$  NMR (300 MHz,  $\text{CDCl}_3$ )  $\delta$  8.65 (s, 1H), 8.42 (d,  $J = 4.2$  Hz, 1H), 7.93 – 7.84 (m, 2H), 7.78 (d,  $J = 2.2$  Hz, 1H), 7.71 – 7.62 (m, 1H), 7.46 – 7.31 (m, 5H), 7.02 (d,  $J = 2.2$  Hz, 1H), 6.66 (s, 1H).

$^{13}\text{C}$  NMR (126 MHz,  $\text{CDCl}_3$ )  $\delta$  156.4, 148.0, 147.9, 145.3, 143.5, 140.4, 137.1, 136.4, 135.5, 128.7, 128.6, 128.2, 127.4, 124.1, 109.2, 101.1.

HRMS (APCI): calcd. for  $C_{18}H_{13}N_3O$   $[M+H]^+ = 288.1131$ ; found  $[M+H]^+ = 288.1132$ .

### Preparative Example 19E

By essentially same procedure set forth in Preparative Example 19C, using 1-methyl-1H-pyrazol-4-amine instead of 5-methylisoxazol-3-amine, the compound given below was prepared.



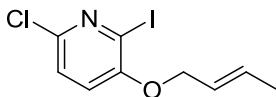
Yellow wax.

$^1H$  NMR (500 MHz,  $CDCl_3$ )  $\delta$  7.89 – 7.84 (m, 2H), 7.75 (d,  $J = 2.2$  Hz, 1H), 7.55 (s, 1H), 7.46 – 7.39 (m, 3H), 7.38 – 7.34 (m, 1H), 6.99 (d,  $J = 2.2$  Hz, 1H), 6.98 (s, 1H), 6.00 (s, 1H), 3.94 (s, 3H).

$^{13}C$  NMR (126 MHz,  $CDCl_3$ )  $\delta$  156.4, 147.5, 146.9, 140.8, 138.8, 136.6, 136.1, 128.6, 128.4, 127.4, 125.9, 121.4, 109.0, 100.0, 39.7.

HRMS (APCI): calcd. for  $C_{17}H_{14}N_4O$   $[M+H]^+ = 291.1240$ ; found  $[M+H]^+ = 291.1237$ .

### Preparative Example 20



To a mixture of the product from Preparative Example 3 (4.34 g; 17.0 mmol) and  $K_2CO_3$  (7.07 g; 51.1 mmol) in *N,N*-dimethylformamide (30 mL) was added under  $N_2$  crotyl bromide (2.6 mL; 25.3 mmol). The resulting reaction mixture was stirred under  $N_2$  at 60 °C for 2 h. Then the solvent was evaporated and the residue was suspended between  $H_2O$  (120 mL) and  $CH_2Cl_2$  (90 mL). The water phase was extracted with  $CH_2Cl_2$  (3×100 mL). The organic extracts were washed with brine (100 mL), dried over  $Na_2SO_4$ , filtered and the solvent was evaporated. The residue was purified by column

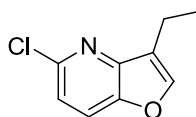
chromatography on silica gel (eluent: hexane/EtOAc – 1:1). So obtained pale yellow solid was washed with cold pentane (3 × 25 mL) to yield the white crystalline product (4.24 g; 81 %).

<sup>1</sup>H NMR (500 MHz, CDCl<sub>3</sub>) δ 7.19-7.11 (m, 1H); 6.93 (d, *J* = 8.46 Hz, 1H); 5.93-5.83 (m, 1H); 5.71-5.61 (m, 1H); 4.52 (d, *J* = 5.49 Hz, 2H); 1.75 (d, *J* = 6.42 Hz, 3H).

<sup>13</sup>C NMR (126 MHz, CDCl<sub>3</sub>) δ 154.4, 141.6, 131.7, 124.7, 123.7, 121.3, 110.0, 70.8, 18.1.

HRMS (APCI): calcd. for C<sub>9</sub>H<sub>10</sub>ClINO [M+H]<sup>+</sup> = 309.9490; found [M+H]<sup>+</sup> = 309.9488.

### Preparative Example 21



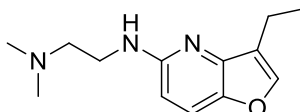
The mixture of the product from Preparative Example 20 (4.24 g; 13.7 mmol), K<sub>2</sub>CO<sub>3</sub> (4.75 g; 34.4 mmol), HCOONa (0.934 g; 13.7 mmol); tetrabutylammonium chloride (4.21 g; 15.1 mmol) and Pd(OAc)<sub>2</sub> (0.185 g; 0.82 mmol) in *N,N*-dimethylformamide (30 mL) was stirred under N<sub>2</sub> at 80 °C for 3 h. Then the solvent was evaporated and the residue was suspended between H<sub>2</sub>O (180 mL) and CH<sub>2</sub>Cl<sub>2</sub> (100 mL). The aqueous phase was extracted with CH<sub>2</sub>Cl<sub>2</sub> (3×100 mL). The organic extracts were washed with brine (100 mL), dried over Na<sub>2</sub>SO<sub>4</sub>, filtered and the solvent was evaporated. The residue was purified by column chromatography on silica gel (eluent: hexane/EtOAc – 30:1) to yield the product as a pale yellow solid (0.774 g; 31 %).

<sup>1</sup>H NMR (500 MHz, CDCl<sub>3</sub>) δ 7.66-7.62 (m, 2H); 7.19 (d, *J* = 8.55 Hz, 1H); 2.76 (dq, *J* = 1.23 Hz, 7.51 Hz, 2H); 1.33 (t, *J* = 7.52 Hz, 3H).

<sup>13</sup>C NMR (126 MHz, CDCl<sub>3</sub>) δ 147.8, 147.4, 146.6, 146.2, 123.6, 120.9, 119.2, 16.0, 13.5.

HRMS (APCI): calcd. for C<sub>9</sub>H<sub>9</sub>ClINO [M+H]<sup>+</sup> = 182.0367; found [M+H]<sup>+</sup> = 182.0365.

### Preparative Example 22



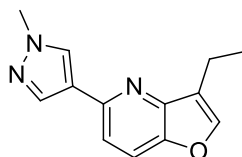
To a freshly prepared solution of (*S*)-1-[(*R<sub>p</sub>*)-2-(dicyclohexylphosphino)ferrocenyl]ethyl-di-*tert*-butylphosphine (0.022 g; 0.039 mmol) and Pd(OAc)<sub>2</sub> (0.009 g; 0.039 mmol) in anhydrous 1,2-dimethoxyethane (2 mL) were added the product from Preparative Example 21 (0.087 g; 0.48 mmol), *t*-BuONa (0.064 g; 0.66 mmol) and *N,N*-dimethylethylenediamine (0.063 mL; 0.57 mmol) and the resulting mixture was stirred under N<sub>2</sub> at 100 °C for 15 h. Then it was cooled to 25 °C, diluted with EtOAc (15 mL), poured into brine (25 mL) and extracted with EtOAc (3×15 mL). The organic extracts were dried over MgSO<sub>4</sub>, filtered and the solvent was evaporated. The residue was purified by column chromatography on silica gel (eluent: CH<sub>2</sub>Cl<sub>2</sub>/7N NH<sub>3</sub> in MeOH – 15:1) to yield the product as an orange oil (0.081 g; 73 %).

<sup>1</sup>H NMR (500 MHz, CDCl<sub>3</sub>) δ 7.46-7.41 (m, 2H); 6.32 (d, *J* = 8.87 Hz, 1H); 5.00-4.89 (m, 1H); 3.42 (dd, *J* = 5.69 Hz, 11.45 Hz, 2H); 2.68 (dq, *J* = 1.14 Hz, 7.51 Hz, 2H); 2.58 (t, *J* = 6.06 Hz, 2H); 2.28 (s, 6H); 1.31 (t, *J* = 7.51 Hz, 3H).

<sup>13</sup>C NMR (126 MHz, CDCl<sub>3</sub>) δ 156.7, 145.3, 143.7, 143.2, 123.0, 120.4, 104.5, 58.6, 45.5, 40.2, 16.2, 13.5.

HRMS (APCI): calcd. for C<sub>13</sub>H<sub>20</sub>N<sub>3</sub>O [M+H]<sup>+</sup> = 234.1601; found [M+H]<sup>+</sup> = 234.1601.

### Preparative Example 23



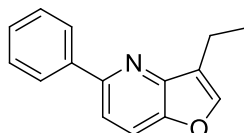
To a mixture of the product from Preparative Example 21 (0.053 g; 0.29 mmol), 1-methylpyrazole-4-boronic acid pinacol ester (0.074 g; 0.36 mmol), K<sub>3</sub>PO<sub>4</sub> (0.262 g; 1.23 mmol) and PdCl<sub>2</sub>.dppf (0.013 g; 0.017 mmol) were added under N<sub>2</sub> 1,2-dimethoxyethane (2 mL) and water (0.5 mL). The reaction mixture was refluxed for 19 h. Then it was cooled to 25 °C, diluted with EtOAc (15 mL), poured into brine (25 mL) and extracted with EtOAc (3×15 mL). The organic extracts were dried over Na<sub>2</sub>SO<sub>4</sub>, filtered and the solvent was evaporated. The residue was purified by column chromatography on silica gel (eluent: CH<sub>2</sub>Cl<sub>2</sub>/MeOH – 10:1) to yield the product as a brown semi – solid (0.055 g; 83 %).

<sup>1</sup>H NMR (500 MHz, CDCl<sub>3</sub>) δ 8.04-7.91 (m, 2H); 7.64 (d, *J* = 8.49 Hz, 1H); 7.58 (s, 1H); 7.36 (d, *J* = 8.51 Hz, 1H); 3.94 (s, 3H); 2.81 (q, *J* = 7.35 Hz, 2H); 1.37 (t, *J* = 7.49 Hz, 3H).

$^{13}\text{C}$  NMR (126 MHz,  $\text{CDCl}_3$ )  $\delta$  148.1, 147.5, 147.1, 145.1, 137.7, 129.0, 124.3, 123.7, 118.9, 115.7, 39.3, 16.2, 13.5.

HRMS (APCI): calcd. for  $\text{C}_{13}\text{H}_{14}\text{N}_3\text{O}$   $[\text{M}+\text{H}]^+ = 228.1131$ ; found  $[\text{M}+\text{H}]^+ = 228.1133$ .

### Preparative Example 24



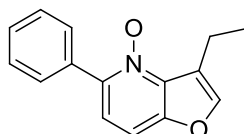
To a mixture of the product from Preparative Example 21 (1.43 g; 7.85 mmol), phenylboronic acid (1.24 g; 10.2 mmol),  $\text{K}_3\text{PO}_4$  (6.86 g; 32.3 mmol) and  $\text{PdCl}_2\cdot\text{dppf}$  (0.530 g; 0.72 mmol) were added under  $\text{N}_2$  1,2-dimethoxyethane (50 mL) and water (10 mL). The reaction mixture was refluxed under  $\text{N}_2$  for 18 h. Then it was cooled to 25 °C, diluted with EtOAc (70 mL), poured into brine (100 mL) and extracted with EtOAc (3 $\times$ 70 mL). The organic extracts were dried over  $\text{Na}_2\text{SO}_4$ , filtered and the solvent was evaporated. The residue was purified by column chromatography on silica gel (eluent: hexane/EtOAc – 15:1) to yield the product as a pale yellow solid (1.59 g; 91 %).

$^1\text{H}$  NMR (500 MHz,  $\text{CDCl}_3$ )  $\delta$  8.04 (d,  $J = 7.51$  Hz, 2H); 7.73 (d,  $J = 8.54$  Hz, 1H); 7.63 (d,  $J = 8.51$  Hz, 2H); 7.51-7.43 (m, 2H); 7.42-7.35 (m, 1H); 2.86 (q,  $J = 7.48$  Hz, 2H); 1.41 (t,  $J = 7.37$  Hz, 3H).

$^{13}\text{C}$  NMR (126 MHz,  $\text{CDCl}_3$ )  $\delta$  153.8, 147.9, 147.7, 145.2, 140.4, 128.9, 128.6, 127.4, 124.1, 118.7, 116.6, 16.2, 13.6.

HRMS (APCI): calcd. for  $\text{C}_{15}\text{H}_{14}\text{NO}$   $[\text{M}+\text{H}]^+ = 224.107$ ; found  $[\text{M}+\text{H}]^+ = 224.1068$ .

### Preparative Example 25



To a stirred solution of the product from Preparative Example 24 (1.59 g, 7.12 mmol) in anhydrous  $\text{CH}_2\text{Cl}_2$  (20 ml) was added MCPBA (2.22 g, 12.9 mmol) and the resulting mixture was stirred under

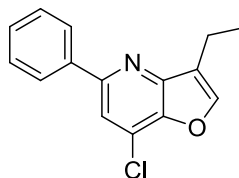
N<sub>2</sub> at 25 °C for 72 h. Then it was poured into saturated aqueous solution of NaHCO<sub>3</sub> (150 mL) and extracted with CH<sub>2</sub>Cl<sub>2</sub> (3×80 mL). The organic extracts were washed with brine (80 mL), dried over Na<sub>2</sub>SO<sub>4</sub>, filtered, and the solvent was evaporated. The residue was purified by column chromatography on silica gel (eluent: CH<sub>2</sub>Cl<sub>2</sub>/EtOAc – 5:1) to yield the product as a pale yellow solid (0.545 g; 32 %).

<sup>1</sup>H NMR (500 MHz, CDCl<sub>3</sub>) δ 7.83-7.76 (m, 2H); 7.50-7.35 (m, 5H); 7.27 (d, *J* = 8.60 Hz, 1H); 3.07 (q, *J* = 7.37 Hz, 2H); 1.34 (t, *J* = 7.41, 3H).

<sup>13</sup>C NMR (126 MHz, CDCl<sub>3</sub>) δ 151.0, 145.4, 144.0, 137.7, 133.1, 129.9, 129.3, 128.4, 122.2, 110.4, 18.1, 14.9.

HRMS (APCI): calcd. for C<sub>15</sub>H<sub>14</sub>NO<sub>2</sub> [M+H]<sup>+</sup> = 240.1019; found [M+H]<sup>+</sup> = 240.1017.

### Preparative Example 26



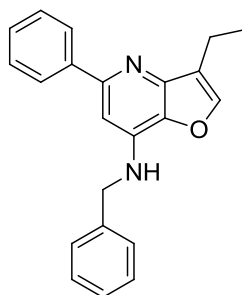
To a stirred solution of the product from Preparative Example 25 (0.713 g, 2.98 mmol) in CHCl<sub>3</sub> (15 ml) was added POCl<sub>3</sub> (6 mL, 64.4 mmol) and the resulting mixture was refluxed under N<sub>2</sub> for 1 hr. Then, the CHCl<sub>3</sub> and POCl<sub>3</sub> were evaporated under reduced pressure. The dark oily residue was diluted with CH<sub>2</sub>Cl<sub>2</sub> (50 mL), poured into saturated aqueous solution of NaHCO<sub>3</sub> (200 mL) and extracted with CH<sub>2</sub>Cl<sub>2</sub> (3×50 mL). The organic extracts were washed with water (50 mL), with brine (80 mL), dried over Na<sub>2</sub>SO<sub>4</sub>, filtered and the solvent was evaporated. The residue was purified by column chromatography on silica gel (eluent: hexane/CH<sub>2</sub>Cl<sub>2</sub> – 2:1) to yield the product as a white solid (0.282 g; 37 %).

<sup>1</sup>H NMR (500 MHz, CDCl<sub>3</sub>) δ 8.07-7.98 (m, 2H); 7.69-7.64 (m, 2H); 7.52-7.36 (m, 3H); 2.84 (dd, *J* = 6.89 Hz, 14.36 Hz, 2H); 1.45-1.39 (m, 3H).

<sup>13</sup>C NMR (126 MHz, CDCl<sub>3</sub>) δ 155.0, 149.1, 145.8, 144.2, 139.3, 129.1, 129.0, 127.4, 126.3, 124.8, 117.1, 16.3, 13.5.

HRMS (APCI): calcd. for C<sub>15</sub>H<sub>13</sub>ClNO [M+H]<sup>+</sup> = 258.0680; found [M+H]<sup>+</sup> = 258.0678.

### Preparative Example 27A



To a solution of the product from Preparative Example 26 (0.202 g; 0.78 mmol), (*R*)-BINAP (0.032 g; 0.052 mmol), Pd<sub>2</sub>(dba)<sub>3</sub> (0.044 g; 0.048 mmol) and *t*-BuOK (0.146 g; 1.30 mmol) in anhydrous toluene (4 mL) was added benzylamine (0.100 mL; 0.92 mmol) and the resulting mixture was stirred under N<sub>2</sub> at 80 °C for 17 h. Then it was cooled to 25 °C, diluted with EtOAc (10 mL), poured into water (25 mL) and extracted with EtOAc (3×10 mL). The organic extracts were washed with brine (15 mL), dried over MgSO<sub>4</sub>, filtered and the solvent was evaporated. The residue was purified by column chromatography on silica gel (eluent: CH<sub>2</sub>Cl<sub>2</sub>/ MeOH – 20:1) to yield a brownish solid (0.168 g; 65 %).

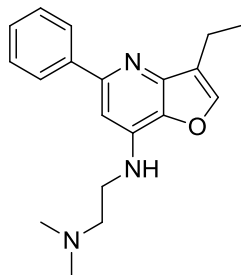
<sup>1</sup>H NMR (500 MHz, CDCl<sub>3</sub>) δ 7.94-7.89 (m, 2H); 7.49-7.46 (m, 1H); 7.43-7.27 (m, 8H); 6.85 (s, 1H); 4.89 (brs, 1H); 4.58 (d, *J* = 5.67 Hz, 2H); 2.83 (dd, *J* = 1.08 Hz, 7.49 Hz, 2H); 1.38 (t, *J* = 7.51 Hz, 3H).

<sup>13</sup>C NMR (126 MHz, CDCl<sub>3</sub>) δ 155.7, 146.6, 143.1, 141.4, 139.6, 138.3, 137.2, 129.1, 128.7, 128.3, 128.0, 127.7, 127.6, 124.6, 99.3, 47.4, 16.4, 13.6.

HRMS (APCI): calcd. for C<sub>22</sub>H<sub>21</sub>N<sub>2</sub>O [M+H]<sup>+</sup> = 329.1648; found [M+H]<sup>+</sup> = 329.1650.

### Preparative Example 27B

By essentially same procedure set forth in Preparative Example 27A, using *N,N*-dimethylethylenediamine instead of benzylamine, the compound given below was prepared.



Yellow wax.

$^1\text{H}$  NMR (500 MHz,  $\text{CDCl}_3$ )  $\delta$  7.99-7.95 (m, 2H); 7.48-7.46 (m, 1H); 7.45-7.40 (m, 2H); 7.37-7.32 (m, 1H); 6.81 (s, 1H); 5.19-5.11 (m, 1H); 3.41 (dd,  $J = 5.16$  Hz, 11.70 Hz, 2H); 2.82 (qd,  $J = 1.20$  Hz, 7.50 Hz, 2H); 2.66-2.59 (m, 2H); 2.28 (s, 6H); 1.38 (t,  $J = 7.51$  Hz, 3H).

$^{13}\text{C}$  NMR (126 MHz,  $\text{CDCl}_3$ )  $\delta$  155.6, 146.7, 142.9, 141.6, 139.9, 137.3, 128.7, 128.2, 127.6, 124.5, 99.3, 57.9, 45.4, 40.3, 16.4, 13.6.

HRMS (APCI): calcd. for  $\text{C}_{19}\text{H}_{24}\text{N}_3\text{O}$   $[\text{M}+\text{H}]^+ = 310.1914$ ; found  $[\text{M}+\text{H}]^+ = 310.1915$ .

### Preparative Example 28



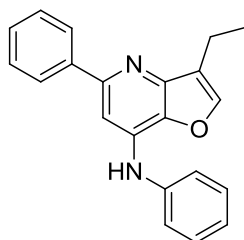
To a stirred solution of the product from Preparative Example 27A (0.052 g, 0.16 mmol) in hot EtOH (2 ml) were added  $\text{Pd}(\text{OH})_2$  (37 mg) and ammonium formate (0.059 g; 0.94 mmol) and the resulting mixture was refluxed under  $\text{N}_2$  for 42 h. Then it was cooled to 25 °C, filtered, and the solvent was evaporated. The residue was purified by preparative TLC (eluent:  $\text{CH}_2\text{Cl}_2/\text{NH}_3$  in MeOH – 50:1) to yield the product as a white solid (0.012 g; 32 %).

$^1\text{H}$  NMR (500 MHz,  $\text{CDCl}_3$ )  $\delta$  7.96 (d,  $J = 7.43$  Hz, 2H); 7.50 (s, 1H); 7.46-7.39 (m, 2H); 7.38-7.31 (m, 1H); 6.92 (s, 1H); 4.36 (brs, 2H); 2.82 (q,  $J = 7.26$  Hz, 2H); 1.38 (t,  $J = 7.45$  Hz, 3H).

$^{13}\text{C}$  NMR (126 MHz,  $\text{CDCl}_3$ )  $\delta$  155.3, 147.7, 143.6, 140.9, 138.1, 137.4, 128.7, 128.3, 127.4, 124.5, 103.0, 16.4, 13.6.

HRMS (APCI): calcd. for  $C_{15}H_{15}N_2O$   $[M+H]^+ = 239.1179$ ; found  $[M+H]^+ = 239.1179$ .

### Preparative Example 29



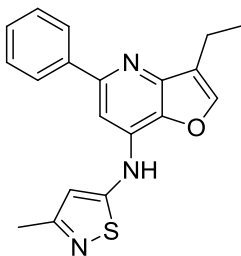
To a freshly prepared solution of xantphos (0.022 g; 0.038 mmol) and  $Pd_3(dba)_2$  (0.042 g; 0.046 mmol) in anhydrous 1,2-dimethoxyethane (2 mL) were added the product from Preparative Example 26 (0.104 g; 0.40 mmol), *t*-BuOK (0.097 g; 0.86 mmol) and aniline (0.048 mL; 0.53 mmol) and the resulting mixture was stirred under  $N_2$  at 100 °C for 16 h. Then it was cooled to 25 °C, diluted with EtOAc (15 mL), poured into brine (25 mL) and extracted with EtOAc ( $3 \times 15$  mL). The organic extracts were dried over  $MgSO_4$ , filtered and the solvent was evaporated. The residue was purified by column chromatography on silica gel (eluent: hexane/EtOAc – 15:1) to yield the product as a pale solid (0.064 g; 51 %).

$^1H$  NMR (500 MHz,  $CDCl_3$ )  $\delta$  7.96-7.91 (m, 2H); 7.56-7.53 (m, 1H); 7.45-7.27 (m, 8H); 7.17-7.12 (m, 1H); 6.40 (brs, 1H); 2.86 (qd,  $J = 1.15$  Hz, 7.50 Hz, 2H); 1.41 (t,  $J = 7.51$  Hz, 3H).

$^{13}C$  NMR (126 MHz,  $CDCl_3$ )  $\delta$  155.5, 147.7, 143.5, 141.1, 139.8, 137.6, 136.1, 129.9, 128.7, 128.4, 127.6, 124.8, 124.2, 121.5, 100.9, 16.4, 13.6.

HRMS (APCI): calcd. for  $C_{21}H_{19}N_2O$   $[M+H]^+ = 315.1492$ ; found  $[M+H]^+ = 315.1492$ .

### Preparative Example 30



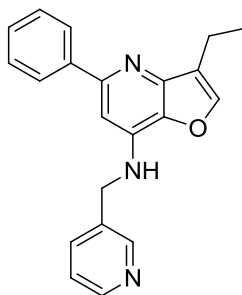
To a freshly prepared solution of xantphos (0.023 g; 0.039 mmol) and Pd<sub>3</sub>(dba)<sub>2</sub> (0.036 g; 0.039 mmol) in anhydrous 1,2-dimethoxyethane (2 mL) were added the product from Preparative Example 26 (0.104 g; 0.40 mmol), *t*-BuOK (0.158 g; 1.40 mmol) and 5-amino-3-methyl-isothiazole hydrochloride (0.115 g; 0.76 mmol) and the resulting mixture was stirred under N<sub>2</sub> at 100 °C for 22 h. Then it was cooled to 25 °C, diluted with EtOAc (15 mL), poured into brine (25 mL) and extracted with EtOAc (3×15 mL). The organic extracts were dried over MgSO<sub>4</sub>, filtered, and the solvent was evaporated. The residue was purified by column chromatography on silica gel (eluent: CH<sub>2</sub>Cl<sub>2</sub>/MeOH – 20:1). So obtained oil was further purified by preparative TLC (eluent: CH<sub>2</sub>Cl<sub>2</sub>/MeOH – 30:1) to yield the product as a pale orange solid (0.053 g; 39 %).

<sup>1</sup>H NMR (500 MHz, DMSO-d<sub>6</sub>) δ 8.15-8.12 (m, 1H); 8.03-7.98 (m, 2H); 7.94-7.88 (m, 1H); 7.56-7.50 (m, 3H); 7.47-7.43 (m, 1H); 7.37 (s, 1H); 2.77 (qd, *J* = 1.05 Hz, 7.48 Hz, 2H); 2.32 (s, 3H); 1.35 (t, *J* = 7.51 Hz, 3H).

<sup>13</sup>C NMR (126 MHz, DMSO-d<sub>6</sub>) δ 168.4, 152.7, 146.4, 146.0, 143.9, 138.9, 130.6, 128.7, 128.6, 126.6, 122.8, 121.5, 110.6, 53.9, 20.0, 15.5, 13.3.

HRMS (APCI): calcd. for C<sub>19</sub>H<sub>18</sub>N<sub>3</sub>OS [M+H]<sup>+</sup> = 336.1165; found [M+H]<sup>+</sup> = 336.1164.

### Preparative Example 31A



To a freshly prepared solution (*S*)-1-[(*R<sub>p</sub>*)-2-(dicyclohexylphosphino)ferrocenyl]ethyl-di-*tert*-butylphosphine (0.011 g; 0.021 mmol) and Pd(OAc)<sub>2</sub> (0.006 g; 0.028 mmol) in anhydrous 1,2-dimethoxyethane (2 mL) were added the product from Preparative Example 26 (0.109 g; 0.42 mmol), *t*-BuONa (0.060 g; 0.62 mmol) and 3-picolylamine (0.045 mL; 0.44 mmol) and the resulting mixture was stirred under N<sub>2</sub> at 100 °C for 17 h. Then it was cooled to 25 °C, diluted with EtOAc (15 mL), poured into brine (25 mL) and extracted with EtOAc (3×15 mL). The organic extracts were dried over MgSO<sub>4</sub>, filtered and the solvent was evaporated. The residue was purified by column

chromatography on silica gel (eluent: CH<sub>2</sub>Cl<sub>2</sub>/MeOH – 10:1). So obtained oil was further purified by preparative TLC (eluent: CH<sub>2</sub>Cl<sub>2</sub>/NH<sub>3</sub> in MeOH – 30:1) to yield the product as a pale yellow solid (0.081 g; 58 %).

<sup>1</sup>H NMR (500 MHz, CDCl<sub>3</sub>) δ 8.67 (s, 1H); 8.55 (d, *J* = 4.20 Hz, 1H); 7.92-7.86 (m, 2H); 7.73-7.68 (m, 1H); 7.48 (s, 1H); 7.43-7.37 (m, 2H); 7.36-7.31 (m, 1H); 7.29-7.25 (m, 1H); 6.81 (s, 1H); 5.01-4.90 (m, 1H); 4.62 (d, *J* = 5.83 Hz, 2H); 2.82 (qd, *J* = 0.84 Hz, 7.45, 2H); 1.38 (t, *J* = 7.51 Hz, 3H).

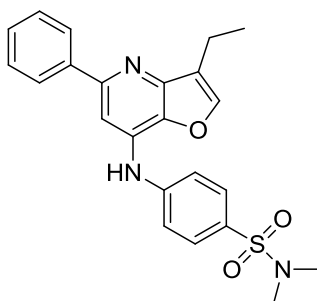
<sup>13</sup>C NMR (126 MHz, CDCl<sub>3</sub>) δ 155.7, 149.5, 149.3, 146.9, 143.3, 141.1, 139.2, 137.1, 135.2, 133.9, 128.7, 128.4, 127.5, 124.6, 123.9, 99.4, 45.0, 16.4, 13.6.

HRMS (APCI): calcd. for C<sub>21</sub>H<sub>20</sub>N<sub>3</sub>O [M+H]<sup>+</sup> = 330.1601; found [M+H]<sup>+</sup> = 330.1598.

### Preparative Examples 31B-31D

By essentially same procedure set forth in Preparative Example 31A, using proper amines instead of 3-picolyamine, the compounds given below were prepared.

#### Preparative Example 31B



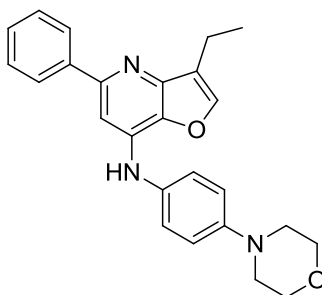
Pale yellow solid.

<sup>1</sup>H NMR (500 MHz, CDCl<sub>3</sub>) δ 7.97-7.91 (m, 2H); 7.78-7.73 (m, 2H); 7.59-7.55 (m, 1H); 7.50 (s, 1H); 7.46-7.32 (m, 5H); 6.90 (brs, 1H); 2.86 (qd, *J* = 0.86 Hz, 7.44 Hz, 2H); 2.76-2.70 (m, 6H); 1.40 (t, *J* = 7.51 Hz, 3H).

<sup>13</sup>C NMR (126 MHz, CDCl<sub>3</sub>) δ 155.3, 148.1, 144.6, 144.3, 140.1, 138.0, 133.9, 129.9, 129.3, 128.9, 127.6, 126.6, 124.7, 118.7, 103.1, 38.2, 16.4, 13.6.

HRMS (APCI): calcd. for  $C_{23}H_{24}N_3O_3S$   $[M+H]^+ = 422.1533$ ; found  $[M+H]^+ = 422.1534$ .

### Preparative Example 31C



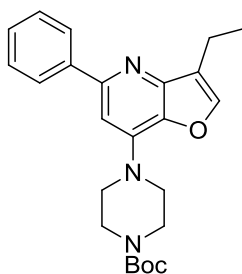
Brown solid.

$^1H$  NMR (500 MHz,  $CDCl_3$ )  $\delta$  7.92-7.86 (m, 2H); 7.55-7.52 (m, 1H); 7.42-7.30 (m, 4H); 7.23-7.20 (m, 1H); 7.17-7.13 (m, 1H); 6.98-6.92 (m, 2H); 6.31 (brs, 1H); 3.90-3.84 (m, 4H); 3.20-3.14 (m, 4H); 2.87 (q,  $J = 7.42$  Hz, 2H); 1.39 (t,  $J = 7.50$  Hz, 3H).

$^{13}C$  NMR (126 MHz,  $CDCl_3$ )  $\delta$  155.3, 149.0, 143.5, 137.3, 131.6, 128.7, 128.5, 127.7, 124.6, 124.6, 124.5, 123.8, 117.0, 116.4, 100.3, 67.1, 49.8, 16.5, 13.6.

HRMS (APCI): calcd. for  $C_{25}H_{26}N_3O_2$   $[M+H]^+ = 400.2020$ ; found  $[M+H]^+ = 400.2019$ .

### Preparative Example 31D



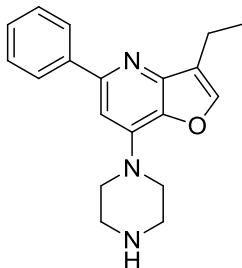
Brown solid foam.

$^1H$  NMR (500 MHz,  $CDCl_3$ )  $\delta$  7.98-7.93 (m, 2H); 7.53-7.50 (m, 1H); 7.46-7.40 (m, 2H); 7.39-7.33 (m, 1H); 6.92 (s, 1H); 3.66-3.56 (m, 8H); 2.84 (q,  $J = 7.39$  Hz, 2H); 1.48 (s, 9H); 1.38 (t,  $J = 7.51$  Hz, 3H).

$^{13}\text{C}$  NMR (126 MHz,  $\text{CDCl}_3$ )  $\delta$  155.4, 154.9, 143.0, 142.2, 138.4, 128.8, 128.5, 127.6, 124.2, 102.8, 80.4, 48.1, 28.6, 16.3, 13.6.

HRMS (APCI): calcd. for  $\text{C}_{24}\text{H}_{30}\text{N}_3\text{O}_3$   $[\text{M}+\text{H}]^+ = 408.2282$ ; found  $[\text{M}+\text{H}]^+ = 408.2281$ .

### Preparative Example 32



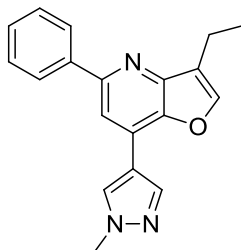
To a stirred solution of the product from Preparative Example 31D (0.088 g; 0.22 mmol) in ethanol (2 mL) was added aqueous HCl (3 M; 1.4 mL; 4.2 mmol) and the resulting mixture was stirred under  $\text{N}_2$  at 60 °C for 17 h. Then, the ethanol and HCl were evaporated and the oily residue was mixed with  $\text{CH}_2\text{Cl}_2$  (2 mL), MeOH (1mL) and  $\text{Na}_2\text{CO}_3$  (200 mg) and the mixture was stirred at 25 °C. After 20 min., the solvents were evaporated and the solid residue was purified by column chromatography on silica gel (eluent:  $\text{CH}_2\text{Cl}_2/7\text{N NH}_3$  in MeOH – 15:1) to yield the product as a pale solid (0.048 g; 72 %).

$^1\text{H}$  NMR (500 MHz,  $\text{CDCl}_3$ )  $\delta$  7.99-7.94 (m, 2H); 7.51-7.48 (m, 1H); 7.46-7.40 (m, 2H); 7.38-7.32 (m, 1H); 6.93 (s, 1H); 3.63-3.56 (m, 4H); 3.11-3.04 (m, 4H); 2.82 (qd,  $J = 1.22$  Hz, 7.50 Hz, 2H); 2.04 (brs, 1H); 1.37 (t,  $J = 7.51$  Hz, 3H).

$^{13}\text{C}$  NMR (126 MHz,  $\text{CDCl}_3$ )  $\delta$  155.4, 148.4, 142.7, 142.6, 141.3, 138.5, 128.7, 128.3, 127.5, 124.2, 102.5, 49.3, 46.1, 16.3, 13.6.

HRMS (APCI): calcd. for  $\text{C}_{19}\text{H}_{22}\text{N}_3\text{O}$   $[\text{M}+\text{H}]^+ = 308.1757$ ; found  $[\text{M}+\text{H}]^+ = 308.1755$ .

### Preparative Example 33



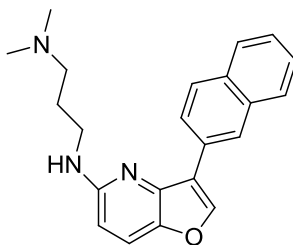
To a mixture of the product from Preparative Example 26 (0.047 g; 0.18 mmol), 1-methylpyrazole-4-boronic acid pinacol ester (0.045 g; 0.22 mmol),  $K_3PO_4$  (0.163 g; 0.77 mmol) and  $PdCl_2(dppf)$  (0.009 g; 0.013 mmol) were added under  $N_2$  1,2-dimethoxyethane (2 mL) and water (0.5 mL). The reaction mixture was refluxed for 15 hrs. Then it was cooled to 25 °C, diluted with EtOAc (15 mL), poured into brine (20 mL) and extracted with EtOAc (3×15 mL). The organic extracts were dried over  $Na_2SO_4$ , filtered and the solvent was evaporated. The residue was purified by column chromatography on silica gel (eluent:  $CH_2Cl_2/EtOAc$  – 10:1). So obtained oil was further purified by preparative TLC (eluent:  $CH_2Cl_2$ ) to yield the product as a white solid (0.024 g; 43 %).

$^1H$  NMR (500 MHz,  $CDCl_3$ )  $\delta$  8.14 (d,  $J = 3.08$  Hz, 2H); 8.07-8.02 (m, 2H); 7.73 (s, 1H); 7.67-7.64 (m, 1H); 7.50-7.44 (m, 2H); 7.41-7.36 (m, 1H); 3.99 (s, 3H); 2.87 (qd,  $J = 1.10$  Hz, 7.49 Hz, 2H); 1.41 (t,  $J = 7.52$  Hz, 3H).

$^{13}C$  NMR (126 MHz,  $CDCl_3$ )  $\delta$  154.4, 148.2, 144.7, 144.2, 140.4, 138.4, 130.5, 128.9, 128.6, 127.5, 124.3, 124.2, 116.1, 112.5, 39.5, 16.3, 13.6.

HRMS (APCI): calcd. for  $C_{19}H_{18}N_3O$   $[M+H]^+ = 304.1444$ ; found  $[M+H]^+ = 304.1444$ .

### Preparative Example 34A



Into a 10 mL flask were placed 1,2-dimethoxyethane (3 mL),  $Pd(OAc)_2$  (1.8 mg, 0.008 mmol) and CyPF(t-Bu) (4.4 mg, 0.008 mmol) and the mixture was stirred at 25 °C under  $N_2$  for 5 min. Then, the

product from Preparative Example 5A (55 mg, 0.20 mmol),  $N^1,N^1$ -dimethylpropane-1,3-diamine (24 mg, 0.24 mmol) and t-BuONa (28 mg, 0.30 mmol) were added and the mixture was refluxed for 22 h. Brine (30 mL) was added and the mixture was extracted with EtOAc (30+20+20 mL). The organic phase was dried over  $\text{Na}_2\text{SO}_4$ , filtered, and the solvent was evaporated. The residue was purified by preparative TLC on silica gel ( $\text{CH}_2\text{Cl}_2/7$  M solution of  $\text{NH}_3$  in MeOH; 30:1). The product was obtained as a green solid (24 mg, 35 %).

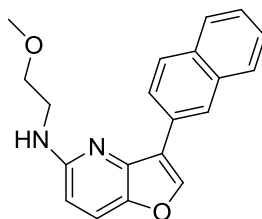
$^1\text{H}$  NMR (500 MHz,  $\text{CDCl}_3$ )  $\delta$  8.09 (s, 1H), 8.04 (dd,  $J = 8.5, 1.7$  Hz, 1H), 7.94 – 7.86 (m, 2H), 7.84 (d,  $J = 7.9$  Hz, 1H), 7.56 (d,  $J = 8.9$  Hz, 1H), 7.52 – 7.43 (m, 2H), 6.42 (d,  $J = 8.9$  Hz, 1H), 3.56 (t,  $J = 6.6$  Hz, 2H), 2.53 (t,  $J = 6.9$  Hz, 2H), 2.31 (s, 6H), 1.94 (p,  $J = 6.8$  Hz, 2H).

$^{13}\text{C}$  NMR (126 MHz,  $\text{CDCl}_3$ )  $\delta$  156.9, 144.02, 143.7, 143.4, 133.8, 132.6, 128.9, 128.3, 128.1, 127.7, 126.1, 125.8, 125.7, 124.8, 120.7, 120.6, 105.0, 58.0, 45.4, 41.5, 27.0.

HRMS (ESI): calcd. for  $\text{C}_{22}\text{H}_{23}\text{N}_3\text{O}$   $[\text{M}+\text{H}]^+ = 346.1914$ ; found  $[\text{M}+\text{H}]^+ = 346.1912$ .

### Preparative Example 34B

By essentially same procedure set forth in Preparative Example 34A, using 2-methoxyethanamine instead of  $N^1,N^1$ -dimethylpropane-1,3-diamine, the compound given below was prepared.



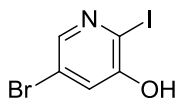
Dark red solid.

$^1\text{H}$  NMR (500 MHz,  $\text{CDCl}_3$ )  $\delta$  8.84 (s, 1H), 8.10 (s, 1H), 8.04 (dd,  $J = 8.5, 1.7$  Hz, 1H), 7.96 – 7.87 (m, 2H), 7.87 – 7.81 (m, 1H), 7.59 (d,  $J = 8.9$  Hz, 1H), 7.53 – 7.44 (m, 2H), 6.46 (d,  $J = 8.9$  Hz, 1H), 3.72 (s, 4H), 3.43 (s, 3H).

$^{13}\text{C}$  NMR (126 MHz,  $\text{CDCl}_3$ )  $\delta$  156.5, 144.3, 143.9, 133.9, 132.8, 128.8, 128.4, 128.2, 127.8, 126.2, 125.9, 125.8, 124.9, 121.0, 120.8, 105.6, 71.6, 58.9, 42.4.

HRMS (APCI): calcd. for  $C_{20}H_{18}N_2O_2$   $[M+H]^+ = 319.1441$ ; found  $[M+H]^+ = 319.1437$ .

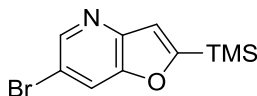
### Preparative Example 35



5-bromopyridin-3-ol (1.1 g, 6.3 mmol), iodine (1.6 g, 6.3 mmol),  $Na_2CO_3$  (1.4 g, 13.2 g) and  $H_2O$  (21 mL) were placed into a 100 mL round bottom flask. The mixture was stirred under  $N_2$  at 25 °C for 3 h. The mixture was neutralized with 1 M aqueous solution of HCl and extracted with EtOAc (60+40+40 mL). The organic phase was washed with brine (50 mL), dried over  $MgSO_4$  and filtered. The product was obtained as a brown solid (1.89 g; 100 %).

$^1H$  NMR (300 MHz,  $CDCl_3$ )  $\delta$  8.08 (d,  $J = 2.1$  Hz, 1H), 7.38 (d,  $J = 2.1$  Hz, 1H), 5.39 (s, 1H).

### Preparative Example 36



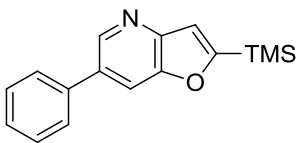
The product from Preparative Example 35 (1.88 g, 6.27 mmol), 1,4-dioxane (12 mL) and TEA (12 mL) were placed into a 100 mL round bottom flask. The mixture was purged with  $N_2$ , then ethynyltrimethylsilane (1.15 mL, 8.15 mmol),  $PdCl_2(PPh_3)_2$  (132 mg, 0.188 mmol) and CuI (71 mg, 0.376 mmol) were added. The mixture was stirred under  $N_2$  at 45 °C for 3 h. The solvent was evaporated and the residue was purified by column chromatography on silica gel (EtOAc/hexane; 1:15). The product was obtained as an orange solid (1.04 g, 61 %).

$^1H$  NMR (500 MHz,  $CDCl_3$ )  $\delta$  8.58 (d,  $J = 1.9$  Hz, 1H), 7.91 (dd,  $J = 1.9, 1.0$  Hz, 1H), 7.10 (d,  $J = 1.0$  Hz, 1H), 0.37 (s, 9H).

$^{13}C$  NMR (126 MHz,  $CDCl_3$ )  $\delta$  170.2, 150.9, 147.1, 146.8, 121.1, 117.1, 115.2, -1.9.

HRMS (APCI): calcd. for  $C_{10}H_{12}BrNOSi$   $[M+H]^+ = 269.9944$ ; found  $[M+H]^+ = 269.9954$ .

### Preparative Example 37



The product from Preparative Example 36 (47 mg, 0.174 mmol), phenylboronic acid (28 mg, 0.226 mmol), 1,2-dimethoxyethane (8 mL), TEA (1 mL) and H<sub>2</sub>O (2 mL) were placed into a 25 mL round bottom flask and the mixture was purged with N<sub>2</sub>. Then, PdCl<sub>2</sub>(dppf) (3.8 mg, 5.2 μmol) was added and the mixture was refluxed under N<sub>2</sub> for 75 min. After addition of brine (25 mL), the mixture was extracted with EtOAc (3×20 mL). The organic phase was dried over MgSO<sub>4</sub>, filtered, and the solvent was evaporated. The residue was purified by column chromatography on silica gel (EtOAc/hexane; 1:10). The product was obtained as a white solid (39 mg, 84 %).

<sup>1</sup>H NMR (300 MHz, CDCl<sub>3</sub>) δ 8.78 (d, *J* = 1.8 Hz, 1H), 7.93 (d, *J* = 0.7 Hz, 1H), 7.69 – 7.59 (m, 2H), 7.55 – 7.35 (m, 3H), 7.17 (d, *J* = 0.8 Hz, 1H), 0.40 (s, 9H).

<sup>13</sup>C NMR (126 MHz, CDCl<sub>3</sub>) δ 169.6, 151.2, 147.5, 145.1, 138.5, 132.9, 129.7, 129.2, 127.9, 127.6, 117.1, 116.4, 115.5, -1.8.

HRMS (APCI): calcd. for C<sub>16</sub>H<sub>17</sub>NOSi [M+H]<sup>+</sup> = 268.1152; found [M+H]<sup>+</sup> = 268.1160.

### Preparative Example 38



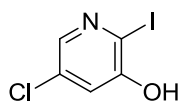
The product from Preparative Example 36 (47 mg, 0.174 mmol), 1-methyl-4-(4,4,5,5-tetramethyl-1,3,2-dioxaborolan-2-yl)-1H-pyrazole (47 mg, 0.226 mmol), 1,2-dimethoxyethane (8 mL), TEA (1 mL) and H<sub>2</sub>O (2 mL) were placed into a 25 mL round bottom flask and the mixture was purged with N<sub>2</sub>. Then, PdCl<sub>2</sub>(dppf) (3.8 mg, 5.2 μmol) was added and the mixture was refluxed under N<sub>2</sub> for 70 min. After addition of brine (25 mL), the mixture was extracted with EtOAc (3×20 mL). The organic phase was dried over MgSO<sub>4</sub>, filtered, and the solvent was evaporated. The residue was purified by column chromatography on silica gel (CH<sub>2</sub>Cl<sub>2</sub>/MeOH; 20:1). The product was obtained as a yellow wax (51 mg, 99 %).

$^1\text{H}$  NMR (500 MHz,  $\text{CDCl}_3$ )  $\delta$  8.67 (d,  $J = 1.7$  Hz, 1H), 7.79 (m, 2H), 7.68 (s, 1H), 7.12 (d,  $J = 1.0$  Hz, 1H), 3.97 (s, 3H), 0.37 (s, 9H).

$^{13}\text{C}$  NMR (126 MHz,  $\text{CDCl}_3$ )  $\delta$  168.9, 151.3, 146.7, 143.8, 137.1, 127.3, 124.6, 120.5, 117.2, 114.6, 39.3, -1.9.

HRMS (APCI): calcd. for  $\text{C}_{14}\text{H}_{17}\text{N}_3\text{OSi}$   $[\text{M}+\text{H}]^+ = 272.1214$ ; found  $[\text{M}+\text{H}]^+ = 272.1219$ .

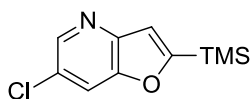
### Preparative Example 39



5-chloropyridin-3-ol (5.12 g, 39.7 mmol), iodine (10.1 g, 39.7 mmol),  $\text{Na}_2\text{CO}_3$  (8.83 g, 83.3 mmol) and  $\text{H}_2\text{O}$  (80 mL) were placed into a 500 mL round bottom flask and the mixture was stirred under  $\text{N}_2$  at 25 °C for 3.5 h. The mixture was neutralized with 1 M aqueous solution of HCl (ca. 120 mL) and extracted with EtOAc (120+70+70 mL). The organic phase was washed with brine (80 mL), dried over  $\text{MgSO}_4$  and filtered. The product was obtained as a brown solid (10.13 g; 100 %).

$^1\text{H}$  NMR (300 MHz, DMSO)  $\delta$  11.38 (s, 1H), 7.95 (d,  $J = 2.3$  Hz, 1H), 7.17 (d,  $J = 2.3$  Hz, 1H).

### Preparative Example 40



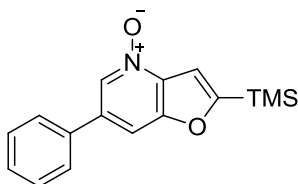
The product from Preparative Example 39 (8.34 g, 32.7 mmol), ethynyltrimethylsilane (6.0 mL, 42.5 mmol),  $\text{PdCl}_2(\text{PPh}_3)_2$  (688 mg, 0.98 mmol), CuI (373 mg, 1.96 mmol), 1,4-dioxane (25 mL) and TEA (25 mL) were placed into a 250 mL round bottom flask. The mixture was stirred under  $\text{N}_2$  at 45 °C for 2.5 h. The solvent was evaporated and the residue was purified by column chromatography on silica gel (EtOAc/hexane; 1:15). The product was obtained as an orange solid (4.37 g, 59 %).

$^1\text{H}$  NMR (500 MHz,  $\text{CDCl}_3$ )  $\delta$  8.52 (dd,  $J = 1.9, 1.4$  Hz, 1H), 7.81 – 7.76 (m, 1H), 7.16 – 7.12 (m, 1H), 0.40 (d,  $J = 1.0$  Hz, 9H).

$^{13}\text{C}$  NMR (126 MHz,  $\text{CDCl}_3$ )  $\delta$  170.3, 150.5, 146.9, 144.9, 127.2, 118.3, 117.1, -1.9.

HRMS (APCI): calcd. for  $C_{10}H_{12}ClNOSi$   $[M+H]^+ = 226.0449$ ; found  $[M+H]^+ = 226.0458$ .

### Preparative Example 41



The product from Preparative Example 37 (1.60 g, 5.98 mmol),  $CH_2Cl_2$  (12 mL) and *m*CPBA (1.86 g, 10.8 mmol) were placed into a 100 mL round bottom flask and the mixture was stirred under  $N_2$  at 25 °C for 3 h. The mixture was neutralized with saturated aqueous solution of  $NaHCO_3$  (30 mL) and extracted with  $CH_2Cl_2$  (3×25 mL). The organic phase was dried over  $MgSO_4$  and filtered. The solvent was evaporated and the residue was purified by column chromatography on silica gel (EtOAc/acetone; 9:1). The product was obtained as a white solid (1.38 g, 82 %).

$^1H$  NMR (500 MHz,  $CDCl_3$ )  $\delta$  8.46 (d,  $J = 1.1$  Hz, 1H), 7.62 (m, 1H), 7.57 (m, 2H), 7.49 (m, 2H), 7.45 (m, 1H), 7.41 (d,  $J = 0.9$  Hz, 1H), 0.39 (s, 9H).

$^{13}C$  NMR (126 MHz,  $CDCl_3$ )  $\delta$  169.6, 154.5, 137.7, 136.3, 135.3, 133.4, 129.5, 129.0, 127.4, 111.1, 109.3, -2.0.

HRMS (APCI): calcd. for  $C_{16}H_{17}NO_2Si$   $[M+H]^+ = 284.1101$ ; found  $[M+H]^+ = 284.1099$ .

### Preparative Example 42



The product from Preparative Example 41 (1.35 g, 4.75 mmol), chloroform (10 mL) and  $POCl_3$  (7.96 mL, 8.54 mmol) were placed into a 100 mL round bottom flask and the mixture was refluxed under  $N_2$  for 1 h. The solvent and  $POCl_3$  were evaporated and the residue was mixed with saturated aqueous solution of  $NaHCO_3$  (50 mL) and extracted with  $CH_2Cl_2$  (50+25+25 mL). The organic phase was dried over  $MgSO_4$  and filtered. The solvent was evaporated and the residue was purified by column

chromatography on silica gel (EtOAc/CH<sub>2</sub>Cl<sub>2</sub>; 1:20). The product was obtained as a white solid (0.824 g, 57 %).

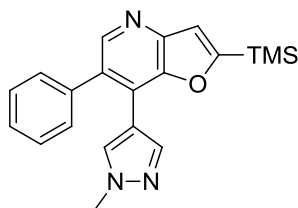
<sup>1</sup>H NMR (500 MHz, CDCl<sub>3</sub>) δ 8.49 (s, 1H), 7.55 – 7.42 (m, 5H), 7.20 (s, 1H), 0.42 (s, 9H).

<sup>13</sup>C NMR (126 MHz, CDCl<sub>3</sub>) δ 170.4, 148.3, 147.9, 147.6, 135.6, 132.0, 130.1, 128.5, 128.3, 124.3, 117.7, -1.8.

HRMS (APCI): calcd for C<sub>16</sub>H<sub>16</sub>ClNOSi [M+H]<sup>+</sup> = 302.0762; found [M+H]<sup>+</sup> = 302.0765.

The structural integrity of this compound was also confirmed by X-ray crystallography.

### Preparative Example 43



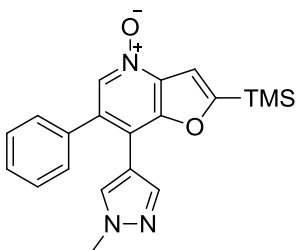
Pd(OAc)<sub>2</sub> (16.7 mg, 74 μmol), SPhos (40 mg, 99 μmol) and 1-butanol (5 mL) were placed into a 25 mL flask and stirred for 5 min. The product from Preparative Example 42 (750 mg, 2.48 mmol), 1-methyl-4-(4,4,5,5-tetramethyl-1,3,2-dioxaborolan-2-yl)-1H-pyrazole (724 mg, 3.48 mmol), TEA (10.4 mL, 74 mmol) and H<sub>2</sub>O (1 mL) were added and the mixture was refluxed for 15 h. The solvent was evaporated and the residue was purified by column chromatography on silica gel (EtOAc/CH<sub>2</sub>Cl<sub>2</sub>; 1:10). The product was obtained as a pale yellow solid (427 mg, 50 %).

<sup>1</sup>H NMR (500 MHz, CDCl<sub>3</sub>) δ 8.41 (s, 1H), 7.58 (s, 1H), 7.47 – 7.41 (m, 3H), 7.38 – 7.32 (m, 2H), 7.27 (s, 1H), 7.20 (s, 1H), 3.84 (s, 3H), 0.42 (s, 9H).

<sup>13</sup>C NMR (126 MHz, CDCl<sub>3</sub>) δ 168.5, 148.0, 147.8, 147.6, 140.9, 139.1, 131.4, 130.3, 130.1, 128.9, 128.0, 122.5, 117.5, 114.3, 39.2, -1.7.

HRMS (APCI): calcd. for C<sub>20</sub>H<sub>21</sub>N<sub>3</sub>OSi [M+H]<sup>+</sup> = 348.1527; found [M+H]<sup>+</sup> = 348.1529.

#### Preparative Example 44



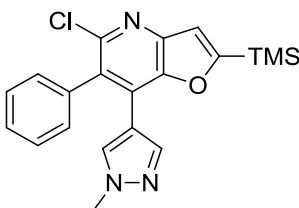
The product from Preparative Example 43 (420 mg, 1.21 mmol),  $\text{CH}_2\text{Cl}_2$  (5 mL) and *m*CPBA (375 mg, 2.18 mmol) were placed into a 25 mL round bottom flask and the mixture was stirred under  $\text{N}_2$  at 25 °C for 1 h. The mixture was mixed with saturated aqueous solution of  $\text{NaHCO}_3$  (40 mL), brine (30 mL) was added and the mixture was extracted with  $\text{CH}_2\text{Cl}_2$  (50+25+25 mL). The organic phase was dried over  $\text{MgSO}_4$  and filtered. The solvent was evaporated and the residue was purified by column chromatography on silica gel (EtOAc/acetone; 2:1). The product was obtained as a light yellow semi-solid (357 mg, 81 %).

$^1\text{H}$  NMR (500 MHz,  $\text{CDCl}_3$ )  $\delta$  8.13 (s, 1H), 7.49 (s, 1H), 7.47 – 7.42 (m, 4H), 7.34 – 7.28 (m, 2H), 7.15 (s, 1H), 3.82 (s, 3H), 0.42 (s, 9H).

$^{13}\text{C}$  NMR (126 MHz,  $\text{CDCl}_3$ )  $\delta$  168.8, 151.0, 140.1, 137.5, 136.8, 135.5, 132.2, 130.6, 129.7, 129.1, 128.8, 116.2, 113.5, 111.4, 39.2, -1.9.

HRMS (APCI): calcd. for  $\text{C}_{20}\text{H}_{21}\text{N}_3\text{O}_2\text{Si}$   $[\text{M}+\text{H}]^+ = 364.1476$ ; found  $[\text{M}+\text{H}]^+ = 364.1478$ .

#### Preparative Example 45



The product from Preparative Example 44 (351 mg, 0.966 mmol) and  $\text{POCl}_3$  (4 mL) were placed into a 25 mL round bottom flask and the mixture was stirred under  $\text{N}_2$  at 100 °C for 25 min. The  $\text{POCl}_3$  was evaporated, the residue was mixed with saturated aqueous solution of  $\text{NaHCO}_3$  (25 mL) and extracted with  $\text{CH}_2\text{Cl}_2$  (20+15+15 mL). The organic phase was dried over  $\text{MgSO}_4$  and filtered. The

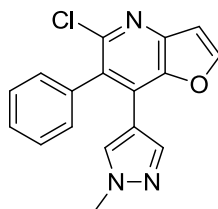
solvent was evaporated and the residue was purified by column chromatography on silica gel (EtOAc/hexane; 1:1). The product was obtained as a white solid (316 mg, 86 %).

$^1\text{H}$  NMR (500 MHz,  $\text{CDCl}_3$ )  $\delta$  7.53 – 7.47 (m, 4H), 7.28 – 7.26 (m, 1H), 7.26 – 7.25 (m, 1H), 7.13 (s, 1H), 6.96 (s, 1H), 3.78 (s, 3H), 0.42 (s, 9H).

$^{13}\text{C}$  NMR (126 MHz,  $\text{CDCl}_3$ )  $\delta$  169.6, 147.4, 147.3, 146.9, 140.9, 138.5, 131.6, 130.3, 129.2, 128.5, 127.8, 126.0, 116.9, 114.5, 39.2, -1.8.

HRMS (APCI): calcd. for  $\text{C}_{20}\text{H}_{20}\text{ClN}_3\text{OSi}$   $[\text{M}+\text{H}]^+ = 382.1137$ ; found  $[\text{M}+\text{H}]^+ = 382.1141$ .

### Preparative Example 46



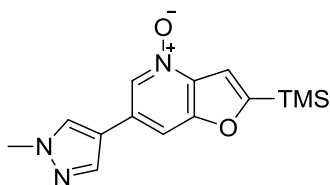
The product from Preparative Example 45 (285 mg, 0.746 mmol), KF (130 mg, 2.24 mmol) and MeOH (16 mL) were placed into a 50 mL round bottom flask and the mixture was stirred under  $\text{N}_2$  at 62 °C for 43 h.. The solvent was evaporated and the residue was purified by column chromatography on silica gel (EtOAc/hexane; 1:1). The product was obtained as a white solid (213 mg, 92 %).

$^1\text{H}$  NMR (500 MHz,  $\text{CDCl}_3$ )  $\delta$  7.93 (d,  $J = 2.3$  Hz, 1H), 7.52 – 7.47 (m, 3H), 7.31 – 7.26 (m, 3H), 7.21 (s, 1H), 7.00 (d,  $J = 2.3$  Hz, 1H), 3.80 (s, 3H).

$^{13}\text{C}$  NMR (126 MHz,  $\text{CDCl}_3$ )  $\delta$  149.4, 148.0, 146.0, 144.4, 140.7, 138.2, 131.9, 130.3, 129.2, 128.6, 128.3, 126.6, 114.0, 108.3, 39.2.

HRMS (APCI): calcd. for  $\text{C}_{18}\text{H}_{12}\text{ClN}_3\text{O}$   $[\text{M}+\text{H}]^+ = 310.0742$ ; found  $[\text{M}+\text{H}]^+ = 310.0750$ .

### Preparative Example 47



The product from Preparative Example 38 (2.36 g, 8.7 mmol),  $\text{CH}_2\text{Cl}_2$  (15 mL) and *m*CPBA (2.1 g, 15.7 mmol) were placed into a 100 mL round bottom flask and the mixture was stirred under  $\text{N}_2$  at 25 °C for 45 h. Then, additional *m*CPBA (0.62 g, 3.6 mmol) was added and the mixture was stirred for additional 4 h. The mixture was mixed with saturated aqueous solution of  $\text{NaHCO}_3$  (20 mL), brine (30 mL) was added, and the mixture was extracted with  $\text{CH}_2\text{Cl}_2$  (3×70 mL). The organic phase was dried over  $\text{MgSO}_4$  and filtered. The solvent was evaporated and the residue was purified by column chromatography on silica gel (EtOAc/MeOH; from 20:1 to 5:1). The product was obtained as a light yellow solid (1.67 g, 66 %).

$^1\text{H}$  NMR (300 MHz,  $\text{CDCl}_3$ )  $\delta$  8.36 (d,  $J = 0.9$  Hz, 1H), 7.76 (s, 1H), 7.63 (s, 1H), 7.49 (s, 1H), 7.36 (d, 1H), 3.98 (s, 3H), 0.38 (s, 9H).

$^{13}\text{C}$  NMR (126 MHz,  $\text{CDCl}_3$ )  $\delta$  168.9, 154.6, 137.1, 131.9, 127.6, 126.8, 118.6, 111.1, 107.4, 39.5, -2.0.

HRMS (APCI): calcd. for  $\text{C}_{14}\text{H}_{17}\text{N}_3\text{O}_2\text{Si}$   $[\text{2M}+\text{H}]^+ = 575.2253$ ; found  $[\text{2M}+\text{H}]^+ = 575.2255$ .

### Preparative Example 48



The product from Preparative Example 47 (1.67 g, 5.81 mmol), chloroform (12 mL) and  $\text{POCl}_3$  (9.75 mL, 105 mmol) were placed into a 100 mL round bottom flask and the mixture was refluxed under  $\text{N}_2$  for 45 min. The solvent and  $\text{POCl}_3$  were evaporated and the residue was mixed with saturated aqueous solution of  $\text{NaHCO}_3$  (40 mL) and extracted with  $\text{CH}_2\text{Cl}_2$  (50+30+30 mL). The organic phase

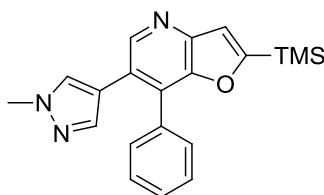
was dried over  $\text{MgSO}_4$  and filtered. The solvent was evaporated and the residue was purified by column chromatography on silica gel ( $\text{CH}_2\text{Cl}_2/\text{MeOH}$ ; 14:1). The product was obtained as a white solid (1.15 g, 65 %).

$^1\text{H}$  NMR (500 MHz,  $\text{CDCl}_3$ )  $\delta$  8.58 (s, 1H), 7.87 (s,  $J = 0.6$  Hz, 1H), 7.83 (s, 1H), 7.15 (s, 1H), 4.00 (s, 3H), 0.40 (s, 9H).

$^{13}\text{C}$  NMR (126 MHz,  $\text{CDCl}_3$ )  $\delta$  169.9, 148.2, 147.3, 146.4, 139.0, 129.8, 123.5, 123.2, 117.7, 116.5, 39.3, -1.9.

HRMS (APCI): calcd. for  $\text{C}_{14}\text{H}_{16}\text{N}_3\text{OSi}$   $[\text{M}+\text{H}]^+ = 306.0824$ ; found  $[\text{M}+\text{H}]^+ = 306.0825$ .

#### Preparative Example 49



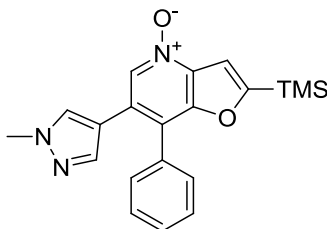
$\text{Pd}(\text{OAc})_2$  (25 mg, 113  $\mu\text{mol}$ ), SPhos (62 mg, 150  $\mu\text{mol}$ ) and 1-butanol (8 mL) were placed into a 50 mL flask and stirred for 5 min. The product from Preparative Example 48 (1.15 g, 3.76 mmol), phenylboronic acid (688 mg, 5.64 mmol), TEA (15.7 mL, 113 mmol) and  $\text{H}_2\text{O}$  (1.6 mL) were added and the mixture was refluxed under  $\text{N}_2$  for 90 min. The solvent was evaporated and the residue was purified by column chromatography on silica gel ( $\text{EtOAc}/\text{MeOH}$ ; from 20:1 to 15:1). The product was obtained as a light grey solid (1.32 g, 100 %).

$^1\text{H}$  NMR (500 MHz,  $\text{CDCl}_3$ )  $\delta$  8.64 (s, 1H), 7.45 – 7.39 (m, 5H), 7.25 (d,  $J = 0.6$  Hz, 1H), 7.17 (s, 1H), 7.04 (s, 1H), 3.81 (s, 3H), 0.32 (s, 9H).

$^{13}\text{C}$  NMR (126 MHz,  $\text{CDCl}_3$ )  $\delta$  169.0, 149.3, 147.1, 146.8, 139.1, 133.5, 130.1, 130.1, 129.2, 128.5, 128.5, 122.8, 118.7, 117.3, 39.0, -1.8.

HRMS (APCI): calcd. for  $\text{C}_{20}\text{H}_{21}\text{N}_3\text{OSi}$   $[\text{M}+\text{H}]^+ = 348.1527$ ; found  $[\text{M}+\text{H}]^+ = 348.1530$ .

### Preparative Example 50



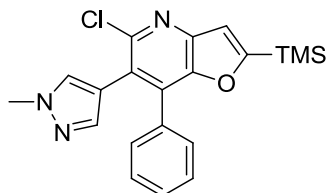
The product from Preparative Example 49 (1.3 g, 3.74 mmol),  $\text{CH}_2\text{Cl}_2$  (10 mL) and *m*CPBA (1.16 g, 6.73 mmol) were placed into a 50 mL round bottom flask and the mixture was stirred under  $\text{N}_2$  at 25 °C for 135 min. The mixture was mixed with saturated aqueous solution of  $\text{NaHCO}_3$  (40 mL) and then extracted with  $\text{CH}_2\text{Cl}_2$  (50+40+40 mL). The organic phase was dried over  $\text{MgSO}_4$  and filtered. The solvent was evaporated and the residue was purified by column chromatography on silica gel (EtOAc/MeOH; from 10:1 to 7:1). The product was obtained as a white semi-solid (1.13 g, 83 %).

$^1\text{H}$  NMR (500 MHz,  $\text{CDCl}_3$ )  $\delta$  8.33 (s, 1H), 7.47 – 7.40 (m, 4H), 7.40 – 7.33 (m, 2H), 7.21 (s, 1H), 7.00 (s, 1H), 3.81 (s, 3H), 0.31 (s, 9H).

$^{13}\text{C}$  NMR (126 MHz,  $\text{CDCl}_3$ )  $\delta$  169.2, 152.6, 138.9, 136.9, 134.2, 132.4, 130.2, 129.5, 128.8, 128.7, 125.3, 123.3, 116.9, 111.2, 39.2, -2.0.

HRMS (APCI): calcd. for  $\text{C}_{20}\text{H}_{21}\text{N}_3\text{O}_2\text{Si}$   $[\text{M}+\text{H}]^+ = 364.1476$ ; found  $[\text{M}+\text{H}]^+ = 364.1479$ .

### Preparative Example 51



The product from Preparative Example 50 (1.13 g, 3.11 mmol) and  $\text{POCl}_3$  (6 mL) were placed into a 50 mL round bottom flask and the mixture was stirred under  $\text{N}_2$  at 100 °C for 20 min. The  $\text{POCl}_3$  was evaporated, the residue was mixed with saturated aqueous solution of  $\text{NaHCO}_3$  (100 mL) and extracted with  $\text{CH}_2\text{Cl}_2$  (60+40+40 mL). The organic phase was dried over  $\text{MgSO}_4$  and filtered. The solvent was evaporated and the residue was purified by column chromatography on silica gel (EtOAc/hexane; 1:2). The product was obtained as a white solid (1.02 g, 86 %).

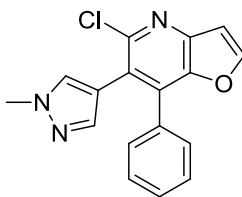
$^1\text{H}$  NMR (300 MHz,  $\text{CDCl}_3$ )  $\delta$  7.38 – 7.32 (m, 3H), 7.31 – 7.26 (m, 3H), 7.14 (s, 1H), 7.10 (s, 1H), 3.83 (s, 3H), 0.32 (s, 9H).

$^{13}\text{C}$  NMR (126 MHz,  $\text{CDCl}_3$ )  $\delta$  170.8, 148.5, 147.6, 146.6, 141.0, 134.6, 133.4, 131.2, 130.2, 128.5, 128.2, 121.5, 116.7, 116.5, 39.0, -1.9.

HRMS (APCI): calcd. for  $\text{C}_{20}\text{H}_{20}\text{ClN}_3\text{OSi}$   $[\text{M}+\text{H}]^+ = 382.1137$ ; found  $[\text{M}+\text{H}]^+ = 382.1141$ .

### Preparative Example 52

By essentially same procedure set forth in Preparative Example 46, using the product from Preparative Example 51, the compound given below was prepared.



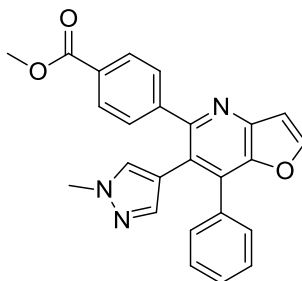
White solid.

$^1\text{H}$  NMR (500 MHz,  $\text{CDCl}_3$ )  $\delta$  7.83 (d,  $J = 2.3$  Hz, 1H), 7.38 – 7.35 (m, 3H), 7.29 – 7.26 (m, 3H), 7.17 (s, 1H), 6.98 (d,  $J = 2.3$  Hz, 1H), 3.83 (s, 3H).

$^{13}\text{C}$  NMR (126 MHz,  $\text{CDCl}_3$ )  $\delta$  150.3, 148.0, 145.6, 140.9, 135.2, 133.0, 131.1, 130.0, 128.8, 128.4, 122.2, 116.2, 108.1, 39.1.

HRMS (APCI): calcd. for  $\text{C}_{17}\text{H}_{12}\text{ClN}_3\text{O}$   $[\text{M}+\text{H}]^+ = 310.0742$ ; found  $[\text{M}+\text{H}]^+ = 310.0746$ .

### Preparative Example 53



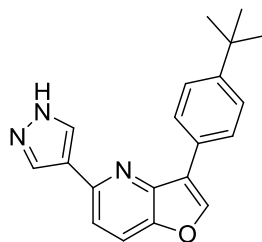
The product from Preparative Example 52 (30 mg, 0.969 mmol), 1,2-dimethoxyethane (2 mL),  $K_3PO_4$  (61.7 mg, 0.291 mmol), (4-(methoxycarbonyl)phenyl)boronic acid (26.1 mg, 0.145 mmol) and  $PdCl_2(dppf)$  (4.3 mg, 5.8  $\mu$ mol) were placed into a 25 mL round bottom flask. The mixture was refluxed under  $N_2$  for 25 h, then additional  $PdCl_2(dppf)$  (5 mg, 6  $\mu$ mol) and  $H_2O$  (0.4 mL) were added and the mixture was refluxed for additional 14 h. The solvent was evaporated and the residue was purified by column chromatography on silica gel (EtOAc/hexane; 1:1). The product was obtained as a colorless wax (17 mg, 43 %).

$^1H$  NMR (500 MHz,  $CDCl_3$ )  $\delta$  8.00 – 7.94 (m, 2H), 7.85 (d,  $J$  = 1.7 Hz, 1H), 7.48 – 7.43 (m, 2H), 7.39 – 7.35 (m, 3H), 7.32 – 7.27 (m, 2H), 7.08 (s, 1H), 6.80 (s, 1H), 6.63 (s, 1H), 3.91 (s, 3H), 3.65 (s, 3H).

$^{13}C$  NMR (126 MHz,  $CDCl_3$ )  $\delta$  171.2, 167.1, 155.4, 149.9, 146.5, 146.2, 145.8, 140.7, 133.3, 133.1, 130.9, 130.1, 129.9, 129.3, 129.1, 128.5, 128.4, 121.9, 117.5, 108.6, 52.2, 38.9.

HRMS (APCI): calcd. for  $C_{25}H_{19}N_3O_3$   $[M+H]^+$  = 410.1499; found  $[M+H]^+$  = 410.1492.

### Preparative Example 54



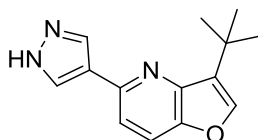
The product from Preparative Example 5D (40 mg, 0.14 mmol), tert-butyl 4-(4,4,5,5-tetramethyl-1,3,2-dioxaborolan-2-yl)-1H-pyrazole-1-carboxylate (49 mg, 0.168 mmol),  $K_3PO_4$  (104 mg, 0.49 mmol), 1,2-dimethoxyethane (2.4 mL),  $H_2O$  (0.6 mL) and  $PdCl_2(dppf)$  (6.2 mg, 8.4  $\mu$ mol) were placed into a 10 mL round bottom flask and the mixture was refluxed under  $N_2$  for 22 h. Then, additional  $PdCl_2(dppf)$  (8 mg, 10.9  $\mu$ mol) was added and the mixture was refluxed for additional 4 h. The solvent was evaporated and the residue was purified by column chromatography on silica gel (EtOAc/hexane; 1:1). The product was obtained as a white solid (18.5 mg, 42 %).

$^1\text{H}$  NMR (500 MHz, DMSO- $d_6$ )  $\delta$  13.04 (s, 1H), 8.74 (s, 1H), 8.52 – 8.10 (m, 4H), 8.05 (d,  $J$  = 8.6 Hz, 1H), 7.73 (d,  $J$  = 8.7 Hz, 1H), 7.54 (d,  $J$  = 8.2 Hz, 2H), 1.35 (s, 9H).

$^{13}\text{C}$  NMR (126 MHz, DMSO- $d_6$ )  $\delta$  149.8, 148.8, 146.7, 146.1, 144.8, 128.7, 127.7, 126.3, 125.4, 122.4, 119.9, 119.5, 115.9, 34.3, 31.1.

HRMS (APCI): calcd. for  $\text{C}_{20}\text{H}_{19}\text{N}_3\text{O}$   $[\text{M}+\text{H}]^+ = 318.1601$ ; found  $[\text{M}+\text{H}]^+ = 318.1599$ .

### Preparative Example 55



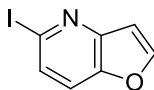
The product from Preparative Example 5E (11 mg, 52.5  $\mu\text{mol}$ ), degassed 1,2-dimethoxyethane (2 mL) and  $\text{H}_2\text{O}$  (0.5 mL) were placed into a 5 mL round bottom flask. Then,  $\text{K}_3\text{PO}_4$  (39 mg, 0.184 mmol), tert-butyl 4-(4,4,5,5-tetramethyl-1,3,2-dioxaborolan-2-yl)-1H-pyrazole-1-carboxylate (18.5 mg, 63  $\mu\text{mol}$ ) and  $\text{PdCl}_2(\text{dppf})$  (2 mg, 2.6  $\mu\text{mol}$ ) were added and the mixture was stirred under  $\text{N}_2$  at 60  $^\circ\text{C}$  for 16 h. Then, additional  $\text{PdCl}_2(\text{dppf})$  (2 mg, 2.6  $\mu\text{mol}$ ), the mixture was refluxed for additional 5 h, another portion of  $\text{PdCl}_2(\text{dppf})$  (2 mg, 2.6  $\mu\text{mol}$ ) and the mixture was refluxed for additional 4 h. The solvent was evaporated and the residue was purified by column chromatography on silica gel (EtOAc/hexane; 1:1). The product was obtained as a yellow wax (2 mg, 15 %).

$^1\text{H}$  NMR (500 MHz,  $\text{CDCl}_3$ )  $\delta$  8.24 (b,  $J$  = 47.6 Hz, 2H), 7.66 (d,  $J$  = 8.2 Hz, 1H), 7.52 (s, 1H), 7.37 (d,  $J$  = 8.1 Hz, 1H), 1.52 (s, 9H).

$^{13}\text{C}$  NMR (126 MHz,  $\text{CDCl}_3$ )  $\delta$  147.7, 143.5, 131.1, 118.7, 115.2, 31.2, 29.8.

HRMS (APCI): calcd. for  $\text{C}_{14}\text{H}_{15}\text{N}_3\text{O}$   $[\text{M}+\text{H}]^+ = 242.1288$ ; found  $[\text{M}+\text{H}]^+ = 242.1292$ .

### Preparative Example 56



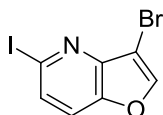
The product from Preparative Example 11 (1.78 g, 11.6 mmol) and degassed 1,4-dioxane (62 mL) were placed into a 250 mL round bottom flask, then AcCl (0.825 mL, 11.6 mmol) was added and the mixture was stirred under N<sub>2</sub> at 25 °C. After 3 min, NaI (17.4 g, 116 mmol) was added, the flask was wrapped with aluminum foil and the mixture was stirred at 106 °C for 70 h. Additional portions of AcCl were added at these times: 15 h, (0.70 mL, 9.8 mmol); 24 h, (0.80 mL, 11.2 mmol); 40 h (0.80 mL, 11.2 mmol); 48 h (0.825 mL, 11.6 mmol); 64 h (0.825 mL, 11.6 mmol). The solvent was evaporated, the residue was mixed with saturated solution of NaHCO<sub>3</sub> (50 mL) and with Na<sub>2</sub>S<sub>2</sub>O<sub>3</sub> (5 g), and extracted with CH<sub>2</sub>Cl<sub>2</sub> (3x90 mL). The organic phase was dried over MgSO<sub>4</sub> and filtered. The mixture was concentrated to the volume of 75 mL and hexane (25 mL) was added. To the solution, upon cooling in ice bath, HCl (15 mL, 1 M solution in Et<sub>2</sub>O) was added. The precipitate was collected by filtration. To the solid, TEA (1.9 mL, 14 mmol) and CH<sub>2</sub>Cl<sub>2</sub> (20 mL) were added, the mixture was cooled in ice bath, H<sub>2</sub>O (60 mL) was added, and the mixture was extracted with CH<sub>2</sub>Cl<sub>2</sub> (3x60 mL). The organic phase was dried over MgSO<sub>4</sub>, filtered, and the solvent was evaporated. The product was obtained as a white solid (1.90 g, 67 %).

<sup>1</sup>H NMR (500 MHz, CDCl<sub>3</sub>) δ 7.81 (d, *J* = 2.3 Hz, 1H), 7.60 (d, *J* = 8.5 Hz, 1H), 7.47 (dd, *J* = 8.5, 0.9 Hz, 1H), 6.96 (dd, *J* = 2.3, 0.9 Hz, 1H).

<sup>13</sup>C NMR (126 MHz, CDCl<sub>3</sub>) δ 149.7, 149.5, 147.5, 129.5, 120.4, 112.0, 108.0.

HRMS (APCI): calcd. for C<sub>7</sub>H<sub>4</sub>INO [M+H]<sup>+</sup> = 245.9410; found [M+H]<sup>+</sup> = 245.9407.

### Preparative Example 57



The product from Preparative Example 56 (1.86 g, 7.60 mmol) and CCl<sub>4</sub> (20 mL) were placed into a 100 mL round bottom flask and the mixture was cooled to -18 °C. Then, bromine (6.49 mL, 114 mmol) was added slowly. The mixture was stirred under N<sub>2</sub> while allowed to warm up to 25 °C for 90

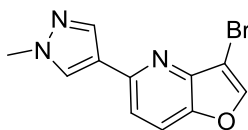
min. The mixture was poured into a mixture of water (100 mL), ice (50 mL) and Na<sub>2</sub>S<sub>2</sub>O<sub>5</sub> (30 g). The resulting mixture was extracted with CH<sub>2</sub>Cl<sub>2</sub> (2x100 mL) and EtOAc (100 mL). The organic phase was washed with brine (100 mL), dried over MgSO<sub>4</sub>, filtered, and the solvent was evaporated. Toluene (24 mL) and DBU (3.4 mL, 22.8 mmol) were added to the residue and the mixture was stirred under N<sub>2</sub> at 80 °C for 45 min. The solvent was evaporated and the residue was and purified by column chromatography on silica gel (EtOAc/hexane; from 1:7 to 1:5). The product was obtained as a white solid (1.77 g, 72 %).

<sup>1</sup>H NMR (500 MHz, CDCl<sub>3</sub>) δ 7.85 (s, 1H), 7.69 (d, *J* = 8.5 Hz, 1H), 7.47 (d, *J* = 8.5 Hz, 1H).

<sup>13</sup>C NMR (126 MHz, CDCl<sub>3</sub>) δ 147.4, 147.2, 146.8, 131.1, 120.9, 113.0, 98.9.

HRMS (APCI): calcd. for C<sub>7</sub>H<sub>3</sub>BrINO [M+H]<sup>+</sup> = 323.8515; found [M+H]<sup>+</sup> = 323.8512.

### Preparative Example 58



A mixture of the product from Preparative Example 57 (167 mg, 0.515 mmol), 1-methyl-4-(4,4,5,5-tetramethyl-1,3,2-dioxaborolan-2-yl)-1H-pyrazole (113 mg, 0.54 mmol), K<sub>3</sub>PO<sub>4</sub> (383 mg, 1.80 mmol), and PdCl<sub>2</sub>(dppf) (18.8 mg, 26 μmol) in 1,2-dimethoxyethane (2 mL) and H<sub>2</sub>O (0.5 mL) was stirred under N<sub>2</sub> at 25 °C for 2.5 h. The solvent was evaporated and the residue was purified by column chromatography on silica gel (hexane/EtOAc; 2:3). The product was obtained as an orange solid (80 mg; 56 %).

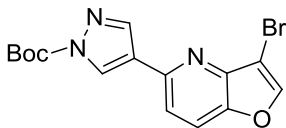
<sup>1</sup>H NMR (500 MHz, CDCl<sub>3</sub>) δ 8.04 (s, 1H), 7.97 (s, 1H), 7.85 (s, 1H), 7.73 (d, *J* = 8.6 Hz, 1H), 7.46 (d, *J* = 8.6 Hz, 1H), 3.96 (s, 3H).

<sup>13</sup>C NMR (126 MHz, CDCl<sub>3</sub>) δ 149.9, 146.6, 146.3, 144.6, 137.6, 129.3, 123.6, 119.6, 116.9, 99.6, 39.3.

HRMS (APCI): calcd. for C<sub>11</sub>H<sub>8</sub>BrN<sub>3</sub>O [M+H]<sup>+</sup> = 277.9924; found [M+H]<sup>+</sup> = 277.9920.

### Preparative Example 59

By essentially same procedure set forth in Preparative Example 58, using tert-butyl 4-(4,4,5,5-tetramethyl-1,3,2-dioxaborolan-2-yl)-1H-pyrazole-1-carboxylate instead of 1-methyl-4-(4,4,5,5-tetramethyl-1,3,2-dioxaborolan-2-yl)-1H-pyrazole, the compound given below was prepared.



White solid.

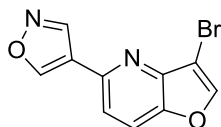
$^1\text{H}$  NMR (500 MHz,  $\text{CDCl}_3$ )  $\delta$  8.65 (s, 1H), 8.27 (s, 1H), 7.90 (s, 1H), 7.79 (d,  $J = 8.6$  Hz, 1H), 7.54 (d,  $J = 8.6$  Hz, 1H), 1.69 (s, 9H).

$^{13}\text{C}$  NMR (126 MHz,  $\text{CDCl}_3$ )  $\delta$  148.2, 147.6, 147.1, 146.7, 145.0, 142.5, 128.7, 125.7, 119.8, 117.5, 99.7, 86.0, 28.1.

HRMS (APCI): calcd. for  $\text{C}_{15}\text{H}_{14}\text{BrN}_3\text{O}_3$   $[\text{M}+\text{H}]^+ = 364.0291$ ; found  $[\text{M}+\text{H}]^+ = 364.0294$ .

The structural integrity of this compound was also confirmed by X-ray crystallography.

### Preparative Example 60



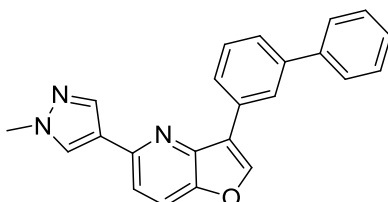
A mixture of the product from Preparative Example 57 (127 mg, 0.393 mmol),  $\text{K}_3\text{PO}_4$  (292 mg, 1.38 mmol), 4-(4,4,5,5-tetramethyl-1,3,2-dioxaborolan-2-yl)isoxazole (80.5 mg, 0.413 mmol), and  $\text{PdCl}_2(\text{dppf})$  (14.4 mg, 19.7  $\mu\text{mol}$ ) in 1,2-dimethoxyethane (2.8 mL) and  $\text{H}_2\text{O}$  (0.7 mL) was stirred under  $\text{N}_2$  at 40  $^\circ\text{C}$  for 25 h. The solvent was evaporated and the residue was purified by column chromatography on silica gel ( $\text{CH}_2\text{Cl}_2/\text{EtOAc}$ ; 20:1). The product was obtained as a white solid (51 mg; 49 %).

$^1\text{H}$  NMR (500 MHz,  $\text{CDCl}_3$ )  $\delta$  9.00 (s, 1H), 8.88 (s, 1H), 7.93 (s, 1H), 7.82 (d,  $J = 8.6$  Hz, 1H), 7.50 (d,  $J = 8.6$  Hz, 1H).

$^{13}\text{C}$  NMR (126 MHz,  $\text{CDCl}_3$ )  $\delta$  155.7, 148.4, 147.5, 146.8, 146.1, 145.3, 122.2, 119.9, 117.8, 99.7.

HRMS (APCI): calcd. for  $\text{C}_{10}\text{H}_5\text{BrN}_2\text{O}_2$   $[\text{M}+\text{H}]^+ = 264.9607$ ; found  $[\text{M}+\text{H}]^+ = 264.9603$ .

### Preparative Example 61



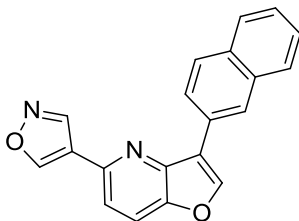
Degassed 1-butanol (2.0 mL) and  $\text{H}_2\text{O}$  (0.4 mL) were placed into a 10 mL round bottom flask,  $\text{Pd}(\text{OAc})_2$  (1 mg, 4  $\mu\text{mol}$ ) and SPhos (2.2 mg, 5.4  $\mu\text{mol}$ ) were added and the mixture was stirred at 25  $^\circ\text{C}$  for 3 min. Then, the product from Preparative Example 58 (25 mg, 90  $\mu\text{mol}$ ), [1,1'-biphenyl]-3-ylboronic acid (25 mg, 0.126 mmol) and TEA (1.0 mL, 7.2 mmol) were added. The mixture was stirred under  $\text{N}_2$  at 40  $^\circ\text{C}$  for 1 h, then at 50  $^\circ\text{C}$  for 2 h. The solvent was evaporated and the residue purified by column chromatography on silica gel (hexane/EtOAc; 1:1) and then by preparative TLC (hexane/acetone; 10:7). The product was obtained as a white solid (7 mg; 22 %).

$^1\text{H}$  NMR (500 MHz,  $\text{CDCl}_3$ )  $\delta$  8.57 – 8.53 (m, 1H), 8.18 (s, 1H), 8.14 – 8.10 (m, 1H), 8.03 (s, 1H), 8.00 (s, 1H), 7.77 (d,  $J = 8.6$  Hz, 1H), 7.75 – 7.71 (m, 2H), 7.63 – 7.54 (m, 2H), 7.53 – 7.44 (m, 3H), 7.42 – 7.37 (m, 1H), 3.99 (s, 3H).

$^{13}\text{C}$  NMR (126 MHz,  $\text{CDCl}_3$ )  $\delta$  148.8, 147.6, 145.8, 145.2, 141.7, 141.4, 137.7, 131.3, 129.2, 128.9, 128.9, 127.5, 127.3, 126.5, 126.2, 125.9, 124.3, 121.4, 119.2, 115.7, 39.3.

HRMS (APCI): calcd. for  $\text{C}_{23}\text{H}_{17}\text{N}_3\text{O}$   $[\text{M}+\text{H}]^+ = 352.1444$ ; found  $[\text{M}+\text{H}]^+ = 352.1449$ .

### Preparative Example 62



The product from Preparative Example 60 (21 mg, 79.2  $\mu\text{mol}$ ),  $\text{Pd}(\text{OAc})_2$  (1 mg, 4  $\mu\text{mol}$ ), SPhos (2 mg, 4.8  $\mu\text{mol}$ ), naphthalen-2-ylboronic acid (17.7 mg, 103  $\mu\text{mol}$ ), 1-butanol (2 mL),  $\text{H}_2\text{O}$  (0.4 mL) and TEA (1.0 mL, 7.17 mmol) were placed into a 10 mL round bottom flask. The mixture was stirred under  $\text{N}_2$  at 45  $^\circ\text{C}$  for 3 h. The solvent was evaporated, the residue was purified by column chromatography (hexane/EtOAc; 3:1) and then by preparative TLC ( $\text{CH}_2\text{Cl}_2/\text{EtOAc}$ ; 30:1). The product was obtained as a colorless wax (2.5 mg; 10 %).

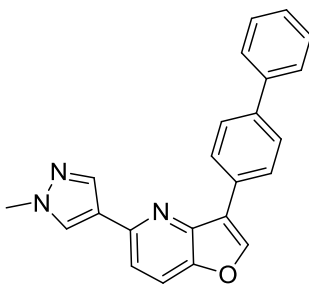
$^1\text{H}$  NMR (500 MHz,  $\text{CDCl}_3$ )  $\delta$  9.02 (s, 1H), 8.94 (s, 1H), 8.87 (s, 1H), 8.30 (s, 1H), 8.09 (dd,  $J = 8.5$ , 1.6 Hz, 1H), 8.00 – 7.93 (m, 2H), 7.91 – 7.85 (m, 2H), 7.57 – 7.50 (m, 3H).

$^{13}\text{C}$  NMR (126 MHz,  $\text{CDCl}_3$ )  $\delta$  155.2, 148.5, 146.5, 146.1, 145.1, 133.8, 133.1, 128.5, 128.5, 127.9, 127.7, 126.6, 126.4, 126.3, 124.8, 122.8, 121.6, 119.5, 116.9.

HRMS (APCI): calcd. for  $\text{C}_{20}\text{H}_{12}\text{N}_2\text{O}_2$   $[\text{M}+\text{H}]^+ = 313.0972$ ; found  $[\text{M}+\text{H}]^+ = 313.0975$ .

### Preparative Example 63

By essentially same procedure set forth in Preparative Example 61, using [1,1'-biphenyl]-4-ylboronic acid instead of [1,1'-biphenyl]-3-ylboronic acid, the compound given below was prepared.



White solid.

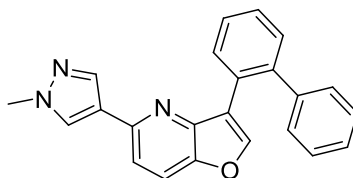
$^1\text{H}$  NMR (500 MHz,  $\text{CDCl}_3$ )  $\delta$  8.28 – 8.24 (m, 2H), 8.16 (s, 1H), 8.04 (d,  $J = 2.9$  Hz, 2H), 7.77 (d,  $J = 8.6$  Hz, 1H), 7.76 – 7.72 (m, 2H), 7.70 – 7.66 (m, 2H), 7.50 – 7.45 (m, 3H), 7.40 – 7.35 (m, 1H), 4.00 (s, 3H).

$^{13}\text{C}$  NMR (126 MHz,  $\text{CDCl}_3$ )  $\delta$  148.8, 147.6, 145.8, 145.1, 141.0, 140.5, 137.7, 129.9, 129.0, 128.9, 127.6, 127.5, 127.4, 127.1, 124.3, 121.3, 119.2, 115.8, 39.3.

HRMS (APCI): calcd. for  $\text{C}_{23}\text{H}_{17}\text{N}_3\text{O}$   $[\text{M}+\text{H}]^+ = 352.1441$ ; found  $[\text{M}+\text{H}]^+ = 352.1442$ .

### Preparative Example 64

By essentially same procedure set forth in Preparative Example 61, using [1,1'-biphenyl]-2-ylboronic acid instead of [1,1'-biphenyl]-3-ylboronic acid, the compound given below was prepared.



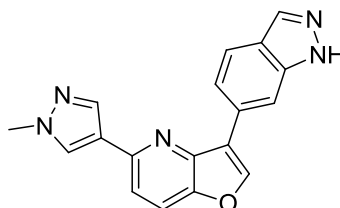
Colorless wax.

$^1\text{H}$  NMR (500 MHz,  $\text{CDCl}_3$ )  $\delta$  8.18 (d,  $J = 7.6$  Hz, 1H), 7.98 – 7.91 (m, 2H), 7.67 (d,  $J = 8.6$  Hz, 1H), 7.54 – 7.48 (m, 1H), 7.47 – 7.42 (m, 2H), 7.38 (d,  $J = 8.6$  Hz, 1H), 7.35 – 7.30 (m, 2H), 7.30 – 7.22 (m, 3H), 7.17 (s, 1H), 3.97 (s, 3H).

$^{13}\text{C}$  NMR (126 MHz,  $\text{CDCl}_3$ )  $\delta$  148.5, 147.5, 146.6, 146.1, 142.2, 141.6, 137.7, 130.9, 130.6, 129.5, 129.1, 128.6, 128.3, 127.8, 127.6, 127.1, 124.1, 120.8, 119.0, 115.5, 39.3.

HRMS (APCI): calcd. for  $\text{C}_{23}\text{H}_{17}\text{N}_3\text{O}$   $[\text{M}+\text{H}]^+ = 352.1444$ ; found  $[\text{M}+\text{H}]^+ = 352.1448$ .

### Preparative Example 65



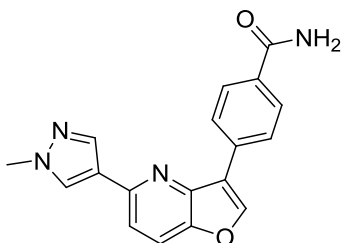
Degassed 1-BuOH (2.5 mL) and H<sub>2</sub>O (0.5 mL) were placed into a 10 mL round bottom flask, then the product from Preparative Example 58 (40 mg, 144 μmol), 6-(4,4,5,5-tetramethyl-1,3,2-dioxaborolan-2-yl)-1H-indazole (49.2 mg, 0.201 mmol), Pd(PPh<sub>3</sub>)<sub>4</sub> (8.3 mg, 7.2 μmol) and K<sub>3</sub>PO<sub>4</sub> (92 mg, 0.432 mmol) were added. The mixture was stirred under N<sub>2</sub> at 90 °C for 18 h. The solvent was evaporated and the residue was purified by column chromatography on silica gel (MeOH/EtOAc; 1:10) and then by preparative TLC (CH<sub>2</sub>Cl<sub>2</sub>/acetone; 3:2). The product was obtained as a white solid (10 mg; 22 %).

<sup>1</sup>H NMR (500 MHz, acetone-d<sub>6</sub>) δ 12.35 (b, 1H), 9.06 (d, *J* = 1.0 Hz, 1H), 8.66 (s, 1H), 8.27 (s, 1H), 8.14 (s, 1H), 8.06 (d, *J* = 0.9 Hz, 1H), 7.95 (d, *J* = 8.7 Hz, 1H), 7.89 – 7.84 (m, 2H), 7.68 (d, *J* = 8.6 Hz, 1H), 3.98 (s, 3H).

<sup>13</sup>C NMR (126 MHz, acetone-d<sub>6</sub>) δ 150.2, 148.5, 147.3, 146.5, 142.0, 138.4, 134.8, 129.9, 129.9, 124.9, 123.6, 122.0, 121.6, 120.5, 120.3, 116.8, 109.7, 39.4.

HRMS (APCI): calcd. for C<sub>18</sub>H<sub>12</sub>N<sub>5</sub>O [M+H]<sup>+</sup> = 316.1193; found [M+H]<sup>+</sup> = 316.1197.

### Preparative Example 66



Degassed 1-butanol (2.0 mL) and H<sub>2</sub>O (0.4 mL) were placed into a 5 mL round bottom flask. Then, the product from Preparative Example 58 (30 mg, 108 μmol), (4-carbamoylphenyl)boronic acid (26.7 mg, 0.162 mmol), Pd(PPh<sub>3</sub>)<sub>4</sub> (6.2 mg, 5.4 μmol) and K<sub>3</sub>PO<sub>4</sub> (68.6 mg, 0.323 mmol) were added. The mixture was stirred under N<sub>2</sub> at 80 °C for 45 min. The solvent was evaporated and the residue was purified by column chromatography on silica gel (MeOH/EtOAc; 1:10) and then by preparative TLC (MeOH/EtOAc; 1:10). The product was obtained as a white solid (12 mg; 35 %).

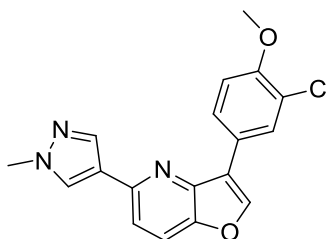
<sup>1</sup>H NMR (500 MHz, acetone-d<sub>6</sub>) δ 8.68 (s, 1H), 8.50 – 8.45 (m, 2H), 8.28 (s, 1H), 8.10 – 8.05 (m, 3H), 7.95 (d, *J* = 8.7 Hz, 1H), 7.69 (d, *J* = 8.7 Hz, 1H), 3.97 (s, 3H).

<sup>13</sup>C NMR (126 MHz, acetone-d<sub>6</sub>) δ 168.8, 150.5, 148.5, 147.8, 146.2, 138.2, 135.1, 134.3, 130.0, 128.9, 127.6, 124.8, 121.3, 120.4, 116.9, 39.4.

HRMS (APCI): calcd. for  $C_{18}H_{14}N_4O_2$   $[M+H]^+ = 319.1190$ ; found  $[M+H]^+ = 319.1187$ .

### Preparative Example 67

By essentially same procedure set forth in Preparative Example 66, using (3-chloro-4-methoxyphenyl)boronic acid instead of (4-carbamoylphenyl)boronic acid, the compound given below was prepared.



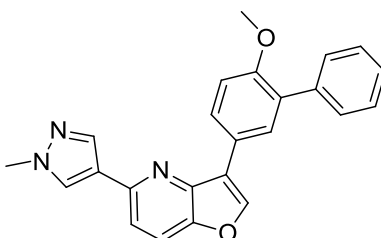
White solid.

$^1H$  NMR (500 MHz, acetone- $d_6$ )  $\delta$  8.56 (s, 1H), 8.43 (d,  $J = 2.1$  Hz, 1H), 8.34 (dd,  $J = 8.6, 2.2$  Hz, 1H), 8.22 (s, 1H), 8.07 (d,  $J = 0.6$  Hz, 1H), 7.92 (d,  $J = 8.7$  Hz, 1H), 7.66 (d,  $J = 8.7$  Hz, 1H), 7.25 (d,  $J = 8.6$  Hz, 1H), 3.97 (d,  $J = 2.0$  Hz, 6H).

$^{13}C$  NMR (126 MHz, acetone- $d_6$ )  $\delta$  155.5, 150.2, 148.3, 146.5, 146.2, 138.2, 129.8, 129.3, 127.6, 125.6, 124.8, 123.1, 120.4, 120.3, 116.8, 113.7, 56.7, 39.4.

HRMS (APCI): calcd. for  $C_{18}H_{14}ClN_3O_2$   $[M+H]^+ = 340.0847$ ; found  $[M+H]^+ = 340.0842$ .

### Preparative Example 68



Degassed 1-butanol (2.0 mL) and H<sub>2</sub>O (0.4 mL) were placed into a 10 mL round bottom flask. Then, the product from Preparative Example 67 (25 mg, 0.074 mmol), phenylboronic acid (11.7 mg, 95.7 μmol), Pd(OAc)<sub>2</sub> (1.0 mg, 3.7 μmol), SPhos (1.8 mg, 44 μmol) and K<sub>3</sub>PO<sub>4</sub> (46.9 mg, 0.220 mmol) were added. The mixture was stirred under N<sub>2</sub> at 80 °C for 4 h. The solvent was evaporated and the residue was purified by column chromatography on silica gel (EtOAc) and then by preparative TLC (CH<sub>2</sub>Cl<sub>2</sub>/EtOAc; 2:1; 3 runs). The product was obtained as a colorless wax (9 mg; 32 %).

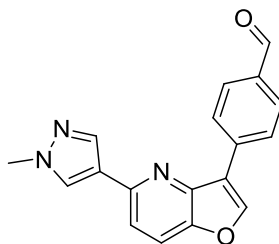
<sup>1</sup>H NMR (300 MHz, acetone-d<sub>6</sub>) δ 8.56 (s, 1H), 8.43 – 8.33 (m, 2H), 8.19 (s, 1H), 8.05 (d, *J* = 0.6 Hz, 1H), 7.90 (d, *J* = 8.7 Hz, 1H), 7.70 – 7.61 (m, 3H), 7.50 – 7.33 (m, 3H), 7.24 (d, *J* = 8.5 Hz, 1H), 3.96 (s, 3H), 3.89 (s, 3H).

<sup>13</sup>C NMR (75 MHz, acetone-d<sub>6</sub>) δ 157.2, 150.0, 148.4, 146.6, 146.2, 139.9, 138.2, 131.7, 130.6, 130.4, 129.8, 129.0, 128.3, 127.9, 125.0, 124.8, 121.5, 120.1, 116.6, 112.9, 56.2, 39.4.

HRMS (APCI): calcd. for C<sub>24</sub>H<sub>19</sub>N<sub>3</sub>O<sub>2</sub> [M+H]<sup>+</sup> = 382.1550; found [M+H]<sup>+</sup> = 382.1547.

### Preparative Example 69

By essentially same procedure set forth in Preparative Example 66, using (4-formylphenyl)boronic acid MIDA ester instead of (4-carbamoylphenyl)boronic acid, the compound given below was prepared.



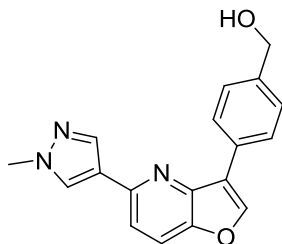
White solid.

<sup>1</sup>H NMR (500 MHz, acetone-d<sub>6</sub>) δ 10.11 (s, 1H), 8.78 (s, 1H), 8.65 (d, *J* = 8.3 Hz, 2H), 8.32 (s, 1H), 8.11 (s, 1H), 8.09 – 8.04 (m, 2H), 7.99 (d, *J* = 8.7 Hz, 1H), 7.73 (d, *J* = 8.7 Hz, 1H), 3.99 (s, 3H).

<sup>13</sup>C NMR (126 MHz, acetone-d<sub>6</sub>) δ 192.6, 192.5, 150.7, 148.6, 148.6, 146.0, 138.3, 136.7, 130.9, 130.1, 128.2, 124.7, 121.0, 120.5, 117.1, 39.4.

HRMS (APCI): calcd. for C<sub>18</sub>H<sub>13</sub>N<sub>3</sub>O<sub>2</sub> [M+H]<sup>+</sup> = 304.1081; found [M+H]<sup>+</sup> = 304.1079.

### Preparative Example 70



The product from Preparative Example 69 (31 mg, 0.102 mmol), NaBH<sub>4</sub> (8 mg, 0.204 mmol) and MeOH (7 mL) were placed into a 10 mL round bottom flask. The mixture was stirred under N<sub>2</sub> at 25 °C for 90 min. Aqueous saturated solution of NH<sub>4</sub>Cl (10 mL) was added and the mixture was extracted with EtOAc (2x20 mL). The organic phase was washed with brine (10 mL), dried over MgSO<sub>4</sub> and filtered. The solvent was evaporated and the residue was purified by column chromatography on silica gel (MeOH/EtOAc; 1:12). The product was obtained as a white solid (26 mg; 84 %).

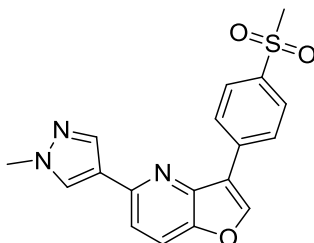
<sup>1</sup>H NMR (500 MHz, acetone-d<sub>6</sub>) δ 8.54 (s, 1H), 8.33 – 8.29 (m, 2H), 8.25 (s, 1H), 8.06 (d, *J* = 0.6 Hz, 1H), 7.92 (d, *J* = 8.7 Hz, 1H), 7.66 (d, *J* = 8.7 Hz, 1H), 7.52 – 7.47 (m, 2H), 4.72 – 4.68 (m, 2H), 3.96 (s, 3H).

<sup>13</sup>C NMR (126 MHz, acetone-d<sub>6</sub>) δ 150.2, 148.4, 146.7, 146.5, 142.9, 138.2, 130.6, 129.9, 127.8, 127.8, 124.9, 122.0, 120.2, 116.7, 64.7, 39.4.

HRMS (APCI): calcd. for C<sub>18</sub>H<sub>15</sub>N<sub>3</sub>O<sub>2</sub> [M+H]<sup>+</sup> = 306.1237; found [M+H]<sup>+</sup> = 306.1242.

### Preparative Example 71

By essentially same procedure set forth in Preparative Example 66, using (4-(methylsulfonyl)phenyl)boronic acid instead of (4-carbamoylphenyl)boronic acid, the compound given below was prepared.



White solid.

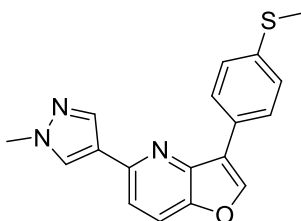
$^1\text{H}$  NMR (300 MHz, acetone- $d_6$ )  $\delta$  8.78 (s, 1H), 8.70 – 8.63 (m, 2H), 8.31 (s, 1H), 8.12 – 8.02 (m, 3H), 7.98 (d,  $J = 8.7$  Hz, 1H), 7.71 (d,  $J = 8.7$  Hz, 1H), 3.97 (s, 3H), 3.17 (s, 3H).

$^{13}\text{C}$  NMR (75 MHz, acetone- $d_6$ )  $\delta$  150.7, 148.7, 148.5, 145.9, 141.0, 138.2, 137.4, 130.1, 128.7, 128.3, 124.6, 120.6, 120.4, 117.1, 44.6, 39.4.

HRMS (APCI): calcd. for  $\text{C}_{18}\text{H}_{15}\text{N}_3\text{O}_3\text{S}$   $[\text{M}+\text{H}]^+ = 354.0907$ ; found  $[\text{M}+\text{H}]^+ = 354.0901$ .

### Preparative Example 72

By essentially same procedure set forth in Preparative Example 66, using (4-(methylthio)phenyl)boronic acid instead of (4-carbamoylphenyl)boronic acid, the compound given below was prepared.



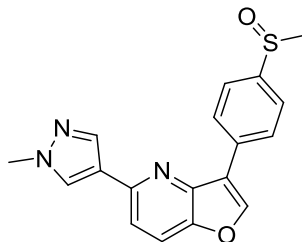
White solid.

$^1\text{H}$  NMR (500 MHz, acetone- $d_6$ )  $\delta$  8.55 (s, 1H), 8.35 – 8.29 (m, 2H), 8.24 (s, 1H), 8.06 (d,  $J = 0.5$  Hz, 1H), 7.91 (d,  $J = 8.7$  Hz, 1H), 7.65 (d,  $J = 8.6$  Hz, 1H), 7.43 – 7.38 (m, 2H), 3.96 (s, 3H), 2.55 (s, 3H).

$^{13}\text{C}$  NMR (126 MHz, acetone- $d_6$ )  $\delta$  150.2, 148.4, 146.7, 146.4, 139.0, 138.2, 129.9, 128.8, 128.3, 127.5, 124.9, 121.5, 120.2, 116.7, 39.4, 15.7.

HRMS (ACPI): calcd. for  $\text{C}_{18}\text{H}_{25}\text{N}_3\text{O}_3\text{S}$   $[\text{M}+\text{H}]^+ = 322.1009$ ; found  $[\text{M}+\text{H}]^+ = 322.1003$ .

### Preparative Example 73



The product from Preparative Example 72 (13 mg, 40.4  $\mu\text{mol}$ ) and  $\text{CH}_2\text{Cl}_2$  (2 mL) were placed into a 5 mL round bottom flask. The mixture was cooled to 0  $^\circ\text{C}$ , then *m*CPBA (7.0 mg, 40.4 mmol) was added and the mixture was stirred under  $\text{N}_2$  at 0  $^\circ\text{C}$  for 45 min. Aqueous saturated solution of  $\text{NaHCO}_3$  (5 mL) and  $\text{H}_2\text{O}$  (5 mL) were added and the mixture was extracted with  $\text{CH}_2\text{Cl}_2$  ( $2 \times 10$  mL). The organic phase was dried over  $\text{MgSO}_4$  and filtered. The solvent was evaporated and the residue was purified by preparative TLC on silica gel (EtOAc/MeOH; 20:1). The product was obtained as a yellow wax (5 mg; 38 %).

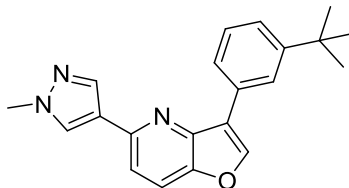
$^1\text{H}$  NMR (300 MHz, acetone- $d_6$ )  $\delta$  8.70 (s, 1H), 8.63 – 8.55 (m, 2H), 8.29 (s, 1H), 8.09 (s, 1H), 7.96 (d,  $J = 8.7$  Hz, 1H), 7.81 (d,  $J = 8.6$  Hz, 2H), 7.69 (d,  $J = 8.7$  Hz, 1H), 3.97 (s, 3H), 2.76 (s, 3H).

$^{13}\text{C}$  NMR (75 MHz, acetone- $d_6$ )  $\delta$  150.4, 148.4, 147.8, 147.1, 146.1, 138.2, 134.6, 130.0, 128.4, 124.8, 124.7, 120.9, 120.4, 116.9, 44.4, 39.3.

HRMS (APCI): calcd. for  $\text{C}_{18}\text{H}_{15}\text{N}_3\text{O}_3\text{S}$   $[\text{M}+\text{H}]^+ = 338.0958$ ; found  $[\text{M}+\text{H}]^+ = 338.0955$ .

### Preparative Example 74

By essentially same procedure set forth in Preparative Example 66, using (3-(tert-butyl)phenyl)boronic acid instead of (4-carbamoylphenyl)boronic acid, the compound given below was prepared.



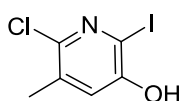
Colorless wax.

$^1\text{H}$  NMR (500 MHz,  $\text{CDCl}_3$ )  $\delta$  8.41 (d,  $J = 0.9$  Hz, 1H), 8.12 (s, 1H), 8.04 (s, 1H), 7.97 (s, 1H), 7.84 (m, 1H), 7.74 (d,  $J = 8.6$  Hz, 1H), 7.42 (m, 3H), 3.97 (s, 3H), 1.44 (s, 9H).

$^{13}\text{C}$  NMR (126 MHz,  $\text{CDCl}_3$ )  $\delta$  151.7, 148.6, 147.6, 145.9, 145.0, 137.7, 130.4, 128.8, 128.5, 124.8, 124.7, 124.4, 124.1, 122.0, 119.1, 115.6, 35.0, 31.6, 31.0.

HRMS (APCI): calcd. for  $\text{C}_{21}\text{H}_{21}\text{N}_3\text{O}$   $[\text{M}+\text{H}]^+ = 332.1757$ ; found  $[\text{M}+\text{H}]^+ = 332.1754$ .

### Preparative Example 75



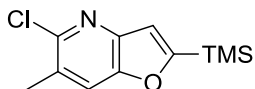
6-chloro-5-iodopyridin-3-ol (2.51 g, 17.5 mmol), iodine (4.44 g, 17.5 mmol),  $\text{H}_2\text{O}$  (35 mL), THF (30 mL) and  $\text{Na}_2\text{CO}_3$  (3.90 g, 36.8 mmol) were placed into a 100 mL round bottom flask. The mixture was stirred under  $\text{N}_2$  at 25 °C for 18 h. The solvent was evaporated and the solution was neutralized with 1 M aqueous solution of HCl (38 mL). Then, saturated aqueous solution of  $\text{NH}_4\text{Cl}$  (30 mL) and  $\text{H}_2\text{O}$  (100 mL) were added and the mixture was extracted with  $\text{CH}_2\text{Cl}_2$  (80 mL) and EtOAc (2×80 mL). The organic phase was washed with brine (30 mL), dried over  $\text{MgSO}_4$ , filtered, and the solvent was evaporated. The product was obtained as a white solid (4.24 g; 90 %).

$^1\text{H}$  NMR (500 MHz,  $\text{CDCl}_3$ )  $\delta$  7.12 (d,  $J = 0.7$  Hz, 1H), 2.31 (d,  $J = 0.7$  Hz, 3H).

$^{13}\text{C}$  NMR (126 MHz,  $\text{CDCl}_3$ )  $\delta$  124.8, 19.3.

HRMS (APCI): calcd. for  $\text{C}_6\text{H}_5\text{ClINO}$   $[\text{M}+\text{H}]^+ = 269.9178$ ; found  $[\text{M}+\text{H}]^+ = 269.9179$ .

### Preparative Example 76



The product from Preparative Example 75 (2.2 g, 8.16 mmol), degassed 1,4-dioxane (17 mL) and TEA (17 mL) were placed into a 100 mL round bottom flask. Then, ethynyltrimethylsilane (1.49 mL, 10.6 mmol), CuI (78 mg, 0.408 mmol) and  $\text{PdCl}_2(\text{PPh}_3)_2$  (114 mg, 0.163 mmol) were added. The mixture was stirred under  $\text{N}_2$  at 45 °C for 3 h. The solvent was evaporated and the residue was

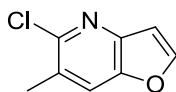
purified by column chromatography on silica gel (hexane/EtOAc; 10:1). The product was obtained as an orange solid (930 mg, 47 %).

$^1\text{H}$  NMR (500 MHz,  $\text{CDCl}_3$ )  $\delta$  7.62 (s, 1H), 7.01 (d,  $J = 0.8$  Hz, 1H), 2.48 (s, 3H), 0.36 (s, 9H).

$^{13}\text{C}$  NMR (126 MHz,  $\text{CDCl}_3$ )  $\delta$  169.5, 150.4, 147.1, 146.1, 127.3, 121.1, 116.5, 20.6, -1.9.

HRMS (APCI): calcd. for  $\text{C}_{11}\text{H}_{14}\text{ClNOSi}$   $[\text{M}+\text{H}]^+ = 240.0606$ ; found  $[\text{M}+\text{H}]^+ = 240.0604$ .

### Preparative Example 77



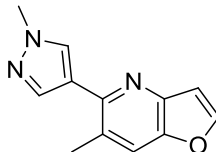
The product from Preparative Example 76 (0.90 g, 3.75 mmol), MeOH (28 mL) and KF (654 mg, 11.3 mmol) were placed into a 100 mL round bottom flask. The mixture was stirred under  $\text{N}_2$  at 25 °C for 14 h, then at 60 °C for additional 8 h. The solvent was evaporated and the residue was purified by column chromatography on silica gel (hexane/EtOAc; from 10:1 to 5:1). The product was obtained as a white solid (560 mg, 88 %).

$^1\text{H}$  NMR (500 MHz,  $\text{CDCl}_3$ )  $\delta$  7.79 (d,  $J = 2.0$  Hz, 1H), 7.65 (s, 1H), 6.89 (m, 1H), 2.49 (s, 3H).

$^{13}\text{C}$  NMR (126 MHz,  $\text{CDCl}_3$ )  $\delta$  149.3, 147.6, 147.4, 145.3, 127.8, 121.4, 107.7, 20.6.

HRMS (APCI): calcd. for  $\text{C}_8\text{H}_6\text{ClNO}$   $[\text{M}+\text{H}]^+ = 168.0211$ ; found  $[\text{M}+\text{H}]^+ = 168.0209$ .

### Preparative Example 78



Degassed 1,2-dimethoxyethane (4.0 mL) and  $\text{H}_2\text{O}$  (1.0 mL) were placed into a 25 mL round bottom flask. Then, the product from Preparative Example 77 (160 mg, 0.94 mmol), 1-methyl-4-(4,4,5,5-

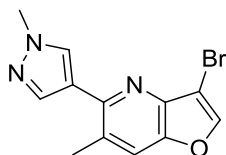
tetramethyl-1,3,2-dioxaborolan-2-yl)-1H-pyrazole (294 mg, 1.42 mmol), PdCl<sub>2</sub>(dppf) (34 mg, 47 μmol) and K<sub>3</sub>PO<sub>4</sub> (599 mg, 2.82 mmol) were added. The mixture was stirred under N<sub>2</sub> at 80 °C for 5 h. The solvent was evaporated and the residue was purified by column chromatography on silica gel (EtOAc/MeOH; from 1:0 to 10:1) and then by another column chromatography (EtOAc). The product was obtained as a white solid (120 mg; 60 %).

<sup>1</sup>H NMR (500 MHz, CDCl<sub>3</sub>) δ 7.90 (s, 1H), 7.82 (s, 1H), 7.76 (d, *J* = 2.3 Hz, 1H), 7.60 (s, 1H), 6.92 (dd, *J* = 2.2, 0.9 Hz, 1H), 3.97 (s, 3H), 2.56 (s, 3H).

<sup>13</sup>C NMR (126 MHz, CDCl<sub>3</sub>) δ 148.6, 146.9, 145.3, 139.3, 137.0, 130.3, 126.6, 123.2, 120.4, 108.0, 39.1, 21.6.

HRMS (APCI): calcd. for C<sub>12</sub>H<sub>11</sub>N<sub>3</sub>O [M+H]<sup>+</sup> = 214.0975; found [M+H]<sup>+</sup> = 214.0972.

### Preparative Example 79



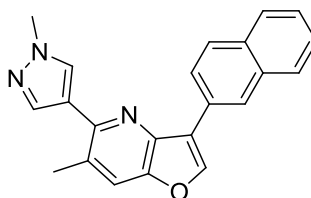
The product from Preparative Example 78 (115 mg, 0.54 mmol) and CCl<sub>4</sub> (5 mL) were placed into a 100 mL round bottom flask. The mixture was cooled to -18 °C, then bromine (0.56 mL, 10.8 mmol) was added slowly. The mixture was allowed to warm to 12 °C and stirred under N<sub>2</sub> for 60 min. The mixture was poured into a mixture of water (30 mL), ice (20 mL) and Na<sub>2</sub>S<sub>2</sub>O<sub>5</sub> (2 g). The resulting mixture was extracted with CH<sub>2</sub>Cl<sub>2</sub> (20 mL) and EtOAc (2×15 mL). The organic phase was dried over MgSO<sub>4</sub>, filtered, and the solvent was evaporated. Toluene (12 mL) and DBU (0.241 mL, 1.62 mmol) were added to the residue and the mixture was stirred under N<sub>2</sub> at 80 °C for 45 min. The solvent was evaporated and the residue was purified by column chromatography on silica gel (EtOAc/hexane; 1:1) and then by preparative TLC (EtOAc/hexane; 2:1). The product was obtained as a white solid (19 mg, 12 %).

<sup>1</sup>H NMR (500 MHz, CDCl<sub>3</sub>) δ 7.93 (d, *J* = 2.3 Hz, 2H), 7.80 (s, 1H), 7.61 (s, 1H), 3.98 (s, 3H), 2.60 (s, 3H).

<sup>13</sup>C NMR (126 MHz, CDCl<sub>3</sub>) δ 149.2, 146.5, 146.1, 142.5, 139.3, 130.9, 127.9, 122.98 (s), 121.0, 99.5, 39.2, 21.7.

HRMS (APCI): calcd. for  $C_{12}H_{10}BrN_3O$   $[M+H]^+ = 292.0080$ ; found  $[M+H]^+ = 292.0075$ .

### Preparative Example 80



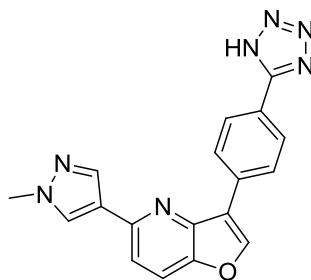
Degassed 1-butanol (2.0 mL) and  $H_2O$  (0.4 mL) were placed into a 10 mL round bottom flask. Then, the product from Preparative Example 79 (15 mg, 51.3  $\mu\text{mol}$ ), naphthalen-2-ylboronic acid (13.3 mg, 77  $\mu\text{mol}$ ),  $Pd(PPh_3)_4$  (3.0 mg, 2.6  $\mu\text{mol}$ ) and  $K_3PO_4$  (32.7 mg, 0.154 mmol) were added. The mixture was stirred under  $N_2$  at 80  $^\circ\text{C}$  for 70 min. The solvent was evaporated and the residue was purified by column chromatography on silica gel (EtOAc/ $CH_2Cl_2$ ; 1:2) and then by preparative TLC (EtOAc/ $CH_2Cl_2$ ; 2:3). The product was obtained as a colorless wax (8.5 mg; 49 % yield).

$^1H$  NMR (300 MHz,  $CDCl_3$ )  $\delta$  8.88 (s, 1H), 8.18 (s, 1H), 8.14 – 8.07 (m, 2H), 7.97 – 7.84 (m, 4H), 7.64 (d,  $J = 0.5$  Hz, 1H), 7.55 – 7.44 (m, 2H), 4.03 (s, 3H), 2.64 (s, 3H).

$^{13}C$  NMR (75 MHz,  $CDCl_3$ )  $\delta$  148.1, 148.0, 144.9, 143.9, 139.8, 133.9, 133.0, 130.5, 128.6, 128.5, 128.4, 127.9, 126.5, 126.4, 126.3, 126.1, 125.0, 123.9, 121.4, 120.7, 39.3, 21.9.

HRMS (APCI): calcd. for  $C_{22}H_{17}N_3O$   $[M+H]^+ = 340.1444$ ; found  $[M+H]^+ = 340.1440$ .

### Preparative Example 81



Degassed 1-butanol (2.0 mL) and  $H_2O$  (0.4 mL) were placed into a 10 mL round bottom flask. Then, the product from Preparative Example 58 (23.8 mg, 85.6  $\mu\text{mol}$ ), (4-(1H-tetrazol-5-yl)phenyl)boronic

acid (19.5 mg, 0.103 mmol), Pd(PPh<sub>3</sub>)<sub>4</sub> (5.0 mg, 4.3 μmol) and K<sub>3</sub>PO<sub>4</sub> (54.5 mg, 0.257 mmol) were added. The mixture was refluxed under N<sub>2</sub> for 150 min. The solvent was evaporated and the residue purified by column chromatography on silica gel (EtOAc/MeOH; from 3:1 to 2:1) and then by preparative TLC (THF/MeOH; 2:1). The product was obtained as a colorless semi-solid (12 mg; 41 %).

<sup>1</sup>H NMR (300 MHz, CD<sub>3</sub>OD) δ 8.44 (s, 1H), 8.37 – 8.30 (m, 2H), 8.20 – 8.13 (m, 3H), 8.05 (d, *J* = 0.7 Hz, 1H), 7.83 (d, *J* = 8.7 Hz, 1H), 7.57 (d, *J* = 8.7 Hz, 1H), 3.96 (s, 3H).

<sup>13</sup>C NMR (75 MHz, CD<sub>3</sub>OD) δ 149.9, 148.9, 147.3, 146.6, 138.4, 132.7, 130.7, 130.0, 128.2, 127.9, 126.5, 125.4, 122.0, 120.3, 116.9, 39.1.

HRMS (APCI): calcd. for C<sub>18</sub>H<sub>13</sub>N<sub>7</sub>O [M+H]<sup>+</sup> = 344.1254; found [M+H]<sup>+</sup> = 344.1252.

### ASSAYS:

*In vitro* essays were performed by the company Merck Millipore in their KinaseProfiler radiometric protein kinase assay as paid commercial service. The compounds' IC<sub>50</sub> values for inhibition of individual protein kinases were determined. Dose-response curves were plotted from inhibition data generated, each in duplicate, from 10 point serial dilutions of inhibitory compounds. Concentration of compound was plotted against % kinase activity. To generate IC<sub>50</sub> values, the dose-response curves were fitted to a standard sigmoidal curve and IC<sub>50</sub> values were derived by standard nonlinear regression analysis.

All tested compounds were prepared in 100% DMSO to final assay concentrations either 0.5 mM (for the concentration row A, see below) or 0.05 mM (for the concentration row B). This working stock of the compound was added to the assay well as the first component in the reaction, followed by the remaining components as detailed below. The stock solution was added to the individual assay wells in such amounts that the concentrations of the compound were either in the row A (0.001 μM, 0.003 μM, 0.01 μM, 0.03 μM, 0.1 μM, 0.3 μM, 1.0 μM, 3.0 μM, and 10.0 μM) or in the row B (0.0001 μM, 0.0003 μM, 0.001 μM, 0.003 μM, 0.01 μM, 0.03 μM, 0.1 μM, 0.3 μM, and 1.0 μM). There was no pre-incubation step between the compound and the kinase prior to initiation of the reaction.

The positive control wells contained all components of the reaction, except the compound of interest; however, DMSO (at a final concentration of 2%) was included in these wells to control for solvent effects. The blank wells contained all components of the reaction, with staurosporine as a reference inhibitor replacing the compound of interest. This abolished kinase activity and established the baseline (0% kinase activity remaining).

### **CLK2 assay**

CLK2 (h) was diluted in the buffer (20 mM MOPS (3-(N-morpholino)propanesulfonic acid), 1 mM EDTA (ethylenediaminetetraacetic acid), 0.01% Brij-35 (detergent), 5% Glycerol, 0.1%  $\beta$ -mercaptoethanol, 1 mg/mL BSAs) to the concentration of 1.01 mg/mL prior to addition to the reaction mix.

The above stock solution of CLK2(h) was added to a mixture containing 8 mM MOPS pH 7.0, 0.2 mM EDTA, and 20  $\mu$ M YRRAAVPPSPSLSRHSSPHQS(p) EDEEE in such amount that the resulting concentration of CLK2(h) was 2.1 nM. This mixture was added to the stock solution of the tested compound. The reaction was initiated by the addition of the MgATP mix in such amount that the resulting concentration of Mg acetate in the reaction mixture was 10 mM and [ $\gamma$ -<sup>33</sup>P-ATP] (specific activity approx. 500 cpm/pmol) was 15  $\mu$ M. After incubation for 40 minutes at room temperature, the reaction was stopped by the addition of 3% phosphoric acid solution. 10  $\mu$ L of the reaction was then spotted onto a P30 filtermat and washed three times for 5 minutes in 75 mM phosphoric acid and once in methanol prior to drying and scintillation counting.

### **CLK4 assay**

CLK4 (h) was diluted in the buffer (20 mM MOPS, 1 mM EDTA, 0.01% Brij-35, 5% Glycerol, 0.1%  $\beta$ -mercaptoethanol, 1 mg/mL BSAs) to the concentration of 1.01 mg/mL prior to addition to the reaction mix.

The above stock solution of CLK4(h) was added to a mixture containing 8 mM MOPS pH 7.0, 0.2 mM EDTA, and 200  $\mu$ M YRRAAVPPSPSLSRHSSPHQS(p) EDEEE in such amount that the resulting concentration of CLK4(h) was 140.8 nM. This mixture was added to the stock solution of the tested compound. The reaction was initiated by the addition of the MgATP mix in such amount that the resulting concentration of Mg acetate in the reaction mixture was 10 mM and [ $\gamma$ -<sup>33</sup>P-ATP]

(specific activity approx. 500 cpm/pmol) was 15  $\mu\text{M}$ . After incubation for 40 minutes at room temperature, the reaction was stopped by the addition of 3% phosphoric acid solution. 10  $\mu\text{L}$  of the reaction was then spotted onto a P30 filtermat and washed three times for 5 minutes in 75 mM phosphoric acid and once in methanol prior to drying and scintillation counting.

### **HIPK1 assay**

HIPK1(h) was diluted in the buffer (20 mM MOPS, 1 mM EDTA, 0.01% Brij-35, 5% Glycerol, 0.1%  $\beta$ -mercaptoethanol, 1 mg/mL BSAs) to the concentration of 1.01 mg/mL prior to addition to the reaction mix.

The above stock solution of HIPK1(h) was added to a mixture containing 8 mM MOPS pH 7.0, 0.2 mM EDTA, and 0.33 mg/mL myelin basic protein in such amount that the resulting concentration of HIPK1(h) was 4.7 nM. This mixture was added to the stock solution of the tested compound. The reaction was initiated by the addition of the MgATP mix in such amount that the resulting concentration of Mg acetate in the reaction mixture was 10 mM and [ $\gamma$ - $^{33}\text{P}$ -ATP] (specific activity approx. 500 cpm/pmol) was 45  $\mu\text{M}$ . After incubation for 40 minutes at room temperature, the reaction was stopped by the addition of 3% phosphoric acid solution. 10  $\mu\text{L}$  of the reaction was then spotted onto a P30 filtermat and washed three times for 5 minutes in 75 mM phosphoric acid and once in methanol prior to drying and scintillation counting.

### **HIPK2 assay**

HIPK2(h) was diluted in the buffer (20 mM MOPS, 1 mM EDTA, 0.01% Brij-35, 5% Glycerol, 0.1%  $\beta$ -mercaptoethanol, 1 mg/mL BSAs) to the concentration of 1.01 mg/mL prior to addition to the reaction mix.

The above stock solution of HIPK2(h) was added to a mixture containing 8 mM MOPS pH 7.0, 0.2 mM EDTA, and 0.33 mg/mL myelin basic protein in such amount that the resulting concentration of HIPK2(h) was 1.4 nM. This mixture was added to the stock solution of the tested compound. The reaction was initiated by the addition of the MgATP mix in such amount that the resulting concentration of Mg acetate in the reaction mixture was 10 mM and [ $\gamma$ - $^{33}\text{P}$ -ATP] (specific activity approx. 500 cpm/pmol) was 10  $\mu\text{M}$ . After incubation for 40 minutes at room temperature, the reaction was stopped by the addition of 3% phosphoric acid solution. 10  $\mu\text{L}$  of the reaction was then spotted

onto a P30 filtermat and washed three times for 5 minutes in 75 mM phosphoric acid and once in methanol prior to drying and scintillation counting.

### **HIPK3 assay**

HIPK3(h) was diluted in the buffer (20 mM MOPS, 1 mM EDTA, 0.01% Brij-35, 5% Glycerol, 0.1%  $\beta$ -mercaptoethanol, 1 mg/mL BSAs) to the concentration of 1.01 mg/mL prior to addition to the reaction mix.

The above stock solution of HIPK3(h) was added to a mixture containing 8 mM MOPS pH 7.0, 0.2 mM EDTA, and 1.0 mg/mL myelin basic protein in such amount that the resulting concentration of HIPK3(h) was 6.4 nM. This mixture was added to the stock solution of the tested compound. The reaction was initiated by the addition of the MgATP mix in such amount that the resulting concentration of Mg acetate in the reaction mixture was 10 mM and [ $\gamma$ -<sup>33</sup>P-ATP] (specific activity approx. 500 cpm/pmol) was 15  $\mu$ M. After incubation for 40 minutes at room temperature, the reaction was stopped by the addition of 3% phosphoric acid solution. 10  $\mu$ L of the reaction was then spotted onto a P30 filtermat and washed three times for 5 minutes in 75 mM phosphoric acid and once in methanol prior to drying and scintillation counting.

### **FLT3 assay**

FLT3(h) was diluted in the buffer (20 mM MOPS, 1 mM EDTA, 0.01% Brij-35, 5% Glycerol, 0.1%  $\beta$ -mercaptoethanol, 1 mg/mL BSAs) to the concentration of 1.01 mg/mL prior to addition to the reaction mix.

The above stock solution of Flt3(h) was added to a mixture containing 8 mM MOPS pH 7.0, 0.2 mM EDTA, and 50  $\mu$ M EAIYAAPFAKKK, in such amount that the resulting concentration of FLT3(h) was 28.3 nM. This mixture was added to the stock solution of the tested compound. The reaction was initiated by the addition of the MgATP mix in such amount that the resulting concentration of Mg acetate in the reaction mixture was 10 mM and [ $\gamma$ -<sup>33</sup>P-ATP] (specific activity approx. 500 cpm/pmol) was 200  $\mu$ M. After incubation for 40 minutes at room temperature, the reaction was stopped by the addition of 3% phosphoric acid solution. 10  $\mu$ L of the reaction was then spotted onto a P30 filtermat and washed three times for 5 minutes in 75 mM phosphoric acid and once in methanol prior to drying and scintillation counting.

### **TRKA assay**

TRKA(h) was diluted in the buffer (20 mM MOPS, 1 mM EDTA, 0.01% Brij-35, 5% Glycerol, 0.1%  $\beta$ -mercaptoethanol, 1 mg/mL BSAs) to the concentration of 1.01 mg/mL prior to addition to the reaction mix.

The above stock solution of TRKA(h) was added to a mixture containing 8 mM MOPS pH 7.0, 0.2 mM EDTA, and 250  $\mu$ M KKKSPGEYVNIEFG, in such amount that the resulting concentration of TRKA(h) was 28.2 nM. This mixture was added to the stock solution of the tested compound. The reaction was initiated by the addition of the MgATP mix in such amount that the resulting concentration of Mg acetate in the reaction mixture was 10 mM and [ $\gamma$ - $^{33}$ P-ATP] (specific activity approx. 500 cpm/pmol) was 120  $\mu$ M. After incubation for 40 minutes at room temperature, the reaction was stopped by the addition of 3% phosphoric acid solution. 10  $\mu$ L of the reaction was then spotted onto a P30 filtermat and washed three times for 5 minutes in 75 mM phosphoric acid and once in methanol prior to drying and scintillation counting.

## Results

A: IC<sub>50</sub> < 0.100 μM

B: IC<sub>50</sub> < 1.00 μM

C: IC<sub>50</sub> < 5.00 μM

compound	CLK2	CLK4	FLT3	HIPK1	HIPK2	HIPK3	DYRK2	TRKA
6A	B	A		B	B	C	C	
6D	C	B		C	C			
7A	A	A		B	B	B		
7B	A	A		A	A	A	C	
7C	C	C			C			
7D	C	C		C	B	C		
7F	B	B		B	A			
8B	B		B					C
8C		C	C					C
8D			C					
8E		C	C					C
9	A	A		A	A	B	C	

compound	CLK2	CLK4	FLT3	HIPK1	HIPK2	HIPK3	DYRK2	TRKA
12B	C	B						
17E			C					C
23	B	B					C	
54	C	C		B	B			
55	B	B						
61	A	A		B	A		C	
62	C	C		B	B			
65	A			B			B	
66	B			B			C	
70	B			B			C	
71	B			C			C	
73	C						C	
74	B			C				
80	B							
81	C			C			C	

## Part 4a

### Syntheses of 5'-amino-2',5'-dideoxy-2',2'-difluorocytidine derivatives as novel anticancer nucleoside analogs\*

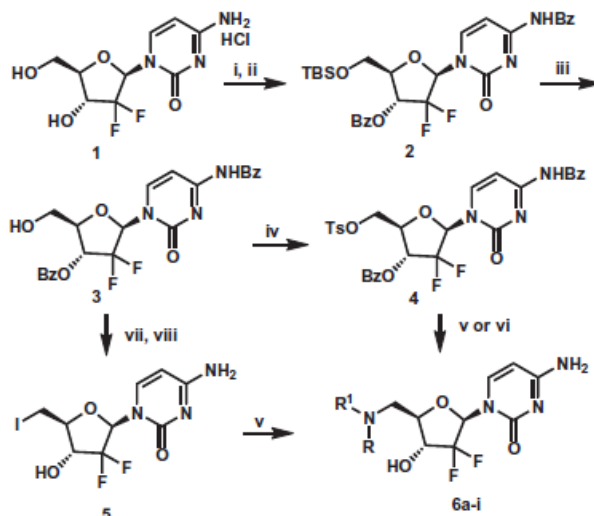
\*published as:

Labroli, M.; Dwyer, M. P.; Shen, R.; Popovici-Muller, J.; Pu, Q.; Richard, J.; Rosner, K.; Paruch, K.; Guzi, T. J. Syntheses of 5'-amino-2',5'-dideoxy-2',2'-difluorocytidine Derivatives as Novel Anticancer Nucleoside Analogs. *Tetrahedron Lett.* **2014**, *55*, 598.

2'-Deoxy-2', 2'-difluorocytidine, the antimetabolite nucleoside known as gemcitabine (**1**), is approved for the treatment of pancreatic, breast, and non-small cell lung cancers either as a single agent or in combination with other chemotherapeutic agents.<sup>1</sup> Gemcitabine acts as a prodrug which is intracellularly phosphorylated to its active diphosphate and triphosphate intermediates.<sup>2</sup> Gemcitabine triphosphate competes with deoxycytidine triphosphate for incorporation into DNA which results in termination of DNA polymerization.<sup>3</sup> The diphosphate intermediate effectively inhibits ribonucleotide reductase (RRM1) which leads to the depletion of the deoxynucleotide pool and halt of DNA synthesis.<sup>4</sup> Since the discovery of gemcitabine by Hertel et al.,<sup>5</sup> numerous gemcitabine derivatives have been synthesized in search for new anticancer or antiviral agents. For example, the base-modified gemcitabine derivatives include adenosine, guanine, and uracil analogs.<sup>6</sup> The ribose-modified derivatives include 4'-azido analogs,<sup>7</sup> 4'-allene substituted analogs,<sup>8</sup> 3'-deoxy analogs,<sup>9</sup> and thio/aza/carbocyclic analogs.<sup>10</sup> However, to our knowledge, the 5'-amino derivatives of gemcitabine, a novel and potentially biologically interesting class of compounds, have not been actively investigated. As part of our program to identify novel and selective anticancer compounds, we initiated efforts to develop efficient syntheses of 5'- amino-2',5'-dideoxy-2',2'-difluorocytidine derivatives in order to profile this novel series. Herein, we describe our chemistry efforts to prepare 5'-amino derivatives of gemcitabine.<sup>11</sup>

Our initial route to the 5'-amino-2',5'-dideoxy-2',2'-difluorocytidine analogs is outlined in Scheme 1. The synthesis began with protection of the 5'-hydroxy group of gemcitabine hydrochloride (**1**) as the tert-butyldimethylsilyl (TBDMS) ether followed by global benzoyl protection to afford compound **2**. Desilylation of the silyl ether was achieved with TBAF at 0 °C to provide alcohol **3**<sup>12</sup> which was converted to tosylate **4** under standard conditions. Treatment of intermediate **4** with excess amine

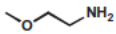
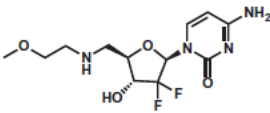
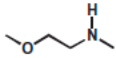
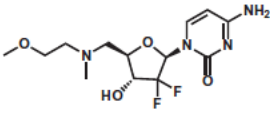
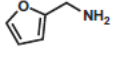
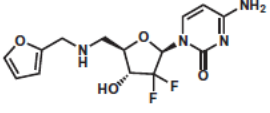
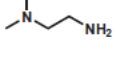
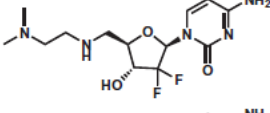
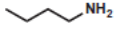
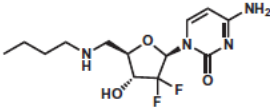
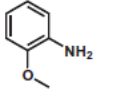
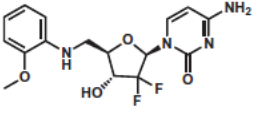
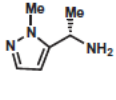
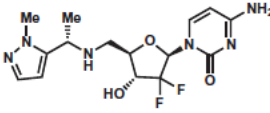
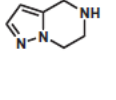
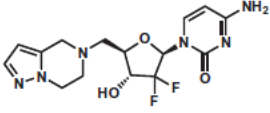
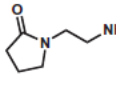
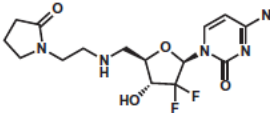
coupling partner at 100 °C promoted both tosylate displacement and benzoyl group cleavage to afford products **6a-d,i** (Table 1).



**Scheme 1.** Reagents and conditions: (i) TBSCl, imidazole, DMF, rt, 12 h, 92%; (ii) BzCl, DMAP, pyridine, rt, 12 h, 90%; (iii) TBAF, THF, 0 °C, 3.5 h then AcOH, 85%; (iv) TsCl, pyridine, Et<sub>3</sub>N, 85%; (v) HNRR<sup>1</sup>, DMF, 90–100 °C; (vi) NH<sub>3</sub>, MeOH, 58%; HNRR<sup>1</sup>, DMF; (vii) MeP(OPh)<sub>3</sub>I, DMF, 60 °C, 84%; (viii) NH<sub>3</sub>, MeOH, 92%.

Alternatively, this protocol could be carried out in a step-wise fashion by first removing the benzoyl groups of **4** by treatment with 7 N ammonia in methanol to provide the penultimate product. Treatment of the resulting tosylate with excess amine provided the desired compounds **6e,f** (Table 1). While the displacement reaction with the amine coupling afforded modest yields of the desired products (Table 1), multiple purifications were required to completely remove the resultant TsOH from desired product. In order to circumvent this issue, alcohol **3** was converted to the iodide intermediate **5** using methyltriphenoxyphosphonium iodide followed by benzoyl deprotection. Treatment of iodide **5** with 3 equiv of amines at 90 °C provided 5'-amino-2',5'-dideoxy-2',2'-difluorocytidine **6g,h** in respectable yields (Table 1).

**Table 1.** Preparation of **6a-i** by SN2 substitution.

Entry	Amines	Product	Yield (%)
6a			20 <sup>a</sup>
6b			54 <sup>a</sup>
6c			32 <sup>a</sup>
6d			19 <sup>a</sup>
6e			84 <sup>a,c</sup>
6f			13 <sup>a</sup>
6g			53 <sup>b</sup>
6h			55 <sup>b</sup>
6i			53 <sup>a</sup>

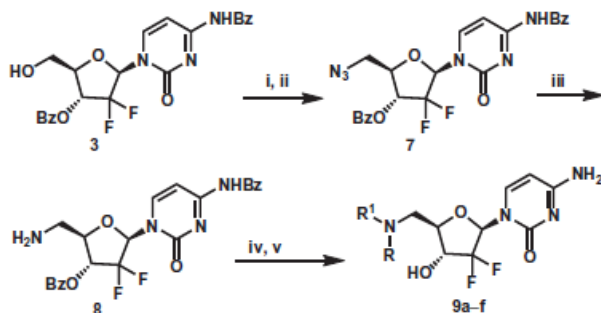
a Yield for one step.

b Combined yield for two steps.

c Rxn heated at 40 °C.

The use of iodide **5** allowed us to scale back the number of equivalents of amine for the displacement reaction while making the purification of the final analogs much easier.

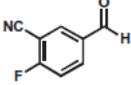
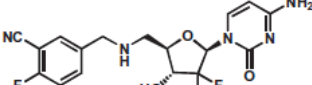
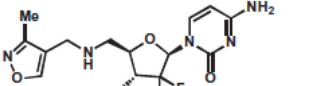
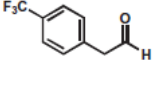
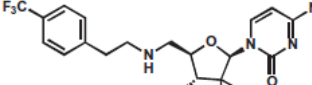
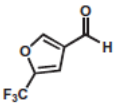
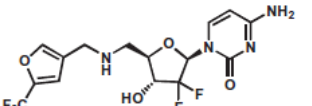
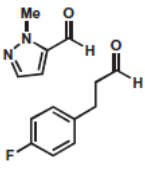
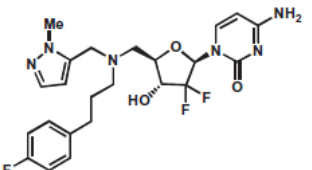
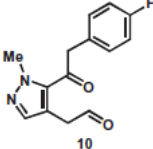
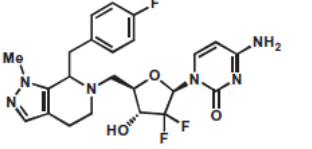
While the SN2 strategy depicted in Scheme 1 represented a concise preparation of 5'-amino-2',5'-dideoxy-2',2'-difluorocytidine derivatives, we decided to pursue other alternatives due to the poor to modest yields for the final compounds. Toward this end, a reductive amination approach was explored not only to improve the yield of the final 5'-amino-2',5'-dideoxy-2',2'-difluorocytidine analogs but to broaden the scope of coupling partners. As shown in Scheme 2, alcohol **3** was converted to the mesylate followed by treatment with NaN<sub>3</sub> to afford the corresponding azide **7**. Treatment of azide **7** with trimethylphosphine provided amine intermediate **8** which was used directly without silica gel purification to prevent benzoyl transfer to the 5'-amino group.



**Scheme 2.** Reagents and conditions: (i) MsCl, Et<sub>3</sub>N, pyridine, 89%; (ii) NaN<sub>3</sub>, DMF, 70 °C, 98%; (iii) Me<sub>3</sub>P, MeCN/H<sub>2</sub>O, 85%; (iv) RCHO, NaBH<sub>3</sub>CN, MeOH, AcOH, 35–75%; (v) 7 M NH<sub>3</sub>/MeOH, 45–85%.

Treatment of **8** with various aldehydes under reductive amination conditions (NaBH<sub>3</sub>CN) afforded the N-alkylated products which were treated with 7 M NH<sub>3</sub> in MeOH to afford 5'-substituted amino analogs **9a-f** shown in Table 2. The reductive amination/deprotection protocol worked well for both aromatic and aliphatic aldehydes (entries **9a-d**) with respectable yields observed for both steps (Table 2). Additionally, this protocol was adapted to a stepwise format by employing two distinct aldehydes to afford **9e** or by employing a dicarbonyl substrate **10** to afford bicyclic derivative **9f**.

**Table 2.** Reductive amination protocol/deprotection from **8** to afford **9a-f** (Scheme 2).

Entry	Aldehydes	Product	Yield (%) of step iv <sup>a</sup> /step v
<b>8a</b>			72/82
<b>b</b>			66/70
<b>c</b>			68/45
<b>d</b>			69/84
<b>e</b>			59 <sup>b</sup> /50
<b>f</b>			35/85

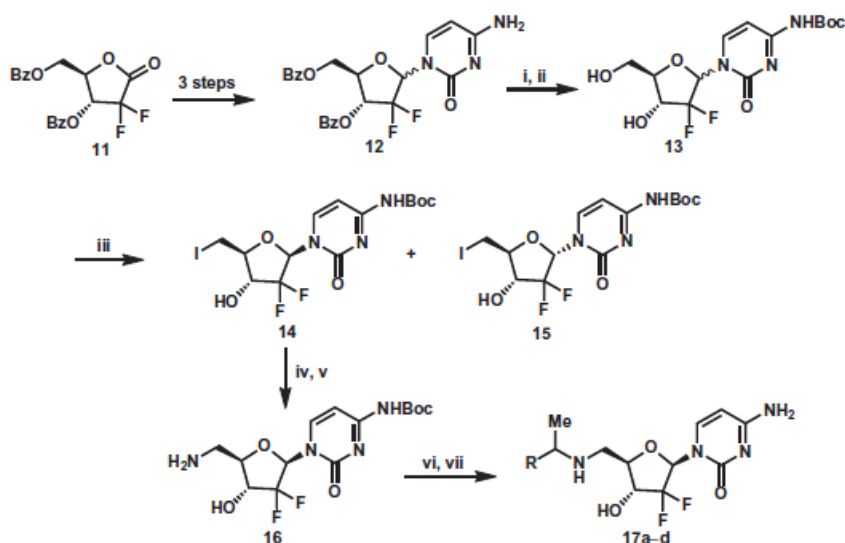
<sup>a</sup> Amine **8** was used as the crude product of reduction of azide **7**.

<sup>b</sup> Prepared by one-pot stepwise reductive amination.

While the reductive amination approach utilizing amine **8** proceeded well with aldehydes, this protocol yielded very low yields of  $\alpha$ -substituted amine products when ketones were used as coupling partners. Owing to the reduced electrophilicity and increased steric hindrance of the ketone coupling partners, it was rationalized that a strong Lewis acid may be required to promote the initial imine formation for these substrates. It was rationalized that one might need an alternative 5'-amino intermediate with a suitable protecting group for harsher imine formation conditions due to potentially labile 3'-benzoate of **8**. Additionally, it was desirable to develop a flexible route which could allow for rapid base modification (other than cytosine) while at the same time circumventing the need to use expensive gemcitabine as a starting material. Based on the above considerations, a

second reductive amination synthetic route was developed to prepare 5'-amino-2',5'-dideoxy-2',2'-difluorocytidine derivatives derived from ketone coupling partners.

The synthesis started with commercially available 2-deoxy-2,2-difluoro-D-*erythro*-pentafuranous-1-ulose-3,5-dibenzoate (**11**) (Scheme 3). Following the protocol described by Chou et al.,<sup>13</sup> lactone **11** was converted to nucleoside **12** in three steps as a mixture of both anomers ( $\alpha:\beta = 1:1.5$ ). The 4-amino group of the cytosine was protected as the Boc derivative followed by hydrolysis of the 3',5'-dibenzoate under mild basic conditions to provide diol **13**. Based on the selective iodination protocol of thymidine reported by Verheyden and Moffatt,<sup>14</sup> treatment of diol **13** with methyltriphenoxyphosphonium iodide afforded only the 5'-iodo nucleoside anomers **14** and **15**.

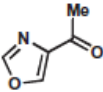
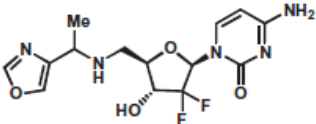
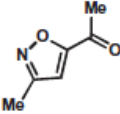
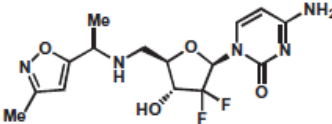
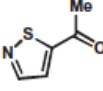
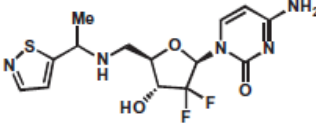
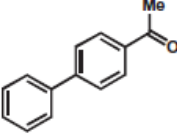
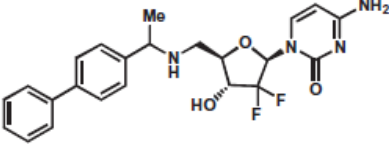


**Scheme 3.** Reagents and conditions: (i)  $\text{Boc}_2\text{O}$ , DMAP, THF, 75%; (ii)  $\text{Et}_3\text{N}/\text{MeOH}/\text{H}_2\text{O}$ , rt, 12 h, 92%; (iii)  $\text{MeP}(\text{OPh})_3\text{I}$ , DMF, rt, 1 h, 31% (**14**), 45% (**15**); (iv)  $\text{NaN}_3$ , DMF, 40 °C, quant.; (v)  $\text{Me}_3\text{P}$ ,  $\text{MeCN}/\text{H}_2\text{O}$ , 73%; (vi)  $\text{RCOMe}$ ,  $\text{Ti}(\text{i-OPr})_4$ , then  $\text{NaBH}_3\text{CN}$ , 51–68%; (vii) TFA,  $\text{CH}_2\text{Cl}_2$ , 71–98%.

Presumably, the selectivity of this transformation is driven by the reduced nucleophilicity of the 3'-hydroxyl caused by the geminal di-fluorine atoms which yields only the 5'-iodo products. Fortunately, the 5'-iodo anomers **14** and **15** could be separated by regular silica gel chromatography. Treatment of  $\alpha$ -anomer **14** with sodium azide followed by reduction furnished the 5'-amino intermediate **16**. Treatment of amine **16** with aromatic ketones in the presence of  $\text{Ti}(\text{i-OPr})_4$ <sup>15</sup>

followed by treatment with  $\text{NaBH}_3\text{CN}$  and Boc deprotection leads to  $\alpha$ -methylated 5'-amino compounds **17a–d** as a mixture of diastereomers in moderate to good yields (Scheme 3). The specific yields for the reductive amination step as well as deprotection are detailed in Table 3.

**Table 3.** Reductive amination/deprotection protocol from **16** to afford **17a–d** (Scheme 3).

Entry	Ketones	Product	Yield (%) of step vi <sup>2</sup> /step vii
17a			68/71
17b			60/95
17c			50/71
17d			51/98

In summary, we have described three unique synthetic routes for the syntheses of a novel class of 5'-amino-2',5'-dideoxy-2',2'-difluorocytidine derivatives. The first route relied upon a  $\text{S}_{\text{N}}2$  displacement of either a 5'-tosylate or 5'-iodide intermediate using excess amine as coupling partners. To circumvent the modest yields and challenging purifications of final products using the first route, a second route was developed which relied upon a reductive amination of a 5'-amino derivative with aldehydes to afford a wide variety of 5'-N-alkylated derivatives. Finally, the final route relies upon a reductive amination step with ketones but also offers the ability to change the base with fewer manipulation of protecting groups than the previous routes. While the 5'-amino intermediates **8** and **16** were critical components for the reductive amination protocols described, one could envision the utility of these materials for preparation of such non-basic analogs such as amides, sulfonamides, and ureas. The biological activity associated with this novel class of 5'-amino-2',5'-dideoxy-2',2'-difluorocytidine derivatives will be reported in due course.<sup>16</sup>

## References and notes

1. (a) Burris, H. A., III; Moore, M. J.; Andersen, J.; Green, M. R.; Rothenberg, M. L.; Modiano, M. R.; Cripps, M. C.; Portenoy, R. K.; Storniolo, A. M.; Tarassoff, P.; Nelson, R.; Dorr, F. A.; Stephens, C. D.; Von Hoff, D. D. *J. Clin. Oncol.* **1997**, *15*, 2403; (b) Manegold, C. *Expert Rev. Anticancer Ther.* **2004**, *4*, 345; (c) Heinemann, V. *Expert Rev. Anticancer Ther.* **2005**, *5*, 429.
2. Heinemann, V.; Hertel, L. W.; Grindey, G. B.; Plunkett, W. *Cancer Res.* **1988**, *48*, 4024.
3. Huang, P.; Chubb, S.; Hertel, L. W.; Grindey, G. B.; Plunkett, W. *Cancer Res.* **1991**, *51*, 6110.
4. (a) van der Donk, W. A.; Yu, G.; Pérez, L.; Sanchez, R. J.; Stubbe, J.; Samano, V.; Robins, M. J. *Biochemistry* **1998**, *37*, 6419; (b) Artin, E.; Wang, J.; Lohman, G. J. S.; Yokoyama, K.; Yu, G.; Griffin, R. G.; Bar, G.; Stubbe, J. *Biochemistry* **2009**, *48*, 11622.
5. Hertel, L. W.; Kroin, J. S.; Misner, J. W.; Tustin, J. M. *J. Org. Chem.* **1988**, *53*, 2406.
6. (a) Hertel, L. W.; Grossman, C. S.; Kroin, J. S.; Mineishib, S.; Chubb, S.; Nowak, B.; Plunkett, W. *Nucleos. Nucleot.* **1989**, *8*, 951; (b) Fahrig, R.; Lohmann, D.; Rolfs, A.; Dieks, H.; Teubner, J.; Heinrich, J.-C. *WO 2008017515*; *Chem. Abstr.* **2008**, *148*, 239457.
7. Smith, D. B.; Kalayanov, G.; Sund, C.; Winqvist, A.; Maltseva, T.; Leveque, V. J.-P., et al *J. Med. Chem.* **2009**, *52*, 2971.
8. Qiu, Y.-L.; Wang, C.; Peng, X.; Ying, L.; Or, Y. S. *WO 2010030858*; *Chem. Abstr.* **2010**, *152*, 335423.
9. Hertel, L. W.; Grossman, C. S.; Kroin, J. S. *EP 329348*, 1989; *Chem. Abstr.* **1989**, *112*, 56592.
10. (a) Qiu, X.-L.; Xu, X.-H.; Qing, F.-L. *Tetrahedron* **2010**, *66*, 789; (b) Devos, R.; Dymock, B. W.; Hobbs, C. J.; Jiang, W.-R.; Martin, J. A.; Merrett, J. H.; Najera, I.; Shimma, N.; Tsukuda, T. *WO 2002018404*; *Chem. Abstr.* **2002**, *136*, 217007.
11. Guzi, T. J.; Parry, D. A.; Labroli, M. A.; Dwyer, M. P.; Paruch, K.; Rosner, K. E.; Shen, R.; Popovici-Muller, J. *WO 2009061781*; *Chem. Abstr.* **2009**, *150*, 515402.
12. It was necessary to maintain the desilylation reaction of **2** at low temperature and higher dilution while quenching the reaction with acetic acid to suppress gemcitabine 3',5',4-tribenzoate formation as a side product. This side product could be formed by intermolecular benzoyl transfer from the less stable 3'-benzoate to 5'-hydroxyl group.
13. Chou, T. S.; Heath, P. C.; Patterson, L. E.; Poteet, L. M.; Lakin, R. E.; Hunt, A. H. *Synthesis* **1992**, 565.
14. Verheyden, J. P. H.; Moffatt, J. G. *J. Org. Chem.* **1970**, *35*, 2319.
15. Mattson, R. J.; Pham, K. M.; Leuck, D. J.; Cowen, K. A. *J. Org. Chem.* **1990**, *55*, 2552.

16. Labroli, M. A.; Dwyer, M. P.; Shen, R.; Popovici-Muller, J.; Pu, Q.; Wyss, D.; McCoy, M.; Barrett, D.; Davis, N.; Seghezzi, W.; Shanahan, F.; Taricani, L.; Parry, D.; Guzi, T. J. *Bioorg. Med. Chem.* submitted for publication.

**Note:** Experimental details can be found in our publicly available patent WO 2009/061781 A1.



## Part 4b

### New carbocyclic nucleosides: synthesis of carbocyclic pseudoisocytidine and its analogs\*

\*published as:

Maier, L.; Hylse, O.; Nečas, M.; Trbušek, M.; Ytre-Arne, M.; Dalhus, B.; Bjarås, M.; Paruch, K. \* New Carbocyclic Nucleosides: Synthesis of Carbocyclic Pseudoisocytidine and its Analogs. *Tetrahedron Lett.* **2014**, *55*, 3713.

Nucleoside analogs represent a diverse group of organic compounds. Appropriate modifications of the nucleoside scaffold can result in significantly altered biological activity.<sup>1</sup> As natural nucleosides contain the relatively labile amination motif (structure **A** in Figure 1), significant effort has been invested in order to identify more stable analogs.

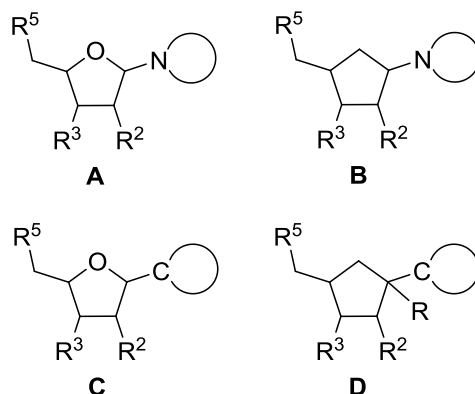
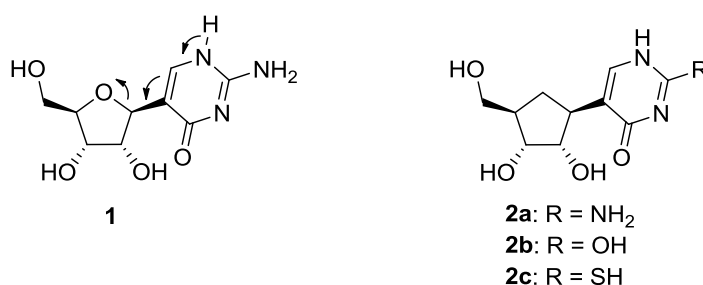


**Figure 1.** The common scaffold of natural nucleosides (**A**) and the structures of their analogs **B**, **C**, **D**.

One strategy consists of replacing the tetrahydrofuran ring with an appropriate carbocyclic isostere. The resulting carbanucleosides have been synthesized by diverse synthetic methods,<sup>2</sup> and in many cases, it has been observed that the tetrahydrofuran ring can be replaced with cyclopentane (structure **B** in Figure 1) without significant loss of biological activity.<sup>3</sup> Naturally occurring representatives of this series include aristeromycin and its unsaturated analog (-)-neplanocin A.<sup>4</sup> Another strategy is based on attachment of the heterocyclic base to the tetrahydrofuran via a C-C bond linkage (structure **C** in Figure 1). While the resulting C-nucleosides are in general more stable than natural nucleosides, the synthesis of even relatively simple systems (e.g., tiazofurin and its analogs) in this series is often not trivial.<sup>5</sup> In addition, some C-nucleosides can still undergo ring-opening of the furan (see below). Structure **D** in Figure 1 combines elements of structures **B** and **C**: carbocyclic C-nucleosides with a

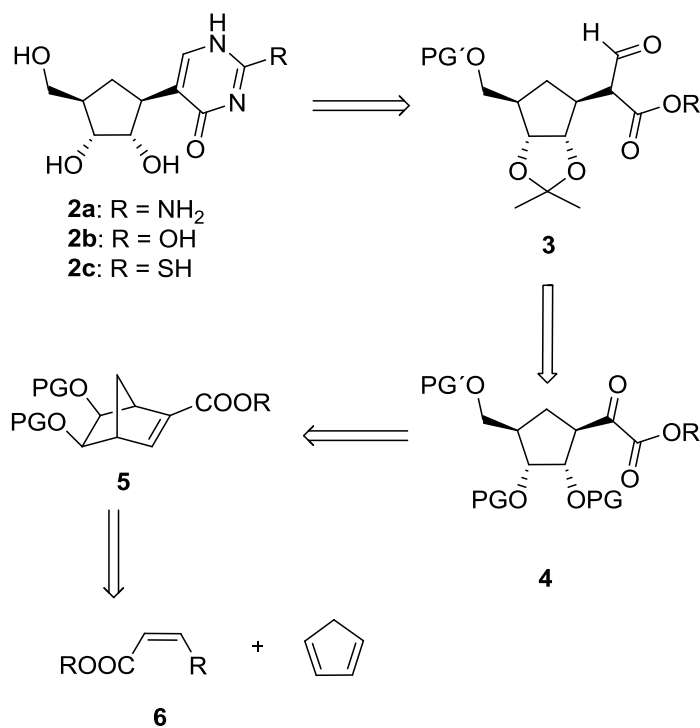
C-C connection between the (heterocyclic) base and the carbocyclic scaffold. It is conceivable that, at least in some cases, these compounds might be more robust versions of nucleoside analogs **B** and **C**. Furthermore, the installation of certain substituents (e.g., R = OH) is meaningful only in this series, as this would lead to chemically unstable ketals and aminals in the other series. Interestingly, compounds with general structure **D** (where R = H) are quite rare<sup>6</sup> and we have been unable to find any analogs of type **D** (containing R = OH) with nucleoside-like substitution patterns.

One attractive biologically active candidate for the tetrahydrofuran-cyclopentane replacement is pseudoisocytidine (**1**), which has been shown to be active against cytarabine-resistant leukemias,<sup>7</sup> but hepatotoxic in vivo,<sup>8</sup> which may be the result of opening of the tetrahydrofuran core (Scheme 1).<sup>9</sup>



**Scheme 1.** Opening of pseudoisocytidine **1** and the structures of its direct carbocyclic analog **2a** and related compounds **2b** and **2c**.

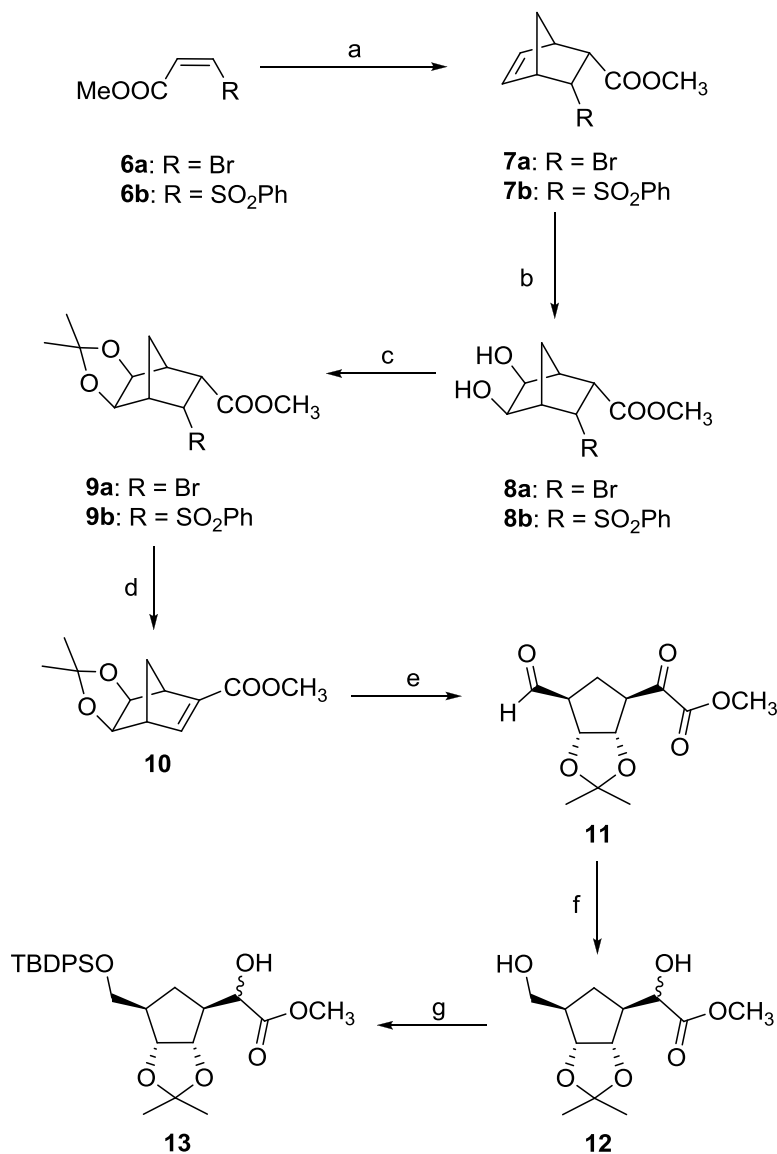
The direct carbocyclic analog **2a** cannot undergo such a ring-opening process and its toxicological profile might therefore be superior to that of pseudoisocytidine, while its biological activity could be retained (Scheme 1). Herein, we report the first synthesis of the previously unknown carbocyclic pseudoisocytidine analog **2a** and its derivatives **2b** and **2c**.



**Scheme 2.** Retrosynthetic analysis of pseudoisocytidine analogs (PG = protecting group).

The overall retrosynthetic strategy is depicted in Scheme 2. It includes the previously described substituted norbornene intermediate **5**,<sup>10</sup> which could yield ketoester **4** after oxidative cleavage. The desired stereochemistry of **4** is dictated by the geometry of the bicyclo[2.2.1]heptene scaffold produced in a Diels-Alder reaction between cyclopentadiene and appropriately substituted dienophile **6**, possessing a leaving group that is utilized in a subsequent elimination-diastereoselective *cis*-dihydroxylation sequence. Compound **4** was envisioned as a precursor to the novel aldehyde-ester **3**, which upon reaction with urea, thiourea or guanidine, and global deprotection would provide the target compounds **2a-c**.

The synthesis started from commercially available methyl propiolate, which was converted into methyl (*Z*)-3-bromo-2-propenoate (**6a**) (Scheme 3).<sup>11</sup>

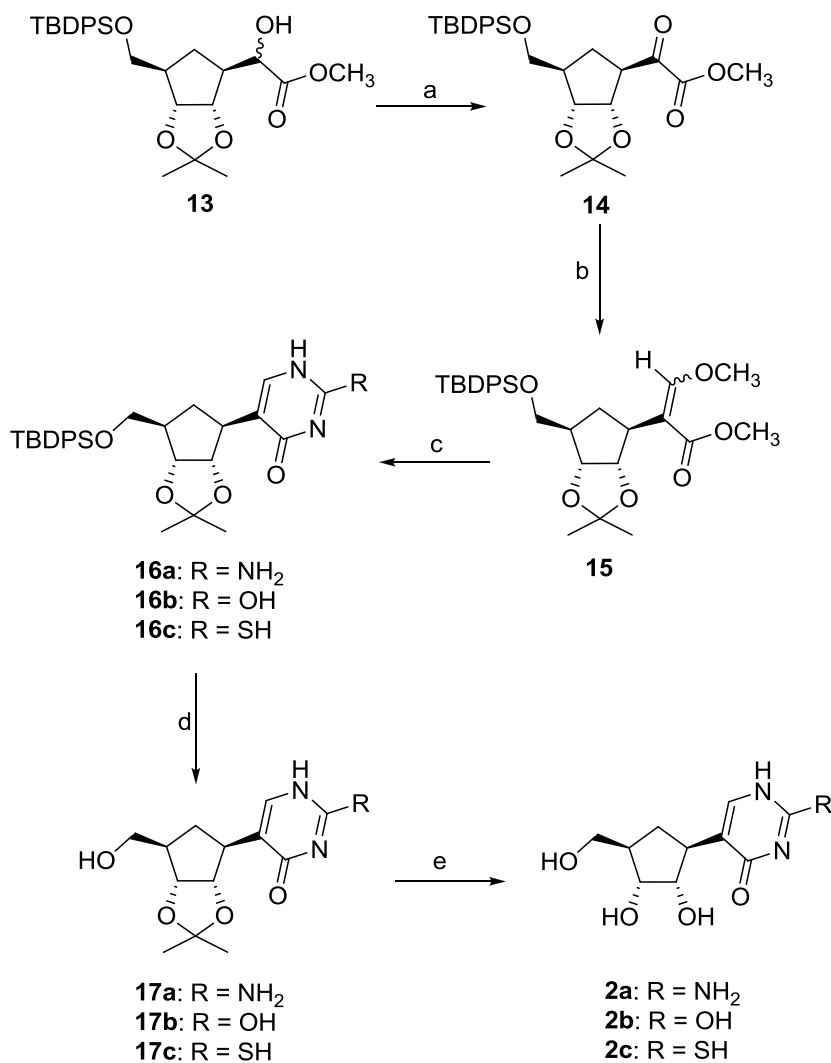


**Scheme 3.** Reagents and conditions: a) EtAlCl<sub>2</sub>, cyclopentadiene, CH<sub>2</sub>Cl<sub>2</sub>, 0 °C; 80% for **7a**, 70-95% for **7b**. b) OsO<sub>4</sub>, NMO, acetone:H<sub>2</sub>O (4:1), 40 °C; 80% for **8a**, 90% for **8b**. c) Me<sub>2</sub>CH(OMe)<sub>2</sub>, cat. TsOH, acetone, r. t.; 99% for **9a** and **9b**. d) DBU, Et<sub>2</sub>O, 0 °C to r. t.; 95%, for **9a**, DBU, CH<sub>3</sub>CN, 90 °C; 86% for **9b**. e) O<sub>3</sub>, CH<sub>2</sub>Cl<sub>2</sub>, -78 °C then Me<sub>2</sub>S -78 °C to room temp. f) Li(Al-O-*t*Bu)<sub>3</sub>H, THF, 0 °C to r. t.; 50-80% from **10**. g) TBDPSCI, imidazole, CH<sub>2</sub>Cl<sub>2</sub>, r. t.; 70-92%.

Since we have found that the bromo compound **6a** irritates skin (especially upon repeated exposure), we have utilized an alternative starting material for the Diels-Alder reaction, sulfone **6b**.<sup>12</sup> Thermal Diels-Alder reaction between cyclopentadiene and **6a** was very sluggish - the conversion after 24 hours in refluxing benzene or toluene was negligible and significant dimerization of cyclopentadiene occurred. On the other hand, the reaction proceeded smoothly at low temperature (0 °C), catalysed by

EtAlCl<sub>2</sub>, with very good diastereoselectivity (9:1 *endo:exo*). Sulfone **6b** underwent an uncatalyzed Diels-Alder reaction quite efficiently (60% yield, r. t., 14 h), although a higher conversion and yield were obtained in the presence of the catalyst (EtAlCl<sub>2</sub>). The structure of the major *endo* diastereomer **7b** was confirmed by X-ray crystallography (see Supporting Information). Diastereoselective *cis*-dihydroxylation of both adducts **7a** and **7b** provided the corresponding diols **8a** and **8b**, which were subsequently protected as acetonides. Elimination of the bromide or phenylsulfonyl group under basic conditions afforded the key intermediate **10**, which underwent ozonolytic cleavage to produce the rather unstable aldehyde **11** that was immediately used in the next step without purification. It should be noted that, in principle, compound **10** could be prepared more directly by dihydroxylation and protection of the Diels-Alder adduct of methyl propiolate and cyclopentadiene, which we prepared in 60-80% yield (cat. AlCl<sub>3</sub>, PhH, 0 °C). Attempted dihydroxylations of the adduct, however, yielded complex hydroxylation mixtures that contained the desired product together with the unwanted diastereomer, the regioisomer with a dihydroxylated double bond in the vicinity of the ester group as well as a tetrahydroxylated product. In accordance with the published results,<sup>10</sup> our attempts to selectively reduce the aldehyde in the presence of an  $\alpha$ -ketoester were not successful. On the other hand, reduction with excess Li(Al-O-*t*-Bu)<sub>3</sub>H yielded an inseparable mixture of epimeric diols in which the primary hydroxyl group could be selectively silylated to provide  $\alpha$ -hydroxyester **13** (Scheme 3).

Oxidation of the hydroxyl group in **13** proved challenging. Many standard methods (e.g., MnO<sub>2</sub>, PDC, KMnO<sub>4</sub>, Swern oxidation) including RuO<sub>2</sub> plus NaIO<sub>4</sub> conditions that were previously used for a structurally similar intermediate,<sup>10</sup> failed to give the desired product **14** in acceptable yield. Fortunately, oxidation with Dess-Martin periodinane yielded pure  $\alpha$ -ketoester **14** in very good yield and purity (Scheme 4).

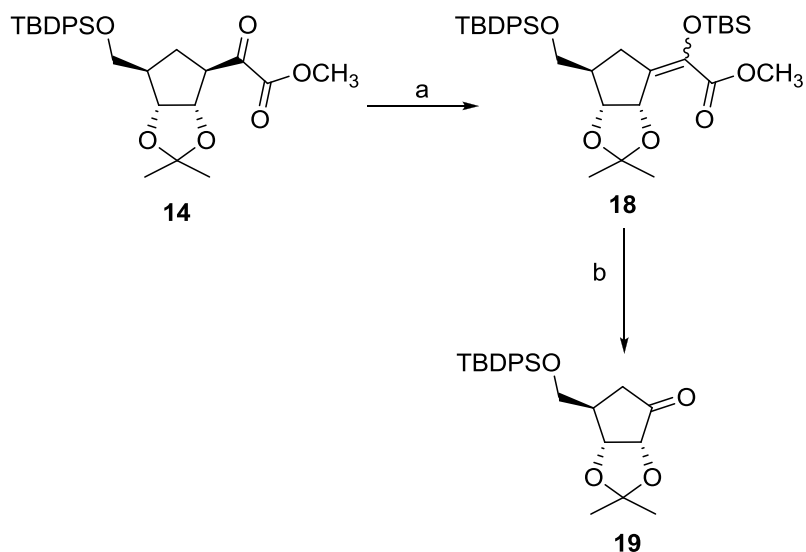


**Scheme 4.** Reagents and conditions: a) Dess-Martin periodinane, CH<sub>2</sub>Cl<sub>2</sub>, 0 °C to r. t.; 80-90%. b) Ph<sub>3</sub>P<sup>+</sup>CH<sub>2</sub>OMeCl<sup>-</sup>, LDA, THF, 0 °C to r. t.; 37-65% (*Z*:*E* 7:5). c) guanidinium.HCl for compound **16a** (20-35%), urea for **16b** (30-45%) and thiourea for **16c** (40-50%), *t*-BuOK, *t*-BuOH, reflux. d) TBAF, wet THF, r. t.; 90% for **17a**, 96% for **17b**, 90% for **17c**. e) HCl:H<sub>2</sub>O:MeOH 1:1:1, r. t.; 69% for **17a**, 76% for **17b**, 71% for **17c**.

One-carbon homologation was accomplished via the Wittig reaction with methoxymethylenetriphenylphosphorane. The reaction produced enol ether **15** in 37-65% yield as a separable mixture of *Z* and *E* isomers (*Z*:*E* ~7:5). It should be noted that the Wittig olefination was rather sensitive to the type and quality of base. Generation of the phosphonium ylide with LDA gave the most consistent and reproducible results, while reactions with LiHMDS, KHMDS, or *t*-BuOK afforded olefination products in substantially lower yields. Attempts to hydrolyze selectively enol ether **15** into the desired aldehyde **3** in the presence of the acetonide and TBPDS groups met with

only limited success. With PPTS or acetic acid, partial cleavage of the acetonide and/or TBDPS groups was observed, while the enol ether moiety remained intact. We thus attempted direct transformation of **15** into pyrimidine **16b** by reaction with urea. With sodium ethoxide in ethanol or NaH in THF, we observed mainly cleavage of the TBDPS group and the desired product **16b** was formed in very low yield. However, using *t*-BuOK in *t*-BuOH as the base, the desired product was formed in good yield. Reactions of **15** with thiourea and guanidine under similar conditions yielded compounds **16c** and **16a**, respectively. Selective deprotection of the TBDPS group in pyrimidines **16a-c** with TBAF revealed the primary hydroxyl group, which could be utilized for further selective derivatization, e.g., the preparation of phosphates and its isosteres. Final hydrolysis of the acetonide under acidic conditions provided the target compounds **2a**, **2b** and **2c** in good overall yields. The relative configurations of **2a-c** were confirmed by 2D NMR experiments (shown in Supporting Information). We were able to separate the enantiomers of intermediates **17b** and **17c** as well as **16a** by HPLC on a chiral stationary phase (see Supporting Information).

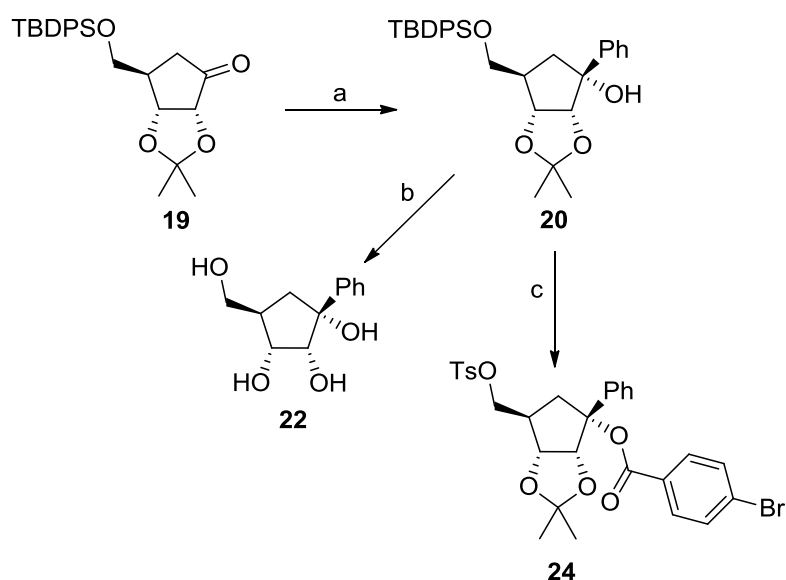
Clearly, the strategy described above can only be applied to construct the (hetero)cyclic bases by elaboration of the ketoester **14**. In order to target compounds that are inaccessible by the methodology described above, we envisioned a different and perhaps more general route that utilizes a versatile cyclopentanone intermediate (**19**, Scheme 5).



**Scheme 5.** Reagents and conditions: a) LiHMDS, TBSOTf, THF, -78 °C. b) O<sub>3</sub>, CH<sub>2</sub>Cl<sub>2</sub>, -78 °C, then Me<sub>2</sub>S -78 °C to r. t.; 52 % from **14**.

In order to access quickly and evaluate the potential of compound **19**, we converted one of the synthetic intermediates, ketoester **14**, into the corresponding silyl enol ether **18**. Subsequent

ozonolysis of this, rather unusual,<sup>13</sup> substrate afforded **19** in an acceptable yield (Scheme 5). The two-step sequence provided sufficient amounts of material for preliminary studies. We initially studied the introduction of a phenyl group using PhMgBr or PhLi under a variety of conditions (e.g., variable temperature and solvent, presence or absence of CeCl<sub>3</sub>) and found that the best results were obtained when PhLi was added to a solution of **19** in THF at 0 °C. Under these conditions, a single diastereomer of addition product **20**, resulting from attack of the reagent from the less sterically hindered side of **19**, was obtained in 75% yield (Scheme 6). We were unable to detect the other diastereomer by NMR spectroscopy.



**Scheme 6.** Reagents and conditions: a) PhLi, THF, 0 °C; 75% b) TBAF, wet THF, r. t.; then PPTS, MeOH r. t.; 42% from **20**. c) TBAF, wet THF, r. t., then TsCl, Et<sub>3</sub>N, DMAP, CH<sub>2</sub>Cl<sub>2</sub>, 0 °C; then NaH, BrPhCOCl, THF, 0 °C to r. t., 42% from **20**.

The relative stereochemistry of the addition product **20** (supported by 2D NMR; see Supporting Information) was unambiguously assigned by X-ray crystallography of its *p*-bromobenzoyl derivative **24** (Scheme 6 and Figure 3).

We tested the effect of compounds **2a**, **2b** and **2c** on the viability of leukemia cell lines that were available to us: SU-DHL-4 (diffuse large B-cell lymphoma, del/mut TP53), JEKO-1 (mantle cell lymphoma, del/mut TP53), and JVM-3 (mantle cell lymphoma, wt-TP53). The viability of SU-DHL-4 and JEKO-1 was not affected by 10 μM nor 100 μM concentrations of the compounds. However,

JVM-3 was more sensitive: 90% viability was observed upon treatment with 100  $\mu\text{M}$  **2c**; with 10  $\mu\text{M}$  and 100  $\mu\text{M}$  **2a** we observed 90% and 83% viability, respectively.

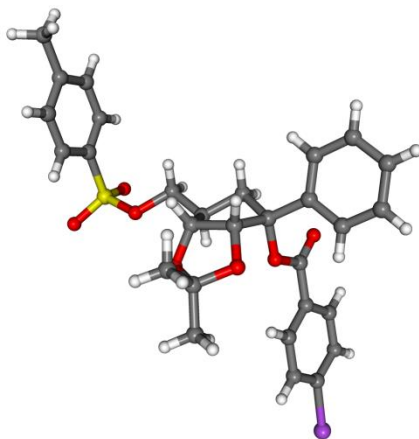


**Figure 3.** X-ray crystal structure of compound **24** (CCDC ref. No. 937690)

Since the arrangement around the tertiary alcohol carbon of compound **22** mimics that of the acetal product of glycosylase-mediated cleavage,<sup>14</sup> this compound was tested against glycosylases NEIL1, NEIL2, NTH1, and hOGG1, and was found to inhibit selectively NEIL1 in a dose-dependent manner: at 1 mM we observed 46% inhibition, and at 0.5 mM and 0.125 mM concentrations 22% and 2% inhibition, respectively.

In summary, we have completed the first syntheses of three new racemic carbocyclic nucleoside analogs (**2a-c**) of pseudoisocytidine, each in 13 steps. The synthetic approach builds on a user-friendly preparation of sulfone **7b**, which can be diastereoselectively dihydroxylated and ultimately elaborated into tetrasubstituted chiral cyclopentanes **11** with good diastereoselectivity. While Diels-Alder reactions between cyclopentadiene with a beta-sulfonyl enoate are known,<sup>15</sup> the strategic elaboration of readily accessed sulfones **7b** into cyclopentanes seems largely undeveloped, and can be used for the construction of nucleoside analogs and for target directed syntheses. Analogs of  $\alpha$ -ketoester intermediate **14** have been previously used for the construction of the heterocyclic ring directly,<sup>6d</sup> or after a two carbon homologation;<sup>6f</sup> our one-carbon homologation enables the synthesis of additional (hetero)cycles. Furthermore, we have performed preliminary studies towards a potentially more versatile strategy for the preparation of carbocyclic nucleoside analogs that utilizes highly diastereoselective additions of organometallic reagents onto cyclopentanone **19**, which itself is available in two-steps from  $\alpha$ -ketoester intermediate **14**. While analogs of **19** are known and have been used in synthesis of carbocyclic nucleosides,<sup>16</sup> tetraol **22**, to our knowledge, is the only carbocyclic C-nucleoside represented by generic structure **D**, where R is an oxygenated substituent.

Unlike the analogs in the series **A**, **B**, and **C** (Figure 1), compounds such as **22** are stable and their biological evaluation should enable mapping of part of the chemical space that is currently inaccessible. Along this line, we have tested the prepared carbocyclic analogs in three leukemia cell lines, and compounds **2a** and **2c** were found to be moderately active against wt-TP53 - mantle cell lymphoma cell line JVM-3, which is generally the most sensitive to chemotherapeutic treatment. The ability of compound **22** to inhibit glycosylase NEIL1 has served as the starting point for a more thorough exploration of the biological activity of this series of novel carbocyclic nucleoside analogs. Further studies are currently in progress and the results will be published elsewhere.

## References and notes

1. *Modified Nucleosides in Biochemistry, Biotechnology and Medicine*; Herdewijn, P., Ed.; Wiley-VCH, 2008.
2. a) Agrofoglio, L.; Suhas, E.; Farese, A.; Condom, R.; Challand, R. S.; Earl, R. A.; Guedj, R. *Tetrahedron* **1994**, *50*, 10611; b) Hildbrand, S.; Troxler, T.; Scheffold, R. *Helv. Chim. Acta* **1994**, *77*, 1236; c) Altmann, K. H.; Kesselring, R. *Synlett* **1994**, 853; d) Crimmins, M. T. *Tetrahedron* **1998**, *54*, 9229; e) Zhu, X.-F. *Nucleosides, Nucleotides, Nucleic Acids* **2000**, *19*, 651; f) Agrofoglio, L. *Curr. Org. Chem.* **2006**, *10*, 333.
3. a) Borchardt, R. T.; Wu, Y. S.; Huber, J. A.; Wycpalek, A. F. *J. Med. Chem.* **1976**, *19*, 1104; b) Secrist, J. A.; Clayton, S. J.; Montgomery, J. A. *J. Med. Chem.* **1984**, *27*, 534; c) Neres, J.; Labello, N. P.; Somu, R. V.; Boshoff, H. I.; Wilson, D. J.; Vannada, J.; Chen, L.; Barry, C. E.; Bennett, E. M.; Aldrich, C. A. *J. Med. Chem.* **2008**, *51*, 5349; d) Choi, W. J.; Chung, H.; Chandra, G.; Alexander, V.; Zhao, L. X.; Lee, H. W.; Nayak, A.; Majik, M. S.; Kim, H. O.; Kim, J.-H.; Lee, Y. B.; Ahn, C. H.; Lee, S. K.; Jeong, L. S. *J. Med. Chem.* **2012**, *55*, 4521.
4. a) Arita, M.; Adachi, K.; Ito, Y.; Sawai, H.; Ohno, M. *J. Am. Chem. Soc.* **1983**, *105*, 4049; b) Arai, Y.; Hayashi, Y.; Yamamoto, M.; Takayema, H.; Koizumi, T. *J. Chem. Soc., Perkin Trans. I* **1988**, 3133.
5. a) Popsavin, M.; Spaic, S.; Svirčev, M.; Kojic, V.; Bogdanovic, G.; Popsavin, V. *Bioorg. Med. Chem. Lett.* **2006**, *16*, 5317; b) Štambaský, J.; Hocek, M.; Kočovský, P. *Chem. Rev.* **2009**, *109*, 6729; c) Bárta, J.; Slavětínská, L.; Klepetářová, B.; Hocek, M. *Eur. J. Org. Chem.* **2010**, 5432.
6. a) Playtis, A. J.; Fissekis, J. D. *J. Org. Chem.* **1975**, *40*, 2488; b) Chu, C. K. I.; Wempfen, I.; Watanabe, K. A.; Fox, J. J. *J. Org. Chem.* **1976**, *41*, 2793; c) Just, G.; Kim, S. *Tetrahedron Lett.* **1976**, *14*, 1063; d) Just, G.; Kim, S. *Can. J. Chem.* **1977**, *55*, 427; e) Saksena, A. K.; Ganguly, A. K. *Tetrahedron Lett.* **1981**, *22*, 5227; f) Takahashi, T.; Kotsubo, H.; Koizumi, T. *Tetrahedron*

- Asymmetry* **1991**, 2, 1035; g) Dishington, A. P.; Humber, D. C.; Stoodley, R. J. *J. Chem., Soc. Perkin Trans. 1* **1993**, 57; h) Díaz, M.; Ortuño, R. M. *Tetrahedron: Asymmetry* **1997**, 8, 3421.
7. Burchenal, J. H.; Ciovacco, K.; Kalaher, K.; O'Toole, T.; Kiefner, R.; Dowling, M. D.; Chu, C. K.; Watanabe, K. A.; Wempen, I.; Fox, J. J. *Cancer Res.* **1976**, 36, 1520.
  8. Woodcock, T. M.; Chou, T. C.; Tan, C. T. C.; Sternberg, S. S.; Philips, F. S.; Young, C. W.; Burchenal, J. H. *Cancer Res.* **1980**, 40, 4243.
  9. Grierson, J. R.; Shields, A. F.; Zheng, M.; Kozawa, S. M.; Courter, J. H. *Nucl. Med. Biol.* **1995**, 22, 671.
  10. a) Just, G.; Reader, G. *Tetrahedron Lett.* **1973**, 17, 1521; b) Just, G.; Reader, G.; Faure, B. C. *Can. J. Chem.* **1975**, 54, 849.
  11. a) Ma, S.; Lu, X. *Org. Synth.* **1999**, 9, 415; b) Rossi, R.; Bellina, F.; Catanese, A.; Mannina, L.; Valensin, D. *Tetrahedron* **2000**, 56, 479.
  12. Hirst, G. C.; Parsons, P. J. *Org. Synth.* **1990**, 69, 169.
  13. We have been unable to find any examples of the ozonolysis of such tetrasubstituted alkenes.
  14. a) Slupphaug, G.; Mol, C. D.; Kavli, B.; Arvai, A. S.; Krokan, H. E.; Tainer, J. A. *Nature* **1996**, 384, 87; b) Parikh, S. S.; Mol, C. D.; Slupphaug, G.; Bharati, S.; Krokan, H. E.; Tainer, J. A. *EMBO J.* **1998**, 17, 5214.
  15. Downey, C. W. .; Craciun, S.; Viveló, C. A.; Neferu, A. M.; Mueller, C. J.; Corsi, S. *Tetrahedron Lett.* **2012**, 53, 5766.
  16. Tanaka, M.; Yoshioka, M.; Sakai, K. *Tetrahedron: Asymmetry* **1993**, 4, 981.

## Experimental Section

### General

All reagents and solvents were of reagent grade and were used without further purification. Anhydrous solvents (THF, dichloromethane, CH<sub>3</sub>CN) were used from commercial suppliers (Aldrich, Acros) or distilled and stored over 4Å molecular sieves. All reactions were carried out in oven-dried glassware and under N<sub>2</sub> atmosphere. Column chromatography was carried on silica gel (230-400 mesh). TLC plates were visualized under UV and with phosphomolybdic acid or KMnO<sub>4</sub> solution.

NMR spectra were recorded on Bruker Avance 300 and 500 MHz instruments, with operating frequencies 300.13, 500.13 MHz for <sup>1</sup>H a 75.48, 125.77 MHz for <sup>13</sup>C. The <sup>1</sup>H and <sup>13</sup>C NMR chemical shifts (δ in ppm) were referenced to the residual signals of solvents: CDCl<sub>3</sub> [7.24 (<sup>1</sup>H) and 77.23 (<sup>13</sup>C)] and DMSO-*d*<sub>6</sub> [2.50 (<sup>1</sup>H) and 39.51 (<sup>13</sup>C)]. Structural assignments of resonances has been

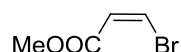
performed with the help of 2D NMR gradients experiments (COSY, multiplicity edited  $^1\text{H}$ - $^{13}\text{C}$  HSQC,  $^1\text{H}$ - $^{13}\text{C}$  HMBC, NOESY,  $^1\text{H}$ - $^{15}\text{N}$  HSQC and  $^1\text{H}$ - $^{15}\text{N}$  HMBC).

Diffraction data were collected on KM4CCD four-circle area diffractometer (Oxford Diffraction, Abingdon, UK) equipped with an Oxford Cryosystems, Oxford, UK. The crystallographic package ShelXTL was used to solve and refine the structures and to prepare the figures.

High resolution mass spectra have been measured on Agilent 6224 Accurate-Mass TOF LC-MS with dual electrospray/chemical ionization mode with mass accuracy greater than 2 ppm, applied mass range from 25 to 20,000 Da.

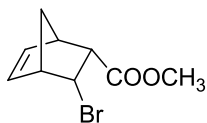
IR spectra ( $4000$ - $400\text{ cm}^{-1}$ ) were collected on an EQUINOX 55/S/NIR FTIR spectrometer. Samples were prepared as KBr pellets.

**(Z)-methyl 3-bromoacrylate (6a)**<sup>11</sup>:



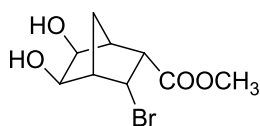
The compound was prepared according to the literature procedure<sup>11</sup> for synthesis of ethyl-(Z)-3-bromo-2-propenoate. LiBr (1.303 g, 15.0 mmol) was dissolved in anhydrous  $\text{CH}_3\text{CN}$  (11 mL). Methyl propiolate (1.074 mL, 12.0 mmol) and AcOH (0.839 mL, 15 mmol) were added under  $\text{N}_2$  and the resulting mixture was refluxed under  $\text{N}_2$  for 24 h. After cooling down water (10 mL) was added and the mixture was carefully neutralized by 200 mg of solid  $\text{K}_2\text{CO}_3$ . The aqueous phase was subsequently extracted with  $\text{Et}_2\text{O}$  (3x 15 mL). Organic extracts were dried with  $\text{MgSO}_4$ , filtered and the solvents were evaporated under reduced pressure to yield a colourless oil (1.58 g, 80%). The crude product was used without further purification. GC-MS and  $^1\text{H}$ ,  $^{13}\text{C}$  NMR analysis indicated the presence of (Z)-isomer only. NMR data were consistent with the literature.<sup>11</sup> GC-MS:  $m/z = 164$  [ $\text{M}^+$ ], 166 [ $\text{M}^+$ ], 133 [ $\text{M}^+$ -OMe], 85 [ $\text{M}^+$ -Br].  $^1\text{H}$  NMR (300 MHz,  $\text{CDCl}_3$ ):  $\delta = 6.97$  (d,  $J = 8.3$  Hz, 1H), 6.60 (d,  $J = 8.3$  Hz, 1H), 3.74 (s, 3H) ppm.  $^{13}\text{C}$  NMR (75 MHz,  $\text{CDCl}_3$ ):  $\delta = 164.47$  (-COOMe), 124.35, 121.63, 51.79 (-OMe) ppm.

**(1R\*,2R\*,3R\*,4S\*)-methyl 3-bromobicyclo[2.2.1]hept-5-ene-2-carboxylate (7a)**:



Methyl-(Z)-3-bromo-2-propenoate **5** (1.789 g, 10.84 mmol) was dissolved in anhydrous CH<sub>2</sub>Cl<sub>2</sub> (15 mL). The resulting mixture was cooled with ice bath to 0°C and EtAlCl<sub>2</sub> (1.8M solution in toluene, 3 mL, 5.42 mmol, 0.5 equiv) was added dropwise over period of 5 minutes. The reaction mixture was stirred for 30 min at 0°C. Freshly distilled cyclopentadiene (4.5 mL, 54.2 mmol) was then added in one portion. The resulting mixture was stirred for an additional 1 hour while maintaining reaction temperature between 0-5°C. The ratio of endo:exo isomers of the product in an aliquot was determined to be 9:1 by GC-MS analysis. The reaction mixture was cautiously poured into a mixture of 15 mL of 10% HCl, 50 g of ice and 50 mL of Et<sub>2</sub>O and stirred at 0°C till a white solid precipitated from the mixture. The precipitate was removed by filtration and the resulting filtrate was extracted with Et<sub>2</sub>O (5x 30 mL). Combined organic extracts were dried over MgSO<sub>4</sub>, filtered and the solvent was removed under vacuum to produce yellow viscous oil. The residue was purified by flash column chromatography (hexane/EtOAc 10:1) to yield pure endo diastereomer as colourless oil which solidified upon freezing to white solid (1.88 g, 75%); m.p.: 31-32°C. GC-MS: m/z = 232 [M<sup>+</sup>], 230 [M<sup>+</sup>], 199 [M<sup>+</sup>-OMe], 133 [M<sup>+</sup>-OMe], 165, 151, 66 [cyclopentadiene]. <sup>1</sup>H NMR (300 MHz, CDCl<sub>3</sub>): δ = 6.53 (dd, *J* = 5.4, 3.0 Hz, 1H), 6.10 (dd, *J* = 5.4, 3.0 Hz, 1H), 4.61 (dd, *J* = 9.2, 3.0 Hz, 1H), 3.66 (s, 3H), 3.20 (dd, *J* = 9.2, 3.0 Hz, 1H), 3.20 (br s, 1H), 3.09 (br s, 1H), 1.64 (d, *J* = 9.2 Hz, 1H), 1.37 (d, *J* = 9.2 Hz, 1H) ppm. <sup>13</sup>C NMR (126 MHz, CDCl<sub>3</sub>): δ = 171.75, 136.94, 134.32, 51.71, 51.32, 50.15, 50.01, 47.70, 40.05 ppm. IR (KBr): ν<sub>max</sub> = 3452, 2987, 1733, 1430, 1189, 1039, 835, 746 cm<sup>-1</sup>. HR-MS (ESI): calcd for C<sub>9</sub>H<sub>11</sub>BrO<sub>2</sub> [M+H]<sup>+</sup>: 231.0014. Found 231.0018.

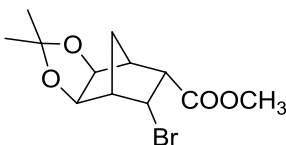
**(1R\*,2S\*,3S\*,4R\*,5S\*,6R\*)-methyl 3-bromo-5,6-dihydroxybicyclo[2.2.1]heptane-2-carboxylate (8a):**



Into a solution of **7a** (1.056 g, 4.57 mmol) in acetone/water (12 mL, 4:1) was added NMO (4.57 mmol, 0.5354 g) and 4% solution of OsO<sub>4</sub> in water (0.036 mmol, 0.227 mL). The reaction mixture was stirred at 40°C, after 14 h solid Na<sub>2</sub>S<sub>2</sub>O<sub>5</sub> (0.5 g) was added and the resulting black solution was stirred for additional 30 min at room temperature. Volatiles were removed under reduced pressure and the black residue was preadsorbed on silica gel and then purified by flash column chromatography (petrolether/EtOAc 2:1) to yield a white crystalline solid (969 mg, 80%). m.p. = 144-146°C. <sup>1</sup>H NMR (300 MHz, CDCl<sub>3</sub>): δ = 4.90-4.87 (m, 1H), 4.49-4.44 (m, 2H), 3.68 (s, 3H), 3.09 (dd, *J* = 11.2, 3.2 Hz, 1H); 2.87 (d, *J* = 5.2 Hz, -OH, 1H), 2.63 (d, *J* = 5.5 Hz, -OH, 1H), 2.51 (d, 1H, *J* = 3.5 Hz), 2.37 (br s, 1H), 2.07 (dm, *J* = 11.1 Hz, 1H), 1.27 (dm, *J* = 11.1 Hz, 1H) ppm. <sup>13</sup>C NMR

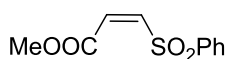
(75 MHz, CDCl<sub>3</sub>):  $\delta$  = 170.93, 71.62, 68.53, 51.79, 50.82, 48.39, 48.02, 46.52, 33.13 ppm. IR (KBr):  $\tilde{\nu}_{\text{max}}$  = 3382, 3263, 2981, 1738, 1430, 1367, 1170, 1047, 860 cm<sup>-1</sup>. HR-MS (APCI): calcd for C<sub>9</sub>H<sub>13</sub>BrO<sub>4</sub> [M-H<sub>2</sub>O+H]<sup>+</sup> = 246.9964. Found 246.9964.

**(3aR\*,4R\*,5S\*,6S\*,7R\*,7aS\*)-methyl 6-bromo-2,2-dimethylhexahydro-4,7-methanobenzo[d][1,3]dioxole-5-carboxylate (9a):**



Diol **8a** (1.1302 g; 4.26 mmol) was dissolved in acetone (12 mL), 2,2-dimethoxypropane (1.776 g, 4 eq., 17.05 mmol) and 3 mg of TsOH were added and the resulting mixture was stirred at room temp. till the TLC indicated disappearance of the starting material (30-60 min). The remaining 2,2-dimethoxypropane and acetone were evaporated under reduced pressure yield crude acetone **9a**, whose purity (analyzed by GC-MS, <sup>1</sup>H NMR and <sup>13</sup>C NMR) was satisfactory and it was therefore used without further purification directly in the next step. GC-MS: m/z = 289 [M<sup>+</sup> -Me], 275 [M<sup>+</sup> -OMe], 229 [M<sup>+</sup> -OOCMe<sub>2</sub>], 135, 79. <sup>1</sup>H NMR (300 MHz, CDCl<sub>3</sub>):  $\delta$  = 4.01-3.94 (m, 3H); 3.69 (s, 3H); 2.61-2.54 (m, 3H), 2.08-2.04 (dm, 1H); 1.89-1.85 (dm, 1H); 1.43 (s, 3H), 1.25 (s, 3H) ppm. <sup>13</sup>C NMR (75 MHz, CDCl<sub>3</sub>):  $\delta$  = 171.02, 110.72, 80.79, 79.98, 51.96, 51.11, 48.80, 47.25, 43.54, 29.44, 25.56, 24.36 ppm.

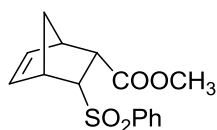
**(Z)-methyl 3-(phenylsulfonyl)acrylate (6b):**



Compound **6b** was prepared by a slightly modified literature procedure.<sup>12</sup> Into a solution of sodium benzenesulfinate (3.671g, 22.36 mmol) and Bu<sub>4</sub>NHSO<sub>4</sub> (1.138 g 3.354 mmol) in H<sub>2</sub>O/THF 1:1 (80 mL), were added methyl propiolate (1.88 g, 22.36 mmol) followed by H<sub>3</sub>BO<sub>3</sub> (2.074 g, 33.54 mmol). The mixture was vigorously stirred at room temp. for 48 h. After that pH was adjusted by 1M HCl to pH = 4 and the mixture was extracted with CH<sub>2</sub>Cl<sub>2</sub> (4x 50 mL). The organic phase was washed with brine (1x 30 mL), dried with MgSO<sub>4</sub>, filtered and the solvents were removed under reduced pressure. The resulting yellow oil was purified by flash column chromatography (petrolether/EtOAc 3:2) to

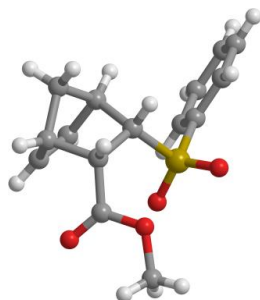
afford both isomers as white crystals (101 mg, 2% of E isomer and 2.93 g, 58% of Z isomer **6b**). E isomer: m.p. = 99-100°C. <sup>1</sup>H NMR (300 MHz, CDCl<sub>3</sub>): δ = 7.91-7.89 (m, 2H), 7.69-7.54 (m, 3H), 7.32 (d, *J* = 15.2 Hz, 1H), 6.82 (d, *J* = 15.2 Hz, 1H), 3.78 (s, 3H) ppm. <sup>13</sup>C NMR (75 MHz, CDCl<sub>3</sub>): δ = 164.11, 143.71, 138.75, 134.60, 130.73, 129.86, 128.56, 52.98 ppm. Z isomer: m.p. = 64-65°C. <sup>1</sup>H NMR (300 MHz, CDCl<sub>3</sub>): δ = 7.99-7.97 (m, 2H), 7.67-7.53 (m, 3H), 6.54 (d, *J* = 11.5 Hz, 1H), 6.48 (d, 1H, *J* = 11.5 Hz), 3.88 (s, 3H) ppm. <sup>13</sup>C NMR (75 MHz, CDCl<sub>3</sub>): δ = 164.53, 139.40, 135.60, 134.22, 131.73, 129.46, 128.24, 52.83 ppm. IR (KBr): ν<sub>max</sub> = 3456, 3037, 2954, 1734, 1633, 1340, 1311, 1238, 1153, 763, 731 cm<sup>-1</sup>.

**(1R\*,2R\*,3R\*,4S\*)-methyl 3-(phenylsulfonyl)bicyclo[2.2.1]hept-5-ene-2-carboxylate (7b):**



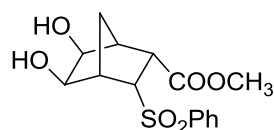
EtAlCl<sub>2</sub> (15.92 mmol, 8.85 ml of 1.8M solution in toluene) was added dropwise over the period of 5 min to a cooled (ice bath, 0°C) solution of compound **6b** (7.206 g, 31.85 mmol) in anhydrous CH<sub>2</sub>Cl<sub>2</sub> (30 mL). The reaction mixture was stirred for 30 min, then freshly distilled cyclopentadiene (1.32 mL, 159.25 mmol) was added. The mixture was stirred for additional 1 h at 0°C, then it was poured onto 10% HCl (80 mL) with ice (200 g). The mixture was filtered to remove white polymeric byproducts, to the filtrate was added brine (200 mL) and it was extracted with CH<sub>2</sub>Cl<sub>2</sub> (4x 100 mL). The organic extracts were dried with MgSO<sub>4</sub>, filtered and concentrated in a vacuum to afford a yellow oil. The product was precipitated by addition of Et<sub>2</sub>O (20 mL); the resulting white crystalline solid was filtered and washed with Et<sub>2</sub>O (3x 15 mL). The product (pure endo diastereomer by NMR) was dried in a vacuum and used directly without further purification. Analytically pure material was isolated by flash column chromatography (petrolether/EtOAc 3:1) as white crystals (7.72 g, 83 %). m.p. = 150-151°C. <sup>1</sup>H NMR (300 MHz, CDCl<sub>3</sub>): δ = 7.93-7.84 (m, 2H), 7.67-7.51 (m, 3H), 6.59 (dd, *J* = 5.3, 3.0 Hz, 1H), 6.26 (dd, *J* = 5.3, 3.0 Hz, 1H), 4.12 (dd, *J* = 10.0, 3.1 Hz, 1H), 3.42 (dd, *J* = 10.0, 3.1 Hz, 1H), 3.21 (br s, 1H), 3.02 (br s, 1H), 1.47 (dm, *J* = 8.9 Hz, 1 H), 1.25 (dm, *J* = 8.9 Hz, 1 H) ppm. <sup>13</sup>C NMR (75 MHz, CDCl<sub>3</sub>): δ = 170.87, 141.40, 137.70, 133.40, 132.13, 129.07, 127.86, 69.17, 51.87, 49.16, 48.12, 47.07, 46.64 ppm. HR-MS (APCI): calcd for C<sub>15</sub>H<sub>16</sub>O<sub>4</sub>S [M+H]<sup>+</sup>: 293.0842. Found 293.0841.

Crystal data for **7b**: CCDC ref. No. 929386. Crystallized from CH<sub>2</sub>Cl<sub>2</sub>, C<sub>15</sub>H<sub>16</sub>O<sub>4</sub>S, *M*<sub>rel</sub> = 292.35, *T* = 120 K, space group P-1, *a* = 8.2134(4) Å, *b* = 8.3868(4) Å, *c* = 10.7465(6) Å, α = 108.251(5), β = 94.702(4), γ = 99.040(4), *V* = 687.466 Å<sup>3</sup>, *R* = 0.031.



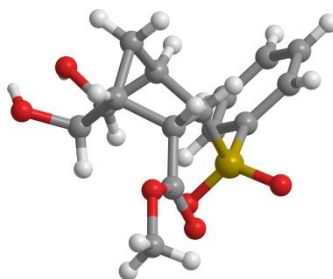
X-ray crystal structure of compound **7b**

**(1R\*,2S\*,3S\*,4R\*,5S\*,6R\*)-methyl 5,6-dihydroxy-3-(phenylsulfonyl)bicyclo[2.2.1]heptane-2-carboxylate (8b):**



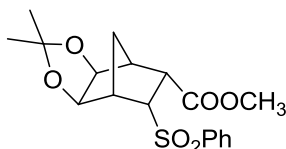
To a stirred solution of alkene **7b** (4.511 g, 15.4 mmol) in acetone/H<sub>2</sub>O (45 mL, 4:1) were added NMO (1.8 g, 15.4 mmol) followed by OsO<sub>4</sub> (700 μL, 4% wt. solution in H<sub>2</sub>O, 0.12 mmol). The yellow solution was stirred for 14 h at 40°C. Solid Na<sub>2</sub>S<sub>2</sub>O<sub>5</sub> (0.5 g) was then added and the resulting black mixture was stirred for 30 min. Volatiles were removed under reduced pressure and the black residue was preadsorbed on silica gel. Flash column chromatography (EtOAc) yielded a white crystalline compound (4.52 g, 90 %). m.p.: 144-145°C. <sup>1</sup>H NMR (500 MHz, CDCl<sub>3</sub>): δ = 7.93-7.85 (m, 2H), 7.66-7.51 (m, 3H), 4.96-4.89 (m, 1H), 4.78-4.70 (m, 1H), 3.76 (dd, *J* = 11.9, 4.1 Hz, 1H), 3.18 (d, *J* = 4.9 Hz, 1H), 3.11 (dd, *J* = 11.9, 4.1 Hz, 1H), 3.06 (d, *J* = 4.9 Hz, 1H), 2.56 (br s, 1H), 2.43 (br s, 1H), 2.09 (d, *J* = 10.9 Hz, 1H), 1.14 (d, *J* = 10.9 Hz, 1H) ppm. <sup>13</sup>C NMR (126 MHz, CDCl<sub>3</sub>): δ = 170.13, 141.25, 133.85, 129.39, 128.00, 77.48, 77.23, 76.98, 69.32, 68.39, 64.65, 52.31, 48.00, 47.90, 44.73, 33.24 ppm. IR (KBr): ν<sub>max</sub> = 3456, 1747, 1637, 1385, 1144, 752, 721 cm<sup>-1</sup>. HR-MS (ESI): calcd for C<sub>15</sub>H<sub>18</sub>O<sub>6</sub>S [M+H]<sup>+</sup>: 327.0897. Found 327.0892.

Crystal data for **8b**: CCDC ref. No. 929387. Crystallized from CH<sub>2</sub>Cl<sub>2</sub>, C<sub>15</sub>H<sub>18</sub>O<sub>6</sub>S, *M*<sub>rel</sub> = 326.36, *T* = 120 K, space group P-1, *a* = 10.4471(4) Å, *b* = 11.4450(6) Å, *c* = 13.4617(6) Å, α = 65.794(4), β = 87.155(3), γ = 82.891(4), *V* = 1456.77 Å<sup>3</sup>, *R* = 0.030.



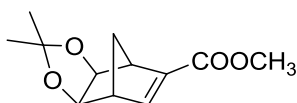
X-ray crystal structure of compound **8b**

**(3aR\*,4R\*,5S\*,6S\*,7R\*,7aS\*)-methyl 2,2-dimethyl-6-(phenylsulfonyl)hexahydro-4,7-methanobenzo[d][1,3]dioxole-5-carboxylate (9b):**



To a solution of diol **8b** (2.00 g, 6.13 mmol) in acetone (24 mL) were added 2,2-dimethoxypropane (3.1 mL, 24.5 mmol) and TsOH (2 mg). The reaction mixture was stirred at room temp. till the starting material was not detected by TLC (petrolether/EtOAc 1:1); within ca. 30 min. The reaction mixture was evaporated to dryness (orange oil) and the crude product was used without further purification directly in the next step. Pure product could be obtained by flash column chromatography (petrolether/EtOAc 1:1) as colourless crystals (2.22 g, 99%). m.p.: 149-150°C. <sup>1</sup>H NMR (500 MHz, CDCl<sub>3</sub>): δ = 7.90 (m, 2H), 7.63 (m, 1H), 7.55 (m, 1H), 5.18 (d, *J* = 5.4 Hz, 1H), 4.97 (d, *J* = 5.4 Hz, 1H), 3.75 (dd, *J* = 11.7, 4.1 Hz, 1H), 3.71 s (3H), 3.17 (dd, *J* = 11.7, 4.1 Hz, 1H), 2.69 (m, 1H), 2.53 (m, 1H), 1.99 (m, 1H), 1.41 (s, 3H), 1.33 (s, 3H), 1.04 (m, 1H) ppm. <sup>13</sup>C NMR (126 MHz, CDCl<sub>3</sub>): δ = 169.69, 141.35, 133.83, 129.41, 128.05, 108.88, 77.29, 76.06, 64.27, 52.35, 45.11, 45.07, 44.01, 32.86, 25.46, 24.52 ppm. IR (KBr): ν<sub>max</sub> = 3456, 1747, 1637, 1385, 1144, 752, 721 cm<sup>-1</sup>. HR-MS (ESI): calcd for C<sub>18</sub>H<sub>22</sub>O<sub>6</sub>S [M+H]<sup>+</sup>: 367.1210. Found 367.1214.

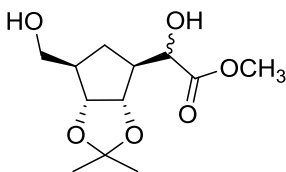
**(3aR\*,4R\*,7S\*,7aS\*)-methyl 2,2-dimethyl-3a,4,7,7a-tetrahydro-4,7-methanobenzo[d][1,3]dioxole-5-carboxylate (10):**



Method a) Into a solution of acetonide **9a** (1.299 g; 4.26 mmol) in anhydrous Et<sub>2</sub>O (10 mL) was added DBU (1.6 mL, 10.65 mmol) at 0°C. The resulting mixture was allowed to warm to room temp. and then it was stirred for 16 h. The resulting suspension was filtered to remove the solid residue. The glass filter was rinsed by Et<sub>2</sub>O (3x 15 mL). The filtrates were collected, the solvents were evaporated under reduced pressure and the resulting yellow viscous liquid was purified by flash column chromatography (hexane/EtOAc 3:1) to yield a white solid (908 mg, 95% from **8a**).

Method b) Into a stirred solution of crude acetonide **9b** (1.37 g, 6.13 mmol) in dry MeCN (10 mL) was added dropwise DBU (2.8 mL, 18.4 mmol). The reaction mixture was then stirred at 90°C for 1 h (monitored by TLC with hexane/EtOAc 3:1). The solvent was then evaporated and the orange residue was purified by flash column chromatography (hexane/EtOAc 3:1) to afford a colourless oil which upon freezing crystallized to white crystals (1.18 g, 86% from **8b**). m.p.: 61-62°C. <sup>1</sup>H NMR (300 MHz, CDCl<sub>3</sub>): δ = 6.91 (d, *J* = 3.1 Hz, 1H), 4.27 (d, *J* = 5.3 Hz, 1H), 4.21 (d, *J* = 5.3 Hz, 1H), 3.70 (s, 3H), 3.14 (br s, 1H), 2.93 (br s, 1H), 2.05 (m, 1H), 1.79 (m, 1H), 1.46 (s, 3H), 1.31 (s, 3H) ppm. <sup>13</sup>C NMR (75 MHz, CDCl<sub>3</sub>): δ = 164.65, 147.55, 142.37, 114.40, 80.23, 80.15, 51.76, 47.40, 45.81, 42.99, 26.19, 24.59 ppm. IR (KBr): ν<sub>max</sub> = 3452, 3000, 2931, 1712, 1643, 1597, 1267, 1062, 856, 756 cm<sup>-1</sup>. HR-MS (ESI): calcd for C<sub>12</sub>H<sub>16</sub>O<sub>4</sub> [M+H]<sup>+</sup>: 225.1121. Found 225.1124.

**(R\*)-methyl 2-hydroxy-2-((3aR\*,4R\*,6S\*,6aS\*)-6-(hydroxymethyl)-2,2-dimethyltetrahydro-3aH-cyclopenta[d][1,3]dioxol-4-yl)acetate (12):**

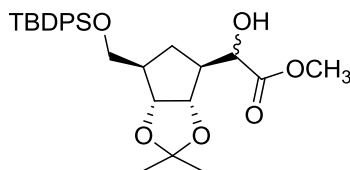


O<sub>3</sub>/O<sub>2</sub> mixture (5mL/min oxygen flow, ozonolysis rate ~ 12 mmol/5min) was bubbled through a cooled solution (-78°C) of compound **10** (2.7447 g, 12.24 mmol) in CH<sub>2</sub>Cl<sub>2</sub> (35 mL) till the TLC (hexane/EtOAc 3:1) indicated disappearance of the starting material and blue colour of the reaction mixture persisted. After that N<sub>2</sub> was bubbled through the reaction mixture to remove residual ozone and oxygen. Me<sub>2</sub>S (4.5 mL, 61.2 mmol) was added in one portion and the reaction mixture was stirred for 4 h while allowed to warm to room temperature. Brine (20 mL) was then added and the mixture was extracted with CH<sub>2</sub>Cl<sub>2</sub> (1x 30 mL). Organic phase was washed with brine (2x 10 mL), dried with MgSO<sub>4</sub>, filtered and the solvent was evaporated. The resulting colourless oil was immediately used in the next step without additional purification. The purity of crude aldehyde **11** was satisfactory by <sup>1</sup>H

NMR (the main impurity is DMSO as a product of Me<sub>2</sub>S oxidation, see below). Attempts to purify the compound by standard flash column chromatography failed due to the compound's instability.

Into a cooled (ice bath, 0°C) solution of crude aldehyde **11** (1.742 g, 6.8 mmol) in anhydrous THF (15 mL) was added Li(AlO-*t*Bu)<sub>3</sub>H (3.98g, 15.64 mmol) portionwise. The reaction mixture was then stirred overnight while allowed to warm to room temp. It was then poured into 5% aqueous solution of NaHSO<sub>4</sub> (50 mL) with crushed ice (50 g). The resulting white liquid was then diluted with brine (30 mL) and extracted with EtOAc (4x 50 mL). The organic phase was dried with MgSO<sub>4</sub>, filtered and concentrated in a vacuum to give a yellow oil. Flash column chromatography (CH<sub>2</sub>Cl<sub>2</sub>/MeOH 15:1) yielded a colourless oil (620 mg, 65 % from compound **10**) as a mixture of both epimers with the ratio of 5:2 based on <sup>1</sup>H NMR. <sup>1</sup>H NMR (500 MHz, CDCl<sub>3</sub>): δ = 4.62 (dd, 1H major epimer), 4.43 dd, 0.4 H minor epimer), 4.39 (d), 4.34 (m), 4.15 (d), 3.78 (s), 3.77 (s), 3.65 (m), 3.01 (br s), 2.46 (m), 2.23 (m), 2.02 (m), 1.76 (m), 1.48 (s), 1.44 (s), 1.29 (s), 1.26 (s) ppm. <sup>13</sup>C NMR (126 MHz, CDCl<sub>3</sub>): δ = 174.98, 112.91, 83.53, 83.49, 82.24, 80.95, 70.97, 70.19, 64.85, 64.73, 53.61, 52.92, 52.80, 49.04, 48.50, 47.48, 30.66, 27.89, 27.86, 27.46, 25.56, 25.46 ppm. HR-MS (ESI): calcd for C<sub>12</sub>H<sub>20</sub>O<sub>6</sub> [M+H]<sup>+</sup>: 261.1333. Found 261.1330, calcd for C<sub>12</sub>H<sub>20</sub>O<sub>6</sub> [M<sub>1</sub>+Na]<sup>+</sup>: 283.1152. Found 283.1156.

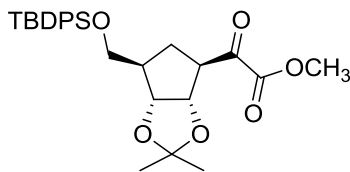
**methyl 2-((3aR\*,4R\*,6S\*,6aS\*)-6-(((tert-butyldiphenylsilyl)oxy)methyl)-2,2-dimethyltetrahydro-3aH-cyclopenta[d][1,3]dioxol-4-yl)-2-hydroxyacetate (**13**):**



Into a solution of starting material **12** (692 mg, 2.66 mmol) in anhydrous CH<sub>2</sub>Cl<sub>2</sub> (8 mL) was added in one portion TBDPSCl (691 μL, 2.79 mmol) followed by imidazole (453 mg, 6.65 mmol). The reaction mixture was then stirred overnight at room temp. The solvent was evaporated and the viscous residue was purified by flash column chromatography (hexane/EtOAc 3:1) to yield a colourless oil (1.07 g, 81%) as a mixture of epimers with the ratio of 5:2 based on <sup>1</sup>H NMR. <sup>1</sup>H NMR (500 MHz, CDCl<sub>3</sub>): δ = 7.66-7.60 (m), 7.43-7.32 (m), 4.57-4.51 (m), 4.43-4.30 (m), 4.18-4.14 (m), 3.76 (s), 3.73-3.64 (m), 2.84 d (0.4 H, minor epimer), 2.74 (d, 1H, major epimer), 2.45-2.35 (m), 2.29-2.19 (m), 2.01-1.94 (m), 1.71-1.64 (m), 1.61-1.53 (m), 1.47 ((-C(CH<sub>3</sub>)<sub>2</sub>), major epimer), 1.43 ((-C(CH<sub>3</sub>)<sub>2</sub>), minor epimer), 1.27 ((-C(CH<sub>3</sub>)<sub>2</sub>), major epimer), 1.24 ((-C(CH<sub>3</sub>)<sub>2</sub>), minor epimer), 1.04 ppm. <sup>13</sup>C NMR (126 MHz, CDCl<sub>3</sub>): δ = 175.23, 175.15, 135.87, 133.92, 133.89, 129.86, 127.88, 112.67, 82.59,

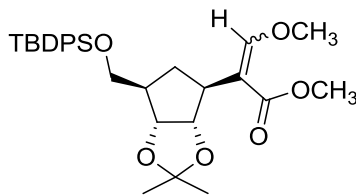
82.48, 81.86, 80.76, 70.83, 70.71, 70.11, 69.99, 65.02, 64.94, 52.87, 52.71, 49.36, 48.87, 47.10, 46.62, 30.70, 28.00, 27.97, 27.67, 27.12, 25.66, 25.54, 19.55 ppm. IR (KBr):  $\tilde{\nu}_{\max}$  = 3452, 2933, 2858, 1740, 1639, 1429, 1211, 1112, 704  $\text{cm}^{-1}$ . HR-MS (ESI): calcd  $\text{C}_{28}\text{H}_{38}\text{O}_6\text{Si}$   $[\text{M}+\text{Na}]^+$ : 521.2330. Found 521.2334.

**methyl 2-((3aR\*,4S\*,6S\*,6aS\*)-6-(((tert-butyl)diphenylsilyl)oxy)methyl)-2,2-dimethyltetrahydro-3aH-cyclopenta[d][1,3]dioxol-4-yl)-2-oxoacetate (14):**



Into a cooled (0°C, ice bath) solution of starting material **13** (487 mg, 0.977 mmol) in anhydrous  $\text{CH}_2\text{Cl}_2$  (8 mL) was added Dess-Martin periodinane (581 mg, 1.37 mmol). The reaction mixture was then allowed to warm to room temp. and then stirred for 14 h. The solvent was evaporated, the residue was suspended in cold  $\text{Et}_2\text{O}$  (50 mL) and the solid was removed by filtration. The filtrate was washed with saturated aqueous  $\text{NaHCO}_3$  solution (2x 10 mL), dried with  $\text{MgSO}_4$ , filtered and concentrated in a vacuum to provide a colourless oil (412 mg, 85%) which solidified upon freezing. Attempts to purify the compound by column chromatography failed due to partial epimerization and decomposition on silica gel. m.p.: 76-78°C.  $^1\text{H}$  NMR (500 MHz,  $\text{CDCl}_3$ ):  $\delta$  = 7.65-7.56 (m, 4H), 7.43-7.31 (m, 6H), 4.82-4.76 (m, 1H), 4.41 (dd,  $J$  = 6.0, 3.6Hz, 1H), 3.85 (s, 3H), 3.69-3.53 (m, 3H), 2.41-2.29 (m, 2H), 1.82-1.75 (m, 1H), 1.47 (s, 3H), 1.26 (s, 3H), 1.02 (s, 9H) ppm.  $^{13}\text{C}$  NMR (126 MHz,  $\text{CDCl}_3$ ):  $\delta$  = 194.60, 161.73, 135.81, 133.68, 129.94, 127.94, 112.66, 82.70, 81.74, 64.18, 54.18, 53.24, 47.69, 30.98, 27.68, 27.09, 25.27, 19.50 ppm. IR (KBr):  $\tilde{\nu}_{\max}$  = 3448, 3415, 2956, 2933, 1738, 1714, 1259, 1114, 1032, 708  $\text{cm}^{-1}$ . HR-MS (ESI): calcd for  $\text{C}_{28}\text{H}_{36}\text{O}_6\text{Si}$   $[\text{M}+\text{Na}]^+$  : 519.2173. Found 519.2176.

**Methyl 2-((3aR\*,4R\*,6S\*,6aS\*)-6-(((tert-butyl)diphenylsilyl)oxy)methyl)-2,2-dimethyltetrahydro-3aH-cyclopenta[d][1,3]dioxol-4-yl)-3-methoxyacrylate (15):**



Into a cooled (0°C, ice bath) suspension of (methoxymethyl)triphenylphosphonium chloride (1.929g, 5.63 mmol) in anhydrous THF (15 mL) was added under N<sub>2</sub> atmosphere LDA (2.63 mL of 2M solution in THF, 5.26 mmol) dropwise over the period of 10 min. The resulting orange mixture was stirred at 0°C for 30 min. and then a solution of ketone **14** (932 mg, 1.88 mmol) in anhydrous THF (20 mL) was added in one portion. The yellow mixture was stirred for additional 3 h while allowed to warm to room temp., then it was quenched with saturated aqueous solution of NH<sub>4</sub>Cl (15 mL). The aqueous phase was extracted with EtOAc (3x 20 mL), the combined organic parts were dried with MgSO<sub>4</sub>, filtered and volatiles were evaporated. The dark brown residue was purified by flash column chromatography (CH<sub>2</sub>Cl<sub>2</sub>/EtOAc 20:1) to afford two isomeric enol ethers in the overall yield of 503 mg (51%) with ratio of Z:E ~7:5. Z isomer (293 mg, 30%, yellow oil): <sup>1</sup>H NMR (500 MHz, CDCl<sub>3</sub>): δ = 7.63 (m, 4H), 7.36 (m, 6H), 6.51 (s, 1H), 4.59 (m, 1H), 4.41 (m, 1H), 3.79 (s, 3H), 3.77 (m, 1H), 3.70 (s, 3H), 3.68 (m, 1H), 2.61 (m, 1H), 2.20 (m, 1H), 1.97 (m, 1H), 1.83 (dd, J = 12.24, 11.98 Hz, 1H), 1.47 (s, 3H), 1.27 (s, 3H), 1.04 (s, 9H) ppm. <sup>13</sup>C NMR (126 MHz, CDCl<sub>3</sub>): δ = 166.60, 157.05, 135.85, 135.84, 134.01, 129.80, 127.83, 112.60, 108.56, 84.56, 82.37, 65.02, 62.21, 51.27, 47.78, 47.34, 34.85, 28.14, 27.11, 25.61, 19.56 ppm. HR-MS (ESI): calcd for C<sub>30</sub>H<sub>40</sub>O<sub>6</sub>Si [M+H]<sup>+</sup> : 525.2667. Found 525.2671.

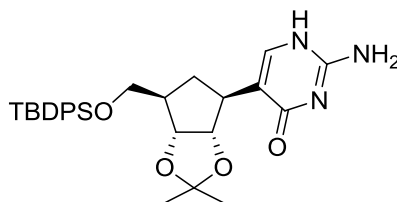
E isomer (210 mg, 21%, yellow oil): <sup>1</sup>H NMR (500 MHz, CDCl<sub>3</sub>): δ = 7.64 (m, 4H), 7.36 (m, 6H), 7.33 (s, 1H), 4.74 (m, 1H), 4.44 (m, 1H), 3.79 (s, 3H), 3.79 (m, 1H), 3.69 (s, 1H), 3.66 (s, 3H), 3.27 (m, 1H), 2.24 (m, 1H), 1.94 (m, 2H), 1.48 (s, 3H), 1.26 (s, 3H), 1.04 (s, 9H) ppm. <sup>13</sup>C NMR (126 MHz, CDCl<sub>3</sub>): δ = 168.30, 160.08, 135.87, 134.13, 134.11, 129.76, 127.82, 112.47, 110.71, 84.37, 82.52, 65.13, 61.76, 51.30, 48.20, 40.88, 33.65, 28.23, 27.11, 25.78, 19.59 ppm. IR both isomers (KBr): ν<sub>max</sub> = 3450, 2935, 2858, 1693, 1639, 1429, 1378, 1211, 1113, 704, 505 cm<sup>-1</sup>. HR-MS (ESI): calcd for C<sub>30</sub>H<sub>40</sub>O<sub>6</sub>Si [M+Na]<sup>+</sup> : 547.2486. Found 547.2485.

### General procedure for synthesis of compounds **16a-16c**

To a 0.05 M solution of starting material **15** (mixture of Z+E enol ethers) in anhydrous *t*-BuOH was added urea (or thiourea or guanidinium.HCl) (3 equiv.) and *t*-BuOK (6 equiv. for **16a** and 4 equiv. for **16b** and **16c** ). The resulting solution was refluxed for 14 h. The reaction mixture was cooled to room

temp., diluted with H<sub>2</sub>O (15 mL) and pH was adjusted to 6-7 with 1M HCl. The resulting solution was extracted with EtOAc (4x 20 mL). Combined organic extracts were dried with Na<sub>2</sub>SO<sub>4</sub>, filtered and concentrated in a vacuum. The resulting brown oil was purified by flash column chromatography (CH<sub>2</sub>Cl<sub>2</sub>/MeOH 15:1 for **16a** and 20:1 for **16b** and **16c**).

**2-amino-5-((3aR\*,4R\*,6S\*,6aS\*)-6-(((tert-butyl)diphenylsilyl)oxy)methyl)-2,2-dimethyltetrahydro-3aH-cyclopenta[d][1,3]dioxol-4-yl)pyrimidin-4(1H)-one (**16a**):**

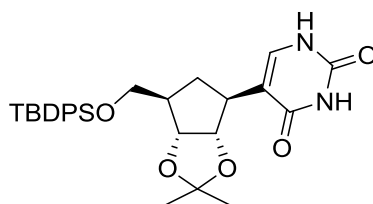


Colourless amorphous solid (166 mg, 43%). <sup>1</sup>H NMR (500 MHz, DMSO-*d*<sub>6</sub>): δ = 10.83 (br s, 1H), 7.61 (m, 4H), 7.44 (m, 6H), 6.34 (br s, 2H), 4.64 (m, 1H), 4.38 (m, 1H), 3.68 (m, 2H), 2.83 (m, 1H), 2.18 (m, 1H), 1.95 (m, 1H), 1.80 (m, 1H), 1.39 (s, 3H), 1.18 (s, 3H), 1.00 (s, 9H) ppm. <sup>13</sup>C NMR (126 MHz, DMSO-*d*<sub>6</sub>): δ = 161.80\*, 155.08, 134.99, 133.15, 129.73, 127.79, 114.27\*, 111.38, 83.20, 81.83, 64.89, 47.26, 44.07, 33.58, 27.72, 26.61, 25.21, 18.84 ppm.\* - these resonances were indirectly detected by <sup>1</sup>H-<sup>13</sup>C HMBC experiment. HR-MS (ESI): calcd for C<sub>29</sub>H<sub>37</sub>N<sub>3</sub>O<sub>4</sub>Si [M-H]<sup>-</sup>: 518.2481. Found 518.2481.

Separation of enantiomers of **16a**:

Chiralpak AD 4.6x250 mm column; hexane/2-propanol 90:10; 1mL/min; UV detection (254 nm)

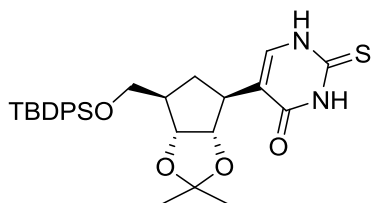
**5-((3aR\*,4R\*,6S\*,6aS\*)-6-(((tert-butyl)diphenylsilyl)oxy)methyl)-2,2-dimethyltetrahydro-3aH-cyclopenta[d][1,3]dioxol-4-yl)pyrimidine-2,4(1H,3H)-dione (**16b**):**



Slightly yellow amorphous solid (85 mg, 38%). <sup>1</sup>H NMR (500 MHz, CDCl<sub>3</sub>): δ = 9.23 (br s, 1H), 8.82 (s, 1H), 7.63 (m, 4H), 7.37 (m, 6H), 7.08 (d, *J* = 6.49 Hz, 1H), 4.63 (m, 1H), 4.46 (dd, *J* = 6.8,

5.2 Hz, 1H), 3.73 (ddd,  $J = 16.4, 10.2, 5.7$  Hz, 2H), 2.87 (m, 1H), 2.31 (m, 1H), 2.13 (dd,  $J = 12.9, 6.8$  Hz, 1H), 1.89 (dd,  $J = 24.3, 12.9$  Hz, 1H), 1.48 (s, 3H), 1.26 (s, 3H), 1.05 (s, 9H) ppm.  $^{13}\text{C}$  NMR (126 MHz,  $\text{CDCl}_3$ ):  $\delta = 163.50, 152.09, 136.83, 135.86, 133.93, 129.89, 127.90, 114.64, 113.09, 83.33, 82.37, 65.01, 47.45, 45.49, 33.68, 28.00, 27.14, 25.48, 19.57$  ppm. HR-MS (ESI): calcd for  $\text{C}_{29}\text{H}_{36}\text{N}_2\text{O}_5\text{Si}$  [M-H]<sup>-</sup>: 519.2321. Found 519.2303.

**5-((3aR\*,4R\*,6S\*,6aS\*)-6-(((tert-butylidiphenylsilyl)oxy)methyl)-2,2-dimethyltetrahydro-3aH-cyclopenta[d][1,3]dioxol-4-yl)-2-thioxo-2,3-dihydropyrimidin-4(1H)-one (16c):**

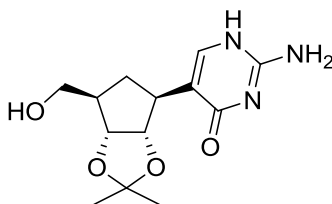


Yellow amorphous solid (198 mg, 45%).  $^1\text{H}$  NMR (300 MHz,  $\text{CDCl}_3$ ):  $\delta = 10.66$  (br s, 1H), 10.21 (s, 1H), 7.63 (m, 4H), 7.38 (m, 6H), 7.07 (d,  $J = 5.2$  Hz, 1H), 4.70 (dd,  $J = 6.60, 13.61$  Hz, 1H), 4.48 (dd,  $J = 6.60, 11.77$  Hz, 1H), 3.74 (m, 2H), 2.90 (m, 1H), 2.34 (m, 1H), 2.10 (m, 1H), 1.90 (m, 1H), 1.51 (s, 3H), 1.29 (s, 3H), 1.05 (s, 9H) ppm.  $^{13}\text{C}$  NMR (75 MHz,  $\text{CDCl}_3$ ):  $\delta = 174.93, 160.80, 137.14, 135.84, 133.86, 129.92, 127.92, 119.13, 113.38, 83.01, 82.43, 64.97, 47.33, 45.72, 33.41, 28.02, 27.14, 25.54, 19.56$  ppm. HR-MS (ESI): calcd for  $\text{C}_{29}\text{H}_{36}\text{N}_2\text{O}_4\text{SSi}$  [M+Na]<sup>+</sup>: 559.2057. Found 559.2021.

**General procedure for synthesis of compounds 17a-c**

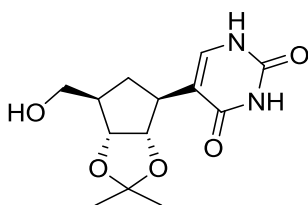
To a 0.1 M solution of starting material **16b-c** in wet THF was added TBAF (1.1 equiv., 1 M solution in THF) and the reaction mixture was stirred at room temp for 14h. THF was evaporated and the brown oily residue was purified on a short silica gel column ( $\text{CH}_2\text{Cl}_2/\text{MeOH}$  2:1 for **17a** and 10:1 for **17b** and **17c**).

**2-amino-5-((3aR\*,4R\*,6S\*,6aS\*)-6-(hydroxymethyl)-2,2-dimethyltetrahydro-3aH-cyclopenta[d][1,3]dioxol-4-yl)pyrimidin-4(1H)-one (17a):**



White crystalline solid (80 mg, 90%). m.p.: > 250°C, decomp.  $^1\text{H}$  NMR (500 MHz,  $\text{DMSO-}d_6$ ):  $\delta$  = 10.80 (s, 1H), 7.43 (s, 1H), 6.33 (s, 2H), 4.63 (m, 1H), 4.54 (m, 1H), 4.32 (m, 1H), 3.40 (m, 2H), 2.79 (m, 1H), 2.04 (m, 1H), 1.89 (m, 1H), 1.65 (m, 1H), 1.40 (s, 3H), 1.19 (s, 3H) ppm.  $^{13}\text{C}$  NMR (126 MHz,  $\text{DMSO-}d_6$ ):  $\delta$  = 162.04\*, 155.03, 153.10\*, 114.52\*, 111.28, 83.10, 82.21, 62.57, 47.41, 44.31, 33.84, 27.72, 25.19 ppm. \* - resonances were indirectly detected through  $^1\text{H-}^{13}\text{C}$  HSQC or  $^1\text{H-}^{13}\text{C}$  HMBC experiments. IR (KBr):  $\tilde{\nu}_{\text{max}}$  = 3434, 3097, 2983, 2736, 1670, 1614, 1562, 1207, 1051, 867  $\text{cm}^{-1}$ . HR-MS (ESI): calcd for  $\text{C}_{13}\text{H}_{19}\text{N}_3\text{O}_4$   $[\text{M}+\text{H}]^+$ : 282.1448. Found 282.1447

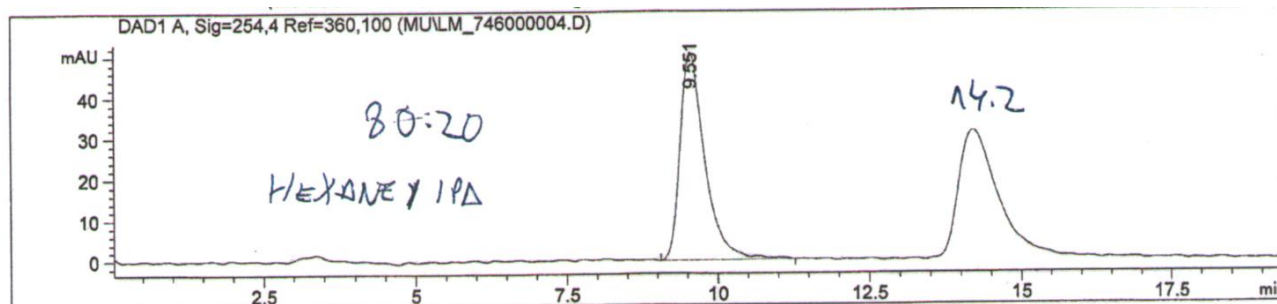
**5-((3aR\*,4R\*,6S\*,6aS\*)-6-(hydroxymethyl)-2,2-dimethyltetrahydro-3aH-cyclopenta[d][1,3]dioxol-4-yl)pyrimidine-2,4(1H,3H)-dione (17b):**



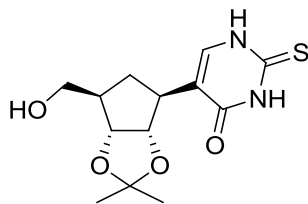
White crystalline solid (89 mg, 96%). m.p.: 246-247°C, decomp.  $^1\text{H}$  NMR (500 MHz,  $\text{DMSO-}d_6$ ):  $\delta$  = 10.99 (s, 1H), 10.70 (br s, 1H), 7.30 (s, 1H), 4.58 (m, 2H), 4.33 (dd,  $J$  = 5.3, 12 Hz, 1H), 3.40 (m, 2H), 2.83 (m, 1H), 2.04 (m, 1H), 1.94 (m, 1H), 1.56 (m, 1H), 1.40 (s, 3H), 1.20 (s, 3H) ppm.  $^{13}\text{C}$  NMR (126 MHz,  $\text{DMSO-}d_6$ ):  $\delta$  = 164.00, 151.06, 137.93, 111.99, 111.43, 82.94, 82.05, 62.40, 47.24, 43.43, 33.83, 27.66, 25.18 ppm. IR (KBr):  $\tilde{\nu}_{\text{max}}$  = 3490, 3228, 2933, 1720, 1666, 1384, 1377, 1065, 1040, 860, 791  $\text{cm}^{-1}$ . HR-MS (ESI): calcd for  $\text{C}_{13}\text{H}_{18}\text{N}_2\text{O}_5$   $[\text{M}-\text{H}]^-$ : 283.1288. Found 283.1287.

Separation of enantiomers of **17b**:

Chiralpak AD 4.6x250 mm column; hexane/2-propanol 80:20; 1mL/min; UV detection (254 nm)



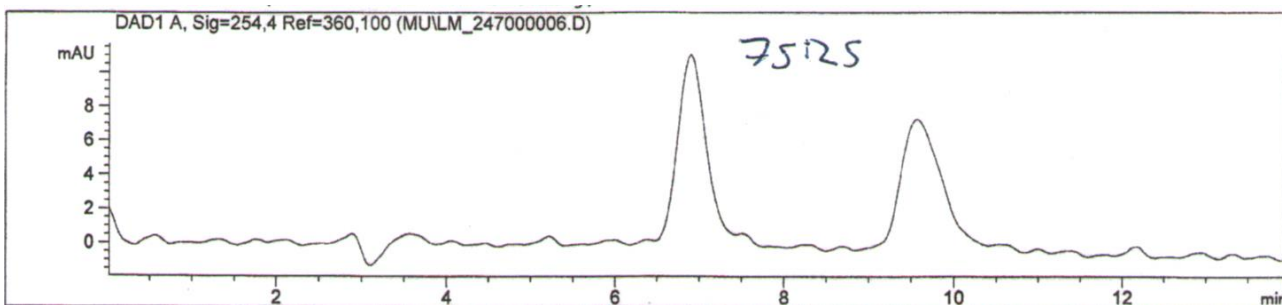
**5-((3aR\*,4R\*,6S\*,6aS\*)-6-(hydroxymethyl)-2,2-dimethyltetrahydro-3aH-cyclopenta[d][1,3]dioxol-4-yl)-2-thioxo-2,3-dihydropyrimidin-4(1H)-one (17c):**



White crystalline solid (99 mg, 90%). m.p. 199-201°C.  $^1\text{H}$  NMR (500 MHz,  $\text{DMSO-}d_6$ ):  $\delta$  = 12.41 (s, 1H), 12.24 (br s, 1H), 7.35 (s, 1H), 4.59 (m, 1H), 4.58 (m, 1H), 4.34 (dd,  $J$  = 5.20, 12 Hz, 1H), 3.40 (m, 2H), 2.88 (m, 1H), 2.05 (m, 1H), 1.96 (m, 1H), 1.56 (dd, 1H,  $J$  = 12, 23.7 Hz), 1.40 (s, 3H), 1.20 (s, 3H) ppm.  $^{13}\text{C}$  NMR (126 MHz,  $\text{DMSO-}d_6$ ):  $\delta$  = 174.59, 160.97, 137.86, 117.78, 111.53, 82.78, 82.06, 62.31, 47.18, 43.36, 33.44, 27.63, 25.19 ppm. IR (KBr):  $\tilde{\nu}_{\text{max}}$  = 3450, 3263, 2927, 1658, 1541, 1456, 1383, 1371, 1213, 1155, 866  $\text{cm}^{-1}$ . HR-MS (ESI): calcd for  $\text{C}_{13}\text{H}_{18}\text{N}_2\text{O}_4\text{S}$  [M-H] $^-$ : 297.0915. Found: 297.0904.

Separation of enantiomers of **17c**:

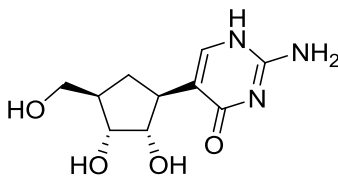
Chiralpak AD 4.6x250 mm column; hexane/2-propanol 75:25; 1mL/min; UV detection (254 nm)



### General procedure for synthesis of compounds **2a-c**

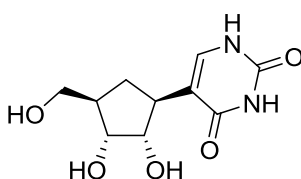
To a 0.2 M solution of starting material **17a-c** in MeOH were added 35% HCl (1 mL) and  $\text{H}_2\text{O}$  (1 mL) and the reaction mixture was stirred at room temp for 30 min. The solvents were evaporated in a vacuum and the resulting brown solid was purified by flash column chromatography ( $\text{CH}_2\text{Cl}_2/7\text{ N NH}_3$  in MeOH 5:1 for compound **2a** and  $\text{CH}_2\text{Cl}_2/\text{MeOH}$  5:1 to 1:1 for compounds **2b** and **2c**).

**2-amino-5-((1R\*,2R\*,3S\*,4S\*)-2,3-dihydroxy-4-(hydroxymethyl)cyclopentyl)pyrimidin-4(1H)-one (2a):**



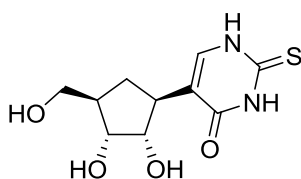
White crystalline solid (46 mg, 69 %). m.p.: > 250°C, decomp.  $^1\text{H}$  NMR (500 MHz,  $\text{DMSO-}d_6$ ):  $\delta$  = 10.94 (br s, 1H), 7.37 (s, 1H), 6.33 (br s 2H), 4.73 (br s –OH), 4.45 (m, 1H), 4.09 (br s – OH), 3.81 (m, 1H), 3.67 (m, 1H), 3.36 (m, 2H), 2.76 (m, 1H), 1.91 (m, 1H), 1.84 (m, 1H), 1.25 (m, 1H).  $^{13}\text{C}$  NMR (126 MHz,  $\text{DMSO-}d_6$ ):  $\delta$  = 164.10\*, 155.40, 151.76\*, 115.31, 75.14, 73.33, 63.39, 46.66, 42.42, 29.12.\*- these resonances were indirectly detected through  $^1\text{H-}^{13}\text{C}$  HSQC or  $^1\text{H-}^{13}\text{C}$  HMBC experiments. IR (KBr):  $\tilde{\nu}_{\text{max}}$  = 3421, 2921, 1652, 1606, 1486, 1118, 1043, 777  $\text{cm}^{-1}$ . HR-MS (ESI): calcd for  $\text{C}_{10}\text{H}_{15}\text{N}_3\text{O}_4[\text{M-H}]^-$ : 240.0990. Found: 240.0969.

**5-((1R\*,2R\*,3S\*,4S\*)-2,3-dihydroxy-4-(hydroxymethyl)cyclopentyl)pyrimidine-2,4(1H,3H)-dione (2b):**



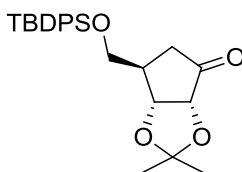
White solid (60 mg, 76 %). m.p. > 300°C, decomp.  $^1\text{H}$  NMR (500 MHz,  $\text{DMSO-}d_6$ ):  $\delta$  = 10.94 (br s, 1H), 10.62 (br s, 1H), 7.15 (s, 1H), 4.46 (m, 1H), 4.37 (d,  $J$  = 6.40 Hz, 1H), 4.22 (d,  $J$  = 4.19 Hz, 1H), 3.79 (m, 1H), 3.68 (m, 1H), 3.34 (m, 2H), 2.76 (m, 1H), 1.91 (m, 2H), 1.11 (m, 1H) ppm.  $^{13}\text{C}$  NMR (126 MHz,  $\text{DMSO-}d_6$ ):  $\delta$  = 164.52, 151.07, 137.32, 113.18, 74.41, 73.03, 63.13, 46.36, 41.35, 29.50. IR (KBr):  $\tilde{\nu}_{\text{max}}$  = 3448, 2926, 1709, 1659, 1446, 1225, 1113, 766,  $\text{cm}^{-1}$ . HR-MS (ESI): calcd for  $\text{C}_{10}\text{H}_{14}\text{N}_2\text{O}_5[\text{M-H}]^-$ : 241.0830. Found: 241.0833.

**5-((1R\*,2R\*,3S\*,4S\*)-2,3-dihydroxy-4-(hydroxymethyl)cyclopentyl)-2-thioxo-2,3-dihydropyrimidin-4(1H)-one (2b):**



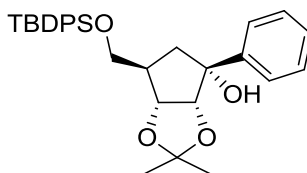
White solid (60 mg, 71 %). m.p: 172-175°C, decomp.  $^1\text{H}$  NMR (500 MHz,  $\text{DMSO-}d_6$ ):  $\delta$  = 12.34 (br s, 1H), 12.18 (br s, 1H), 7.20 (s, 1H), 4.49 (m, 1H), 4.43 (d,  $J$  = 6.44 Hz, 1H), 4.25 (d,  $J$  = 4.47 Hz, 1H), 3.81 (m, 1H), 3.69 (m, 1H), 3.34 (m, 2H), 2.81 (m, 1H), 1.93 (m, 2H), 1.12 (m, 1H) ppm.  $^{13}\text{C}$  NMR (126 MHz,  $\text{DMSO-}d_6$ ):  $\delta$  = 174.30, 161.40, 137.33, 119.02, 74.24, 73.03, 63.09, 46.37, 41.40, 29.12 ppm. IR (KBr):  $\tilde{\nu}_{\text{max}}$  = 3437, 3162, 3070, 2931, 1654, 1587, 1463, 1232, 1033, 766  $\text{cm}^{-1}$ . HR-MS (ESI): calcd for  $\text{C}_{10}\text{H}_{14}\text{N}_2\text{O}_4\text{S}[\text{M-H}]^-$ : 257.0602 Found:257.0608.

**(3aR\*,6R\*,6aR\*)-6-(((tert-butyl)diphenylsilyloxy)methyl)-2,2-dimethyldihydro-3aH-cyclopenta[d][1,3]dioxol-4(5H)-one (19):**



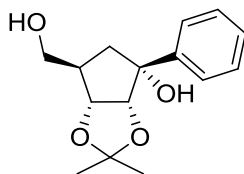
LiHMDS (280  $\mu$ L of 1 M solution in THF, 0.28 mmol) followed by TBDMSOTf (0.28 mmol, 64  $\mu$ L) were added dropwise to a cooled (-78°C) solution of starting material **14** (140 mg, 0.28 mmol) in THF (2 mL) and the resulting mixture was stirred for additional 2 h at -78°C. All volatiles were evaporated and the crude mixture was immediately dissolved in anhydrous CH<sub>2</sub>Cl<sub>2</sub> (6 mL) and cooled to -78°C. O<sub>3</sub>/O<sub>2</sub> mixture (5 mL/min oxygen flow) was bubbled through the solution until TLC (hexane/EtOAc 10:1) indicated disappearance of starting material and blue colour of the reaction mixture persisted. Then N<sub>2</sub> was bubbled through the reaction mixture to remove residual ozone and oxygen. Me<sub>2</sub>S (120  $\mu$ L, 1.4 mmol) was added in one portion and the reaction mixture was stirred for 4 h while allowed to warm to room temperature. Brine (10 mL) was then added and the mixture was extracted with CH<sub>2</sub>Cl<sub>2</sub> (2x 15 mL). The organic phase was washed with brine (2x 10 mL), dried with MgSO<sub>4</sub>, filtered and the solvents were evaporated. The resulting yellow oil was purified by flash column chromatography (hexane/EtOAc 5:1) to yield a white crystalline solid (62 mg, 52 %). m.p: 96-97°C. <sup>1</sup>H NMR (500 MHz, CDCl<sub>3</sub>):  $\delta$  = 7.60-7.57 (m, 4H), 7.45-7.36 (m, 6H), 4.61 (d, *J* = 5.4 Hz, 1H), 4.33 (d, *J* = 5.4 Hz, 1H), 3.78 (dd, *J* = 10.2, 2.8 Hz, 1H), 3.59 (dd, *J* = 10.2, 2.8 Hz, 1H), 2.73 (dd, *J* = 18.4, 9.0 Hz, 1H), 2.47 (m, 1H), 2.17 (m, 1H), 1.41 (s, 3H), 1.32 (s, 3H), 1.00 (s, 9H) ppm. <sup>13</sup>C NMR (126 MHz, CDCl<sub>3</sub>):  $\delta$  = 213.41, 135.94, 135.82, 132.97, 132.61, 130.24, 130.19, 128.09, 111.48, 81.79, 79.32, 77.48, 77.23, 76.98, 66.13, 39.31, 37.49, 27.05, 27.02, 24.89, 19.35. IR (KBr):  $\tilde{\nu}_{\text{max}}$  = 3486, 2933, 1755, 1589, 1429, 1108, 705.85 cm<sup>-1</sup>. HR-MS (ESI): calcd for C<sub>25</sub>H<sub>32</sub>O<sub>4</sub>Si [M+Na]<sup>+</sup>: 447.1962 Found:447.1962.

**(3aR\*,4R\*,6R\*,6aR\*)-6-(((tert-butyl)diphenylsilyloxy)methyl)-2,2-dimethyl-4-phenyltetrahydro-3aH-cyclopenta[d][1,3]dioxol-4-ol (20):**



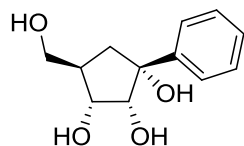
PhLi (138  $\mu$ L of 1.8 M solution in Bu<sub>2</sub>O, 0.25 mmol) was added dropwise to a cooled (0°C, ice bath) solution of ketone **19** (70 mg, 0.17 mmol) in THF (4 mL) and the resulting mixture was stirred for 1h at 0°C. Then it was quenched with saturated aqueous solution of NH<sub>4</sub>Cl (15 mL). The aqueous phase was extracted with EtOAc (3x 15 mL), the combined organic parts were dried with MgSO<sub>4</sub>, filtered and volatiles were evaporated. The dark brown residue was purified by flash column chromatography (hexane/EtOAc 10:1) to yield a colourless oil (125 mg, 75%). <sup>1</sup>H NMR (500 MHz, CDCl<sub>3</sub>):  $\delta$  = 7.69-7.62 (m, 4H), 7.47-7.33 (m, 10H), 7.28-7.23 (m, 1H), 4.70-4.63 (m, 2H), 3.87 (dd, *J* = 10.3, 5.0 Hz, 1H), 3.79 (dd, *J* = 10.3, 4.4 Hz, 1H), 3.32 (d, *J* = 1.5 Hz, 1H), 2.73-2.66 (m, 1H), 2.31 (dd, *J* = 13.6, 6.8 Hz, 1H), 2.18 (dd, 13.6, 1.5 Hz, 1H), 1.59 (s, 3H), 1.35 (s, 3H), 1.08 (s, 9H) ppm. <sup>13</sup>C NMR (126 MHz, CDCl<sub>3</sub>):  $\delta$  = 145.25, 135.86, 135.84, 133.85, 133.81, 129.92, 128.53, 127.93, 127.92, 127.26, 125.32, 114.74, 87.11, 82.23, 78.57, 64.46, 46.14, 42.73, 27.16, 26.61, 24.89, 19.60.

**(3aR\*,4R\*,6R\*,6aR\*)-6-(hydroxymethyl)-2,2-dimethyl-4-phenyltetrahydro-3aH-cyclopenta[d][1,3]dioxol-4-ol (21)**



To a solution of compound **20** (72 mg, 0.14 mmol) in wet THF (3 mL) was added TBAF (154  $\mu$ L of 1 M solution in THF, 154 mmol) and the reaction mixture was stirred at 25°C for 14h. The solvent was evaporated and the brown oily residue was purified on a short silica gel column (CH<sub>2</sub>Cl<sub>2</sub>/MeOH 20:1) to yield a white crystalline solid (33 mg, 87%). <sup>1</sup>H NMR (500 MHz, CDCl<sub>3</sub>):  $\delta$  = 7.480-7.42 (m, 2H), 7.36-7.31 (m, 2H), 7.26-7.22 (m, 1H), 4.70-4.63 (m, 1H), 3.83 (dd, *J* = 10.7, 5.0 Hz, 1H), 3.67 (dd, *J* = 10.7, 6.7 Hz, 1H), 3.38 (d, *J* = 1.5 Hz, 1H), 2.73-2.65 (m, 1H), 2.32 (dd, *J* = 13.5, 6.6 Hz, 1H), 1.97 (dd, *J* = 13.5, 1.5 Hz, 1H), 1.60 (s, 3H), 1.37 (s, 3H) ppm. <sup>13</sup>C NMR (126 MHz, CDCl<sub>3</sub>):  $\delta$  = 144.87, 128.52, 127.36, 125.32, 115.08, 86.83, 83.11, 78.29, 64.06, 46.33, 42.28, 26.57, 24.93.

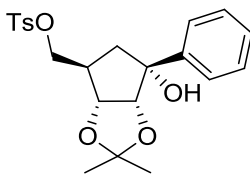
**(1R\*,2R\*,3R\*,4R\*)-4-(hydroxymethyl)-1-phenylcyclopentane-1,2,3-triol (22)**



To a solution of compound **21** (33 mg, 0.124 mmol) in MeOH (4 mL) was added PPTS (156 mg, 0.620 mmol) and the mixture was stirred at 25°C for 24h. The solvent was evaporated and the residue

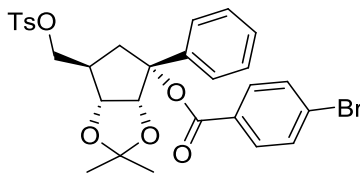
was purified by flash column chromatography (CH<sub>2</sub>Cl<sub>2</sub>/MeOH 20:1 to 2:1) to yield a white crystalline solid (14 mg, 48 %). m.p: 141.3-143°C. <sup>1</sup>H NMR (500 MHz, DMSO-*d*<sub>6</sub>): δ = 7.49-7.44 (m, 2H), 7.33-7.27 (m, 2H), 7.22-7.17 (m, 1H), 4.66 (s, 1H), 4.58 (d, *J* = 6.09 Hz, 1H), 4.55 (m, 1H), 4.44 (d, *J* = 7.68 Hz, 1H), 3.82 (dd, *J* = 14.14, 6.83 Hz, 1H), 3.79 (m, 1H), 2.81 (m, 1H), 2.22 (m, 1H), 1.95 (dd, *J* = 13.5, 8.4 Hz, 1H), 1.66 (dd, *J* = 13.5, 10.07 Hz, 1H) ppm. <sup>13</sup>C NMR (126 MHz, DMSO-*d*<sub>6</sub>): δ = 146.27, 127.55, 126.03, 125.33, 80.73, 77.89, 72.91, 62.70, 46.85 ppm. IR (KBr): ν<sup>max</sup> = 3465, 3272, 2960, 2933, 1645, 1417, 1130, 1022, 700 cm<sup>-1</sup>. HR-MS (ESI): calcd for C<sub>12</sub>H<sub>6</sub>O<sub>4</sub> [M+H]<sup>+</sup>: 224.0976 Found:224.0970.

**((3aR\*,4R\*,6R\*,6aR\*)-6-hydroxy-2,2-dimethyl-6-phenyltetrahydro-3aH-cyclopenta[d][1,3]dioxol-4-yl)methyl 4-methylbenzenesulfonate (23)**



To a cooled (0°C, ice bath) solution of compound **21** (73 mg, 0.276 mmol) in CH<sub>2</sub>Cl<sub>2</sub> (5 mL) were added Et<sub>3</sub>N (154 μL, 1.1), DMAP (3 mg, 0.028 mmol) and TsCl (58 mg, 0.304 mmol). The mixture was stirred at 25°C for 3h. The solvent was evaporated and the residue was purified by flash column chromatography (CH<sub>2</sub>Cl<sub>2</sub>/EtOAc 20:1) to yield a colourless solid (107 mg, 93 %). m.p: 141.3-143°C. <sup>1</sup>H NMR (500 MHz, CDCl<sub>3</sub>): δ = 7.81-7.76 (m, 2H), 7.44-7.27 (m, 6H), 7.26-7.21 (m, 1H), 4.64 (d, *J* = 7.90 Hz, 1H), 4.53 (m, 1H), 4.22 (dd, *J* = 10.10, 4.74 Hz 1H), 4.10 (dd, *J* = 10.10, 4.84 Hz, 1H), 3.28 (brs, 1H), 2.79-2.72 (m, 1H), 2.43 (s, 3H), 2.24 (dd, *J* = 13.6, 6.6 Hz, 1H), 1.97 (m, *J* = 13.6 Hz, 1H), 1.55 (s, 3H), 1.31 (s, 3H) ppm. <sup>13</sup>C NMR (126 MHz, CDCl<sub>3</sub>): δ = 145.19, 144.32, 130.16, 128.61, 128.20, 125.29, 115.39, 86.43, 81.60, 78.08, 70.71, 43.46, 42.08, 26.51, 24.92, 21.85 ppm.

**(3aR\*,4R\*,6R\*,6aR\*)-2,2-dimethyl-4-phenyl-6-(tosyloxymethyl)tetrahydro-3aH-cyclopenta[d][1,3]dioxol-4-yl 4-bromobenzoate (24)**



To a cooled (0°C, ice bath) stirred suspension of NaH (60%, 5 mg, 0.135 mmol) in anhydrous THF (2 mL) was added a solution of compound **23** (47 mg, 0.113 mmol) in anhydrous THF (1 mL) dropwise.

The resulting mixture was vigorously stirred at 25°C for 2 h. Then, 4-bromobenzoyl chloride (27 mg, 0.124 mmol) was added in one portion and the mixture was stirred at 25°C for additional 24 h. The reaction was quenched with saturated aqueous NH<sub>4</sub>Cl (0.2 mL) and the solvent was evaporated. The residue was dissolved in CH<sub>2</sub>Cl<sub>2</sub> (1 mL) and purified using preparative TLC (silica gel, CH<sub>2</sub>Cl<sub>2</sub>) to give benzoate **24** as a white solid (35 mg, 51 % yield). <sup>1</sup>H NMR (500 MHz, CDCl<sub>3</sub>): δ = 7.85 (m, 2H), 7.73 (m, 2H), 7.52 (m, 2H), 7.40 (m, 2H), 7.34-7.23 (m, 5H), 4.82 (d, *J* = 7.00 Hz, 1H), 4.51 (dd, *J* = 7.1, 4.4 Hz, 1H), 3.96 (m, 2H), 3.04 (dd, *J* = 13.9, 7.1 Hz 1H), 2.56 (m, 1H), 2.43 (s, 3H), 2.19 (dd, *J* = 13.9, 10.2 Hz, 1H), 1.56 (s, 3H), 1.33 (s, 3H) ppm. <sup>13</sup>C NMR (126 MHz, CDCl<sub>3</sub>): δ = 164.63, 145.24, 131.85, 131.42, 130.29, 130.16, 128.73, 128.36, 128.19, 125.96, 114.30, 86.83, 85.57, 81.11, 70.34, 42.33, 37.35, 26.67, 25.09, 21.85 ppm. Crystal data for **24**: CCDC ref. No. 937690. Crystallized from toluene, C<sub>29</sub>H<sub>29</sub>BrO<sub>7</sub>S, *M*<sub>rel</sub> = 601.51, *T* = 120 K, space group P-1, *a* = 8.0723(4) Å, *b* = 12.4224(5) Å, *c* = 13.9348(6) Å, *α* = 92.267(4), *β* = 96.617(4), *γ* = 106.814(4), *V* = 1324.79 Å<sup>3</sup>, *R* = 0.026.

#### WST-1 assay of compounds **2a**, **2b**, and **2c**

The following B-lymphoid cell lines were used: SU-DHL-4 (diffuse large B-cell lymphoma, del/mut TP53), JEKO-1 (mantle cell lymphoma, del/mut TP53), and JVM-3 (mantle cell lymphoma, wt-TP53). Cells were seeded in 96-well plates in duplicates (1 × 10<sup>5</sup> cells per well, volume 200 μl) and subjected to 72 h exposure of the studied compounds at 10 μM and 100 μM concentrations (the concentrations used were obtained by dilution of 50 mM stock solutions of the compounds in DMSO). DMSO was added to mock control. The cell viability was assessed by the metabolic WST-1 assay (Roche) using spectrophotometer 1420 Multilabel Counter Victor (PerkinElmer).

#### Glycosylase activity assays

Samples	Positive control (Enzyme + DMSO)	Enzyme + compound	Negative Control
Protein extract	1 μl	1 μl	-
milliQ-filtered H <sub>2</sub> O	3 μl	3 μl	4 μl
Compound	-	1 μl	-
DMSO	1 μl	-	1 μl

DMSO was added to the compounds to give 10 mM stock solutions. 1 μl of the stock solution was added to each sample for initial testing (final concentration 1 mM). Compounds that decreased enzyme activity were further diluted with DMSO to 5 mM, 2.5 mM and 1 mM (which gave compound concentrations of 0.5 mM, 0.25 mM and 0.1 mM, respectively, after adding 1 μl to the samples).

Protein extracts were diluted to the desired concentration using protein dilution buffer.

A master mix containing reaction buffer and substrate (labelled oligonucleotide) was made for the appropriate number of reactions.

**Neil1 (bifunctional glycosylase)**

Enzyme concentration: 7-10 nM

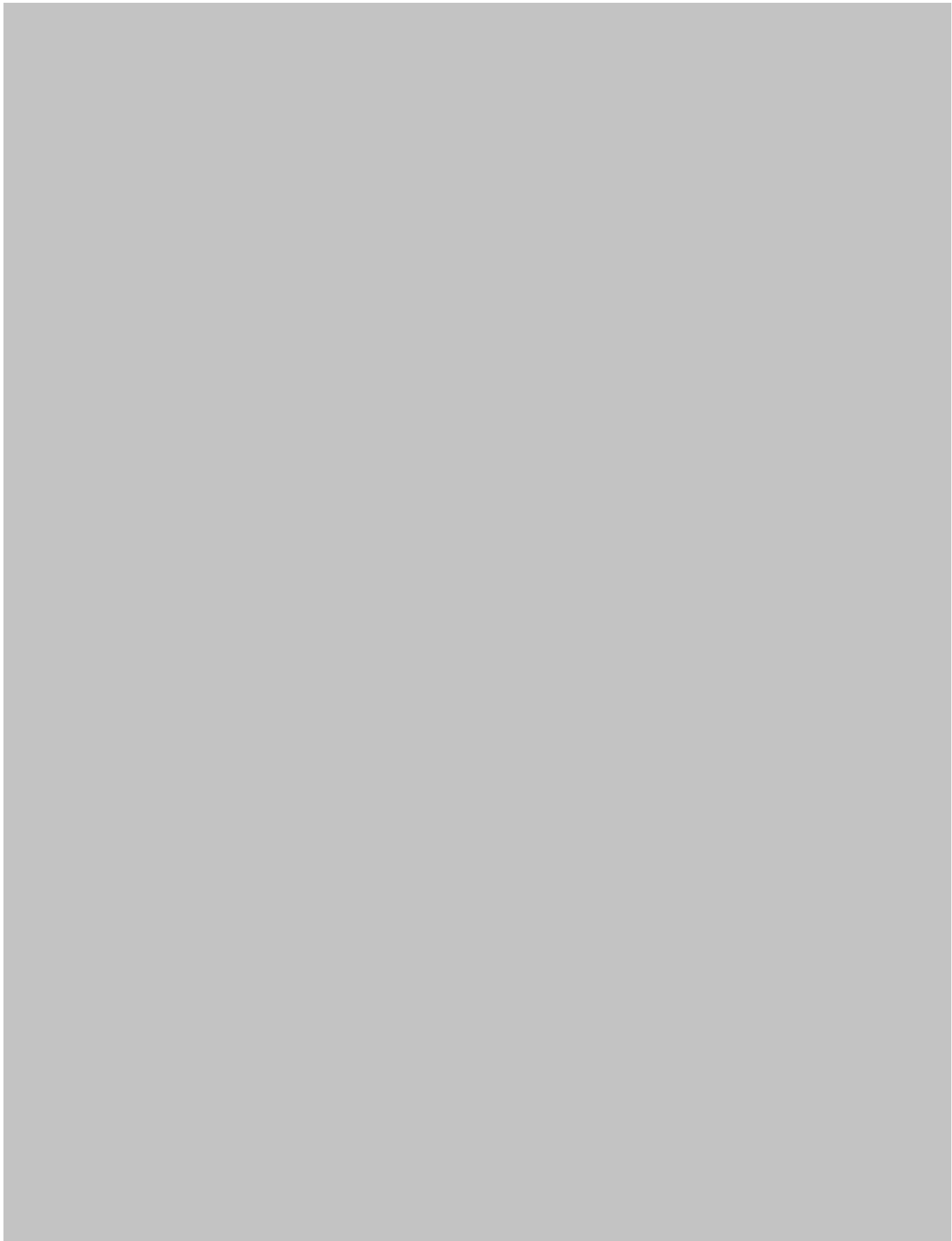
Substrate: 5ohU/G

Samples were prepared according to the table above.

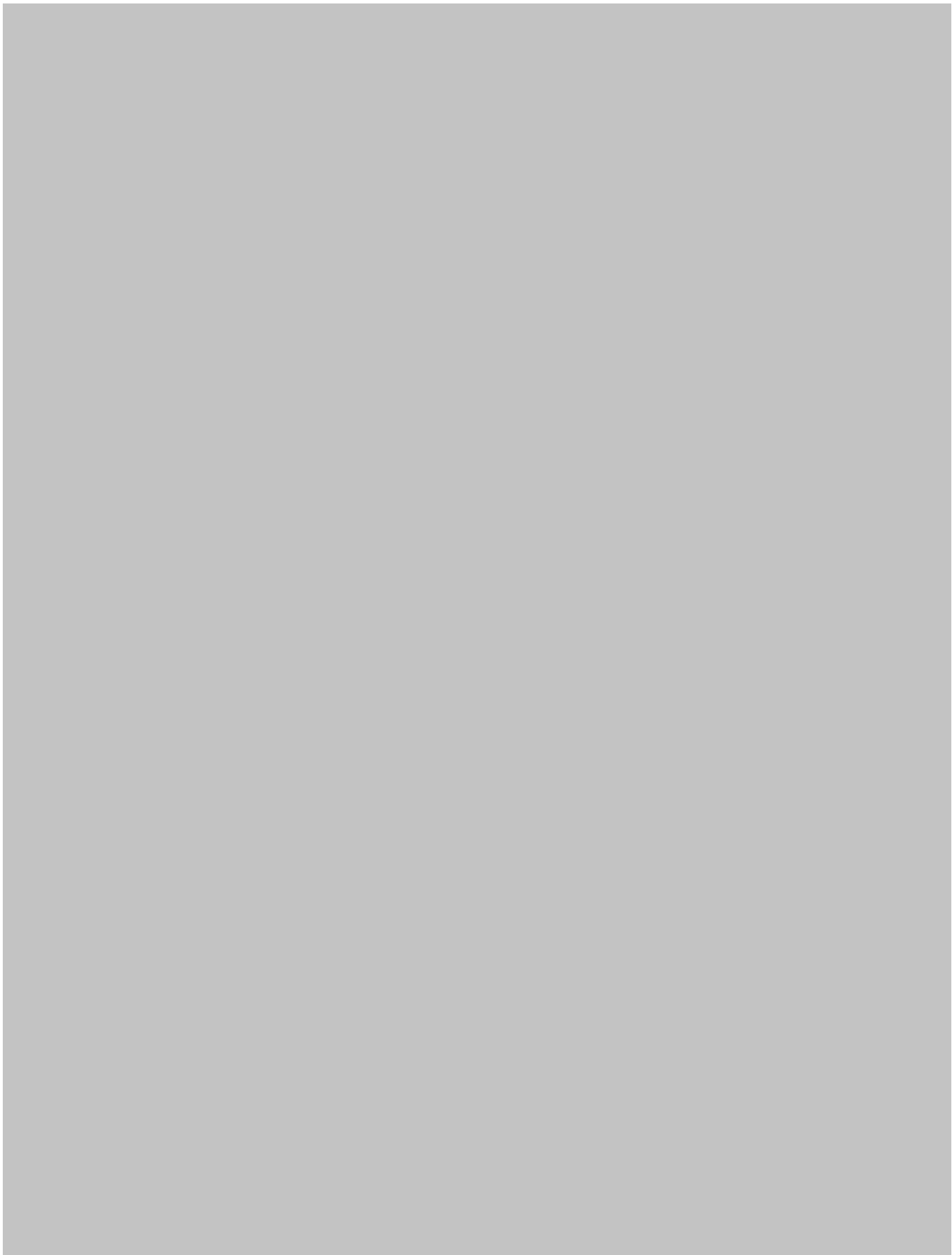
5 µl mastermix was added to each sample. Incubated at 37°C for 10 minutes.

10 µl glycosylase stop solution was added to each sample followed by incubation at 95°C for 5 minutes. Samples were analyzed on 20% denaturing urea gels. Gels were run at 200 volt for 50 minutes. The gels were transferred to 3M paper and dried at 80°C for 45 minutes. The dry gels were placed in a storage phosphor screen over night, and subsequently scanned on the Typhoon 9410 Variable Mode Image. ImageQuant TL Version 2003.02 (Amersham Biosciences) was used to analyze the results.





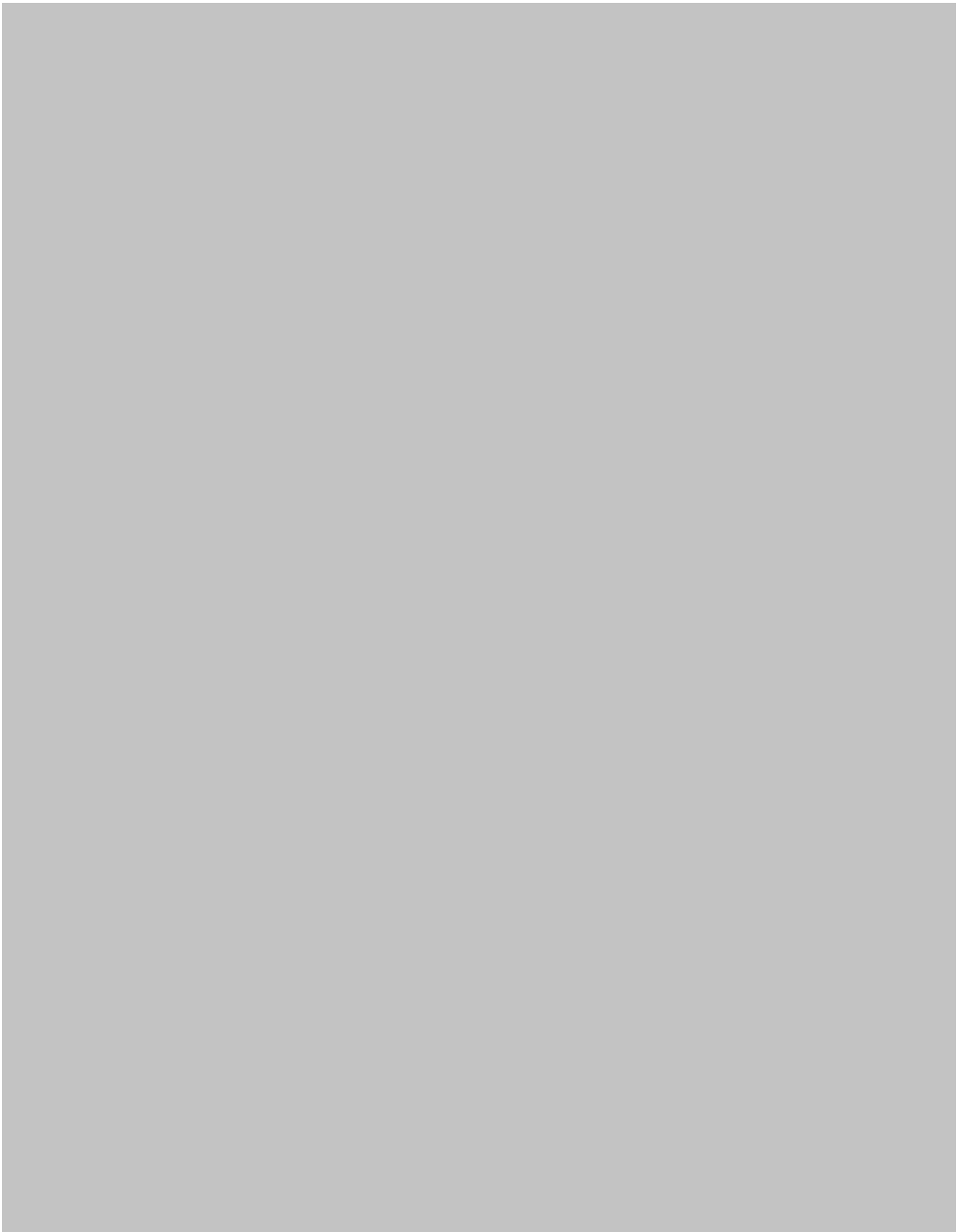


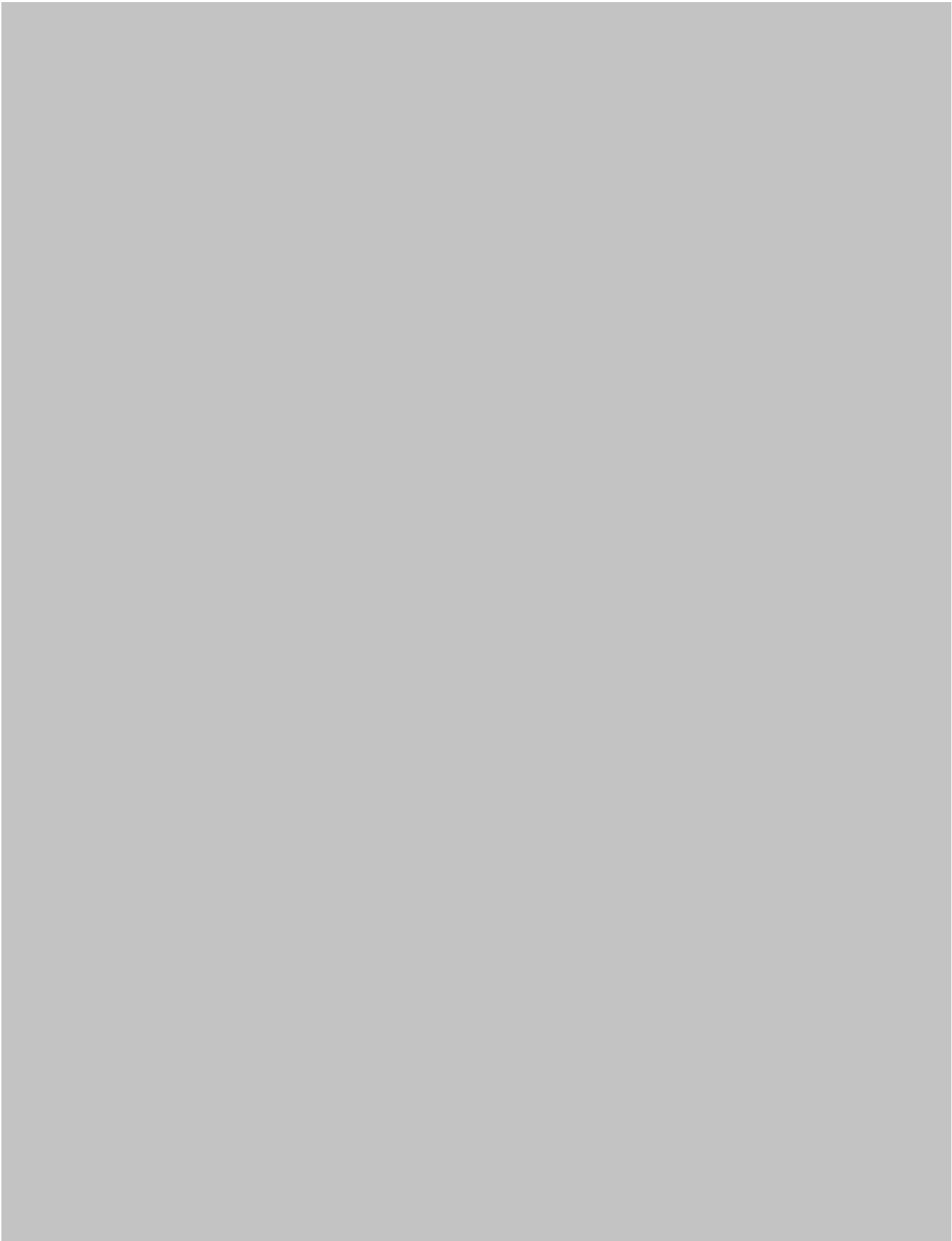




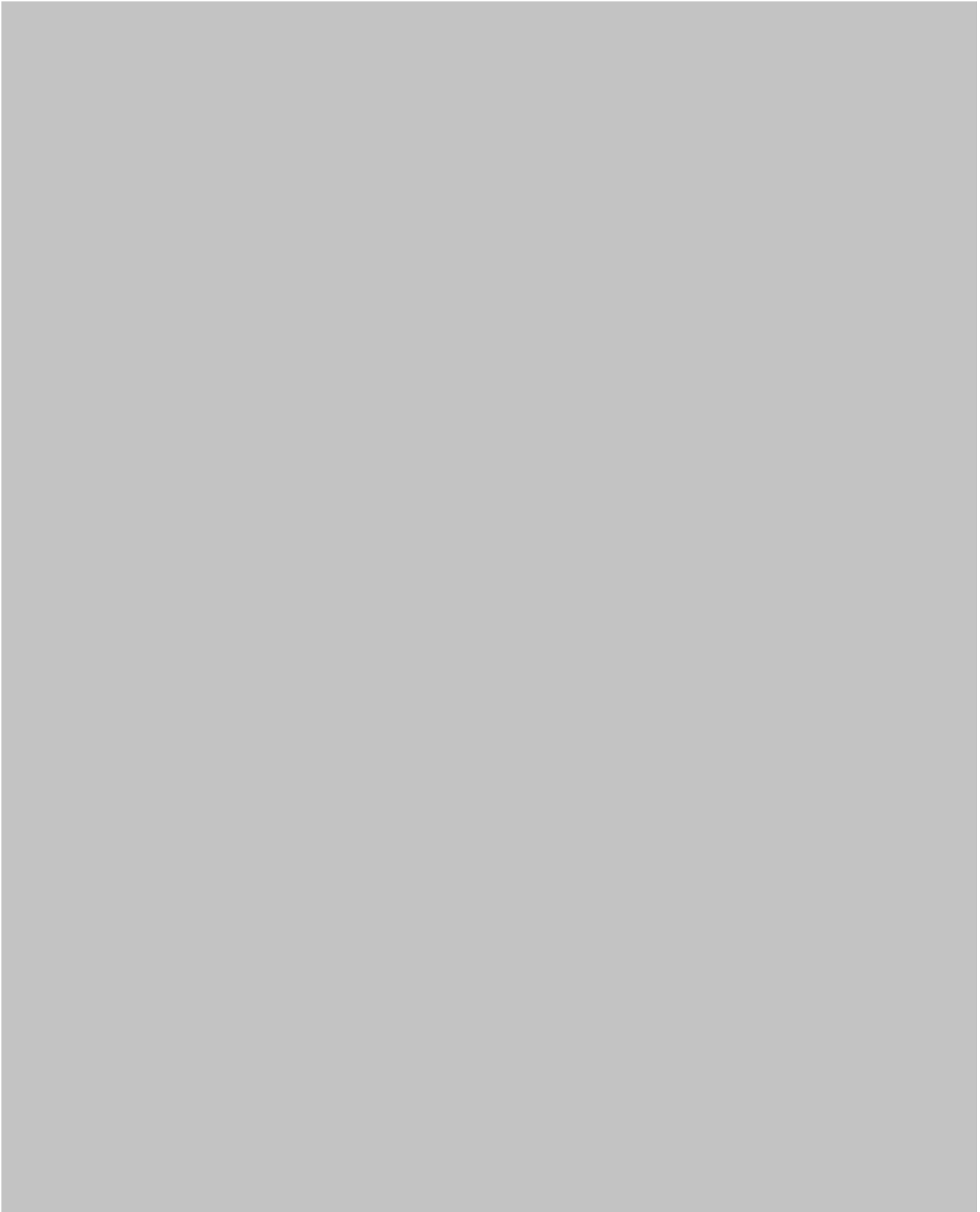








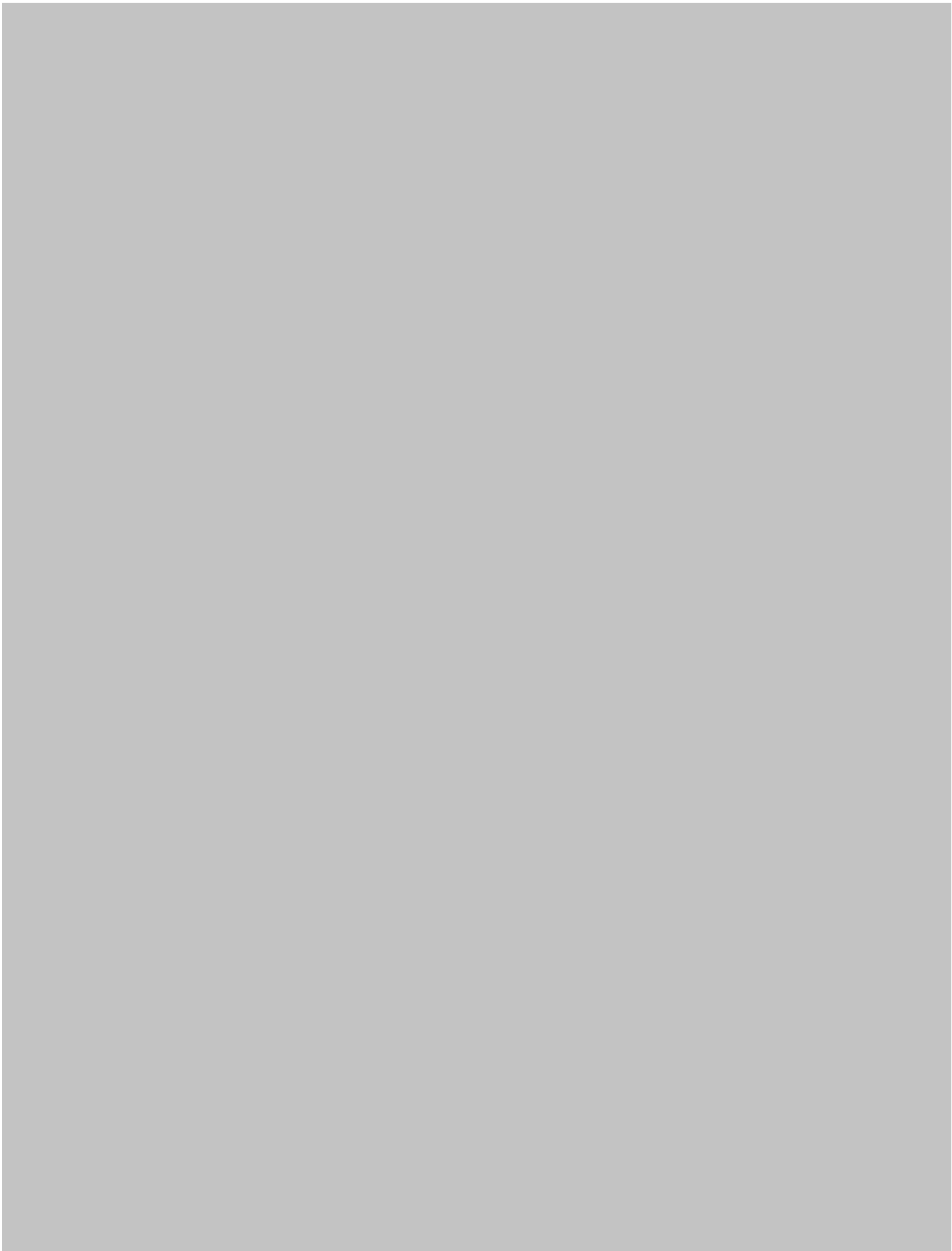














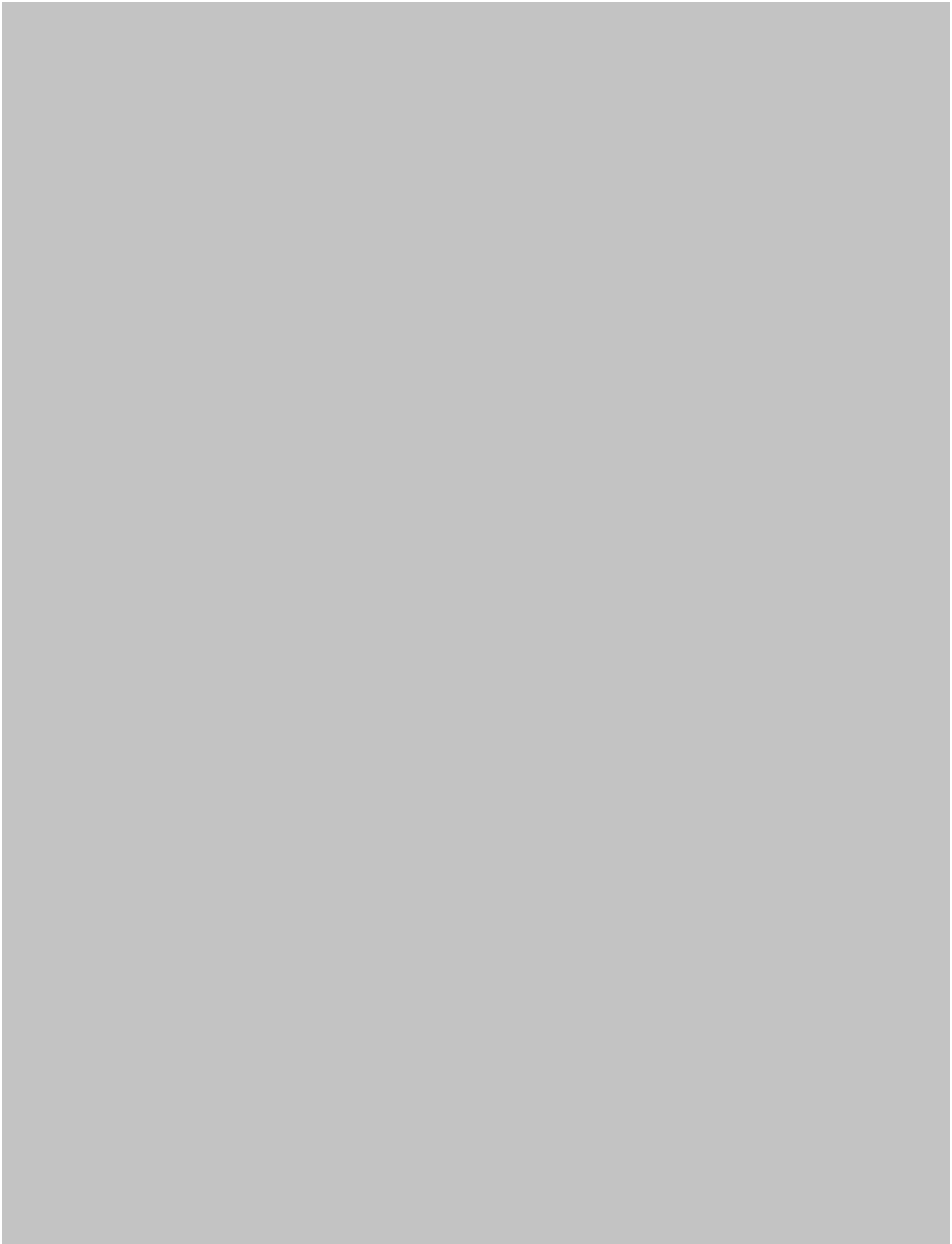






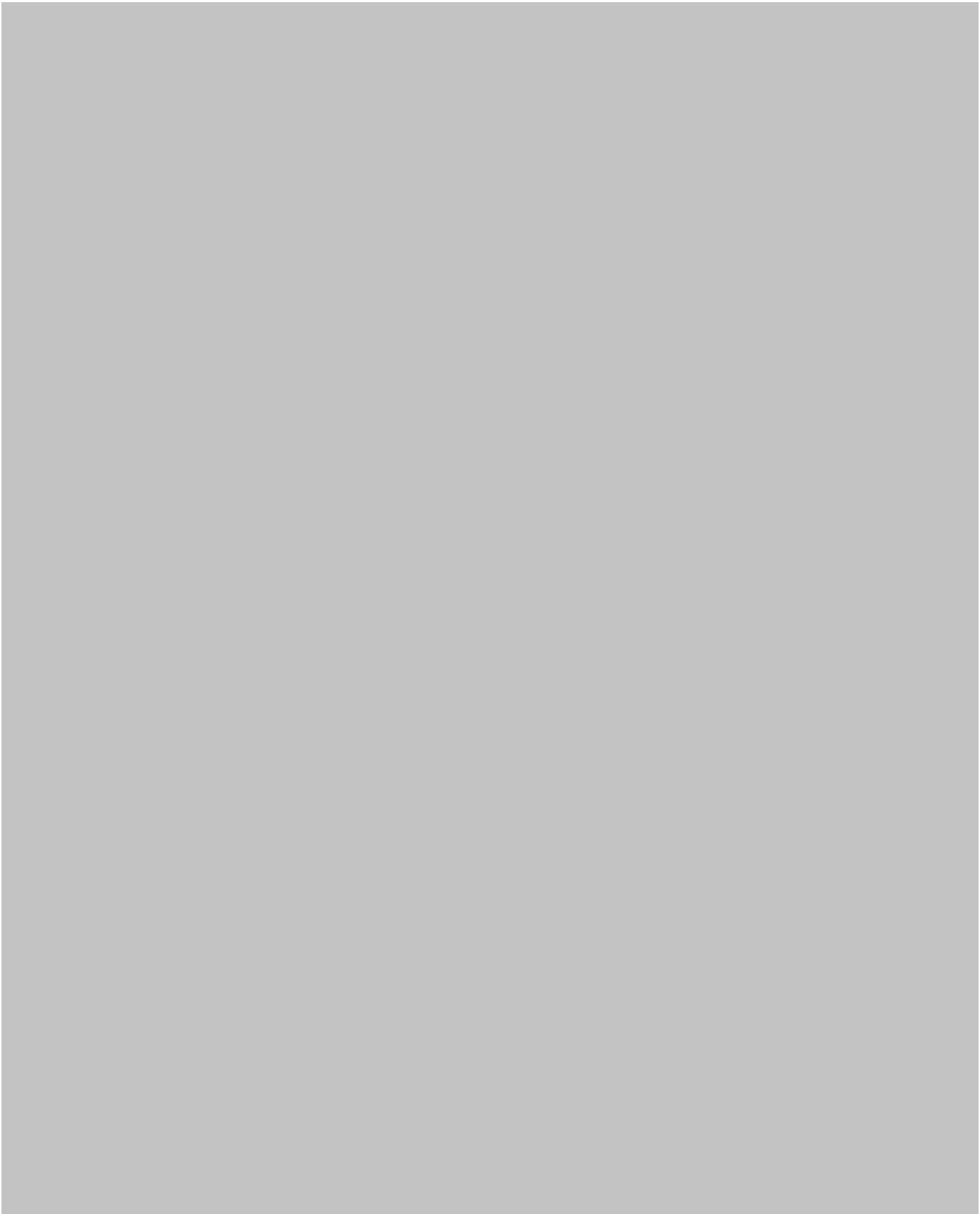
















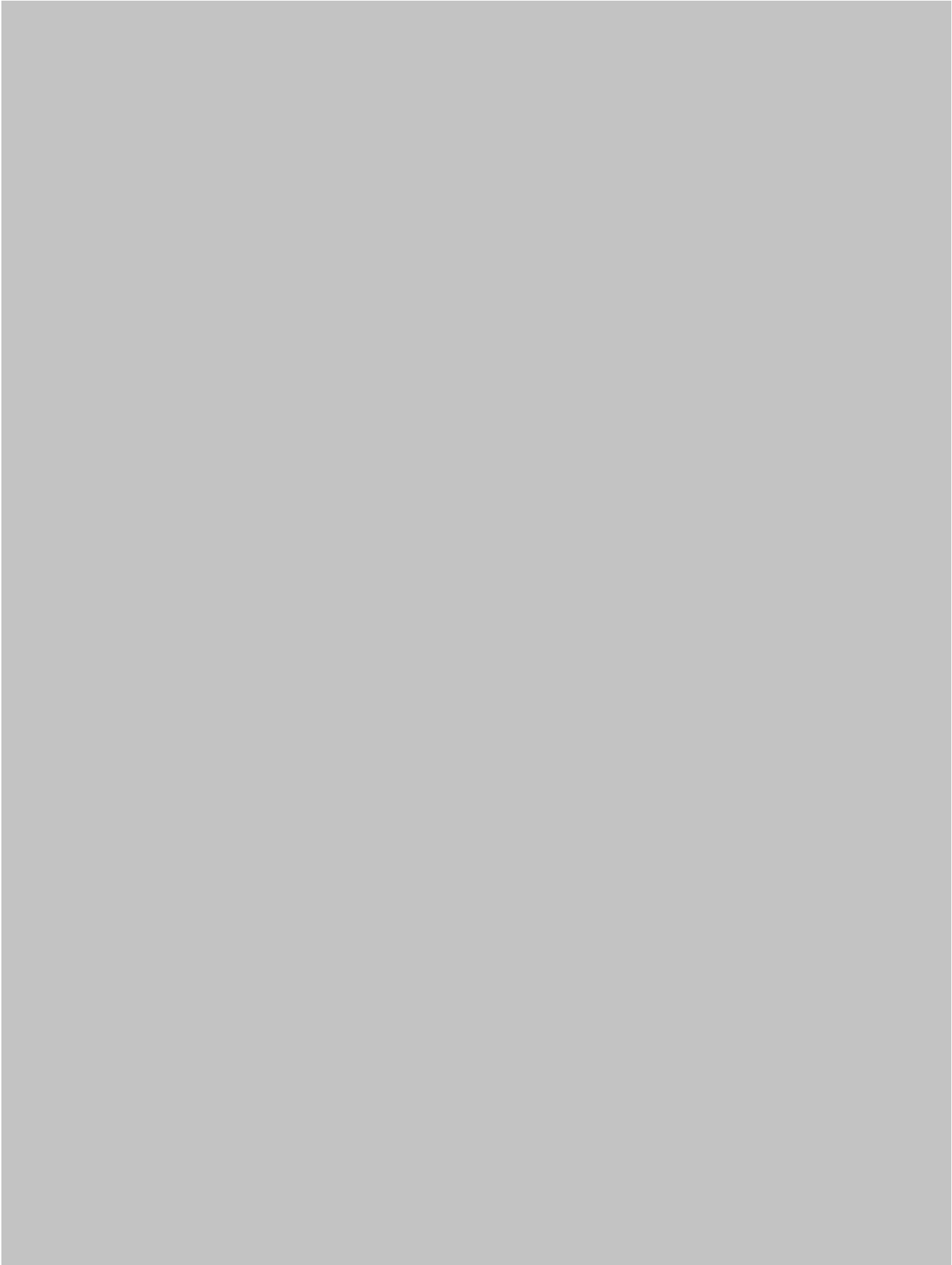






















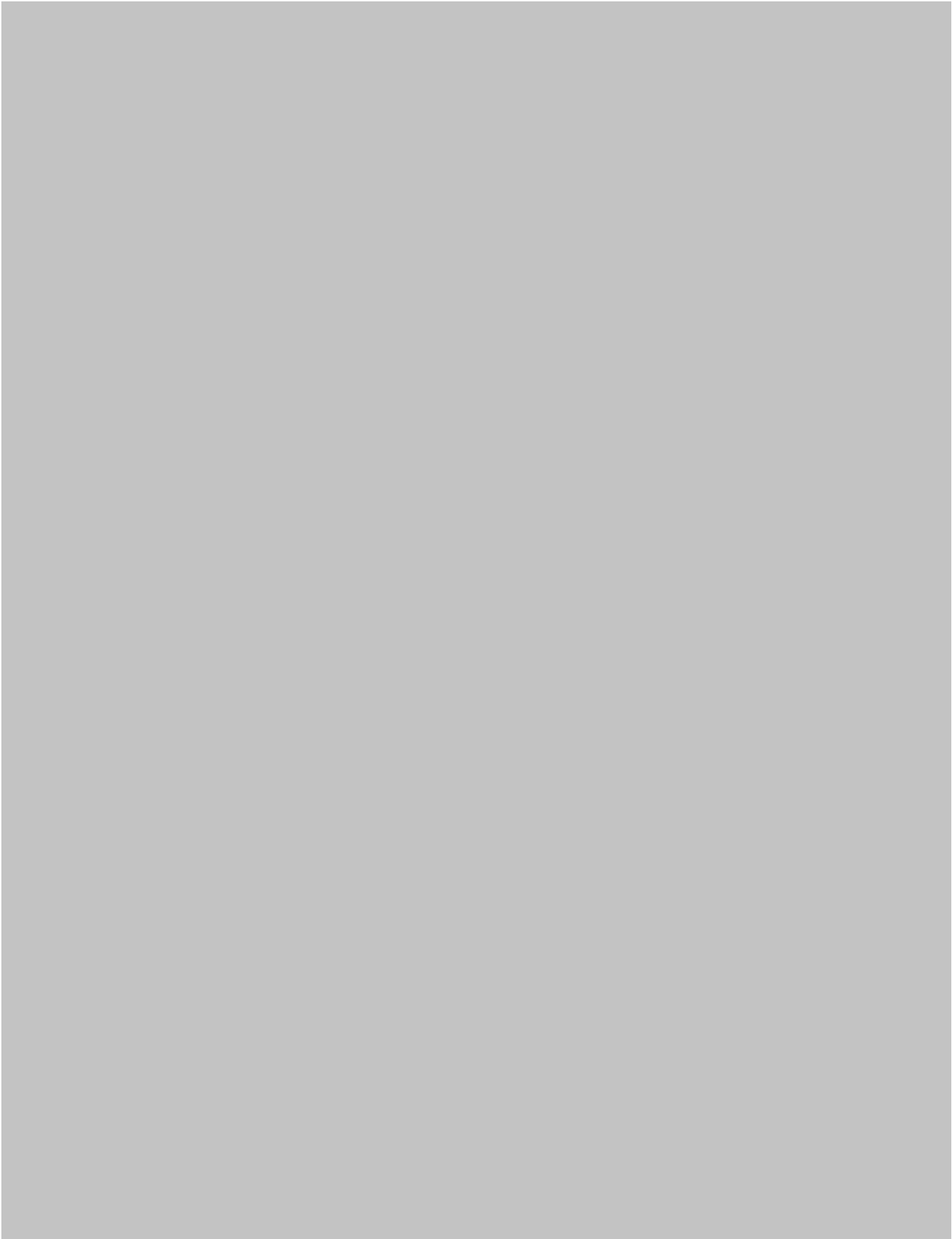


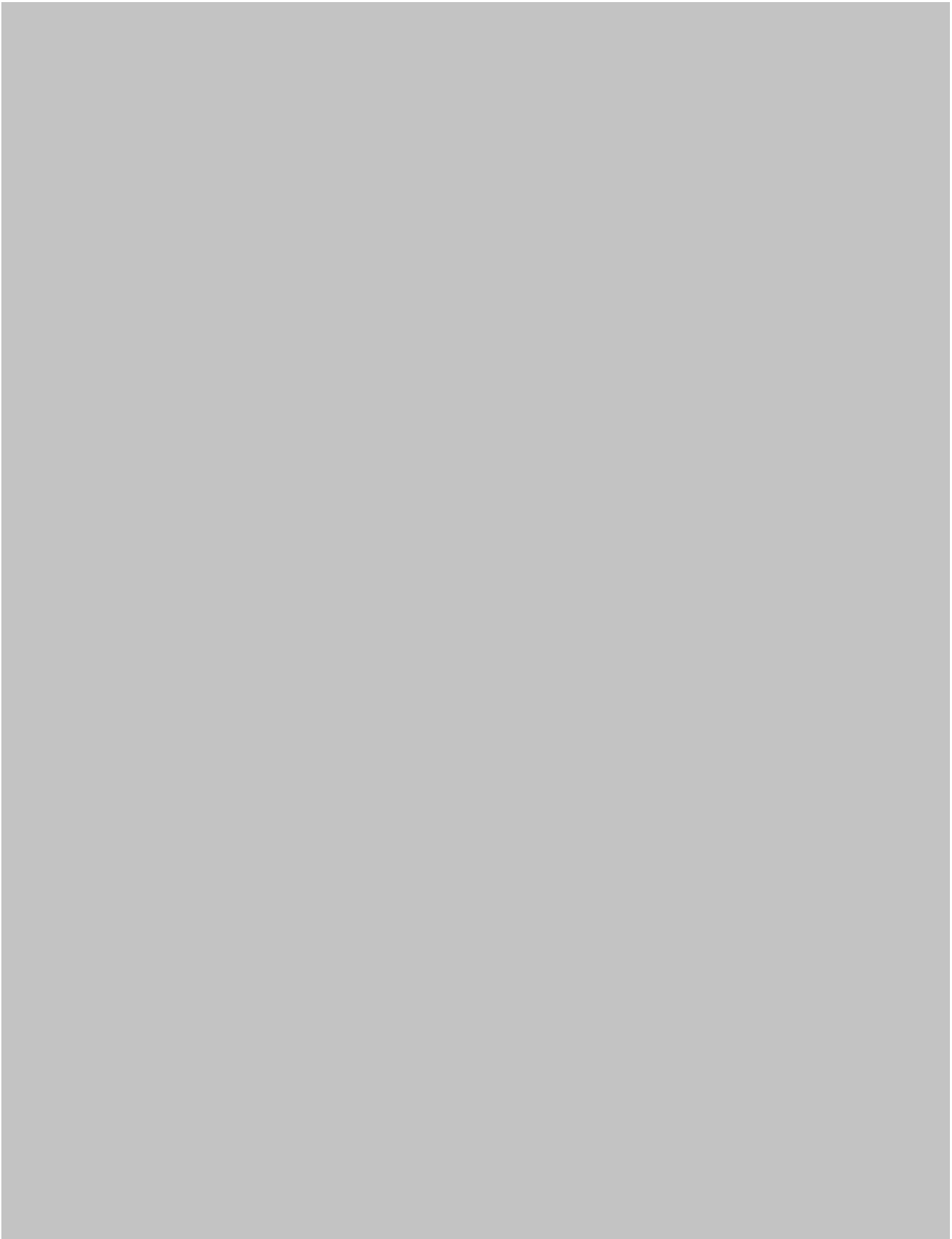


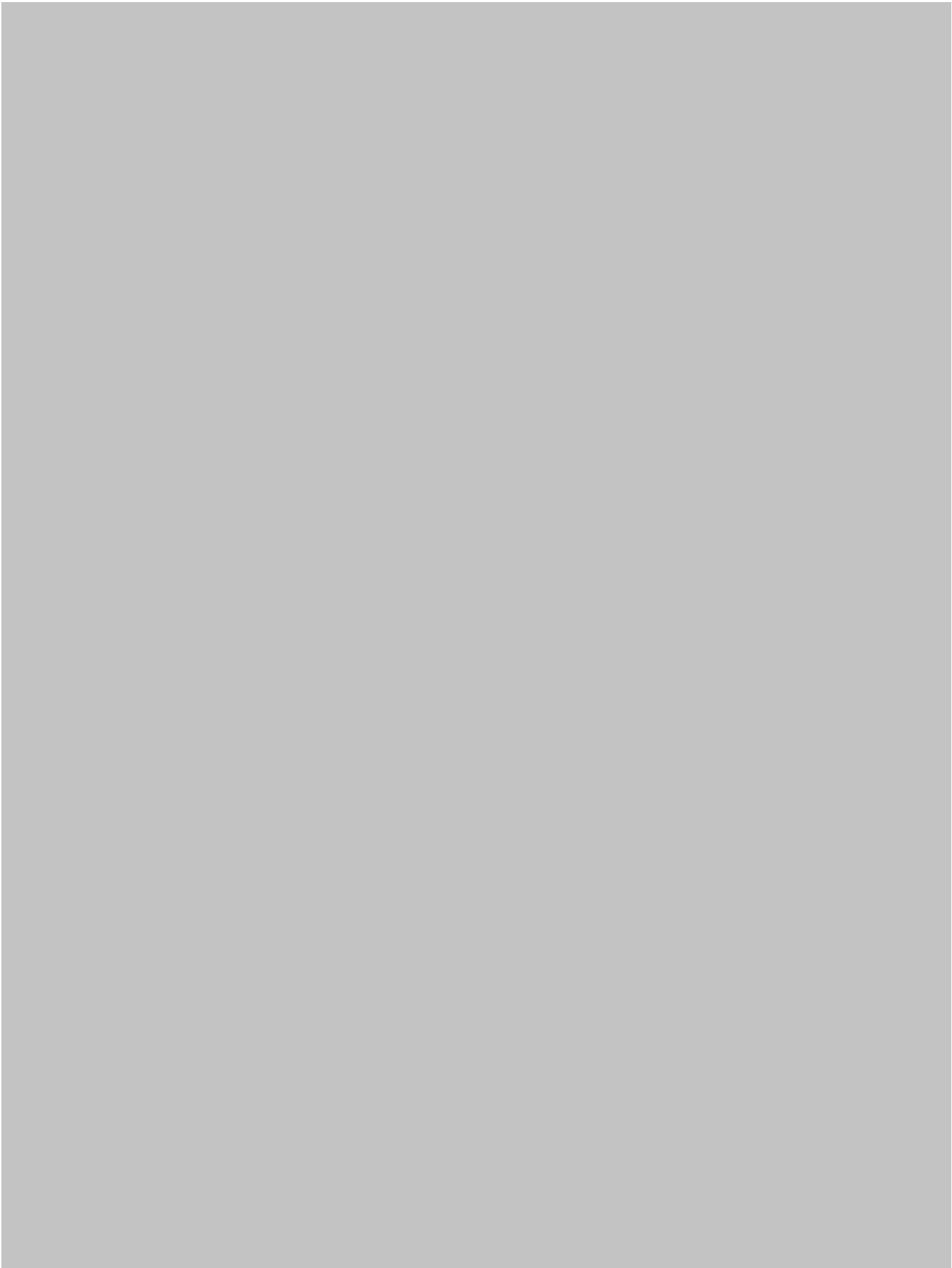








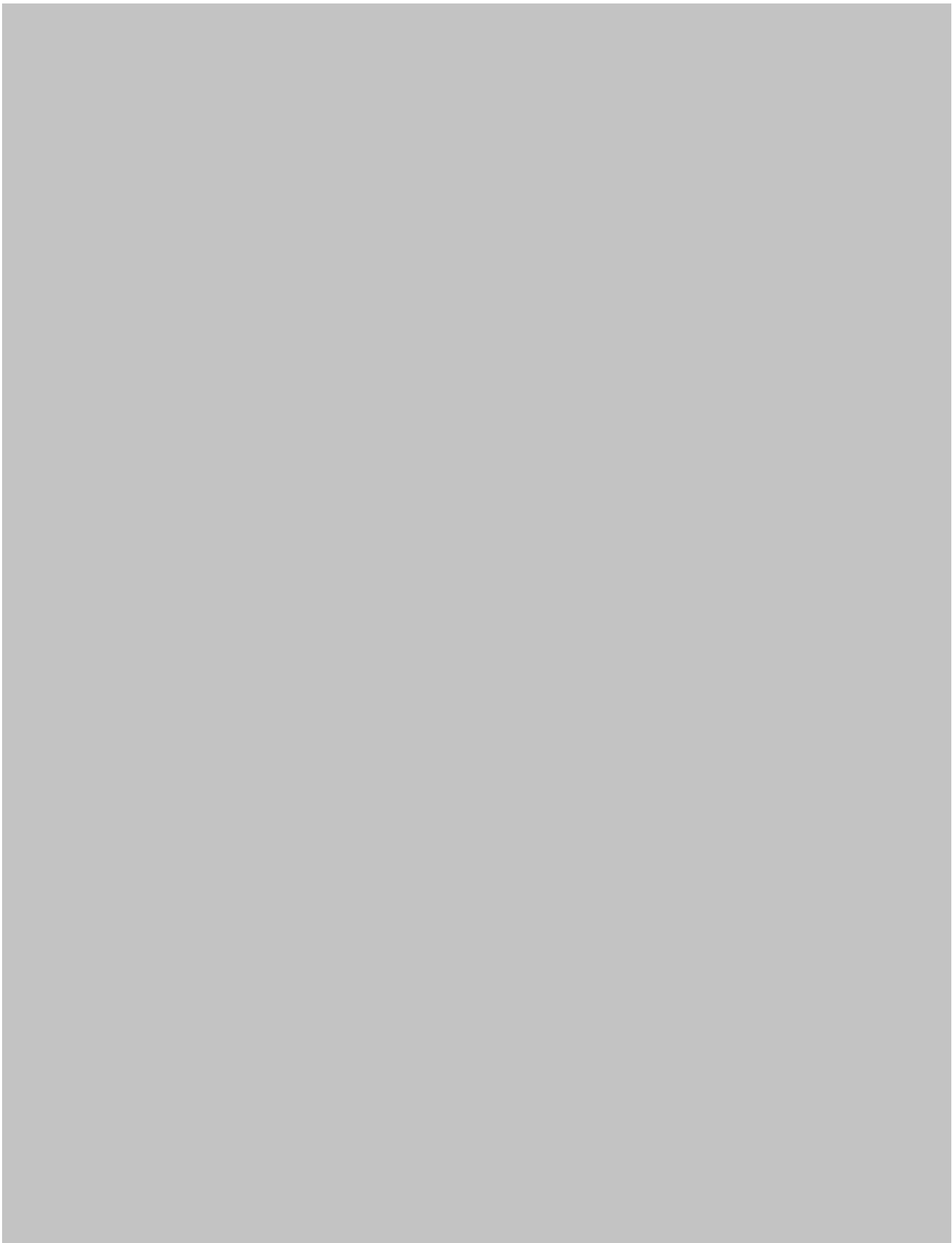












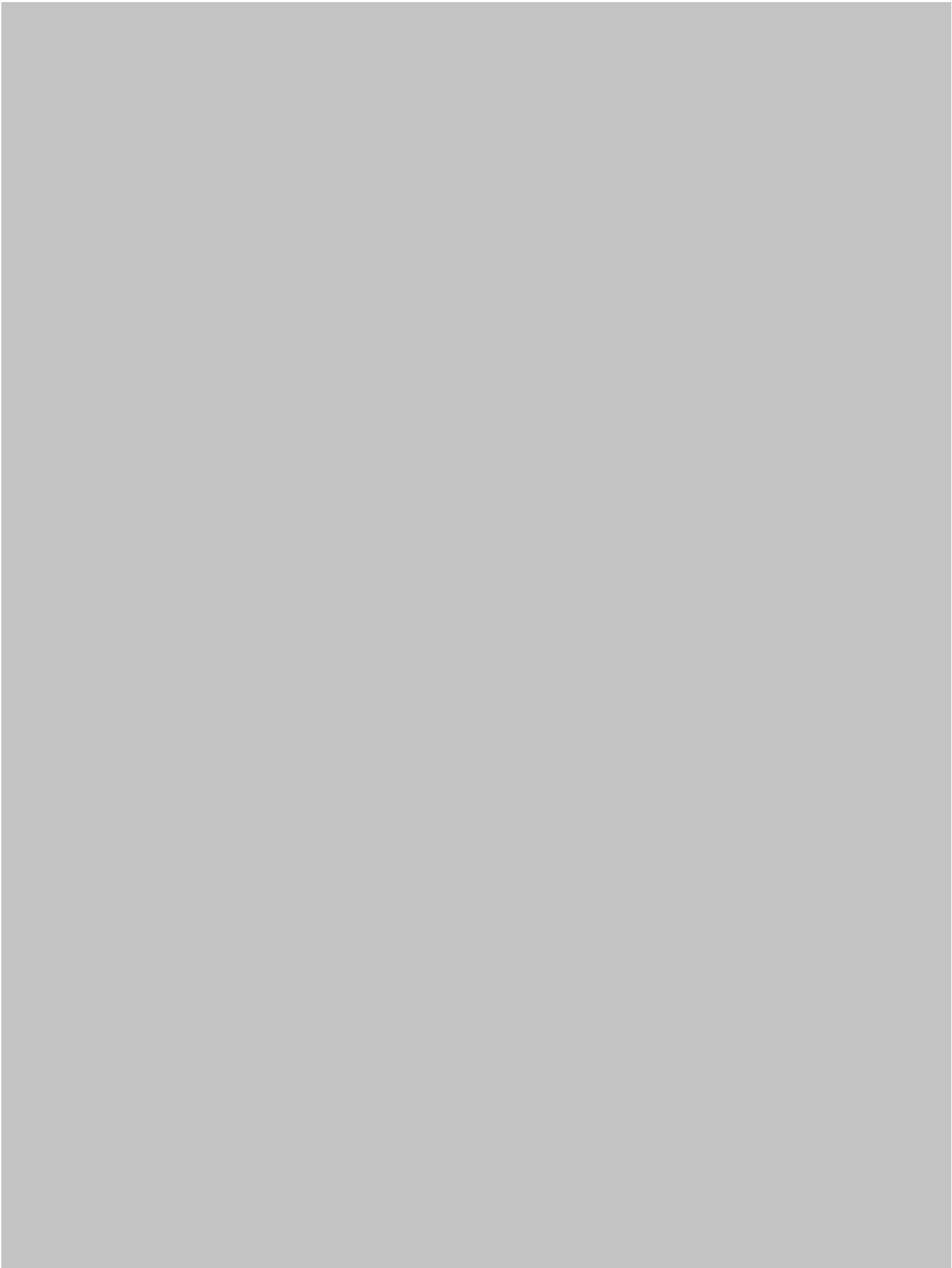








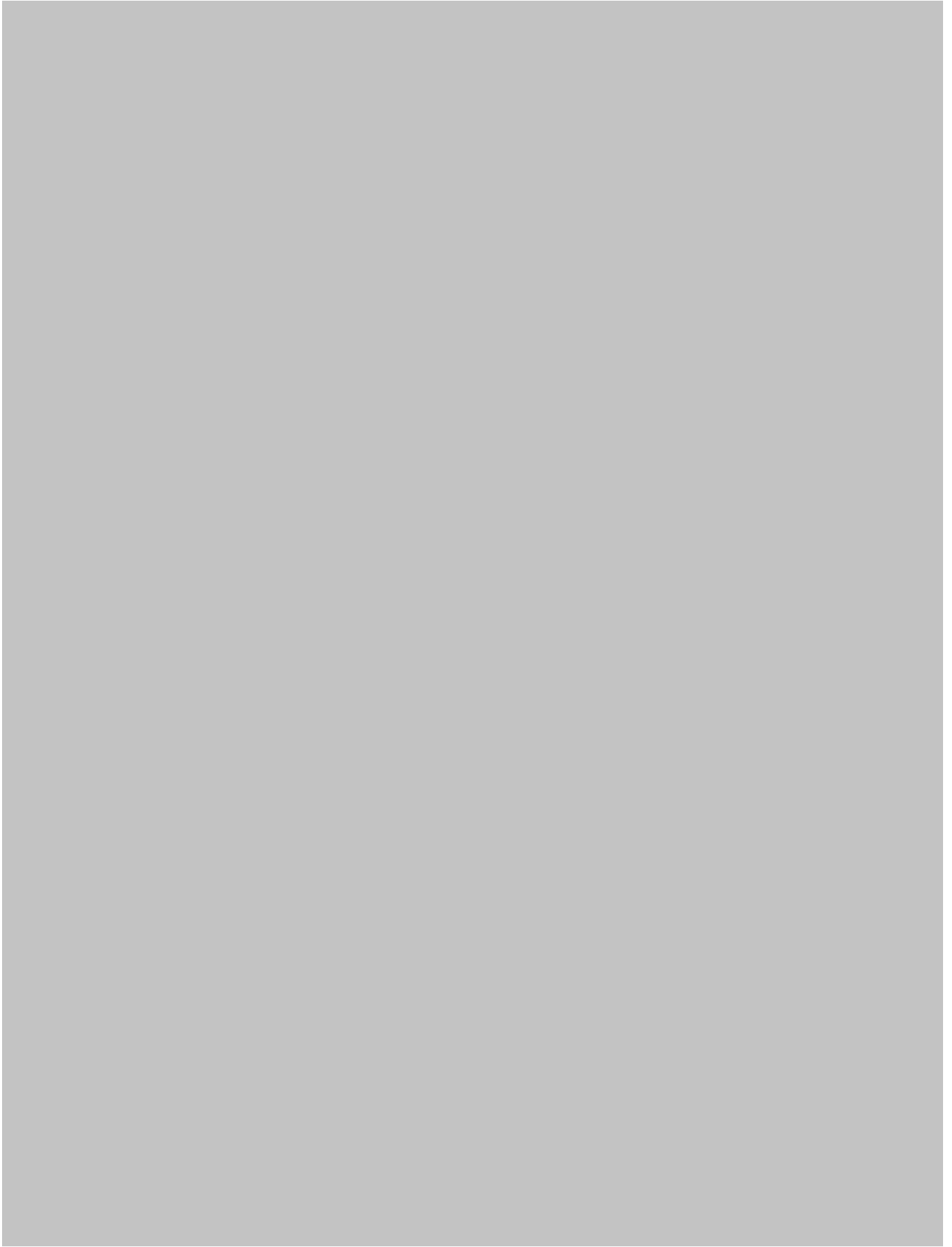




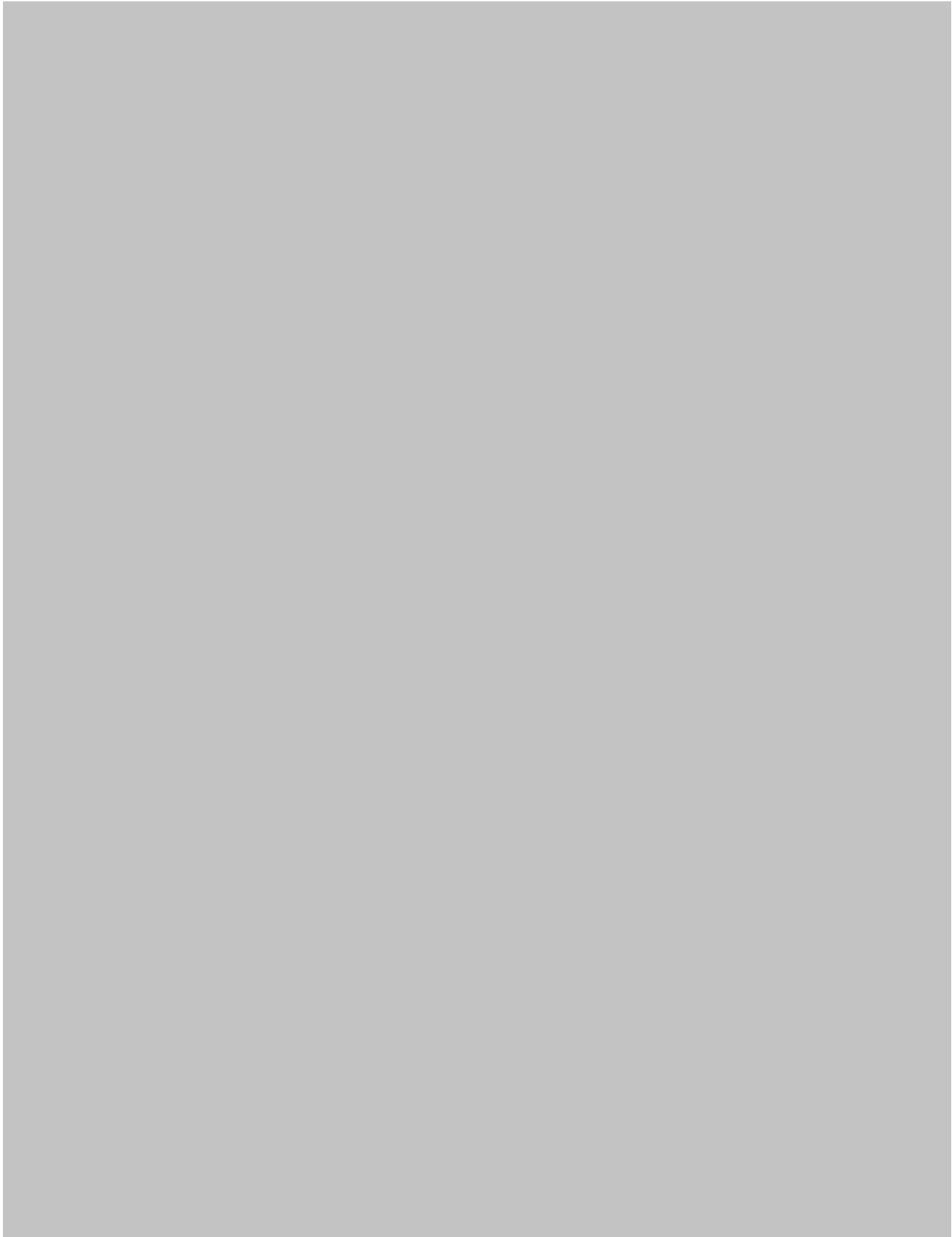




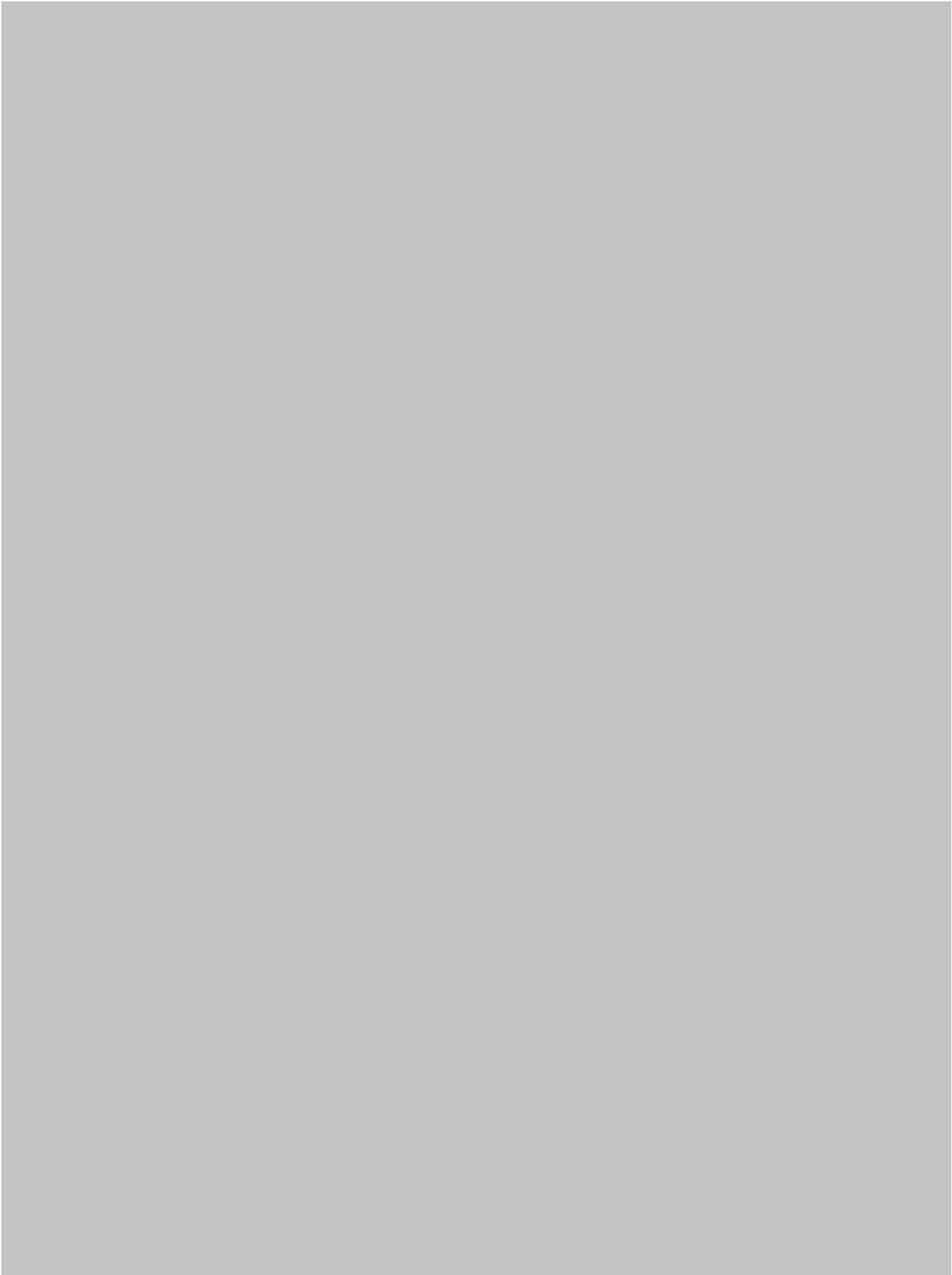






















## Part 5

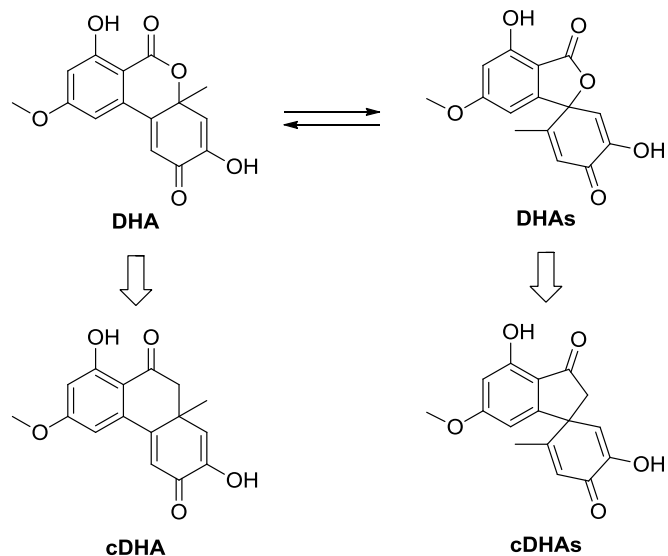
### Synthesis of carbocyclic analogs of dehydroaltenusin: identification of a stable inhibitor of calf DNA polymerase $\alpha$ \*

\*published as:

Kováčová, S.; Adla, S. K.; Maier, L.; Babiak, M.; Mizushina, Y.; Paruch, K.\* Synthesis of Carbocyclic Analogs of Dehydroaltenusin: Identification of a Stable Inhibitor of Calf DNA Polymerase  $\alpha$ . *Tetrahedron* **2015**, *71*, 7575.

#### 1. Introduction

Proteins and pathways involved in DNA damage/repair continue to be intensely studied, especially in the context of development of new cancer therapeutic agents.<sup>1</sup> The inhibition of DNA polymerases (pols) seems to be a proper component of synthetic lethal combination therapy.<sup>2</sup> Specifically, deletion of pol  $\alpha$  was found to be synthetic lethal with elimination or inhibition of CHK1 kinase, but elimination of additional pols (delta and epsilon) resulted in significantly weaker synthetic lethal response.<sup>3</sup> Selective inhibitors of pol  $\alpha$  could therefore be of considerable therapeutic potential. Of the compounds that are known to inhibit this enzyme,<sup>1</sup> only two seem to be sufficiently selective: nucleoside analog BuPdGTP and its derivatives,<sup>4</sup> and dehydroaltenusin.<sup>5</sup> Both substances possess suboptimal pharmacological properties: BuPdGTP exhibits only weak activity in the cell,<sup>6</sup> while chemical stability of dehydroaltenusin is limited, as it undergoes a rearrangement in aqueous solutions to give a mixture of the spirocyclic and non-spirocyclic forms (structures **DHAs** and **DHA** in Scheme 1; absolute configurations are not known).<sup>7</sup> It is not clear which of these forms is active and it has been suggested that the rearrangement o-quinone intermediate might be also responsible for the inhibitory activity.<sup>8</sup> In order to help elucidate this issue, we decided to carry out bioisosteric replacement of the lactone ring oxygen by methylene group and prepare the carbocyclic analogs of the spirocyclic and non-spirocyclic forms of dehydroaltenusin - **cdHAs** and **cdHA**, respectively (Scheme 1). These compounds were envisioned to be significantly more stable and resistant to the rearrangement.

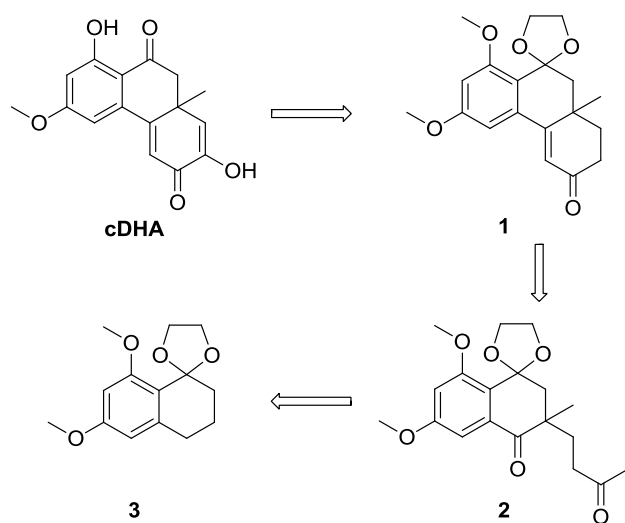


**Scheme 1.** Spirocyclic and non-spirocyclic isomers of dehydroaltenusin and their carbocyclic analogs.

Of note, the central scaffolds of both **cDHA** and **cDHAs** are only sporadically documented in the literature.

## 2. Results and Discussion

The retrosynthetic analysis of **cDHA**, depicted in Scheme 2, relies on benzylic oxidation and alkylation of protected tetralone **3** to provide intermediate **2** possessing the required quaternary center, aldol cyclization forming the tricyclic scaffold **1**, and final oxidation and deprotection to yield the target compound (**cDHA**).



**Scheme 2.** Retrosynthetic analysis of **cDHA**. Construction of the quaternary center and the tricyclic scaffold.

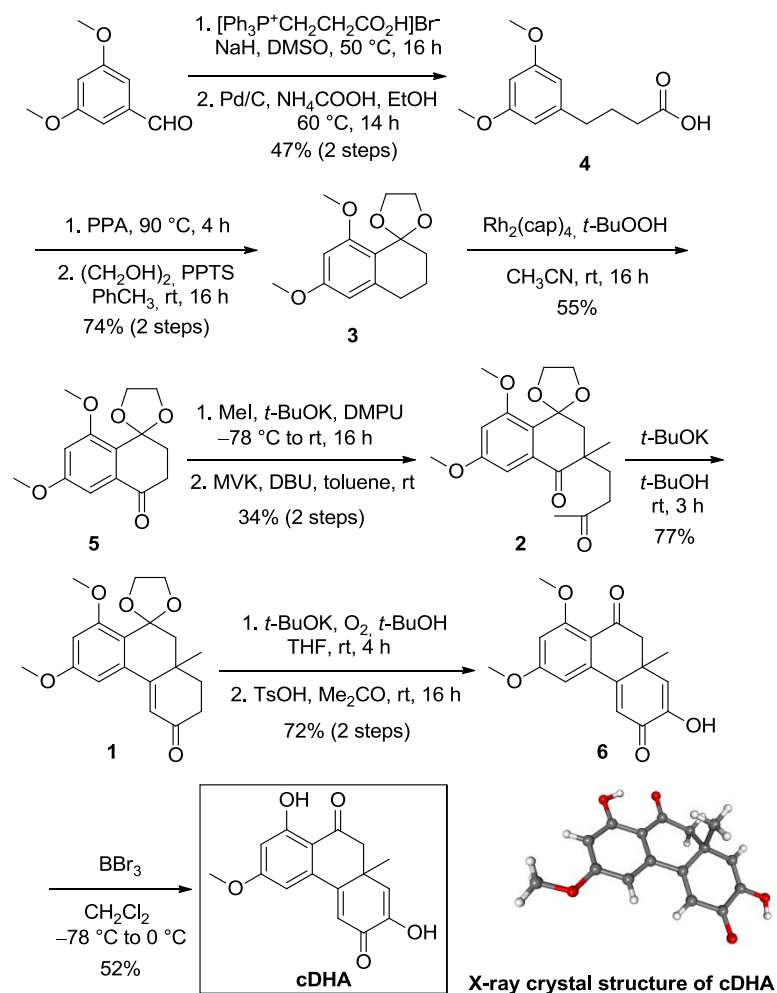
Starting from 3,5-dimethoxybenzaldehyde, Wittig reaction followed by hydrogenation afforded acid **4**, whose intramolecular Friedel-Crafts cyclization gave the required tetralone (not shown).<sup>9</sup> Attempted protections of the tetralone using ethanediol, 2-methoxy-1,3-dioxolane, ethanediol plus CH(OCH<sub>3</sub>)<sub>3</sub>, or 2-methoxy-1,3-dioxolane in the presence of TsOH did not provide the desired product **3** in acceptable yields, likely due to the sensitivity of the substance to strong acids. However, reaction with ethanediol in the presence of PPTS in refluxing benzene afforded **3** in satisfactory yield (Scheme 3).

Benzylic oxidation of **3** using Cr(CO)<sub>6</sub> or PDC with *tert*-butylhydroperoxide<sup>10</sup> afforded the desired ketone **5** in modest yields (10% and 35%, respectively). Best result (55%) was obtained with dirhodium caprolactamate plus *tert*-butylhydroperoxide in acetonitrile, buffered with NaHCO<sub>3</sub>.<sup>11</sup>

Methylation (*t*-BuOK, MeI) of **5** led to a mixture of mono- and di-methylated ketones, along with the unreacted starting material. Reasonable yield (55%) of the desired mono-methylated product was obtained when the alkylation was carried out in the presence of DMPU. Subsequent reaction with methyl vinyl ketone (MVK) proved difficult and out of many conditions tried, only the method by von Doering<sup>12</sup> afforded the desired diketone **2** in acceptable (61%) yield.

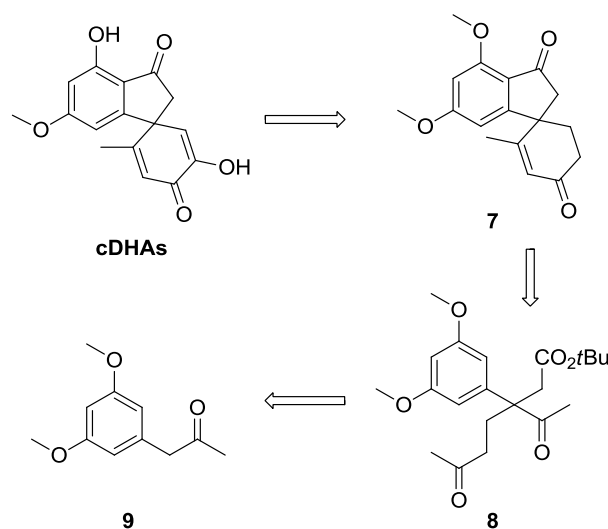
Intramolecular aldol condensation of **2** using *t*-BuOH/*t*-BuOK provided tricyclic ketone **1**. Subsequent oxidation with oxygen under basic conditions, followed by acidic cleavage of the ketal provided compound **6** in good overall yield (Scheme 3).

Finally, selective demethylation of **6** using BBr<sub>3</sub> gave the desired target compound **cDHA**, whose structure was confirmed by X-ray crystallography (Scheme 3).



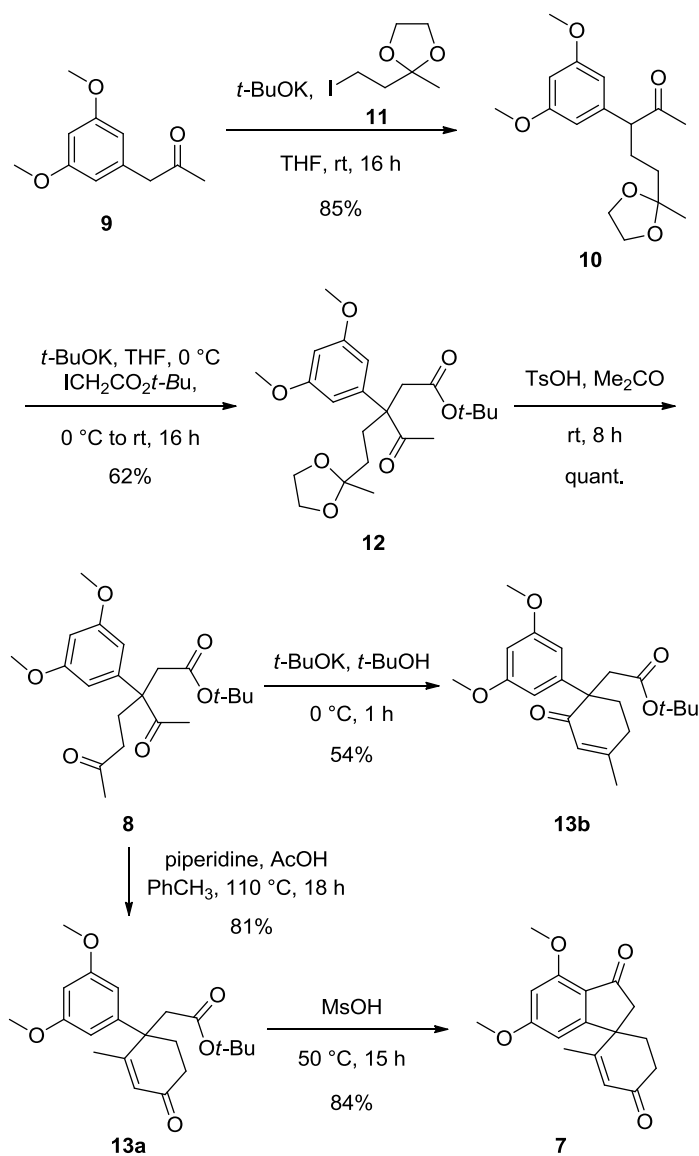
**Scheme 3.** Synthesis and structural assignment of **cDHA**.

The retrosynthetic analysis of **cDHAs** (depicted in Scheme 4) relies on double alkylation of ketone **9**, regioselective ring closure of **8** leading to the spirocyclic intermediate **7**, and final oxidation and selective demethylation to afford **cDHAs**.



**Scheme 4.** Retrosynthetic analysis of **cDHAs**. Construction of the spirocyclic core.

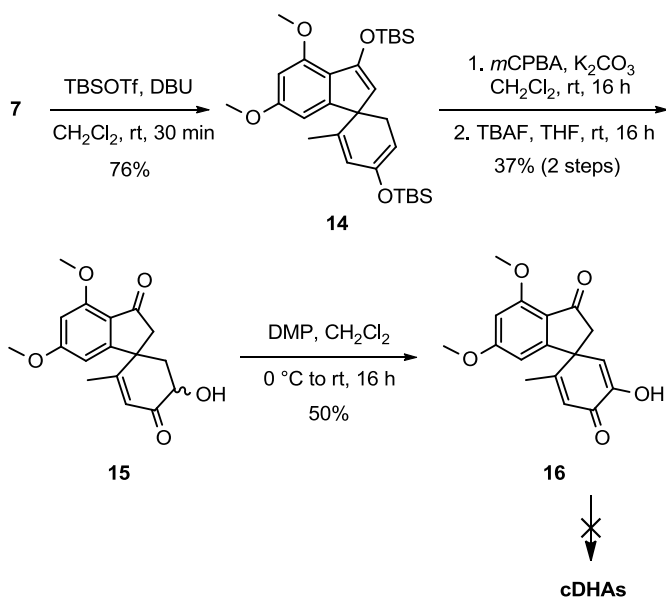
Ketone **9** was prepared in two steps by condensation of 3,5-dimethoxybenzaldehyde with nitroethane, followed by reduction with iron in AcOH.<sup>13</sup> Because our subsequent attempts to add MVK to **9** failed under a variety of conditions and in most cases lead only to the recovery of the starting material, we attempted alkylations with MVK equivalents. Best results were obtained with iodide **11**, which we prepared in 80% yield by modification of the procedure published for the analogous bromide.<sup>14</sup> This way we obtained intermediate **10** that underwent second alkylation with *t*-butyl-2-iodoacetate.<sup>15</sup> The resulting ester **12** was then deprotected to give diketone **8**, which was used for the subsequent intramolecular aldol closure (Scheme 5).



**Scheme 5.** Construction of the spirocyclic scaffold.

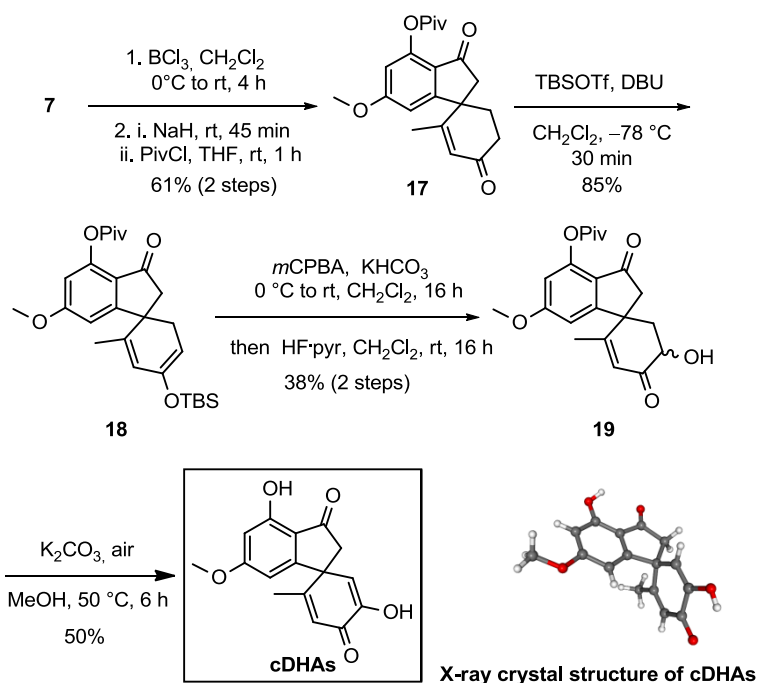
The regioselectivity of the aldol closure proved very dependent on the reaction conditions. Condensation using piperidine/AcOH in toluene,<sup>16</sup> which may proceed *via* enamine formation at the less sterically hindered carbonyl, afforded the desired enone **13a** (81%). In contrast, when carried out under basic conditions ( $t\text{-BuOK}$ /THF), the condensation yielded exclusively the isomer **13b** (Scheme 5). Construction of the spirocyclic scaffold was completed by intramolecular Friedel-Crafts reaction of **13a** in the presence of MsOH, which provided the spirocyclic enone **7** in good yield (Scheme 5). In contrast to the non-spirocyclic series, we were not able to oxidize enone **7** directly. We thus attempted to convert it into a silyl enol ether that could be used for subsequent Rubottom oxidation. In accordance with the literature,<sup>17</sup> regioselective formation of the desired silyl enol ether proved non-

trivial: numerous attempts to carry out mono-silylation of **7** yielded only mixtures of the desired product, often along with its exocyclic isomer, bis-silyl enol ether **14** and unreacted **7**. However, with excess of TBSOTf the bis-silylation of **7** proceeded cleanly and the subsequent epoxidation occurred predominantly at the six membered ring (Scheme 6). The resulting hydroxyketone **15** (as ca. 5:1 mixture of diastereomers) was oxidized to **16**. However, all our attempts to cleave the phenolic methyl ether in the vicinity of indanone carbonyl (e.g., using  $\text{BBr}_3$  or  $\text{BCl}_3$ ) failed and yielded complex mixtures that contained only traces of the desired product **cDHAs**.



**Scheme 6.** Attempted conversion of enone **7** into **cDHAs**.

Fortunately, selective demethylation was possible at the stage of spirocyclic enone **7**, which enabled us to introduce an alternative protecting group that could be cleaved more easily at the end of the synthesis (Scheme 7). Along this line we decided to prepare pivaloyl ester **17**. Interestingly (and in contrast to **7**), ester **17** underwent clean *mono*-silylation to afford enol ether **18**, which was then oxidized to hydroxyketone **19**. Exposure of methanolic solution of **19** to air and  $\text{K}_2\text{CO}_3$ , which effected the desired oxidation and cleavage of the pivaloate, afforded the target compound **cDHAs**, whose structure was again unambiguously confirmed by X-ray crystallography (Scheme 7).



**Scheme 7.** Completion of synthesis of **cDHAs**.

In the biochemical assay we developed previously,<sup>18</sup> we tested both **cDHA** and **cDHAs** against the following mammalian pols: calf pol  $\alpha$  and human pols  $\gamma$ ,  $\kappa$ , and  $\lambda$ , which belong to the B-, A-, Y-, and X-family of pols, respectively. As shown in Table 1, **cDHA** specifically inhibits pol  $\alpha$ . In contrast, **cDHAs** inhibits none of the tested pols.

**Table 1.**  $\text{IC}_{50}$  values of **cDHA** and **cDHAs** for mammalian DNA polymerases.<sup>a</sup>

polymerase	$\text{IC}_{50}$ value ( $\mu\text{M}$ )	
	<b>cDHA</b>	<b>cDHAs</b>
calf pol $\alpha$	$5.5 \pm 0.29$	> 100
human pol $\gamma$	> 100	> 100
human pol $\kappa$	> 100	> 100
human pol $\lambda$	> 100	> 100

<sup>a</sup> Data are shown as the means  $\pm$  SE of three independent experiments. Description of the assay is given in Experimental Section.

### 3. Conclusions

In conclusion, we prepared racemic novel carbocyclic analogs of dehydroaltenusin **cDHA** and **cDHAs** in 11 and 13 steps, respectively, starting from 3,5-dimethoxybenzaldehyde. While **cDHA** is approximately eight times weaker inhibitor than dehydroaltenusin itself (previously reported  $IC_{50}$  value for dehydroaltenusin against calf pol  $\alpha$  is 0.68  $\mu\text{M}$ ),<sup>5</sup> it is stable and can be stored in the solid state as well as in aqueous DMSO solution for at least four weeks without noticeable decomposition. In addition, the enantiomers of **cDHA** can be efficiently separated by HPLC on chiral stationary phase (details given in Supporting Information). Bioisosteric replacement of oxygen atom by the methylene group is commonly used in medicinal chemistry;<sup>19</sup> however, in the context of this project, it enabled not only identification of more stable analogs, but also provided significant (albeit indirect) information on which of the dehydroaltenusin isomers is responsible for its biological activity. Our observation of the dramatic difference in activities of **cDHA** and **cDHAs** strongly suggests that dehydroaltenusin's inhibitory activity toward pols is due to its non-spirocyclic form **DHA** and while the presence reactive o-quinone intermediate may contribute to dehydroaltenusin's inhibitory activity, it may not be absolutely required.

We believe the methodology presented above will enable preparation of additional analogs possessing the rare and non-trivial tricyclic central motifs. In addition, our results could be used to guide further development of potent and selective inhibitors of mammalian polymerases, namely pol  $\alpha$ , exploiting the recently published crystal structure.<sup>20</sup>

### 4. Experimental Section

#### General

All reagents and solvents were of reagent grade and used without further purification. Anhydrous solvents (THF, dichloromethane,  $\text{CH}_3\text{CN}$ ) were purchased from commercial suppliers (Aldrich, Acros) and stored over 4Å molecular sieves. All reactions were carried out in oven-dried glassware and under  $\text{N}_2$  atmosphere unless stated otherwise. Column chromatography was carried on silica gel (230-400 mesh). TLC plates were visualized under UV and stained with phosphomolybdic acid or  $\text{KMnO}_4$  solution or Vaughn's reagent ( $(\text{NH}_4)_6\text{Mo}_7\text{O}_{24}\cdot 4\text{H}_2\text{O}/\text{Ce}(\text{SO}_4)_2\cdot 4\text{H}_2\text{O}/\text{conc. H}_2\text{SO}_4/\text{H}_2\text{O}$ ).

NMR spectra were recorded on Bruker Avance 300 and 500 MHz spectrometers, with operating frequencies 300.13, 500.13 MHz for  $^1\text{H}$  and 75.48, 125.77 MHz for  $^{13}\text{C}$ . The  $^1\text{H}$  and  $^{13}\text{C}$  NMR chemical shifts ( $\delta$  in ppm) were referenced to the residual signals of solvents:  $\text{CDCl}_3$  [7.24 ( $^1\text{H}$ ) and

77.23 ( $^{13}\text{C}$ )]. Structural assignments of resonances have been performed with the help of 2D NMR gradients experiments (HSQC, HMBC, NOESY).

High resolution mass spectra were measured on Agilent 6224 Accurate-Mass TOF LC-MS with dual electrospray/chemical ionization mode with mass accuracy greater than 2 ppm, applied mass range was from 25 to 20,000 Da.

IR spectra ( $4000\text{--}400\text{ cm}^{-1}$ ) were collected on an EQUINOX 55/S/NIR FTIR spectrometer. Samples were prepared as KBr pellets.

The diffraction data for sample **cDHA** (CCDC number 1012667) were collected with a KUMA KM-4  $\kappa$ -axis diffractometer equipped with a Sapphire2 CCD detector and a Cryostream Cooler (Oxford Cryosystems, UK). Mo  $K\alpha$  radiation ( $\lambda = 0.71073\text{ \AA}$ , fine-focus sealed tube, graphite monochromator) was used.

The diffraction data for sample **cDHAs** (CCDC number 1012668) were collected with a Rigaku partial  $\chi$  geometry diffractometer equipped with a Saturn 944+ HG CCD detector and a Cryostream Cooler (Oxford Cryosystems, UK). Cu  $K\alpha$  radiation ( $\lambda = 1.54184\text{ \AA}$ , MicroMax-007HF rotating anode source, multilayer optic VariMax) was used. Data reduction and final cell refinement were carried out using the CrysAlisPro software ( $^{\text{C}}\text{CrysAlisPro}$ ] CrysAlisPRO, Agilent Technologies UK Ltd).

#### **4.1. 4-(3,5-dimethoxyphenyl)but-3-enoic acid**

To NaH (60% suspension in mineral oil, 1.90 g, 49.7 mmol) was added dry DMSO (36 mL) and the mixture was stirred and heated at  $70\text{ }^{\circ}\text{C}$ . After the evolution of bubbles ceased, the mixture was cooled to  $10\text{ }^{\circ}\text{C}$ . To this mixture, a solution of (2-carboethoxy)triphenylphosphonium bromide (11.00 g, 26.5 mmol) in DMSO (26 mL) was added dropwise. To the resulting dark red reaction mixture, a solution of 3,5-dimethoxybenzaldehyde (2.0 g, 12.0 mmol) in DMSO (5 mL) was added. The reaction mixture was stirred at  $50\text{ }^{\circ}\text{C}$  for 16 h, then cooled, poured into ice-water (200 mL), acidified with conc. HCl to  $\text{pH} < 4$ , and extracted with EtOAc (4 x 50 mL). The combined organic layers were washed with  $\text{H}_2\text{O}$  (2 x 50 mL), dried over  $\text{Na}_2\text{SO}_4$  and concentrated. The product was purified by column chromatography (silica gel, EtOAc/hexane (1:1)) to obtain the title 4-(3,5-dimethoxyphenyl)but-3-enoic acid as a yellow solid (1.80 g, 66%). mp  $58\text{--}60\text{ }^{\circ}\text{C}$ ;  $^1\text{H NMR}$  (300 MHz,  $\text{CDCl}_3$ )  $\delta = 6.55$  (d,  $J = 2.3\text{ Hz}$ , 2H), 6.47 (d,  $J = 15.9\text{ Hz}$ , 1H), 6.39 (t,  $J = 2.3\text{ Hz}$ , 1H), 6.28 (dt,  $J = 15.9\text{ Hz}$ ,  $J = 7.2\text{ Hz}$ , 1H), 3.80 (s, 6H), 3.30 (d,  $J = 7.2\text{ Hz}$ , 2H).  $^1\text{H NMR}$  spectrum was identical with the published literature.<sup>21</sup>

#### 4.2. 4-(3,5-dimethoxyphenyl)butanoic acid (**4**)

A solution of 4-(3,5-dimethoxyphenyl)but-3-enoic acid (2.00 g, 9.0 mmol) in EtOH (24 mL) was added to Pd/C (10% Pd, 478 mg) and ammonium formate (1.70 g, 27.0 mmol). The reaction mixture was stirred at 60 °C for 14 h, then cooled, filtered through a pad of Celite, and concentrated under reduced pressure. The residue was diluted with H<sub>2</sub>O (100 mL), acidified with conc. HCl to pH=4, and extracted with EtOAc (3 x 50 mL). The combined organic extracts were dried over Na<sub>2</sub>SO<sub>4</sub> and concentrated. The residue was purified by column chromatography (silica gel, EtOAc/hexane (1:1)) to afford **4** as a white solid (1.44 g, 71%). mp 63-65 °C; <sup>1</sup>H NMR (300 MHz, CDCl<sub>3</sub>) δ = 6.35 (d, *J* = 2.0 Hz, 2H), 6.32 (dd, *J* = 2.0 Hz, 1H), 3.78 (s, 6H), 2.62 (t, *J* = 7.6 Hz, 2H), 2.38 (t, *J* = 7.4 Hz, 2H), 2.02 – 1.90 (m, 2H).

#### 4.3. 6,8-dimethoxy-3,4-dihydronaphthalen-1(2*H*)-one

A mixture of **4** (1.44 g, 6.42 mmol) and polyphosphoric acid (14 mL) was stirred at 90 °C for 4 h, then it was poured into ice-water (250 mL) and extracted with EtOAc (3 x 100 mL). The combined organic extracts were washed with saturated aqueous solution of NaHCO<sub>3</sub> (2 x 50 mL) and dried over Na<sub>2</sub>SO<sub>4</sub>. Removal of the solvent under reduced pressure afforded the product as a yellow solid (1.24 g, 93%). mp 62-63 °C; <sup>1</sup>H NMR (300 MHz, CDCl<sub>3</sub>) δ = 6.35 – 6.30 (m, 3H), 3.87 (s, 2H), 3.84 (s, 3H), 2.87 (t, *J* = 6.0 Hz, 2H), 2.57 (t, *J* = 6.5 Hz, 2H), 2.07 – 1.96 (m, 2H). <sup>1</sup>H NMR spectrum was identical with the published literature.<sup>22</sup>

#### 4.4. 6',8'-dimethoxy-3',4'-dihydro-2'*H*-spiro[[1,3]dioxolane-2,1'-naphthalene] (**3**)

A mixture of 6,8-dimethoxy-3,4-dihydronaphthalen-1(2*H*)-one (206 mg, 1.00 mmol), pyridinium *p*-toluenesulfonate (25 mg, 0.01 mmol), and ethylene glycol (170 μl, 3.00 mmol) in benzene (25 mL) was heated at reflux in a flask equipped with a Dean-Stark apparatus for 14 h. The mixture was cooled to 25 °C, K<sub>2</sub>CO<sub>3</sub> (100 mg) was added, and the solvent was evaporated. The residue was purified by column chromatography (silica gel, EtOAc/hexane/Et<sub>3</sub>N (100:50:1)) to afford **3** as a white solid (200 mg, 80%), which was used immediately in the next step. mp 85 °C (dec.); <sup>1</sup>H NMR (500 MHz, CDCl<sub>3</sub>) δ = 6.33 (d, *J* = 2.4 Hz, 1H), 6.21 (d, *J* = 2.4 Hz, 1H), 4.25 – 4.18 (m, 2H), 4.08 – 4.01 (m, 2H), 3.80 (s, 3H), 3.76 (s, 3H), 2.75 – 2.70 (m, 2H), 1.96 – 1.91 (m, 2H) 1.86 – 1.79 (m, 2H); <sup>13</sup>C NMR (126 MHz, CDCl<sub>3</sub>) δ = 160.2, 160.0, 142.3, 117.8, 108.1, 104.3, 98.0, 65.3 (2C), 55.8, 55.1, 36.8, 31.1, 21.1; HRMS (APCI): calcd. for C<sub>14</sub>H<sub>19</sub>O<sub>4</sub> [M+H]<sup>+</sup>: 251.1283, found: 251.1348.

#### 4.5. 6',8'-dimethoxy-2'*H*-spiro[[1,3]dioxolane-2,1'-naphthalen]-4'(3'*H*)-one (**5**)

Rh<sub>2</sub>(cap)<sub>4</sub> (9 mg, 0.01 mol) and *t*-BuOOH (5.5 M in decane, 900 μL, 4.95 mmol) were added to a mixture of **3** (250 mg, 1.00 mmol) and NaHCO<sub>3</sub> (42 mg, 0.50 mmol) in CH<sub>3</sub>CN (2 mL). The reaction mixture was stirred at 25 °C for 16 h, then concentrated, and purified by column chromatography (silica gel, EtOAc/hexane (1:2)) to yield **5** as a white solid (145 mg, 55%). mp 81 °C (dec.); <sup>1</sup>H NMR (300 MHz, CDCl<sub>3</sub>) δ = 7.11 (d, *J* = 2.5 Hz, 1H), 6.71 (d, *J* = 2.5 Hz, 1H), 4.31 – 4.23 (m, 2H), 4.13 – 4.05 (m, 2H), 3.86 (s, 3H), 3.84 (s, 3H), 2.79 (m, 2H), 2.28 (m, 2H); <sup>13</sup>C NMR (75 MHz, CDCl<sub>3</sub>) δ = 197.3, 161.0, 159.1, 135.2, 123.4, 106.8, 106.0, 100.9, 65.8 (2C), 56.3, 55.6, 36.2, 34.4; IR (KBr):  $\tilde{\nu}$  = 2962 cm<sup>-1</sup> (m), 2939 (w), 2887 (w), 1685 (s), 1603 (s), 1466 (m), 1430 (w), 1354 (s), 1321 (s), 1300 (s), 1217 (s), 1163 (s), 1114 (s), 1040 (s), 980 (w), 916 (m), 842 (m); HRMS (APCI): calcd. for C<sub>14</sub>H<sub>17</sub>O<sub>5</sub> [M+H]<sup>+</sup>: 265.1071, found: 265.1068.

#### 4.6. 6',8'-dimethoxy-3'-methyl-2'*H*-spiro[[1,3]dioxolane-2,1'-naphthalen]-4'(3'*H*)-one:

A solution of compound **5** (100 mg, 0.38 mmol) and 1,3-dimethyltetrahydropyrimidin-2(1*H*)-one (330 μL) in THF (1 mL) was cooled to -78 °C, *t*-BuOK (46.8 mg, 0.42 mmol) was added, and the mixture was stirred at -78 °C for 45 min. Iodomethane (30 μL, 0.48 mmol) was added, the mixture was allowed to warm to 25 °C and stirred for 16 h, then diluted with H<sub>2</sub>O (50 mL), and extracted with CH<sub>2</sub>Cl<sub>2</sub> (3 x 20 mL). The combined organic extracts were dried over Na<sub>2</sub>SO<sub>4</sub> and concentrated. The residue was purified by column chromatography (silica gel, EtOAc/hexane (1:2)) to yield 6',8'-dimethoxy-3'-methyl-2'*H*-spiro[[1,3]dioxolane-2,1'-naphthalen]-4'(3'*H*)-one as a white solid (58 mg, 55%). mp 99 °C (dec.); <sup>1</sup>H NMR (500 MHz, CDCl<sub>3</sub>) δ = 7.11 (d, *J* = 2.6 Hz, 1H), 6.70 (d, *J* = 2.6 Hz, 1H), 4.33 – 4.24 (m, 2H), 4.17 – 4.13 (m, 1H), 4.11 – 4.06 (m, 1H), 3.86 (s, 3H), 3.85 (s, 3H), 3.00 – 2.92 (m, 1H) 2.25 (m, 1H), 2.12 (m, 1H), 1.22 (d, *J* = 6.7 Hz, 3H); <sup>13</sup>C NMR (126 MHz, CDCl<sub>3</sub>) δ = 199.6, 161.0, 159.1, 135.4, 123.0, 106.7, 105.5, 100.9, 65.9, 65.8, 56.1, 55.5, 42.7, 39.9, 14.6; IR (KBr):  $\tilde{\nu}$  = 2987 cm<sup>-1</sup> (w), 2968 (m), 2893 (m), 2860 (m), 2839 (w), 1680 (s), 1603 (s), 1470 (m), 1456 (s), 1365 (m), 1323 (s), 1300 (s), 1229 (s), 1207 (s), 1157 (m), 1115 (s), 1082 (m), 1041 (m), 964 (m), 949 (w), 941 (w), 839 (s); HRMS (APCI): calcd. for C<sub>15</sub>H<sub>19</sub>O<sub>5</sub> [M+H]<sup>+</sup>: 279.1227, found: 279.1227.

#### 4.7. 6',8'-dimethoxy-3'-methyl-3'-(3-oxobutyl)-2'*H*-spiro[[1,3]dioxolane-2,1'-naphthalen]-4'(3'*H*)-one (2)

A stream of nitrogen saturated by MVK was bubbled through a solution of 6',8'-dimethoxy-3'-methyl-2'*H*-spiro[[1,3]dioxolane-2,1'-naphthalen]-4'(3'*H*)-one (40 mg, 0.14 mmol) and DBU (22 μL, 0.14 mmol) in toluene (1 mL). Upon completion, indicated by TLC (silica gel, EtOAc/hexane (1:2)), the solvent was evaporated. The crude residue was purified by column chromatography (silica gel,

EtOAc/hexane (1:2)) to afford **2** as a colorless wax (29.7 mg, 61%). <sup>1</sup>H NMR (300 MHz, CDCl<sub>3</sub>) δ = 7.10 (d, *J* = 2.5 Hz, 1H), 6.71 (d, *J* = 2.5 Hz, 1H), 4.33 – 4.20 (m, 2H), 4.16 – 4.05 (m, 2H), 3.84 (s, 6H), 2.57 – 2.44 (m, 1H), 2.39 – 2.27 (m, 1H), 2.22 (d<sub>AB</sub>, *J* = 14.4 Hz, 1H), 2.12 (s, 3H), 2.10 (d<sub>AB</sub>, *J* = 14.4 Hz, 1H), 2.06 – 1.85 (m, 2H), 1.20 (s, 3H); <sup>13</sup>C NMR (75 MHz, CDCl<sub>3</sub>) δ = 208.1, 201.5, 161.2, 159.1, 133.9, 122.4, 105.8, 105.6, 101.3, 65.64, 65.56, 56.1, 55.5, 44.9, 44.5, 38.6, 31.3, 29.8, 23.1; IR (KBr):  $\tilde{\nu}$  = 2964 cm<sup>-1</sup> (w), 2937 (w), 2899 (w), 1713 (s), 1687 (s), 1601 (s), 1464 (m), 1356 (m), 1323 (s), 1296 (s), 1221 (m), 1159 (s), 1115 (m), 1090 (m), 1045 (m), 1011 (w), 948 (w), 848 (w); HRMS (APCI): calcd. for C<sub>19</sub>H<sub>25</sub>O<sub>6</sub> [M+H]<sup>+</sup>: 349.1646, found: 349.1647.

#### 4.8. 6',8'-dimethoxy-10a'-methyl-10',10a'-dihydro-1'H-spiro[[1,3]dioxolane-2,9'-phenanthren]-3'(2'H)-one (**1**)

*t*-BuOK (57.9 mg, 0.52 mmol) was added to a solution of **2** (150 mg, 0.43 mmol) in *t*-BuOH (2 mL), the reaction mixture was stirred at 25 °C for 3 h. H<sub>2</sub>O (5 mL) was added and the mixture was extracted with EtOAc (3 x 10 mL). The combined organic extracts were dried over Na<sub>2</sub>SO<sub>4</sub>, filtered, and concentrated in a vacuum to afford **1** as a white solid (110 mg, 77%), which was used in the next step without further purification. mp 126 °C (dec.); <sup>1</sup>H NMR (300 MHz, CDCl<sub>3</sub>) δ = 6.70 (d, *J* = 2.3 Hz, 1H), 6.60 (d, *J* = 2.3 Hz, 1H), 6.47 (br. s, 1H), 4.37 – 4.27 (m, 1H), 4.23 – 4.04 (m, 3H), 3.86 (s, 3H), 3.82 (s, 3H), 2.70 – 2.54 (m, 1H), 2.48 – 1.39 (m, 1H), 2.14 – 1.85 (m, 4H), 1.30 (s, 3H); <sup>13</sup>C NMR (75 MHz, CDCl<sub>3</sub>) δ = 199.6, 162.2, 160.9, 160.0, 135.6, 121.9, 118.7, 106.3, 102.9, 101.3, 65.8, 65.2, 56.0, 55.4, 49.3, 36.8, 35.6, 33.2, 21.7; IR (KBr):  $\tilde{\nu}$  = 2950 cm<sup>-1</sup> (m), 2922 (w), 2890 (w), 1660 (s), 1603 (s), 1579 (s), 1466 (s), 1425 (m), 1356 (s), 1327 (s), 1296 (s), 1275 (s), 1207 (s), 1157 (s), 1134 (s), 1101 (s), 1147 (s), 1020 (m), 989 (m), 950 (m), 849 (w), 837 (m), 821 (w); HRMS (APCI): calcd. for C<sub>19</sub>H<sub>23</sub>O<sub>5</sub> [M+H]<sup>+</sup>: 331.1540, found: 331.1543.

#### 4.9. 2-hydroxy-6,8-dimethoxy-10a-methyl-10,10a-dihydrophenanthrene-3,9-dione (**6**)

*t*-BuOK (110 mg, 0.30 mmol) was added to a solution of **1** (186 mg, 0.33 mmol) in *t*-BuOH (2 mL) and THF (2 mL) and the mixture was stirred under O<sub>2</sub> atmosphere at 25 °C for 4 h. The reaction mixture was diluted with saturated aqueous solution of NH<sub>4</sub>Cl (30 mL) and extracted with CH<sub>2</sub>Cl<sub>2</sub> (3 x 20 mL). The combined organic phases were dried over Na<sub>2</sub>SO<sub>4</sub>, filtered, and the solvent was evaporated. The residue was dissolved in acetone (5 mL), TsOH (10 mg, 0.05 mmol) was added, and the mixture was stirred at 25 °C for 16 h. The solvent was removed under reduced pressure and the residue was purified by column chromatography (silica gel, EtOAc/CH<sub>2</sub>Cl<sub>2</sub> (1:1)) to afford **6** (71 mg, 72%) as a white solid. mp 218-220 °C; <sup>1</sup>H NMR (300 MHz, CDCl<sub>3</sub>) δ = 6.84 (s, 1H), 6.73 (d, *J* = 2.3 Hz, 1H), 6.61 (d, *J* = 2.3 Hz, 1H), 6.37 (br. s, 1H), 6.13 (s, 1H), 3.95 (s, 3H), 3.94 (s, 3H), 2.83 (d<sub>AB</sub>, *J*

= 16.1 Hz, 1H), 2.57 (d<sub>AB</sub>, *J* = 16.1 Hz, 1H), 1.34 (s, 3H); <sup>13</sup>C NMR (126 MHz, CDCl<sub>3</sub>) δ = 192.0, 181.7, 164.8, 162.6, 162.3, 146.5, 141.8, 123.8, 122.3, 114.0, 102.5, 101.1, 56.3, 55.7, 51.0, 42.0, 25.8; IR (KBr):  $\tilde{\nu}$  = 3234 cm<sup>-1</sup> (w), 3018 (w), 2972 (w), 2931 (w), 1657 (s), 1606 (s), 1589 (s), 1558 (s), 1477 (m), 1454 (m), 1407 (m), 1377 (w), 1342 (s), 1306 (w), 1265 (s), 1245 (s), 1215 (s), 1207 (s), 1165 (s), 1115 (s), 1026 (w), 999 (m), 957 (w), 895 (w), 850 (w), 839 (w); HRMS (APCI): calcd. for C<sub>17</sub>H<sub>17</sub>O<sub>5</sub> [M+H]<sup>+</sup>: 301.1071, found: 301.1067.

#### 4.10. 2,8-dihydroxy-6-methoxy-10a-methyl-10,10a-dihydrophenanthrene-3,9-dione (cDHA)

BBr<sub>3</sub> (1 M in CH<sub>2</sub>Cl<sub>2</sub>, 0.2 mL, 0.2 mmol) was added dropwise to a solution of **6** (30 mg, 0.1 mmol) in anhydrous CH<sub>2</sub>Cl<sub>2</sub> (3 mL) at -78 °C. The reaction mixture was stirred at -78 °C for 1 h, then allowed to warm to 0 °C, and quenched with aqueous 10% NaOH (1 mL). The mixture was acidified with 1 M HCl to pH=6 and extracted with CH<sub>2</sub>Cl<sub>2</sub> (2 x 10 mL). The combined organic extracts were dried over Na<sub>2</sub>SO<sub>4</sub>, filtered, and concentrated. The residue was purified by preparative TLC (CH<sub>2</sub>Cl<sub>2</sub>/EtOAc (1:1)) to afford **cDHA** (15 mg, 52%) as a pale yellow solid. mp 199 °C (dec.); <sup>1</sup>H NMR (300 MHz, CDCl<sub>3</sub>) δ = 12.61 (s, 1H), 6.84 (s, 1H), 6.72 (d, *J* = 2.3 Hz, 1H), 6.54 (d, *J* = 2.3 Hz, 1H), 6.38 (s, 1H), 6.13 (s, 1H), 3.90 (s, 3H), 2.85 (d<sub>AB</sub>, *J* = 17.0 Hz, 1H), 2.67 (d<sub>AB</sub>, *J* = 17.0 Hz, 1H), 1.35 (s, 3H); <sup>13</sup>C NMR (126 MHz, CDCl<sub>3</sub>) δ = 199.1, 181.5, 166.5, 165.5, 160.4, 146.6, 139.6, 123.0, 122.3, 109.1, 105.5, 102.8, 55.9, 48.8, 41.6, 26.3; IR (KBr):  $\tilde{\nu}$  = 3375 cm<sup>-1</sup> (m), 2964 (w), 2926 (w), 1632 (s), 1564 (w), 1479 (w), 1454 (w), 1429 (m), 1389 (m), 1365 (m), 1343 (w), 1292 (s), 1238 (m), 1203 (s), 1159 (s), 1126 (w), 1101 (w), 1067 (w), 978 (w), 903 (w), 879 (w); HRMS (APCI): calcd. for C<sub>16</sub>H<sub>15</sub>O<sub>5</sub> [M+H]<sup>+</sup>: 287.0914, found: 287.0912.

Crystal data for **cDHA**: CCDC ref. No. 1012667. Crystallized from CHCl<sub>3</sub>.

#### 4.11. 1,3-dimethoxy-5-(2-nitroprop-1-en-1-yl)benzene

A mixture of 3,5-dimethoxybenzaldehyde (10.0 g, 60.18 mmol), nitroethane (45 mL, 630.68 mmol) and NH<sub>4</sub>OAc (3.36 g, 43.57 mmol) was stirred and heated at reflux for 4 h (oil bath 130 °C). The reaction mixture was cooled to 25 °C, diluted with Et<sub>2</sub>O (200 mL), and washed with brine (4 x 150 mL). The organic layer was dried over Na<sub>2</sub>SO<sub>4</sub>, filtered, and the solvent was evaporated. 1,3-Dimethoxy-5-(2-nitroprop-1-en-1-yl)benzene (13.04 g, 97%) was obtained as a yellow solid. mp 86-87 °C; <sup>1</sup>H NMR (300 MHz, CDCl<sub>3</sub>) δ = 7.99 (br. s, 1H), 6.54 (d, *J* = 2.2 Hz, 2H), 6.51 (d, *J* = 2.2 Hz, 1H), 3.81 (s, 6H), 2.43 (d, *J* = 0.9 Hz, 3H).

#### 4.12. 1-(3,5-dimethoxyphenyl)propan-2-one (**9**)

Fe powder (1.60 g, 28.7 mmol) was added to a solution of 1,3-dimethoxy-5-(2-nitroprop-1-en-1-yl)benzene (493 mg, 2.21 mmol) in AcOH (13.9 mL, 221.0 mmol) and the mixture was heated at reflux for 3 h. The mixture was cooled to 25 °C, filtered, diluted with water (70 mL), and extracted with CH<sub>2</sub>Cl<sub>2</sub> (3 x 30 mL). Combined organic extracts were washed with aqueous 5% NaOH (2 x 30 mL), brine (2 x 30 mL), dried over Na<sub>2</sub>SO<sub>4</sub>, and concentrated. The crude residue was purified by column chromatography (silica gel, EtOAc/hexane (2:1)) to provide **9** (303 mg, 71%) as a colorless oil. <sup>1</sup>H NMR (300 MHz, CDCl<sub>3</sub>) δ = 6.37 – 6.31 (m, 3H), 3.74 (s, 6H), 3.57 (s, 2H), 2.11 (s, 3H).

#### 4.13. 2-(2-iodoethyl)-2-methyl-1,3-dioxolane (**11**)

Iodotrimethylsilane (1.7 mL, 12 mmol) was added dropwise at 0 °C to a mixture of methyl vinyl ketone (90%, 833 μL, 10 mmol) and ethylene glycol (1.24 mL, 22 mmol). The reaction mixture was stirred for 2 h while allowed to warm to 25 °C, then it was diluted with pentane (20 mL) and washed successively with 5% aqueous Na<sub>2</sub>CO<sub>3</sub> (10 mL) and 5% aqueous Na<sub>2</sub>S<sub>2</sub>O<sub>3</sub> (10 mL). The organic layer was dried over K<sub>2</sub>CO<sub>3</sub> and concentrated under reduced pressure to provide **11** (1.93 g, 80%) as a pale yellow oil, which was used directly in the next step without further purification. <sup>1</sup>H NMR (300 MHz, CDCl<sub>3</sub>) δ = 4.01 – 3.87 (m, 4H), 3.21 – 3.12 (m, 2H), 2.35 – 2.24 (m, 2H), 1.30 (s, 3H).

#### 4.14. 3-(3,5-dimethoxyphenyl)-5-(2-methyl-1,3-dioxolan-2-yl)pentan-2-one (**10**)

*t*-BuOK (677 mg, 6.04 mmol) was added to a solution of **9** (1.02 g, 5.24 mmol) in anhydrous THF (12 mL) and the reaction mixture was stirred at 25 °C for 1 h. **11** (1.7 g, 7.02 mmol) was added dropwise over the period of 5 min and the reaction mixture was stirred at 25 °C for 16 h. Saturated aqueous solution of NaHCO<sub>3</sub> (1 mL) was added, the solvents were evaporated and the residue was directly loaded onto a column and purified by column chromatography (silica gel, EtOAc/hexane (1:2)). **10** (1.37 g, 85%) was obtained as a pale yellow oil. <sup>1</sup>H NMR (300 MHz, CDCl<sub>3</sub>) δ = 6.35 (s, 3H), 3.94 – 3.84 (m, 4H), 3.77 (s, 6H), 3.54 (t, *J* = 7.4 Hz, 1H), 2.16 – 2.02 (m, 1H), 2.05 (s, 3H), 1.86 – 1.71 (m, 1H), 1.64 – 1.43 (m, 2H), 1.29 (s, 3H); <sup>13</sup>C NMR (CDCl<sub>3</sub>, 75 MHz) δ = 207.9, 161.2 (2C), 141.2, 109.9, 106.4 (2C), 99.2, 64.61, 64.58, 59.7, 55.3 (2C), 36.6, 28.8, 26.0, 23.8; IR (KBr):  $\tilde{\nu}$  = 2958 cm<sup>-1</sup> (w), 2941 (w), 1712 (s), 1670 (w), 1605 (s), 1595 (s), 1460 (m), 1431 (m), 1352 (w), 1205 (s), 1157 (s), 1065 (s), 858 (w), 837 (w); HRMS (ESI): calcd. for C<sub>17</sub>H<sub>24</sub>O<sub>5</sub>Na [M+Na]<sup>+</sup>: 331.1516, found: 331.1517.

#### 4.15. *tert*-butyl 3-acetyl-3-(3,5-dimethoxyphenyl)-5-(2-methyl-1,3-dioxolan-2-yl)pentanoate (**12**)

*t*-BuOK (580 mg, 5.17 mmol) was added to a solution of **10** (1.39 g, 4.50 mmol) in THF (16 mL) at 0 °C and the resulting yellow mixture was stirred at 0 °C for 1 h. Then, *t*-butyl-2-iodoacetate (2.0 g, 5.85 mmol) was added, the mixture was allowed to warm to 25 °C and stirred for 20 h. Reaction was quenched by saturated solution of NaHCO<sub>3</sub> (1 mL). The solvents were evaporated and the residue was purified by column chromatography (silica gel, EtOAc/hexane (1:4 to 1:1)) to yield **12** (924 mg, 62%) as a colorless oil. <sup>1</sup>H NMR (300 MHz, CDCl<sub>3</sub>) δ = 6.36 – 6.33 (m, 3H), 3.93 – 3.80 (m, 2H), 3.76 (s, 6H), 2.96 (d<sub>AB</sub>, *J* = 14.7 Hz, 1H), 2.81 (d<sub>AB</sub>, *J* = 14.7 Hz, 1H), 2.40 – 2.27 (m, 1H), 2.07 – 1.96 (m, 3H), 1.98 (s, 3H), 1.45 – 1.37 (m, 2H), 1.35 (s, 9H), 1.30 (s, 3H); <sup>13</sup>C NMR (75 MHz, CDCl<sub>3</sub>) δ = 207.8, 170.2, 161.0 (2C), 142.6, 109.8, 105.2 (2C), 98.9, 81.0, 64.6, 64.5, 57.4, 55.3 (2C), 39.5, 33.2, 27.8 (3C), 27.5, 25.4, 23.7; IR (KBr):  $\tilde{\nu}$  = 2978 cm<sup>-1</sup> (w), 2937 (w), 2885 (w), 1726 (s), 1713 (s), 1598 (s), 1458 (m), 1425 (m), 1369 (m), 1352 (m), 1296 (w), 1205 (s), 1157 (s), 1064 (m), 858 (w), 845 (w); HRMS (ESI): calcd. for C<sub>23</sub>H<sub>34</sub>O<sub>7</sub>Na [M+Na]<sup>+</sup>: 445.2197, found: 445.2198.

#### 4.16. *tert*-butyl 3-acetyl-3-(3,5-dimethoxyphenyl)-6-oxoheptanoate (**8**)

TsOH (75 mg, 0.17 mmol) was added to a solution of **12** (721 mg, 1.71 mmol) in acetone (10 mL) and the mixture was stirred at 25 °C for 8 h. The solvent was evaporated, the residue was dissolved in Et<sub>2</sub>O (20 mL) and washed with saturated aqueous solution of NaHCO<sub>3</sub> (10 mL). The aqueous phase was re-extracted with Et<sub>2</sub>O (2 x 10 mL). The combined organic extracts were washed with H<sub>2</sub>O (10 mL), dried over Na<sub>2</sub>SO<sub>4</sub> and concentrated in a vacuum to yield **8** (641 mg, 100%) as a white solid. mp 94–97 °C; <sup>1</sup>H NMR (500 MHz, CDCl<sub>3</sub>) δ = 6.36 (t, *J* = 2.2 Hz, 1H), 6.30 (d, *J* = 2.2 Hz, 2H), 3.76 (s, 6H), 2.98 (d, *J* = 14.3 Hz, 1H), 2.79 (d, *J* = 14.3 Hz, 1H), 2.48 – 2.42 (m, 1H), 2.29 – 2.15 (m, 3H), 2.07 (s, 3H), 1.97 (s, 3H), 1.35 (s, 9H); <sup>13</sup>C NMR (126 MHz, CDCl<sub>3</sub>) δ = 207.6, 207.4, 170.0, 161.2 (2C), 142.2, 105.0 (2C), 99.0, 81.4, 57.1, 55.4 (2C), 39.8, 38.5, 29.8, 27.8 (3C), 27.5, 25.6; IR (KBr):  $\tilde{\nu}$  = 2975 cm<sup>-1</sup> (w), 2939 (w), 1720 (s), 1707 (s), 1593 (s), 1466 (m), 1427 (m), 1365 (m), 1352 (s), 1311 (s), 1292 (m), 1211 (s), 1146 (s), 1068 (m), 1051 (m), 924 (w), 840 (w); HRMS (ESI): calcd. for C<sub>21</sub>H<sub>30</sub>O<sub>6</sub>Na [M+Na]<sup>+</sup>: 401.1935, found: 401.1935.

#### 4.17. *tert*-butyl 2-(3',5'-dimethoxy-6-methyl-4-oxo-1,2,3,4-tetrahydro-[1,1'-biphenyl]-1-yl)acetate (**13a**)

AcOH (0.12 mL, 2.13 mmol) and piperidine (0.19 mL, 1.93 mmol) were added to a solution of **8** (732 mg, 1.93 mmol) in toluene (10 mL) and the mixture was heated at reflux (oil bath 110 °C) for 18 h. The solvent was evaporated in a vacuum, the residue was dissolved in EtOAc (150 mL) and washed

with H<sub>2</sub>O (100 mL) and then with brine (100 mL). The organic layer was dried over Na<sub>2</sub>SO<sub>4</sub>, concentrated, and the residue was purified by column chromatography (silica gel, EtOAc/hexane (1:2)) to afford **13a** as a white semi-solid (563 mg, 81%). <sup>1</sup>H NMR (300 MHz, CDCl<sub>3</sub>) δ = 6.40 (d, *J* = 2.1 Hz, 2H), 6.36 (t, *J* = 2.1 Hz, 1H), 6.16 (br. s, 1H), 3.76 (s, 6H), 2.91 (s, 2H), 2.72 – 2.60 (m, 1H), 2.32 – 2.01 (m, 3H), 1.98 (d, *J* = 1.2 Hz, 3H), 1.43 (s, 9H); <sup>13</sup>C NMR (75 MHz, CDCl<sub>3</sub>) δ = 198.7, 169.8, 163.5, 161.0 (2C), 144.7, 130.4, 105.7 (2C), 96.1, 81.4, 55.3 (2C), 46.8, 43.8, 35.7, 34.2, 28.0 (3C), 21.7; IR (KBr):  $\tilde{\nu}$  = 2976 cm<sup>-1</sup> (w), 2937 (w), 1724 (s), 1672 (s), 1601 (s), 1456 (s), 1425 (m), 1369 (m), 1348 (m), 1310 (m), 1207 (s), 1159 (s), 1068 (w), 1043 (w), 841 (w); HRMS (ESI): calcd. for C<sub>21</sub>H<sub>28</sub>O<sub>5</sub>Na [M+Na]<sup>+</sup>: 383.1829, found: 383.1829.

#### 4.18. *tert*-butyl 2-(3',5'-dimethoxy-4-methyl-6-oxo-1,2,3,6-tetrahydro-[1,1'-biphenyl]-1-yl)acetate (**13b**)

*t*-BuOK (14.6 mg, 0.13 mmol) was added to a solution of **8** (50 mg, 0.13 mmol) in THF (1 mL) at 0 °C. The reaction mixture was stirred at 0 °C for 1 h, then saturated aqueous solution of NaHCO<sub>3</sub> (1 mL) was added. The solvent was evaporated and the residue was loaded directly onto a column and purified by column chromatography (silica gel, EtOAc/hexane (1:2)) to give **13b** as a colorless oil (25.2 mg, 54%). <sup>1</sup>H NMR (500 MHz, CDCl<sub>3</sub>) δ = 6.40 (d, *J* = 2.2 Hz, 2H), 6.34 (t, *J* = 2.1 Hz, 1H), 5.95 (br. s, 1H), 3.75 (s, 6H), 2.93 (d<sub>AB</sub>, *J* = 16.2, 1H), 2.73 – 2.66 (m, 1H), 2.56 (d<sub>AB</sub>, *J* = 16.2, 1H), 2.51 – 2.45 (m, 1H), 2.34 – 2.24 (m, 1H), 2.17 – 2.10 (m, 1H), 1.84 (s, 3H), 1.36 (s, 9H); <sup>13</sup>C NMR (126 MHz, CDCl<sub>3</sub>) δ = 199.2, 170.6, 161.4, 160.8 (2C), 141.8, 126.4, 105.3 (2C), 96.7, 80.4, 55.3 (2C), 50.9, 45.1, 31.3, 28.7 (3C), 28.2, 24.1; IR (KBr):  $\tilde{\nu}$  = 2974 cm<sup>-1</sup> (w), 2931 (w), 1730 (s), 1668 (s), 1637 (w), 1595 (s), 1458 (s), 1425 (m), 1367 (m), 1348 (m), 1308 (m), 1294 (w), 1205 (s), 1159 (s), 1080 (w), 1063 (w), 1049 (w), 843 (w); HRMS (APCI): calcd. for C<sub>21</sub>H<sub>29</sub>O<sub>5</sub> [M+H]<sup>+</sup>: 361.2010, found: 361.2004.

#### 4.19. 4',6'-dimethoxy-2-methylspiro[cyclohex[2]ene-1,1'-indene]-3',4(2'*H*)-dione (**7**)

A solution of **13a** (415 mg, 1.15 mmol) in MsOH (4.2 mL) was heated at 50 °C for 15 h. The mixture was cooled to 25 °C, poured into cold saturated solution of NaHCO<sub>3</sub> (30 mL), and extracted with EtOAc (5 x 30 mL). The combined organic extracts were dried over Na<sub>2</sub>SO<sub>4</sub>, evaporated, and the residue was purified by gradient column chromatography (silica gel, EtOAc/hexane (1:2 to pure EtOAc)) to afford **7** (275 mg, 84%) as a pale brown solid. mp 159-164 °C; <sup>1</sup>H NMR (300 MHz, CDCl<sub>3</sub>) δ = 6.37 (d, *J* = 1.9 Hz, 2H), 6.32 (d, *J* = 1.9 Hz, 1H), 6.00 (br. s, 1H), 3.93 (s, 3H), 2.86 (s,

3H), 2.82 (d<sub>AB</sub>, *J* = 18.5, 1H), 2.65 (d<sub>AB</sub>, *J* = 18.5, 1H), 2.56 – 2.48 (m, 2H), 2.46 – 2.29 (m, 1H), 2.06 – 1.97 (m, 1H), 1.64 (d, *J* = 1.2 Hz, 3H); <sup>13</sup>C NMR (75 MHz, CDCl<sub>3</sub>) δ = 199.2, 197.9, 167.5, 163.8, 162.5, 159.5, 128.4, 118.8, 100.4, 98.3, 55.91, 55.89, 47.4, 46.7, 37.2, 34.9, 20.4; IR (KBr):  $\tilde{\nu}$  = 2953 cm<sup>-1</sup> (w), 2927 (w), 1697 (s), 1664 (s), 1576 (s), 1460 (m), 1439 (w), 1427 (w), 1350 (w), 1315 (s), 1234 (s), 1203 (s), 1159 (s), 1107 (w), 1053 (m), 1026 (w), 860 (m); HRMS (APCI): calcd. for C<sub>17</sub>H<sub>19</sub>O<sub>4</sub> [M+H]<sup>+</sup>: 287.1278, found: 287.1279.

#### 4.20. 4'-hydroxy-6'-methoxy-2-methylspiro[cyclohex[2]ene-1,1'-indene]-3',4(2'H)-dione

BCl<sub>3</sub> (1 M solution in CH<sub>2</sub>Cl<sub>2</sub>, 0.96 mL, 0.96 mmol) was added dropwise to a solution of **7** (275 mg, 0.96 mmol) in CH<sub>2</sub>Cl<sub>2</sub> (10 mL) at 0 °C and the mixture was stirred at 0 °C. Additional five 0.96 mL portions of 1M BCl<sub>3</sub> in CH<sub>2</sub>Cl<sub>2</sub> (total volume of 4.8 mL, 4.8 mmol) were added in one hour intervals and then the mixture was stirred for 16 h while allowed to warm to 25 °C. Then the reaction mixture was cooled to 0 °C, additional four 2.88 mL portions of 1M BCl<sub>3</sub> in CH<sub>2</sub>Cl<sub>2</sub> (total volume of 11.5 mL, 11.5 mmol) were added in three hour intervals and the mixture was stirred for additional 16 h while allowed to warm to 25 °C. Then it was quenched with cold saturated aqueous solution of NaHCO<sub>3</sub> (50 mL), and extracted with CH<sub>2</sub>Cl<sub>2</sub> (3 x 50 mL). The combined organic extracts were dried over Na<sub>2</sub>SO<sub>4</sub>, filtered, and concentrated. The residue was purified by column chromatography (silica gel, EtOAc/hexane (2:1)) to afford 4'-hydroxy-6'-methoxy-2-methylspiro[cyclohex[2]ene-1,1'-indene]-3',4(2'H)-dione (170 mg, 65%) as a white solid. mp 128-129 °C; <sup>1</sup>H NMR (300 MHz, CDCl<sub>3</sub>) δ = 9.07 (s, 1H), 6.34 (d, *J* = 1.9 Hz 1H), 6.31 (d, *J* = 1.9 Hz, 1H), 5.98 (br. s, 1H), 3.82 (s, 3H), 2.85 (d<sub>AB</sub>, *J* = 18.9 Hz, 1H), 2.69 (d<sub>AB</sub>, *J* = 18.9 Hz, 1H), 2.61 – 2.46 (m, 2H), 2.44 – 2.28 (m, 1H), 2.10 – 2.00 (m, 1H), 1.64 (d, *J* = 1.2 Hz, 3H); <sup>13</sup>C NMR (75 MHz, CDCl<sub>3</sub>) δ = 204.0, 197.7, 168.4, 162.0, 160.5, 159.1, 128.3, 116.2, 102.8, 100.1, 55.9, 47.6, 46.9, 36.7, 34.8, 20.3; IR (KBr):  $\tilde{\nu}$  = 3433 cm<sup>-1</sup> (w), 2976 (w), 2928 (w), 2918 (w), 1672 (s), 1659 (s), 1624 (s), 1597 (s), 1491 (m), 1443 (m), 1367 (s), 1325 (m), 1254 (m), 1205 (m), 1151 (s), 1022 (w), 989 (w), 962 (w), 864 (w), 849 (w); HRMS (APCI): calcd. for C<sub>16</sub>H<sub>17</sub>O<sub>4</sub> [M+H]<sup>+</sup>: 273.1121, found: 273.1125.

#### 4.21. 6'-methoxy-2-methyl-3',4-dioxo-2',3'-dihydrospiro[cyclohex[2]ene-1,1'-inden]-4'-yl pivalate (**17**)

A solution of 4'-hydroxy-6'-methoxy-2-methylspiro[cyclohex[2]ene-1,1'-indene]-3',4(2'H)-dione (295 mg, 1.08 mmol) in dry THF (5 mL) was added to NaH (60% dispersion in mineral oil, 65 mg, 1.63 mmol) and the mixture was stirred at 25 °C for 45 min. Pivaloyl chloride (189 μL, 1.52 mmol) was added and the mixture was stirred for additional 1 h. Water (50 mL) was added and the mixture was extracted with EtOAc (3 x 50 mL). The combined organic extracts were dried over Na<sub>2</sub>SO<sub>4</sub>, filtered,

and concentrated. The residue was purified by column chromatography (silica gel, EtOAc/hexane (1:1)) to afford **17** (352 mg, 92%) as a white solid. mp 136-138 °C; <sup>1</sup>H NMR (300 MHz, CDCl<sub>3</sub>) δ = 6.63 (br. s, 1H), 6.59 (br. s, 1H), 6.00 (br. s, 1H), 3.86 (s, 3H), 2.81 (d<sub>AB</sub>, *J* = 18.7 Hz, 1H), 2.64 (d<sub>AB</sub>, *J* = 18.9 Hz, 1H), 2.57 – 2.30 (m, 3H), 2.11 - 2.01 (m, 1H), 1.64 (br. s, 3H); 1.40 (s, 9H); <sup>13</sup>C NMR (75 MHz, CDCl<sub>3</sub>) δ = 198.2, 197.6, 176.0, 166.5, 162.14, 162.09, 149.5, 128.5, 121.9, 109.1, 106.6, 55.1, 47.4, 46.8, 39.1, 37.1, 34.9, 27.1 (3C), 20.4; IR (KBr):  $\tilde{\nu}$  = 2978 cm<sup>-1</sup> (w), 2956 (w), 2931 (w), 1759 (s), 1711 (s), 1670 (s), 1591 (m), 1481 (m), 1438 (m), 1340 (w), 1332 (w), 1310 (s), 1261 (m), 1244 (m), 1142 (s), 1109 (s), 1084 (s), 1036 (m), 1009 (m), 897 (w), 856 (w); HRMS (APCI): calcd. for C<sub>21</sub>H<sub>25</sub>O<sub>5</sub> [M+H]<sup>+</sup>: 357.1697, found: 357.1695.

#### 4.22. 4-((*tert*-butyldimethylsilyloxy)-6'-methoxy-2-methyl-3'-oxo-2',3'-dihydrospiro-[cyclohexa[2,4]diene-1,1'-inden]-4'-yl pivalate (**18**)

TBSOTf (143 μL, 0.61 mmol) was added to a solution of **17** (135 mg, 0.38 mmol) in CH<sub>2</sub>Cl<sub>2</sub> (1 mL) at -78 °C, then DBU (92 μL, 0.61 mmol) was added dropwise and the reaction mixture was stirred at -78 °C for 30 min, filtered through a pad of silica gel (1 cm height, 2 cm diameter), and the pad was quickly washed with EtOAc (100 mL). After evaporation of the solvents from the filtrate, **18** (152 mg, 85%) was obtained as a colorless semi-solid, which was used in the next step without any further purification. Analytically pure sample was obtained by preparative TLC (silica gel, EtOAc/hexane (1:2)); <sup>1</sup>H NMR (300 MHz, CDCl<sub>3</sub>) = 6.84 (d, *J* = 2.0 Hz, 1H), 6.54 (d, *J* = 2.0 Hz, 1H), 5.67 (br. s, 1H), 4.85 – 4.79 (m, 1H), 3.88 (s, 3H), 2.81 (d<sub>AB</sub>, *J* = 18.3 Hz, 1H), 2.74 (dd, *J* = 16.9 Hz, *J* = 2.6 Hz, 1H), 2.45 (d<sub>AB</sub>, *J* = 18.3 Hz, 1H), 2.26 (dd, *J* = 16.9 Hz, *J* = 5.8 Hz, 1H), 1.53 (s, 3H), 1.41 (s, 9H), 0.95 (s, 9H), 0.16 (s, 6H); <sup>13</sup>C NMR (126 MHz, CDCl<sub>3</sub>) δ = 200.3, 176.2, 166.1, 163.9, 149.1, 148.9, 141.0, 124.2, 122.0, 108.6, 107.3, 99.0, 56.0 (2C), 48.4, 46.4, 39.1, 38.6, 27.2 (3C), 25.7 (3C), 19.5, 18.1, - 4.4; IR (KBr):  $\tilde{\nu}$  = 2958 cm<sup>-1</sup> (m), 2931 (m), 2856 (w), 1761 (s), 1711 (s), 1674 (s), 1610 (s), 1589 (s), 1479 (m), 1462 (m), 1461 (m), 1441 (m), 1396 (w), 1340 (m), 1310 (s), 1273 (m), 1244 (m), 1194 (w), 1144 (s), 1109 (s), 1186 (s), 1036 (m), 862 (w), 839 (w); HRMS (APCI): calcd. for C<sub>27</sub>H<sub>39</sub>O<sub>5</sub>Si [M+H]<sup>+</sup>: 471.2561, found: 471.2560.

#### 4.23. 5-hydroxy-6'-methoxy-2-methyl-3',4'-dioxo-2',3'-dihydrospiro[cyclohex[2]ene-1,1'-inden]-4'-yl pivalate (**19**)

*m*CPBA (77%, 110 mg, 0.49 mmol) was added to a mixture of **18** (155 mg, 0.33 mmol) and KHCO<sub>3</sub> (77 mg, 0.77 mmol) in CH<sub>2</sub>Cl<sub>2</sub> (5 mL) at 0 °C and the reaction mixture was stirred at 25 °C for 16 h. EtOAc (50 mL) was added and the mixture was washed with saturated aqueous solution of NaHCO<sub>3</sub> (20 mL), then with H<sub>2</sub>O (30 mL), dried over Na<sub>2</sub>SO<sub>4</sub>, filtered, and concentrated in a vacuum. The

residue was dissolved in CH<sub>2</sub>Cl<sub>2</sub> (10 mL), pyr.HF (1 mL) was added, and the mixture was stirred at 25 °C for 16 h. The mixture was diluted with H<sub>2</sub>O (10 mL) and extracted with EtOAc (3 x 30 mL). The combined organic extracts were dried over Na<sub>2</sub>SO<sub>4</sub>, filtered, and concentrated under reduced pressure. The residue was purified by preparative TLC (silica gel, EtOAc/hexane (2:1)) to afford **19** (45 mg, 37%) as a colorless semi solid. <sup>1</sup>H NMR (500 MHz, CDCl<sub>3</sub>) δ = 6.71 (d, *J* = 2.0 Hz, 1H), 6.63 (d, *J* = 2.0 Hz, 1H), 6.16 – 6.15 (m, 1H), 4.57 (dd, *J* = 12.9 Hz, *J* = 5.8 Hz, 1H), 3.87 (s, 3H), 3.08 (d<sub>AB</sub>, *J* = 18.7 Hz, 1H), 2.56 (d<sub>AB</sub>, *J* = 18.7 Hz, 1H), 2.50 (dd, *J* = 13.2 Hz, *J* = 5.8 Hz, 1H), 2.27 (dd, *J* = 13.2 Hz, *J* = 12.9 Hz, 1H), 1.78 (d, *J* = 1.2 Hz, 3H), 1.43 (s, 9H); <sup>13</sup>C NMR (126 MHz, CDCl<sub>3</sub>) δ = 198.4, 198.1, 176.1, 166.3, 163.5, 159.0, 150.1, 125.9, 121.3, 109.0, 107.6, 69.0, 56.2, 51.1, 48.2, 44.1, 39.2, 27.2 (3C), 20.1; IR (KBr):  $\tilde{\nu}$  = 2976 cm<sup>-1</sup> (w), 2933 (w), 1759 (s), 1711 (s), 1684 (s), 1608 (s), 1587 (s), 1479 (w), 1440 (w), 1340 (m), 1308 (m), 1244 (m), 1142 (s), 1109 (s), 1053 (w), 1032 (w), 899 (w), 867 (w); HRMS (APCI): calcd. for C<sub>21</sub>H<sub>25</sub>O<sub>6</sub> [M+H]<sup>+</sup>: 373.1646, found: 373.1641.

#### 4.24. 4',5-dihydroxy-6'-methoxy-2-methylspiro[cyclohexa[2,5]diene-1,1'-indene]-3',4(2'*H*)-dione (cDHAs)

K<sub>2</sub>CO<sub>3</sub> (44.5 mg, 0.322 mmol) was added to a solution of **19** (38 mg, 0.107 mmol) in MeOH (4 mL), and the mixture was stirred in an open flask at 50 °C for 6 h. MeOH was then evaporated and the residue was dissolved in H<sub>2</sub>O (10 mL) and the pH was adjusted to 7 with 1 M HCl. The mixture was extracted with EtOAc (4 x 10 mL), the combined organic extracts were dried over Na<sub>2</sub>SO<sub>4</sub>, filtered, and the solvent was evaporated. The residue was purified by preparative TLC (silica gel, CH<sub>2</sub>Cl<sub>2</sub>/EtOAc (2:1)) to afford **cDHAs** (14.5 mg, 50%) as a white solid. mp 177 °C (dec.); <sup>1</sup>H NMR (300 MHz, CDCl<sub>3</sub>) δ = 9.02 (br. s, 1H), 6.42 – 6.33 (m, 3H), 6.14 (d, *J* = 1.7 Hz, 1H), 6.03, (s, 1H), 3.83 (s, 3H), 2.92 (s, 2H), 1.75 (s, 3H); <sup>13</sup>C NMR (126 MHz, CDCl<sub>3</sub>) δ = 203.4, 181.6, 168.8, 162.8, 159.3, 156.8, 146.0, 125.5, 120.0, 116.0, 102.6, 101.0, 56.1, 50.8, 47.3, 19.5; IR (KBr):  $\tilde{\nu}$  = 3387 cm<sup>-1</sup> (w), 2955 (w), 2922 (m), 2850 (w), 1680 (s), 1639 (s), 1628 (s), 1433 (w), 1420 (w), 1377 (m), 1311 (m), 1205 (s), 1176 (m), 1148 (s), 1105 (w), 1022 (w), 887 (w); HRMS (APCI): calcd. for C<sub>16</sub>H<sub>15</sub>O<sub>5</sub> [M+H]<sup>+</sup>: 287.0914, found: 287.0912.

Crystal data for **cDHAs**: CCDC ref. No. 1012668. Crystallized from CHCl<sub>3</sub>.

### Measurement of inhibitory activities of mammalian pols

The four mammalian pols  $\alpha$ ,  $\gamma$ ,  $\kappa$ , and  $\lambda$  were prepared, and the reaction mixtures for these pols, as described previously.<sup>23</sup> Briefly, poly(dA)/oligo(dT)<sub>18</sub> (A/T, 2:1) and [<sup>3</sup>H]-dTTP (100 cpm/pmol) were used as the DNA template-primer substrate and nucleotide (dNTP; 2'-deoxynucleotide-5'-triphosphate) substrate, respectively. The tested compounds were dissolved in distilled dimethyl sulfoxide (DMSO) at concentrations 0 – 200  $\mu$ M. Subsequently, 4- $\mu$ L aliquots were mixed with 16  $\mu$ L of each enzyme (0.05 units) in 50 mM Tris-HCl (at pH 7.5) containing 1 mM dithiothreitol, 50% glycerol (v/v), and 0.1 mM ethylenediaminetetraacetic acid, and were held at 0°C for 10 min. Subsequently, 8  $\mu$ L of these inhibitor-enzyme mixtures were added to 16- $\mu$ L aliquots of enzyme standard reaction mixture containing 50 mM Tris-HCl (at pH 7.5), 1 mM dithiothreitol, 1 mM MgCl<sub>2</sub>, 15% glycerol, 5  $\mu$ M poly(dA)/oligo(dT)<sub>18</sub> (A/T, 2:1) and 10  $\mu$ M [<sup>3</sup>H]-dTTP, and were incubated at 37 °C for 60 min. The enzyme activity in the absence of inhibitor was taken as 100% (the activity without the enzyme was considered 0%), and the inhibitory activity was determined for each inhibitor concentration. One unit of pol activity was defined as the amount of each enzyme that catalyzed incorporation of 1 nmol dTTP into synthetic DNA template-primers in 60 min at 37 °C, under standard reaction conditions.<sup>24</sup> The 50% inhibitory concentration (IC<sub>50</sub> value) of the enzyme inhibitor was determined by constructing a dose-response curve and examining the effect of different concentrations of inhibitor on reversing enzyme activity (functional antagonist assay).

## References

- [1] Ljungman, M. *Chem. Rev.* **2009**, *109*, 2929-2950.
- [2] Martin, S. A.; McCabe, N.; Mullarkey, M.; Cummings, R.; Burgess, D. J.; Nakabeppu, Y.; Oka, S.; Kay, E.; Lord, C. J.; Ashworth, A. *Cancer Cell* **2010**, *17*, 235-248.
- [3] Taricani, L.; Shanahan, F.; Parry, D. *Cell Cycle* **2009**, *8*, 482-489.
- [4] Wright, G. E.; Hubschner, U.; Khan, N. N.; Focher, F.; Verri, A. *FEBS Letters* **1994**, *341*, 128-130.
- [5] (a) Mizushina, Y.; Kamisuki, S.; Mizuno, T.; Takemure, M.; Asahara, H.; Linn, S.; Yamaguchi, T.; Matsukage, A.; Hanaoka, F.; Yoshida, S.; Saneyoshi, M.; Sugawara, F.; Sakaguchi, K. *J. Biol. Chem.* **2000**, *275*, 33957-33961; (b) Mizushina, Y. *Biosci. Biotechnol. Biochem.* **2009**, *73*, 1239-1251.
- [6] Jackson, D. A. *Nucleic Acid Res.* **1990**, *18*, 753-758.
- [7] Kamisuki, S.; Takahashi, S.; Mizushina, Y.; Sakaguchi, K.; Nakata, T.; Sugawara, F. *Bioorg. Med. Chem.* **2004**, *12*, 5355-5359.
- [8] Kuramochi, K.; Fukudome, K.; Kuryama, I.; Takeuchi, T.; Sato, Y.; Kamisuki, S.; Tsubaki, K.; Sugawara, F.; Yoshida, H.; Mizushina, Y. *Bioorg. Med. Chem.* **2009**, *17*, 7227-7238.
- [9] Beugelmans, R.; Chastanet, J.; Ginsburg, H.; Quintero-Cortes, L.; Roussi, G. *J. Org. Chem.* **1985**, *50*, 4933-4938.
- [10] Chidambaram, N.; Chandrasekaran, S. *J. Org. Chem.* **1987**, *52*, 5048-5051.
- [11] Catino, J. A.; Nichols, M. J.; Choi, H.; Gottipamula, S.; Doyle, M. P. *Org. Lett.* **2005**, *7*, 5167-5170.
- [12] Doering, W. v. E.; Benkhoff, J.; Shao, L. *J. Am. Chem. Soc.* **1999**, *121*, 962-968.
- [13] Hoye, T. R.; Chen, M.; Hoang, B.; Mi, L.; Priest, O. P. *J. Org. Chem.* **1999**, *64*, 7184-7201.
- [14] Singh, S.; Guiry, P. J. *J. Org. Chem.* **2009**, *74*, 5758-5761.
- [15] Jiang, S.; Li, P.; Lai, C. C.; Kelley, J. A.; Roller, P. P. *J. Org. Chem.* **2006**, *71*, 7307-7314.
- [16] Srikrishna, A.; Ramasastry, S. S. V. *Tetrahedron Lett.* **2005**, *46*, 7373-7376.
- [17] (a) Krafft, M. E.; Holton, R. A. *J. Am. Chem. Soc.* **1984**, *106*, 7619-7621; (b) Ihara, M.; Ishida, Y.; Fukumoto, K.; Kametani, T. *Chem. Phar. Bull.* **1985**, *33*, 4102-4105; (c) Jung, Y. C.; Yoon, C. H.; Turos, E.; Yoo, K. S.; Jung, K. W. *J. Org. Chem.* **2007**, *72*, 10114-10122.
- [18] Myobatake, Y.; Takeuchi, T.; Kuramochi, K.; Kuriyama, I.; Ishido, T.; Hirano, K.; Sugawara, F.; Yoshida, H.; Mizushina, Y. *J. Nat. Prod.* **2012**, *75*, 135-141.
- [19] *Bioisosteres in Medicinal Chemistry*; Brown, N., Ed.; Wiley-VCH, 2012.
- [20] Baranovskiy, A. G.; Babayeva, N. D.; Suwa, Y.; Gu, J.; Pavlov, Y. I.; Tahirov, T. H. *Nucleic Acids Res.* **2014**, *42*, 14013-14021.

- [21] Findlay, J. A.; Kwan, D. *Can. J. Chem.* **1973**, *51*, 3299-3301.
- [22] El-Feraly, F. S.; Cheatham, S. F.; McChesney, J. D. *Can. J. Chem.* **1985**, *63*, 2232-2236.
- [23] (a) Mizushina, Y.; Tanaka, N.; Yagi, H.; Kurosawa, T.; Onoue, M.; Seto, H.; Horie, T.; Ayoagi, N.; Yamaoka, M.; Matsukage, A.; Yoshida, S.; Sakaguchi, K. *Biochim. Biophys. Acta* **1996**, *1308*, 256-262; (b) Mizushina, Y.; Yoshida, S.; Matsukage, A.; Sakaguchi, K. *Biochim. Biophys. Acta* **1997**, *1336*, 509-521; (c) Myobatake, Y.; Takeuchi, T.; Kuramochi, K.; Kuriyama, I.; Ishido, T.; Hirano, K.; Sugawara, F.; Yoshida, H.; Mizushina, Y. *J. Nat. Prod.* **2012**, *75*, 135-141.

## Supporting information

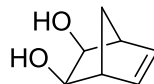
### Highly Diastereoselective Flexible Synthesis of New Carbocyclic C-nucleosides

Lukáš Maier,<sup>a,b#</sup> Prashant Khirsariya,<sup>a,b#</sup> Ondřej Hylse,<sup>a,b</sup> Santosh Kumar Adla,<sup>a</sup> Lenka Černová,<sup>a</sup> Michal Poljak,<sup>a</sup> Soňa Krajčovičová,<sup>a</sup> Erik Weis,<sup>a</sup> Stanislav Drápela,<sup>b,c</sup> Karel Souček,<sup>b,c</sup> and Kamil Paruch<sup>a,b\*</sup>

### Table of contents

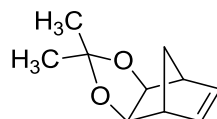
1. Experimental procedures.....	2
2. <sup>1</sup> H, <sup>13</sup> C NMR spectra related to key cyclopentanone synthesis.....	16
3. <sup>1</sup> H, <sup>13</sup> C NMR spectra related to nucleophilic addition pathway.....	77
4. <sup>1</sup> H, <sup>13</sup> C NMR spectra related to enol triflate pathway.....	126
5. <sup>1</sup> H, <sup>13</sup> C NMR spectra related to 5' and 2' modifications.....	214
6. <sup>1</sup> H, <sup>13</sup> C NMR spectra related to the preparation of optically active intermediates.....	236
7. Selected IR spectra, HPLC chromatograms and CD spectra.....	245
8. Cell-based assays.....	260

**(1R\*,2R\*,3S\*,4S\*)-bicyclo[2.2.1]hept-5-ene-2,3-diol (S-1).**



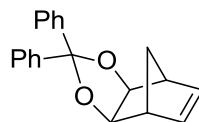
NMO (19.06 g, 162.8 mmol) and OsO<sub>4</sub> (4% wt. in H<sub>2</sub>O, 2.04 mL, 0.2 mol %) were added to a solution of norbornadiene (15.0 g, 162.8 mmol) in acetone and H<sub>2</sub>O (200 + 50 mL) and the reaction mixture was stirred at 40 °C for 14 h. After cooling to 25 °C, Na<sub>2</sub>S<sub>2</sub>O<sub>5</sub> (1.00 g) was added and the reaction mixture was stirred at 25 °C for another 30 min. All volatiles were removed under reduced pressure and the black residue was purified by flash column chromatography (hexane/EtOAc = 2:1) to afford **S-1** as a white crystalline solid (8.42 g, 41%). <sup>1</sup>H NMR (500 MHz, CDCl<sub>3</sub>): δ = 6.04 (m, 2H), 3.71 (m, 2H), 2.95 (m, 2H), 2.70 (m, 2H), 1.89 (dm, *J* = 9.2 Hz, 1H), 1.63 (dm, *J* = 9.2 Hz, 1H) ppm. <sup>13</sup>C NMR (126 MHz, CDCl<sub>3</sub>): δ = 136.56, 69.18, 48.21, 42.37 ppm. The spectral data were consistent with the literature.<sup>7</sup>

**(exo, exo)-5,6-dimethylmethylenedioxy-bicyclo[2.2.1]hept-2-ene (6a).**



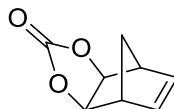
2,2-dimethoxypropane (26.0 mL, 196.6 mmol) and TsOH (5 mg) were added to a solution of diol **S-1** (6.2 g, 49.2 mmol) in acetone (75 mL). The reaction mixture was stirred at 25 °C for 20 min., the solvent was evaporated and the residue was purified on a short pad of silica gel (hexane/EtOAc = 20:1) to afford **6a** as a colorless oil which solidified upon standing at -20 °C (7.86 g, 95 %). <sup>1</sup>H NMR (500 MHz, CDCl<sub>3</sub>): δ = 6.05 (m, 2H), 4.18 (d, *J* = 1.6 Hz, 2H), 2.76 (m, 2H), 1.97 (m, 1H), 1.67 (m, 1H), 1.47 (s, 3H), 1.32 (s, 3H) ppm. <sup>13</sup>C NMR (126 MHz, CDCl<sub>3</sub>): δ = 136.89, 113.81, 80.63, 45.35, 43.02, 26.32, 24.58 ppm. The spectral data were consistent with the literature.<sup>7</sup>

**(3aR\*,4R\*,7S\*,7aS\*)-2,2-diphenyl-3a,4,7,7a-tetrahydro-4,7-methanobenzo[d][1,3]dioxole (6b).**



Benzophenone dimethyl ketal (2.08 g, 9.15 mmol) was added to a solution of **S-1** (0.800 g, 6.34 mmol) in CH<sub>2</sub>Cl<sub>2</sub> (8 mL), followed by addition of TsOH (1 mg), and the reaction mixture was stirred at 25 °C for 18 h. The solvent was evaporated and the residue was purified by flash column chromatography (hexane/EtOAc = 20:1) to afford **6b** (1.60 g) contaminated with residual benzophenone and benzophenone dimethyl ketal as a white crystalline solid. This material was used for the next step (preparation of compound **S-3**) without further purification. An analytical sample could be obtained by repeated flash column chromatography with slow gradient elution (hexane to hexane/EtOAc = 20:1) as a white crystalline solid. m.p. = 123-127 °C. <sup>1</sup>H NMR (500 MHz, CDCl<sub>3</sub>): δ = 7.58-7.56 (m, 2H), 7.51-7.49 (m, 2H), 7.37-7.34 (m, 2H), 7.31-7.26 (m, 4H), 6.05 (m, 2H), 4.13 (d, *J* = 1.6 Hz, 2H), 2.97 (m, 2H), 2.21 (dm, *J* = 8.9 Hz, 1H), 1.77 (dm, *J* = 8.9 Hz, 1H). <sup>13</sup>C NMR (126 MHz, CDCl<sub>3</sub>): δ = 143.03, 141.71, 137.06, 128.46, 128.40, 128.28, 128.07, 126.73, 126.24, 114.41, 81.31, 45.43, 43.78 ppm. IR ( $\tilde{\nu}_{\text{max}}$ ) = 2979 (w), 2946 (w), 2924 (w), 1489 (m), 1270 (m), 1203 (m), 1019 (s), 747 (s), 703 (s), 694 (s) cm<sup>-1</sup>. HR-MS (EI) calculated for C<sub>20</sub>H<sub>18</sub>O<sub>2</sub>: 290.1307. Found: 290.1311.

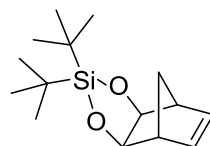
**(3aR\*,4R\*,7S\*,7aS\*)-3a,4,7,7a-tetrahydro-4,7-methanobenzo[d][1,3]dioxol-2-one (6c).**



1,1'-carbonyldiimidazole (0.250 g, 1.98 mmol) was added to a solution of starting material **S-1** (0.200 g, 1.58 mmol) in anhydrous toluene (6 mL) and the reaction mixture was stirred at 55 °C for 16 h. The reaction mixture was then cooled to 25 °C and the solvent was evaporated. The residue was purified by flash column chromatography (hexane/EtOAc = 5:1) to afford **6-c** as a white crystalline solid (0.191 g, 80%). m.p. = 86-

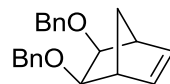
88 °C.  $^1\text{H}$  NMR (500 MHz,  $\text{CDCl}_3$ ):  $\delta$  = 6.12 (m, 2H), 4.56 (d,  $J$  = 1.4 Hz, 2H), 3.14 (m, 2H), 1.90-1.82 (m, 2H) ppm.  $^{13}\text{C}$  NMR (126 MHz,  $\text{CDCl}_3$ ):  $\delta$  = 156.53, 136.17, 78.92, 45.79, 41.15 ppm. IR ( $\tilde{\nu}_{\text{max}}$ ) = 3011 (w), 1777 (s), 1367 (m), 1160 (s), 1055 (s), 1014 (s), 742 (s), 697 (s)  $\text{cm}^{-1}$ . HR-MS (ESI) calculated for  $\text{C}_8\text{H}_8\text{O}_3$  [ $\text{M}+\text{Na}$ ] $^+$  : 175.0371. Found: 175.0370.

**(1R\*,4S\*,5S\*,6R\*)-5,6-bis(triisopropylsilyloxy)bicyclo[2.2.1]hept-2-ene (6d).**



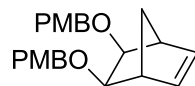
Imidazole (1.78 g, 26.16 mmol) was added to a cooled solution (0 °C, ice bath) of **S-1** (1 g, 7.93 mmol) in anhydrous DMF (10 mL) followed by dropwise addition of di-tert-butylsilyl bis(trifluoromethanesulfonate) (2.84 mL, 8.72 mmol). The reaction mixture was stirred while allowed to warm to 25 °C for 14 h.  $\text{H}_2\text{O}$  (60 mL) was added slowly and the mixture was extracted with  $\text{Et}_2\text{O}$  ( $3 \times 50$  mL). The organic extracts were dried over  $\text{Na}_2\text{SO}_4$ , filtered, and the solvent was evaporated. The residue was purified by flash column chromatography (hexane/ $\text{EtOAc}$  = 20:1) to afford **6d** as a colorless oil (1.42 g, 78%).  $^1\text{H}$  NMR (500 MHz,  $\text{CDCl}_3$ ):  $\delta$  = 6.06 (m, 2H), 4.15 (d,  $J$  = 1.5 Hz, 2H), 2.79 (m, 2H), 2.20 (dm,  $J$  = 9.2 Hz, 1H), 1.64 (dm,  $J$  = 9.2 Hz, 1H), 1.12 (s, 9H), 1.05 (s, 9H) ppm.  $^{13}\text{C}$  NMR (126 MHz,  $\text{CDCl}_3$ ):  $\delta$  = 137.51, 78.53, 47.20, 42.51, 28.30, 27.73, 22.88, 20.62 ppm. IR ( $\tilde{\nu}_{\text{max}}$ ) = 2933 (w), 2858 (w), 1475 (m), 1171 (w), 1036 (s), 1021 (s), 853 (s), 823 (s), 704 (m), 648 (m)  $\text{cm}^{-1}$ . HR-MS (ESI) calculated for  $\text{C}_{15}\text{H}_{27}\text{O}_2\text{Si}$  [ $\text{M}+\text{H}$ ] $^+$  : 267.1780. Found: 267.1779.

**(1R\*,4S\*,5S\*,6R\*)-5,6-bis(benzyloxy)bicyclo[2.2.1]hept-2-ene (6e).**



A solution of diol **S-1** (4.88 g, 38.70 mmol) in DMF (40 mL) was added dropwise to a suspension of NaH (60% dispersion in mineral oil, 4.64 g, 116.11 mmol) in DMF (20 mL). The reaction mixture was stirred at 25 °C for 20 min, benzyl bromide (11.05 mL, 92.9 mmol) was slowly added, followed by a solution of tetra-*N*-butyl ammonium iodide (1.43 g, 3.87 mmol) in DMF (10 mL). The reaction mixture was stirred at 25 °C for additional 14 h and then quenched by dropwise addition of H<sub>2</sub>O (5 mL). H<sub>2</sub>O (100 mL) was added and the mixture was extracted with Et<sub>2</sub>O (4 × 100 mL). The combined organic extracts were dried over Na<sub>2</sub>SO<sub>4</sub>, filtered, and the solvent was evaporated. The resulting yellow oil was purified by flash column chromatography (hexane/EtOAc = 20:1) to afford **6e** as a white crystalline solid (9.08 g, 77%), m.p. = 65.9-66.1 °C. <sup>1</sup>H NMR (500 MHz, CDCl<sub>3</sub>): δ = 7.37-7.26 (m, 10H), 6.01 (m, 2H), 4.69-4.63 (m, 4H), 3.53 (m, 2H), 2.85 (m, 2H), 2.20 (m, 1H), 1.67 (m, 1H) ppm. <sup>13</sup>C NMR (126 MHz, CDCl<sub>3</sub>): δ = 139.23, 137.02, 128.48, 128.00, 127.59, 77.19, 72.50, 45.88, 44.18 ppm. IR (ν<sub>max</sub>) = 3063 (w), 3029 (w), 1496 (w), 1453 (m), 1343 (w), 1114 (m), 733 (s), 696 (s) cm<sup>-1</sup>. HR-MS (ESI) calculated for C<sub>21</sub>H<sub>22</sub>O<sub>2</sub> [M+Na]<sup>+</sup>: 329.1517. Found: 329.1524.

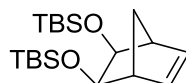
**(1R\*,4S\*,5S\*,6R\*)-5,6-bis(4-methoxybenzyloxy)bicyclo[2.2.1]hept-2-ene (6f).**



A solution of diol **S-1** (1.18 g, 9.37 mmol), in DMF (20 mL), was added dropwise to a suspension of NaH (60% dispersion in mineral oil, 1.12 g, 28.11 mmol) in DMF (20 mL). The reaction mixture was stirred at 25 °C for 20 min, 4-methoxybenzyl chloride (2.8 mL, 20.62 mmol) was slowly added, followed by a solution of tetra-*N*-butyl ammonium iodide (0.346 g, 0.94 mmol) in DMF (10 mL). The reaction mixture was stirred at 25 °C for additional 14 h and then quenched by dropwise addition of H<sub>2</sub>O (5 mL). H<sub>2</sub>O (100 mL) was added and the mixture was extracted with Et<sub>2</sub>O (4 × 100 mL). The combined organic extracts were dried over Na<sub>2</sub>SO<sub>4</sub>, filtered, and the solvent was evaporated. The resulting yellow oil was purified by flash column chromatography (hexane/EtOAc = 15:1) to afford **6f** as a white wax (3.2 g, 93%). <sup>1</sup>H NMR (500 MHz, CDCl<sub>3</sub>): δ = 7.27 (d, *J* = 8.6 Hz, 4H), 6.85 (d, *J* = 8.6 Hz, 4H), 5.99 (m, 2H), 4.58 (d, *J* = 11.7 Hz, 2H), 4.53 (d, *J* = 11.7 Hz, 2H), 3.80 (s, 6H), 3.48 (d, *J* =

1.8 Hz, 2H), 2.80 (m, 2H), 2.16-2.14 (m, 1H), 1.64-1.62 (m, 1H) ppm.  $^{13}\text{C}$  NMR (126 MHz,  $\text{CDCl}_3$ ):  $\delta$  = 159.29, 137.01, 131.35, 129.59, 113.89, 76.98, 76.79, 72.10, 55.50, 45.87, 44.17 ppm. IR ( $\tilde{\nu}_{\text{max}}$ ) = 2991 (w), 2952 (w), 1402 (m), 1257 (m), 1109 (s), 741 (s), 694, 650 ( $\text{cm}^{-1}$ ).

**(1R\*,4S\*,5S\*,6R\*)-5,6-bis(tert-butyldimethylsilyloxy)bicyclo[2.2.1]hept-2-ene (6g).**



Imidazole (0.558 g, 8.21 mmol) and TBSCl (0.544 g, 3.61 mmol) were added to a solution of **S-1** (0.207 g, 1.64 mmol) in  $\text{CH}_2\text{Cl}_2$  (15 mL) and the reaction mixture was stirred at 25 °C for 14 h. The solvent was evaporated and the residue was purified by flash column chromatography (hexane/EtOAc = 10:1) to afford **6g** as a white semi-solid (0.44 g, 76%).  $^1\text{H}$  NMR (500 MHz,  $\text{CDCl}_3$ ):  $\delta$  = 6.00 (m, 2H), 3.64 (m, 2H), 2.53 (m, 2H), 2.14 (dm,  $J$  = 8.2 Hz, 1H), 1.56 (dm,  $J$  = 8.2 Hz, 1H) 0.91 (s, 18H), 0.07 (s, 6H), 0.05 (s, 6H) ppm.  $^{13}\text{C}$  NMR (126 MHz,  $\text{CDCl}_3$ ):  $\delta$  = 136.95, 70.98, 49.65, 43.41, 26.30, 18.60, -4.02, -4.65 ppm. IR ( $\tilde{\nu}_{\text{max}}$ ) = 1481 (w), 1103 (m), 759 (s), 693 ( $\text{cm}^{-1}$ ).

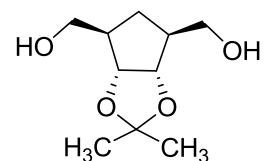
**(1R\*,4S\*,5S\*,6R\*)-5,6-bis(tert-butyldiphenylsilyloxy)bicyclo[2.2.1]hept-2-ene (6h).**



TBDPSCl (1 mL, 3.96 mmol) and imidazole (0.433 g, 6.36 mmol) were added to a solution of **S-1** (0.200 g, 1.59 mmol) in  $\text{CH}_2\text{Cl}_2$  (10 mL) and the reaction mixture was stirred at 25 °C for 14 h. The solvent was evaporated and the yellow residue was purified by flash column chromatography (hexane/EtOAc = 20:1) to afford **6h** as a white crystalline solid (0.24 g, 25 %), along with the mono-silylated side-product (0.417 g, 43%). m.p. = 133-136 °C.  $^1\text{H}$  NMR (500 MHz,  $\text{CDCl}_3$ ):  $\delta$  = 7.76-7.72 (m, 8H), 7.41-7.31 (m, 12H), 5.53 (m, 2H), 3.87 (d,  $J$  = 1.5 Hz, 2H), 2.32 (dm,  $J$  = 8.6 Hz, 1H), 2.24 (m, 2H), 1.38 (dm,  $J$  = 8.6 Hz, 1H), 1.10 (s, 18H) ppm.  $^{13}\text{C}$  NMR (126 MHz,  $\text{CDCl}_3$ ):  $\delta$  = 136.63, 136.27,

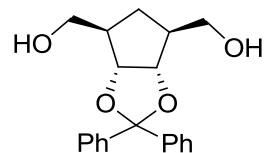
136.15, 135.28, 134.70, 129.71, 129.60, 127.68, 127.67, 72.30, 48.87, 42.96, 27.43, 19.60 ppm. IR ( $\tilde{\nu}_{\max}$ ) = 1472 (w), 1102 (m), 1086 (m), 697 (s), 499 (s), 481 (s)  $\text{cm}^{-1}$ . HR-MS (ESI) calculated for  $\text{C}_{39}\text{H}_{46}\text{O}_2\text{Si}_2$   $[\text{M}+\text{Na}]^+$ : 625.29285. Found: 625.29285.

**((3aR\*,4R\*,6S\*,6aS\*)-2,2-dimethyltetrahydro-3aH-cyclopenta[d][1,3]dioxol-4,6-diyl)dimethanol (S-2).**



Prepared by general procedure A using 6.2 g (37.32 mmol) of **6a**; flash column chromatography ( $\text{CH}_2\text{Cl}_2/\text{MeOH} = 20:1$  to  $10:1$ ) afforded **S-2** as a colorless oil (5.11 g, 67%).  $^1\text{H}$  NMR (500 MHz,  $\text{CDCl}_3$ ):  $\delta = 4.41$  (m, 2H), 3.69 (m, 4H), 2.28 (m, 2H), 2.08 (m, 1H), 1.68 (br s, 2H), 1.51 (s, 3H), 1.32 (s, 3H), 1.26 (m, 1H) ppm.  $^{13}\text{C}$  NMR (126 MHz,  $\text{CDCl}_3$ ):  $\delta = 112.66$ , 83.67, 64.51, 47.63, 30.66, 27.75, 25.32 ppm. HR-MS (APCI) calculated for  $\text{C}_{10}\text{H}_{18}\text{O}_4$   $[\text{M}+\text{H}]^+$ : 203.1278. Found: 203.1276. The spectral data were consistent with the literature.<sup>7</sup>

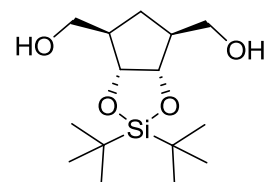
**((3aR\*,4R\*,6S\*,6aS\*)-2,2-diphenyltetrahydro-3aH-cyclopenta[d][1,3]dioxole-4,6-diyl)dimethanol (S-3).**



Prepared by general procedure A using 2.59 g (7.92 mmol) of **6b**; flash column chromatography ( $\text{CH}_2\text{Cl}_2/\text{MeOH} = 20:1$ ) afforded **S-3** as a colorless oil (0.950 g, 37%).  $^1\text{H}$  NMR (500 MHz,  $\text{CDCl}_3$ ):  $\delta = 7.54$ -7.52 (m, 2H), 7.47-7.45 (m, 2H), 7.36-7.26 (m, 6H), 4.41-4.38 (m, 2H), 3.73-3.66 (m, 4H), 2.49-2.45 (m, 2H), 2.17-2.12 (m, 1H), 1.67 (br s, 2H), 1.40-1.33 (m, 1H) ppm.  $^{13}\text{C}$  NMR (126 MHz,  $\text{CDCl}_3$ ):  $\delta = 142.60$ , 142.29,

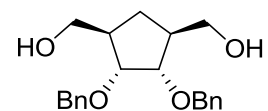
128.50, 128.39, 128.22, 126.70, 126.64, 113.25, 84.42, 64.78, 47.32, 31.01 ppm. IR ( $\tilde{\nu}_{\max}$ ) = 3307 (m), 2924 (m), 1446 (m), 1261 (m), 1086 (m), 1067 (m), 1052 (m), 973 (m), 695 (s), 635 (m)  $\text{cm}^{-1}$ . HR-MS (ESI) calculated for  $\text{C}_{20}\text{H}_{22}\text{O}_4$   $[\text{M}+\text{H}]^+$  : 327.1591. Found: 327.1581.

**((3aR\*,4R\*,6S\*,6aS\*)-2,2-di-tert-butyltetrahydro-3aH-cyclopenta[d][1,3,2]dioxasilole-4,6-diyl)dimethanol (S-4).**



Prepared by general procedure A using 1.19 g (4.49 mmol) of **6c**; flash column chromatography ( $\text{CH}_2\text{Cl}_2/\text{MeOH} = 20:1$ ) afforded **S-4** as a white solid (0.643 g, 62 %). m.p. = 99-103 °C.  $^1\text{H}$  NMR (500 MHz,  $\text{CDCl}_3$ ):  $\delta = 4.29\text{-}4.25$  (m, 2H), 3.76 (d,  $J = 6.1$  Hz, 2H), 2.17 (m, 2H), 1.88 (m, 1H), 1.08 (s, 9H), 1.08 (overlapped, m, 1H), 1.02 (s, 9H) ppm.  $^{13}\text{C}$  NMR (126 MHz,  $\text{CDCl}_3$ ):  $\delta = 81.86, 65.15, 49.47, 28.35, 27.70, 27.03, 22.11, 19.66$  ppm. IR ( $\tilde{\nu}_{\max}$ ) = 3298 (br), 2886 (m), 2858 (m), 1472 (m), 1065 (s), 1032 (s), 849 (m), 819 (m), 651 (m)  $\text{cm}^{-1}$ . HR-MS (ESI) calculated for  $\text{C}_{15}\text{H}_{30}\text{O}_4\text{Si}$   $[\text{M}+\text{Na}]^+$  : 325.18056. Found: 325.18060.

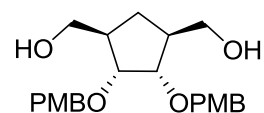
**((1R\*,3S\*,4S\*,5R\*)-4,5-bis(benzyloxy)cyclopentan-1,3-diyl)dimethanol (S-5).**



Prepared by general procedure A using 9.08 g (29.60 mmol) of **6e**; flash column chromatography ( $\text{CH}_2\text{Cl}_2/\text{MeOH} = 20:1$ ) afforded **S-5** as a colorless oil (8.95 g, 88%).  $^1\text{H}$  NMR (500 MHz,  $\text{CDCl}_3$ ):  $\delta = 7.36\text{-}7.28$  (m, 2H), 4.59 (d, AB,  $J = 11.8$  Hz, 2H), 4.52 (d, AB,  $J = 11.8$  Hz, 2H), 3.71 (m, 2H), 3.64 (m, 2H), 3.52 (m, 2H), 2.45 (m, 2H), 1.96 (m, 1H), 1.77 (br s, 2H), 0.93 (m, 1H) ppm.  $^{13}\text{C}$  NMR (126 MHz,  $\text{CDCl}_3$ ):  $\delta =$

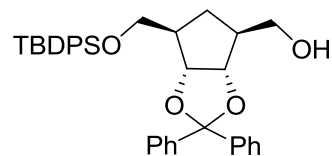
138.51, 128.62, 128.21, 127.93, 81.16, 71.39, 65.42, 43.99, 25.51 ppm. IR ( $\tilde{\nu}_{\max}$ ) = 3310 (m), 2928 (m), 1431 (m), 1250 (m), 1060 (m), 973 (m), 670 (s)  $\text{cm}^{-1}$ . HR-MS (APCI) calculated for  $\text{C}_{21}\text{H}_{26}\text{O}_4$   $[\text{M}+\text{H}]^+$  : 343.1904. Found: 343.1900.

**((1R\*,3S\*,4S\*,5R\*)-4,5-bis(4-methoxybenzyloxy)cyclopentane-1,3-diyl)dimethanol (S-6).**



Prepared by general procedure A using 3.20 g (8.74 mmol) of **6f**; flash column chromatography ( $\text{CH}_2\text{Cl}_2/\text{MeOH} = 20:1$ ) afforded **S-6** as a colorless oil (1.81 g, 56%).  $^1\text{H}$  NMR (500 MHz,  $\text{CDCl}_3$ ):  $\delta = 7.28$  (m, 4H), 6.87 (m, 4H), 4.52 (d, AB,  $J = 11.8$  Hz, 2H), 4.43 (d, AB,  $J = 11.8$  Hz, 2H), 3.81 (s, 6H), 3.67-3.60 (m, 4H), 3.51-3.47 (m, 2H), 2.41 (m, 2H), 1.94 (m, 1H), 1.85 (br s, 2H), 0.90 (m, 1H) ppm.  $^{13}\text{C}$  NMR (126 MHz,  $\text{CDCl}_3$ ):  $\delta = 159.49$ , 130.60, 129.79, 129.61, 114.02, 80.78, 70.93, 65.49, 55.50, 43.97, 25.51. IR ( $\tilde{\nu}_{\max}$ ) = 3367 (b), 2924 (w), 2858 (w), 1448 (m), 1203 (m), 1084 (s), 735 (s), 696 (s)  $\text{cm}^{-1}$ .

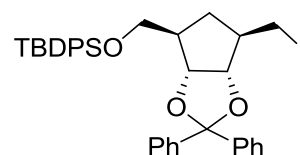
**((3aS\*,4S\*,6R\*,6aR\*)-6-((tert-butyldiphenylsilyloxy)methyl)-2,2-diphenyltetrahydro-3aH-cyclopenta[d][1,3]dioxol-4-yl)methanol (S-7):**



The compound was prepared by essentially same procedure used for compound **7a** from 0.571 g (1.75 mmol) of **S-3**; flash column chromatography (hexane/EtOAc = 5:1) afforded **S-7** as a colorless oil (0.742 g, 75 %).  $^1\text{H}$  NMR (500 MHz,  $\text{CDCl}_3$ ):  $\delta = 7.65$ -7.63 (m, 4H), 7.53-

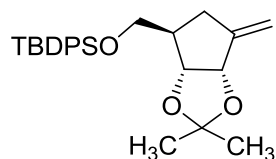
7.51 (m, 2H), 7.48-7.46 (m, 2H), 7.42-7.40 (m, 2H), 7.38-7.27 (m, 10H), 4.40 (dd,  $J = 7.1, 4.9$  Hz, 1H), 4.31 (dd,  $J = 7.1, 5.6$  Hz, 1H), 3.70 (dd,  $J = 6.25, 1.92$  Hz, 2H), 3.66 (m, 2H), 2.51 (m, 1H), 2.42 (m, 1H), 1.05 (s, 9H) ppm.  $^{13}\text{C}$  NMR (126 MHz,  $\text{CDCl}_3$ ):  $\delta = 142.87, 142.48, 135.86, 135.84, 133.89, 129.87, 128.39, 128.35, 128.19, 128.12, 127.89, 126.67, 126.59, 113.14, 84.25, 83.93, 65.26, 65.01, 47.60, 47.00, 31.15, 27.10, 19.54$ . IR ( $\tilde{\nu}_{\text{max}}$ ) = 2930 (w), 1449 (w), 1427 (w), 1264 (m), 1105 (m), 1064 (m), 733 (s), 698 (s)  $\text{cm}^{-1}$ . HR-MS (ESI) calculated for  $\text{C}_{36}\text{H}_{40}\text{O}_4\text{Si}$   $[\text{M}+\text{H}]^+$ : 565.2769. Found: 565.2762.

**tert-butyl(((3aR\*,4R\*,6R\*,6aS\*)-6-(iodomethyl)-2,2-diphenyltetrahydro-3aH-cyclopenta[d][1,3]dioxol-4-yl)methoxy)diphenylsilane (S-8).**



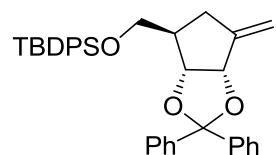
The compound was prepared by essentially same procedure used for compound **8a** from 0.735 g (1.3 mmol) of **S-7**; flash column chromatography (hexane/EtOAc = 40:1) afforded **S-8** as a colorless oil (0.685 g, 78 %).  $^1\text{H}$  NMR (500 MHz,  $\text{CDCl}_3$ ):  $\delta = 7.65\text{-}7.63$  (m, 4H), 7.52-7.50 (m, 2H), 7.47-7.41 (m, 4H), 7.38-7.28 (m, 10H), 4.44 (dd,  $J = 7.2, 5.04$  Hz, 1H), 4.18 (dd,  $J = 7.2, 6.28$  Hz, 1H), 3.74-3.65 (m, 2H), 3.35 (dd,  $J = 9.9, 5.6$  Hz 1H), 3.25 (dd,  $J = 9.9, 7.0$  Hz), 2.51 (m, 1H), 2.37 (m, 1H), 2.11 (m, 1H), 1.40 (m, 1H), 1.06 (s, 9H) ppm.  $^{13}\text{C}$  NMR (126 MHz,  $\text{CDCl}_3$ ):  $\delta = 142.78, 135.87, 135.85, 133.80, 129.91, 128.43, 128.41, 128.23, 128.19, 127.91, 126.57, 126.49, 113.34, 86.00, 84.06, 64.95, 46.96, 46.65, 35.88, 27.12, 19.55, 10.06$  ppm. IR ( $\tilde{\nu}_{\text{max}}$ ) = 2929 (w), 2856 (w), 1489 (w), 1471 (w), 1109 (m), 737 (m), 698 (s), 503 (m)  $\text{cm}^{-1}$ . HR-MS (ESI) calculated for  $\text{C}_{39}\text{H}_{39}\text{IO}_3\text{Si}$   $[\text{M}+\text{Na}]^+$ : 697.1603. Found: 697.1606.

**tert-butyl(((3aR\*,4R\*,6aS\*)-2,2-dimethyl-6-methylenetetrahydro-3aH-cyclopenta[d][1,3]dioxol-4-yl)methoxy)diphenylsilane (S-9).**



DBU (1.04 mL, 7.54 mmol) was added to a solution of **8a** (1.54 g, 2.78 mmol) in toluene (10 mL) and the reaction mixture was stirred at 90 °C for 4 h. The solvent was evaporated under reduced pressure and the residue was purified by flash column chromatography (hexane/EtOAc = 20:1) to afford **S-9** as a colorless oil (0.855 g, 72 %). <sup>1</sup>H NMR (500 MHz, CDCl<sub>3</sub>): δ = 7.65-7.63 (m, 4H), 7.45-7.36 (m, 6H), 5.17 (m, 1H), 5.07 (m, 1H), 4.63 (d, *J* = 5.6 Hz, 1H), 4.50 (d, *J* = 5.6 Hz, 1H), 3.48 (m, 2H), 2.78-2.73 (m, 1H), 2.38 (m, 1H), 2.15 (dm, *J* = 15.9, Hz, 1H), 1.47 (s, 3H), 1.32 (s, 3H), 1.05 (s, 9H) ppm. <sup>13</sup>C NMR (126 MHz, CDCl<sub>3</sub>): δ = 149.83, 135.83, 133.77, 133.75, 129.91, 129.90, 127.90, 112.65, 110.56, 82.74, 81.96, 64.62, 45.85, 32.74, 27.07, 26.99, 24.69, 19.46 ppm. IR ( $\tilde{\nu}_{\max}$ ) = 2930 (m), 1732 (w), 1478 (w), 1222 (w), 1127 (s), 679 (s) cm<sup>-1</sup>.

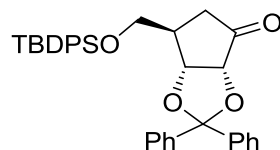
**tert-butyl(((3aR\*,4R\*,6aS\*)-6-methylene-2,2-diphenyltetrahydro-3aH-cyclopenta[d][1,3]dioxol-4-yl)methoxy)diphenylsilane (S-10).**



The compound was prepared by essentially same procedure used for compound **S-9** from 0.685 g (1.015 mmol) of **S-8**; flash column chromatography (hexane/EtOAc = 20:1) afforded **S-10** as a colorless oil (0.433 g, 78 %). <sup>1</sup>H NMR (500 MHz, CDCl<sub>3</sub>): δ = 7.59-7.55 (m, 6H), 7.42-7.31 (m, 14H), 5.21 (m, 1H), 4.47 (d, *J* = 5.90 Hz, 1H), 4.41 (d, *J* = 5.9 Hz, 1H), 3.44 (m, 2H), 2.85 (m, 1H), 2.57 (m, 1H), 2.18 (m, 1H), 1.03 (s, 9H) ppm. <sup>13</sup>C NMR (126 MHz, CDCl<sub>3</sub>): δ = 147.24, 138.94, 138.82, 135.85, 135.82, 134.02, 129.81, 129.79, 128.51, 128.45, 128.15,

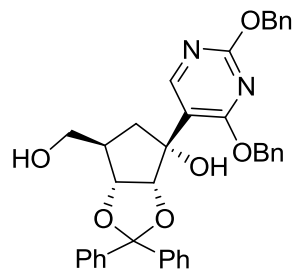
128.00, 127.86, 127.65, 112.32, 110.93, 80.39, 79.53, 71.77, 69.65, 64.04, 43.66, 30.15, 27.11, 19.60 ppm. HR-MS (APCI) calculated for  $C_{36}H_{38}O_3Si$   $[M+H]^+$ : 547.2663 Found: 547.2664.

**(3aR\*,6R\*,6aR\*)-6-((tert-butyldiphenylsilyloxy)methyl)-2,2-diphenyldihydro-3aH-cyclopenta[d][1,3]dioxol-4(5H)-one (S-11).**



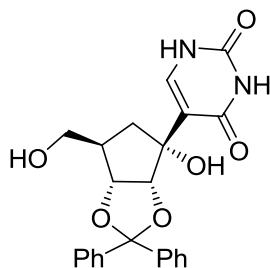
Prepared by general procedure B using 0.43 g (0.792 mmol) alkene **S-10**; flash column chromatography (hexane/EtOAc = 5:1) afforded **S-11** as a white crystalline solid (0.40 g, 92%). m.p. > 250 °C.  $^1H$  NMR (500 MHz,  $CDCl_3$ ):  $\delta$  = 7.58-7.53 (m, 4H), 7.51 (m, 2H), 7.44-7.26 (m, 14H), 4.57 (d,  $J$  = 6.03, 1H), 4.36 (d,  $J$  = 5.6, 1H), 3.76 (dd,  $J$  = 10.08, 2.77 Hz, 1H), 3.58 (dd,  $J$  = 10.08, 3.26 Hz, 1H), 2.76 (dd,  $J$  = 18.18, 9.20 Hz, 1H), 2.66 (m, 1H), 2.19 (d,  $J$  = 18.18 Hz, 1H), 0.99 (s, 9H) ppm.  $^{13}C$  NMR (126 MHz):  $\delta$  = 212.05, 141.74, 141.09, 135.93, 135.73, 132.84, 132.53, 130.21, 130.13, 128.69, 128.57, 128.48, 128.29, 128.06, 128.00, 126.58, 126.45, 112.05, 82.70, 79.51, 66.17, 39.64, 38.13, 27.04, 19.30 ppm. IR ( $\tilde{\nu}_{max}$ ) = 2961 (w), 1756 (s), 1104 (m), 1068 (s), 699 (s), 502 (m)  $cm^{-1}$ . HR-MS (ESI) calculated for:  $C_{35}H_{36}O_4Si[M+Na]^+$ : 571.2271. Found: 571.2274.

**(3aR\*,4R\*,6R\*,6aR\*)-4-(2,4-bis(benzyloxy)pyrimidin-5-yl)-6-(hydroxymethyl)-2,2-diphenyltetrahydro-3aH-cyclopenta[d][1,3]dioxol-4-ol (S-12).**



Prepared by essentially same procedure used for compound **17**, from bromide **11** (0.152 g, 0.41 mmol) and ketone **S-11** (0.150 g, 0.273 mmol); flash column chromatography (SiO<sub>2</sub>, hexane/EtOAc 10:1) afforded the adduct (0.170 g, 75 %), which was directly dissolved in THF (4 mL) and deprotected with TBAF (1.0 M in THF, 338 μL, 0.338 mmol) according to general procedure D. Flash column chromatography (CH<sub>2</sub>Cl<sub>2</sub>/EtOAc = 1:1) afforded compound **S-12** as a colorless glassy solid (0.085 g, 73%). <sup>1</sup>H NMR (500 MHz, CDCl<sub>3</sub>): δ = 8.48 (s, 1H), 7.46-7.42 (m, 6H), 7.36-7.20 (m, 14H), 5.41 (AB dd, *J* = 12.2, 0.8 Hz, 2H), 5.38 (m, 2H), 4.48 (d, *J* = 7.8 Hz, 1H), 4.58 (dd, *J* = 7.8, 5.5 Hz), 3.67 (m, 1H), 3.53 (m, 1H), 3.44 (d, *J* = 1Hz, 1H, -OH), 2.83 (m, 1H), 2.24 (m, 1H), 2.13 (dd, *J* = 13.5, 7.2 Hz, 1H) ppm. <sup>13</sup>C NMR (126 MHz, CDCl<sub>3</sub>): δ = 167.31, 164.47, 157.20, 141.71, 140.90, 136.89, 135.88, 128.96, 128.83, 128.67, 128.60, 128.52, 128.44, 128.36, 128.23, 126.51, 126.49, 117.58, 115.22, 84.50, 83.57, 76.39, 69.38, 68.98, 64.07, 45.60, 40.89 ppm. IR (ν<sub>max</sub>) = 2929 (w), 1592 (m), 1560 (m), 1422 (s), 1066 (s), 695 (s) cm<sup>-1</sup>. HR-MS (ESI) calculated for C<sub>37</sub>H<sub>34</sub>O<sub>6</sub>N<sub>2</sub> [M+H]<sup>+</sup>: 603.24896. Found: 603.24908.

**5-((3aR\*,4R\*,6R\*,6aR\*)-4-hydroxy-6-(hydroxymethyl)-2,2-diphenyltetrahydro-3aH-cyclopenta[d][1,3]dioxol-4-yl)pyrimidine-2,4(1H,3H)-dione (S-13).**



Prepared by general procedure C using using compound **S-12** (67 mg, 0.111 mmol), Pd/C (0.002 g, 0.022 mmol), H<sub>2</sub> (1 bar) in EtOH; flash column chromatography (CH<sub>2</sub>Cl<sub>2</sub>/MeOH = 5:1) afforded **S-13** as a colorless semi-solid (38 mg, 81%). <sup>1</sup>H NMR (500 MHz, DMSO-*d*<sub>6</sub>): δ = 11.06 (br s, 1H, N-H), 10.85 (br s, 1H, N-H), 7.47-7.32 (m, 10H), 4.75 (d, *J* = 8.0 Hz, 1H), 4.64 (m, 1H), 4.32 (d, *J* = 4.2 Hz, 1H, -OH), 4.28 (dd, *J* = 7.9, 5.5 Hz, 1H), 3.46 (m, 2H), 2.62 (m, 1H), 2.27 (m, 1H), 1.74 (dd, *J* = 13.1, 6.8 Hz, 1H), 1.68 (dd, *J* = 12.2, 6.0 Hz, 1H) ppm. <sup>13</sup>C NMR (126 MHz, DMSO-*d*<sub>6</sub>): δ = 163.37, 151.11, 142.06, 141.23, 138.77, 128.25, 128.02, 127.77, 126.53, 125.96, 114.12, 113.52, 82.83, 82.74, 76.04, 62.04, 44.87, 40.64 ppm. IR ( $\tilde{\nu}_{\max}$ ) = 1708 (s), 1679 (s), 1455 (w), 1212 (m), 1100 (w), 722 (s) cm<sup>-1</sup>. HR-MS (ESI) calculated for C<sub>23</sub>H<sub>22</sub>N<sub>2</sub>O<sub>6</sub> [M+Na]<sup>+</sup>: 445.1359. Found: 445.1436.

**7-bromo-*N,N*-bis((2-(trimethylsilyl)ethoxy)methyl)pyrrolo[2,1-*f*][1,2,4]triazin-4-amine (S-14).**



A solution of 7-bromopyrrolo[1,2-*f*][1,2,4]triazin-4-amine (0.500 g, 2.34 mmol) in DMF (4 mL) was added to a suspension of NaH (60 % in mineral oil, 0.234 g, 5.86 mmol) in DMF (1.5 mL) and the mixture was stirred at 25 °C for 30 min. SEM-Cl (0.872 mL, 4.92 mmol) was added

dropwise and the mixture was stirred at 25 °C for 5 h. The reaction mixture was quenched with water (10 mL) and extracted with EtOAc (3 × 25 mL). The organic phase was washed with brine (15 mL), dried over MgSO<sub>4</sub>, filtered, and concentrated under reduced pressure. The residue was purified by flash column chromatography (hexane/EtOAc 20 : 1) to afford **S-14** (0.650 g, 58 %) as a colorless oil. <sup>1</sup>H NMR (500 MHz, CDCl<sub>3</sub>): δ = 8.08 (s, 1H), 7.08 (d, AB, *J* = 4.8 Hz, 1H), 6.76 (d, AB, *J* = 4.8 Hz, 1H), 5.21 (s, 4H), 3.68 (m, 4H), 0.98 (m, 4H), 0.01 (s, 9H) ppm. <sup>13</sup>C NMR (126 MHz, CDCl<sub>3</sub>): δ = 156.09, 147.52, 115.99, 113.96, 106.86, 102.09, 77.82, 66.32, 18.41, -1.18 ppm. IR (ν<sub>max</sub>) = 2954 (w), 1582 (w), 1517 (w), 1264 (m), 1074 (m), 858 (m), 732 (s) cm<sup>-1</sup>. HR-MS (ESI) calculated for C<sub>18</sub>H<sub>34</sub>N<sub>4</sub>O<sub>2</sub>Si<sub>2</sub>Br [M+H]<sup>+</sup>: 473.1403. Found: 473.1402.

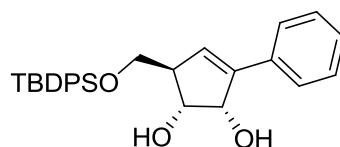
**(4-(bis((2-(trimethylsilyl)ethoxy)methyl)amino)pyrrolo[2,1-f][1,2,4]triazin-7-yl)boronic acid (29).**



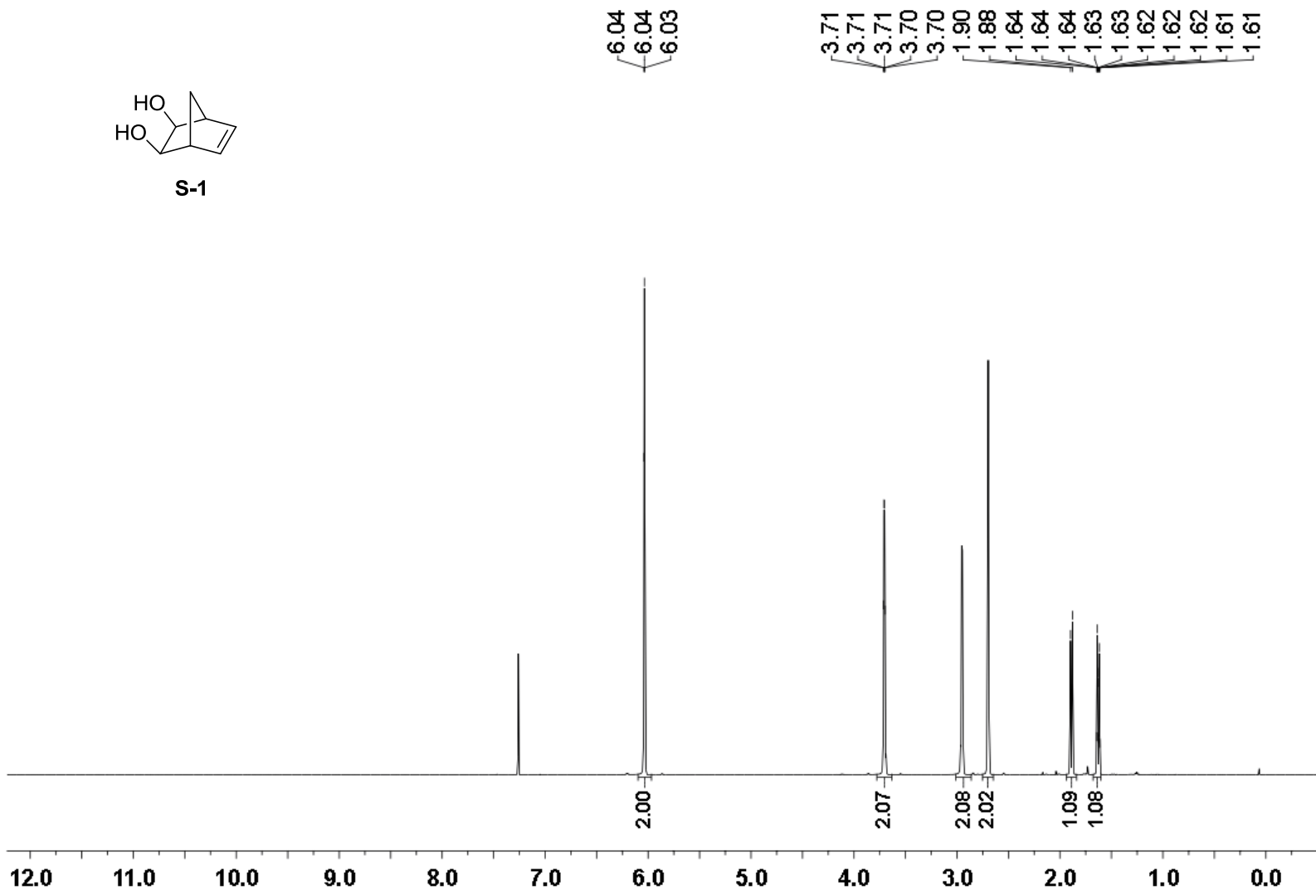
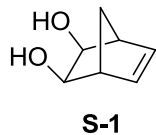
*n*-BuLi (1.6 M in hexanes, 2.4 mL, 3.84 mmol) was added to a solution of **S-14** (0.909 g, 1.919 mmol) in THF (6 mL) at -78 °C and the mixture was stirred at -78 °C for 30 min. 2-isopropoxy-4,4,5,5-tetramethyl-1,3,2-dioxaborolane (0.515 mL, 2.303 mmol) was added dropwise to the reaction mixture at -78 °C. The reaction mixture was then allowed to warm to 25 °C and stirred for 1 h. Saturated aqueous solution of NH<sub>4</sub>Cl (10 mL) was added and the mixture was extracted with EtOAc (3 × 30 mL). The organic phase was washed with brine (15 mL), dried over MgSO<sub>4</sub>, filtered, and concentrated under reduced pressure to yield the crude boronate. The boronate hydrolyzed during the purification by flash column chromatography on silica gel (CH<sub>2</sub>Cl<sub>2</sub>/EtOAc = 9:1) to afford **29** (0.418 g, 50 %) as a yellow wax. <sup>1</sup>H NMR (500 MHz, DMSO-*d*<sub>6</sub>): δ = 8.35 (s, 2H, -B(OH)<sub>2</sub>), 8.16 (s, 1H), 7.20 (d, AB, *J* = 4.5 Hz, 1H), 7.01 (d, AB, *J* = 4.8 Hz, 1H), 5.22 (s, 4H), 3.65 (app t, *J* = 8.13 Hz, 4H), 0.91 (app t, *J* = 8.13 Hz, 4H), -0.03 (s, 18H) ppm. <sup>13</sup>C NMR (126 MHz, DMSO-*d*<sub>6</sub>): δ = 155.74, 146.08, 126.25 (br, C-B(OH)<sub>2</sub>, detected through <sup>1</sup>H-<sup>13</sup>C

HMBC), 120.16, 116.92, 106.21, 77.62, 65.07, 17.52, -1.45 ppm.  $^{11}\text{B}$  NMR (160.5 MHz,  $\text{DMSO-}d_6$ ):  $\delta = 25.90$  (br) ppm. IR ( $\tilde{\nu}_{\text{max}}$ ) = 2952 (m), 1585 (m), 1517 (w), 1370 (m), 1248 (m), 1075 (s), 856 (s), 832 (s)  $\text{cm}^{-1}$ . HR-MS (ESI) calculated for  $\text{C}_{18}\text{H}_{34}\text{N}_4\text{O}_4\text{BSi}_2$  [M-H] $^-$ : 437.22171. Found: 437.22107.

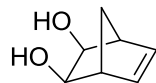
**(1R\*,2S\*,5R\*)-5-((tert-butyldiphenylsilyloxy)methyl)-3-phenylcyclopent-3-ene-1,2-diol (S-15).**



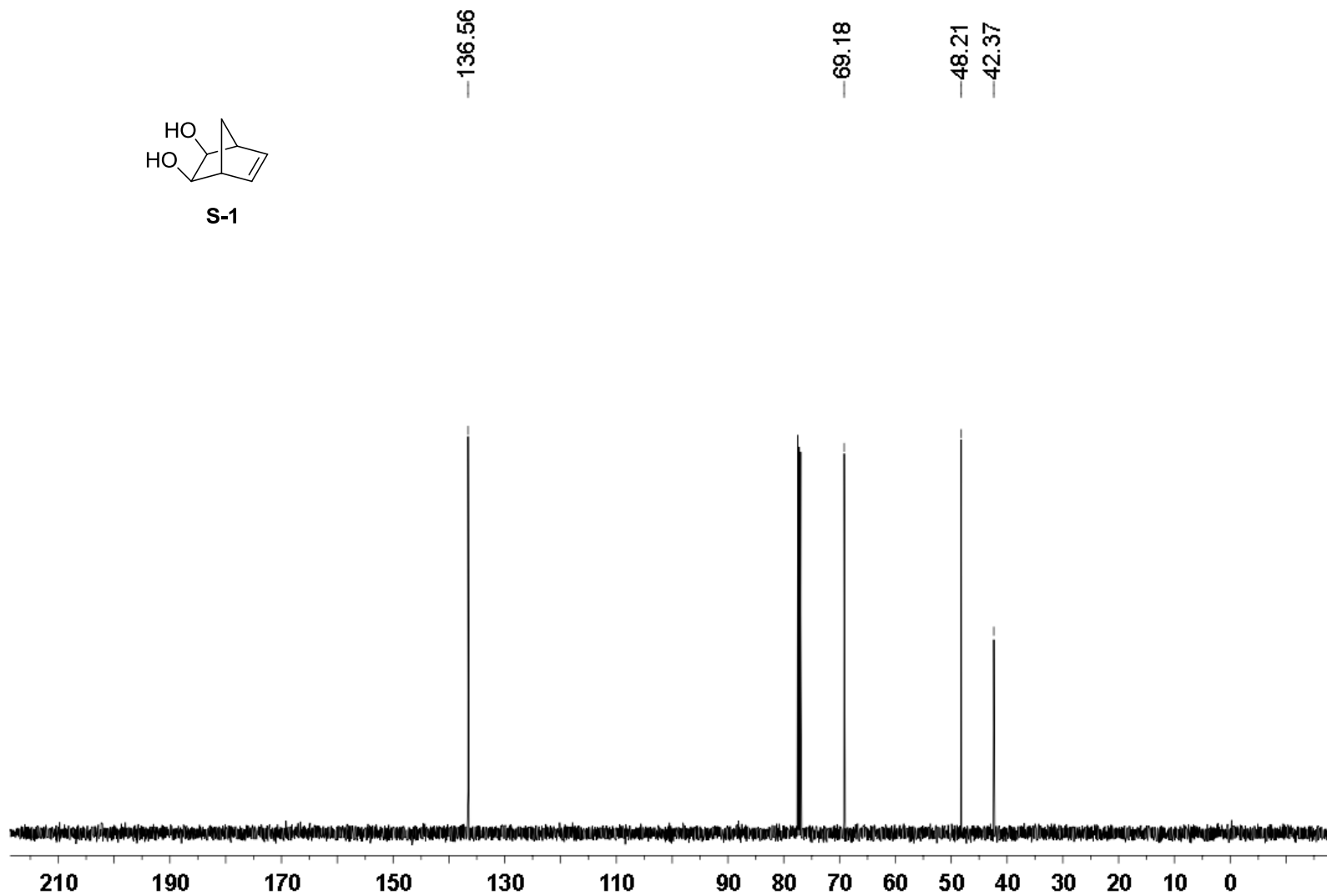
Freshly prepared PPTS (0.111 g, 0.443 mmol) was added to a solution of **23a** (0.043 g, 0.089 mmol) in MeOH (3 mL). The reaction mixture was stirred at 25 °C for 96 h. The solvent was evaporated and the residue was purified by flash column chromatography (gradient elution from hexane/EtOAc 10:1 to initially elute starting material - 18 mg, 33% recovered to  $\text{CH}_2\text{Cl}_2/\text{EtOAc} = 10:1$ ) to afford product **S-15** as a white semi-solid (0.015 g, 38 %).  $^1\text{H}$  NMR (500 MHz,  $\text{CDCl}_3$ ):  $\delta = 7.67\text{-}7.62$  (m, 4H), 7.54-7.50 (m, 2H), 7.44-7.31 (m, 8H), 7.26 (m, 1H), 6.09 (d,  $J = 2.2$  Hz, 1H), 4.96 (m, 1H), 4.22 (dd,  $J = 9.9, 4.9$  Hz, 1H), 3.86 (dd,  $J = 10.0, 5.5$  Hz, 1H), 3.79 (dd,  $J = 10.0, 5.5$  Hz, 1H), 2.99 (m, 1H), 2.69 (d,  $J = 5.1$  Hz, 1H, -OH), 2.43 (d,  $J = 4.7$  Hz, 1H, -OH), 1.04 (s, 9H) ppm.  $^{13}\text{C}$  NMR (126 MHz,  $\text{CDCl}_3$ ):  $\delta = 143.55, 135.83, 135.79, 134.69, 133.60, 133.54, 129.99, 129.31, 128.78, 128.05, 127.98, 127.96, 126.26, 75.75, 74.77, 65.09, 54.00, 27.09, 19.45$  ppm. IR ( $\tilde{\nu}_{\text{max}}$ ) = 3300 (m), 2940 (w), 1215 (s), 1182 (s), 765 (s)  $\text{cm}^{-1}$ .



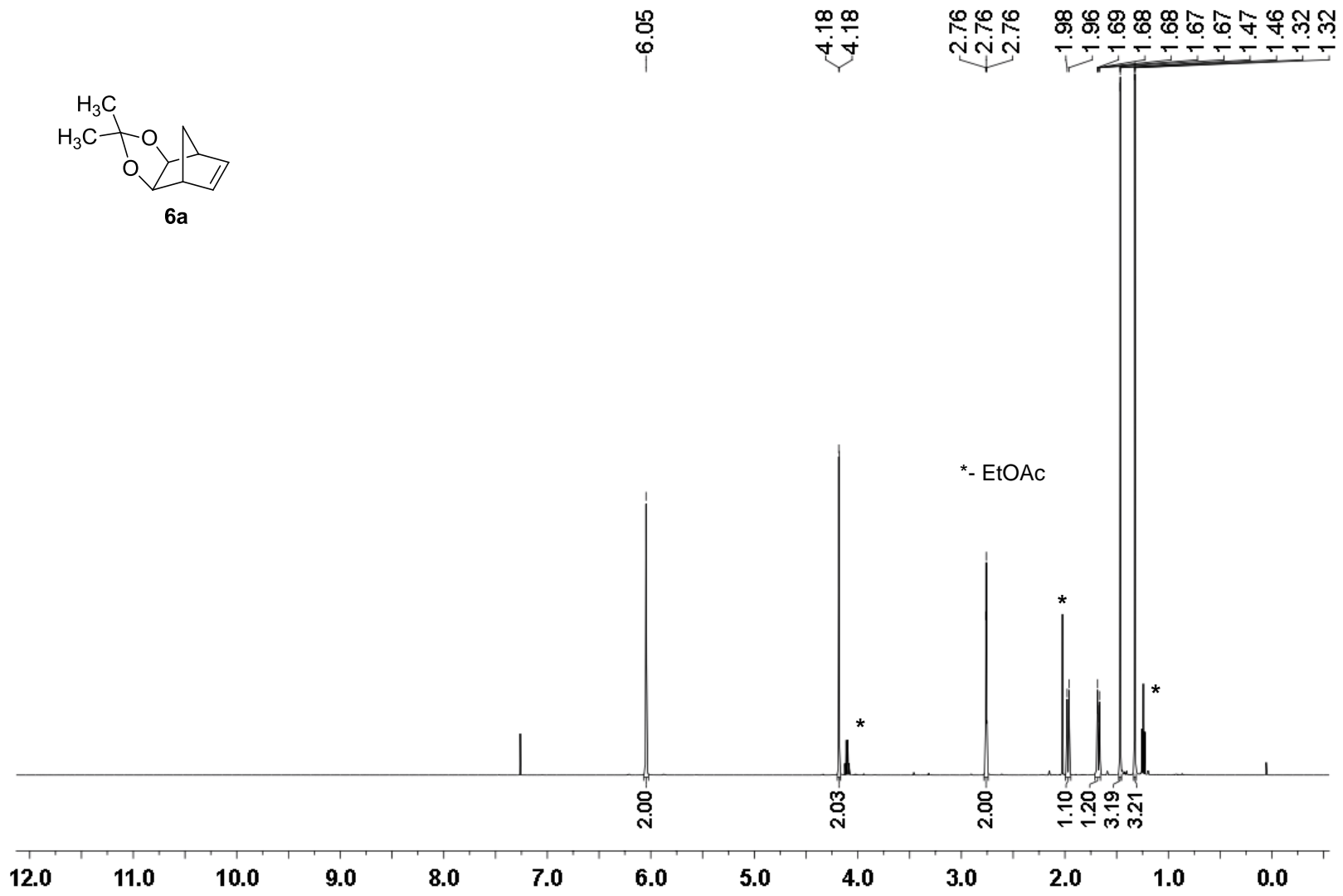
<sup>1</sup>H NMR (500MHz) spectrum of **S-1** in CDCl<sub>3</sub>



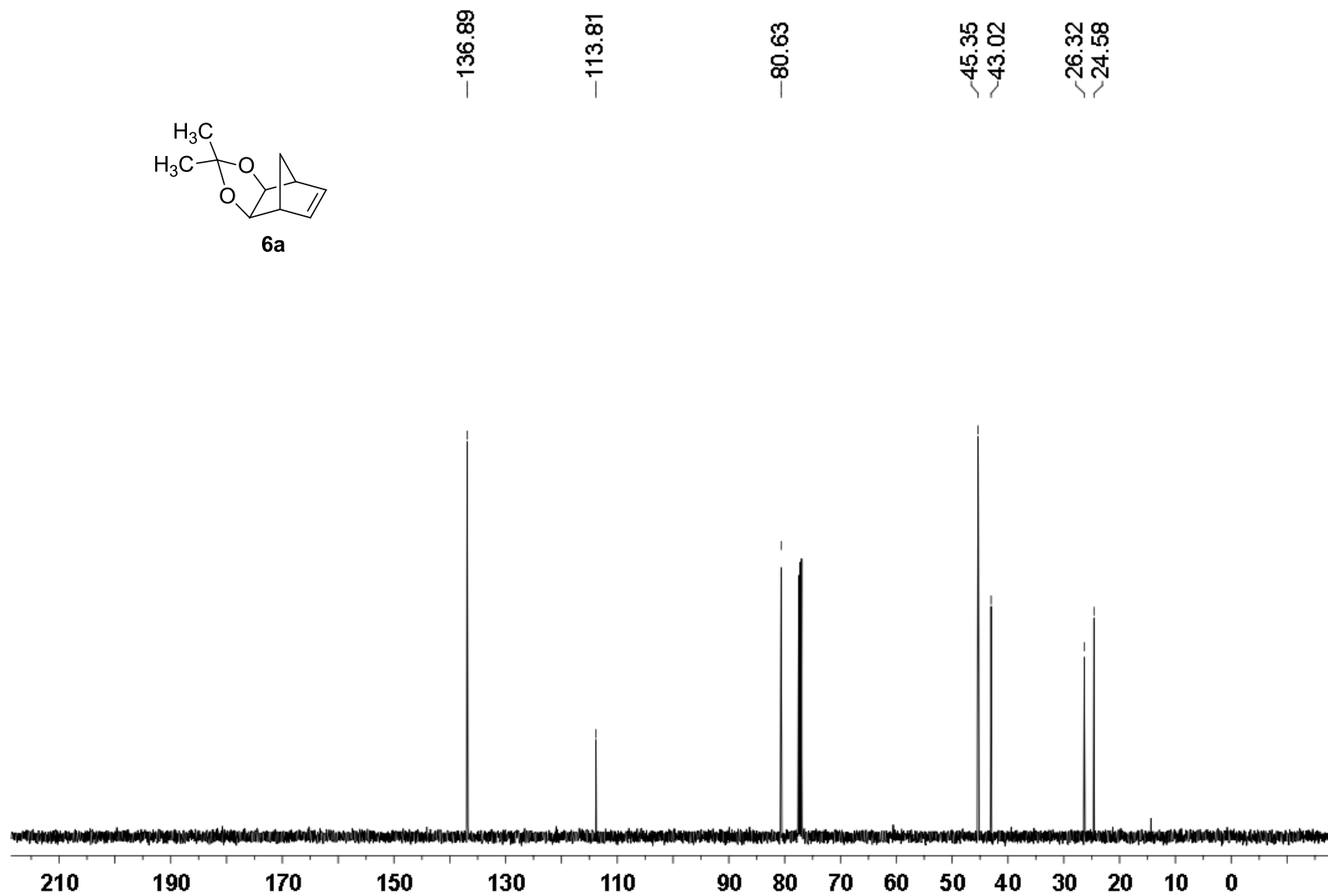
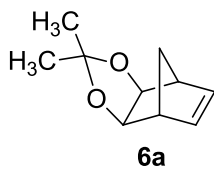
**S-1**



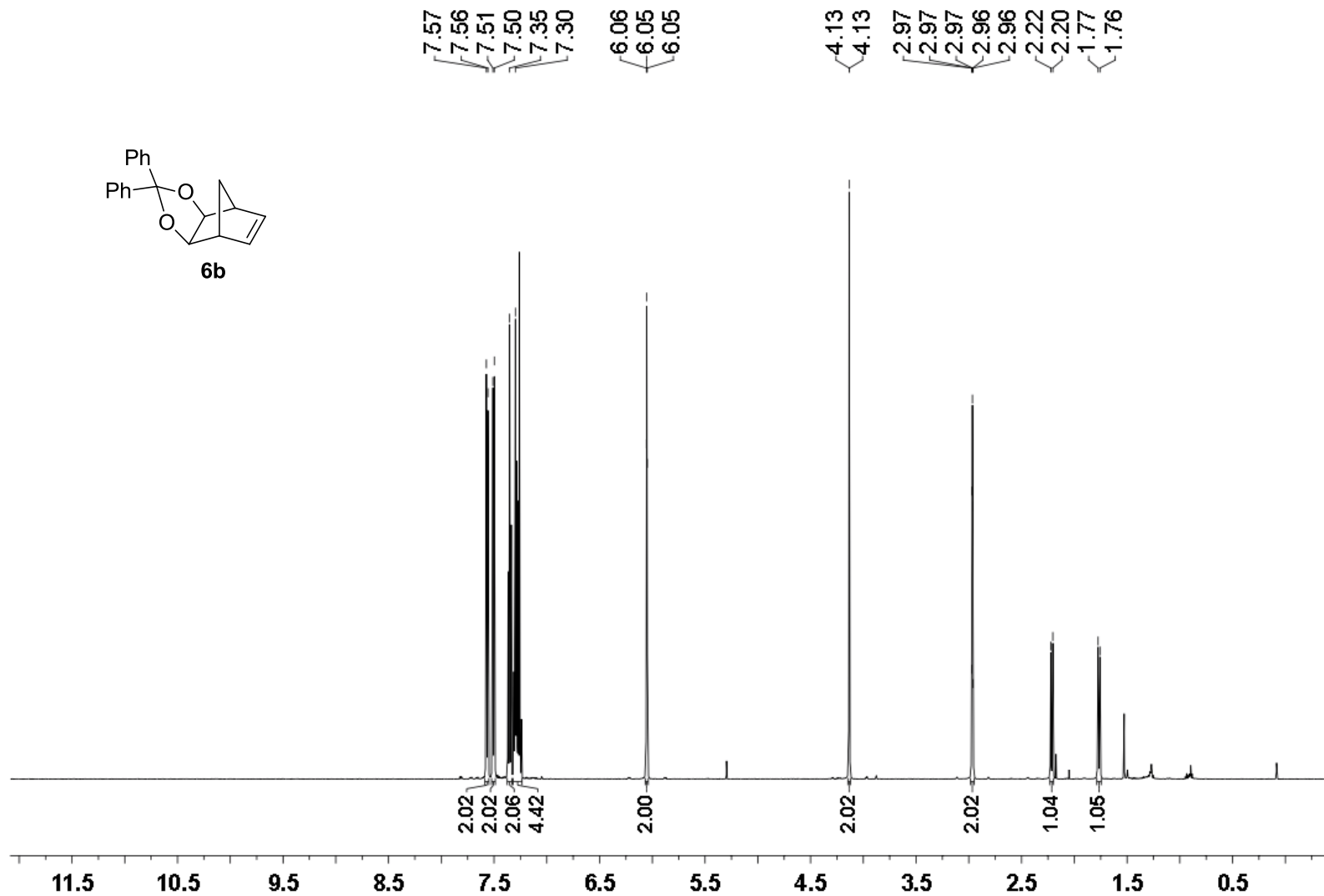
$^{13}\text{C}$  NMR (126 MHz) spectrum of **S-1** in  $\text{CDCl}_3$



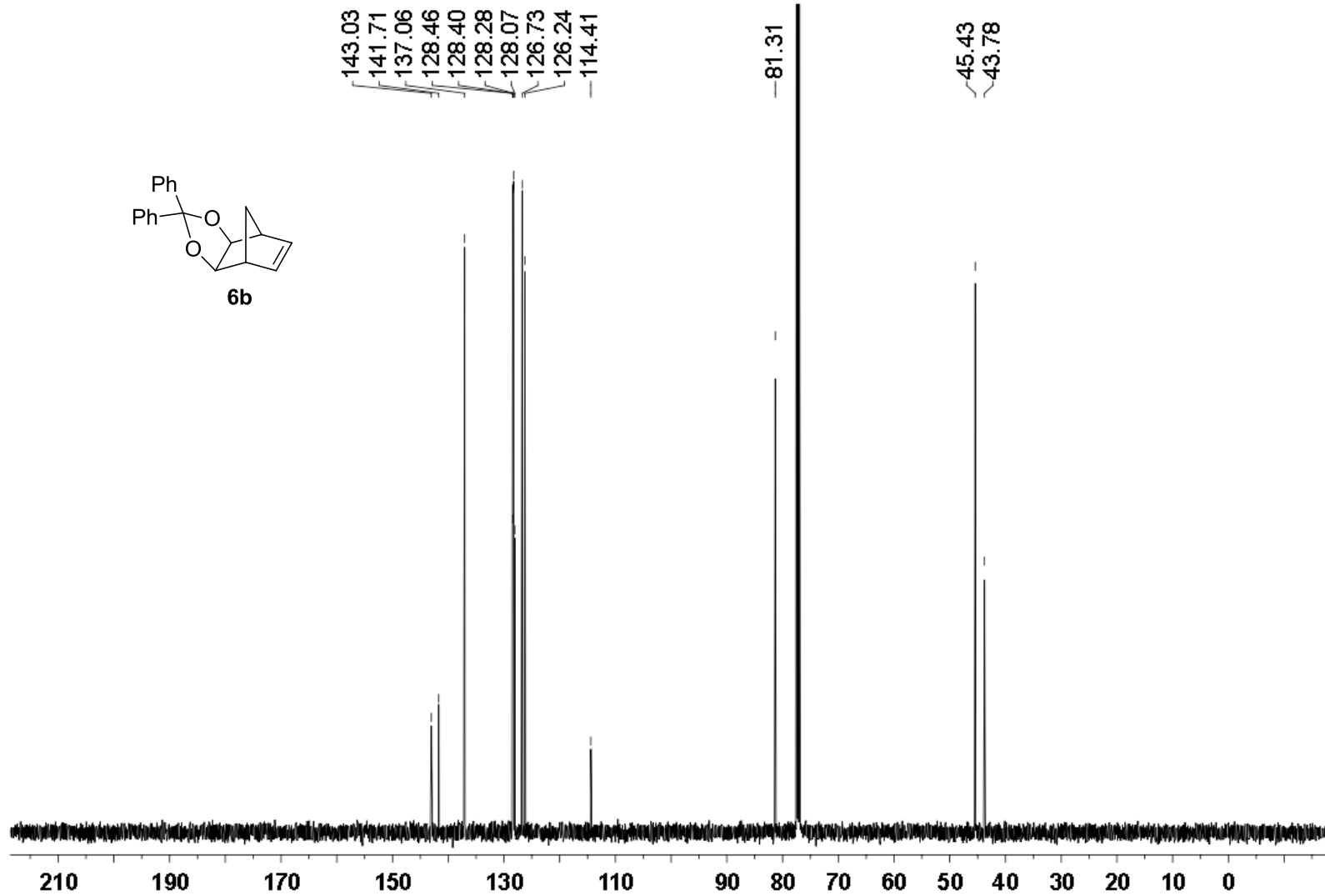
<sup>1</sup>H NMR (500 MHz) spectrum of **6a** in CDCl<sub>3</sub>



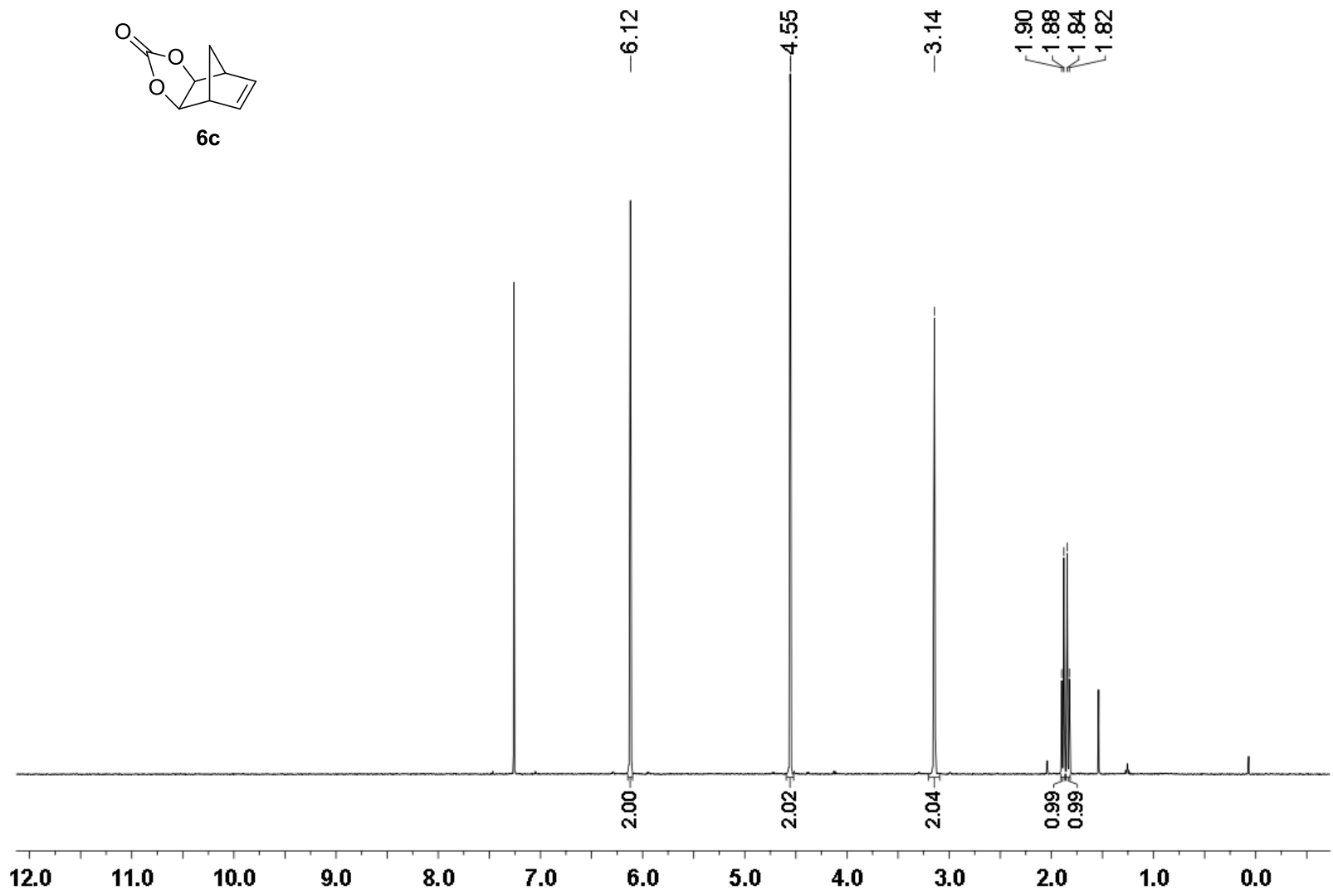
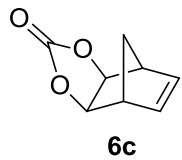
$^{13}\text{C}$  NMR (126 MHz) spectrum of **6a** in  $\text{CDCl}_3$



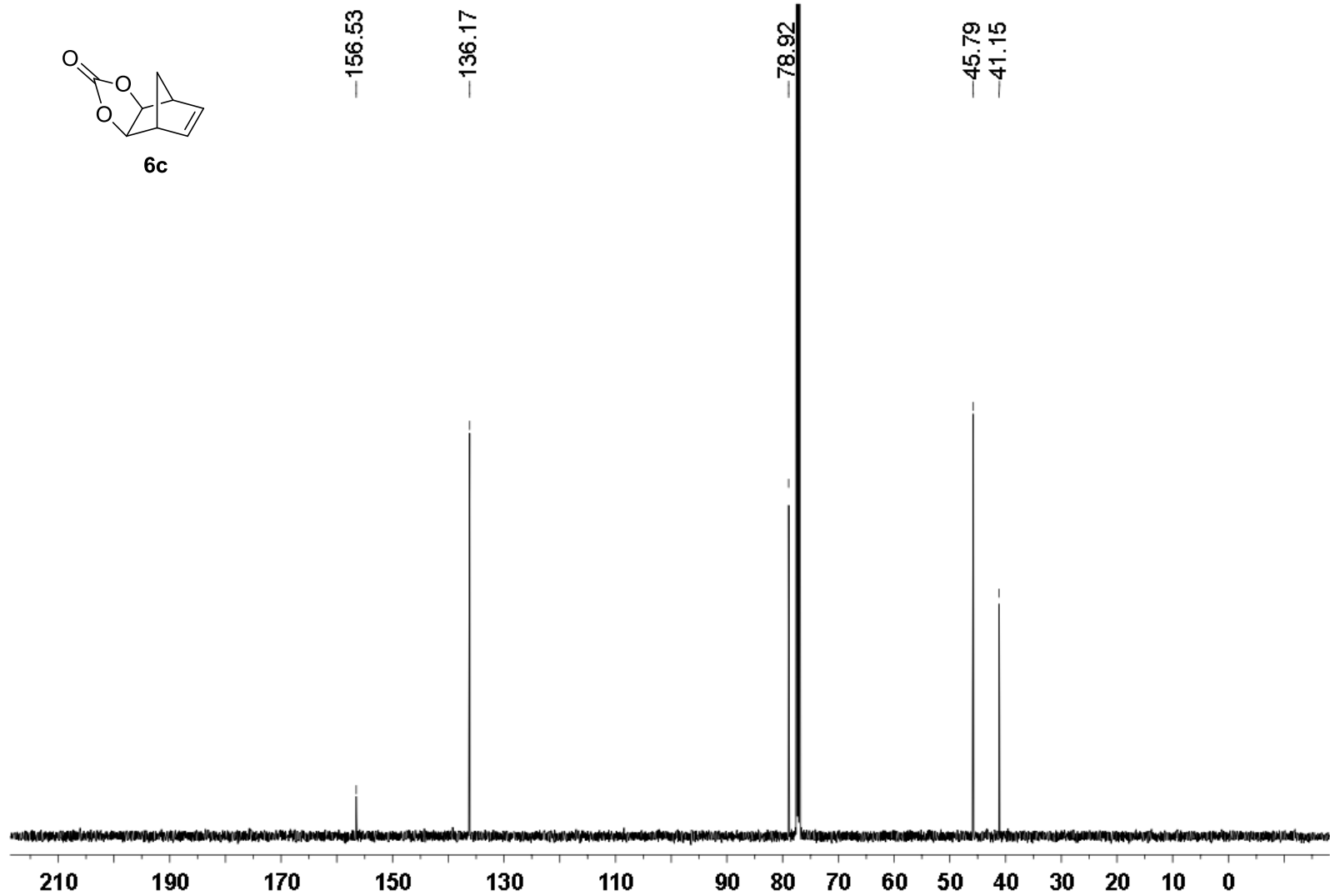
$^1\text{H}$  NMR (500 MHz) spectrum of **6b** in  $\text{CDCl}_3$



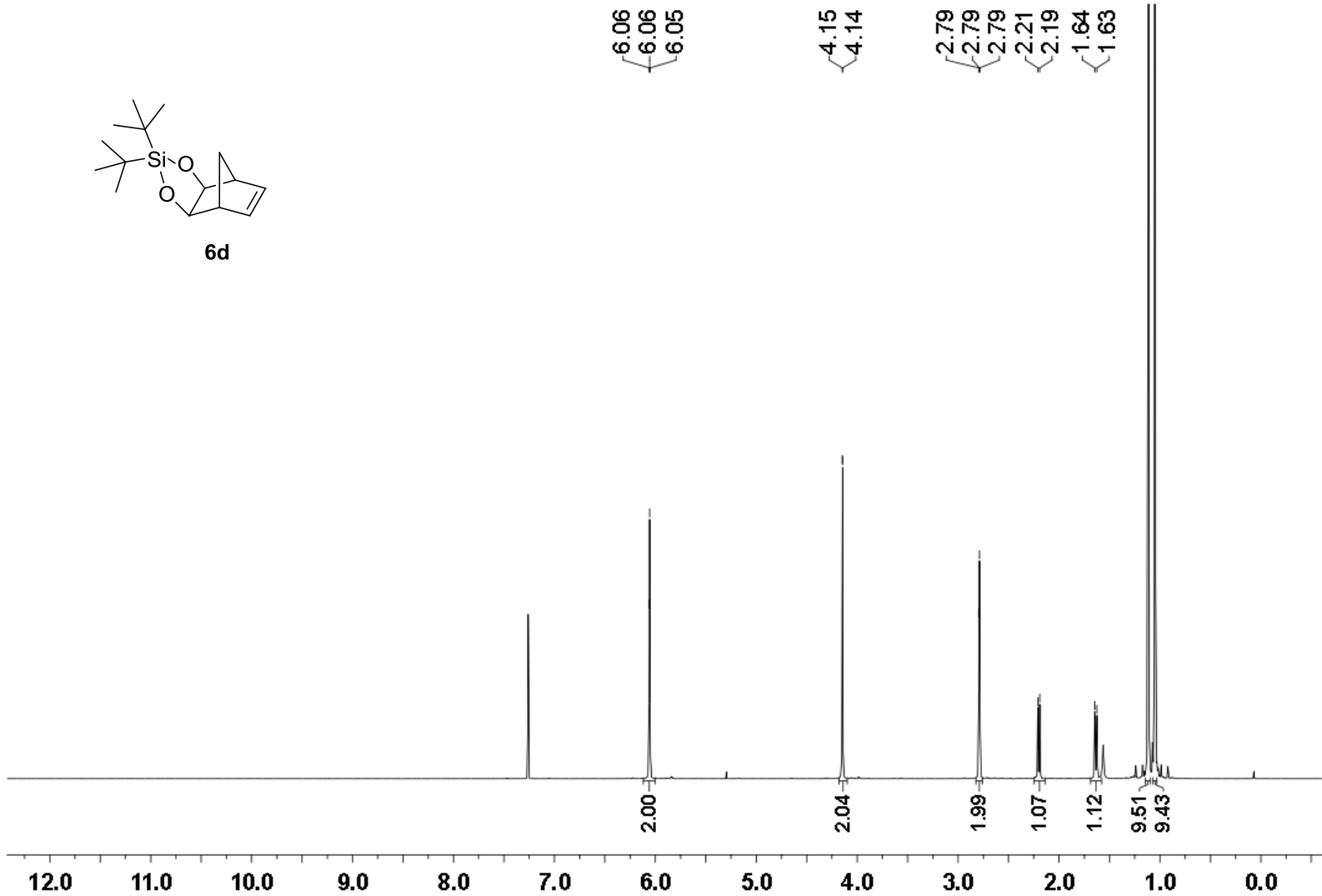
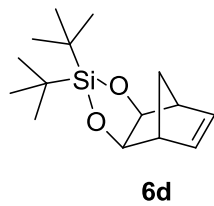
$^{13}\text{C}$  NMR (126 MHz) spectrum of **6b** in  $\text{CDCl}_3$



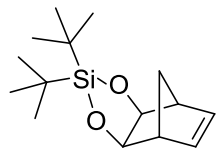
$^1\text{H}$  NMR (500 MHz) spectrum of **6c** in  $\text{CDCl}_3$



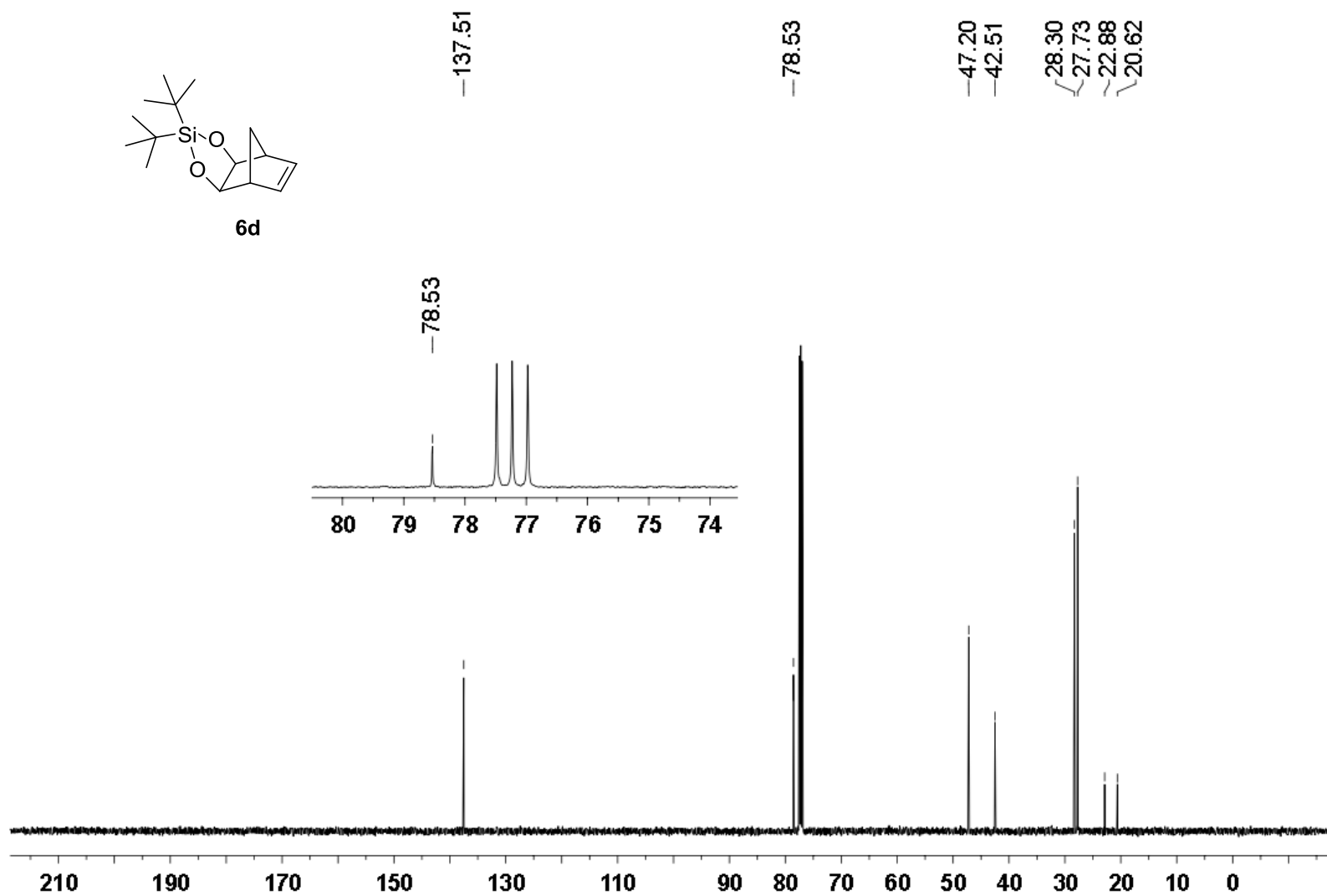
$^{13}\text{C}$  NMR (126 MHz) spectrum of **6c** in  $\text{CDCl}_3$



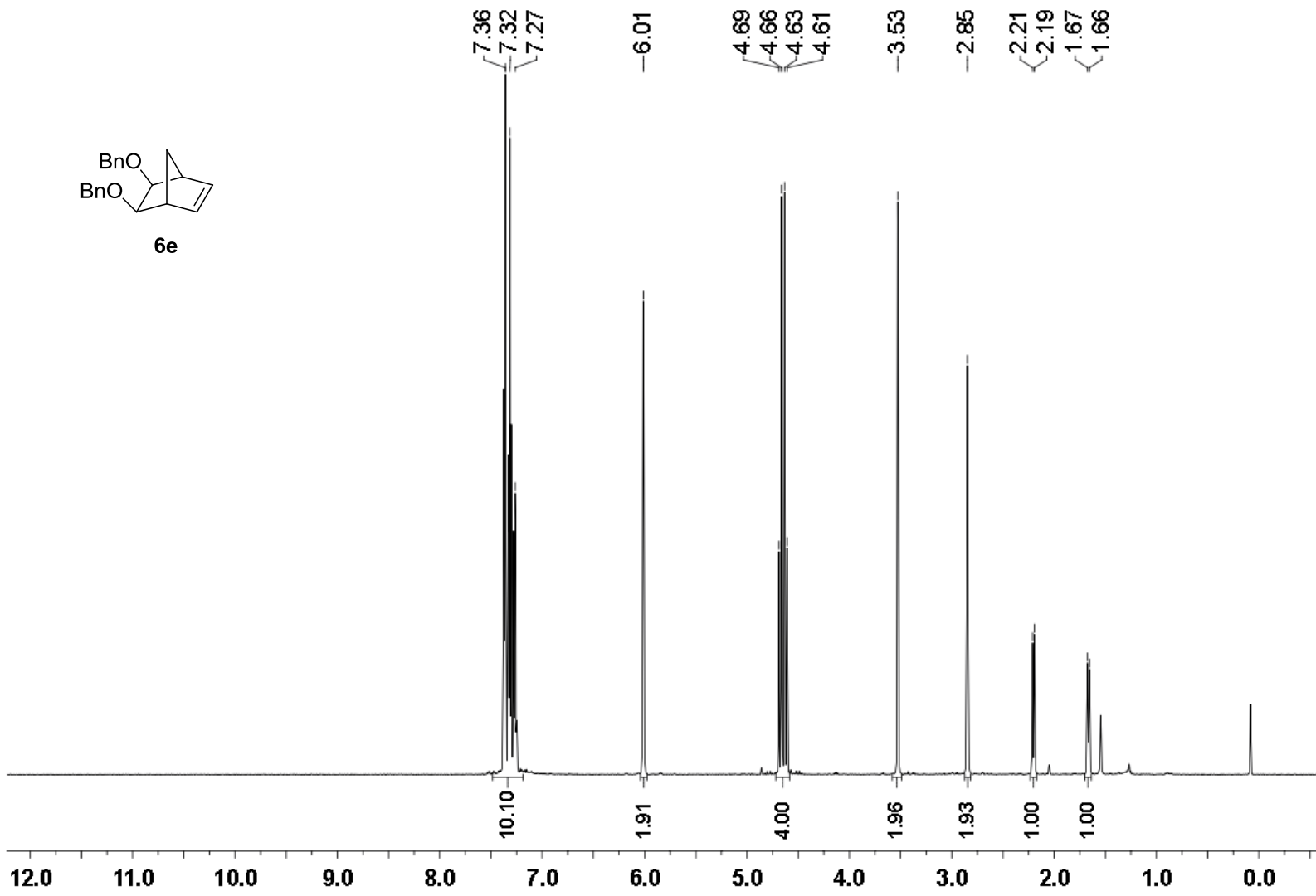
<sup>1</sup>H NMR (500 MHz) spectrum of **6d** in CDCl<sub>3</sub>



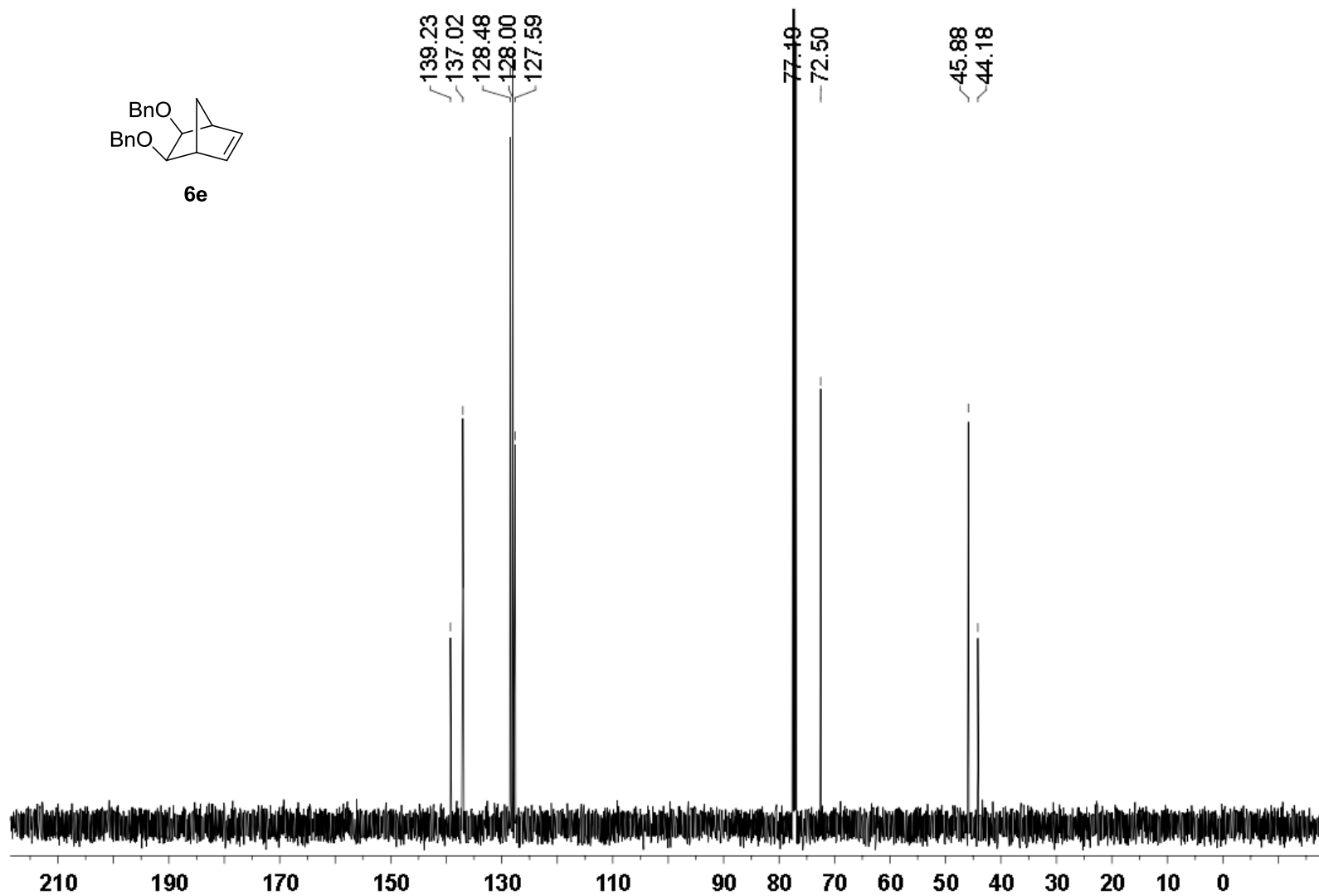
**6d**



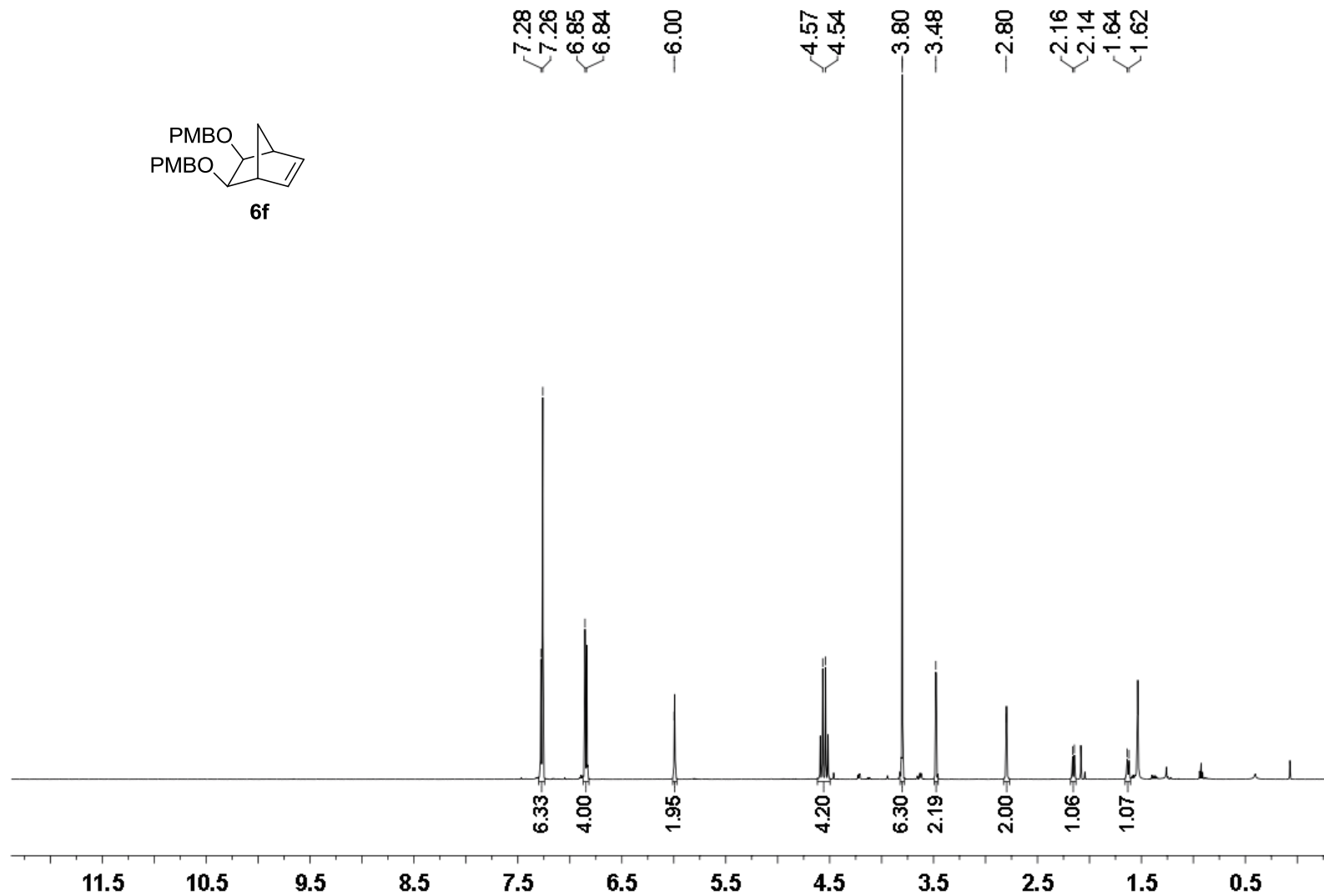
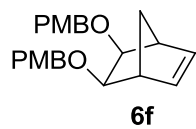
<sup>13</sup>C NMR (126 MHz) spectrum of **6d** in CDCl<sub>3</sub>



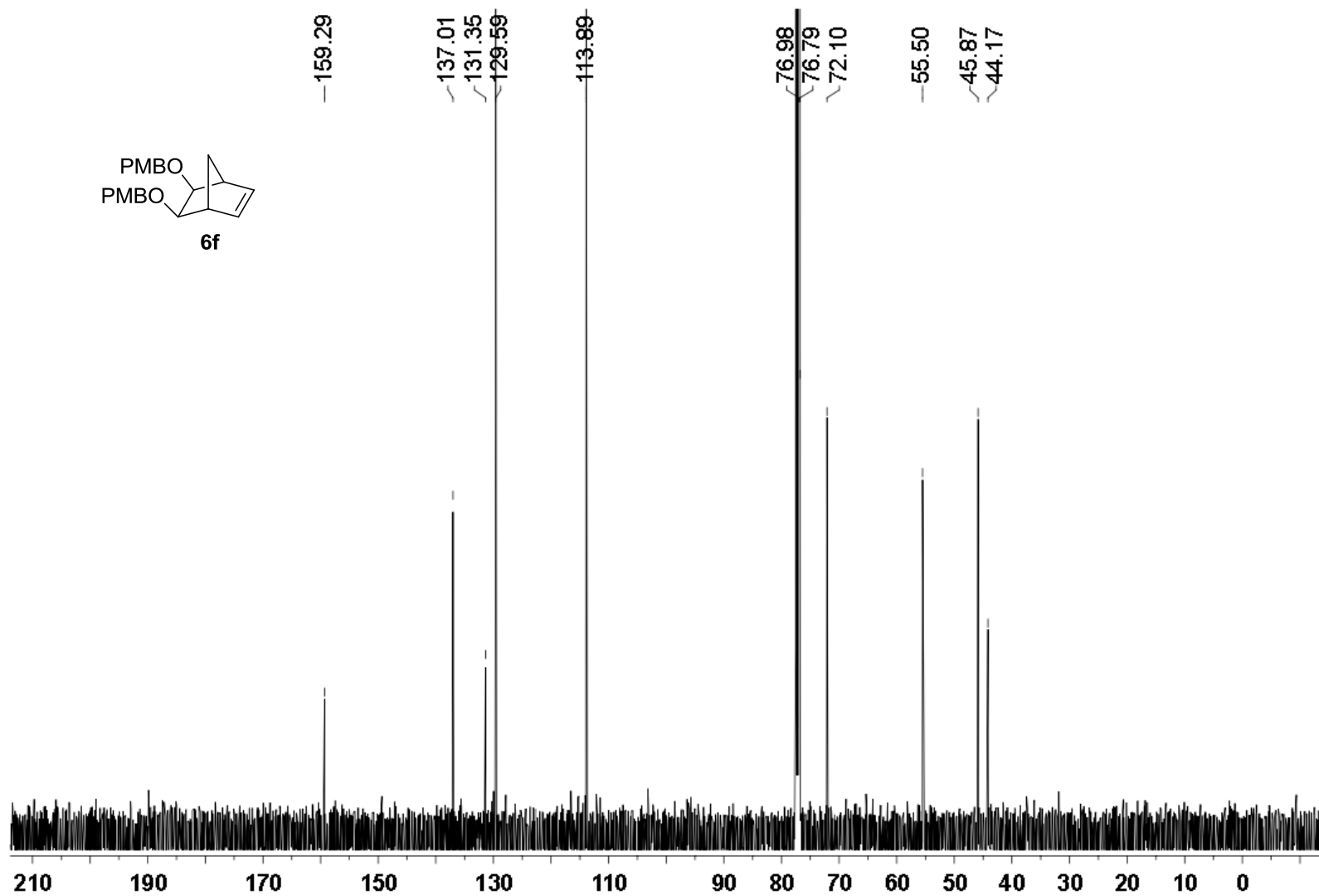
$^1\text{H}$  NMR (500MHz) spectrum of **6e** in  $\text{CDCl}_3$



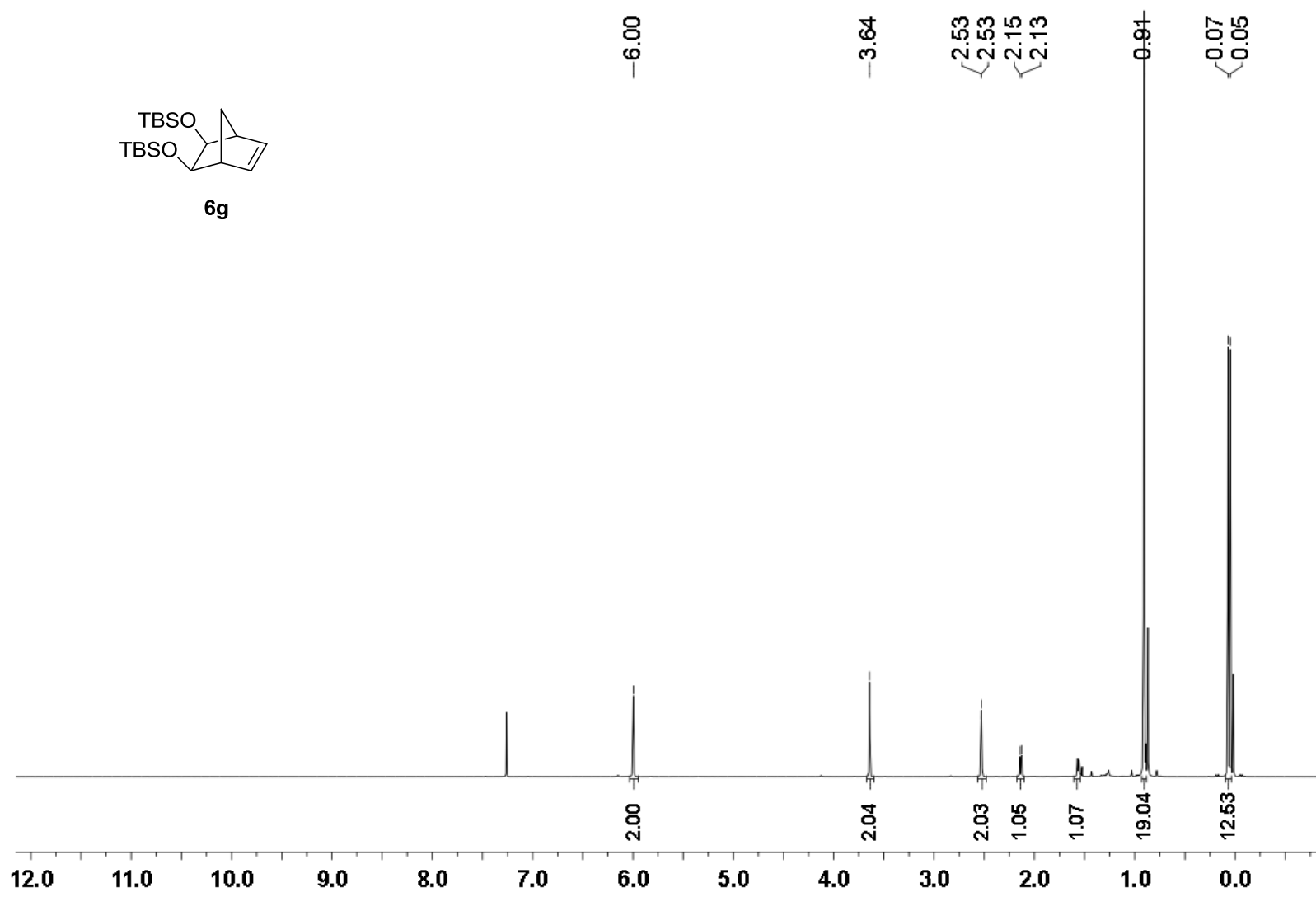
$^{13}\text{C}$  NMR (126 MHz) spectrum of **6e** in  $\text{CDCl}_3$



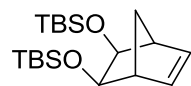
<sup>1</sup>H NMR (500 MHz) spectrum of **6f** in CDCl<sub>3</sub>



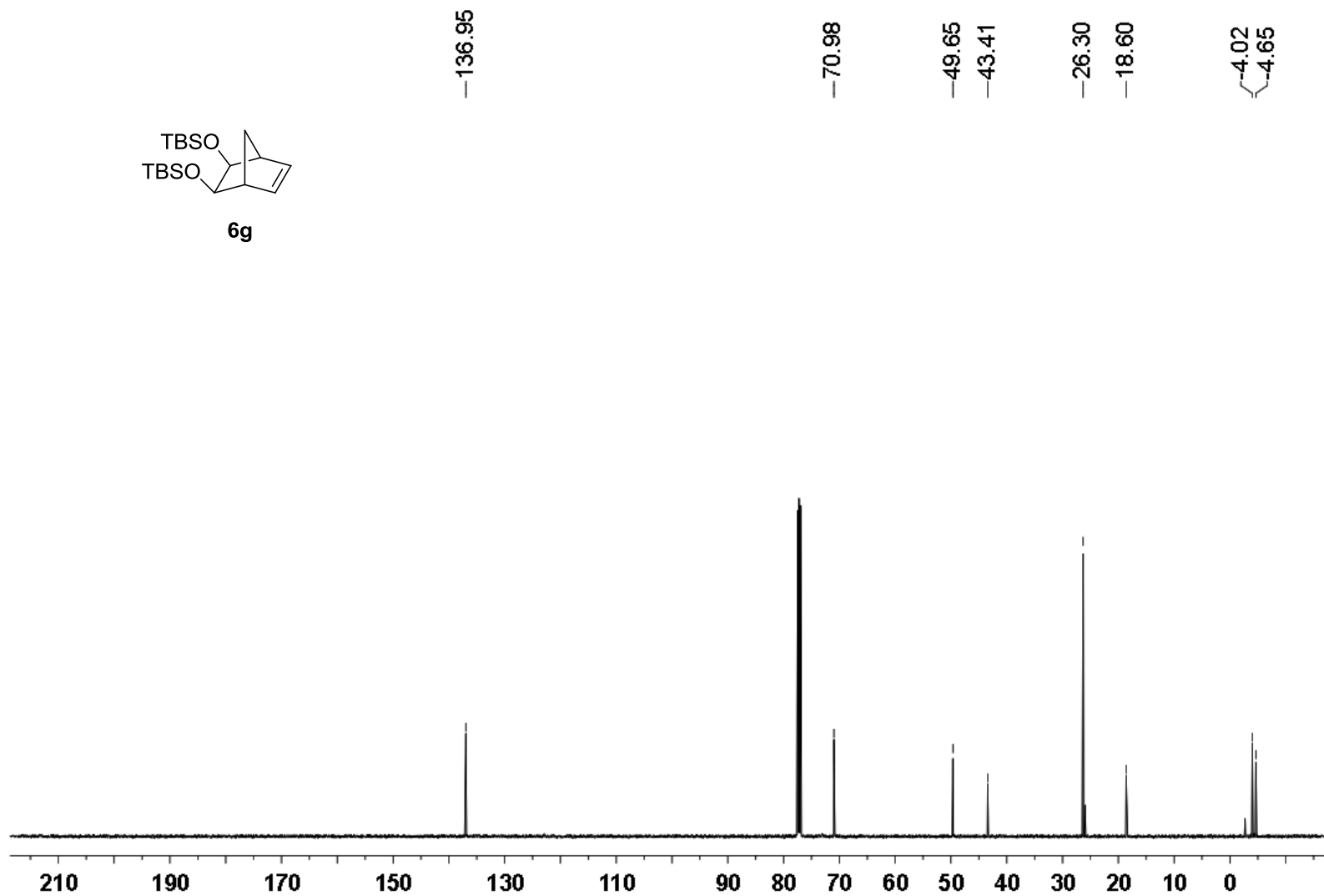
$^{13}\text{C}$  NMR (126 MHz) spectrum of **6f** in  $\text{CDCl}_3$



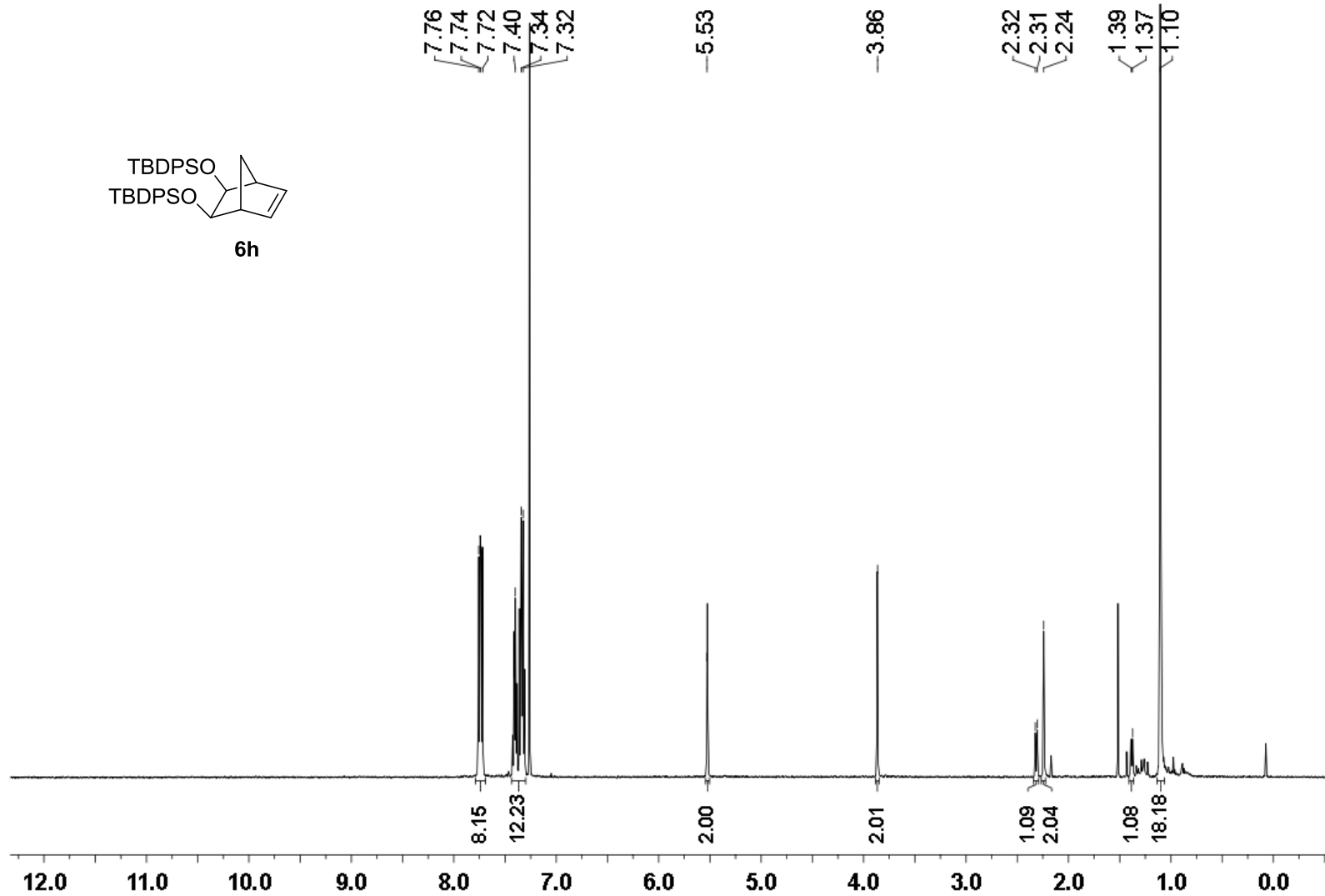
$^1\text{H}$  NMR (500 MHz) spectrum of **6g** in  $\text{CDCl}_3$



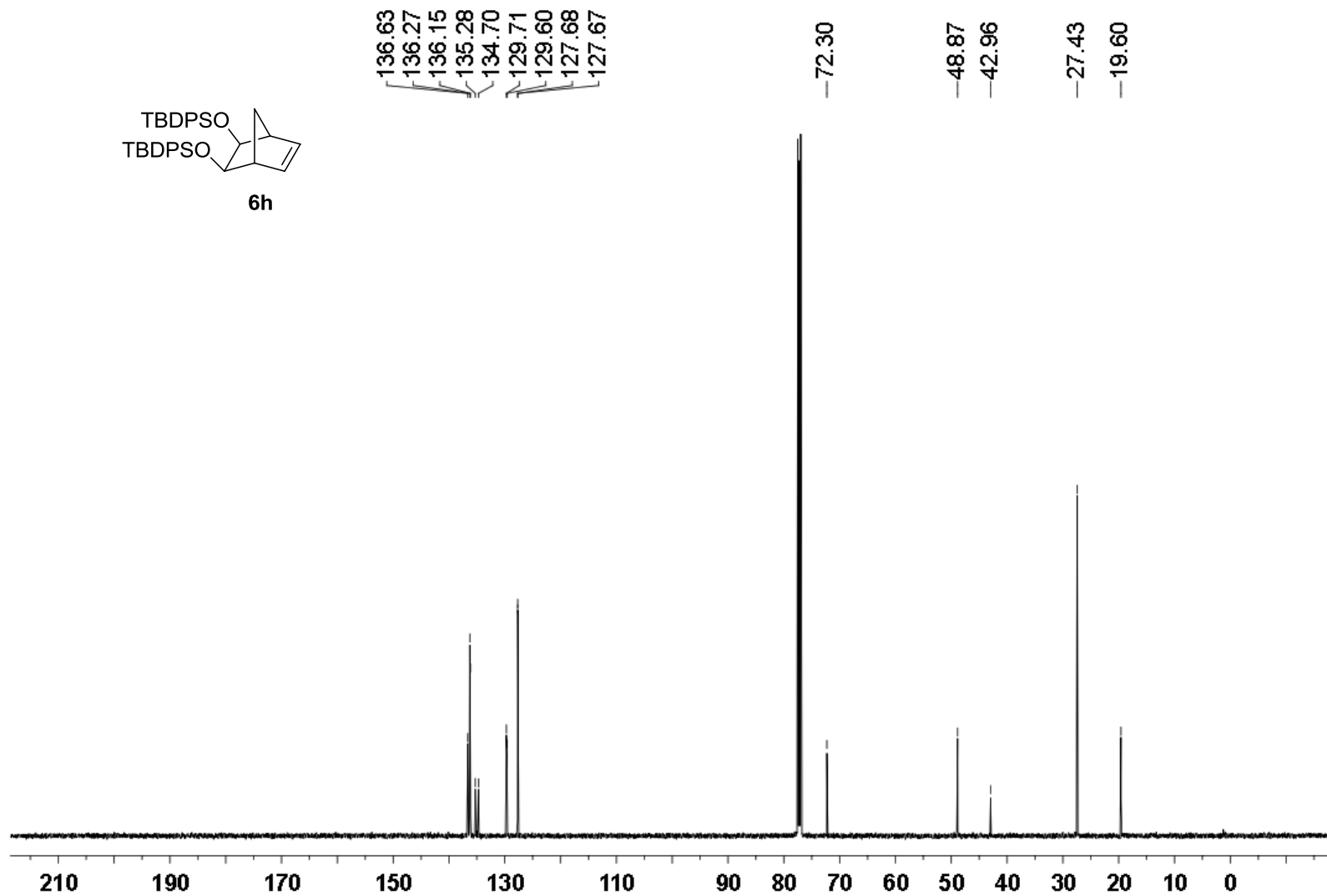
**6g**



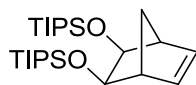
$^{13}\text{C}$  NMR (126 MHz) spectrum of **6g** in  $\text{CDCl}_3$



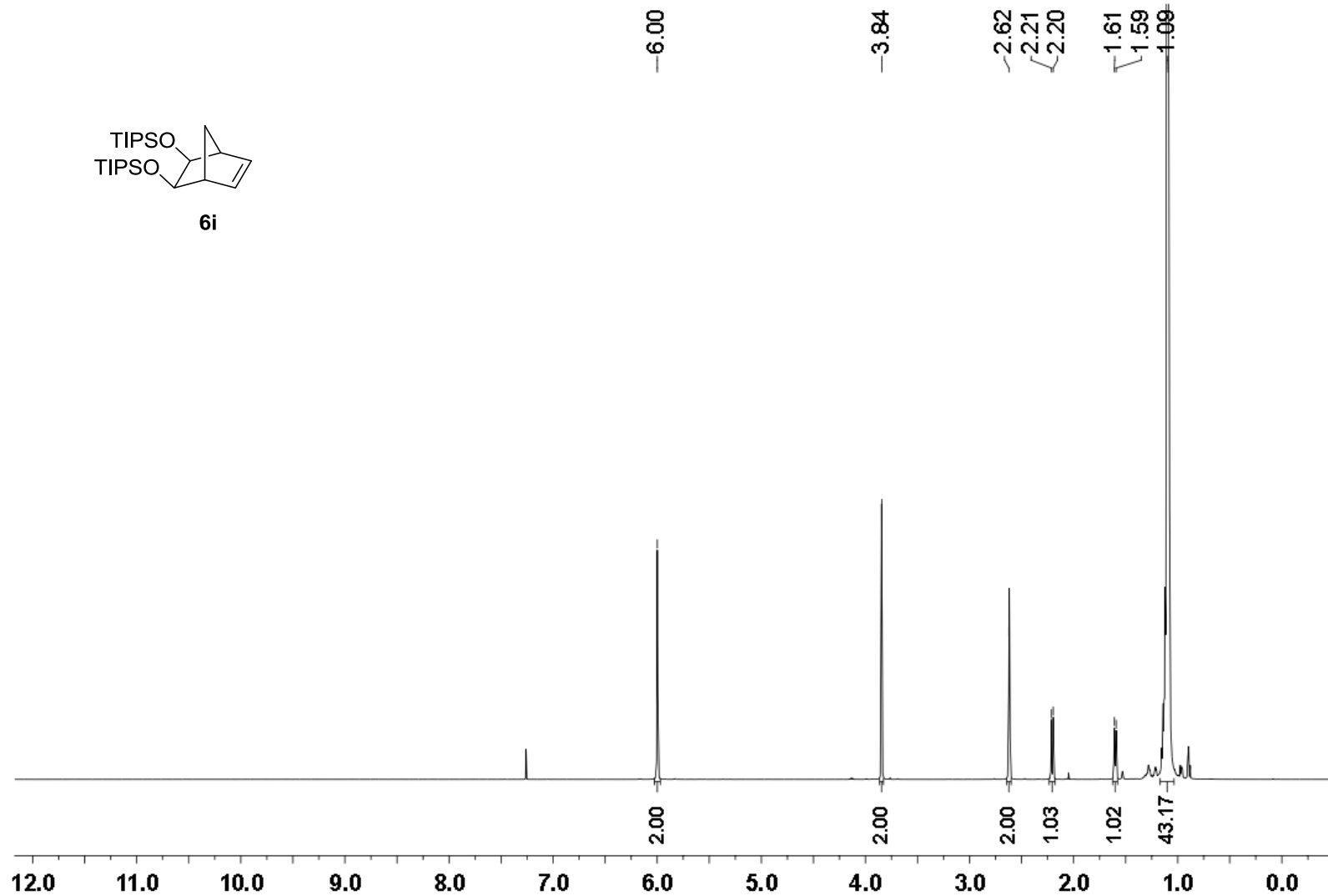
$^1\text{H}$  NMR (500 MHz) spectrum of **6h** in  $\text{CDCl}_3$



$^{13}\text{C}$  NMR (126 MHz) spectrum of **6h** in  $\text{CDCl}_3$

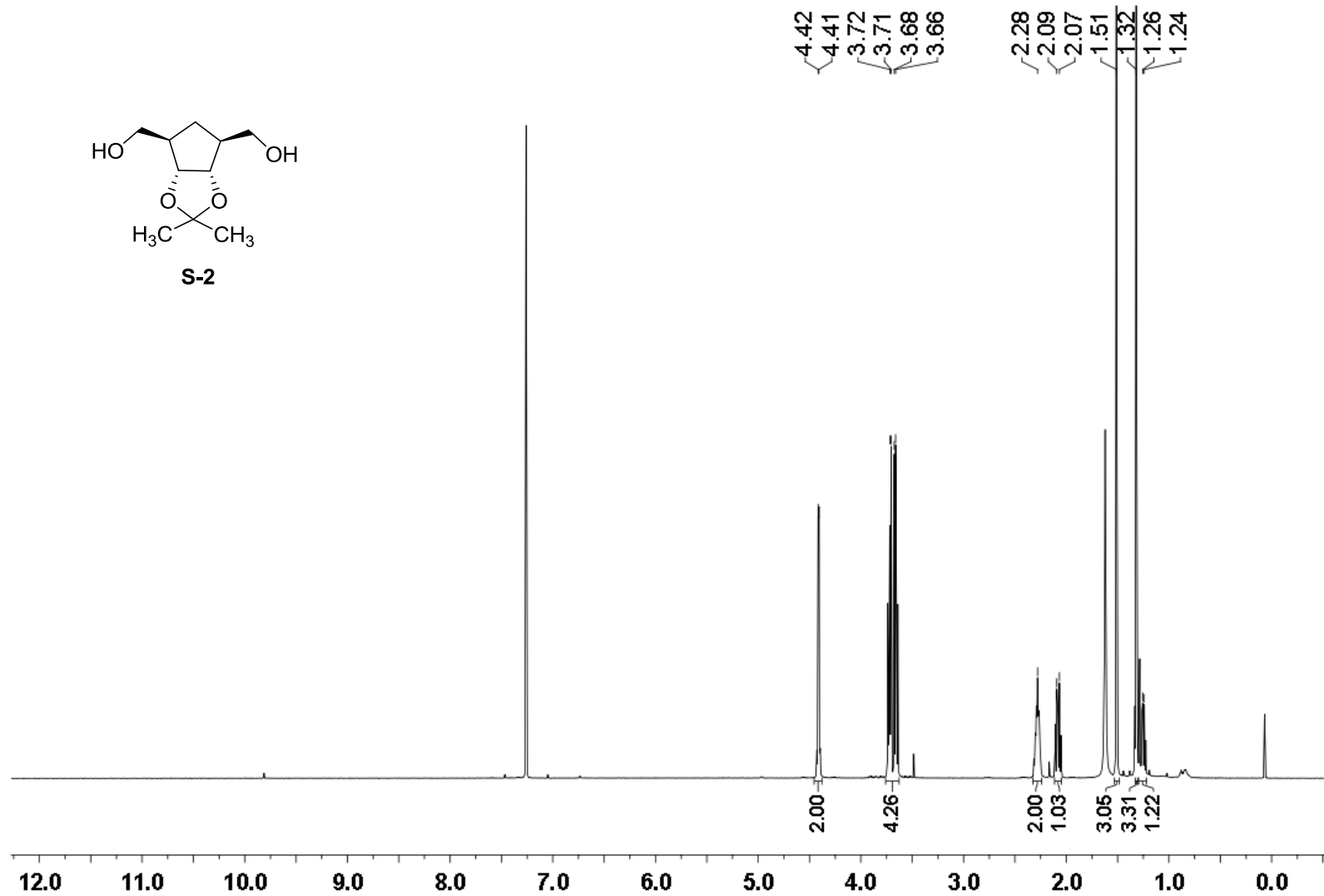
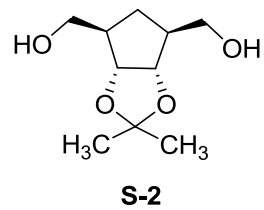


**6i**

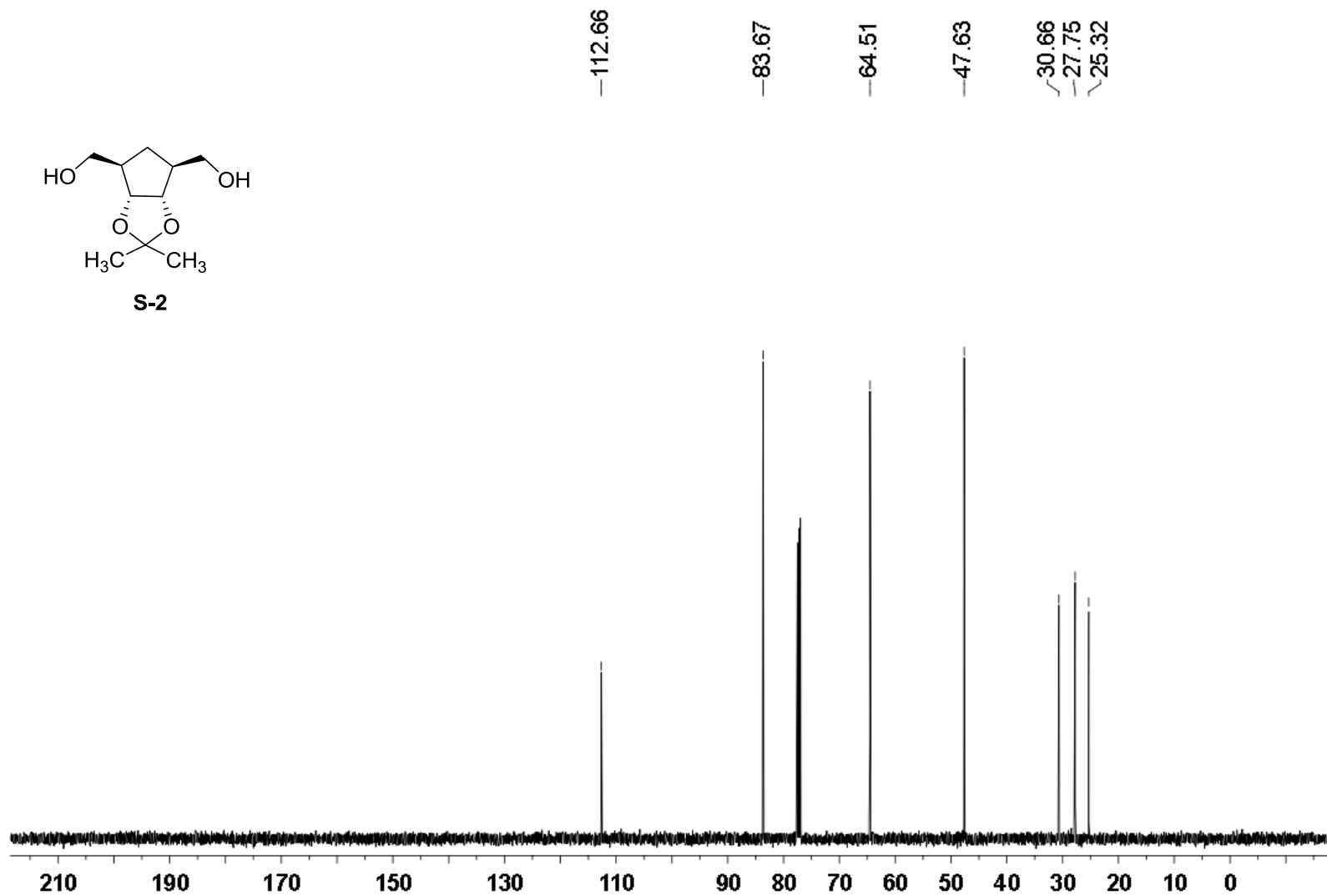
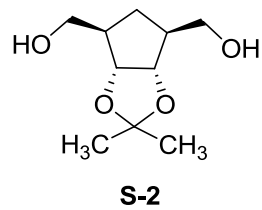


$^1\text{H}$  NMR (500 MHz) spectrum of **6i** in  $\text{CDCl}_3$

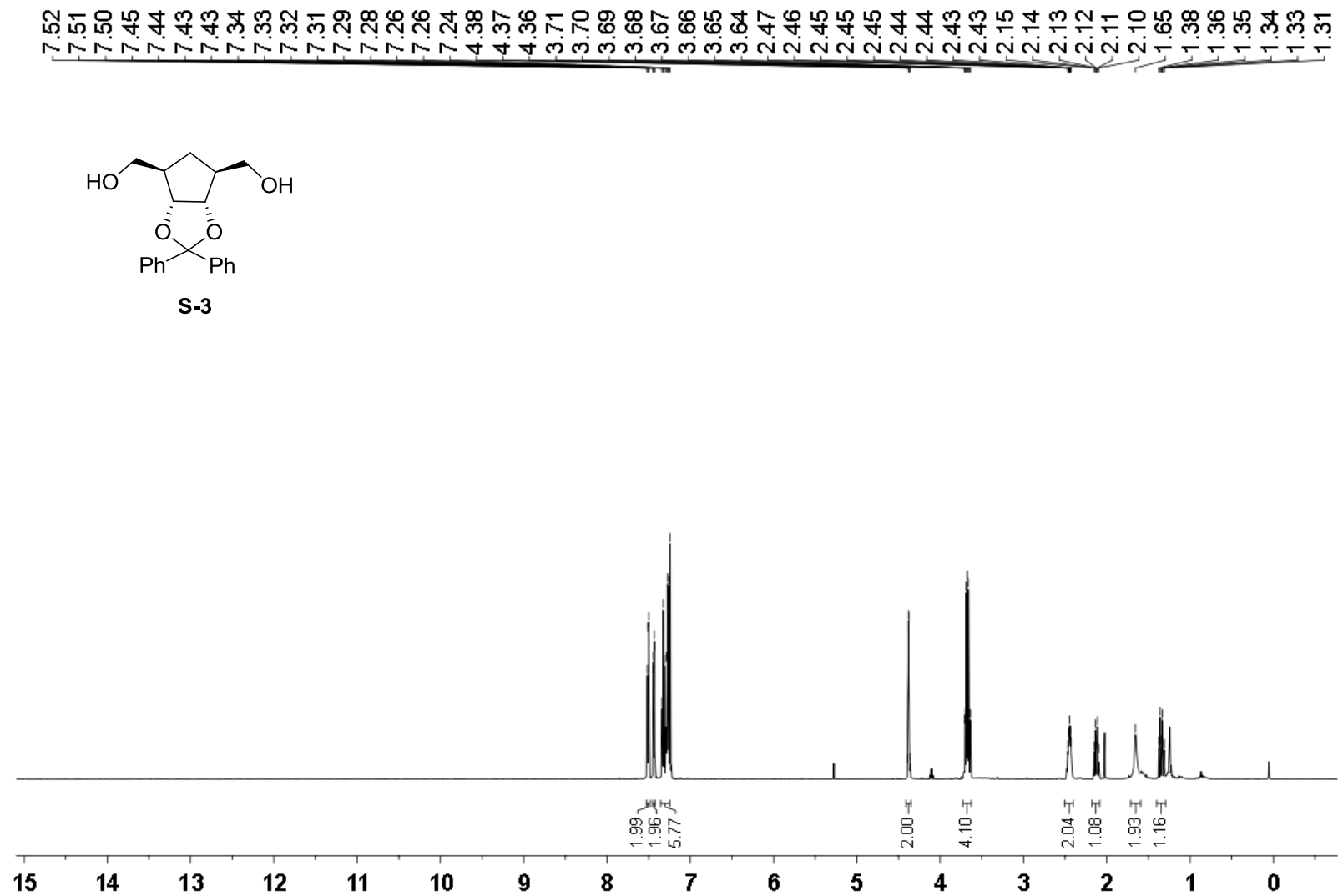




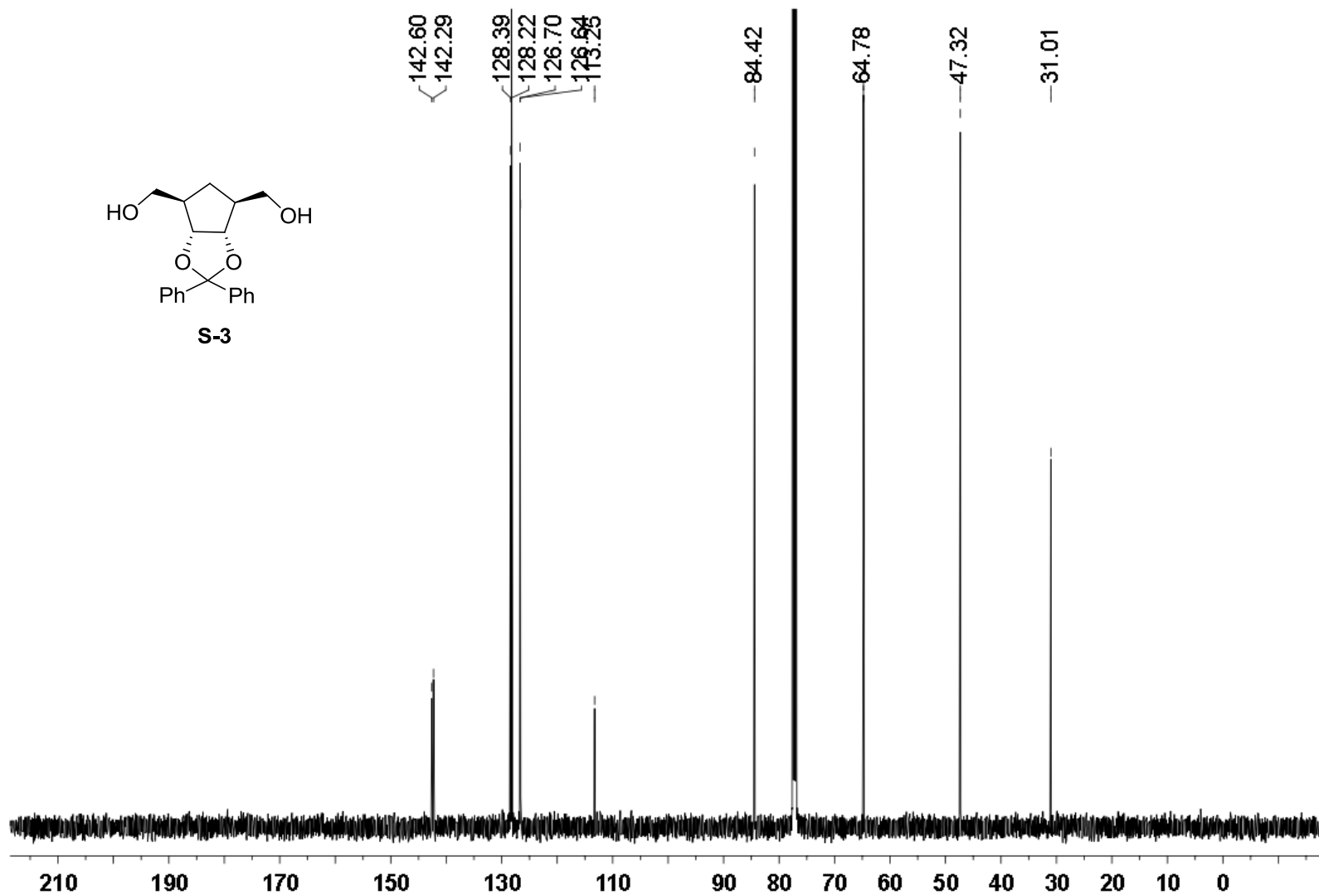
<sup>1</sup>H NMR (500 MHz) spectrum of S-2 in CDCl<sub>3</sub>



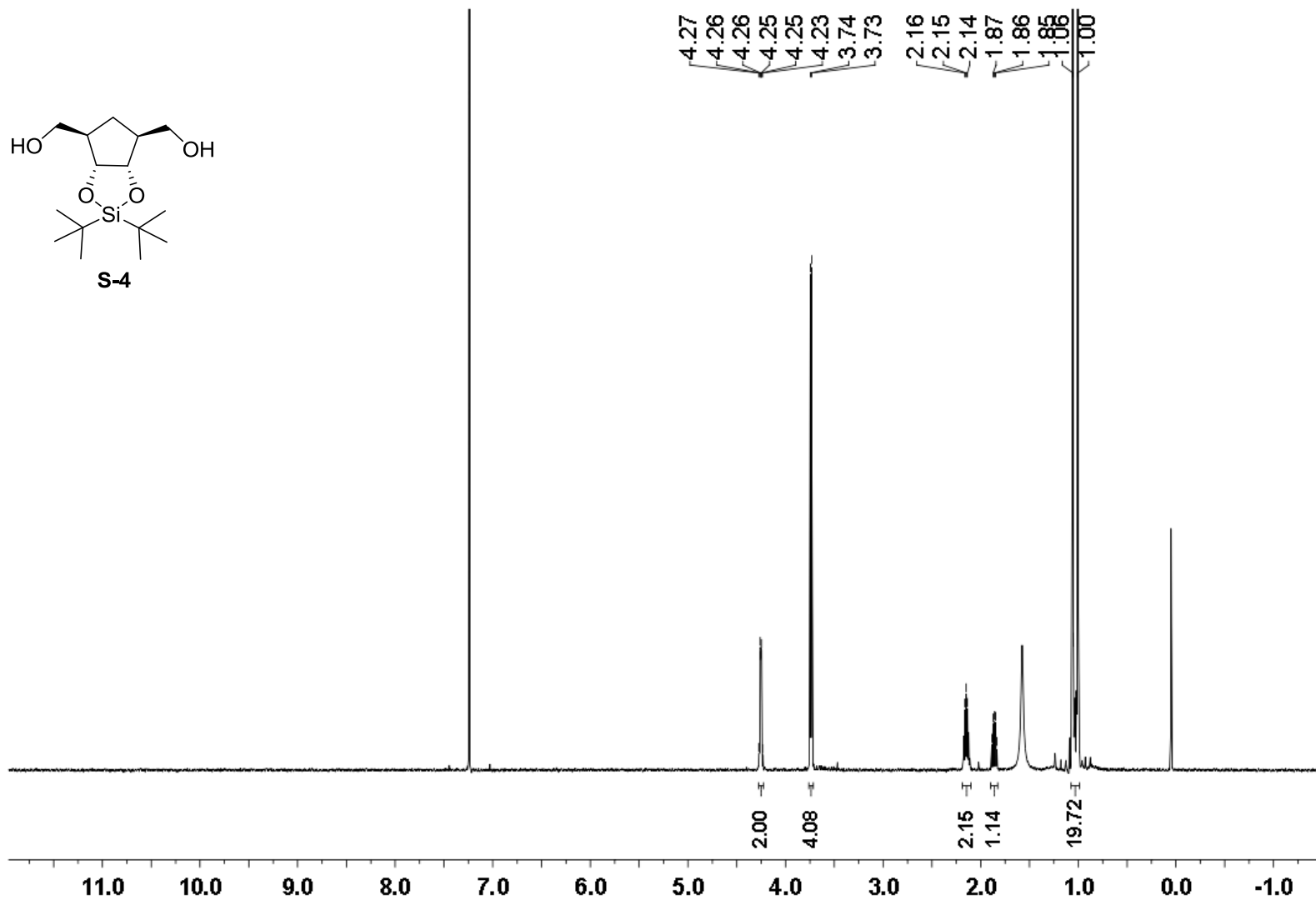
$^{13}\text{C}$  NMR (126 MHz) spectrum of S-2 in  $\text{CDCl}_3$



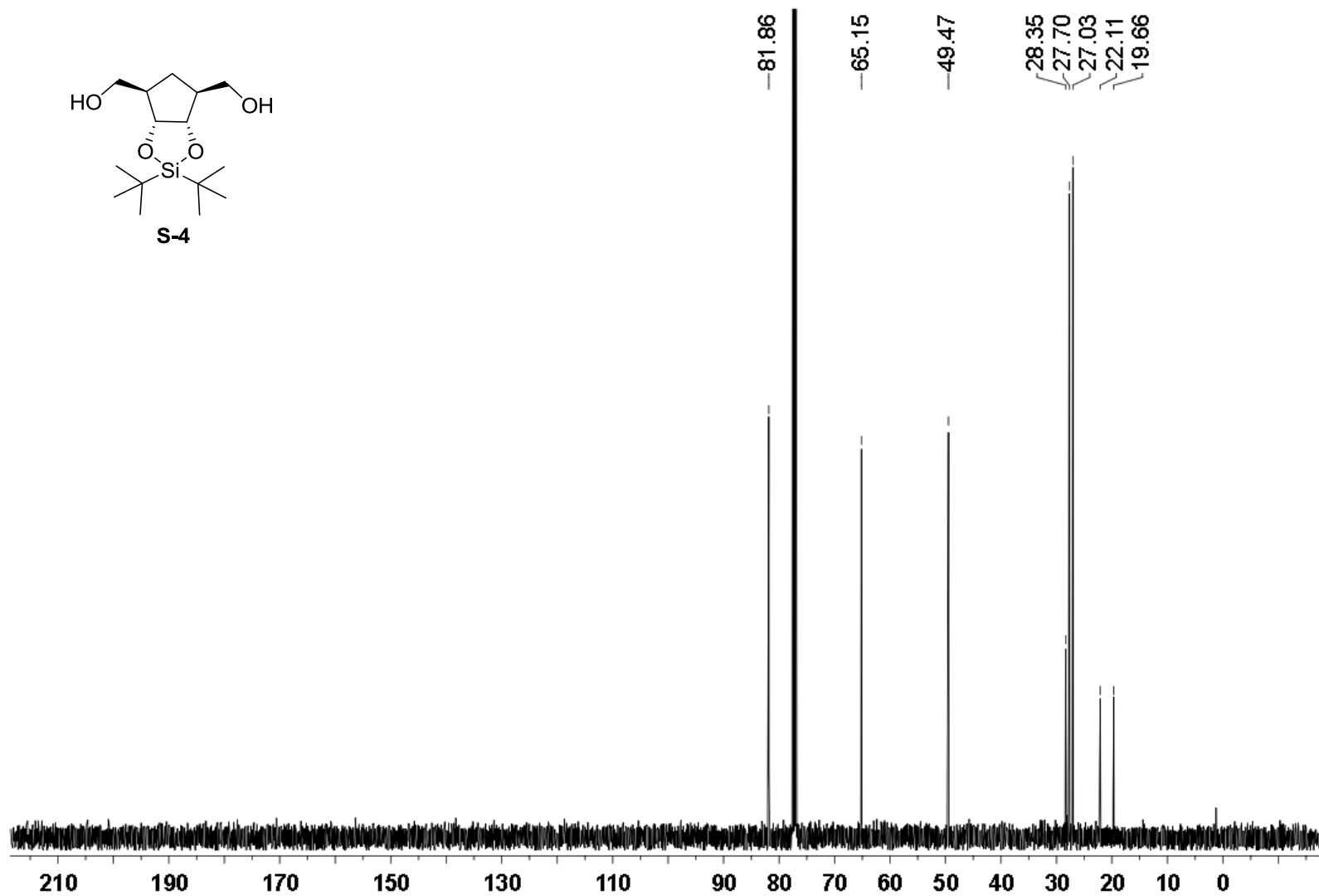
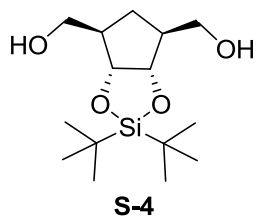
<sup>1</sup>H NMR (500 MHz) spectrum of **S-3** in CDCl<sub>3</sub>



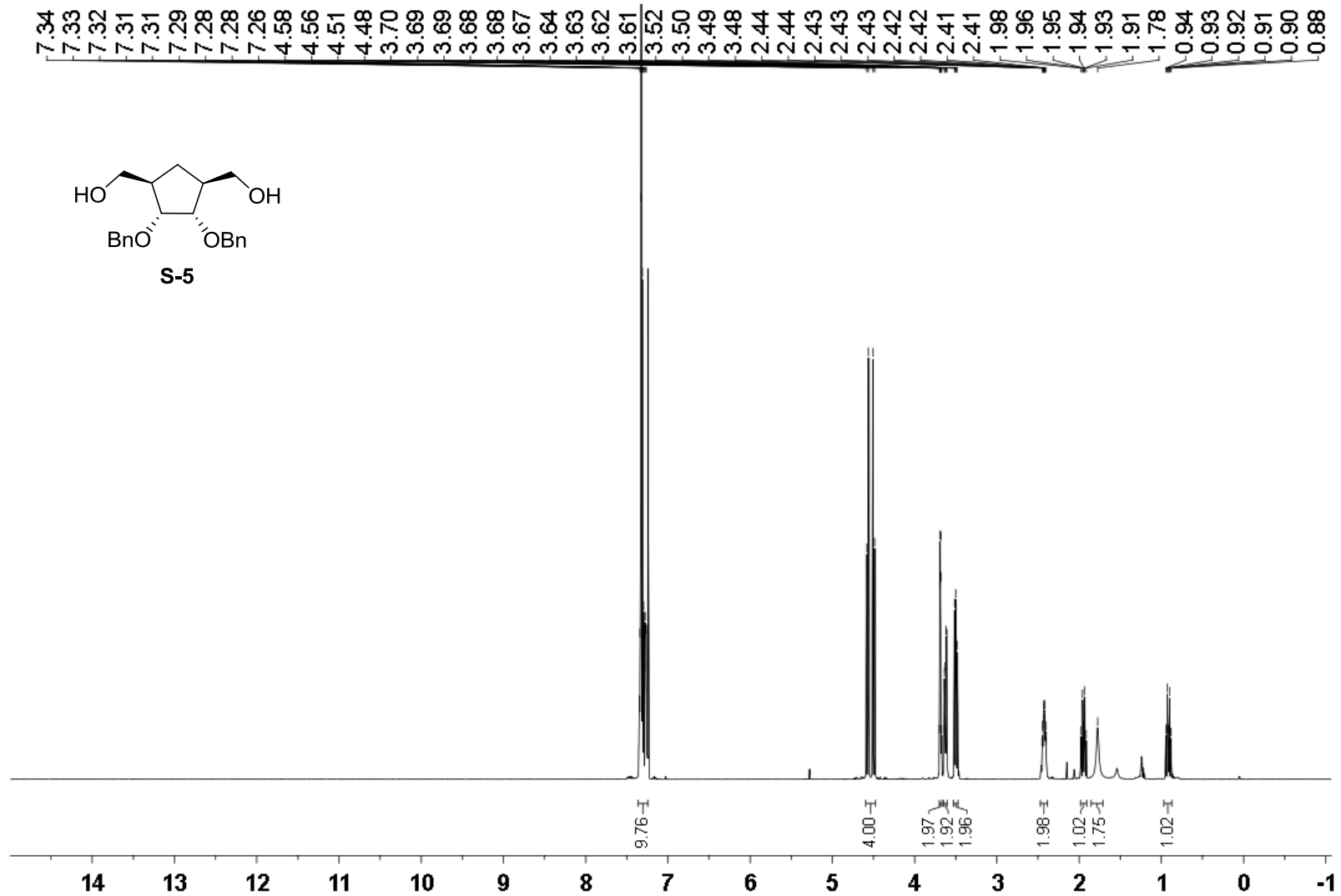
$^{13}\text{C}$  NMR (126 MHz) spectrum of **S-3** in  $\text{CDCl}_3$



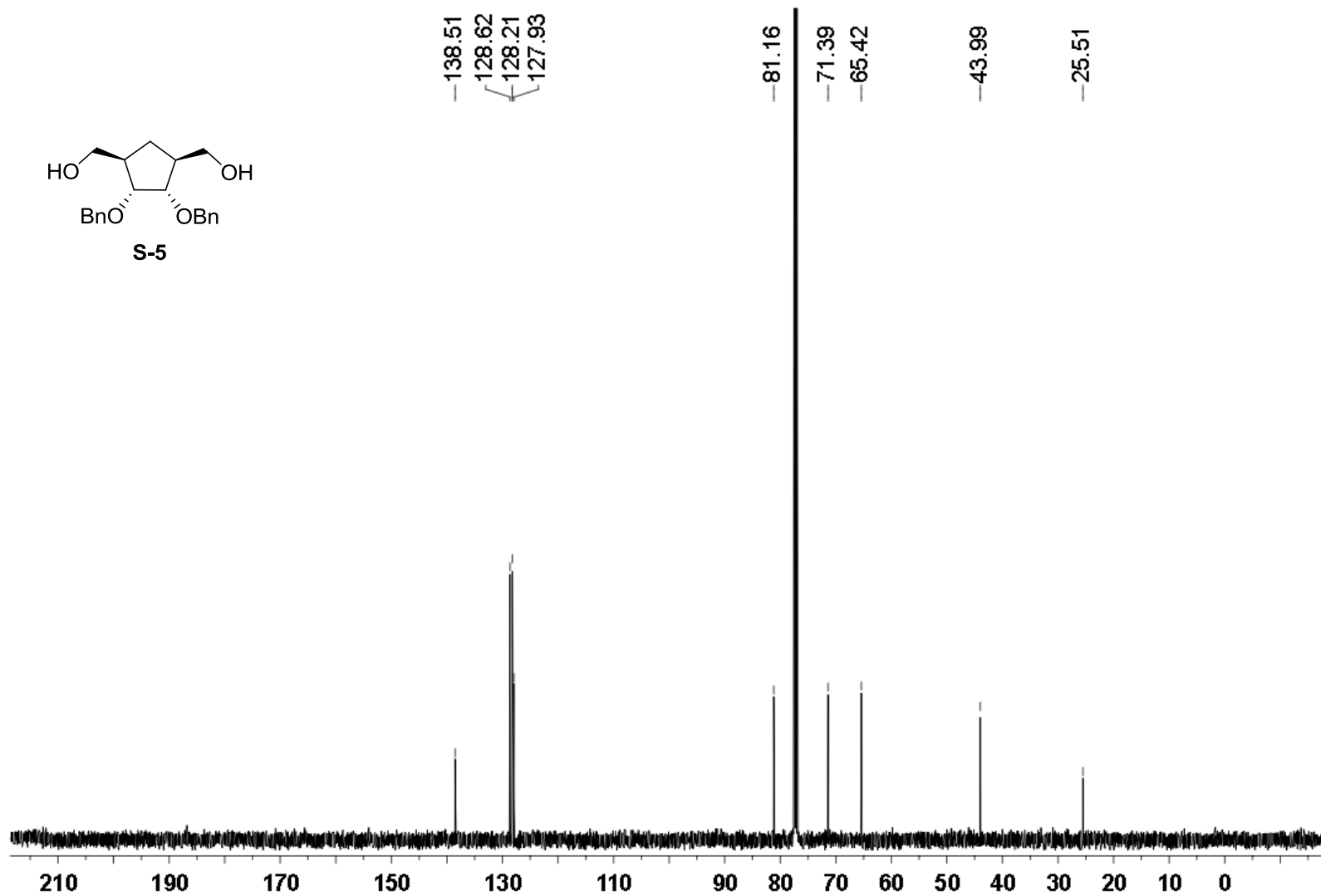
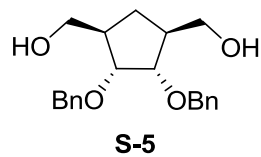
<sup>1</sup>H NMR (500 MHz) spectrum of S-4 in CDCl<sub>3</sub>



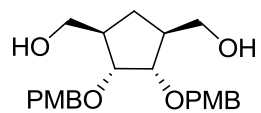
$^{13}\text{C}$  NMR (126 MHz) spectrum of **S-4** in  $\text{CDCl}_3$



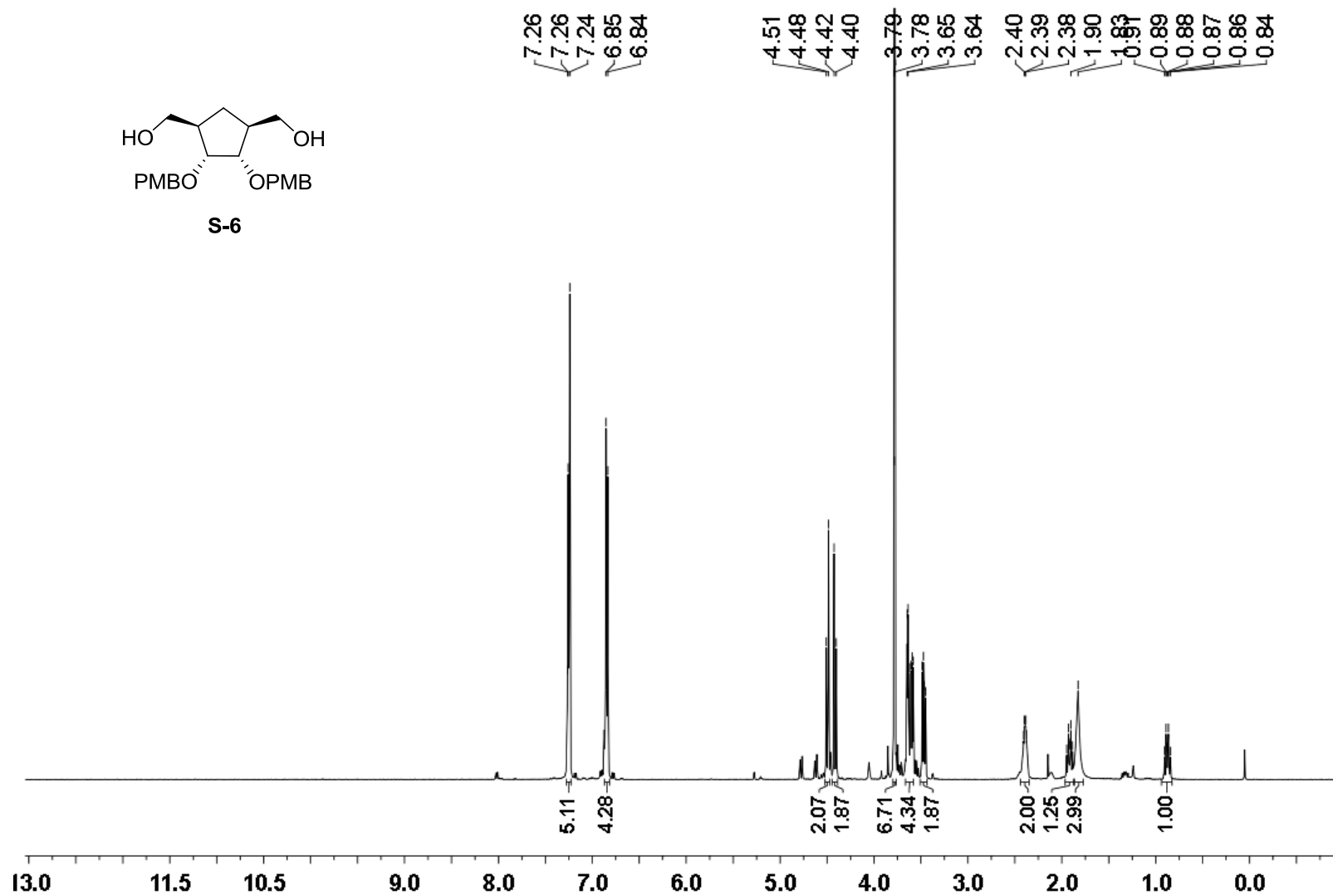
<sup>1</sup>H NMR (500 MHz) spectrum of **S-5** in CDCl<sub>3</sub>



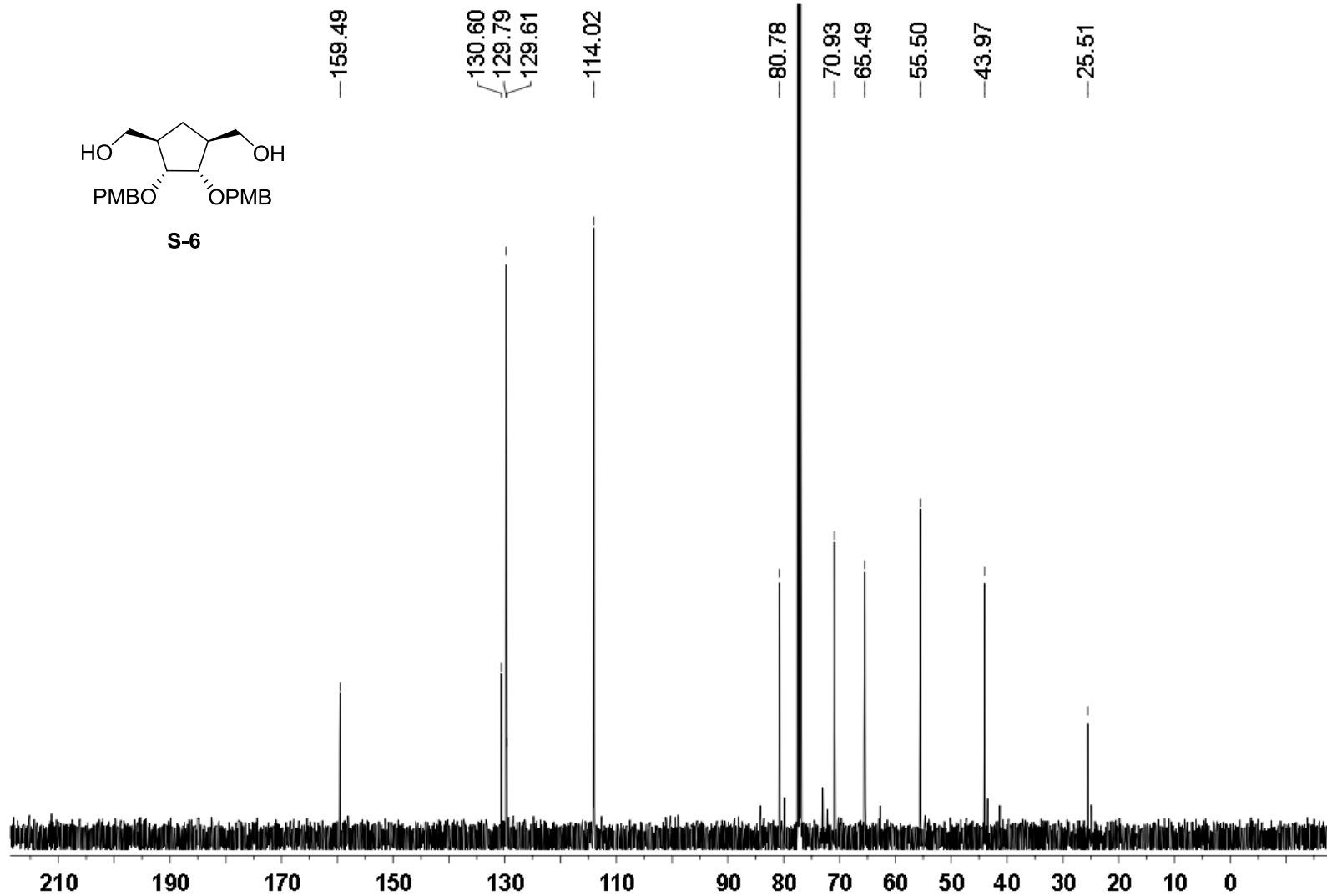
$^{13}\text{C}$  NMR (126 MHz) spectrum of **S-5** in  $\text{CDCl}_3$



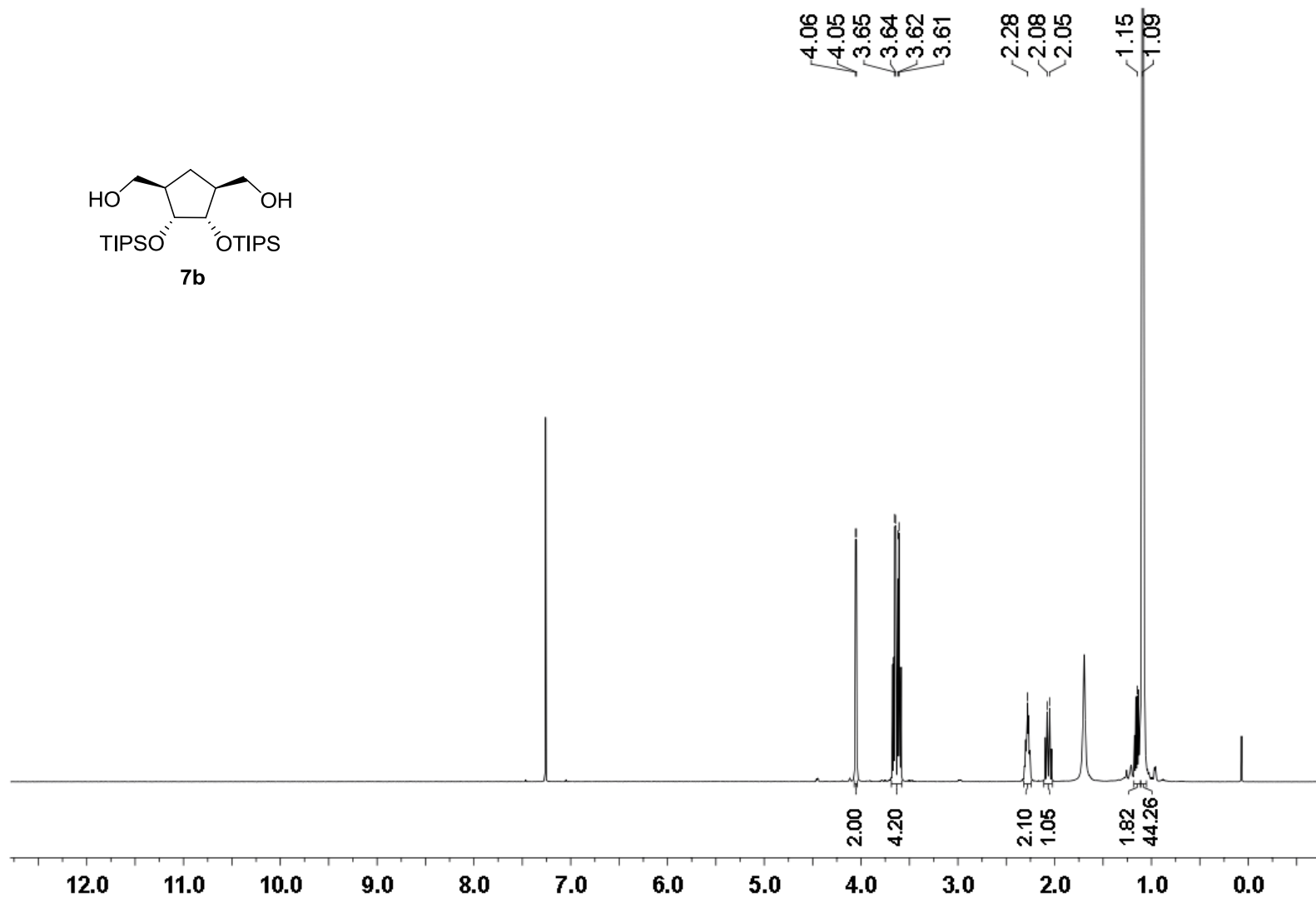
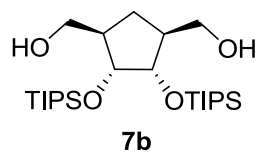
S-6



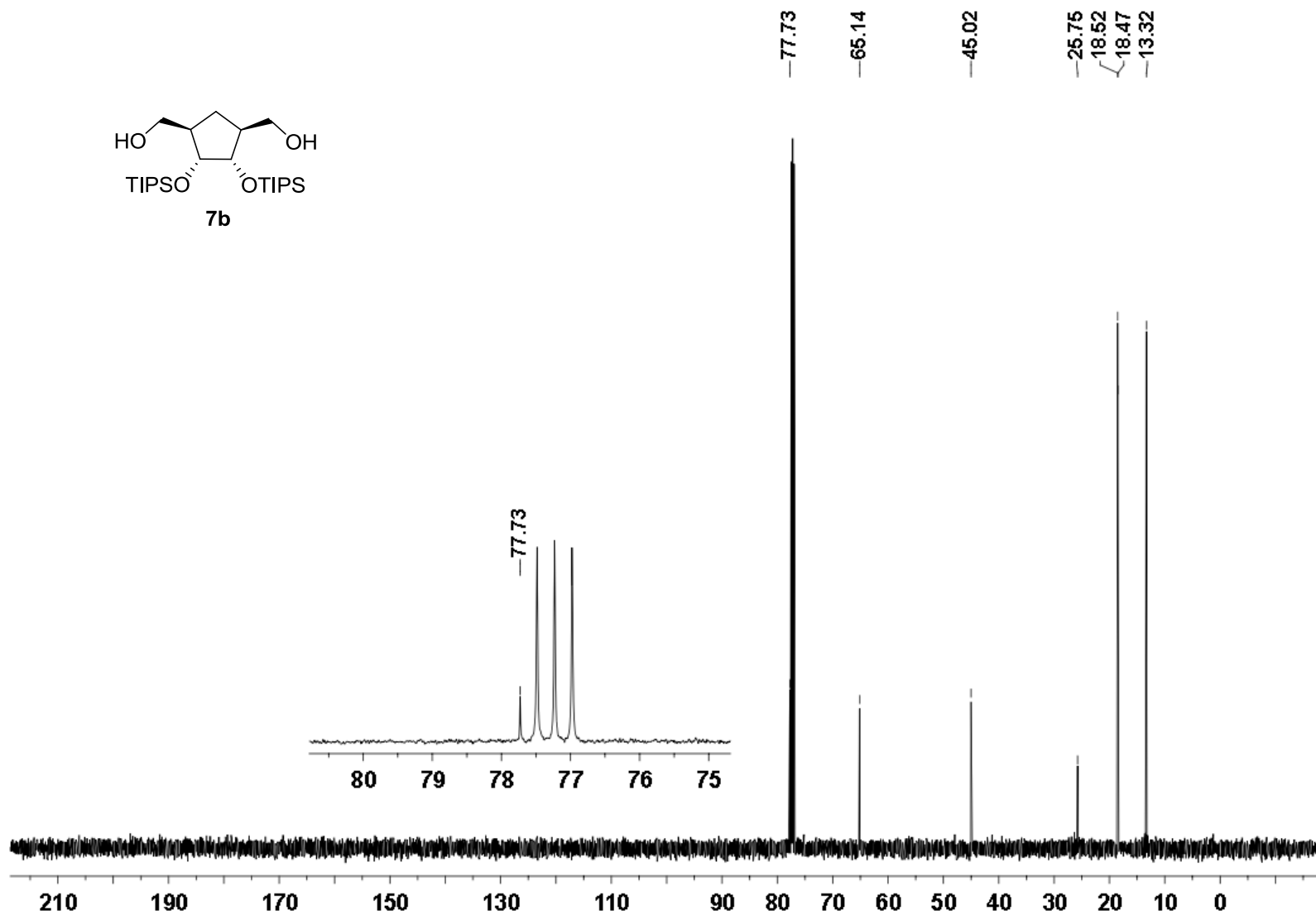
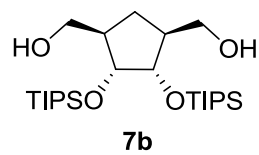
<sup>1</sup>H NMR (500 MHz) spectrum of S-6 in CDCl<sub>3</sub>



$^{13}\text{C}$  NMR (126 MHz) spectrum of **S-6** in  $\text{CDCl}_3$



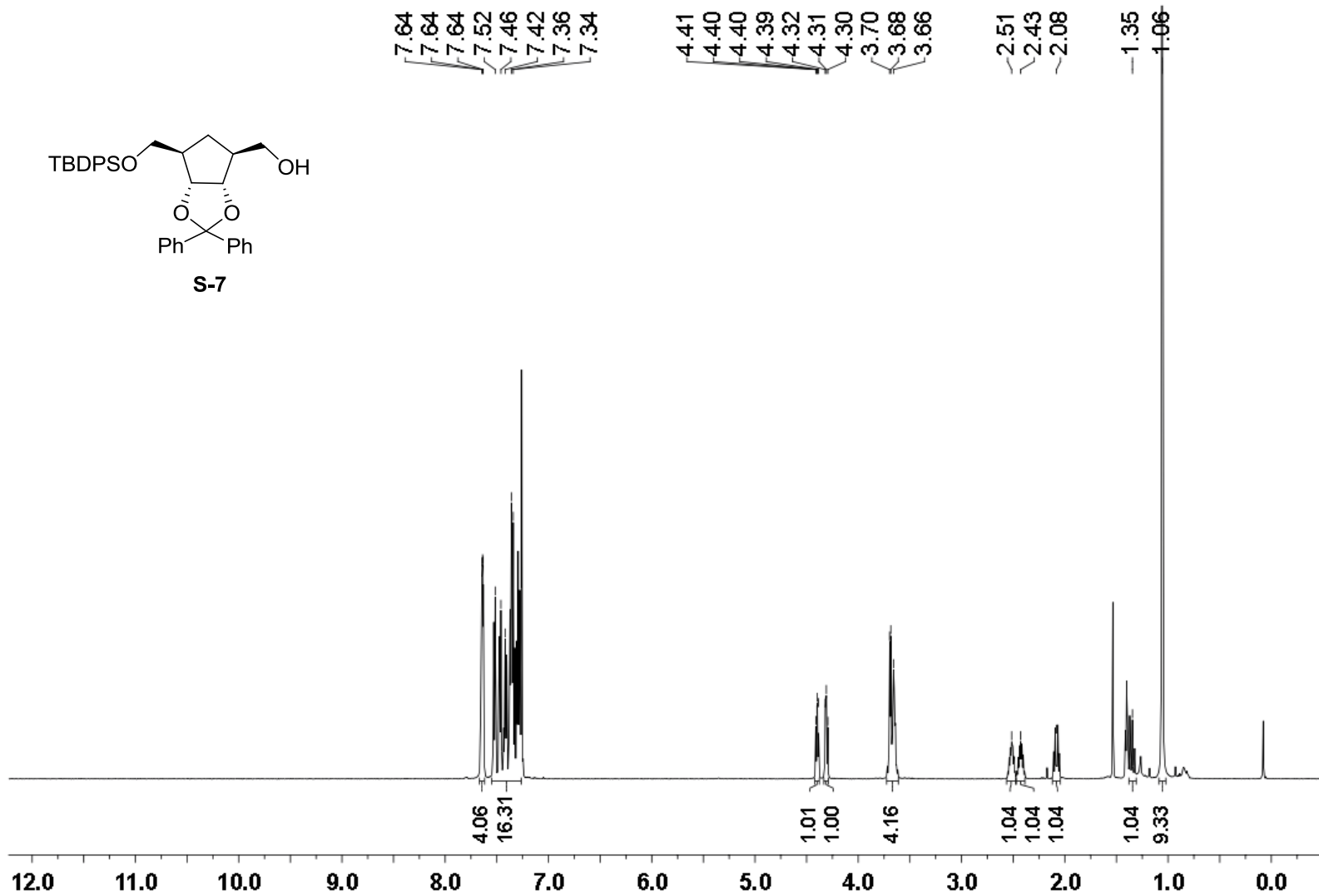
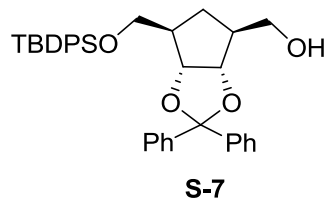
$^1\text{H}$  NMR (500 MHz) spectrum of **7b** in  $\text{CDCl}_3$



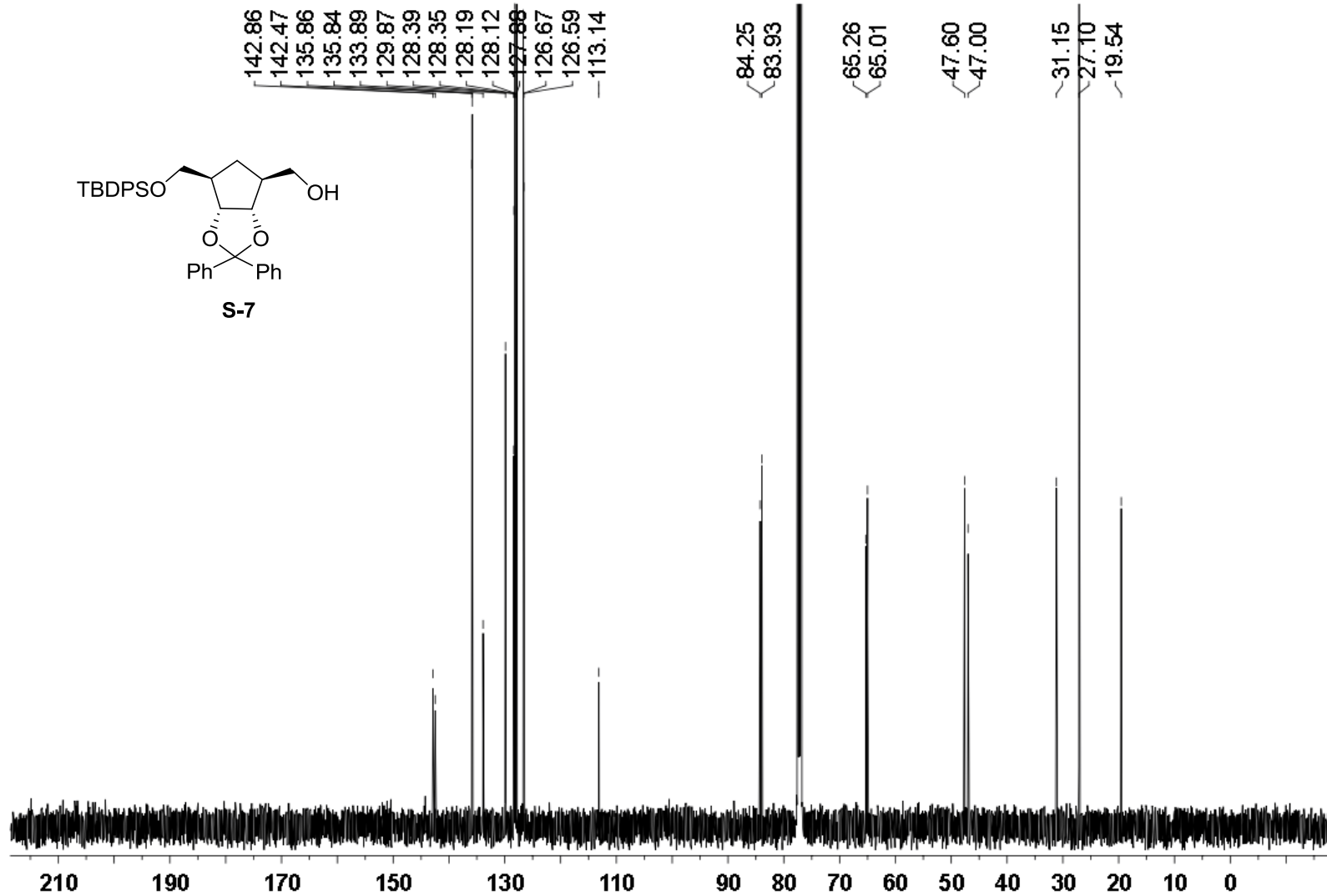
<sup>13</sup>C NMR (126 MHz) spectrum of **7b** in CDCl<sub>3</sub>



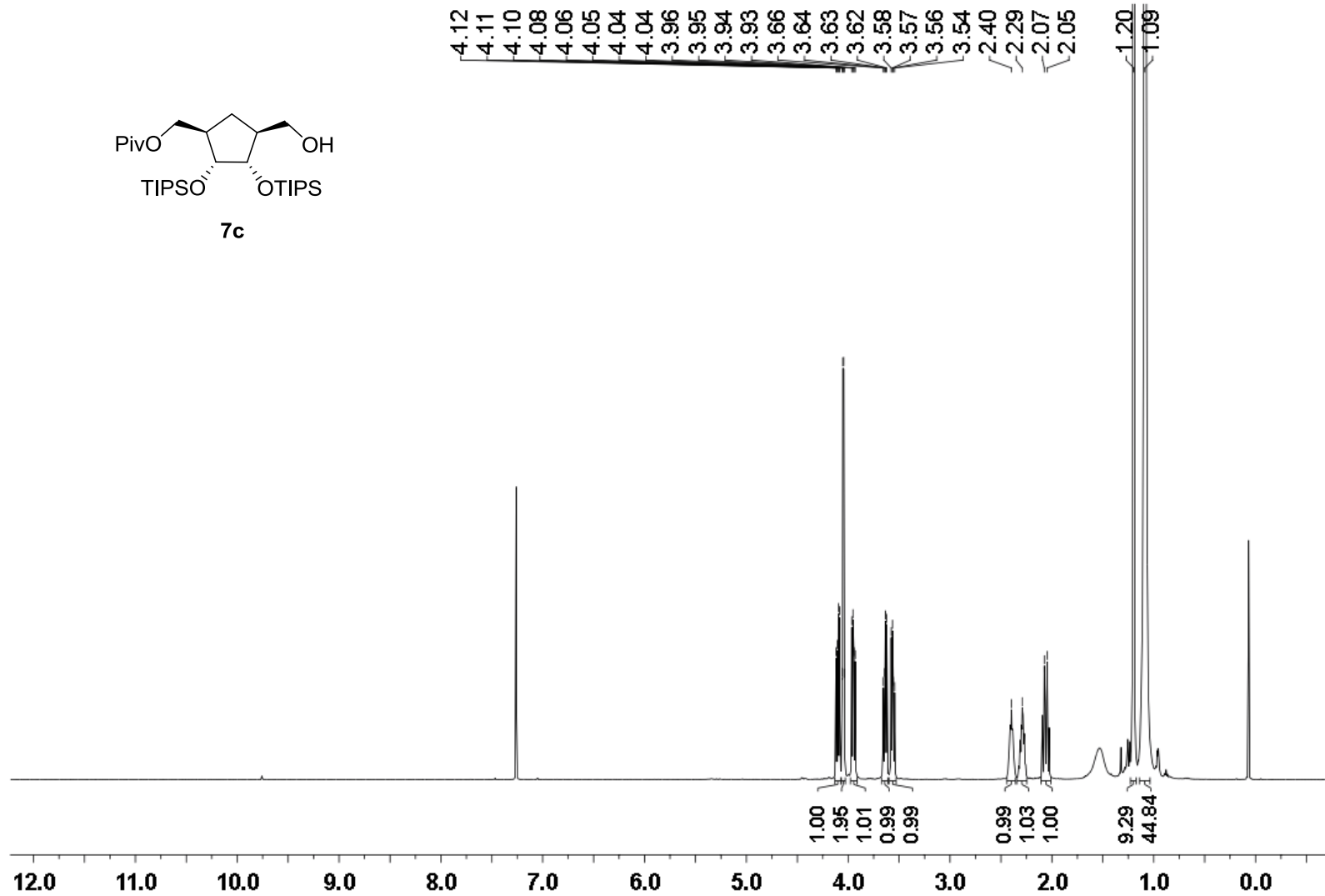




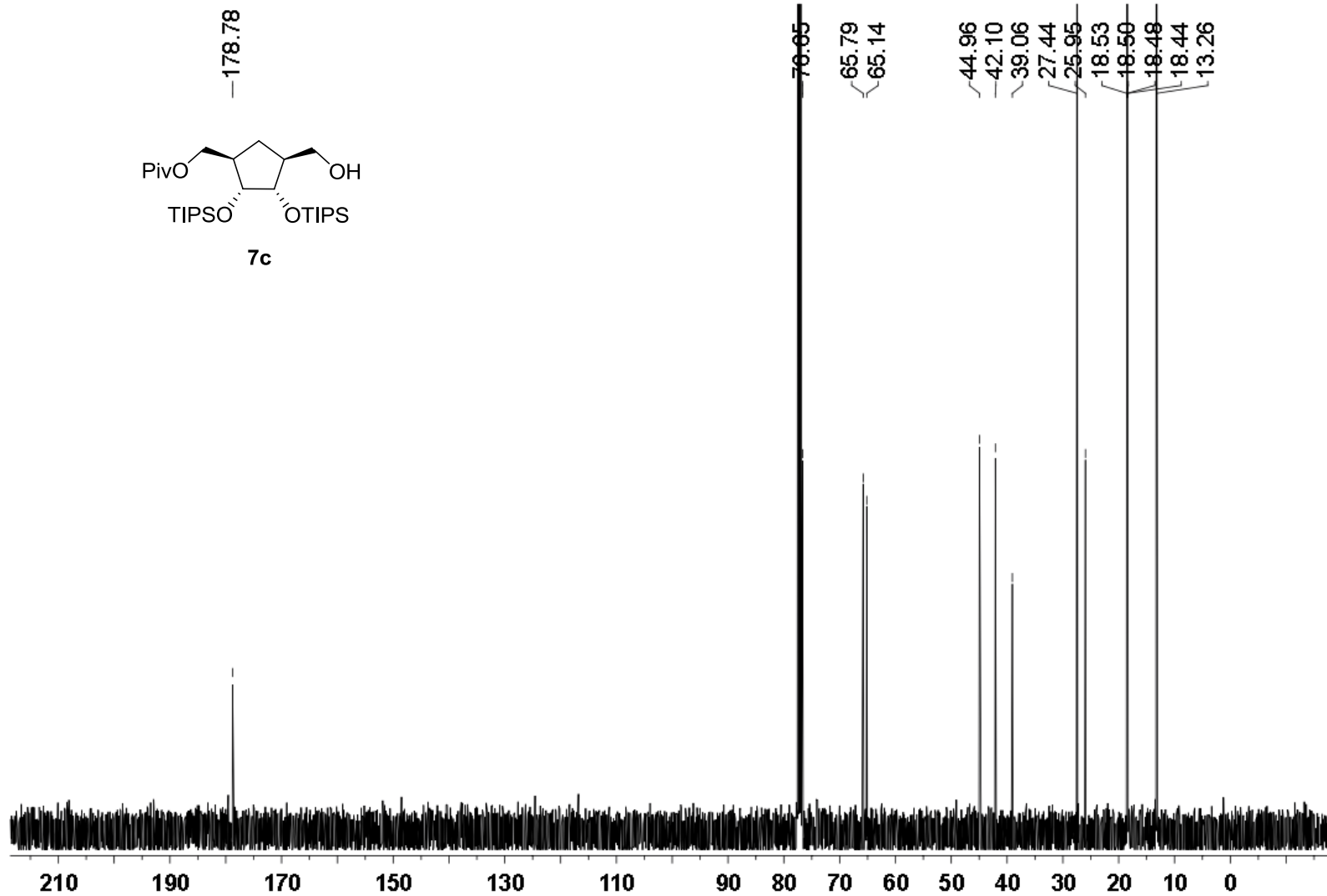
<sup>1</sup>H NMR (500MHz) spectrum of **S-7** in CDCl<sub>3</sub>



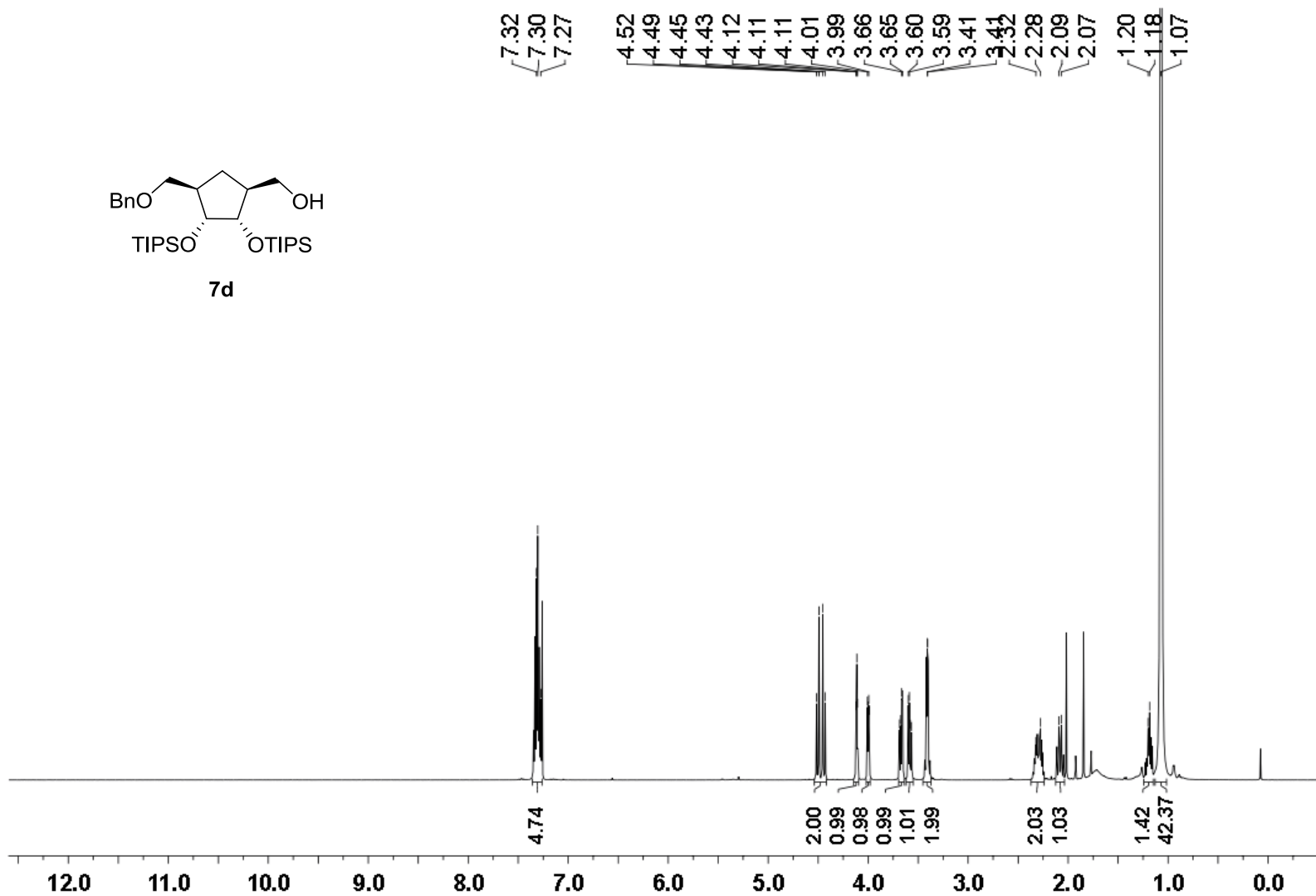
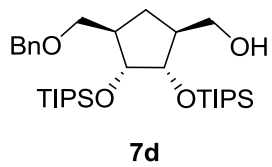
$^{13}\text{C}$  NMR (126 MHz) spectrum of **S-7** in  $\text{CDCl}_3$



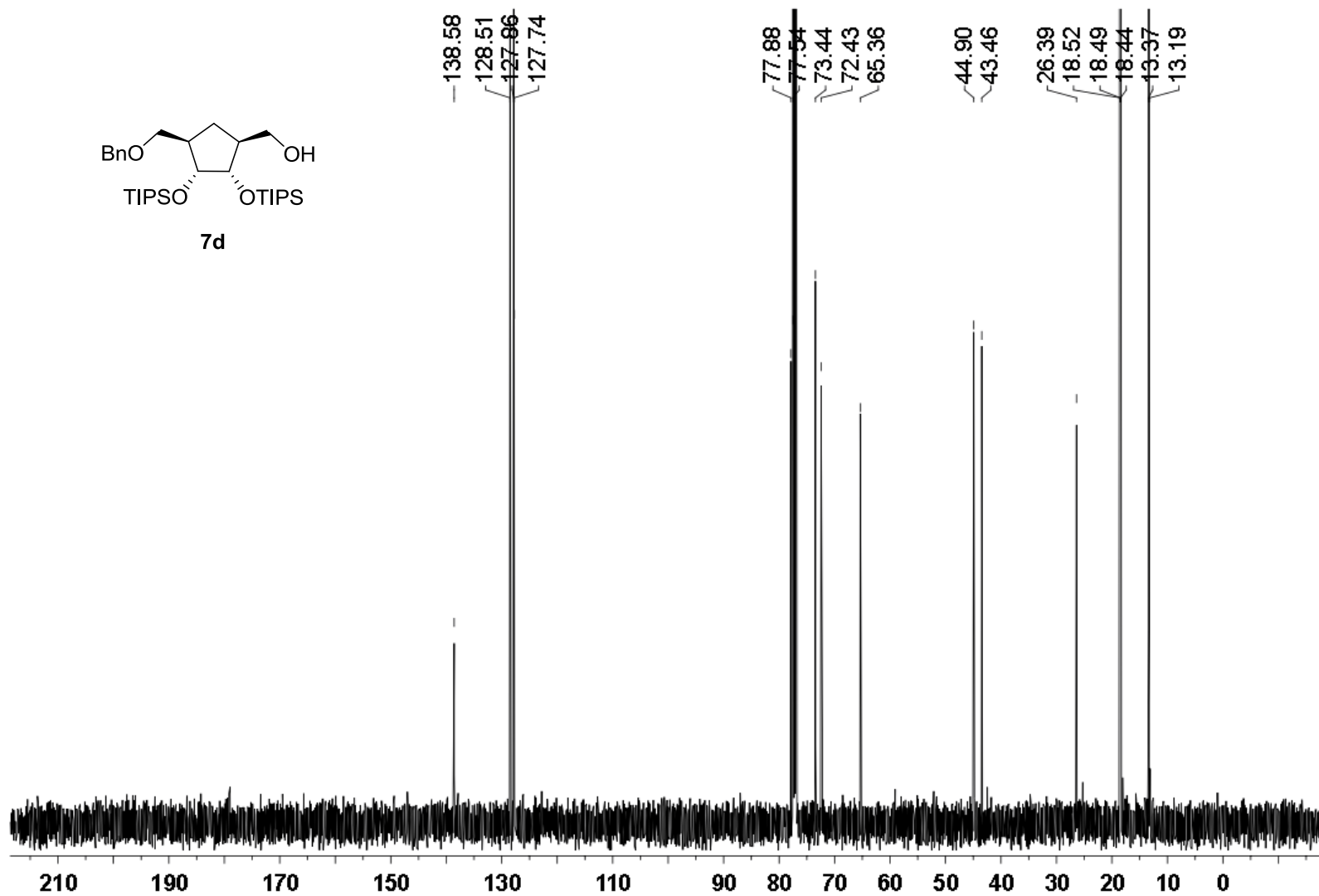
<sup>1</sup>H NMR (500MHz) spectrum of **7c** in CDCl<sub>3</sub>



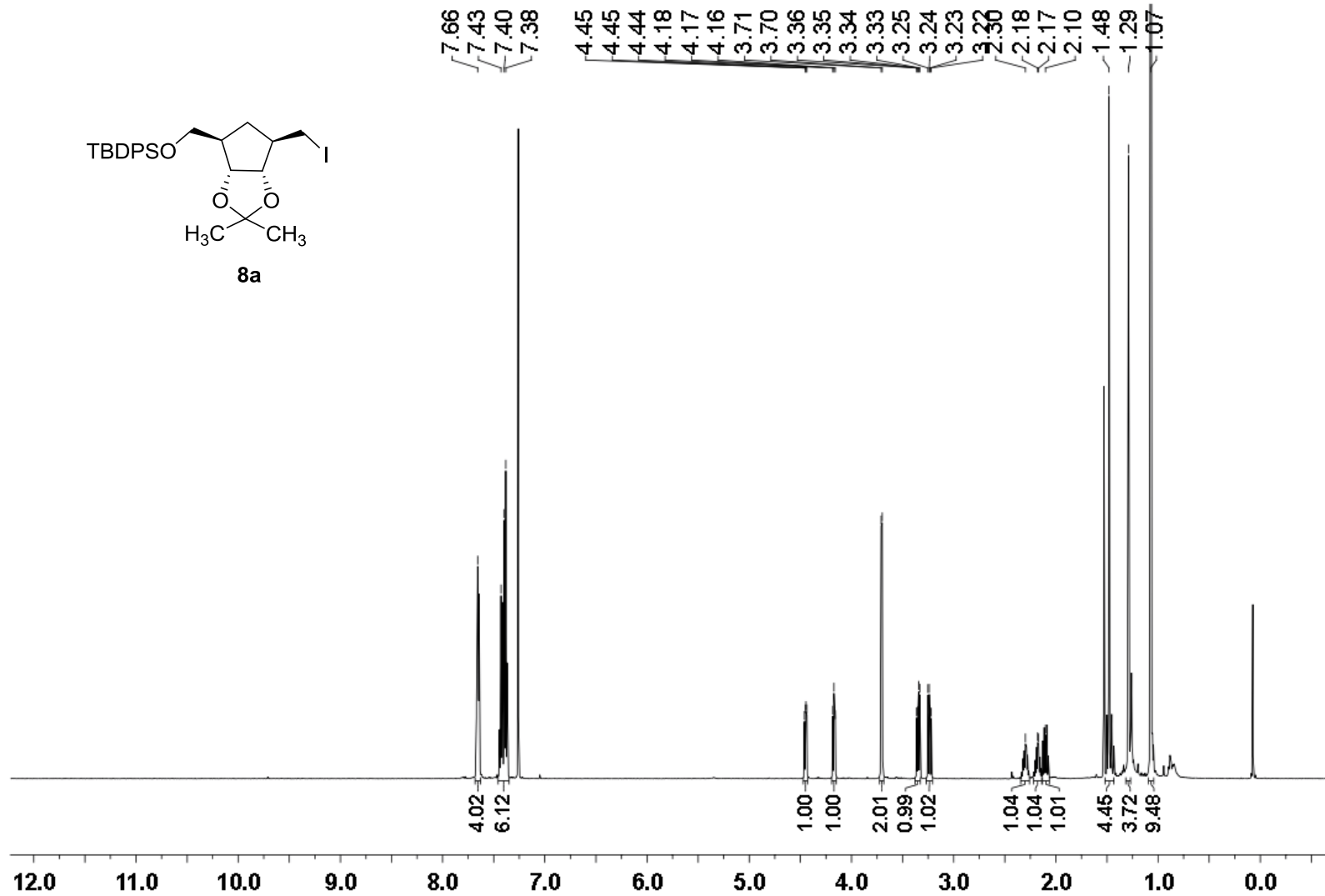
$^{13}\text{C}$  NMR (126 MHz) spectrum of **7c** in  $\text{CDCl}_3$



$^1\text{H}$  NMR (500MHz) spectrum of **7d** in  $\text{CDCl}_3$

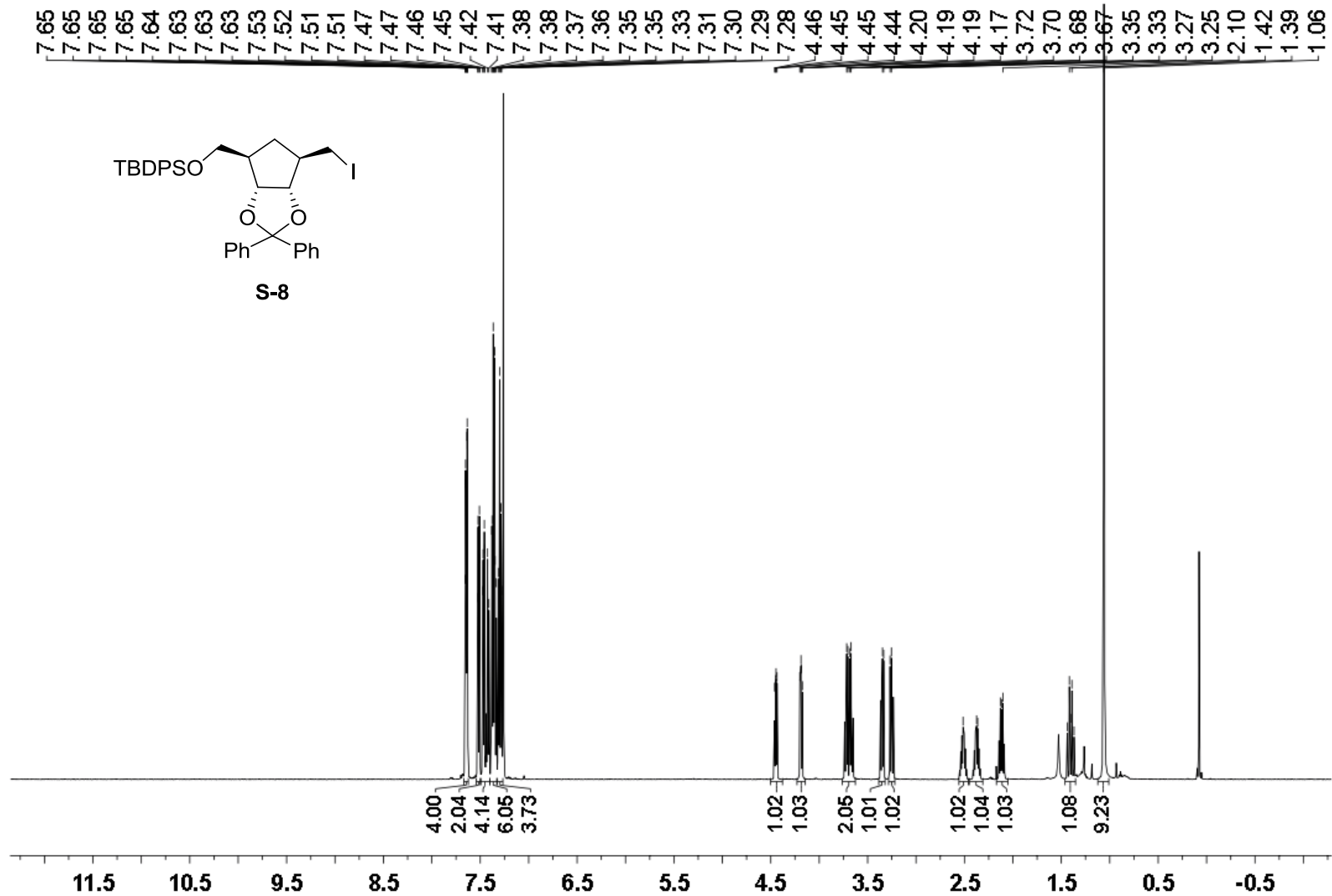


$^{13}\text{C}$  NMR (126 MHz) spectrum of **7d** in  $\text{CDCl}_3$



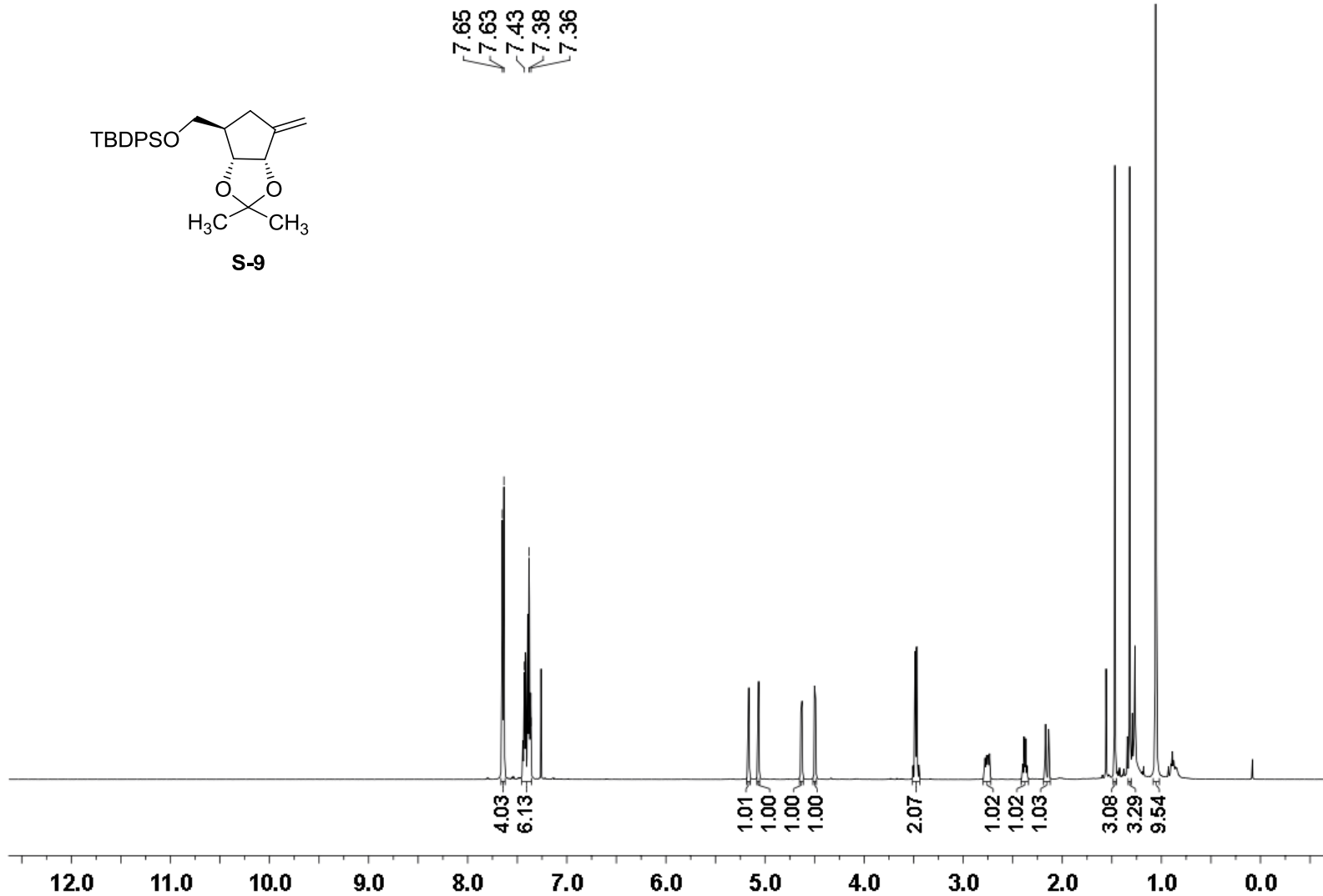
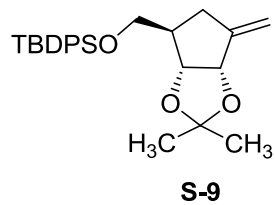
<sup>1</sup>H NMR (500 MHz) spectrum of **8a** in CDCl<sub>3</sub>



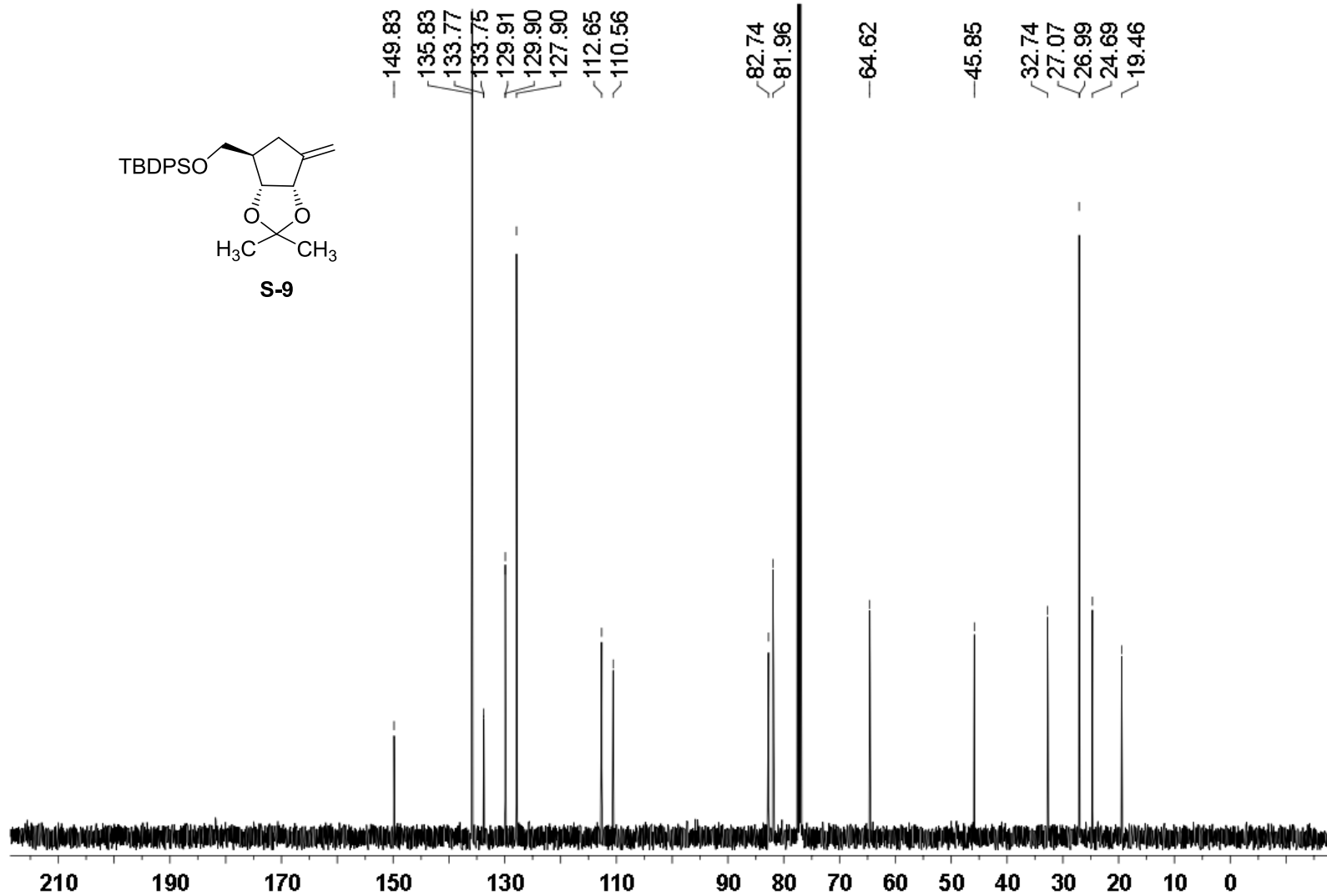


<sup>1</sup>H NMR (500 MHz) spectrum of **S-8** in CDCl<sub>3</sub>

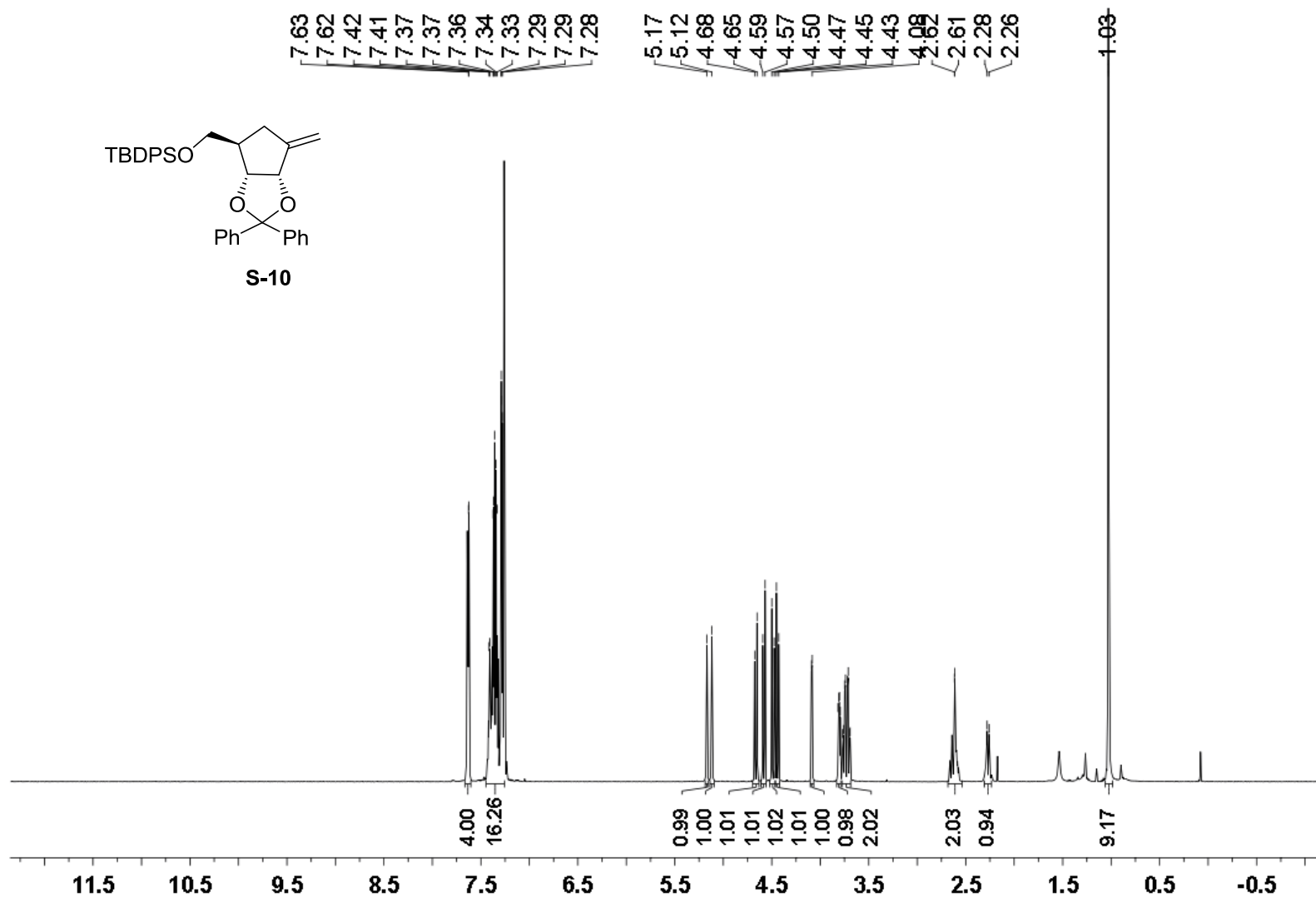




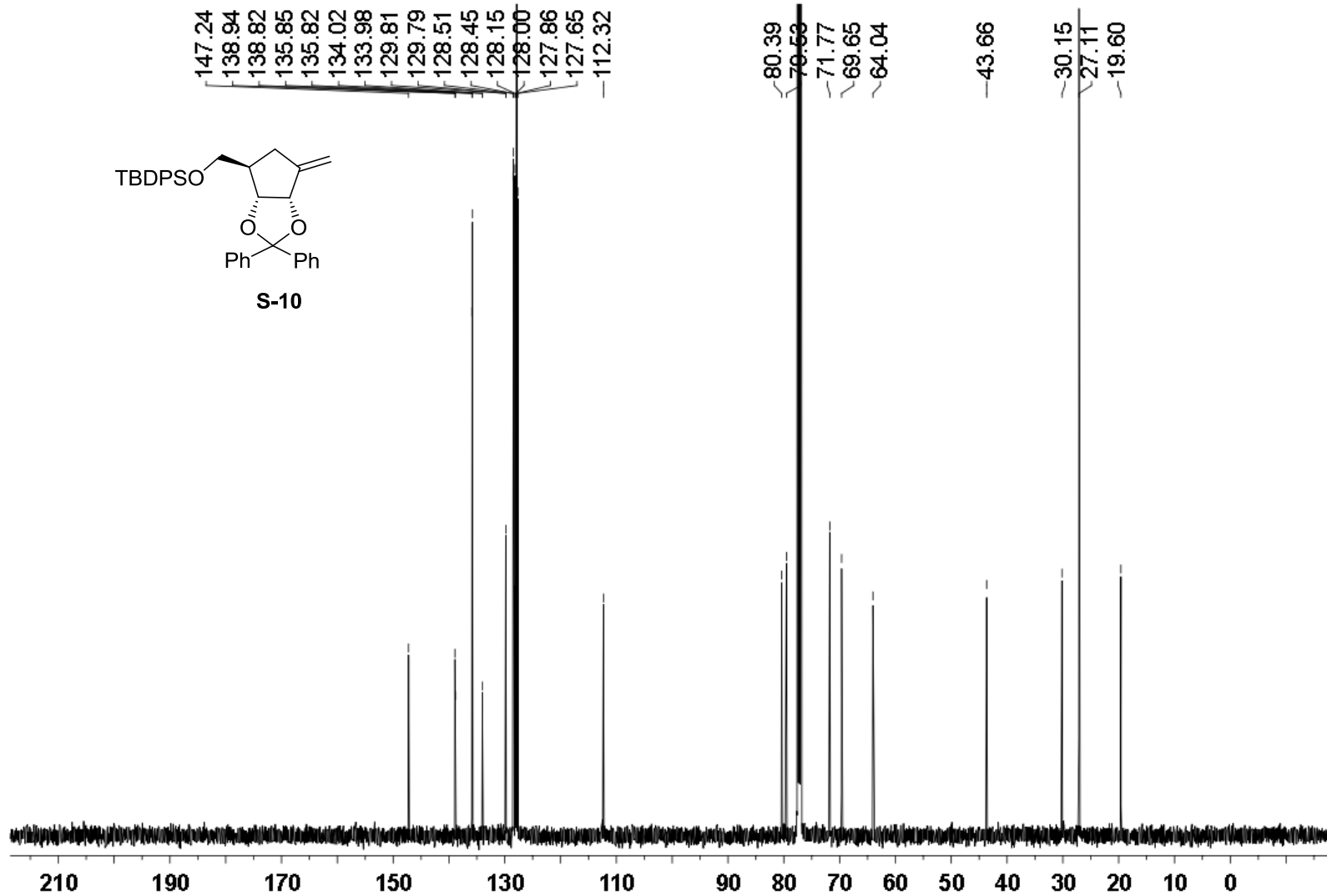
$^1\text{H}$  NMR (500 MHz) spectrum of **S-9** in  $\text{CDCl}_3$



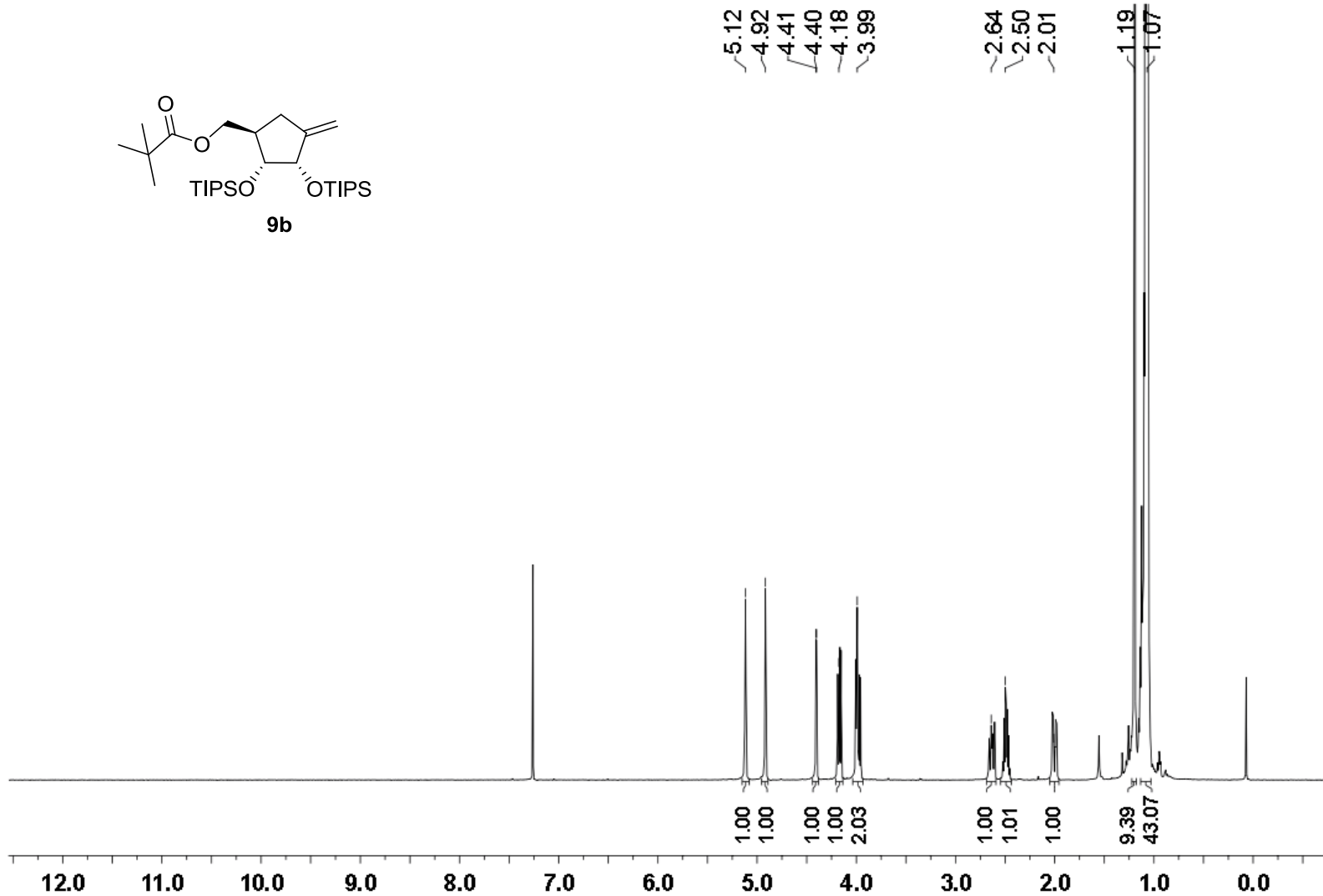
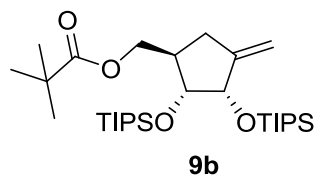
$^{13}\text{C}$  NMR (126 MHz) spectrum of **S-9** in  $\text{CDCl}_3$



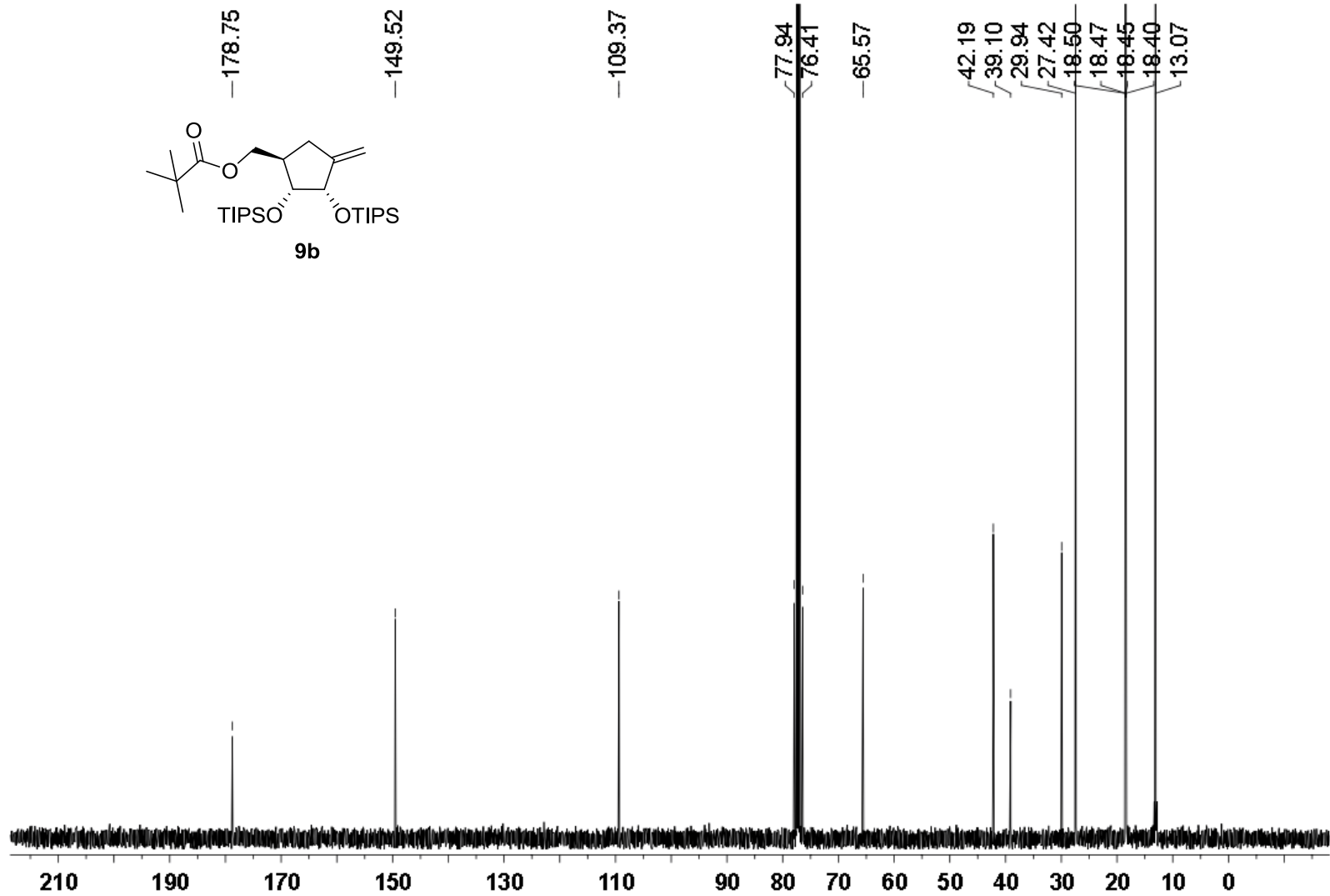
<sup>1</sup>H NMR (500 MHz) spectrum of **S-10** in CDCl<sub>3</sub>



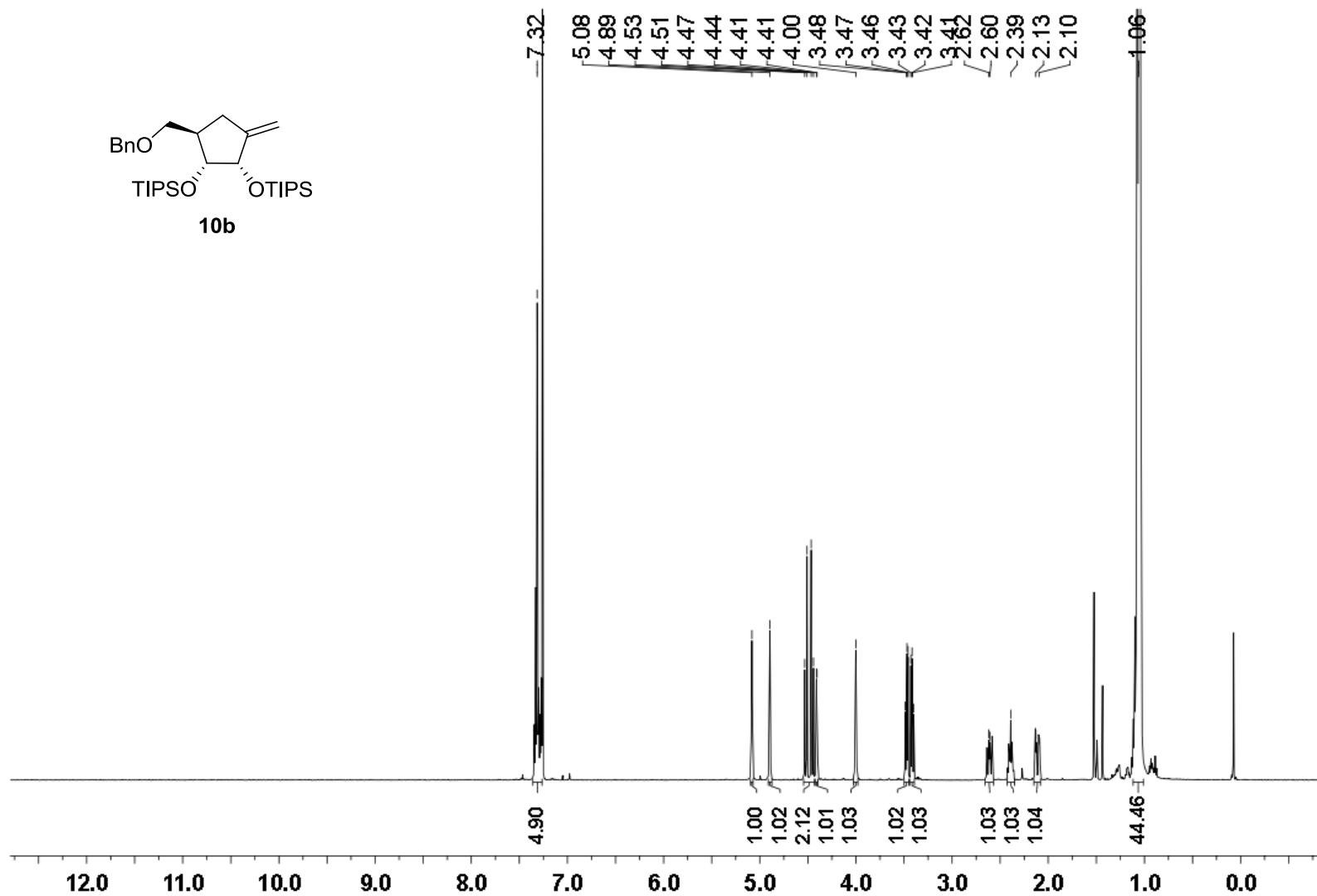
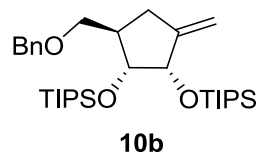
$^{13}\text{C}$  NMR (126 MHz) spectrum of **S-10** in  $\text{CDCl}_3$



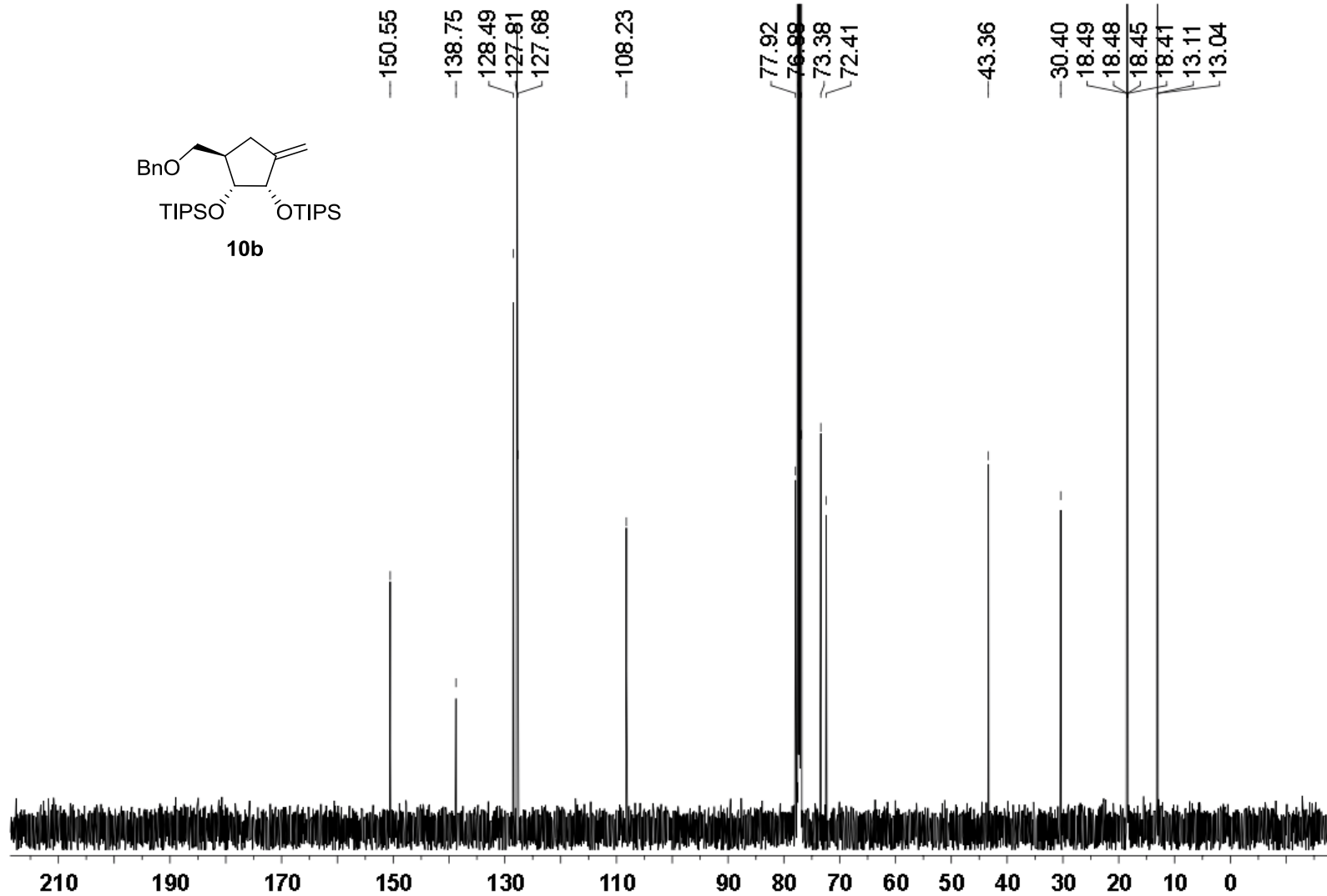
$^1\text{H}$  NMR (500 MHz) spectrum of **9b** in  $\text{CDCl}_3$



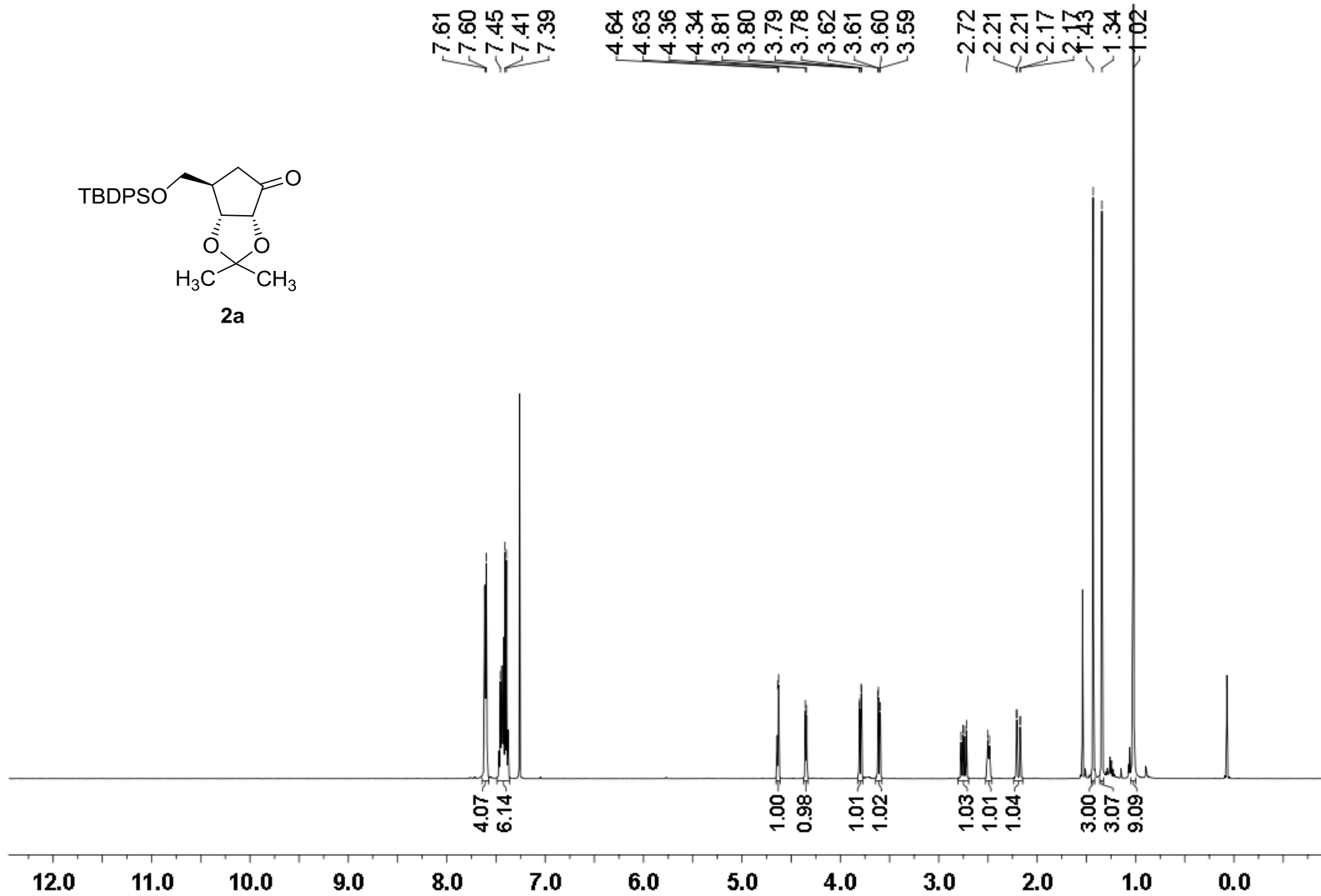
$^{13}\text{C}$  NMR (126 MHz) spectrum of **9b** in  $\text{CDCl}_3$



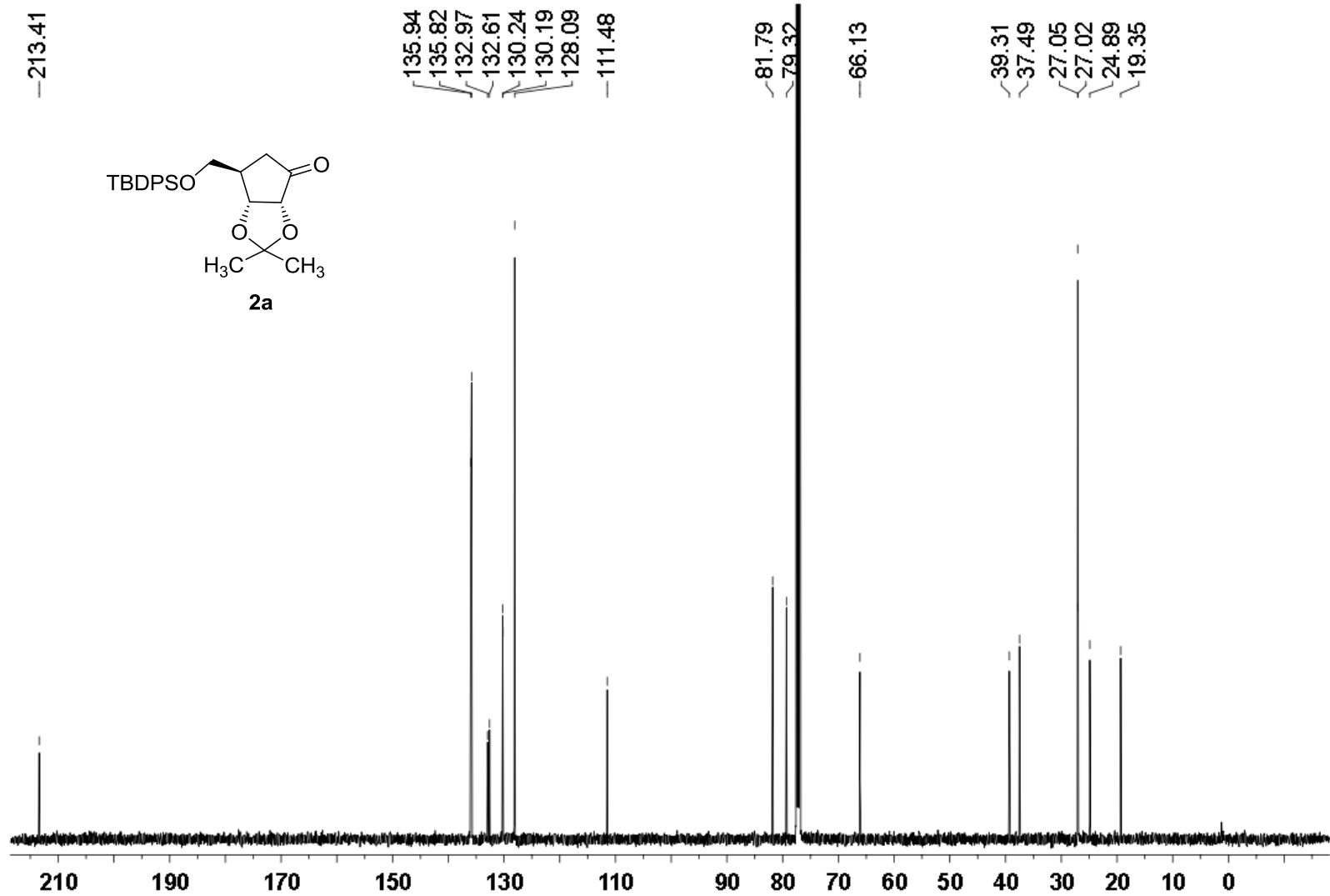
$^1\text{H}$  NMR (500 MHz) spectrum of **10b** in  $\text{CDCl}_3$



$^{13}\text{C}$  NMR (126 MHz) spectrum of **10b** in  $\text{CDCl}_3$

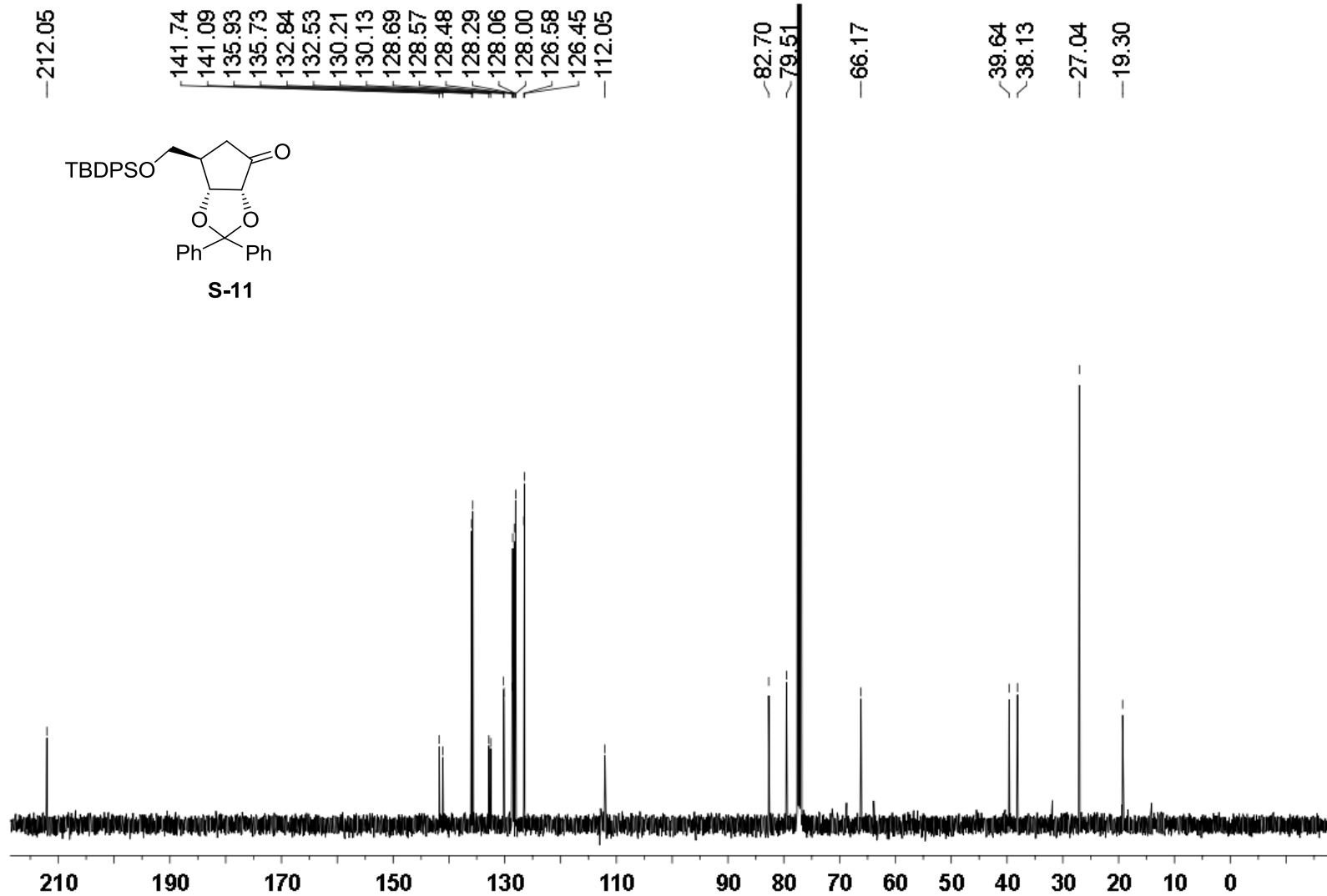


<sup>1</sup>H NMR (500 MHz) spectrum of **2a** in CDCl<sub>3</sub>

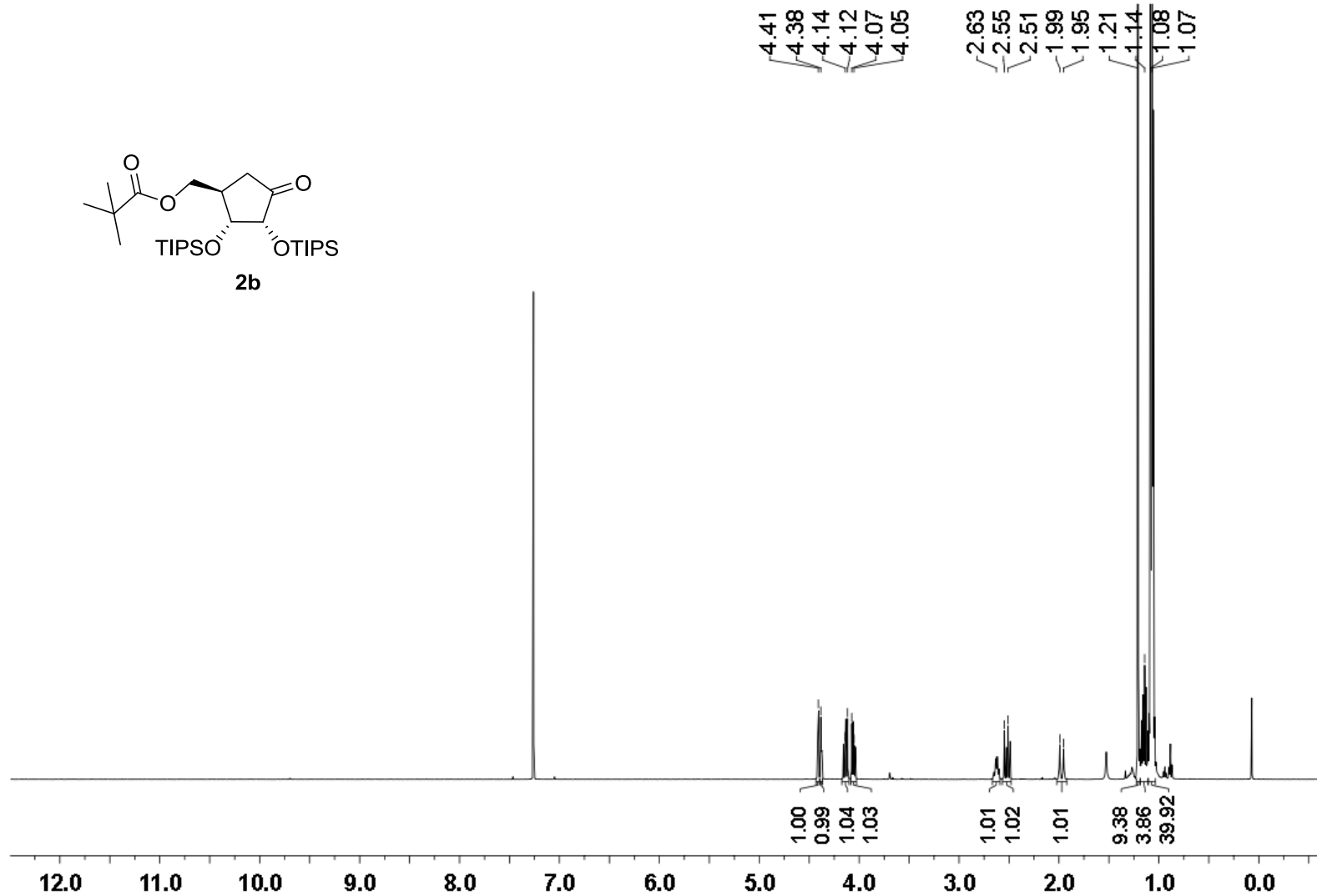
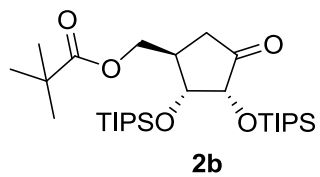


$^{13}\text{C}$  NMR (126 MHz) spectrum of **2a** in  $\text{CDCl}_3$

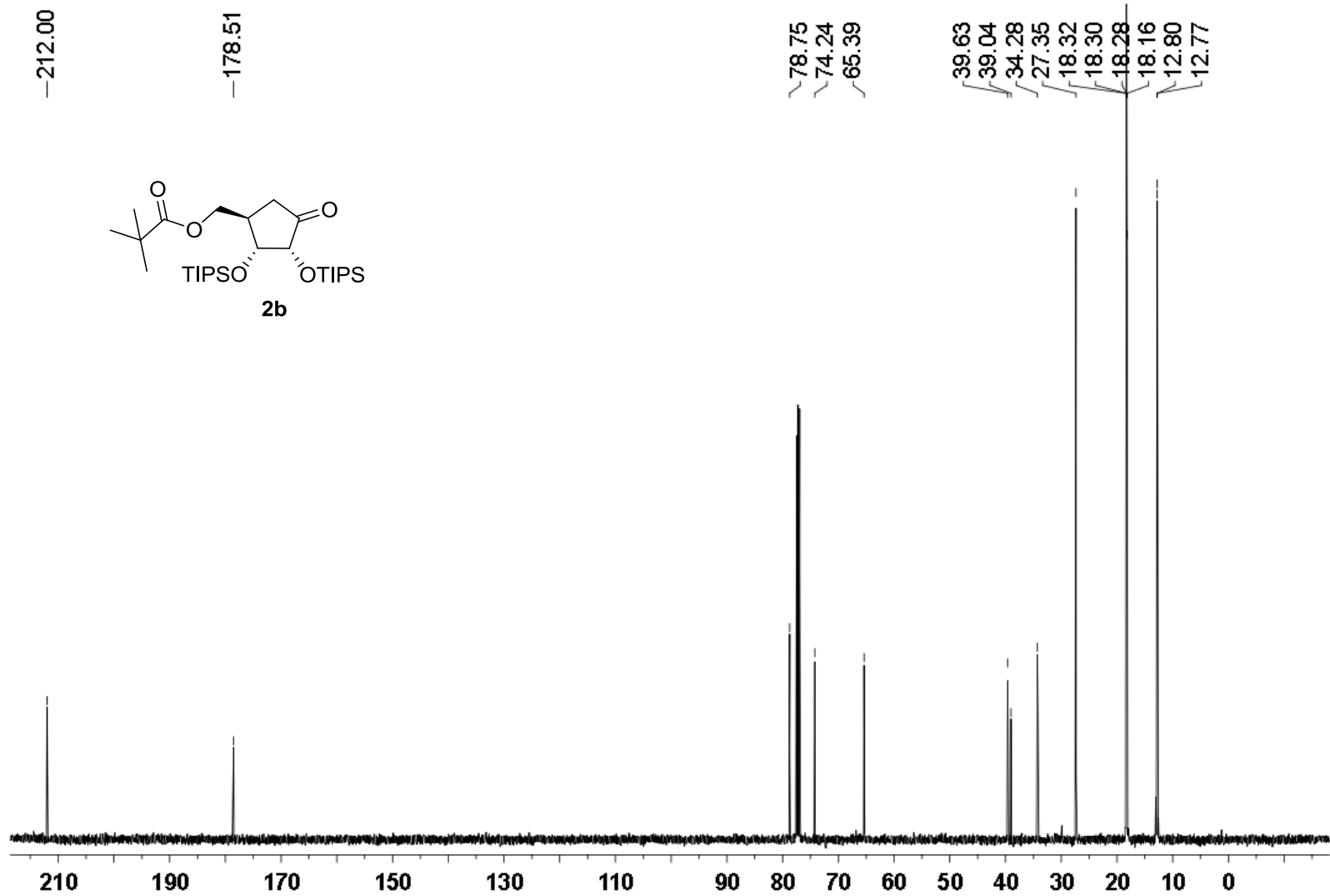




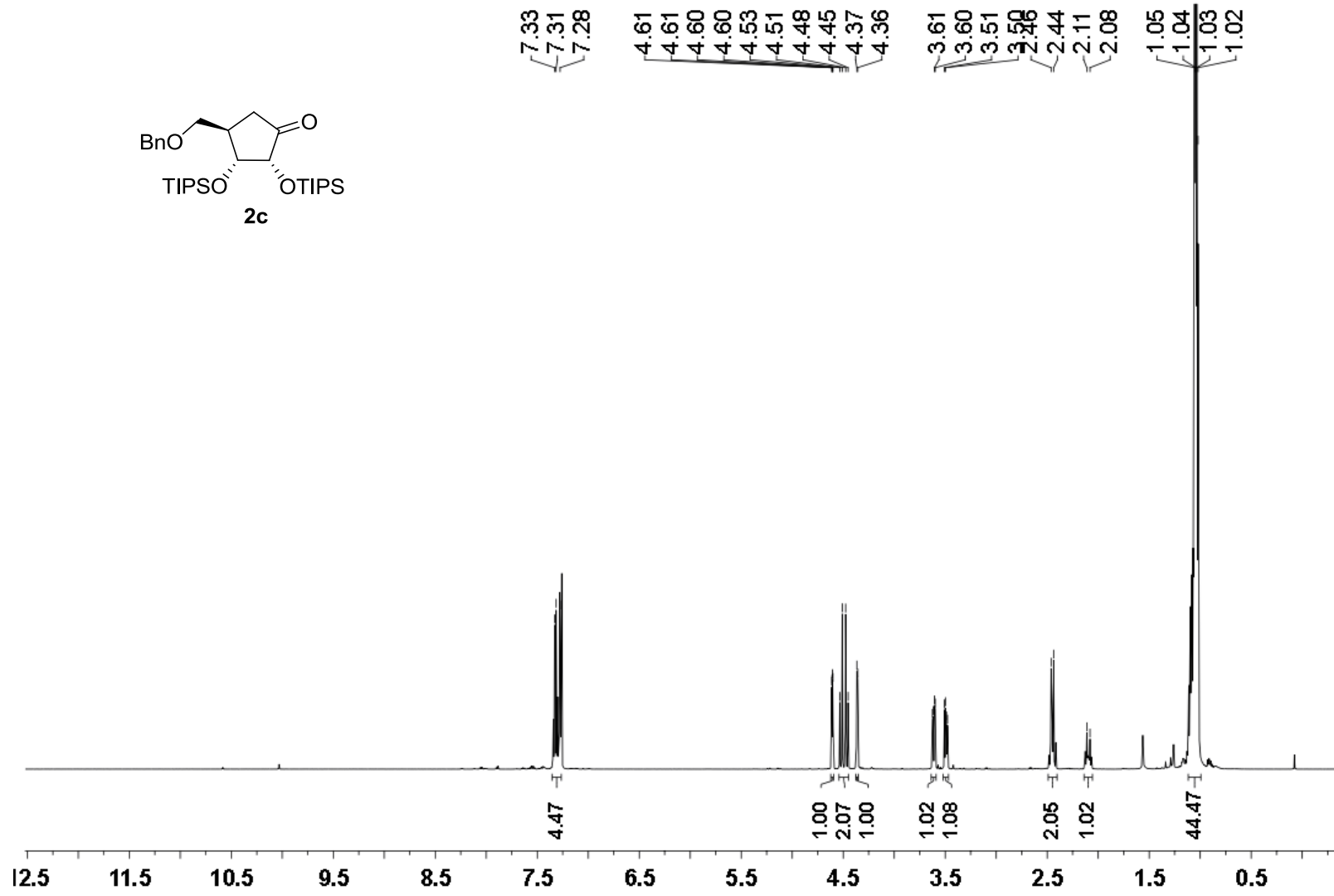
<sup>13</sup>C NMR (126 MHz) spectrum of **S-11** in CDCl<sub>3</sub>



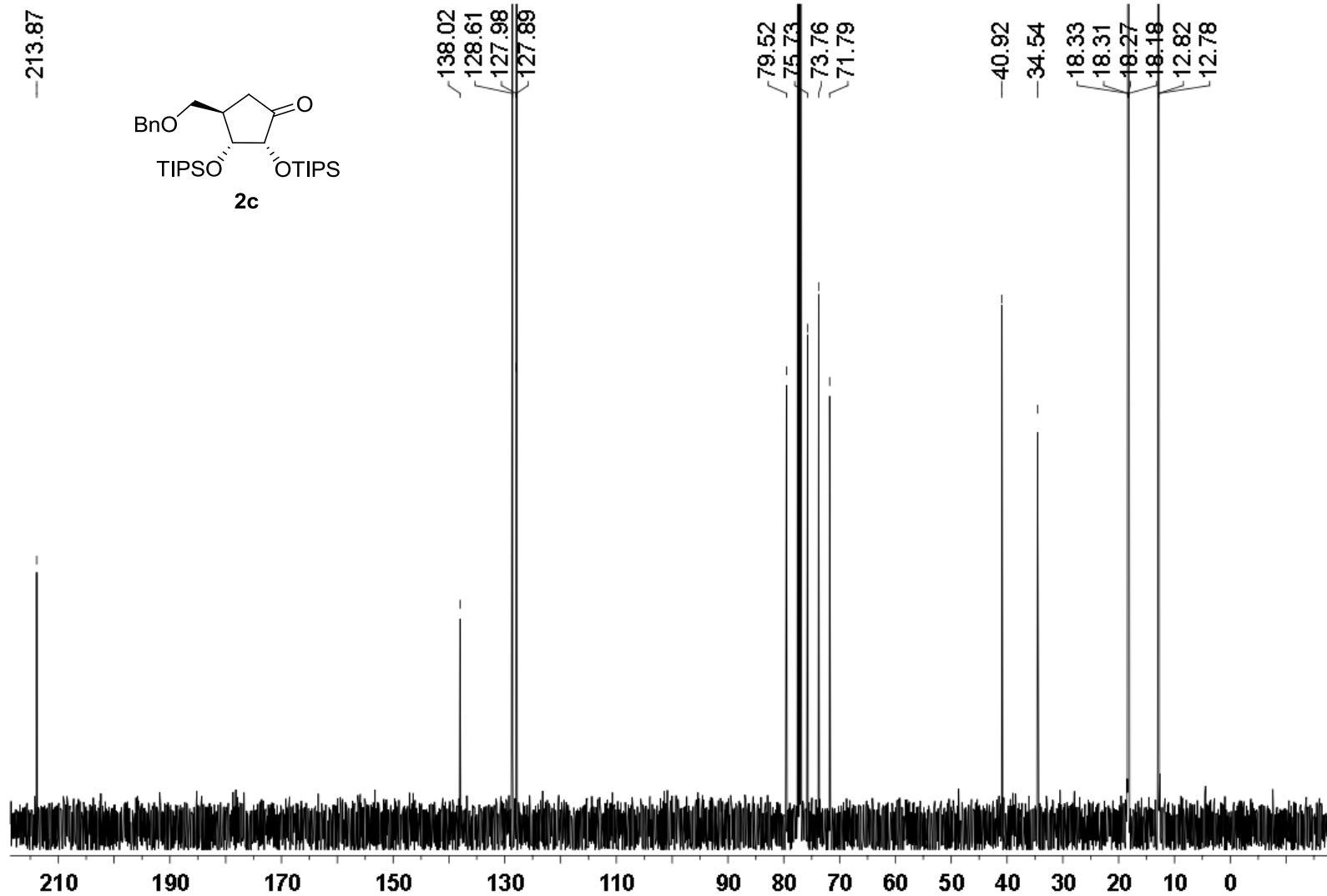
<sup>1</sup>H NMR (500 MHz) spectrum of **2b** in CDCl<sub>3</sub>



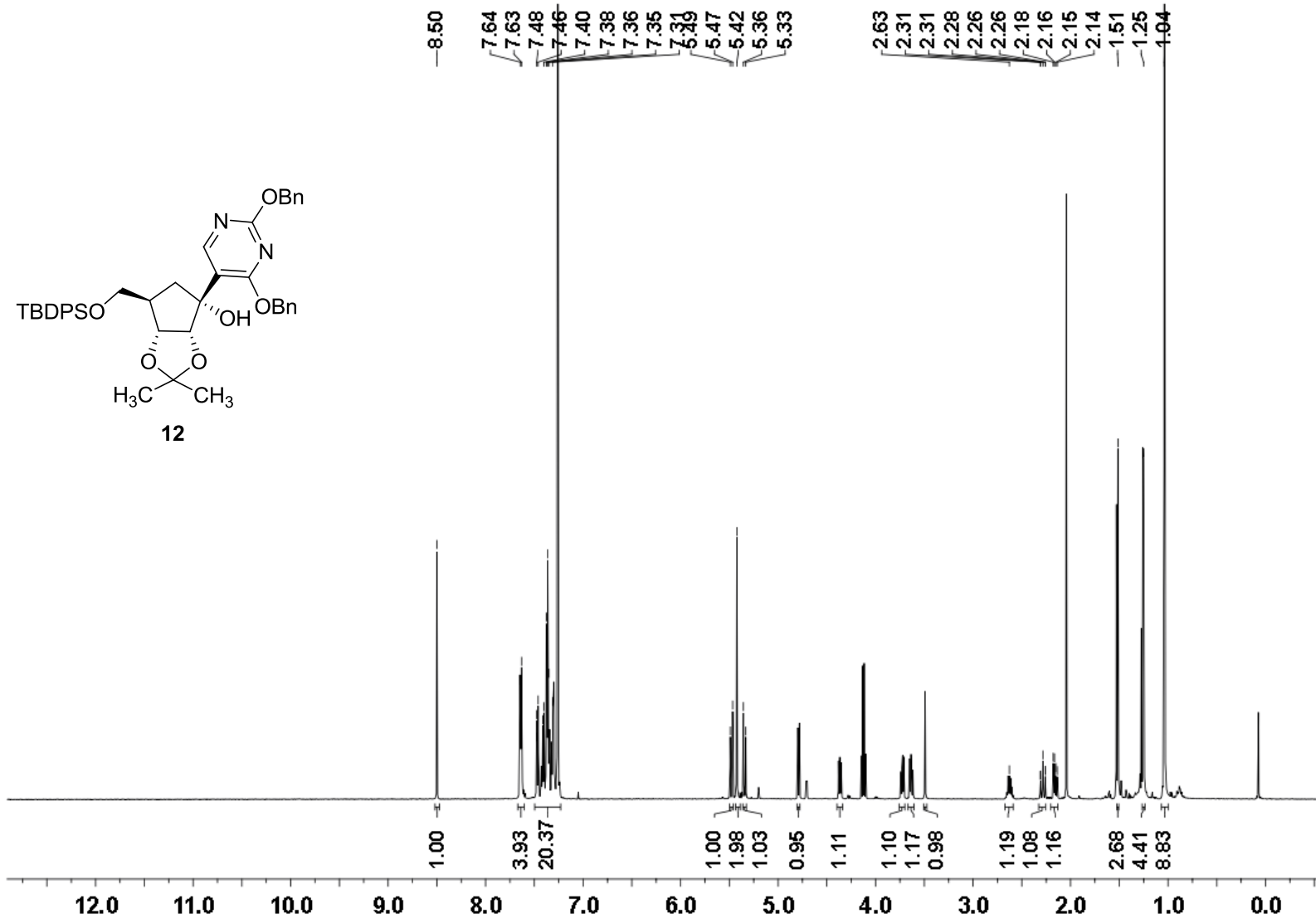
$^{13}\text{C}$  NMR (126 MHz) spectrum of **2b** in  $\text{CDCl}_3$



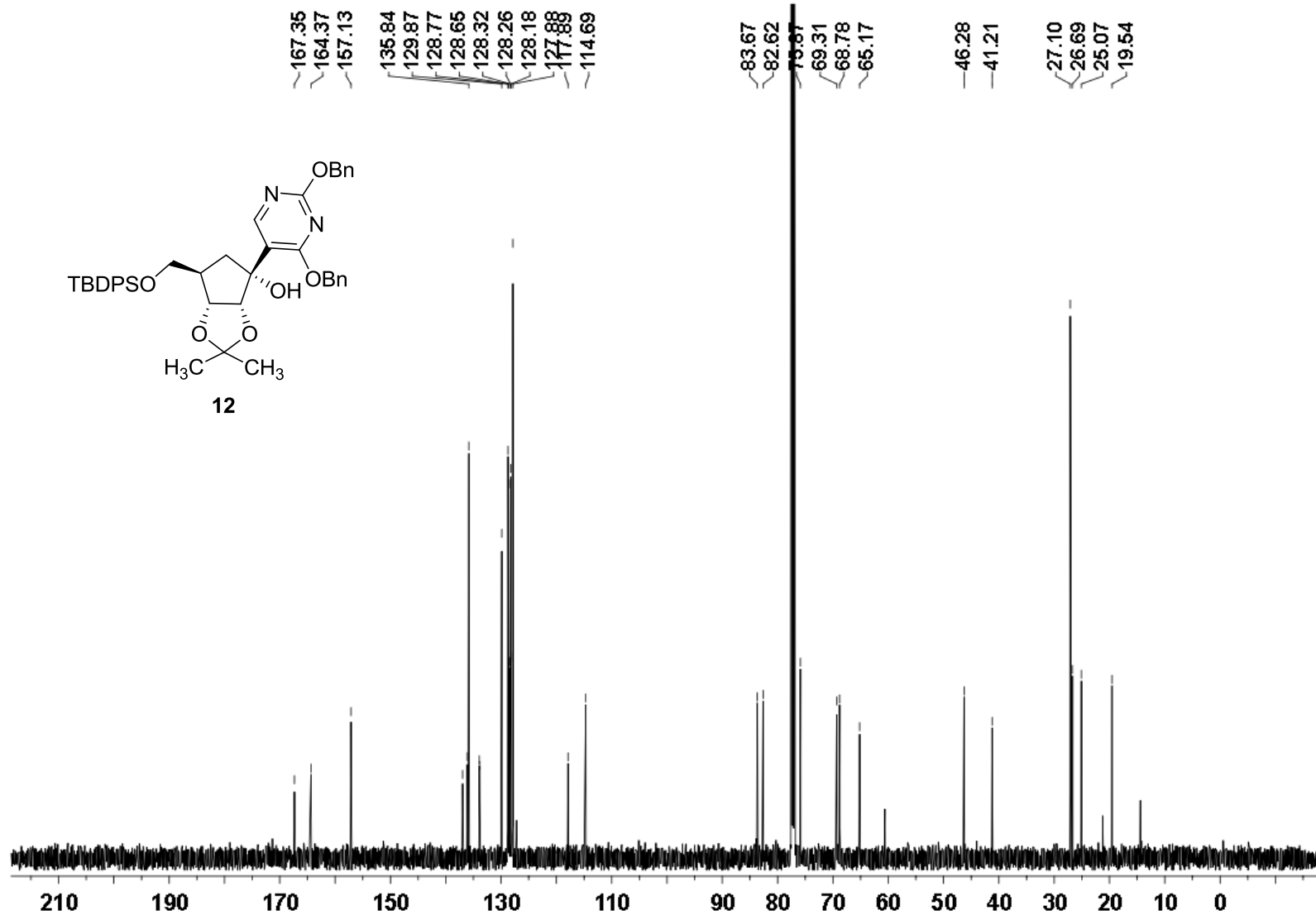
<sup>1</sup>H NMR (500 MHz) spectrum of **2c** in CDCl<sub>3</sub>



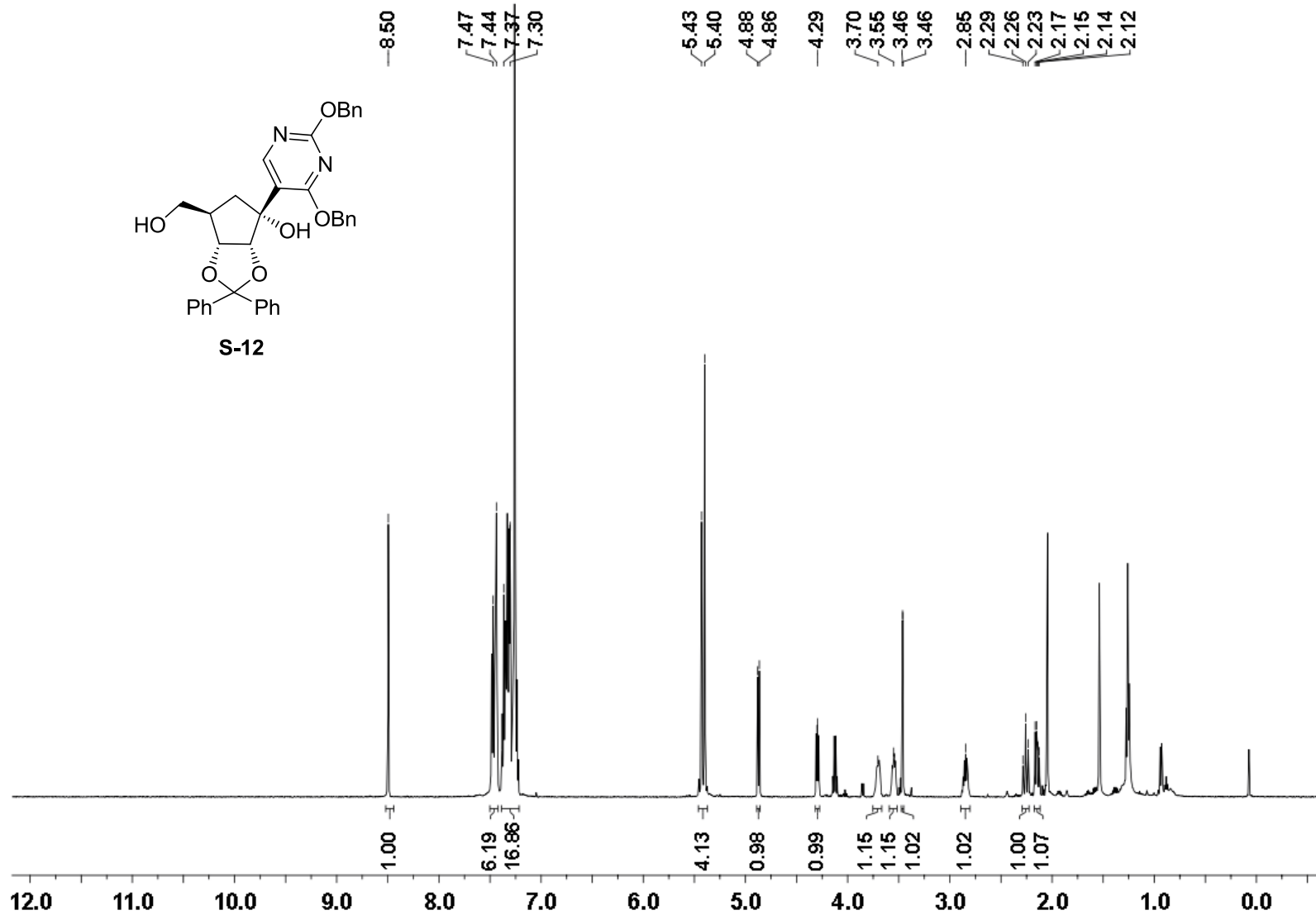
$^{13}\text{C}$  NMR (126 MHz) spectrum of **2c** in  $\text{CDCl}_3$



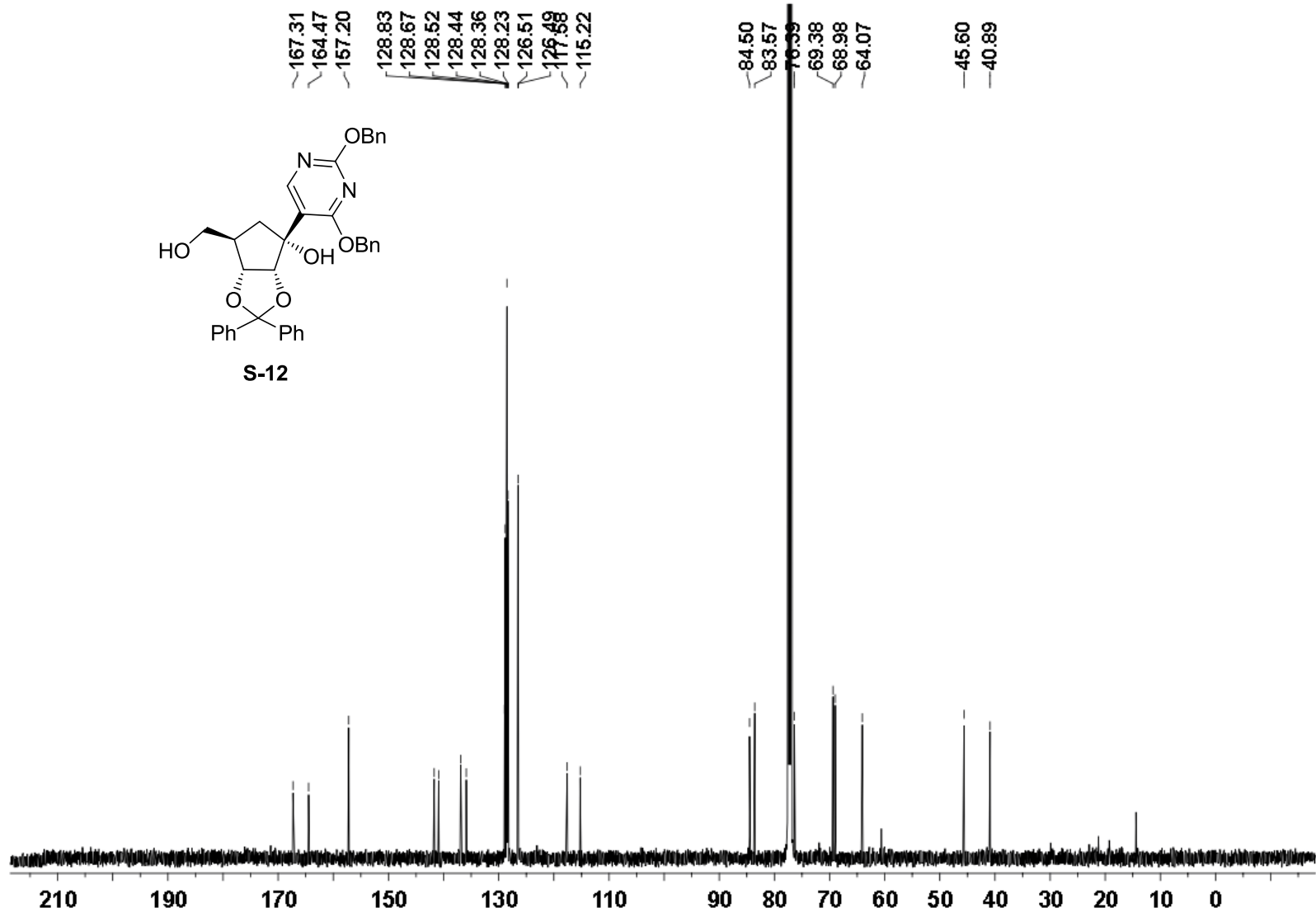
<sup>1</sup>H NMR (500 MHz) spectrum of **12** in CDCl<sub>3</sub>



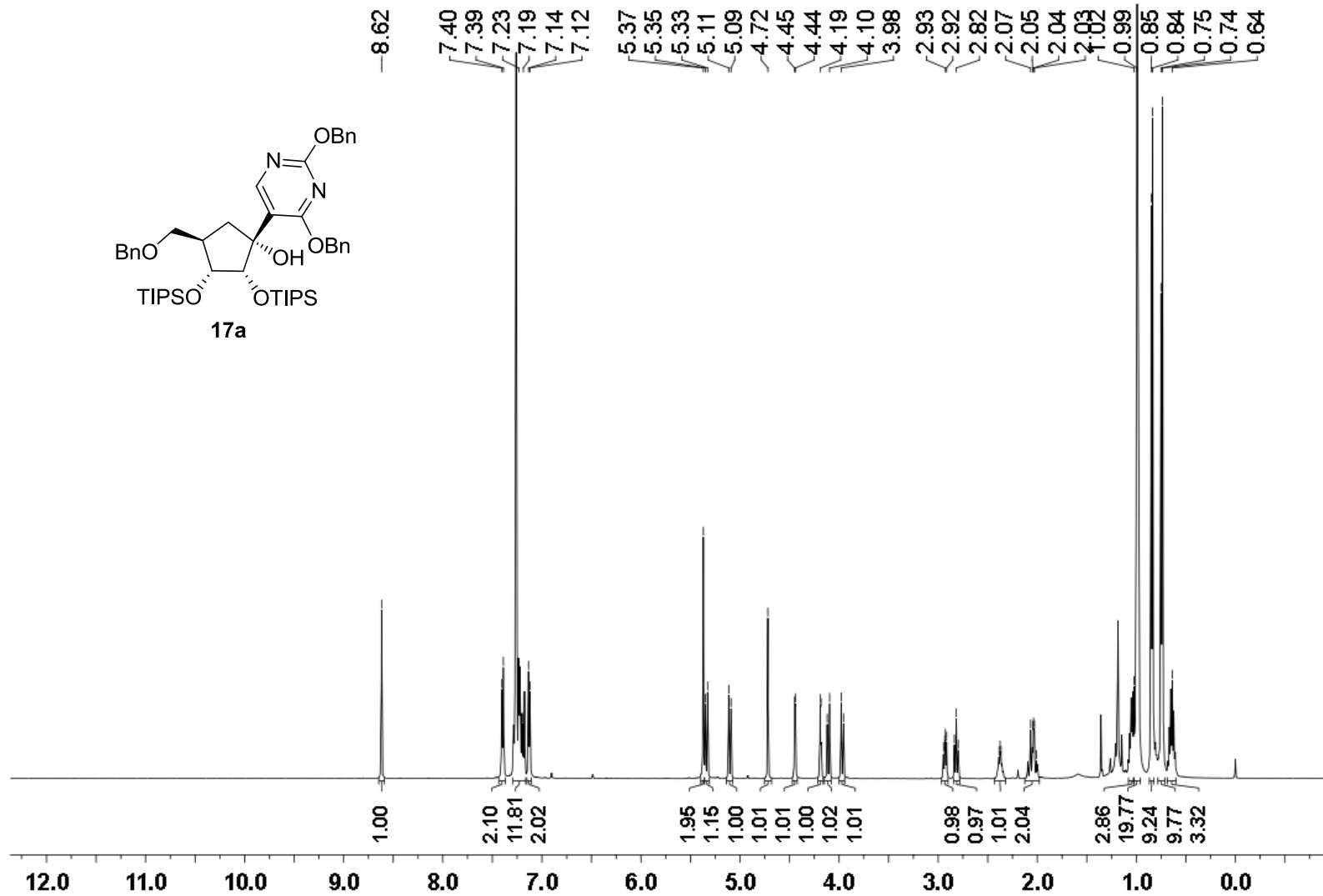
$^{13}\text{C}$  NMR (126 MHz) spectrum of **12** in  $\text{CDCl}_3$



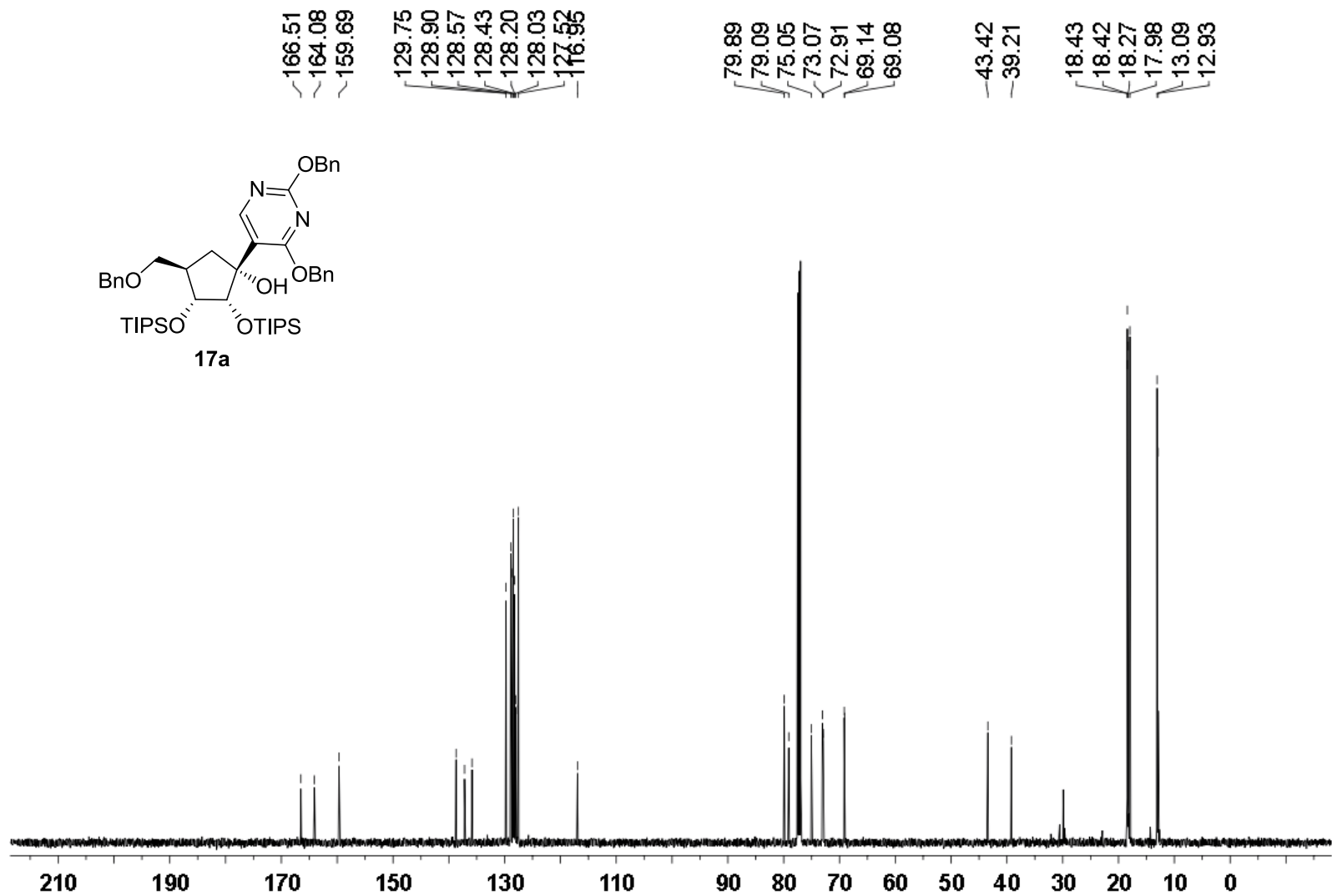
<sup>1</sup>H NMR (500 MHz) spectrum of S-12 in CDCl<sub>3</sub>



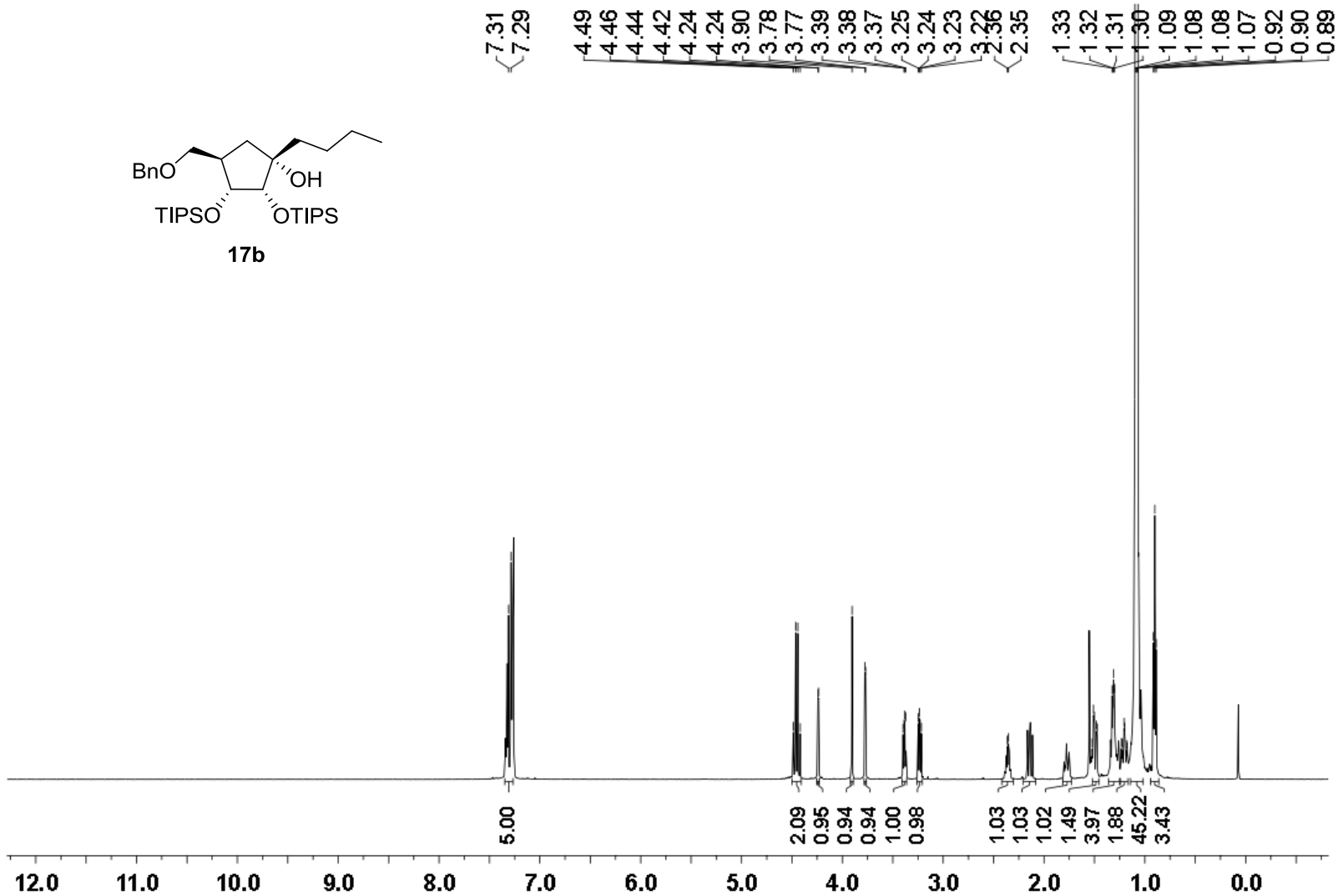
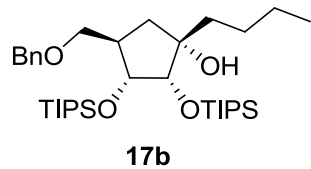
<sup>13</sup>C NMR (126 MHz) spectrum of **S-12** in CDCl<sub>3</sub>



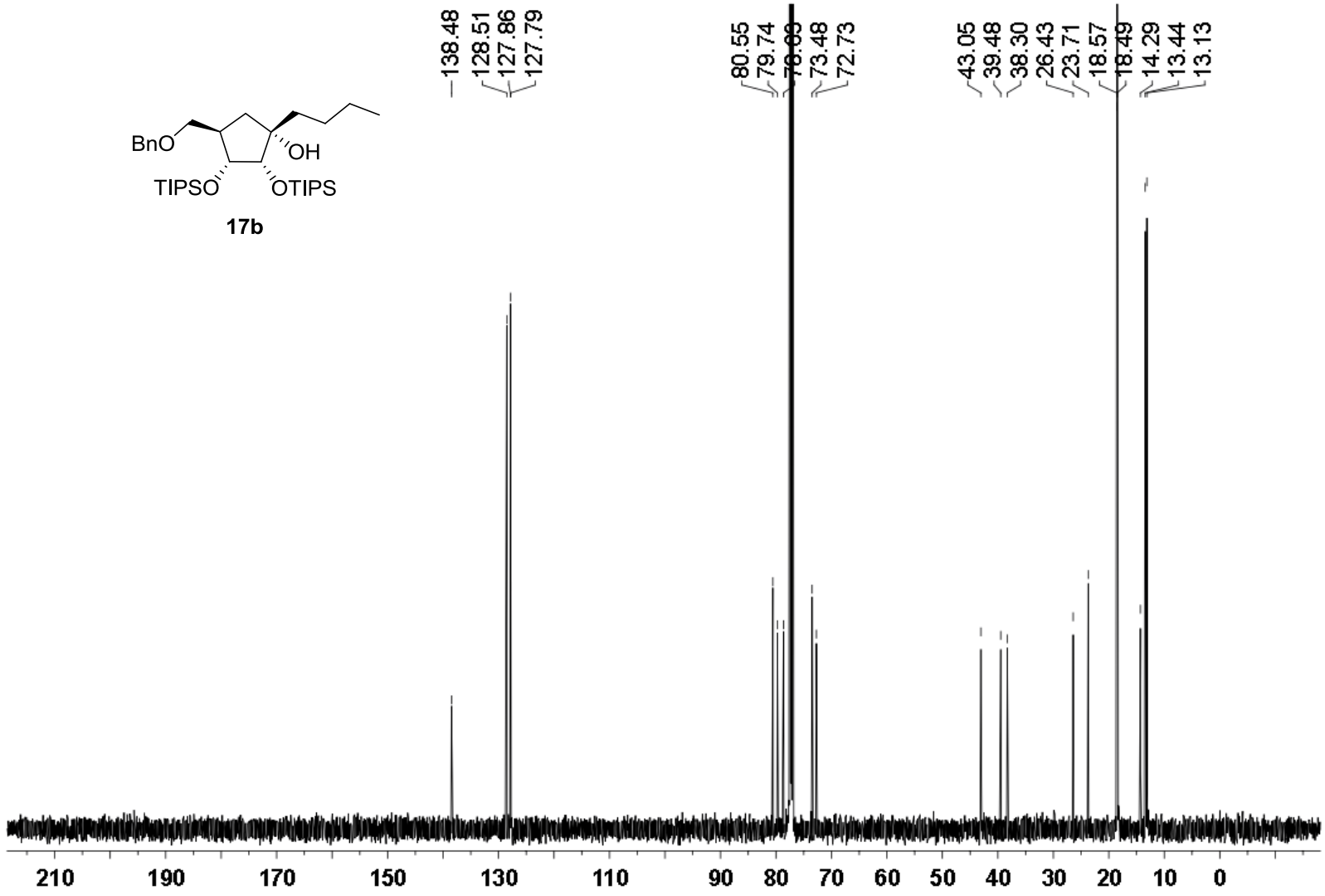
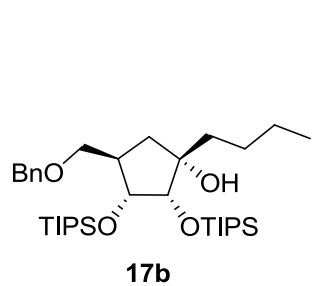
<sup>1</sup>H NMR (500 MHz) spectrum of **17a** in CDCl<sub>3</sub>



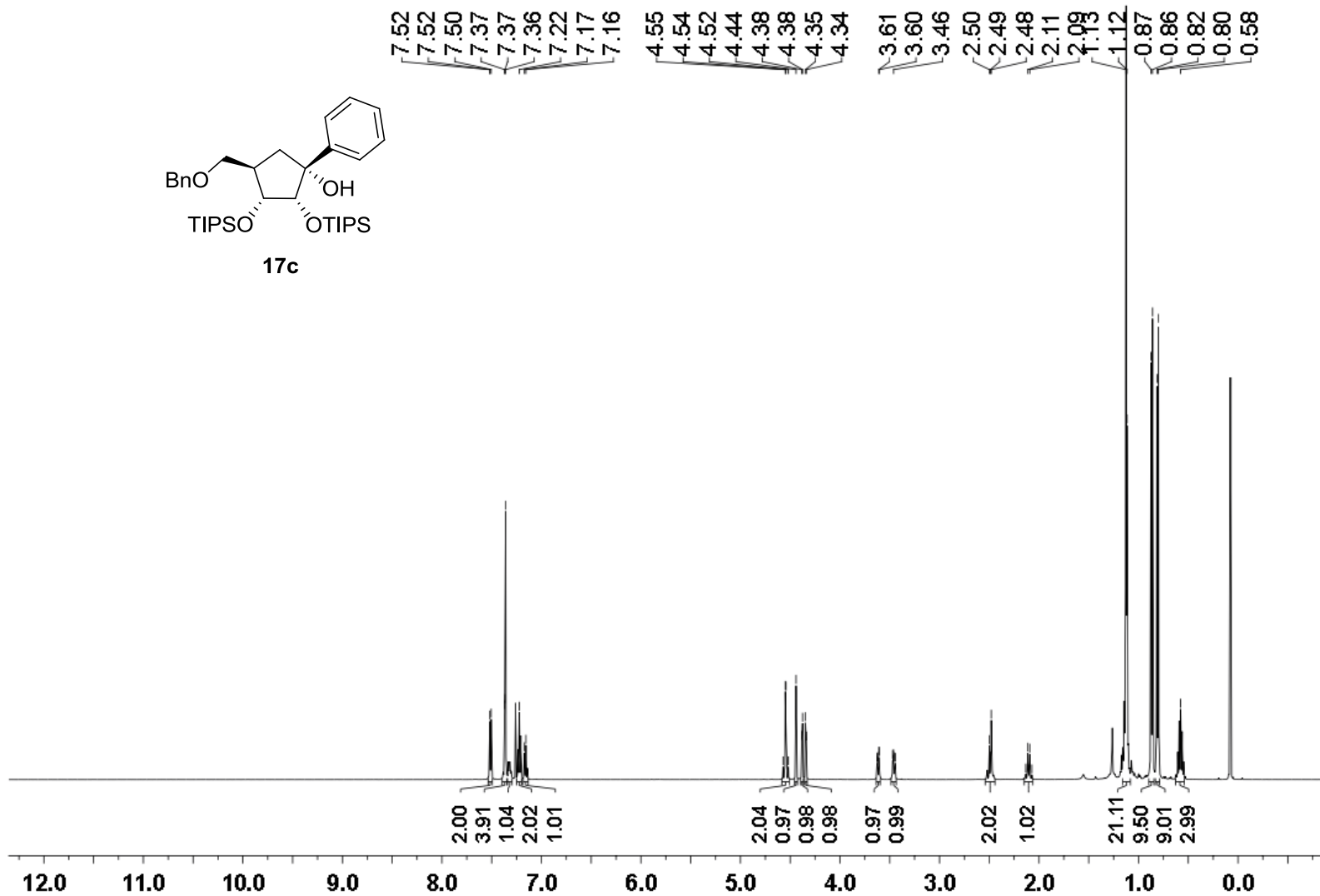
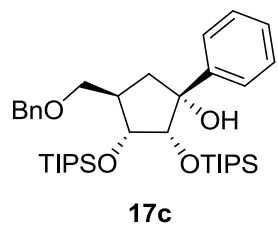
<sup>13</sup>C NMR (126 MHz) spectrum of **17a** in CDCl<sub>3</sub>



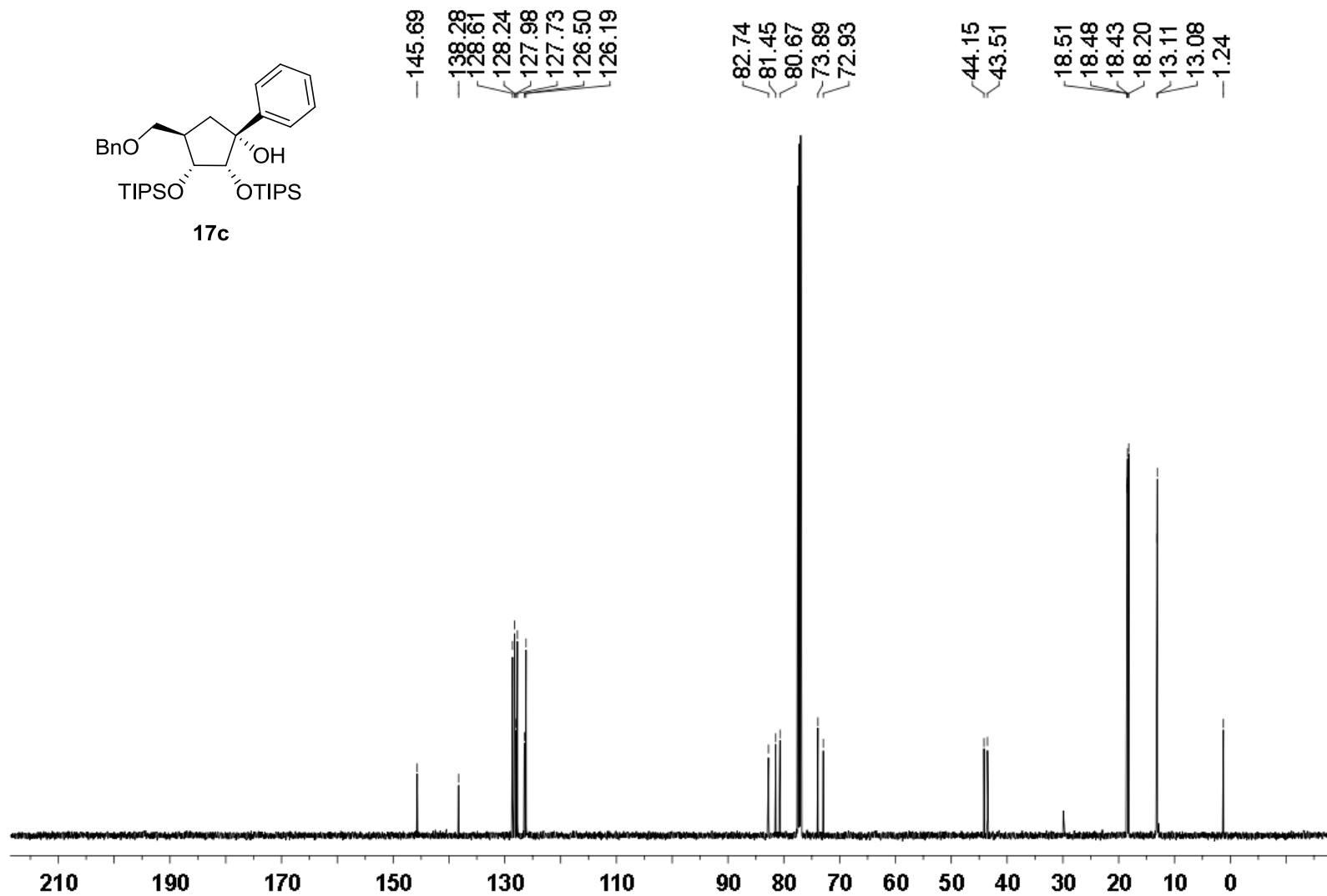
$^1\text{H}$  NMR (500 MHz) spectrum of **17b** in  $\text{CDCl}_3$



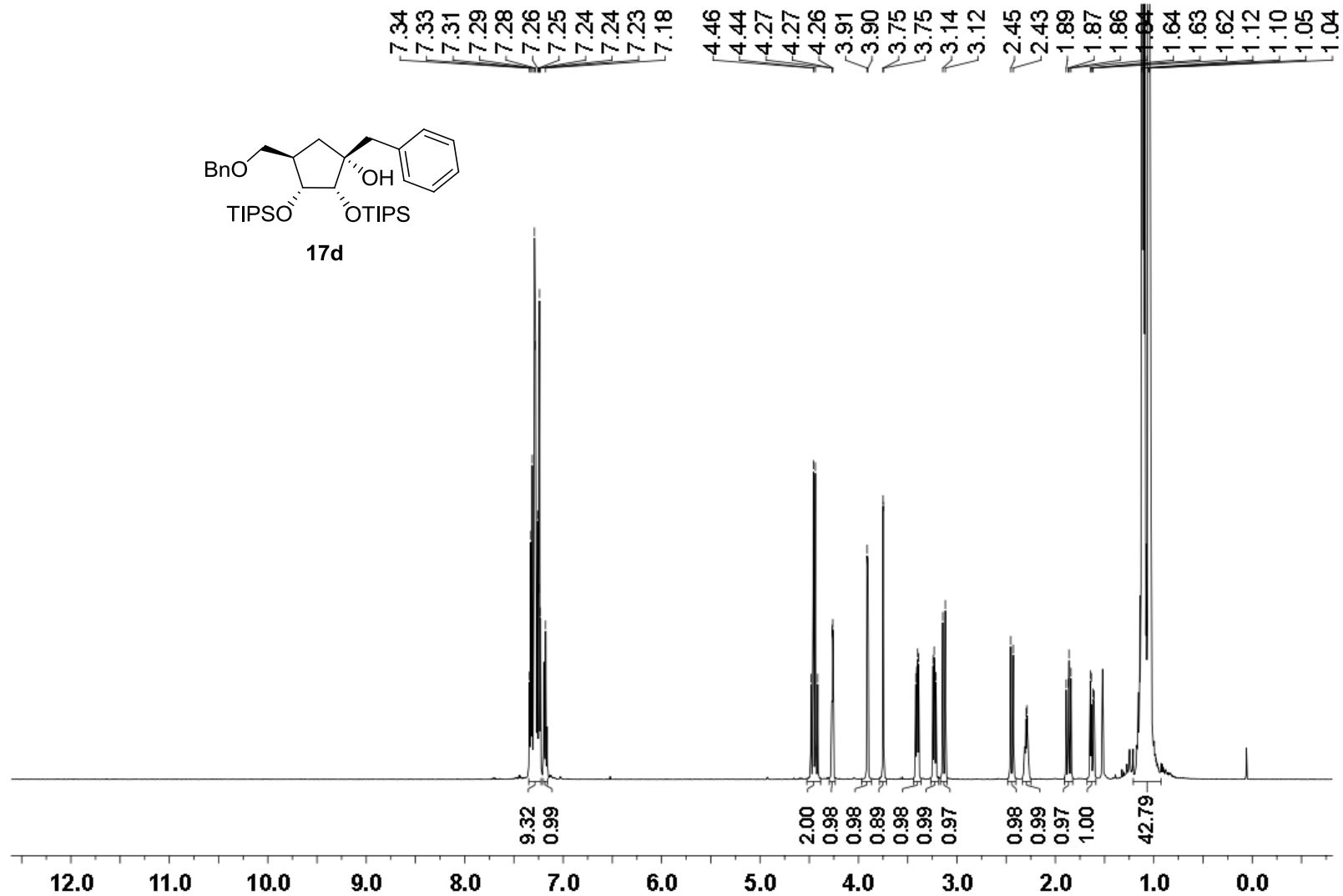
$^{13}\text{C}$  NMR (126 MHz) spectrum of **17b** in  $\text{CDCl}_3$



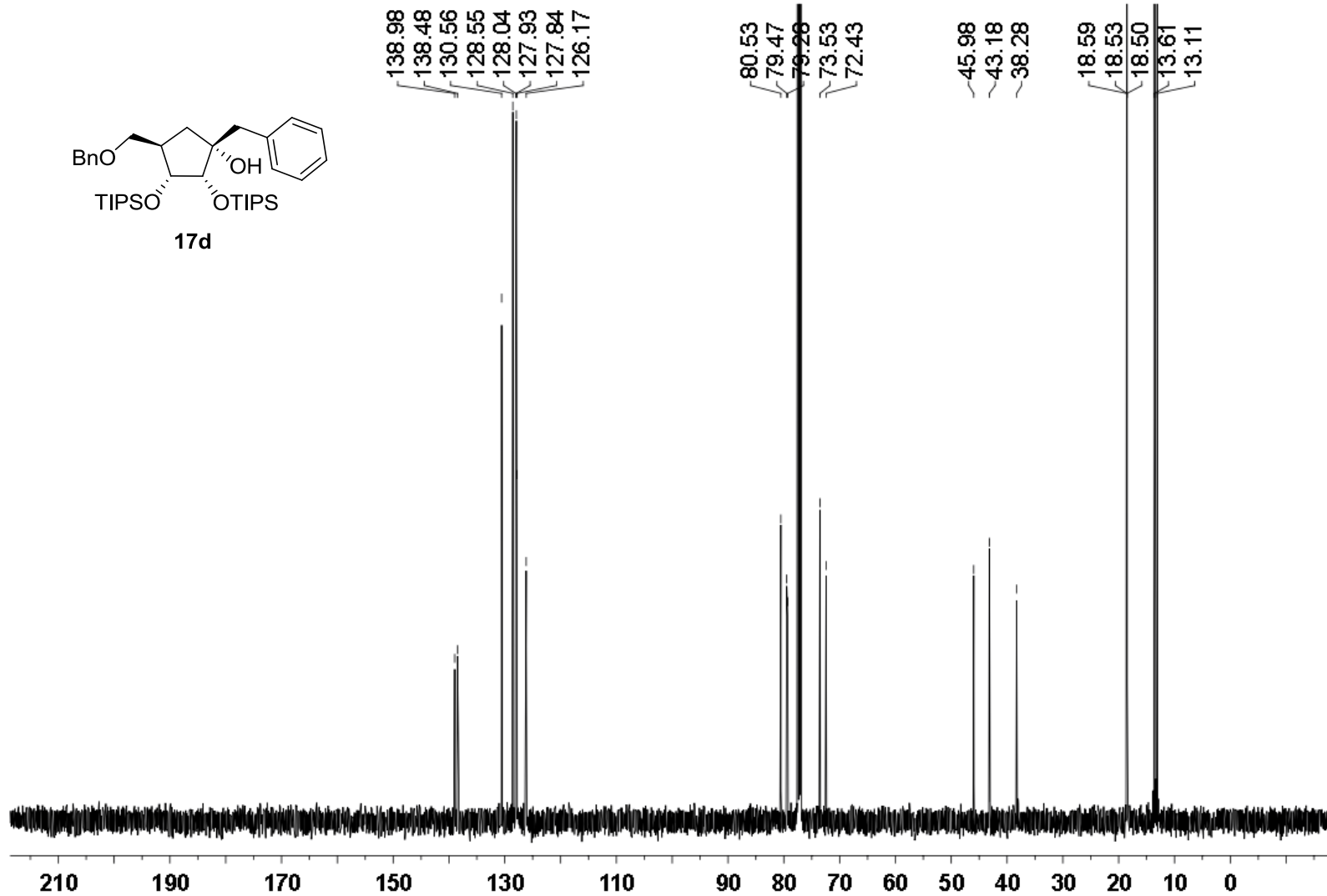
<sup>1</sup>H NMR (500 MHz) spectrum of **17c** in CDCl<sub>3</sub>



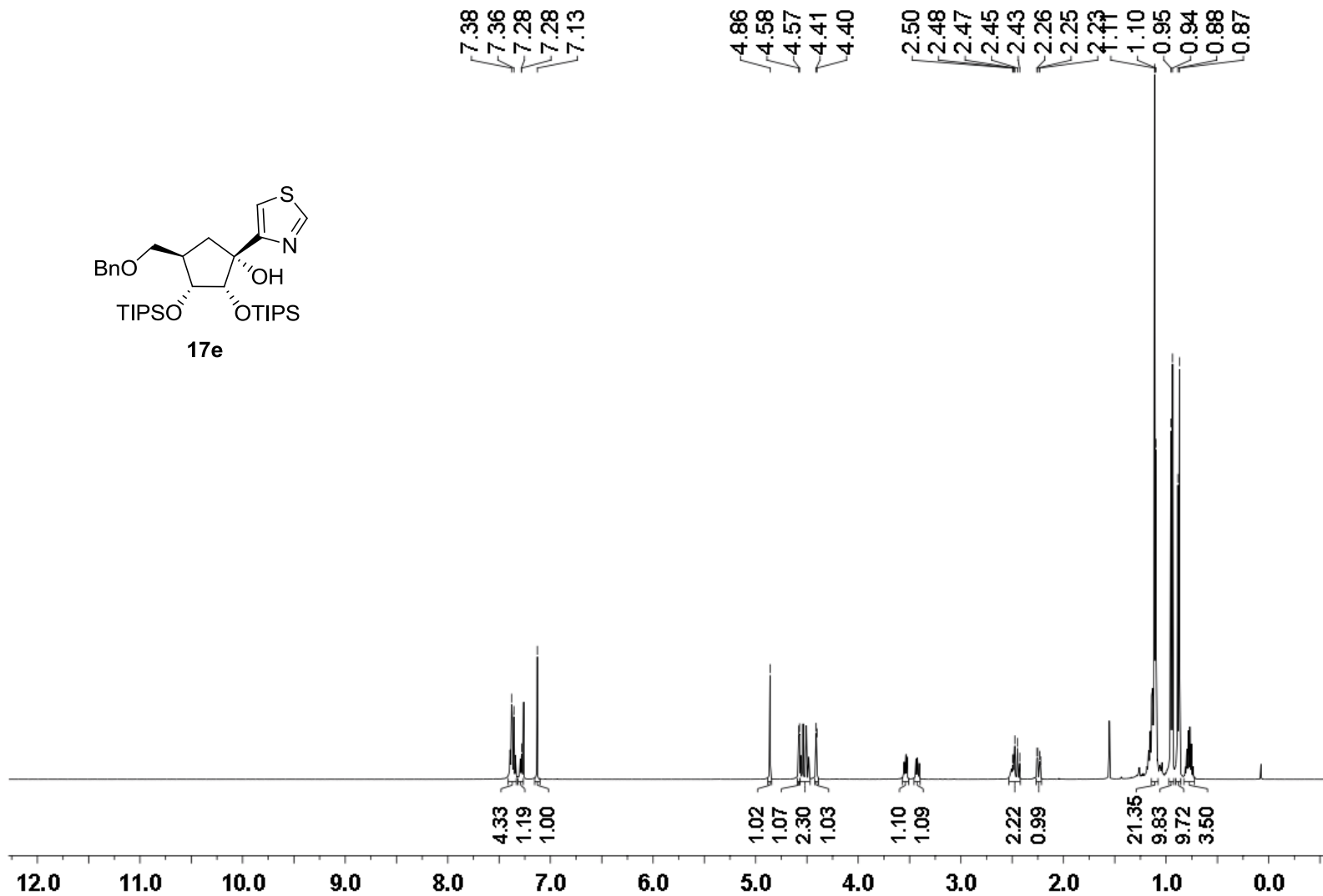
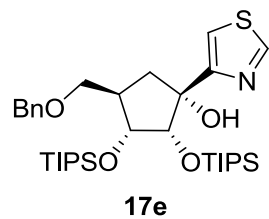
$^{13}\text{C}$  NMR (126 MHz) spectrum of **17c** in  $\text{CDCl}_3$



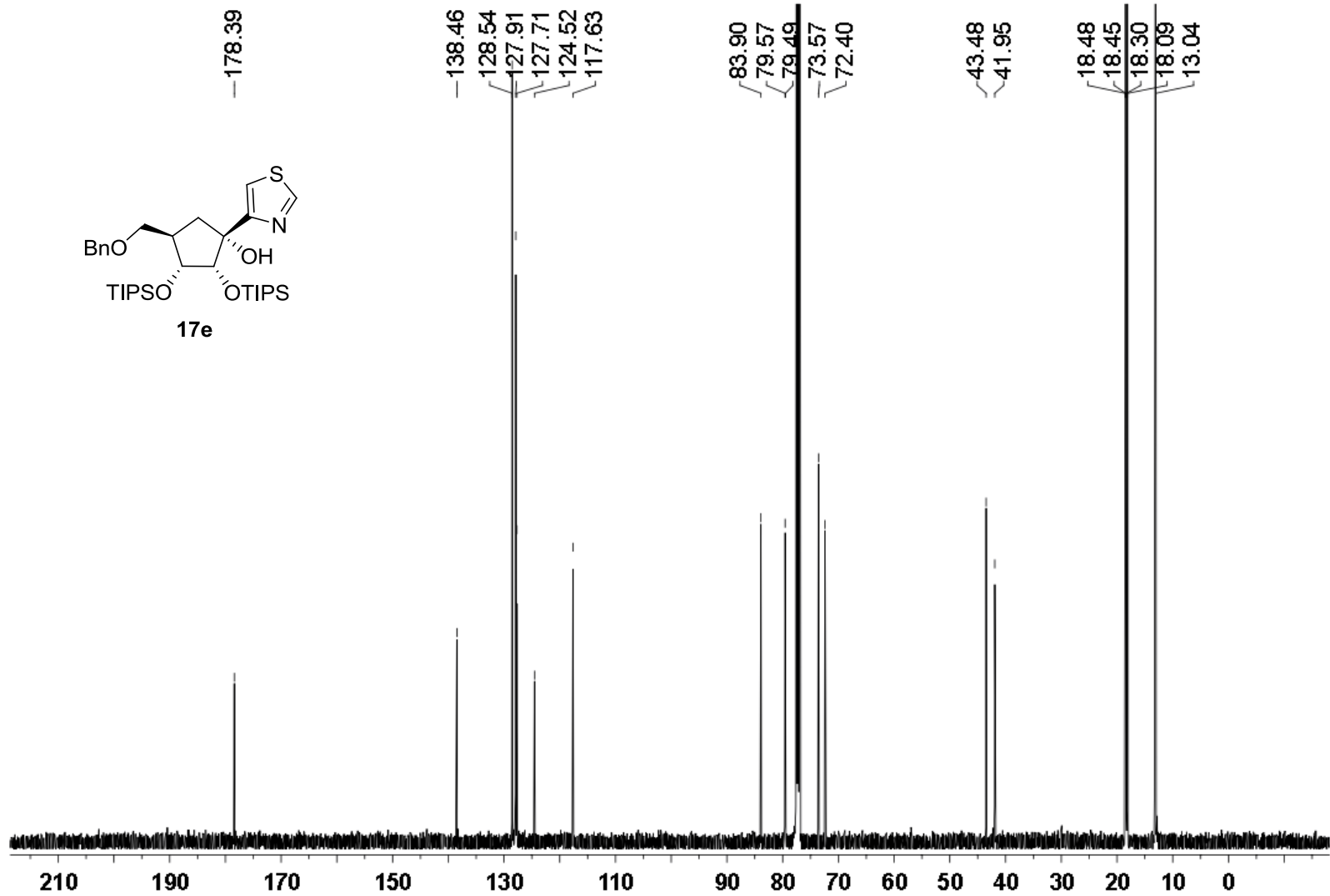
<sup>1</sup>H NMR (500 MHz) spectrum of **17d** in CDCl<sub>3</sub>



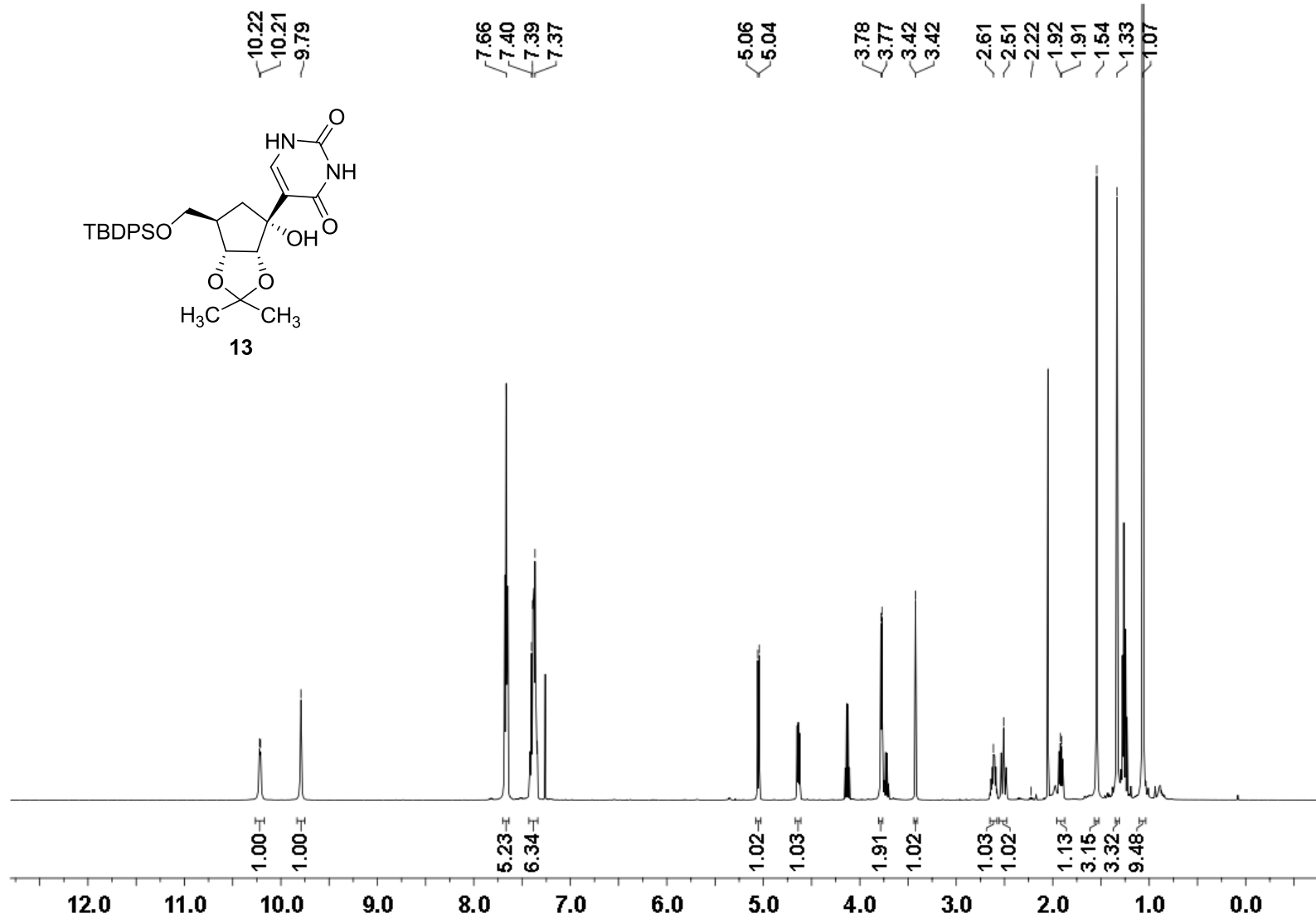
$^{13}\text{C}$  NMR (126 MHz) spectrum of **17d** in  $\text{CDCl}_3$



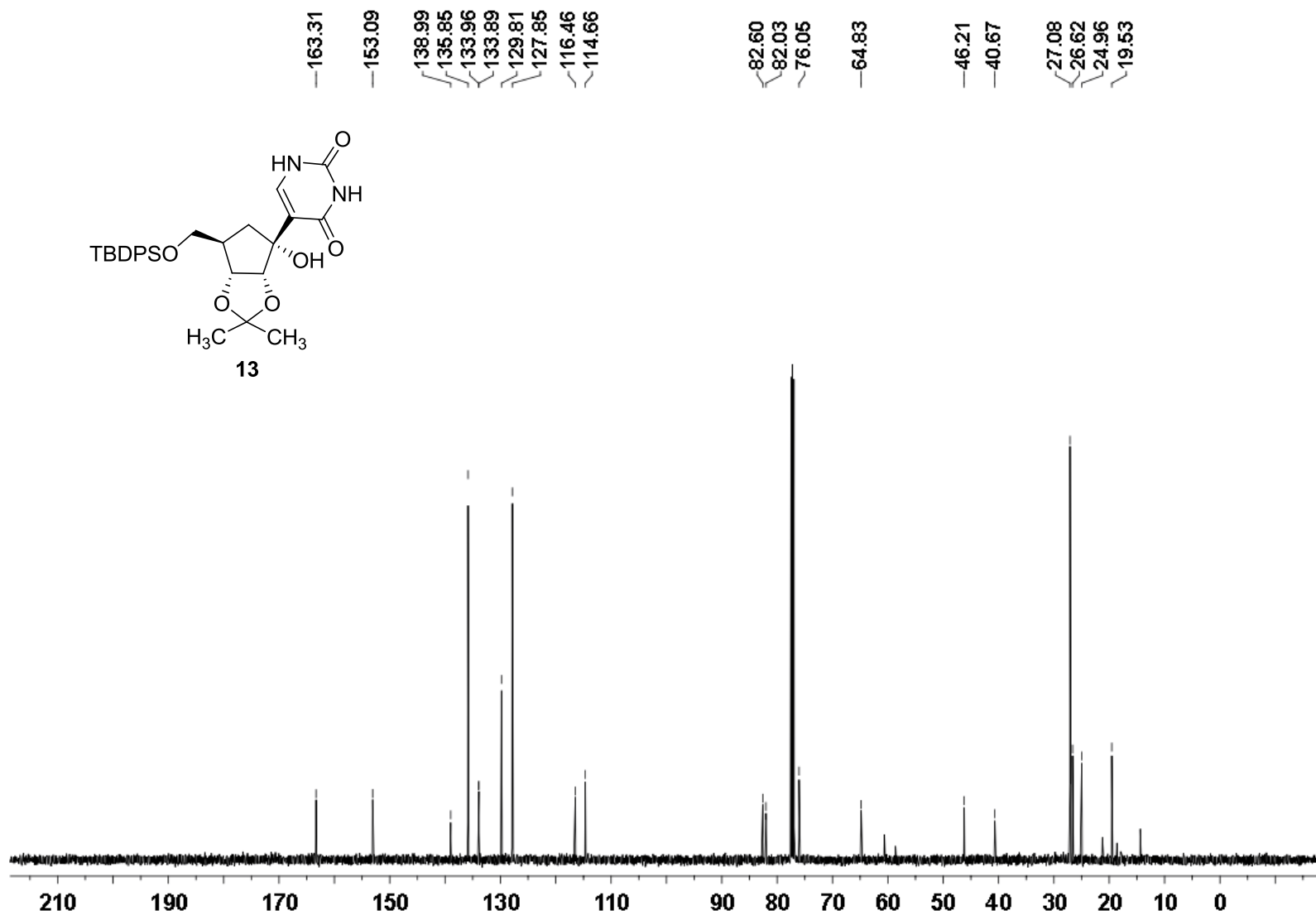
$^1\text{H}$  NMR (500 MHz) spectrum of **17e** in  $\text{CDCl}_3$



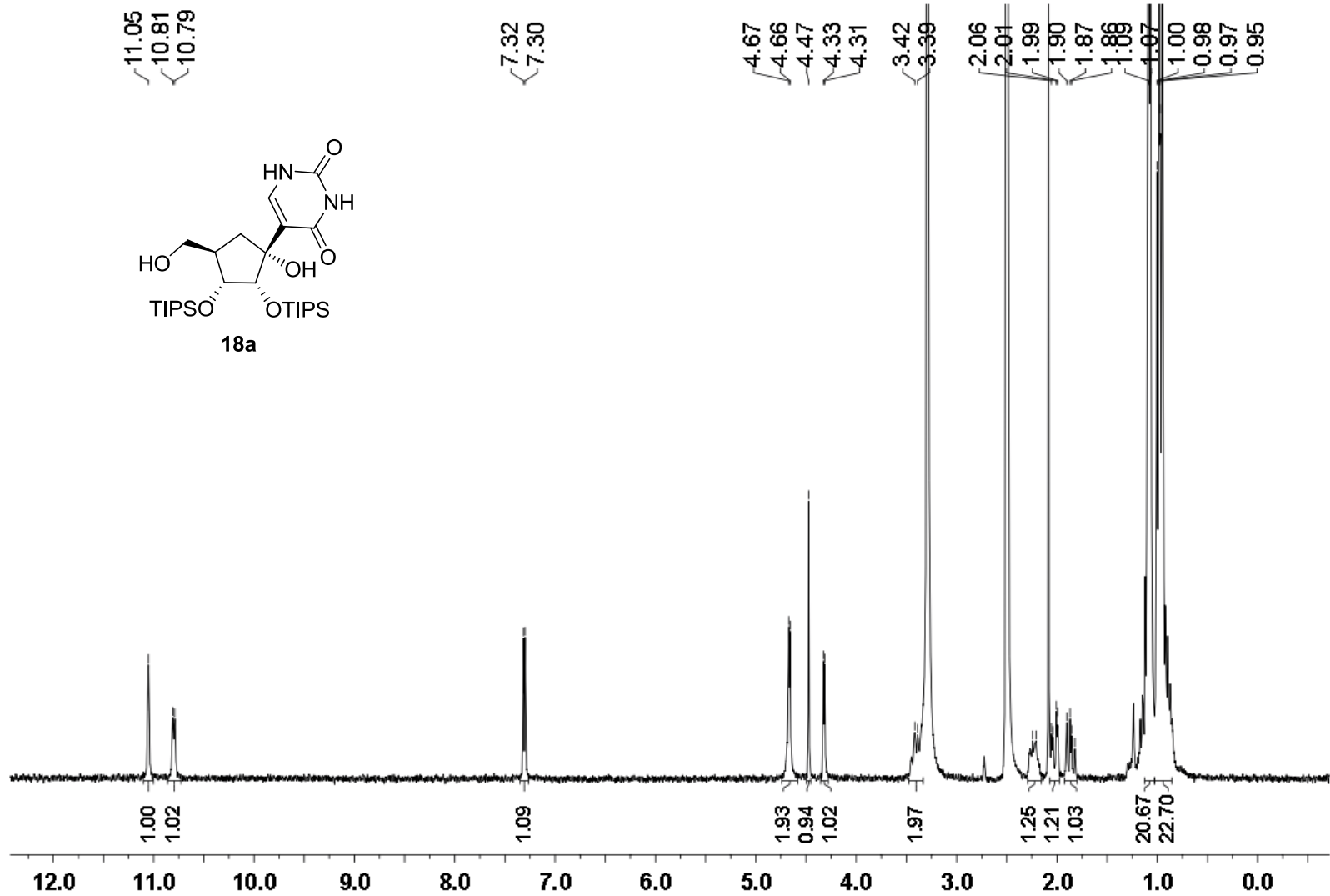
$^{13}\text{C}$  NMR (126 MHz) spectrum of **17e** in  $\text{CDCl}_3$



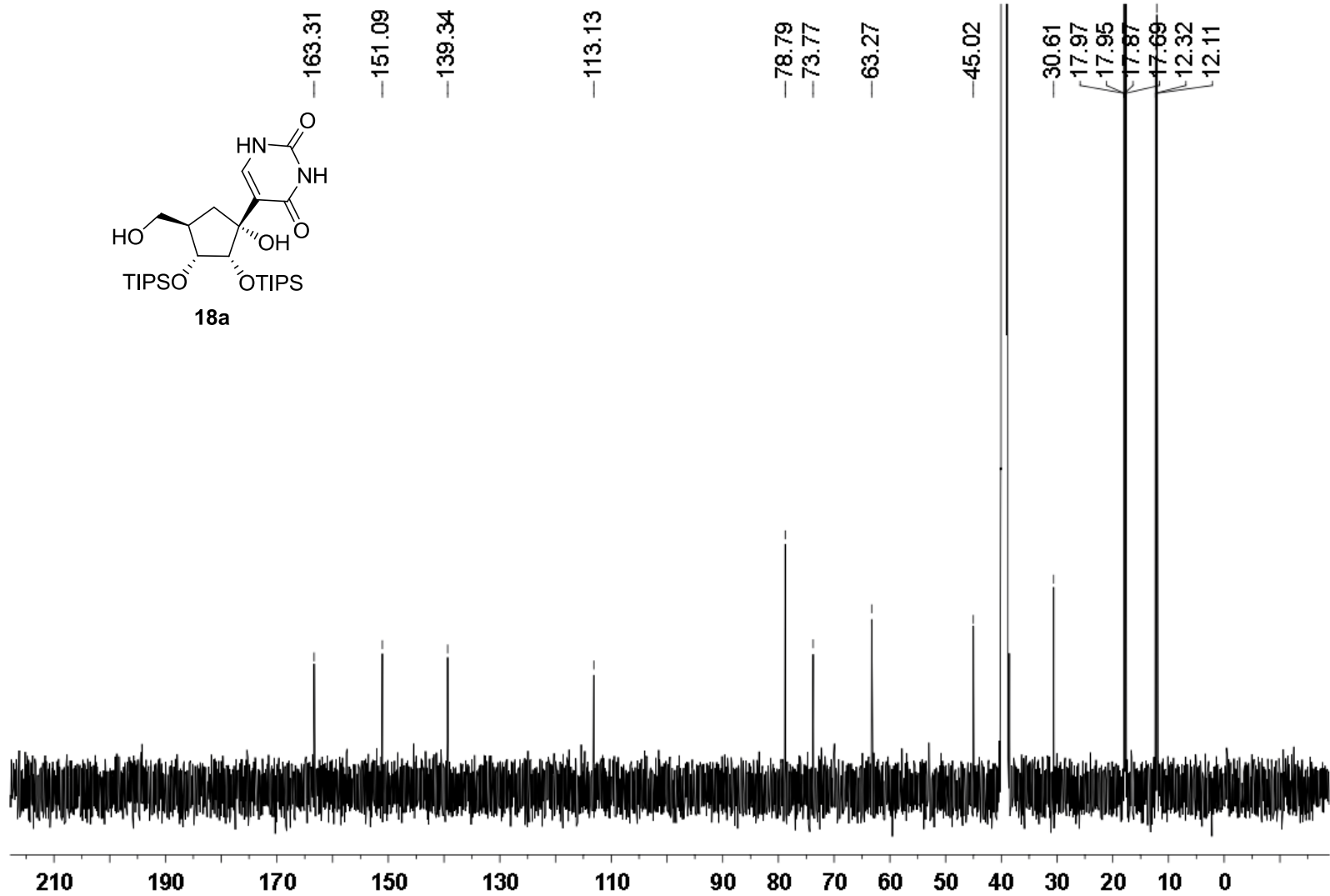
$^1\text{H}$  NMR (500 MHz) spectrum of **13** in  $\text{CDCl}_3$



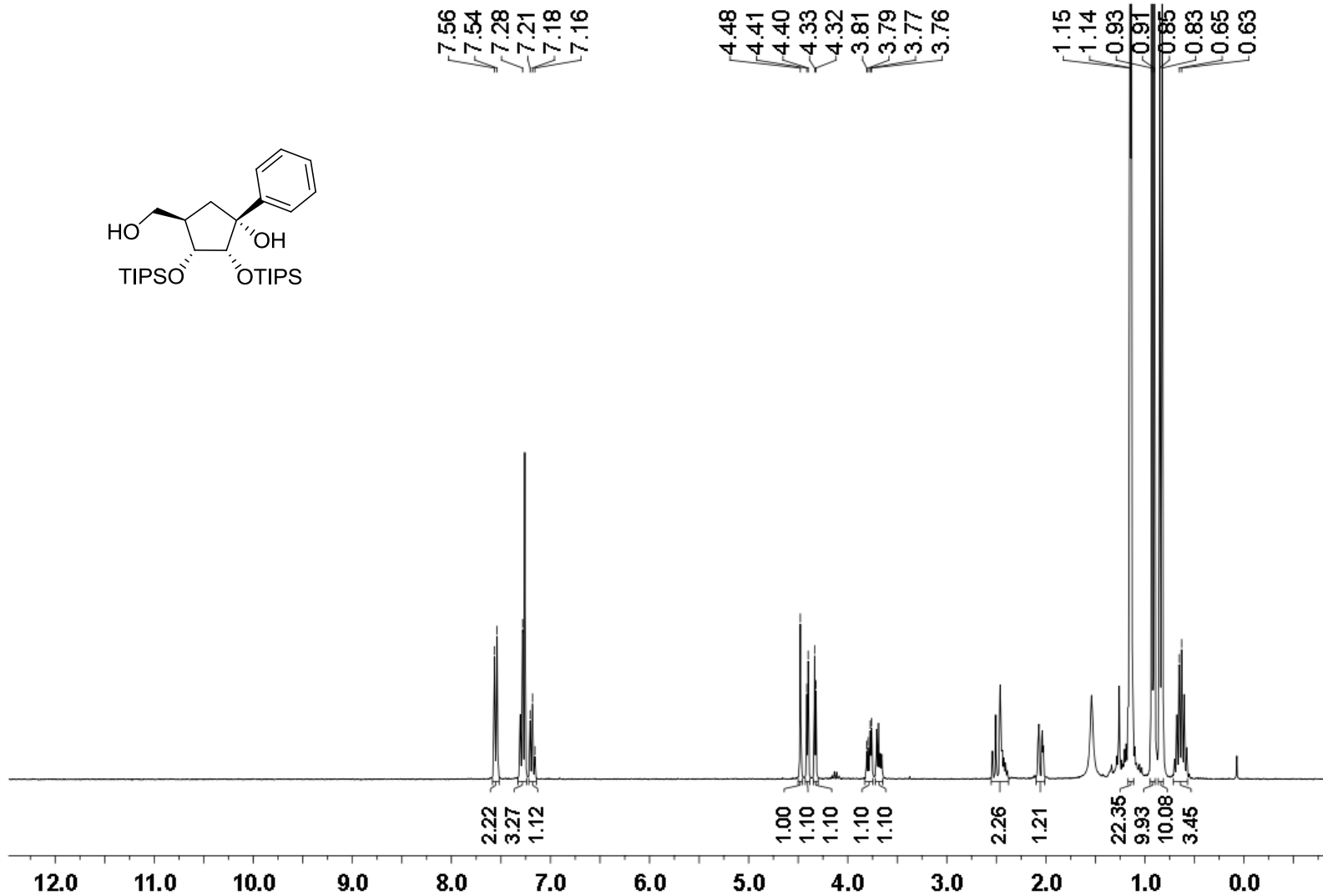
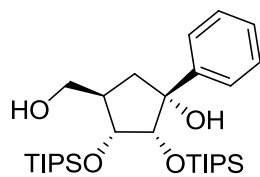
<sup>13</sup>C NMR (126 MHz) spectrum of **13** in CDCl<sub>3</sub>



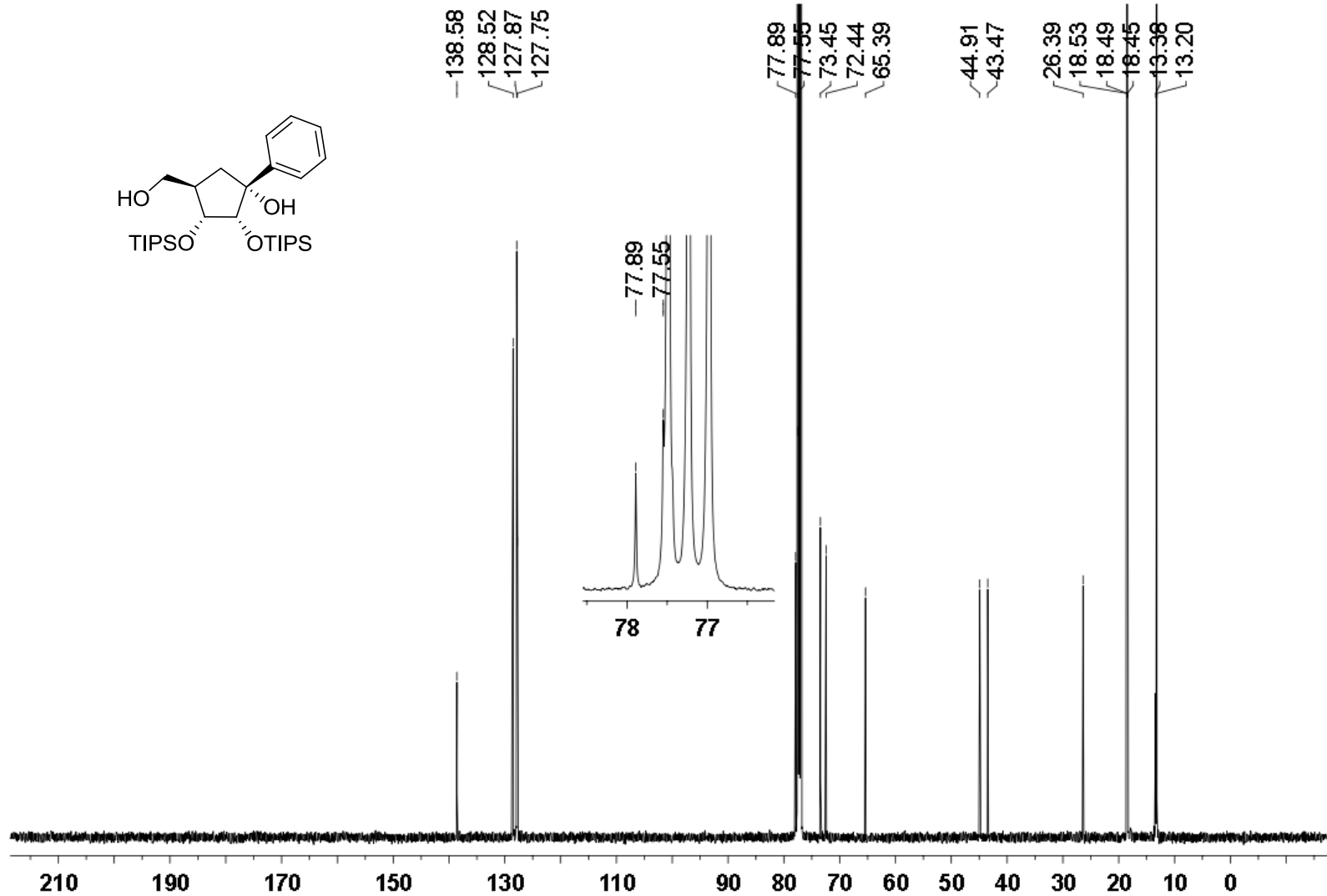
<sup>1</sup>H NMR (300 MHz) spectrum of **18a** in CDCl<sub>3</sub>



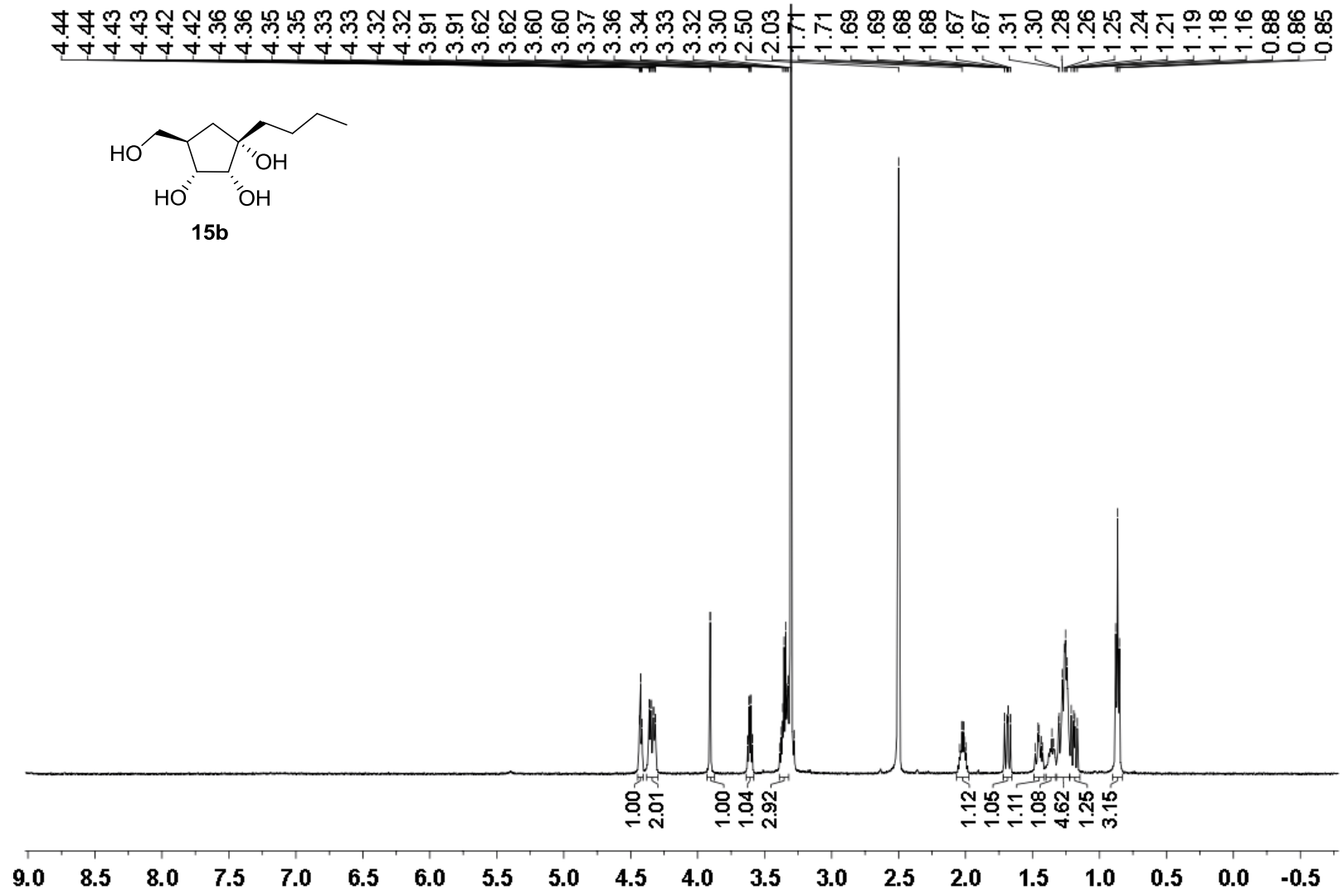
<sup>13</sup>C NMR (126 MHz) spectrum of **18a** in CDCl<sub>3</sub>



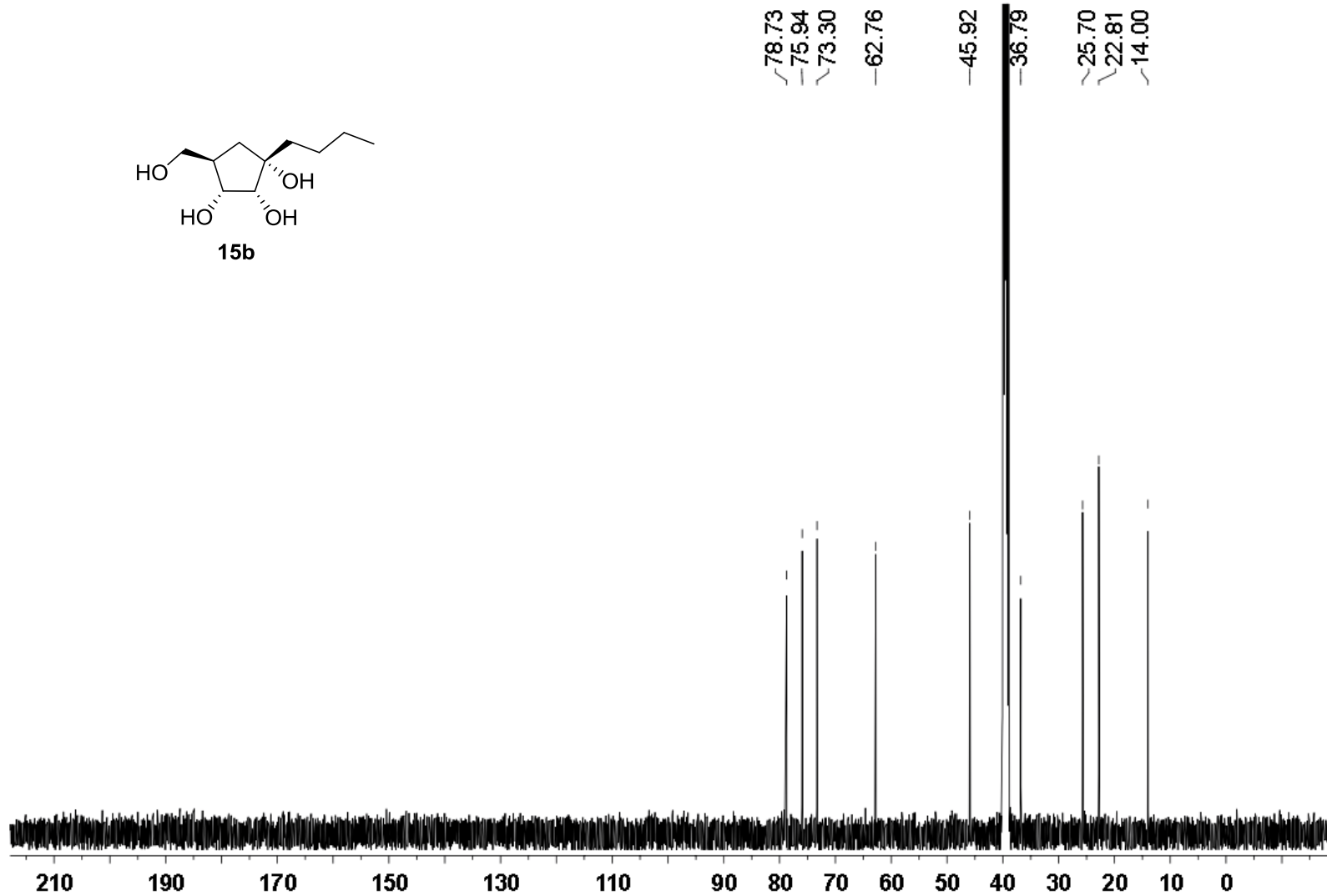
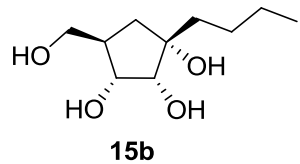
<sup>1</sup>H NMR (300 MHz) spectrum in CDCl<sub>3</sub>



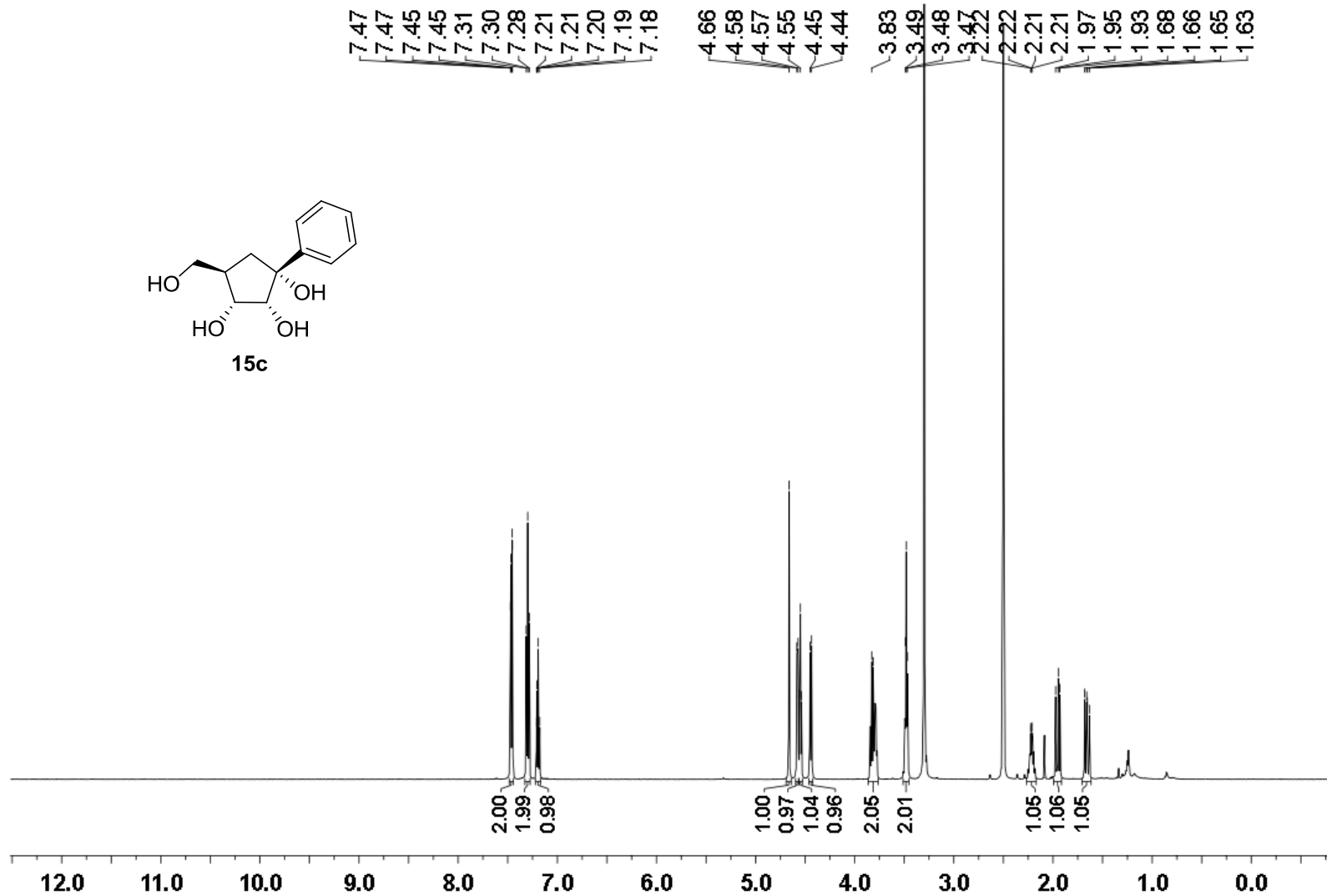
$^{13}\text{C}$  NMR (126 MHz) spectrum in  $\text{CDCl}_3$



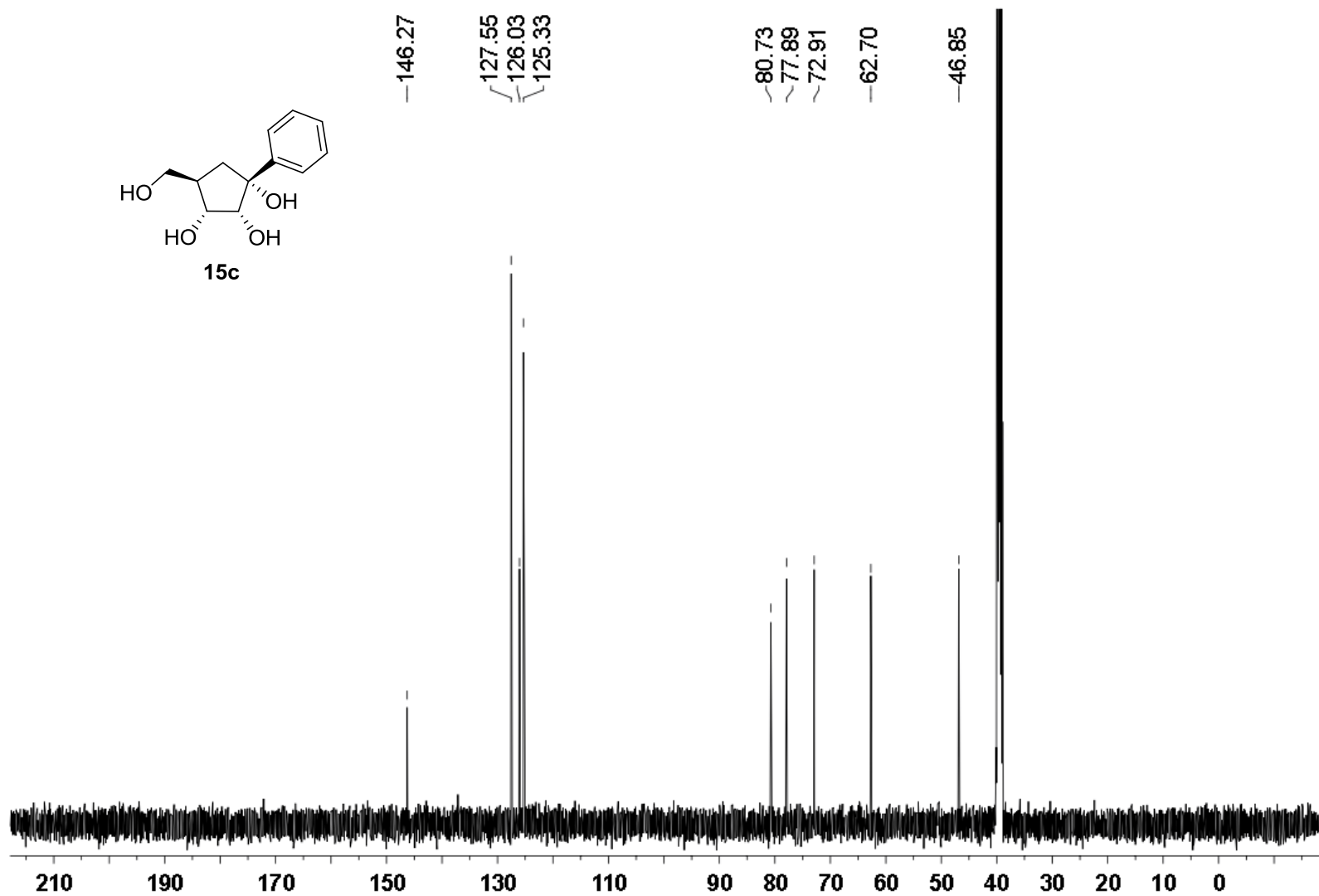
<sup>1</sup>H NMR (500 MHz) spectrum of **15b** in DMSO-*d*<sub>6</sub>



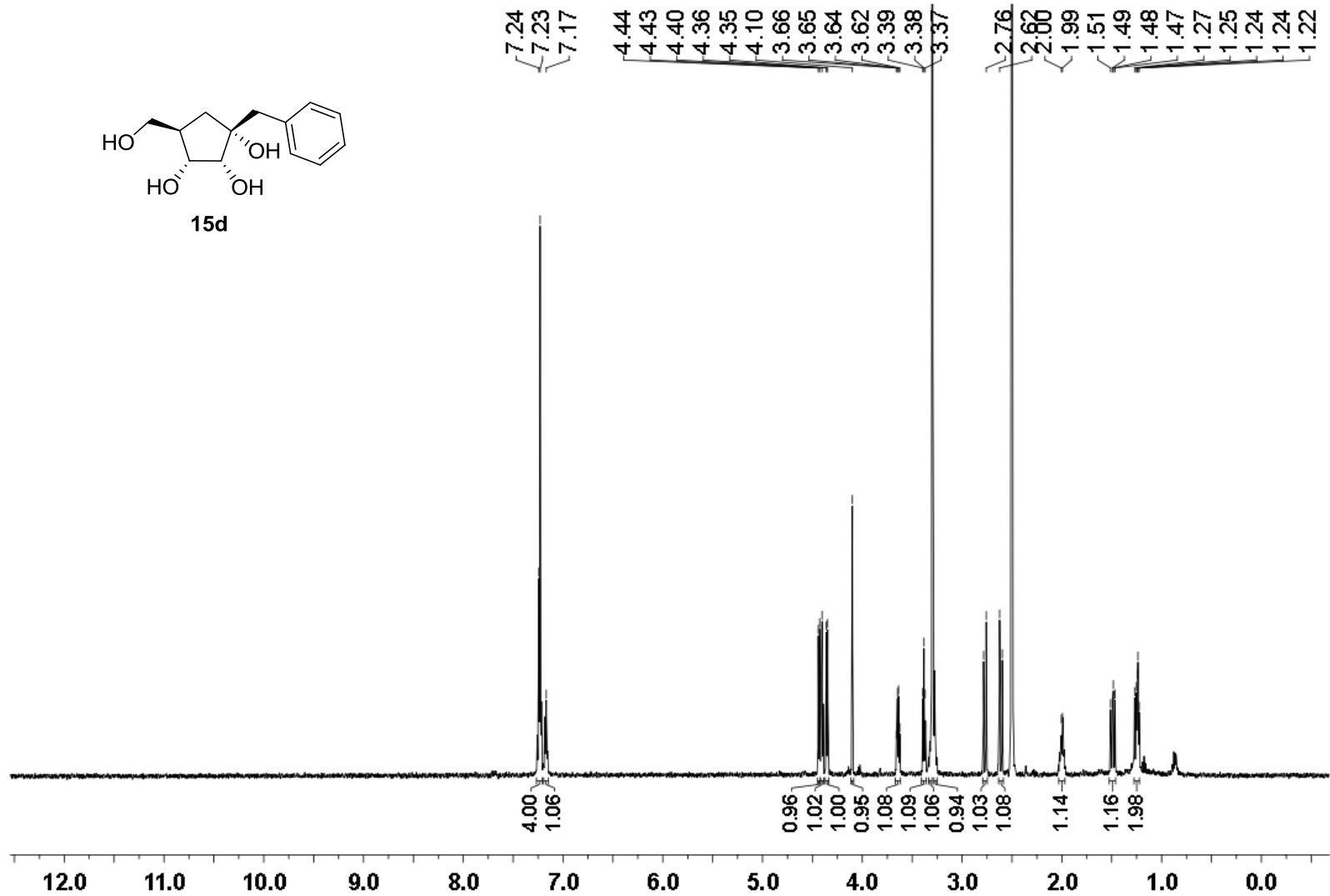
$^{13}\text{C}$  NMR (126 MHz) spectrum of **15b** in  $\text{DMSO-}d_6$



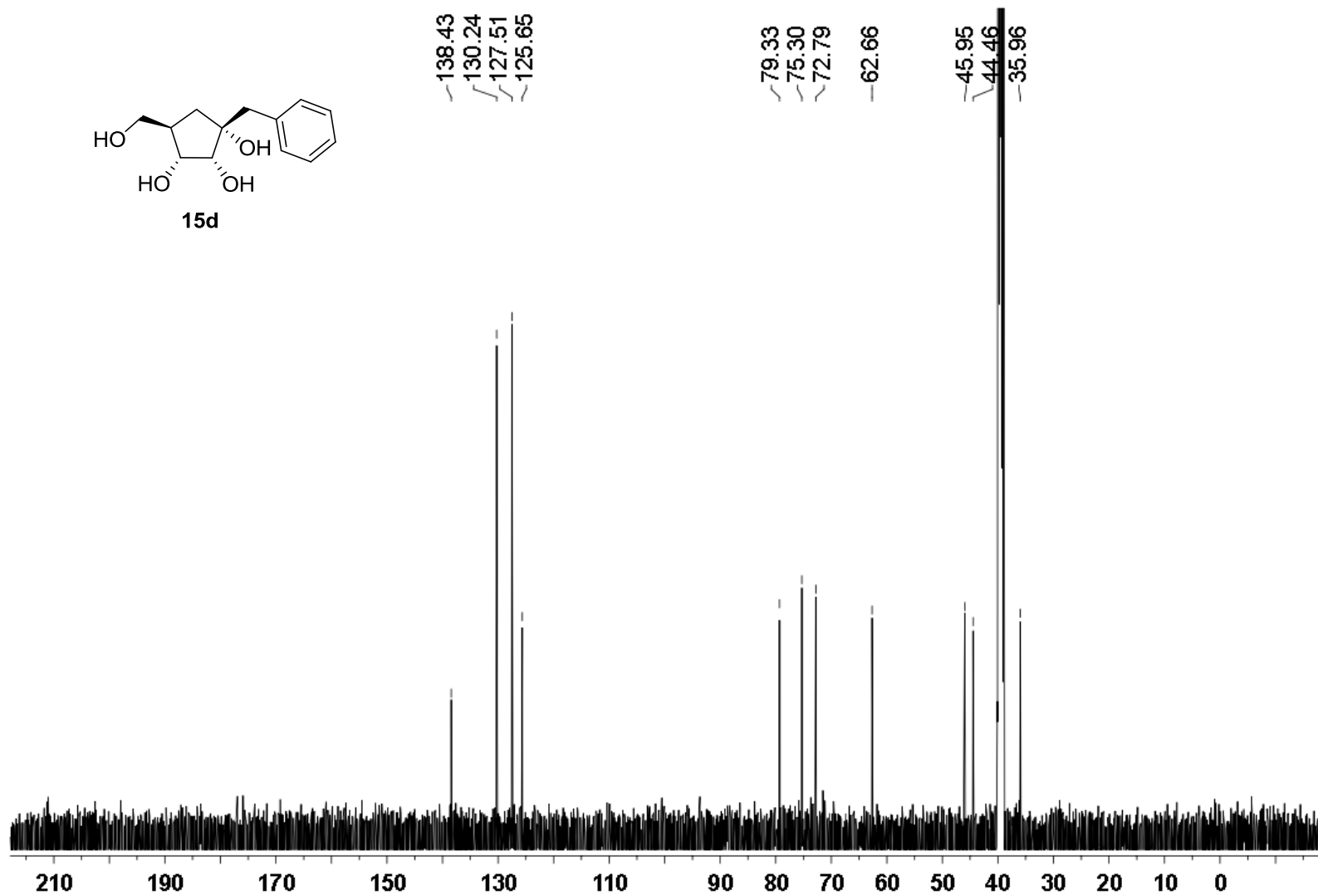
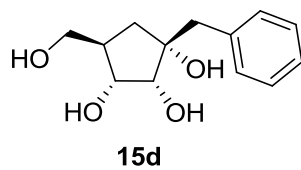
$^1\text{H}$  NMR (500 MHz) spectrum of **15c** in  $\text{DMSO-}d_6$



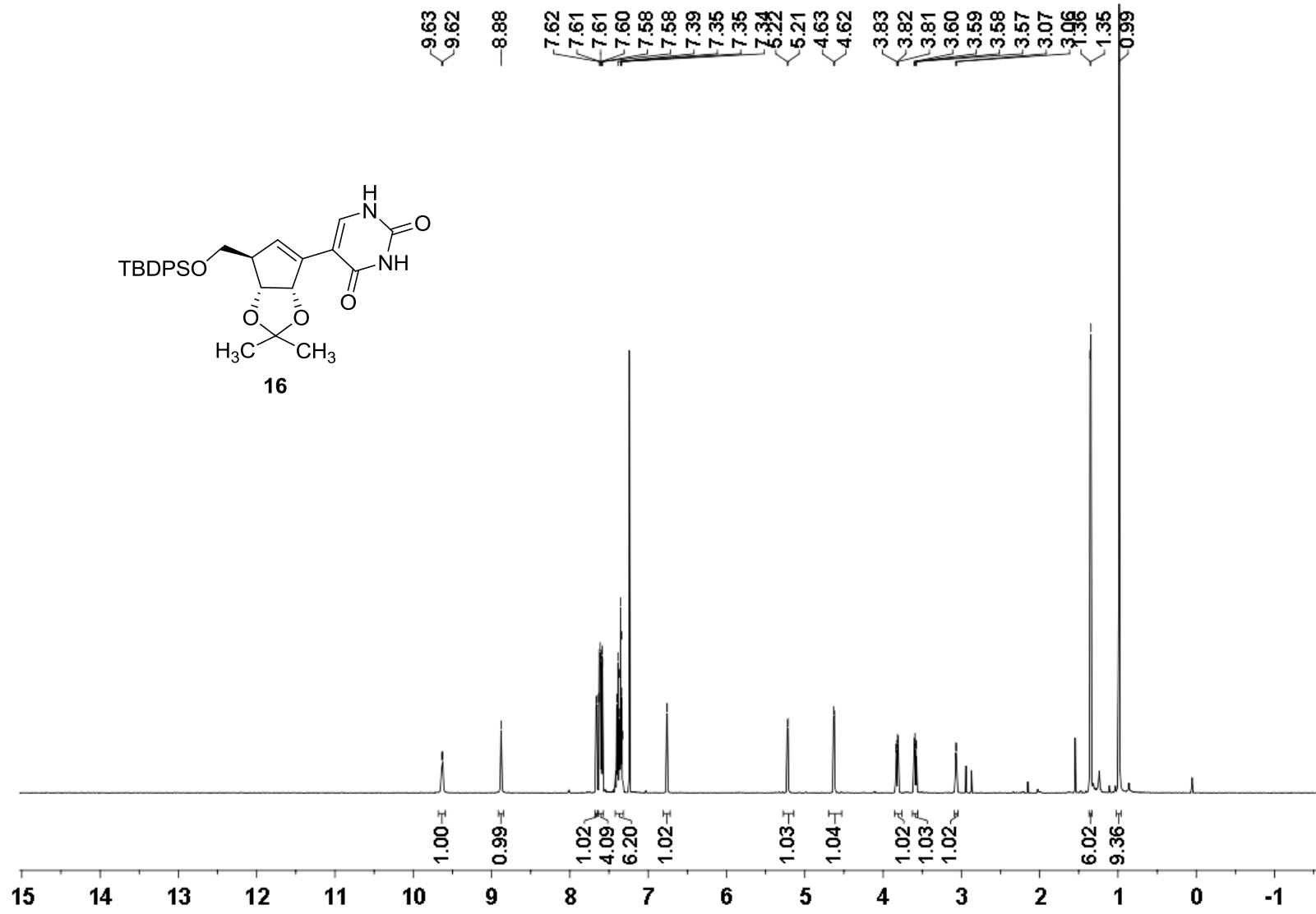
$^{13}\text{C}$  NMR (126 MHz) spectrum of **15c** in  $\text{DMSO-}d_6$



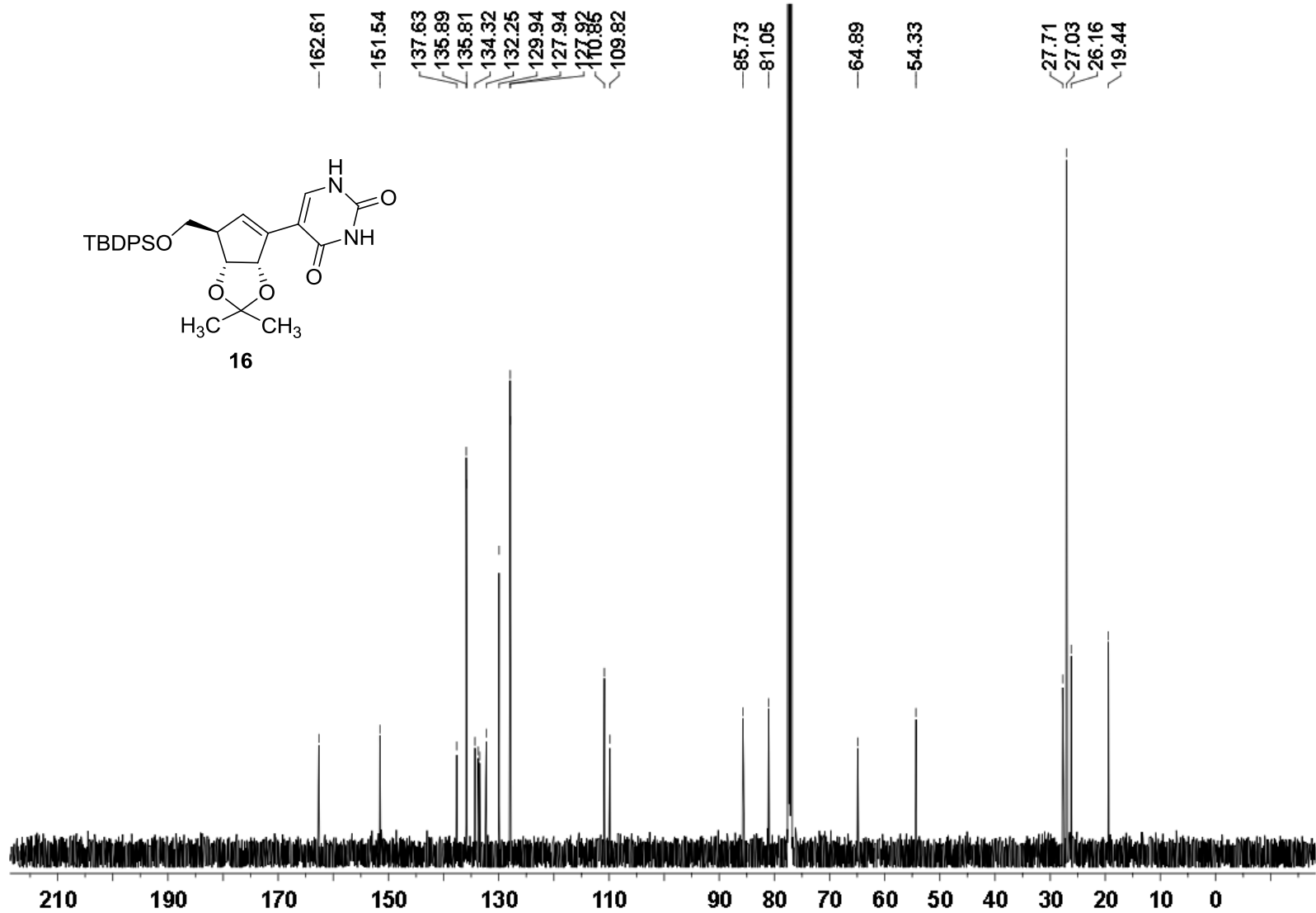
<sup>1</sup>H NMR (500 MHz) spectrum of **15d** in DMSO-*d*<sub>6</sub>



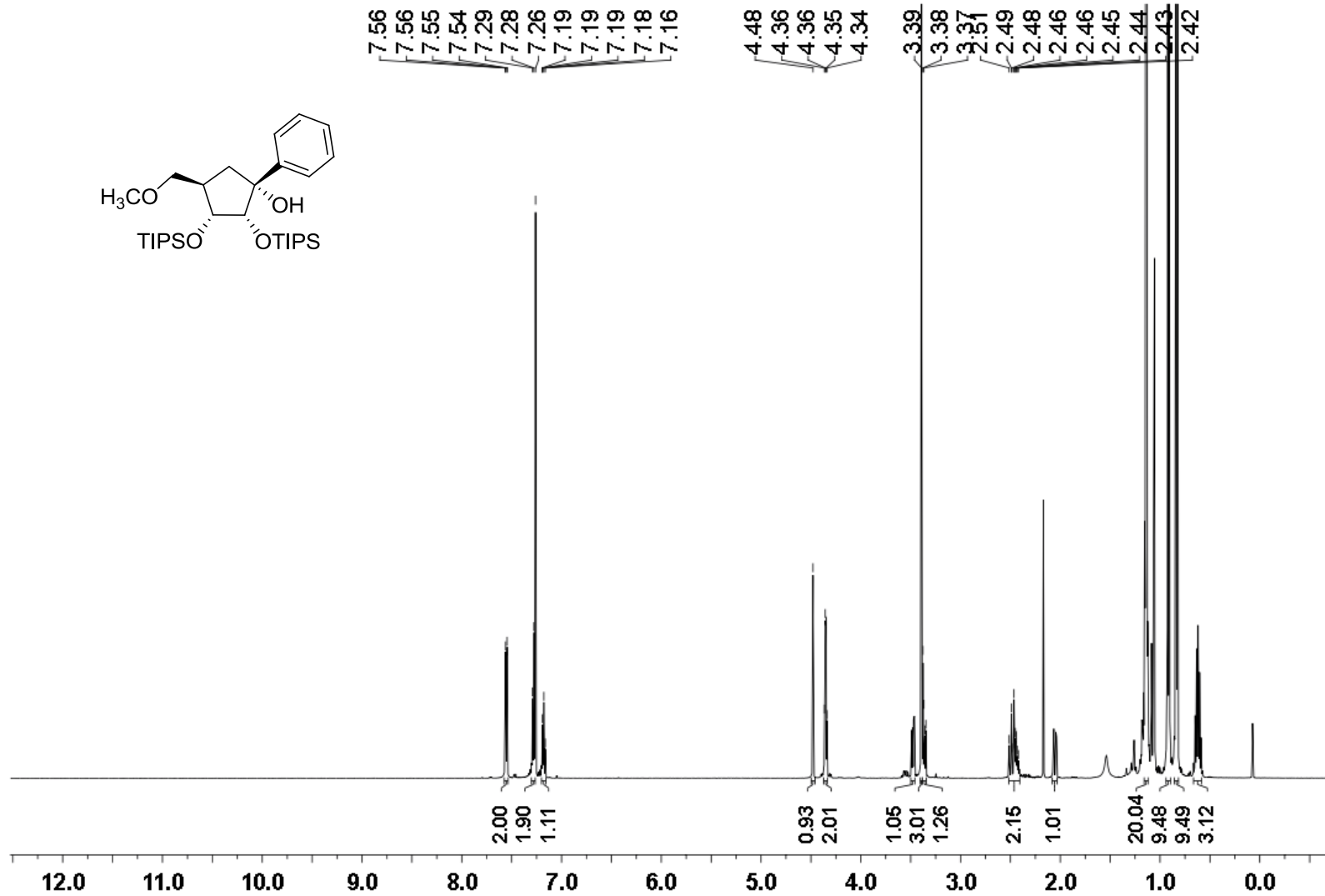
$^{13}\text{C}$  NMR (126 MHz) spectrum of **15d** in  $\text{DMSO-}d_6$



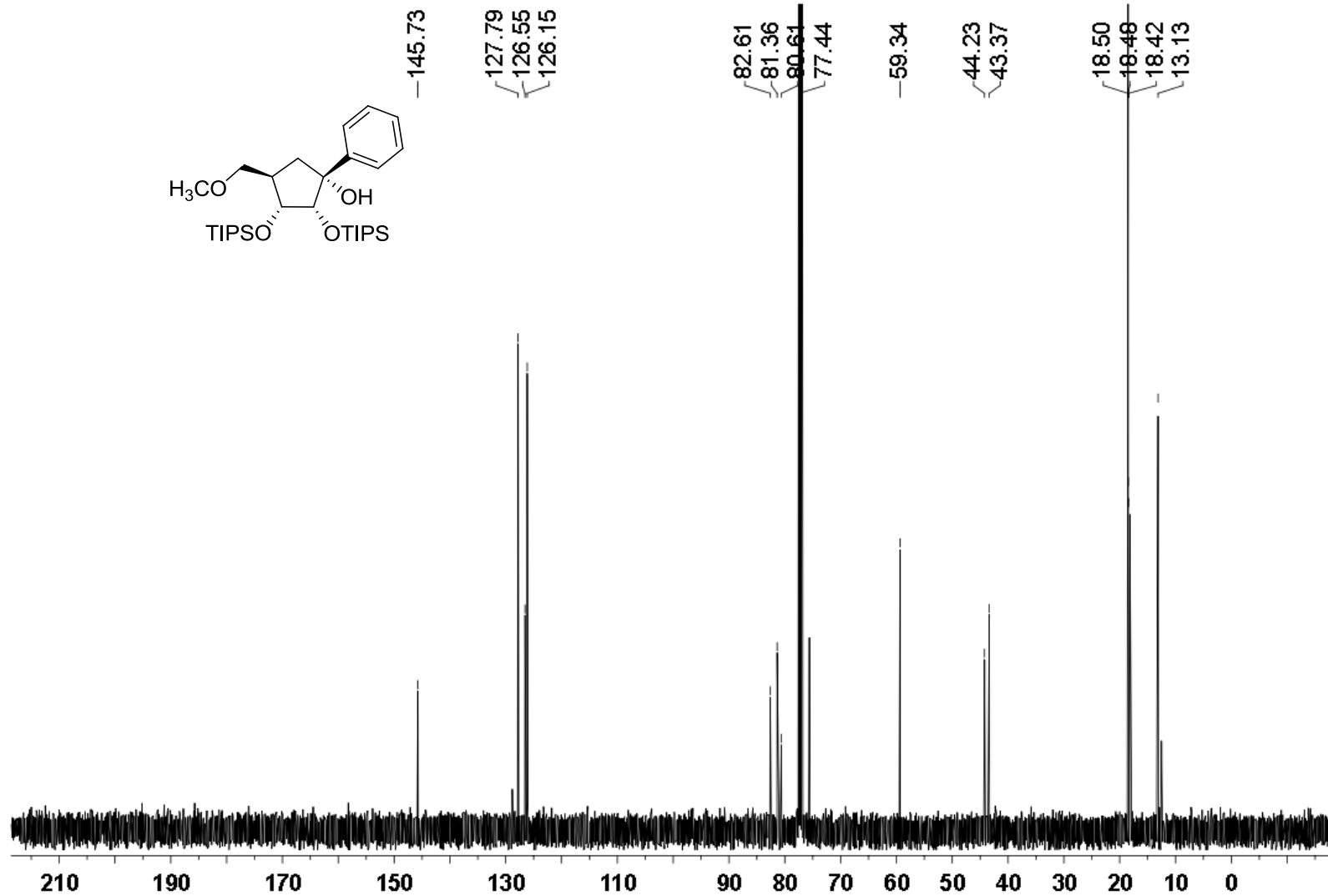
<sup>1</sup>H NMR (500 MHz) spectrum of **16** in CDCl<sub>3</sub>



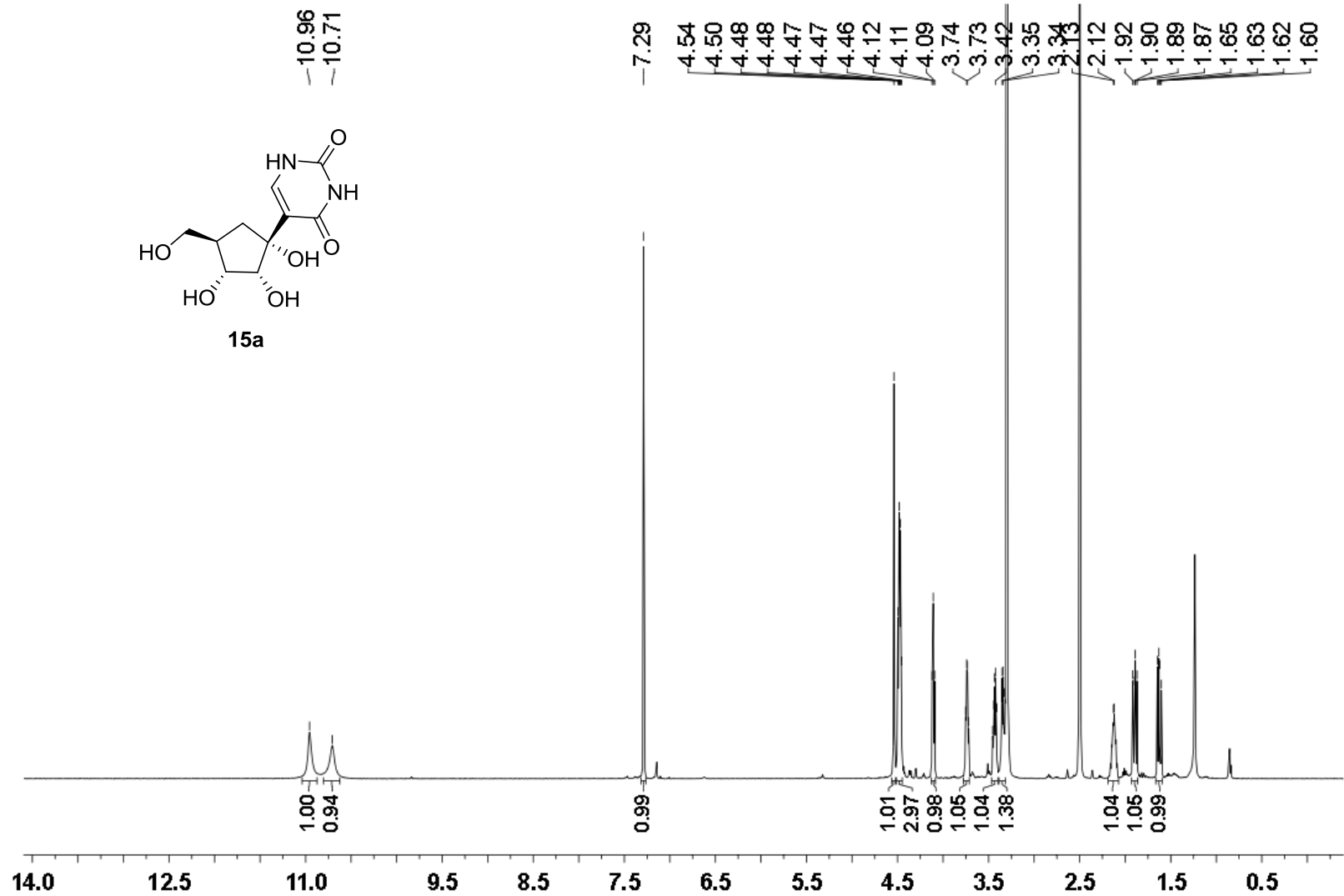
$^{13}\text{C}$  NMR (126 MHz) spectrum of **16** in  $\text{CDCl}_3$



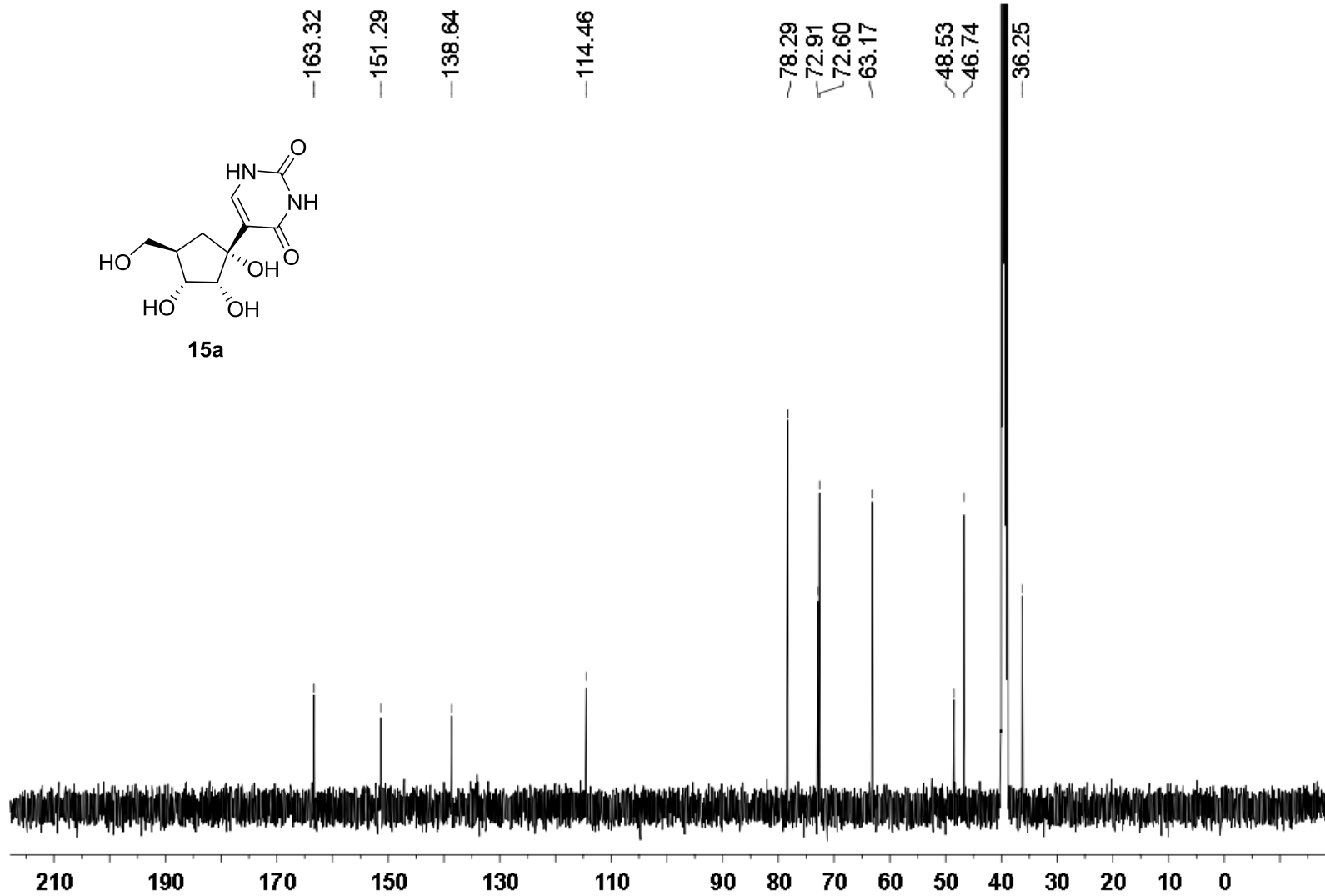
$^1\text{H}$  NMR (500 MHz) spectrum in  $\text{CDCl}_3$



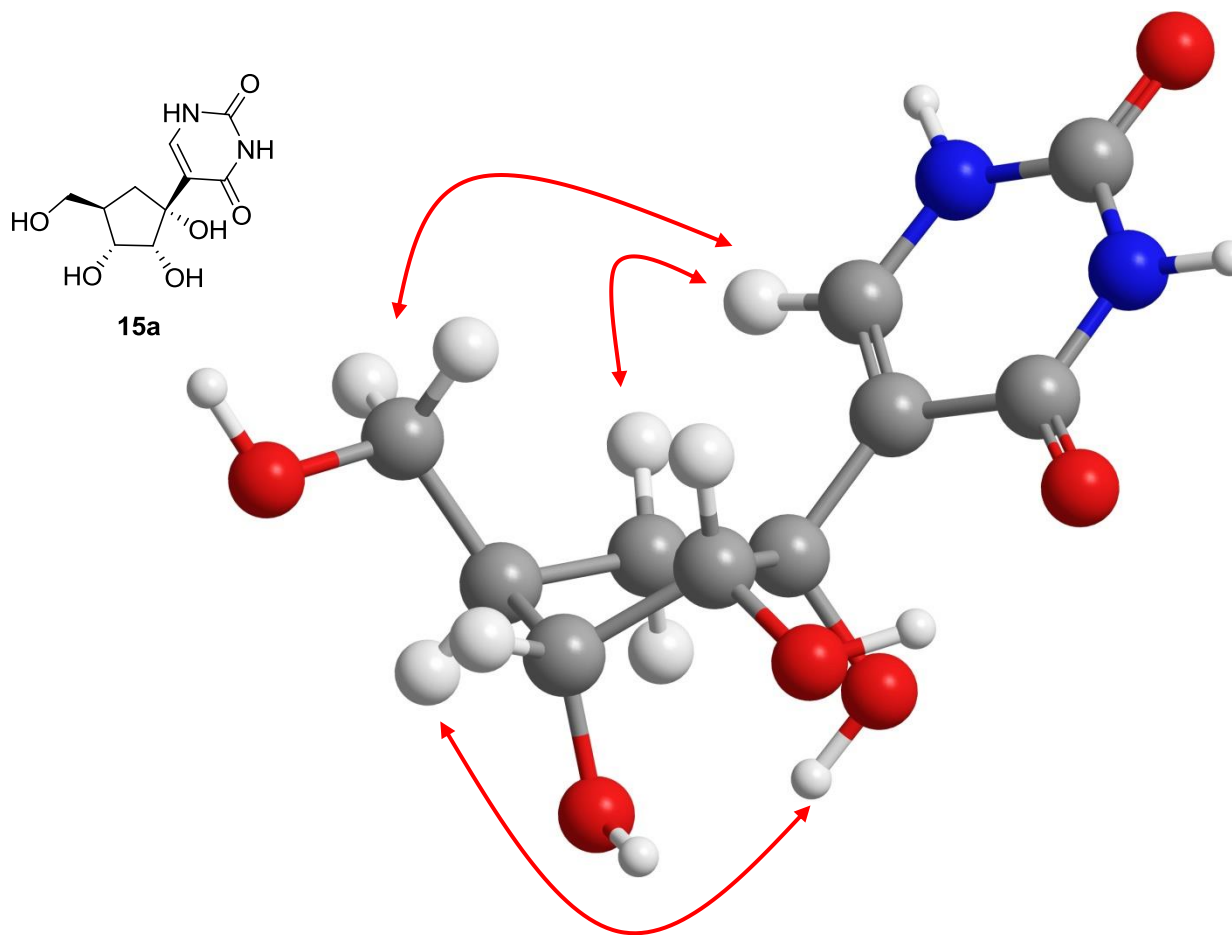
$^{13}\text{C}$  NMR (126 MHz) spectrum in  $\text{CDCl}_3$



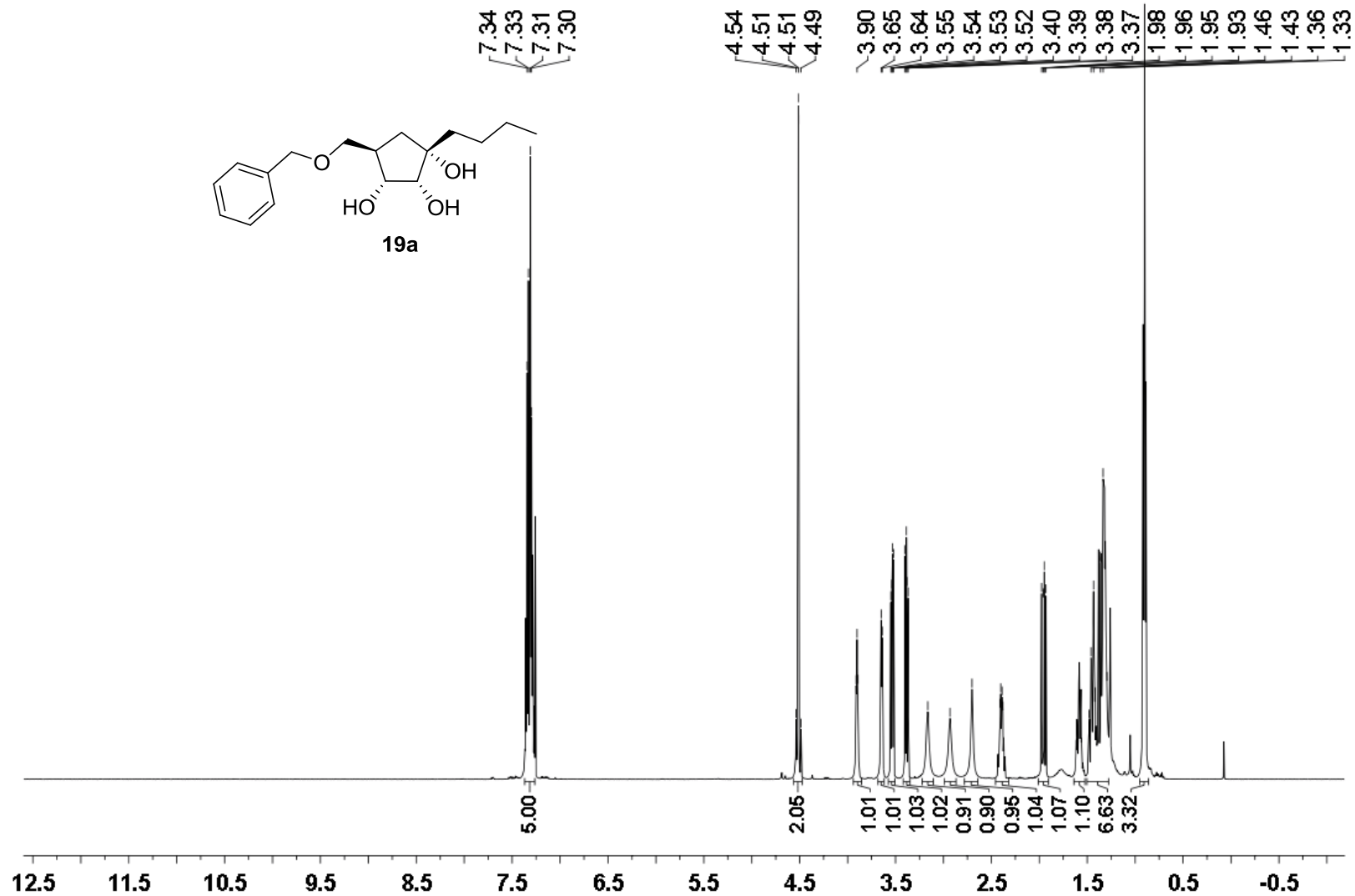
<sup>1</sup>H NMR (500 MHz) spectrum of **15a** in DMSO-*d*<sub>6</sub>



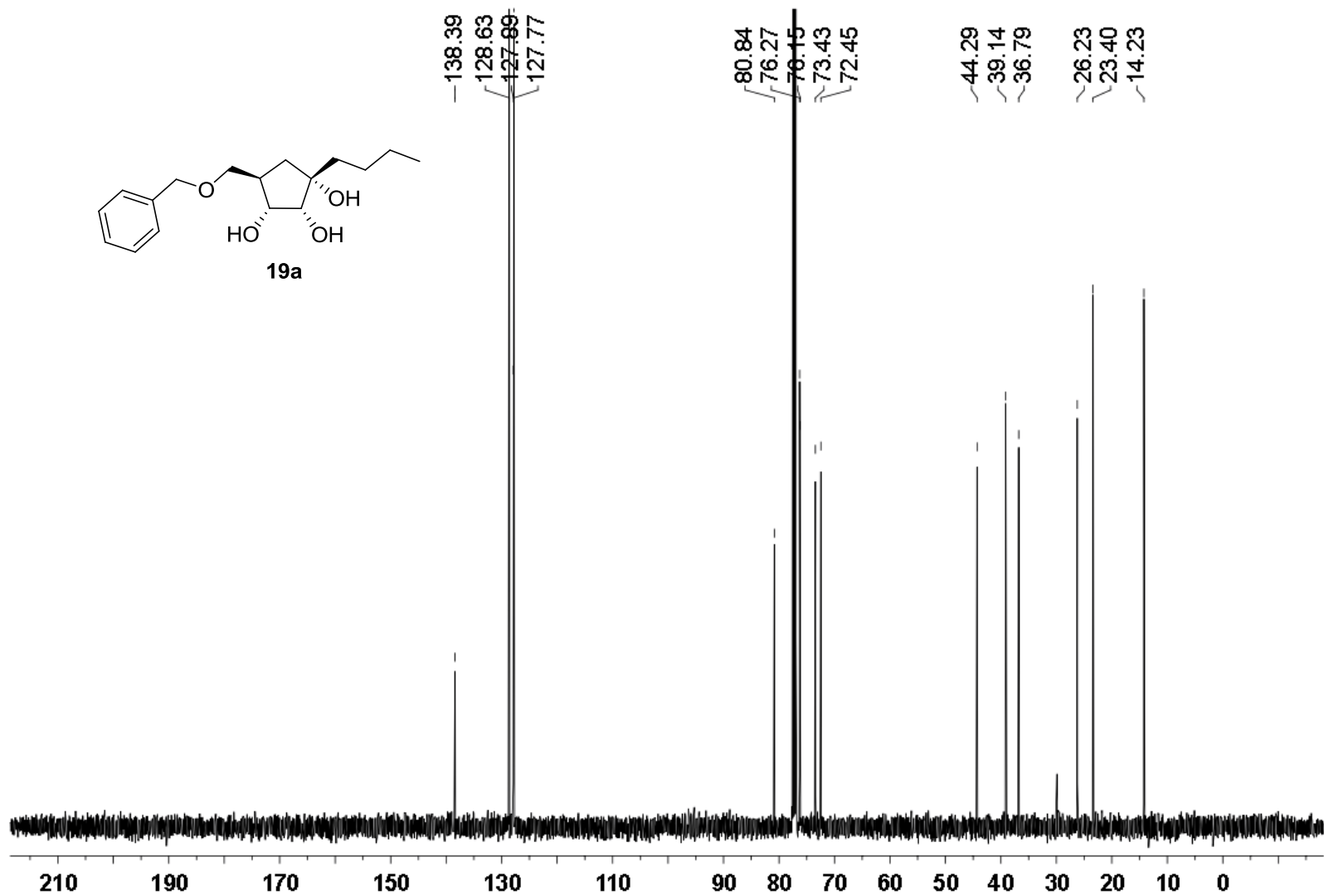
$^{13}\text{C}$  NMR (126 MHz) spectrum of **15a** in  $\text{DMSO-}d_6$



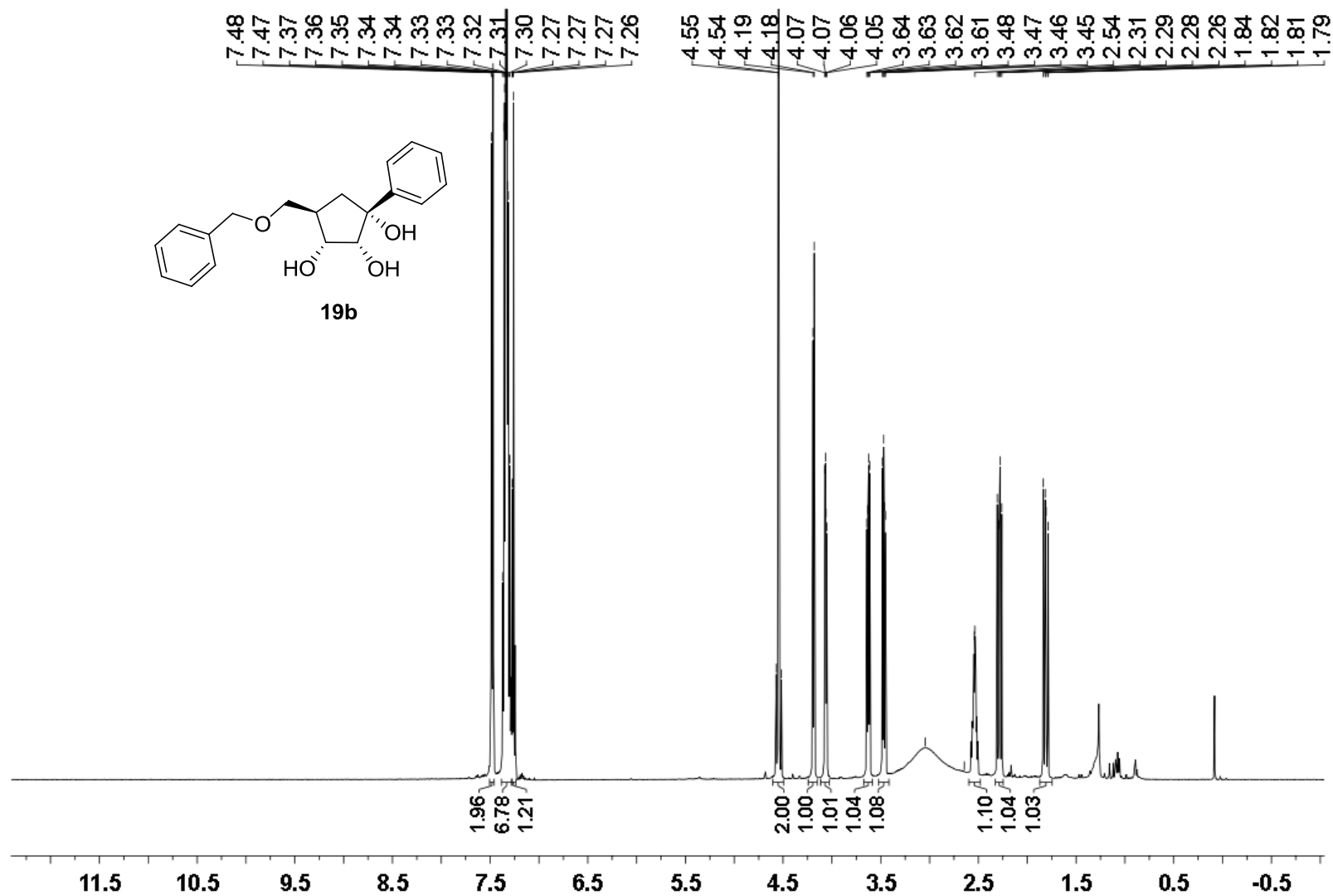
Key NOE interactions observed in molecule **15a**



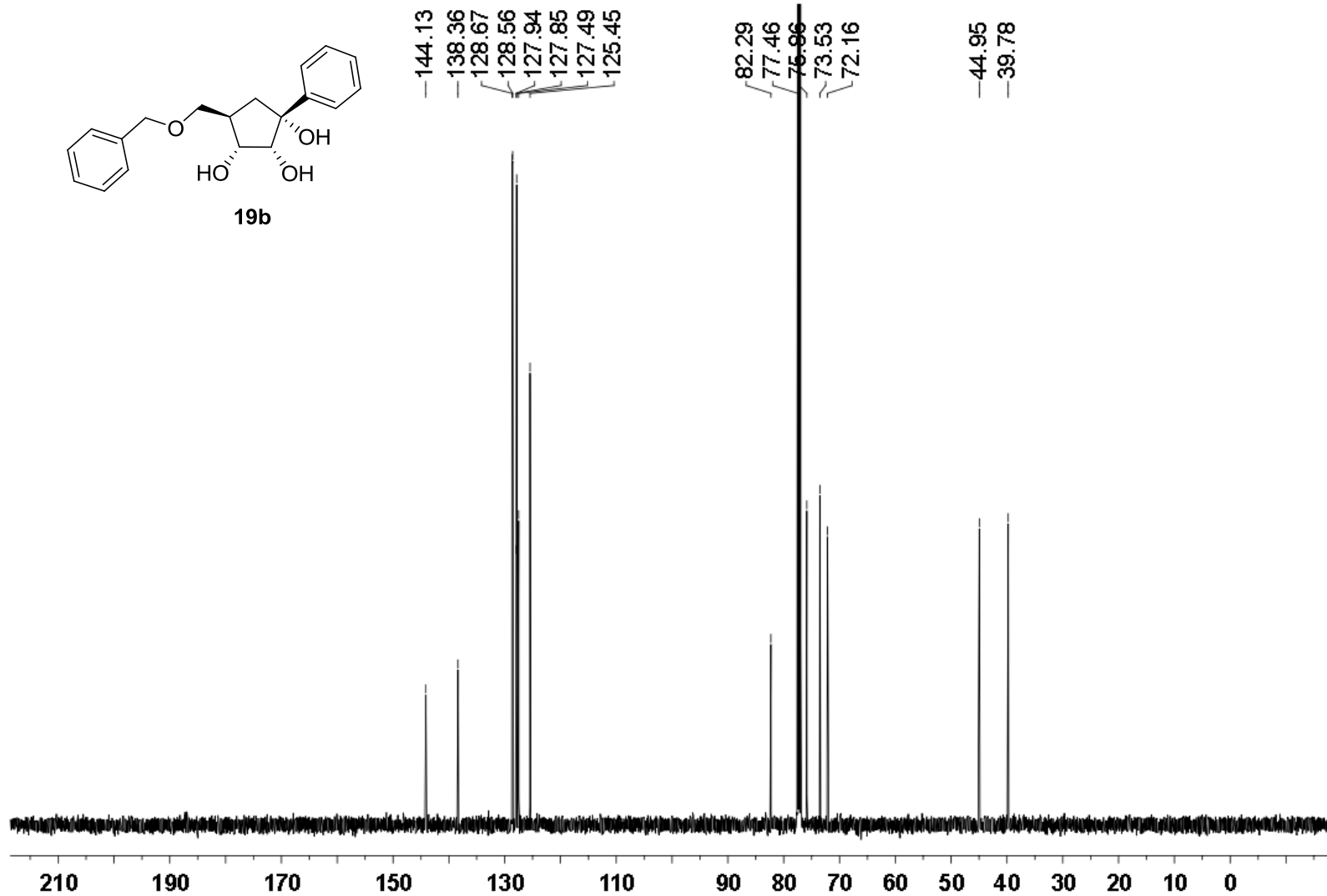
$^1\text{H}$  NMR (500 MHz) spectrum of **19a** in  $\text{CDCl}_3$



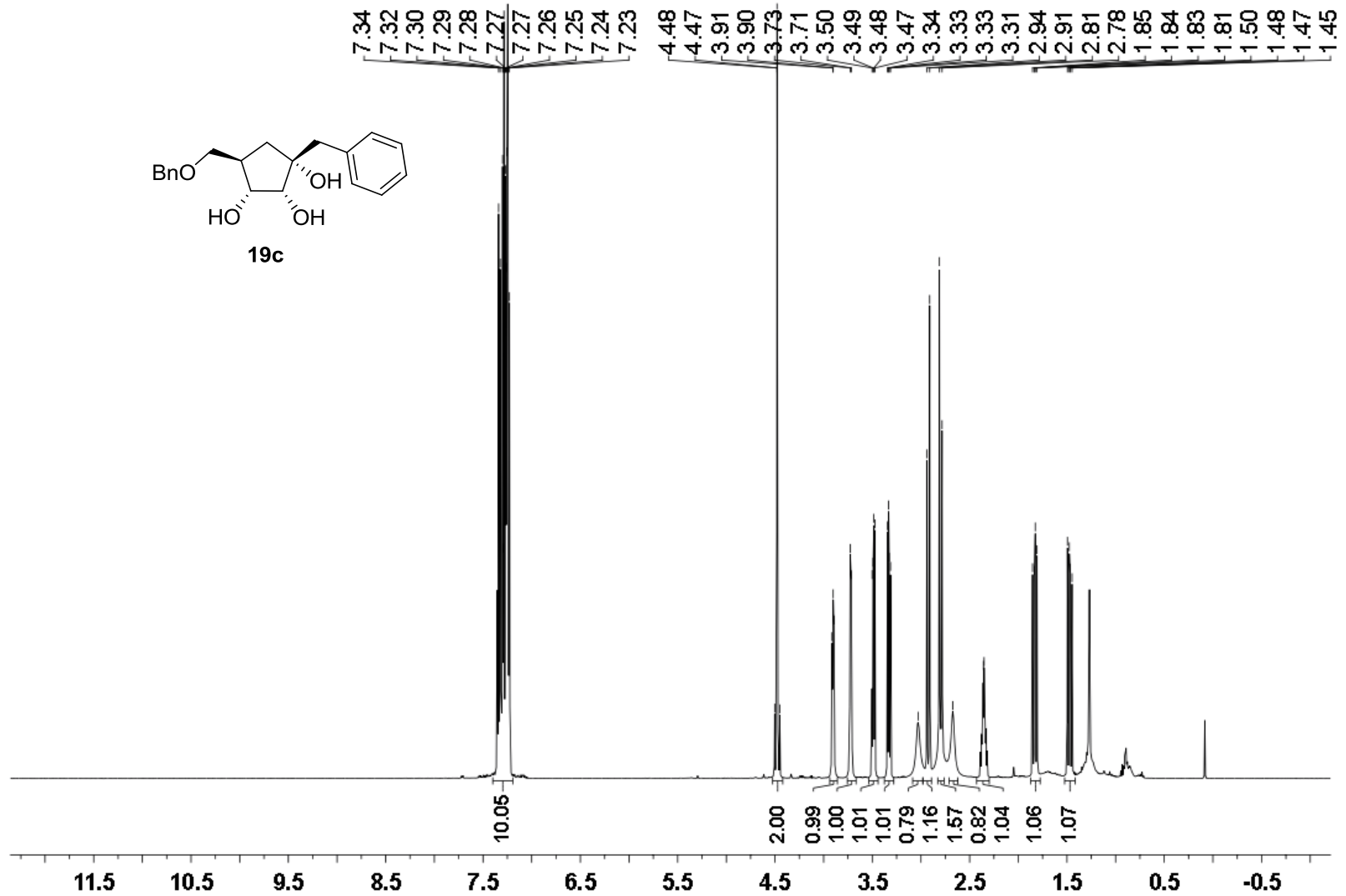
$^{13}\text{C}$  NMR (126 MHz) spectrum of **19a** in  $\text{CDCl}_3$



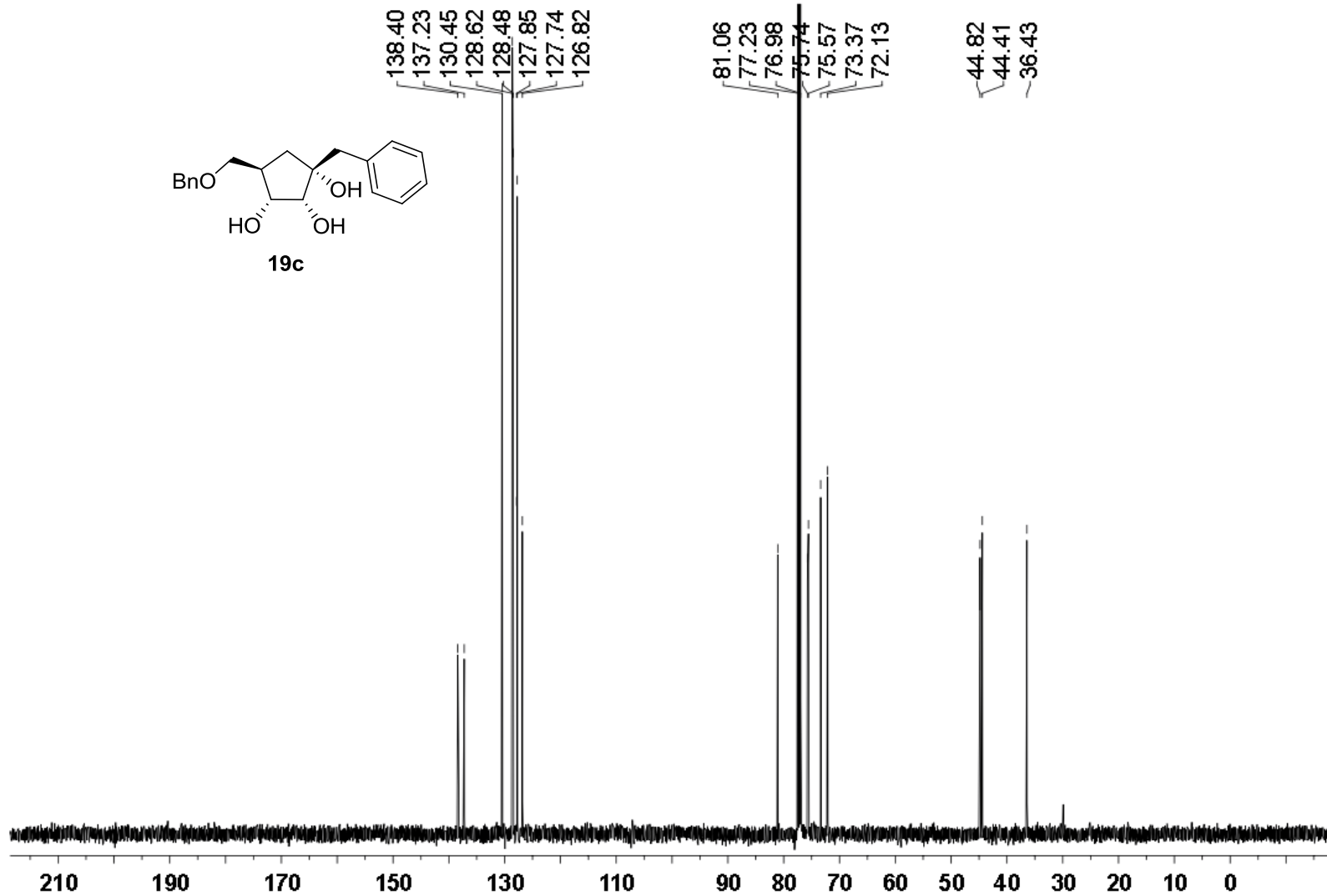
<sup>1</sup>H NMR (500 MHz) spectrum of **19b** in CDCl<sub>3</sub>



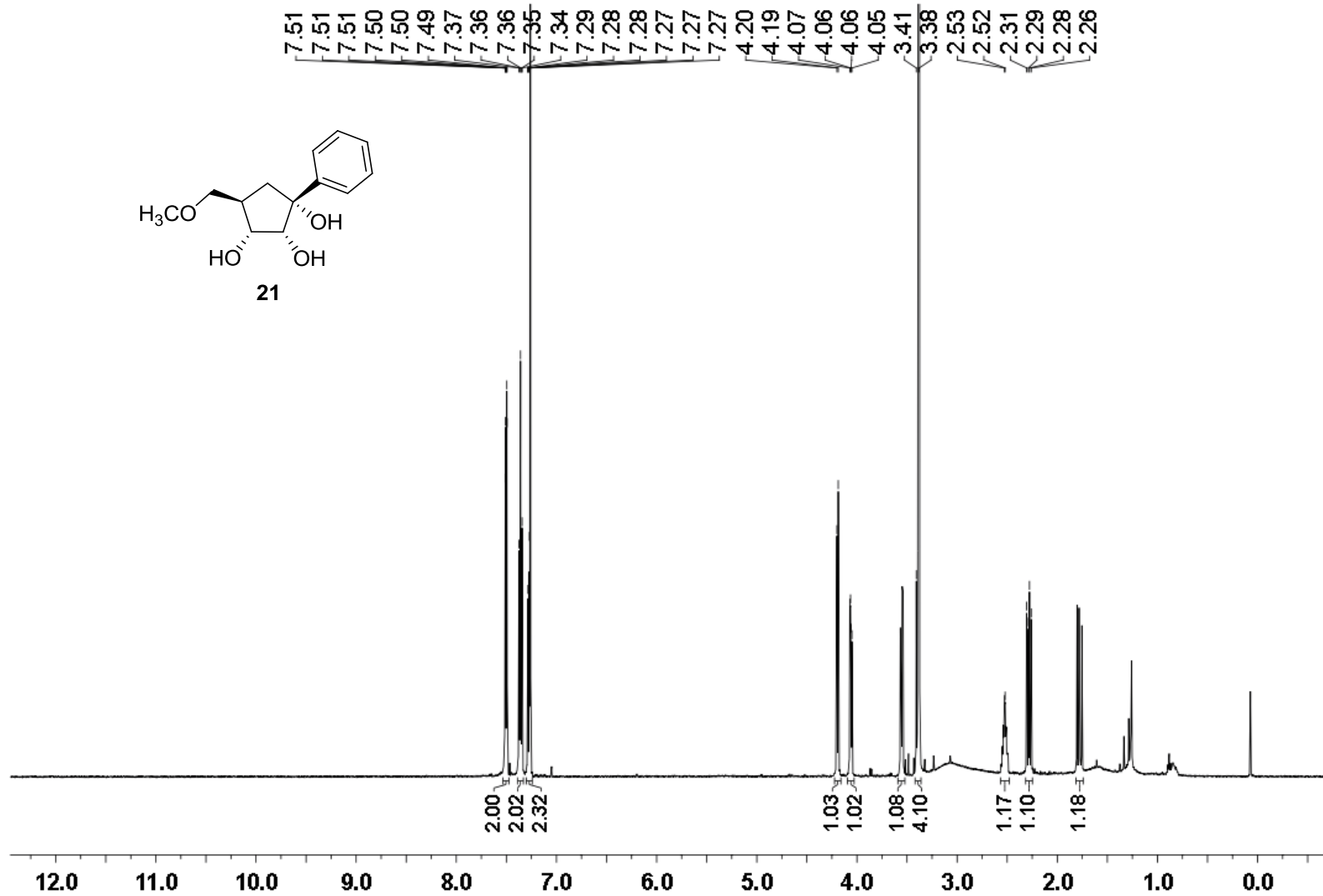
$^{13}\text{C}$  NMR (126 MHz) spectrum of **19b** in  $\text{CDCl}_3$



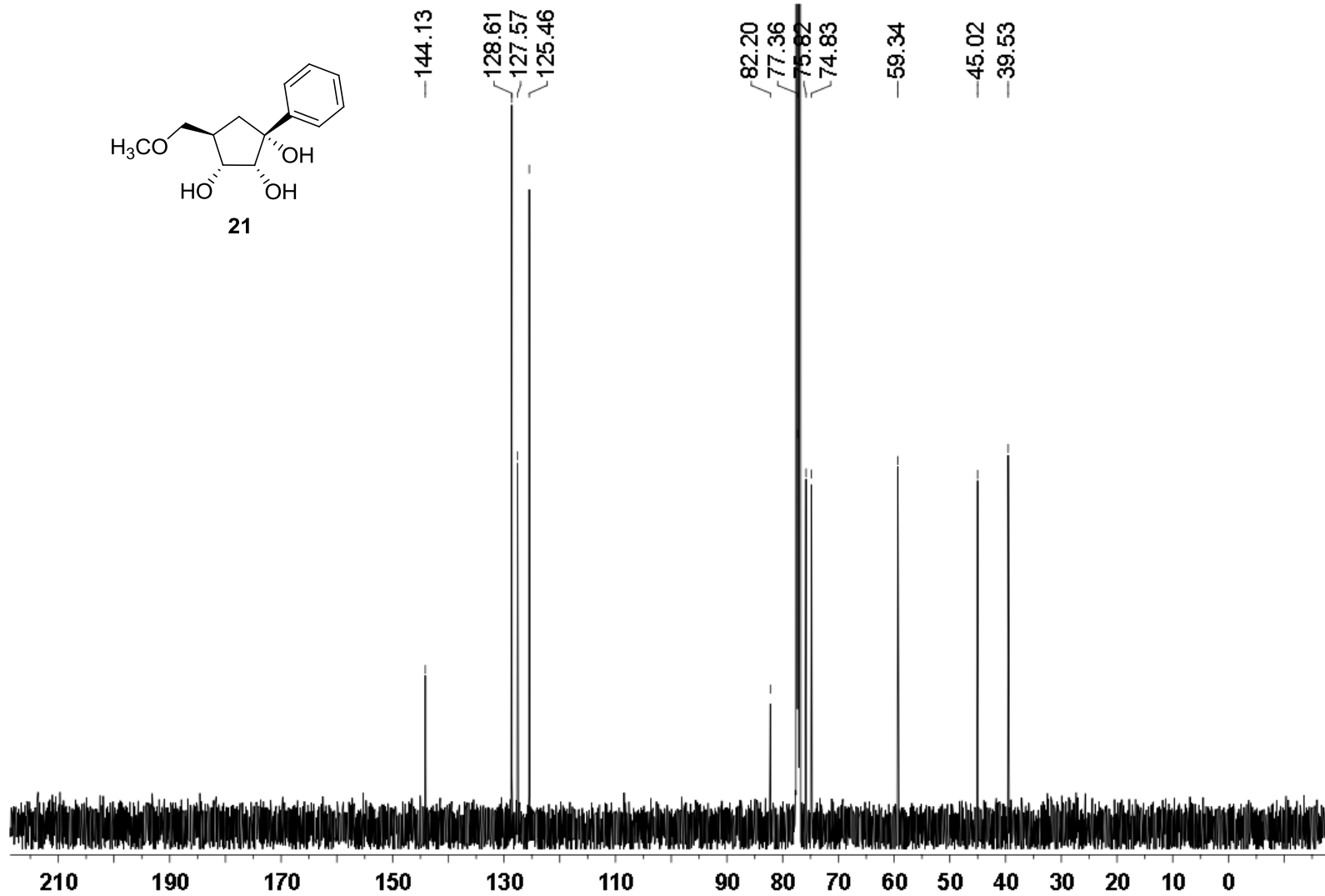
<sup>1</sup>H NMR (126 MHz) spectrum of **19c** in CDCl<sub>3</sub>



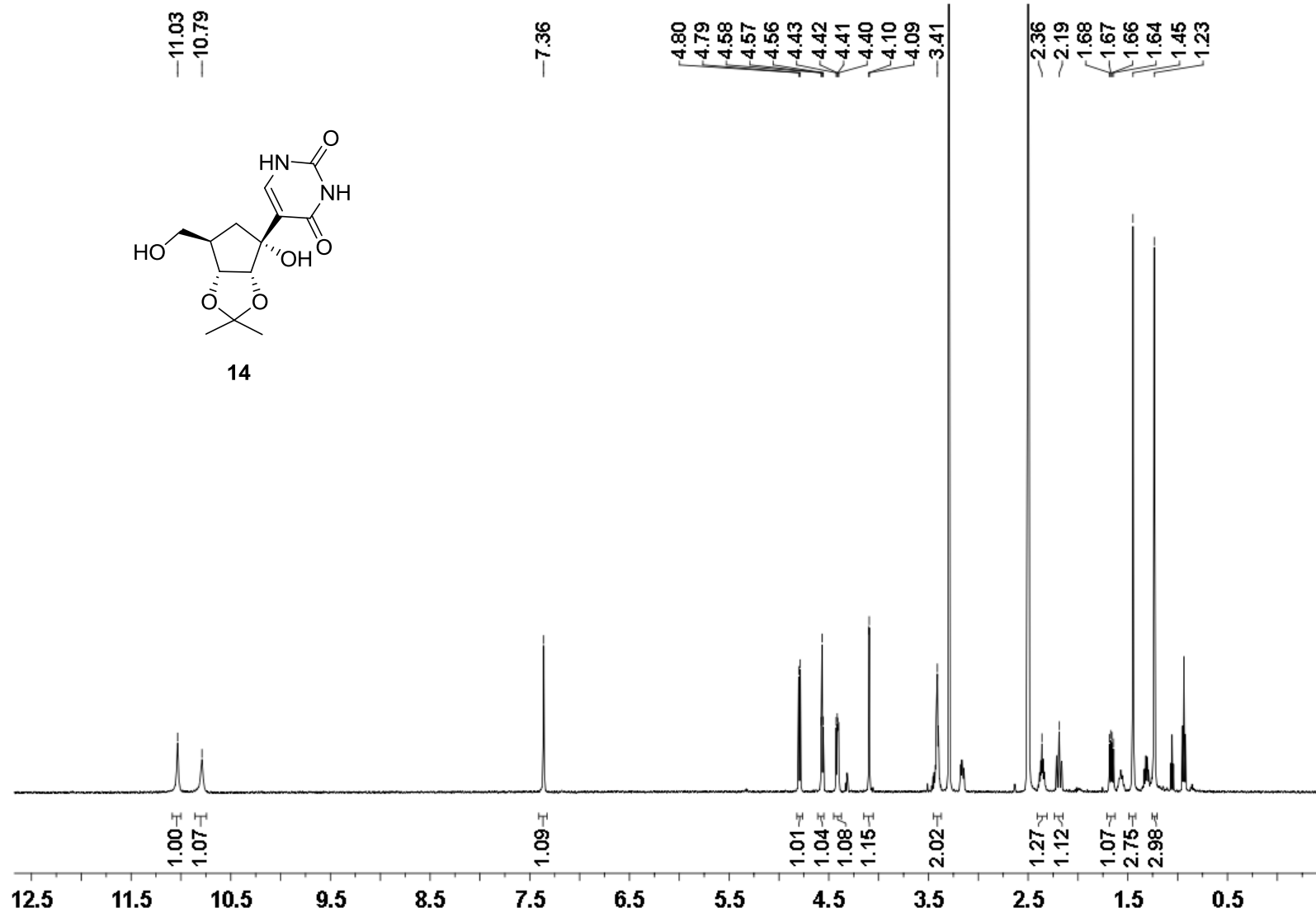
$^{13}\text{C}$  NMR (126 MHz) spectrum of **19c** in  $\text{CDCl}_3$



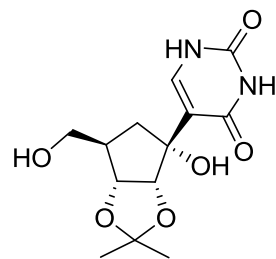
<sup>1</sup>H NMR (126 MHz) spectrum of **21** in CDCl<sub>3</sub>



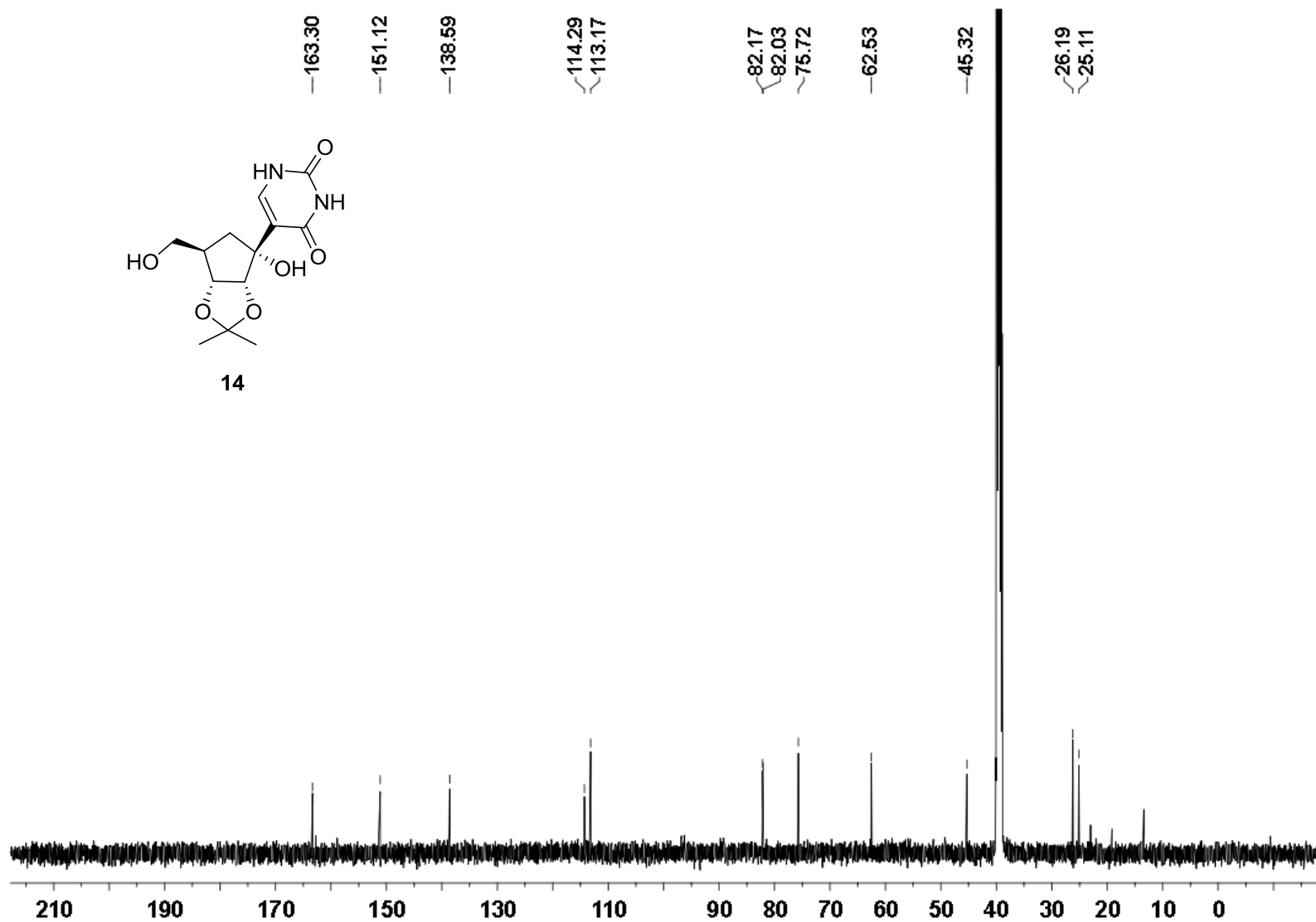
<sup>13</sup>C NMR (126 MHz) spectrum of **21** in CDCl<sub>3</sub>



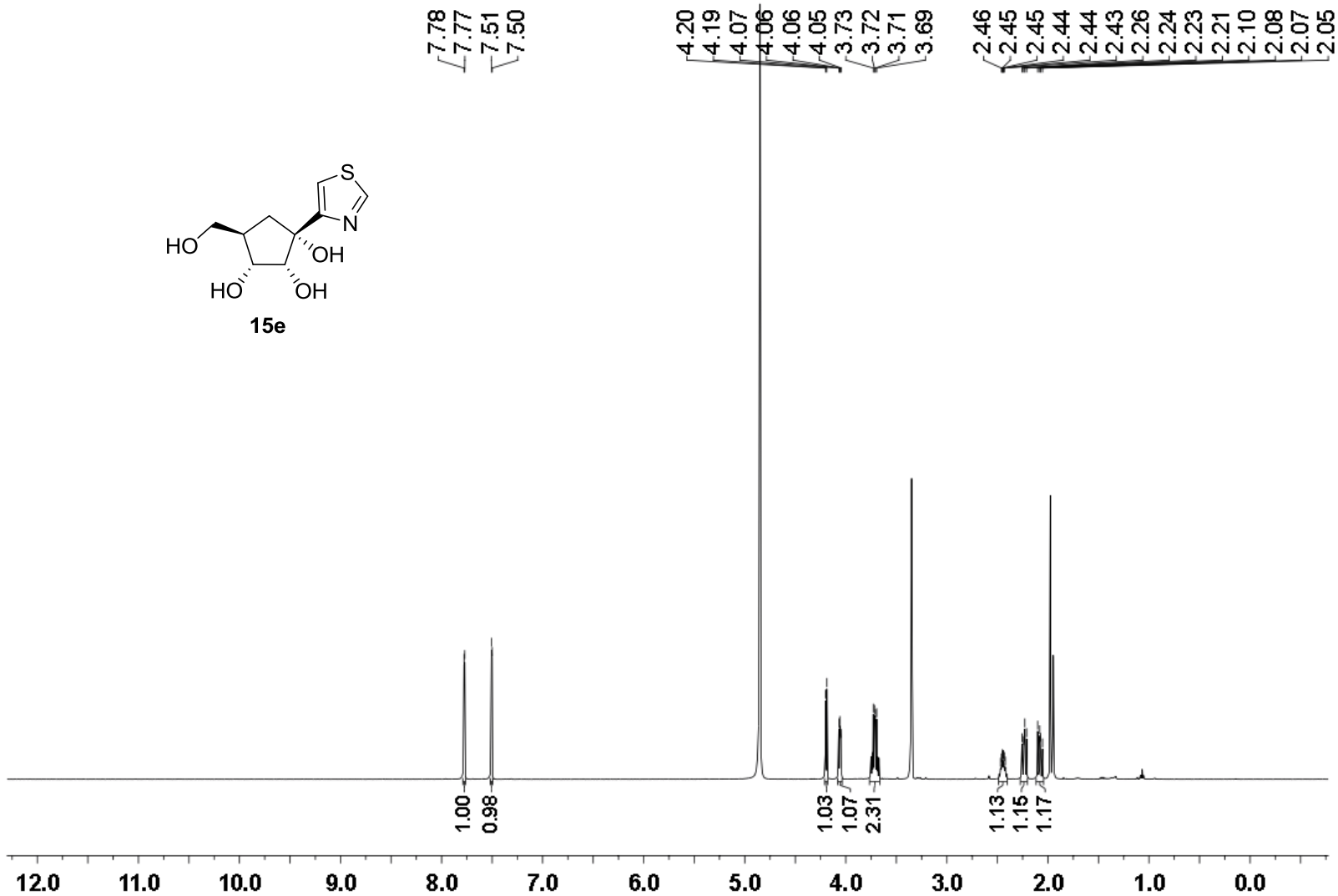
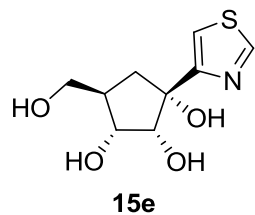
$^1\text{H NMR}$  (500 MHz) spectrum of **14** in  $\text{DMSO-}d_6$



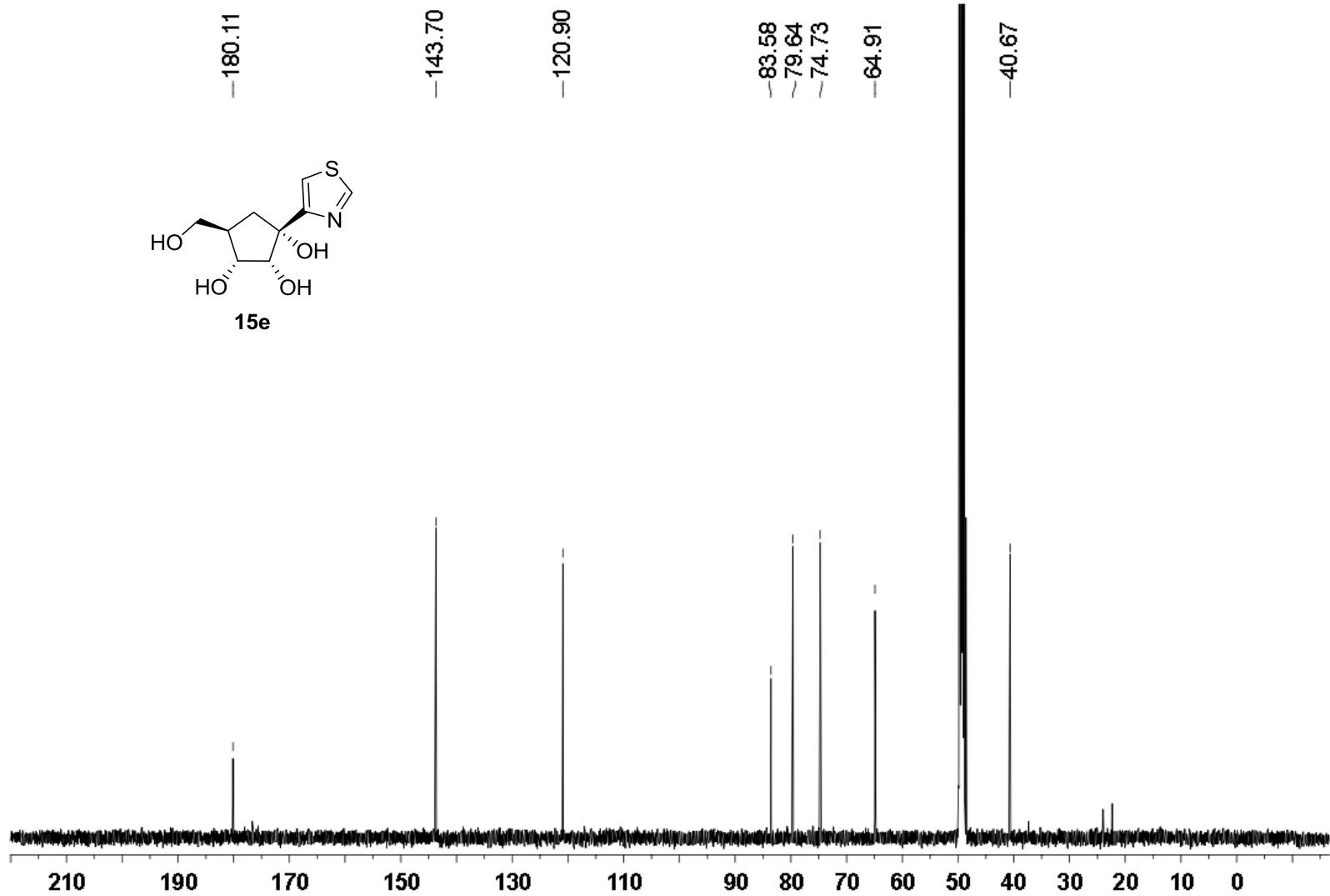
14



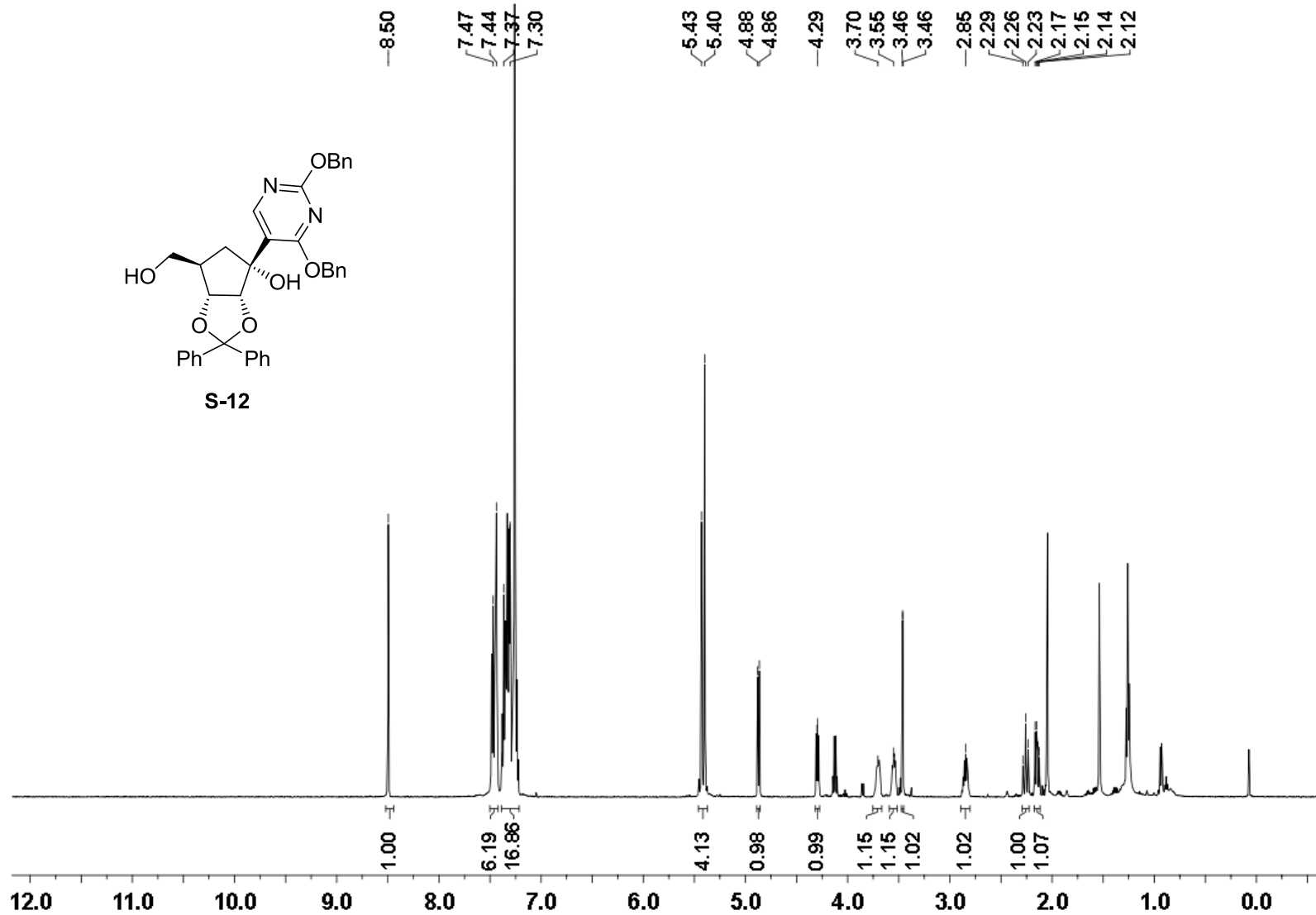
$^{13}\text{C}$  NMR (126 MHz) spectrum of 14 in  $\text{DMSO-}d_6$



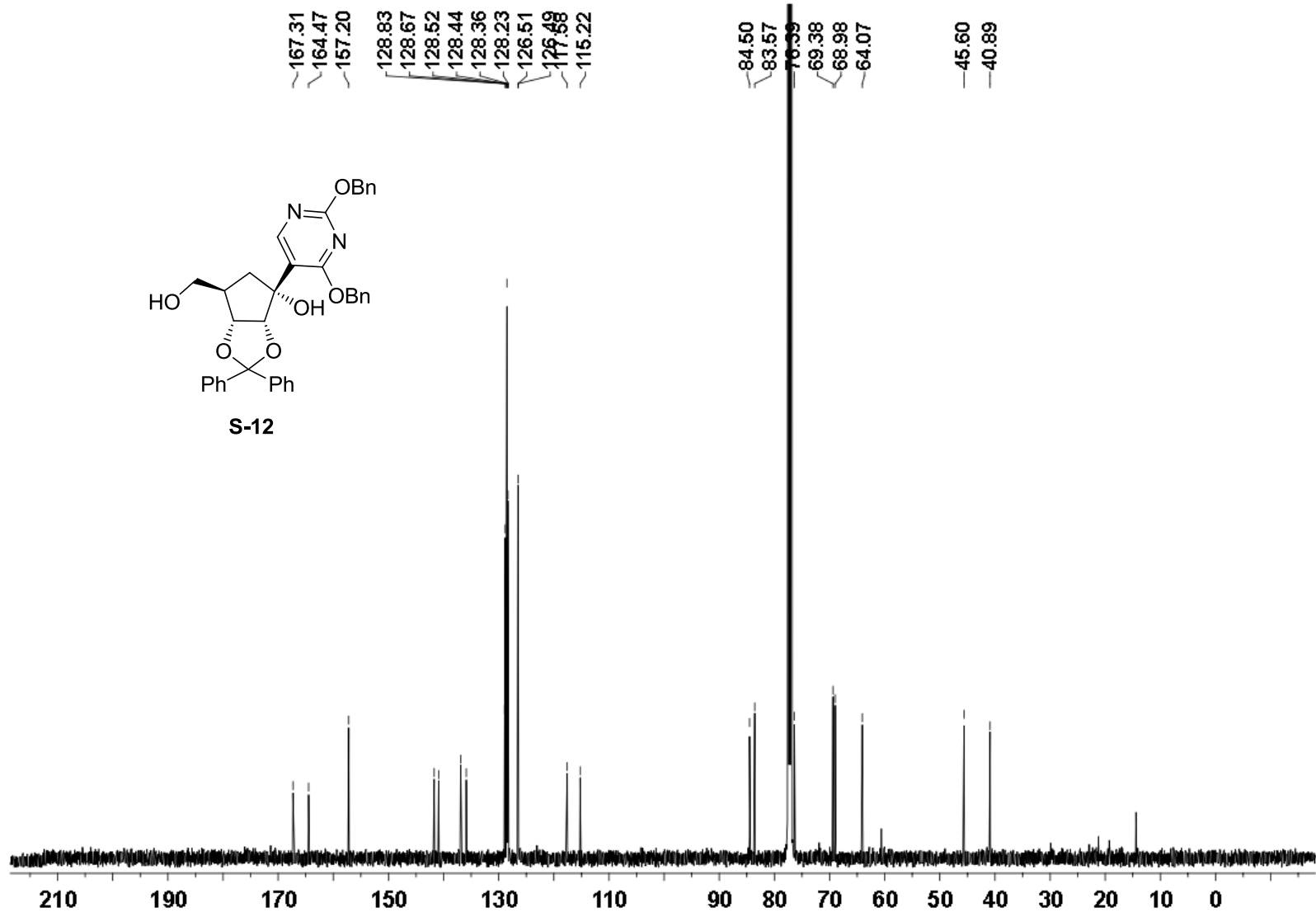
$^1\text{H}$  NMR (126 MHz) spectrum of **15e** in  $\text{CD}_3\text{OD}$



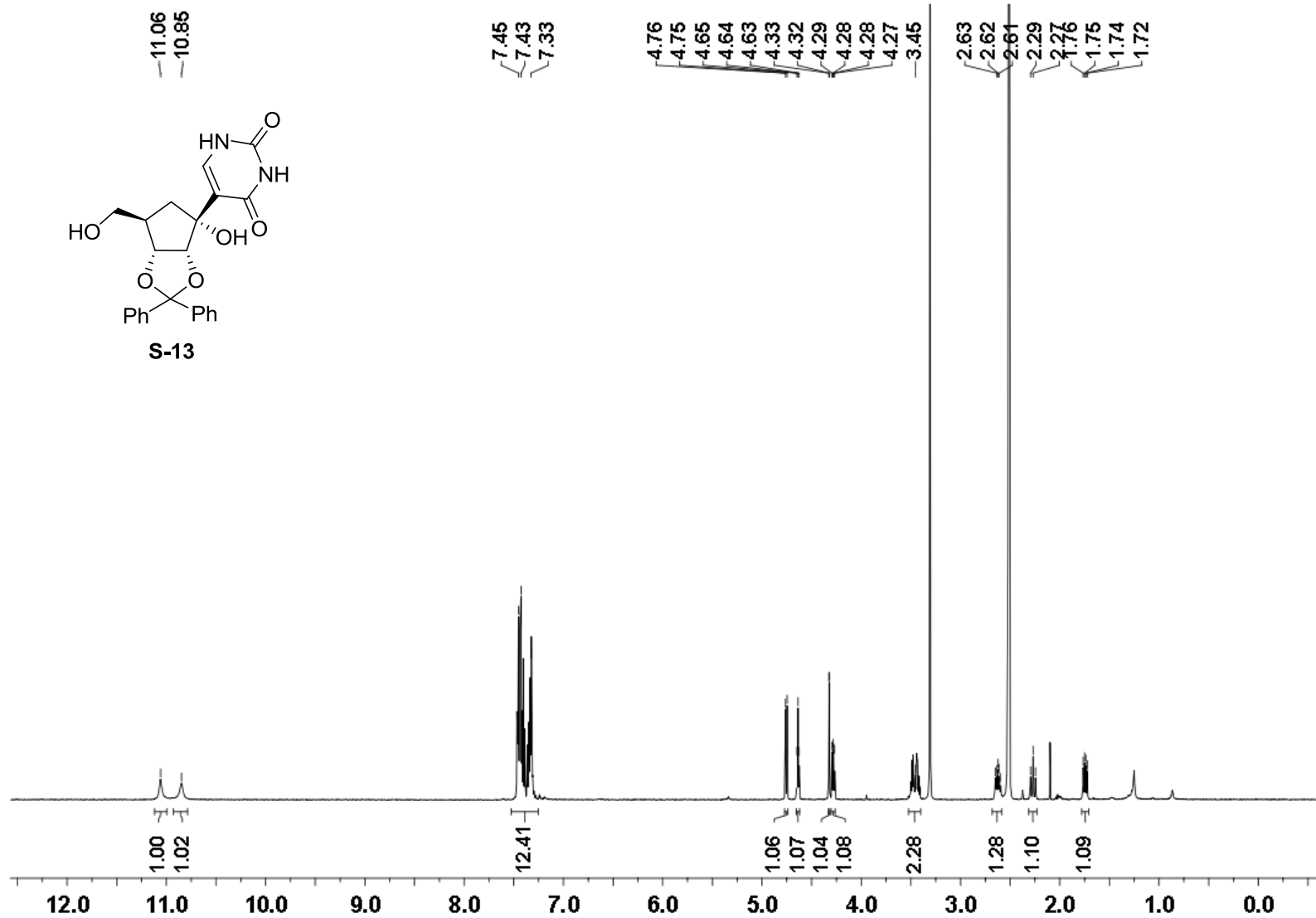
$^{13}\text{C}$  NMR (126 MHz) spectrum of **15e** in  $\text{CD}_3\text{OD}$



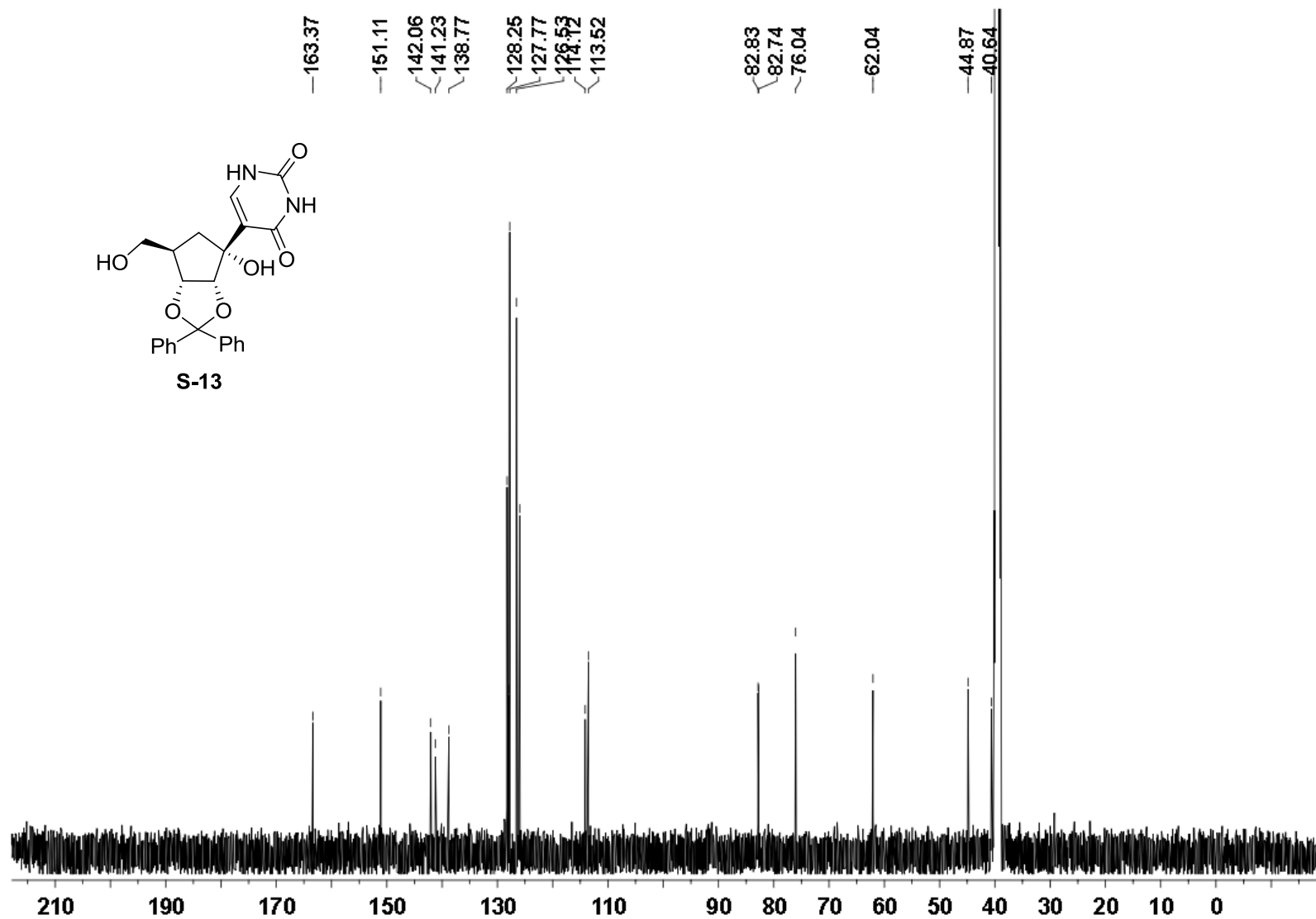
<sup>1</sup>H NMR (500 MHz) spectrum of S-12 in CDCl<sub>3</sub>



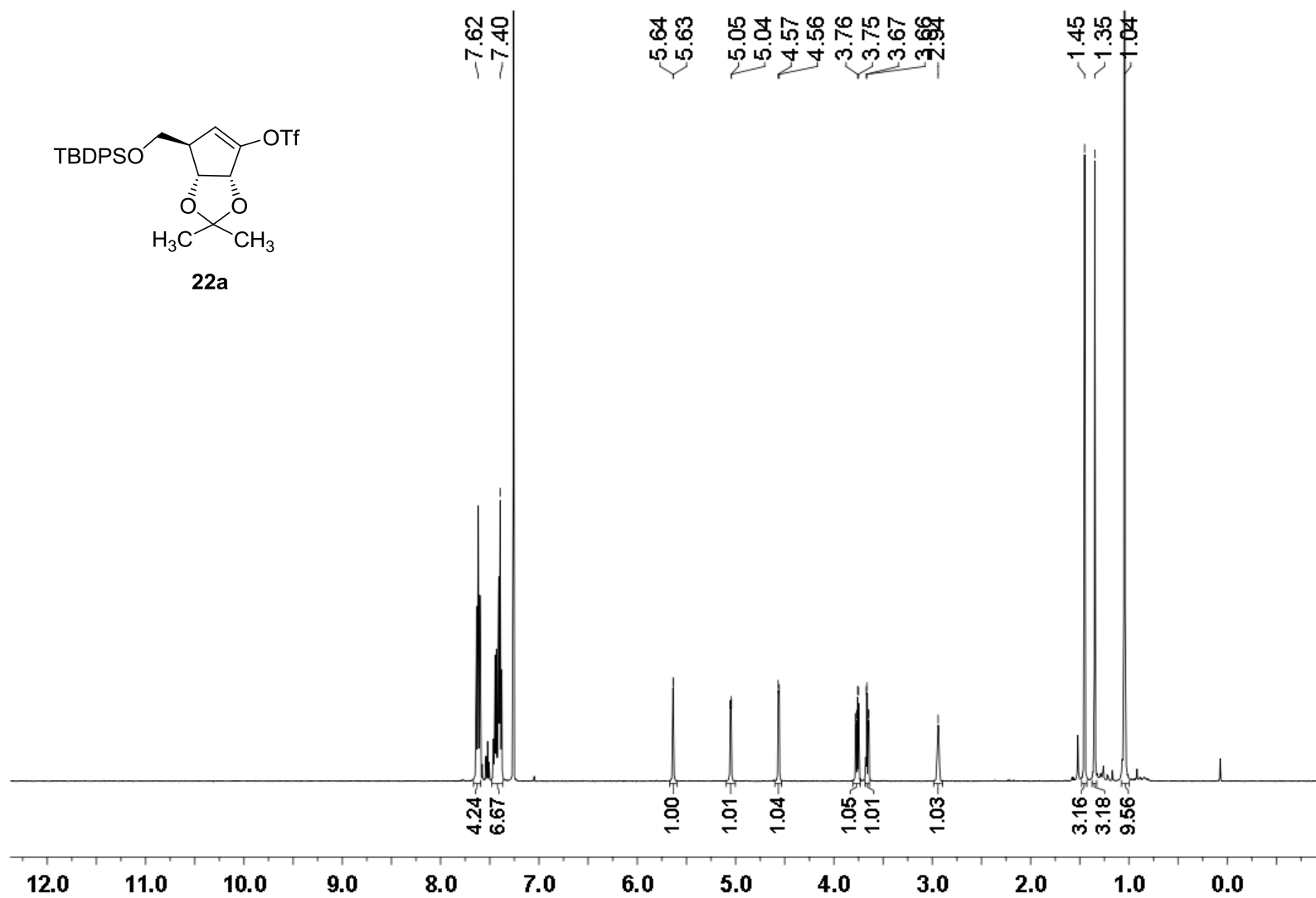
$^{13}\text{C}$  NMR (126 MHz) spectrum of **S-12** in  $\text{CDCl}_3$



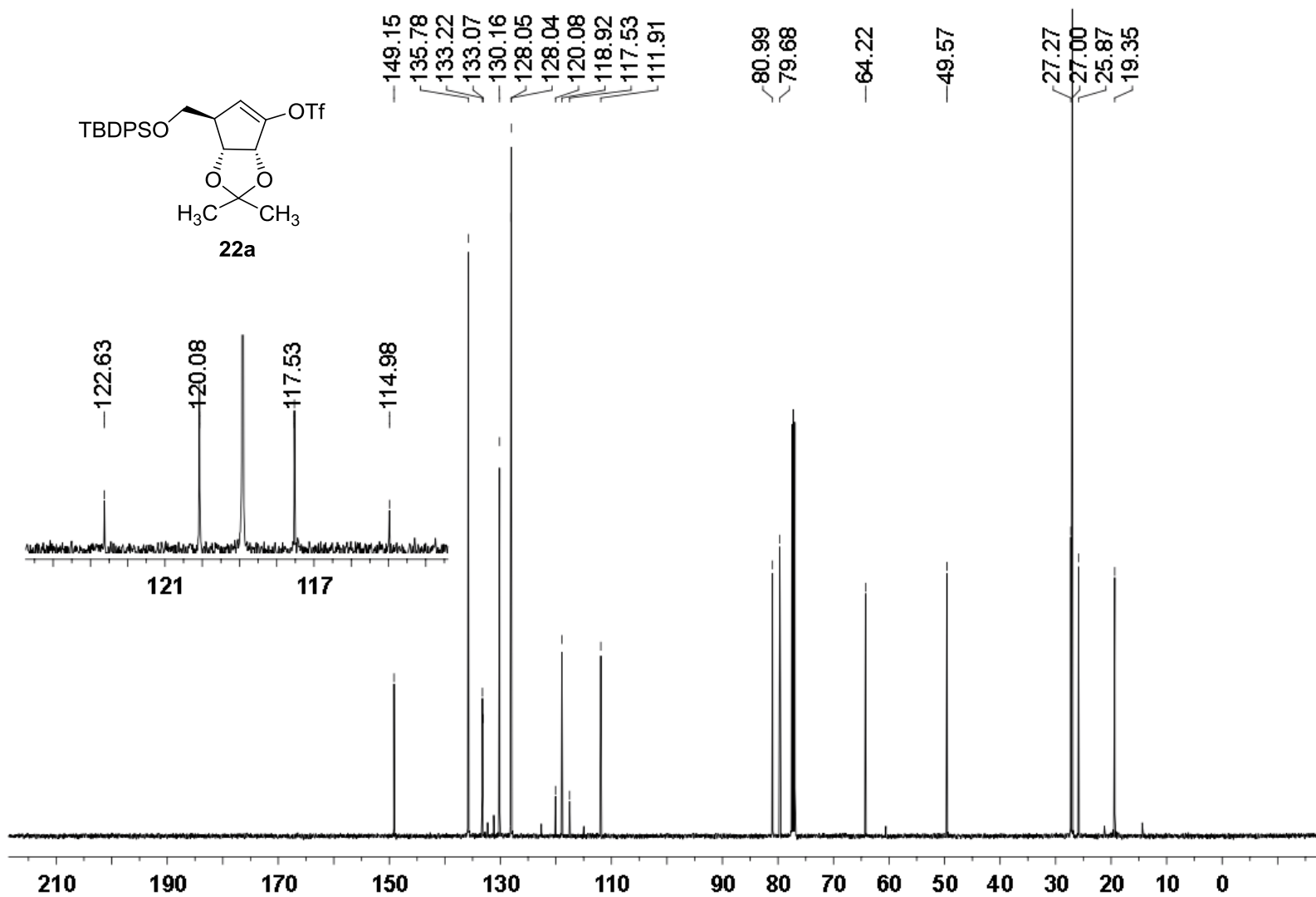
<sup>1</sup>H NMR (500 MHz) spectrum of **S-13** in DMSO-*d*<sub>6</sub>



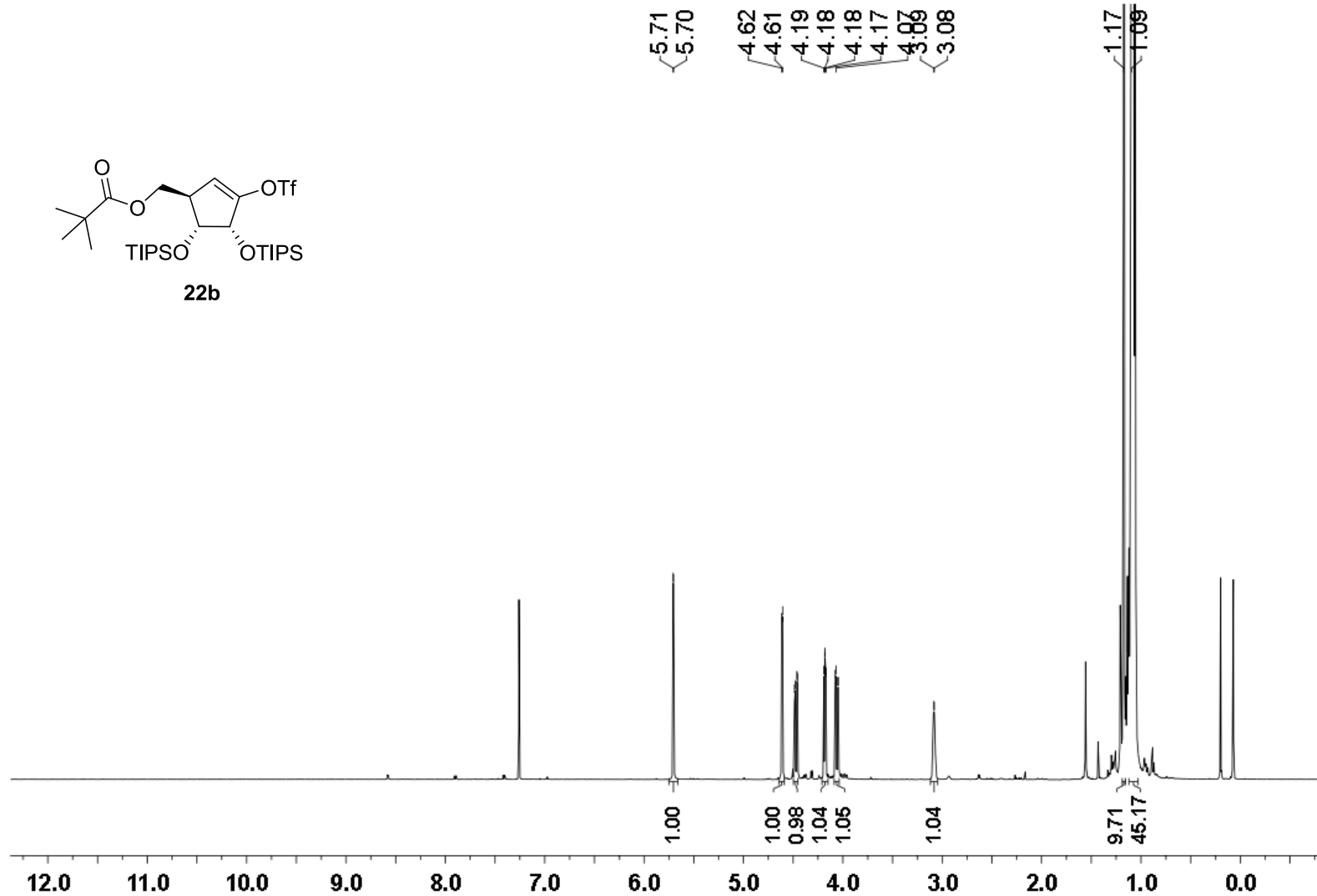
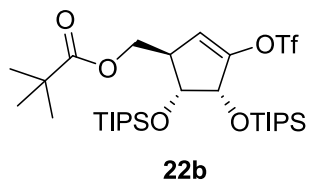
$^{13}\text{C}$  (126 MHz) NMR spectra of S-13 in  $\text{DMSO-}d_6$



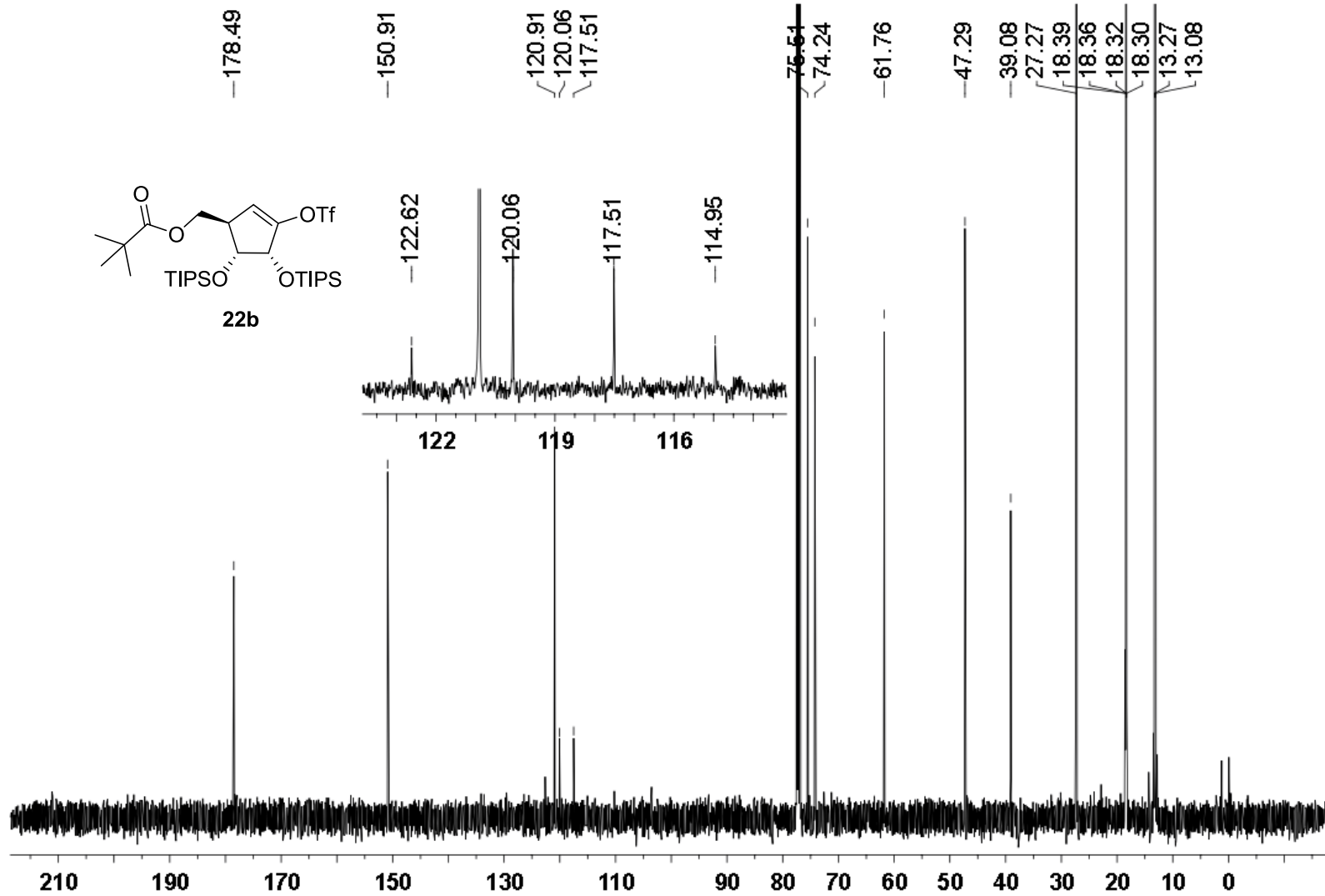
<sup>1</sup>H NMR (500 MHz) spectrum of **22a** in CDCl<sub>3</sub>



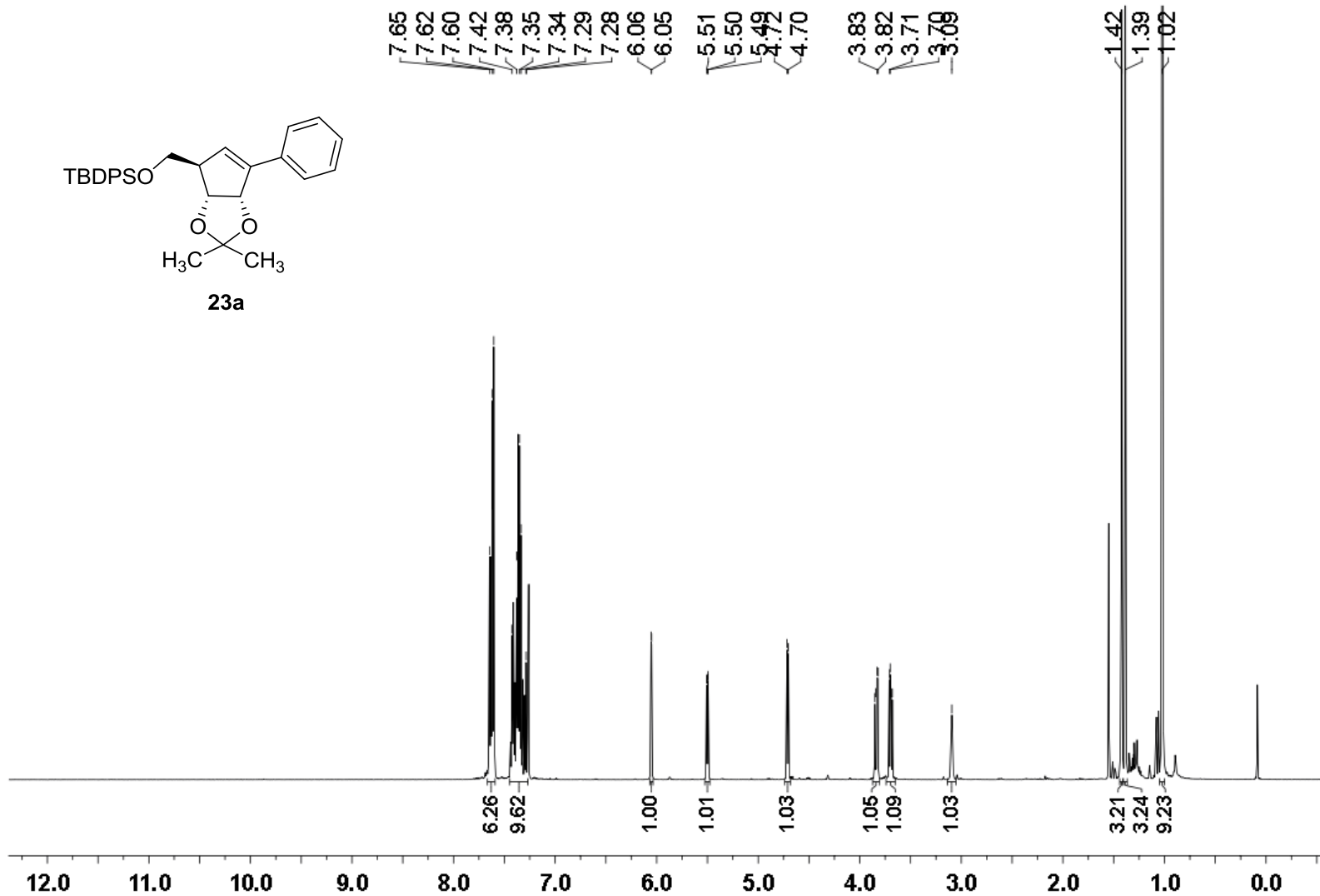
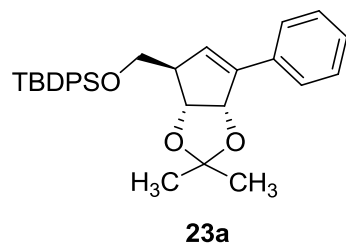
$^{13}\text{C}$  NMR (126 MHz) spectrum of **22a** in  $\text{CDCl}_3$



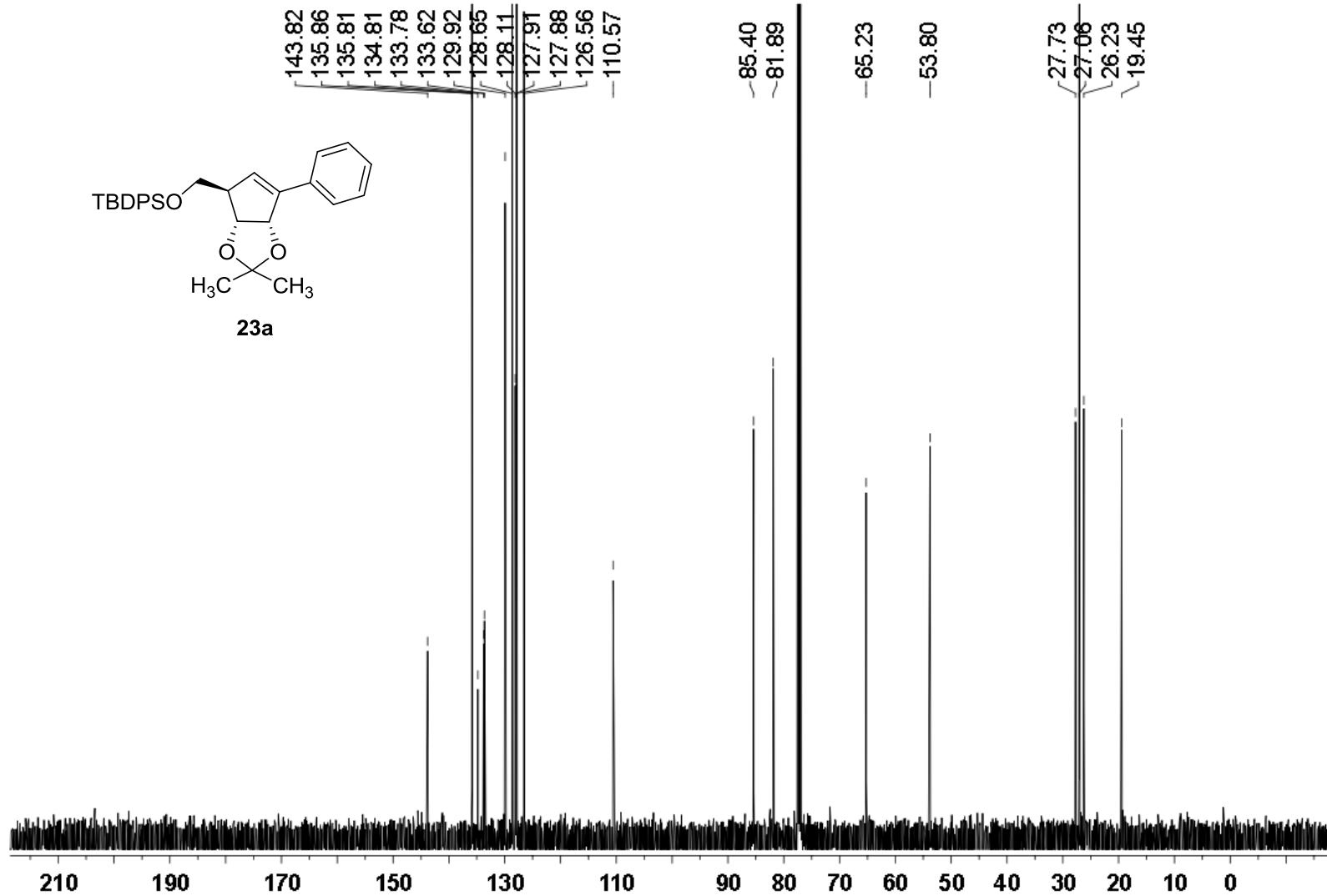
$^1\text{H}$  NMR (500 MHz) spectrum of **22b** in  $\text{CDCl}_3$



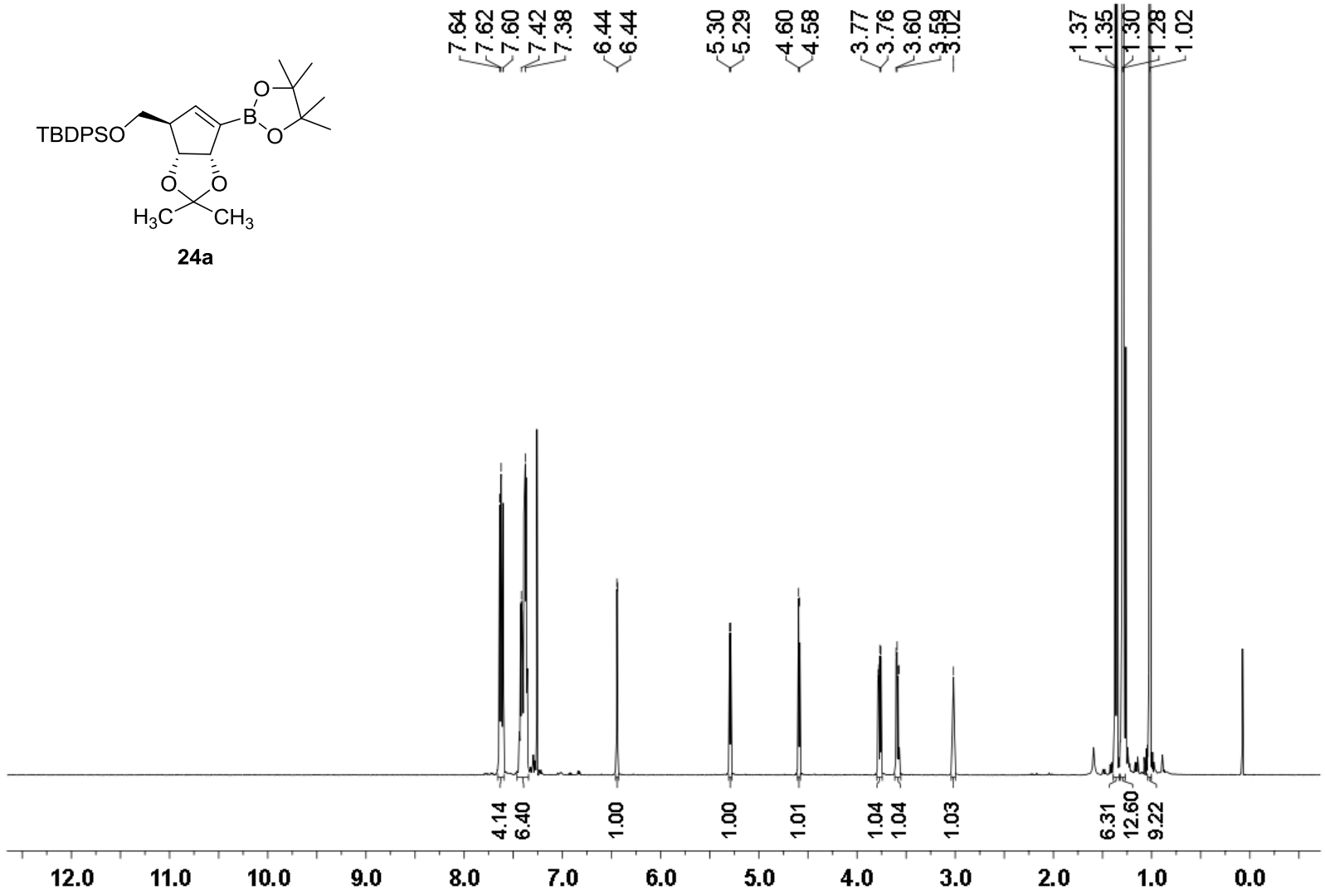
$^{13}\text{C}$  NMR (126 MHz) spectrum of **22b** in  $\text{CDCl}_3$



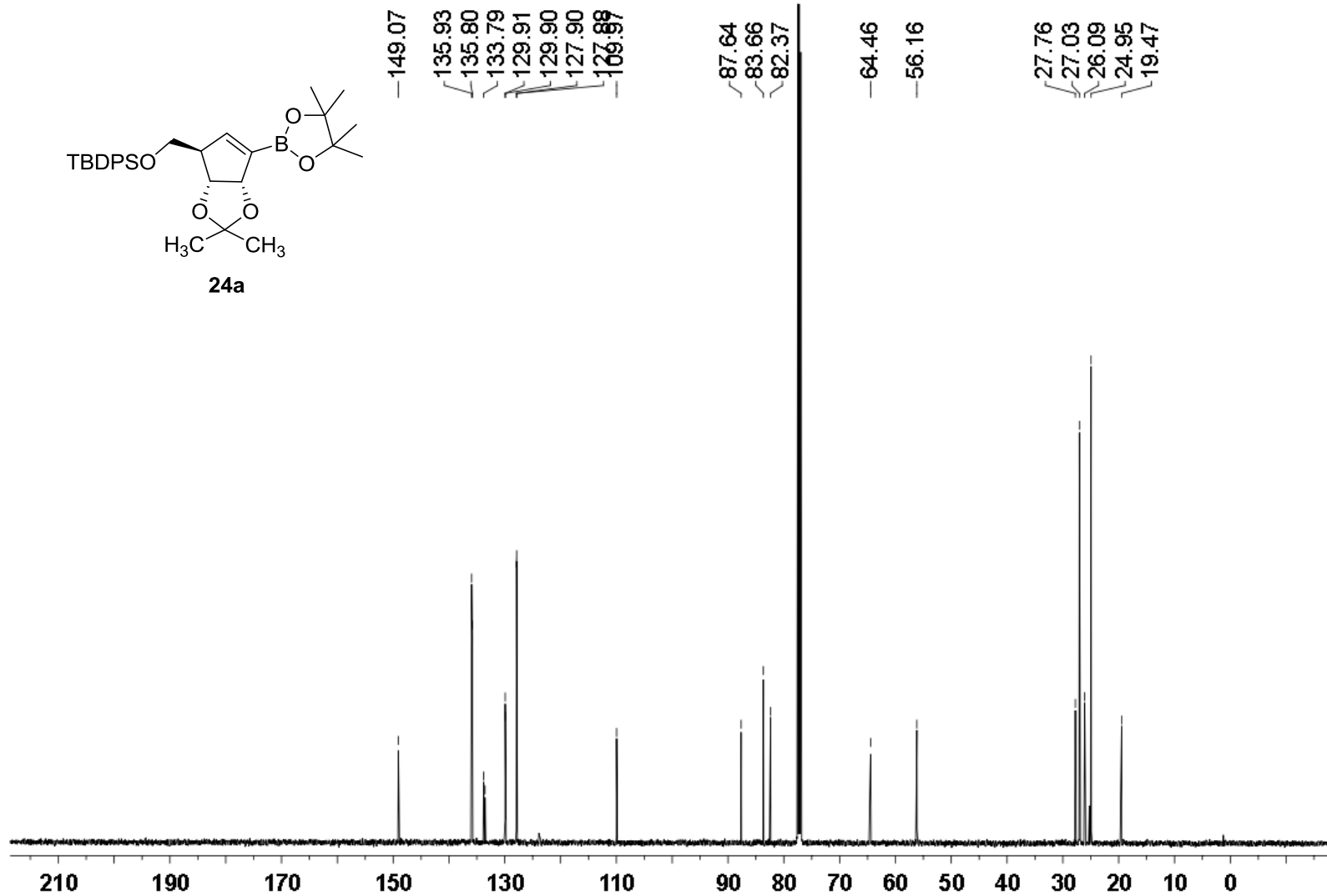
$^1\text{H}$  NMR (500 MHz) spectrum of **23a** in  $\text{CDCl}_3$



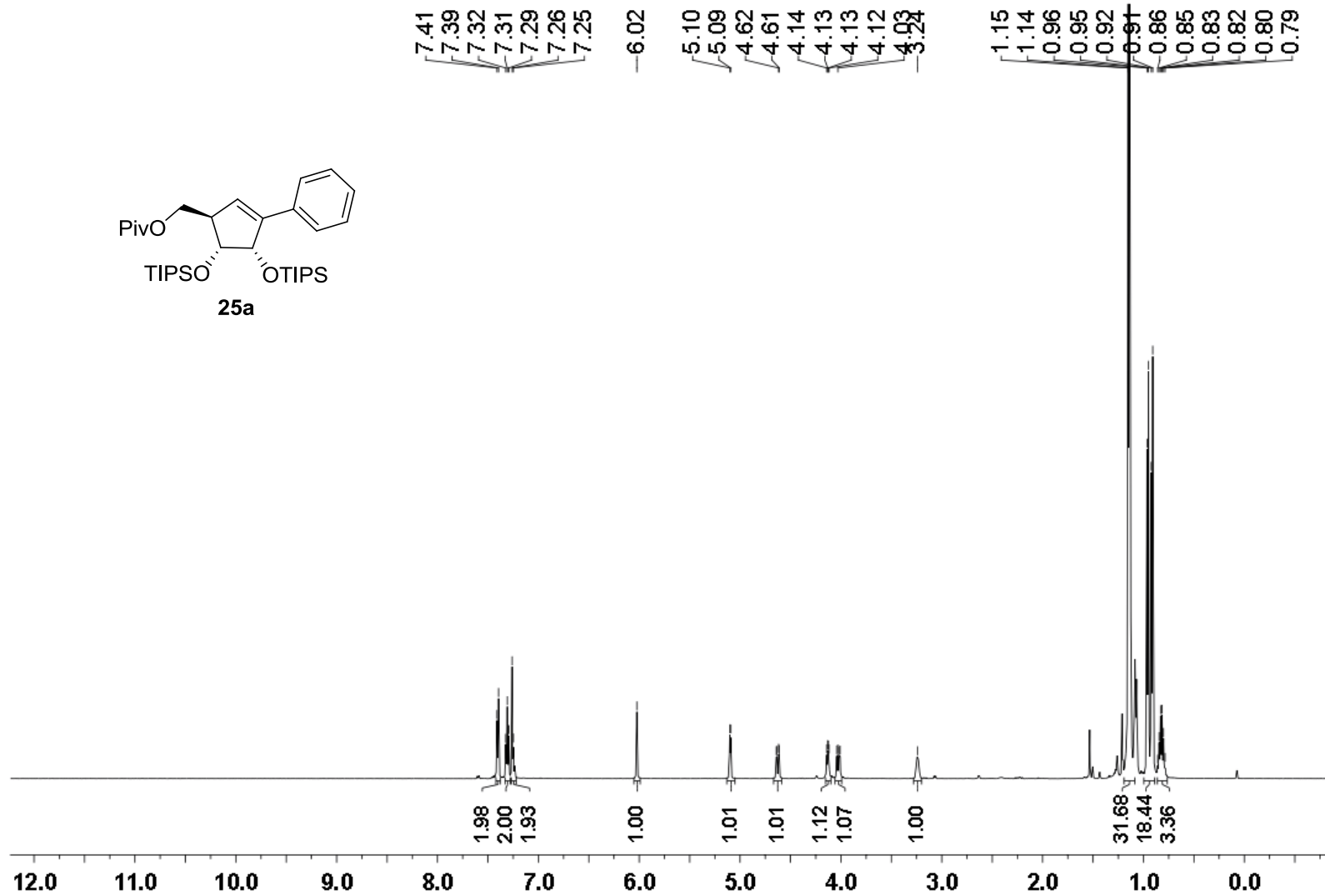
$^{13}\text{C}$  NMR (126 MHz) spectrum of **23a** in  $\text{CDCl}_3$



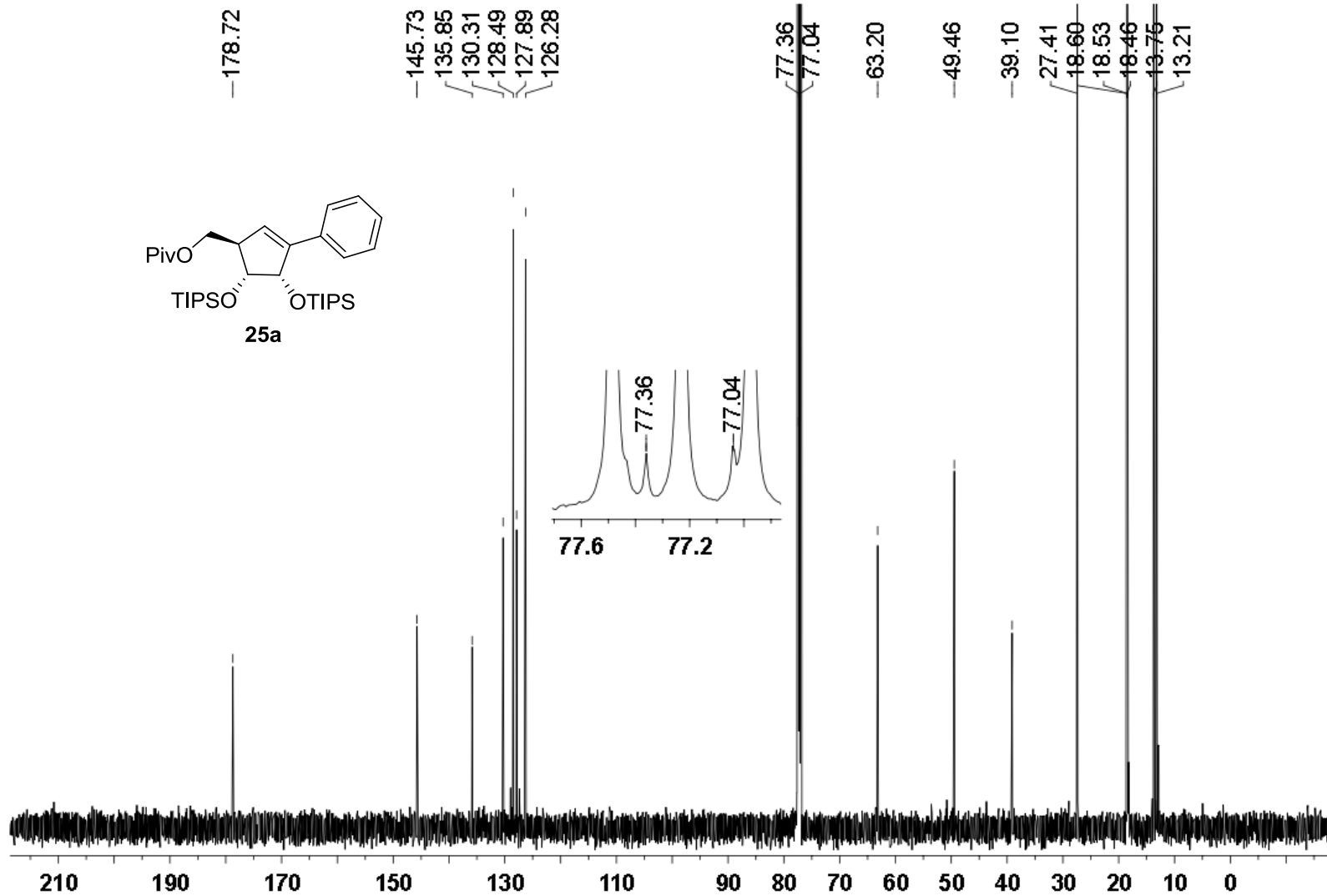
$^1\text{H}$  NMR (500 MHz) spectrum of **24a** in  $\text{CDCl}_3$



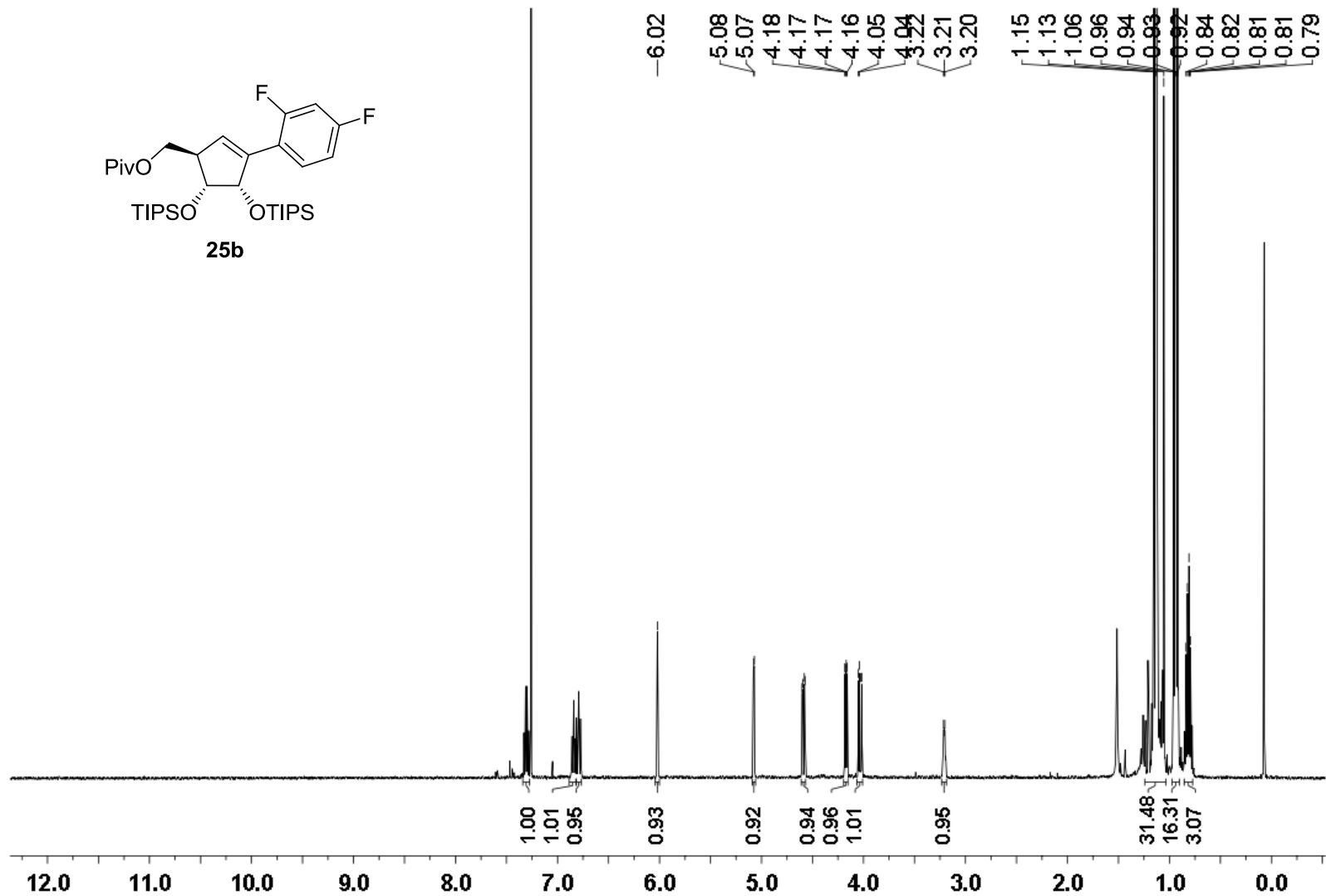
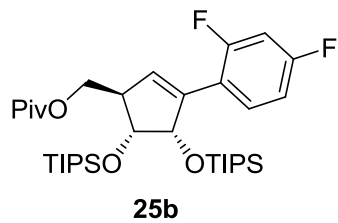
$^{13}\text{C}$  NMR (126 MHz) spectrum of **24a** in  $\text{CDCl}_3$



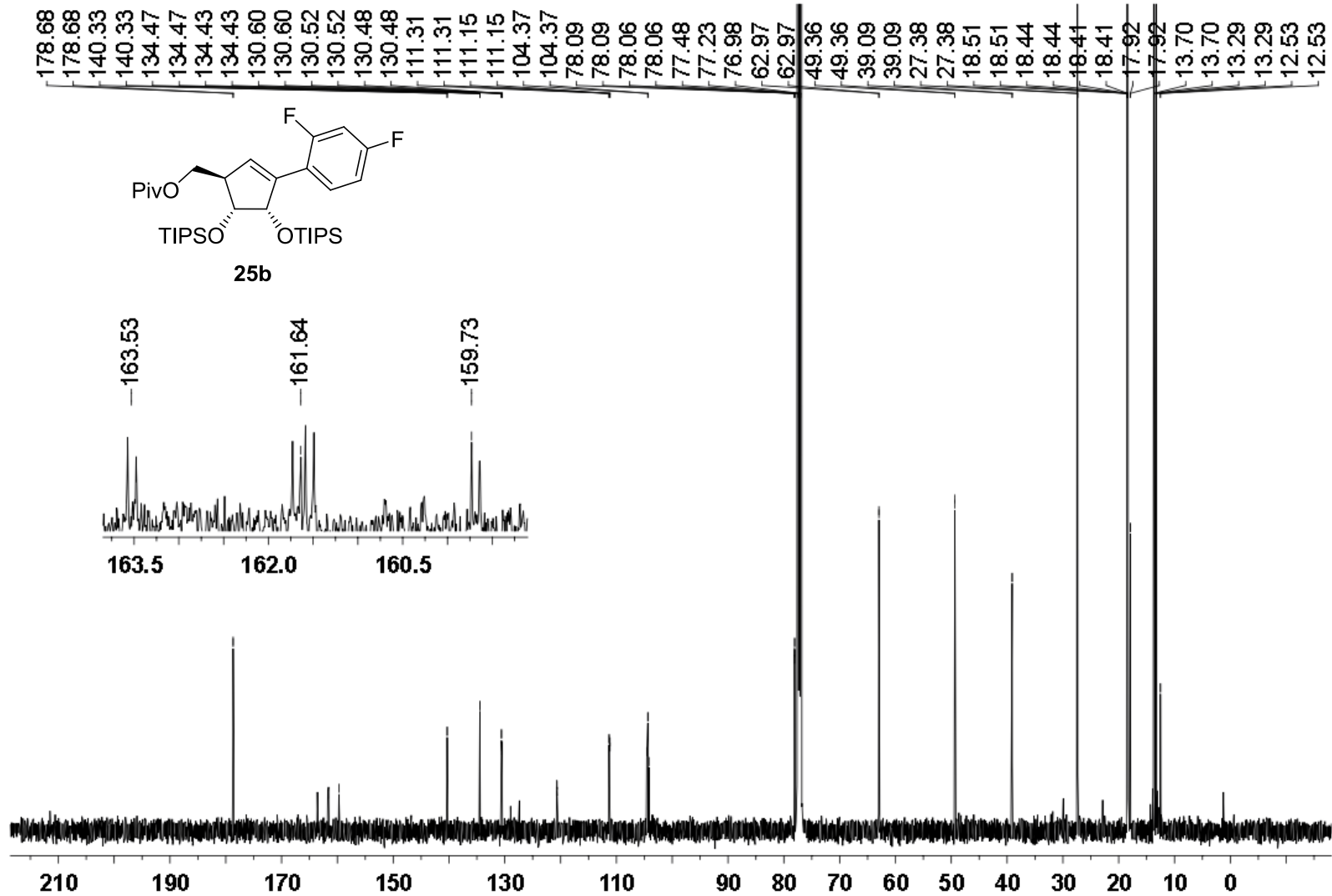
<sup>1</sup>H NMR (500 MHz) spectrum of **25a** in CDCl<sub>3</sub>



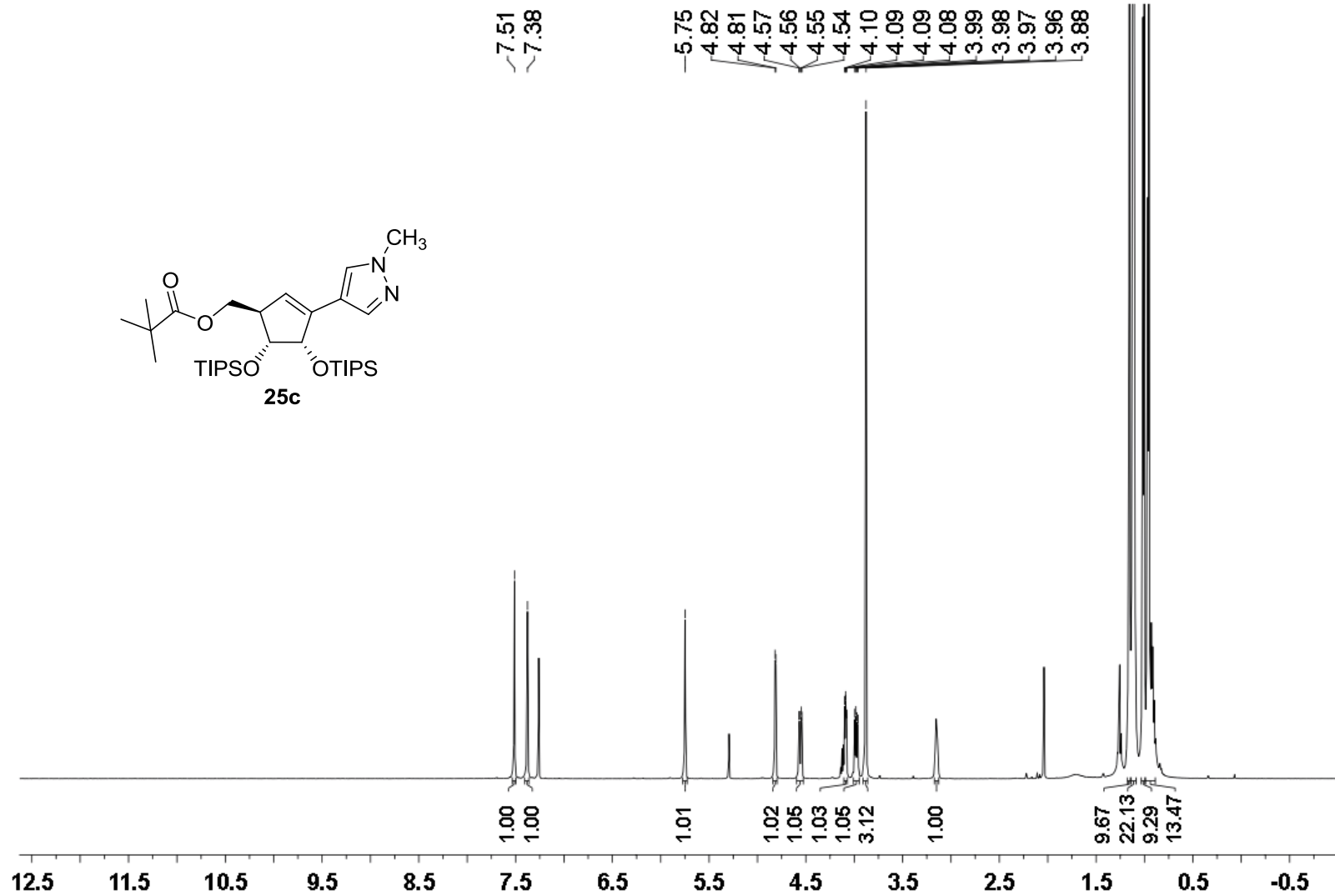
$^{13}\text{C}$  NMR (126 MHz) spectrum of **25a** in  $\text{CDCl}_3$



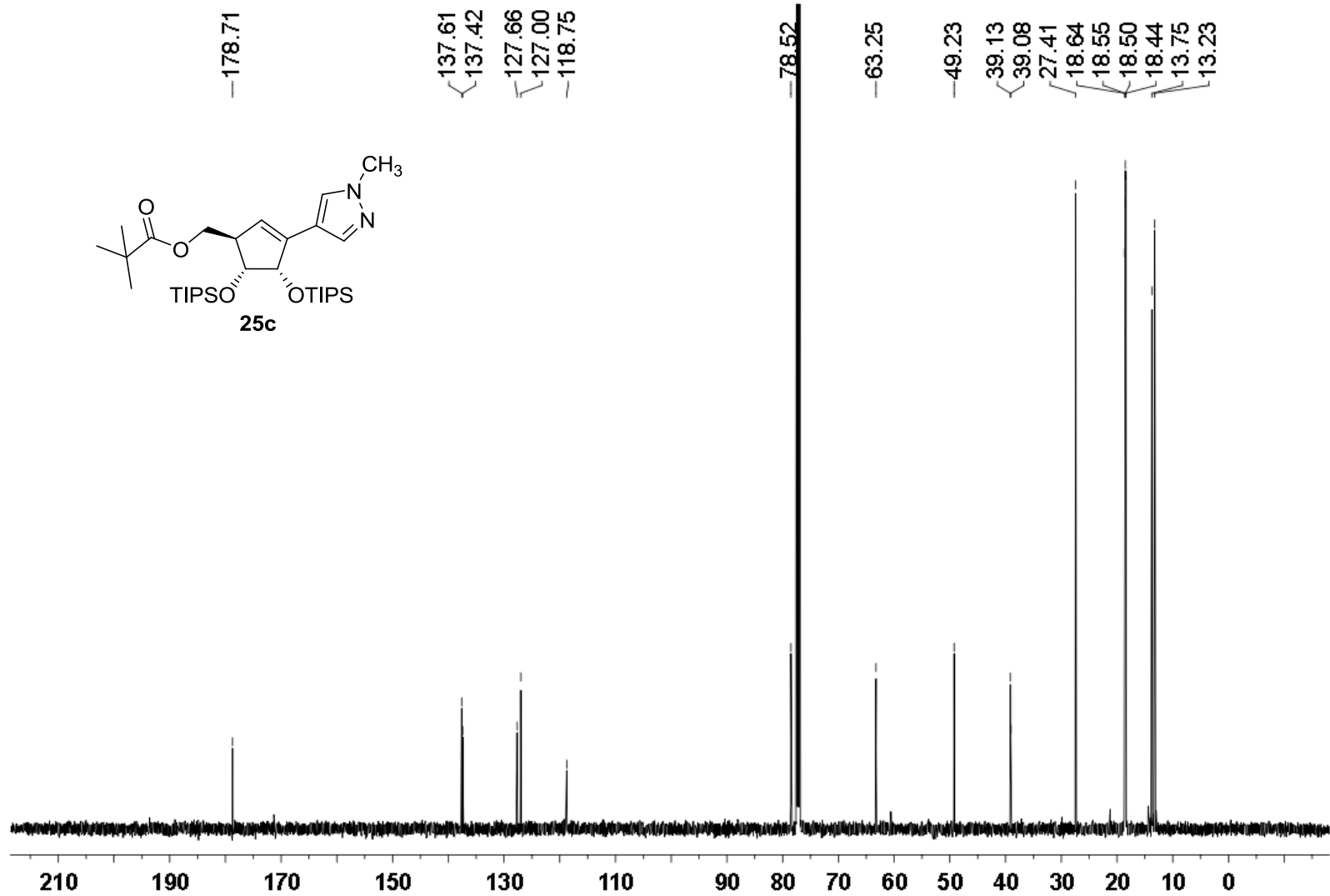
$^1\text{H}$  NMR (500 MHz) spectrum of **25b** in  $\text{CDCl}_3$



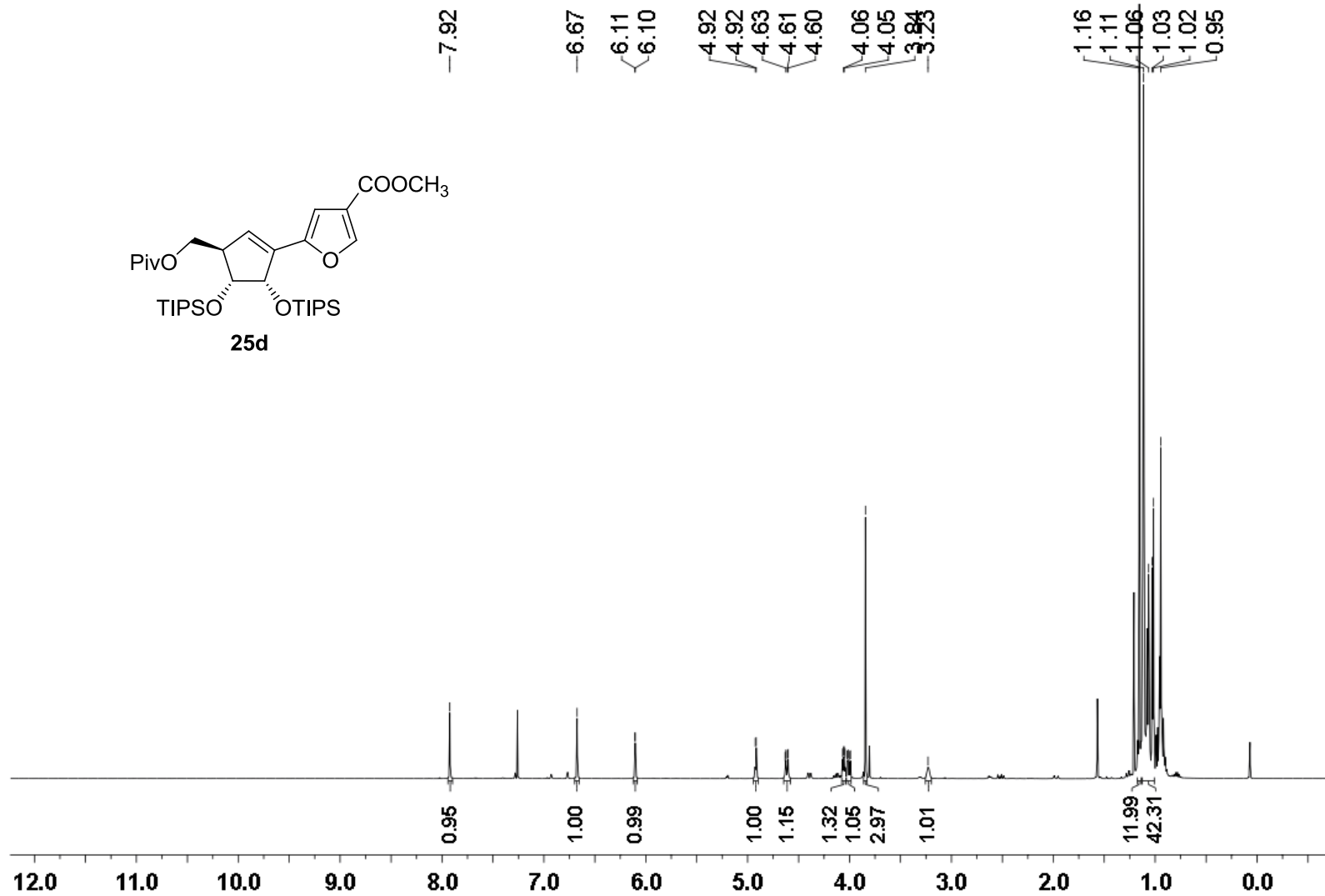
<sup>13</sup>C NMR (126 MHz) spectrum of **25b** in CDCl<sub>3</sub>



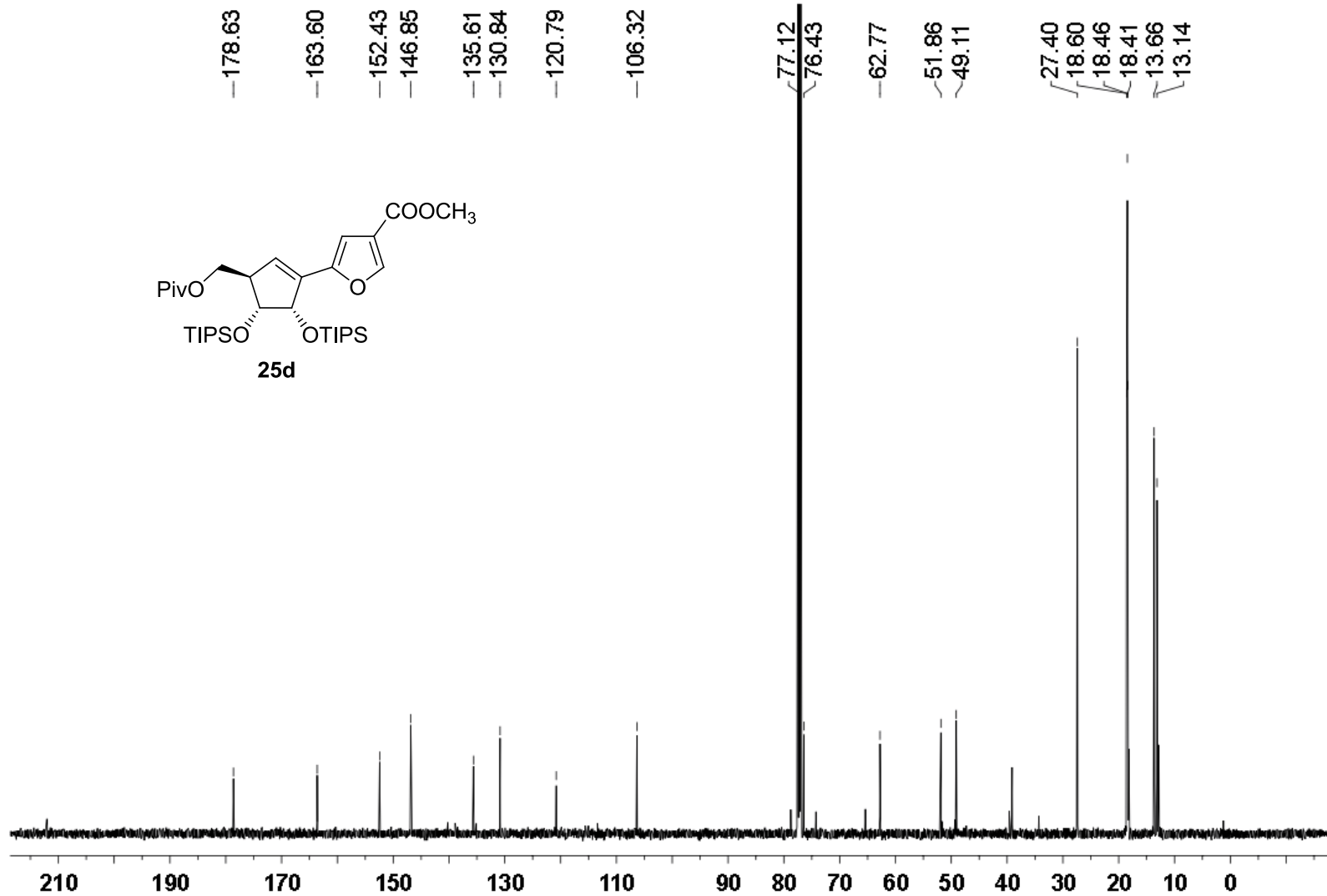
$^1\text{H}$  NMR (500 MHz) spectrum of **25c** in  $\text{CDCl}_3$



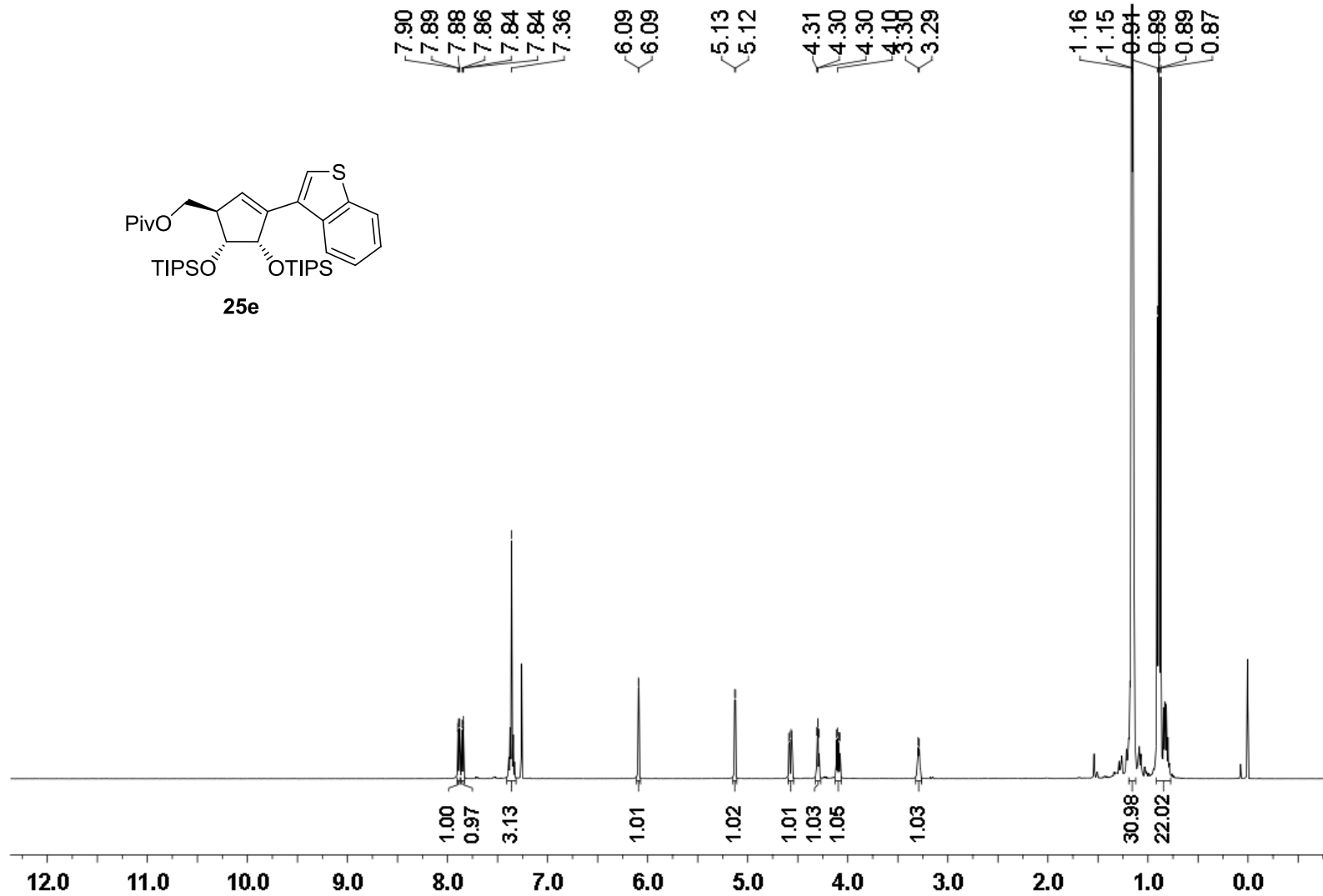
<sup>13</sup>C NMR (126 MHz) spectrum of **25c** in CDCl<sub>3</sub>



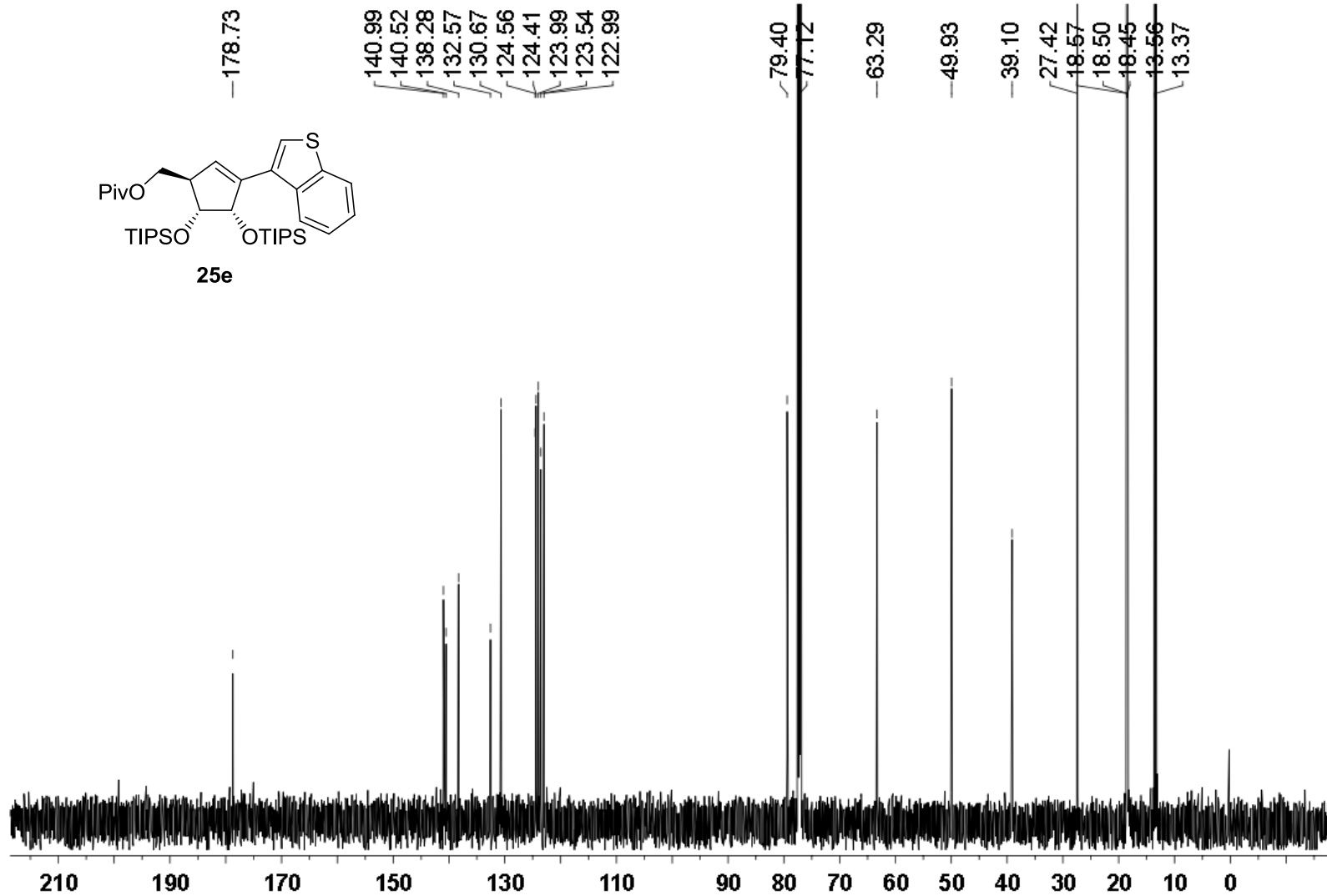
<sup>1</sup>H NMR (500 MHz) spectrum of **25d** in CDCl<sub>3</sub>



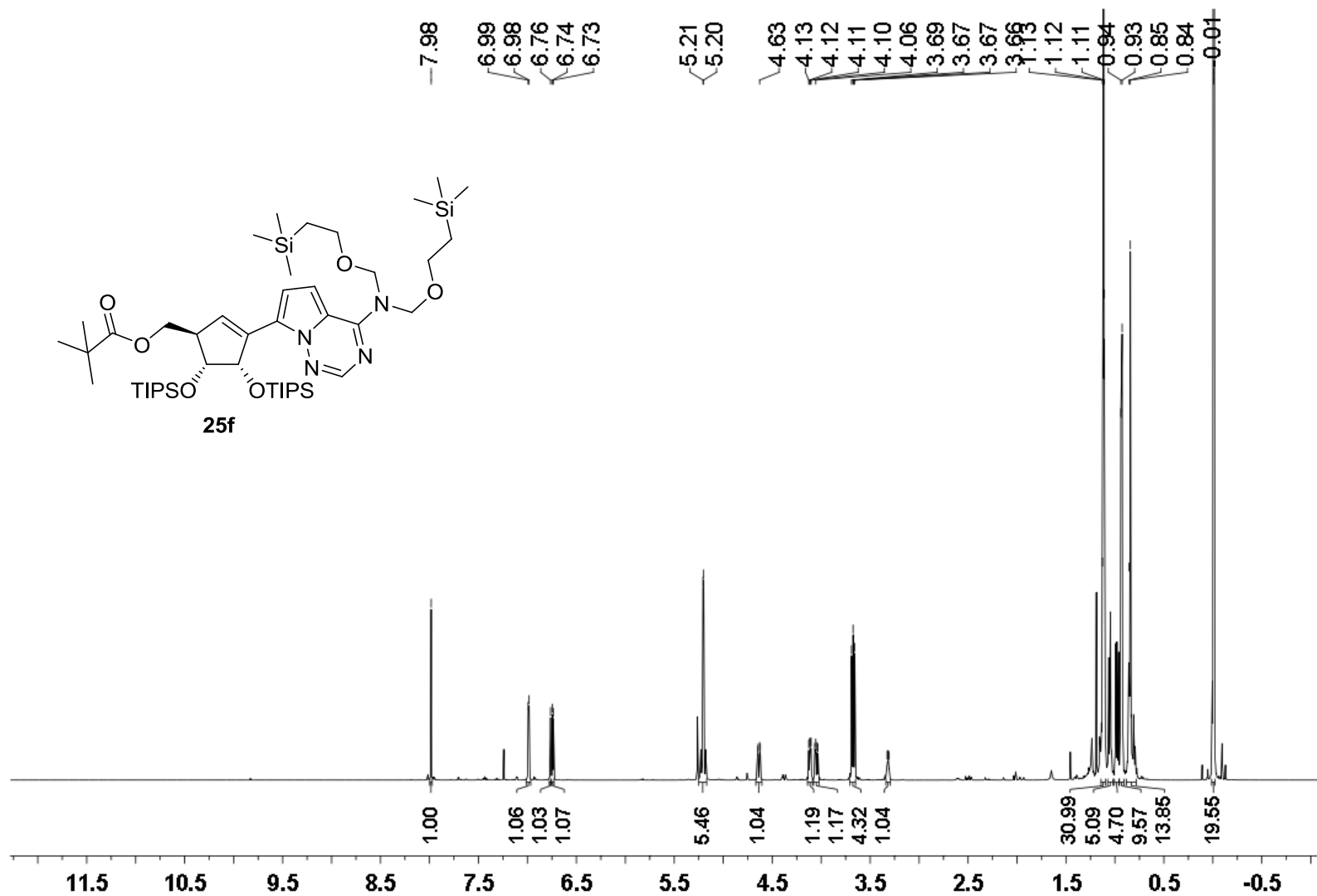
<sup>13</sup>C NMR (126 MHz) spectrum of **25d** in CDCl<sub>3</sub>



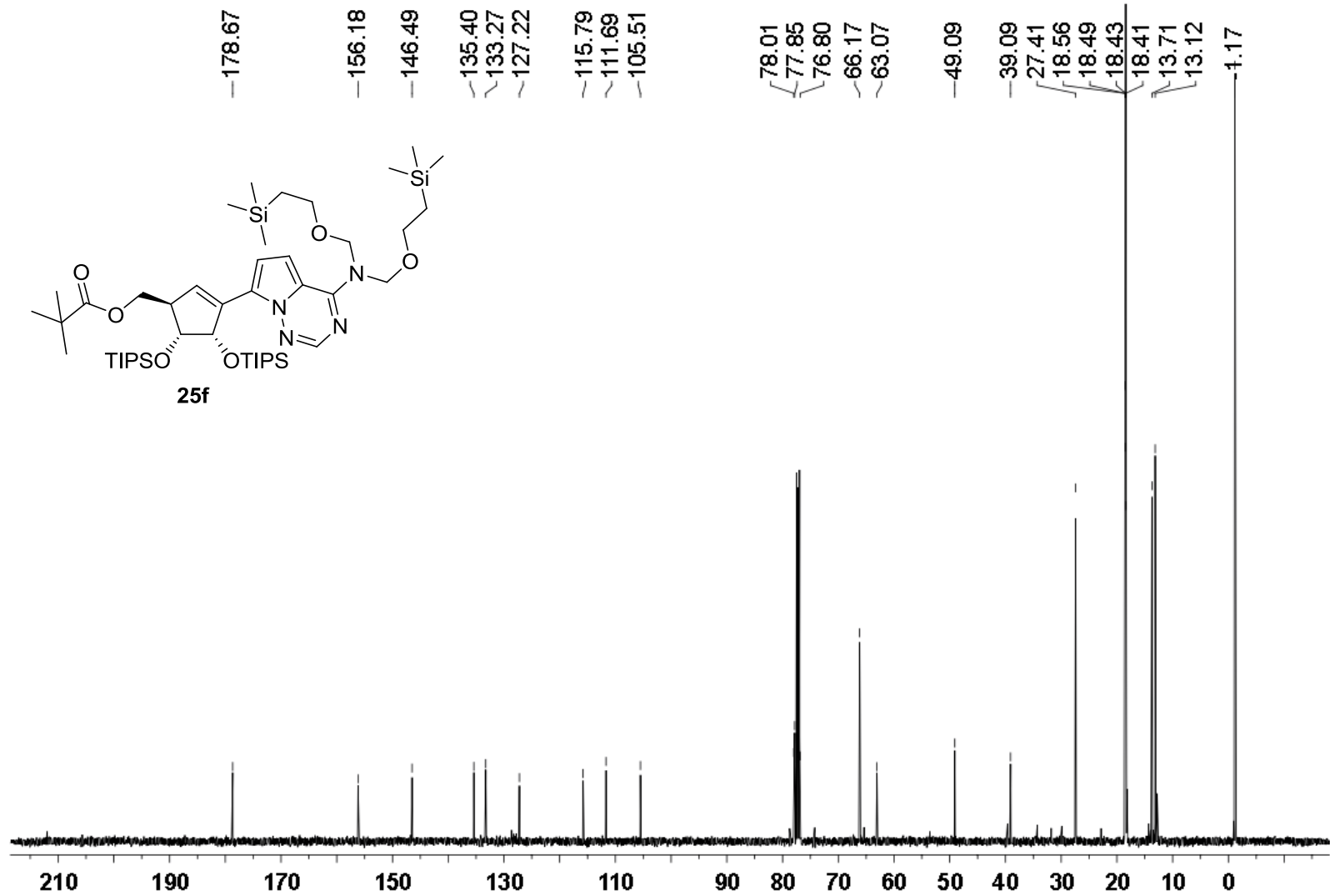
$^1\text{H}$  NMR (500 MHz) spectrum of **25e** in  $\text{CDCl}_3$



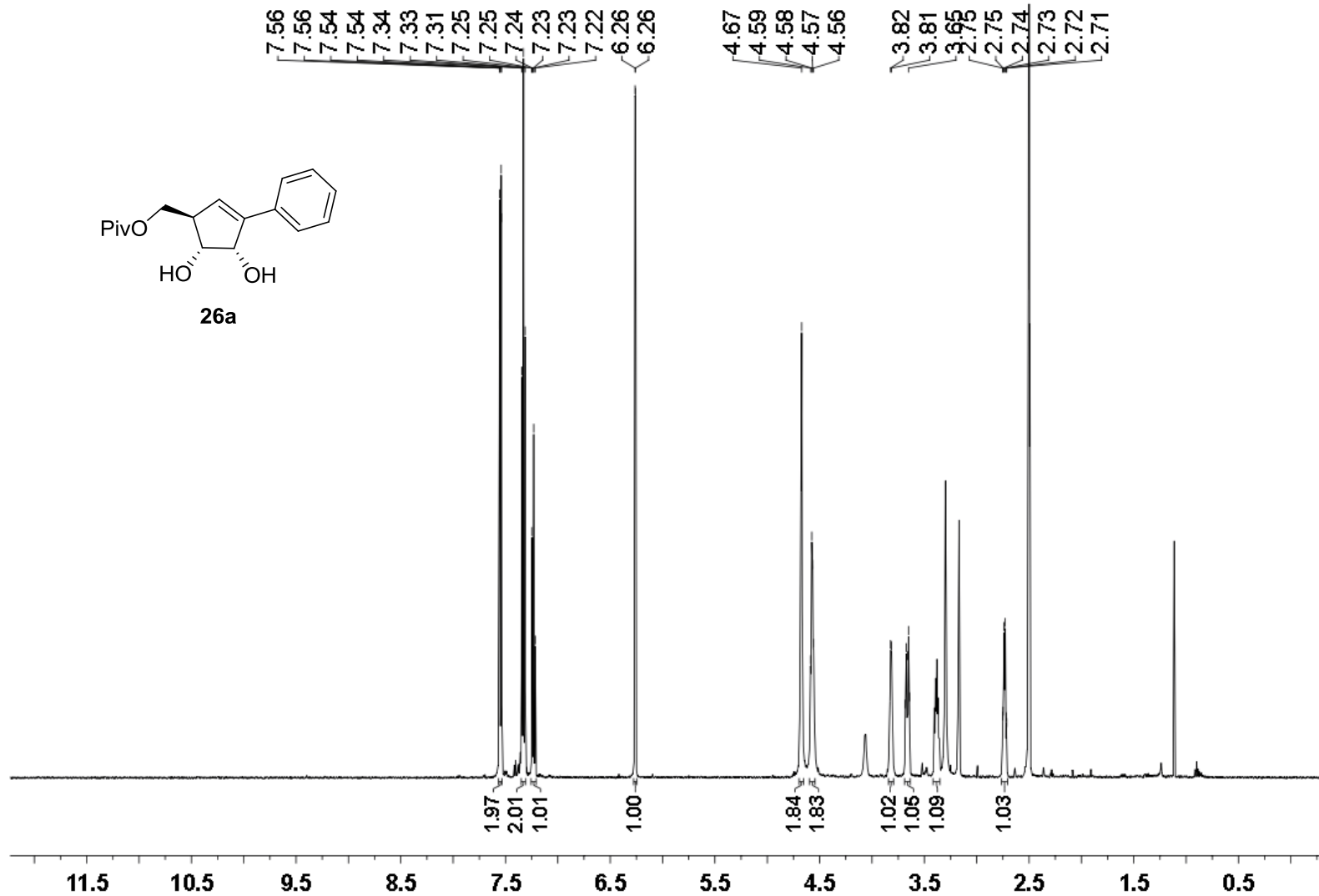
<sup>13</sup>C NMR (126 MHz) spectrum of **25e** in CDCl<sub>3</sub>

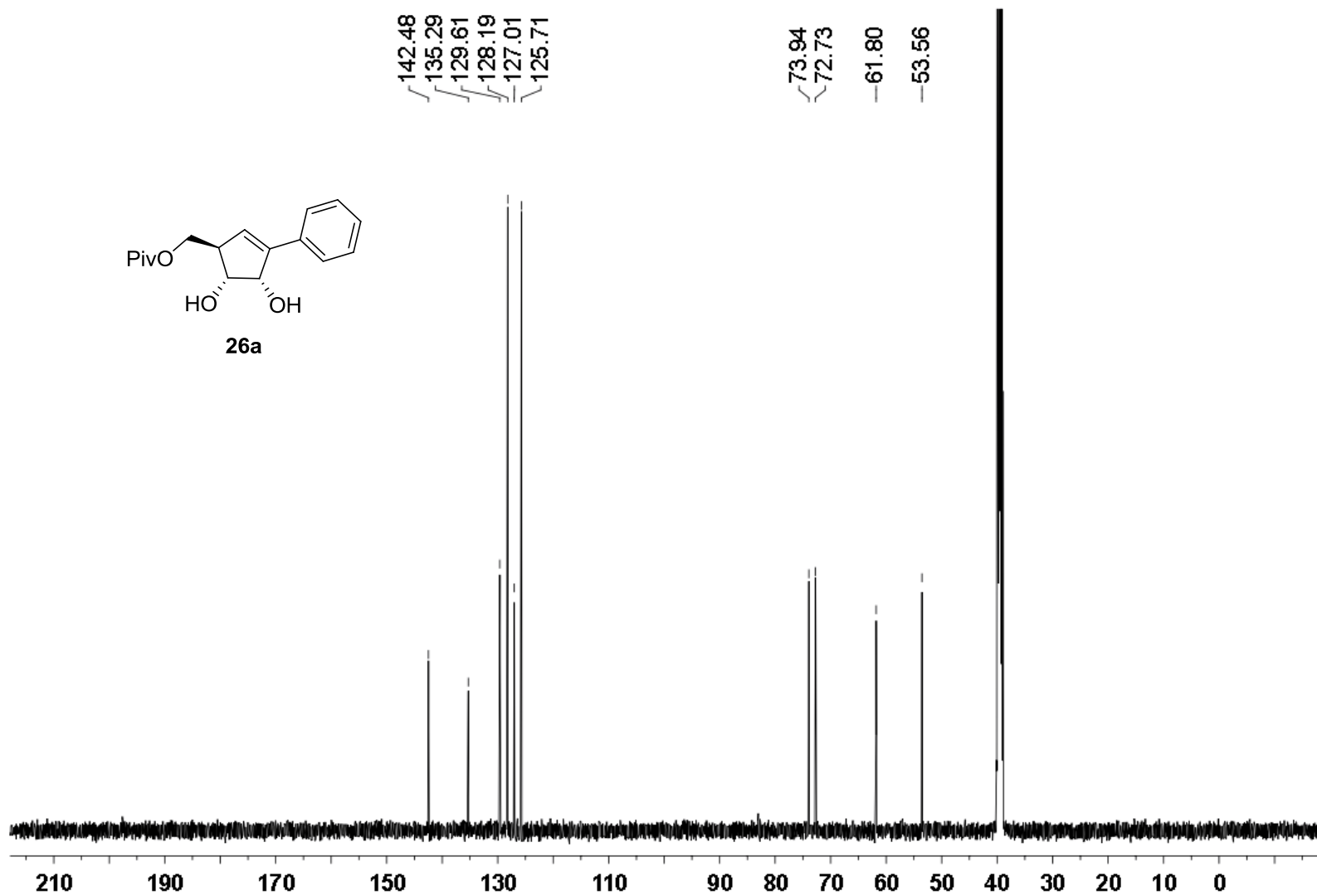


<sup>1</sup>H NMR (500 MHz) spectrum of **25f** in CDCl<sub>3</sub>

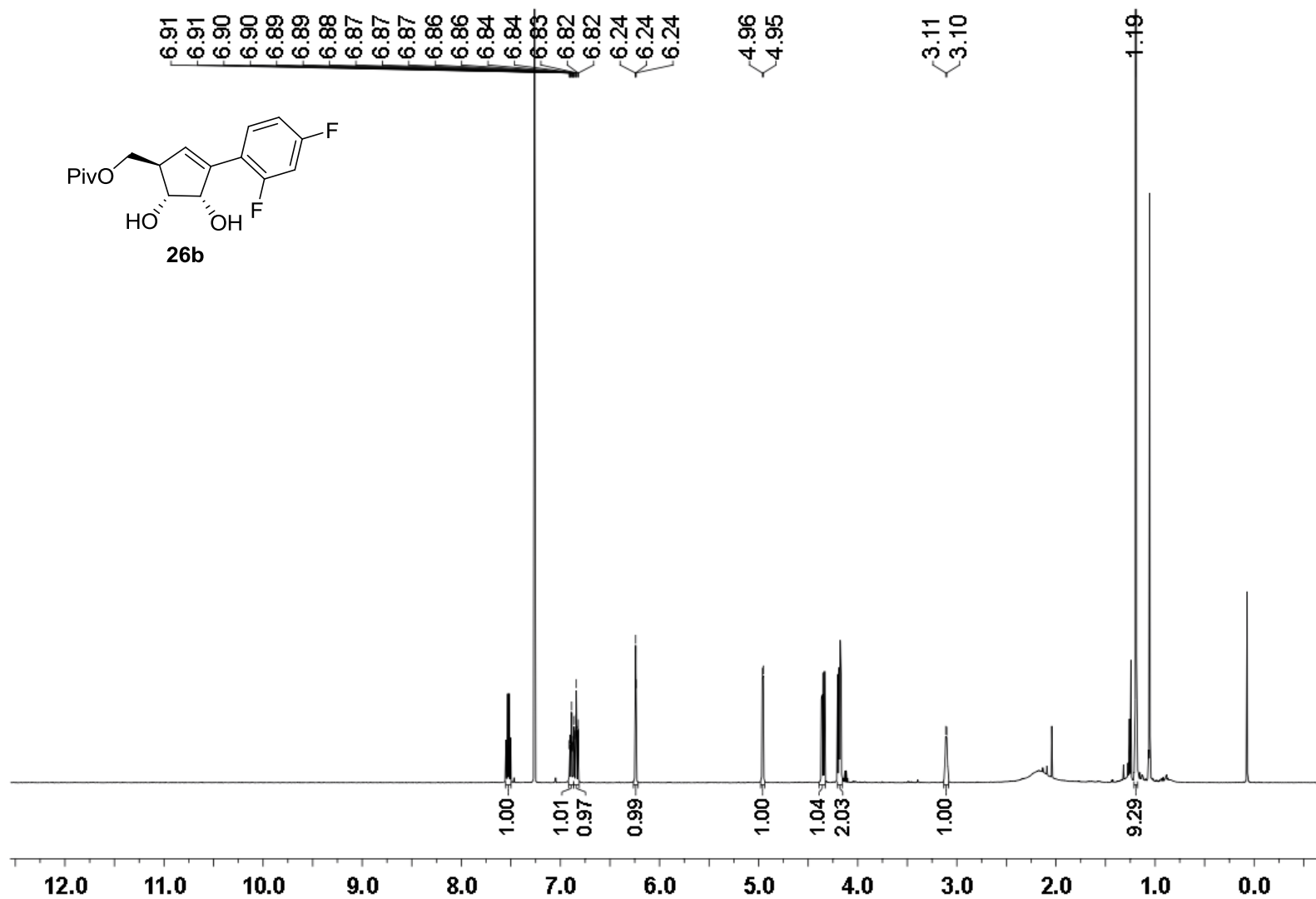


$^{13}\text{C}$  NMR (126 MHz) spectrum of **25f** in  $\text{CDCl}_3$

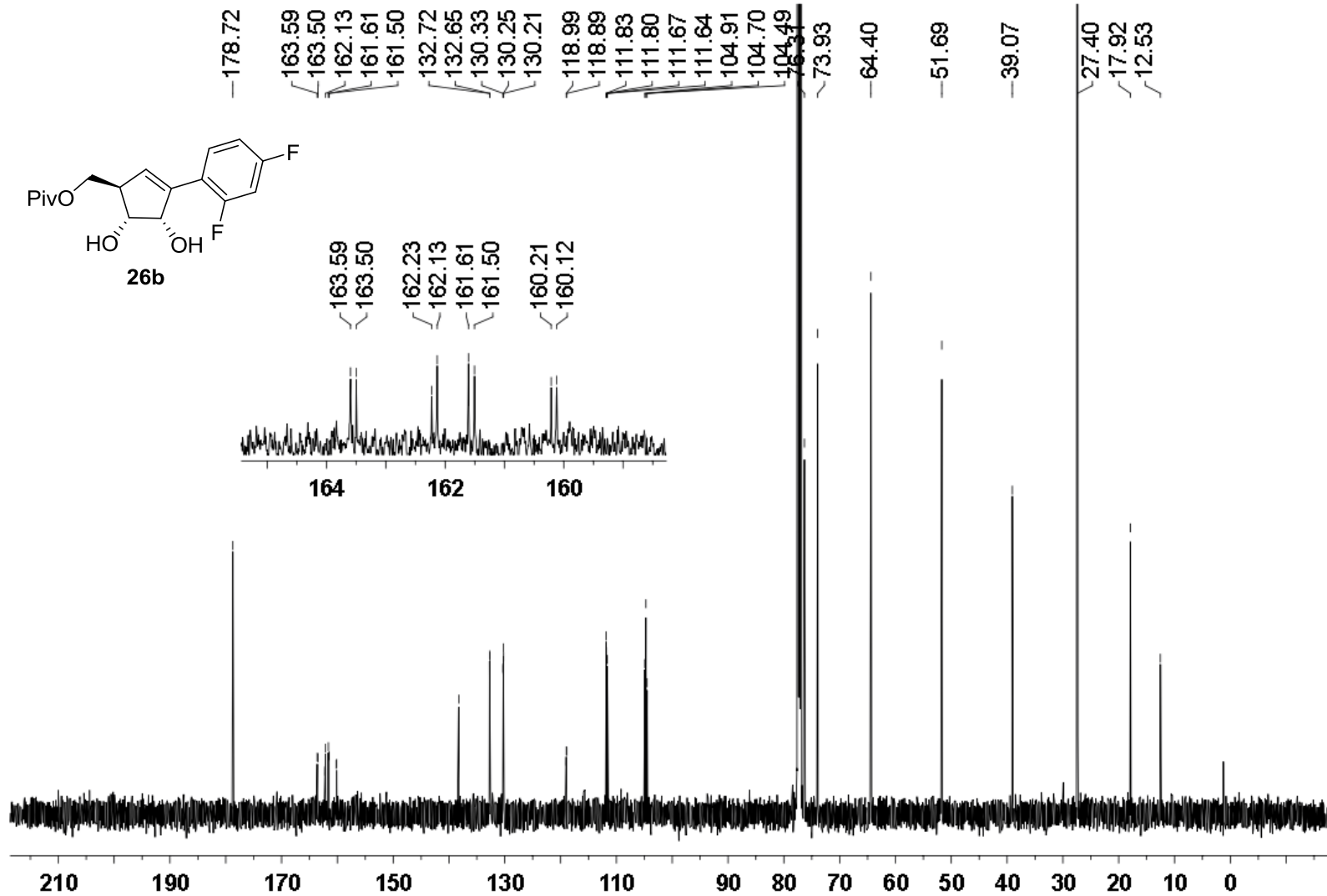




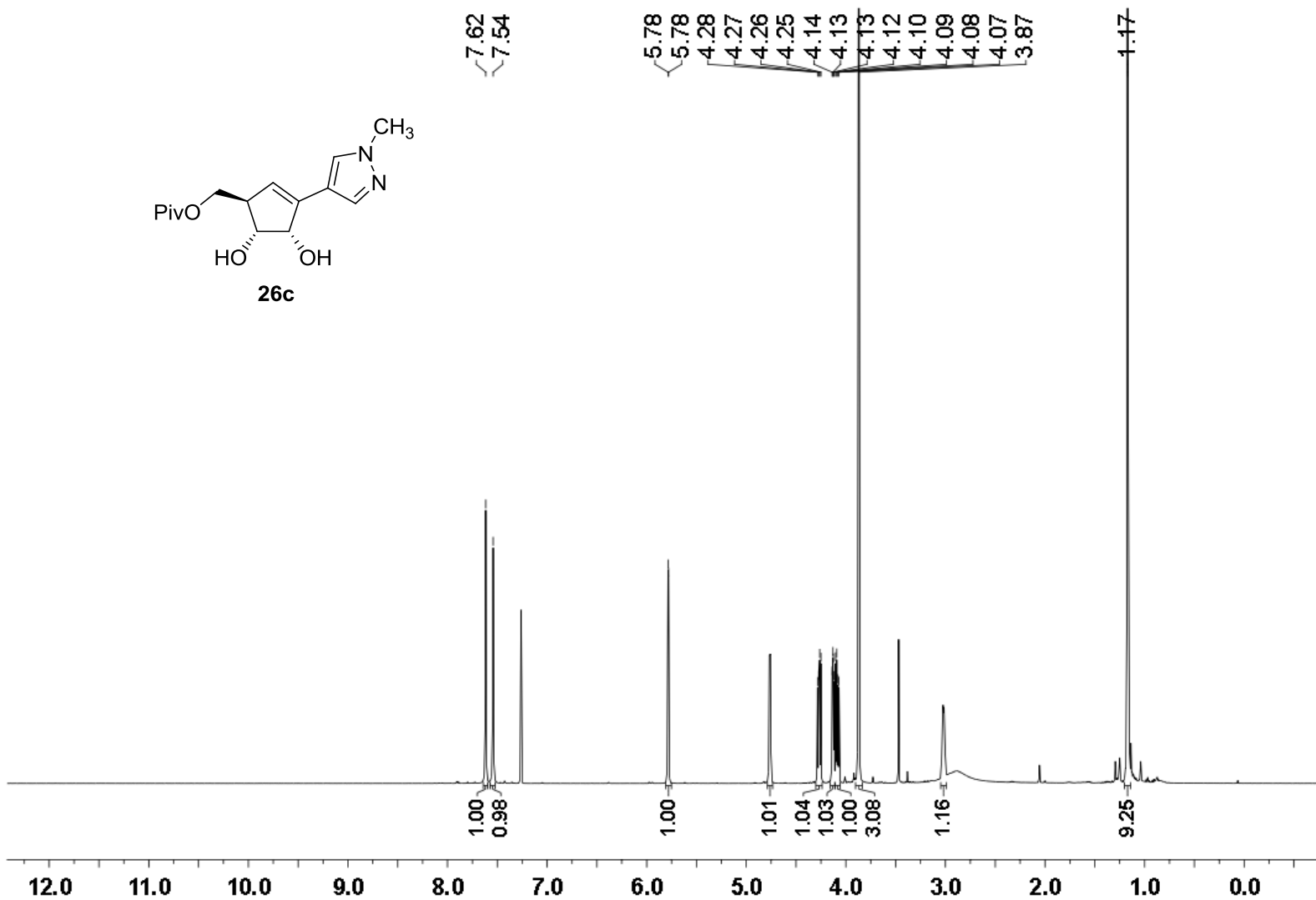
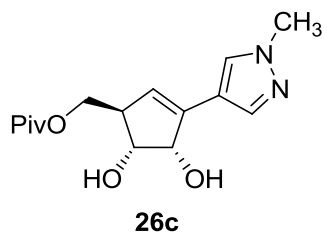
$^{13}\text{C}$  NMR (126 MHz) spectrum of **26a** in  $\text{DMSO-}d_6$



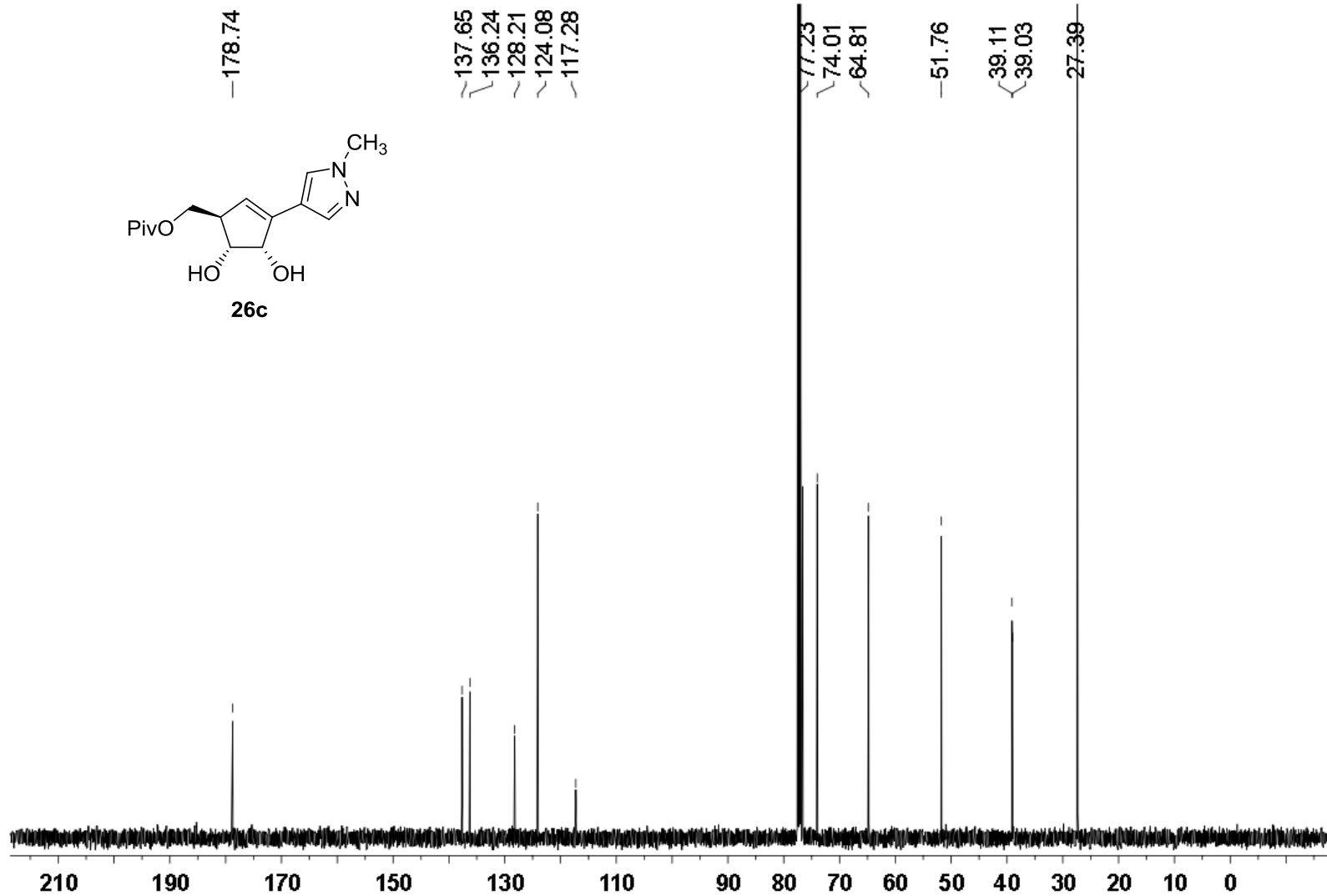
$^1\text{H}$  NMR (500 MHz) spectrum of **26b** in  $\text{CDCl}_3$



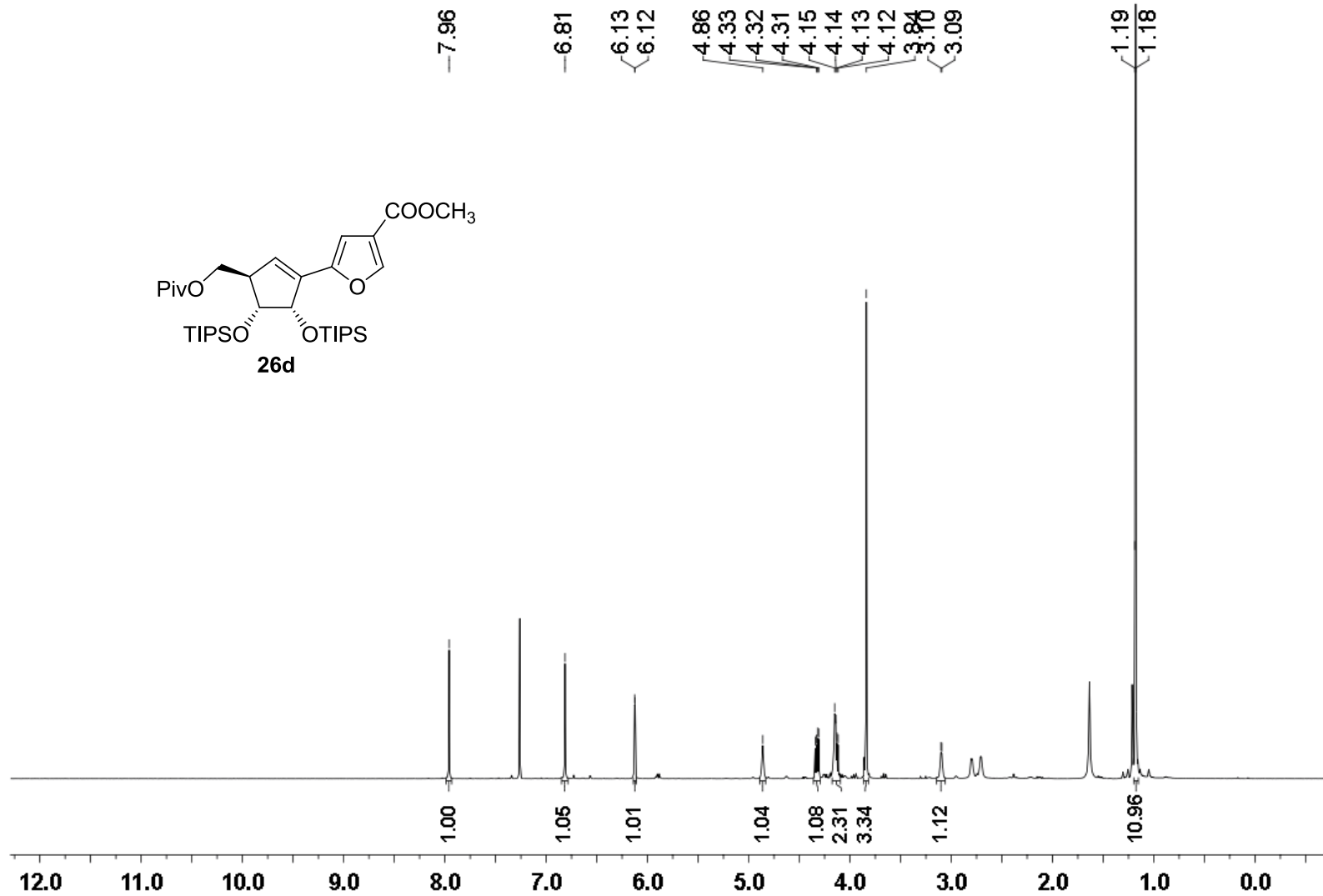
<sup>13</sup>C NMR (126 MHz) spectrum of **26b** in CDCl<sub>3</sub>



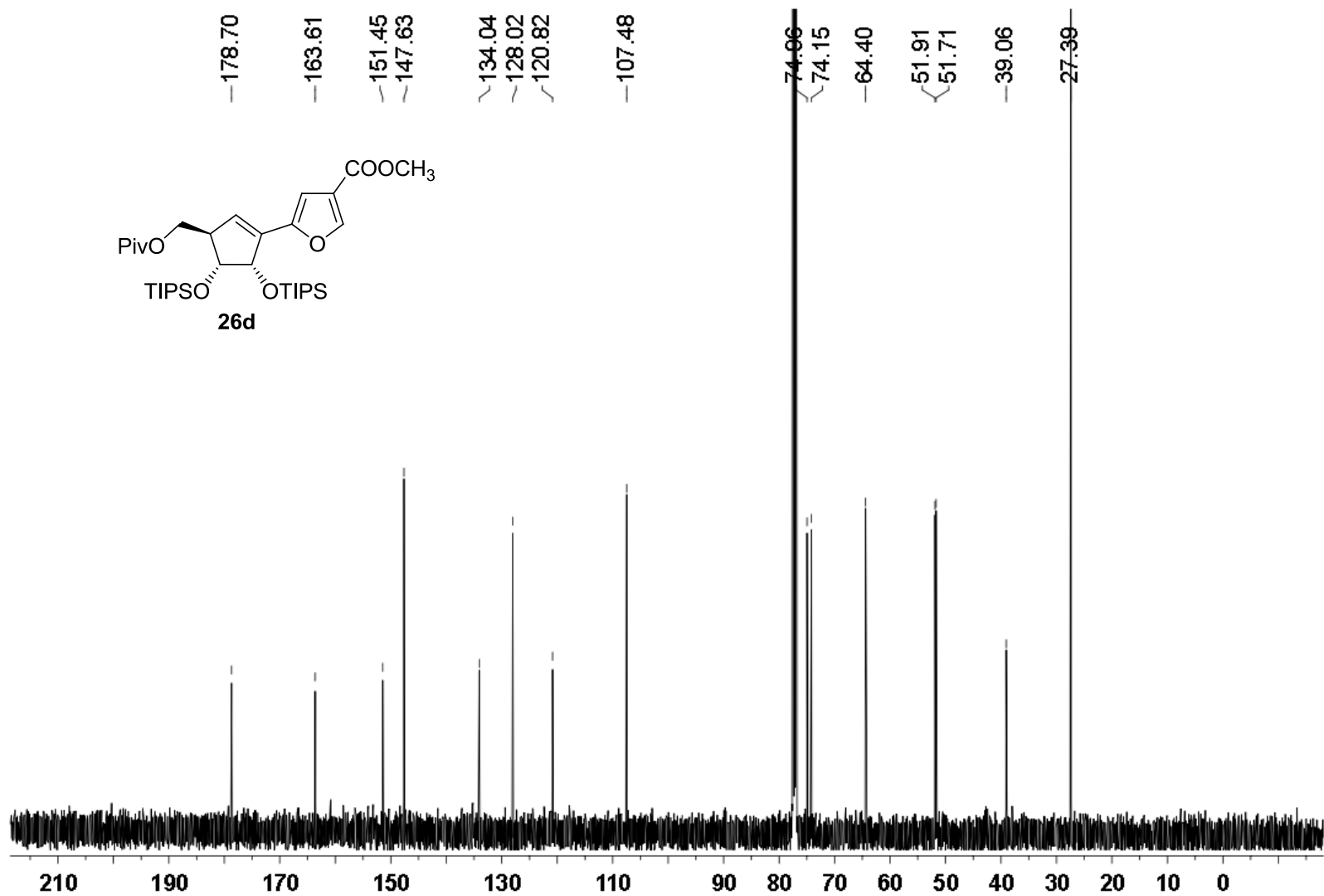
<sup>1</sup>H NMR (500 MHz) spectrum of **26c** in CDCl<sub>3</sub>



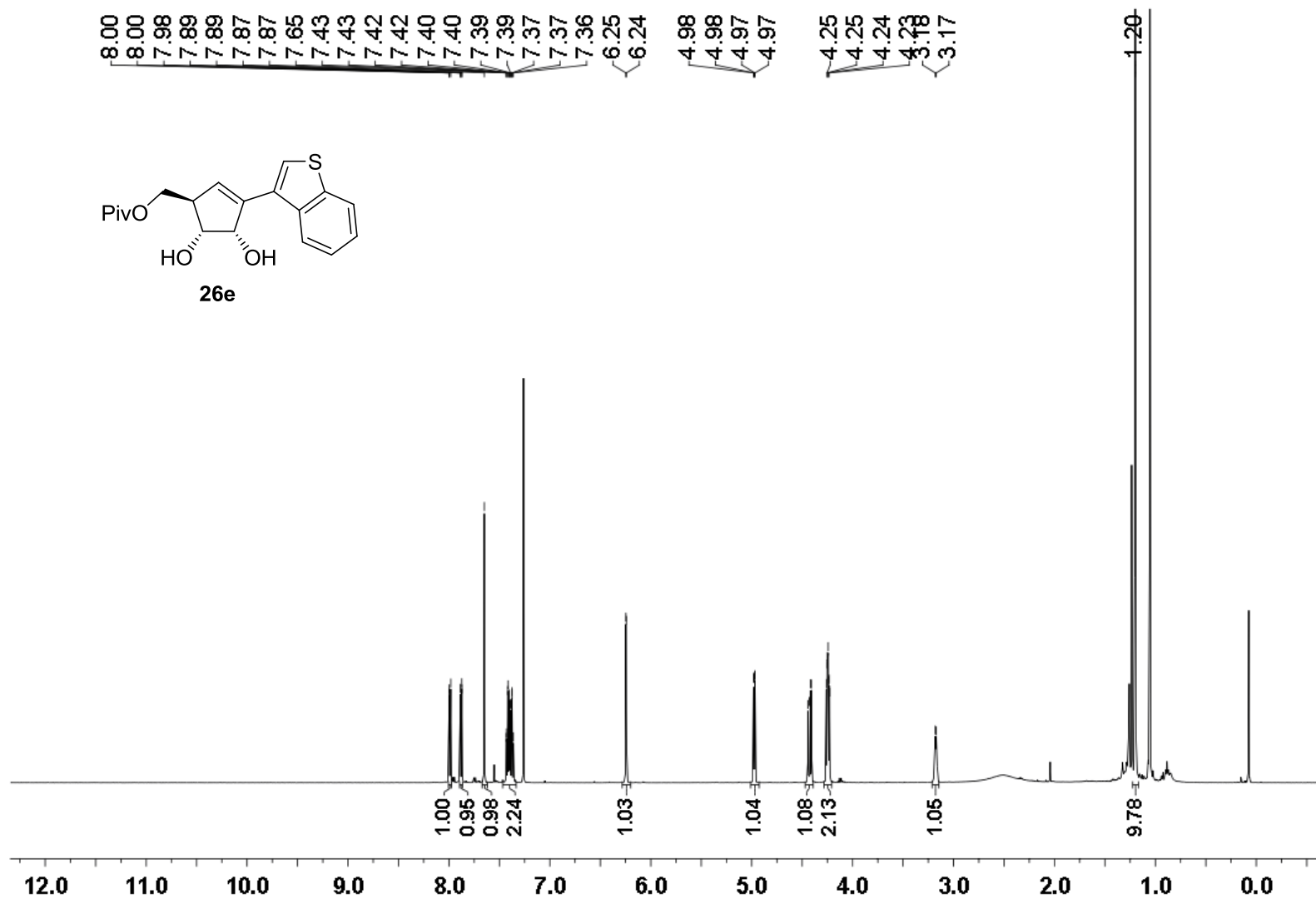
$^{13}\text{C}$  NMR (126 MHz) spectrum of **26c** in  $\text{CDCl}_3$



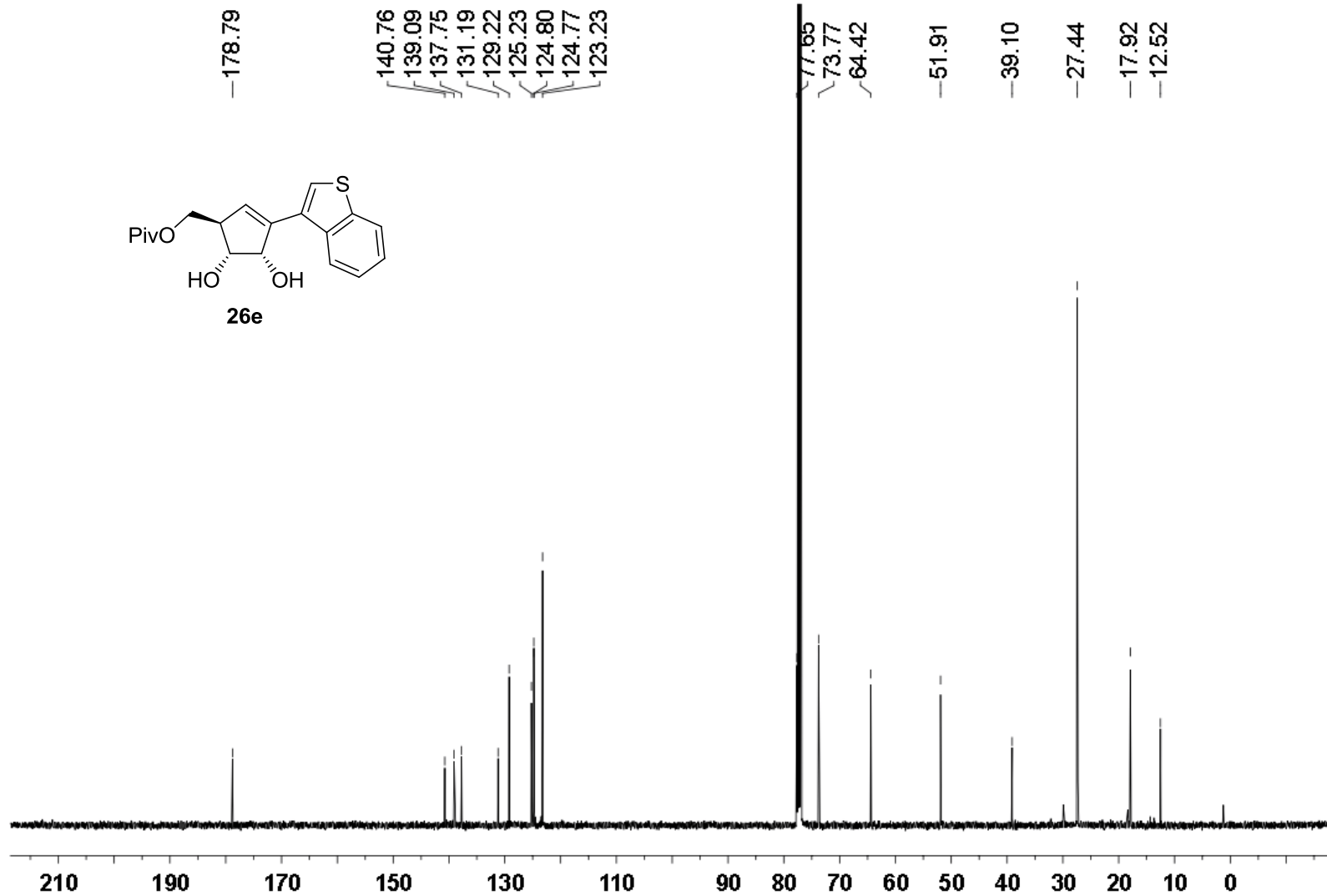
$^1\text{H}$  NMR (500 MHz) spectrum of **26d** in  $\text{CDCl}_3$



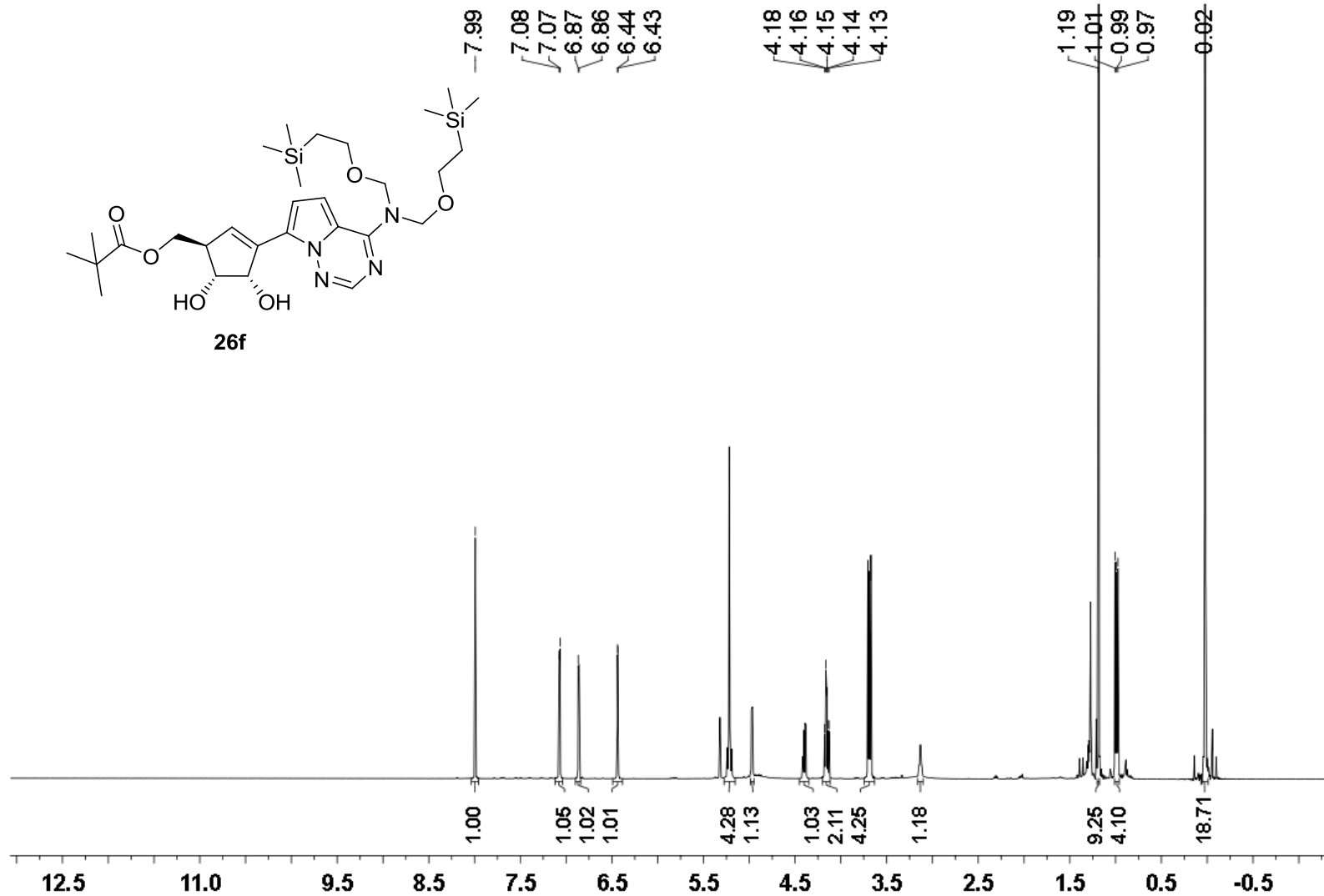
<sup>13</sup>C NMR (126 MHz) spectrum of **26d** in CDCl<sub>3</sub>



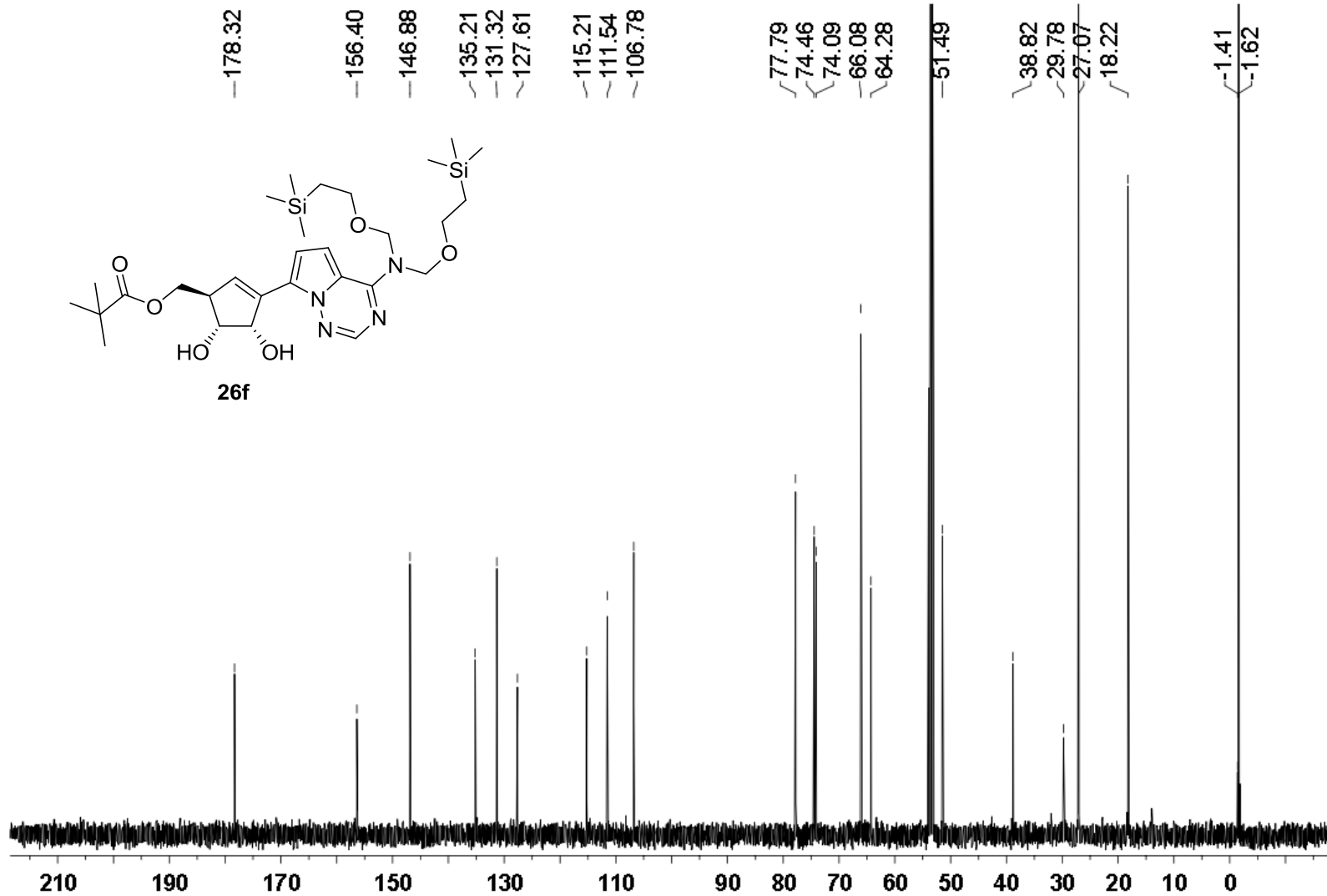
<sup>1</sup>H NMR (500 MHz) spectrum of **26e** in CDCl<sub>3</sub>



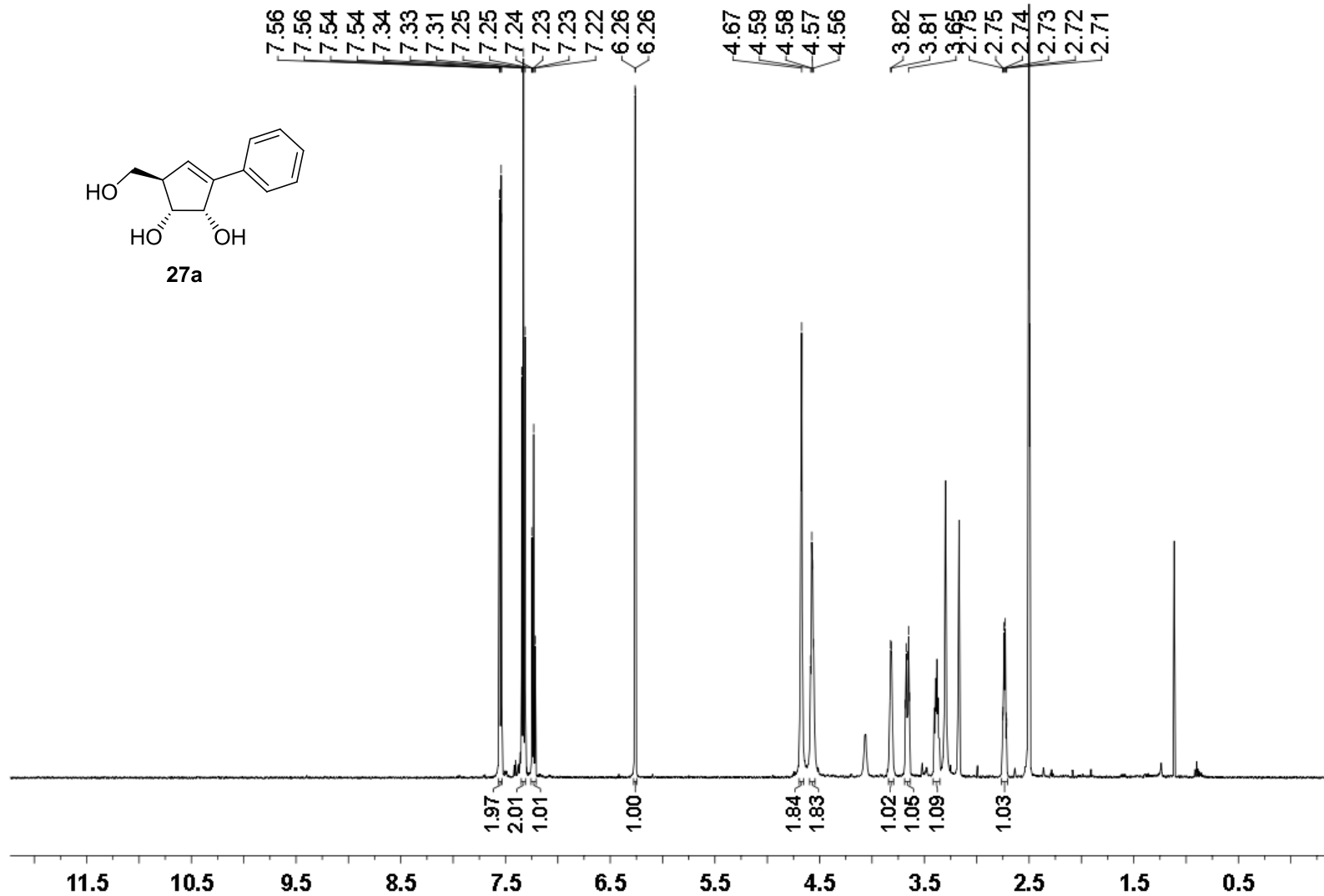
<sup>13</sup>C NMR (126 MHz) spectrum of **26e** in CDCl<sub>3</sub>



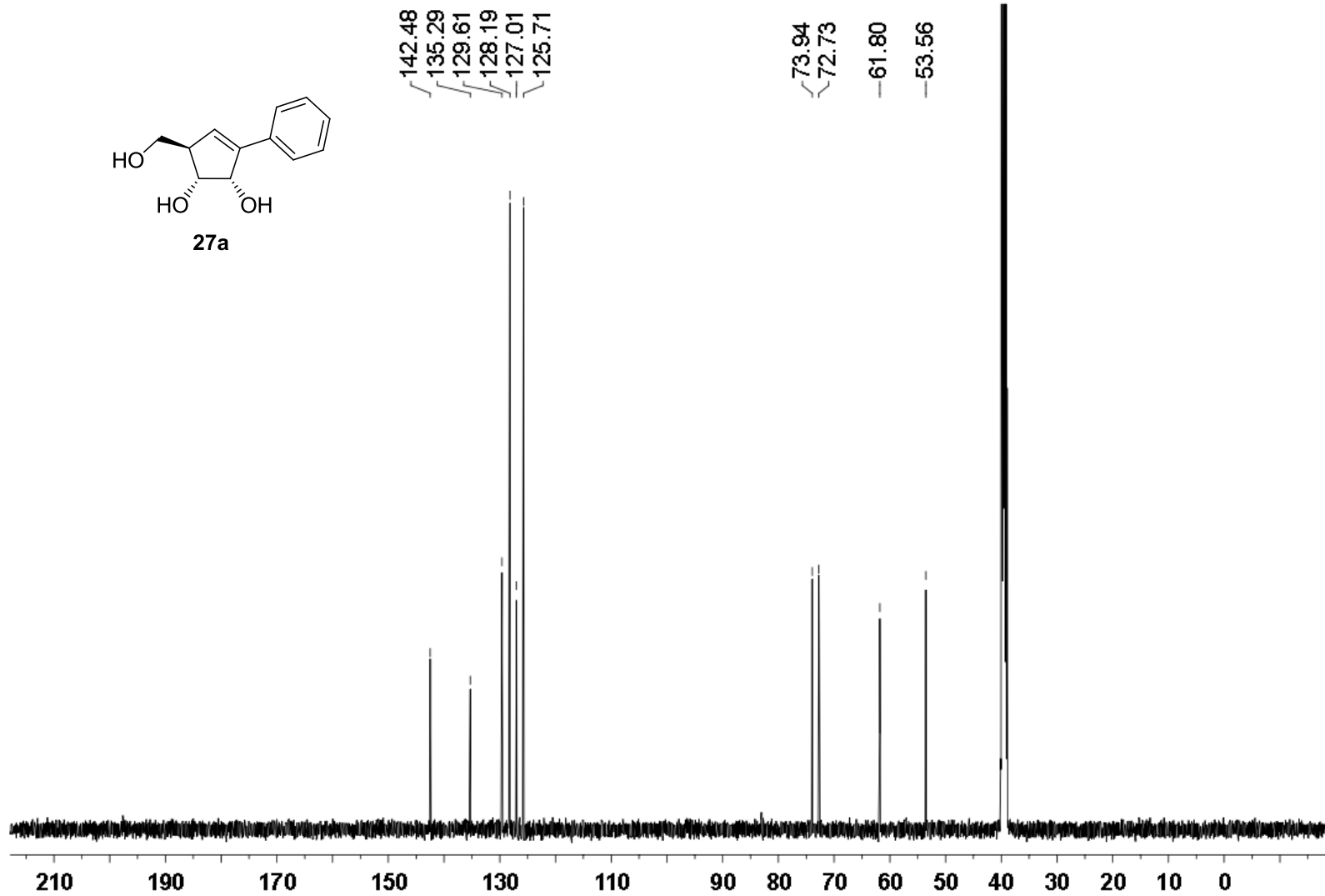
$^1\text{H}$  NMR (500 MHz) spectrum of **26f** in  $\text{CD}_2\text{Cl}_2$



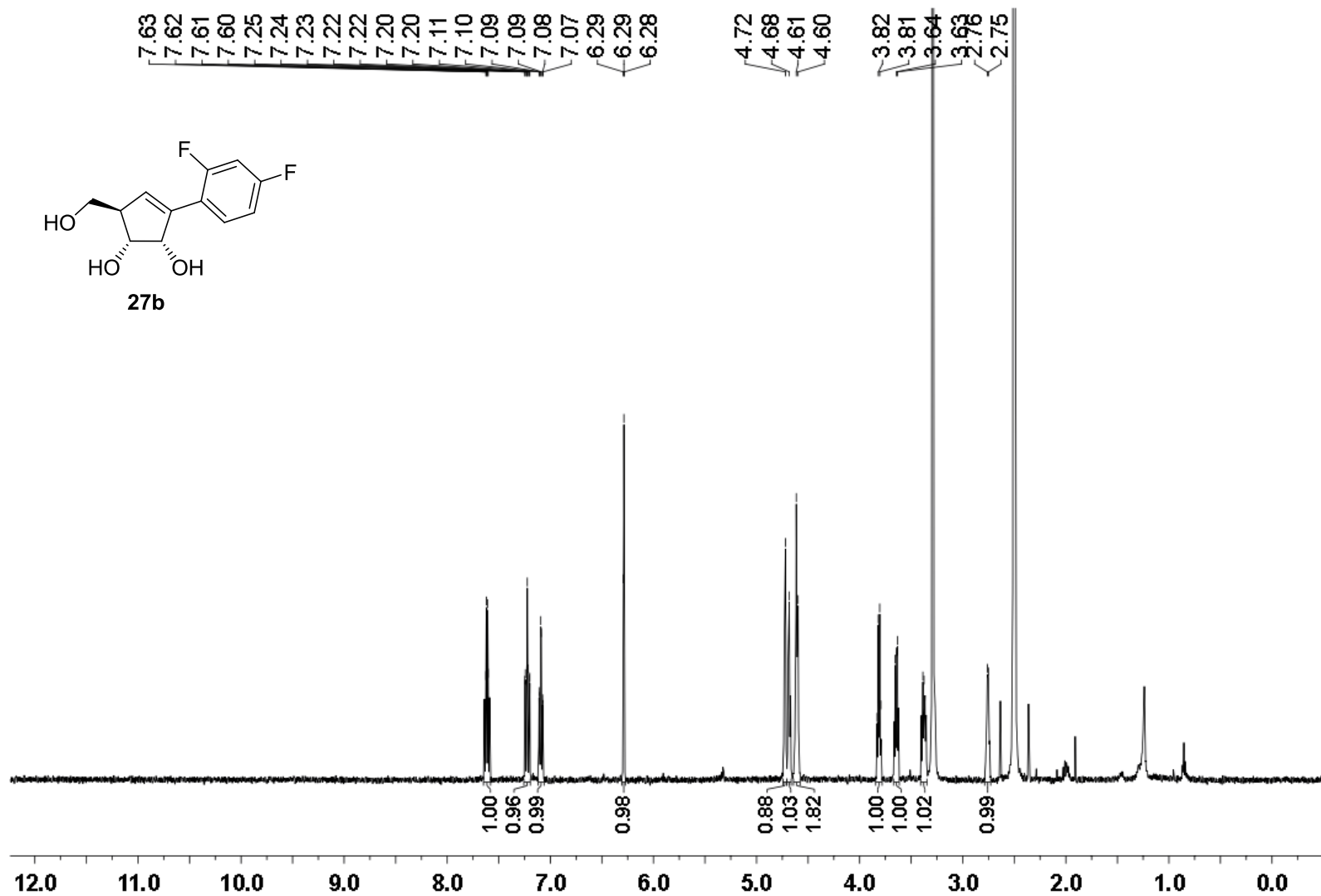
<sup>13</sup>C NMR (126 MHz) spectrum of **26f** in CD<sub>2</sub>Cl<sub>2</sub>



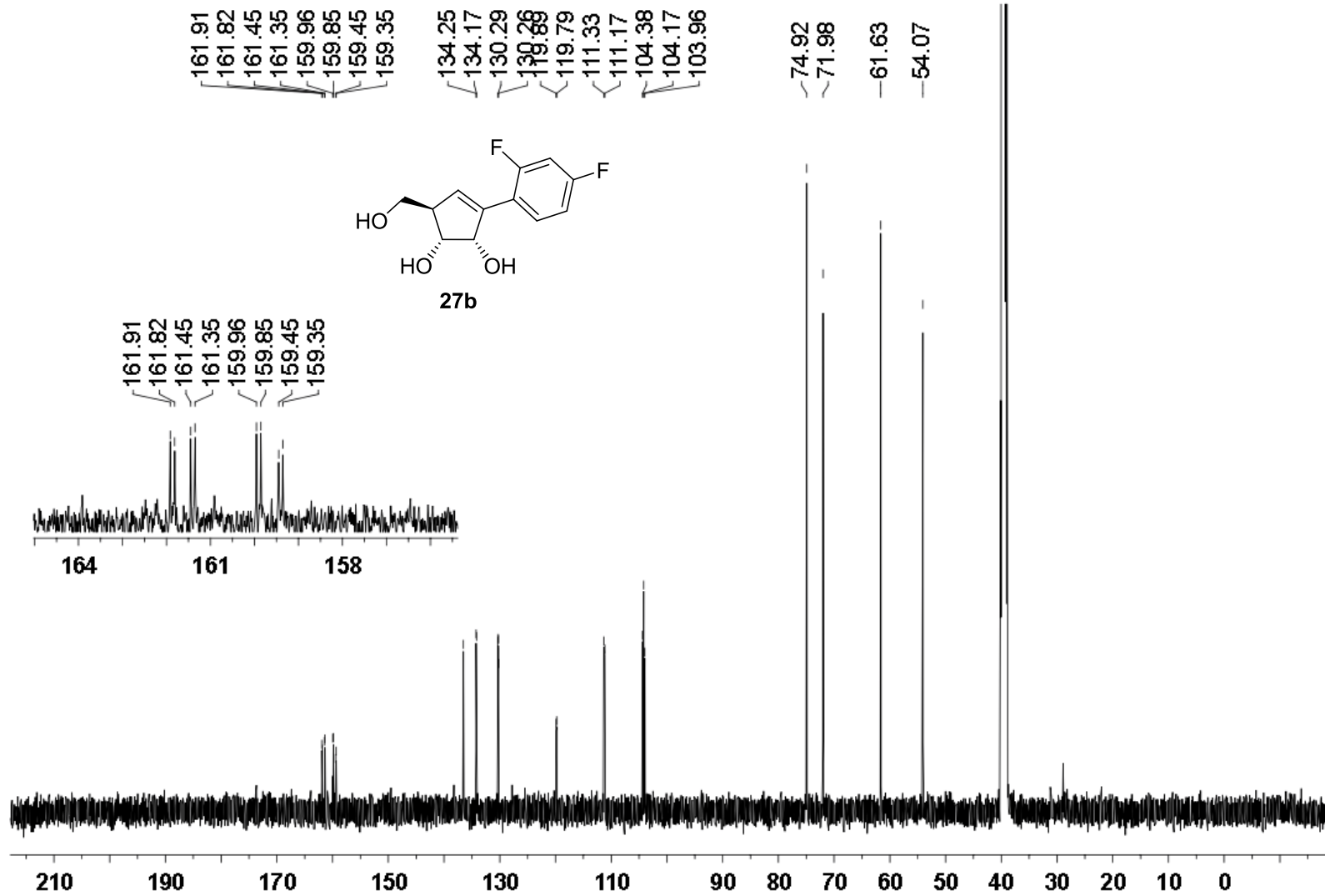
<sup>1</sup>H NMR (500 MHz) spectrum of **27a** in DMSO-*d*<sub>6</sub>



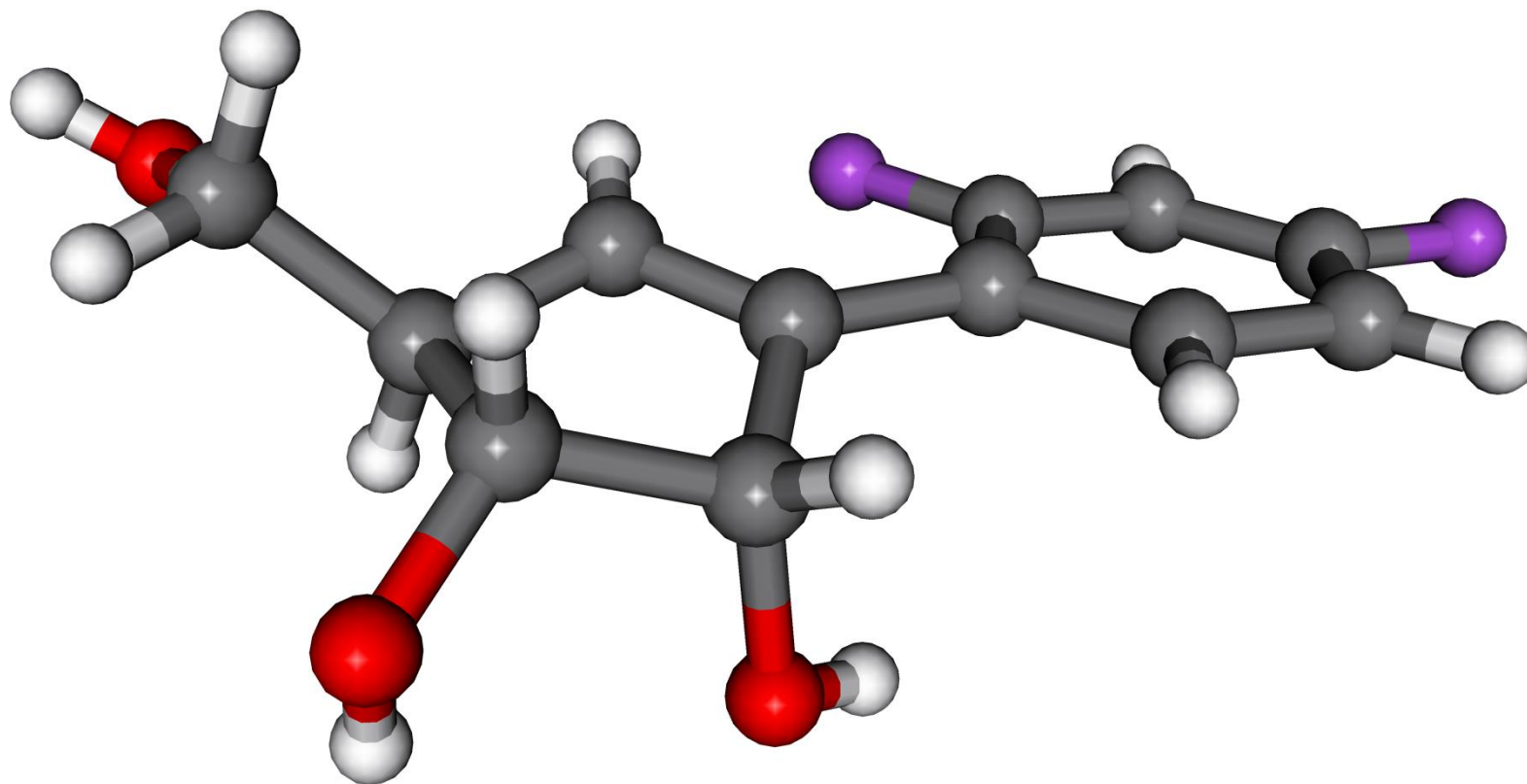
$^{13}\text{C}$  NMR (126 MHz) spectrum of **27a** in  $\text{DMSO-}d_6$



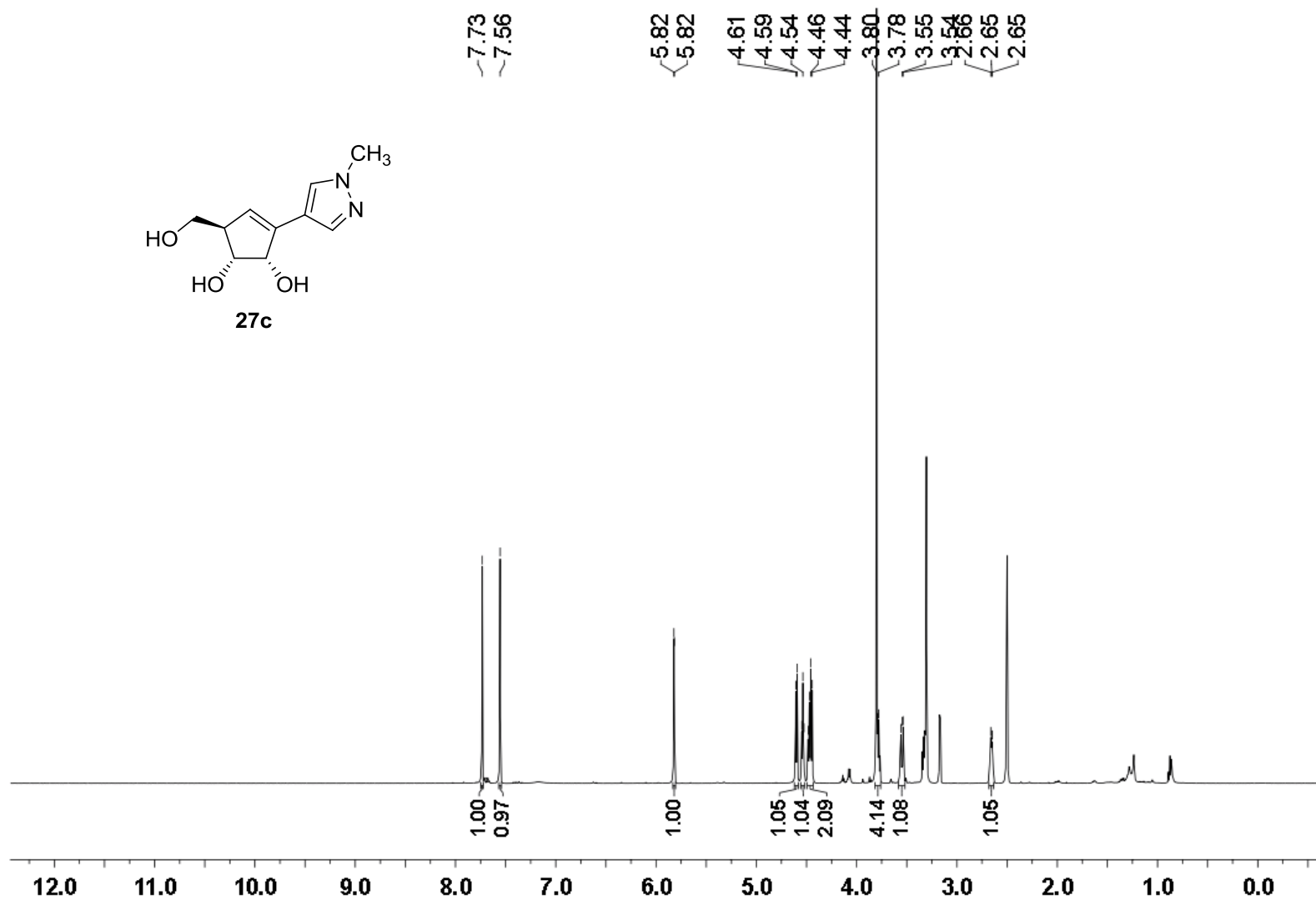
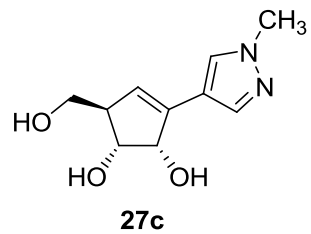
<sup>1</sup>H NMR (500 MHz) spectrum of **27b** in DMSO-*d*<sub>6</sub>



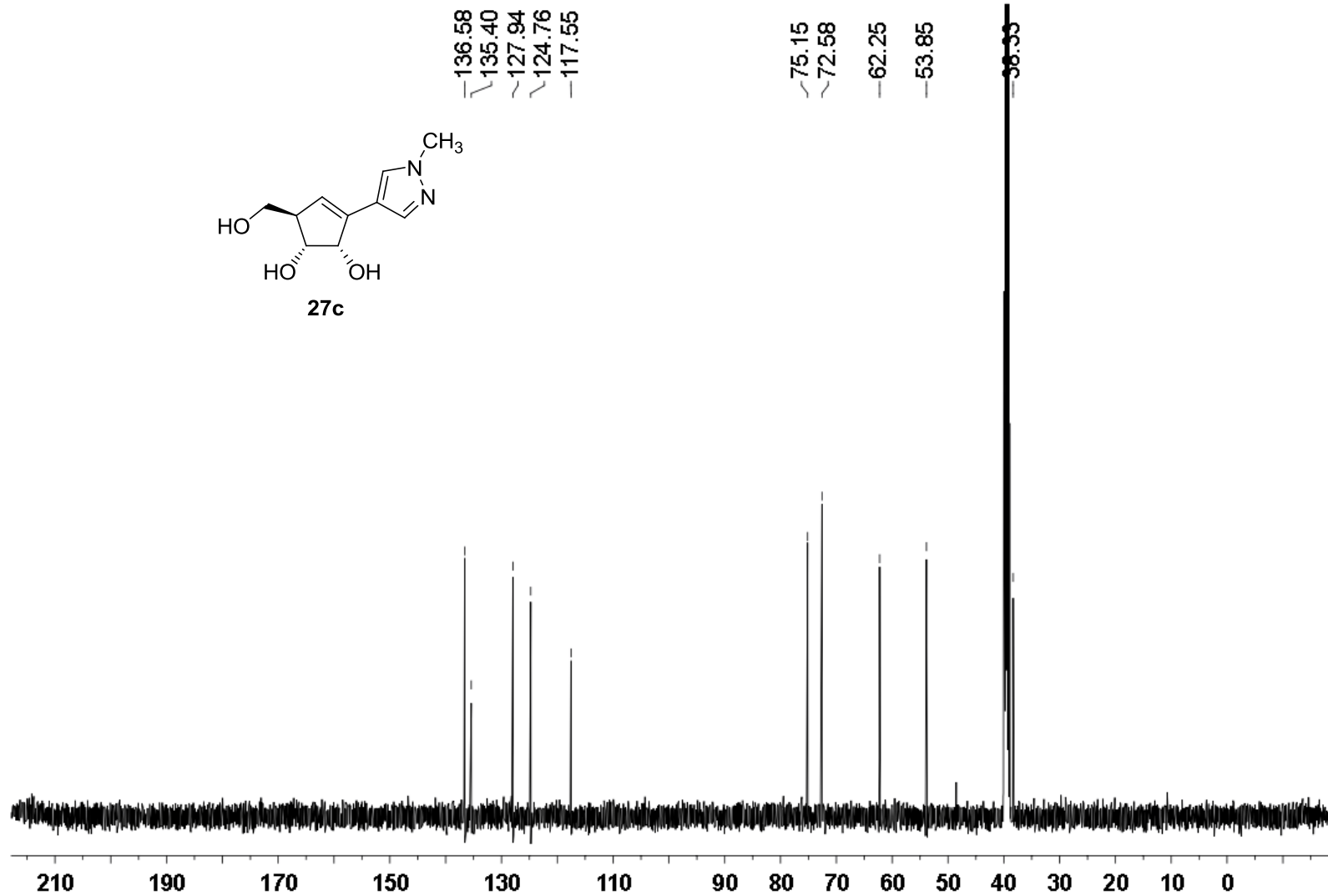
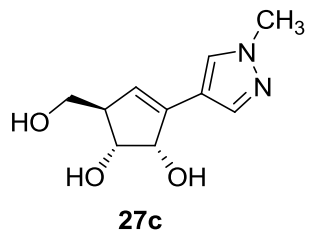
<sup>13</sup>C NMR (126 MHz) spectrum of **27b** in DMSO-*d*<sub>6</sub>



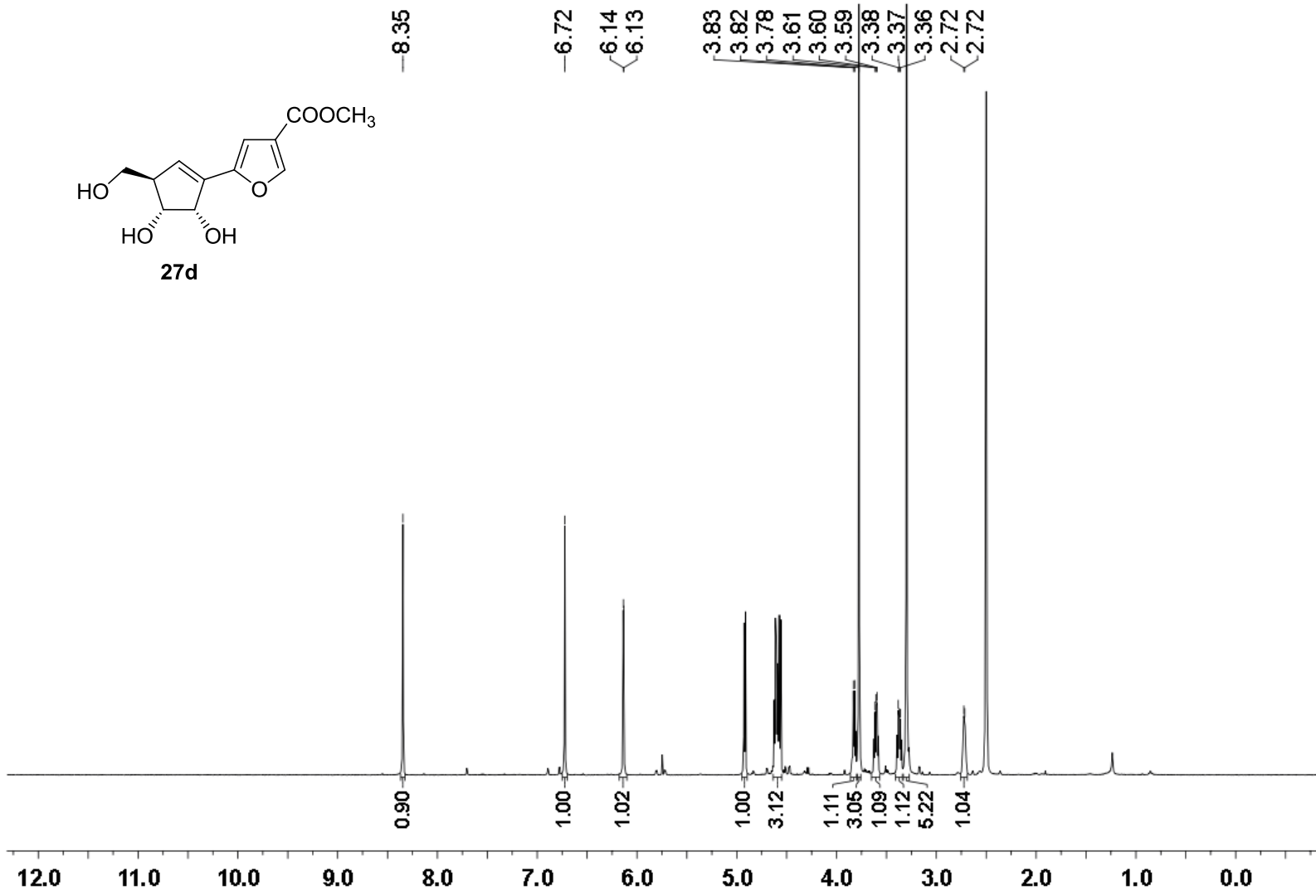
X-ray structure of **27b**



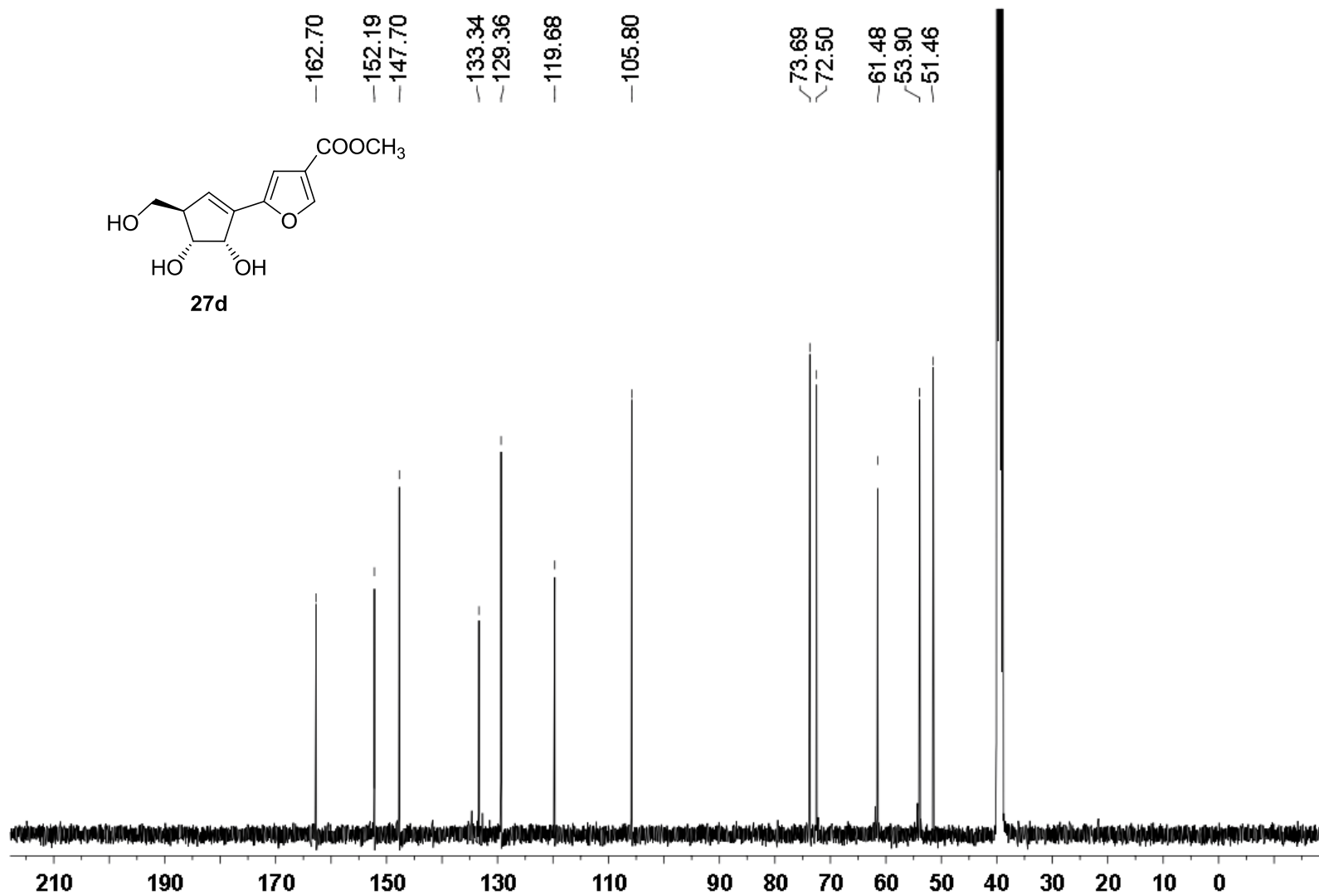
$^1\text{H}$  NMR (500 MHz) spectrum of **27c** in  $\text{DMSO-}d_6$



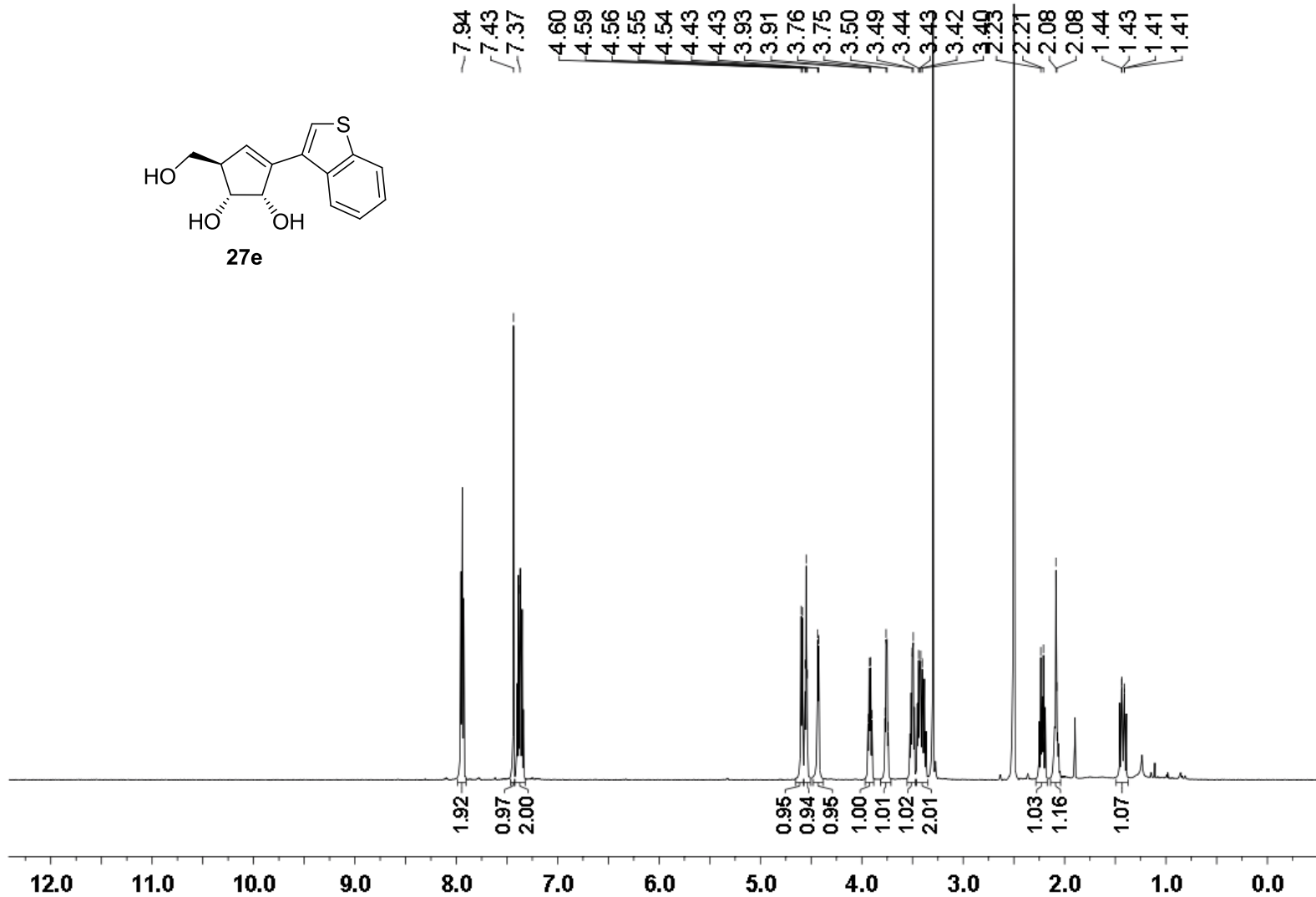
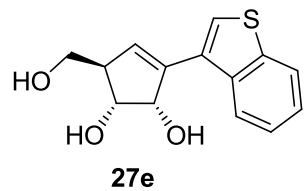
$^{13}\text{C}$  NMR (126 MHz) spectrum of **27c** in  $\text{DMSO-}d_6$



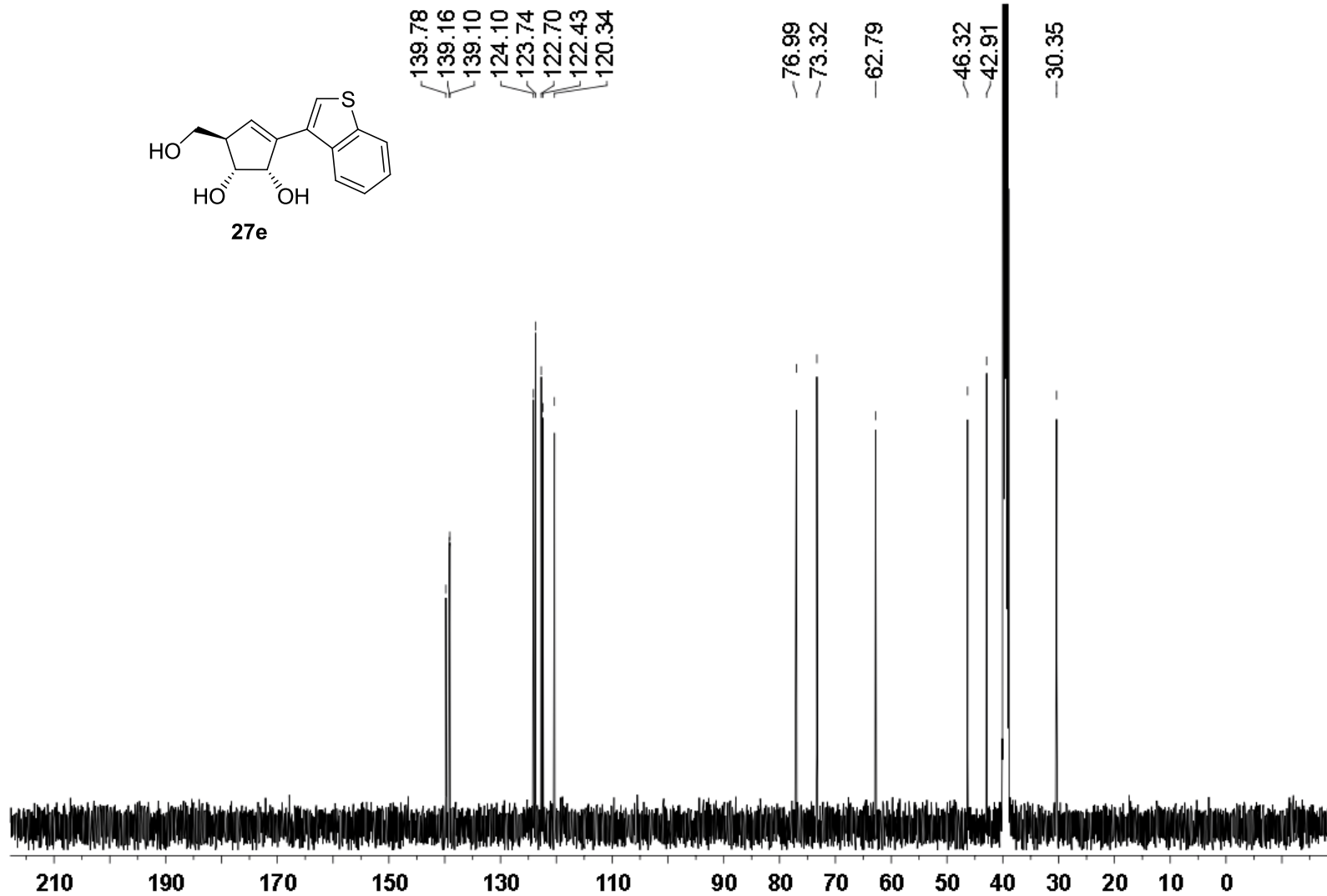
<sup>1</sup>H NMR (500 MHz) spectrum of **27d** in DMSO-*d*<sub>6</sub>



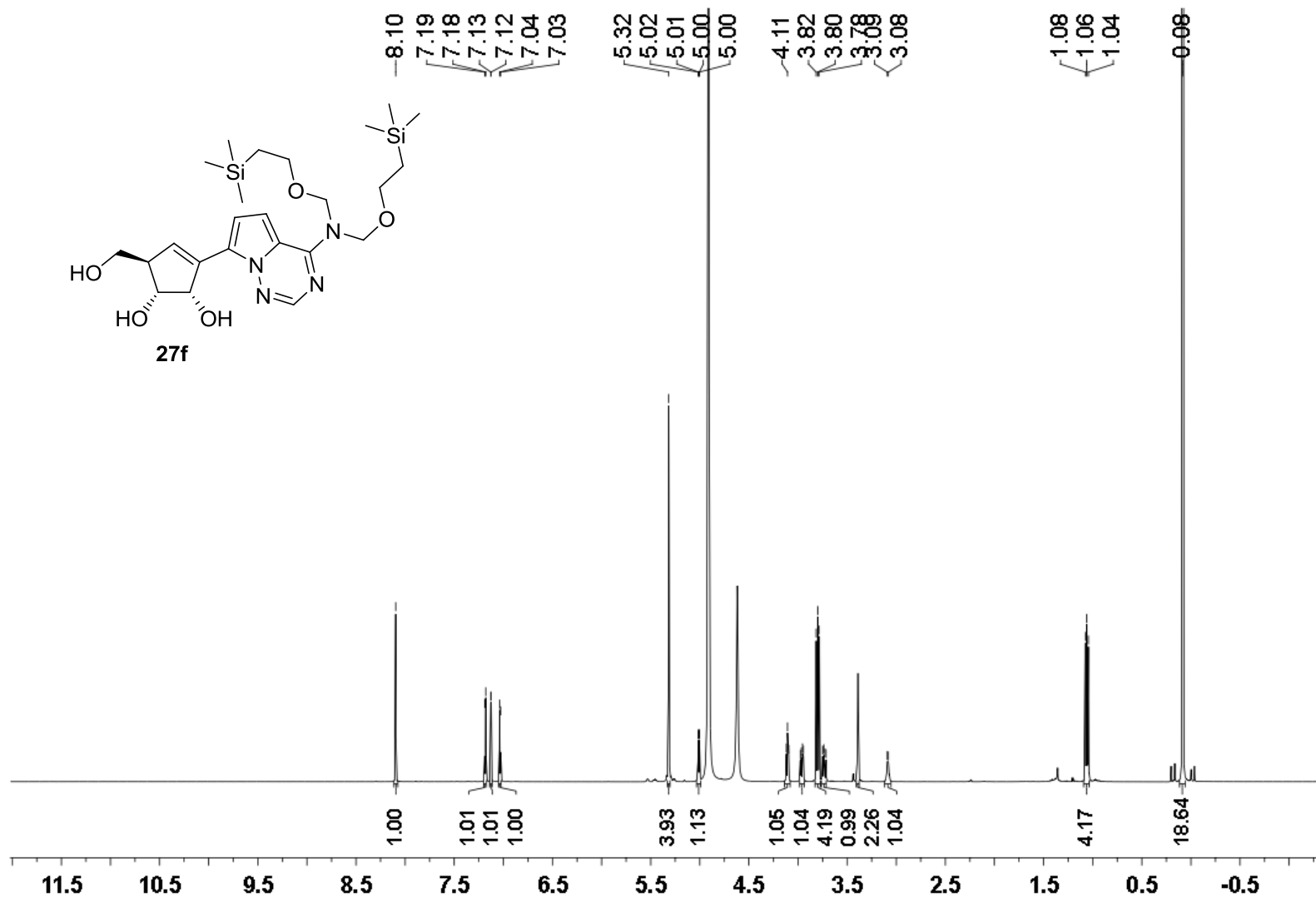
$^{13}\text{C}$  NMR (126 MHz) spectrum of **27d** in  $\text{DMSO-}d_6$



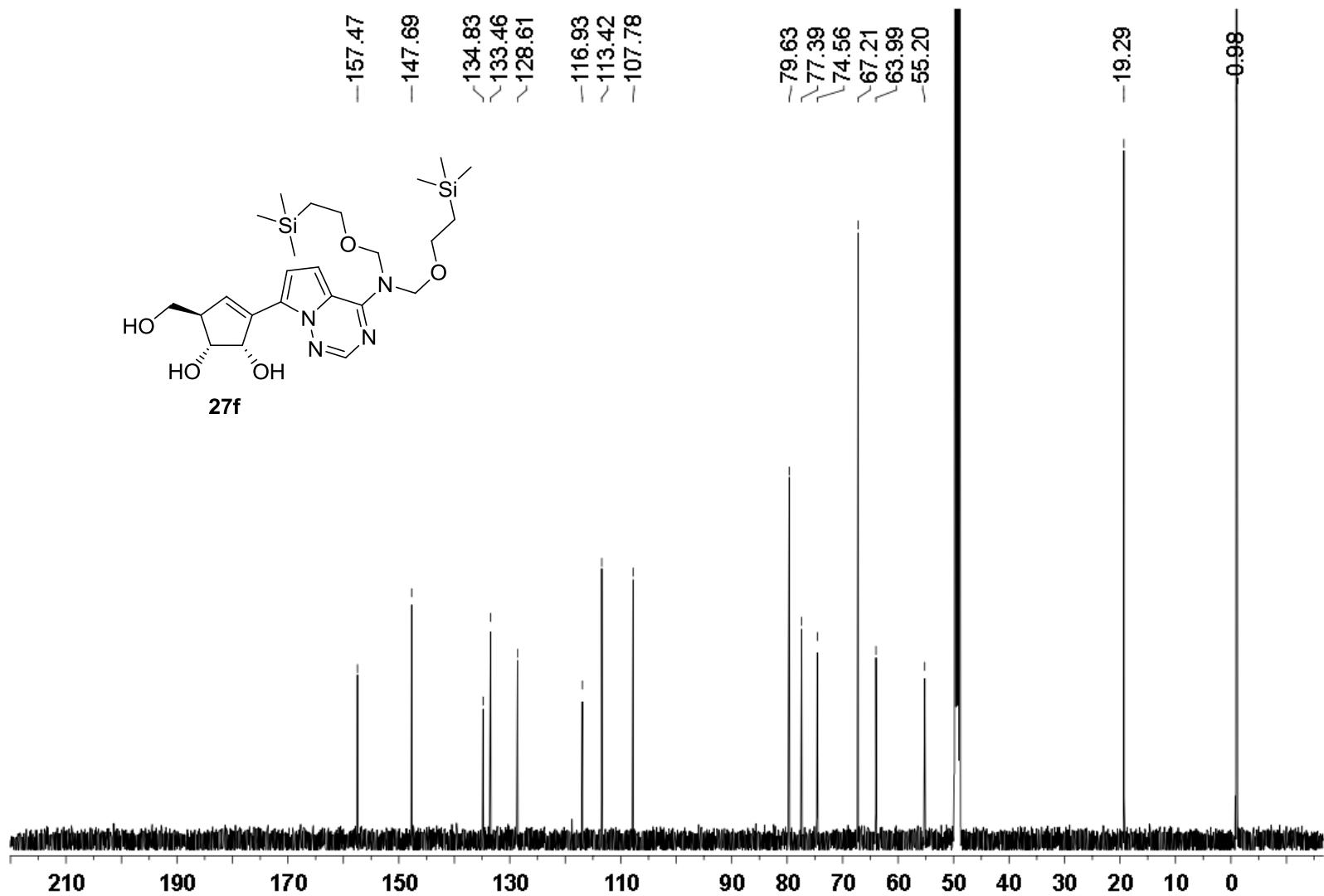
<sup>1</sup>H NMR (500 MHz) spectrum of **27e** in DMSO-*d*<sub>6</sub>



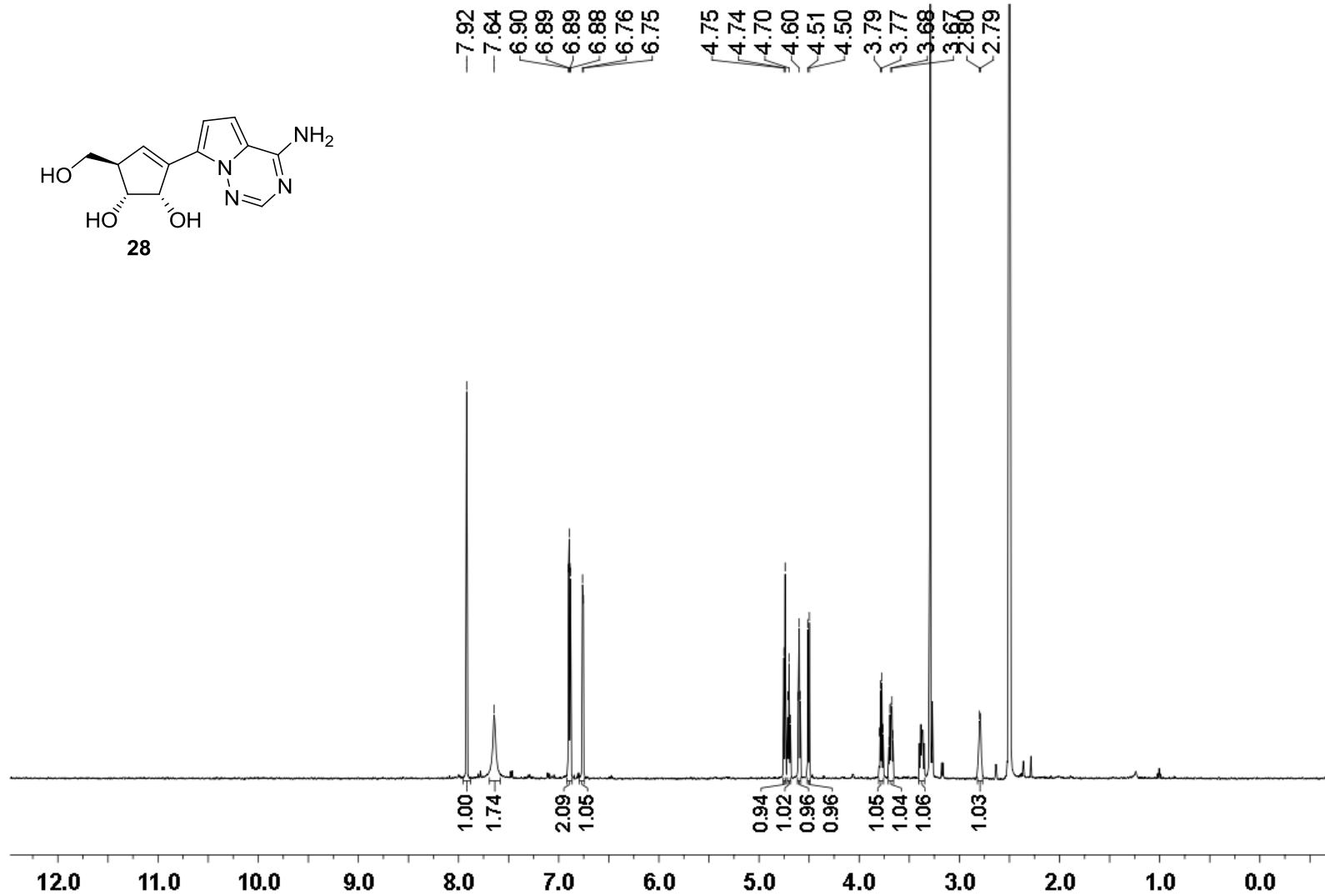
$^{13}\text{C}$  NMR (126 MHz) spectrum of **27e** in  $\text{DMSO-}d_6$



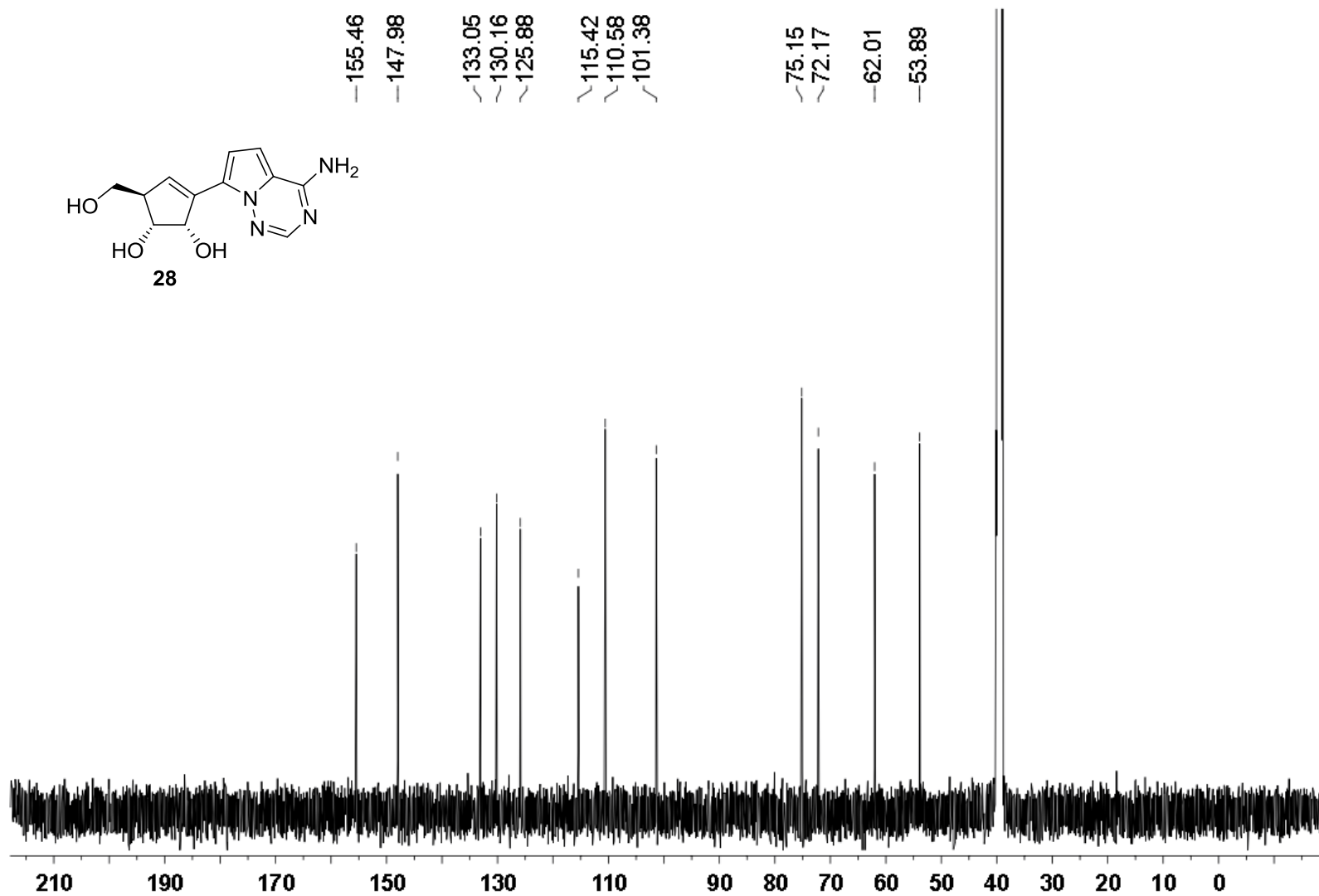
$^1\text{H}$  NMR (500 MHz) spectrum of **27f** in  $\text{CD}_3\text{OD}$



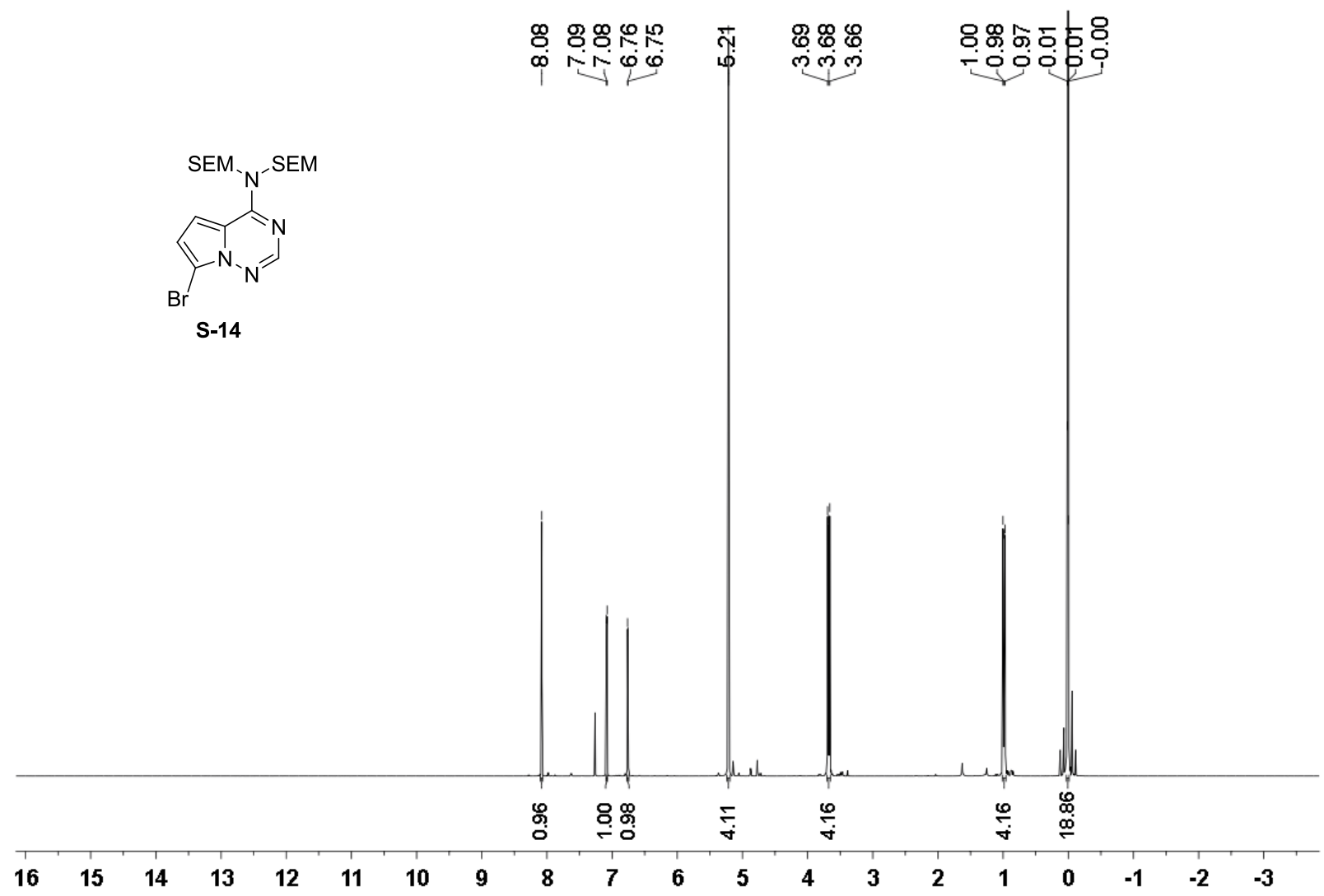
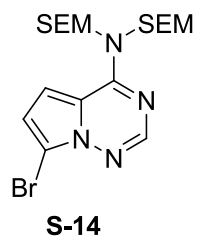
$^{13}\text{C}$  NMR (126 MHz) spectrum of **27f** in  $\text{CD}_3\text{OD}$



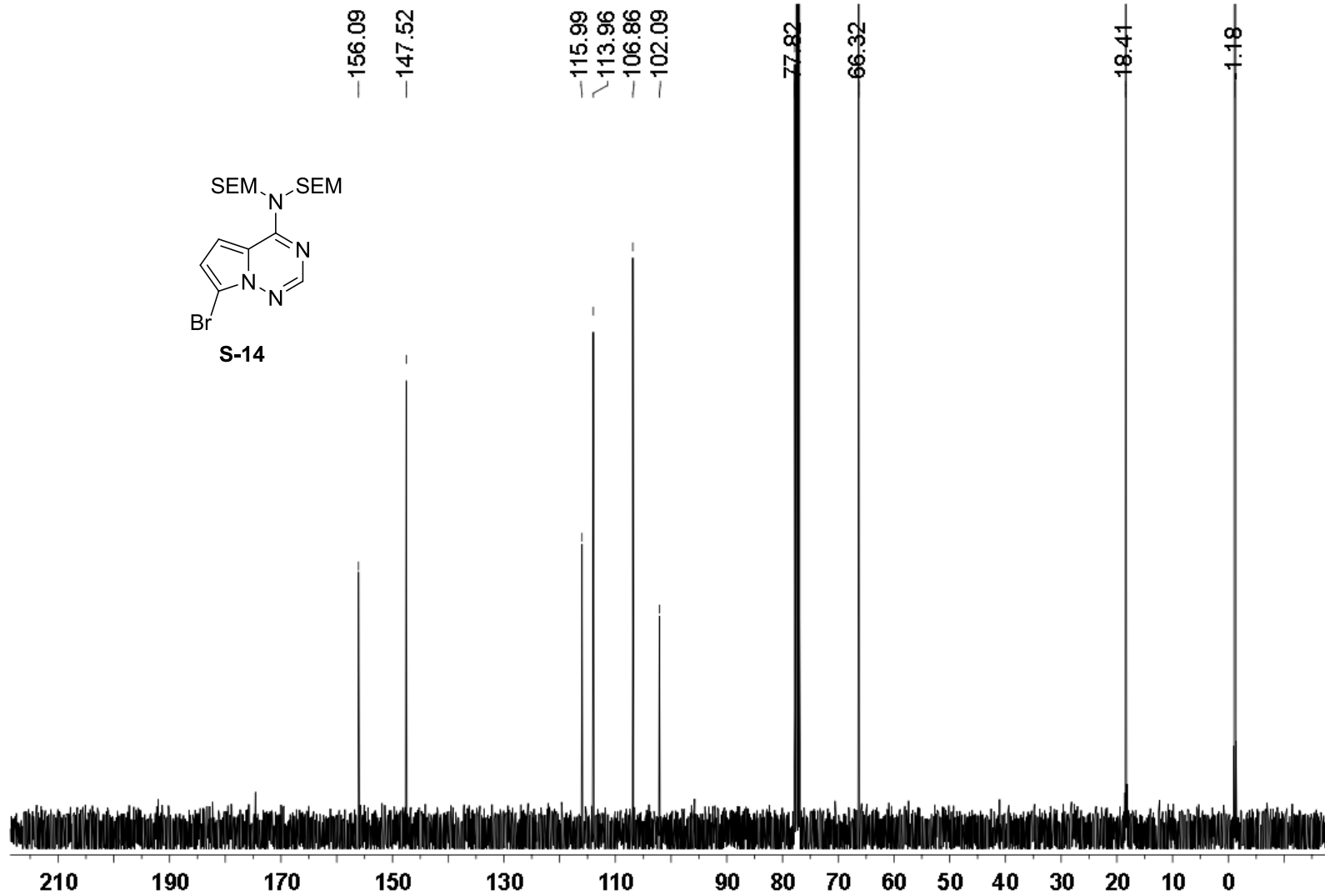
<sup>1</sup>H NMR (500 MHz) spectrum of **28** in DMSO-*d*<sub>6</sub>



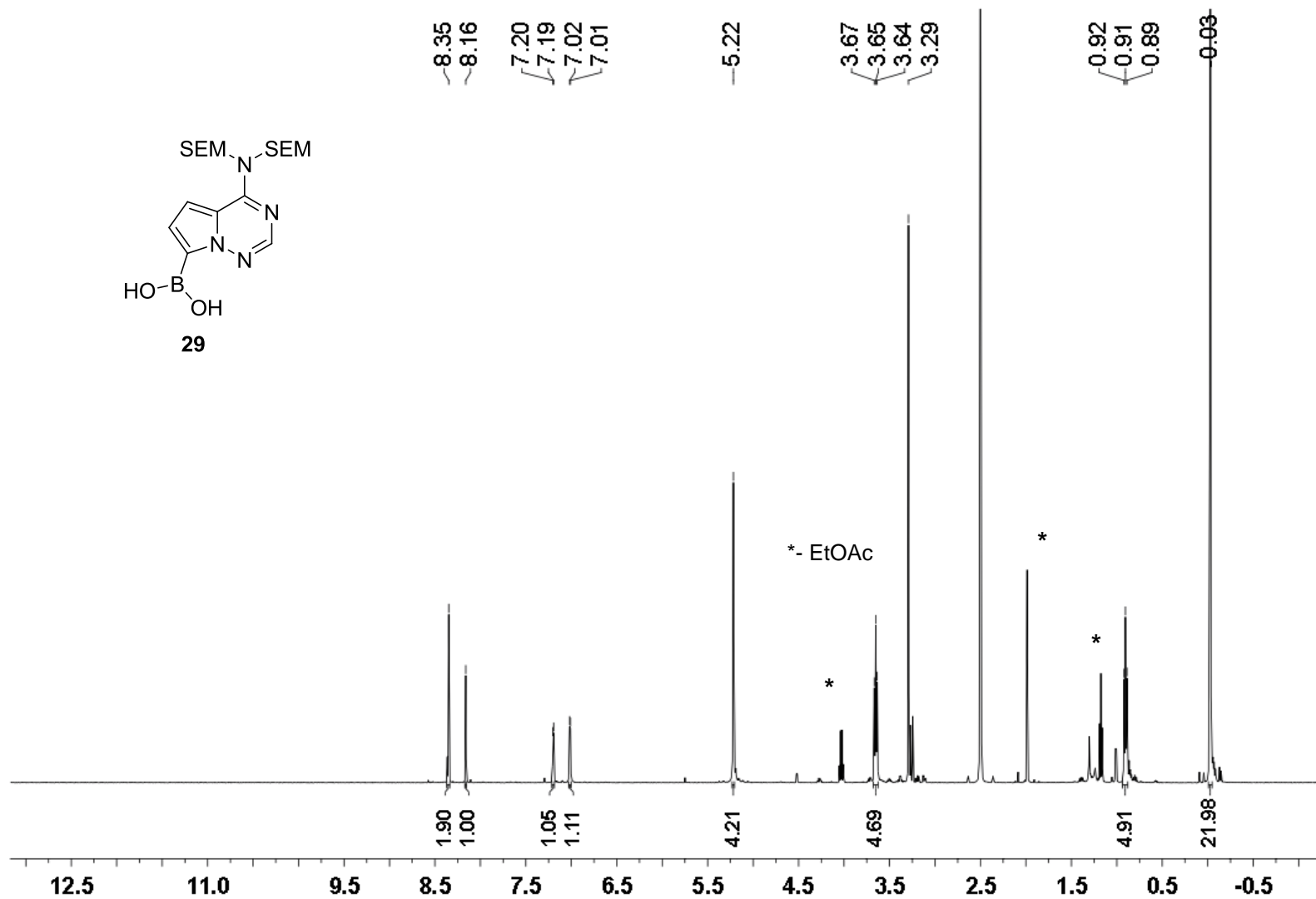
$^{13}\text{C}$  NMR (500 MHz) spectrum of **28** in  $\text{DMSO-}d_6$



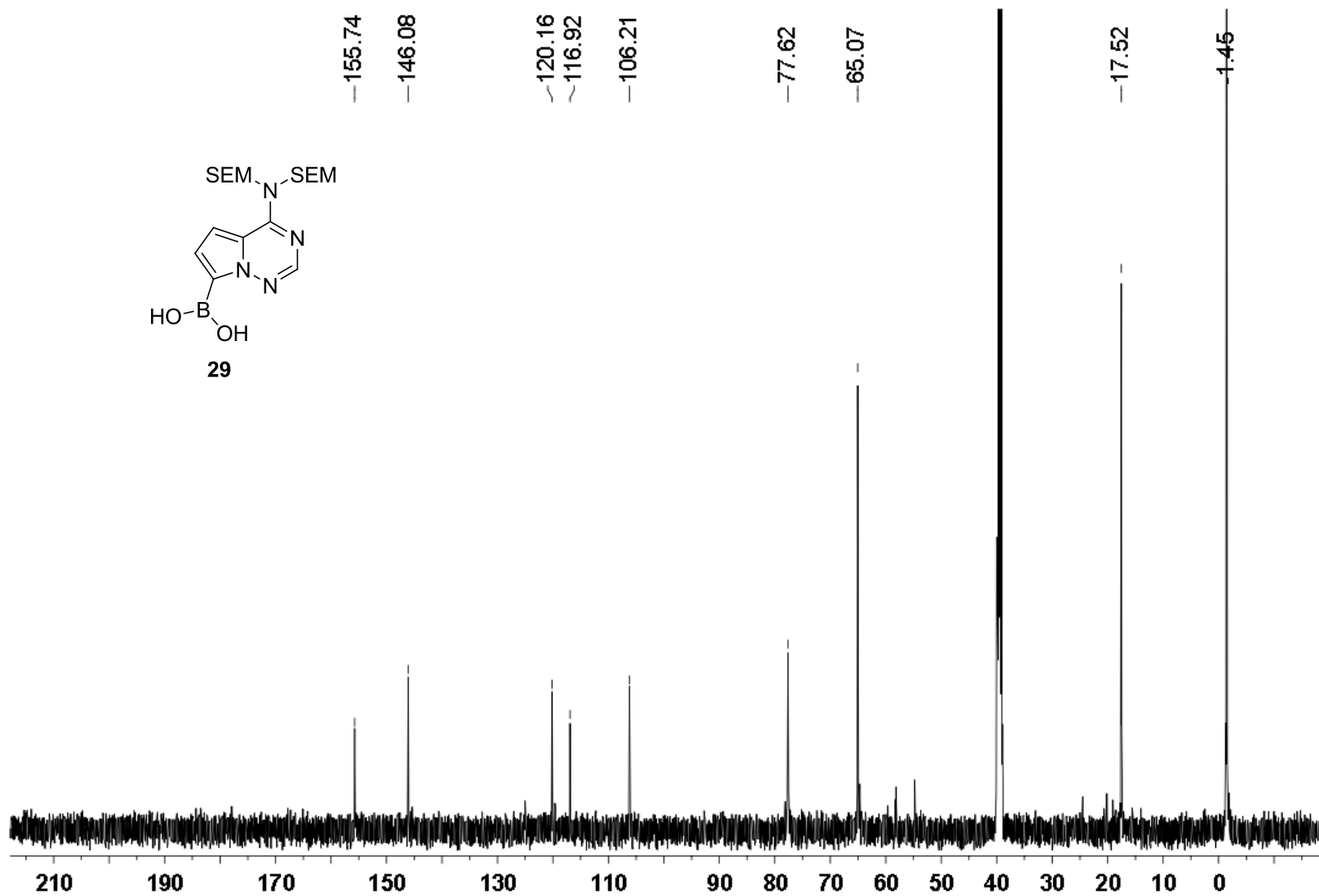
<sup>1</sup>H NMR (500 MHz) spectrum of S-14 in CDCl<sub>3</sub>



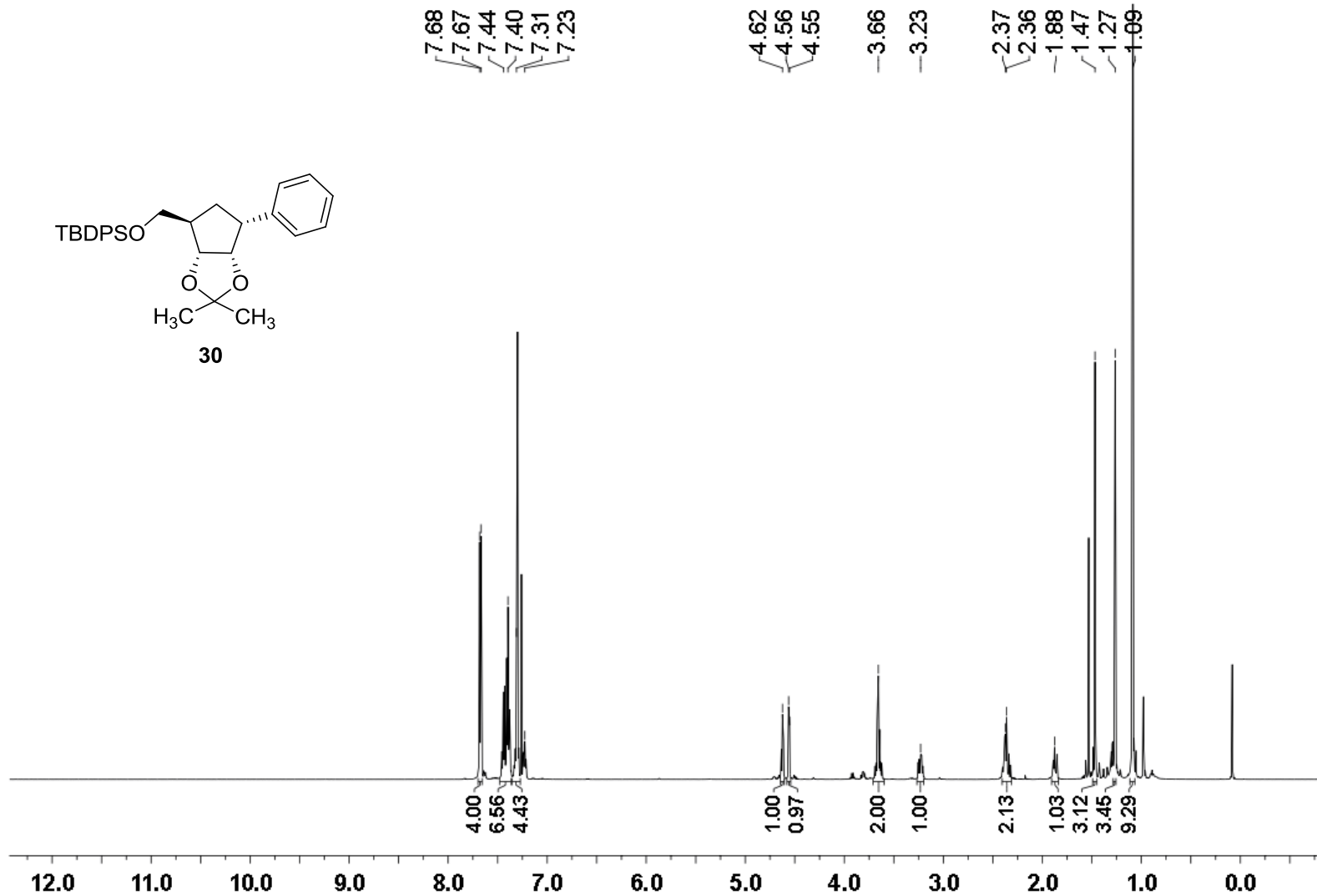
$^{13}\text{C}$  NMR (126 MHz) spectrum of **S-14** in  $\text{CDCl}_3$



$^1\text{H}$  NMR (500 MHz) spectrum of **29** in  $\text{DMSO-}d_6$

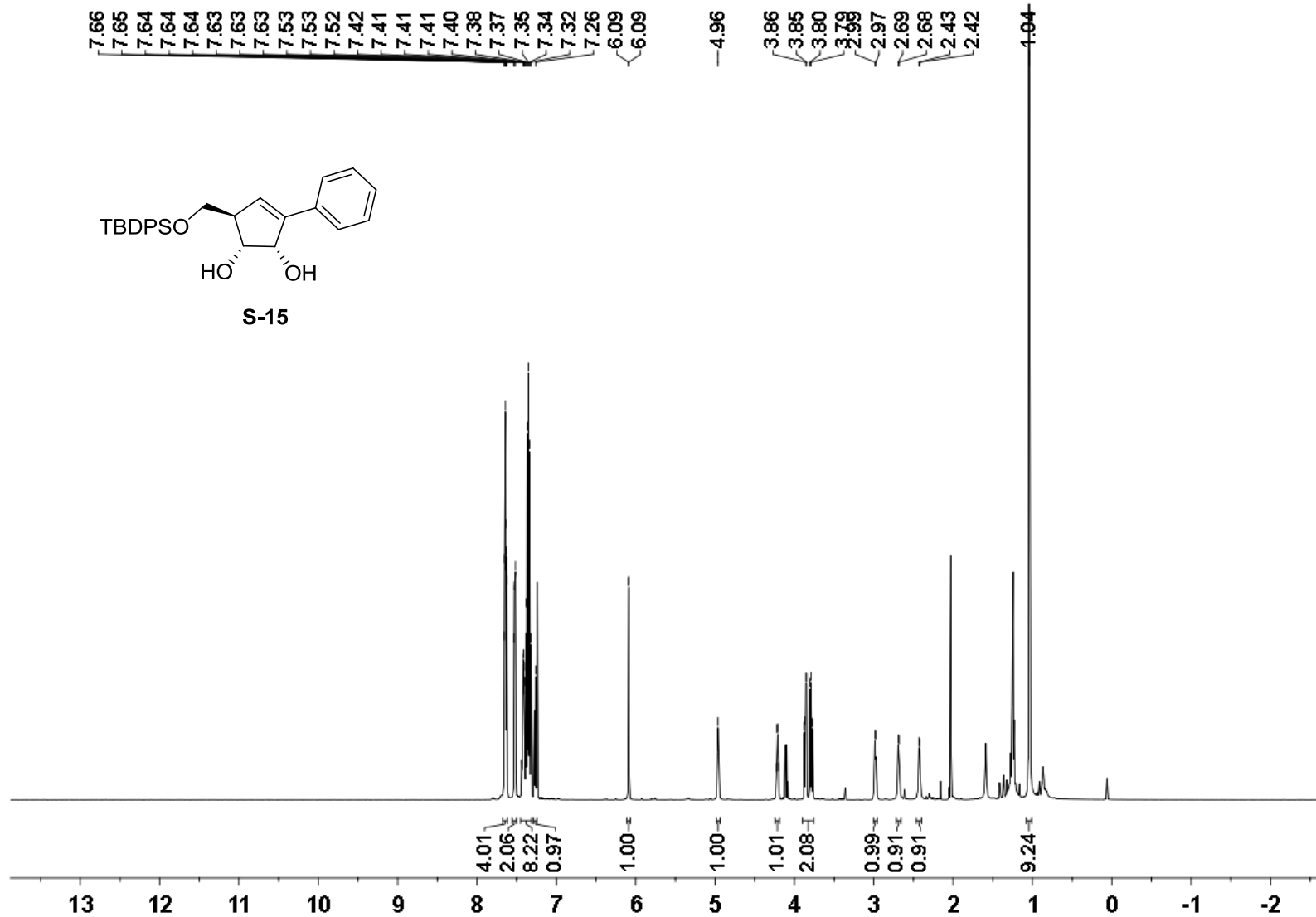


$^{13}\text{C}$  NMR (126 MHz) spectrum of **29** in  $\text{DMSO-}d_6$



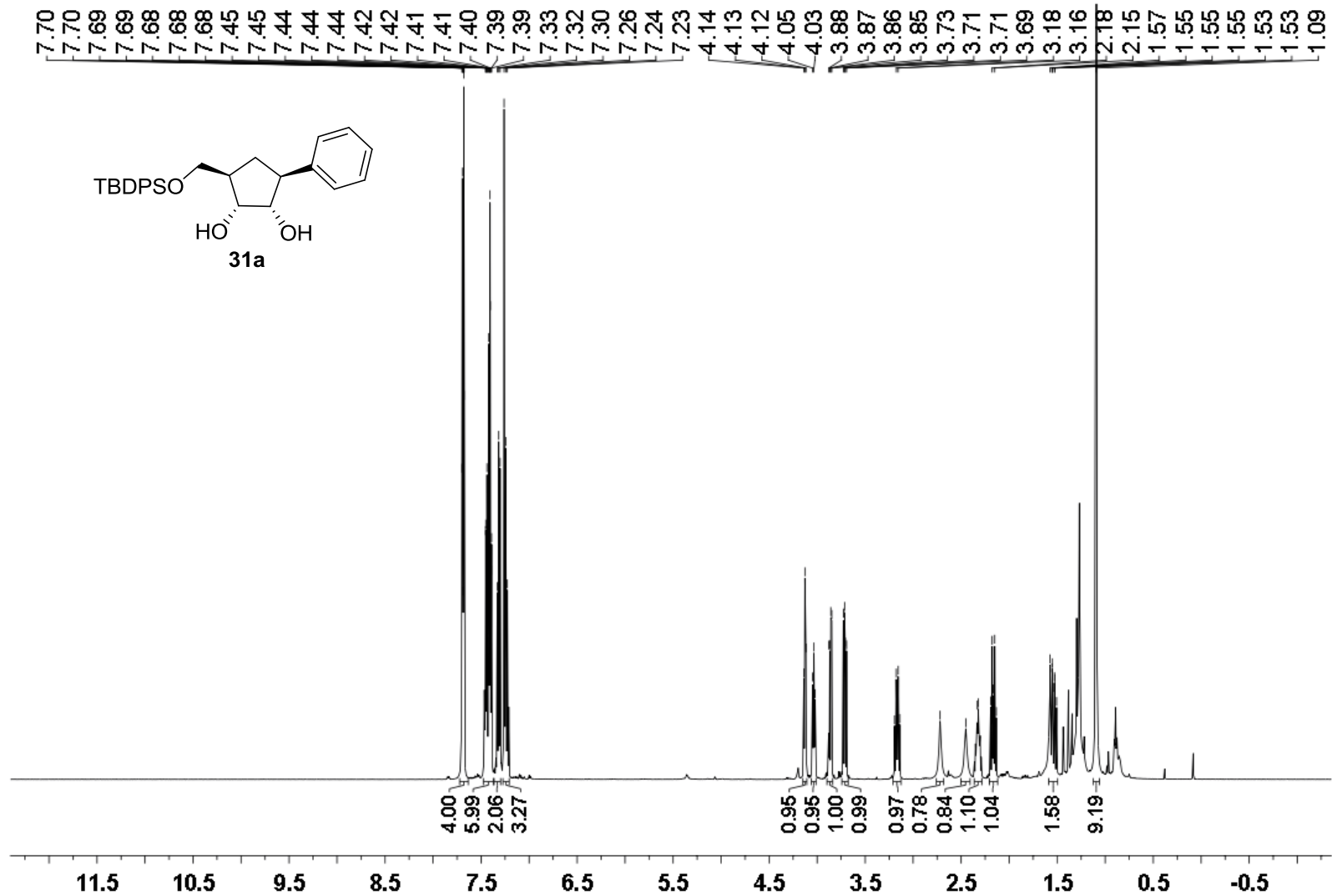
$^1\text{H}$  NMR (500 MHz) spectrum of **30** in  $\text{CDCl}_3$



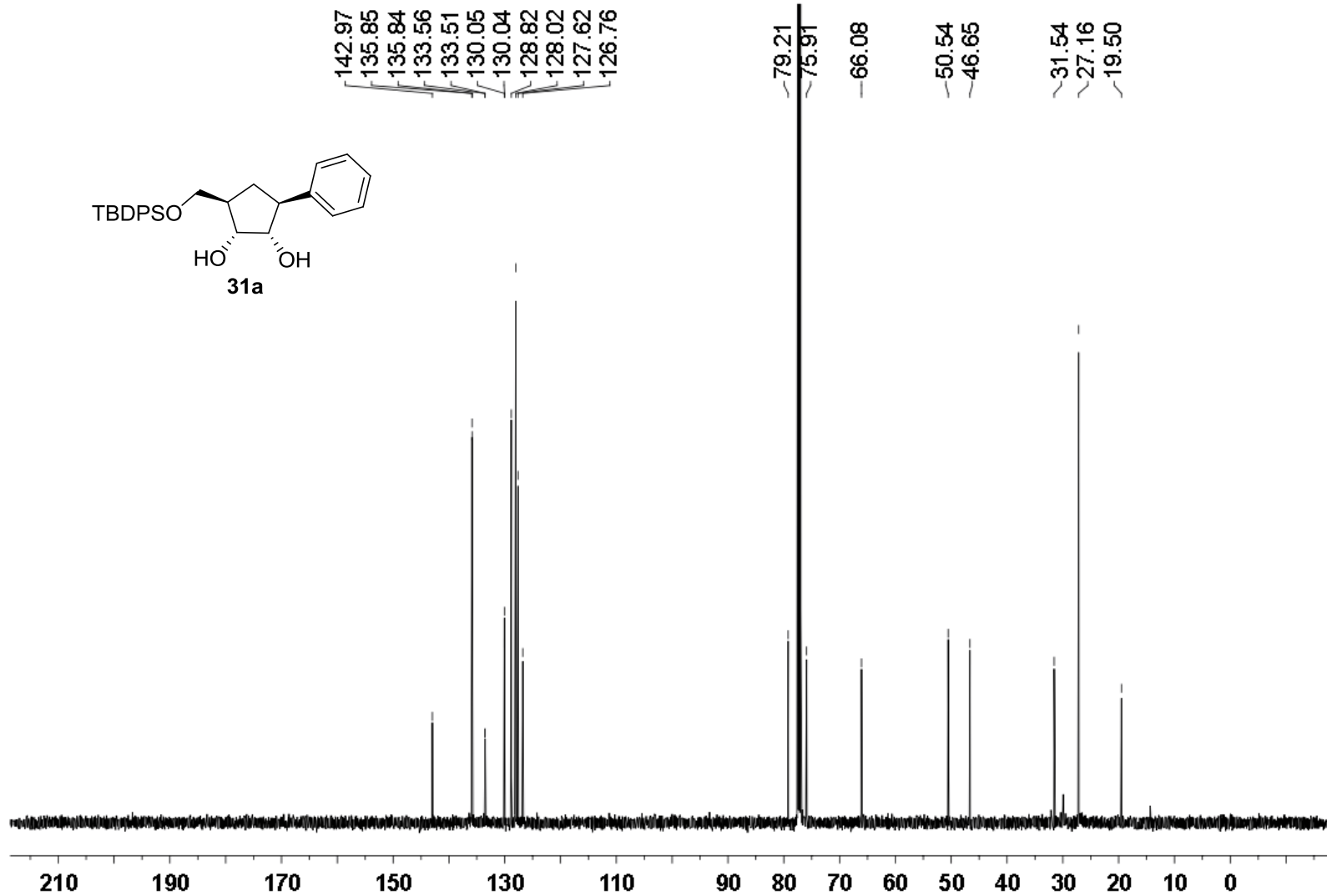


<sup>1</sup>H NMR (500 MHz) spectrum of **S-15** in CDCl<sub>3</sub>

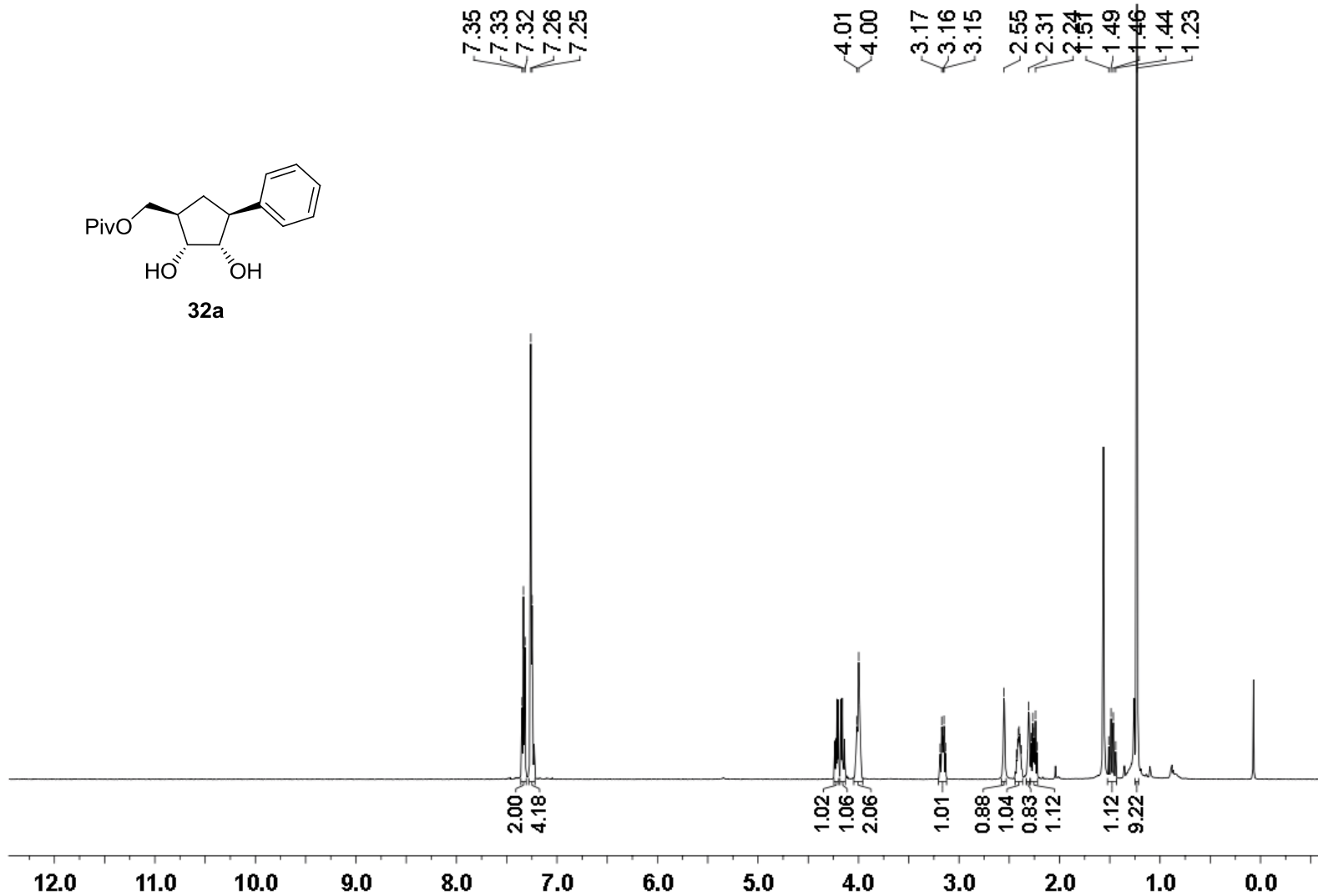
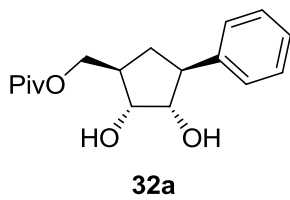




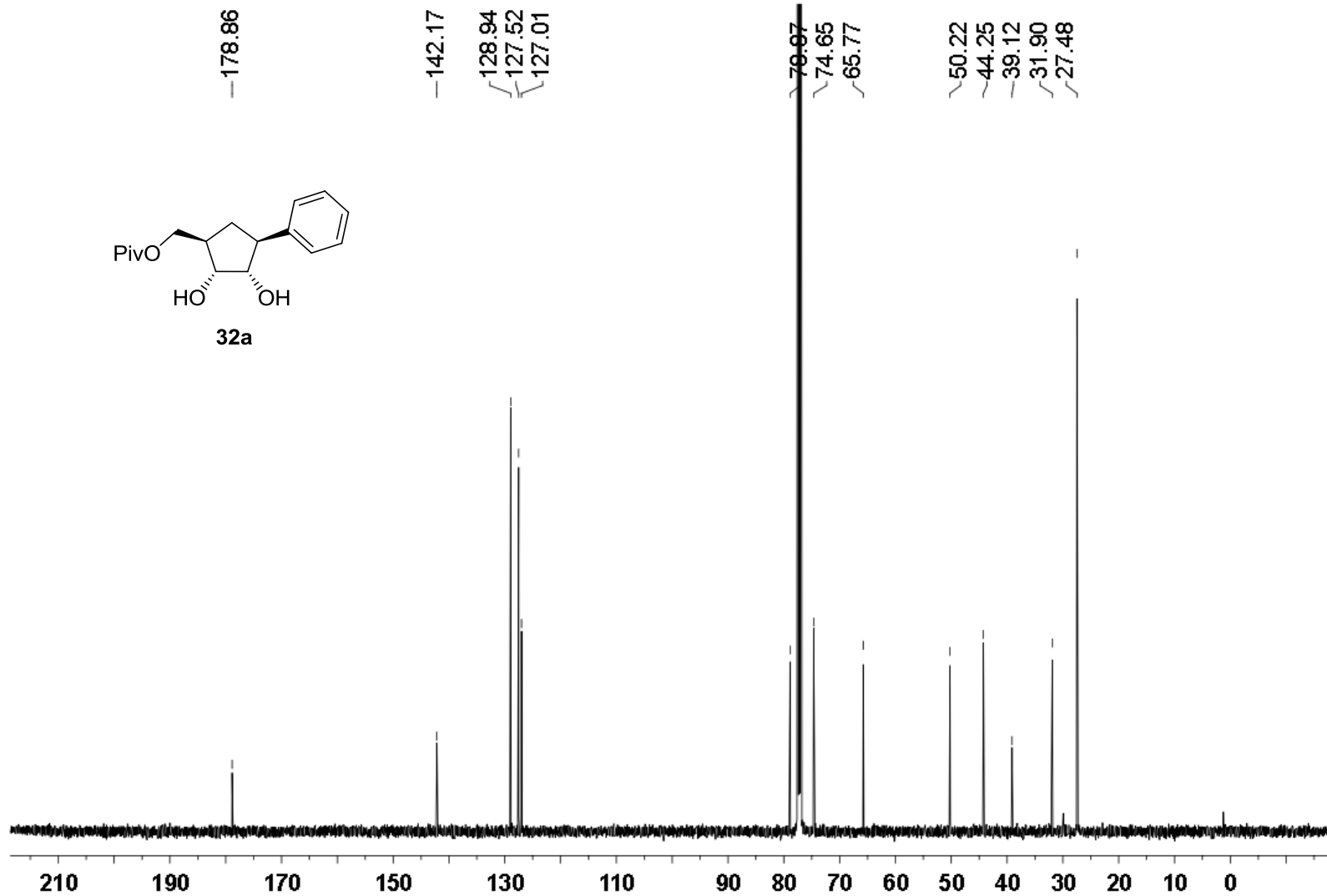
<sup>1</sup>H NMR (500 MHz) spectrum of **31a** in CDCl<sub>3</sub>



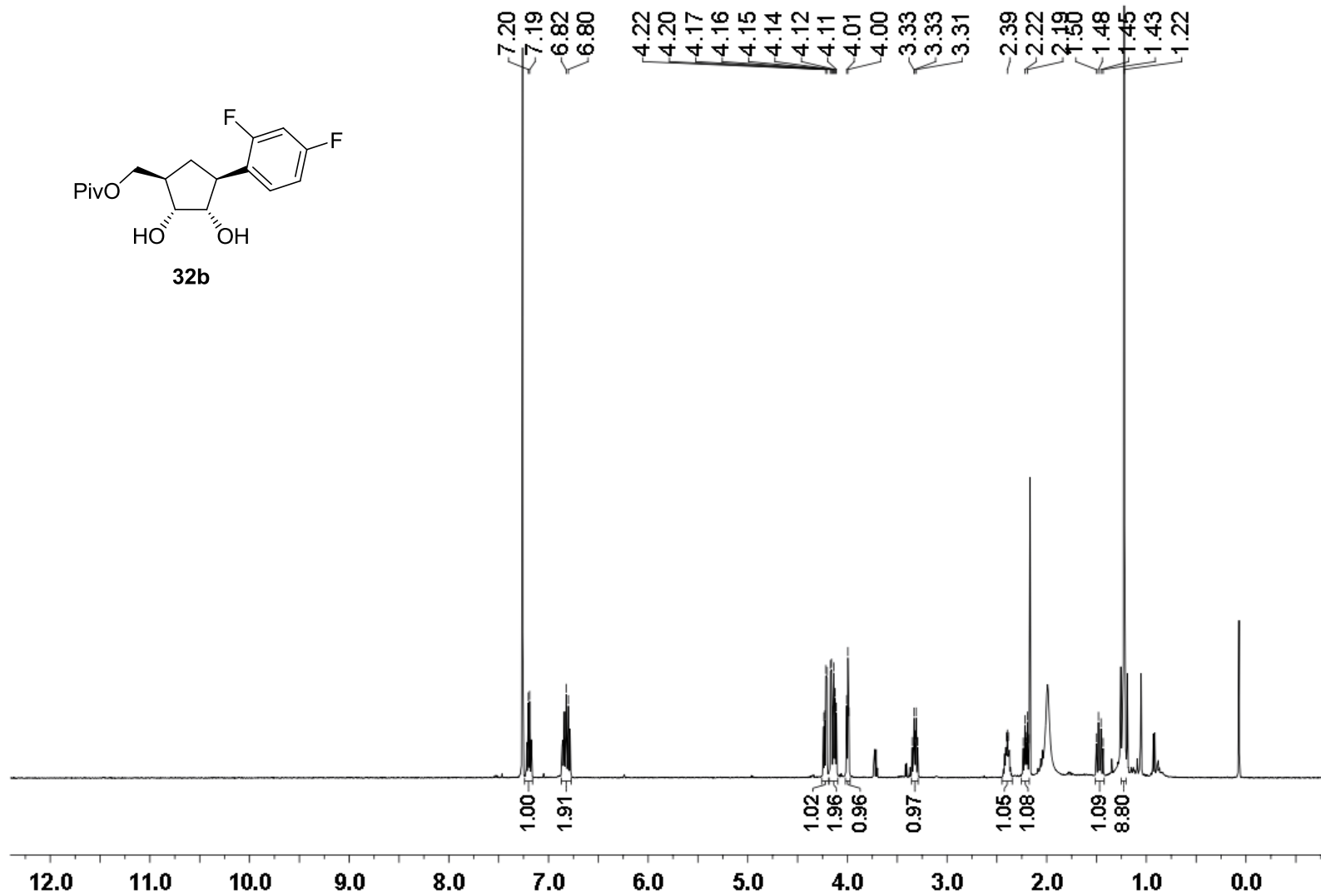
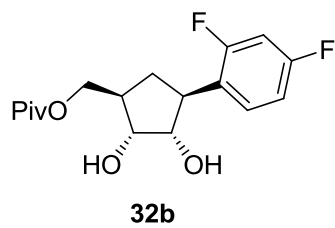
$^{13}\text{C}$  NMR (126 MHz) spectrum of **31a** in  $\text{CDCl}_3$



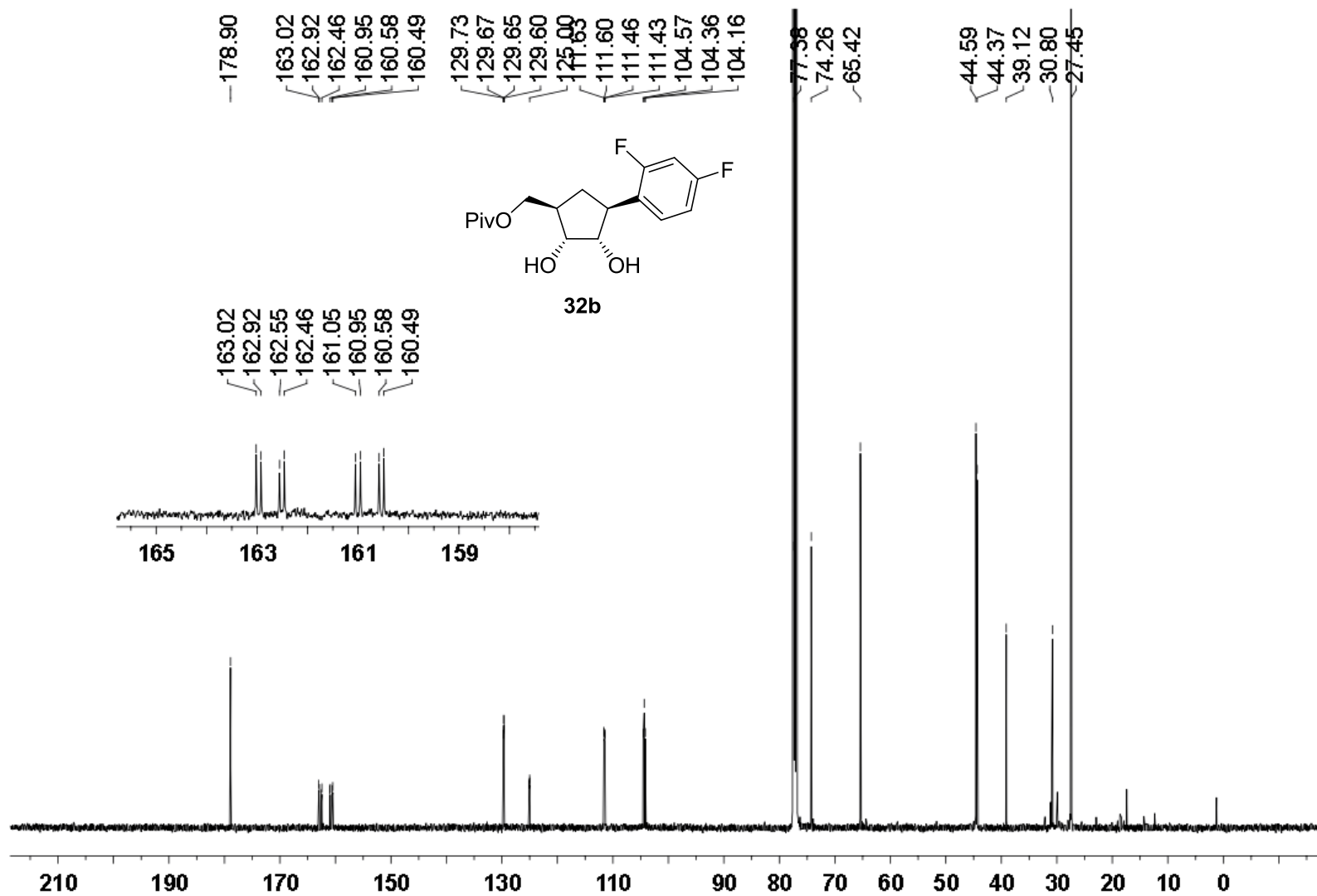
<sup>1</sup>H NMR (500 MHz) spectrum of **32a** in CDCl<sub>3</sub>



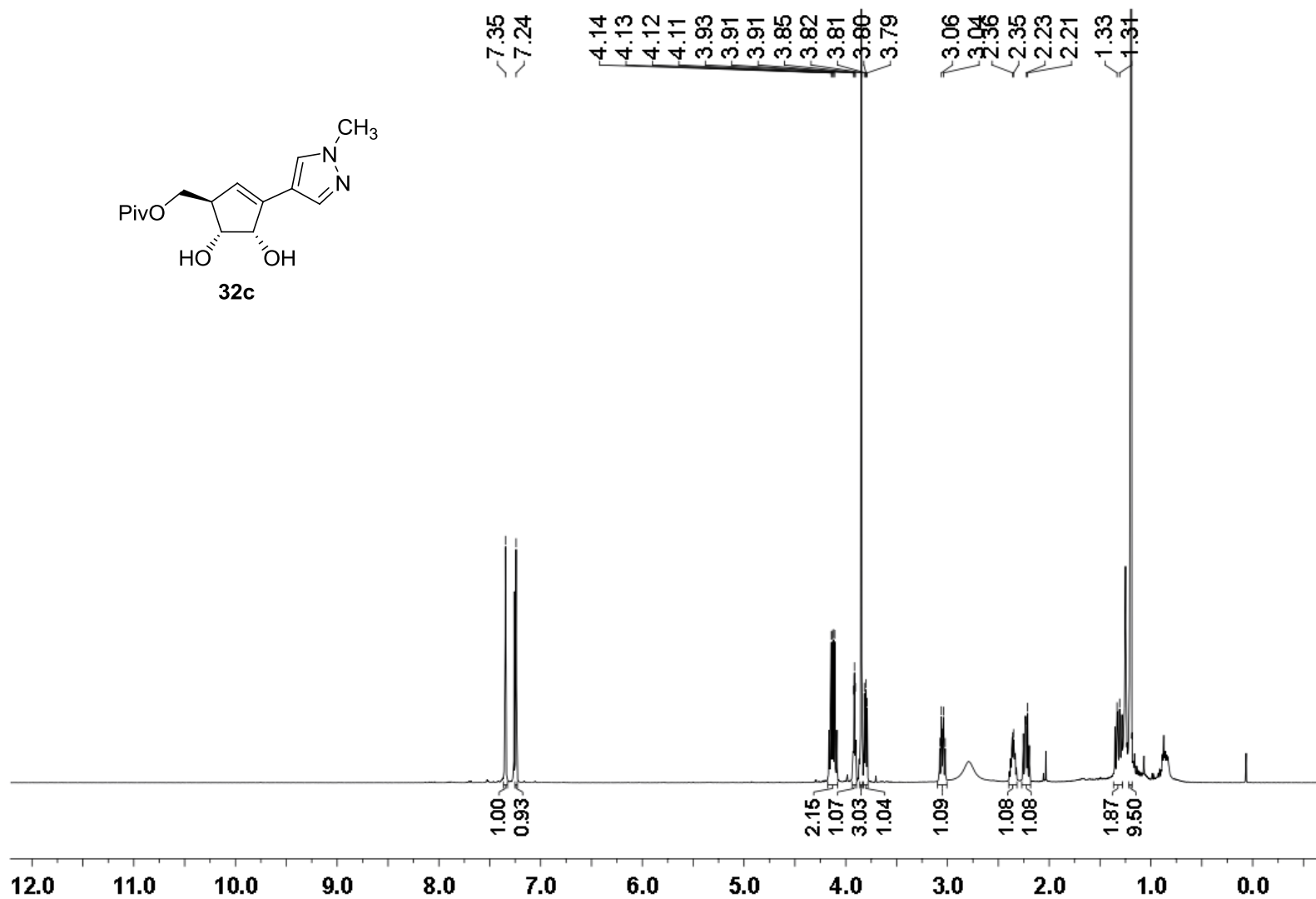
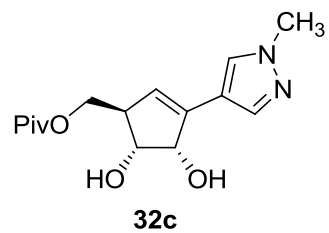
<sup>13</sup>C NMR (126 MHz) spectrum of **32a** in CDCl<sub>3</sub>



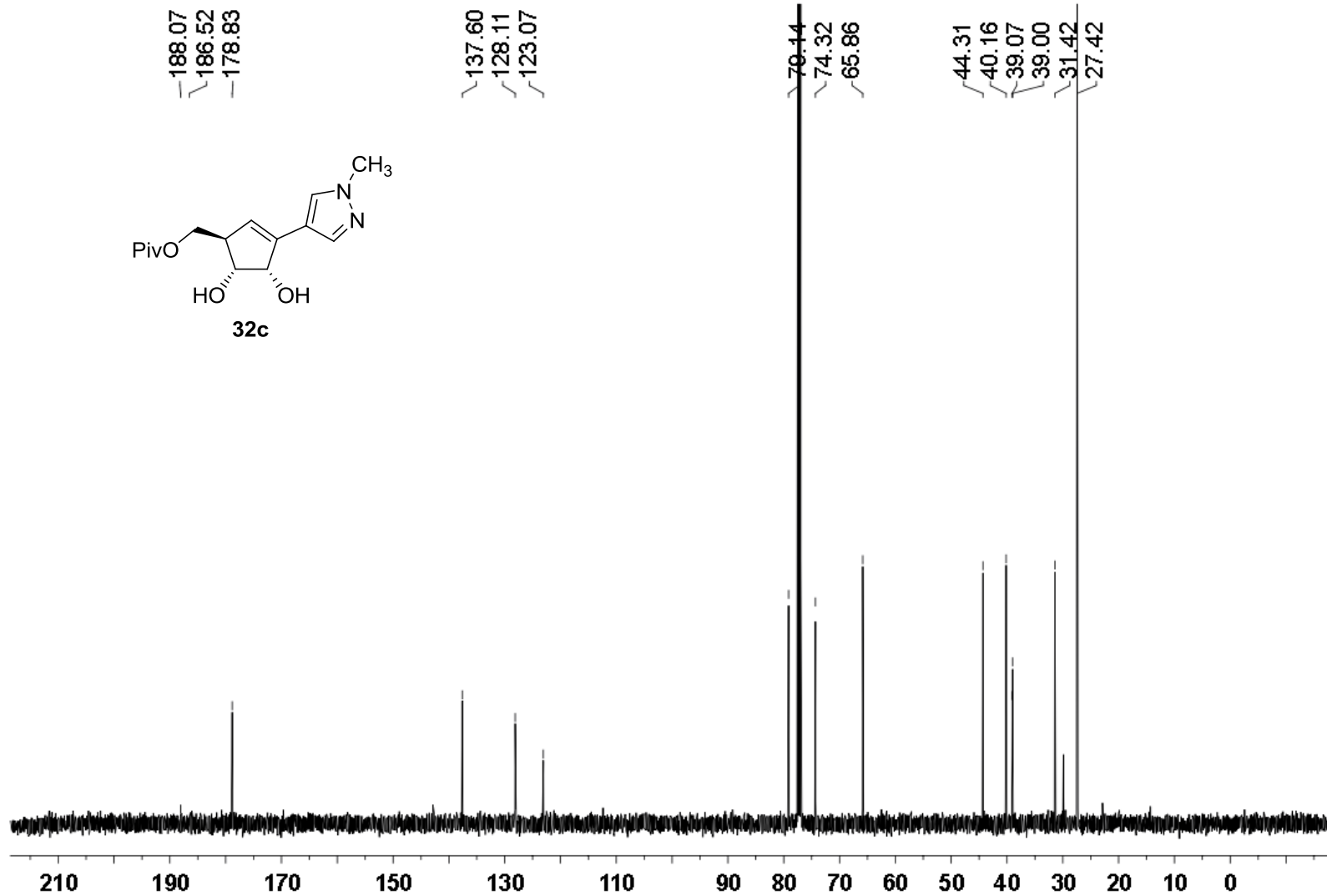
<sup>1</sup>H NMR (500 MHz) spectrum of **32b** in CDCl<sub>3</sub>



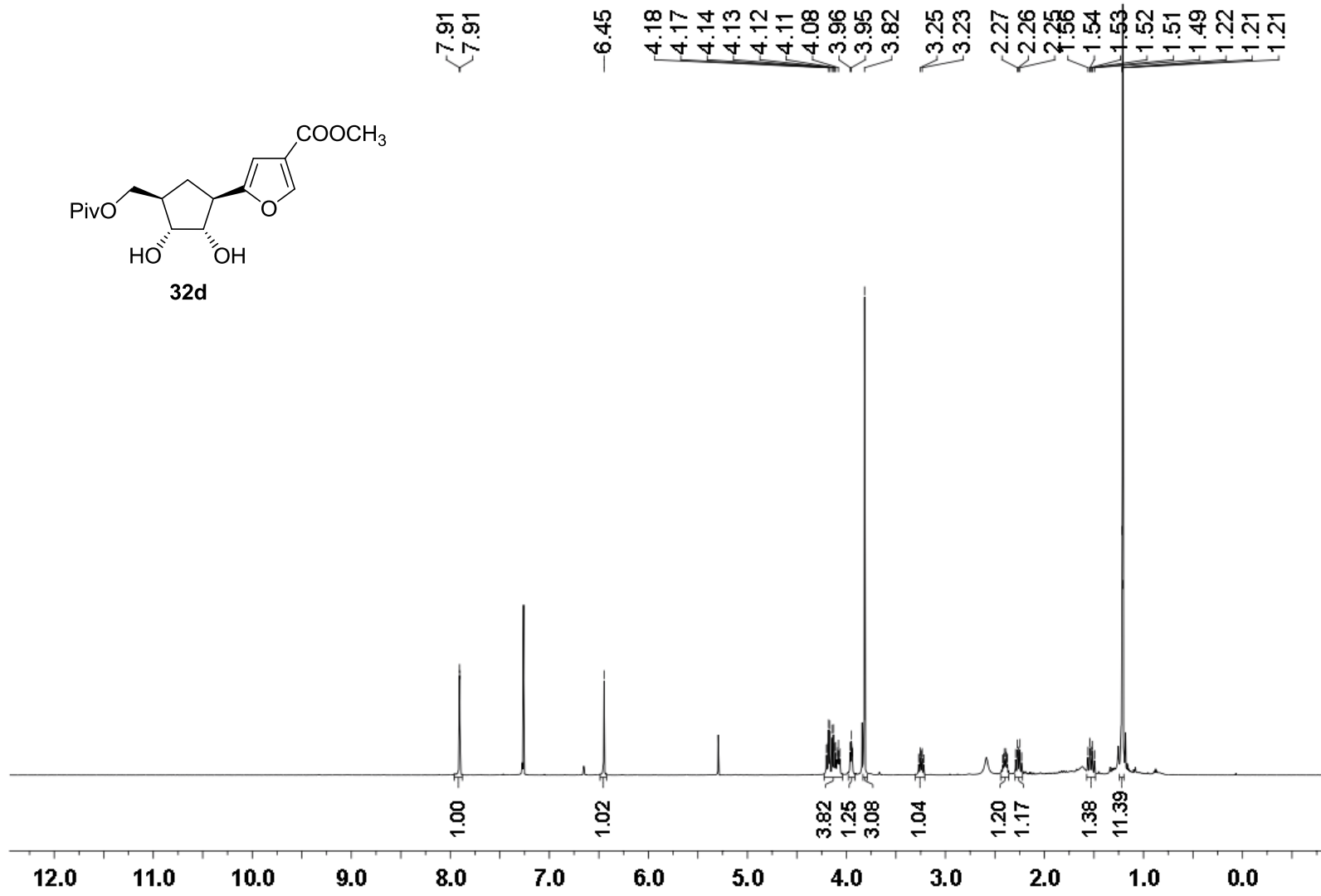
<sup>13</sup>C NMR (126 MHz) spectrum of **32b** in CDCl<sub>3</sub>



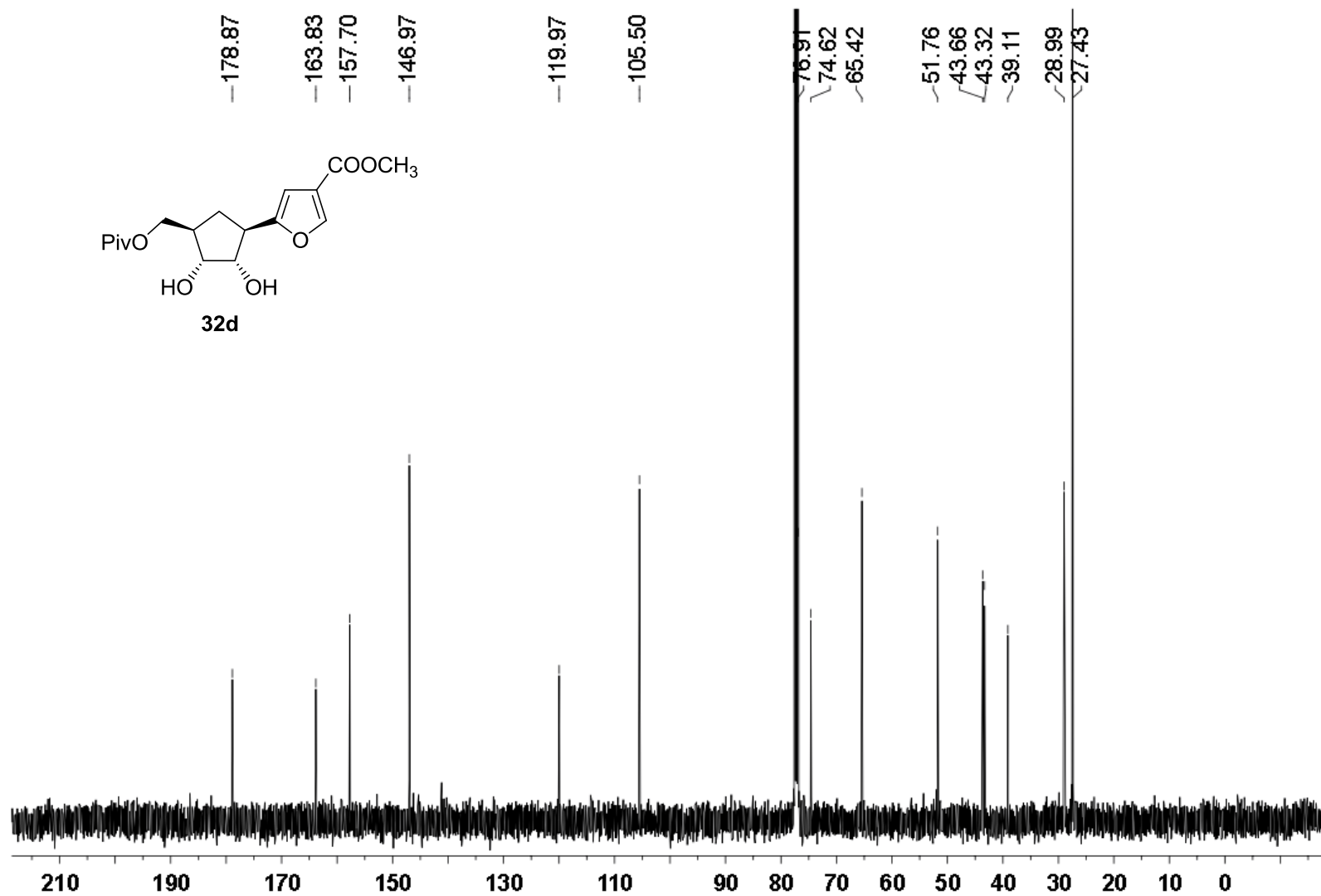
$^1\text{H}$  NMR (500 MHz) spectrum of **32c** in  $\text{CDCl}_3$



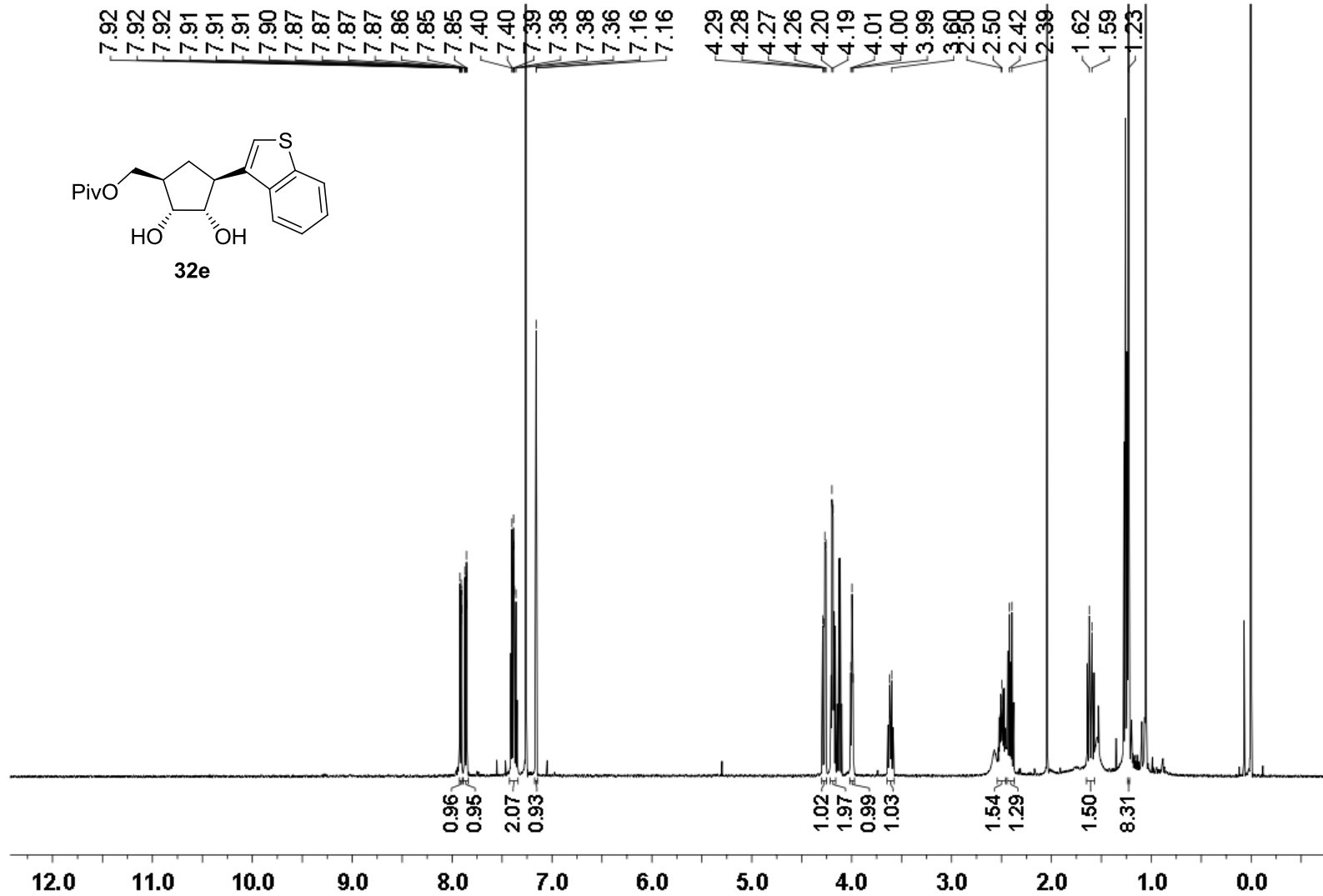
$^{13}\text{C}$  NMR (126 MHz) spectrum of **32c** in  $\text{CDCl}_3$



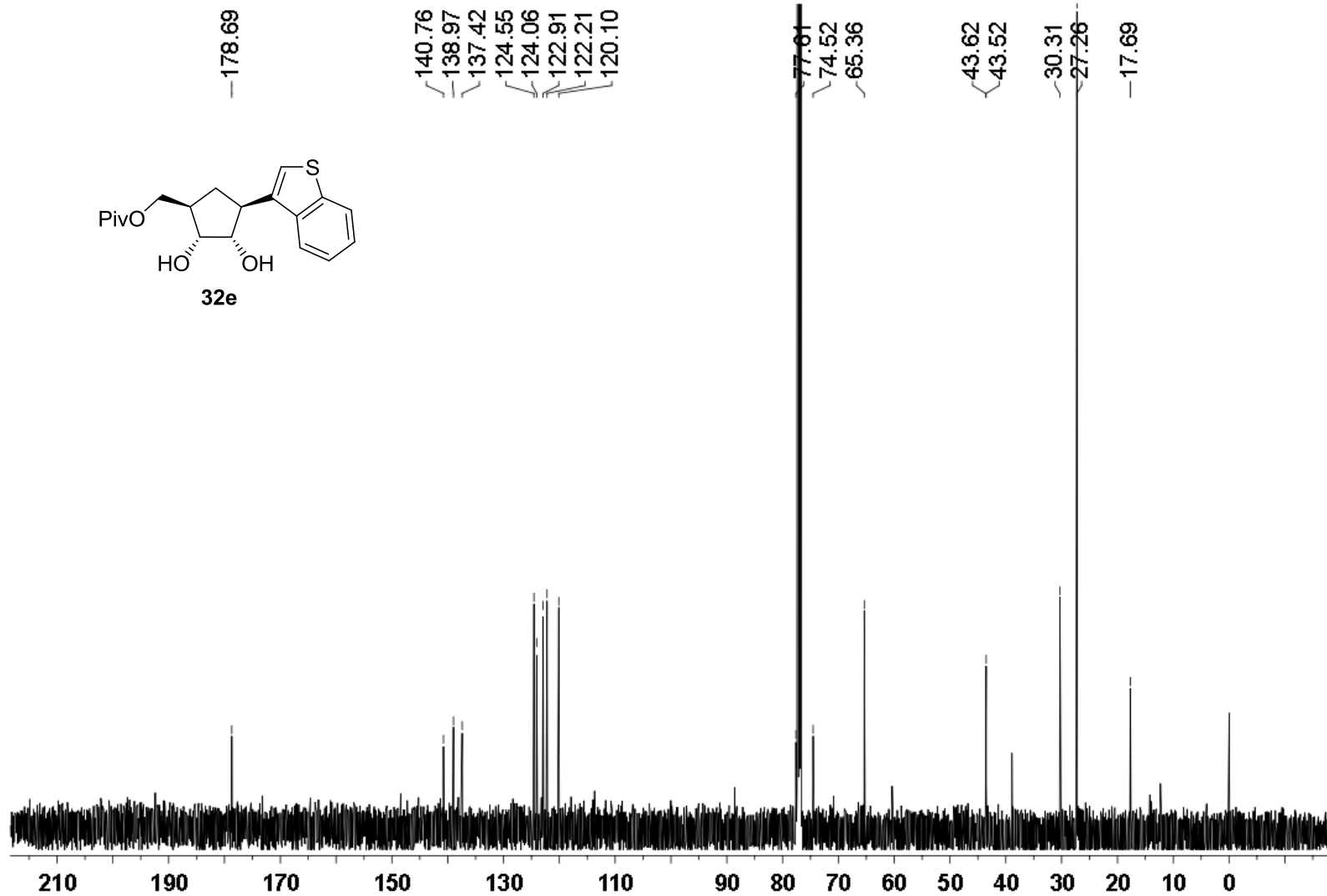
$^1\text{H}$  NMR (500 MHz) spectrum of **32d** in  $\text{CDCl}_3$



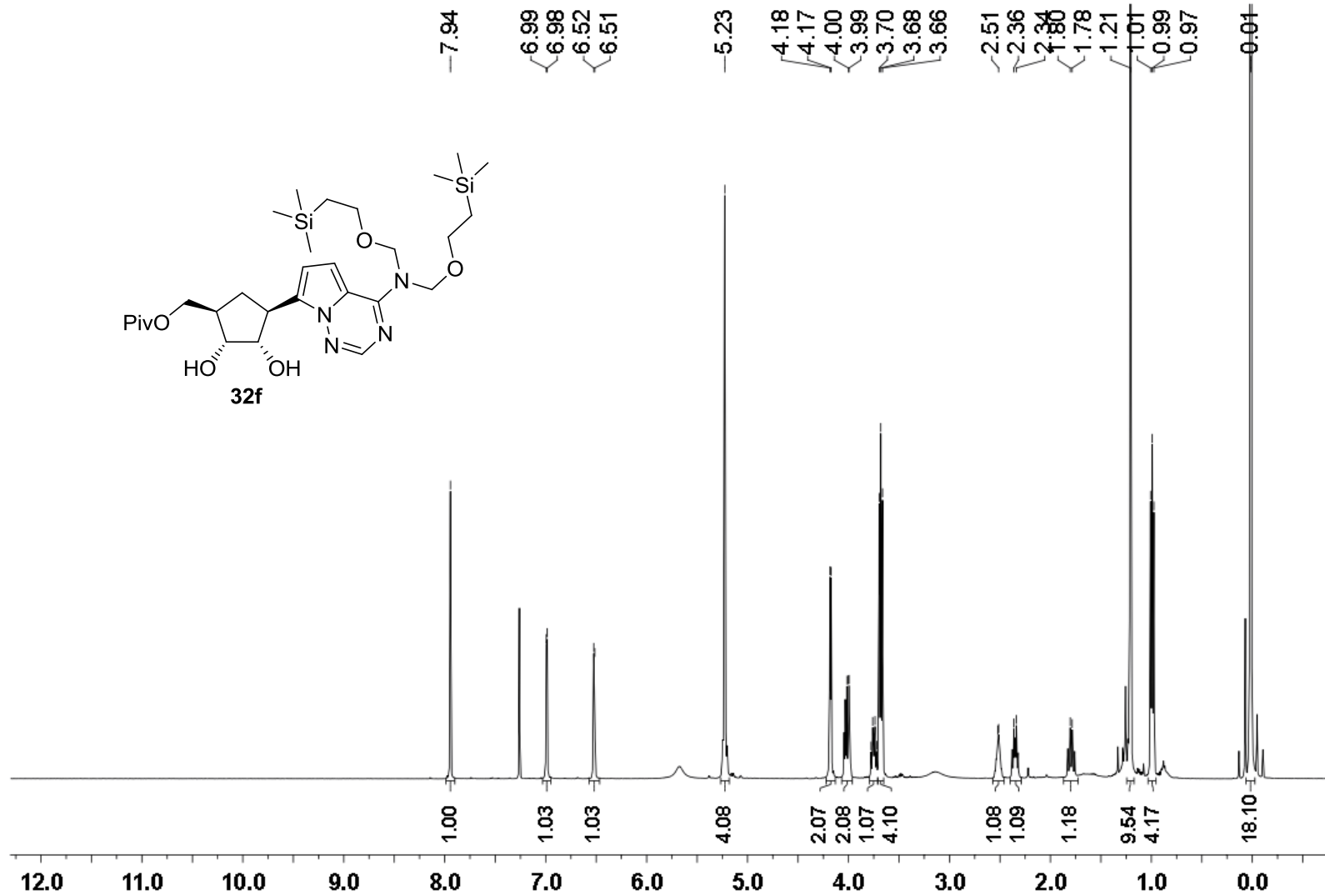
<sup>13</sup>C NMR (126 MHz) spectrum of **32d** in CDCl<sub>3</sub>



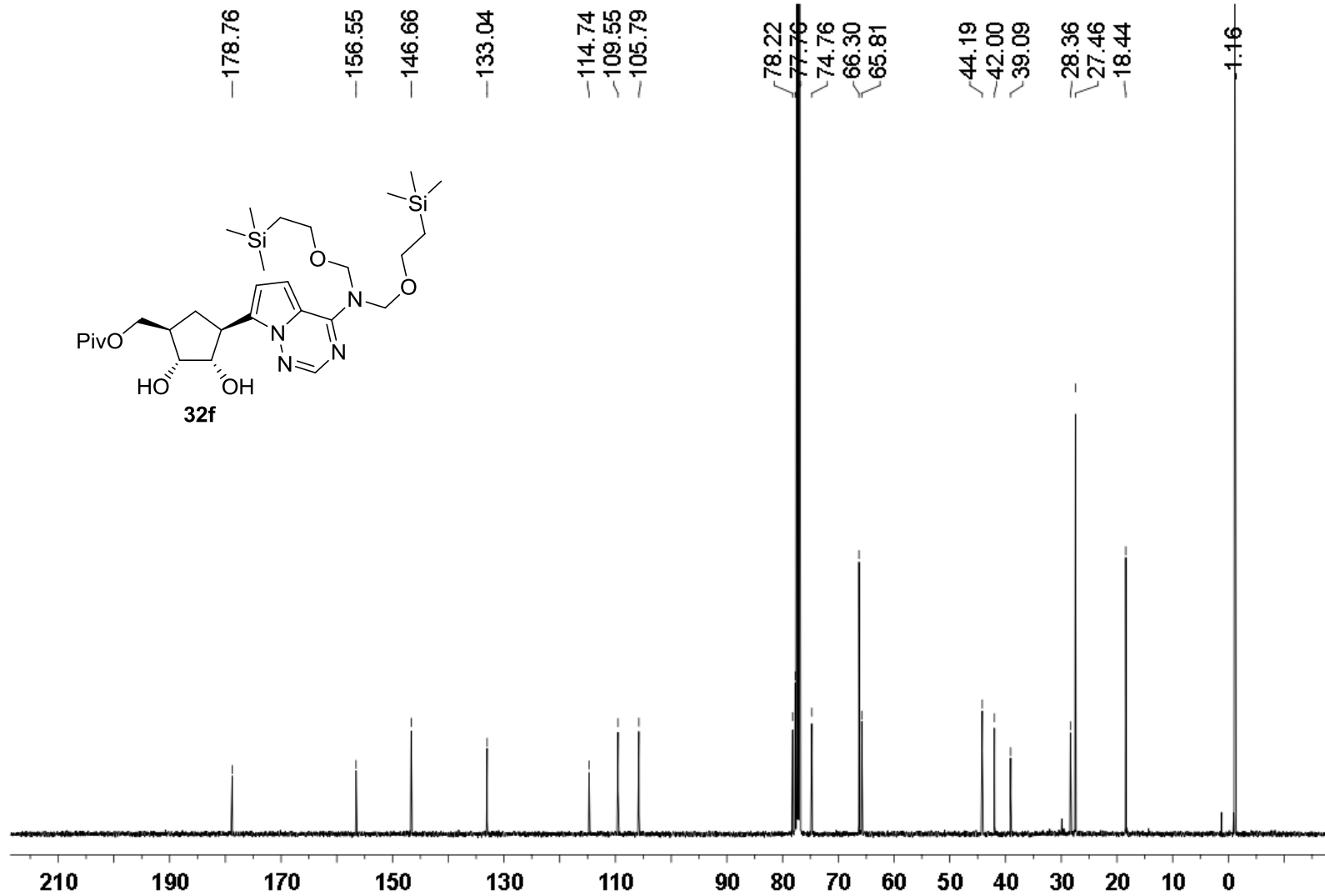
<sup>1</sup>H NMR (500 MHz) spectrum of **32e** in CDCl<sub>3</sub>



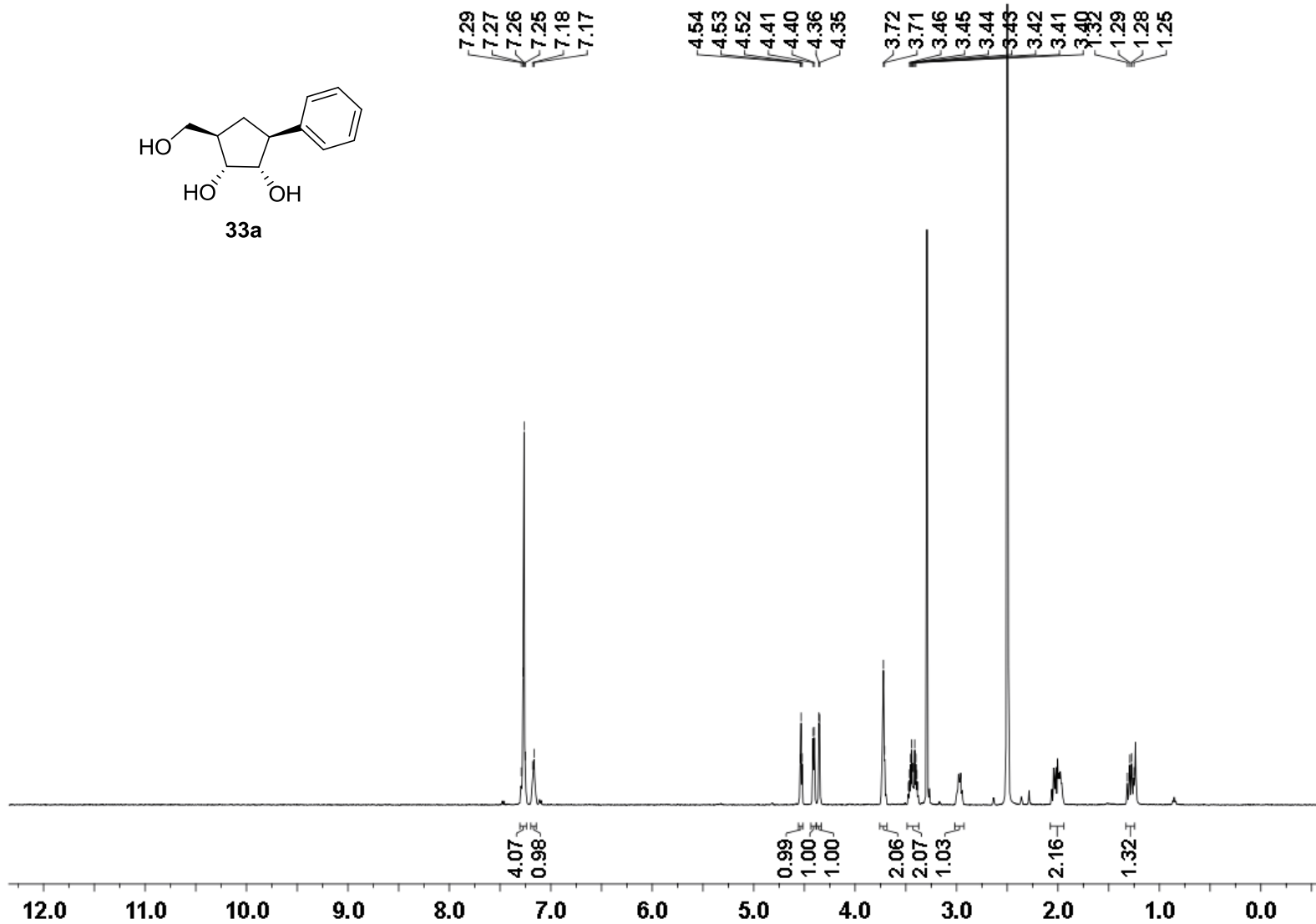
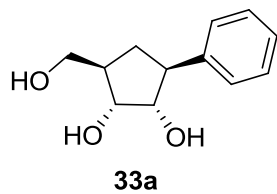
$^{13}\text{C}$  NMR (126 MHz) spectrum of **32e** in  $\text{CDCl}_3$



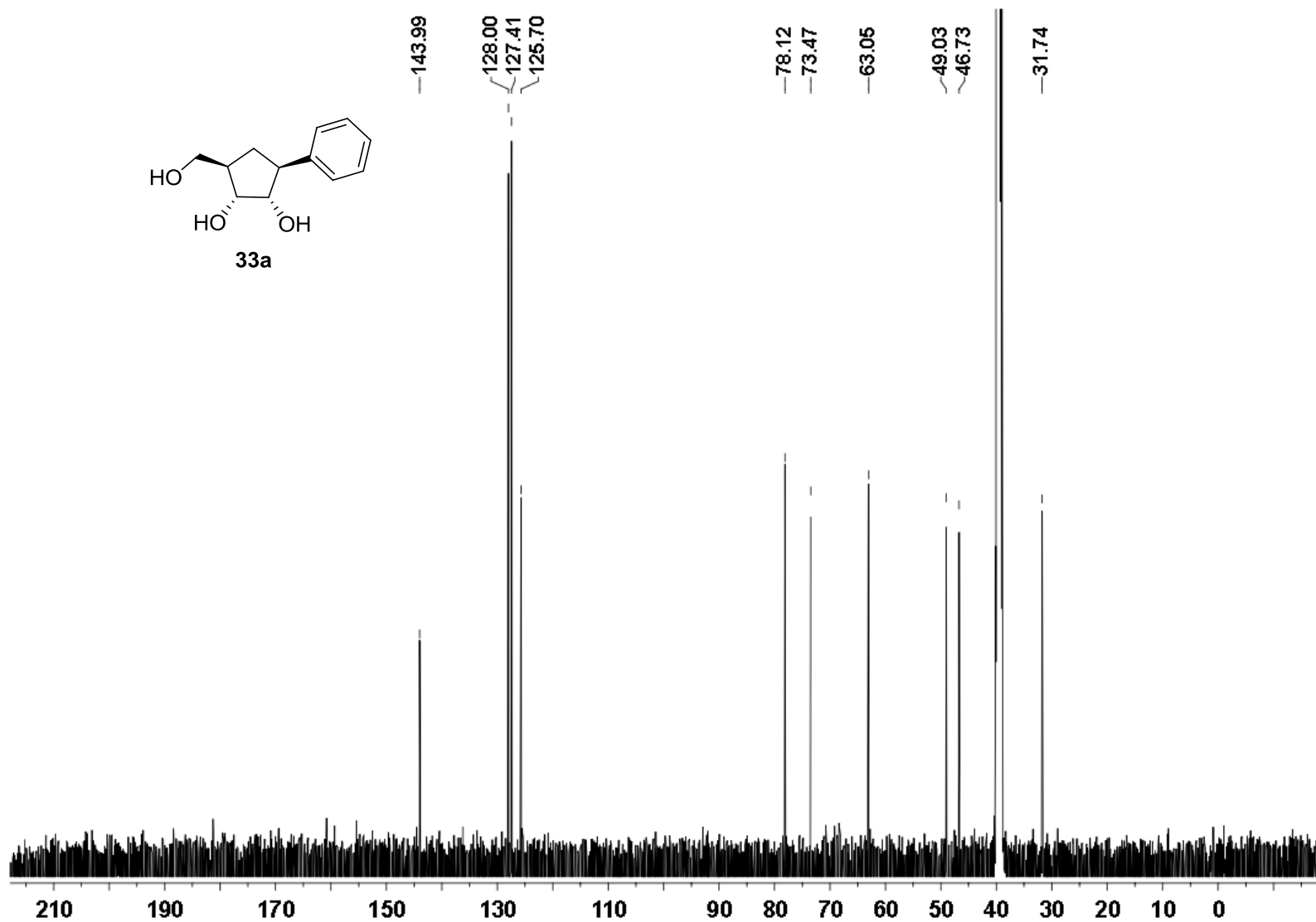
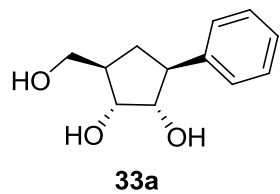
$^1\text{H}$  NMR (500 MHz) spectrum of **32f** in  $\text{CDCl}_3$



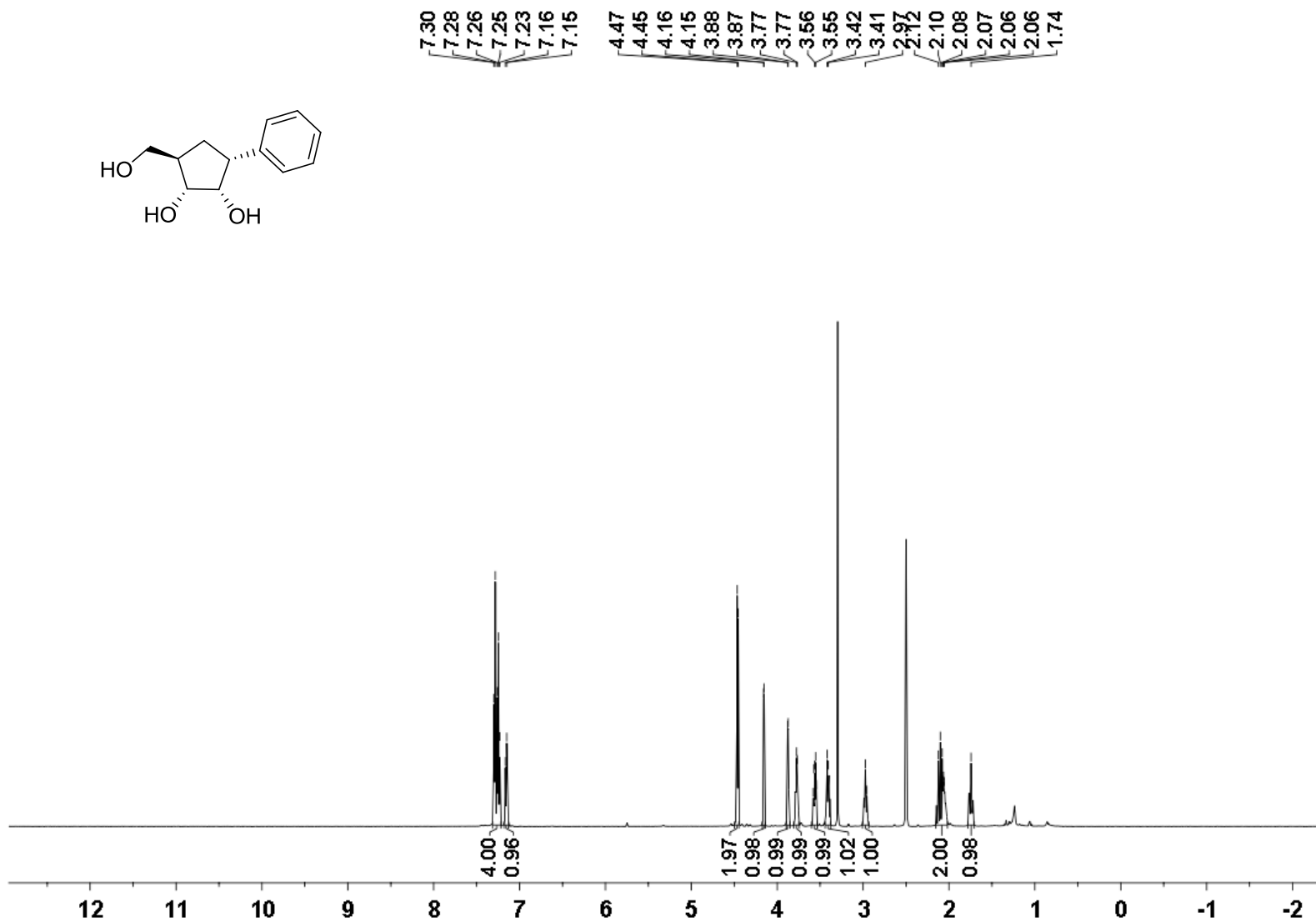
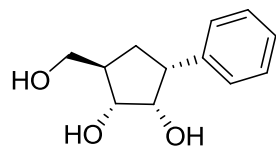
$^{13}\text{C}$  NMR (500 MHz) spectrum of **32f** in  $\text{CDCl}_3$



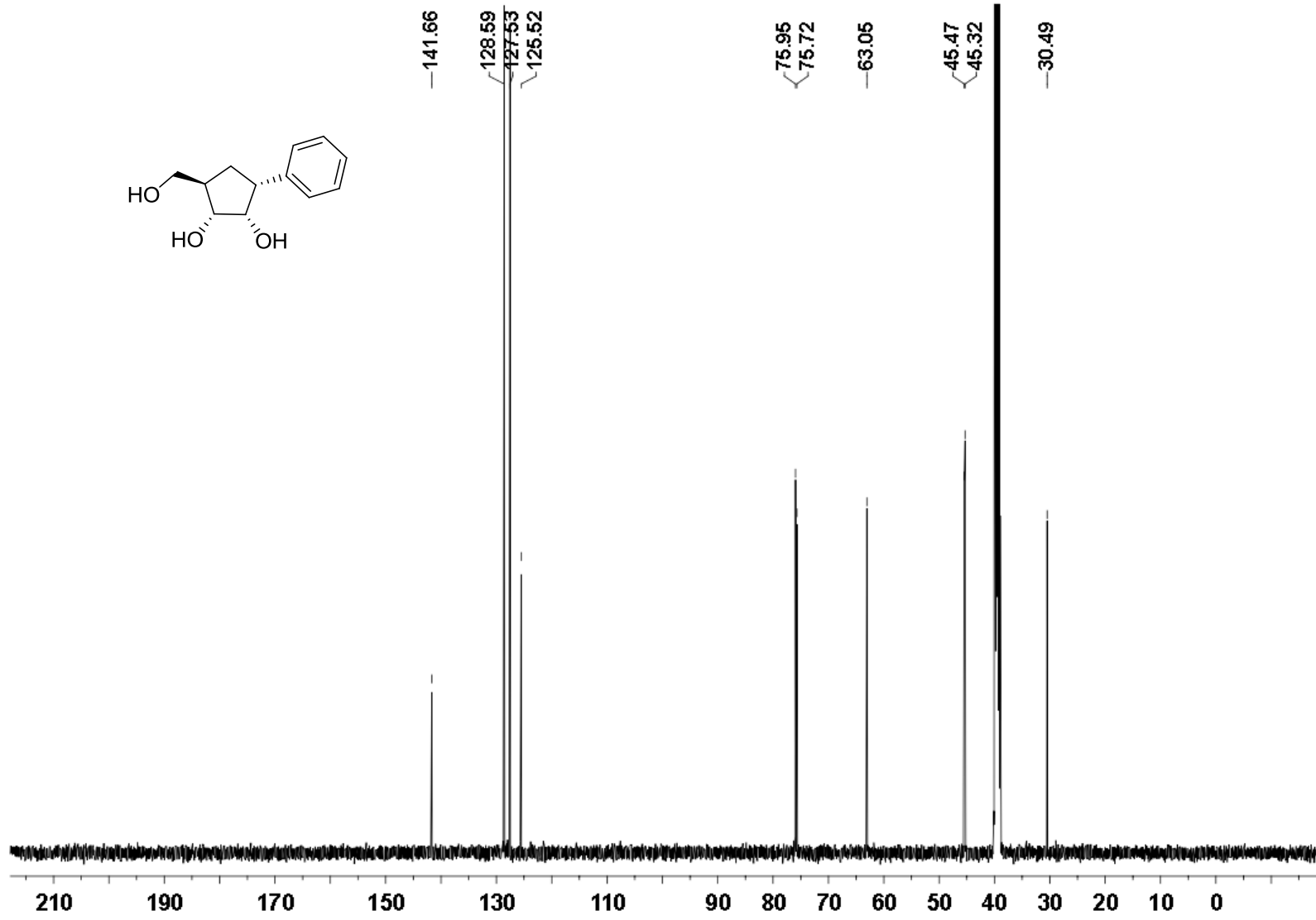
$^1\text{H}$  NMR (500 MHz) spectrum of **33a** in  $\text{DMSO-}d_6$



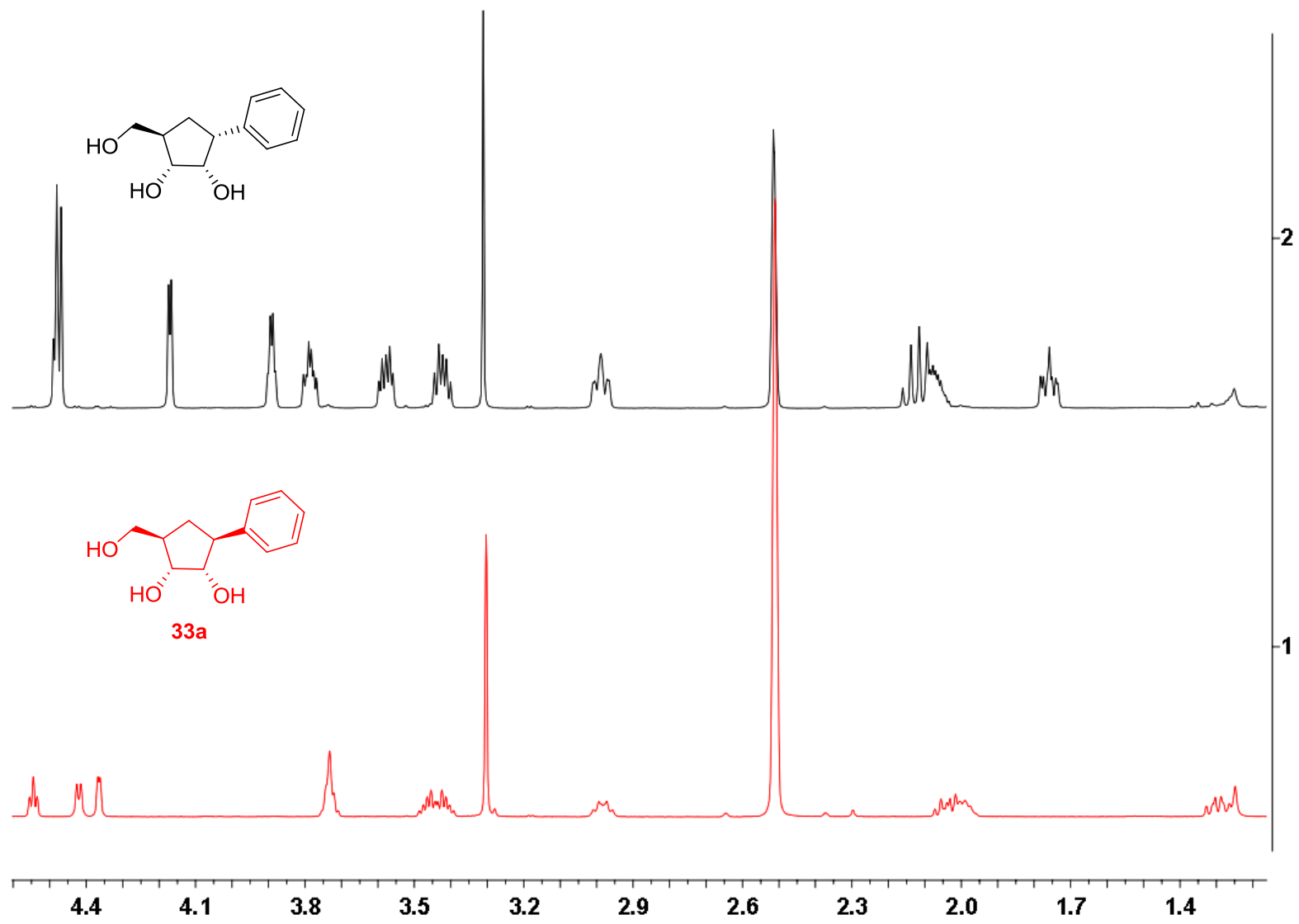
$^{13}\text{C}$  NMR (126 MHz) spectrum of **33a** in  $\text{DMSO-}d_6$



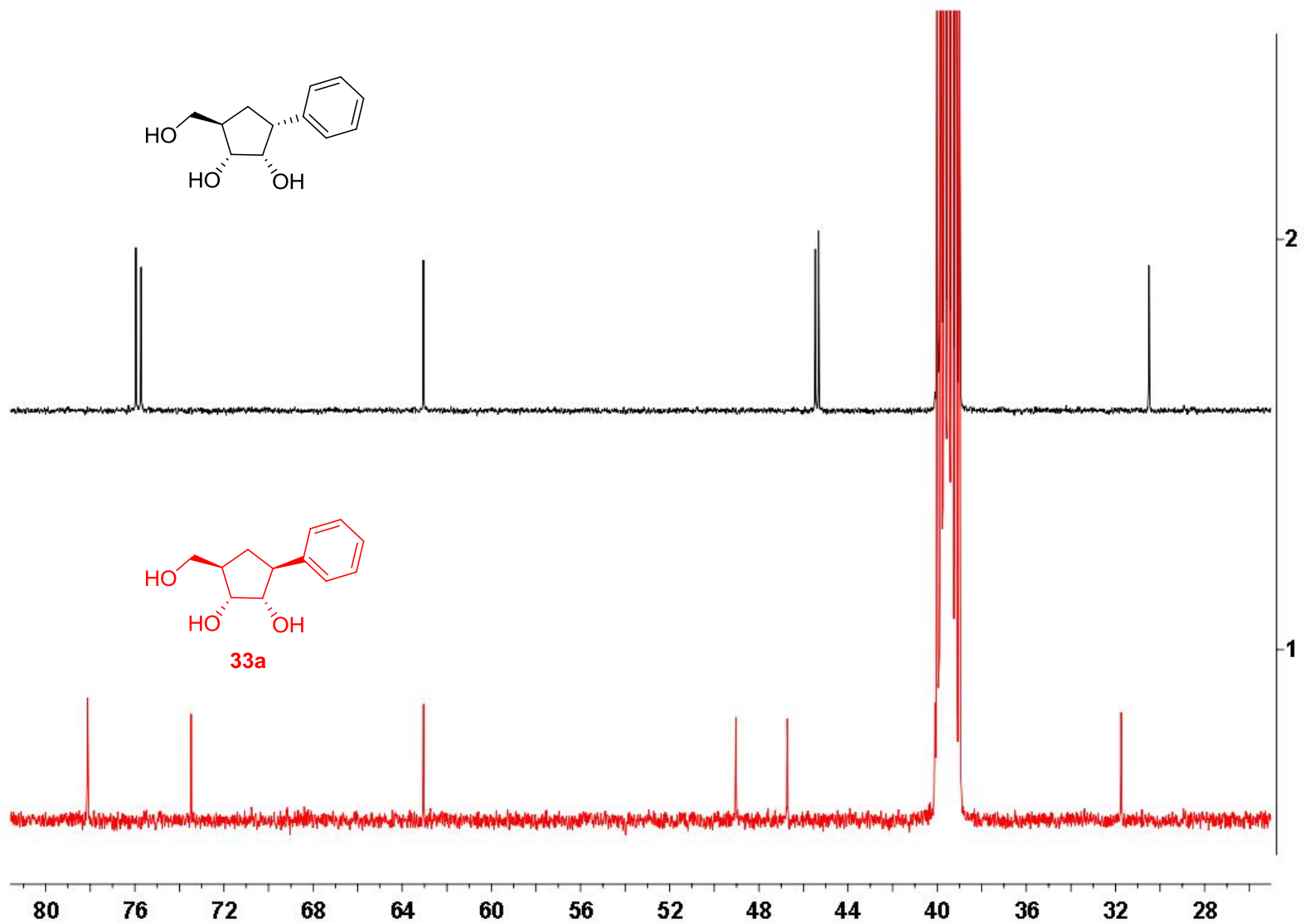
$^1\text{H}$  NMR (500 MHz) spectrum in  $\text{DMSO-}d_6$



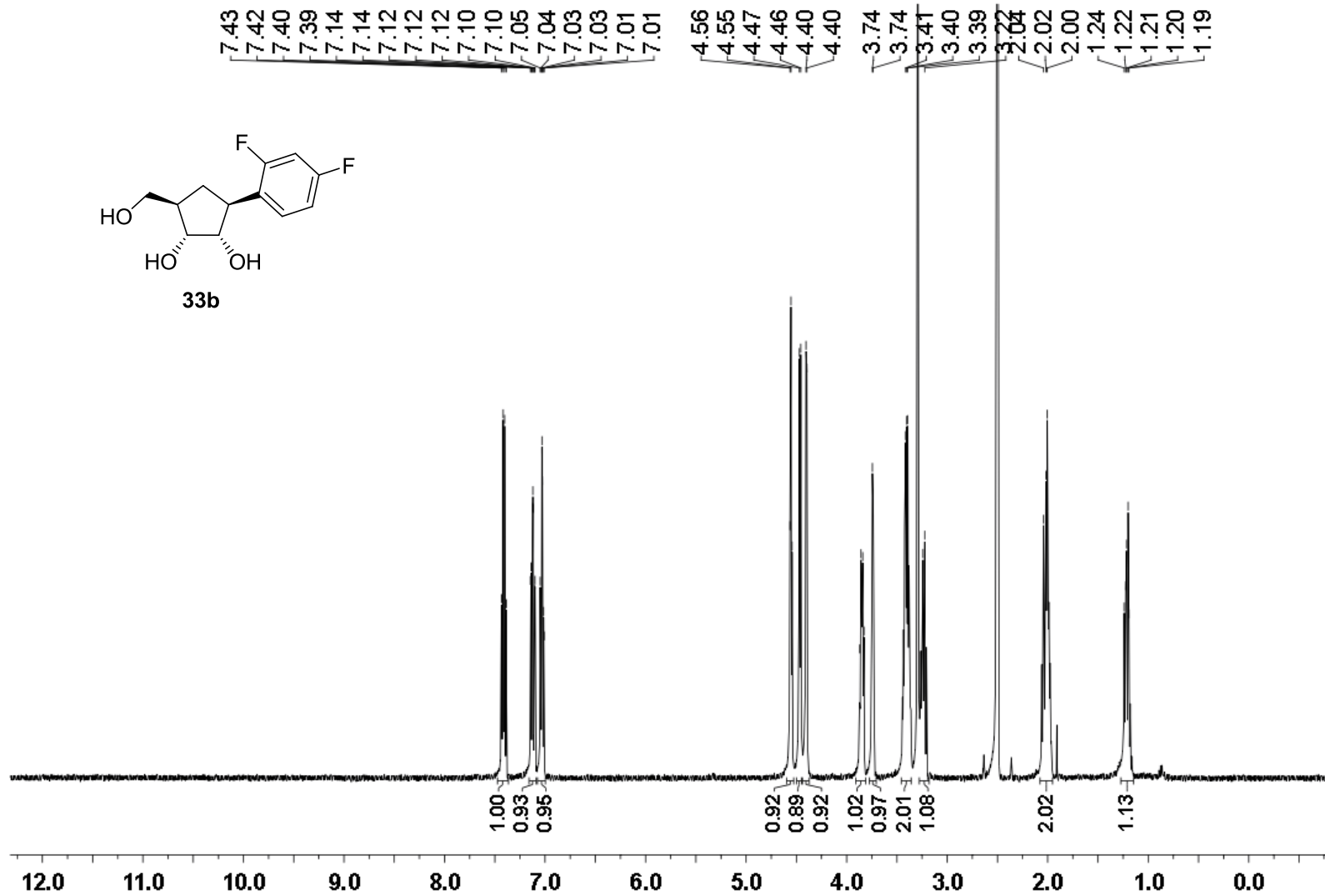
$^{13}\text{C}$  NMR (126 MHz) spectrum in  $\text{DMSO-}d_6$



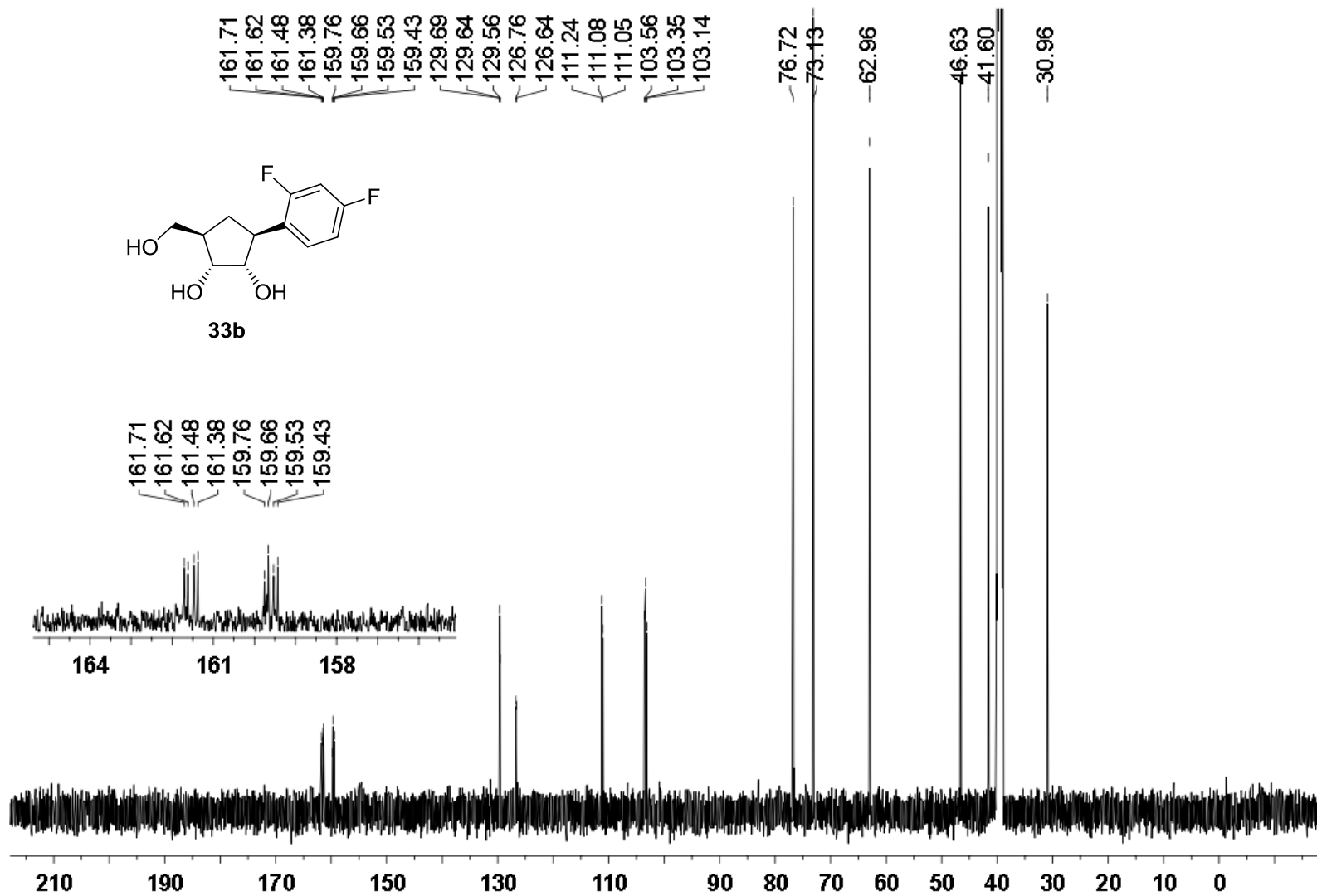
Comparison of <sup>1</sup>H NMR resonances for **33a** and corresponding epimer



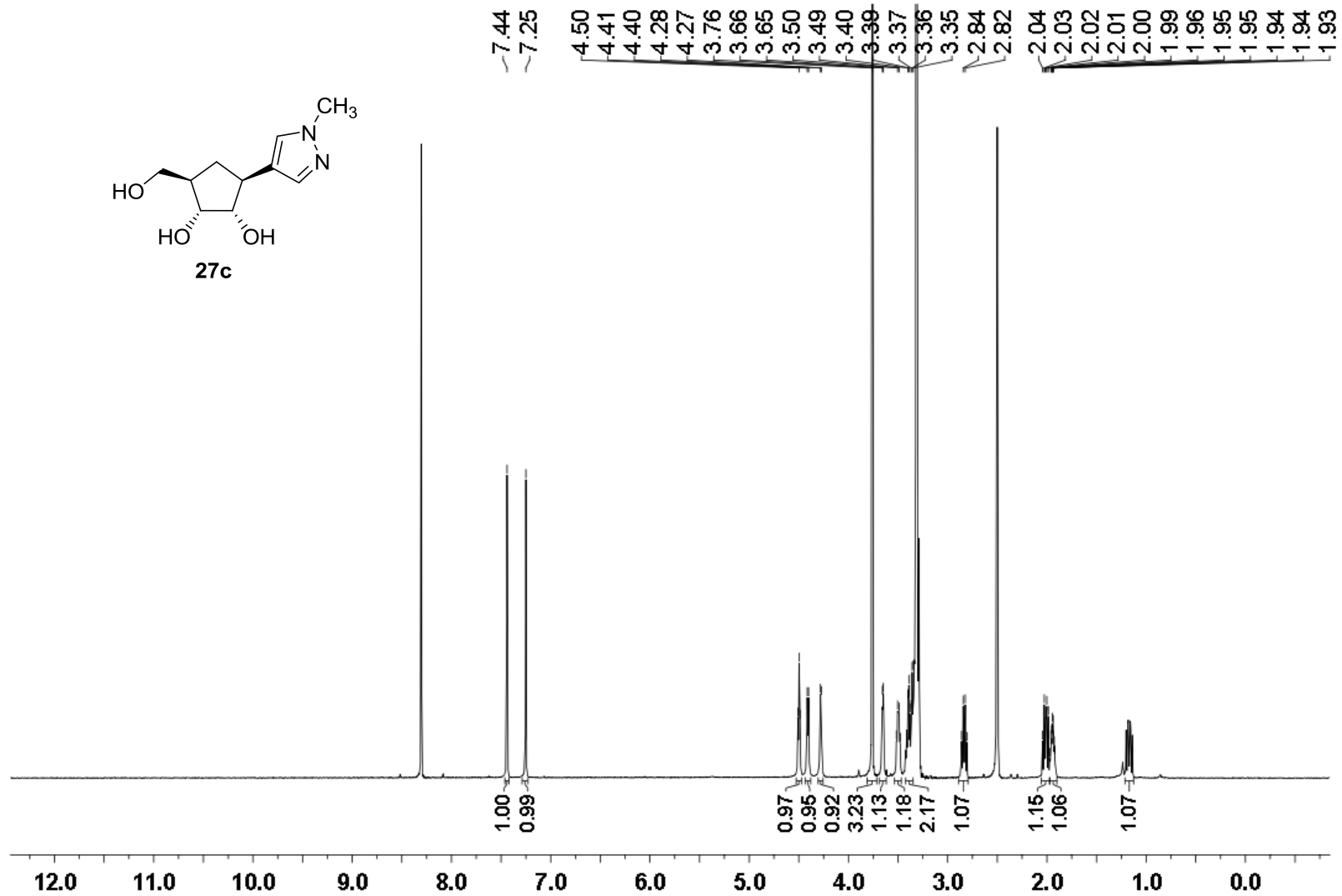
Comparison of <sup>13</sup>C NMR resonances for **33a** and corresponding epimer



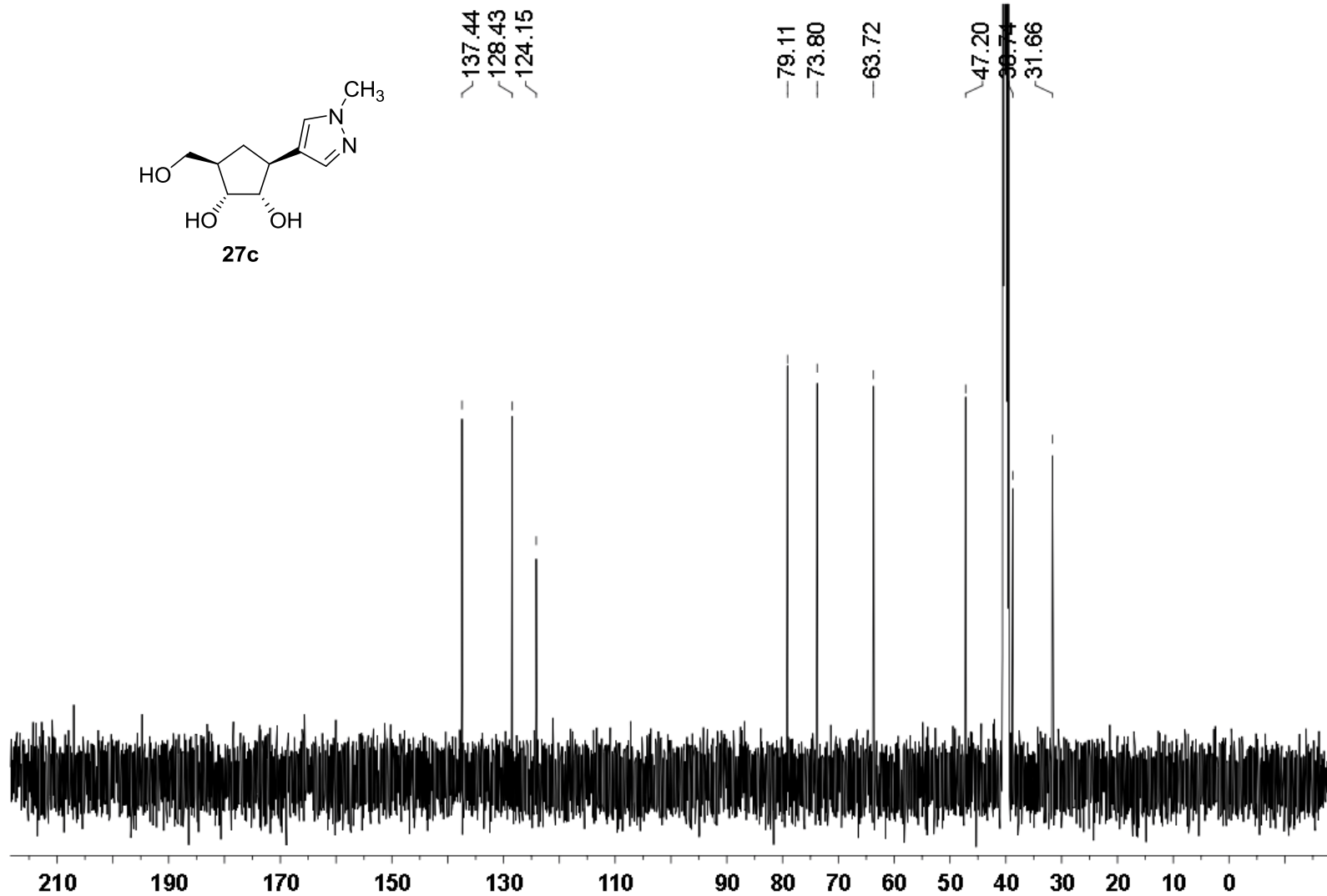
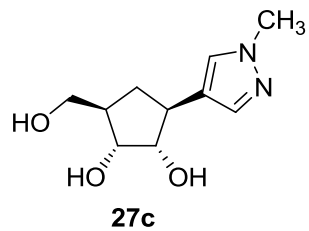
<sup>1</sup>H NMR (500 MHz) spectrum of **33b** in DMSO-*d*<sub>6</sub>



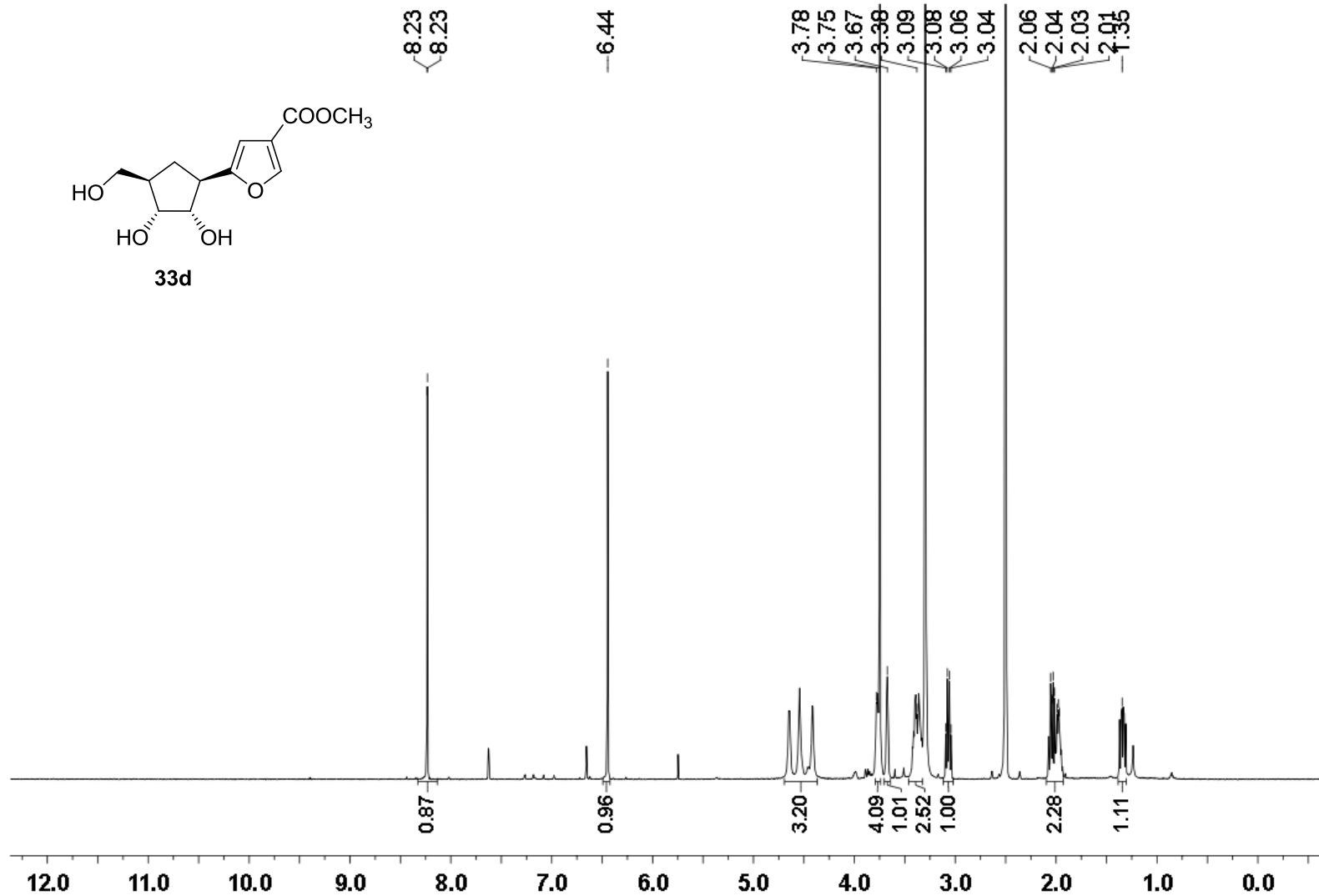
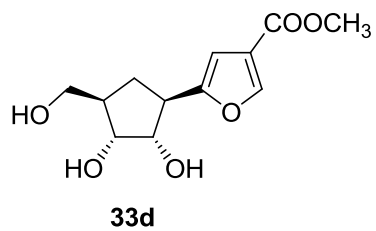
$^{13}\text{C}$  NMR (126 MHz) spectrum of **33b** in  $\text{DMSO-}d_6$



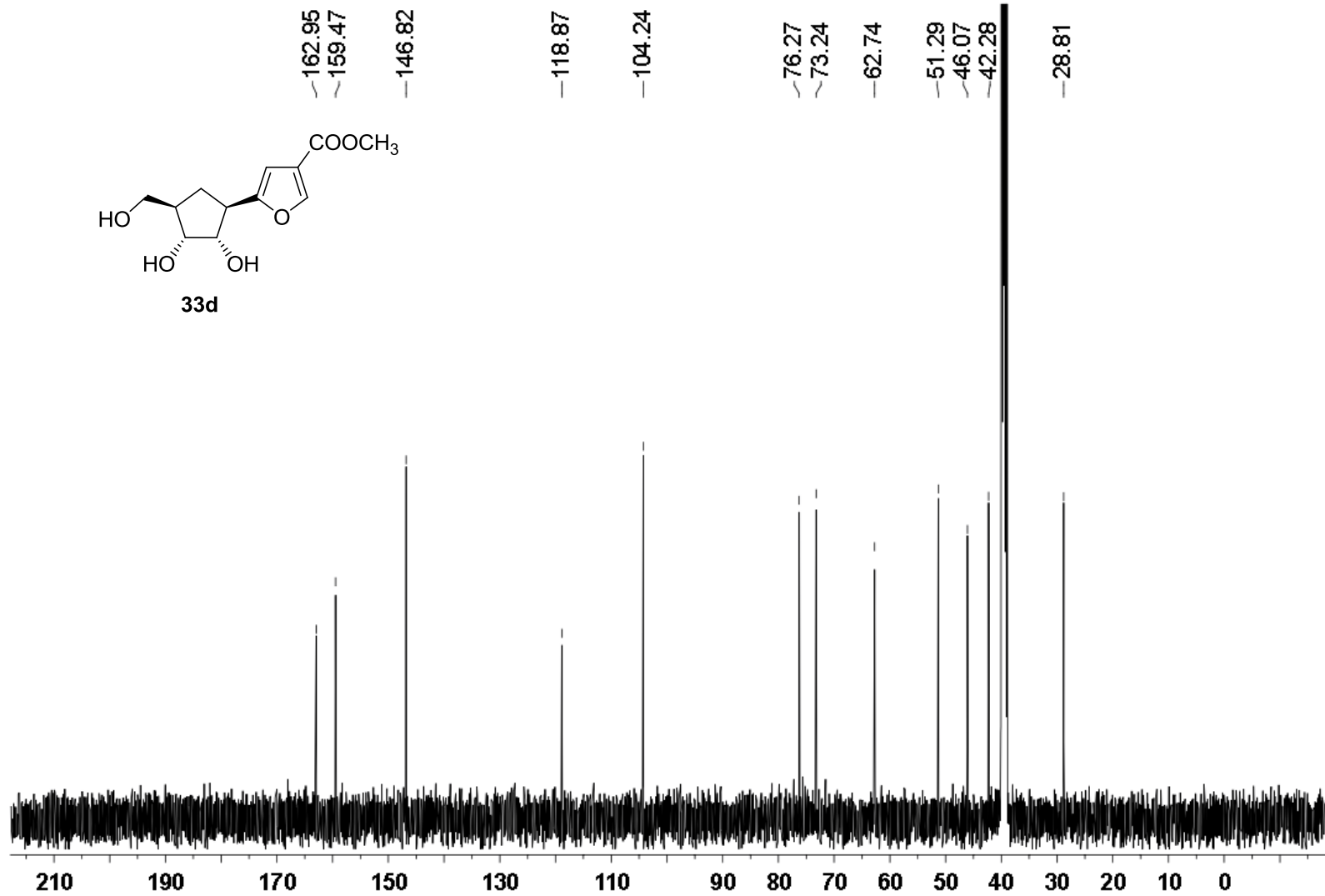
<sup>1</sup>H NMR (500 MHz) spectrum of **27c** in DMSO-*d*<sub>6</sub> + CDCl<sub>3</sub>



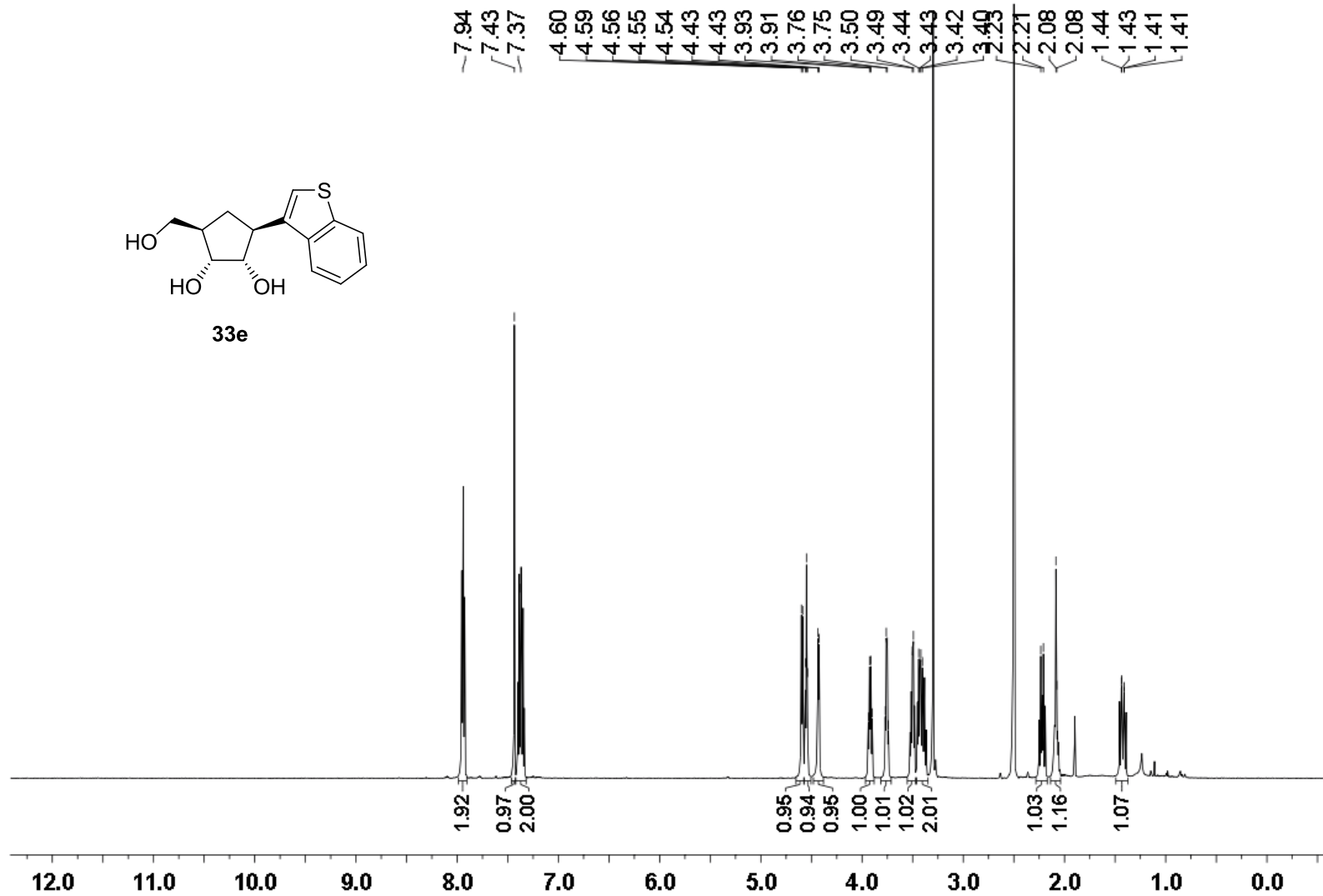
$^{13}\text{C}$  NMR (126 MHz) spectrum of **27c** in DMSO- $d_6$  +  $\text{CDCl}_3$



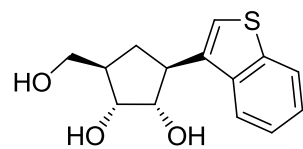
$^1\text{H}$  NMR (500 MHz) spectrum of **33d** in  $\text{DMSO-}d_6$



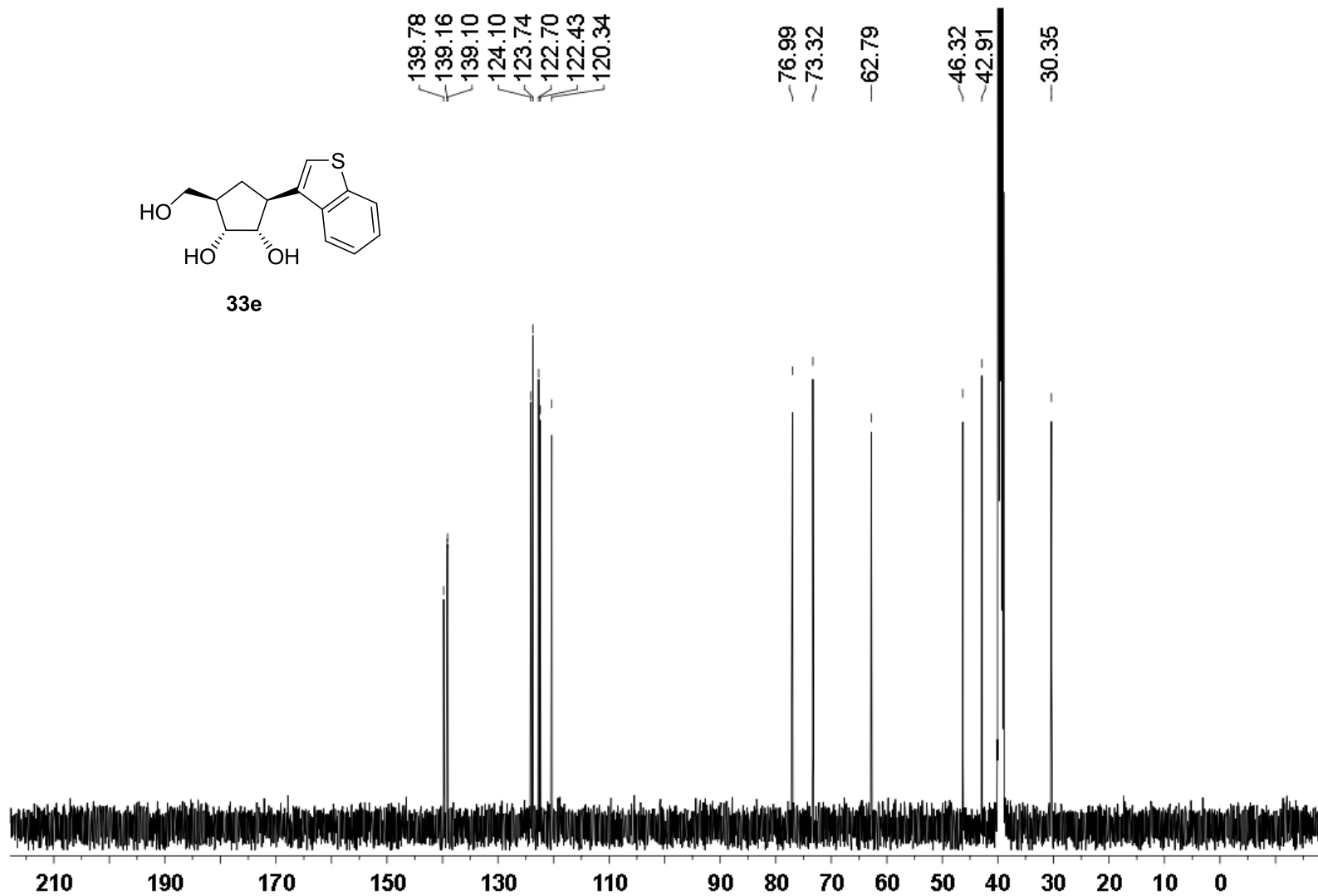
$^{13}\text{C}$  NMR (126 MHz) spectrum of **33d** in  $\text{DMSO-}d_6$



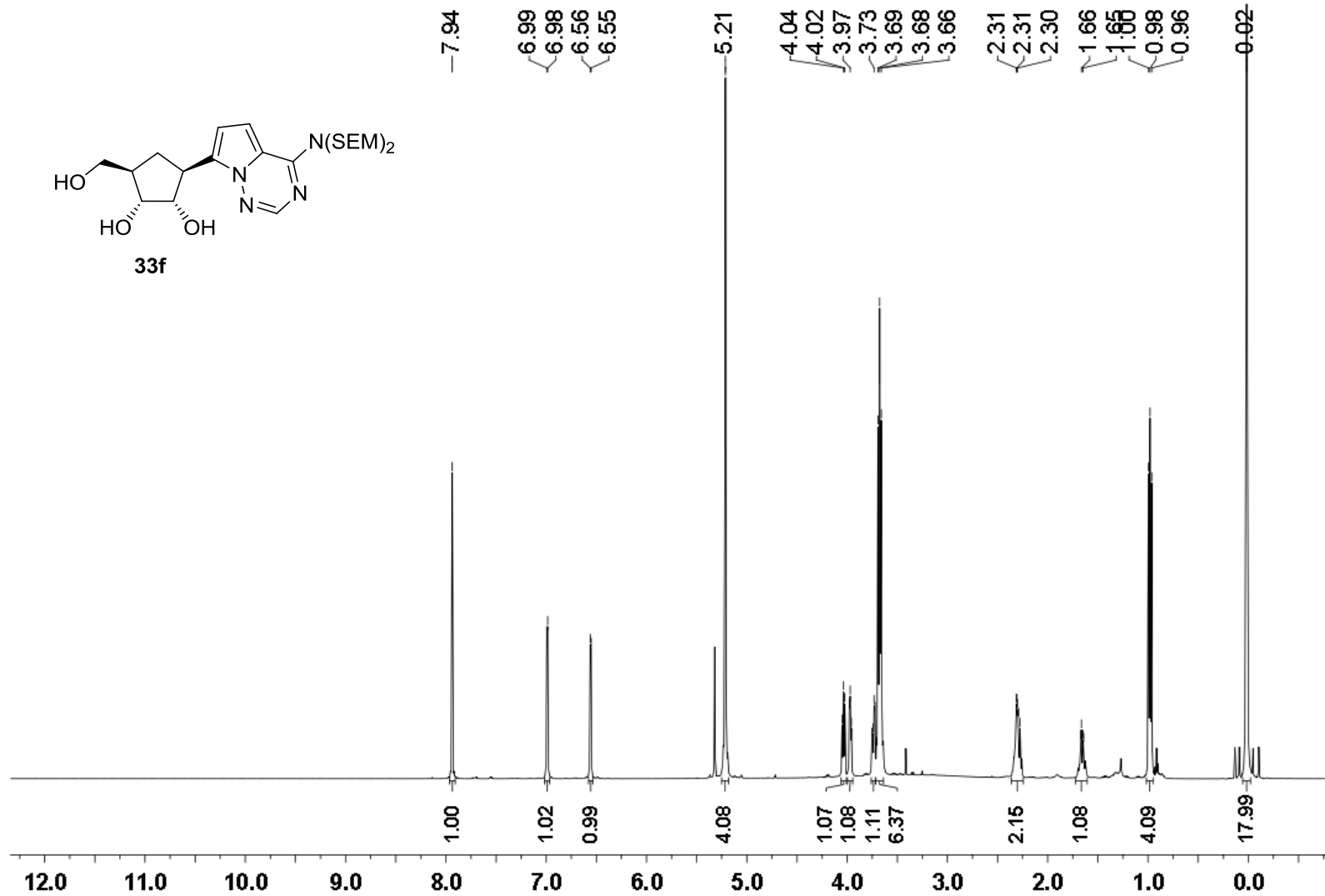
<sup>1</sup>H NMR (500 MHz) spectrum of **33e** in DMSO-*d*<sub>6</sub>



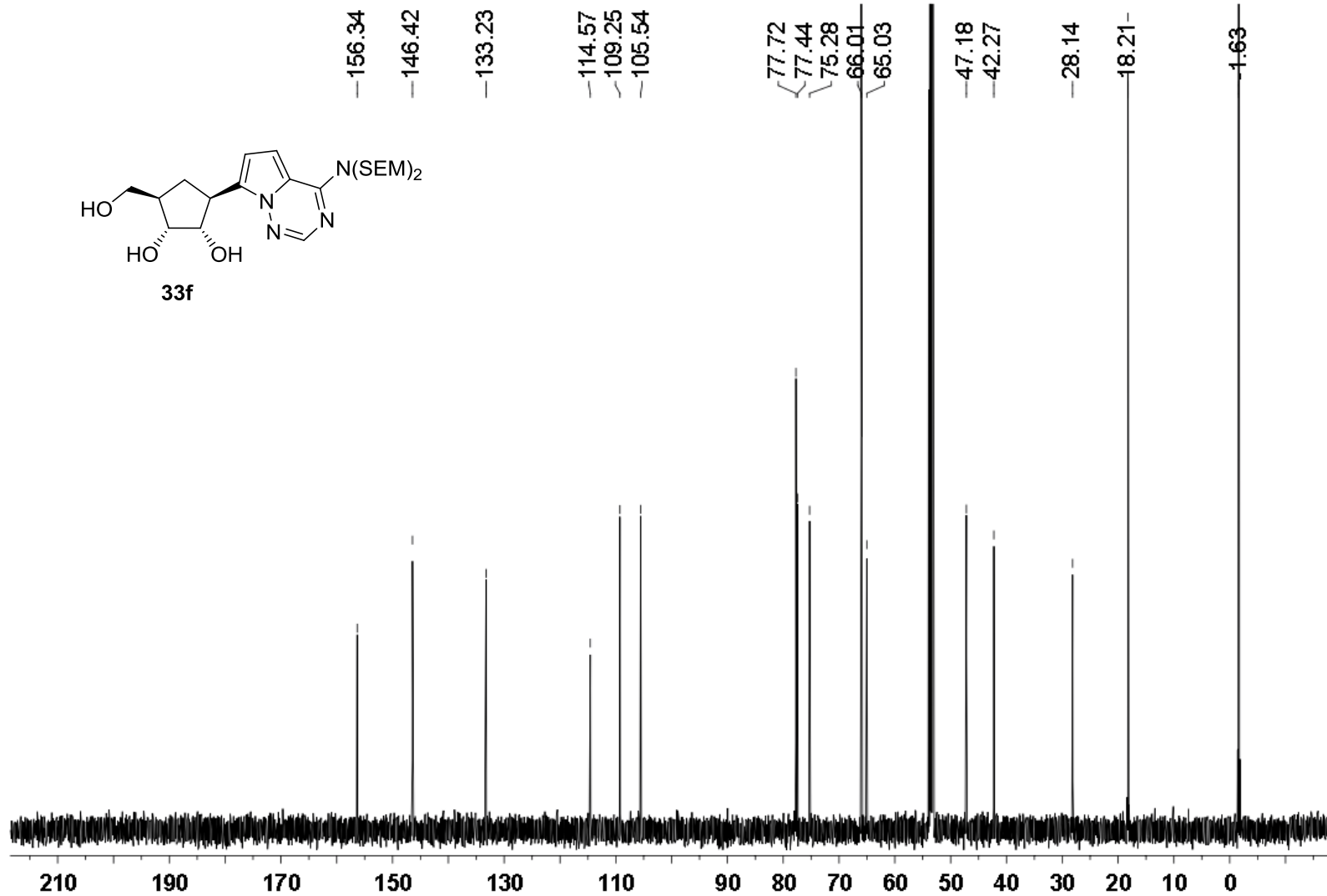
**33e**



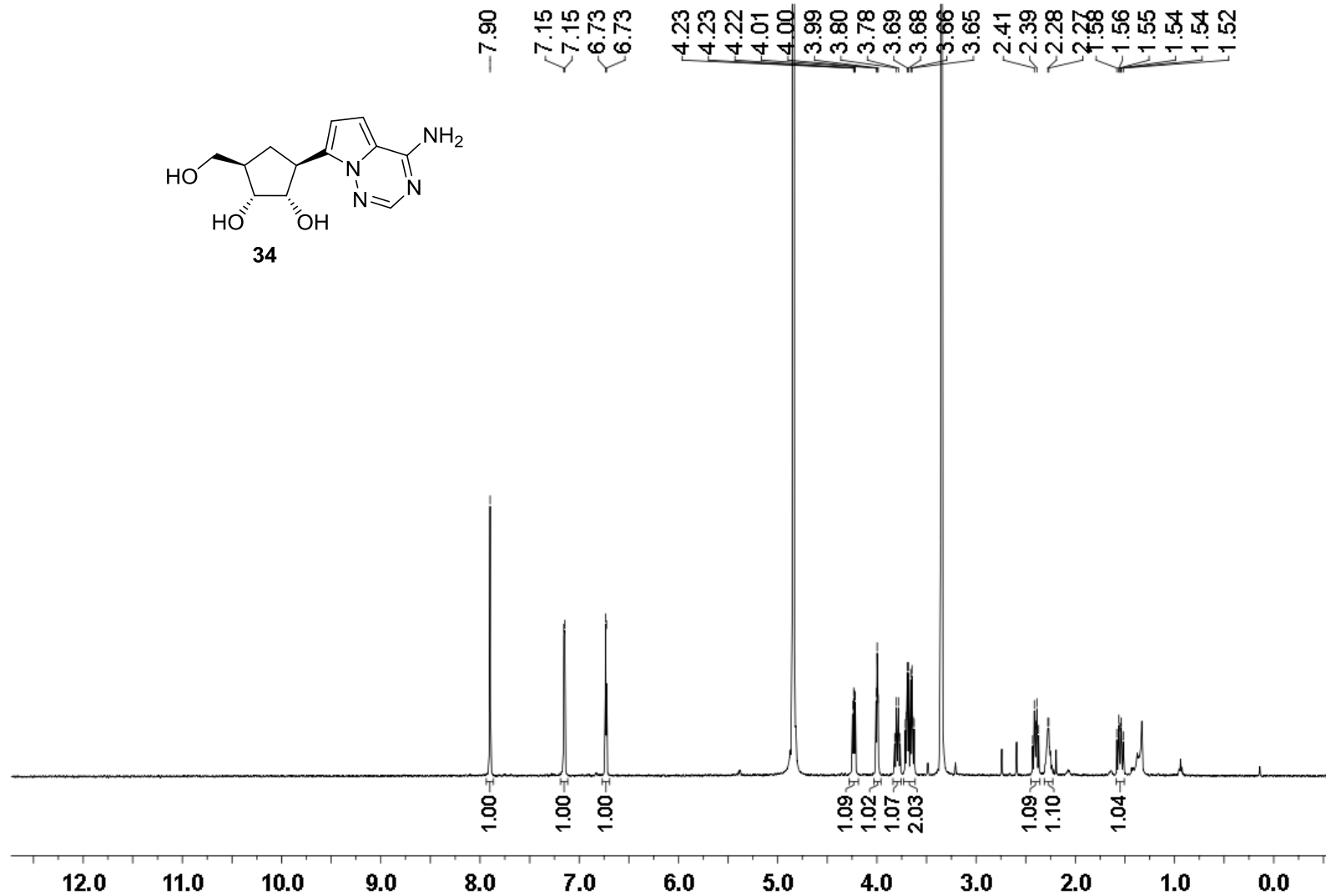
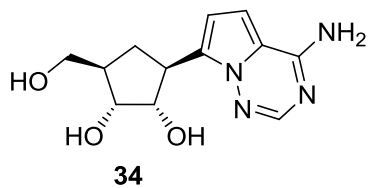
$^{13}\text{C}$  NMR (126 MHz) spectrum of **33e** in  $\text{DMSO-}d_6$



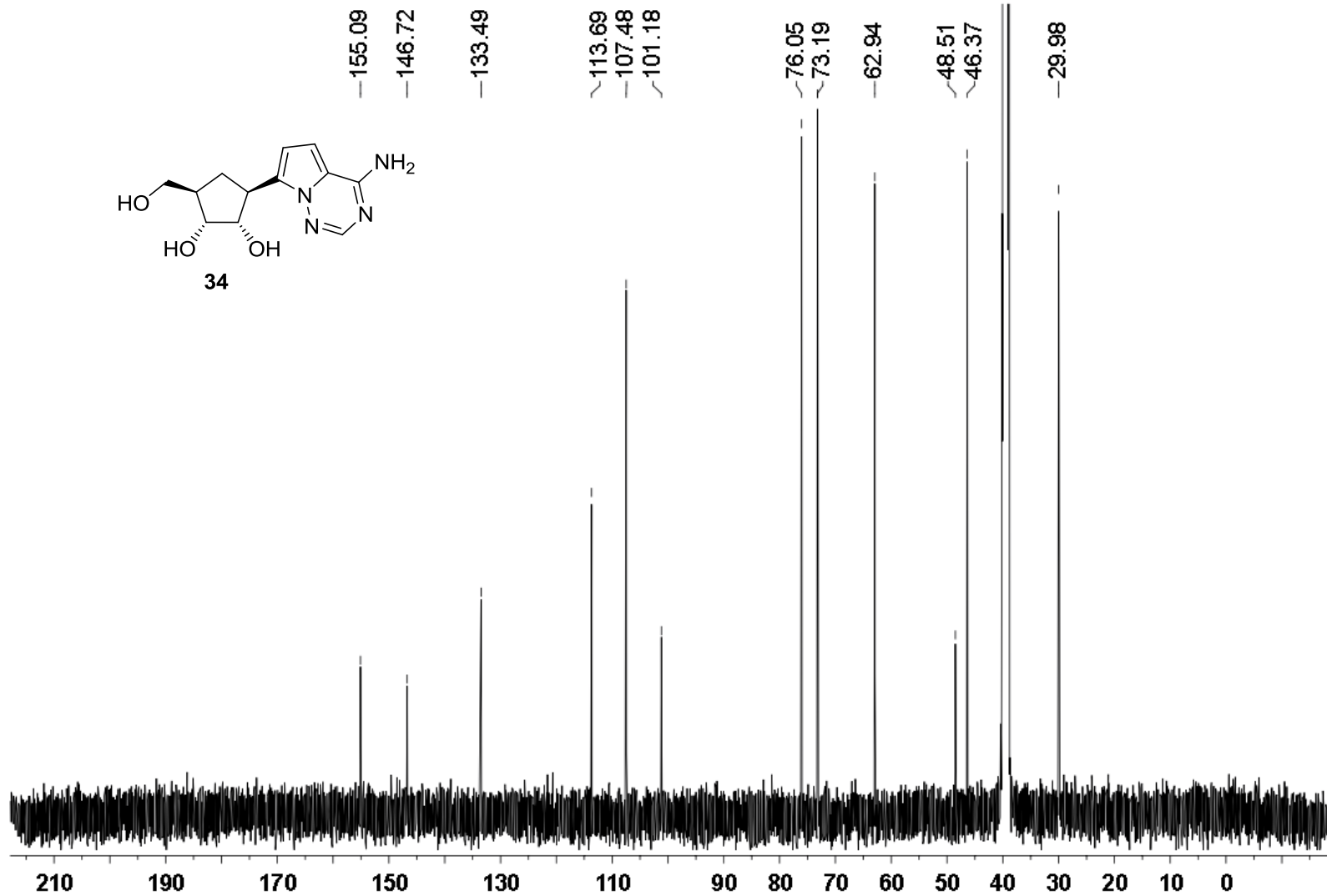
$^1\text{H}$  NMR (500 MHz) spectrum of **33f** in  $\text{CD}_2\text{Cl}_2$



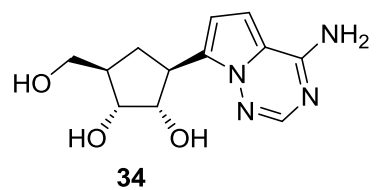
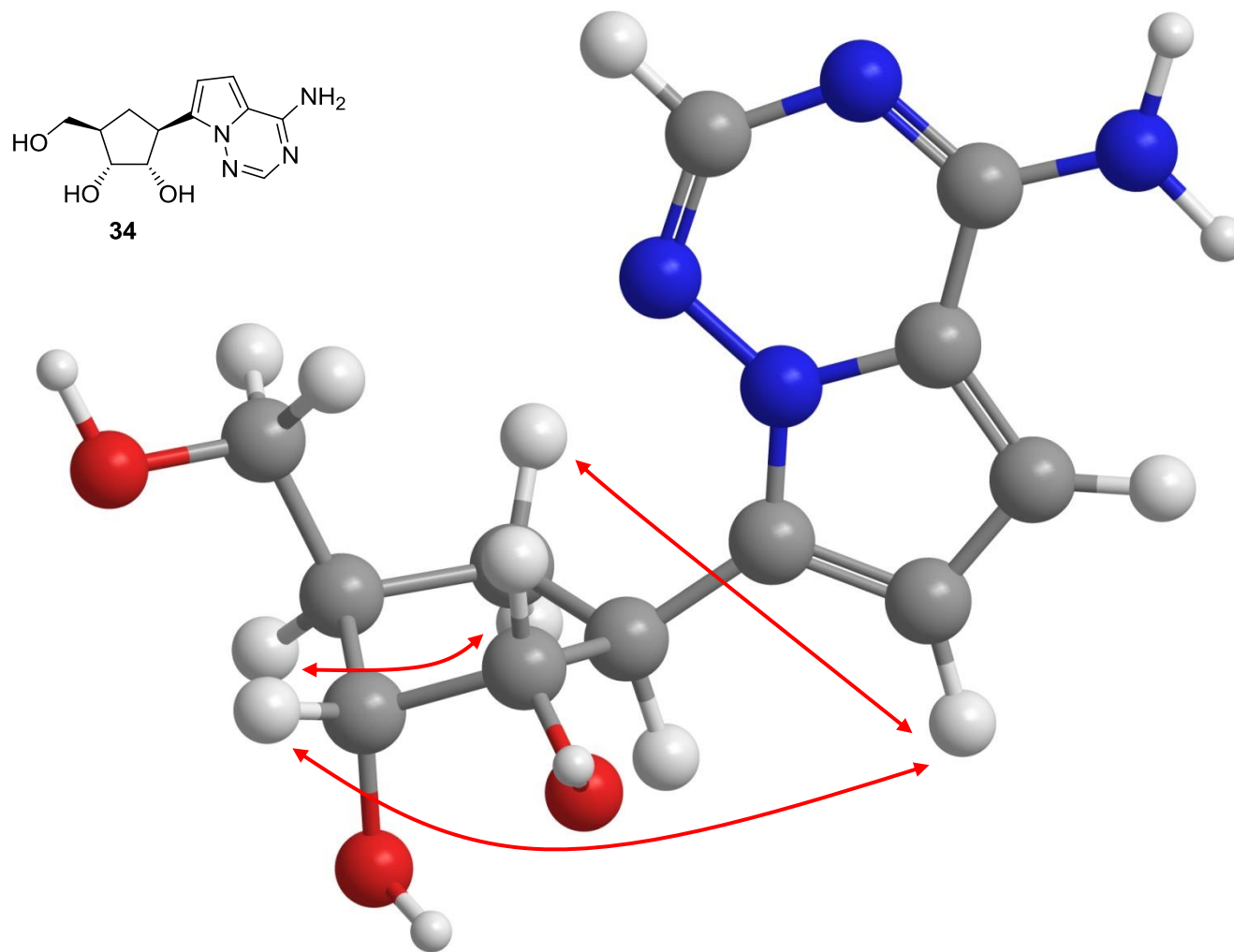
<sup>13</sup>C NMR (126 MHz) spectrum of **33f** in CD<sub>2</sub>Cl<sub>2</sub>



$^1\text{H}$  NMR (500 MHz) spectrum of **34** in  $\text{CD}_3\text{OD}$

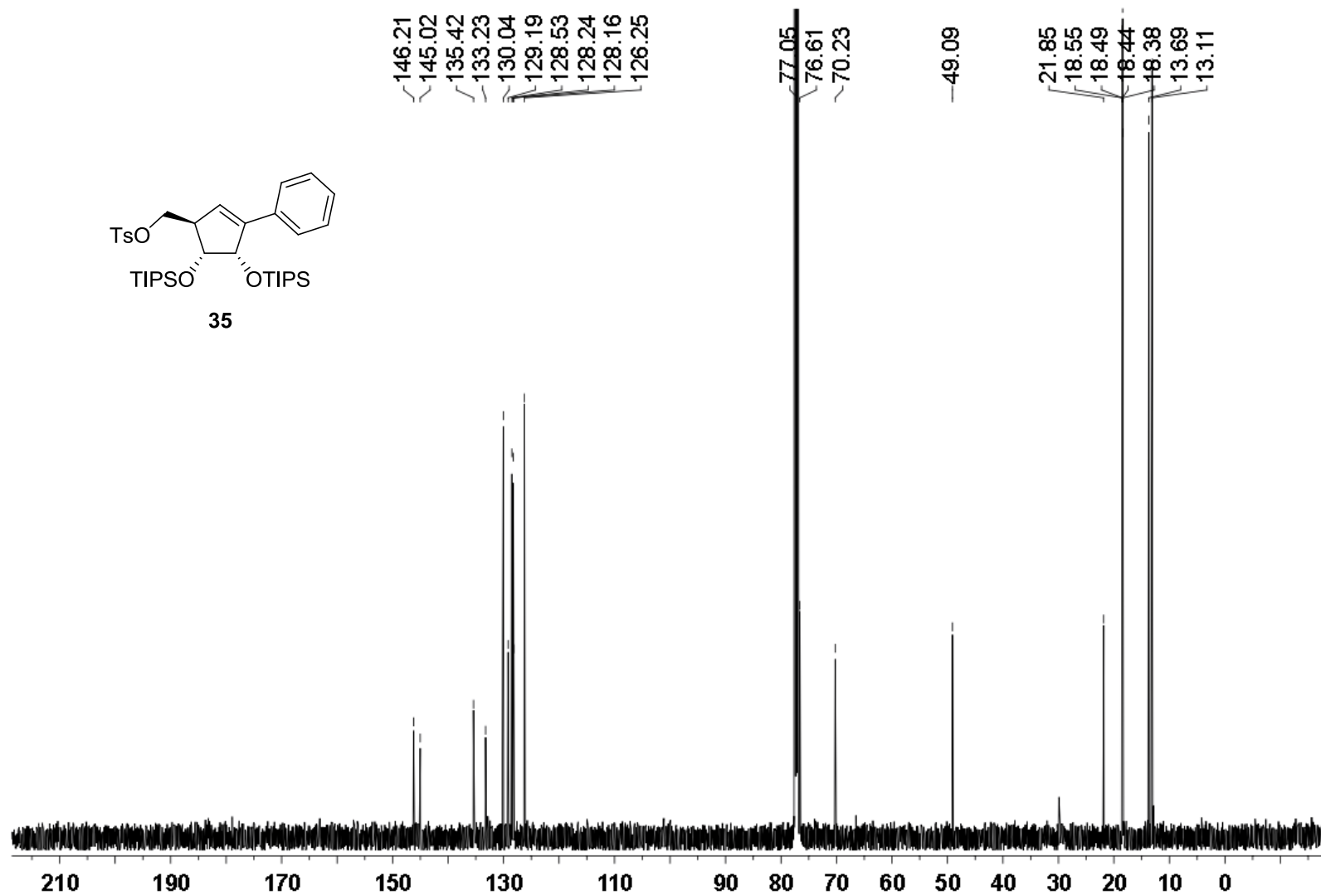


$^{13}\text{C}$  NMR (126 MHz) spectrum of **34** in  $\text{DMSO-}d_6$

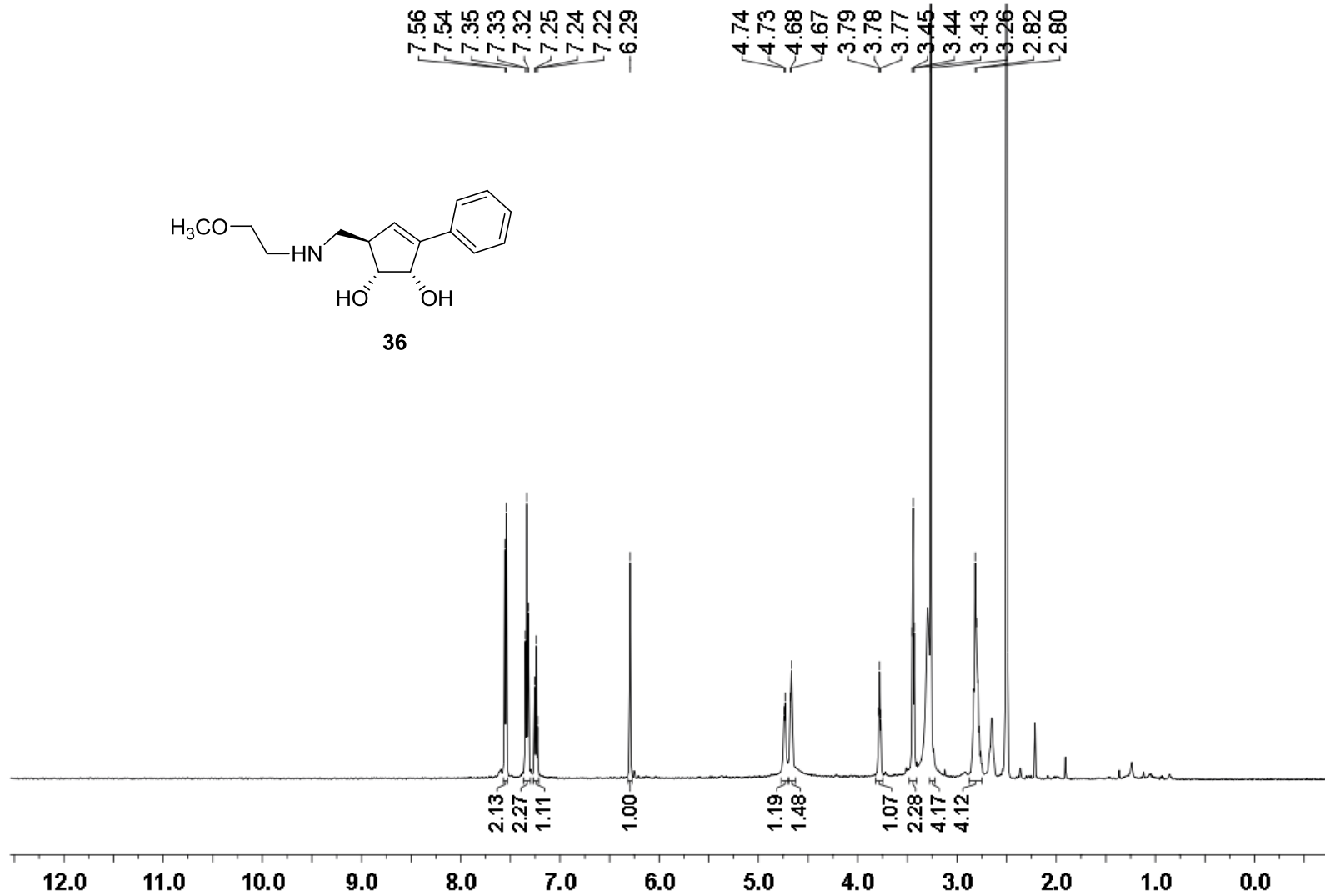


Important NOE interactions observed in compound **34**

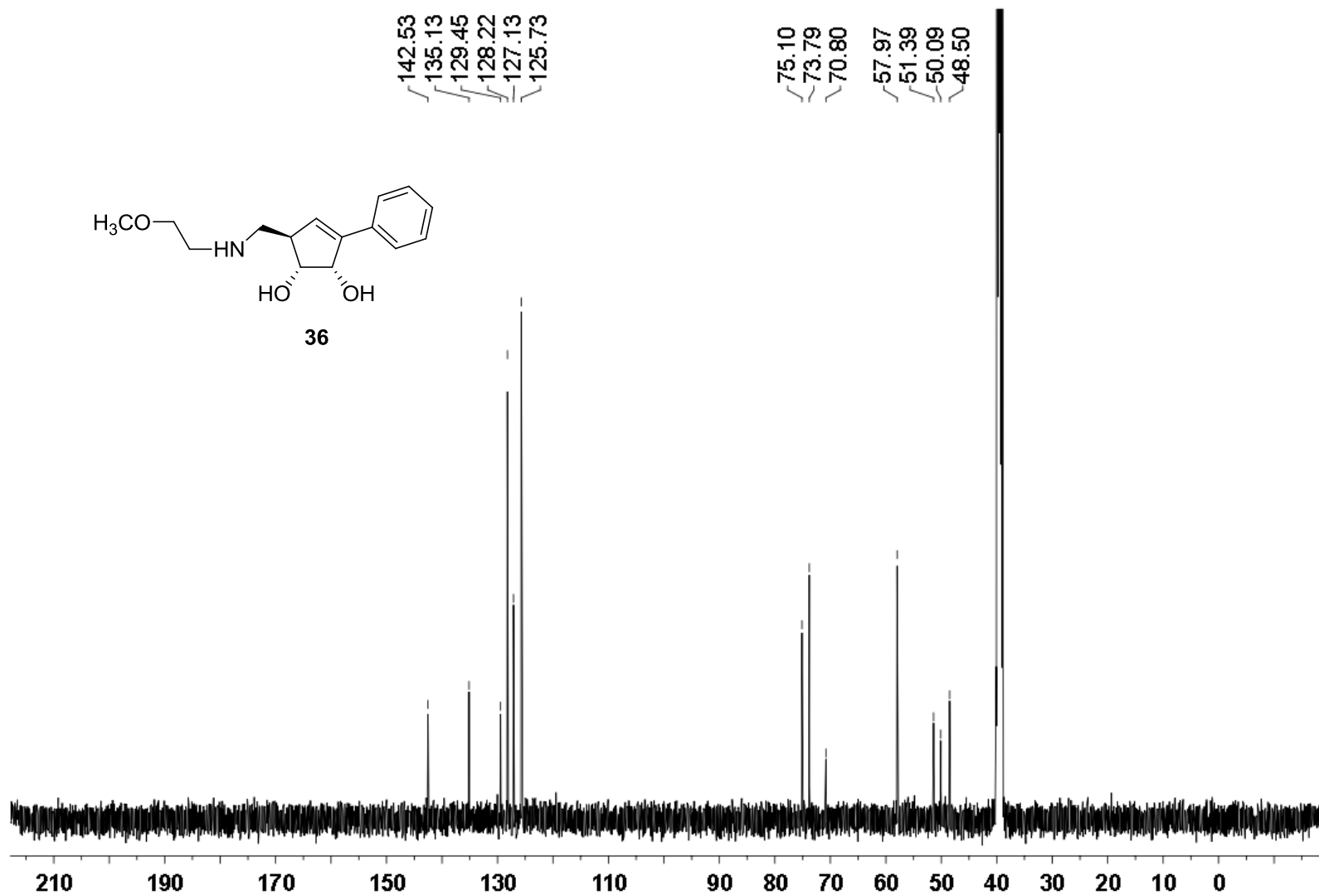




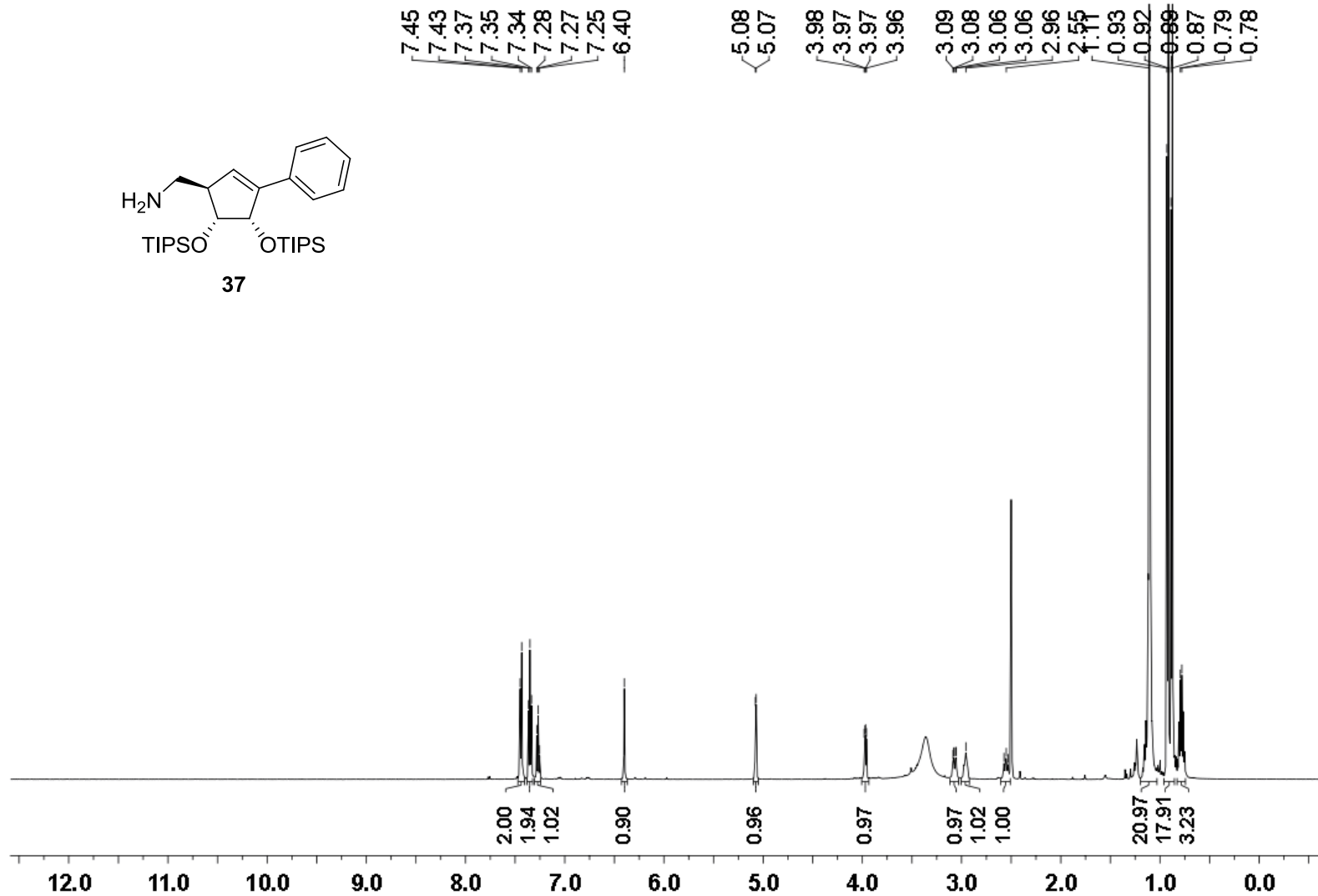
<sup>13</sup>C NMR (126 MHz) spectrum of **35** in CDCl<sub>3</sub>



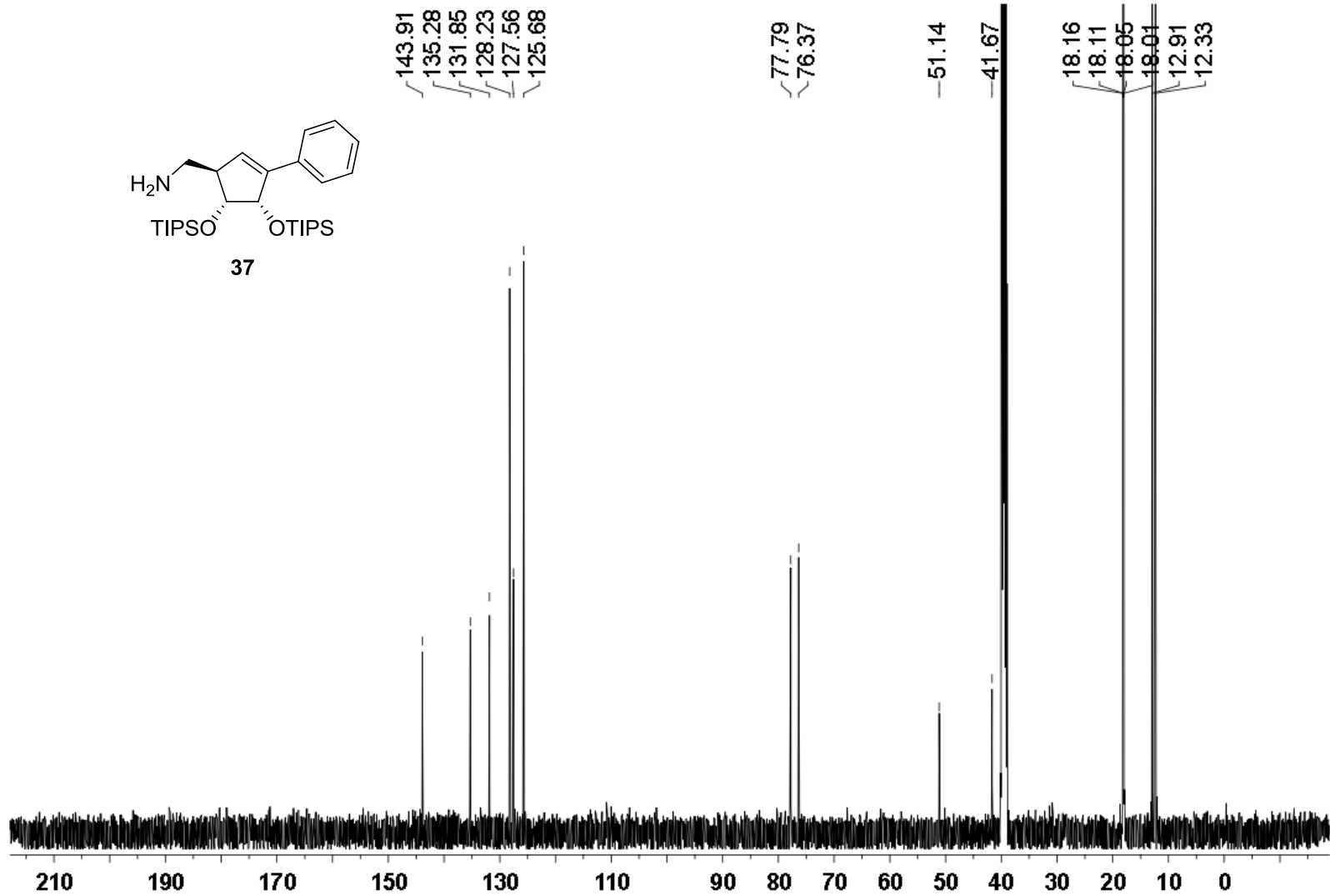
<sup>1</sup>H NMR (500 MHz) spectrum of **36** in DMSO-*d*<sub>6</sub>



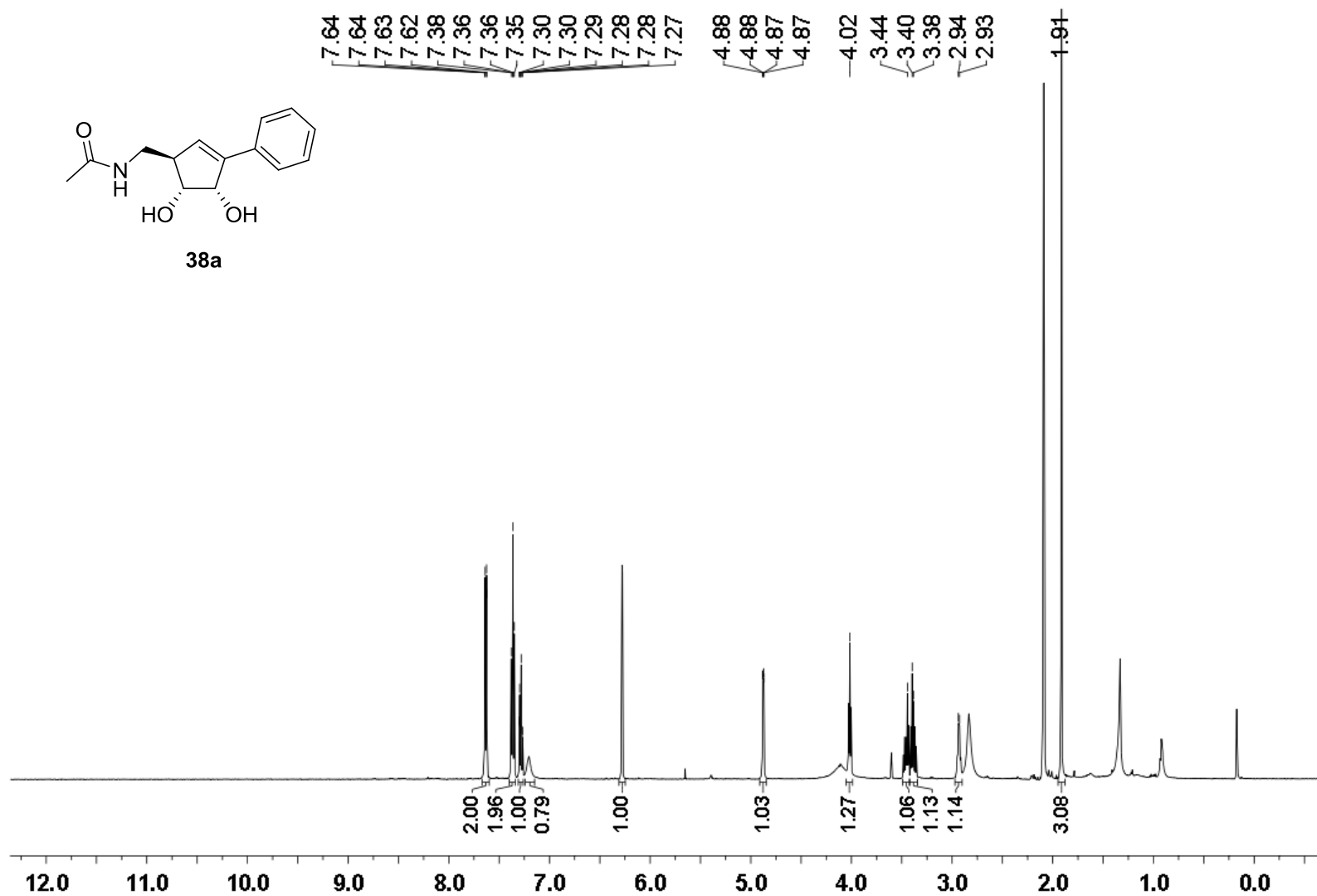
$^{13}\text{C}$  NMR (126 MHz) spectrum of **36** in  $\text{DMSO-}d_6$



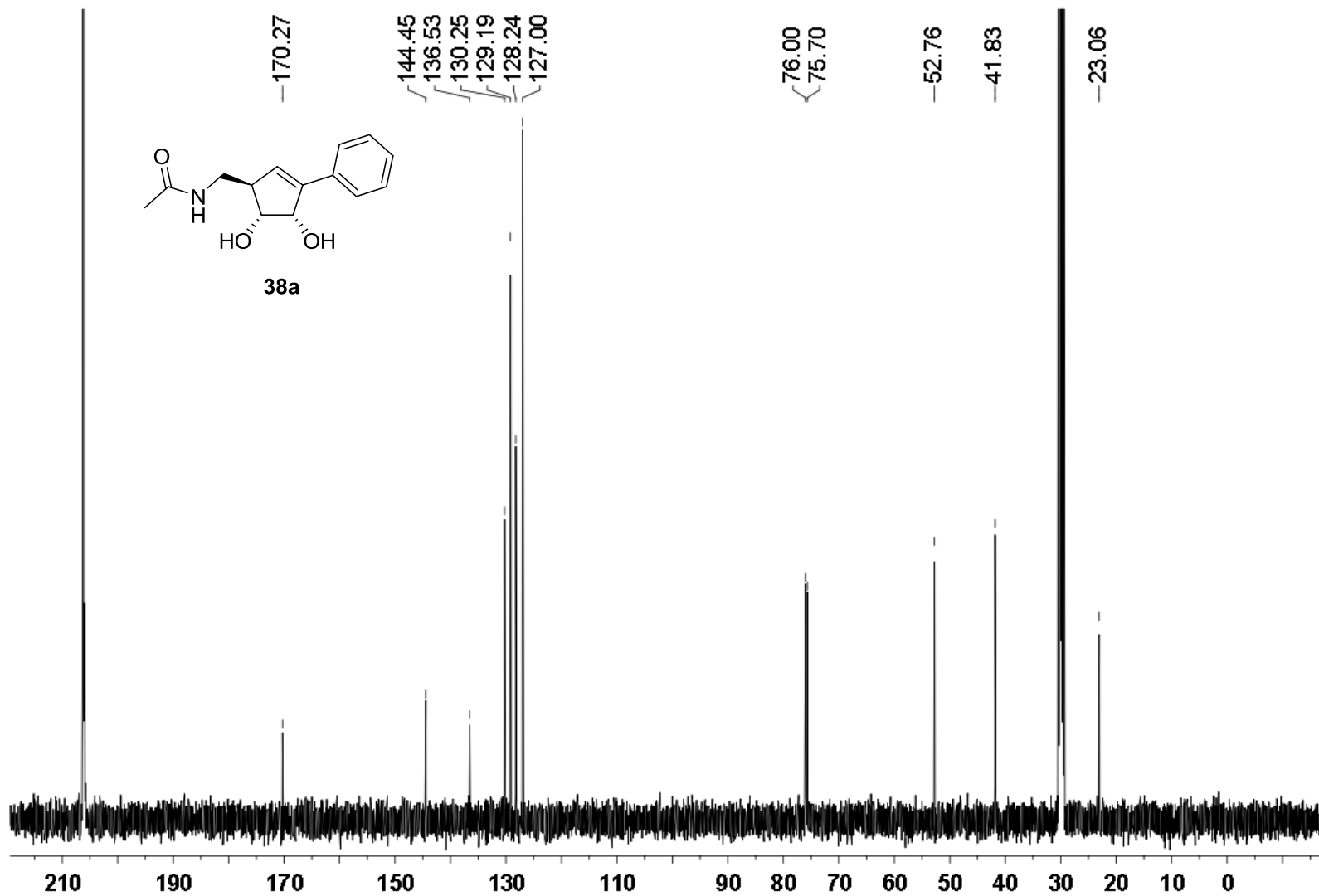
<sup>1</sup>H NMR (500 MHz) spectrum of **37** in DMSO-*d*<sub>6</sub>



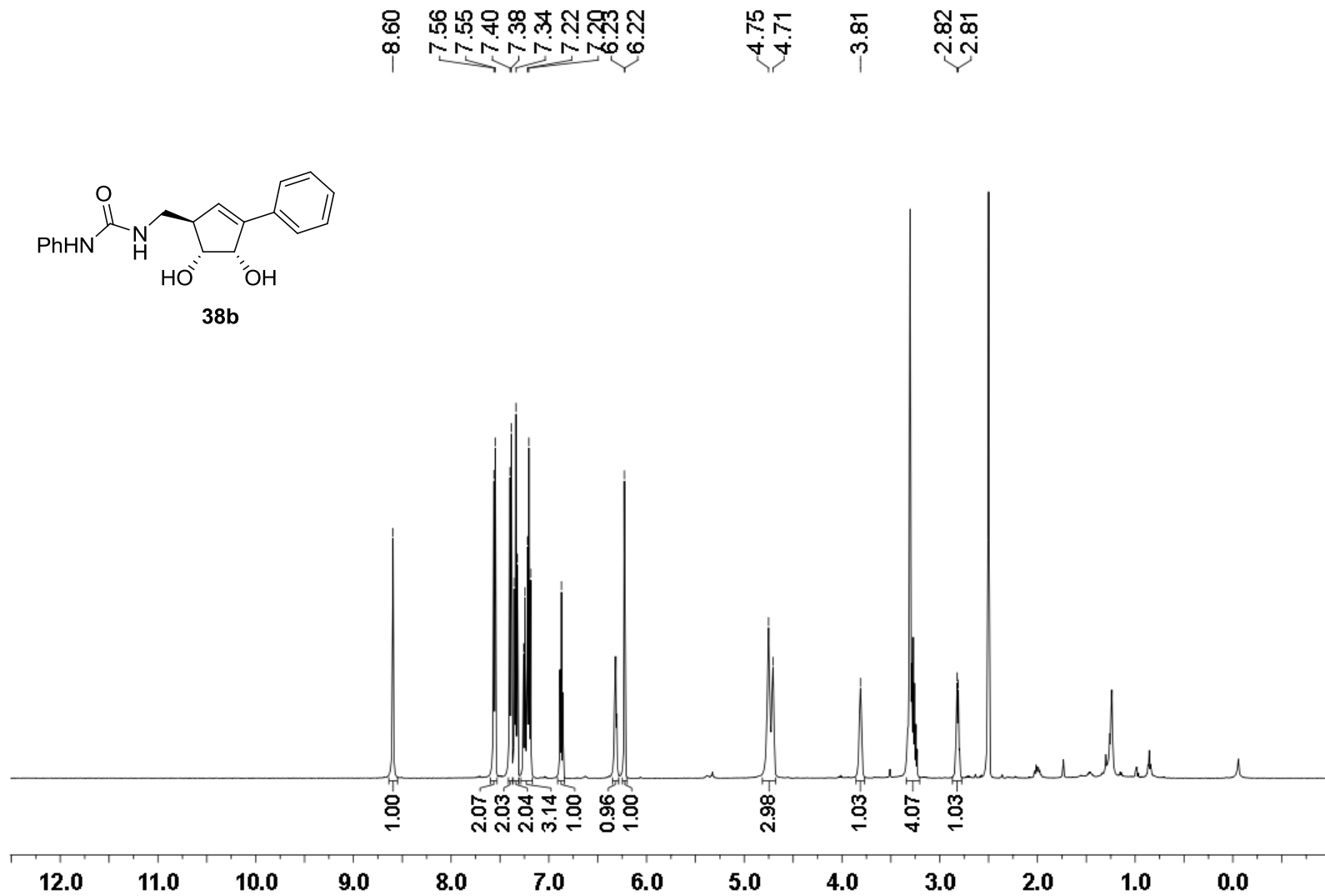
$^{13}\text{C}$  NMR (126 MHz) spectrum of **37** in  $\text{DMSO-}d_6$



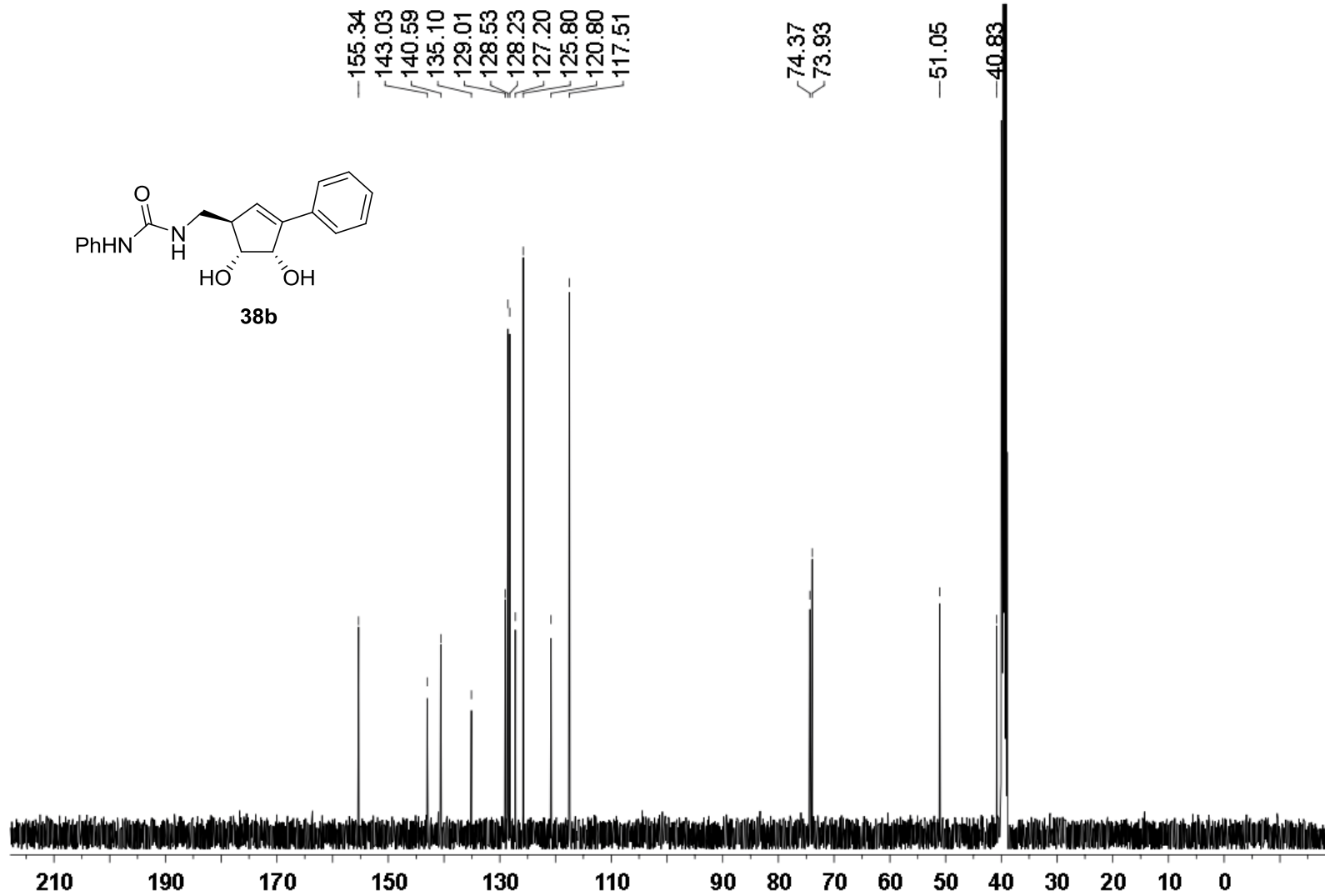
<sup>1</sup>H NMR (500 MHz) spectrum of **38a** in acetone-*d*<sub>6</sub>



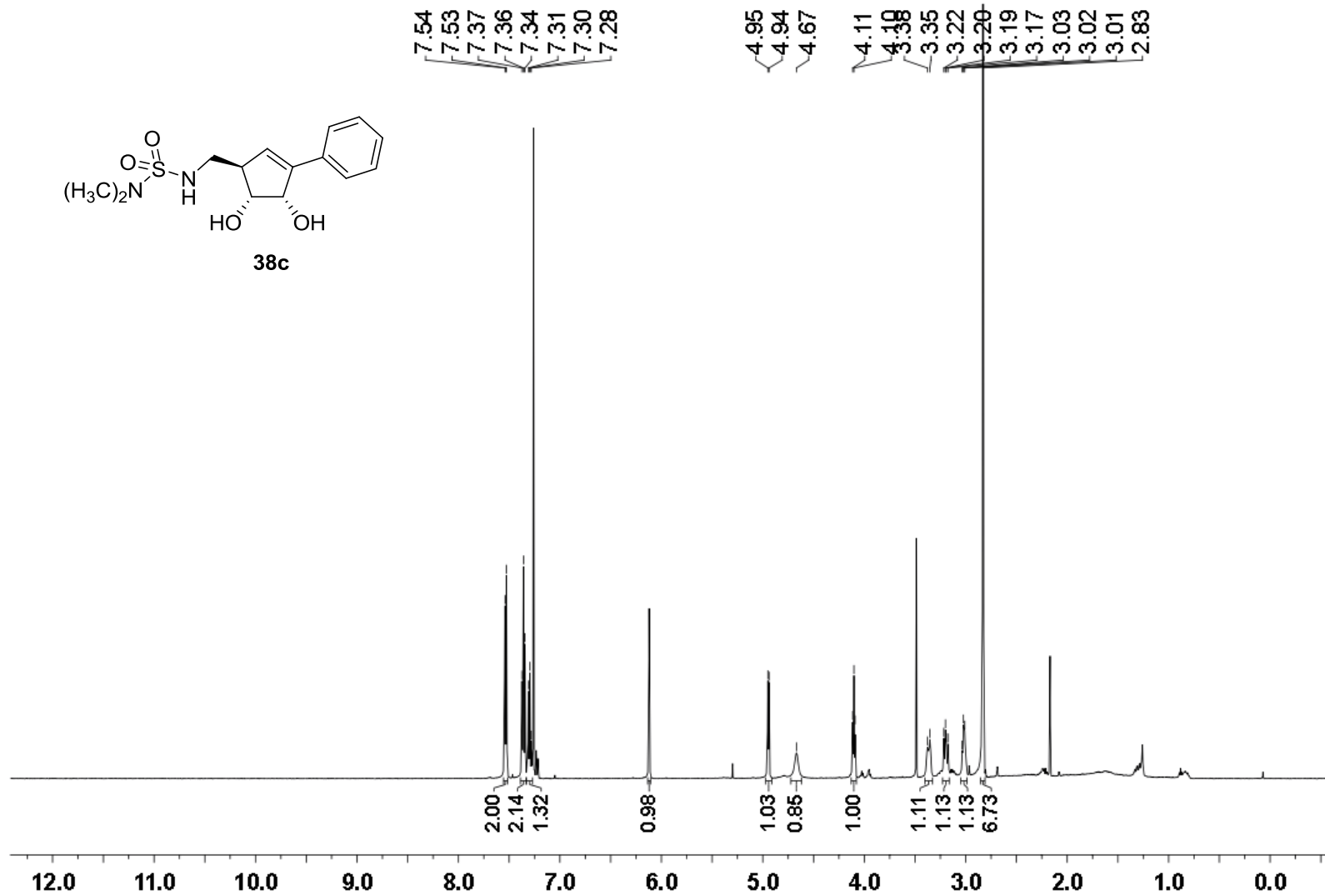
$^{13}\text{C}$  NMR (126 MHz) spectrum of **38a** in acetone- $d_6$



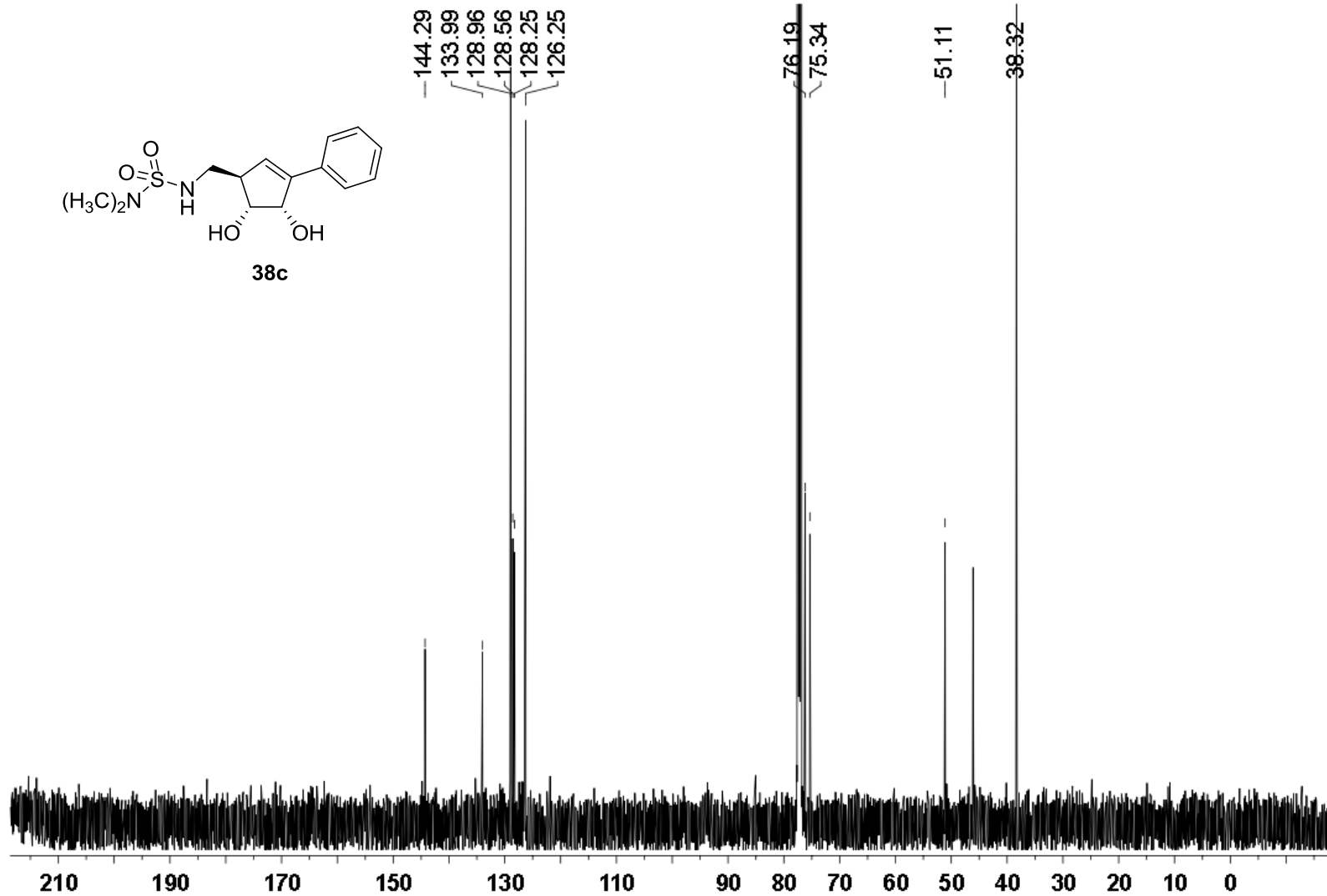
<sup>1</sup>H NMR (500 MHz) spectrum of **38b** in DMSO-*d*<sub>6</sub>



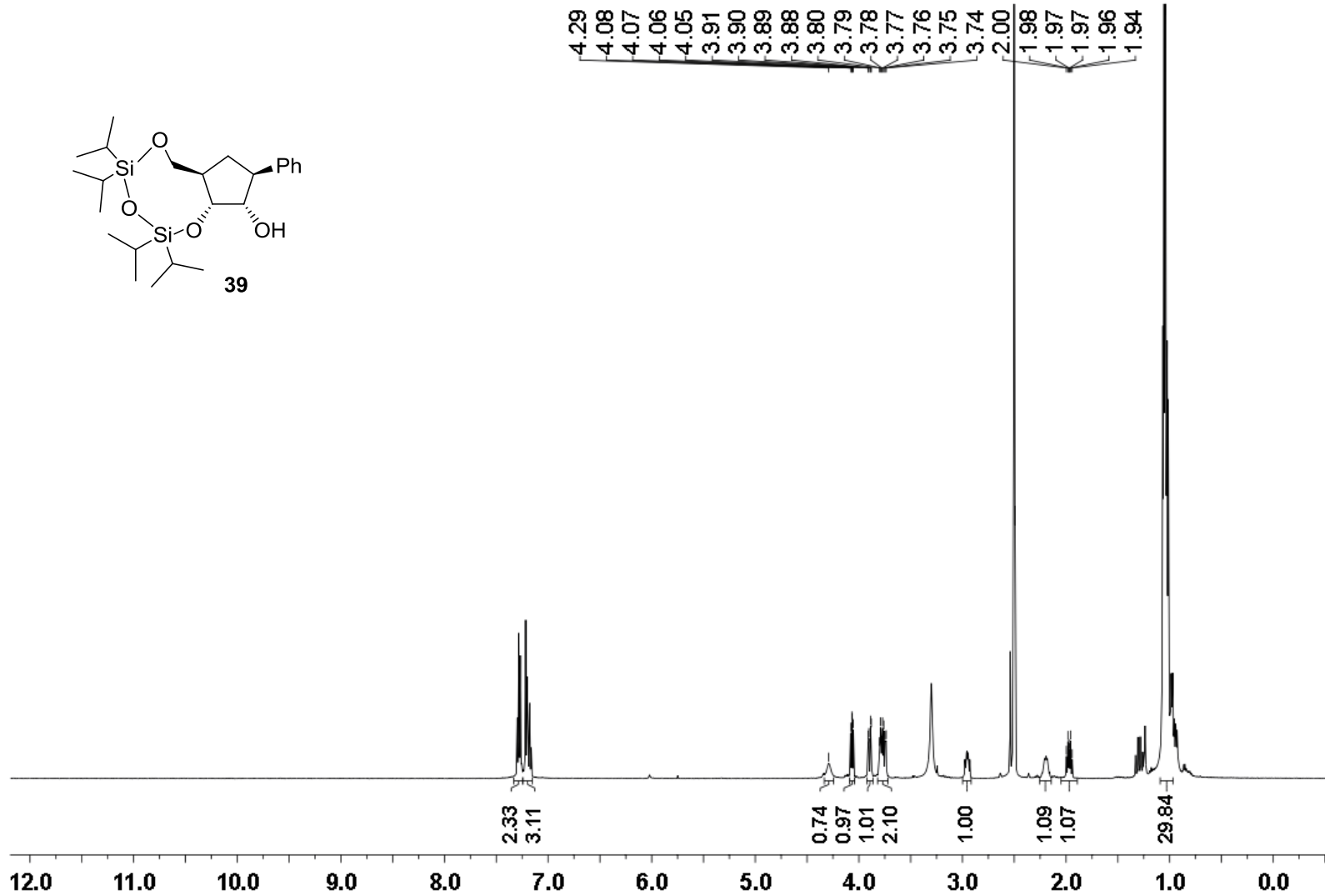
$^{13}\text{C}$  NMR (126 MHz) spectrum of **38b** in  $\text{DMSO-}d_6$



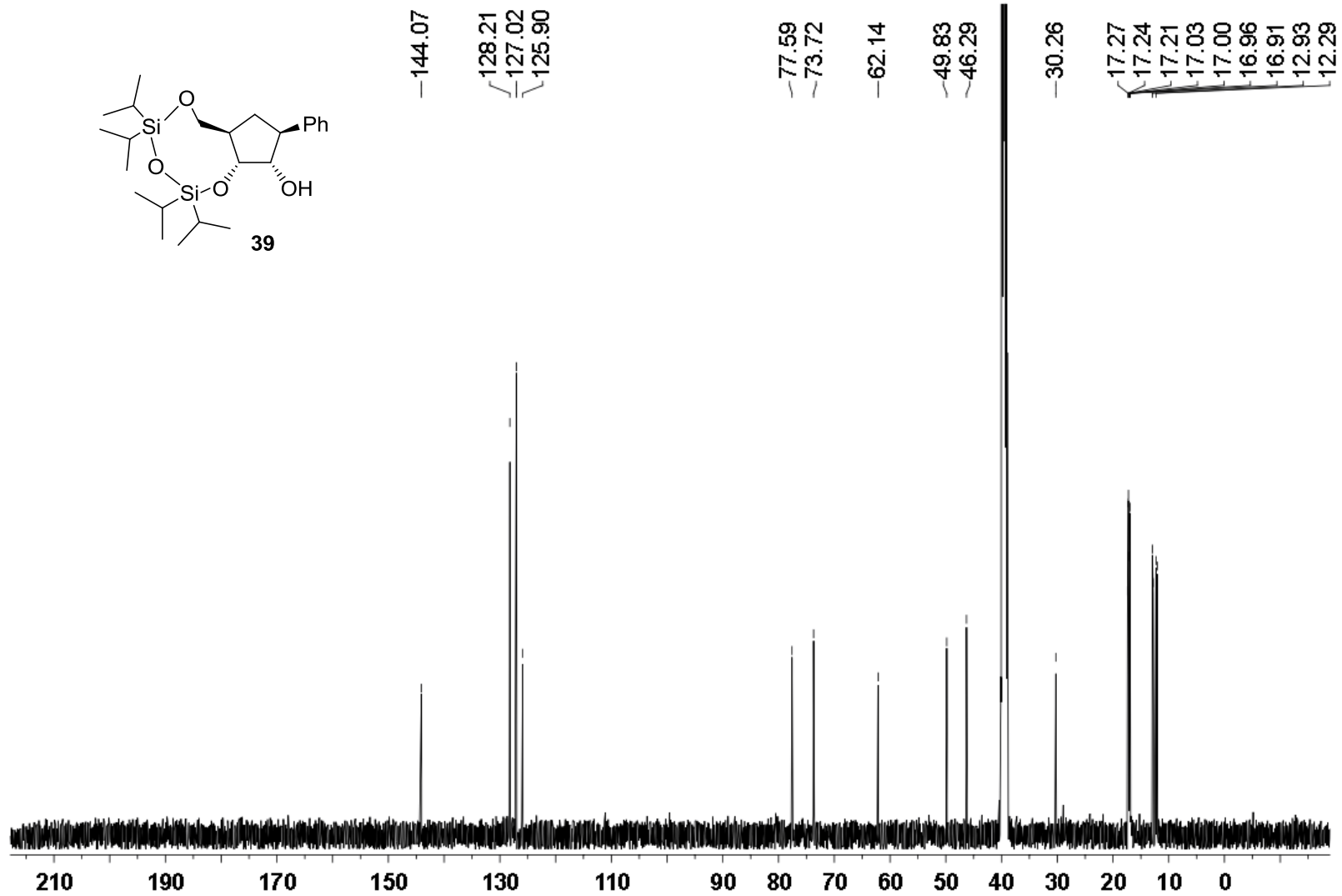
$^1\text{H}$  NMR (500 MHz) spectrum of **38c** in  $\text{CDCl}_3$



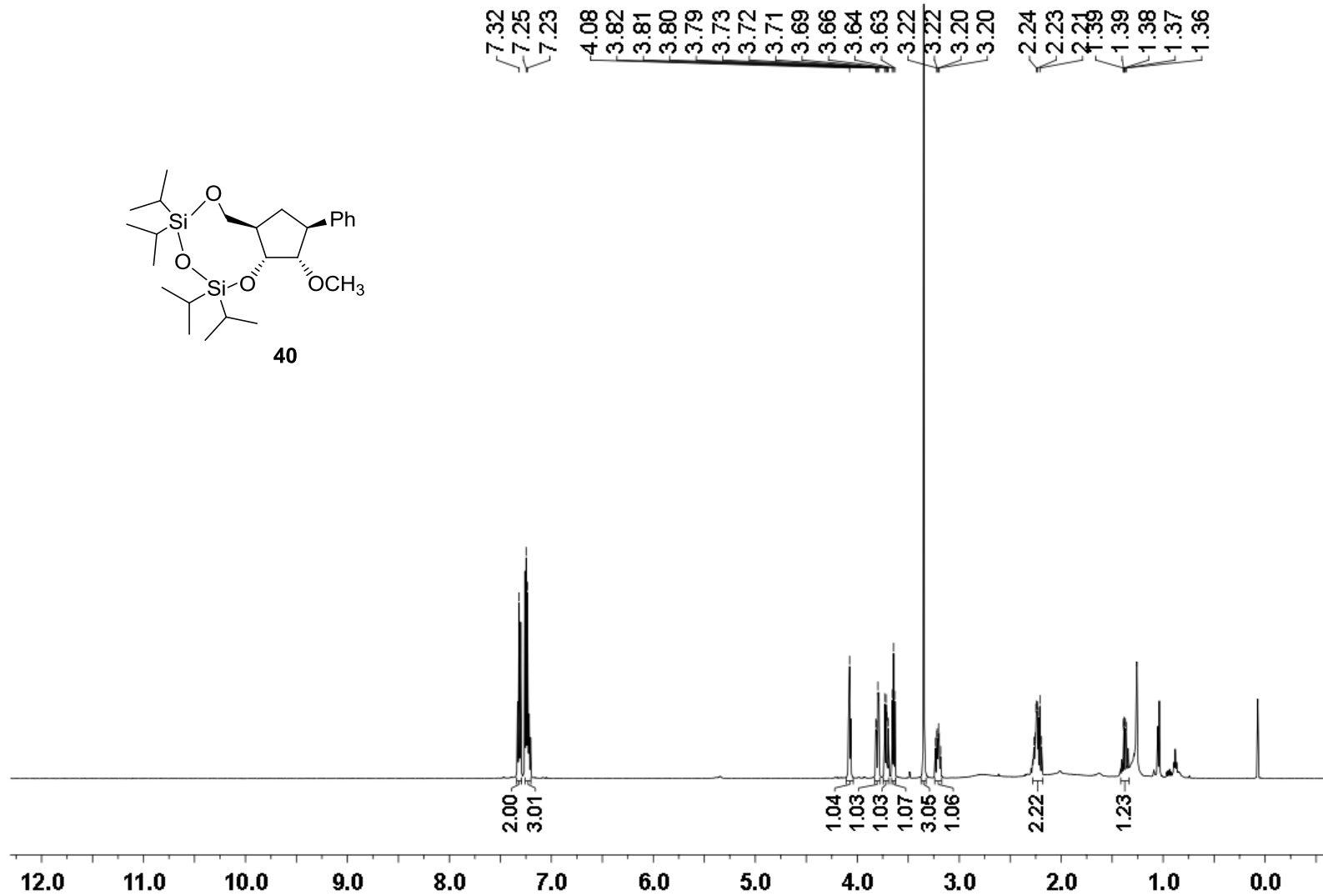
$^{13}\text{C}$  NMR (126 MHz) spectrum of **38c** in  $\text{CDCl}_3$



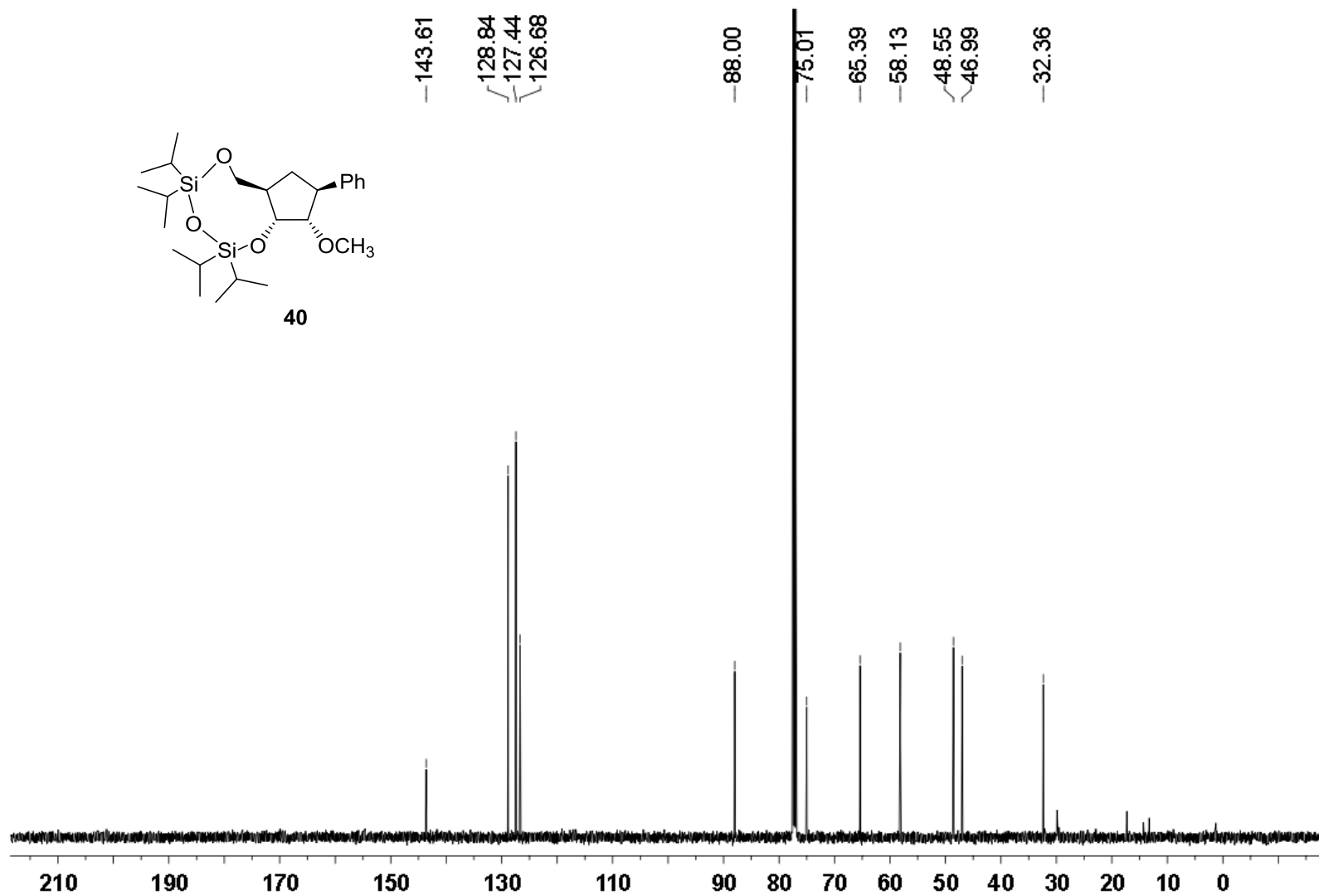
$^1\text{H NMR}$  (500 MHz) spectrum of **39** in  $\text{DMSO-}d_6$



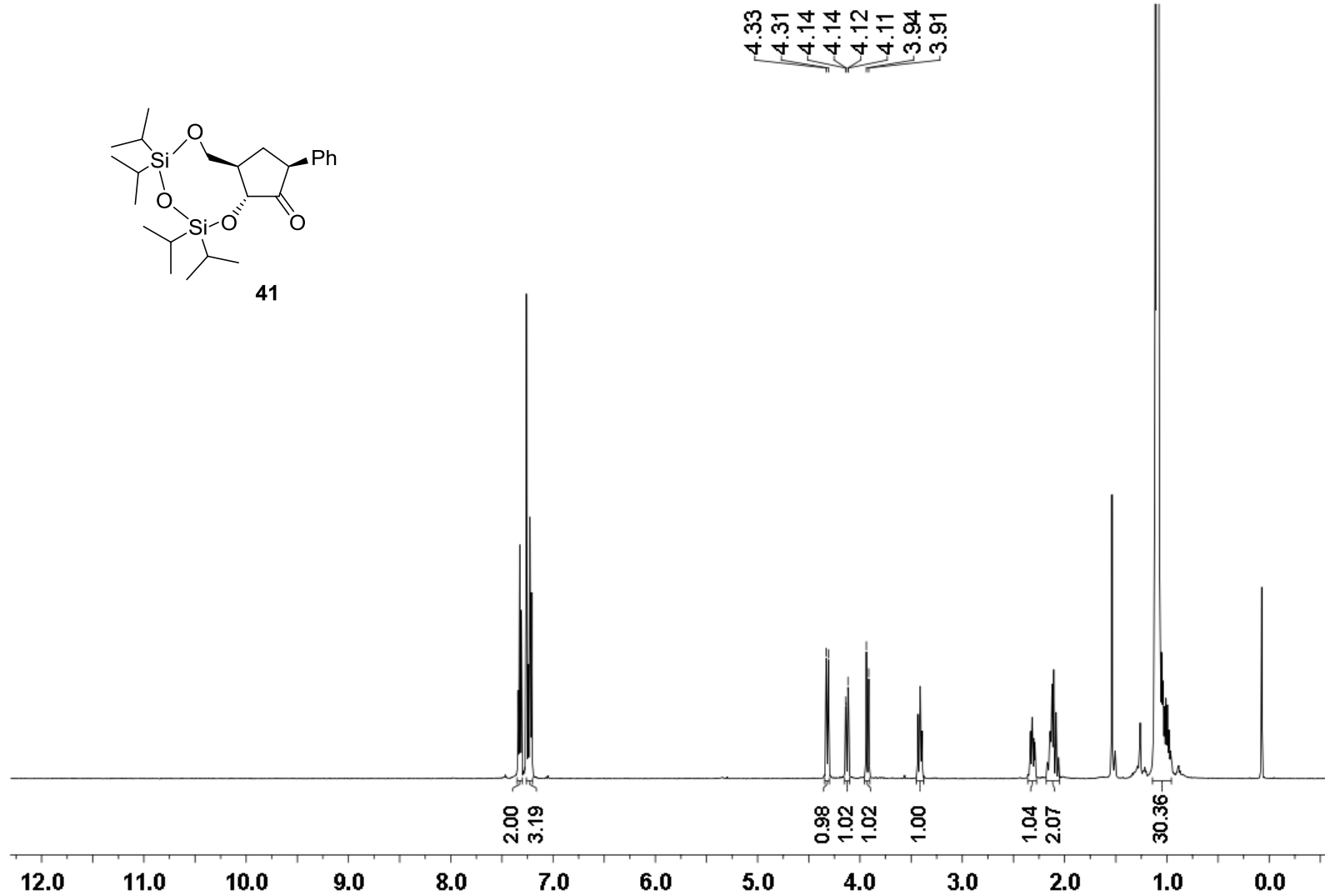
$^{13}\text{C}$  NMR (126 MHz) spectrum of **39** in  $\text{DMSO-}d_6$



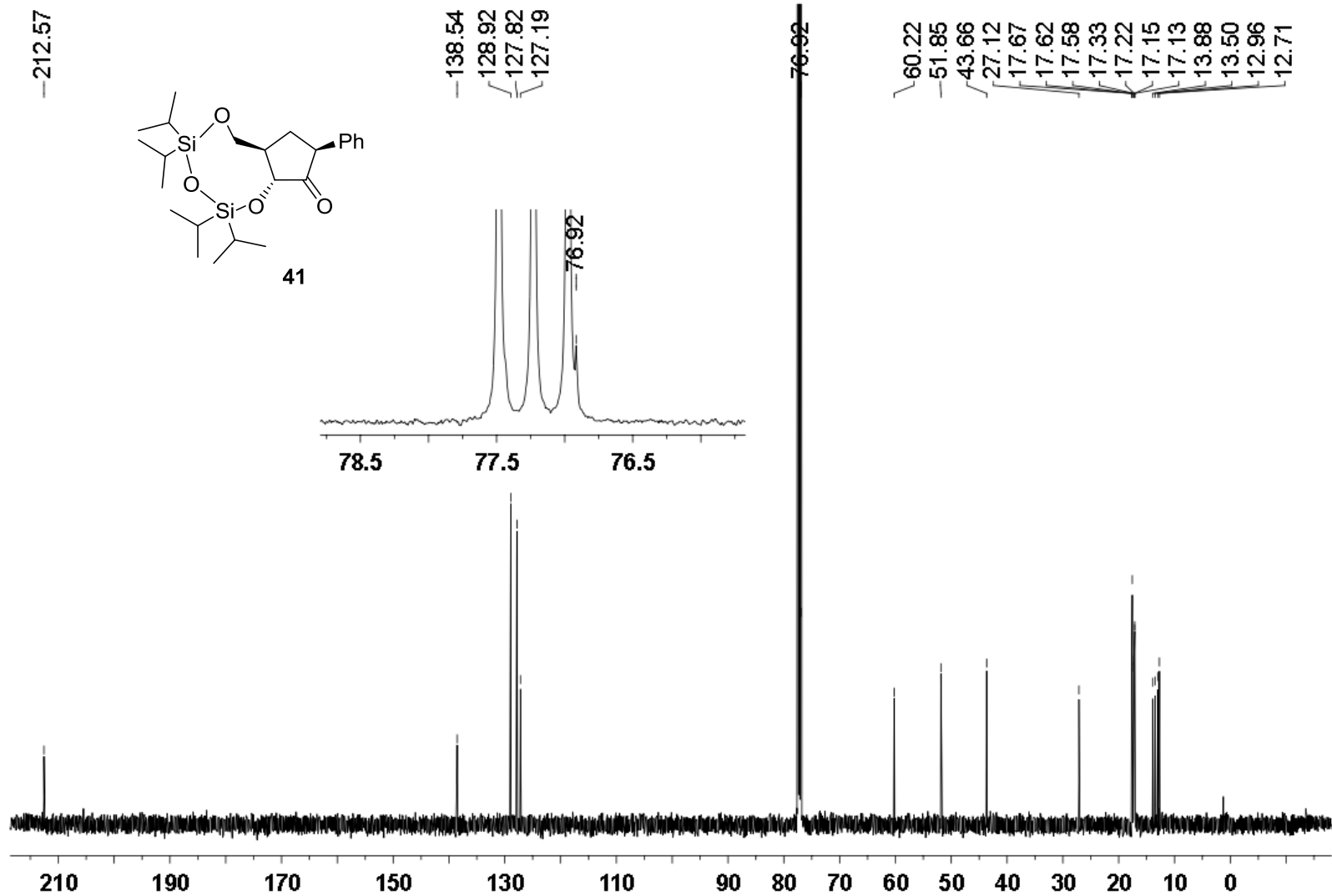
<sup>1</sup>H NMR (500 MHz) spectrum of **40** in CDCl<sub>3</sub>



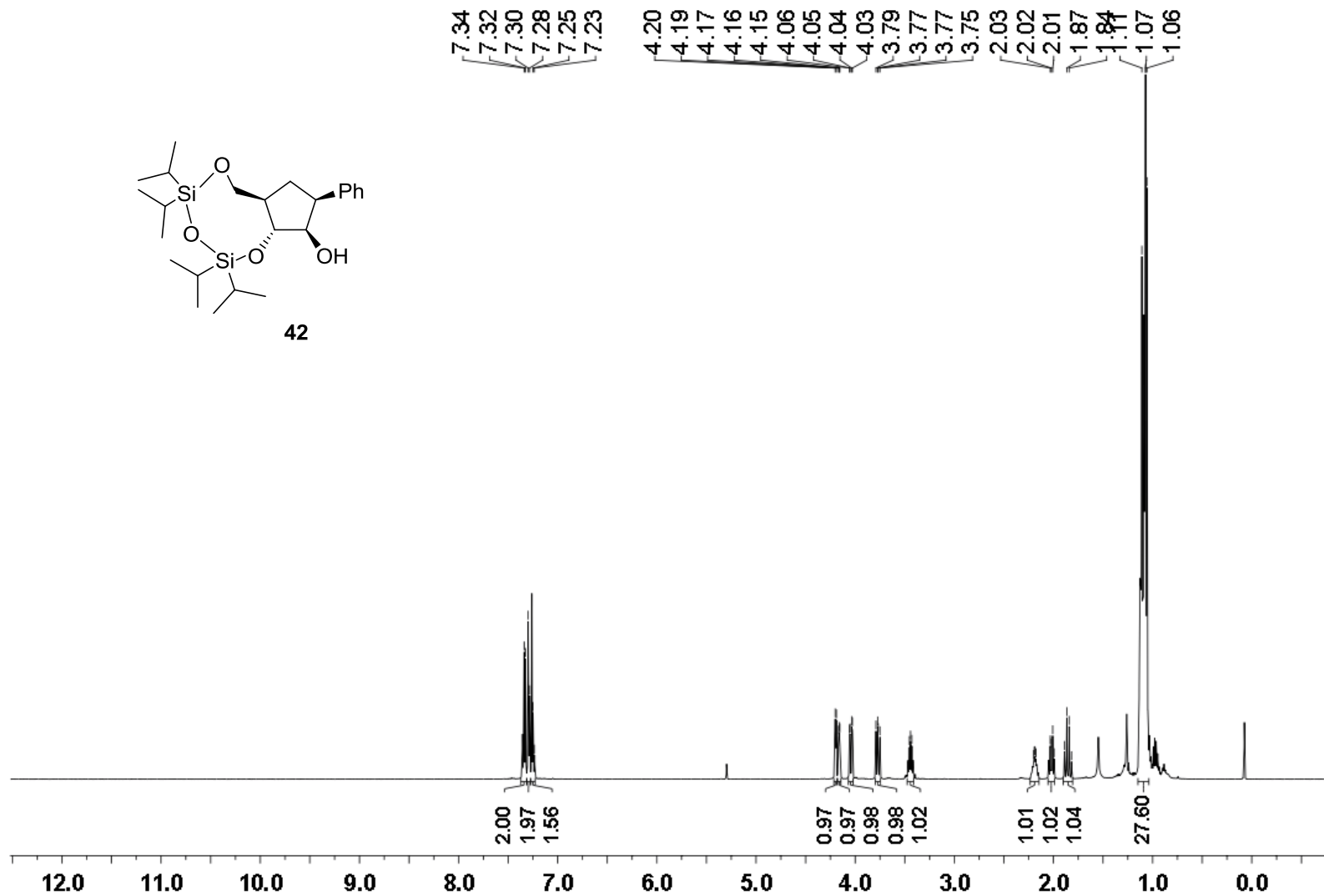
<sup>13</sup>C NMR (126 MHz) spectrum of **40** in CDCl<sub>3</sub>



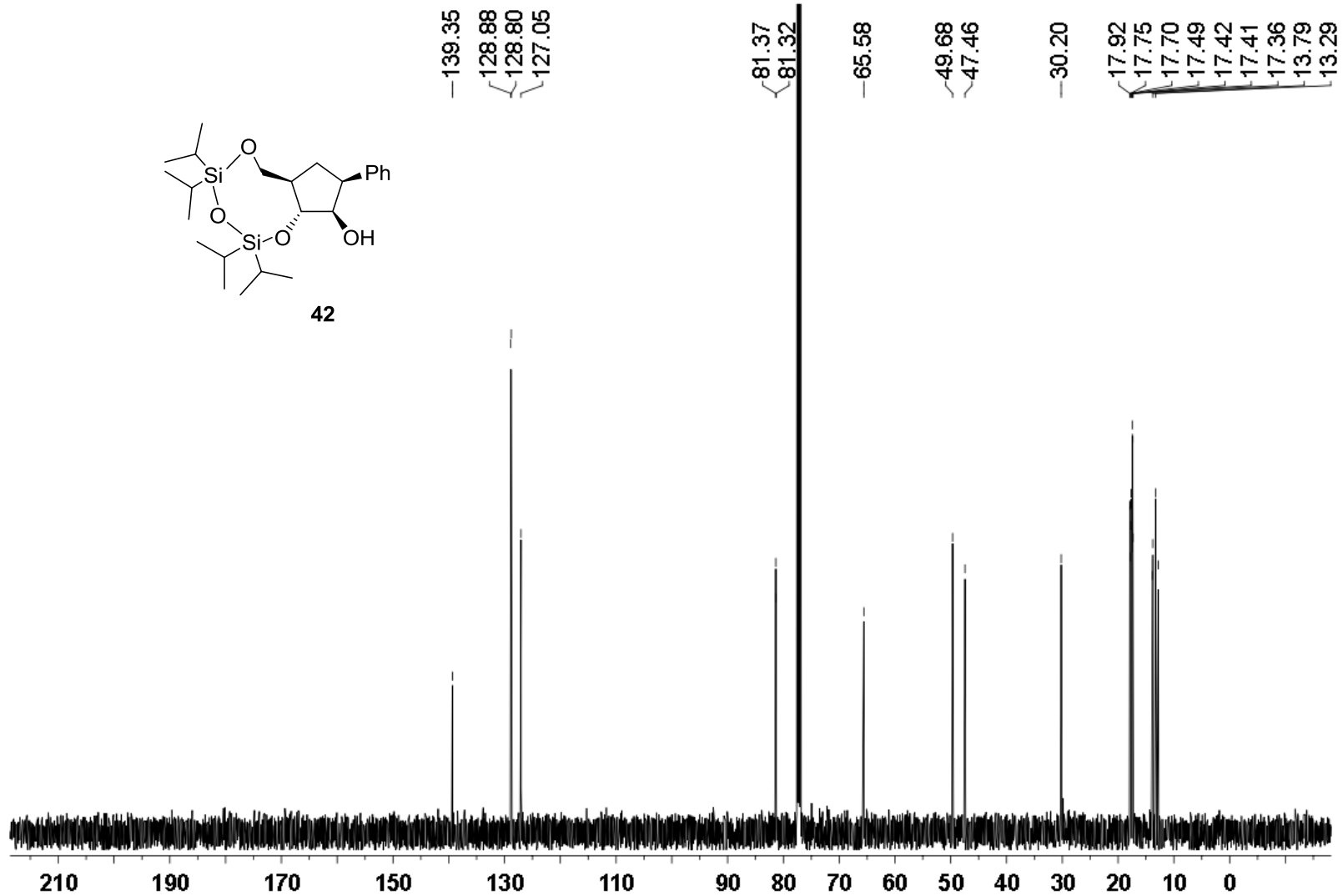
$^1\text{H}$  NMR (500 MHz) spectrum of **41** in  $\text{CDCl}_3$



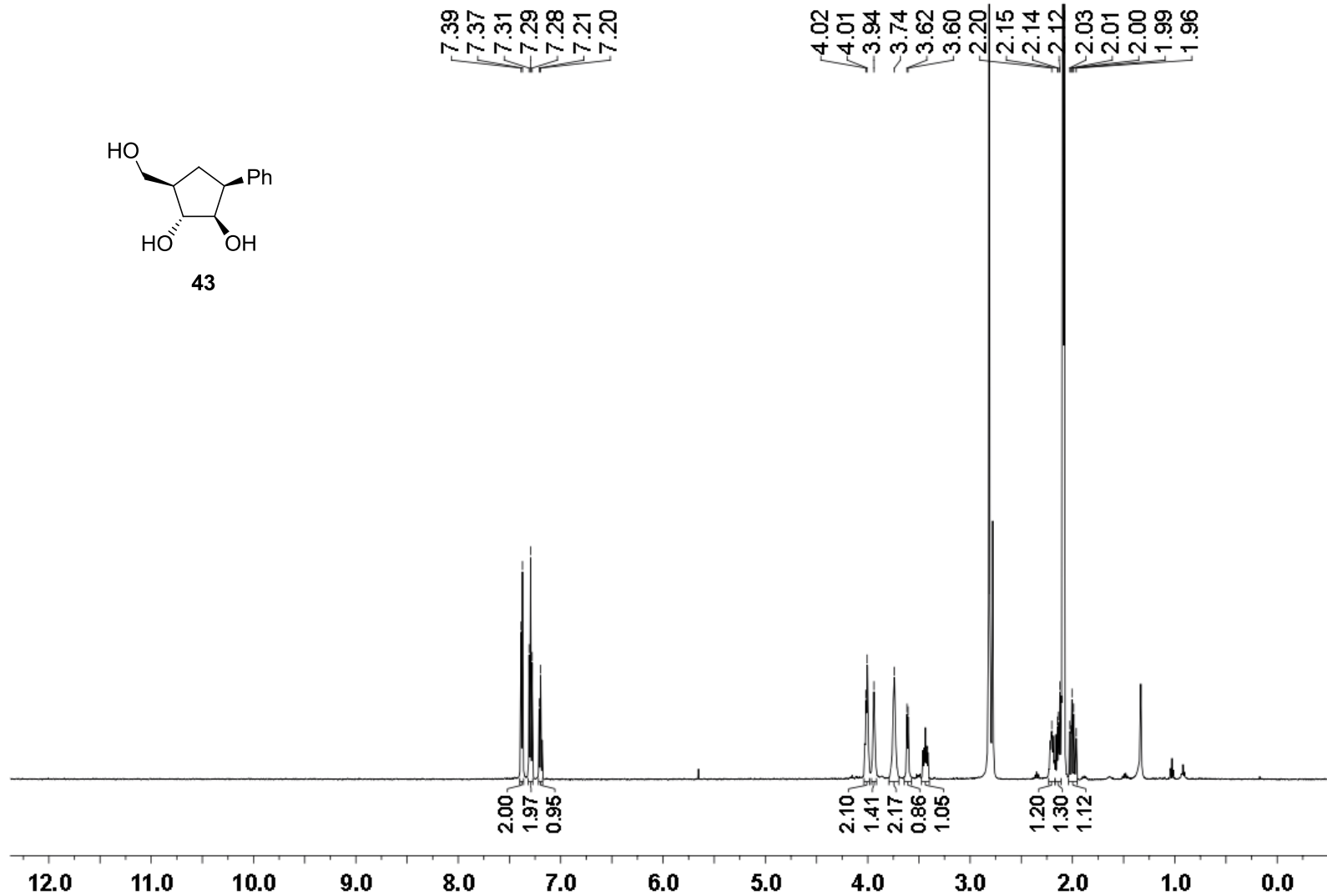
$^{13}\text{C}$  NMR (126 MHz) spectrum of **41** in  $\text{CDCl}_3$



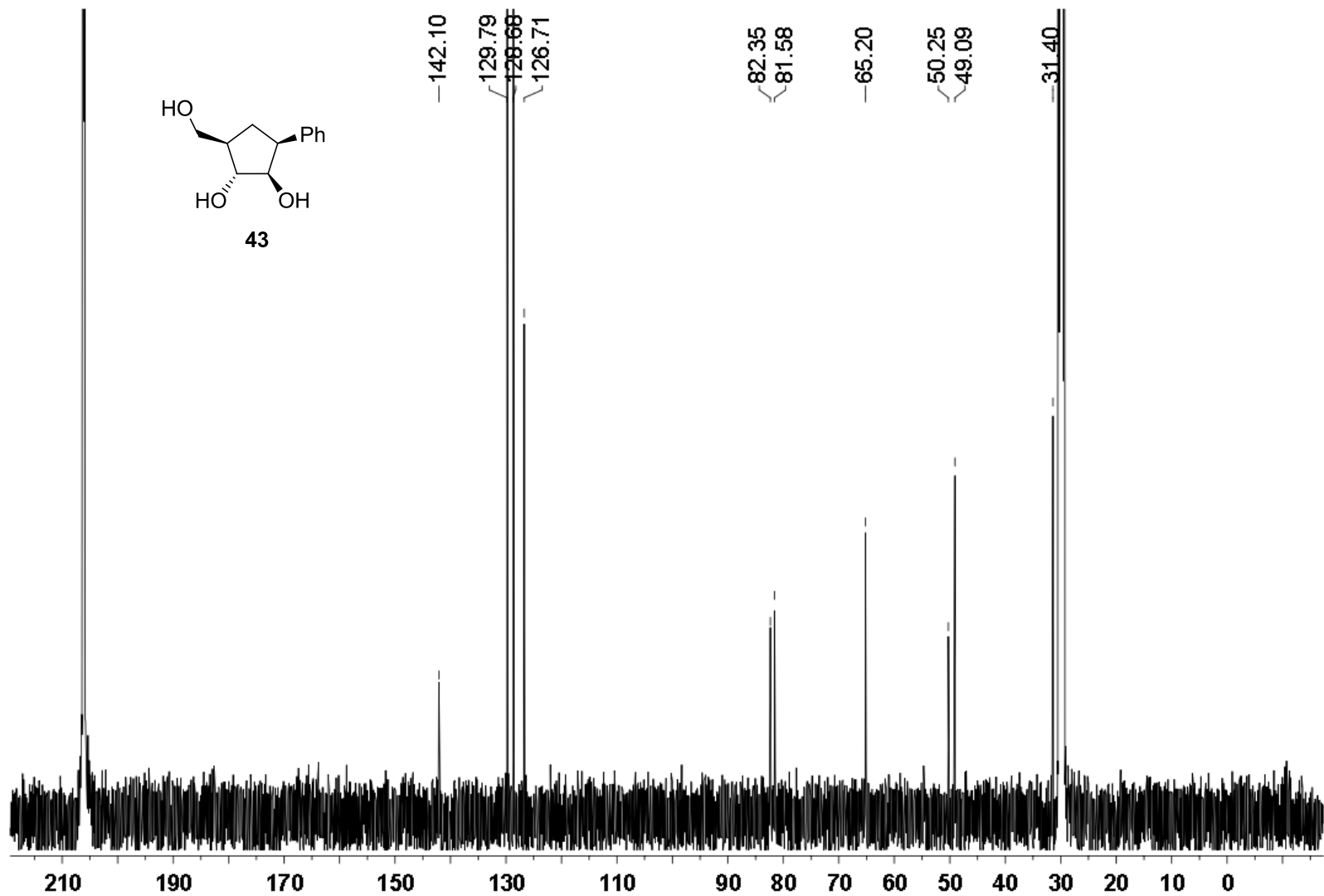
<sup>1</sup>H NMR (500 MHz) spectrum of **42** in CDCl<sub>3</sub>



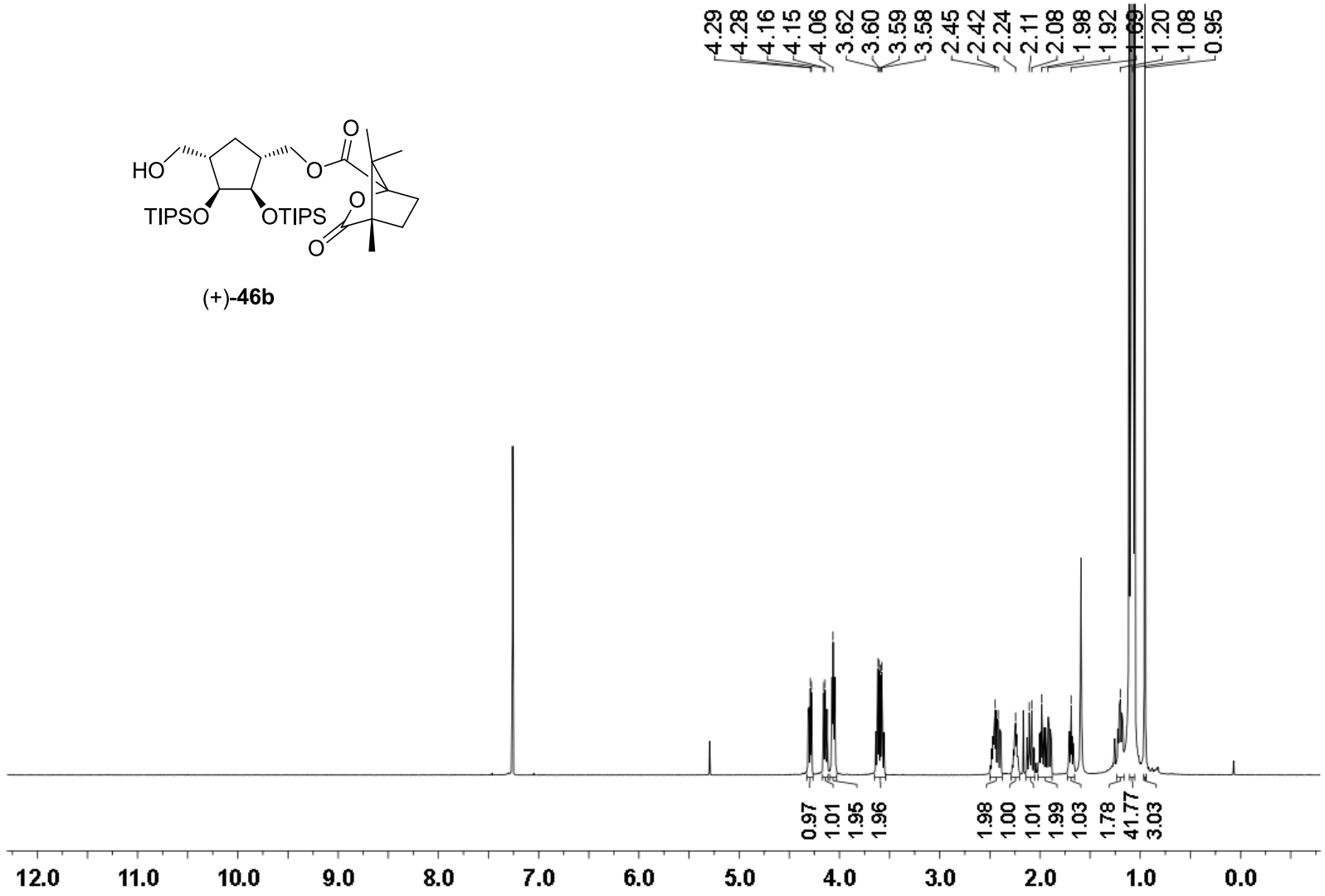
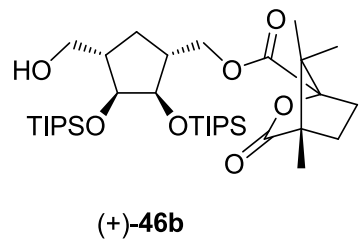
<sup>13</sup>C NMR (126 MHz) spectrum of **42** in CDCl<sub>3</sub>



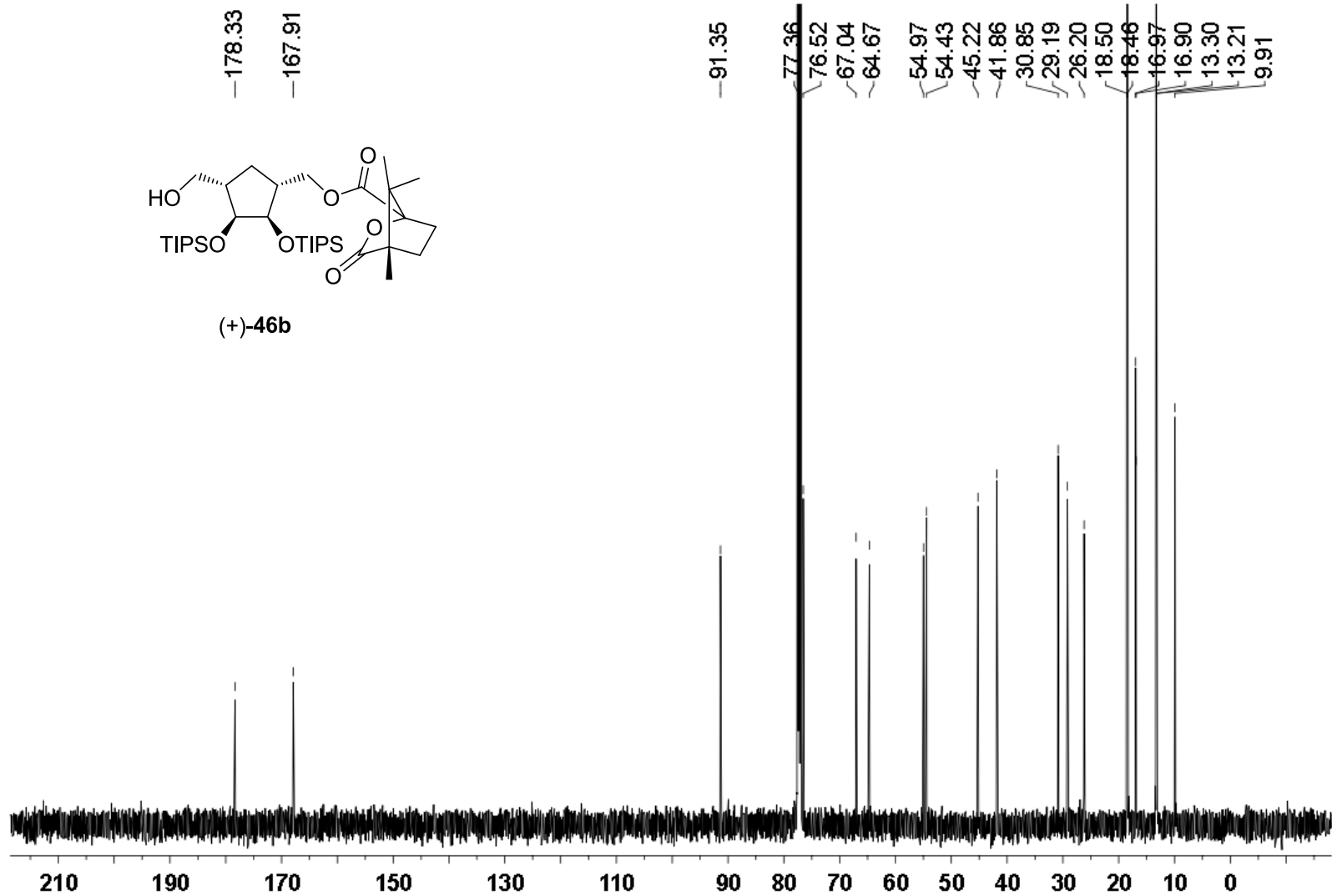
$^1\text{H}$  NMR (500 MHz) spectrum of **43** in acetone- $d_6$



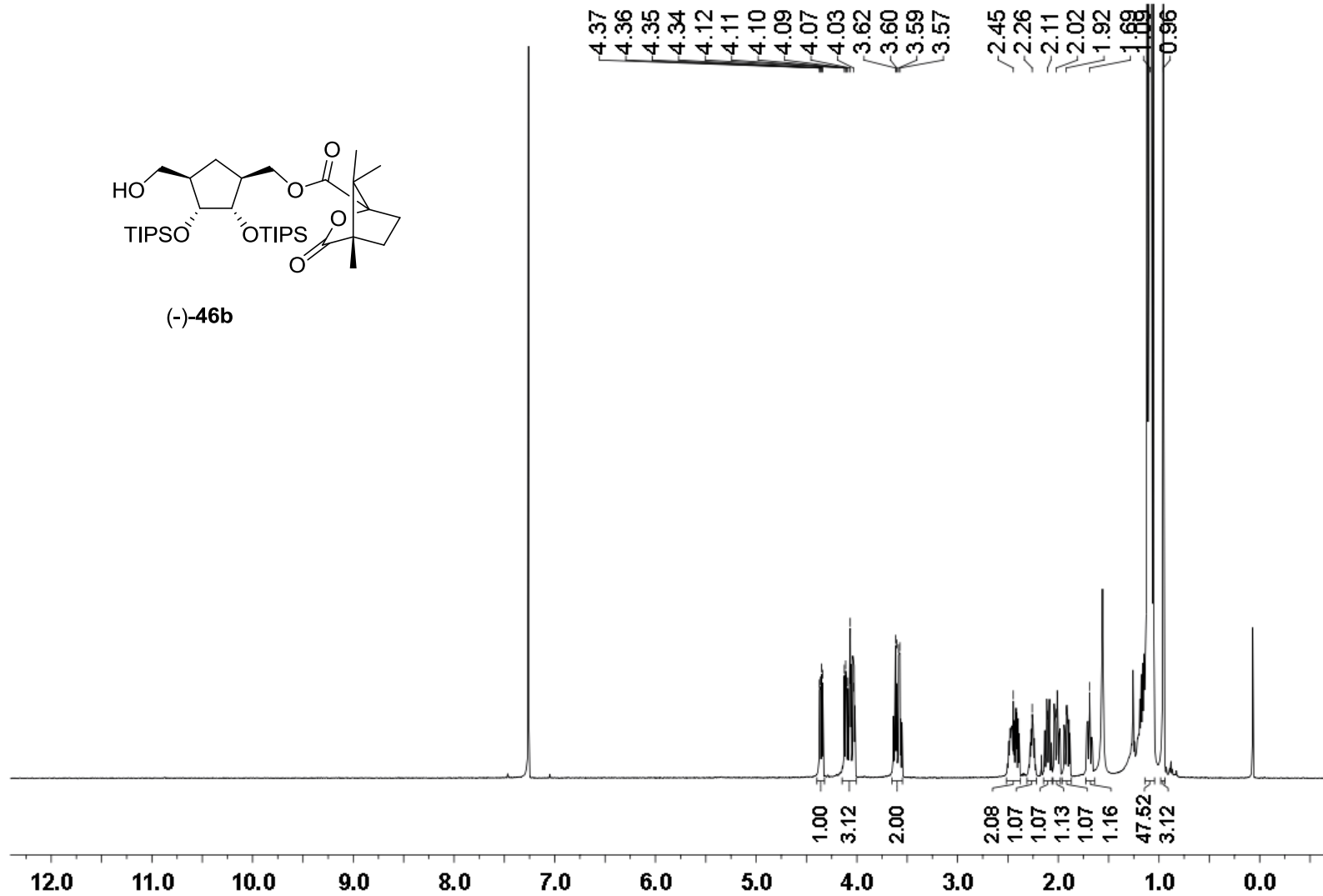
$^{13}\text{C}$  NMR (126 MHz) spectrum of **43** in acetone- $d_6$



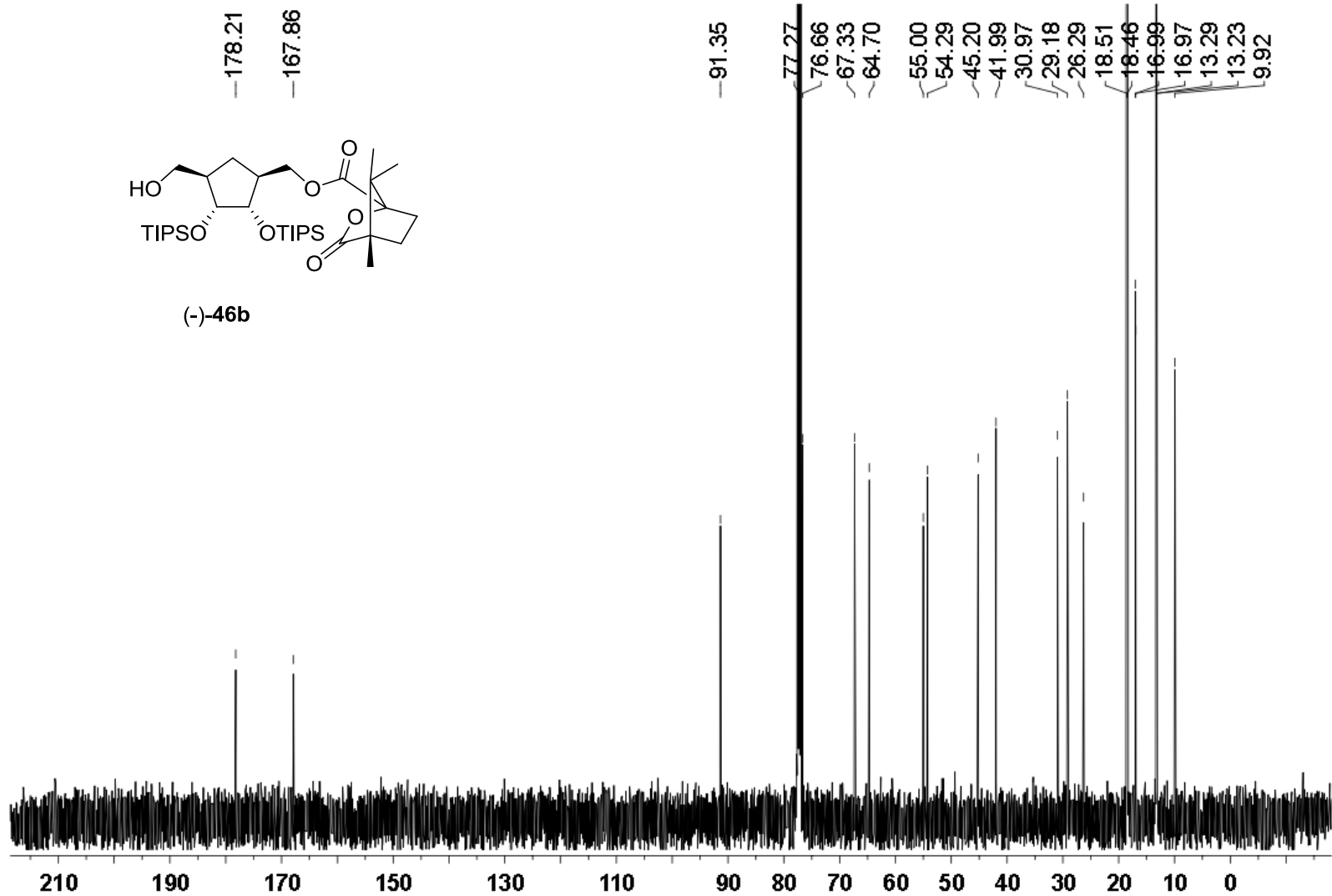
<sup>1</sup>H NMR (500 MHz) spectrum of (+)-46b in CDCl<sub>3</sub>



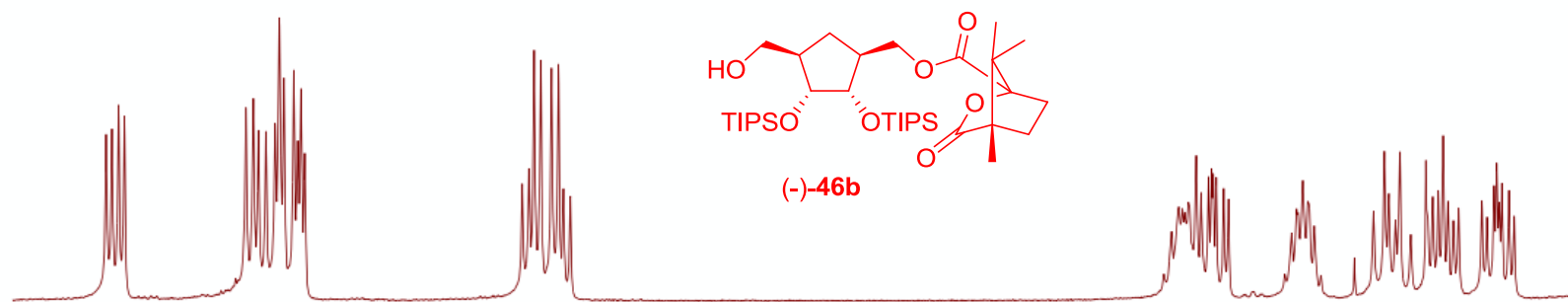
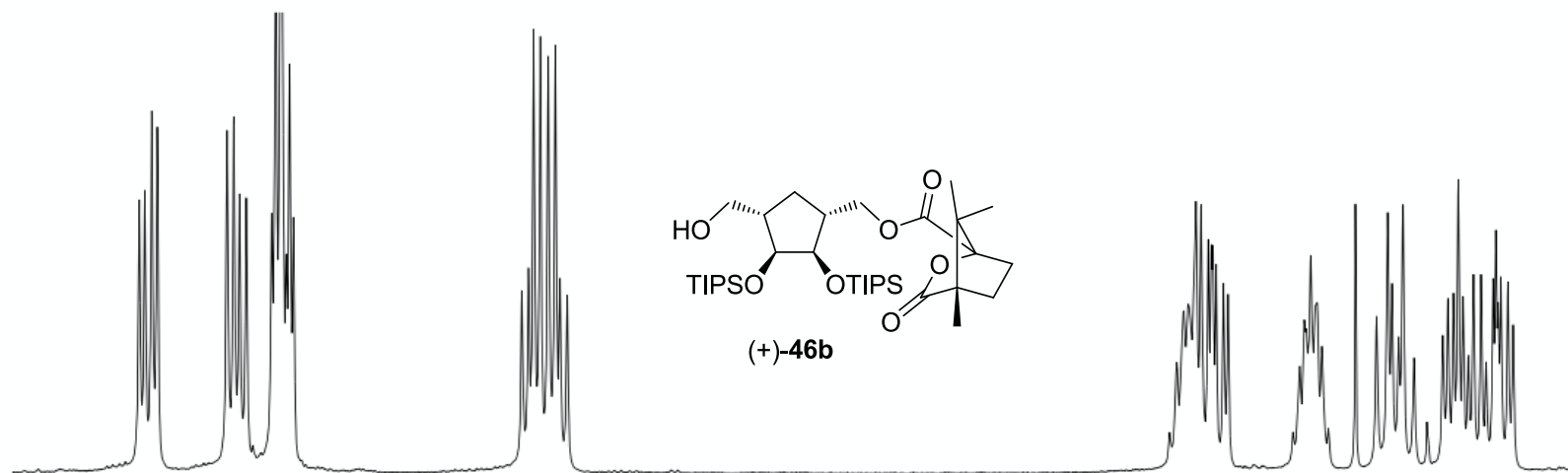
<sup>13</sup>C NMR (126 MHz) spectrum of (+)-46b in CDCl<sub>3</sub>



$^1\text{H}$  NMR (500 MHz) spectrum of (-)-46b in  $\text{CDCl}_3$



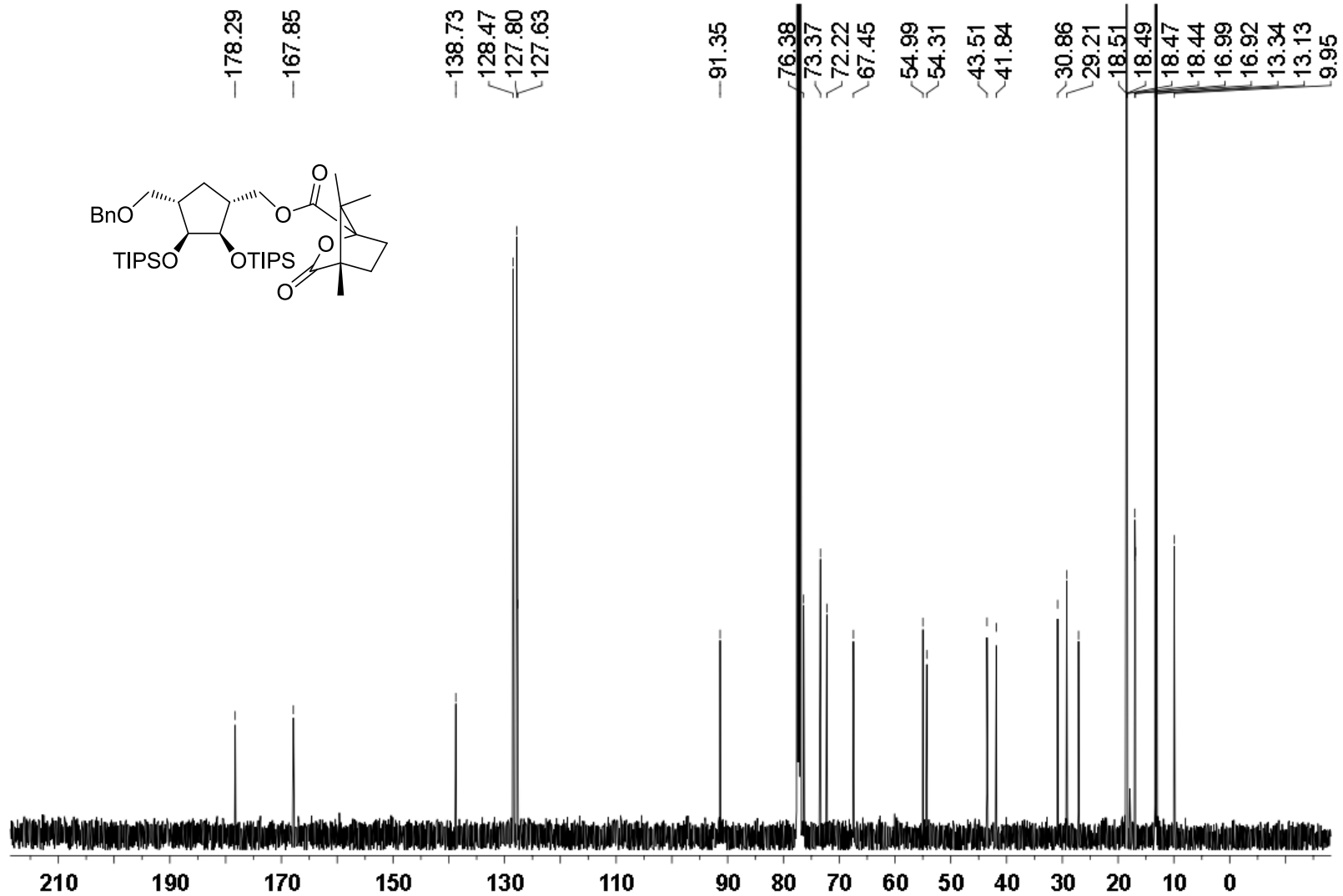
$^{13}\text{C}$  NMR (126 MHz) spectrum of (-)-46b in  $\text{CDCl}_3$



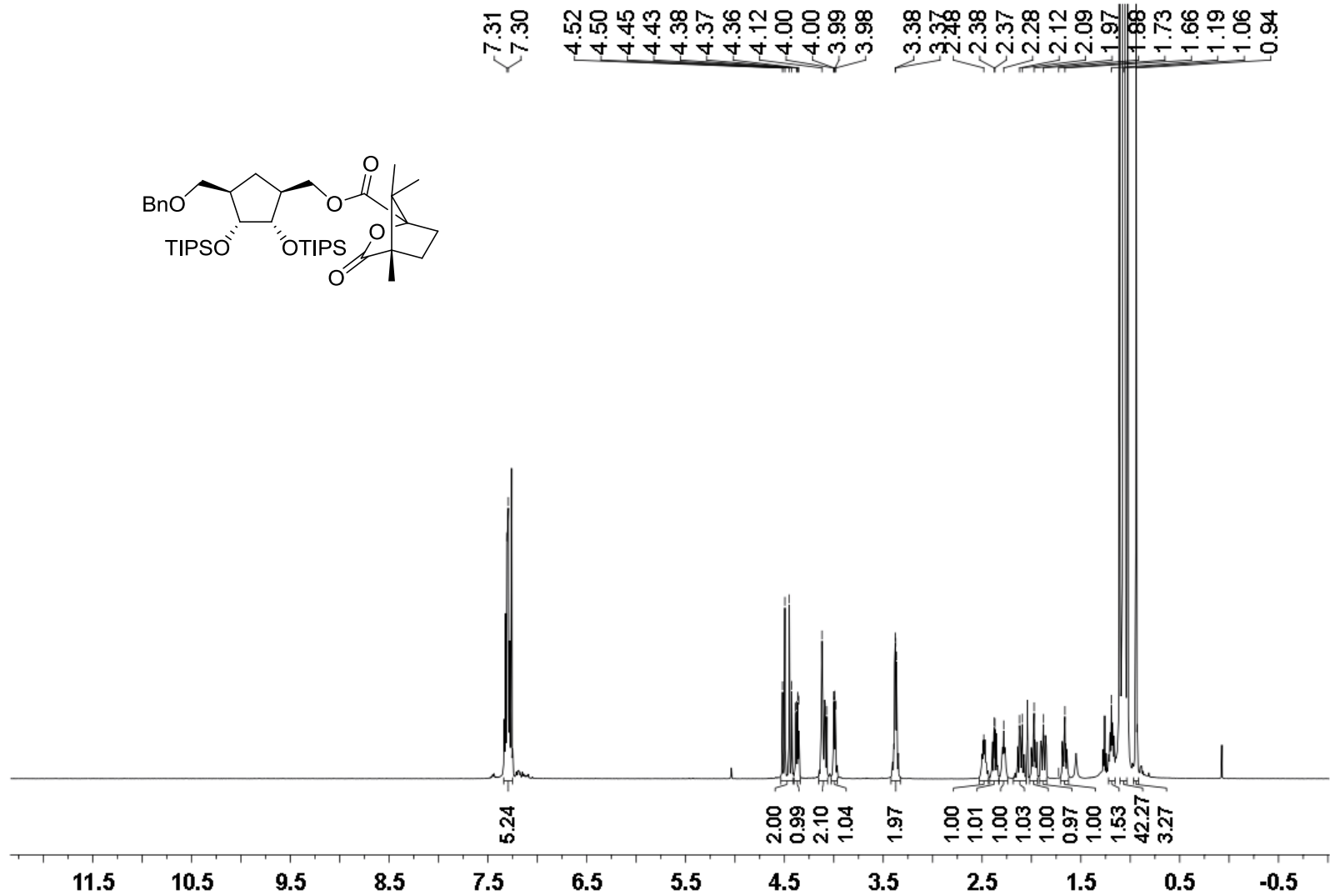
4.5 4.3 4.1 3.9 3.7 3.5 3.3 3.1 2.9 2.7 2.5 2.3 2.1 1.9

Portion of <sup>1</sup>H NMR spectrum of diastereomers **46b**



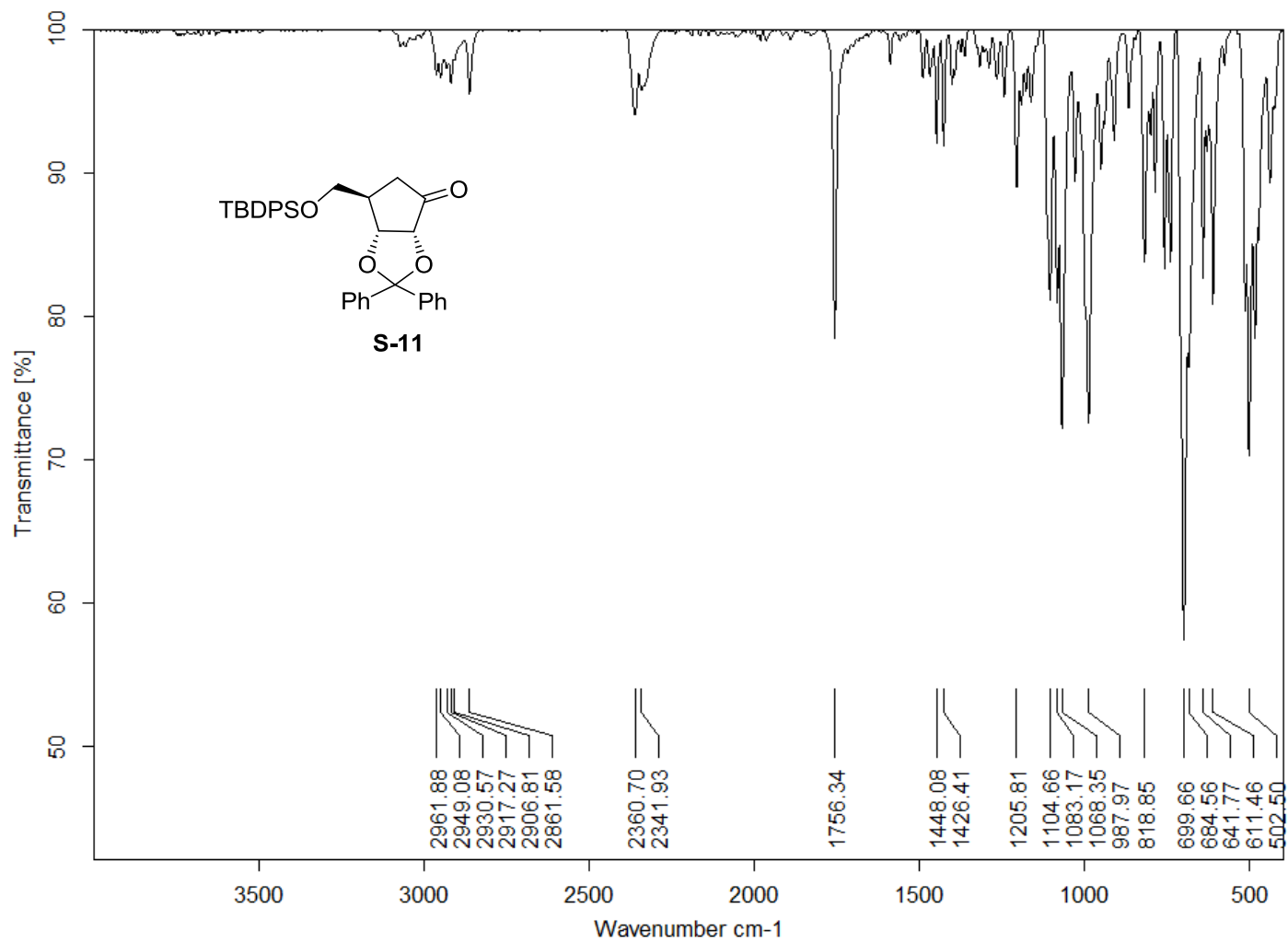


$^{13}\text{C}$  NMR (126 MHz) spectrum in  $\text{CDCl}_3$



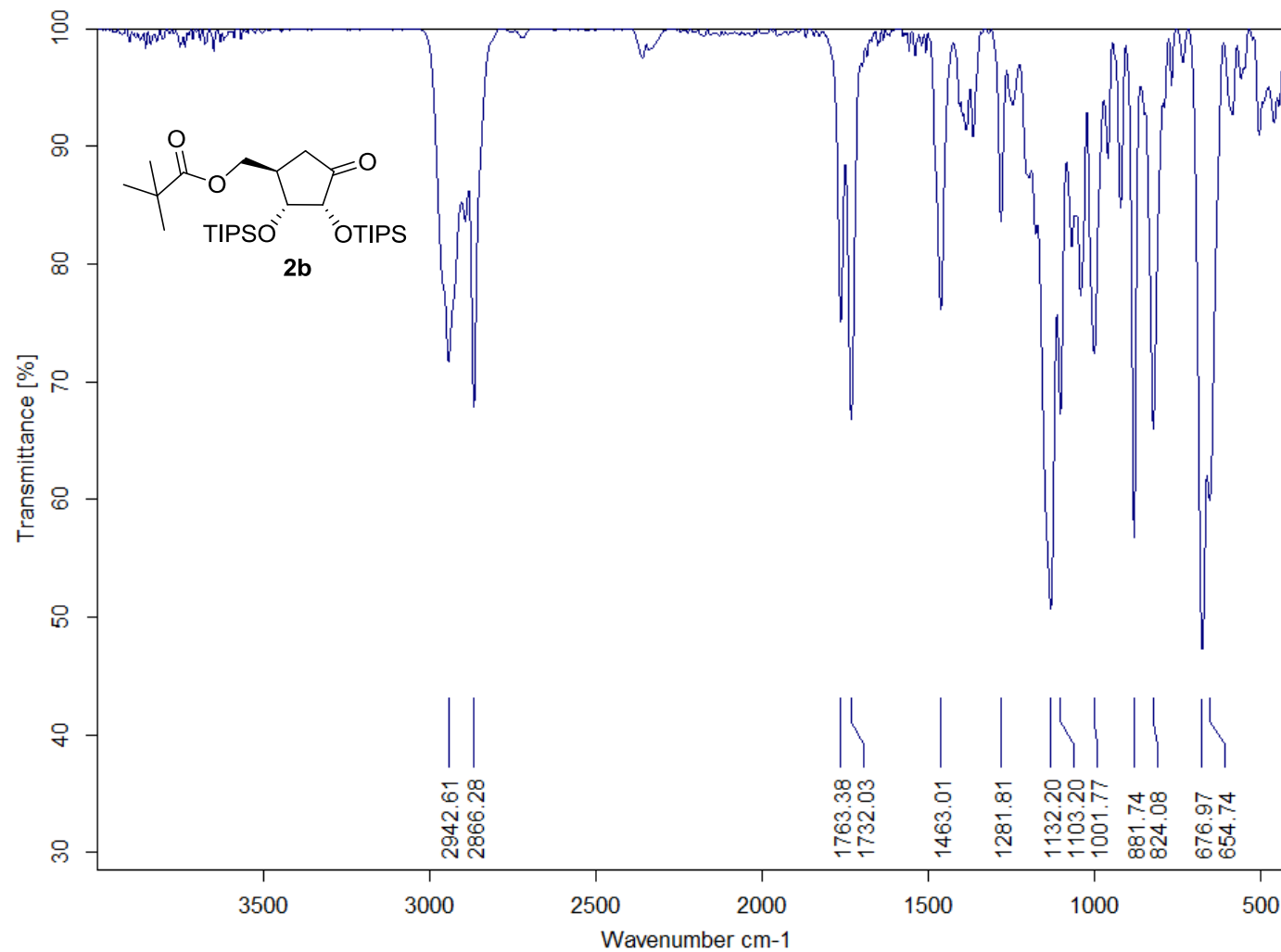
<sup>1</sup>H NMR (500 MHz) spectrum in CDCl<sub>3</sub>





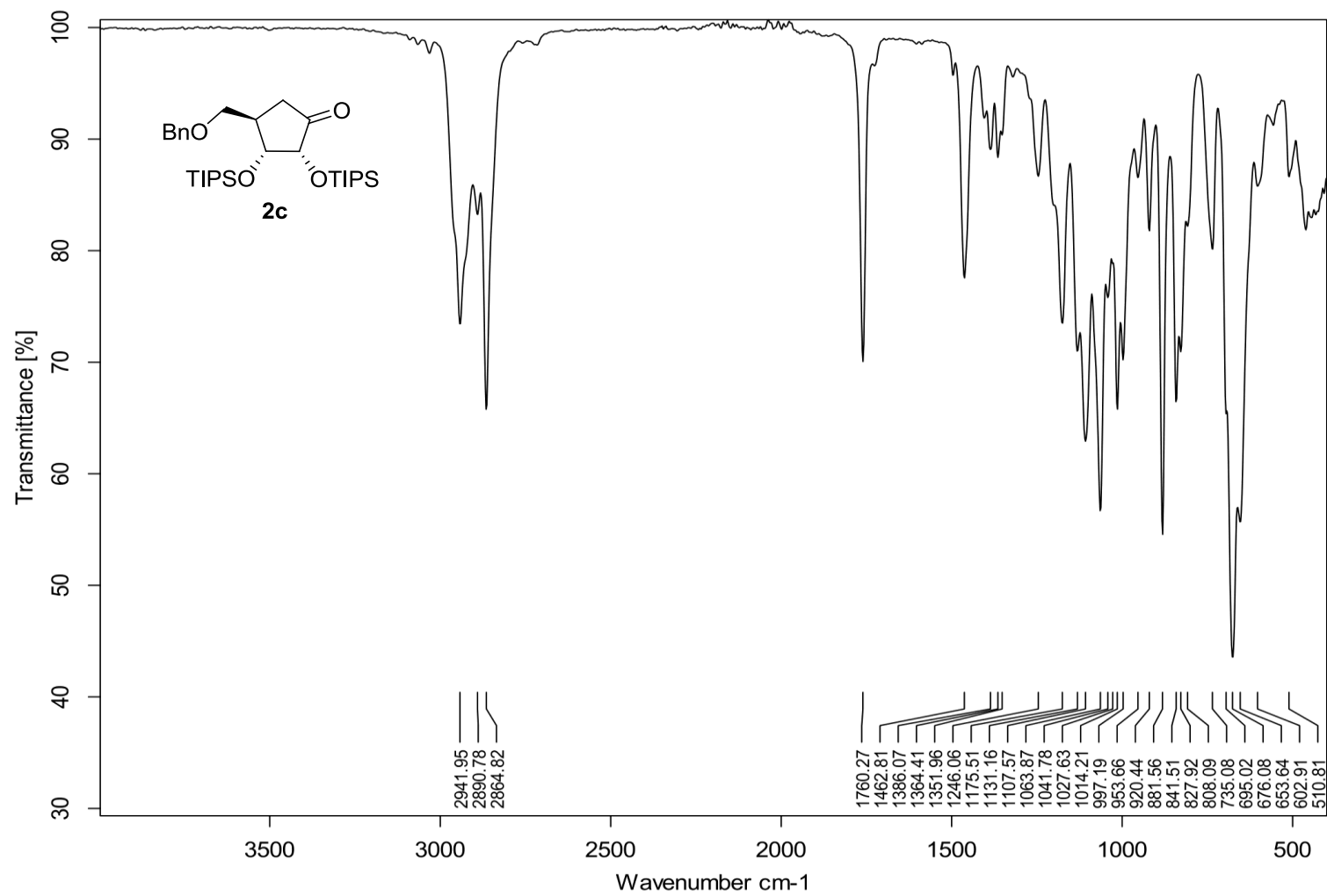
Page 1 of 1

IR spectrum (neat) of S-11

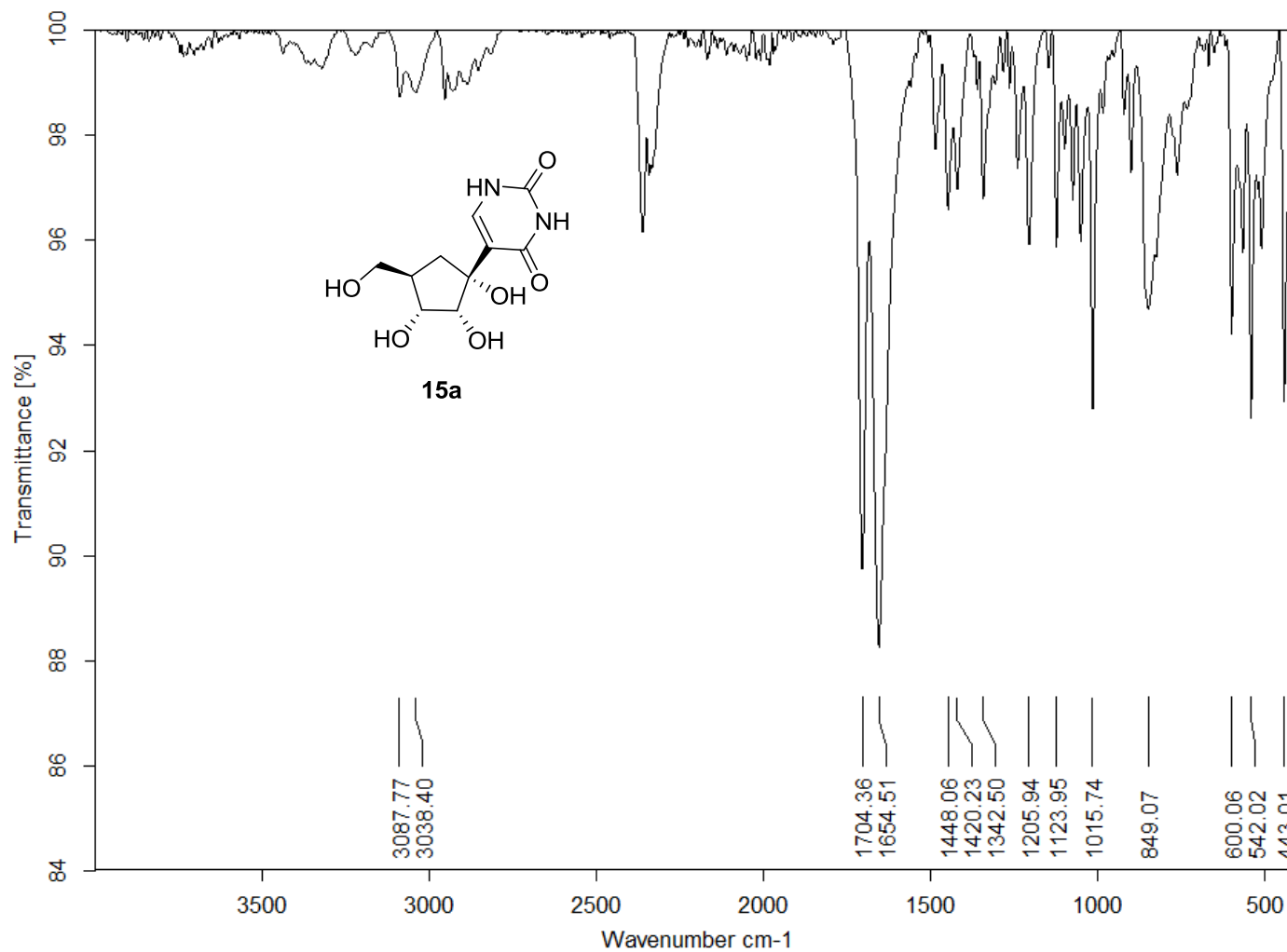


Page 1 of 1

IR spectrum (neat) of **2b**

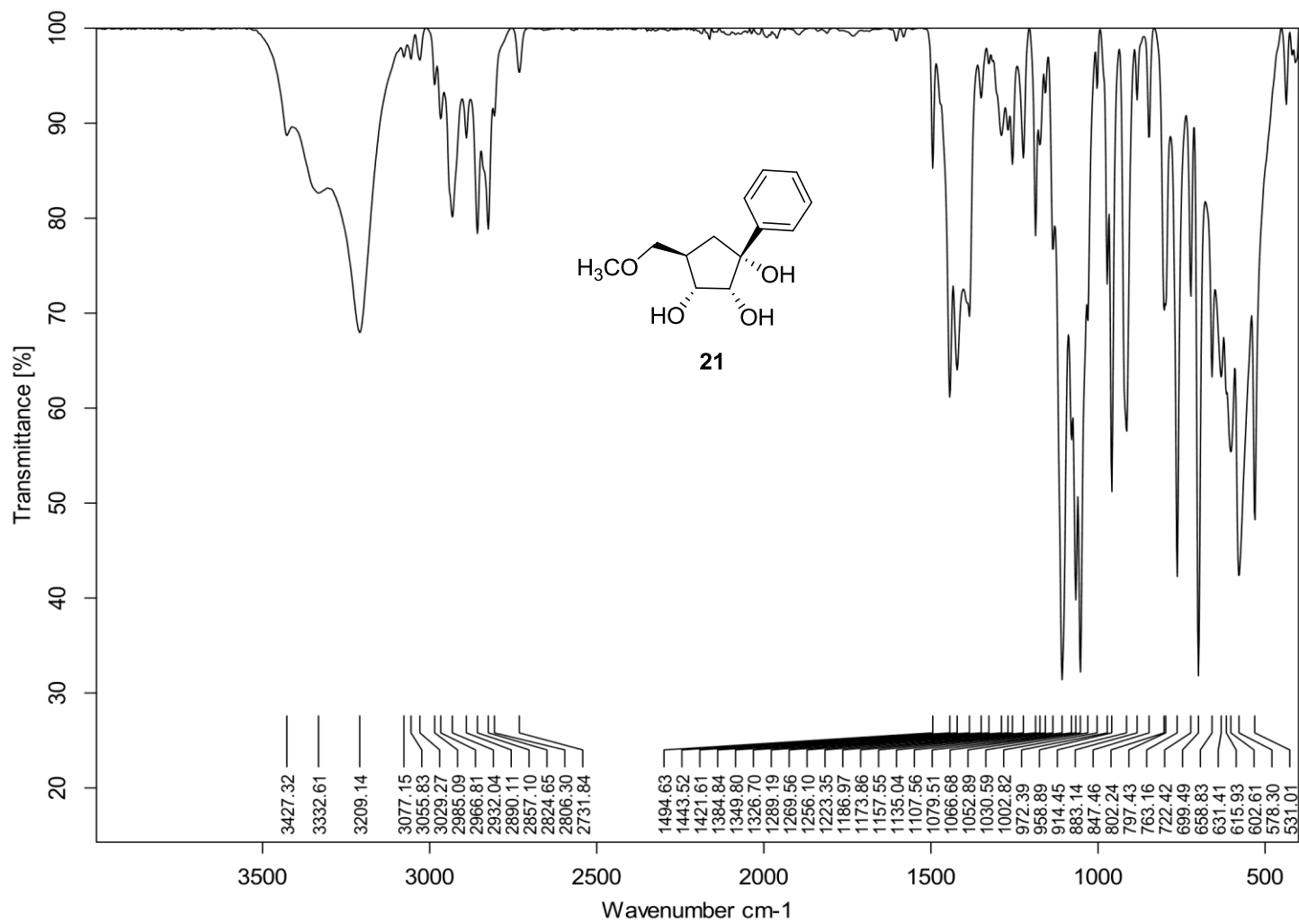


IR spectrum (neat) of **2c**

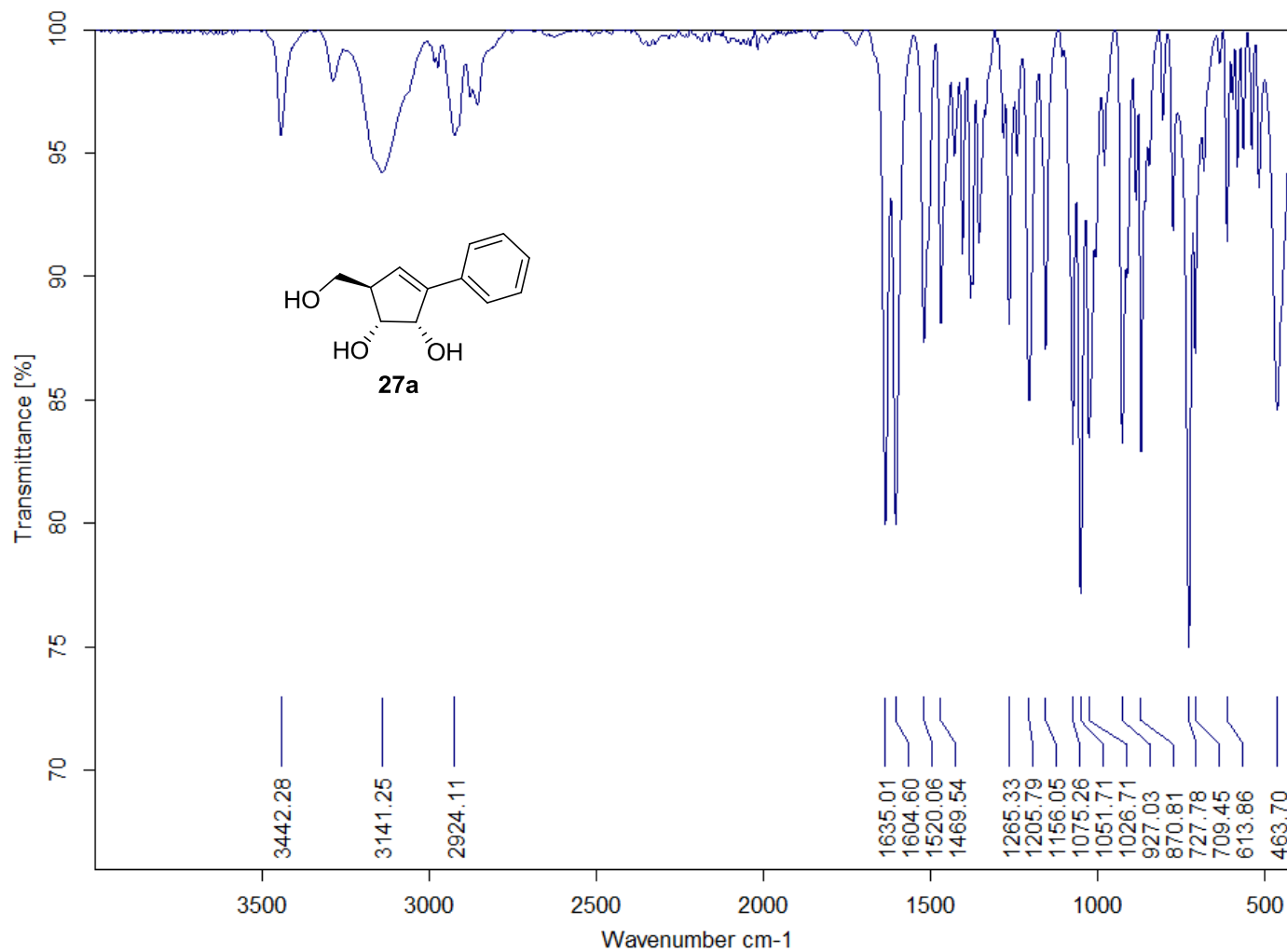


Page 1 of 1

IR spectrum (neat) of **15a**

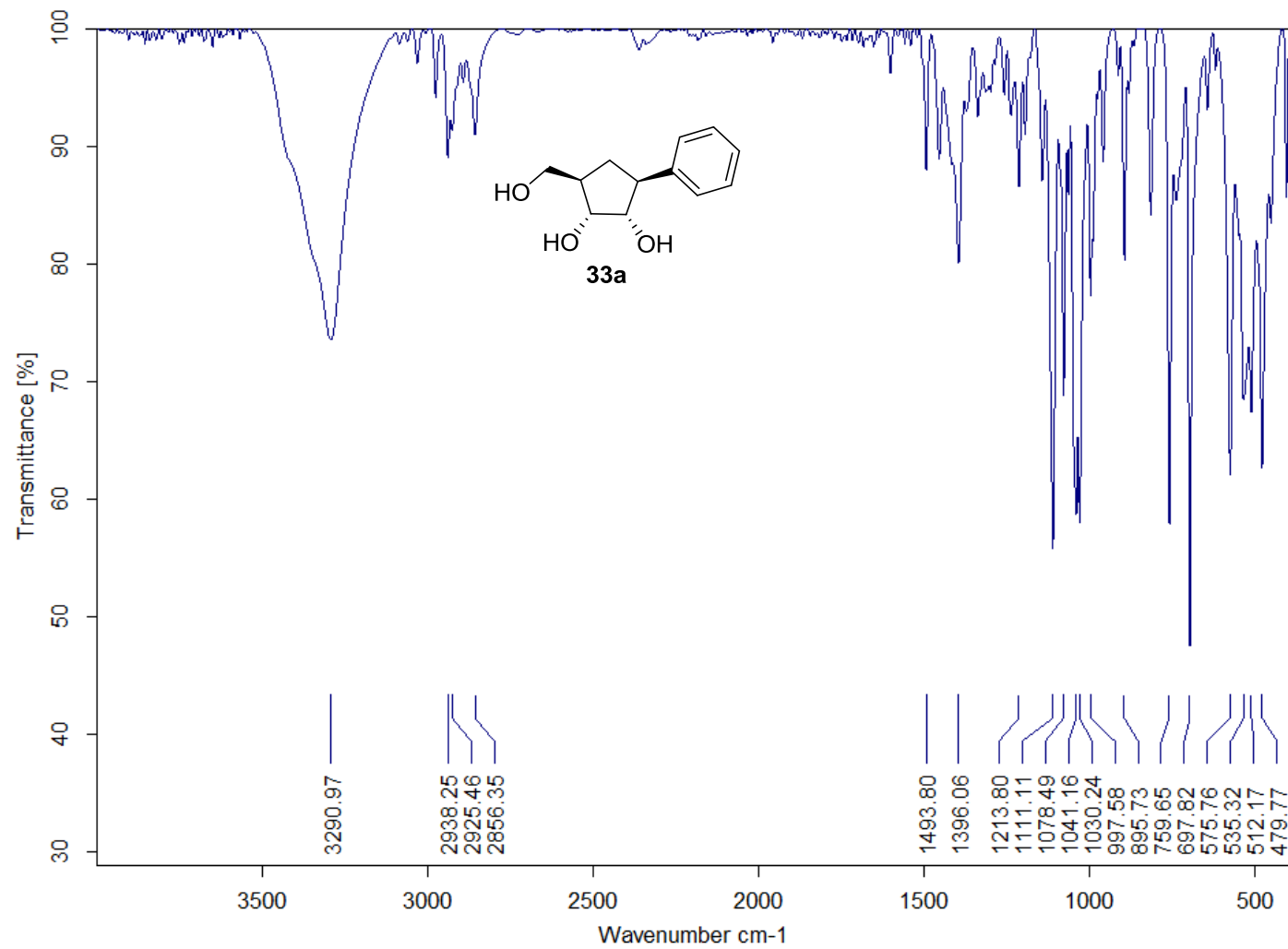


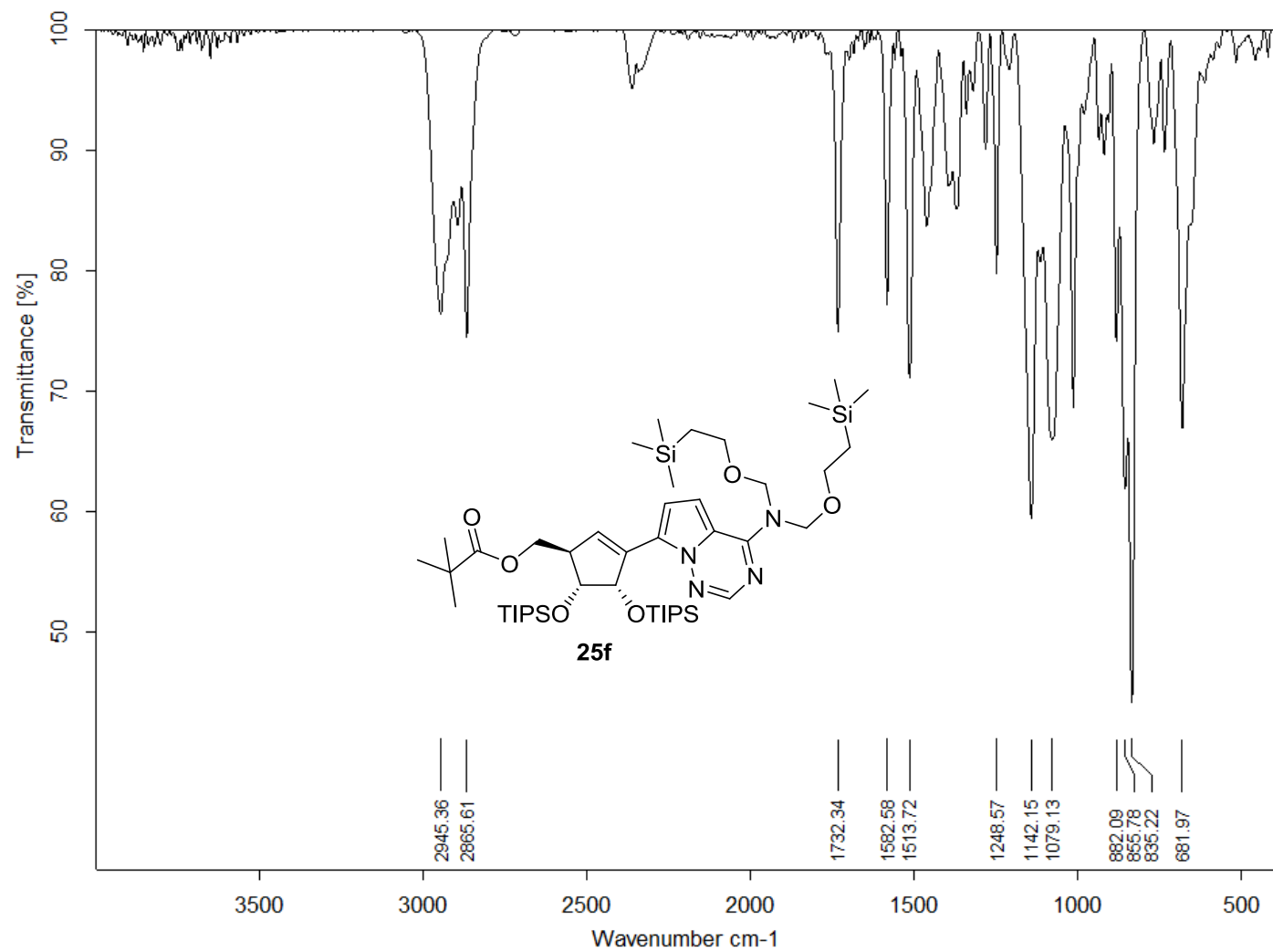
IR spectrum (neat) of **21**



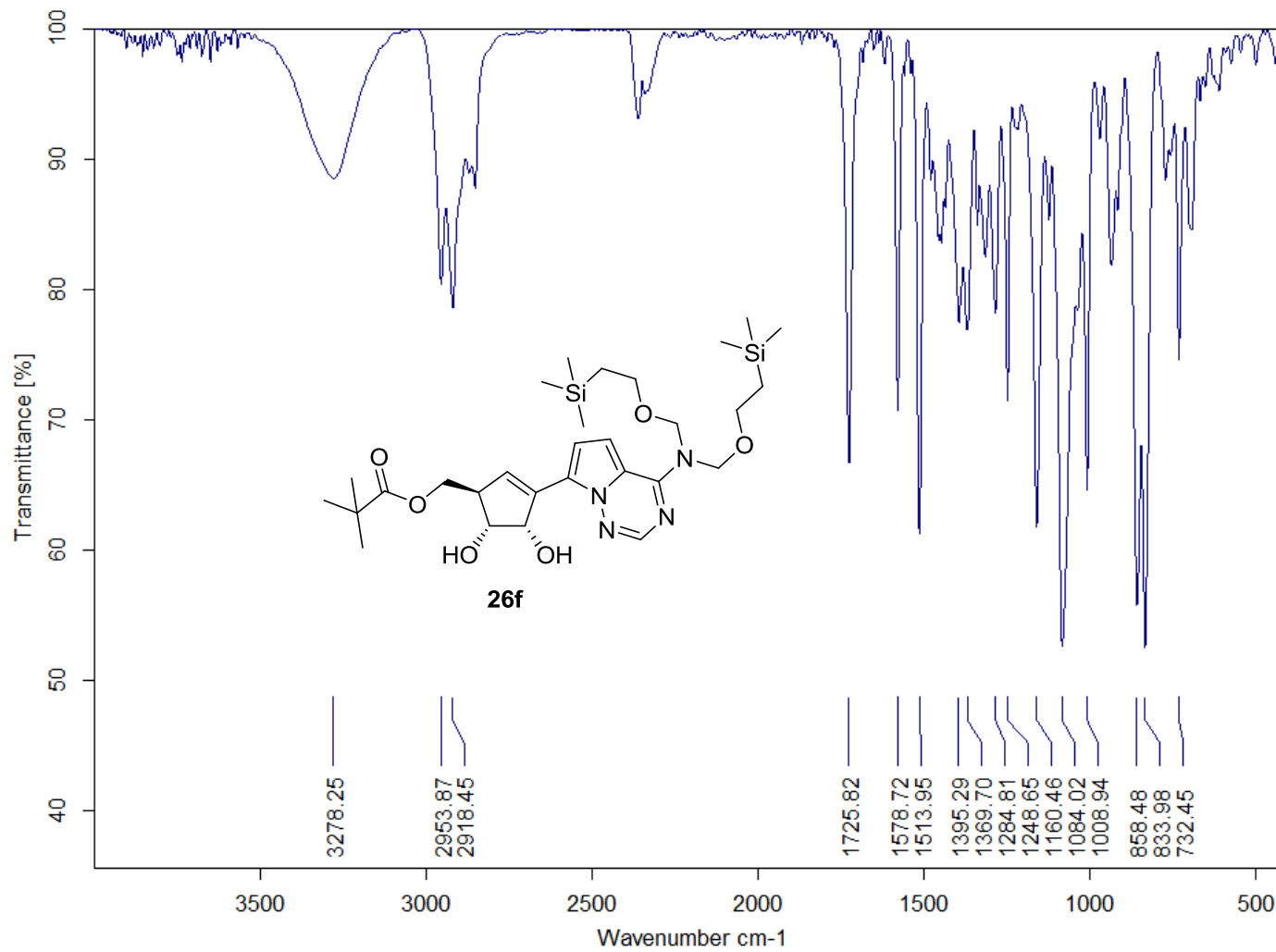
Page 1 of 1

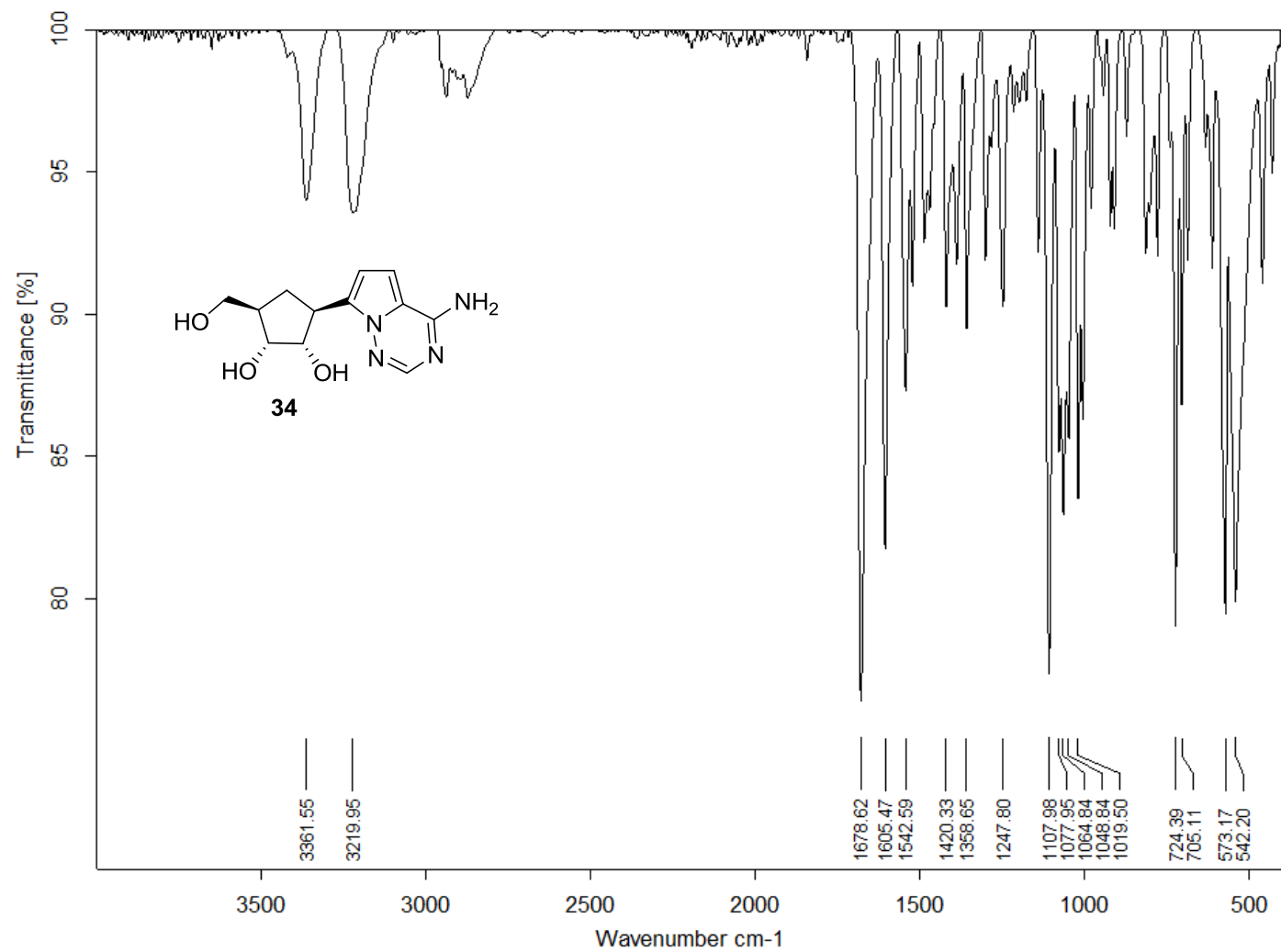
IR spectrum (neat) of **27a**





IR spectrum (neat) of **25f**

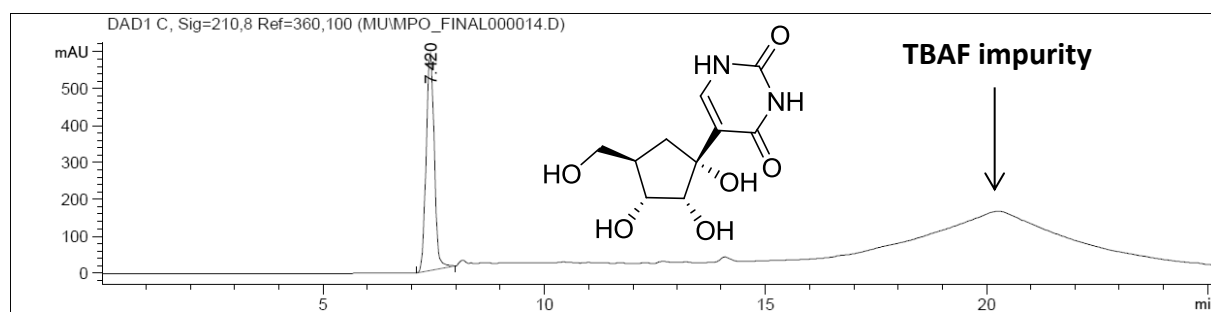




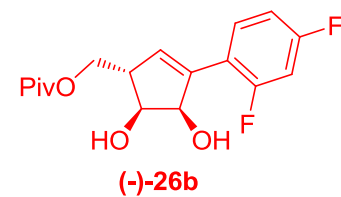
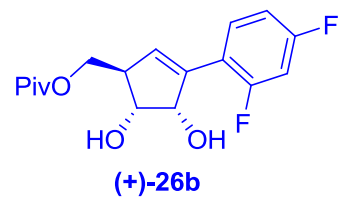
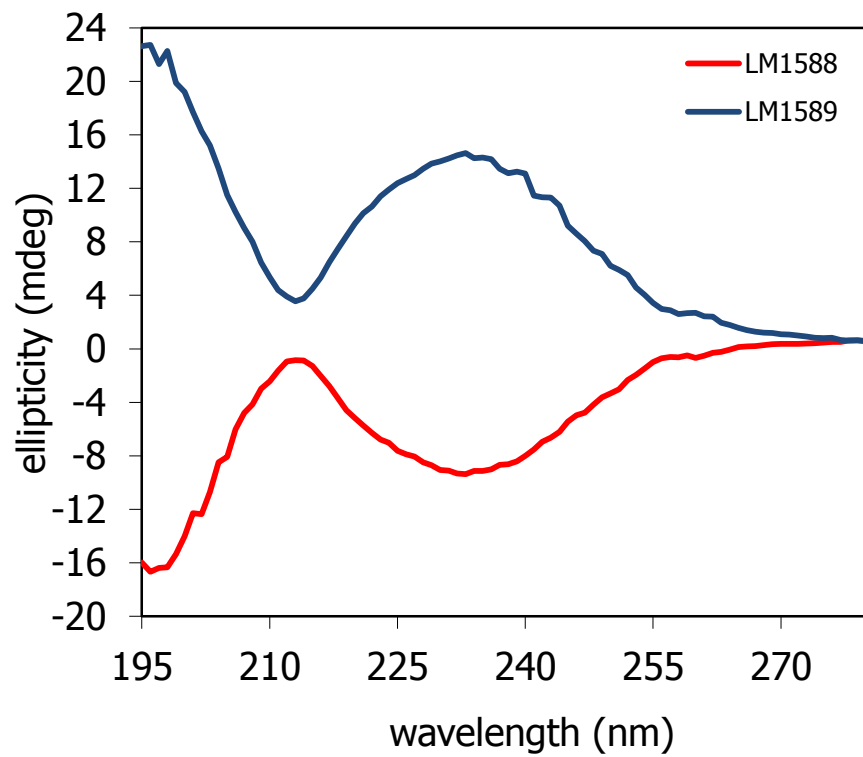
IR spectrum (neat) of **34**

**Table 1. Gradient elution profile for RP-HPLC (Nucleodur<sup>®</sup> C18 HTec, 5 $\mu$ m, 250 mm  $\times$  50 mm) purification of 15a and 15e (solvent A – MeOH, solvent B – H<sub>2</sub>O).**

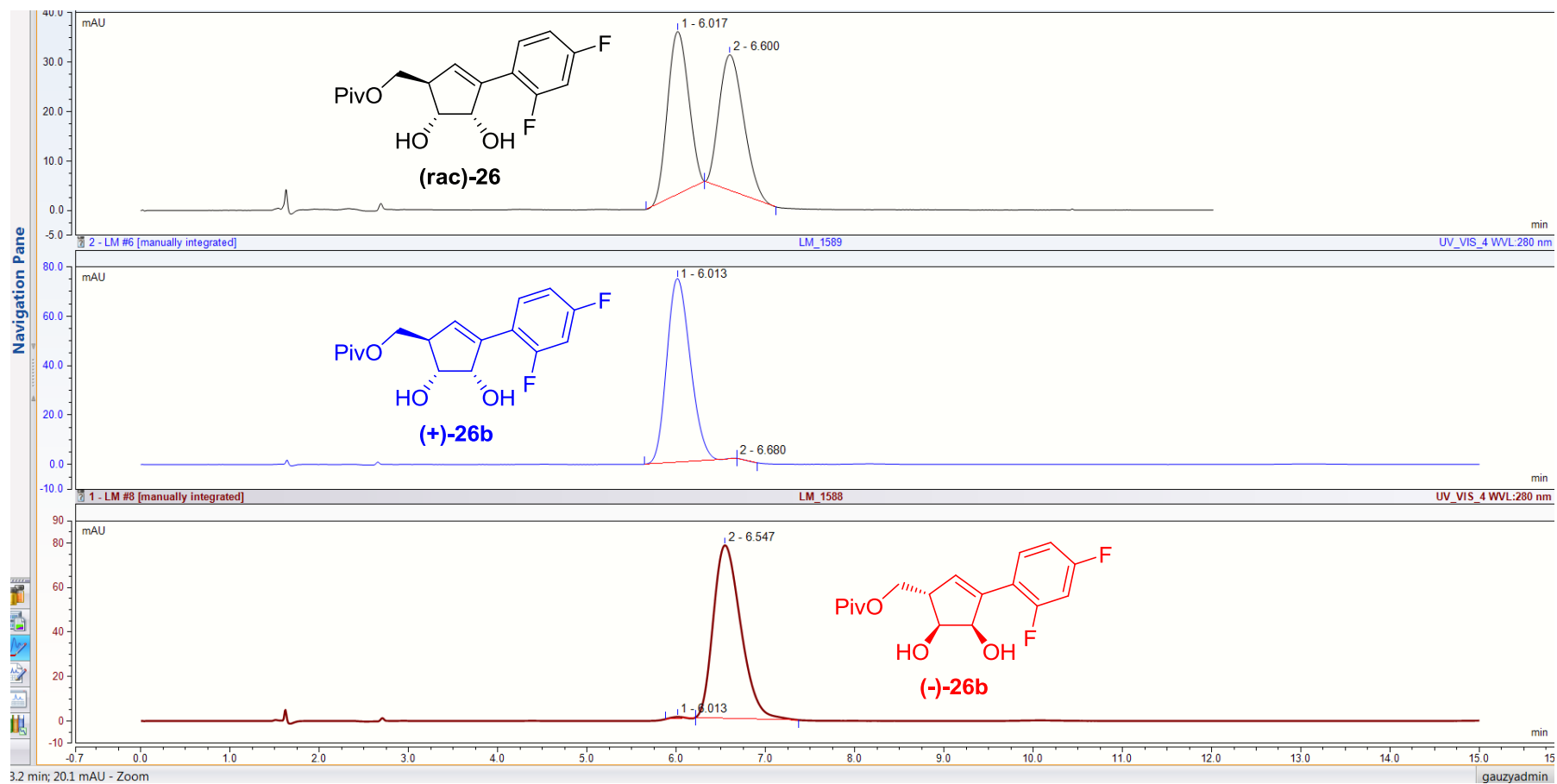
Time [min]	Solvent B [%]	Flow [ml/min]
0.00	90.0	10.00
2.00	60.0	10.00
4.00	55.0	10.00
6.00	50.0	10.00
8.00	45.0	10.00
10.00	40.0	10.00
12.00	30.0	10.00
14.00	15.0	10.00
25.00	90.0	10.00



HPLC Chromatogram of compound **15a** (UV detection at 210 nm).



CD spectra of enantiomers of compound **26** (EtOH,  $10^{-3}$  M)

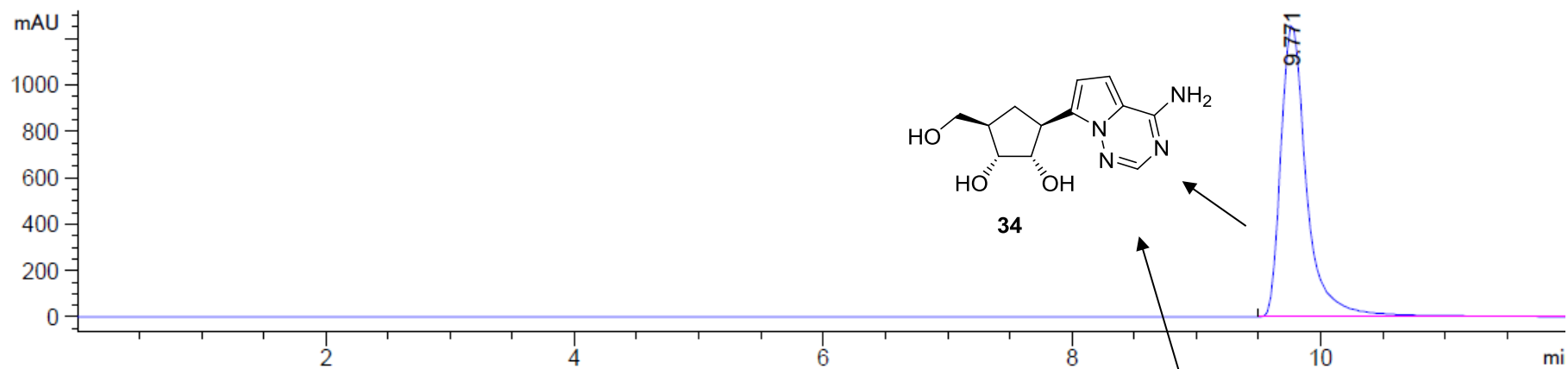


HPLC chromatogram of racemic compound 27 and corresponding HPLC analysis of enantiomers **(+)-26b** and **(-)-27b**. (Daicel-CHIRALPAK AS 4.6 mm × 250 mm; hexane/EtOH = 96.5 / 3.5; 2 mL/min;  $t_r$ ;  $t_R$  = 6.02 min for **(+)-26b**, 6.60 min for **(-)-26b**).

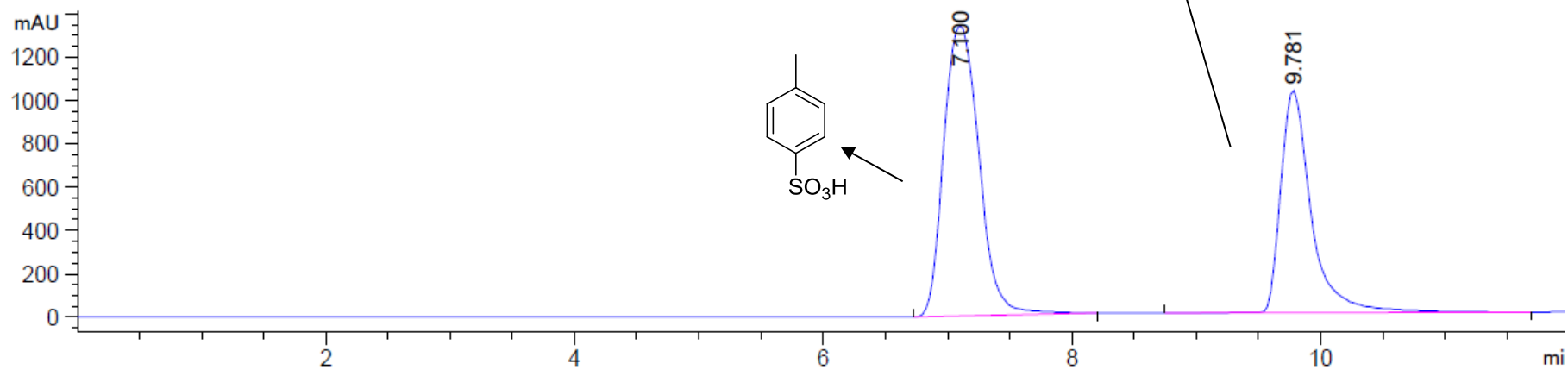
**Table 2. Gradient elution profile for RP-HPLC (Nucleodur<sup>®</sup> C18 HTec, 5µm, 250 mm × 50 mm) purification of compounds 28 and 34 (solvent A – MeOH, solvent B – H<sub>2</sub>O).**

<b>Time [min]</b>	<b>Solvent B [%]</b>	<b>Flow [ml/min]</b>
0.00	90.0	10.00
2.00	65.0	10.00
4.00	55.0	10.00
6.00	52.0	10.00
8.00	50.0	10.00
10.00	45.0	10.00
13.00	90.0	10.00

DAD1 A, Sig=254,4 Ref=360,100 (MULM\_1500\_X000094.D)



DAD1 C, Sig=210,8 Ref=360,100 (MULM\_1500\_X000094.D)



HPLC chromatogram of tubercidine analog **34**

## Cell cultures

MCF7 breast cancer cells was cultivated in Minimum Essential Media (MEM) with L-Glutamine, Proline and Pyruvate (Gibco) supplemented with penicillin (100 U/mL), streptomycin (0.1 mg/mL) and 10% fetal bovine serum (Gibco).

Human foreskin fibroblasts HFF1 were maintained in Dulbecco's Modified Eagle's Medium (DMEM) supplemented with 15% fetal bovine serum (Gibco).

All cells were harvested after a brief incubation in 0.05% ethylenediaminetetraacetic acid (EDTA) in phosphate-buffered saline (PBS), followed by trypsinization (0.25% w/v trypsin/0.53 mM EDTA in PBS). They were then counted by using a CASY TT automatic cell counter (Roche Diagnostics, Prague, Czech Republic), diluted in the appropriate volume and seeded for experimental procedure.

MCF7 and HFF1 cell lines were obtained from American Type Culture Collection (LGC Standards, Warsaw, Poland).

## Cell proliferation assays

For cytotoxicity screening the cells were seeded at the density of 20 000 cells/cm<sup>2</sup> on black Corning 96 well plates with clear flat bottom. After 24 hrs, cells were treated with tubercidine or compound **34** (3 wells per concentration, range 0,0015 uM to 100 uM using 9 points). Vehicle (DMSO) was added at the same time as the control. The cells were grown during next 24 hrs. The medium was then gently removed, the cells were refurbished with fresh medium and allowed to proliferate for 48 hrs. Finally, the cells were harvested and analysed using the CyQuant assay. The CyQuant cell proliferation assay (Invitrogen) was performed according to the manufacturer's recommendations and the results were analysed using a Fluostar Galaxy reader (BMG Labtech, Ortenberg, Germany).

## Data analysis

The data were evaluated as % of viable cell normalized to the control (DMSO). For calculation of IC<sub>50</sub> values, a four-parameter logistic dose-response model with a sigmoidal shape was used:  $Y = \text{Bottom} + (\text{Top} - \text{Bottom}) / (1 + (x / \text{IC}_{50})^{\text{HillSlope}})$  where IC<sub>50</sub> denoted the concentration of the inhibitor that gave a response that was halfway between Bottom and Top. HillSlope described the steepness of the curve, and the Top and Bottom denoted plateaus in the units of the Y-axis. Lower and upper bound of a 95% confidence interval for IC<sub>50</sub> was calculated.